

Glass Property-Composition Models for Support of Hanford WTP LAW Facility Operation

March 2022

John D. Vienna
Alejandro Heredia-Langner
Scott K. Cooley
Aimee E. Holmes
Dong-Sang Kim
Nicholas A. Lumetta

DISCLAIMER

This report was prepared as an account of work sponsored by an agency of the United States Government. Neither the United States Government nor any agency thereof, nor Battelle Memorial Institute, nor any of their employees, makes any warranty, express or implied, or assumes any legal liability or responsibility for the accuracy, completeness, or usefulness of any information, apparatus, product, or process disclosed, or represents that its use would not infringe privately owned rights. Reference herein to any specific commercial product, process, or service by trade name, trademark, manufacturer, or otherwise does not necessarily constitute or imply its endorsement, recommendation, or favoring by the United States Government or any agency thereof, or Battelle Memorial Institute. The views and opinions of authors expressed herein do not necessarily state or reflect those of the United States Government or any agency thereof.

PACIFIC NORTHWEST NATIONAL LABORATORY
operated by
BATTELLE
for the
UNITED STATES DEPARTMENT OF ENERGY
under Contract DE-AC05-76RL01830

Printed in the United States of America
Available to DOE and DOE contractors from the
Office of Scientific and Technical Information,
P.O. Box 62, Oak Ridge, TN 37831-0062;
ph: (865) 576-8401
fax: (865) 576-5728
email: reports@adonis.osti.gov
Available to the public from the National Technical Information Service
5301 Shawnee Rd., Alexandria, VA 22312
ph: (800) 553-NTIS (6847)
email: orders@ntis.gov <<https://www.ntis.gov/about>>
Online ordering: <http://www.ntis.gov>

Glass Property-Composition Models for Support of Hanford WTP LAW Facility Operation

March 2022

John D. Vienna
Alejandro Heredia-Langner
Scott K. Cooley
Aimee E. Holmes
Dong-Sang Kim
Nicholas A. Lumetta

Prepared for
the U.S. Department of Energy
under Contract DE-AC05-76RL01830

Pacific Northwest National Laboratory
Richland, Washington 99354

Abstract

Current plans for the River Protection Project at Hanford envision starting to vitrifying low-activity waste (LAW) by 2023 using a Direct Feed Low-Activity Waste (DFLAW) approach.¹ The Waste Treatment and Immobilization Plant (WTP) LAW Facility will be operated and controlled using a LAW glass formulation algorithm (GFA), which requires several inputs based on research and development results. LAW glass property-composition models for several product quality and processing properties are key inputs for the LAW GFA.

It is envisioned that the preliminary LAW GFA discussed by Kim and Vienna (2012)² will be used for commissioning and initial radioactive operations of the WTP LAW Facility under Bechtel National, Inc. using the DFLAW approach. Then, an updated LAW GFA will be developed for implementation by the WTP operating contractor that takes over after WTP LAW Facility commissioning. This report documents the enhanced LAW glass property-composition models developed for use in the updated LAW GFA. The properties for which models were developed include Product Consistency Test (PCT) response, Vapor Hydration Test (VHT) response, viscosity at 1150 °C, electrical conductivity at 1150 °C, melter SO₃ tolerance at 1150 °C, and K-3 refractory corrosion at 1208 °C. Table S.1 lists the tables in this report that contain the recommended models for each of these properties. The model types recommended include partial quadratic mixture (PQM) models for viscosity, electrical conductivity, melter SO₃ tolerance and K-3 corrosion, bias corrected PQM model (bcPQM) for PCT, and logistic PQM model for VHT. The fits of model and validation subsets were found to be well predicted by the recommended models.

Table S.1. Report Tables Containing the Recommended Property-Composition Models and Their Variance-Covariance Matrices

LAW Glass Property	Model Form	Report Table Containing Recommended Model	Report Table Containing Variance-Covariance Matrix for Recommended Model
PCT, B and Na normalized losses (g/m ²)	bcPQM	Table 3.7 (B), Table 3.11 (Na)	Table D.2, Table D.4
VHT (pass/fail)	Logistic PQM model	Table 4.6	Table D.6
Viscosity at 1150 °C (poise)	PQM model	Table 5.5	Table D.8
Electrical conductivity at 1150 °C (S/cm)	PQM model	Table 6.5	Table D.10
Melter SO ₃ tolerance (wt%)	PQM model	Table 7.5	Table D.12
K-3 refractory corrosion (inches)	PQM model	Table 8.5	Table D.14

¹ Tilanus SN, LM Bergman, RO Lokken, AJ Schubick, EB West, RT Jasper, SL Orcutt, TM Holh, AN Praga, MN Wells, KW Burnett, CS Smalley, JK Bernards, SD Reaksecker, and TL Waldo. 2017. *River Protection Project System Plan*. ORP-11242, Rev. 8. U.S. Department of Energy, Office of River Protection, Richland, Washington.

² Kim DS and JD Vienna. 2012. *Preliminary ILAW Formulation Algorithm Description*. 24590 LAW RPT-RT-04-0003, Rev. 1, ORP-56321, River Protection Project, Hanford Waste Treatment and Immobilization Plant, Richland, Washington.

Quality Assurance

This work was performed under the U.S. Department of Energy (DOE) Office of River Protection Inter-Entity Work Order # M0ORV00020 and in accordance with the Pacific Northwest National Laboratory (PNNL) Nuclear Quality Assurance Program (NQAP) Quality Assurance Manual (NQAP-2012) and associated quality assurance procedures. The NQAP is based on the requirements of NQA-1-2012, *Quality Assurance Requirements for Nuclear Facility Application*, graded on the approach presented in NQA-1-2012, Subpart 4.2.1, *Guidance on Graded Application of Nuclear Quality Assurance (NQA) Standard for Research and Development*.

The NQAP works in conjunction with PNNL's laboratory-level Quality Management Program, which is based upon the requirements as defined in the DOE Order 414.1D, *Quality Assurance*, and 10 CFR 830, *Nuclear Safety Management*, Subpart A, *Quality Assurance Requirements*. PNNL implements these requirements with a graded approach using the consensus standard ASME NQA-1-2000, *Quality Assurance Requirements for Nuclear Facility Applications*, graded on the approach presented in NQA-1-2000, Subpart 4.2, *Guidance on Graded Application of Quality Assurance (QA) Standard for Nuclear-Related Research and Development*.

This work was graded and performed to support production and operation of technology, unless otherwise noted.

Acknowledgments

The authors gratefully acknowledge the financial support provided by the U.S. Department of Energy Office of River Protection. The organization of this report and some of its text were adapted from the organization and text in Piepel et al. (2007). A special thanks to Greg Piepel (PNNL-retired) who adapted and drafted material in Sections 1, 2, 4, 6, and 7, and the appendices but chose not to be listed as a co-author because of retiring before the report was completed. Stephen Walsh (PNNL/MSU) and Xiaonan Lu (PNNL), along with the authors, performed the tedious job of checking data and calculations; for which we are greatly indebted. We also thank Renee Russell, Charmayne Lonergan, Tony Jin, and David MacPherson for PNNL internal reviews of this report. We also acknowledge Matt Wilburn for editing and formatting the report. We thank Will Eaton (PNNL) and Renee Russell (PNNL) for programmatic support during the conduct of this work. This report was also reviewed by a number of technical reviewers outside of PNNL to whom we are grateful: Pavel Hrma (ORP), Paul Bingham (SHU), Sofie Schuller (CEA).

The data used in modeling of the glass properties in this study were supplied by the Vitreous State Laboratory at the Catholic University of America (VSL), PNNL, and SRNL. We are grateful for the data and those who carefully collected and documented it. We have acknowledged the data more specifically by citing each data source where appropriate.

Finally, we are indebted to Albert Kruger (ORP) for his vision and oversight (both technical and programmatic) of this effort.

Abbreviations

3TS	three-time saturation
ANN	artificial neural network
bc	bias correction(ed)
BCa	bias corrected accelerated (method for bootstrap analysis)
bcPQM	bias corrected partial quadratic mixture
BS	batch saturation (method for measuring SO ₃ solubility)
Bub	bubbling (method for measuring SO ₃ solubility)
CCC	container centerline cooled(ing)
CI	confidence interval (two-sided)
DF	degrees of freedom
DFLAW	Direct Feed Low-Activity Waste
DOE	U.S. Department of Energy
EC	electrical conductivity
EWG	enhanced waste glass
FLM	full linear mixture
GCR	glass composition region
GFA	glass formulation algorithm
GLM	generalized linear model
GLS	generalized least squares
GPR	Gaussian process regression
HLW	high-level waste
HiNa ₂ O	high-waste-loading LAW glass with high Na ₂ O
HiSO ₃	high-waste-loading LAW glass with high SO ₃ , but not high Na ₂ O
ICP-OES	inductively coupled plasma-optical emission spectroscopy
ID	identification
IHLW	immobilized high-level waste
IL	inner layer
ILAW	immobilized low-activity waste
KNN	k-nearest neighbors
LAW	low-activity waste
LCI	lower confidence interval
LLR	local linear regression
LM	linear mixture
LOF	lack of fit
LP123	PNNL LAW Phases 1, 2, and 3

LP2OL	PNNL LAW Phase 2 outer layer
MAXR	maximum R^2 improvement
MCC	multiple-component constraint
mf	mass fraction
MSE	mean squared error (from regression)
MT	melter tolerance
NQA	nuclear quality assurance
NQAP	nuclear quality assurance program
OL	outer layer
OLS	ordinary least squares
ORP	DOE Office of River Protection
P	poise
Pa·s	Pascal-second
PCT	Product Consistency Test
P/F	pass/fail
PI	prediction interval
PNNL	Pacific Northwest National Laboratory
PQM	partial quadratic mixture
PvM	predicted versus measured
QA	quality assurance
QAP	Quality Assurance Plan
REFMIX	reference mixture
RLM	reduced linear mixture
%RSD	percent relative standard deviation
SCC	single-component constraint
SD	standard deviation
SR	saturation-remelt (method of measuring SO_3 solubility)
SSE	sum-of-squared errors
SVM	support vector machine
UCI	upper confidence interval
VHT	Vapor Hydration Test
VFT	Vogel-Fulcher-Tammann
VSL	Vitreous State Laboratory at the Catholic University of America
WTP	Waste Treatment and Immobilization Plant
XRF	X-ray fluorescence

Symbols

A	glass surface area
β_i	coefficient for the i^{th} model component
$\boldsymbol{\beta}$	vector of model coefficients
\mathbf{b}	vector of model coefficient estimates
c	bias correction cutoff estimate
C	bias correction cutoff
c_j	elemental concentration of the j^{th} element in the PCT leachate
C_3	offset for 3TS SO ₃ solubility methods in melter SO ₃ tolerance models
C_S	offset for BS and SR SO ₃ solubility methods in melter SO ₃ tolerance models
\mathbf{d}	vector of component concentrations normalized after removing SO ₃
\mathbf{D}	matrix of \mathbf{d} vectors for all glasses in modeling set
D	Vapor Hydration Test response, alteration depth after 24-day test
e	random error for each point
E	preexponential term in VFT equation
ε	melt electrical conductivity
ε_{1150}	melt electrical conductivity at 1150°C (S/cm)
F	temperature coefficient in VFT equation
f_j	mass fraction of the j^{th} element in the glass
\mathbf{g}	vector of component concentrations in mass fraction
\mathbf{G}	matrix of \mathbf{g} vectors for all glasses in modeling set
g_i	mass fraction of i^{th} component in glass
g_j	mass fraction of j^{th} component in glass
H_3	SO ₃ solubility method counter (1 if the method was 3TS, 0 otherwise)
H_S	SO ₃ solubility method counter (1 if the method was BS or SR, 0 otherwise)
i	used as a counter in variables that take on several values (e.g., g_i vector)
j	used as a counter in variables that take on several values (e.g., g_j vector)
K	a multiplier that reflects the desired confidence level and DF
k_{1208}	K-3 corrosion neck loss in 6-day test at 1208°C (inches)
L	lower limit
L_i	lower limit for i^{th} glass component concentration
LV	leachate (deionized water) volume used in the PCT
η	melt viscosity
η_{1150}	melt viscosity at 1150°C (P or Pa·s)
n	number of datapoints
n_i	mass fraction of i^{th} component in glass, with SO ₃ normalized out
MSE	mean squared error
M_{SO_3}	measured mass fraction of SO ₃
P	transformed property
PCT_B^{NL}	normalized loss (g/m ²) of boron after 7-day PCT
PCT_{Na}^{NL}	normalized loss (g/m ²) of sodium after 7-day PCT
PCT_j^{NL}	normalized loss (g/m ²) of j^{th} element after 7-day PCT, $j = \text{B, Na, and/or Si}$

ρ	glass density
q	number of terms
R^2	R-squared (coefficient of determination)
R_A^2	R-squared adjusted
R_{Eval}^2	R-squared for evaluation set
R_P^2	R-squared predicted (aka press)
R_V^2	R-squared validation
r_a^{VHT}	alteration rate (g/m ² /d) by 200 °C VHT
$RMSE$	root mean squared error
$RMSE_{Eval}$	root mean squared error for evaluation set
$RMSE_V$	root mean squared error, validation
s	bias correction slope estimate
s_0	initial bias correction slope estimate
Δs	change in bias correction slope estimate
S	bias correction slope
S_0	initial bias correction slope
ΔS	change in bias correction slope
SO_3-m	measured mass fraction of SO ₃ in a LAW glass
SO_3-sol	estimated soluble mass fraction of SO ₃ in a LAW glass
SO_3-t	target mass fraction of SO ₃ in a LAW glass
t	VHT test duration
T_0	temperature independent parameter in VFT equation
T_j	target mass fraction of the j^{th} glass component
T_K	absolute temperature in VFT equation
U	upper limit
U_i	upper limit for i^{th} glass component concentration
v_λ	unbiased variance estimate for the term λ
V_λ	variance for the term λ
\mathbf{V}_P	variance-covariance matrix for property P
$w_{SO_3}^{MT}$	melter SO ₃ tolerance
x_i	normalized mass fraction of the i^{th} glass oxide or halogen component after removing SO_3-m from glass composition
Z_i	coefficient for i^{th} glass component in multi-component concentration limit

Contents

Abstract.....	iii
Quality Assurance.....	iv
Acknowledgments.....	v
Abbreviations.....	vi
Symbols	viii
Contents	x
Figures	xvi
Tables	xxv
1.0 Introduction.....	1.1
1.1 Glass Property-Composition Models and Associated Constraints.....	1.2
1.1.1 PCT Normalized Losses of B and Na (PCT_B^{NL} , PCT_{Na}^{NL}) (g/m ²)	1.2
1.1.2 VHT Alteration Rate (r_a^{VHT}) (g m ⁻² d ⁻¹).....	1.2
1.1.3 Viscosity at 1150 °C (η_{1150}) (P) and Electrical Conductivity at 1150 °C (ϵ_{1150}) (S/cm).....	1.3
1.1.4 Melter SO ₃ Tolerance Model at 1150 °C ($w_{SO_3}^{MT1150}$) (wt%)	1.3
1.1.5 K-3 Refractory Corrosion Neck Loss at 1208 °C (k_{1208}) (inch).....	1.3
1.1.6 Goal of LAW Glass Property-Composition Modeling	1.3
1.1.7 Property-Composition Model Validity Constraints.....	1.4
2.0 LAW Glass Property-Composition Data for Modeling	2.1
2.1 LAW Glass Database.....	2.1
2.2 Accounting for SO ₃ Incorporated into LAW Glass Compositions	2.3
2.3 LAW Glass Data for Property Modeling	2.5
2.3.1 Viscosity and Electrical Conductivity	2.6
2.3.2 Product Consistency Test Response	2.9
2.3.3 Vapor Hydration Test Response.....	2.9
2.3.4 Melter SO ₃ Tolerance	2.10
2.3.5 Data Subgroups	2.10
2.3.6 Tabulation of All Data.....	2.11
2.4 Subsets of LAW Glass Compositions Used to Evaluate Prediction Performance of and Validate Property-Composition Models	2.11
2.5 Glass Composition for Example Calculations	2.13
3.0 Models Relating Normalized PCT Boron and Sodium Losses to Composition of LAW Glasses	3.1
3.1 Normalized PCT Loss Data from LAW Glasses Used for Model Development, Evaluation, and Validation.....	3.1

3.1.1	Model Development Data for Normalized PCT Boron and Sodium Losses from LAW Glasses	3.1
3.1.2	Model Validation Approach and Data for the PCT on LAW Glasses.....	3.19
3.1.3	Subsets of LAW Glasses to Evaluate Prediction Performance of Models for B and Na Normalized Losses from the PCT.....	3.19
3.2	Model Forms for Boron and Sodium Normalized PCT Losses from LAW Glasses	3.20
3.2.1	Mixture Experiment Model Forms for Normalized PCT Boron and Sodium Losses from LAW Glasses.....	3.20
3.2.2	Normalization and Transformation of Boron and Sodium Losses on the PCT from LAW Glasses.....	3.21
3.3	Property-Composition Model Results for Normalized PCT Boron Loss from LAW Glasses	3.22
3.3.1	Results from the 20-Component Full Linear Mixture Model for the Natural Logarithm of Normalized PCT Boron Loss from LAW Glasses	3.22
3.3.2	Results from the 15-Component Reduced Linear Mixture Model for the Natural Logarithm of Normalized Boron Loss from the PCT on LAW Glasses.....	3.25
3.3.3	Results from a Reduced Partial Quadratic Mixture Model for the Natural Logarithm of Normalized PCT Boron Loss from LAW Glasses	3.29
3.3.4	Screening of Model Types for Predicting Natural Logarithm of Normalized PCT Boron Loss from LAW Glasses	3.33
3.3.5	Results from a Bias Corrected Partial Quadratic Mixture Model for the Natural Logarithm of Normalized PCT Boron Loss from LAW Glasses	3.36
3.4	Property-Composition Model Results for PCT Sodium Normalized Loss from LAW Glasses	3.43
3.4.1	Results from the 20-Component Full Linear Mixture Model for the Natural Logarithm of Normalized PCT Sodium Loss from LAW Glasses.....	3.43
3.4.2	Results from the 15-Component Reduced Linear Mixture Model for the Natural Logarithm of Normalized PCT Sodium Loss from LAW Glasses.....	3.46
3.4.3	Results from a Reduced Partial Quadratic Mixture Model for the Natural Logarithm of Normalized PCT Sodium Loss from LAW Glasses.....	3.50
3.4.4	Screening of Model Types for Predicting Natural Logarithm of Normalized PCT Sodium Loss from LAW Glasses	3.54
3.4.5	Results from a Bias Corrected Partial Quadratic Mixture Model for the Natural Logarithm of Normalized PCT Sodium Loss from LAW Glasses.....	3.55
3.5	Recommended Model for the Natural Logarithm of Normalized PCT Boron and Sodium Loss from LAW Glasses	3.61
3.6	Example Illustrating Model Predictions and Statistical Intervals for the Natural Logarithm of Normalized PCT Boron and Sodium Loss from LAW Glasses	3.62

3.6.1	Optimization of Glass Composition using bcPQM	3.68
3.7	Suitability of the Recommended Models for Natural Logarithm of Normalized PCT Boron and Sodium Loss from LAW Glasses	3.68
4.0	Models Relating Vapor Hydration Test Results to LAW Glass Compositions	4.1
4.1	VHT Data from LAW Glasses Used for Model Development, Evaluation, and Validation.....	4.1
4.1.1	Model Development Data for Pass/Fail VHT on LAW Glasses	4.1
4.1.2	Model Validation Approach and Data for the VHT on LAW Glasses	4.12
4.1.3	Subsets of LAW Glasses to Evaluate Prediction Performance of Pass/Fail VHT Models.....	4.13
4.2	Model Forms and Accuracy Measures for the Vapor Hydration Test on LAW Glasses	4.13
4.2.1	Mixture Experiment Model Forms for a Binary Pass/Fail VHT Response on LAW Glasses.....	4.14
4.3	Property-Composition Model Results for a Pass/Fail VHT Response on LAW Glasses	4.15
4.3.1	Results from the 20-Component Full Linear Mixture Logistic Model for the Pass/Fail Response for the VHT on LAW Glasses	4.15
4.3.2	Results from the Development of a 19-Term Partial Quadratic Mixture Model for Pass/Fail VHT on LAW Glasses	4.20
4.3.3	Recommended Model for Pass/Fail VHT on LAW Glasses	4.26
4.4	Example Illustrating VHT Model Predictions and Statistical Intervals.....	4.27
4.5	Suitability of the Recommended Model for Pass/Fail VHT Responses for Application by the WTP LAW Facility	4.29
5.0	Models Relating Viscosity at 1150 °C to LAW Glass Composition	5.1
5.1	Viscosity at 1150 °C Data Used for Model Development, Evaluation, and Validation.....	5.1
5.1.1	Model Development Data for Viscosity at 1150 °C.....	5.1
5.1.2	Model Validation Approach and Data for Viscosity at 1150 °C of LAW Glasses.....	5.11
5.1.3	Subsets of LAW Glasses to Evaluate Prediction Performance of Models for Viscosity at 1150 °C	5.12
5.2	Model Forms for Viscosity at 1150 °C of LAW Glasses	5.12
5.2.1	Mixture Experiment Model Forms for Viscosity at 1150 °C of LAW Glasses.....	5.12
5.2.2	Transformation of Viscosity at 1150 °C for LAW Glasses.....	5.13
5.3	Property-Composition Model Results for Viscosity at 1150 °C of LAW Glasses	5.14
5.3.1	Results from the 20-Component Full Linear Mixture Model for the Natural Logarithm of Viscosity at 1150 °C with LAW Glasses.....	5.14
5.3.2	Results from a Reduced Linear Mixture Model for the Natural Logarithm of Viscosity at 1150 °C with LAW Glasses	5.18

5.3.3	Results from a Reduced Partial Quadratic Mixture Model for the Natural Logarithm of Viscosity at 1150 °C with LAW Glasses	5.24
5.3.4	Recommended Model for the Natural Logarithm of Viscosity at 1150 °C for LAW Glasses	5.30
5.4	Example Illustrating Model Predictions and Statistical Intervals for Viscosity at 1150 °C	5.31
5.5	Suitability of the Recommended Viscosity at 1150 °C Model for Application by the WTP LAW Facility	5.35
6.0	Models Relating Electrical Conductivity at 1150 °C to LAW Glass Composition	6.1
6.1	Electrical Conductivity at 1150 °C Data Used for Model Development, Evaluation, and Validation.....	6.1
6.1.1	Model Development Data for Electrical Conductivity at 1150 °C.....	6.1
6.1.2	Model Validation Approach and Data for Electrical Conductivity at 1150 °C of LAW Glasses	6.11
6.1.3	Subsets of LAW Glasses to Evaluate Prediction Performance of Models for Electrical Conductivity at 1150 °C	6.12
6.2	Model Forms for Electrical Conductivity at 1150 °C of LAW Glasses	6.12
6.2.1	Mixture Experiment Model Forms for Electrical Conductivity at 1150 °C of LAW Glasses	6.12
6.2.2	Transformation of Electrical Conductivity at 1150 °C for LAW Glasses.....	6.13
6.3	Property-Composition Model Results for Electrical Conductivity at 1150 °C of LAW Glasses	6.14
6.3.1	Results from the 20-Component Full Linear Mixture Model for the Natural Logarithm of Electrical Conductivity at 1150 °C of LAW Glasses.....	6.14
6.3.2	Results from a Reduced Linear Mixture Model for Electrical Conductivity at 1150 °C for LAW Glasses.....	6.18
6.3.3	Results from a Reduced Partial Quadratic Mixture Model for the Natural Logarithm of Electrical Conductivity at 1150 °C with LAW Glasses.....	6.24
6.3.4	Recommended Model for the Natural Logarithm of Electrical Conductivity at 1150 °C for LAW Glasses.....	6.30
6.4	Example Illustrating Model Predictions and Statistical Intervals for Electrical Conductivity at 1150 °C	6.31
6.5	Suitability of the Recommended Electrical Conductivity at 1150 °C Model for Application by the WTP LAW Facility	6.35
7.0	Models Relating Melter SO ₃ Tolerance at 1150 °C to LAW Glass Composition	7.1
7.1	Melter SO ₃ Tolerance and Solubility at 1150 °C Data Used for Melter SO ₃ Tolerance Model Development, Evaluation, and Validation.....	7.1
7.1.1	Model Development Data for Melter SO ₃ Tolerance at 1150 °C	7.1
7.1.2	Model Validation Approach and Data for Melter SO ₃ Tolerance Model at 1150 °C of LAW Glasses	7.13

7.1.3	Subsets of LAW Glasses to Evaluate Prediction Performance of Models for Melter SO ₃ Tolerance at 1150 °C	7.13
7.2	Model Forms for Melter SO ₃ Tolerance at 1150 °C of LAW Glasses.....	7.14
7.2.1	Mixture Experiment Model Forms for Melter SO ₃ Tolerance at 1150 °C of LAW Glasses	7.14
7.2.2	Offsets for Melter SO ₃ Tolerance Model at 1150 °C for LAW Glasses.....	7.15
7.3	Property-Composition Model Results for Melter SO ₃ Tolerance at 1150 °C of LAW Glasses	7.16
7.3.1	Results from the 19-Component Full Linear Mixture Model for Melter SO ₃ Tolerance at 1150 °C with LAW Glasses	7.17
7.3.2	Results from a Reduced Linear Mixture Model for the Melter SO ₃ Tolerance at 1150 °C with LAW Glasses.....	7.22
7.3.3	Results from a Reduced Partial Quadratic Mixture Model for Melter SO ₃ Tolerance at 1150 °C with LAW Glasses	7.28
7.3.4	Recommended Model for Melter SO ₃ Tolerance at 1150 °C for LAW Glasses.....	7.34
7.4	Example Illustrating Model Predictions and Statistical Intervals for Melter SO ₃ Tolerance at 1150 °C	7.35
7.5	Suitability of the Recommended Melter SO ₃ Tolerance at 1150 °C Model for Application by the WTP LAW Facility	7.39
8.0	Models Relating K-3 Refractory Corrosion to LAW Glass Composition	8.1
8.1	K-3 Corrosion at 1208 °C Data Used for Model Development, Evaluation, and Validation.....	8.1
8.1.1	Model Development Data for K-3 Corrosion at 1208 °C.....	8.1
8.1.2	Model Validation Approach and Data for K-3 Corrosion at 1208 °C of LAW Glasses.....	8.9
8.1.3	Subsets of LAW Glasses to Evaluate Prediction Performance of Models for K-3 Corrosion at 1208 °C	8.9
8.2	Model Forms for K-3 Corrosion at 1208 °C of LAW Glasses	8.10
8.2.1	Mixture Experiment Model Forms for K-3 Corrosion at 1208 °C of LAW Glasses.....	8.10
8.2.2	Transformation of K-3 Corrosion at 1208 °C for LAW Glasses.....	8.11
8.3	Property-Composition Model Results for K-3 Corrosion at 1208 °C of LAW Glasses	8.11
8.3.1	Results from the 20-Component Full Linear Mixture Model for the Natural Logarithm of K-3 Corrosion at 1208 °C with LAW Glasses	8.11
8.3.2	Results from a Reduced Linear Mixture Model for the Natural Logarithm of K-3 Corrosion at 1208 °C with LAW Glasses	8.16
8.3.3	Results from a Reduced Partial Quadratic Mixture Model for the Natural Logarithm of K-3 Corrosion at 1208 °C with LAW Glasses	8.22
8.3.4	Recommended Model for the Natural Logarithm of K-3 Corrosion at 1208 °C for LAW Glasses.....	8.28

8.4	Example Illustrating Model Predictions and Statistical Intervals for K-3 Corrosion at 1208 °C	8.29
8.5	Suitability of the Recommended K-3 Corrosion at 1208 °C Model for Application by the WTP LAW Facility	8.33
9.0	Summary and Conclusions for LAW Glass Property-Composition Models	9.1
9.1	Summary of LAW Glass PCT Modeling	9.2
9.2	Summary of LAW VHT Modeling	9.3
9.3	Summary of LAW Viscosity Modeling	9.4
9.4	Summary of LAW Electrical Conductivity Modeling	9.5
9.5	Summary of LAW Melter SO ₃ Tolerance Modeling	9.6
9.6	Summary of LAW K-3 Refractory Corrosion Modeling	9.7
9.7	Summary of Model Validity Regions for Recommended LAW Glass Property Models	9.8
9.8	Component Effects on Properties	9.13
9.9	Additional Constraints	9.15
9.9.1	Slow-Cooled Glass Crystallization Constraint	9.15
9.9.2	Melt Crystallization Constraint	9.16
9.9.3	Lithia and Zirconia Targets	9.16
9.10	Status and Recommendation of Future Work	9.17
10.0	References	10.1
Appendix A	Appendix A – LAW Glass Data for Developing Property-Composition Models	A.1
Appendix B	Statistical Methods to Develop, Evaluate, and Validate Property-Compositions Models Fit to Experimental Data	B.1
Appendix C	LAW Glass Numbers in Each of the Six Evaluation Subsets	C.1
Appendix D	Variance-Covariance Matrices Associated with the Estimated Coefficients of LAW Glass Property-Composition	D.1
Appendix E	Appendix E Example Temperature and Composition Models for Viscosity and Electrical Conductivity	E.1

Figures

Figure 2.1. Measured versus Target SO ₃ Concentrations (wt%) in 589 Glasses with Independently Measured SO ₃ Concentration Data. The 54 Glasses Marked in Red Were Removed before Fitting Eq. (2.1). The solid curved line represents the fitted model from Eq. (2.1).....	2.5
Figure 3.1. Distributions of 20 Main Components (in mass fractions) for 703 LAW Glass Compositions with Data for normalized PCT Losses of B or Na. The vertical lines (when present) represent the lower and upper limits for each component from the PNNL LAW Phase 1 (blue lines) and Phase 2 (pink lines) outer-layer studies (see Table 2.1). In cases where two limits are the same, pink lines over-plot the blue lines.....	3.3
Figure 3.2. Distributions of 22 Minor Components (in mass fractions) for 703 LAW Glass Compositions with Data for normalized PCT Losses of B or Na.	3.4
Figure 3.3. Distributions of 20 Main Components (in mass fractions) for 691 LAW Glass Compositions with Data for Normalized PCT Losses of B or Na that Remain after Excluding the 12 Glasses in Table 3.1. The vertical lines (when present) represent the lower and upper limits for each component from the PNNL LAW Phase 1 (blue lines) and Phase 2 (pink lines) outer-layer studies (see Table 2.1). In cases where two limits are the same, pink lines over-plot the blue lines.	3.6
Figure 3.4. Distributions of 22 Minor Components (in mass fractions) for 691 LAW Glass Compositions with Data for Normalized PCT Losses of B or Na that Remain after Excluding the 12 Glasses in Table 3.1.....	3.7
Figure 3.5. Scatterplot Matrix of 20 Components (mass fractions) for 691 LAW Glasses with Data for Normalized PCT Losses (g/m ²) of B and Na that Remain after Excluding the 12 Glasses in Table 3.1	3.9
Figure 3.6. Predicted versus Measured Plot for the 690-Glass Modeling Dataset Using the 20-Component Full Linear Mixture Model on the Natural Logarithm of PCT _B ^{NL} from LAW Glasses. The red lines represent the WTP contract limit of 2 g/m ² , or 0.6931 ln(g/m ²).	3.24
Figure 3.7. Response Trace Plot for the 20-Component Full Linear Mixture Model on the Natural Logarithm of Normalized PCT Boron Loss from LAW Glasses.....	3.25
Figure 3.8. Predicted versus Measured Plot for the 690-Glass Modeling Dataset Using the 15-Component Reduced Linear Mixture Model on the Natural Logarithm of PCT _B ^{NL} from LAW Glasses. The red lines represent the WTP contract limit of 2 g/m ² , or 0.6931 ln(g/m ²).	3.28
Figure 3.9. Response Trace Plot for the 15-Component Reduced Linear Mixture Model on the Natural Logarithm of Normalized PCT Boron Loss from LAW Glasses.....	3.29
Figure 3.10. Predicted versus Measured Plot for the 690-Glass Modeling Dataset Using the 19-Term Partial Quadratic Mixture Model on the Natural Logarithm of PCT _B ^{NL} from LAW Glasses. The red lines represent the WTP contract limit of 2 g/m ² , or 0.6931 ln(g/m ²).	3.32
Figure 3.11. Response Trace Plot for the 19-Term Partial Quadratic Mixture Model on the Natural Logarithm of Normalized PCT Boron Loss from LAW Glasses.....	3.33

Figure 3.12. Predicted versus Measured Plot for a 22-term Partial Quadratic Generalized Mixture Model with Four Higher-order Terms on the Natural Logarithm of PCT_B^{NL} from LAW Glasses. The red lines represent the WTP contract limit of $0.6931 \ln(g/m^2)$. For Information Only	3.35
Figure 3.13. Standardized Residuals Plot for the 22-Term bcPQM Model on the Natural Logarithm of Normalized PCT Boron Loss from LAW Glasses.....	3.40
Figure 3.14. Predicted versus Measured Plot for the 690-glass Modeling Dataset Using the 22-Term bcPQM Model on the Natural Logarithm of Normalized PCT Boron Loss from LAW Glasses	3.41
Figure 3.15. Predicted versus Measured Plots for the Six Evaluation Subsets Using the 22-Term bcPQM Model on the Natural Logarithm of Normalized PCT Boron Loss from LAW Glasses	3.42
Figure 3.16. Response Trace Plot for 22-Term bcPQM Model on the Natural Logarithm of Normalized PCT Boron Loss from LAW Glasses.....	3.43
Figure 3.17. Predicted versus Measured Plot for the 690-Glass Modeling Dataset Using the 20-Component Full Linear Mixture Model on the Natural Logarithm of PCT_{Na}^{NL} from LAW Glasses. The red lines represent the WTP contract limit of $2 g/m^2$, or $0.6931 \ln(g/m^2)$	3.45
Figure 3.18. Response Trace Plot for the 20-Component Full Linear Mixture Model on the Natural Logarithm of Normalized PCT Sodium Loss from LAW Glasses	3.46
Figure 3.19. Predicted versus Measured Plot for the 690-Glass Modeling Dataset Using the 15-Component Reduced Linear Mixture Model on the Natural Logarithm of PCT_{Na}^{NL} from LAW Glasses. The red lines represent the WTP contract limit of $2 g/m^2$, or $0.6931 \ln(g/m^2)$	3.49
Figure 3.20. Response Trace Plot for the 15-Component Reduced Linear Mixture Model on the Natural Logarithm of Normalized PCT Sodium Loss from LAW Glasses	3.50
Figure 3.21. Predicted versus Measured Plot for the 690-Glass Modeling Dataset Using the 19-Term Partial Quadratic Mixture Model on the Natural Logarithm of PCT_{Na}^{NL} from LAW Glasses. The red lines represent the WTP contract limit of $2 g/m^2$, or $0.6931 \ln(g/m^2)$	3.53
Figure 3.22. Response Trace Plot for the 19-Term Partial Quadratic Mixture Model on the Natural Logarithm of Normalized PCT Sodium Loss from LAW Glasses	3.54
Figure 3.23. Standardized Residuals Plot for the 22-Term bcPQM Model on the Natural Logarithm of Normalized PCT Sodium Loss from LAW Glasses	3.58
Figure 3.24. Predicted versus Measured Plot for the 690-glass Modeling Dataset Using the 22-Term bcPQM Model on the Natural Logarithm of Normalized PCT Sodium Loss from LAW Glasses	3.59
Figure 3.25. Predicted versus Measured Plots for the Six Evaluation Subsets Using the 22-Term bcPQM Model on the Natural Logarithm of Normalized PCT Sodium Loss from LAW Glasses	3.60
Figure 3.26. Response Trace Plot for 22-Term bcPQM Model on the Natural Logarithm of Normalized PCT Sodium Loss from LAW Glasses	3.61

Figure 3.27. Distribution of Δs Values for 100,000 Samples of Glasses and Corresponding $\ln(\text{PCT}_B^{\text{NL}})$ Values Obtained from the Available 690 Glasses Used To Model $\ln(\text{PCT}_B^{\text{NL}})$	3.65
Figure 4.1. Distributions of 20 Main Components (in mass fractions) for 699 LAW Glass Compositions with Pass/Fail VHT Data. The vertical lines (when present) represent the lower and upper limits for each component from the PNNL LAW Phase 1 (blue lines) and Phase 2 (pink lines) outer-layer studies (see Table 2.1). In cases where two limits are the same, pink lines over plot the blue lines.....	4.3
Figure 4.2. Distributions of 21 Minor Components (in mass fraction) for 699 LAW Glass Compositions with Pass/Fail VHT Data. The vertical lines (when present) represent the lower and upper limits for each component from the PNNL LAW Phase 1 (blue lines) and Phase 2 (pink lines) outer-layer studies (see Table 2.1). In cases where two limits are the same, pink lines over plot the blue lines.....	4.4
Figure 4.3. Distributions of 20 Main Components (in mass fractions) for 686 LAW Glass Compositions with Data for Pass/Fail VHT that Remain after Excluding the 13 Glasses in Table 4.1. The vertical lines (when present) represent the lower and upper limits for each component from the PNNL LAW Phase 1 (blue lines) and Phase 2 (pink lines) outer-layer studies (see Table 2.1). In cases where two limits are the same, pink lines over plot the blue lines.	4.6
Figure 4.4. Distributions of 21 Minor Components (in weight percent) for 686 LAW Glass Compositions with Data for Pass/Fail VHT that Remain after Excluding the 13 Glasses in Table 4.1. The vertical lines (when present) represent the lower and upper limits for each component from the PNNL LAW Phase 1 (blue lines) and Phase 2 (pink lines) outer-layer studies (see Table 2.1). In cases where two limits are the same, pink lines over plot the blue lines.	4.7
Figure 4.5. Scatterplot Matrix of 20 Components (mass fractions) for the 686 LAW Glasses with Pass/Fail Data that Remain after Excluding the 13 Glasses in Table 4.1	4.8
Figure 4.6. Scores (y-axes) for Glasses that Pass (upper panel) and Fail (lower panel) Generated by the 20-term VHT FLM. The x-axes show glasses on an index to avoid overcrowding. The 0.3 threshold value for classification (used for illustration purposes only) is shown as a red horizontal line.	4.18
Figure 4.7. Plots of the Scores Produced by the 20-term FLM for Six Sets of Glasses that Pass the Vapor Hydration Constraint. The 0.3 threshold value for classification (used for illustration purposes only) is shown as a red horizontal line.	4.19
Figure 4.8. Plots of the Scores Produced by the 20-term FLM for Six Sets of Glasses that Fail the Vapor Hydration Constraint. The 0.3 threshold value for classification (used for illustration purposes only) is shown as a red horizontal line.	4.20
Figure 4.9. Scores (y-axes) for Glasses that Pass (upper panel) and Fail (lower panel) Generated by the 19-term VHT PQM. The x-axes show glasses on an index to avoid overcrowding. The 0.19 value used as threshold for classification is shown as a red horizontal line.	4.23
Figure 4.10. Model Scores (y-axes) Produced by the 19-term PQM Pass/Fail VHT Model for the Pass Glasses in Six Different Evaluation Sets. Glasses below the 0.19 threshold are correctly classified as Pass.....	4.24

Figure 4.11. Model Scores (y-axes) Produced by the 19-term PQM Pass/Fail VHT Model for the Fail Glasses in Six Different Evaluation Sets. Glasses above the 0.19 threshold are correctly classified as Fail.....	4.25
Figure 4.12. Response Trace Plot for the 19-term PQM Pass/Fail VHT Model.....	4.26
Figure 5.1. Distributions of 20 Main Components (in mass fractions) for 549 LAW Glass Compositions with Data for Viscosity at 1150 °C. The vertical lines (when present) represent the lower and upper limits for each component from the PNNL LAW Phase 1 outer-layer study (blue lines), Phase 2 outer-layer study (pink lines), and Phase 3 study (also shown by the same pink lines), as shown in Table 2.1. In cases where two limits are the same, pink lines over plot the blue lines. The x-axis represents the mass fraction values of a LAW glass component. The y-axis shows an index value representing each LAW glass composition, which aids in spreading out the data points to avoid over-plotting.	5.3
Figure 5.2. Distributions of 17 Minor Components (in mass fractions) for the 549 LAW Glass Compositions with Data for Viscosity at 1150 °C. The x-axis represents the mass fraction values of a LAW glass component. The y-axis shows an index value representing each LAW glass composition, which aids in spreading out the data points to avoid over-plotting.	5.4
Figure 5.3. Distributions of 20 Main Components (in mass fractions) for 534 LAW Glass Compositions with Data for Viscosity at 1150 °C that Remain after Excluding the 15 Glasses in Table 5.1. The vertical lines (when present) represent the lower and upper limits for each component from the PNNL LAW Phase 1 outer-layer study (blue lines), Phase 2 outer-layer study (pink lines), and Phase 3 study (pink lines), as shown in Table 2.1. In cases where two limits are the same, pink lines over plot the blue lines. The x-axis represents the mass fraction values of a LAW glass component. The y-axis shows an index value representing each LAW glass composition, which aids in spreading out the data points to avoid over-plotting.	5.6
Figure 5.4. Distributions of 17 Minor Components (in mass fractions) for the 534 LAW Glass Compositions with Data for Viscosity at 1150 °C that Remain after Excluding the 15 Glasses in Table 5.1. The x-axis represents the mass fraction values of a LAW glass component. The y-axis shows an index value representing each LAW glass composition, which aids in spreading out the data points to avoid over-plotting.	5.7
Figure 5.5. Scatterplot Matrix of 20 Components (mass fractions) for the 534 LAW Glasses with Viscosity at 1150°C Data that Remain after Excluding the 15 Glasses in Table 5.1	5.8
Figure 5.6. Predicted versus Measured Plot for the 534-Glass Modeling Dataset Using the 20-Component Full Linear Mixture Model on the Natural Logarithm of Viscosity at 1150 °C for LAW Glasses. The red lines represent the WTP LAW Facility operating limits for viscosity at 1150 °C (20 to 100 poise).	5.16
Figure 5.7. Predicted versus Measured Plots for the Six Evaluation Subsets Using the 20-Component Full Linear Mixture Model on the Natural Logarithm of Viscosity at 1150 °C for LAW Glasses	5.17
Figure 5.8. Response Trace Plot for the 20-Component Full Linear Mixture Model on the Natural Logarithm of Viscosity at 1150 °C for LAW Glasses	5.18

Figure 5.9. Standardized Residuals Plot for the 18-Component Reduced Linear Mixture Model on the Natural Logarithm of Viscosity at 1150 °C for LAW Glasses	5.21
Figure 5.10. Predicted versus Measured Plot for the 534-Glass Modeling Dataset Using the 18-Component Reduced Linear Mixture Model on the Natural Logarithm of Viscosity at 1150 °C for LAW Glasses. The red lines represent the WTP LAW Facility operating limits for viscosity at 1150 °C (20 to 100 poise).	5.22
Figure 5.11. Predicted versus Measured Plots for the Six Evaluation Subsets Using the 18-Component Reduced Linear Mixture Model on the Natural Logarithm of Viscosity at 1150 °C for LAW Glasses	5.23
Figure 5.12. Response Trace Plot for the 18-Component Reduced Linear Mixture Model on the Natural Logarithm of Viscosity at 1150 °C for LAW Glasses	5.24
Figure 5.13. Standardized Residuals Plot for the 21-Term Reduced Partial Quadratic Mixture Model on the Natural Logarithm of Viscosity at 1150 °C for LAW Glasses	5.27
Figure 5.14. Predicted versus Measured Plot for the 516-glass Modeling Dataset Using the 21-term Reduced Partial Quadratic Mixture Model on the Natural Logarithm of Viscosity at 1150 °C for LAW glasses. The red lines represent the WTP LAW Facility operating limits for viscosity at 1150 °C (20 to 100 poise).	5.28
Figure 5.15. Predicted versus Measured Plots for the Six Evaluation Subsets Using the 21-term Reduced Partial Quadratic Mixture Model on the Natural Logarithm of Viscosity at 1150 °C for LAW Glasses	5.29
Figure 5.16. Response Trace Plot for 21-Term Reduced Partial Quadratic Mixture Model on the Natural Logarithm of Viscosity at 1150 °C for LAW Glasses	5.30
Figure 5.17. Prediction Standard Deviations versus Predicted Values over the LAW Glass Compositions in the 534-Glass Modeling Dataset for the Recommended 21-term PQM Model for the Natural Logarithm of Viscosity at 1150 °C.....	5.38
Figure 6.1. Distributions of 20 Main Components (in mass fractions) for 542 LAW Glass Compositions with Data for Electrical Conductivity at 1150 °C. The vertical lines (when present) represent the lower and upper limits for each component from the PNNL LAW Phase 1 outer-layer study (blue lines), Phase 2 outer-layer study (pink lines), and Phase 3 study (pink lines), as shown in Table 2.1. In cases where two limits are the same, pink lines over plot the blue lines. The x-axis represents the mass fraction values of a LAW glass component. The y-axis shows an index value representing each LAW glass composition, which aids in spreading out the data points to avoid over-plotting.....	6.3
Figure 6.2. Distributions of 17 Minor Components (in mass fractions) for 542 LAW Glass Compositions with Data for Electrical Conductivity at 1150 °C. The x-axis represents the mass fraction values of a LAW glass component. The y-axis shows an index value representing each LAW glass composition, which aids in spreading out the data points to avoid over-plotting.....	6.4
Figure 6.3. Distributions of 20 Main Components (in mass fractions) for 526 LAW Glass Compositions with Data for Electrical Conductivity at 1150 °C that Remain after Excluding the 16 Glasses in Table 6.1. The vertical lines (when present) represent the lower and upper limits for each component from the PNNL LAW Phase 1 outer-layer study (blue lines), Phase 2 outer-layer study (pink lines), and Phase 3 study (pink lines), as shown in Table 2.1. In cases where two limits are the same, pink lines over plot the blue lines. The x-axis represents the mass	

fraction values of a LAW glass component. The y-axis shows an index value representing each LAW glass composition, which aids in spreading out the data points to avoid over-plotting.....	6.6
Figure 6.4. Distributions of 17 Minor Components (in mass fractions) for 526 LAW Glass Compositions with Data for Electrical Conductivity at 1150 °C that Remain after Excluding the 16 Glasses in Table 6.1. The x-axis represents the mass fraction values of a LAW glass component. The y-axis shows an index value representing each LAW glass composition, which aids in spreading out the data points to avoid over-plotting.....	6.7
Figure 6.5. Scatterplot Matrix of 20 Components (mass fractions) for 526 LAW Glasses with Electrical Conductivity at 1150 °C Data that Remain after Excluding the 16 Glasses in Table 6.1	6.8
Figure 6.6. Predicted versus Measured Plot for the 526-Glass Modeling Dataset Using the 20-Component Full Linear Mixture Model on the Natural Logarithm of Electrical Conductivity at 1150 °C of LAW Glasses. The red lines represent WTP LAW Facility operating limits for electrical conductivity at 1150 °C (0.105 to 0.671 S/cm).....	6.16
Figure 6.7. Predicted versus Measured Plots for the Six Evaluation Subsets Using the 20-Component Full Linear Mixture Model on the Natural Logarithm of Electrical Conductivity at 1150 °C for LAW Glasses.....	6.17
Figure 6.8. Response Trace Plot for 20-Component Full Linear Mixture Model on the Natural Logarithm of Electrical Conductivity at 1150 °C for LAW Glasses	6.18
Figure 6.9. Standardized Residuals Plot for the 11-Component Reduced Linear Mixture Model on the Natural Logarithm of Electrical Conductivity at 1150 °C for LAW Glasses	6.21
Figure 6.10. Predicted versus Measured Plot for the 526-Glass Modeling Dataset Using the 11-Component Reduced Linear Mixture Model on the Natural Logarithm of Electrical Conductivity at 1150 °C for LAW Glasses. The red lines represent the WTP LAW Facility operating limits for electrical conductivity at 1150 °C (0.105 to 0.671 S/cm).....	6.22
Figure 6.11. Predicted versus Measured Plots for the Six Evaluation Sets Using the 11-Component Reduced Linear Mixture Model on the Natural Logarithm of Electrical Conductivity at 1150 °C for LAW Glasses	6.23
Figure 6.12. Response Trace Plot for 11-Component Reduced Linear Mixture Model on the Natural Logarithm of Electrical Conductivity at 1150 °C for LAW Glasses	6.24
Figure 6.13. Standardized Residuals Plot for the 13-Term Reduced Partial Quadratic Mixture Model on the Natural Logarithm of Electrical Conductivity at 1150 °C for LAW Glasses	6.27
Figure 6.14. Predicted versus Measured Plot for the 526-glass Modeling Dataset Using the 13-term Reduced Partial Quadratic Mixture Model on the Natural Logarithm of Electrical Conductivity at 1150 °C for LAW Glasses. The red lines represent the WTP LAW Facility operating limits for electrical conductivity at 1150 °C (0.105 – 0.671 S/cm).....	6.28
Figure 6.15. Predicted versus Measured Plots for the Six Evaluation Sets Using the 13-Term Reduced Partial Quadratic Mixture Model on the Natural Logarithm of Electrical Conductivity at 1150 °C for LAW Glasses.....	6.29

Figure 6.16. Response Trace Plot for 13-Term Reduced Partial Quadratic Mixture Model on the Natural Logarithm of Electrical Conductivity at 1150 °C for LAW Glasses	6.30
Figure 6.17. Prediction Standard Deviations versus Predicted Values over the LAW Glass Compositions in the 518-Glass Modeling Dataset for the Recommended 13-Term PQM Model for the Natural Logarithm of Electrical Conductivity at 1150 °C.....	6.37
Figure 7.1. Distributions of 20 Main Components (in mass fractions) for 601 LAW Glass Compositions with Melter SO ₃ Tolerance and Solubility Measurements at 1150 °C. The vertical lines (when present) represent the lower and upper limits for each component from the PNNL LAW Phase 1 outer-layer study (blue lines), LAW Phase 2 outer-layer study (pink lines), and LAW Phase 3 study (pink lines), as shown in Table 2.1. In cases where two limits are the same, blue lines over plot the pink lines.....	7.4
Figure 7.2. Distributions of 16 Minor Components (in mass fractions) for the 601 LAW Glasses with Melter SO ₃ Tolerance and Solubility Values at 1150 °C.....	7.5
Figure 7.3. Distributions of 20 Main Components (in mass fractions) for 576 LAW Glass Compositions with Melter SO ₃ Tolerance and Solubility Measurements at 1150 °C that Remain after Excluding the 25 Glasses in Table 7.1. The vertical lines (when present) represent the lower and upper limits for each component from the PNNL LAW Phase 1 outer-layer study (blue lines), LAW Phase 2 outer-layer study (pink lines), and LAW Phase 3 study (pink lines), as shown in Table 2.1. In cases where two limits are the same, blue lines over plot the pink lines.	7.7
Figure 7.4. Distributions of 10 Minor Components (in mass fractions) for the 576 LAW Glass Compositions with Data for Melter SO ₃ Tolerance and Solubility at 1150 °C that Remain after Excluding the 25 Glasses in Table 7.1	7.8
Figure 7.5. Scatterplot Matrix of 20 Components (mass fractions) for the 576 LAW Glasses with Melter SO ₃ Tolerance and Solubility at 1150 °C Data that Remain after Excluding the 25 Glasses in Table 7.1	7.10
Figure 7.6. Predicted versus Measured Plot for the 576-Glass Modeling Dataset Using the 19-Component Full Linear Mixture Model on Melter SO ₃ Tolerance at 1150 °C for LAW Glasses	7.19
Figure 7.7. Predicted versus Measured Plots for the Six Evaluation Subsets Using the 19-Component Full Linear Mixture Model on the Melter SO ₃ Tolerance at 1150 °C for LAW Glasses	7.20
Figure 7.8. Response Trace Plot for the 19-Component Full Linear Mixture Model on Melter SO ₃ Tolerance at 1150 °C for LAW Glasses	7.21
Figure 7.9. Standardized Residuals Plot for the 10-Component Reduced Linear Mixture Model on Melter SO ₃ Tolerance at 1150 °C for LAW Glasses	7.25
Figure 7.10. Predicted versus Measured Plot for the 576-Glass Modeling Dataset Using the 10-Component Reduced Linear Mixture Model on Melter SO ₃ Tolerance at 1150 °C for LAW Glasses	7.26
Figure 7.11. Predicted versus Measured Plots for the Six Evaluation Subsets Using the 10-Component Reduced Linear Mixture Model on Melter SO ₃ Tolerance at 1150 °C for LAW Glasses	7.27
Figure 7.12. Response Trace Plot for the 10-Component Reduced Linear Mixture Model on Melter SO ₃ Tolerance at 1150 °C for LAW Glasses	7.28

Figure 7.13. Standardized Residuals Plot for the 11-Term Reduced Partial Quadratic Mixture Model on Melter SO ₃ Tolerance at 1150 °C for LAW Glasses	7.31
Figure 7.14. Predicted versus Measured Plot for the 576-Glass Modeling Dataset Using the 11-Term Reduced Partial Quadratic Mixture Model on Melter SO ₃ Tolerance at 1150 °C for LAW Glasses	7.32
Figure 7.15. Predicted versus Measured Plots for the Six Evaluation Subsets Using the 11-Term Reduced Partial Quadratic Mixture Model on Melter SO ₃ Tolerance at 1150 °C for LAW Glasses	7.33
Figure 7.16. Response Trace Plot for 11-Term Reduced Partial Quadratic Mixture Model on Melter SO ₃ Tolerance at 1150 °C for LAW Glasses	7.34
Figure 7.17. Prediction Standard Deviations versus Predicted Values over the LAW Glass Compositions in the 576-Glass Modeling Dataset for the Recommended 11-Term PQM Model for Melter SO ₃ Tolerance at 1150 °C.....	7.40
Figure 8.1. Distributions of 20 Main Components (in mass fractions) for 344 LAW Glass Compositions with Data for K-3 Corrosion at 1208 °C. The vertical lines (when present) represent the lower and upper limits for each component from the PNNL LAW Phase 1 outer-layer study (blue lines), Phase 2 outer-layer study (pink lines), and Phase 3 study (pink lines), as shown in Table 2.1. In cases where two limits are the same, pink lines over plot the blue lines.	8.3
Figure 8.2. Distributions of 20 Main Components (in mass fractions) for 333 LAW Glass Compositions with Data for K-3 Corrosion at 1208 °C that Remain after Excluding the 11 Glasses in Table 8.1. The vertical lines (when present) represent the lower and upper limits for each component from the PNNL LAW Phase 1 outer-layer study (blue lines), Phase 2 outer-layer study (pink lines), and Phase 3 study (pink lines), as shown in Table 2.1. In cases where two limits are the same, pink lines over plot the blue lines.	8.5
Figure 8.3. Scatterplot Matrix of 20 Components (mass fractions) for the 333 LAW Glasses with K-3 Corrosion at 1208 °C Data that Remain after Excluding the 11 Glasses in Table 8.1	8.6
Figure 8.4. Predicted versus Measured Plot for the 333-Glass Modeling Dataset Using the 20-Component Full Linear Mixture Model on the Natural Logarithm of K-3 Corrosion at 1208 °C for LAW Glasses	8.14
Figure 8.5. Predicted versus Measured Plots for the Five Evaluation Subsets Using the 20-Component Full Linear Mixture Model on the Natural Logarithm of K-3 Corrosion at 1208 °C for LAW Glasses	8.15
Figure 8.6. Response Trace Plot for the 20-Component Full Linear Mixture Model on the Natural Logarithm of K-3 Corrosion at 1208 °C for LAW Glasses	8.16
Figure 8.7. Standardized Residuals Plot for the 11-Component Reduced Linear Mixture Model on the Natural Logarithm of K-3 Corrosion at 1208 °C for LAW Glasses	8.19
Figure 8.8. Predicted versus Measured Plot for the 333-Glass Modeling Dataset Using the 11-Component Reduced Linear Mixture Model on the Natural Logarithm of K-3 Corrosion at 1208 °C for LAW Glasses	8.20
Figure 8.9. Predicted versus Measured Plots for the Five Evaluation Subsets Using the 11-Component Reduced Linear Mixture Model on the Natural Logarithm of K-3 Corrosion at 1208 °C for LAW Glasses	8.21

Figure 8.10. Response Trace Plot for the 11-Component Reduced Linear Mixture Model on the Natural Logarithm of K-3 Corrosion at 1208 °C for LAW Glasses	8.22
Figure 8.11. Standardized Residuals Plot for the 13-Term Reduced Partial Quadratic Mixture Model on the Natural Logarithm of K-3 Corrosion at 1208 °C for LAW Glasses	8.25
Figure 8.12. Predicted versus Measured Plot for the 333-Glass Modeling Dataset Using the 13-Term Reduced Partial Quadratic Mixture Model on the Natural Logarithm of K-3 Corrosion at 1208 °C for LAW Glasses	8.26
Figure 8.13. Predicted versus Measured Plots for the Five Evaluation Subsets Using the 13-Term Reduced Partial Quadratic Mixture Model on the Natural Logarithm of K-3 Corrosion at 1208 °C for LAW Glasses	8.27
Figure 8.14. Response Trace Plot for 13-Term Reduced Partial Quadratic Mixture Model on the Natural Logarithm of K-3 Corrosion at 1208 °C for LAW Glasses	8.28
Figure 9.1. Concentrations of NaK ($= g_{\text{Na}_2\text{O}} + 0.66g_{\text{K}_2\text{O}}$) and Li_2O of modeling database in mass fractions.	9.11
Figure 9.2. Concentrations of SiO_2 and Al_2O_3 of modeling database in mass fractions.	9.12
Figure 9.3. Concentrations of Na_2O and SiO_2 of modeling database in mass fractions.....	9.12

Tables

Table 2.1. Single-Component Constraints (SCCs), Multiple-Component Constraints (MCCs), and Center Points (CPs) for PNNL LAW Phase 1 Outer Layer (Ph1-OL), Phase 1 Inner Layer (Ph1-IL), Phase 2 Inner Layer (Ph2-IL), and Phase 2 Outer Layer (Ph2-OL) Studies. The Phase 3 constraints are the same as the Phase 2 OL constraints.	2.2
Table 2.2. Summary of LAW Glass Database Showing Data Group, Report Number, Total Number of Glasses, and Number of Glasses with Values for Each Property	2.7
Table 2.3. REFMIX Composition in Formats Used for Example Calculations and Response Trace Plots	2.13
Table 3.1. Fourteen LAW Glasses with Non-representative Compositions Excluded from the Modeling Datasets for Normalized PCT Losses of B and Na	3.5
Table 3.2. Uncertainty in Normalized PCT Losses (g/m ²) of B for Replicate and Near-Replicate Sets of LAW Glasses	3.11
Table 3.3. Uncertainty in Normalized PCT Losses (g/m ²) of Na for Replicate and Near-Replicate Sets of LAW Glasses	3.15
Table 3.4. Coefficients and Performance Summary for the 20-Component Full Linear Mixture Model on the Natural Logarithm of Normalized Boron Loss from the PCT on LAW Glasses.	3.23
Table 3.5. Coefficients and Performance Summary for the 15-Component Reduced Linear Mixture Model on the Natural Logarithm of Normalized Boron Loss from the PCT on LAW Glasses.	3.27
Table 3.6. Coefficients and Performance Summary for the 19-Term Partial Quadratic Mixture Model on the Natural Logarithm of Normalized Boron Loss from the PCT on LAW Glasses	3.31
Table 3.7. Coefficients and Performance Summary for 22-Term Bias Corrected Partial Quadratic Mixture Model on the Natural Logarithm of Normalized PCT Boron Loss from LAW Glasses	3.39
Table 3.8. Coefficients and Performance Summary for the 20-Component Full Linear Mixture Model on the Natural Logarithm of Normalized PCT Sodium Loss from LAW Glasses	3.44
Table 3.9. Coefficients and Performance Summary for the 15-Component Reduced Linear Mixture Model on the Natural Logarithm of Normalized PCT Sodium Loss from LAW Glasses	3.48
Table 3.10. Coefficients and Performance Summary for the 19-Term Partial Quadratic Mixture Model on the Natural Logarithm of Normalized PCT Sodium Loss from LAW Glasses	3.52
Table 3.11. Coefficients and Performance Summary for 22-Term Bias Corrected Partial Quadratic Mixture Model on the Natural Logarithm of Normalized PCT Sodium Loss from LAW Glasses	3.57

Table 3.12. Performance Summary of Two Models for the Natural Logarithm of PCT Responses of LAW Glasses.....	3.62
Table 3.13. Example Glass Compositions in Formats Used with Models of Natural Logarithm of Normalized PCT Boron and Sodium Losses from LAW Glasses (mass fractions).....	3.67
Table 3.14. Predicted PCTjNL, Standard Deviation, and Statistical Intervals for the Example Glass Compositions Used in Two Models for Natural Logarithm of Normalized PCT Boron and Sodium Losses from LAW Glasses	3.67
Table 3.15. Data Component Concentration Ranges (mass fraction) for LAW Glasses Used in Final Natural Logarithm of Normalized PCT Boron and Sodium Loss Models	3.69
Table 4.1. Thirteen LAW Glasses with Non-representative Compositions Excluded from the Modeling Datasets for Pass/Fail VHT	4.5
Table 4.2. Agreement in the VHT Pass (0)/Fail (1) Response for Replicate and Near-Replicate Glasses	4.9
Table 4.3. Coefficients and Performance Summary for the 20-Component Logistic Full Linear Mixture Model on the Pass/Fail VHT response on LAW Glasses Using a Threshold for Classification of 0.3	4.16
Table 4.4. Coefficients and Performance Summary for the 19-Component Logistic Partially Quadratic Mixture Model on the Pass/Fail VHT response on LAW Glasses Using a Threshold for Classification of 0.19.....	4.22
Table 4.5. REFMIX Composition in Formats Used with Models of $\ln P(g)1-P(g)$ for Predicting Pass/Fail VHT for LAW Glasses	4.28
Table 4.6. Predicted $\ln P(g)1-P(g)$ and $P(g)$ and Confidence Interval for the REFMIX Composition Used in the Recommended 19-term Model for VHT	4.29
Table 4.7. Data Component Concentration Ranges (mass fraction) for LAW Glasses Used in Final VHT Pass/Fail Models.....	4.30
Table 5.1. Fifteen LAW Glasses Excluded from the Modeling Dataset for Viscosity at 1150 °C (η_{1150}).....	5.5
Table 5.2. Uncertainty in Viscosity at 1150 °C Responses for Replicate and Near-Replicate Sets	5.10
Table 5.3. Coefficient Estimates and Performance Summary Statistics for the 20-Component Full Linear Mixture Model on the Natural Logarithm of Viscosity at 1150 °C for LAW Glasses	5.15
Table 5.4. Coefficients and Performance Summary for the 18-Component Reduced Linear Mixture Model on the Natural Logarithm of Viscosity at 1150 °C for LAW Glasses	5.20
Table 5.5. Coefficients and Performance Summary for 21-Term Reduced Partial Quadratic Mixture Model on the Natural Logarithm of Viscosity at 1150 °C for LAW Glasses	5.26
Table 5.6. Performance Summary of Three Models for the Natural Logarithm of Viscosity at 1150 °C for LAW Glasses	5.31
Table 5.7. REFMIX Composition in Formats Used with Models of Natural Logarithm of Viscosity at 1150 °C for LAW Glasses	5.33
Table 5.8. Predicted Viscosity at 1150 °C, Standard Deviation, and Statistical Intervals for the REFMIX Composition Used in Two Models for Viscosity at 1150 °C	5.34

Table 5.9. Data Component Concentration Ranges (mass fraction) for LAW Glasses Used in Final Viscosity Models	5.37
Table 6.1. Sixteen LAW Glasses Excluded from the Modeling Dataset for Electrical Conductivity at 1150 °C (ϵ_{1150}).....	6.5
Table 6.2. Uncertainty in Electrical Conductivity at 1150 °C Responses for Replicate and Near-Replicate Sets.....	6.10
Table 6.3. Coefficients and Performance Summary for the 20-Component Full Linear Mixture Model on the Natural Logarithm of Electrical Conductivity at 1150 °C for LAW Glasses	6.15
Table 6.4. Coefficients and Performance Summary for the 11-Component Reduced Linear Mixture Model on the Natural Logarithm of Electrical Conductivity at 1150 °C for LAW Glasses	6.20
Table 6.5. Coefficients and Performance Summary for the 13-Term Reduced Partial Quadratic Mixture Model on the Natural Logarithm of Electrical Conductivity at 1150 °C for LAW Glasses	6.26
Table 6.6. Performance Summary of Three Models for the Natural Logarithm of Electrical Conductivity at 1150 °C for LAW Glasses.....	6.31
Table 6.7. REFMIX Composition in Formats Used with Models of Natural Logarithm of Electrical Conductivity at 1150 °C for LAW Glasses	6.33
Table 6.8. Predicted Electrical Conductivity at 1150 °C, Standard Deviation, and Statistical Intervals for the REFMIX Composition Used in Two Models for Electrical Conductivity at 1150 °C	6.34
Table 6.9. Data Component Concentration Ranges (mass fraction) for LAW Glasses Used in Final Electrical Conductivity Models	6.38
Table 7.1. Twenty-five LAW Glasses Excluded from the Modeling Dataset for Melter SO ₃ Tolerance and Solubility at 1150 °C.....	7.6
Table 7.2. Uncertainty in SO ₃ Solubility at 1150 °C Responses for Replicate and Near-Replicate Sets.....	7.12
Table 7.3. Coefficients and Performance Summary for the 19-Component Full Linear Mixture Model on the Melter SO ₃ Tolerance at 1150 °C for LAW Glasses	7.18
Table 7.4. Coefficients and Performance Summary for the 10-Component Reduced Linear Mixture Model on the Melter SO ₃ Tolerance at 1150 °C for LAW Glasses	7.23
Table 7.5. Coefficients and Performance Summary for 11-Term Reduced Partial Quadratic Mixture Model on Melter SO ₃ Tolerance at 1150 °C for LAW Glasses.....	7.30
Table 7.6. Performance Summary of Three Models for Melter SO ₃ Tolerance at 1150 °C for LAW Glasses	7.35
Table 7.7. REFMIX Composition in Formats Used with Models of Melter SO ₃ Tolerance at 1150 °C for LAW Glasses	7.37
Table 7.8. Predicted Melter SO ₃ Tolerance at 1150 °C, Standard Deviation, and Statistical Intervals for the REFMIX Composition Used in Two Models for Melter SO ₃ Tolerance at 1150 °C	7.37
Table 7.9. Data Component Concentration Ranges (mass fraction) for LAW Glasses Used in Final Melter SO ₃ Tolerance at 1150 °C Models	7.41

Table 8.1. Eleven LAW Glasses Excluded from the Modeling Dataset for K-3 Corrosion at 1208 °C	8.4
Table 8.2. Uncertainty in K-3 Corrosion at 1208 °C Responses for Replicate and Near-Replicate Sets.....	8.8
Table 8.3. Coefficients and Performance Summary for the 20-Component Full Linear Mixture Model on the Natural Logarithm of K-3 Corrosion at 1208 °C for LAW Glasses.....	8.13
Table 8.4. Coefficients and Performance Summary for the 11-Component Reduced Linear Mixture Model on the Natural Logarithm of K-3 Corrosion at 1208 °C for LAW Glasses	8.18
Table 8.5. Coefficients and Performance Summary for 13-Term Reduced Partial Quadratic Mixture Model on the Natural Logarithm of K-3 Corrosion at 1208 °C for LAW Glasses	8.24
Table 8.6. Performance Summary of Three Models for the Natural Logarithm of K-3 Corrosion at 1208 °C for LAW Glasses	8.29
Table 8.7. REFMIX Glass Composition in Formats Used with Models of Natural Logarithm of K-3 Corrosion at 1208 °C for LAW Glasses	8.31
Table 8.8. Predicted K-3 Corrosion at 1208 °C, Standard Deviation, and Statistical Intervals for the REFMIX Glass Composition Used in Two Models for K-3 Corrosion at 1208 °C	8.32
Table 8.9. Data Component Concentration Ranges (mass fraction) for LAW Glasses Used in Final Natural Logarithm K-3 Corrosion at 1208 °C Models	8.34
Table 9.1. Summary of Melter SO ₃ Tolerance and Solubility Data.....	9.6
Table 9.2. Data Component Concentration Ranges (mass fraction) for LAW Glasses Used in Models	9.10
Table 9.3. Component effect “slopes” for each of the recommended models taken at the REFMIX composition.....	9.14
Table 9.4. General Direction of Component Effects on Properties ^(a) (For Information Only)	9.14

1.0 Introduction

The U.S. Department of Energy's (DOE's) Hanford Site in Washington State is the current storage location for roughly 56 million gallons of highly radioactive wastes stored in underground tanks. The Waste Treatment and Immobilization Plant (WTP) will provide DOE with a capability to treat the waste by vitrification for subsequent disposal. The low-activity waste (LAW) fraction of the tank waste will be vitrified to form an alkali-alumino-boro-silicate immobilized low-activity waste (ILAW) product to be disposed in the Integrated Disposal Facility on the Hanford Site. The ILAW product must satisfy a variety of requirements with respect to protection of the environment before it can be accepted for disposal. Additionally, to be efficiently processed in the WTP, the LAW melts must satisfy process-related properties.

Current plans for the WTP envision vitrifying LAW prior to startup of the WTP high-level waste (HLW) Facility using a Direct Feed Low-Activity Waste (DFLAW) approach (Tilanus et al. 2017). The WTP LAW Facility will be operated and controlled using a LAW glass formulation algorithm (GFA), which requires several inputs based on research and development results, plant operations data, and analyzed compositions. Currently it is envisioned that the preliminary LAW GFA discussed by Kim and Vienna (2012) and the LAW glass property-composition models recommended in Piepel et al. (2007) will be used for commissioning and initial radioactive operations of the LAW Facility under the DFLAW approach. After commissioning and initial operations, an updated LAW GFA being developed at Pacific Northwest National Laboratory (PNNL) and using the models in this report will be implemented by the WTP operations contractor in the WTP LAW Facility.

The updated LAW GFA uses several inputs, including the (i) LAW glass formulation methods and constraints, (ii) LAW glass property constraints, (iii) LAW glass property-composition models and corresponding methods for quantifying uncertainties in model property predictions, and (iv) model validity constraints. Item (i) will be documented in the GFA report and item (ii) remains unchanged. This report documents the results for items (iii) and (iv). The LAW glass properties for which models, model uncertainties, and model validity constraints are reported here include Product Consistency Test (PCT) response, Vapor Hydration Test (VHT) response, viscosity at 1150 °C (η_{1150}), electrical conductivity (EC) at 1150 °C (ϵ_{1150}), melter SO₃ tolerance at 1150 °C, and K-3 refractory corrosion at 1208 °C.

LAW glass property-composition data collected to support modeling, model development, model validation, and model uncertainty results are presented in this report. They represent a significant increase in model validity range, which directly translates to the size of the processing envelope, compared to previously published models (Piepel et al. 2007).

Section 1.1 discusses the LAW glass properties for which property-composition models were developed. Section 1.1 introduces the property-composition models and associated constraints for LAW glass property-composition model development. The LAW glass property-composition data available for modeling are described in Section 2.0. Data sources are summarized in Section 2.1. Section 2.2 describes the treatment of SO₃ and renormalization in glass compositions used for modeling. The mapping of glass data to each property to be modeled is summarized in Section 2.3. Subsets of the data used to evaluate the performance of models for enhanced glass composition region (GCR) are defined in Section 2.4. Section 2.5 describes the reference glass used for example calculations and response trace plots. Models relating PCT boron and sodium normalized losses to LAW glass composition are presented and discussed in Section 3.0. Data and models relating the LAW glass composition to the probability to fail the VHT constraint (alteration rate ≤ 50 g/m²/day) are presented and discussed in Section 4.0. Data and models relating viscosity and EC – at 1150 °C – to LAW glass composition are presented and discussed in

Sections 5.0 and 6.0, respectively. Data and models relating melter SO_3 tolerance at 1150 °C to LAW glass composition are presented and discussed in Section 7.0. Data and models relating K-3 refractory neck corrosion at 1208 °C to LAW glass composition are presented and discussed in Section 8.0. A summary and conclusions from the work to develop, evaluate, and validate the LAW glass property-composition models are presented in Section 9.0 along with recommendations for future development. The references cited in the report are listed in Section 10.0.

The mass fraction compositions and property values of all the LAW glasses used to develop property-composition models are presented in Appendix A. Appendix B discusses the statistical methods applied in the main body of the report. Appendix C lists the glass numbers (Glass #s) associated with each of the six evaluation subsets of data for each LAW glass property-composition model. Appendix D lists the variance-covariance matrices for selected LAW glass property-composition models, which are required to calculate uncertainties of model predictions.

1.1 Glass Property-Composition Models and Associated Constraints

LAW glass produced by the WTP LAW Facility must satisfy constraints for several product quality and processing properties. In most cases, constraints for the LAW glass properties are satisfied using property-composition models. Those LAW glass product quality and processing property constraints that are currently planned to be met using glass property-composition models are discussed below. Other constraints are not met using glass property-composition models typically because either the property does not vary sufficiently to approach the limit (e.g., density, compressive strength, etc.) or because there is insufficient data or mechanistic understanding to model (e.g., melter feed processing rate, crystallization kinetics, etc.).

1.1.1 PCT Normalized Losses of B and Na (PCT_B^{NL} , PCT_{Na}^{NL}) (g/m²)

WTP contract Specification 2.2.2.17.2 requires that PCT normalized losses of B (PCT_B^{NL}), Na (PCT_{Na}^{NL}), and Si (PCT_{Si}^{NL}) from quenched and container centerline cooled (CCC) glasses must be less than 2 g/m² (DOE 2000). Several references (including Piepel et al. 2007; Muller et al. 2014; Vienna et al. 2013, 2016) have shown that PCT_{Si}^{NL} values are always less than PCT_B^{NL} and/or PCT_{Na}^{NL} values. This was also found in this study; thus, it was only necessary to model PCT_B^{NL} and PCT_{Na}^{NL} as functions of LAW glass composition.

1.1.2 VHT Alteration Rate (r_a^{VHT}) (g m⁻² d⁻¹)

WTP contract Specification 2.2.2.17.3 requires that alteration rates of LAW glasses subjected to at least a 7-day VHT run at 200 °C be less than 50 g/m²/d (DOE 2000). The WTP project chose to perform 24-day VHTs for most of the data (Muller et al. 2001). However, some data do exist at 7- and 14-day durations. For LAW glasses with typical densities near the reference value of 2.65 g/cm³, the 50 g/m²/d limit translates to an alteration depth (D) of 453 μm during the 24-day test period (Piepel et al. 2007). In previous reports, D was the VHT response that was modeled (Piepel et al. 2007; Muller et al. 2014; Vienna et al. 2013, 2016) as a function of LAW glass composition. However, in this report it is the binary response of pass corresponding to $r_a^{VHT} < 50$ g/m²/d and fail corresponding to $r_a^{VHT} \geq 50$ g/m²/d that is modeled. This is due to the difficulty in predicting the r_a^{VHT} as functions of composition for the broader range of data needed for this phase of modeling.

1.1.3 Viscosity at 1150 °C (η_{1150}) (P) and Electrical Conductivity at 1150 °C (ϵ_{1150}) (S/cm)

The η_{1150} should fall between 20 and 80 P to ensure sufficient processing rate and flow of LAW glass while minimizing corrosion of melter construction materials (Perez 2006). The EC should fall between 0.1 and 0.7 S/cm over the temperature range from 1100 to 1200 °C to ensure sufficient energy can be supplied by the power source without exceeding current density limits of the power system at nominal throughput. Ideally, viscosity and EC would be modeled as functions of LAW glass composition and melt temperature. Such models would allow prediction of the viscosity and EC for different glass compositions at different melt temperatures. The statistical methods for fitting such models and quantifying prediction uncertainties, although quite complex, have been developed. However, the viscosity and EC models at a fixed temperature are simpler to develop and easier to implement to glass formulation. For this reason, it was decided to model η_{1150} and ϵ_{1150} , the nominal melter operating temperature, rather than to model viscosity and EC as functions of composition and melt temperature. Models for viscosity and EC at temperatures other than 1150 °C could be developed similarly if needed. The current constraints for EC are set at 1100 and 1200 °C. Since the EC constraints span $\pm 50^\circ\text{C}$ from modeled temperature of 1150 °C, adjusted limits for EC at 1150°C should be used as the model constraints to determine compliance. Assuming a relationship between EC and absolute temperature (T_K) of: $\ln(\epsilon) = A + B/T_K$ (where A and B are temperature independent parameters) a predicted ϵ_{1150} can be used to calculate EC across the temperature range. Applying the median B value of -7168 (K/ln(cm/S)), it is straight forward to estimate the limits at a fixed temperature of 1150 °C of $0.120 \leq \epsilon_{1150} \leq 0.590$ S/cm.

1.1.4 Melter SO₃ Tolerance Model at 1150 °C ($w_{SO_3}^{MT1150}$) (wt%)

Melter SO₃ tolerance is the feed SO₃ concentration above which a salt phase accumulates in the melter. The wt% SO₃ in the melter feed should not exceed the melter SO₃ tolerance at the processing temperature of 1150 °C to avoid excessive corrosion of melter construction materials and increased radionuclide volatility from an accumulated salt phase (Vienna et al. 2014; Muller et al. 2015b). A preliminary constraint used to plan the Hanford cleanup mission (Vienna et al. 2013, 2016) has been that the SO₃ target concentration in melter feed (after converting to oxides/halogens) must be lower than the predicted melter SO₃ tolerance at 1150 °C. Hence, this report develops a model for melter SO₃ tolerance at 1150 °C, which is denoted $w_{SO_3}^{MT1150}$.

1.1.5 K-3 Refractory Corrosion Neck Loss at 1208 °C (k_{1208}) (inch)

As the loading of LAW in glass increases, K-3 refractory corrosion becomes an important factor, primarily because of the increasing fraction of glasses with high alkali content. The preliminary constraint used to plan the Hanford cleanup mission (Vienna et al. 2013, 2016) has been that the neck corrosion loss must be less than 0.04 inches per 6-day test at 1208 °C as proposed by Muller et al. (2015b). Although it is challenging to relate this test time and conditions directly to melter operation, it is used since nearly 100% of data available for modeling of K-3 corrosion in typical LAW glass compositions was measured under these conditions. This report develops an enhanced version of the Muller et al. (2018) model for the neck corrosion loss of K-3 refractory, although the basis for the time, temperature, and thickness constraint has not been rigorously developed.

1.1.6 Goal of LAW Glass Property-Composition Modeling

The goal for LAW glass property-composition models is to adequately approximate the true, unknown relationships over a specified LAW GCR. Ideally, this specified GCR should be large enough to include

all LAW glass compositions that (i) may be made from Hanford LAW, and (ii) are inside, near, and somewhat past the boundaries corresponding to property constraints. The models need to be able to discriminate between LAW glass compositions that have acceptable and unacceptable values of properties, as well as adequately approximate the property-composition relationships for LAW glasses with acceptable values of properties.

Depending on the LAW glass property, it sometimes is not possible to adequately approximate the true, unknown property-composition relationship with a single model applicable over the whole LAW GCR of interest. In those cases, it is necessary for one or more properties to (i) develop different models for different subregions of the LAW GCR of interest, (ii) use more advanced property modeling approaches applicable over the whole LAW GCR of interest, or (iii) use logistic regression of constraint pass/fail data. The GCR would ideally be as broad as any compositions desired for processing of LAW in glass. However, it is ultimately limited by the data available for model fitting (the model validity range).

1.1.7 Property-Composition Model Validity Constraints

LAW glass properties are complex functions of glass composition and potentially other factors such as cooling rate and the presence and types of crystals formed on cooling. Property-composition models with mathematical forms that can adequately approximate the true unknown property-composition relationships must be fitted to experimental data to estimate the unknown model coefficients. Hence, the resulting models should only be used to predict properties of LAW glass compositions (i) within the GCR over which the property-composition data used for fitting models were collected, and (ii) for similar cooling schedules and other conditions for which data were collected.

The LAW GCR containing the compositions used for fitting property-composition models is typically specified by lower and/or upper bounds on (i) individual LAW glass components, which are referred to as single-component constraints (SCCs), and (ii) linear combinations of two or more glass components, which are referred to as multiple-component constraints (MCCs). A SCC is of the general form

$$L_i \leq g_i \leq U_i, \quad (1.1)$$

where L_i and U_i are respectively lower and upper bounds on the mass fraction of the i^{th} component (g_i) in a LAW glass with q components, $\sum_{i=1}^q g_i = 1$. A linear MCC is of the general form

$$L \leq \sum_{i=1}^q Z_i g_i \leq U \quad (1.2)$$

where L and U are respectively the lower and upper bounds on the linear combination of component mass fractions with coefficients Z_1, \dots, Z_q . If necessary, nonlinear functions of two or more glass components may also be used to form MCCs. The property-composition model validity constraints will generally be specified using the SCCs and MCCs, which mathematically describe the LAW GCR over which data were used to develop the property-composition models. Other conditions under which modeling data were developed (which may vary by property) must also be represented by model validity constraints. It is important to develop and explicitly specify the validity constraints for each LAW glass property model so that models will only be applied within valid GCRs by the LAW GFA and for other purposes.

In addition to model validity constraints, SCCs and MCCs are also typically applied to avoid composition regions that are prone to undesirable characteristics that are not directly predicted using property-composition models. For example, constraints to limit the propensity to crystallization of the ILAW in the melter and during slow cooling in the glass container have been applied in the past (Vienna et al. 2013, 2016).

Property-composition models and statistical methods for quantifying uncertainties in model predictions will be used in the updated LAW GFA. The GFA in turn will be used to design LAW glasses and verify that associated property constraints are satisfied with sufficient confidence after accounting for uncertainties in property prediction and WTP LAW Facility operations. Hence, statistical methods for quantifying the uncertainties in predicted glass property values were developed. Glass property-composition models and uncertainty methods may also be used to support the following:

- Waste feed qualification by assessing (i) melter feed properties, (ii) decisions on pretreatment operations, and (iii) vitrification process effectiveness.
- River Protection Project mission planning and optimization, considering the waste feed delivery strategy, waste pretreatment requirements, and mission life/cost estimation.

The specific LAW glass properties for which models were developed as functions of LAW glass composition are listed and discussed in Section 2. The discussion addresses why the specific properties were chosen for modeling.

2.0 LAW Glass Property-Composition Data for Modeling

Section 2.1 briefly discusses LAW glass composition and property data compiled from the literature into an Excel™ database for use in developing property-composition models. Section 2.2 describes how the LAW glass compositions were normalized using measured or estimated SO₃ concentrations. Section 2.3 summarizes the LAW glass property-composition data available for modeling. Section 2.4 discusses subsets of the LAW property-composition data used to evaluate the prediction performance of models for the corresponding composition subregions.

2.1 LAW Glass Database

An Excel™ database of LAW glass property-composition data for modeling LAW glass properties as functions of composition was compiled from technical reports published by the Vitreous State Laboratory (VSL) at The Catholic University of America and PNNL. A total of 1075 LAW glass compositions were compiled. The database includes LAW glass compositions from the PNNL Phase 1, 2, and 3 statistically designed studies. Property values available for each glass from the VSL and PNNL studies were compiled in the database. In addition, a separate VSL dataset of 344 LAW glass compositions with K-3 corrosion data were extracted from Muller et al. (2018). Many but not all of these 344 glass compositions are also in the compiled database.

The LAW Phase 1 study at PNNL (Russell et al. 2017) was conducted in two parts. The first part explored the inner layer (IL) of the LAW GCR specified by the Phase 1 IL SCCs and MCCs in Table 2.1. The second part explored the outer layer (OL) of the LAW GCR specified by the Phase 1 OL SCCs and MCCs in Table 2.1. A total of 36 glasses were investigated in both parts of the LAW Phase 1 study, with the corresponding glass property values as documented by Russell et al. (2017).

The LAW Phase 2 study at PNNL (Russell et al. 2020) was conducted in two parts. The first part explored the IL of the LAW GCR specified by the Phase 2 IL SCCs and MCCs in Table 2.1. The second part explored the OL of the LAW GCR specified by the Phase 2 OL SCCs and MCCs in Table 2.1. The LAW Phase 2 IL study consisted of 17 glasses, while the LAW Phase 2 OL study consisted of 25 glasses. Some glasses in the LAW Phase 2 OL study had to have their target compositions (in the statistically selected test matrix) modified, which was discussed by Russell et al. (2020). However, even with modifications, a homogeneous version of one of the OL glasses could not be made. So, the Phase 2 study contained a total of 41 LAW glasses. Russell et al. (2020) presented and discussed the glass compositions and property data from the LAW Phase 2 IL and OL studies conducted at PNNL.

The LAW Phase 3 study at PNNL (Lonergan et al. 2020) explored the same GCR as specified by the LAW Phase 2 OL SCCs and MCCs in Table 2.1. However, to obtain a better coverage of this GCR, a space-filling experimental design approach was used to select 20 Phase 3 glasses to augment the 41 LAW Phase 2 glasses. The specifics are discussed in Section 2.1.1 of Lonergan et al. (2020). Two of the 20 glasses had replicate results, so the LAW Phase 3 study is discussed in this report as investigating 22 glasses even though there were only 20 distinct target glass compositions. The property values for these glasses are documented by Lonergan et al. (2020).

Table 2.1. Single-Component Constraints (SCCs), Multiple-Component Constraints (MCCs), and Center Points (CPs) for PNNL LAW Phase 1 Outer Layer (Ph1-OL), Phase 1 Inner Layer (Ph1-IL), Phase 2 Inner Layer (Ph2-IL), and Phase 2 Outer Layer (Ph2-OL) Studies. The Phase 3 constraints are the same as the Phase 2 OL constraints.

Component	Ph1 OL Min	Ph1 OL Max	Ph1 IL Min	Ph1 IL Max	Ph1 Center Point	Ph2 IL Min	Ph2 IL Max	Ph2 IL Center Point	Ph2 OL & Ph3 Min	Ph2 OL & Ph3 Max	Ph2 OL Center Point
Single-Component Constraints											
Al ₂ O ₃	0.035	0.1385	0.0625	0.115	0.09	0.075	0.1075	0.10	0.06	0.125	0.1000
B ₂ O ₃	0.06	0.1375	0.08	0.1175	0.10	0.08	0.12	0.095	0.06	0.1375	0.0950
CaO	0	0.1224	0.0275	0.09	0.055	0.02	0.08	0.05	0.02	0.11	0.0500
Cr ₂ O ₃	0.0004 ^(a)	0.0031 ^(a)	0.0008 ^(a)	0.0021 ^(a)	0.0014 ^(a)	0.00375	0.00525	0.0045	0.003	0.006	0.0045
Fe ₂ O ₃	0	0.015	0.005	0.0125	0.01	0.002	0.01	0.006	0	0.015	0.0060
K ₂ O	0	0.015	0.002	0.01	0.004	0.005	0.02	0.01	0	0.0575	0.0100
Li ₂ O	0	0.05	0.01	0.035	0.02	0 ^(b)	0 ^(b)	0 ^(b)	0 ^(b)	0 ^(b)	0 ^(b)
MgO	0	0.035	0.005	0.025	0.015	0.003	0.01	0.0065	0	0.0135	0.0065
Na ₂ O	0.10	0.26	0.15	0.23	0.19	0.22	0.245	0.23	0.21	0.26	0.2300
SO ₃	0.001	0.02	0.004	0.013	0.007	0.002	0.008	0.005	0.001	0.02	0.0050
SiO ₂	0.34	0.47	0.3675	0.4325	0.3955	0.37	0.43	0.388	0.349	0.47	0.3880
SnO ₂	0	0.05	0.01	0.035	0.02	0.005	0.025	0.015	0	0.035	0.0150
V ₂ O ₅	0	0.04	0.005	0.03	0.02	0.005	0.02	0.01	0	0.04	0.0100
ZnO	0.01	0.05	0.02	0.04	0.03	0.024	0.032	0.028	0.02	0.036	0.0280
ZrO ₂	0	0.065	0.015	0.0475	0.03	0.03	0.055	0.04	0.0295	0.065	0.0400
Others	0.004	0.03	0.0075	0.02	0.0135	0.01	0.02	0.012	0	0.0269	0.0120
Multiple-Component Constraints											
Expression											
NAlk ^(c)	0.15	0.265	0.195	0.25	NA	— ^(d)	0.25	NA	—	0.26	NA
SO ₃ solubility ^(e)	0	—	0	—	NA	0	—	NA	0	—	NA
η ₁₁₅₀ , poise ^(f)	10	100	30	70	NA	30	70	NA	10	100	NA
SnO ₂ +ZrO ₂	0.03	0.11	0.04	0.08	NA	—	—	NA	—	—	—
Al ₂ O ₃ +SnO ₂ +ZrO ₂	—	—	—	—	NA	—	0.17	NA	—	0.17	NA
NAlk-ZrO ₂ -SnO ₂ -CaO	—	—	—	—	NA	—	0.15	NA	—	0.15	NA

(a) Cr₂O₃ was contained in Others for LAW Phase 1 with a fixed mass fraction of 0.104 of the total amounts of Others, but was a separate, varied component for LAW Phase 2 and Phase 3.

(b) Li₂O was set to zero for the LAW Phase 2 IL and OL studies, and the Phase 3 study.

(c) NAlk = Na₂O + 2(Li₂O) + 0.66(K₂O)

(d) A dash (—) denotes that there was no limit on the expression.

(e) The SO₃ solubility constraint was implemented as 0.01*SL(SO₃) – SO₃ ≥ 0, where SO₃ is the mass fraction of SO₃ in a LAW glass, and SL(SO₃) is a model prediction of melter SO₃ tolerance (in wt%) for that LAW glass. The melter SO₃ tolerance model is discussed by Vienna et al. (2014).

(f) The LAW Phase 1, Phase 2, and Phase 3 studies at PNNL used η₁₁₅₀ constraints in units of Pa·s. The units were converted to poise in this table because those are the units used by in the current GFA. The η₁₁₅₀ constraints were implemented using a model discussed by Piepel et al. (2016) for Phase 1, and a model discussed by Vienna et al. (2016) for Phase 2 and Phase 3.

The GCR for model development is largely controlled by data availability for each specific property. Generally, the data available for each model is surveyed, and frequently it is found that a small number of glasses (one to four) significantly expand the concentration range of one or more component compared to the bulk of data. In those cases, the small number of glasses are excluded from model fitting, leaving the GCR being the range covered by most of the data. The specifics are discussed in the Sections 3.1.1, 4.1.1, 5.1.1, 6.1.1, 7.1.1, and 8.1.1 for PCT, VHT, viscosity, EC, melter SO₃ tolerance, and K-3 corrosion models, respectively.

2.2 Accounting for SO₃ Incorporated into LAW Glass Compositions

Target concentrations (mass fractions) of LAW glass components were used to determine batch and melt amounts of precursor chemicals to yield the target glass compositions. However, a portion of SO₃ may be lost due to (i) volatilization during melting of batch chemicals at 1150 °C or (ii) formation of separated sulfate salts on the melt surface. Thus, the mass fraction of SO₃ incorporated into a glass may be less than the corresponding target mass fraction of SO₃. The concentration (mass fraction) of SO₃ incorporated into the glass was measured (or estimated). The process of estimating the “measured” SO₃ for the glasses without measured SO₃ is described in the subsequent paragraphs. Then, the measured (or an estimated) SO₃ value was substituted for the target SO₃ value for each LAW glass composition. Finally, the remaining target component values were normalized so the total of the component mass fractions (including the measured or estimated SO₃ concentration) summed to 1. The normalization process increased the number of digits in glass component concentrations. The concentrations were rounded to six digits making necessary adjustments such that the sum of component concentrations would be precisely 1.000000. The choice of six digits was made to minimize the impact of rounding on glass property model fitting while maintaining a reasonable number of digits to report in data tables.

The database discussed in Section 2.1 contained 101 LAW glasses without measured SO₃ concentrations. An equation relating measured and target SO₃ concentrations was fitted using the glasses with both target and measured SO₃ values. Then, this fitted equation was used to estimate the “measured” SO₃ concentration in each of the 101 glasses. The following paragraph discusses the data used to fit this measured versus target equation.

Among the 1075 glasses in the database discussed in Section 2.1, 974 glasses had measured SO₃ concentrations, which left 101 glasses without measured SO₃ concentrations (as mentioned previously). Since all the PNNL glasses had measured SO₃ values, these were excluded from the data set to avoid any inter-lab impacts due to preparation conditions. In addition, 83 of the 836 remaining glasses with measured SO₃ involved duplicate data for various reasons (such as CCC glasses that used the same measured SO₃ as the quenched glasses). These 83 glasses with duplicate measured SO₃ values were excluded, which left 753 glasses with independently measured SO₃ for fitting an equation to relate measured SO₃ to target SO₃. However, there were 163 glasses that were tested for properties on samples that were saturated with SO₃ for SO₃ solubility measurement. The SO₃ solubility at 1150 °C results for these 163 glasses were used to obtain normalized glass compositions. However, the data for these 163 glasses were not used to fit the SO₃ measured-target equation because the glasses were prepared with excess target SO₃. One glass (ID# 33, LAWA97S) that was prepared with excess SO₃ did not have a SO₃ solubility value, and so a normalized composition could not be obtained. Hence, that glass was excluded, leaving 589 glasses for fitting the SO₃ measured-target equation.

Figure 2.1 shows the measured SO₃ (SO₃-m) versus target SO₃ (SO₃-t) concentrations in the 589 glasses with independently measured SO₃. Most glasses have SO₃-m values lower than the SO₃-t values because of expected volatile loss and potential loss of SO₃ from salt formation during glass preparation. A slightly higher SO₃-m than SO₃-t in some glasses is possible within testing and analytical experimental errors. However, there are glasses with significantly higher SO₃-m than SO₃-t, which may not be justified by experimental errors. This is especially so for the three glasses with (SO₃-m)/(SO₃-t) ≥ 1.5. Closely examining the glasses with SO₃-m > SO₃-t resulted in the following two findings.

- The three glasses with (SO₃-m)/(SO₃-t) ≥ 1.5 also had SO₃-m even higher than SO₃ solubility (w_{SO_3})¹ at 1150 °C, which suggests that the SO₃-m values are likely in error. In addition, the comparison of

¹ See Section 7 for details on SO₃ solubility methods and data.

w_{SO_3} and SO_3 -m for all 589 glasses found that a large fraction of glasses with SO_3 -m > SO_3 -t also had SO_3 -m > w_{SO_3} . So, it was decided to exclude the 44 glasses with SO_3 -m > w_{SO_3} (data points marked by red open circles in Figure 2.1) from the SO_3 -m versus SO_3 -t fit. However, it was noted that this process also removed some “normal” glasses with SO_3 -m < SO_3 -t.

- In data from Gan et al. (2001), 8 out of 10 glasses with measured SO_3 had SO_3 -m > SO_3 -t. This is unusual and suggests potential analytical bias in this set of glasses. So, it was also decided to exclude these 10 glasses (marked by red open triangles in Figure 2.1) from the SO_3 -m versus SO_3 -t fit.

Ultimately, 535 glasses were used to fit the SO_3 -m versus SO_3 -t equation.

An equation relating SO_3 -m to a second-order polynomial in SO_3 -t was fit to the data using the data from the 535 glasses, resulting in

$$SO_3\text{-m} = 0.955 (SO_3\text{-t}) - 0.170 (SO_3\text{-t})^2. \quad (2.1)$$

Eq. (2.1) does not have a constant (intercept) term because SO_3 -m should be zero when SO_3 -t is zero. The fitted curve fit to 535 data points using Eq. (2.1) is shown as a blue line in Figure 2.1. The figure shows that Eq. (2.1) may tend to over-predict measured SO_3 when the target SO_3 approaches 2 wt%. However, this was judged acceptable because there were a limited number of data points with SO_3 -t > 1.5 wt% to support fitting other model forms that could rectify this issue.

Ultimately, Eq. (2.1) was used to estimate SO_3 -m for the 101 glasses without measured SO_3 and the 54 glasses that had measured SO_3 but were removed from the SO_3 -m versus SO_3 -t fit for the reasons described previously.

Finally, normalized compositions of the LAW glasses were calculated using the equation

$$\begin{aligned} g_j &= \frac{T_j}{\sum_{j \neq SO_3} T_j} (1 - M_{SO_3}) \quad \text{for } j \neq SO_3 \\ &= M_{SO_3} \quad \text{for } j = SO_3 \end{aligned} \quad (2.2)$$

where

- g_j = normalized concentration of the j^{th} component in the glass (mass fraction)
- T_j = target value of the j^{th} component in the glass (mass fraction)
- M_{SO_3} = measured or estimated SO_3 value for the glass (mass fraction).

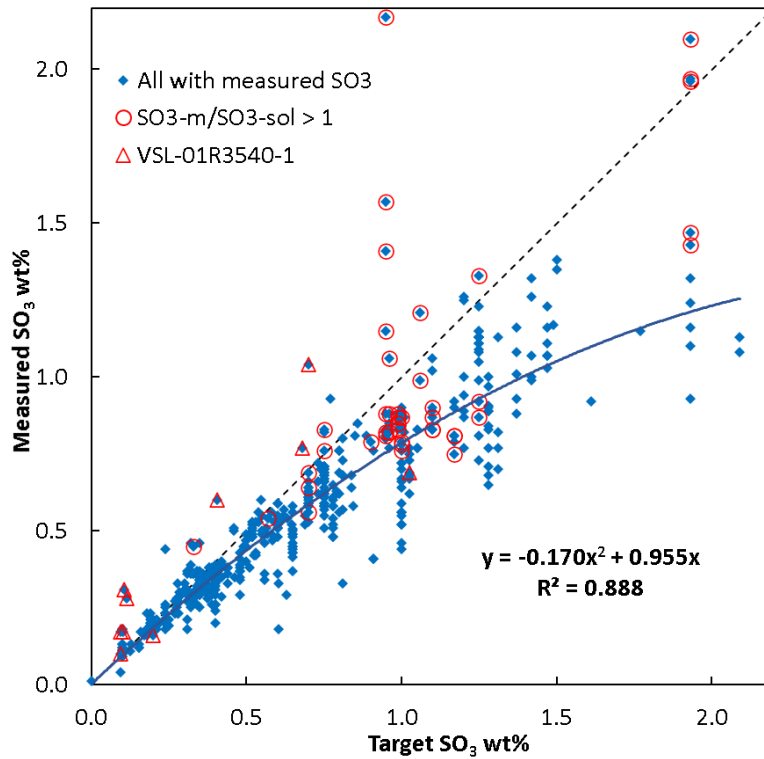


Figure 2.1. Measured versus Target SO₃ Concentrations (wt%) in 589 Glasses with Independently Measured SO₃ Concentration Data. The 54 Glasses Marked in Red Were Removed before Fitting Eq. (2.1). The solid curved line represents the fitted model from Eq. (2.1).

2.3 LAW Glass Data for Property Modeling

Table 2.2 summarizes the LAW glass property-composition data available for developing property-composition models, including the number of LAW glasses and number of property data points from each report that were (i) compiled in the ExcelTM database, including from the PNNL LAW Phase 1, 2, and 3 studies; and (ii) the 344 glasses directly imported from Muller et al. (2018) for k_{1208} only. Initially, the k_{1208} data were also compiled in the ExcelTM database, but later it was found that Muller et al. (2018) included additional data that were not reported in previous publications. So, it was decided to use the as-published k_{1208} data in that report for property-composition modeling. Muller et al. (2018) reported full glass compositions including measured SO₃ for all 344 glasses. Note that the PNNL LAW Phase 1, 2, and 3 studies did not involve k_{1208} testing. The properties listed in Table 2.2 (for which property-composition models were subsequently developed) include η_{1150} , ε_{1150} , PCT, VHT, $w_{SO_3}^{MT}$, and k_{1208} .

As noted in Section 2.1 and seen in Table 2.2, much of the property and composition data for LAW glasses were obtained from VSL reports. The experimental procedures used to (i) prepare and characterize the simulated LAW glasses and (ii) prepare and test glasses made from actual LAW samples are discussed in the reports listed in Table 2.2. Because the LAW glass data for property modeling were developed over many years at VSL and PNNL, sometimes using different methods and instruments, the

property data may be subject to additional sources of long-term (within-lab), short-term (within-lab), and lab-to-lab (i.e., reproducibility) uncertainties.

The following paragraphs discuss whether each property was measured directly or calculated from measured values. If applicable, the calculational process or formula for a given property is briefly discussed.

2.3.1 Viscosity and Electrical Conductivity

The η_{1150} and ε_{1150} values were calculated at 1150 °C from equations fit to viscosity and EC versus temperature data for each LAW glass. The majority of VSL reports do not provide the “original” viscosity and EC versus temperature data. Rather, most VSL reports provide the η_{1150} and ε_{1150} values obtained from fitting the temperature dependent data to the Vogel-Fulcher-Tammann (VFT) equation and calculating values of viscosity and EC at 1150 °C. The VFT equation is given by

$$\ln(\eta) \text{ or } \ln(\varepsilon) = E + \frac{F}{T_K - T_0}, \quad (2.3)$$

where E , F , and T_0 are temperature independent, and composition dependent coefficients and T_K is the temperature in K ($T(^{\circ}\text{C}) + 273.15$). For those LAW glasses with the original data but without reported η_{1150} and ε_{1150} values, (i) the VFT equation was fit to viscosity and EC versus temperature data and (ii) the fitted VFT equations were used to calculate estimated η_{1150} and ε_{1150} values. This latter process was performed for all PNNL data, and for some VSL data. Care was taken to include only data points that were not significantly impacted by phase changes or volatility.

Table 2.2. Summary of LAW Glass Database Showing Data Group, Report Number, Total Number of Glasses, and Number of Glasses with Values for Each Property

				Number of Glasses with Property Values										
				SO ₃ Solubility or Melter Tolerance										
				at 1150 °C (wt%)										
Group ^(a)	Report ^(b)	Reference	# of Glasses	η_{1150} (P)	ε_{1150} (S/cm)	PCT (g/m ²)	VHT		BS ^(d)	SR ^(e)	Bub ^(f)	MT ^(g)	3TS ^(h)	k_{1208} (in)
							r_a (g/m ² /d)	(P/F) (c)						
WTP	VSL-00R3501-1	Matlack et al. 2000	1	(i)		1								
WTP	VSL-01R3501-2	Matlack et al. 2001	4	2	2	2								
WTP	VSL-01R3560-2	Muller et al. 2001	121	58	54	69	30	33	62		3			
WTP	VSL-01R3540-1	Gan et al. 2001	15											
WTP	VSL-01R62N0-1, Rev. 2	Matlack et al. 2003	2	2	2									
WTP	VSL-03R3460-1	Muller and Pegg 2003a	122	48	48	52	48	48	66		1			
WTP	VSL-03R3460-2	Muller and Pegg 2003b	42	20	20	41	17	17	1					
WTP	VSL-03R3470-1	Muller and Pegg 2003c	6	2	2	2	4	4	2					
WTP	VSL-03R3470-2	Muller and Pegg 2003d	10	5	5	7	6	6						
WTP	VSL-03R3470-3	Muller and Pegg 2003e	2			1	2	2						
WTP	VSL-03R4470-1	Muller and Pegg 2003f	3	2	2	1	1	1						
WTP	VSL-04R4470-1	Muller et al. 2004	2			1	1	1						
WTP	VSL-04R4480-1	Rielley et al. 2004	60	21	21	60	52	57		56				
ORP	VSL-04R4960-1	Matlack et al. 2004a	17	1	1	2	3	3		14	1	1		
ORP	VSL-04R4970-1	Matlack et al. 2004b	3	3	3									
WTP	VSL-04R4980-1	Matlack et al. 2004c	1	1	1	1	1	1						
WTP	VSL-05R5460-1	Muller et al. 2005	30	2	2	26	12	12						
ORP	VSL-05R5900-1	Matlack et al. 2006b	6	6	6	6	6	6		4	4	1		
WTP	VSL-06R6480-1	Matlack et al. 2006c	8	8	8	8	8	8						
WTP	VSL-06R6480-2	Muller et al. 2006a	18	9	9	18	18	18						
WTP	VSL-06R6480-3	Muller et al. 2006b	26	14	14	25	25	26						
ORP	VSL-06R6900-1	Matlack et al. 2006b	45	36	36	40	37	44		36	15	2		
ORP	VSL-07R1130-1	Matlack et al. 2007a	78	37	37	45	65	78		41	13	4		
ORP	VSL-07R7480-1	Matlack et al. 2007b	9	9	9	9	9	9						
ORP	VSL-08R1410-1	Muller et al. 2008	56			15	55	56						
ORP	VSL-09R1510-2	Matlack et al. 2009a	50	31	31	46	44	45		40	2	3		
ORP	VSL-10R1790-1	Muller et al. 2010	32	9	9	32	27	31		30	1	2		

Table 2.2. Summary of LAW Glass Database Showing Data Group, Report Number, Total Number of Glasses, and Number of Glasses with Values for Each Property (cont.)

				Number of Glasses with Property Values										
				SO ₃ Solubility or Melter Tolerance at 1150 °C (wt%)										
				VHT									K-3	
Group ^(a)	Report ^(b)	Reference	# of Glasses	η_{1150} (P)	ε_{1150} (S/cm)	PCT (g/m ²)	r_a (g/m ² /d)	(P/F) (^(c))	BS ^(d)	SR ^(e)	Bub ^(f)	MT ^(g)	3TS ^(h)	(in)
ORP	VSL-13R2940-1	Muller et al. 2013	20	18	20	20	18	20		20				
ORP	VSL-14R3050-1	Muller et al. 2014	22	15	20	21	20	20		20				
ORP	VSL-15R3290-1	Muller et al. 2015c	24	11	11	10	15	15		20				
ORP	VSL-16R4000-1	Muller et al. 2016	38	32	32	32	38	38		28	7			
ORP	VSL-17R4140-1	Muller et al. 2017a	19	18	18	17	19	19		14	7			
ORP	VSL-17R4230-1	Muller et al. 2017b	17	15	15	15	16	16		10	3			
ORP	VSL-17R4250-1	Matlack et al. 2017a	11	9	9	6	9	9		11				
ORP	VSL-17R4330-1	Matlack et al. 2017b	8	8	8	5	8	8		8				
ORP	PNNL-26630	Russell et al. 2017	75	36	35	72	36	36					38	
ORP	VSL-18R4360-1 ⁽ⁱ⁾	Muller et al. 2018	9							8				
ORP	PNNL-28838, Rev. 2	Russell et al. 2020	41	41	41	41	39	41					41	
ORP	PNNL-29847	Lonergan et al. 2020	22	20	11	22	14	20					20	
ORP	VSL-18R4360-1 ^(k,l)	Muller et al. 2018												344
Total			1075	549	542	771	703	748	131	360	57	13	99	344

(a) Grouping of datasets as either WTP or ORP (Office of River Protection) (see text for description).

(b) All reports are Rev. 0 unless otherwise noted.

(c) P/F = pass/fail.

(d) BS = batch saturation. Excess sulfate is added to raw materials batch and melted to fabricate glass while saturating glass with sulfur.

(e) SR = saturation re-melting. Pre-melted glass is mixed with excess sulfate and melted to saturate glass.

(f) Bub = bubbling. Molten glass is bubbled with SO₂ and O₂ gas mixture to saturate glass.

(g) MT = melter tolerance. Maximum target SO₃ concentration (glass basis) in the melter feed without salt segregation.

(h) 3TS = Three-time saturation. Like the saturation re-melting method but re-melted three times to fully saturate glass.

(i) Blank cells indicate no data.

(j) This row for VSL-18R4360 includes nine glasses with properties other than K-3 corrosion, although two of the nine glasses do have K-3 corrosion values.

(k) This report includes both WTP and ORP glasses and some glasses that cannot be classified because they were not reported in previous publications.

(l) This report is listed a second time with the number of glasses having K-3 corrosion values = 344.

2.3.2 Product Consistency Test Response

As explained in Section 1.2, it is only necessary to model PCT_B^{NL} and PCT_{Na}^{NL} (g/m²). All measured PCT responses were measured using PCT Method A (ASTM 2014). All LAW glasses that had measured values of one of these PCT responses had measured values of both, so the number of data points are the same. Values of PCT_j^{NL} (where j = B or Na) were calculated via

$$PCT_j^{NL} = \frac{c_j / f_j}{A / LV}, \quad (2.4)$$

where

- c_j = elemental concentration of the j^{th} element in the PCT leachate (mg/L = g/m³)
- f_i = mass fraction of the j^{th} element in the glass (unitless)
- A = surface area of the crushed glass used in the PCT (m²)
- LV = volume of the leachate (deionized water) used in the PCT (m³).

A standard value of the A/LV ratio (2000 m⁻¹) is specified in the PCT method (ASTM 2014).

2.3.3 Vapor Hydration Test Response

The VHT data used in this report for modeling were collected from tests performed at 200 °C for nominal durations between 7 and 24 days. The pass/fail data were all taken from 24-day duration tests. Some of the reported numerical alteration depth data were taken from earlier times and linearly extrapolated to 24 days. However, these alteration depth/reaction rate data were ultimately not used in VHT response modeling. The VHT response modeled in this report is denoted P or F for pass or fail. VHT rate data given in this report and associated database were not directly measured, but were calculated via

$$r_a^{VHT} = \rho D / t, \quad (2.5)$$

where

- r_a^{VHT} = mean glass alteration rate over the test duration (g/m²/d)
- ρ = glass density (g/cm³)
- D = alteration depth/thickness (μm)
- t = test duration (d).

This equation assumes that the altered layer density is not appreciably different from the density of the glass when alteration layer thickness is measured instead of remaining glass thickness. Under this assumption, for a typical density of 2.65 g/cm³, a layer thickness of 453 microns in a 24-day VHT would correspond to a mean glass alteration rate of 50 g/m²/d (Piepel et al. 2007). This value of $D \leq 453$ μm was previously used as the VHT acceptance criteria (Kim and Vienna 2012).

2.3.4 Melter SO₃ Tolerance

The objective of melter SO₃ tolerance models (discussed in Section 7.0) is to predict the maximum SO₃ concentration that can be processed in the melter without forming segregated sulfate salt, referred to as the “melter SO₃ tolerance.” The segregated salt can cause potential problems associated with melter operation (Vienna et al. 2014). Vienna et al. (2014) showed that there is a good correlation between the melter SO₃ tolerance and SO₃ solubility at 1150 °C. Hence, SO₃ solubility data developed primarily from crucible scale tests can be used to predict the melter SO₃ tolerance that can only be obtained from costly melter tests. Values of SO₃ solubility or melter tolerance at 1150 °C for LAW glasses were determined using several different methods, as noted in Table 2.2. The methods are briefly described in the notes of Table 2.2, and in further detail in the reports listed in Table 2.2. Some SO₃ solubility data were extracted from figures in reports when data were not provided in a tabular format. The measured SO₃ solubility at 1150 °C values were obtained by (i) washing a LAW glass sample melted at 1150 °C, and (ii) chemical analysis via X-ray fluorescence (XRF) (for all VSL glasses) or inductively coupled plasma - optical emission spectrometry (ICP-OES) [for all PNNL glasses (Russell et al. 2017, 2020; Lonergan et al. 2020) and selected VSL glasses]. When both XRF and ICP-OES were used for some VSL samples, XRF results were used for consistency.

2.3.5 Data Subgroups

The 39 datasets with 1075 glasses in the LAW property-composition dataset (not including the additional data for k_{1208}) are classified as either WTP or ORP, as seen in Table 2.2. The WTP datasets include glass formulations with conservative waste loadings designed to ensure successful initial startup and operation of the plant. The WTP data were used to develop the models presented by Piepel et al. (2007), which did not include a model for k_{1208} . These models were used in the preliminary LAW GFA by Kim and Vienna (2012). The preliminary LAW GFA is planned to be implemented for commissioning and initial radioactive operations of the WTP LAW Facility. The ORP datasets include the glasses developed to generate the data and models needed to process the full range of LAW compositions at high waste loadings. Note that some reports that were published earlier than Piepel et al. (2007) also include ORP glasses. The dataset for k_{1208} from Muller et al. (2018) in Table 2.2 includes both WTP and ORP glasses, and there were some glasses that cannot be classified because they were not reported in any previous publications.

Figures in subsequent sections have the LAW glass compositions further identified into the following seven groups:

- WTP (lower-waste-loading glasses)
- ORP (high-waste-loading glasses, VSL studies)
- LP1.OL (high-waste-loading glasses, PNNL LAW Phase 1 outer layer)
- LP1.IL (high-waste-loading glasses, PNNL LAW Phase 1 inner layer)
- LP2.OL (high-waste-loading glasses, PNNL LAW Phase 2 outer layer)
- LP2.IL (high-waste-loading glasses, PNNL LAW Phase 2 inner layer)
- LP3 (high-waste-loading glasses, PNNL LAW Phase 3, same region for LAW Phase 2)

The WTP glasses are composed of seven sub-groups, discussed in Sections 2.1 to 2.7 of Piepel et al. (2007), but those sub-groups are not used in this report. The LP1.OL, LP1.IL, LP2.OL, LP2.IL, and LP3 groups represent five statistically designed studies conducted at PNNL from 2016 to 2020. The glass

compositional regions for LAW Phase 2 and Phase 3 (which were the same) were smaller than the glass compositional region for LAW Phase 1 (see Table 2.1). The LP1.OL, LP1.IL, LP2.OL, LP2.IL, and LP3 glasses are also ORP glasses (high waste loading) but are identified separately because they are from recent statistically designed studies for specific high-LAW-loading glass compositional regions of interest.

The LAW glass property-composition dataset includes data for actively designed glasses (by VSL) and statistically designed glasses (by PNNL and VSL). Actively designed glasses result from typical LAW glass formulation efforts with specific objectives, such as developing glass compositions for specific wastes with desired properties. Actively designed glasses sometimes occur in subsets over small composition subregions because of the iterative way a glass for a specific waste was formulated. Glass formulations early in this iterative process usually only have certain properties of primary interest measured. Then, all glass properties are measured when the final glass formulation for a specific waste is selected. Statistically designed glasses result from using statistical experimental design methods and software to well cover specified GCRs of interest.

For most LAW glass formulations, all properties were tested on glasses prepared from dry raw materials, melted in laboratory crucibles, and then quenched in air. Some CCC-treated glasses were tested for PCT and/or VHT. Those data were included in the database but were excluded from modeling. The ExcelTM database also includes a limited number of crucible glasses prepared from actual LAW samples or simulated liquid waste mixed with additive chemicals and minerals. Finally, properties were also tested on selected glasses produced from processing simulated melter feed (simulated waste plus additives) in various scaled melters.

2.3.6 Tabulation of All Data

The LAW glass property-composition dataset available for developing property-composition models of LAW glasses is summarized in Appendix A. Table A.1 lists the range of Glass #s (from 1 to 1075) associated with the data from each literature reference. Table A.2 displays the compositions of the 1075 glasses compiled from the literature, while Table A.3 lists the property values of these glasses (if they were measured) for all properties except k_{1208} . Table A.4 lists the normalized compositions of the 344 LAW glasses with k_{1208} values, which are listed in Table A.5. The glass compositions in Tables A.2 and A.4 are based on 20 components that include 19 components of potential interest for modeling and “Others” that consist of all remaining components. The LAW glass compositions in Tables A.2 and A.4 are normalized to sum to 1 using target concentrations for all components except SO_3 (which used measured or estimated concentrations, as discussed in Section 2.2). The Others component includes (i) minor components that are present in very low concentrations (CdO , NiO , PbO , etc.) and (ii) components that are present only in a very small number of glasses, although sometimes with high concentrations (La_2O_3 , SrO , etc.).

2.4 Subsets of LAW Glass Compositions Used to Evaluate Prediction Performance of and Validate Property-Composition Models

In subsequent sections of this report, property-composition models are developed, evaluated, and validated for each of the LAW glass properties discussed in Section 1.1. Because these models will be used to formulate LAW glasses with higher waste loadings and operate the WTP LAW Facility for such glasses, it is important to evaluate the predictive performance of the models for various subsets of LAW glasses, especially those with higher waste loadings (i.e., higher concentrations of Na_2O or SO_3).

Six subsets of the LAW glasses used to model various properties were chosen to evaluate the predictive performance of the LAW glass property-composition models. These subsets and the notations used to denote them are briefly described below.

- **WTP:** Older LAW glasses with lower waste loadings that were tested by VSL, which were used by Piepel et al. (2007) for property-composition modeling. This classification was assigned when the database of 1075 LAW glasses was compiled (see Section 2.3).
- **ORP:** Newer LAW glasses with higher waste loadings that were tested by VSL. This classification was assigned when the database of 1075 LAW glasses was compiled (see Section 2.3).
- **LP2OL:** LAW glasses that satisfy slightly expanded (described subsequently) versions of the PNNL Phase 2 OL (and Phase 3) constraints specified in Table 2.1. Hence, this subset of evaluation glasses includes the LP2.OL, LP2.IL, and LP3 glasses, as well as any other LAW glasses that satisfy the expanded Phase 2 OL constraints. Note that the glasses in this evaluation set have high Na₂O waste loadings.
- **LP123:** LAW glasses from PNNL Phases 1, 2, and 3.
- **HiNa₂O:** LAW glasses with high concentrations of Na₂O (≥ 0.21 mf).
- **HiSO₃:** LAW glasses with high concentrations of SO₃ (≥ 0.0085 mf).

For the LP2OL evaluation set, the SCCs and MCCs for the Phase 2 OL subregion were slightly expanded to accommodate changes from target glass compositions to normalized glass compositions calculated using measured (or estimated) SO₃ values. The SCCs (lower and upper limits of the components) for these constraints (in Table 2.1) were expanded by a relative 10%. Specifically, where L_i is the lower limit and U_i is the upper limit for the i^{th} component in the Phase 2 OL constraints, the expanded lower and upper limits were $0.9(L_i)$ and $1.1(U_i)$. As an example, the target range for Na₂O was 0.21 to 0.26 mf, with the expanded range 0.189 to 0.286 mf. The MCC constraints (NAlk, SO₃ solubility, SnO₂+ZrO₂, Al₂O₃+SnO₂+ZrO₂, and NAlk-ZrO₂-SnO₂-CaO) for the Phase 2 OL region listed in Table 2.1 had their limiting constant values decreased by 0.01 for lower limits and increased by 0.01 for upper limits. The limits for the η_{1150} constraints were not changed.

Finally, the numbers of LAW glasses in the six evaluation sets differ by glass property, because not all LAW glass properties were measured for every glass. Also, not all of these six subsets of evaluation glasses are distinct. That is, some glasses are in more than one evaluation set. The specific glasses in the six evaluation sets are identified in Appendix C and summarized in Sections 3.0 to 8.0, which discuss the data and models for each LAW glass property.

Ideally, glass property models would be validated by a dataset in the same composition region but that was not used to fit model parameters (called external validation). Due to the lack of data for some properties in the composition region intended for application and the highly non-linear property-composition responses, it was decided to validate the models using a model subset validation approach. Generally, this approach quantitatively validates the model form including terms selected for the model while allowing for the final model coefficients to be determined by the full set of available data appropriate for modeling a given property. The general approach is to combine all replicate glasses in a modeling subset of data then sort remaining data in order of property response values. Roughly one fifth of the data is selected by taking every fifth point for use in a validation set. The model is then fit to the replicate sets and 4/5ths of the remaining data. This model is used to predict the values for the remaining ~1/5th of the data. The removed data points are systematically changed from the 1st to 2nd to 3rd, etc. point in the set so that each non-near replicate glass is in one validation subset. The validation statistics for each validation subset are reported along with their averages.

2.5 Glass Composition for Example Calculations

Throughout the process of model development and reporting, it became necessary to define a reference glass composition. The reference mixture (REFMIX) glass was used. This reference glass composition was developed to represent an average of compositions in the glass property-composition database. Starting with the 1075 glasses listed in Appendix A, all replicate and near-replicate glasses were removed (leaving only one point for each replicate set) along with glass LAWA97S, which has no reported composition. This left 904 compositions. The average for each component concentration in the 904 glasses was taken and the composition was normalized to sum to precisely 1.000000 with six-digit rounding. Table 2.3 lists the 20-component composition of the REFMIX glass. For each recommended glass property-composition model, an example calculation was performed using the REFMIX glass composition. Additionally, property response trace plots (AKA spider plots) were generated for all property models based on the REFMIX composition.

Table 2.3. REFMIX Composition in Formats Used for Example Calculations and Response Trace Plots

REFMIX Composition	
Model Term	(mass fractions)
Al ₂ O ₃	0.075760
B ₂ O ₃	0.097257
CaO	0.052514
Cl	0.003376
Cr ₂ O ₃	0.002041
F	0.001348
Fe ₂ O ₃	0.029727
K ₂ O	0.012064
Li ₂ O	0.014802
MgO	0.016989
Na ₂ O	0.168395
P ₂ O ₅	0.003239
SO ₃	0.005542
SiO ₂	0.424565
SnO ₂	0.007587
TiO ₂	0.008034
V ₂ O ₅	0.007499
ZnO	0.031997
ZrO ₂	0.036219
Others	0.001045

3.0 Models Relating Normalized PCT Boron and Sodium Losses to Composition of LAW Glasses

This section documents the development, evaluation, and validation of property-composition models and corresponding uncertainty expressions for predicting the PCT_B^{NL} and PCT_{Na}^{NL} of LAW glasses. PCT values, as $\ln(PCT_B^{NL})$ and $\ln(PCT_{Na}^{NL})$, are modeled using a combination of full linear mixture (FLM) model, reduced linear mixture (RLM) model, partial quadratic mixture (PQM) model and ultimately bias corrected PQM model (bcPQM) as functions of LAW glass composition. Specification 2.2.2.17.2 in the WTP contract (DOE 2000) sets a 2 g/m² limit on PCT_B^{NL} , PCT_{Na}^{NL} , and PCT_{Si}^{NL} from LAW glasses. However, PCT_{Si}^{NL} was less than PCT_B^{NL} and PCT_{Na}^{NL} for all 703 of the simulated and actual LAW glasses having PCT responses of quenched samples. Because PCT_B^{NL} and PCT_{Na}^{NL} are higher than PCT_{Si}^{NL} , the WTP Project decided that only PCT_B^{NL} and PCT_{Na}^{NL} need be modeled (Piepel et al. 2007). The same reasoning is applicable here. The property-composition models and corresponding uncertainty expressions for $\ln(PCT_B^{NL})$ and $\ln(PCT_{Na}^{NL})$ presented in this section were developed and validated using composition and normalized PCT loss data collected for simulated and actual LAW glasses having PCT responses.

The 703 quenched simulated and actual LAW glass samples available for $\ln(PCT_B^{NL})$ and $\ln(PCT_{Na}^{NL})$ model development, evaluation, and validation are discussed in Section 3.1. Section 3.2 presents the model forms for $\ln(PCT_B^{NL})$ and $\ln(PCT_{Na}^{NL})$ that were investigated. Sections 3.3 and 3.4, respectively, summarize the results for the PCT_B^{NL} and PCT_{Na}^{NL} model forms investigated and the model forms ultimately recommended. Section 3.5 illustrates the calculation of $\ln(PCT_B^{NL})$ and $\ln(PCT_{Na}^{NL})$ predictions and the uncertainties in those predictions using selected models and corresponding uncertainty equations. Section 3.6 discusses the suitability of the recommended $\ln(PCT_B^{NL})$ and $\ln(PCT_{Na}^{NL})$ models for use by the WTP LAW Facility and presents model validity ranges. Appendix B discusses the statistical methods and summary statistics used to develop, evaluate, and validate the several model forms investigated, as well as statistical equations for quantifying the uncertainties in $\ln(PCT_B^{NL})$ and $\ln(PCT_{Na}^{NL})$ predictions.

3.1 Normalized PCT Loss Data from LAW Glasses Used for Model Development, Evaluation, and Validation

The data used to develop $\ln(PCT_B^{NL})$ and $\ln(PCT_{Na}^{NL})$ models as functions of LAW glass composition are discussed in Section 3.1.1. The approaches and data used for evaluating and validating the models are discussed in Sections 3.1.2 and 3.1.3.

3.1.1 Model Development Data for Normalized PCT Boron and Sodium Losses from LAW Glasses

The data available for developing property-composition models for PCT_B^{NL} and PCT_{Na}^{NL} consist of composition (adjusted as described in Section 2.2) and normalized PCT loss data from 703 quenched LAW glass samples. In addition, 68 glasses listed in Appendix A have measured normalized PCT loss data on CCC samples that were not used in model development. Instead, constraints are added to avoid glasses prone to significant changes in PCT response from CCC heat treatments. These glasses and their normalized compositions based on measured (or estimates of measured) SO₃ values are discussed in Section 2.0. The corresponding PCT_B^{NL} and PCT_{Na}^{NL} values are presented in Table A.3 of Appendix A.

3.1.1.1 Assessment of Available LAW Glasses with Boron and Sodium Normalized Losses from the PCT

The database of 703 quenched glasses with PCT_B^{NL} and PCT_{Na}^{NL} values contains statistically designed as well as actively designed glasses. Some actively designed glasses are outside the composition region covered by the majority of the LAW compositions. Such glasses are not ideal for inclusion in a modeling dataset because they can be influential when fitting models to data. Hence, it was decided to

- (i) graphically assess the 703 simulated and actual LAW glass compositions with PCT values and
- (ii) remove from the modeling dataset any compositions considered to be outlying or non-representative of LAW glasses of interest for the WTP LAW Facility.

Figure 3.1 displays plots of the mass fraction values for 19 “main components” plus the Others component (the sum of all remaining components) in the 703 LAW glasses with quenched glass PCT data. These 20 components (including Others) have sufficient ranges and distributions of mass fraction values to support separate model terms if so desired. Figure 3.2 displays similar plots for the remaining “minor components.” On each plot in Figure 3.1 and Figure 3.2, the x-axis represents the mass fraction values of a LAW glass component. The y-axis shows an index value representing each LAW glass composition, which aids in spreading out the data points to avoid over-plotting. The plotting symbols in Figure 3.1 and Figure 3.2 correspond to the seven groups of LAW glasses discussed in Section 2.3. For comparison purposes, the vertical lines in Figure 3.1 and Figure 3.2 represent the ranges over which the LAW glass components were varied in the PNNL (i) LAW Phase 1 outer-layer study (blue lines), (ii) Phase 2 outer-layer study (pink lines), and (iii) Phase 3 study (pink lines), as shown in Table 2.1. Phases 2 and 3 focused on LAW glasses with high Na_2O waste loadings, whereas Phase 1 explored a larger LAW GCR with higher waste loadings.

Figure 3.1 shows several of the 703 glasses have components with outlying mass fraction values compared to the remaining glasses and to the component ranges tested in the PNNL LAW Phase 1, Phase 2, and Phase 3 studies. Figure 3.2 shows what appear to be outliers for some “minor components,” but the values and ranges of those components are small and hence the glass compositions were not considered to be outliers. Table 3.1 lists the 11 LAW glasses excluded from the PCT modeling dataset, and the reason each glass was excluded. One glass (LAWPH3-06) was removed from modeling of PCT_B^{NL} due to a reported response of $< 0.3205 \text{ g/m}^2$. One glass (LAWC14) was removed from modeling PCT_{Na}^{NL} due to an anomalous PCT_{Na}^{NL} value compared to PCT_B^{NL} and was also found to be an influential outlier in $\ln[PCT_{Na}^{NL}]$ modeling. Finally, one glass (New-OL-80309) was identified as an extreme outlier for all candidate bcPQMs, which significantly altered the bias correction slope and goodness of fit and thus was excluded from modeling dataset for both $\ln[PCT_B^{NL}]$ and $\ln[PCT_{Na}^{NL}]$. These 14 glasses were considered non-representative and were excluded from the PCT modeling dataset.

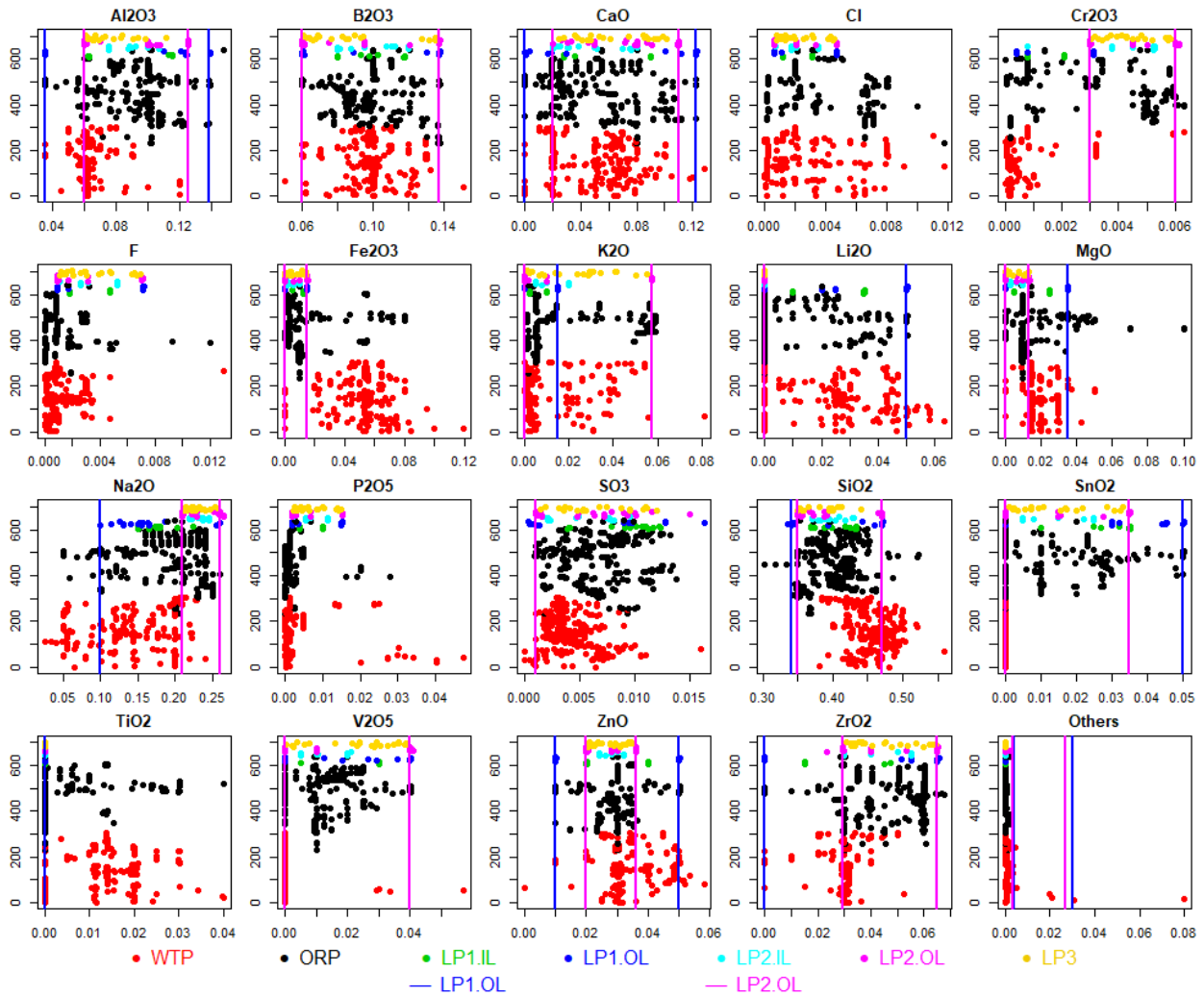


Figure 3.1. Distributions of 20 Main Components (in mass fractions) for 703 LAW Glass Compositions with Data for normalized PCT Losses of B or Na. The vertical lines (when present) represent the lower and upper limits for each component from the PNNL LAW Phase 1 (blue lines) and Phase 2 (pink lines) outer-layer studies (see Table 2.1). In cases where two limits are the same, pink lines over-plot the blue lines.

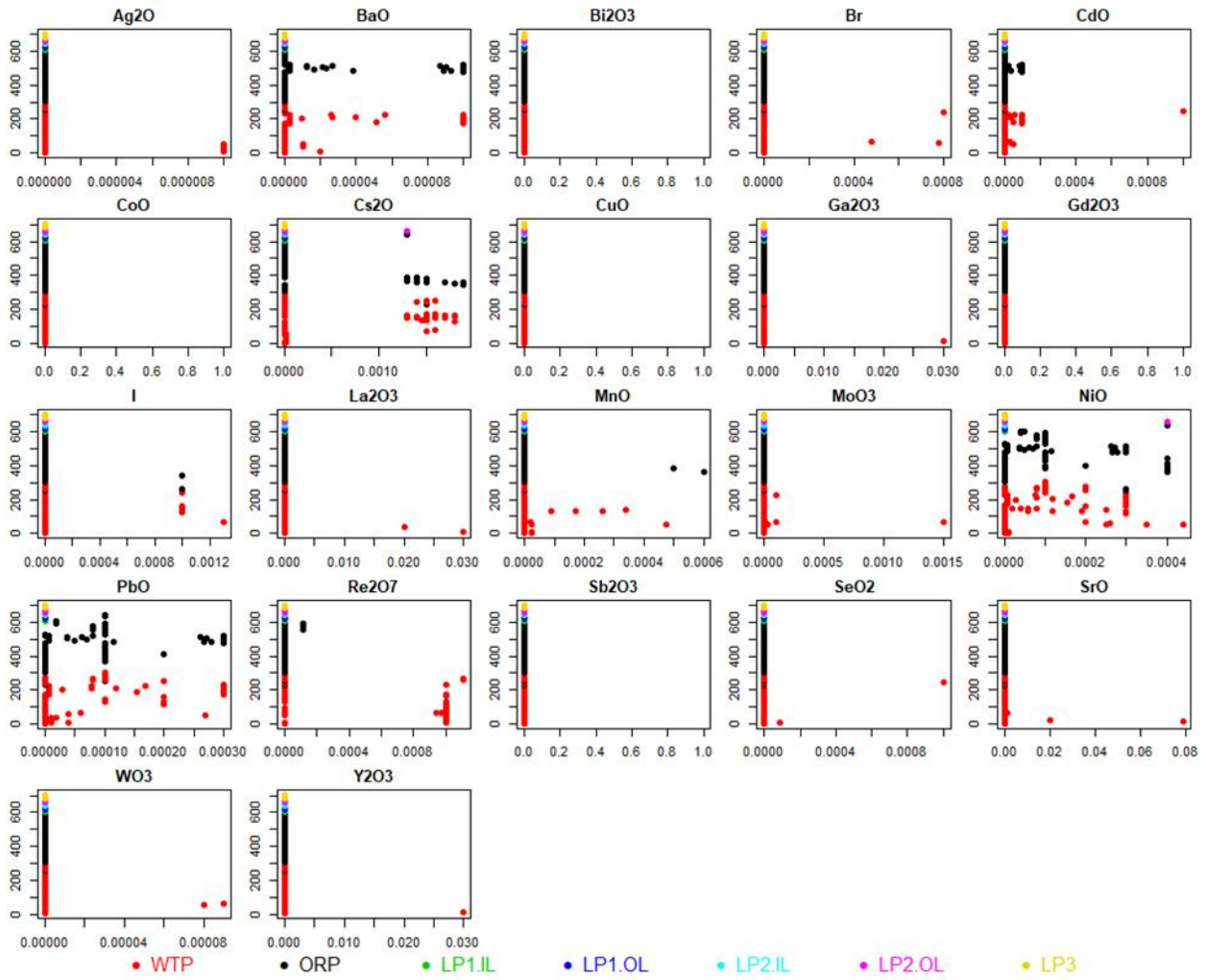


Figure 3.2. Distributions of 22 Minor Components (in mass fractions) for 703 LAW Glass Compositions with Data for normalized PCT Losses of B or Na.

Table 3.1. Fourteen LAW Glasses with Non-representative Compositions Excluded from the Modeling Datasets for Normalized PCT Losses of B and Na

Glass#	Glass ID	Reason Glass Excluded from PCT_B^{NL} and PCT_{Na}^{NL} Modeling Datasets ^(a)
739	ORPLA28	MgO>0.06 (=0.07015) mf
740	ORPLA29	MgO>0.06 (=0.10022) mf
742	ORPLA31	MgO>0.06 (=0.07015) mf
743	ORPLA32	MgO>0.06 (=0.10022) mf
12	LAWA46	Others > 0.02 (= 0.03103) mf
13	LAWA47	Others > 0.02 (= 0.03103) mf
14	LAWA48	Others > 0.02 (= 0.03103) mf
20	LAWA64	Others > 0.02 (= 0.07985) mf
25	LAWA85	Others > 0.02 (= 0.02096) mf
26	LAWA86	Others > 0.02 (= 0.02096) mf
43	LAWABP1	Others \geq 0.02 (= 0.020001) mf
67	LAWC14	Had an outlying PCT_{Na}^{NL} value (compared to PCT_B^{NL} and predicted PCT_{Na}^{NL}) and so was not used for PCT_{Na}^{NL} modeling
1059	LAWPH3-06	Had a reported PCT_B^{NL} value of < 0.3205 g/m ² and so was not used for PCT_B^{NL} modeling
977	New-OL-80309	Was identified as an extreme outlier for all candidate bcPQMs, which significantly altered the bias correction slope and goodness of fit

(a) mf = mass fraction

The combined PCT boron and sodium loss database, after removing outliers, contains 691 glasses. A total of 14 glasses are listed in Table 3.1. Thirteen glasses were removed from each of the PCT_j^{NL} modeling datasets, leaving 690 glasses available for modeling each PCT_j^{NL} . Twelve of the 14 glasses in Table 3.1 were common to both datasets (Glass#'s 12, 13, 14, 20, 25, 26, 43, 739, 740, 742, 743, and 977). Glass# 67 was removed from PCT_{Na}^{NL} dataset and not from the PCT_B^{NL} dataset while glass# 1059 was removed the PCT_B^{NL} dataset and not from the PCT_{Na}^{NL} dataset. Only glasses removed from both datasets were removed from the overall PCT database. Figure 3.3 and Figure 3.4 (corresponding to Figure 3.1 and Figure 3.2, respectively) show plots of component distributions after the 12 outlying and non-representative glasses were removed from the PCT dataset containing 703 glasses. Figure 3.3 shows that, for the remaining 691 LAW glasses, all 19 LAW glass “main components” have sufficient ranges and distributions of values within those ranges to support terms for modeling $\ln(PCT_B^{NL})$ and $\ln(PCT_{Na}^{NL})$. Figure 3.4 confirms than none of the “minor components” have sufficient ranges and distributions of values within their ranges to support model terms for those components. Based on Figure 3.3 and Figure 3.4, it was decided to use 20 components for initial PCT_B^{NL} and PCT_{Na}^{NL} modeling work. These components are Al₂O₃, B₂O₃, CaO, Cl, Cr₂O₃, F, Fe₂O₃, K₂O, Li₂O, MgO, Na₂O, P₂O₅, SO₃, SiO₂, SnO₂, TiO₂, V₂O₅, ZnO, ZrO₂, and Others (the sum of all remaining components); the same components used for modeling other properties.

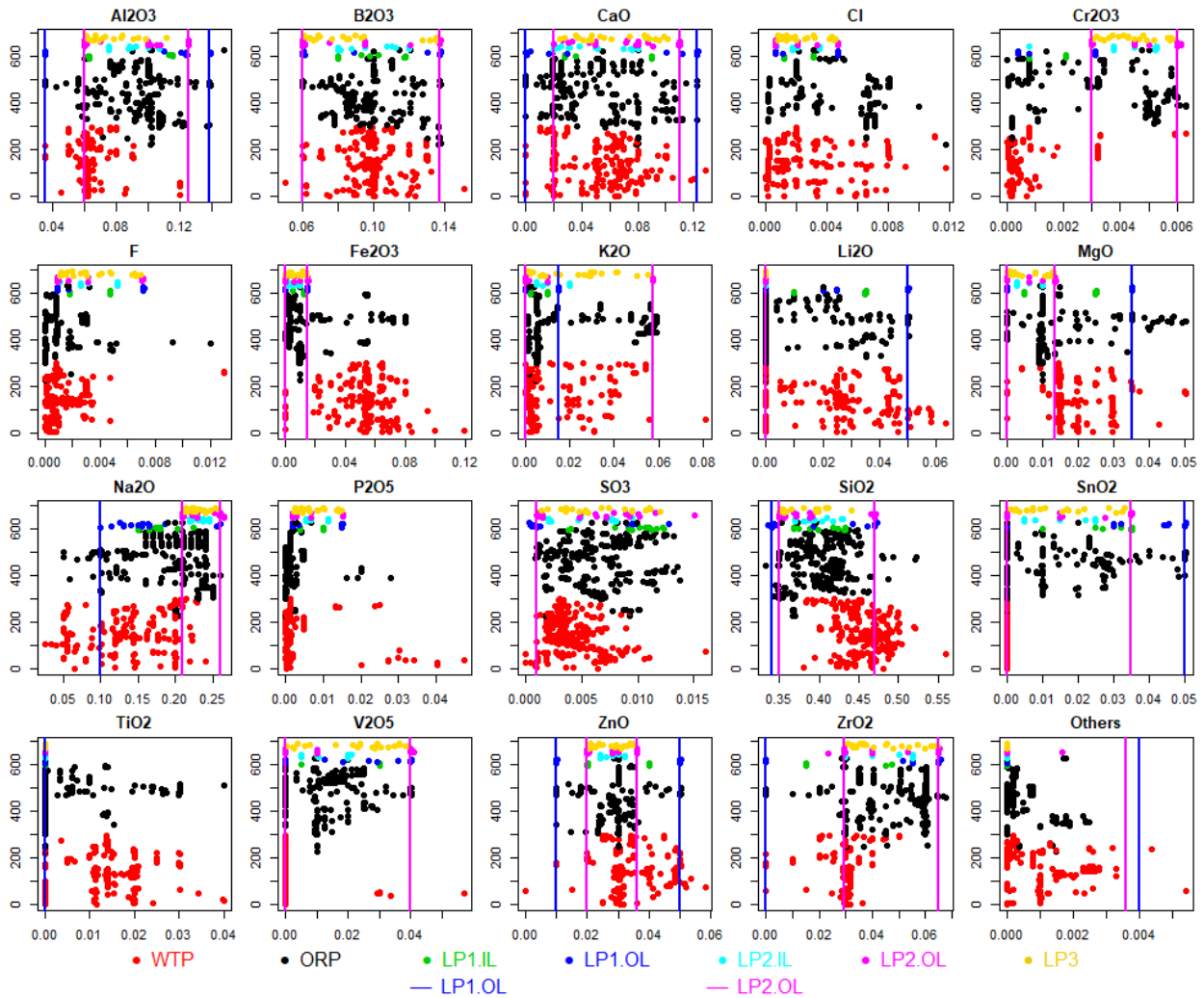


Figure 3.3. Distributions of 20 Main Components (in mass fractions) for 691 LAW Glass Compositions with Data for Normalized PCT Losses of B or Na that Remain after Excluding the 12 Glasses in Table 3.1. The vertical lines (when present) represent the lower and upper limits for each component from the PNNL LAW Phase 1 (blue lines) and Phase 2 (pink lines) outer-layer studies (see Table 2.1). In cases where two limits are the same, pink lines over-plot the blue lines.

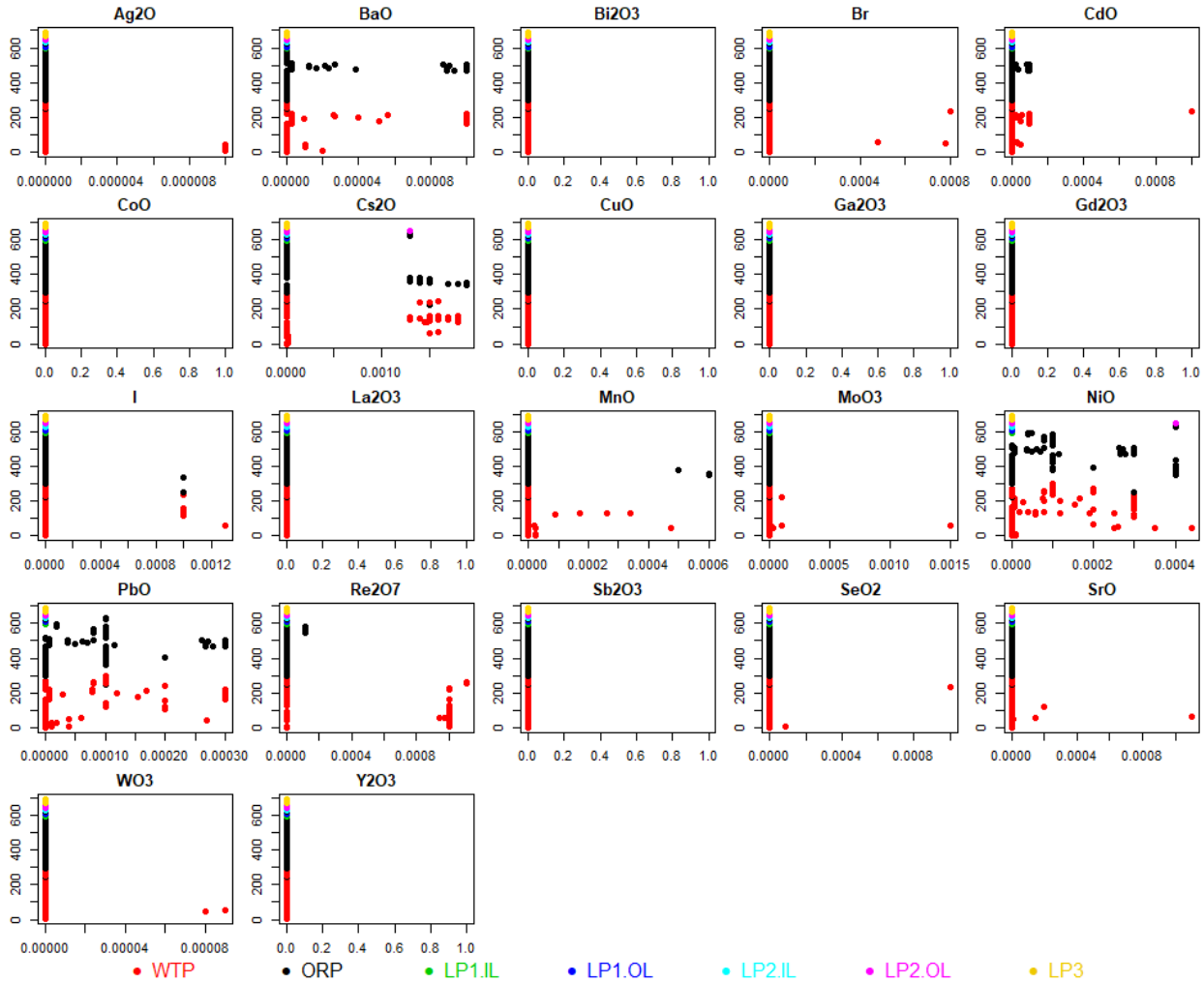


Figure 3.4. Distributions of 22 Minor Components (in mass fractions) for 691 LAW Glass Compositions with Data for Normalized PCT Losses of B or Na that Remain after Excluding the 12 Glasses in Table 3.1.

Figure 3.5 shows a scatterplot matrix of the 691 glasses remaining in the PCT modeling dataset after removing the 12 non-representative compositions. High correlations between pairs of components can create problems with accurately estimating the effect of a component on a response, so pairwise correlation coefficients were calculated. These can vary from -1.0 (perfect negative correlation) to 0 (no correlation) to 1.0 (perfect positive correlation). The only component pairs with correlations larger (in absolute value) than 0.60 were Li_2O and Na_2O , with a correlation of -0.8634 , and Na_2O and SiO_2 , with a correlation -0.6061 . See Section 9.7 for further discussion of these highly correlated pairs. Two other pairs of components, Al_2O_3 and SiO_2 , and Fe_2O_3 and TiO_2 , have correlations of -0.5676 and 0.5794 , respectively. High pairwise correlations can make it difficult for regression methods to properly separate the effects of the components on the response variable (e.g., PCT_B^{NL} or PCT_{Na}^{NL}) and inflate prediction uncertainties. Thus, these high pairwise correlations need to be kept in mind in developing and applying LAW glass property-composition models for PCT_B^{NL} and PCT_{Na}^{NL} .

3.1.1.2 Modeling Dataset for the PCT

Table A.3 in Appendix A lists the Glass ID, as well as PCT_B^{NL} and PCT_{Na}^{NL} values, for the 691 remaining simulated and actual LAW glasses used for model development. The PCT_B^{NL} and PCT_{Na}^{NL} values for non-representative (see Table 3.1) and CCC heat treated glasses excluded from the 691-glass modeling dataset are marked with an asterisk in Table A.3. The compositions for these 691 LAW glasses are included in Table A.2. The glass compositions are the normalized mass fractions (mf) of the 20 components previously identified as having sufficient data to support a separate model term if needed. These components are Al_2O_3 , B_2O_3 , CaO , Cl , Cr_2O_3 , F , Fe_2O_3 , K_2O , Li_2O , MgO , Na_2O , P_2O_5 , SO_3 , SiO_2 , SnO_2 , TiO_2 , V_2O_5 , ZnO , ZrO_2 , and Others. The mass fraction values of the 20 components shown in Table A.2 were normalized so that they sum to precisely 1.000000 for each of the glasses (see Section 2.2).

Section 3.2.2 discusses how the PCT_B^{NL} and PCT_{Na}^{NL} values were calculated from measured elemental releases and target glass compositions. The values of PCT_B^{NL} and PCT_{Na}^{NL} in Table A.3 for the 691 glasses in the modeling dataset range from 0.08 to 17.84 g/m² and 0.10 to 13.41 g/m², to two decimal places, respectively.

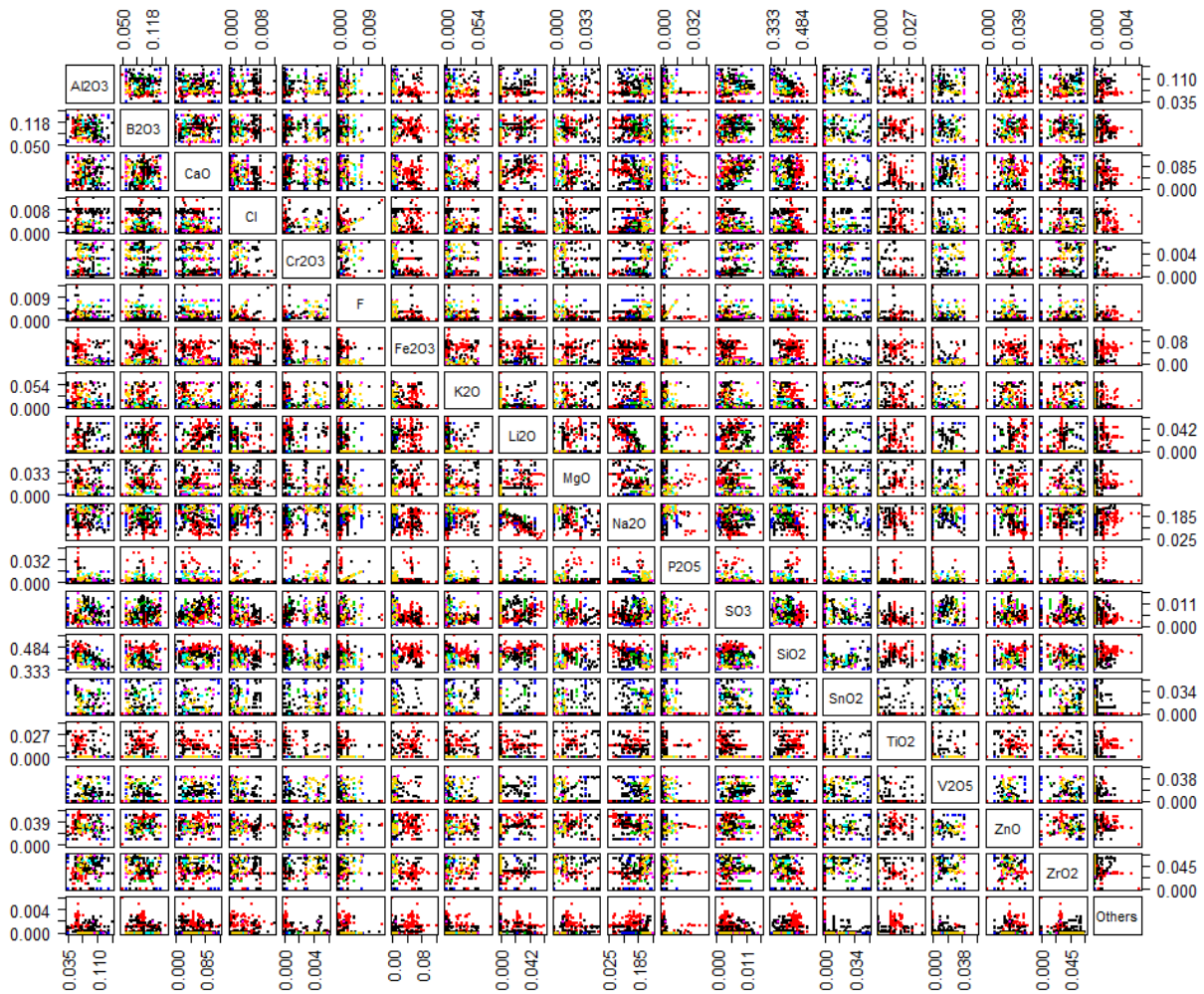


Figure 3.5. Scatterplot Matrix of 20 Components (mass fractions) for 691 LAW Glasses with Data for Normalized PCT Losses (g/m^2) of B and Na that Remain after Excluding the 12 Glasses in Table 3.1

Of the 691 simulated and actual LAW glasses in the PCT modeling dataset, 40 had PCT_B^{NL} and 32 had PCT_{Na}^{NL} values that exceeded the limit of 2 g/m^2 given in Specification 2.2.2.17.2 of the WTP contract. It is desirable to have some glasses in the modeling dataset that have PCT_B^{NL} and PCT_{Na}^{NL} ranging from somewhat below to somewhat above the limit. This allows for more confident use of models in discerning between glasses with acceptable and unacceptable PCT_B^{NL} and PCT_{Na}^{NL} values. However, glass formulations that have PCT_B^{NL} and PCT_{Na}^{NL} values far beyond the limit may not be desirable for model development, because using such glasses could adversely affect model prediction performance for the majority of the glasses. For this reason, dropping from the modeling dataset a few glasses with the highest PCT_B^{NL} and PCT_{Na}^{NL} values was investigated. However, comparing model fits with and without these sets of glasses did not notably change the predictive performance of models for the remaining glasses. Hence, the high normalized PCT losses were outliers but not influential. This conclusion, along with the need to have glasses with higher normalized PCT losses in the modeling dataset, led to the decision not to drop any LAW glasses from the PCT modeling dataset because of “too-large” normalized PCT losses.

3.1.1.3 Replicate and Near-Replicate PCT Data on LAW Glasses

The changes to the LAW glass compositions caused by the renormalization associated with using measured (or estimates of measured) SO_3 values (see Section 2.2) resulted in some replicate glasses not having exactly equal normalized compositions. Such compositions are referred to as near-replicates. For ease of discussion, henceforth both replicates and near-replicates are referred to as replicates.

Table 3.2 lists the replicate sets of LAW glasses in the PCT modeling dataset and the corresponding PCT_B^{NL} values. Table 3.3 lists the replicate sets of LAW glasses in the PCT modeling dataset and the corresponding PCT_{Na}^{NL} values. Table 3.2 and Table 3.3 also list estimates of (i) percent relative standard deviations (%RSDs) [calculated using PCT_B^{NL} and PCT_{Na}^{NL} values in original g/m^2 units] and (ii) standard deviations (SDs) [calculated using $\ln(PCT_B^{NL})$ and $\ln(PCT_{Na}^{NL})$ values in $\ln(\text{g/m}^2)$ units] for each replicate set. Table 3.2 and Table 3.3 also list pooled estimates of %RSD and SD calculated over all the replicate sets. A pooled %RSD or SD combines the separate %RSD or SD estimates from each replicate set, so that a more precise combined estimate of the %RSD or SD is obtained. These pooled %RSDs and SDs include uncertainties due to fabricating glasses, performing the PCT, and chemically analyzing leachates to determine elemental (and then normalized) losses. The pooled SDs in $\ln(\text{g/m}^2)$ units are 0.232 for $\ln(PCT_B^{NL})$ and 0.185 for $\ln(PCT_{Na}^{NL})$. The pooled %RSDs in percentage units are 22.2 for PCT_B^{NL} and 17.9 for PCT_{Na}^{NL} . The pooled SDs (0.232 and 0.185) and pooled %RSDs (22.2 and 17.9) in Table 3.2 and Table 3.3 indicate there is approximately a 20% total relative uncertainty in the PCT_B^{NL} and PCT_{Na}^{NL} values over the replicate glasses.

Table 3.2. Uncertainty in Normalized PCT Losses (g/m²) of B for Replicate and Near-Replicate Sets of LAW Glasses

Replicate Set Glass #s	Replicate Glass IDs	Replicate Set PCT_B^{NL} (g/m ²)	%RSD ^(a)	SD [ln(g/m ²)]	RepSet Number
268	A88Si+15	1.240	50.76	0.5312	1
294	WVE-G-108A	0.585			
269	A88Si-15	0.325	5.66	0.0566	2
295	WVE-G-27D	0.300			
273	C22Si+15	0.635	22.60	0.2280	3
303	WVD-G-25A	0.460			
274	C22Si-15	0.465	33.94	0.3462	4
304	WVC-G-107B	0.285			
993	EWG-LAW-Centroid-1	0.402	0.71	0.0071	5
995	EWG-LAW-Centroid-2	0.398			
4	A100-G-115A	0.480	11.24	0.1151	6
123	A100-G-115A	0.485			
296	WVB-G-124B	0.425			
427	LAWA102R2	0.380			
39	LAWA102S	0.275	31.09	0.3161	8
390	LAWA102R1	0.430			
315	LAWA126	0.598	5.89	0.0590	12
414	AP-101 Actual	0.650			
280	A2-AP101(LAWA126)	0.780	22.00	0.2218	13
426	WVM-G-142C	0.570			
318	LAWA127R1	0.334	6.27	0.0628	14
319	LAWA127R2	0.365			
538	EWV-G-89B	1.060	10.00	0.1002	21
737	ORPLA26	0.920			
9	LAWA44	0.370	26.42	0.2673	24
266	LAWA44(Crucible)	0.540			
28	LAWA88	0.435	31.75	0.3149	34
389	LAWA88R1	0.815			
413	AW-101 Actual	0.570			
267	A88AP101R1	0.685	34.71	0.3544	35
293	WVF-G-21B	0.415			
227	LAWB83	0.305	19.23	0.1908	40
229	LAWB84	0.340			
284	B1-AZ101(LAWB83)	0.390			
299	WVJ-G-109D	0.245			
415	AZ-101 Actual	0.260			

Table 3.2. Uncertainty in Normalized PCT Losses (g/m²) of B for Replicate and Near-Replicate Sets of LAW Glasses, cont.

Replicate Set Glass #s	Replicate Glass IDs	Replicate Set PCT_B^{NL} (g/m ²)	%RSD(a)	SD [ln(g/m ²)]	RepSet Number
311	LAWB88	0.195			
416	AZ-102 Actual	0.200	6.45	0.0636	41
435	AZ-102 Surrogate	0.220			
270	LAWB96	0.275	3.75	0.0376	42
431	GTSD-1126	0.290			
442	LAWC100	0.525			
443	LAWC100R1	0.840	27.42	0.3011	43
447	WVY-G-95A	0.920			
68	LAWC15	0.329	4.37	0.0438	44
418	AN-107 Actual	0.350			
5	C100-G-136B	0.368			
125	C100-G-136B	0.368			
248	C21REV2	0.345	4.60	0.0462	45
437	LAWC21	0.330			
438	LAWC21Rev2	0.350			
419	AN-102 Actual LC Melter	0.210	24.96	0.2522	46
420	AN-102 Actual	0.300			
75	LAWC22	0.518			
249	C22AN107	0.570			
271	LAWC22(Crucible)	0.480	17.09	0.1925	47
272	C22AN107	0.570			
279	C1-AN107(LAWC22)	0.515			
436	12S-G-85C	0.340			
260	LAWC31	0.275	9.61	0.0963	49
305	WVH-G-57B	0.240			
289	C2-AN102C35	0.340	2.05	0.0205	50
440	GTSD-1437	0.350			
456	LAWCrP1	0.276	1.77	0.0177	51
457	LAWCrP1R	0.283			
458	LAWCrP2	0.303	41.88	0.4318	54
459	LAWCrP2R	0.558			
460	LAWCrP3	0.285	19.47	0.1959	55
461	LAWCrP3R	0.376			
462	LAWCrP4	0.436	0.16	0.0016	56
463	LAWCrP4R	0.437			
451	LAW7H	0.535	82.76	0.9480	66
624	FWV-G-63B	0.140			
331	LAWM1	0.075	12.86	0.1289	69
383	LAWM53	0.090			

Table 3.2. Uncertainty in Normalized PCT Losses (g/m²) of B for Replicate and Near-Replicate Sets of LAW Glasses, cont.

Replicate Set Glass #s	Replicate Glass IDs	Replicate Set PCT_B^{NL} (g/m ²)	%RSD(a)	SD [ln(g/m ²)]	RepSet Number
342	LAWM12	14.850	12.92	0.1295	70
385	LAWM55	17.835			
365	LAWM35	5.265	22.81	0.2301	71
386	LAWM56	7.290			
380	LAWM50	0.325	4.22	0.0422	72
381	LAWM51	0.345			
339	LAWM9	0.105	39.01	0.4005	73
384	LAWM54	0.185			
797	LORPM28R1	3.845	2.55	0.0255	78
798	LORPM28R1	3.709			
846	ORLEC12	0.635	19.66	0.1978	85
865	OWV-G-144E	0.840			
848	ORLEC14	0.475	7.86	0.0786	86
887	QWV-G-107B	0.425			
850	ORLEC16	0.435	8.41	0.0842	87
888	PWV-G-130C	0.490			
853	ORLEC19	0.330	7.12	0.0713	88
890	QWV-G-29C	0.365			
856	ORLEC22	0.280	7.19	0.0720	89
891	QWV-G-75B	0.310			
862	ORLEC26	0.365	36.08	0.3689	91
867	OWV-G-109B	0.615			
863	ORLEC27	0.680	48.51	0.5056	92
869	PWV-G-43E	1.390			
864	ORLEC28	0.510	28.28	0.2867	93
871	PWV-G-93A	0.765			
877	ORLEC33	0.740	1.94	0.0194	94
903	RWV-G-9C	0.720			
878	ORLEC34	0.900	5.29	0.0530	95
904	RWV-G-48D	0.970			
893	ORLEC44	0.490	24.47	0.2471	96
905	RWV-G-79C	0.695			
895	ORLEC46	0.345	25.94	0.2624	97
906	RWV-G-120D	0.500			
897	ORLEC48R	0.275	9.59	0.0960	98
907	SWV-G-17A	0.315			
751	ORPLA38-1	0.730	12.78	0.1281	102
767	J10-G-24B	0.875			
589	ORPLC2	1.120	30.66	0.3115	106
591	ORPLC3	1.740			

Table 3.2. Uncertainty in Normalized PCT Losses (g/m²) of B for Replicate and Near-Replicate Sets of LAW Glasses, cont.

Replicate Set Glass #s	Replicate Glass IDs	Replicate Set PCT_B^{NL} (g/m ²)	%RSD(a)	SD [ln(g/m ²)]	RepSet Number
595	ORPLC5	0.850	16.23	0.1630	108
620	S10-G-101B	0.675			
597	ORPLD1	0.660	25.10	0.2357	109
622	T10-G-16A	0.345			
997	LAW-ORP-LD1(1)	0.467			
999	LAW-ORP-LD1(2)	0.424			
1035	LP2-OL-07	0.437			
732	Z10-G-60C	0.625	17.12	0.1721	110
733	10A-G-53C	0.490			
766	ORPLG27	0.665	23.50	0.2372	114
768	I10-G-135A	0.930			
1022	LP2-IL-10	0.441	4.31	0.0429	116
1028	LP2-IL-16	0.486			
1031	LP2-OL-02	0.469			
1049	LP2-OL-21	0.451			
1034	LP2-OL-05	0.160	4.29	0.0429	117
1038	LP2-OL-10-MOD	0.170			
1065	LAWPH3-12	1.360	9.60	0.0961	118
1066	LAWPH3-12-2	1.558			
1071	LAWPH3-17	0.532	7.43	0.0744	119
1072	LAWPH3-17-2	0.591			
Pooled Over 58 Replicate Sets with 78 total DF^(b)			22.1812	0.2317	

(a) %RSD = $100 \times (\text{Standard Deviation} / \text{Mean})$
(b) DF = degrees of freedom

Table 3.3. Uncertainty in Normalized PCT Losses (g/m²) of Na for Replicate and Near-Replicate Sets of LAW Glasses

Replicate Set Glass #s	Replicate Glass IDs	Replicate Set PCT_{Na}^{NL} (g/m ²)	%RSD ^(a)	SD [ln(g/m ²)]	RepSet Number
268	A88Si+15	1.000	45.27	0.4692	1
294	WVE-G-108A	0.515			
269	A88Si-15	0.325	9.27	0.0929	2
295	WVE-G-27D	0.285			
273	C22Si+15	0.830	40.56	0.4173	3
303	WVD-G-25A	0.460			
274	C22Si-15	0.345	19.87	0.2000	4
304	WVC-G-107B	0.260			
993	EWG-LAW-Centroid-1	0.524	0.40	0.0040	5
995	EWG-LAW-Centroid-2	0.527			
4	A100-G-115A	0.458	4.24	0.0429	6
123	A100-G-115A	0.450			
296	WVB-G-124B	0.415			
427	LAWA102R2	0.440			
39	LAWA102S	0.220	35.05	0.3580	8
390	LAWA102R1	0.365			
315	LAWA126	0.524	15.18	0.1524	12
414	AP-101 Actual	0.650			
280	A2-AP101(LAWA126)	0.560	5.24	0.0524	13
426	WVM-G-142C	0.520			
318	LAWA127R1	0.342	2.24	0.0224	14
319	LAWA127R2	0.353			
538	EWV-G-89B	0.950	14.35	0.1440	21
737	ORPLA26	0.775			
9	LAWA44	0.360	18.74	0.1885	24
266	LAWA44(Crucible)	0.470			
28	LAWA88	0.425	20.99	0.2227	34
389	LAWA88R1	0.650			
413	AW-101 Actual	0.590			
267	A88AP101R1	0.585	32.75	0.3336	35
293	WVF-G-21B	0.365			
227	LAWB83	0.265	8.89	0.0921	40
229	LAWB84	0.280			
284	B1-AZ101(LAWB83)	0.265			
299	WVJ-G-109D	0.220			
415	AZ-101 Actual	0.250			

Table 3.3. Uncertainty in Normalized PCT Losses (g/m²) of Na for Replicate and Near-Replicate Sets of LAW Glasses, cont.

Replicate Set Glass #s	Replicate Glass IDs	Replicate Set PCT_{Na}^{NL} (g/m ²)	%RSD(a)	SD [ln(g/m ²)]	RepSet Number
311	LAWB88	0.160			
416	AZ-102 Actual	0.160	13.32	0.1288	41
435	AZ-102 Surrogate	0.200			
270	LAWB96	0.285			
431	GTSD-1126	0.280	1.25	0.0125	42
442	LAWC100	0.435			
443	LAWC100R1	0.755	29.30	0.3281	43
447	WVY-G-95A	0.780			
68	LAWC15	0.336			
418	AN-107 Actual	0.420	15.71	0.1578	44
5	C100-G-136B	0.405			
125	C100-G-136B	0.349			
248	C21REV2	0.360	5.96	0.0577	45
437	LAWC21	0.360			
438	LAWC21Rev2	0.360			
419	AN-102 Actual LC Melter	0.260			
420	AN-102 Actual	0.350	20.87	0.2102	46
75	LAWC22	0.469			
249	C22AN107	0.555			
271	LAWC22(Crucible)	0.435			
272	C22AN107	0.555	18.29	0.2003	47
279	C1-AN107(LAWC22)	0.530			
436	12S-G-85C	0.330			
260	LAWC31	0.315			
305	WVH-G-57B	0.245	17.68	0.1777	49
289	C2-AN102C35	0.375			
440	GTSD-1437	0.370	0.95	0.0095	50
456	LAWCrP1	0.326			
457	LAWCrP1R	0.328	0.43	0.0043	51
458	LAWCrP2	0.328			
459	LAWCrP2R	0.519	31.89	0.3245	54
460	LAWCrP3	0.326			
461	LAWCrP3R	0.424	18.48	0.1859	55
462	LAWCrP4	0.409			
463	LAWCrP4R	0.437	4.68	0.0468	56
451	LAWE7H	0.515			
624	FWV-G-63B	0.245	50.24	0.5253	66

Table 3.3. Uncertainty in Normalized PCT Losses (g/m²) of Na for Replicate and Near-Replicate Sets of LAW Glasses, cont.

Replicate Set Glass #s	Replicate Glass IDs	Replicate Set PCT_{Na}^{NL} (g/m ²)	%RSD(a)	SD [ln(g/m ²)]	RepSet Number
331	LAWM1	0.145	5.05	0.0505	69
383	LAWM53	0.135			
342	LAWM12	8.045	24.82	0.2508	70
385	LAWM55	11.470			
365	LAWM35	3.315	27.15	0.2749	71
386	LAWM56	4.890			
380	LAWM50	0.315	9.43	0.0944	72
381	LAWM51	0.360			
339	LAWM9	0.255	22.50	0.2269	73
384	LAWM54	0.185			
797	LORPM28R1	2.094	1.01	0.0101	78
798	LORPM28R1	2.124			
846	ORLEC12	0.605	0.58	0.0058	85
865	OWV-G-144E	0.610			
848	ORLEC14	0.480	1.46	0.0146	86
887	QWV-G-107B	0.490			
850	ORLEC16	0.435	1.61	0.0161	87
888	PWV-G-130C	0.445			
853	ORLEC19	0.365	0.96	0.0096	88
890	QWV-G-29C	0.370			
856	ORLEC22	0.390	2.67	0.0267	89
891	QWV-G-75B	0.405			
862	ORLEC26	0.445	10.31	0.1033	91
867	OWV-G-109B	0.515			
863	ORLEC27	0.640	27.21	0.2756	92
869	PWV-G-43E	0.945			
864	ORLEC28	0.510	9.69	0.0970	93
871	PWV-G-93A	0.585			
877	ORLEC33	0.550	3.29	0.0329	94
903	RWV-G-9C	0.525			
878	ORLEC34	0.680	5.50	0.0550	95
904	RWV-G-48D	0.735			
893	ORLEC44	0.520	13.53	0.1357	96
905	RWV-G-79C	0.630			
895	ORLEC46	0.405	20.20	0.2034	97
906	RWV-G-120D	0.540			

Table 3.3. Uncertainty in Normalized PCT Losses (g/m²) of Na for Replicate and Near-Replicate Sets of LAW Glasses, cont.

Replicate Set Glass #s	Replicate Glass IDs	Replicate Set PCT_{Na}^{NL} (g/m ²)	%RSD(a)	SD [ln(g/m ²)]	RepSet Number
897	ORLEC48R	0.435	6.82	0.0682	98
907	SWV-G-17A	0.395			
751	ORPLA38-1	0.675	14.14	0.1419	102
767	J10-G-24B	0.825			
589	ORPLC2	1.125	9.11	0.0913	106
591	ORPLC3	1.280			
595	ORPLC5	0.745	14.67	0.1472	108
620	S10-G-101B	0.605			
597	ORPLD1	0.720	22.15	0.2221	109
622	T10-G-16A	0.395			
997	LAW-ORP-LD1(1)	0.596			
999	LAW-ORP-LD1(2)	0.517			
1035	LP2-OL-07	0.501			
732	Z10-G-60C	0.790	23.48	0.2370	110
733	10A-G-53C	0.565			
766	ORPLG27	0.770	19.75	0.1988	114
768	I10-G-135A	1.020			
1022	LP2-IL-10	0.573	6.94	0.0691	116
1028	LP2-IL-16	0.599			
1031	LP2-OL-02	0.523			
1049	LP2-OL-21	0.521			
1034	LP2-OL-05	0.363	7.73	0.0774	117
1038	LP2-OL-10-MOD	0.405			
1065	LAWPH3-12	0.960	7.99	0.0800	118
1066	LAWPH3-12-2	1.075			
1071	LAWPH3-17	1.713	18.11	0.1821	119
1072	LAWPH3-17-2	1.324			
Pooled Over 58 Replicate Sets with 78 total DF^(b)			17.88	0.1845	

(a) %RSD = 100 × (Standard Deviation / Mean)
(b) DF = degrees of freedom

The magnitudes of the pooled %RSDs in Table 3.2 and Table 3.3 are approximately the same values for PCT_B^{NL} (22.18%) and PCT_{Na}^{NL} (17.88%) reported in Table 5.4 of Piepel et al. (2007). Although both datasets include a long-term source of variation, the current dataset included data collected over roughly 18 years and includes a between laboratory (The Catholic University of America, PNNL, and Savannah River National Laboratory) source of variance and also includes replicates over a significantly broader composition region.

Consistent results from Table 3.2 and Table 3.3, and those in Piepel et al. (2007), suggest that roughly 20% RSD for replicates is likely to be reflective of what could be expected in future studies. It also suggests that the lower limit of model prediction uncertainties is unlikely to be less than roughly 0.2 (ln[g/m²]) due to variation inherent in data collection.

3.1.2 Model Validation Approach and Data for the PCT on LAW Glasses

The validation approach for the PCT_B^{NL} and PCT_{Na}^{NL} models was based on splitting the two 690-glass datasets for model development into five modeling/validation subsets. The five modeling/validation splits of the 690 glasses in the PCT_B^{NL} and PCT_{Na}^{NL} modeling datasets were formed as follows.

1. The 58 replicate sets (136 glasses) were set aside so they would always be included in each of the five model development datasets. This was done so that replicate pairs would not be split between modeling and validation subsets, thus negating the intent to have validation glasses different than model development glasses.
2. The remaining 554 glasses were ordered from smallest to largest according to their values of PCT_B^{NL} and PCT_{Na}^{NL} (g/m²). The glasses were numbered 1, 2, 3, 4, 5, 1, 2, 3, 4, 5, etc. All of the 1's formed the first model validation set, while all of the remaining points formed the first model development dataset. Similarly, all of the 2's, 3's, 4's, and 5's respectively formed the second, third, fourth, and fifth model validation sets. In each case, the remaining non-2's, non-3's, non-4's, and non-5's formed the second, third, fourth, and fifth model development datasets. Modeling and validation subsets do not necessarily contain the same numbers of glasses, but all the validation sets span the range of normalized PCT values in the region of interest.
3. The 136 replicate glasses were added to each of the split modeling subsets so that each of the five splits contains a relatively balanced number of modeling and validation glasses.

Data splitting was chosen as the validation approach because the PCT modeling dataset contains all compositions that (i) are in the LAW GCR of interest, (ii) meet quality assurance (QA) requirements, and (iii) have PCT_B^{NL} and PCT_{Na}^{NL} data. Having a separate validation dataset not used for modeling is desirable, but that desire was over-ridden by wanting PCT models developed using all appropriate data.

3.1.3 Subsets of LAW Glasses to Evaluate Prediction Performance of Models for B and Na Normalized Losses from the PCT

Section 2.4 discusses six subsets of LAW glasses for evaluating the prediction performance of LAW glass property-composition models, including subsets of glasses with higher waste loadings. The subsets, as discussed in Section 2.4, are denoted WTP, ORP, LP2OL, LP123, HiNa₂O, and HiSO₃. The normalized PCT boron loss modeling dataset of 690 LAW glasses (see Section 3.1.1) contains 289, 309, 120, 92, 232, and 110 in these six evaluation subsets, respectively. The normalized PCT sodium loss modeling dataset of 690 LAW glasses (see Section 3.1.1) contains 288, 309, 121, 93, 233, and 110 in these six evaluation subsets, respectively. The "Glass #s" of these six evaluation subsets of LAW glasses are listed in Table C.1 of Appendix C. The normalized LAW glass compositions and PCT_B^{NL} or PCT_{Na}^{NL} values for the glasses with these "Glass #s" are listed in Tables A.2 and A.3, respectively, of Appendix A. The predictive performance of $\ln(PCT_B^{NL})$ and $\ln(PCT_{Na}^{NL})$ models as functions of LAW glass composition developed in subsequent subsections are evaluated using these subsets of data.

3.2 Model Forms for Boron and Sodium Normalized PCT Losses from LAW Glasses

Mixture models (Cornell 2002) linking LAW glass compositions to PCT_B^{NL} and PCT_{Na}^{NL} are used. Empirical models of this type use existing data to estimate coefficients in a predictive equation such that certain goodness-of-fit criteria are optimized. Section B.1 of Appendix B discusses mixture experiments and several general forms of mixture experiment models.

Section 3.2.1 discusses the forms of mixture experiment models used for PCT responses of LAW glasses. Section 3.2.2 discusses the choice between modeling unnormalized PCT releases and normalized PCT losses.

3.2.1 Mixture Experiment Model Forms for Normalized PCT Boron and Sodium Losses from LAW Glasses

Linear mixture (LM) and PQM model forms introduced in Section B.1 of Appendix B have been used in the past (e.g., Piepel et al. 2007; Muller et al. 2014) to model PCT_B^{NL} and PCT_{Na}^{NL} as functions of LAW glass composition. Hence, these model forms were chosen for modeling $\ln(PCT_B^{NL})$ and $\ln(PCT_{Na}^{NL})$ in this report. The LM model form is given by

$$\ln(PCT_B^{NL}) \text{ or } \ln(PCT_{Na}^{NL}) = \sum_{i=1}^q \beta_i g_i + e \quad (3.1)$$

while the PQM model form is given by

$$\ln(PCT_B^{NL}) \text{ or } \ln(PCT_{Na}^{NL}) = \sum_{i=1}^q \beta_i g_i + \text{Selected} \{ \sum_{i=1}^q \beta_{ii} g_i^2 + \sum_{i < j}^{q-1} \sum_j^q \beta_{ij} g_i g_j \} + e \quad (3.2)$$

In Eqs. (3.1) and (3.2)

- $\ln(PCT_B^{NL})$ = natural logarithm of the PCT_B^{NL} normalized loss (in g/m²)
- $\ln(PCT_{Na}^{NL})$ = natural logarithm of the PCT_{Na}^{NL} normalized loss (in g/m²)
- g_i = normalized mass fraction of the i^{th} glass oxide or halogen component
($i = 1, 2, \dots, q$) such that $\sum_{i=1}^q g_i = 1$
- β_i = coefficient of the i^{th} linear blending term ($i = 1, 2, \dots, q$)
- β_{ii} and β_{ij} = coefficients of selected quadratic (squared) or crossproduct blending terms to be estimated from the data
- e = random error for each data point.

Many statistical methods exist for the case where the e are independent (i.e., not correlated) and normally distributed with mean 0 and standard deviation σ . Other methods, like generalized linear models (GLMs, Myers et al. 2002), offer more flexibility and can be used when the random errors for the data belong to a member of the exponential family of distributions, which includes the case with independent and normally distributed errors. In Eq. (3.2), “Selected” means that only some of the terms in curly brackets are included in the model. The subset is selected using stepwise regression or other variable selection methods (Draper and Smith 1998; Montgomery et al. 2012). PQM models are discussed in more detail and illustrated in Piepel et al. (2002) and Smith (2005).

Numerous forms of the models represented by Eq. (3.2) were fitted to the data, always resulting in biased predictions for some portion of the available PCT_B^{NL} and PCT_{Na}^{NL} range. The region of $\ln(PCT_B^{NL})$ and $\ln(PCT_{Na}^{NL})$ with values within the confidence interval around $0.693 \ln(\text{g/m}^2)$ is of particular interest; therefore, it was decided to focus attention on models with good prediction properties in the region with PCT_B^{NL} and PCT_{Na}^{NL} values near or above 2 g/m^2 limit.

3.2.2 Normalization and Transformation of Boron and Sodium Losses on the PCT from LAW Glasses

A transformation to normalized elemental losses is widely employed in the data analysis and modeling of leaching data (Hrma et al. 1994; Gan et al. 2001). The PCT_j^{NL} values were calculated according to the formula

$$PCT_j^{NL} = \frac{c_j LV}{f_j A} \quad (3.3)$$

where c_j is the concentration of the j^{th} element (B or Na) in solution (g/m^3) from the 7-day PCT, LV is the PCT solution volume (m^3), f_j is the j^{th} element concentration in glass, and A is the glass surface area exposed to solution in the PCT (m^2). For PCT values modeled in this study, a nominal A/LV ratio of 2000 m^{-1} was used. Normalized mass fraction compositions of glasses were calculated as discussed in Section 2.3. As seen in Eq. (3.3), normalizing a PCT elemental response involves dividing the measured leachate concentration for a given element by the fraction of that element in glass and by the surface-area-to-solution volume ratio. This results in a normalized loss value that ideally represents the grams of glass dissolved into solution per unit glass surface area. However, some glass components release faster from glass (i.e., incongruent) while others are held up in the solid alteration products on the surface. Therefore, the PCT_j^{NL} are not all equal for all elements, j . Differences in PCT_j^{NL} give an indication of the degree of incongruence. Past experience has suggested that PCT_B^{NL} , PCT_{Na}^{NL} , and PCT_{Li}^{NL} are generally similar in value and give the best indication of overall glass dissolution behavior (Vienna and Crum 2018, for example). Significant differences between the normalized losses of B, Na, and Li may be an indication of experimental error, as was seen for glass LAW14, which was excluded from the PCT_{Na}^{NL} modeling dataset for that reason.

Based on preliminary modeling work for PCT responses of LAW glasses, Perez-Cardenas et al. (2003) suggested a slight preference for models based on normalized PCT elemental losses as opposed to concentrations or normalized concentrations. The fact that WTP contract Specification 2.2.2.17.2 specifies a limit (2 g/m^2) in terms of normalized elemental losses was the deciding factor in the decision to model normalized PCT elemental losses in this work.

In modeling normalized PCT elemental losses, it is advantageous to model the response using a natural logarithm transformation. The advantages of this transformation include the following:

- For the 691 simulated and actual LAW glasses used for PCT modeling, the PCT_B^{NL} values range from 0.08 to 17.84 g/m^2 and the PCT_{Na}^{NL} values range from 0.1 to 13.41 g/m^2 . The range (i.e., minimum to maximum values) for each normalized loss spans more than an order-of-magnitude difference. In such cases, typically the uncertainty in making glasses, performing the PCT, and analyzing the leachate leads to smaller absolute uncertainties for smaller normalized losses and larger absolute uncertainties for larger normalized losses. Hence, the ordinary least squares (OLS) regression assumption of equal variances for all response variable values (see Section B.2.1 of Appendix B) may

not hold. A logarithmic transformation on the PCT response or the use of a GLM with a log link function may help make variances of normalized PCT elemental losses approximately equal as required for OLS regression.

- Theoretical relationships between glass composition and alteration result in logarithmic corrosion rates being correlated to composition (e.g., Jantzen et al. 1995; Feng et al. 1996; Gin et al. 2020). Although a 7-day PCT is not a measure of corrosion rate, it does obtain corrosion extent at a fixed time.
- A logarithmic transformation tends to linearize the compositional dependence of leach test data and reduce the need for non-linear terms in the model form.
 - A natural logarithm transformation is preferred over a common logarithm (or other base logarithm) transformation because of the approximate relationship

$$SD [\ln(y)] \cong RSD (y) \quad (3.4)$$

where SD denotes standard deviation, RSD denotes relative standard deviation (i.e., the standard deviation divided by the mean), and y denotes PCT_B^{NL} or PCT_{Na}^{NL} . Eq. (3.4) results from applying the first-order variance propagation formula [Eq. (7-7) of Hahn and Shapiro (1967)] to the function $z = \ln(y)$. The relationship in Eq. (3.4) is very useful, in that uncertainties of the natural logarithm of the response variable y can be interpreted as RSDs of the untransformed response variable y .

For these reasons, a natural logarithm function was used on the normalized PCT losses (g/m^2) in modeling PCT_B^{NL} and PCT_{Na}^{NL} .

3.3 Property-Composition Model Results for Normalized PCT Boron Loss from LAW Glasses

This section discusses the results of fitting several different mixture models to the LAW glass $\ln(PCT_B^{NL} [\text{g/m}^2])$ -composition dataset. Sections 3.3.1 and 3.3.2 present the results of modeling $\ln(PCT_B^{NL})$ using 20-component FLM and RLM models, respectively. Section 3.3.3 presents the results of modeling $\ln(PCT_B^{NL})$ using a PQM model based on a reduced set of 15 mixture components. Section 3.3.4 presents the result of modeling $\ln(PCT_B^{NL})$ using a 19-term PQM model with bias correction at high PCT response values.

3.3.1 Results from the 20-Component Full Linear Mixture Model for the Natural Logarithm of Normalized PCT Boron Loss from LAW Glasses

As the initial step in PCT_B^{NL} -composition model development, a FLM model was fit to the modeling data (690 glasses) using OLS with the 20 glass components identified in Section 3.1.1. This model form was a reasonable starting point based on the previous work modeling $\ln(PCT_B^{NL})$ from LAW glasses (Hrma et al. 1994; Piepel et al. 2007) and provided a basis for appropriate model modifications.

Table 3.4 contains the results from the 20-component FLM model for $\ln(PCT_B^{NL})$. Table 3.4 lists the model coefficients, standard deviations of the coefficients, and model performance summaries for the 20-component FLM model using the modeling dataset (690 LAW glasses).

The $R^2 = 0.6979$, $R^2_A = 0.6893$, and $R^2_P = 0.6719$ statistics (see Section B.3 of Appendix B) in Table 3.4 show that (i) the 20-component FLM model does not fit the $\ln(PCT_B^{NL})$ data in the 690-glass modeling dataset well, (ii) there are several unneeded model terms (evidenced by the high standard errors relative to the reported coefficient estimates), and (iii) there are not any highly influential data points (confirmed in the diagnostic graphics described in Section B.3 and by the fact that the R^2 -predicted value is close to the R^2 -adjusted and R^2 values for this model). The RMSE = 0.4587 is significantly larger than the pooled glass batching and PCT_B^{NL} determination uncertainty (SD = 0.2317 in $\ln(\text{g/m}^2)$ units) estimated from replicates in Table 3.2. This suggests that the 20-component FLM model has a statistically significant lack of fit (LOF), which is confirmed by the model LOF p-value < 0.0001 in Table 3.4. See Section B.3 for discussion of the statistical test for model LOF.

Table 3.4. Coefficients and Performance Summary for the 20-Component Full Linear Mixture Model on the Natural Logarithm of Normalized Boron Loss from the PCT on LAW Glasses.

$\ln(PCT_B^{NL})$ 20-Component FLM Model Term	Coefficient Estimate	Coefficient Stand. Err.
Al ₂ O ₃	-18.0821	0.8798
B ₂ O ₃	12.4579	0.9161
CaO	-6.5648	0.6705
Cl	33.6608	7.7478
Cr ₂ O ₃	33.7671	10.7963
F	15.5259	11.5518
Fe ₂ O ₃	2.1789	0.9752
K ₂ O	10.0826	1.1672
Li ₂ O	25.7927	2.1412
MgO	23.3373	2.0069
Na ₂ O	12.7411	0.6304
P ₂ O ₅	-12.7348	3.4435
SO ₃	-21.5444	7.4247
SiO ₂	-7.0147	0.3746
SnO ₂	-12.6129	1.7068
TiO ₂	-20.1107	2.6617
V ₂ O ₅	5.2029	1.8564
ZnO	-1.3986	2.0702
ZrO ₂	-2.7195	1.4352
Others(a)	-44.8943	25.7588
Modeling Data Statistics, 690 Glasses (b)	Value	
R^2	0.6979	
R^2_A	0.6893	
R^2_P	0.6719	
RMSE	0.4587	
Model LOF p-value	<0.0001	
(a) For the 20-component FLM model, the “Others” component includes any components not separately listed.		
(b) The model evaluation statistics are defined in Section B.3 of Appendix B. The model validation statistics are defined in Section B.5.		

Figure 3.6 shows the predicted versus measured (PvM) plot for the 690-glass modeling dataset using the 20-component FLM model for $\ln(PCT_B^{NL})$. The plot illustrates that the 20-component FLM model significantly under-predicts PCT_B^{NL} above the limit of 2 g/m² (shown with red lines). The model also under-predicts glasses with the lowest PCT_B^{NL} values, although this is not a major concern for LAW Facility application.

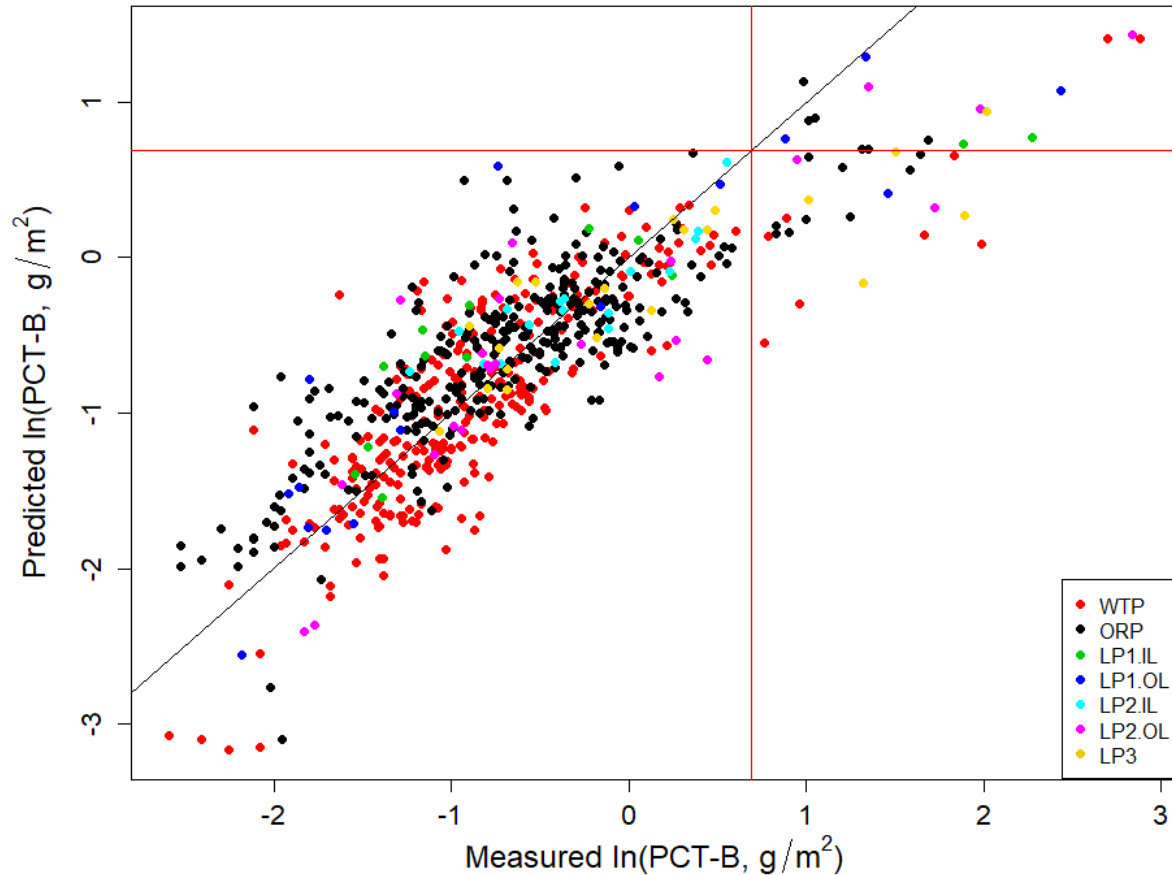


Figure 3.6. Predicted versus Measured Plot for the 690-Glass Modeling Dataset Using the 20-Component Full Linear Mixture Model on the Natural Logarithm of PCT_B^{NL} from LAW Glasses. The red lines represent the WTP contract limit of 2 g/m², or 0.6931 ln(g/m²).

The results in Table 3.4 and Figure 3.6 indicate that the 20-term FLM produces unacceptable results, particularly in the region of PCT_B^{NL} values that are of most interest to the project. The majority of glasses at or above the WTP contract limit of 2 g/m² are underpredicted by the 20-term FLM model.

The model in Table 3.4, fit to the 690-glass PCT_B^{NL} modeling dataset, provides a starting point for improvement (e.g., addition of non-linear terms). The 20-component LM model was used to produce the response trace plot (see Section B.4.1 in Appendix B) shown in Figure 3.7. The average glass composition of the 1074 glasses in the compiled database discussed in Section 2.5 was used as the REFMIX (see Section B.4.1) in response trace plots for every property. The glass composition of the REFMIX is listed in Table 2.3.

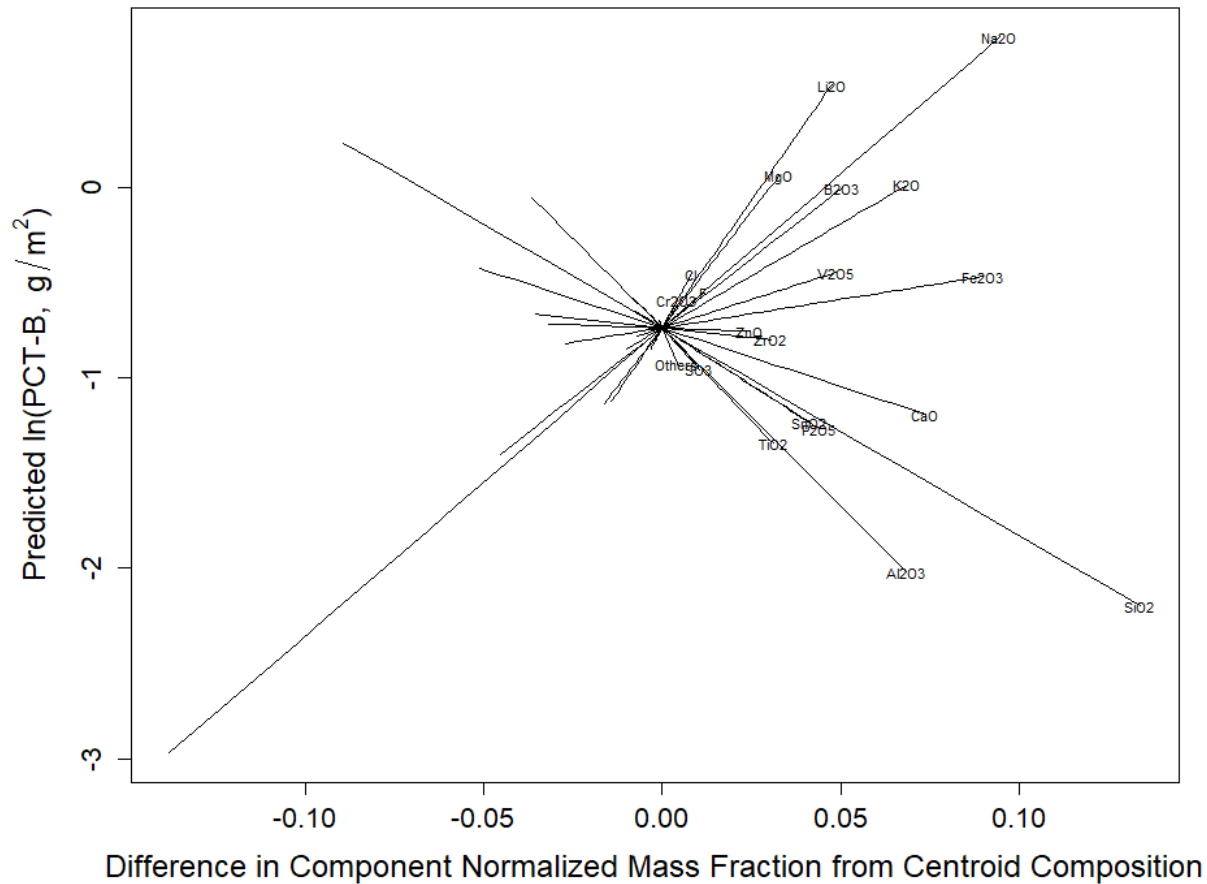


Figure 3.7. Response Trace Plot for the 20-Component Full Linear Mixture Model on the Natural Logarithm of Normalized PCT Boron Loss from LAW Glasses

The response trace plot in Figure 3.7 shows that Li_2O , MgO , Na_2O , B_2O_3 , and K_2O are predicted to increase $\ln(\text{PCT}_B^{NL})$, while CaO , SiO_2 , SnO_2 , P_2O_5 , Al_2O_3 , and TiO_2 are predicted to decrease $\ln(\text{PCT}_B^{NL})$. The impacts of Cr_2O_3 , Cl , SO_3 , and Others are significantly larger than expected based on previous model attempts and knowledge of chemistry impacts on PCT responses. It is likely that the slopes associated with these terms are exaggerated due more to multicollinearity present in the data than actual component effects. To test this hypothesis, the terms Cr_2O_3 , Cl , SO_3 were combined into Others in subsection 3.3.2 to determine if the fit statistics are significantly impacted. If significant impacts are identified, then further research would be required to experimentally verify those results.

Due to the poor predictive performance of the 20-term FLM in the region of interest, no further analysis of this model was carried out, focusing instead on the development of a better model.

3.3.2 Results from the 15-Component Reduced Linear Mixture Model for the Natural Logarithm of Normalized Boron Loss from the PCT on LAW Glasses

The 20-component FLM model for $\ln(\text{PCT}_B^{NL})$ presented in Section 3.3.1 contains components that do not significantly contribute to predicting $\ln(\text{PCT}_B^{NL})$ and some components with unexpectedly strong effects,

so model reduction was performed prior to selection of higher order terms. RLM models for involving fewer than the 20 components were considered. To reduce the number of terms, (i) the sequential F-test model reduction approach (see Section B.4.1 of Appendix B; Piepel and Cooley 2006) and (ii) selection based on knowledge of PCT chemical effect were used. Using the F-test method and a threshold of 0.001, SO_3 , TiO_2 , P_2O_5 , SnO_2 , and F were determined to be the least significant terms and were combined to Others. This resulted in significant and non-defensible effects of Cl and Cr_2O_3 (similar to those in the FLM model in Section 3.3.1). Cl and Cr_2O_3 have the smallest overall concentration ranges ($0.0000 \leq \text{Cl} \leq 0.0117$ and $0.0000 \leq \text{Cr}_2\text{O}_3 \leq 0.0063$, mf). Cl is also volatile to differing extents in glass, with a mean retention of roughly 70% in typical crucible melts (with a broad distribution of retention factors). Neither component is expected to have a significant effect on PCT or increase PCT responses. There is a potential for Cl to slightly decrease pH of PCT solution, thereby slightly reducing PCT responses. With such strong predicted effect of these two components, counter to previous observations, independent experimental verification is needed prior to including in the model. Additionally, the combination of SnO_2 and TiO_2 with Others caused the combined Others term to have a strong negative effect on $\ln(PCT_B^{NL})$ with most other components (including SiO_2) to have positive effects. The F-test method, after forcing Cl and Cr_2O_3 into Others resulted in Cl, Cr_2O_3 , F, P_2O_5 , and SO_3 to be combined with Others resulting in a 15-term RLM model.

Table 3.5 contains the results from the 15-component RLM model for $\ln(PCT_B^{NL})$. Table 3.5 lists the model coefficients, standard deviations of the coefficients, and model performance summaries for the RLM model using the modeling dataset (690 LAW glasses).

The $R^2 = 0.6732$, $R_A^2 = 0.6665$, and $R_P^2 = 0.6508$ statistics (see Section B.3 of Appendix B) in Table 3.5 show that the 15-component FLM model does not fit the $\ln(PCT_B^{NL})$ data in the 690-glass modeling dataset well. The RMSE = 0.4752 is significantly larger than the pooled glass batching and PCT_B^{NL} determination uncertainty ($\text{SD} = 0.2317$ in $\ln(\text{g/m}^2)$ units) estimated from replicates in Table 3.2. This suggests that the 15-component RLM model has a statistically significant LOF, which is confirmed by the model LOF p-value < 0.0001 in Table 3.5. See Section B.3 for discussion of the statistical test for model LOF.

Figure 3.8 shows the PvM plot for the 690-glass modeling dataset using the 15-component RLM model for $\ln(PCT_B^{NL})$. The plot illustrates that the 15-component RLM model significantly under-predicts PCT_B^{NL} above the limit of 2 g/m^2 (shown with red lines). The model also under-predicts glasses with the lowest PCT_B^{NL} values, although this is not a major concern for WTP LAW Facility application.

Table 3.5. Coefficients and Performance Summary for the 15-Component Reduced Linear Mixture Model on the Natural Logarithm of Normalized Boron Loss from the PCT on LAW Glasses.

$\ln(PCT_B^{NL})$ 15-Component RLM Model Term	Coefficient Estimate	Coefficient Stand. Err.
Al ₂ O ₃	-17.5901	0.8971
B ₂ O ₃	11.9640	0.9389
CaO	-6.5749	0.6705
Fe ₂ O ₃	2.1137	0.9616
K ₂ O	10.4441	1.1634
Li ₂ O	25.2325	2.1725
MgO	23.5570	2.0666
Na ₂ O	13.4439	0.6356
SiO ₂	-7.4485	0.3761
SnO ₂	-9.2257	1.6609
TiO ₂	-16.8034	2.6512
V ₂ O ₅	2.9369	1.8297
ZnO	-0.8531	2.1322
ZrO ₂	-1.4873	1.4357
Others ^(a)	-0.0736	2.1993
Modeling Data Statistics, 690 Glasses ^(b)	Value	
R ²	0.6732	
R ² _A	0.6665	
R ² _P	0.6508	
RMSE	0.4752	
Model LOF p-value	<0.0001	

(a) For the 15-component FLM model, the “Others” component includes the Others component from the FLM model plus Cl, Cr₂O₃, F, P₂O₅, and SO₃.

(b) The model evaluation statistics are defined in Section B.3 of Appendix B. The model validation statistics are defined in Section B.5.

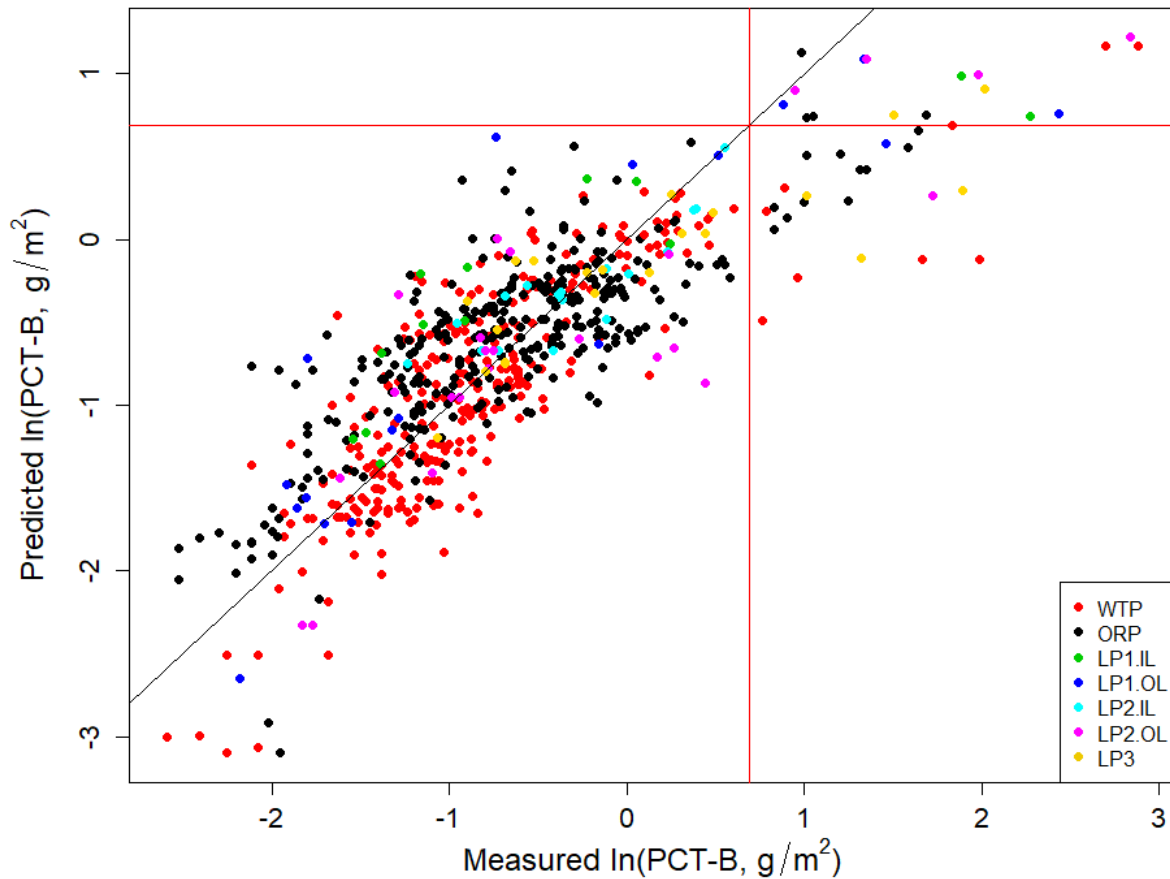


Figure 3.8. Predicted versus Measured Plot for the 690-Glass Modeling Dataset Using the 15-Component Reduced Linear Mixture Model on the Natural Logarithm of PCT_B^{NL} from LAW Glasses. The red lines represent the WTP contract limit of 2 g/m², or 0.6931 ln(g/m²).

The results in Table 3.5 and Figure 3.8 indicate that the 15-term RLM produces unacceptable results, particularly in the region of PCT_B^{NL} values that are of most interest to the project. The majority of glasses at or above the WTP contract limit of 2 g/m² are underpredicted by the 15-term RLM model.

The model in Table 3.5, fit to the 690-glass PCT_B^{NL} modeling dataset, provides a starting point for improvement (e.g., addition of non-linear terms). The 15-component RLM model was used to produce the response trace plot (see Section B.4.1 in Appendix B) shown in Figure 3.9. The average glass composition of the 1074 glasses in the compiled database discussed in Section 2.5 was used as the REFMIX (see Section B.4.1) in response trace plots for every property. The glass composition of the REFMIX is listed in Table 2.3.

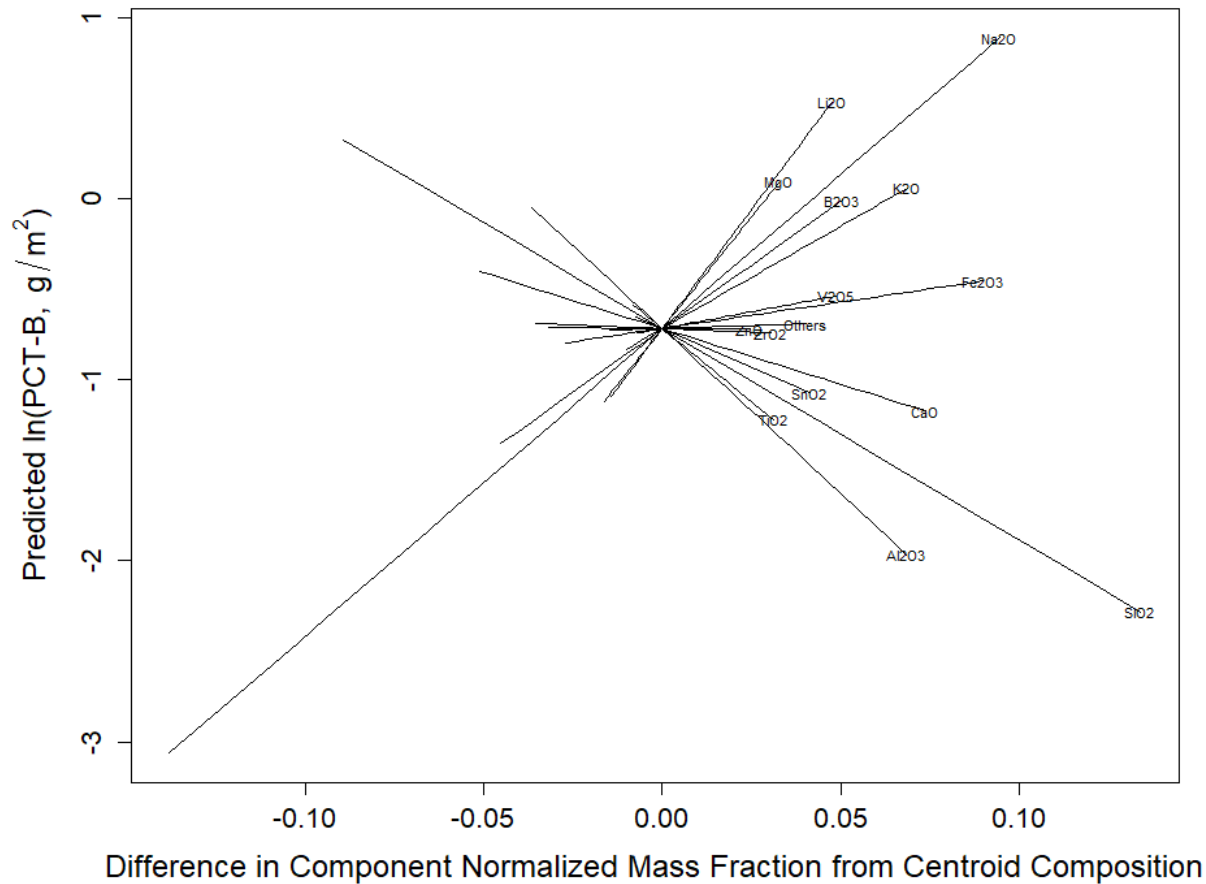


Figure 3.9. Response Trace Plot for the 15-Component Reduced Linear Mixture Model on the Natural Logarithm of Normalized PCT Boron Loss from LAW Glasses

The response trace plot in Figure 3.9 shows that Li_2O , MgO , Na_2O , B_2O_3 , and K_2O are predicted to increase $\ln(\text{PCT}_B^{\text{NL}})$ the most, while Al_2O_3 , TiO_2 , SiO_2 , SnO_2 , and CaO are predicted to decrease $\ln(\text{PCT}_B^{\text{NL}})$ the most. These agree with previous model attempts and knowledge of the chemistry of PCT responses. Due to the poor predictive performance of the 15-term RLM in the region of interest, no further analysis of this model was carried out, focusing instead on the development of a better model based on these same 15 components.

3.3.3 Results from a Reduced Partial Quadratic Mixture Model for the Natural Logarithm of Normalized PCT Boron Loss from LAW Glasses

Reduced PQM models were investigated in an effort to improve the 15-component RLM model for predicting $\ln(\text{PCT}_B^{\text{NL}})$. Past experience with developing and validating PQM models has indicated that adding too many quadratic terms tends to over-fit the model development dataset and degrade predictive performance for new glasses. So, a process of identifying as few as possible second-order terms while improving model fit statistics was performed as follows:

1. Regressions were performed to fit reduced partial quadratic models involving all possible subsets of 1, 2, 3, or 4 second-order terms.

2. The resulting model performance statistics (R-squared and RMSE values) were then examined to see which second-order terms were most beneficial to model performance and how many second-order terms to include.
3. The RMSE values from the top candidate models were plotted as a function of the number of second-order terms (0 to 4) to identify the point of diminishing returns.
4. The reduced PQM model with the number of terms just before the point of diminishing returns was selected as the final reduced PQM model.

The maximum R^2 improvement (MAXR) criterion (see Section B.4.2 of Appendix B) was also attempted as a means of selecting second-order terms. Both methods resulted in the same selection as “best” four second-order terms: $\text{Na}_2\text{O} \times \text{SiO}_2$, $\text{CaO} \times \text{V}_2\text{O}_5$, $\text{Al}_2\text{O}_3 \times \text{Al}_2\text{O}_3$, $\text{CaO} \times \text{CaO}$.

Ultimately, a 19-term PQM model for $\ln(PCT_B^{NL})$ with 15 linear terms and 4 second-order terms (2 quadratic and 2 cross-product) was selected as including enough quadratic terms to improve the model fit, without over-fitting the model development data. Table 3.6 contains the coefficients of the 19-term PQM model for $\ln(PCT_B^{NL})$ and the coefficient standard errors. Table 3.6 also includes model fit summary statistics for the 19-term PQM model.

The $R^2 = 0.7454$, $R_A^2 = 0.7386$, and $R_P^2 = 0.7191$ statistics (see Section B.3 of Appendix B) in Table 3.6 show that the 19-component PQM model fits the $\ln(PCT_B^{NL})$ data in the 690-glass modeling dataset significantly better than the FLM and RLM models. The RMSE = 0.4207 is still significantly larger than the pooled glass batching and PCT_B^{NL} determination uncertainty (SD = 0.2317 in $\ln(\text{g/m}^2)$ units) estimated from replicates in Table 3.2. This suggests that the 19-component PQM model has a statistically significant LOF, which is confirmed by the model LOF p-value < 0.0001 in Table 3.6. See Section B.3 for discussion of the statistical test for model LOF.

Table 3.6. Coefficients and Performance Summary for the 19-Term Partial Quadratic Mixture Model on the Natural Logarithm of Normalized Boron Loss from the PCT on LAW Glasses

ln(PCT-B) 19-Component PQM Model Term	Coefficient Estimate	Coefficient Stand. Err.
Al ₂ O ₃	-57.0952	5.2015
B ₂ O ₃	7.7336	1.0536
CaO	4.9798	2.6276
Fe ₂ O ₃	-1.3429	0.9721
K ₂ O	10.4299	1.1196
Li ₂ O	22.8298	2.0010
MgO	20.3182	1.9193
Na ₂ O	32.8910	2.6479
SiO ₂	-1.5454	0.8087
SnO ₂	-13.0083	1.5958
TiO ₂	-14.8241	2.4431
V ₂ O ₅	15.8120	2.8024
ZnO	-6.0511	2.0309
ZrO ₂	-3.0717	1.4733
Others ^(a)	-2.9975	2.0071
Na ₂ O × SiO ₂	-49.4262	7.1942
CaO × V ₂ O ₅	-247.8584	43.6363
(Al ₂ O ₃) ²	214.2560	31.9372
(CaO) ²	-100.1039	20.1701
Modeling Data Statistics, 690 Glasses ^(b)	Value	
R ²	0.7454	
R ² _A	0.7386	
R ² _P	0.7191	
RMSE	0.4207	
Model LOF p-value	<0.0001	
(a) For the 19-component PQM model, the “Others” component includes the Others component from the FLM model plus Cl, Cr ₂ O ₃ , F, P ₂ O ₅ , and SO ₃ .		
(b) The model evaluation statistics are defined in Section B.3 of Appendix B. The model validation statistics are defined in Section B.5.		

Figure 3.10 shows the PvM plot for the 690-glass modeling dataset using the 19-term PQM model for $\ln(PCT_B^{NL})$. The plot illustrates that the 19-term PQM model significantly under-predicts PCT_B^{NL} above the limit of 2 g/m² (shown with red lines). The model also under-predicts glasses with the lowest PCT_B^{NL} values, although this is not a major concern for WTP LAW Facility application.

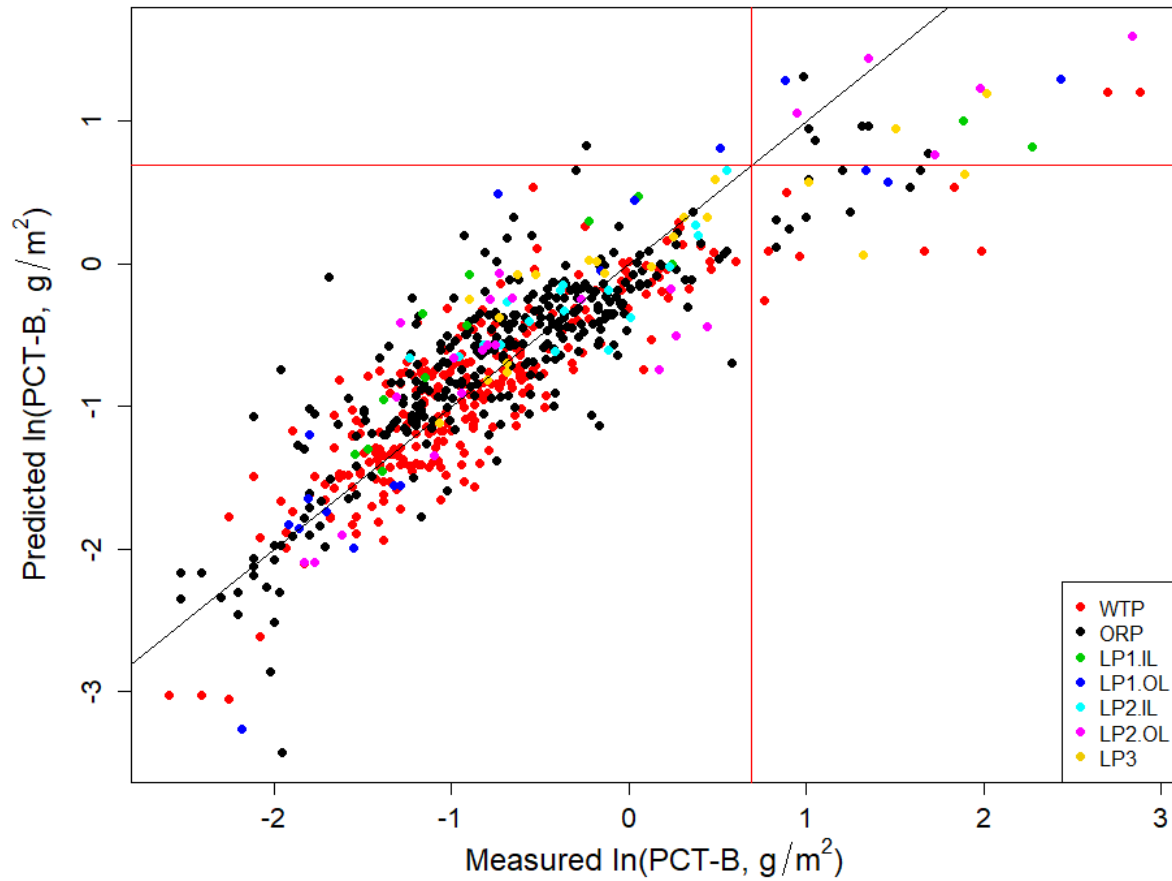


Figure 3.10. Predicted versus Measured Plot for the 690-Glass Modeling Dataset Using the 19-Term Partial Quadratic Mixture Model on the Natural Logarithm of PCT_B^{NL} from LAW Glasses. The red lines represent the WTP contract limit of 2 g/m², or 0.6931 ln(g/m²).

The results in Table 3.6 and Figure 3.10 indicate that the 19-term PQM produces unacceptable results, particularly in the region of PCT_B^{NL} values that are of most interest to the project. The majority of glasses at or above the WTP contract limit of 2 g/m² are underpredicted by the 19-term PQM model.

The 19-term PQM model was used to produce the response trace plot (see Section B.4.1 in Appendix B) shown in Figure 3.11. The average glass composition of the 1074 glasses in the compiled database discussed in Section 2.5 was used as the REFMIX (see Section B.4.1) in response trace plots for every property. The glass composition of the REFMIX is listed in Table 2.3.

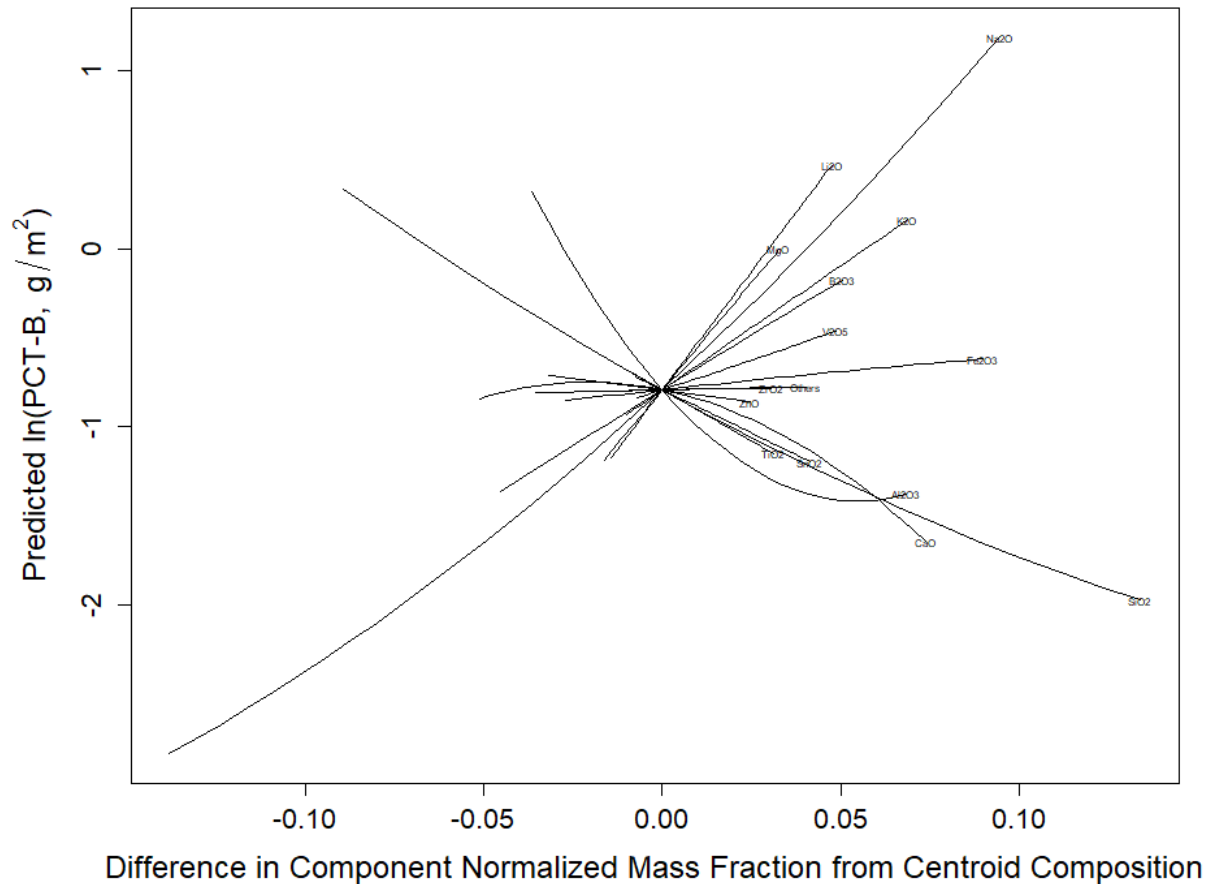


Figure 3.11. Response Trace Plot for the 19-Term Partial Quadratic Mixture Model on the Natural Logarithm of Normalized PCT Boron Loss from LAW Glasses

The response trace plot in Figure 3.11 shows that Li_2O , MgO , Na_2O , K_2O , and B_2O_3 are predicted to increase $\ln(\text{PCT}_B^{NL})$ the most, while Al_2O_3 , TiO_2 , SiO_2 , SnO_2 , and CaO are predicted to decrease $\ln(\text{PCT}_B^{NL})$ the most. These agree with previous model attempts and knowledge of the chemistry of PCT responses. The non-linear impact of Al_2O_3 evident in Figure 3.11 is a well-documented trend (see, for example, Vienna and Crum 2018). Due to the poor predictive performance of the 19-term PQM in the region of interest, no further analysis of this model was carried out, focusing instead on the development of better models.

3.3.4 Screening of Model Types for Predicting Natural Logarithm of Normalized PCT Boron Loss from LAW Glasses

Most waste glass properties are well represented using FLM, RLM, or PQM models over sufficiently narrow composition regions. This was found to be the case for predicting $\ln(\text{PCT}_B^{NL})$ of LAW glasses covering a narrower subset of the current 690-glass dataset. It is apparent by the bias seen at high $\ln(\text{PCT}_B^{NL})$ responses ($>0.5 \ln[\text{g}/\text{m}^2]$) shown in Figure 3.10 that a PQM is insufficient in this case. Therefore, a brief survey of model approaches for modeling properties as non-linear functions of glass composition was undertaken. Several approaches were surveyed for predicting either $\ln(\text{PCT}_B^{NL})$ or categorical pass/fail (P/F) of the WTP contract constraint of $\text{PCT}_B^{NL} \leq 2 \text{ g}/\text{m}^2$ including:

1. Local linear regression (LLR)
2. K-nearest neighbor (KNN) (numerical or P/F)
3. Generalized linear models (GLM)
4. Gaussian process regression (GPR)
5. Artificial neural networks (ANN)
6. Decision tree (P/F)
7. Random forest (P/F)
8. Support vector machine (SVM)(P/F)
9. Linear and partial quadratic logistic regression (P/F)
10. Bias corrected PQM model (bcPQM)

Each of these methods was attempted with the same 690-glass normalized PCT boron response dataset.

LLR improved but did not fully remove the bias prediction in the high PCT_B^{NL} range. The residual bias is likely due to the sparse data in that region. Although the fit did improve, it improved at a cost of significantly larger confidence intervals.

KNN models were fitted to both $\ln(PCT_B^{NL})$ and the categorical P/F PCT data. In either case, 25% of the data was randomly selected for testing of model predictions. The model for $\ln(PCT_B^{NL})$ response used the same set of linear and higher order terms from the PQM model (Section 3.3.3) and resulted in an optimal $k = 2$. Both the training and testing fits were poorer than the associated PQM model (e.g., $R^2 = 0.5685$, $RMSE = 0.5376$) (potentially because only 75% of the data was used to fit the model). The categorical model predicted resulted in a best-fit $k = 3$. The typical fit resulted in a misclassification rate near 0.04 for the fit data and near 0.05 for the test data. Those values varied significantly with random seed, however, suggesting an unstable model form with these data.

GLMs, as well as traditional linear models, can be tuned to reduce the uncertainty in a specific subset of data. An attempt was made to tune a GLM to obtain the lowest RMSE for $\ln(PCT_B^{NL}) \geq 0.6$. The result was greatly improved prediction in this response range, but at the expense of non-intuitive component effects and gross underpredictions in the lower PCT_B^{NL} region (as shown in Figure 3.12).

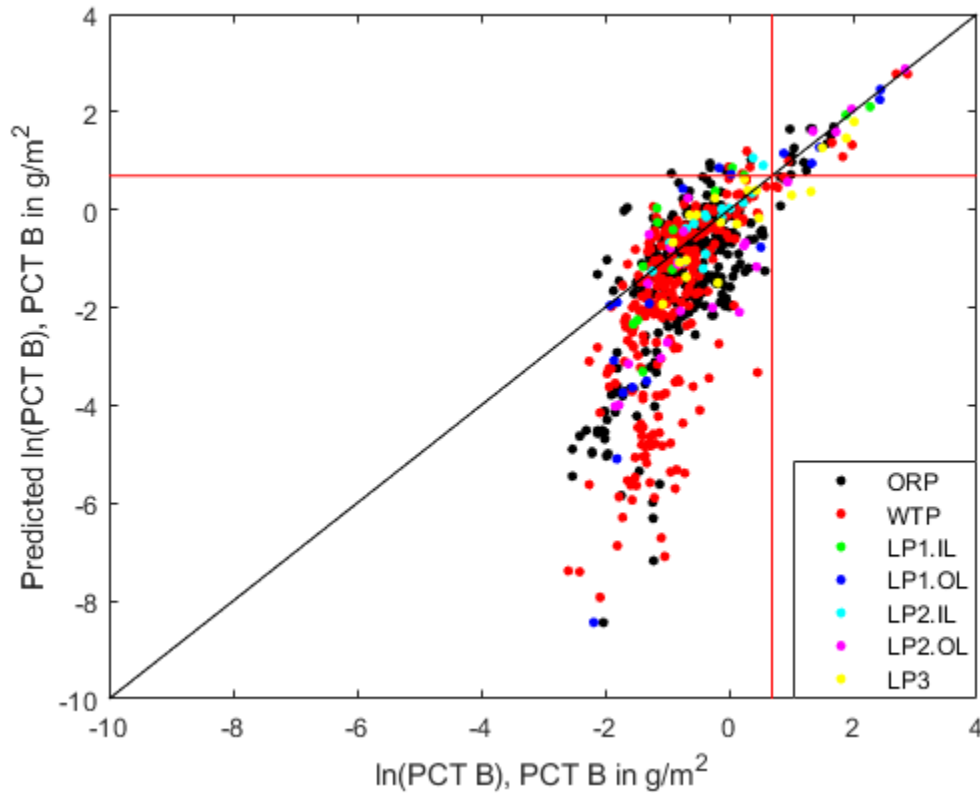


Figure 3.12. Predicted versus Measured Plot for a 22-term Partial Quadratic Generalized Mixture Model with Four Higher-order Terms on the Natural Logarithm of PCT_B^{NL} from LAW Glasses. The red lines represent the WTP contract limit of $0.6931 \ln(\text{g/m}^2)$. For Information Only

GPR was fitted with the 15 terms associated with the RLM model (Section 3.3.2). The 15-term model did not fit the data well and produced unreasonable predictions for a considerable portion of the data. Different tuning parameters were attempted without significant success at improving the behavior of the model. Combined with the computationally expensive property prediction calculations, the GPR approach was not further pursued.

ANN models had previously been used to predict VHT response of LAW glasses (Vienna et al. 2013). An ANN model using the 15 components from the RLM model (Section 3.3.2), a single layer and a TanH transfer function was fitted to the 690-point $\ln(PCT_B^{NL})$ dataset. A good fit was obtained with the data, however, biased, underpredicted estimates at high $\ln(PCT_B^{NL})$ values were observed. The test set (randomly selected 25% of the data) was not well predicted and was also biased in the high $\ln(PCT_B^{NL})$ range. Based on the relatively poor performance for the validation set, the complicated model form, and bias, this model was not pursued further.

A single decision tree was developed to predict PCT P/F categorical data of the 690-glass dataset. The dataset was first split into a training set with randomly selected 75% of the data and the remaining 25% as a test set. Both automated and manual pruning were attempted. Each tree started with a split in Al_2O_3 concentration at 0.055706, which yielded 479 glass branches above the cutoff containing 463 passes and 16 fails. The 46 points below the cutoff contained 17 fails and 29 passes. The misclassification rate was closely matched between the training and testing set. Further spitting of the tree resulted in growing

disparity between training and testing set statistics. Automated function repeatedly converged on this single split value, with relatively poor performance. The single decision tree wasn't pursued further.

The decision tree concept was expanded to a random forest. Like the single tree, the random forest method failed to produce a predictive model that performed well for the testing (validation) set. R^2 values of 0.6440 for the training set and 0.4604 for the validation set were typical. The random forest method wasn't pursued further.

SVM classification models were fitted. The performance of the SVM was similar to the results found with the decision tree and was not pursued further.

Logistic regression of PCT P/F data resulted in relatively poor prediction with a bias to higher false negative rates (FNR = # of fail glasses classified as pass/# of fail glasses in set). A threshold probability can be adjusted to balance the FNR with false positive rates (FPR = # of pass glasses classified as fail/# of pass glasses in set), however this resulted in an unacceptably high level of conservatism (high FPR). Interestingly, of all possible second-order terms, the two found most significant using a logistic model were $Al_2O_3 \times Al_2O_3$ and $CaO \times CaO$, as was the case for PQM models. Logistic regressions were not further pursued.

The PQM models were not successful due to a non-conservative bias at high $\ln(PCT_B^{NL})$ values (≥ 0.6). One approach previously used to correct similar biases in PCT responses of HLW glasses was to add a bias correction (bc) (Piepel et al. 2008). The application of bc to PQM predictions of $\ln(PCT_B^{NL})$ is straightforward, but requires that there are no discontinuities in prediction as the correction threshold is approached. Any prediction discontinuity would cause glass composition optimization routines to fail to converge. The bcPQM approach was compared to the other modeling approaches and ultimately adopted for use in prediction of both $\ln(PCT_B^{NL})$ (Section 3.3.5) and $\ln(PCT_{Na}^{NL})$ (Section 3.4.5).

3.3.5 Results from a Bias Corrected Partial Quadratic Mixture Model for the Natural Logarithm of Normalized PCT Boron Loss from LAW Glasses

The poor performance of the FLM and PQM models, particularly in the region of high PCT values, suggests that a method to correct prediction bias may be useful for producing usable PCT models. Bias correction methods have been investigated and applied before in the modeling of PCT (Piepel et al. 2008; Vienna and Kim 2014). The bias corrected form of the models is given by:

$$\ln(\widehat{PCT}_B^{NL})_{BC} = \begin{cases} \ln(\widehat{PCT}_B^{NL}) & \text{if } \ln(\widehat{PCT}_B^{NL}) \leq c \\ \ln(\widehat{PCT}_B^{NL}) + (\ln(\widehat{PCT}_B^{NL}) - c)s & \text{if } \ln(\widehat{PCT}_B^{NL}) > c \end{cases} \quad (3.5)$$

where

$$\begin{aligned} \ln(\widehat{PCT}_B^{NL}) &= \ln(PCT_B^{NL}) \text{ predicted using a PQM model prior to application of bc (ln[g/m}^2\text{])} \\ c &= \text{estimated bias correction cut-off (ln[g/m}^2\text{])} \\ s &= \text{estimated bias correction slope (unitless). Due to the fitting process, } s \text{ is the sum} \\ &\quad \text{of the initial slope (} s_0 \text{) and the change in slope (} \Delta s \text{) (i.e., } s = s_0 + \Delta s \text{) as} \\ &\quad \text{described in Section 3.6.} \end{aligned}$$

In Eq. (3.5), the bias correction applied to the predicted $\ln(PCT_B^{NL})$ value increases or decreases linearly from zero at the cutoff with a slope given by s . Values of c and s were found using two approaches: (i) fitting Eq. (3.5) to measured $\ln(PCT_B^{NL})$ using the PQM reported in Section 3.3.3, or (ii) simultaneously fitting the PQM model terms with the c and s according to

$$\ln(PCT_B^{NL})_{BC} = \begin{cases} \mathbf{g}^T \boldsymbol{\beta} & \text{if } \mathbf{g}^T \boldsymbol{\beta} \leq C \\ \mathbf{g}^T \boldsymbol{\beta} + (\mathbf{g}^T \boldsymbol{\beta} - C)S & \text{if } \mathbf{g}^T \boldsymbol{\beta} > C \end{cases} + e \quad (3.6)$$

where:

- $\boldsymbol{\beta}$ = the vector of PQM term coefficients including β_i , β_{ii} , and β_{ij} values
- \mathbf{g} = the vector of component concentrations for first order terms followed by component concentrations squared for quadratic terms and concentrations multiplied for cross-product terms (in the same order as $\boldsymbol{\beta}$)
- C = bias correction cut-off ($\ln[\text{g/m}^2]$)
- S = bias correction slope (unitless). Due to the fitting process, S is the sum of the initial slope (S_0) and the change in slope (ΔS) (i.e., $S = S_0 + \Delta S$) similar to what is described in Section 3.6 (except for the parameters, rather than the estimates).
- e = random error for each data point.

Both approaches were attempted, and the second approach was ultimately adopted because it resulted in a better solution with less scatter in the data. The same first-order terms were used as in the RLM model described in Section 3.3.2. Three of the four second-order terms in the PQM model were also selected for the bcPQM model ($\text{Al}_2\text{O}_3 \times \text{Al}_2\text{O}_3$, $\text{CaO} \times \text{CaO}$, and $\text{CaO} \times \text{V}_2\text{O}_5$). The fourth second-order term selected in the bcPQM model was $\text{Al}_2\text{O}_3 \times \text{Li}_2\text{O}$ instead of the $\text{Al}_2\text{O}_3 \times \text{Na}_2\text{O}$ term selected for the PQM model. These terms are generally expected based on past PCT response modeling for LAW glasses that showed second-order terms involving Al_2O_3 , CaO , Li_2O , and Na_2O (Piepel et al. 2007, Vienna et al. 2013, Vienna et al. 2016). Second order terms containing V_2O_5 are not commonly found, but Muller et al. (2014) combined V_2O_5 into others and reported two second-order terms involving Others. Table 3.7 contains the coefficients of the 22-term bcPQM model for $\ln(PCT_B^{NL})$ and the coefficient standard errors. Table 3.7 also includes model performance statistics for the 22-term bcPQM using the (i) 690-glass modeling data, (ii) data-split modeling data (as a model validation approach), and (iii) six evaluation subsets of the modeling glasses discussed in Section 3.1.3 (as a model evaluation approach).

In Table 3.7, the $\ln(PCT_B^{NL})$ model fit statistics $R^2 = 0.7762$, $R_A^2 = 0.7692$, and $\text{RMSE} = 0.3954$ for the 22-term bcPQM model are small improvements over the corresponding statistics for the 19-term PQM model in Table 3.6. The small difference in values between R^2 and R_A^2 suggests that the $\ln(PCT_B^{NL})$ model does not have excess terms. R_p^2 , reported for properties in this report, was not estimated for the $\ln(PCT_B^{NL})$ model due to software limitations.

The RMSE in Table 3.7 is an estimate of the uncertainty [in $\ln(\text{g/m}^2)$ units] in fabricating LAW glasses and useful for determining if the 22-term PCT_B^{NL} bcPQM model has a statistically significant LOF. The $\text{RMSE} = 0.3954$ for the bcPQM model fitted to the 690-glass modeling dataset is slightly smaller than the corresponding value for the 19-term PQM model ($\text{RMSE} = 0.4207$) in Table 3.6, indicating a better fit to the data by bcPQM. The RMSE value is roughly double the pooled replicate SD in $\ln(\text{g/m}^2)$ units of 0.2317 in Table 3.2. These observations suggest that the 22-term bcPQM model does have significant model LOF, which is confirmed by the LOF test p-value < 0.0001 in Table 3.7. See Section B.3 of Appendix B for discussion of the statistical test for model LOF.

At the bottom right of Table 3.7, the average model-fit statistics (R^2 , R^2_A , and RMSE) over the five data-splits are close to the statistics obtained from fitting the 22-term bcPQM model for $\ln(PCT_B^{NL})$ to all 690 glasses in the modeling dataset. The data-split validation statistics (R^2_v and $RMSE_v$) are slightly worse than the bcPQM R^2 and RMSE (i) values from fitting the model to the full dataset, and (ii) averages from fitting the model to the data-split modeling subsets. The difference can be attributed to significant outliers among the high $\ln(PCT_B^{NL})$ data which, when in the validation sets, influenced R^2_v and $RMSE_v$.

The statistics from evaluating the predictive performance of the 22-term reduced PQM model for $\ln(PCT_B^{NL})$ on the six evaluation subsets of modeling glasses (see Section 3.1.3) are given on the right side of Table 3.7. The R^2 statistics for the six evaluation subsets (0.7145 to 0.8491) are similar to the R^2 statistic for the whole modeling dataset (0.7762), with the $HiNa_2O$ set having the lowest $R^2_{Eval} = 0.7145$, which is still relatively high. The LP2OL evaluation set has the highest R^2_{Eval} of 0.8491.

Table 3.7. Coefficients and Performance Summary for 22-Term Bias Corrected Partial Quadratic Mixture Model on the Natural Logarithm of Normalized PCT Boron Loss from LAW Glasses

$\ln(PCT_B^{NL})$ 22-Term bcPQM Model Term	Coefficient Estimate	Coefficient Stand. Err.	Modeling Data Statistic, 690 Glasses ^(a)				Value
Al ₂ O ₃	-29.5323	2.7881	R ²				0.7762
B ₂ O ₃	5.9849	0.5609	R ² _A				0.7692
CaO	8.3534	1.2792	RMSE				0.3954
Fe ₂ O ₃	0.9519	0.4879	Model LOF p-value				<0.0001
K ₂ O	6.7807	0.6464					
Li ₂ O	24.2726	2.0446					
MgO	13.8911	1.1780					
Na ₂ O	8.6740	0.5846					
SiO ₂	-4.4655	0.2632					
SnO ₂	-7.6174	0.8306					
TiO ₂	-8.6853	1.4078					
V ₂ O ₅	9.6149	1.5043					
ZnO	-2.0873	0.9961					
ZrO ₂	0.4532	0.6662					
Others	0.0176	1.0038					
Al ₂ O ₃ ×Al ₂ O ₃	121.2960	15.4798					
Al ₂ O ₃ ×Li ₂ O	-156.1213	21.2580					
CaO×CaO	-96.9262	11.6159					
CaO×V ₂ O ₅	-147.9209	26.0555					
<i>c</i>	-0.7193	0.05273561					
<i>s</i> ₀	1.6836	0.18933406					
Δ <i>s</i>	0.5869	0.1585 ^(d)					
<i>s</i>	2.2705 ^(e)						
Data Splitting Statistic ^(a,f)	DS1	DS2	DS3	DS4	DS5	Average	
R ²	0.7987	0.7807	0.7714	0.7679	0.7906	0.7819	
R ² _A	0.7911	0.7724	0.7628	0.7592	0.7827	0.7736	
RMSE	0.3759	0.3912	0.3985	0.4002	0.3855	0.3903	
R ² _V	0.6451	0.7112	0.7772	0.8234	0.5698	0.7053	
RMSE _V	0.4889	0.4484	0.3978	0.3598	0.5231	0.4436	

Evaluation Set		
(# Glasses) ^(b)	R ² _{Eval}	RMSE _{Eval}
WTP (289)	0.7312	0.3637
ORP (309)	0.7356	0.4108
LP2OL (120)	0.7553	0.4253
LP123 (92)	0.8491	0.5203
HiNa ₂ O (232)	0.7145	0.4020
HiSO ₃ (110)	0.7776	0.4332

(a) The model evaluation statistics are defined in Section B.3 of Appendix B. The model validation statistics are defined in Section B.5.

(b) The six sets of LAW evaluation glasses are discussed in Sections 2.4 and 3.1.3.

(c) For the 22-term bcPQM model, the “Others” component includes any components not separately listed.

(d) The standard error in Δ*s* is described in Section 3.6

(e) *s* = *s*₀ + Δ*s*. The associated error for *s* is obtained by propagation of errors in Section 3.6.

(f) The evaluation and validation statistics calculated for data-splits are defined the same as for separate modeling and validation sets. Section 3.1.2 describes how the modeling dataset was split into modeling and validation subsets.

Figure 3.13 displays for the 22-term bcPQM model of $\ln(PCT_B^{NL})$ the standardized residuals plotted versus the data index (a sequential numbering of the modeling data points), with different plotting symbols representing the different groups of LAW glasses discussed in Section 2.3. Figure 3.13 shows a similar degree of scatter for all data subsets, with slightly broader scatter in WTP dataset near indices 180 to 200 and in the ORP dataset near indices 490 to 510.

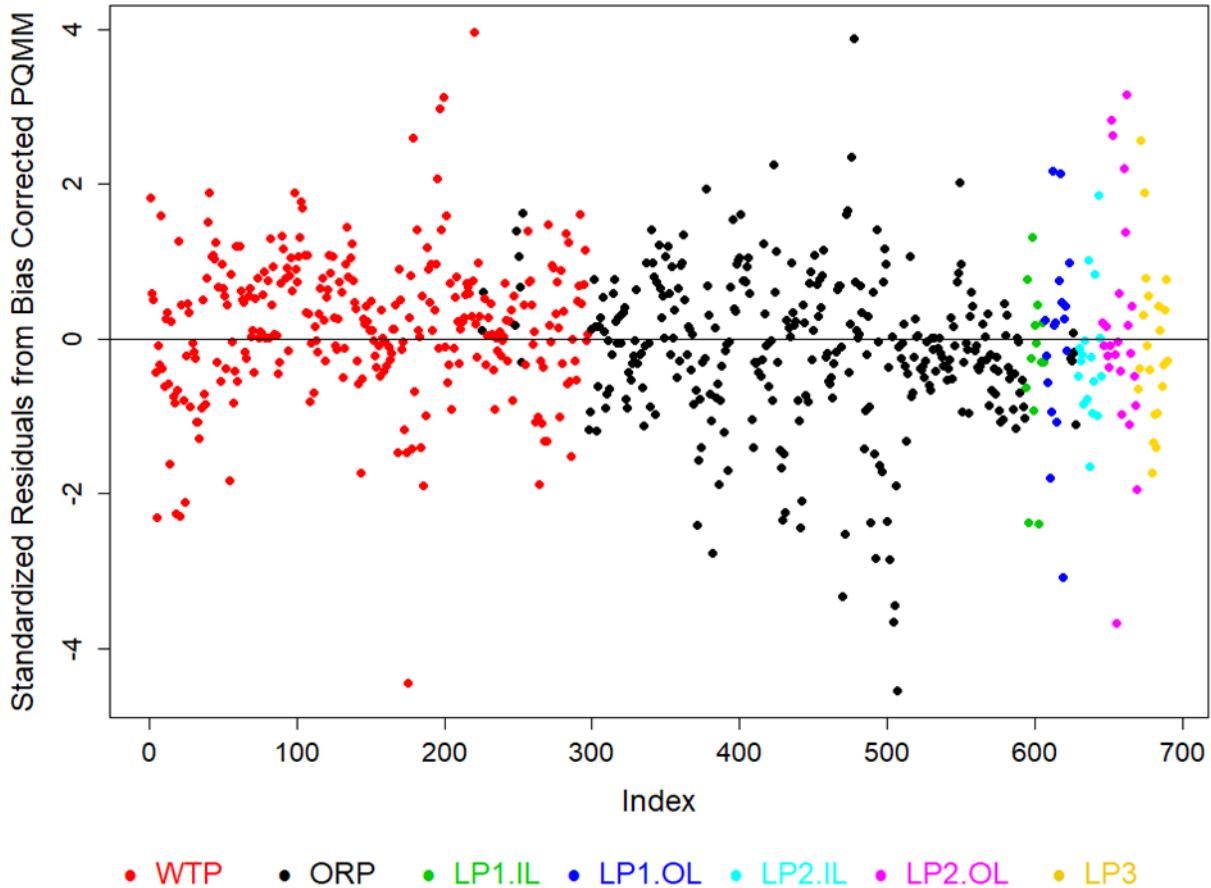


Figure 3.13. Standardized Residuals Plot for the 22-Term bcPQM Model on the Natural Logarithm of Normalized PCT Boron Loss from LAW Glasses

Figure 3.14 displays the PvM plot for the 690-glass modeling dataset using the 22-term bcPQM model on $\ln(PCT_B^{NL})$. Figure 3.14 differs from the PvM plot for the 19-term PQM model in Figure 3.10 in that the higher values ($> 0.6 \ln[g/m^2]$) do not show bias. Also, there is a slightly larger scatter of predicted data about the 45° line in this same region.

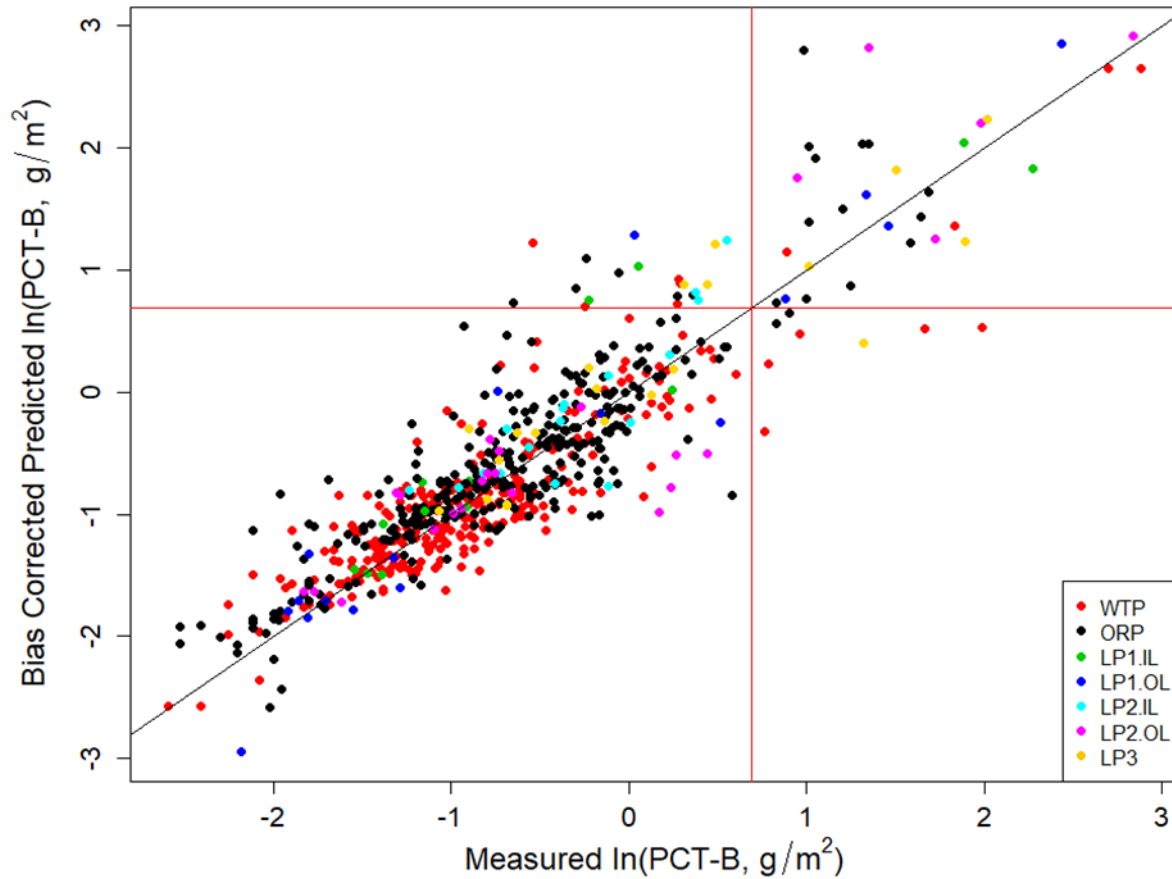


Figure 3.14. Predicted versus Measured Plot for the 690-glass Modeling Dataset Using the 22-Term bcPQM Model on the Natural Logarithm of Normalized PCT Boron Loss from LAW Glasses

Figure 3.15 displays PvM plots using the 22-term bcPQM model in Table 3.7 applied to the five evaluation subsets discussed in Section 3.1.3. Each plot in the figure contains the evaluation R^2 and RMSE values for the corresponding evaluation subset. Figure 3.15 shows that the 22-term bcPQM model fit to the 690-glass modeling dataset generally predicts reasonably well for all the evaluation subsets with R^2_{Eval} values ranging 0.7145 to 0.8491.

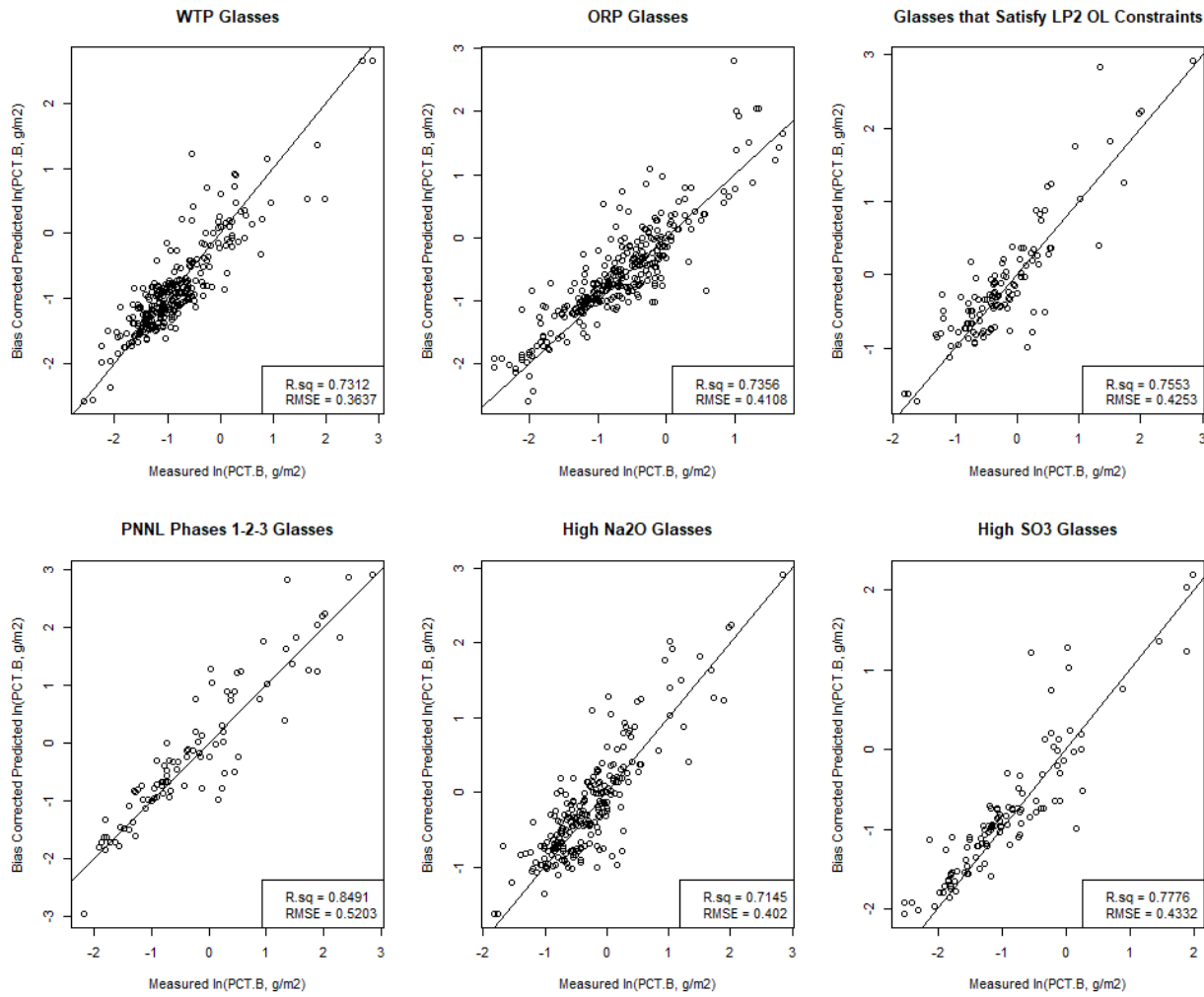


Figure 3.15. Predicted versus Measured Plots for the Six Evaluation Subsets Using the 22-Term bcPQM Model on the Natural Logarithm of Normalized PCT Boron Loss from LAW Glasses

Figure 3.16 displays the response trace plot (see Section B.4.1 of Appendix B) for the 22-term bcPQM model on $\ln(PCT_B^{NL})$. Figure 3.16 shows that MgO , Li_2O , Na_2O , K_2O , and B_2O_3 are predicted to increase $\ln(PCT_B^{NL})$ the most, while Al_2O_3 and SiO_2 are predicted to decrease $\ln(PCT_B^{NL})$ the most. The impact of bias correction is clearly seen in the dramatic change in SiO_2 , Al_2O_3 , MgO , Li_2O , Na_2O , K_2O , and B_2O_3 effects. V_2O_5 , Fe_2O_3 , Others, ZrO_2 , and ZnO have predicted response traces with small to negligible slopes, indicating those components are predicted to have small to negligible effects on $\ln(PCT_B^{NL})$.

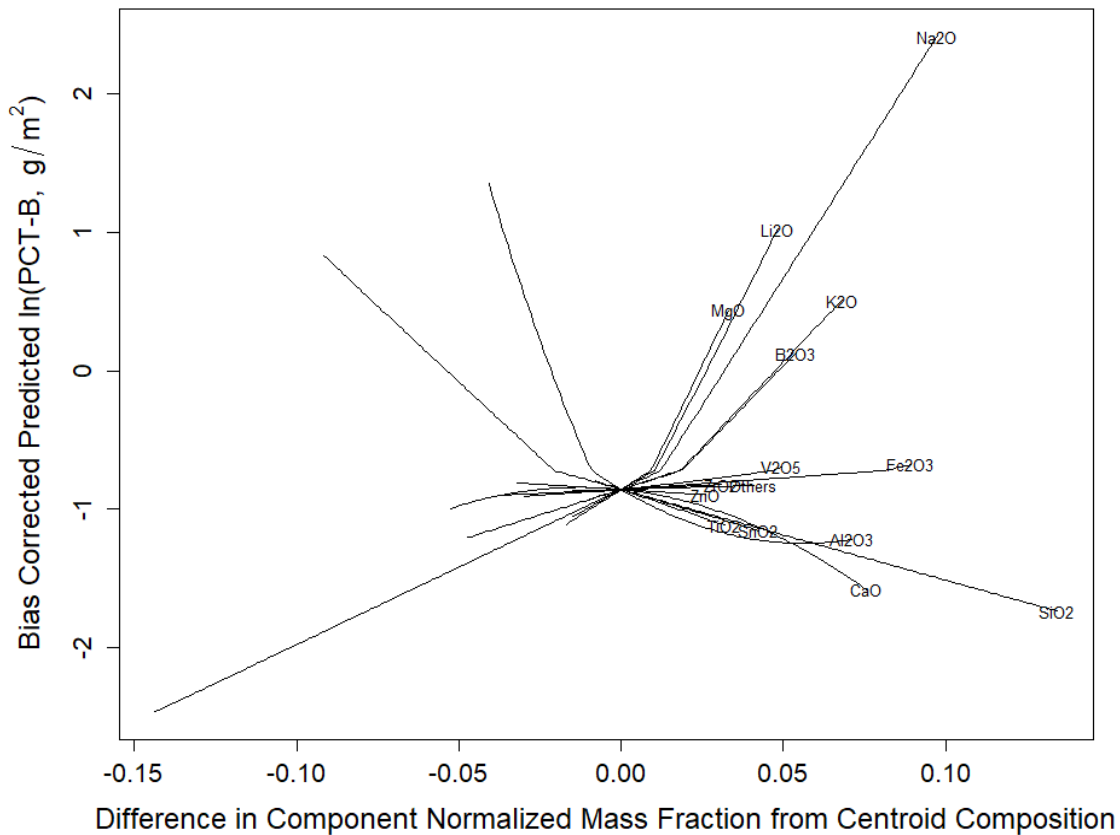


Figure 3.16. Response Trace Plot for 22-Term bcPQM Model on the Natural Logarithm of Normalized PCT Boron Loss from LAW Glasses

3.4 Property-Composition Model Results for PCT Sodium Normalized Loss from LAW Glasses

This section discusses the results of fitting several different mixture models $\ln(PCT_{Na}^{NL} [g/m^2])$ to LAW glass compositions. Sections 3.4.1 and 3.4.2 present the results of modeling $\ln(PCT_{Na}^{NL})$ using 20-component FLM and RLM models, respectively. Section 3.4.3 presents the results of modeling $\ln(PCT_B^{NL})$ using a PQM model based on a reduced set of 15 mixture components. Section 3.4.4 presents the result of modeling $\ln(PCT_{Na}^{NL})$ using a 19-term PQM model with a bias correction at high PCT response values.

3.4.1 Results from the 20-Component Full Linear Mixture Model for the Natural Logarithm of Normalized PCT Sodium Loss from LAW Glasses

As the initial step in PCT_{Na}^{NL} -composition model development, a FLM model in the 20 components identified in Section 3.1.1 was fit to the modeling data (690 glasses) OLS to the 20 glass components. This model form was a reasonable starting point based on the previous work modeling $\ln(PCT_{Na}^{NL})$ from LAW glasses (Hrma et al. 1994; Piepel et al. 2007) and provided a basis for appropriate model modifications.

Table 3.8 contains the results from the 20-component FLM model for $\ln(PCT_{Na}^{NL})$. Table 3.8 lists the model coefficients, standard deviations of the coefficients, and model performance summaries for the 20-component FLM model using the modeling dataset (690 LAW glasses).

The $R^2 = 0.7370$, $R^2_A = 0.7295$, and $R^2_P = 0.7137$ statistics (see Section B.3 of Appendix B) in Table 3.8 show that (i) the 20-component FLM model does not fit the $\ln(PCT_{Na}^{NL})$ data in the 690-glass modeling dataset well, (ii) there are several unneeded model terms (evidenced by the high standard errors relative to the reported coefficient estimates), and (iii) there are not any highly influential data points (confirmed in the diagnostic graphics described in Section B.3 and by the fact that the R^2 -predicted value is close to the R^2 -adjusted and R^2 values for this model). The RMSE = 0.3705 is significantly larger than the pooled glass batching and PCT_{Na}^{NL} determination uncertainty (SD = 0.1845 in $\ln[g/m^2]$ units) estimated from replicates in Table 3.3. This suggests that the 20-component FLM model has a statistically significant LOF, which is confirmed by the model LOF p-value < 0.0001 in Table 3.8. See Section B.3 for discussion of the statistical test for model LOF.

Table 3.8. Coefficients and Performance Summary for the 20-Component Full Linear Mixture Model on the Natural Logarithm of Normalized PCT Sodium Loss from LAW Glasses

$\ln(PCT_{Na}^{NL})$ 20-Component FLM Model Term	Coefficient Estimate	Coefficient Stand. Err.
Al ₂ O ₃	-15.2197	0.7107
B ₂ O ₃	5.0710	0.7410
CaO	-0.1461	0.5395
Cl	14.9347	6.2516
Cr ₂ O ₃	33.4551	8.7126
F	26.0052	9.3366
Fe ₂ O ₃	-0.3571	0.7878
K ₂ O	10.3999	0.9431
Li ₂ O	24.9567	1.7308
MgO	15.9769	1.6210
Na ₂ O	13.3667	0.5093
P ₂ O ₅	-14.2654	2.7815
SO ₃	-25.4051	5.9988
SiO ₂	-6.0002	0.3029
SnO ₂	-10.0191	1.3777
TiO ₂	-12.4034	2.1517
V ₂ O ₅	4.7078	1.5350
ZnO	-2.6238	1.6726
ZrO ₂	-4.6351	1.1585
Others	-56.8364	20.8327
Modeling Data Statistics, 690 Glasses		Value
R^2		0.7370
R^2_A		0.7295
R^2_P		0.7137
RMSE		0.3705
Model LOF p-value		<0.0001
(a) For the 20-component FLM model, the “Others” component includes any components not separately listed.		
(b) The model evaluation statistics are defined in Section B.3 of Appendix B. The model validation statistics are defined in Section B.5.		

Figure 3.17 shows the PvM plot for the 690-glass modeling dataset using the 20-component FLM model for $\ln(PCT_{Na}^{NL})$. The plot illustrates that the 20-component FLM model significantly under-predicts PCT_{Na}^{NL} above the limit of 2 g/m² (shown with red lines). The model also under-predicts glasses with the lowest PCT_{Na}^{NL} values, although this is not a major concern for LAW Facility application.

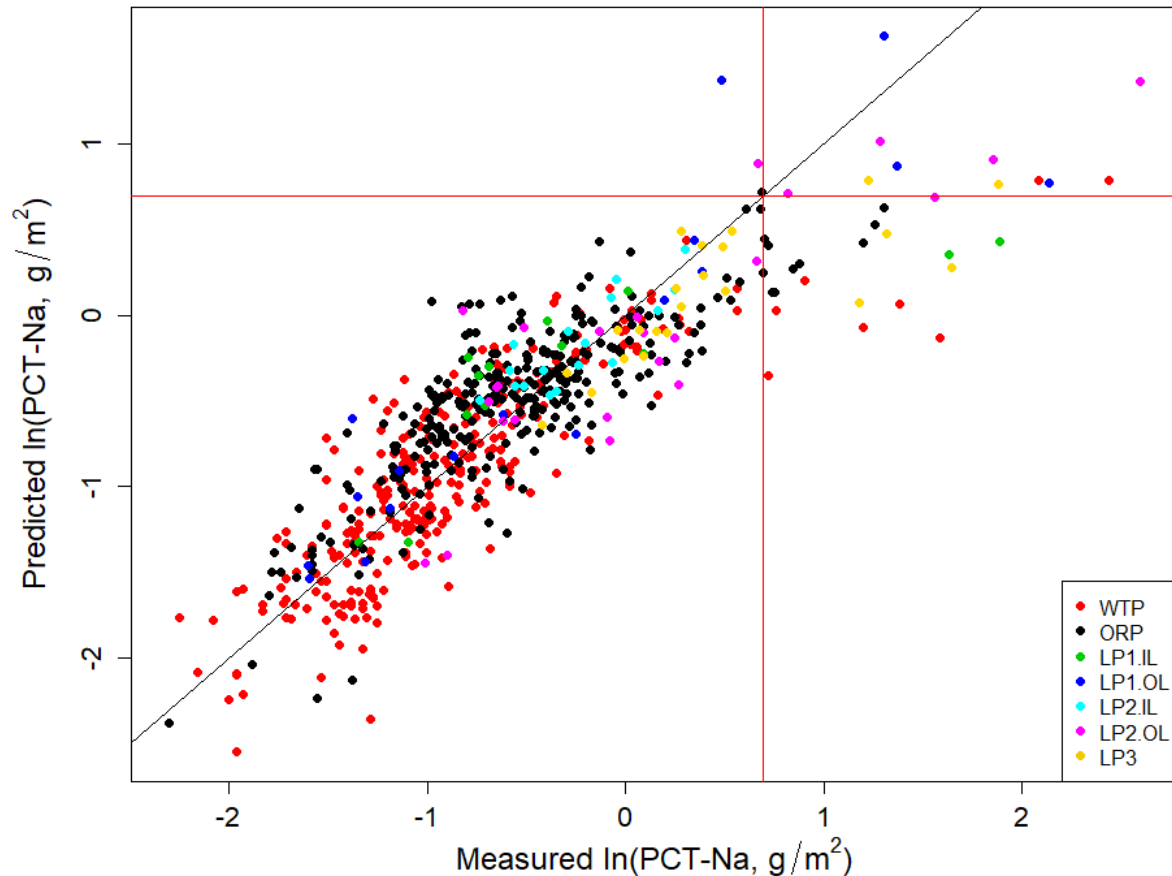


Figure 3.17. Predicted versus Measured Plot for the 690-Glass Modeling Dataset Using the 20-Component Full Linear Mixture Model on the Natural Logarithm of PCT_{Na}^{NL} from LAW Glasses. The red lines represent the WTP contract limit of 2 g/m², or 0.6931 ln(g/m²).

The results in Table 3.8 and Figure 3.17 indicate that the 20-term FLM produces unacceptable results, particularly in the region of PCT_{Na}^{NL} values that are of most interest to the project. The majority of glasses at or above the WTP contract limit of 2 g/m² are underpredicted by the 20-term FLM model.

The model in Table 3.8, fit to the 690-glass PCT_{Na}^{NL} modeling dataset, provides a starting point for improvement (e.g., addition of non-linear terms). The 20-component FLM model was used to produce the response trace plot (see Section B.4.1 in Appendix B) shown in Figure 3.18. The average glass composition of the 1074 glasses in the compiled database discussed in Section 2.5 was used as the REFMIX (see Section B.4.1) in response trace plots for every property. The glass composition of the REFMIX is listed in Table 2.3.

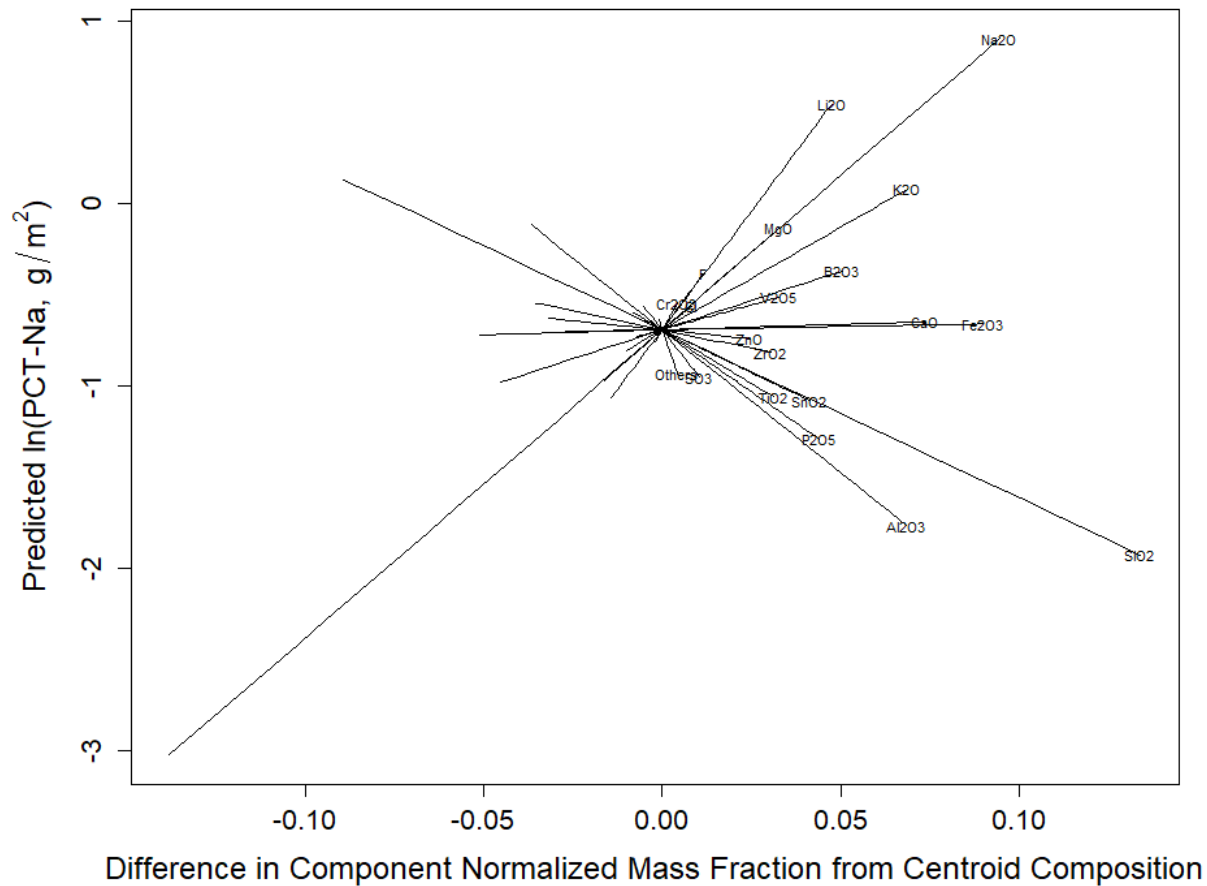


Figure 3.18. Response Trace Plot for the 20-Component Full Linear Mixture Model on the Natural Logarithm of Normalized PCT Sodium Loss from LAW Glasses

The response trace plot in Figure 3.18 shows that Li_2O , Na_2O , MgO , K_2O , and B_2O_3 are predicted to increase $\ln(PCT_{Na}^{NL})$, while Al_2O_3 , P_2O_5 , TiO_2 , SnO_2 , and SiO_2 are predicted to decrease $\ln(PCT_{Na}^{NL})$. The impacts of Cr_2O_3 , F, Cl, SO_3 , and Others are significantly larger than expected based on previous model attempts and knowledge of the chemistry of PCT responses. It is likely that the slopes associated with these terms are exaggerated due more to peculiarities in the data than actual component effects. To test this hypothesis, the terms Cr_2O_3 , F, Cl, and SO_3 were combined into Others in subsection 3.4.2 to determine if the fit statistics are significantly impacted. If significant impacts are identified, then further research would be required to experimentally verify those results.

Due to the poor predictive performance of the 20-term FLM in the region of interest, no further analysis of this model was carried out, focusing instead on the development of a better model.

3.4.2 Results from the 15-Component Reduced Linear Mixture Model for the Natural Logarithm of Normalized PCT Sodium Loss from LAW Glasses

The 20-component FLM model for $\ln(PCT_{Na}^{NL})$ presented in Section 3.4.1 contains components that do not significantly contribute to predicting $\ln(PCT_{Na}^{NL})$ and some components with unexpectedly strong effects, so model reduction was performed prior to selection of higher order terms. RLM models involving fewer

than the 20 components were considered. To reduce the number of terms, (i) the sequential F-test model reduction approach (see Section B.4.1 of Appendix B; Piepel and Cooley 2006) and (ii) selection based on knowledge of PCT chemical effect were used. Using the F-test method and a threshold of 0.001, SO_3 , P_2O_5 , TiO_2 , and SnO_2 were determined to be the least significant terms and were combined to Others. This resulted in significant and non-defensible effects of Cl, Cr_2O_3 , F, and Others (similar to those in the FLM model in Section 3.4.1). Cl, Cr_2O_3 , and F have the smallest overall concentration ranges ($0.0000 \leq \text{Cl} \leq 0.0117$, $0.0000 \leq \text{Cr}_2\text{O}_3 \leq 0.0063$, and $0.0000 \leq \text{F} \leq 0.0130$, mf). Cl is also volatile to differing extents in glass with a mean retention of roughly 70 % in typical crucible melts (with a broad distribution of retention factors). Neither component is expected to have a significant effect on PCT responses. There is a potential for Cl and F to slightly decrease pH of PCT solution, thereby slightly reducing PCT responses. With such strong predicted effect of these three components, counter to previous observations, independent experimental verification is needed prior to including in the model. Additionally, the combination of SnO_2 and TiO_2 with Others caused the combined Others term to have a strong negative effect on $\ln(PCT_{Na}^{NL})$ with most other components to have positive effects. The F-test method, after forcing Cl, Cr_2O_3 , and F into Others resulted in Cl, Cr_2O_3 , F, P_2O_5 , and SO_3 to be combined with Others resulting in a 15-term RLM model.

Table 3.9 contains the results from the 15-component RLM model for $\ln(PCT_{Na}^{NL})$. Table 3.9 lists the model coefficients, standard deviations of the coefficients, and model performance summaries for the RLM model using the modeling dataset (690 LAW glasses).

The $R^2 = 0.7110$, $R_A^2 = 0.7050$, and $R_P^2 = 0.6910$ statistics (see Section B.3 of Appendix B) in Table 3.9 show that the 15-component RLM model does not fit the $\ln(PCT_{Na}^{NL})$ data in the 690-glass modeling dataset well. The $\text{RMSE} = 0.3869$ is significantly larger than the pooled glass batching and PCT_{Na}^{NL} determination uncertainty ($\text{SD} = 0.1845$ in $\ln[\text{g/m}^2]$ units) estimated from replicates in Table 3.3. This suggests that the 15-component RLM model has a statistically significant LOF, which is confirmed by the model LOF p-value < 0.0001 in Table 3.9. See Section B.3 for discussion of the statistical test for model LOF.

Table 3.9. Coefficients and Performance Summary for the 15-Component Reduced Linear Mixture Model on the Natural Logarithm of Normalized PCT Sodium Loss from LAW Glasses

$\ln(PCT_{Na}^{NL})$ 15-Component RLM Model Term	Coefficient Estimate	Coefficient Std. Err.
Al ₂ O ₃	-15.0672	0.7305
B ₂ O ₃	4.5199	0.7657
CaO	-0.1463	0.5439
Fe ₂ O ₃	-0.4765	0.7830
K ₂ O	11.2954	0.9477
Li ₂ O	24.4653	1.7708
MgO	15.8399	1.6825
Na ₂ O	13.8507	0.5177
SiO ₂	-6.3773	0.3067
SnO ₂	-6.6824	1.3495
TiO ₂	-10.3655	2.1608
V ₂ O ₅	3.1413	1.5227
ZnO	-1.8021	1.7360
ZrO ₂	-3.5106	1.1688
Others ^(a)	-2.0976	1.7916
Modeling Data Statistics, 690 Glasses ^(b)	Value	
R ²	0.7110	
R ² _A	0.7050	
R ² _P	0.6910	
RMSE	0.3869	
Model LOF p-value	<0.0001	
<p>(a) For the 15-component FLM model, the “Others” component includes the Others component from the FLM model plus Cl, Cr₂O₃, F, P₂O₅, and SO₃.</p> <p>(b) The model evaluation statistics are defined in Section B.3 of Appendix B. The model validation statistics are defined in Section B.5.</p>		

Figure 3.19 shows the PvM plot for the 690-glass modeling dataset using the 15-component RLM model for $\ln(PCT_{Na}^{NL})$. The plot illustrates that the 15-component RLM model significantly under-predicts PCT_{Na}^{NL} above the limit of 2 g/m² (shown with red lines). The model also under-predicts glasses with the lowest PCT_{Na}^{NL} values, although this is not a major concern for WTP LAW Facility application.

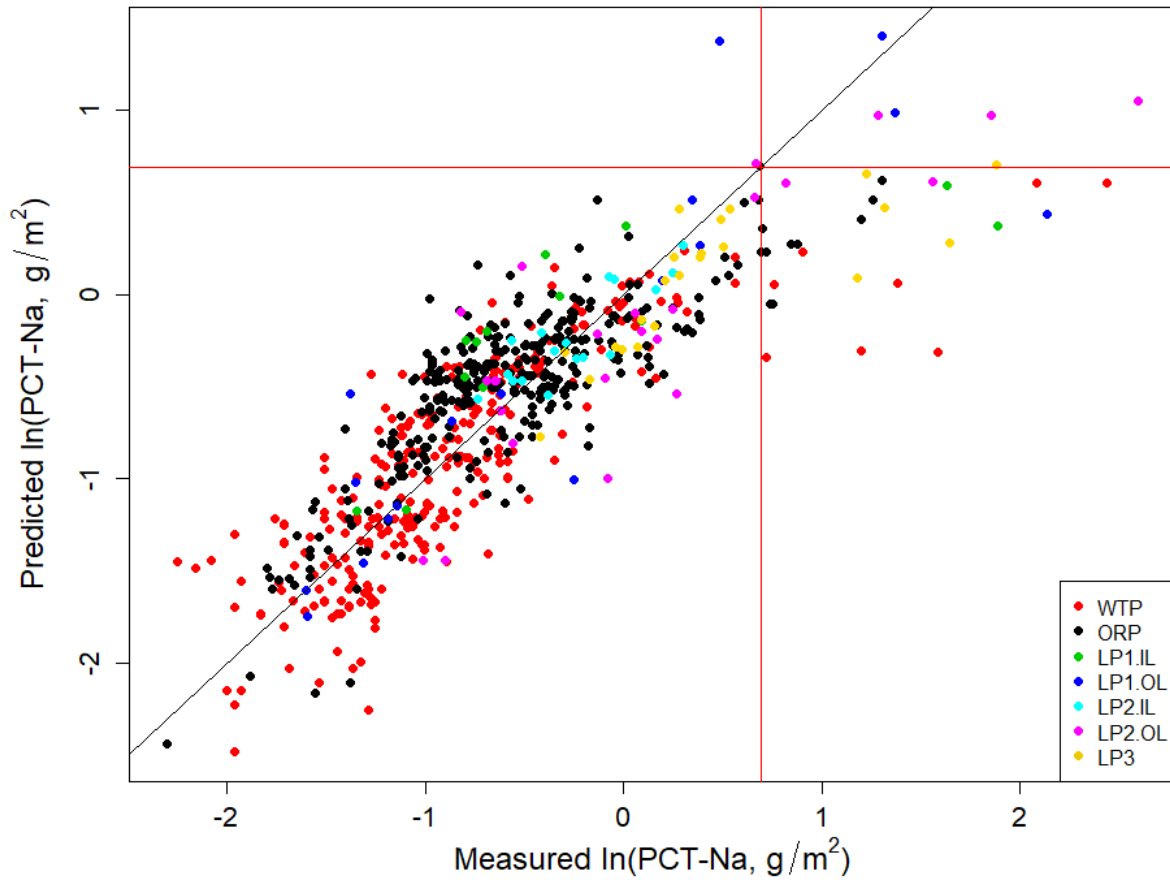


Figure 3.19. Predicted versus Measured Plot for the 690-Glass Modeling Dataset Using the 15-Component Reduced Linear Mixture Model on the Natural Logarithm of PCT_{Na}^{NL} from LAW Glasses. The red lines represent the WTP contract limit of 2 g/m², or 0.6931 ln(g/m²).

The results in Table 3.9 and Figure 3.19 indicate that the 15-term RLM produces unacceptable results, particularly in the region of PCT_{Na}^{NL} values that are of most interest to the project. The majority of glasses at or above the WTP contract limit of 2 g/m² are underpredicted by the 15-term RLM model.

The model in Table 3.9, fit to the 690-glass PCT_{Na}^{NL} modeling dataset, provides a starting point for improvement (e.g., addition of non-linear terms). The 15-component RLM model was used to produce the response trace plot (see Section B.4.1 in Appendix B) shown in Figure 3.20. The average glass composition of the 1074 glasses in the compiled database discussed in Section 2.5 was used as the REFMIX (see Section B.4.1) in response trace plots for every property. The glass composition of the REFMIX is listed in Table 2.3.

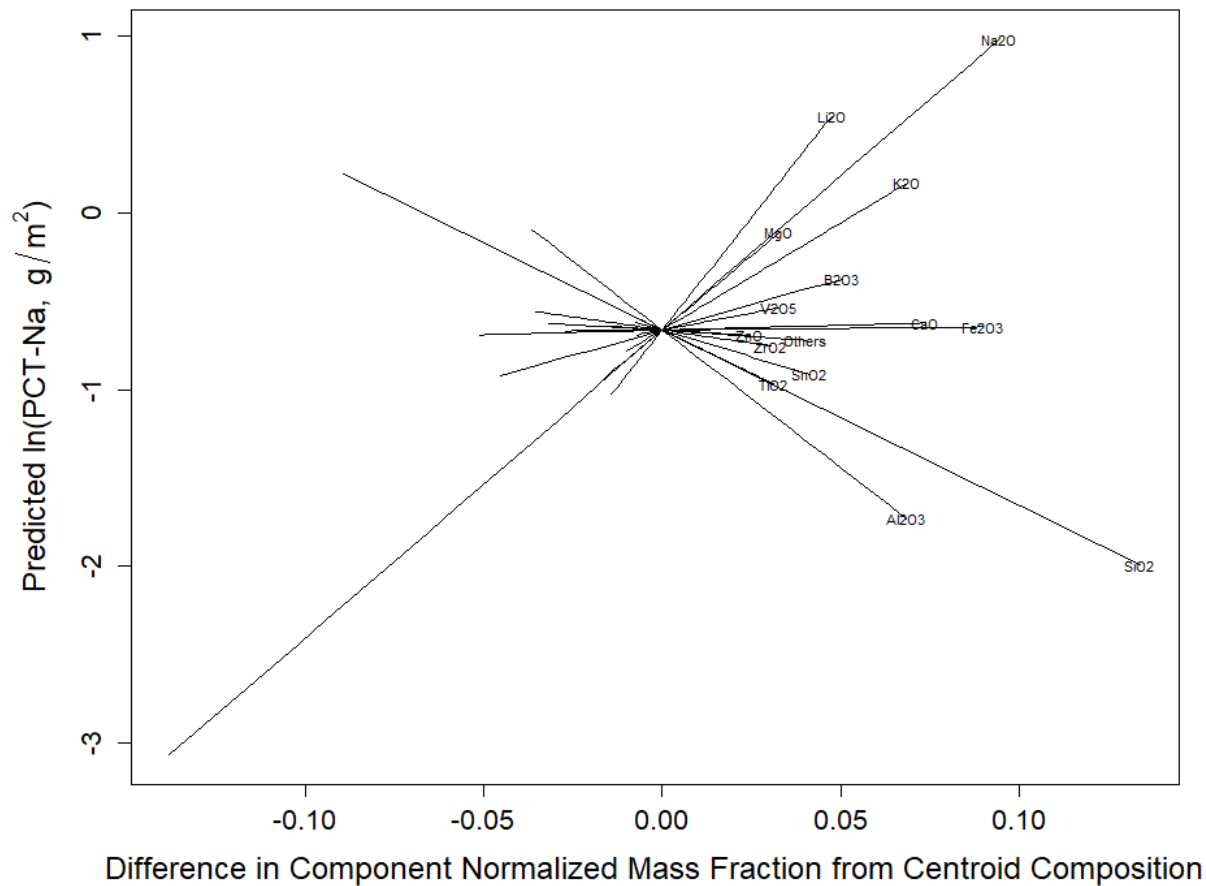


Figure 3.20. Response Trace Plot for the 15-Component Reduced Linear Mixture Model on the Natural Logarithm of Normalized PCT Sodium Loss from LAW Glasses

The response trace plot in Figure 3.20 shows that Li_2O , Na_2O , MgO , K_2O , and B_2O_3 are predicted to increase $\ln(\text{PCT}_{\text{Na}}^{\text{NL}})$ the most, while Al_2O_3 , TiO_2 , SiO_2 , and SnO_2 are predicted to decrease $\ln(\text{PCT}_{\text{Na}}^{\text{NL}})$ the most. These agree with previous model attempts and knowledge of the chemistry of PCT responses. Due to the poor predictive performance of the 15-term RLM in the region of interest, no further analysis of this model was carried out, focusing instead on the development of a better model based on these same 15 components.

3.4.3 Results from a Reduced Partial Quadratic Mixture Model for the Natural Logarithm of Normalized PCT Sodium Loss from LAW Glasses

Reduced PQM models were investigated in an effort to improve the 15-component RLM model for predicting $\ln(\text{PCT}_{\text{Na}}^{\text{NL}})$. Past experience with developing and validating PQM models has indicated that adding too many quadratic terms tends to over-fit the model development dataset and degrade predictive performance for new glasses. So, a process of identifying as few as possible second-order terms while improving model fit statistics was performed as follows:

1. Regressions were performed to fit reduced partial quadratic models involving all possible subsets of 1, 2, 3, or 4 second-order terms.

2. The resulting model performance statistics (R-squared and RMSE values) were then examined to see which second-order terms were most beneficial to model performance and how many second-order terms to include.
3. The RMSE values from the top candidate models were plotted as a function of the number of second order terms (0 to 4) to identify where the point of diminishing returns was.
4. The reduced PQM model with the number of terms just before the point of diminishing returns was selected as the final reduced PQM model.

The MAXR criterion (see Section B.4.2 of Appendix B) was also attempted as a means of selecting second-order terms. Both methods resulted in the same selection as “best” four second-order terms: $\text{Na}_2\text{O} \times \text{SiO}_2$, $\text{CaO} \times \text{V}_2\text{O}_5$, $\text{Al}_2\text{O}_3 \times \text{Al}_2\text{O}_3$, and $\text{V}_2\text{O}_5 \times \text{V}_2\text{O}_5$.

Ultimately, a 19-term PQM model for $\ln(PCT_{Na}^{NL})$ with 15 linear terms and 4 second-order terms (2 quadratic and 2 cross-product) was selected as including enough quadratic terms to improve the model fit, without over-fitting the model development data. Table 3.10 contains the coefficients of the 19-term PQM model for $\ln(PCT_{Na}^{NL})$ and the coefficient standard errors. Table 3.10 also includes model fit summary statistics for the 19-term PQM model.

The $R^2 = 0.7719$, $R_A^2 = 0.7658$, and $R_P^2 = 0.7511$ statistics (see Section B.3 of Appendix B) in Table 3.10 show that the 19-component PQM model fits the $\ln(PCT_{Na}^{NL})$ data in the 690-glass modeling dataset significantly better than the FLM and RLM models. The RMSE = 0.3448 is still significantly larger than the pooled glass batching and PCT_{Na}^{NL} determination uncertainty (SD = 0.1845 in $\ln[\text{g/m}^2]$ units) estimated from replicates in Table 3.3. This suggests that the 19-component PQM model has a statistically significant LOF, which is confirmed by the model LOF p-value < 0.0001 in Table 3.10. See Section B.3 for discussion of the statistical test for model LOF.

Table 3.10. Coefficients and Performance Summary for the 19-Term Partial Quadratic Mixture Model on the Natural Logarithm of Normalized PCT Sodium Loss from LAW Glasses

$\ln(PCT_{Na}^{NL})$ 19-Component PQM Model Term	Coefficient Estimate	Coefficient Stand. Err.
Al ₂ O ₃	-39.3217	4.2228
B ₂ O ₃	1.5635	0.8566
CaO	0.3470	0.8299
Fe ₂ O ₃	-3.9415	0.8109
K ₂ O	10.3966	0.9137
Li ₂ O	22.5371	1.6326
MgO	13.0612	1.5690
Na ₂ O	29.4758	2.1037
SiO ₂	-1.8303	0.6570
SnO ₂	-12.0479	1.2843
TiO ₂	-11.7384	1.9371
V ₂ O ₅	-10.3548	5.0034
ZnO	-5.7262	1.6617
ZrO ₂	-5.0914	1.1849
Others ^(a)	-4.7843	1.6441
Na ₂ O×SiO ₂	-39.2424	5.6951
CaO×V ₂ O ₅	-209.2758	35.1796
(Al ₂ O ₃) ²	130.7351	25.4185
(V ₂ O ₅) ²	689.2301	129.1334
Modeling Data Statistics, 690 Glasses ^(b)	Value	
R ²	0.7719	
R ² _A	0.7658	
R ² _P	0.7511	
RMSE	0.3448	
Model LOF p-value	<0.0001	
(a) For the 19-component PQM model, the “Others” component includes the Others component from the FLM model plus Cl, Cr ₂ O ₃ , F, P ₂ O ₅ , and SO ₃ .		
(b) The model evaluation statistics are defined in Section B.3 of Appendix B. The model validation statistics are defined in Section B.5.		

Figure 3.21 shows the PvM plot for the 690-glass modeling dataset using the 19-term PQM model for $\ln(PCT_{Na}^{NL})$. The plot illustrates that the 19-term PQM model significantly under-predicts PCT_{Na}^{NL} above the limit of 2 g/m² (shown with red lines).

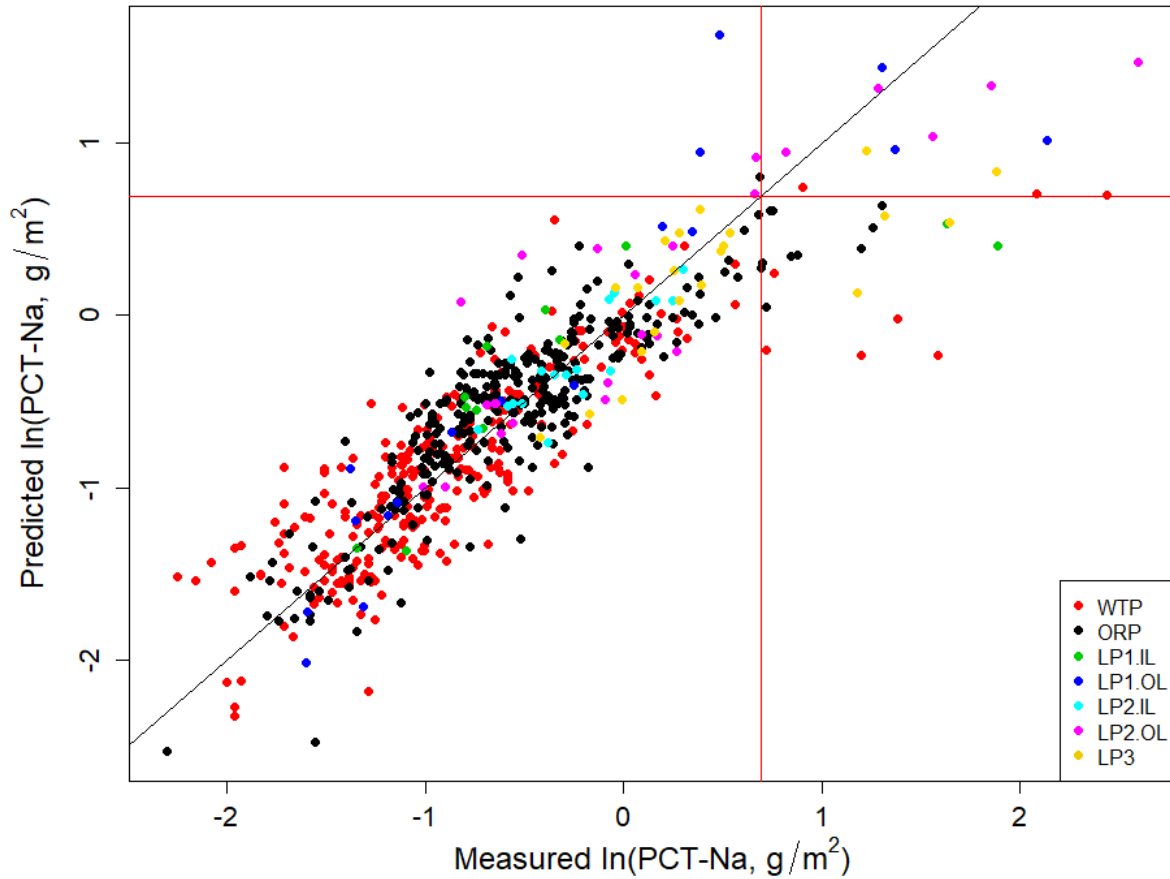


Figure 3.21. Predicted versus Measured Plot for the 690-Glass Modeling Dataset Using the 19-Term Partial Quadratic Mixture Model on the Natural Logarithm of PCT_{Na}^{NL} from LAW Glasses. The red lines represent the WTP contract limit of 2 g/m², or 0.6931 ln(g/m²).

The results in Table 3.10 and Figure 3.21 indicate that the 19-term PQM produces unacceptable results, particularly in the region of PCT_{Na}^{NL} values that are of most interest to the project. The majority of glasses at or above the WTP contract limit of 2 g/m² are underpredicted by the 19-term PQM model.

The 19-term PQM model was used to produce the response trace plot (see Section B.4.1 in Appendix B) shown in Figure 3.22. The average glass composition of the 1074 glasses in the compiled database discussed in Section 2.5 was used as the REFMIX (see Section B.4.1) in response trace plots for every property. The glass composition of the REFMIX is listed in Table 2.3.

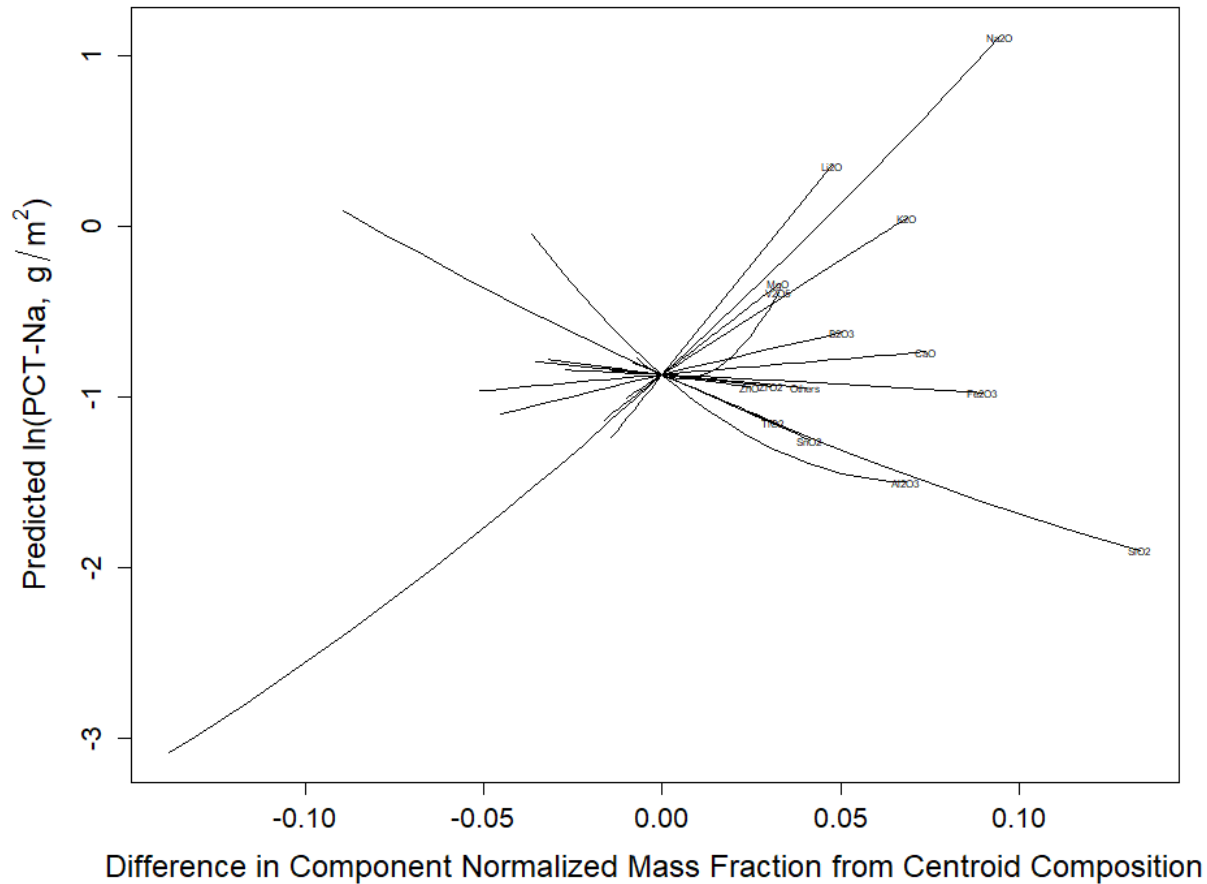


Figure 3.22. Response Trace Plot for the 19-Term Partial Quadratic Mixture Model on the Natural Logarithm of Normalized PCT Sodium Loss from LAW Glasses

The response trace plot in Figure 3.22 shows that Li_2O , Na_2O , MgO , K_2O , and V_2O_5 are predicted to increase $\ln(PCT_{Na}^{NL})$ the most, while Al_2O_3 , TiO_2 , SiO_2 , and SnO_2 are predicted to decrease $\ln(PCT_{Na}^{NL})$ the most. These agree with previous model attempts and knowledge of the chemistry of PCT responses. The non-linear impact of Al_2O_3 evident in Figure 3.22 is a well-documented trend (see, for example, Vienna and Crum 2018). A non-linear impact of V_2O_5 is also evident in Figure 3.22. Due to the poor predictive performance of the 19-term PQM in the region of interest, no further analysis of this model was carried out, focusing instead on the development of a better models.

3.4.4 Screening of Model Types for Predicting Natural Logarithm of Normalized PCT Sodium Loss from LAW Glasses

Most waste glass properties are well represented using FLM, RLM, or PQM models over sufficiently narrow composition regions. This was found to be the case for predicting $\ln(PCT_{Na}^{NL})$ of LAW glasses covering a narrower subset of the current 690 glass dataset. It is apparent by the bias seen at high $\ln(PCT_{Na}^{NL})$ responses ($>0.5 \ln[\text{g}/\text{m}^2]$) shown in Figure 3.21 that PQM is insufficient in this case. Therefore, a brief survey of model approaches for modeling properties as non-linear functions of glass composition was undertaken. Several approaches were surveyed for predicting either $\ln(PCT_{Na}^{NL})$ or categorical pass/fail of the WTP contract constraint of $PCT_{Na}^{NL} \leq 2 \text{ g}/\text{m}^2$ (P/F), including:

1. Local linear regression (LLR)
2. K-nearest neighbor (KNN) (numerical or P/F)
3. Generalized linear models (GLM)
4. Gaussian process regression (GPR)
5. Artificial neural networks (ANN)
6. Decision tree (P/F)
7. Random forest (P/F)
8. Support vector machine (P/F)
9. Linear and partial quadratic logistic regression (P/F)
10. Bias corrected PQM model (bcPQM)

Each of these methods was attempted with the same 690-glass normalized PCT sodium response dataset. The results of these modeling approaches match closely with those described in Section 3.3.4 for normalized PCT boron response. The outcome was that bcPQM models were further pursued for predicting $\ln(PCT_{Na}^{NL})$ of LAW glasses.

3.4.5 Results from a Bias Corrected Partial Quadratic Mixture Model for the Natural Logarithm of Normalized PCT Sodium Loss from LAW Glasses

The poor performance of the FLM and PQM models suggests that a method to correct prediction bias may be useful for producing usable PCT models. Bias correction methods have been investigated and applied before in the modeling of PCT (Piepel et al. 2008; Vienna and Kim 2014). The bias corrected form of the models is given by

$$\ln(\widehat{PCT}_{Na}^{NL})_{BC} = \begin{cases} \ln(\widehat{PCT}_{Na}^{NL}) & \text{if } \ln(\widehat{PCT}_{Na}^{NL}) \leq c \\ \ln(\widehat{PCT}_{Na}^{NL}) + (\ln(\widehat{PCT}_{Na}^{NL}) - c)s & \text{if } \ln(\widehat{PCT}_{Na}^{NL}) > c \end{cases} \quad (3.7)$$

where

$$\begin{aligned} \ln(\widehat{PCT}_{Na}^{NL}) &= \ln(PCT_{Na}^{NL}) \text{ predicted using PQM model prior to application of bc (ln[g/m}^2\text{)]} \\ c &= \text{estimated bias correction cut-off (ln[g/m}^2\text{)]} \\ s &= \text{estimated bias correction slope (unitless). Due to the fitting process, } s \text{ is the sum of the initial slope (} s_0 \text{) and the change in slope (} \Delta s \text{) (i.e., } s = s_0 + \Delta s \text{) as described in Section 3.6.} \end{aligned}$$

In Eq. (3.7), the bias correction applied to the predicted $\ln(\widehat{PCT}_{Na}^{NL})$ value increases or decreases linearly from zero at the cutoff with a slope given by s . Values of c and s (estimates of C and S respectively) were found using two approaches: (i) fitting Eq. (3.7) to measure $\ln(PCT_{Na}^{NL})$ using the PQM reported in Section 3.4.3, or (ii) simultaneously fitting the PQM model terms with the c and s according to

$$\ln(PCT_{Na}^{NL})_{BC} = \begin{cases} \mathbf{g}^T \boldsymbol{\beta} & \text{if } \mathbf{g}^T \boldsymbol{\beta} \leq C \\ \mathbf{g}^T \boldsymbol{\beta} + (\mathbf{g}^T \boldsymbol{\beta} - C)S & \text{if } \mathbf{g}^T \boldsymbol{\beta} > C \end{cases} + e \quad (3.8)$$

where

- β = the vector of PQM term coefficients including β_i , β_{ii} , and β_{ij} values
- \mathbf{g} = the vector of component concentrations for first order terms followed by component concentrations squared for quadratic terms and concentrations multiplied for cross-product terms (in the same order as β)
- C = bias correction cut-off ($\ln[\text{g/m}^2]$)
- S = bias correction slope ((unitless). Due to the fitting process, S is the sum of the initial slope (S_0) and the change in slope (ΔS) (i.e., $S = S_0 + \Delta S$) similar to what is described in Section 3.6 (except for the parameters, rather than the estimates).
- e = random error for each data point.

Both approaches were attempted, and the second approach was ultimately adopted because it resulted in a more optimal solution with less scatter in the data. The same first-order terms were used as in the RLM model described in Section 3.4.2. However, some of the second-order terms differed; best model fit results were obtained with $\text{Al}_2\text{O}_3 \times \text{Al}_2\text{O}_3$, $\text{CaO} \times \text{CaO}$, $\text{Al}_2\text{O}_3 \times \text{Na}_2\text{O}$, and $\text{CaO} \times \text{V}_2\text{O}_5$ (e.g., $\text{CaO} \times \text{CaO}$ replaced $\text{V}_2\text{O}_5 \times \text{V}_2\text{O}_5$). These terms are generally expected based on past PCT response modeling for LAW glasses that showed second-order terms involving Al_2O_3 , CaO , Li_2O , and Na_2O (Piepel et al. 2007, Vienna et al. 2013, Vienna et al. 2016). Second order terms containing V_2O_5 are not commonly found, but Muller et al. (2014) combined V_2O_5 into others and reported two second-order terms involving Others. Table 3.11 contains the coefficients of the 22-term bcPQM model for $\ln(PCT_{Na}^{NL})$ and the coefficient standard errors. Table 3.11 also includes model performance statistics for the 22-term bcPQM using the (i) 690-glass modeling data, (ii) data-split modeling data (as a model validation approach), and (iii) six evaluation subsets of the modeling glasses discussed in Section 3.1.3 (as a model evaluation approach).

In Table 3.11, the $\ln(PCT_{Na}^{NL})$ model fit statistics $R^2 = 0.7621$, $R^2_A = 0.7546$, and $\text{RMSE} = 0.3529$ for the 22-term bcPQM model are a small reduction over the corresponding statistics for the 19-term PQM model in Table 3.10. The small decrease in values from R^2 to R^2_A suggests that the $\ln(PCT_{Na}^{NL})$ model does not have excess terms. R^2_p , reported for other properties in this report, was not estimated for the $\ln(PCT_{Na}^{NL})$ model due to software limitations.

The RMSE in Table 3.11 is an estimate of the uncertainty [in $\ln(\text{g/m}^2)$ units] in fabricating LAW glasses and determining PCT_{Na}^{NL} if the 22-term bcPQM model does not have statistically significant LOF. The $\text{RMSE} = 0.3529$ for the bcPQM model fitted to the 690-glass modeling dataset is slightly larger than the corresponding value for the 19-term PQM model ($\text{RMSE} = 0.3448$) in Table 3.10, indicating a poorer fit to the data by bcPQM. The RMSE value is roughly double the pooled replicate SD in $\ln(\text{g/m}^2)$ units of 0.1845 in Table 3.3. These observations suggest that the 22-term bcPQM model does have a significant model LOF, which is confirmed by the LOF test p-value < 0.0001 in Table 3.11. See Section B.3 of Appendix B for discussion of the statistical test for model LOF.

At the bottom right of Table 3.11, the average model-fit statistics (R^2 , R^2_A , and RMSE) over the five data-splits are close to the statistics obtained from fitting the 22-term bcPQM model for $\ln(PCT_{Na}^{NL})$ to all 690 glasses in the modeling dataset. The data-split validation statistics (R^2_v and RMSE_v) are slightly worse than the R^2 and RMSE values from fitting the model to the full dataset. The difference can be attributed to significant outliers among the high $\ln(PCT_{Na}^{NL})$ data, which, when in the validation sets, influenced R^2_v and RMSE_v .

The statistics from evaluating the predictive performance of the 22-term bias corrected reduced PQM model for $\ln(PCT_{Na}^{NL})$ on the six evaluation subsets of modeling glasses (see Section 3.1.3) are given on

the right side of Table 3.11. The R^2 statistics for five of the six evaluation subsets (0.7166 to 0.8022) are similar to the R^2 statistic for the whole modeling dataset (0.7621). The exception is the WTP evaluation subset, with $R^2_{\text{Eval}} = 0.6756$, which is relatively low. The new models in this report are intended to predict well for LAW glasses with higher waste loadings, and still predict acceptably well for glasses with lower waste loadings (the older WTP glasses).

Table 3.11. Coefficients and Performance Summary for 22-Term Bias Corrected Partial Quadratic Mixture Model on the Natural Logarithm of Normalized PCT Sodium Loss from LAW Glasses

$\ln(PCT_{Na}^{NL})$ 22-Term bcPQM Model Term	Coefficient Estimate	Coefficient Stand. Err.	Modeling Data Statistic, 690 Glasses ^(a)			
Al ₂ O ₃	-31.8140	2.4885	R ²		0.7621	
B ₂ O ₃	3.2631	0.3738	R ² _A		0.7546	
CaO	5.5241	1.0402	RMSE		0.3529	
Fe ₂ O ₃	-0.0973	0.3951	Model LOF p-value		<0.0001	
K ₂ O	7.6834	0.5886				
Li ₂ O	13.4028	1.1441				
MgO	8.8211	0.8748				
Na ₂ O	6.1643	0.6263				
SiO ₂	-3.1590	0.2218				
SnO ₂	-5.3964	0.6736				
TiO ₂	-3.5008	1.0960				
V ₂ O ₅	8.6155	1.2230				
ZnO	-1.1891	0.7800				
ZrO ₂	-0.4027	0.4953				
Others	0.7336	0.8105				
Al ₂ O ₃ ×Al ₂ O ₃	85.1327	13.3262				
CaO×CaO	-41.0621	8.8831				
CaO×V ₂ O ₅	-106.4057	19.0477				
Al ₂ O ₃ ×Na ₂ O	44.4157	6.4474				
<i>c</i>	-0.5891	0.04210215				
<i>s</i> ₀	1.9108	0.20861944				
Δs	0.9457	0.2373 ^(d)				
<i>s</i>	2.8565 ^(e)					
Evaluation Set (# Glasses) ^(b)			R ² _{Eval}	RMSE _{Eval}		
WTP (288)			0.6756	0.3432		
ORP (309)			0.7674	0.3195		
LP2OL (121)			0.7442	0.4191		
LP123 (93)			0.8022	0.5441		
HiNa ₂ O (233)			0.7166	0.3903		
HiSO ₃ (110)			0.7855	0.3978		
Data Splitting Statistic ^(a,f)						
DS1	DS2	DS3	DS4	DS5	Average	
R ²	0.7711	0.7725	0.7697	0.7380	0.7735	0.7650
R ² _A	0.7625	0.7639	0.7610	0.7282	0.7649	0.7561
RMSE	0.3468	0.3447	0.3459	0.3669	0.3464	0.3502
R ² _V	0.7131	0.7547	0.6990	0.8019	0.6128	0.7163
RMSE _V	0.3823	0.3587	0.4027	0.3346	0.4340	0.3824

(a) The model evaluation statistics are defined in Section B.3 of Appendix B. The model validation statistics are defined in Section B.5.

(b) The six sets of LAW evaluation glasses are discussed in Sections 2.4 and 3.1.3.

(c) For the 22-term bcPQM model, the “Others” component includes any components not separately listed.

(d) The standard error in Δs is described in Section 3.6

(e) $s = s_0 + \Delta s$. The associated error for *s* is obtained by propagation of errors in Section 3.6.

(f) The evaluation and validation statistics calculated for data-splits are defined the same as for separate modeling and validation sets. Section 3.1.2 describes how the modeling dataset was split into modeling and validation subsets.

Figure 3.23 displays, for the 22-term bcPQM model of $\ln(PCT_{Na}^{NL})$, the standardized residuals plotted versus the data index (a sequential numbering of the modeling data points), with different plotting symbols representing the different groups of LAW glasses discussed in Section 2.3. Figure 3.23 shows similar scatter for all data subsets.

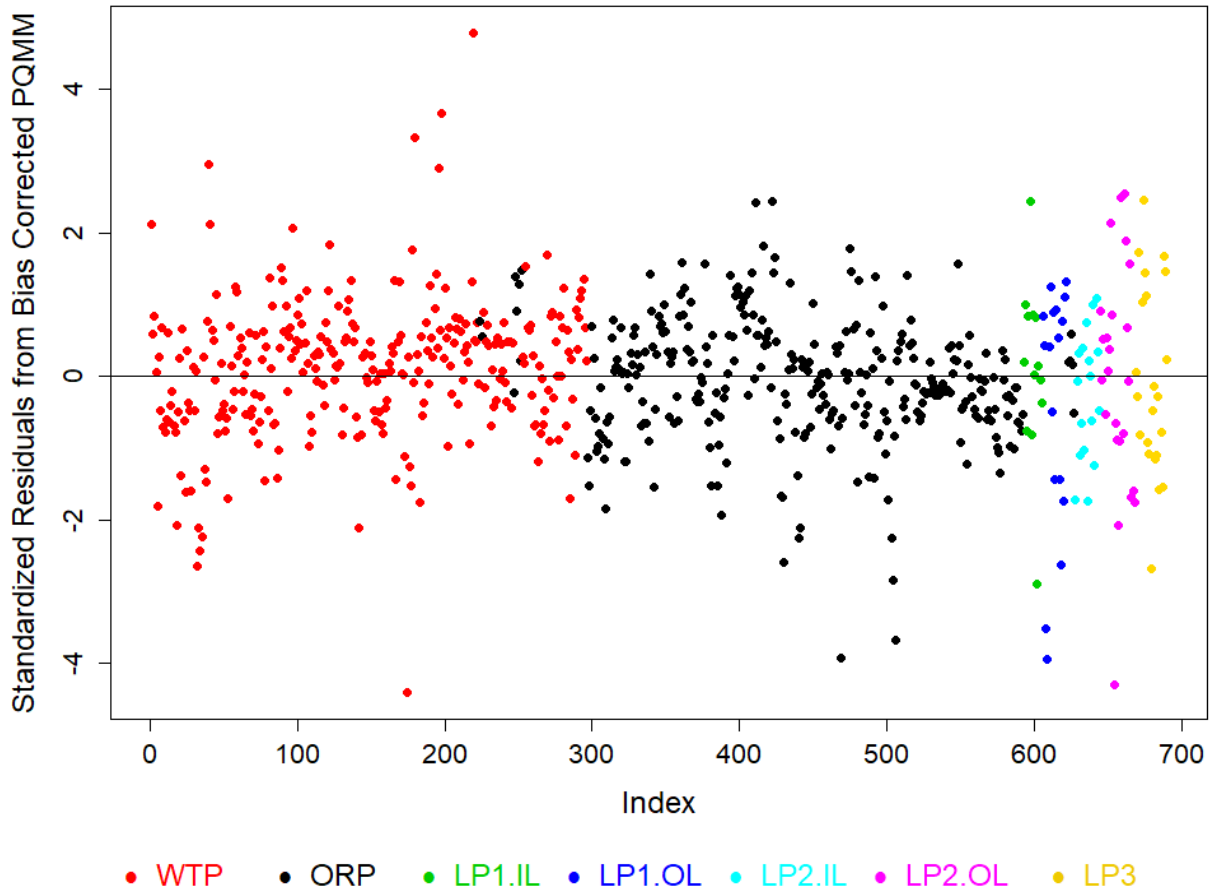


Figure 3.23. Standardized Residuals Plot for the 22-Term bcPQM Model on the Natural Logarithm of Normalized PCT Sodium Loss from LAW Glasses

Figure 3.24 displays the PvM plot for the 690-glass modeling dataset using the 22-term bcPQM model on $\ln(PCT_{Na}^{NL})$. Figure 3.24 differs from the PvM plot for the 19-term PQM model in Figure 3.19 in that the higher values ($> 0.6 \ln[g/m^2]$), which do not show bias, show slightly larger scatter of predicted data about the 45° line in this same region.

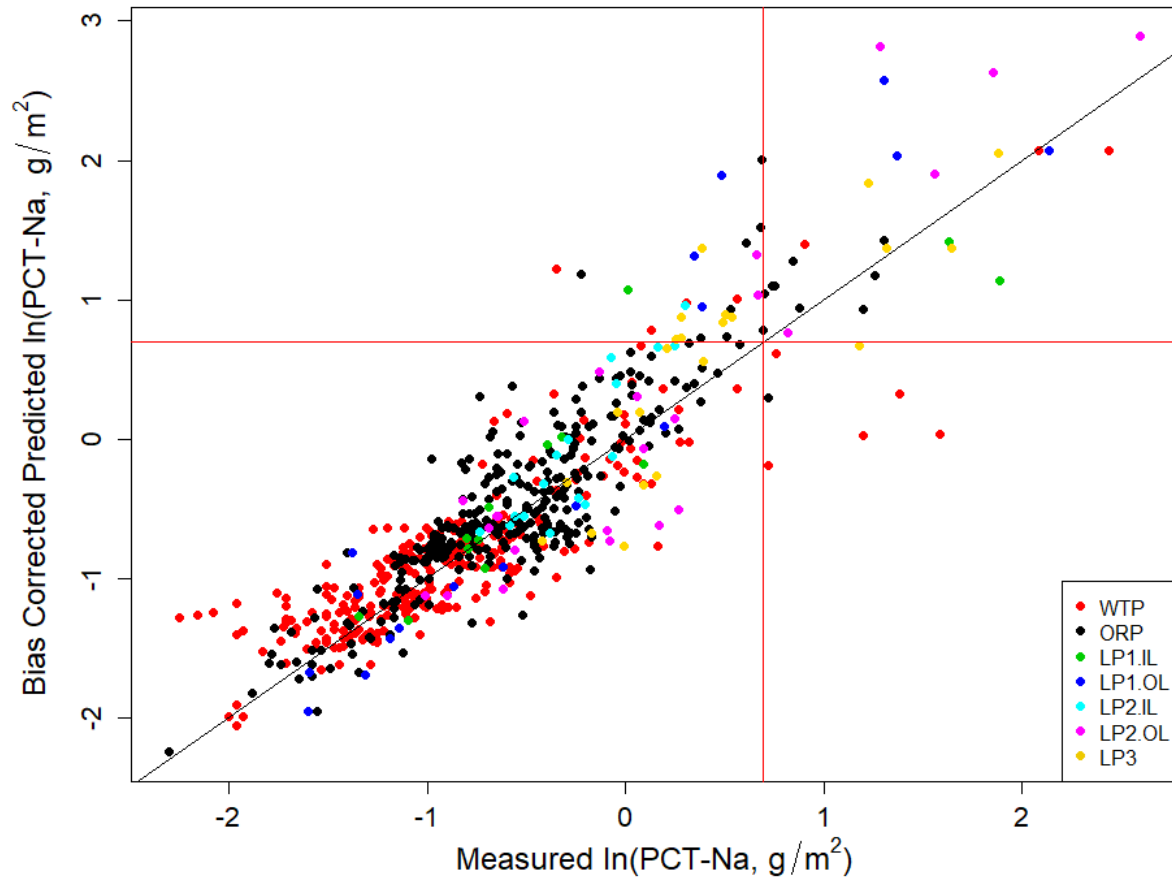


Figure 3.24. Predicted versus Measured Plot for the 690-glass Modeling Dataset Using the 22-Term bcPQM Model on the Natural Logarithm of Normalized PCT Sodium Loss from LAW Glasses

Figure 3.25 displays PvM plots using the 22-term bcPQM model in Table 3.11 applied to the five evaluation subsets discussed in Section 3.1.3. Each plot in the figure contains the evaluation R^2 and RMSE values for the corresponding evaluation subset. Figure 3.25 shows that the 22-term bcPQM model fit to the 690-glass modeling dataset generally predicts reasonably well for all six evaluation subsets.

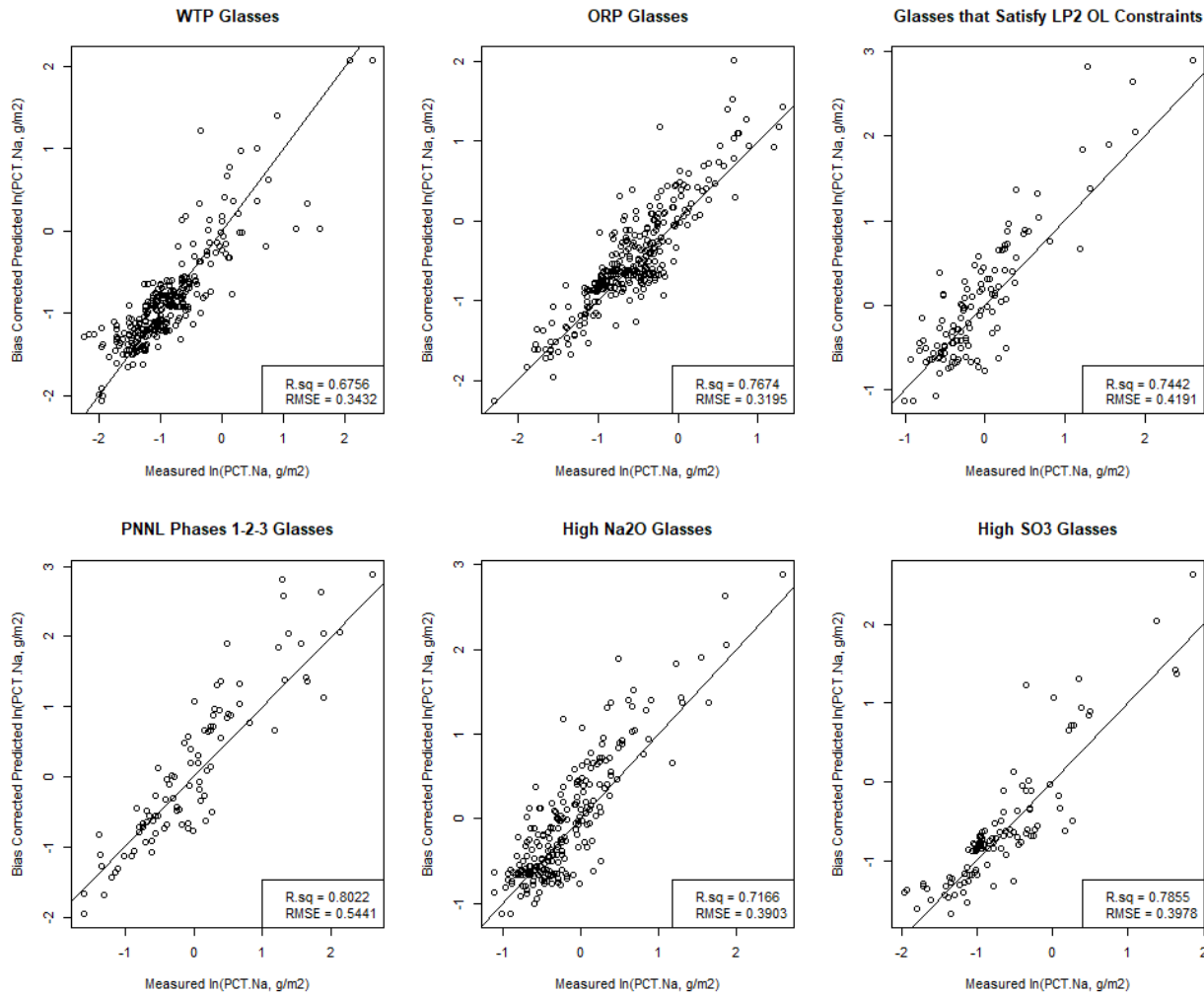


Figure 3.25. Predicted versus Measured Plots for the Six Evaluation Subsets Using the 22-Term bcPQM Model on the Natural Logarithm of Normalized PCT Sodium Loss from LAW Glasses

Figure 3.26 displays the response trace plot (see Section B.4.1 of Appendix B) for the 22-term bcPQM model on $\ln(PCT_{Na}^{NL})$. Figure 3.26 shows that Li_2O , Na_2O , MgO , and K_2O are predicted to increase $\ln(PCT_{Na}^{NL})$ the most, while Al_2O_3 and SiO_2 are predicted to decrease $\ln(PCT_{Na}^{NL})$ the most. The impact of bias correction is clearly seen in the dramatic change in SiO_2 , Al_2O_3 , Li_2O , Na_2O , MgO , and K_2O effects. B_2O_3 , V_2O_5 , Fe_2O_3 , Others, CaO , ZrO_2 , and ZnO have predicted response traces with small to negligible slopes, indicating those components are predicted to have small to negligible effects on $\ln(PCT_{Na}^{NL})$.

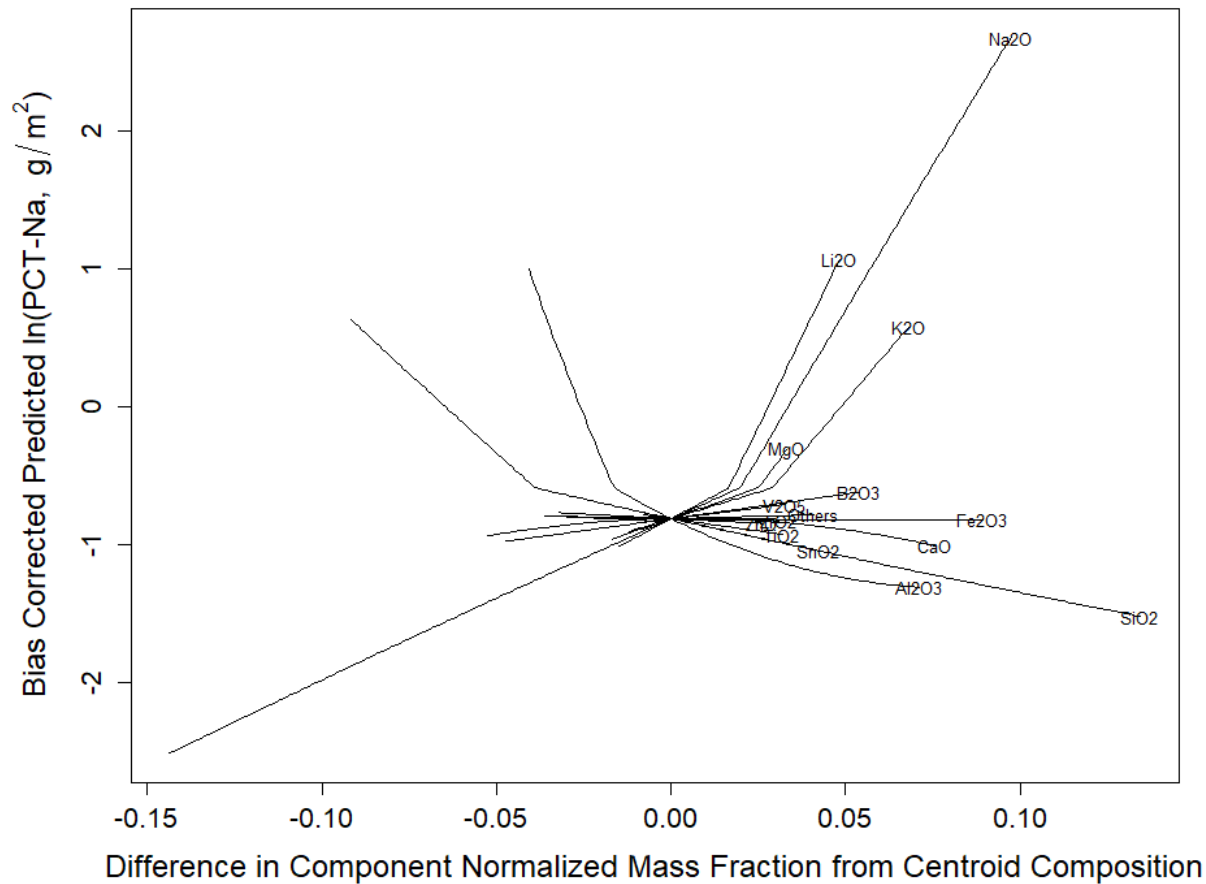


Figure 3.26. Response Trace Plot for 22-Term bcPQM Model on the Natural Logarithm of Normalized PCT Sodium Loss from LAW Glasses

3.5 Recommended Model for the Natural Logarithm of Normalized PCT Boron and Sodium Loss from LAW Glasses

Of the eight models reported to predict natural logarithm of normalized PCT boron and sodium loss, the PQM and bcPQM models fit the data and were validated the best. Table 3.12 summarizes the model evaluation and validation results for the PQM and bcPQM models for predicting $\ln(PCT_B^{NL})$ and $\ln(PCT_{Na}^{NL})$ from LAW glasses. Only the bcPQM models did not display a significant bias at high PCT responses ($> 0.5 \ln(\text{g/m}^2)$). The bcPQM models also displayed the highest fit and validation statistics (with the exception of PQM for $\ln(PCT_{Na}^{NL})$). Therefore, the bcPQM models are recommended for predicting $\ln(PCT_B^{NL})$ and $\ln(PCT_{Na}^{NL})$ of LAW glasses.

Table 3.12. Performance Summary of Two Models for the Natural Logarithm of PCT Responses of LAW Glasses

Model Fit to 690 Glasses ^(a)	PCT-B		PCT-Na	
	PQM	bcPQM	PQM	bcPQM
Section	3.3.3	3.3.5	3.4.3	3.4.5
Summary Table	3.6	3.7	3.10	3.11
R ²	0.7454	0.7762	0.7719	0.7621
R ² _A	0.7386	0.7692	0.7658	0.7546
RMSE	0.4207	0.3954	0.3448	0.3529
LOF p-value	<0.0001	<0.0001	<0.0001	<0.0001
Linear Terms	15	15	15	15
Selected Quadratic Terms in Model	Al ₂ O ₃ ×Al ₂ O ₃ , CaO×CaO, CaO×V ₂ O ₅ , Na ₂ O×SiO ₃	Al ₂ O ₃ ×Al ₂ O ₃ , CaO×CaO, CaO×V ₂ O ₅ , Al ₂ O ₃ ×Li ₂ O	Al ₂ O ₃ ×Al ₂ O ₃ , V ₂ O ₅ ×V ₂ O ₅ , CaO×V ₂ O ₅ , Na ₂ O×SiO ₂	Al ₂ O ₃ ×Al ₂ O ₃ , CaO×CaO, CaO×V ₂ O ₅ , Al ₂ O ₃ ×Na ₂ O
# Data	690	690	690	690
# Model Parameters	19	22	19	22
Validation Summary Statistics Averaged Over 5 Data-Splitting Sets for bcPQM only ^(a)				
R ²	--	0.7819	--	0.7650
R ² _A	--	0.7736	--	0.7561
RMSE	--	0.3903	--	0.3502
R ² _v	--	0.7053	--	0.7163
RMSE _v	--	0.4436	--	0.3824
Summary Statistics for Five Evaluation Subsets of LAW Glasses for bcPQM only ^(b)				
Evaluation Set (# Glasses) ^(b)	bcPQM R ² _{Eval}	bcPQM RMSE _{Eval}	bcPQM R ² _{Eval}	bcPQM RMSE _{Eval}
WTP (B:289, Na:288)	0.7312	0.3637	0.6756	0.3432
ORP (309)	0.7356	0.4108	0.7674	0.3195
LP2OL (B:120, Na:121)	0.7553	0.4253	0.7442	0.4191
LP123 (B:92, Na:93)	0.8491	0.5203	0.8022	0.5441
HiNa ₂ O (233)	0.7145	0.4020	0.7166	0.3903
HiSO ₃ (110)	0.7776	0.4332	0.7855	0.3978

(a) Model validation statistics are defined in Section B.5 of Appendix B.
(b) The model evaluation statistics are defined in Section B.3 of Appendix B.

3.6 Example Illustrating Model Predictions and Statistical Intervals for the Natural Logarithm of Normalized PCT Boron and Sodium Loss from LAW Glasses

This section contains examples to illustrate using the recommended 22-term bcPQM models (Sections 3.3.5 and 3.4.5) to obtain predicted PCT_B^{NL} and PCT_{Na}^{NL} values, respectively, and corresponding 90% simultaneous upper confidence intervals (SUCIs) for a specific LAW glass composition as described in Section B.6 of Appendix B. The 90% confidence levels associated with SUCIs were chosen for illustration purposes only.¹ The WTP LAW Facility can use an appropriate confidence level depending on the use of the $\ln(PCT_j^{NL})$ -composition models and the type of statistical uncertainty expression.

The common glass composition selected for example calculations for all properties in this report (denoted REFMIX) is listed in Table 2.3. Because the bcPQM models were recommended for predicting

¹ Currently, the WTP LAW Facility uses SUCI's with 90% confidence levels (Kim and Vienna 2012).

normalized PCT responses and the REFMIX composition is below the bias correction cutoff, a second glass above the cutoff was also selected for example calculations. The 20-component compositions (mass fractions) for PCT_B^{NL} and PCT_{Na}^{NL} modeling are given in Table 3.13. To apply the 22-term bcPQM models for $\ln(PCT_B^{NL})$ and $\ln(PCT_{Na}^{NL})$ to the glass composition, the mass fractions of the 20 components must be converted to mass fractions (that sum to 1.0) of the 15 LAW glass components contained in both models. This involves adding the mass fractions of the 5 of 20 components not contained in the models (Cl, Cr₂O₃, F, P₂O₅, and SO₃) to the mass fraction of Others (one of the original 20 components) to obtain a new Others (one of the reduced sets of 15 components). Mass fractions of the relevant components are then multiplied to obtain the second-order terms of the 22-term reduced bcPQM models. Table 3.13 contains the compositions of the glasses prepared for use in the $\ln(PCT_B^{NL})$ and $\ln(PCT_{Na}^{NL})$ models for LAW glasses.

For each of the two bcPQM models, initial predicted $\ln(PCT_j^{NL})$, g/m² values are obtained by multiplying the composition in the format needed for that model by the coefficients for that model, then summing the results. That is, the initial values are calculated by

$$\ln(\widehat{PCT}_j^{NL}) = \mathbf{g}^T \mathbf{b} \quad (3.9)$$

where \mathbf{g} is the composition of the example glass formatted to match the terms in a given model (from Table 3.13), the superscript T represents a vector transpose, and \mathbf{b} is the vector of coefficients for a given model. The initial $\ln(\widehat{PCT}_j^{NL})$ values for the two example glasses using the two bcPQM models are listed in the second column of Table 3.14. The initial $\ln(\widehat{PCT}_j^{NL})$ values in $\ln(\text{g/m}^2)$ units are easily converted to \widehat{PCT}_j^{NL} values (g/m²) by exponentiation.

The standard deviation of $\ln(\widehat{PCT}_j^{NL})$ values are given by

$$SD_{\ln(\widehat{PCT}_j^{NL})} = \sqrt{V_{\ln(\widehat{PCT}_j^{NL})}} = \sqrt{\text{MSE}_{\ln(\widehat{PCT}_j^{NL})} \mathbf{g}^T (\mathbf{G}^T \mathbf{G})^{-1} \mathbf{g}} \quad (3.10)$$

where

$$\begin{aligned} V_{\ln(\widehat{PCT}_j^{NL})} &= \text{the variance of } \ln(\widehat{PCT}_j^{NL}) = SD_{\ln(\widehat{PCT}_j^{NL})}^2 \\ \text{MSE}_{\ln(\widehat{PCT}_j^{NL})} &= \text{mean-squared error of associated with a given model} \\ \text{MSE}_{\ln(\widehat{PCT}_j^{NL})} (\mathbf{G}^T \mathbf{G})^{-1} &= \text{the variance-covariance matrix of the model (also denoted as } \mathbf{V}) \\ \mathbf{g} &= \text{the vector of values for the PCT model consisting of the individual mass fractions of the components expanded to the appropriate model form.} \end{aligned}$$

The $SD_{\ln(\widehat{PCT}_j^{NL})}$ values are listed in the third column of Table 3.14. For $\ln(\widehat{PCT}^{NL})$ values above the cutoff (c), a bias correction (bc) is added according to Eqs. (3.6) and (3.8). The variance-covariance matrices, given by $\mathbf{V} = \text{MSE}_{\ln(\widehat{PCT}_j^{NL})} (\mathbf{G}^T \mathbf{G})^{-1}$, are listed in Tables D.1 and D.2 for $\ln(PCT_B^{NL})$ and $\ln(PCT_{Na}^{NL})$, respectively.

The bias corrected value is given in the fourth column of Table 3.14 by adding the bc (bias correction) to $\ln(\widehat{PCT}_j^{NL})$ yielding the final (bias corrected) prediction of $\ln(PCT_j^{NL})$ in the fourth column of Table 3.14.

The standard deviation of bcPQM model prediction is calculated using a propagation of errors approach. The formula to obtain predicted PCT responses for $\mathbf{g}^T \mathbf{b} > c$ (according to Eqs. (3.6) and (3.8)) is

$$\ln(PCT_j^{NL})_{BC} = \mathbf{g}^T \boldsymbol{\beta} + (\mathbf{g}^T \boldsymbol{\beta} - C)S + e \quad (3.11)$$

Since S was developed using a two-part process $S = S_0 + \Delta S$, this becomes:

$$\ln(PCT_j^{NL})_{BC} = \mathbf{g}^T \boldsymbol{\beta} + (\mathbf{g}^T \boldsymbol{\beta} - C)(S_0 + \Delta S) + e. \quad (3.12)$$

Expanding Equation (3.12) yields:

$$\ln(PCT_j^{NL})_{BC} = \mathbf{g}^T \boldsymbol{\beta} + \mathbf{g}^T \boldsymbol{\beta} \cdot S_0 + \mathbf{g}^T \boldsymbol{\beta} \cdot \Delta S - C \cdot S_0 - C \cdot \Delta S + e \quad (3.13)$$

where

- $\boldsymbol{\beta}$ = the vector of PQM term coefficients including β_i , β_{ii} , and β_{ij} values
- \mathbf{g} = the vector of component concentrations for first order terms followed by component concentrations squared for quadratic terms and concentrations multiplied for cross-product terms (in the same order as $\boldsymbol{\beta}$)
- C = bias correction cut-off ($\ln[\text{g/m}^2]$)
- S = bias correction slope ((unitless). Due to the fitting process, S is the sum of the initial slope (S_0) and the change in slope (ΔS) (i.e., $S = S_0 + \Delta S$).
- S_0 = initial bias correction slope (unitless)
- ΔS = change in slope (unitless)
- e = random error for each data point.

This expression involves four product terms. The variance formula for a product $x \cdot y$ is $V(x \cdot y) = X^2 V(y) + Y^2 V(x) + V(x)V(y)$; where X is the true but unknown expected value of x , Y is the true but unknown expected value of y , $V(x)$ is the true but unknown variance of x , and $V(y)$ is the true but unknown variance of y . However, when this formula is implemented using estimates of $V(x)$ and $V(y)$, the results are biased. An unbiased version of this formula is available (Goodman 1960); $\hat{V}(x \cdot y) = x^2 v(y) + y^2 v(x) - v(x)v(y)$; where $v(x)$ is an unbiased estimator of $V(x)$ and $v(y)$ is an unbiased estimator of $V(y)$. This variance estimation formula was used for each of the four product terms in the expression used to calculate $\ln(PCT_j^{NL})$ values for cases in which $\ln(PCT_j^{NL}) > c$:

$$\begin{aligned} \hat{V}_{\ln(\widehat{PCT}_j^{NL})} &= \widehat{SD}(\widehat{PCT}_j^{NL})^2 \\ &= v_{\mathbf{g}^T \mathbf{b}} + (\mathbf{g}^T \mathbf{b})^2 v_{S_0} + S_0^2 v_{\mathbf{g}^T \mathbf{b}} - v_{S_0} v_{\mathbf{g}^T \mathbf{b}} + (\mathbf{g}^T \mathbf{b})^2 v_{\Delta S} + \Delta S^2 v_{\mathbf{g}^T \mathbf{b}} - v_{\Delta S} v_{\mathbf{g}^T \mathbf{b}} \\ &\quad + c^2 v_{S_0} + S_0^2 v_c - v_c v_{S_0} + \Delta S^2 v_c + c^2 v_{\Delta S} - v_c v_{\Delta S} \end{aligned} \quad (3.14)$$

where $v_{g_{Tb}}$ is given in Equation (3.10), v_c is the square of the standard error of c given in Tables 3.7 and 3.11, and v_{s_0} is the square of the standard error of s_0 given in Tables 3.7 and 3.11. A bootstrap method was used to estimate $v_{\Delta s}$. The process of estimating the standard error of Δs consists of sampling, with replacement, 690 composition and $\ln(PCT_B^{NL})$ data from the 690 glasses available for PCT B modeling. Each new sample of glass compositions and $\ln(PCT_B^{NL})$ values are used to calculate a value for Δs . This process is repeated many times to obtain a bias corrected and accelerated (BCa) bootstrap distribution of Δs estimates.

The standard error for Δs can be estimated as the standard deviation of the resampled Δs data. As an example, consider the data for Δs obtained from randomly resampling, with replacement, data and calculating Δs for each new sample 100,000 times. This process produces the distribution for Δs shown in Figure 3.27.

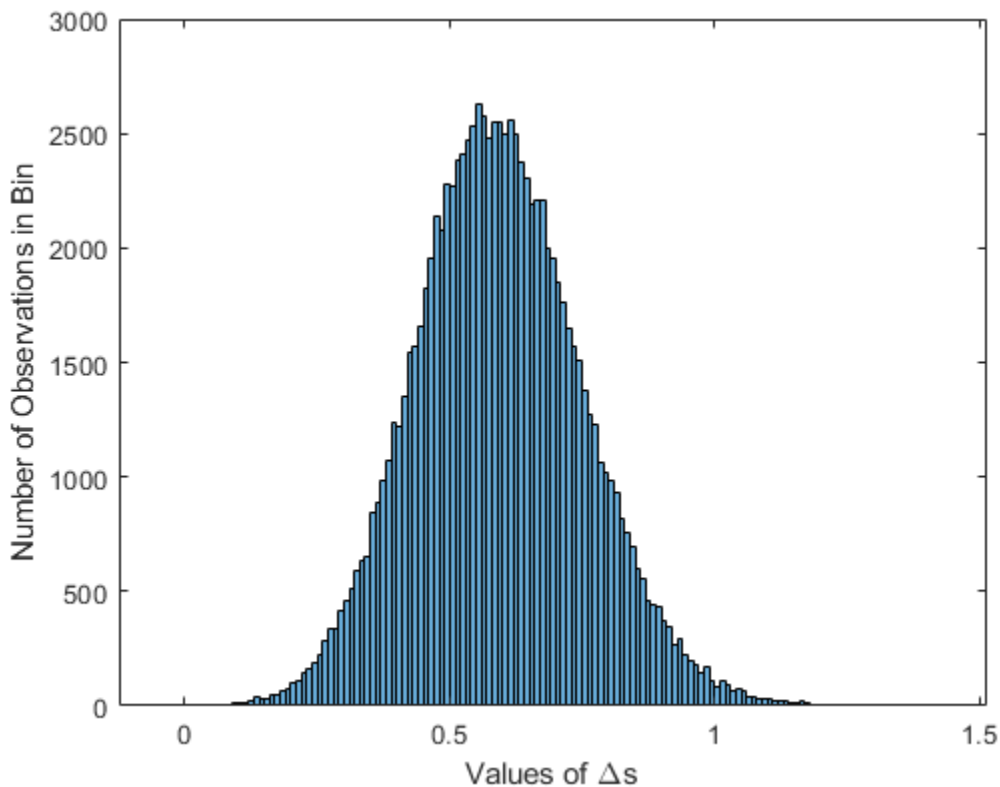


Figure 3.27. Distribution of Δs Values for 100,000 Samples of Glasses and Corresponding $\ln(PCT_B^{NL})$ Values Obtained from the Available 690 Glasses Used To Model $\ln(PCT_B^{NL})$

The distribution in Figure 3.27 appears symmetrically distributed around the mean value of 0.5933. The original Δs value calculated with JMP® is 0.5869. The estimated standard error of Δs obtained as the standard deviation ($SD_{\Delta s}$) of the 100,000 bootstrapped samples shown in Figure 3.27 is 0.1585. This is the estimated standard error of Δs .

The BCa bootstrap method is the preferred technique when using resampled data because it tends to produce good estimates for a variety of statistics. It automatically corrects for skewness in the sampled distribution and it is invariant to transformations. The same BCa was applied to $\ln(PCT_{Na}^{NL})$ data, resulting

in an approximation for Δs of 0.9590, a $SD_{\Delta s} = 0.2373$. The original Δs value for $\ln(PCT_{Na}^{NL})$, calculated with JMP®, is 0.9457.

The variances from Eqn. (3.14) – v_c , v_{s_0} , and $v_{\Delta s}$ – are obtained by squaring the standard errors for their associated terms found in Tables 3.7 and 3.11 for $\ln(PCT_B^{NL})$ and $\ln(PCT_{Na}^{NL})$, respectively.

The calculated standard deviations of the final predicted $\ln(PCT_j^{NL})$ (that is, $SD_{\ln(PCT_j^{NL})}$) when $\mathbf{g}^T \mathbf{b} > c$ are given in the fifth column of Table 3.14.

The general form of the equation for calculating the simultaneous upper confidence interval (SUCI) is

$$SUCI = \ln(\widehat{PCT_j^{NL}}) + K \cdot SD_{\ln(\widehat{PCT_j^{NL}})} \quad (3.15)$$

where K is a multiplier that reflects the desired confidence level as well as the available degrees of freedom. As explained in Appendix B, a one-sided (upper) Working-Hotelling SUCI was used for our example calculations. For this approach, the multiplier K in the SUCI formula having a confidence level of $100(1-\alpha)\%$ is given by

$$K = \sqrt{q F_{1-2\alpha}(q, n - q)} \quad (3.16)$$

where n is the number of glasses used to generate the final bcPQM model, and q is the number of parameters estimated for the final bcPQM model. For the bcPQM models in this report, $q = p + 3$ ($=22$) for all glasses (whether a bias correction was needed or not). This is because the final bcPQM model coefficients (\mathbf{b}), the estimated bias correction cutoff (c), and the estimated initial bias correction slope (s_0) were all determined together via a non-linear optimization routine in JMP®. The estimated delta slope (Δs) was determined separately via a bootstrap simulation including all data.¹

Eq. (3.15) can be applied to obtain SUCI with a confidence level given by $(1-\alpha)$, where α is a small value like 0.1, for a 90% confidence level. The sixth column in Table 3.14 lists $SUCI_{\alpha}^{PCT}$ for each of the example glasses for both $\ln(PCT_B^{NL})$ and $\ln(PCT_{Na}^{NL})$. Exponentiation of $SUCI_{\alpha}^{PCT}$ yields the SUCI on the median PCT_j^{NL} (listed in the seventh column of Table 3.14). For the example in Table 3.14, $n = 690$, $q = 22$, and thus the F-statistic value needed in Eq. (3.16) is 1.247741. The resulting K multiplier for Eqs. (3.15) and (3.16) is 5.239303. The values for the F-statistic and K multiplier are the same for calculations involving both PCT models described in Table 3.14. The following cell formula can be used to obtain the F-statistic value with Excel: $=F.INV(0.8,22,690-22)$.

¹ Note that from the Piepel et al. (2008), Equation C.38 showed a different value for q when working with glasses requiring a bias correction versus those that do not. In particular, that report used $q = p$ = the number of model coefficients for glasses that did not require a bias correction, and $q = p + 1$ for glasses that did require a bias correction. The ‘+1’ was to account for the bias correction slope which was the only additional parameter needed to conduct the bias correction for that work. But for that work, the coefficients of the PQM model used were determined together via regression and the bias correction slope was determined separately. So, it was appropriate to use $q = p + 1$ in the K multiplier for glasses requiring bias correction in the that study.

Table 3.13. Example Glass Compositions in Formats Used with Models of Natural Logarithm of Normalized PCT Boron and Sodium Losses from LAW Glasses (mass fractions)

Glass	REFMIX ^(a)			LAWA42		
	20- Component	19-Term PCT_B^{NL}	19-Term PCT_{Na}^{NL}	20- Component	19-Term PCT_B^{NL}	19-Term PCT_{Na}^{NL}
Al ₂ O ₃	0.075760	0.075760	0.075760	0.062034	0.062034	0.062034
B ₂ O ₃	0.097257	0.097257	0.097257	0.090336	0.090336	0.090336
CaO	0.052514	0.052514	0.052514	0.024042	0.024042	0.024042
Cl	0.003376	NA ^(b)	NA	0.005790	NA	NA
Cr ₂ O ₃	0.002041	NA	NA	0.000170	NA	NA
F	0.001348	NA	NA	0.000360	NA	NA
Fe ₂ O ₃	0.029727	0.029727	0.029727	0.084106	0.084106	0.084106
K ₂ O	0.012064	0.012064	0.012064	0.031012	0.031012	0.031012
Li ₂ O	0.014802	0.014802	0.014802	0.000010	0.000010	0.000010
MgO	0.016989	0.016989	0.016989	0.024022	0.024022	0.024022
Na ₂ O	0.168395	0.168395	0.168395	0.200014	0.200014	0.200014
P ₂ O ₅	0.003239	NA	NA	0.000780	NA	NA
SO ₃	0.005542	NA	NA	0.000956	NA	NA
SiO ₂	0.424565	0.424565	0.424565	0.380026	0.380026	0.380026
SnO ₂	0.007587	0.007587	0.007587	0.000000	0.000000	0.000000
TiO ₂	0.008034	0.008034	0.008034	0.024022	0.024022	0.024022
V ₂ O ₅	0.007499	0.007499	0.007499	0.000000	0.000000	0.000000
ZnO	0.031997	0.031997	0.031997	0.036043	0.036043	0.036043
ZrO ₂	0.036219	0.036219	0.036219	0.036073	0.036073	0.036073
Others	0.001045	0.016591	0.016591	0.000204	0.008260	0.008260
Al ₂ O ₃ ×Al ₂ O ₃	NA	0.00573958	0.00573958	NA	0.00384822	0.00384822
Al ₂ O ₃ ×Li ₂ O	NA	0.00112140	NA	NA	0.00000062	NA
CaO×CaO	NA	0.00275772	0.00275772	NA	0.00057802	0.00057802
CaO×V ₂ O ₅	NA	0.00039380	0.00039380	NA	0.00000000	0.00000000
Al ₂ O ₃ ×Na ₂ O	NA	NA	0.01275761	NA	NA	0.01240767

(a) The composition in mass fractions is from Table 2.3

(b) NA = not applicable, because the model doesn't contain the term.

Table 3.14. Predicted PCT_B^{NL} and PCT_{Na}^{NL} , Standard Deviation, and Statistical Intervals for the Example Glass Compositions Used in Two Recommended Models for Natural Logarithm of Normalized PCT Losses from LAW Glasses

bcPQM Models for $\ln(PCT_j^{NL})^{(a)}$	Initial $\ln(\widehat{PCT}_j^{NL})$ [ln(g/m ²)]	Standard Deviation of $\ln(\widehat{PCT}_j^{NL})$ [ln(g/m ²)]	Bias Corr. $\ln(\widehat{PCT}_j^{NL})$ [ln(g/m ²)]	Std. Dev. of BC $\ln(\widehat{PCT}_j^{NL})$ [ln(g/m ²)]	90% SUCI ^(c) $\ln(\widehat{PCT}_j^{NL})$ [ln(g/m ²)]	90% SUCI ^(c) \widehat{PCT}_j^{NL} [g/m ²]
22-Term $\ln(PCT_B^{NL})$						
REFMIX	-0.8565	0.0250	NA	NA	-0.7256	0.4840
LAWA42	-0.2851	NA	0.7009	0.2410	1.9635	7.1244
22-Term $\ln(PCT_{Na}^{NL})$						
REFMIX	-0.8127	0.0227	NA	NA	-0.6940	0.4996
LAWA42	-0.3518	NA	0.3259	0.2616	1.6967	5.4560

(a) The two bcPQM models in this column are given in Table 3.7 and Table 3.11 for $\ln(PCT_B^{NL})$ and $\ln(PCT_{Na}^{NL})$, respectively.

(b) The standard deviation is for the $\ln(PCT_j^{NL})$ prediction considered to be the mean of such values for the example glass.

(c) SUCI = simultaneous upper confidence interval (see Section B.6 of Appendix B).

3.6.1 Optimization of Glass Composition using bcPQM

As previously mentioned, the form of the bias correction equation (Eqn. 3.12) maintains continuity between the predicted PCT responses above and below the cutoff value (c). However, for $\mathbf{g}^T \mathbf{b} > c$ there are more uncertainty components as shown in Equation (3.14). The additional variance terms cause a discontinuity in $V_{\ln(\widehat{PCT}_j^{NL})}$. This discontinuity creates challenges when attempting to optimize a glass composition with PCT responses near the cutoff values. To facilitate glass optimization, a sigmoid function can be used to generate a smooth approximation for $V_{\ln(\widehat{PCT}_j^{NL})}$ across the cutoff:

$$V_{\ln(\widehat{PCT}_j^{NL})} \cong v_{\mathbf{g}^T \mathbf{b}} + \frac{X}{1 + e^{-k(\mathbf{g}^T \mathbf{b} - c)}} \quad (3.17)$$

$$X = (\mathbf{g}^T \mathbf{b})^2 v_{S_0} + s_0^2 v_{\mathbf{g}^T \mathbf{b}} - v_{S_0} v_{\mathbf{g}^T \mathbf{b}} + (\mathbf{g}^T \mathbf{b})^2 v_{\Delta s} + \Delta s^2 v_{\mathbf{g}^T \mathbf{b}} - v_{\Delta s} v_{\mathbf{g}^T \mathbf{b}} + c^2 v_{S_0} + s_0^2 v_c - v_c v_{S_0} + \Delta s^2 v_c + c^2 v_{\Delta s} - v_c v_{\Delta s}$$

where X combines the additional variance terms and k is a constant related to the steepness of the sigmoid curve and should be selected based on the optimization routine selected (typically by trial and error).

3.7 Suitability of the Recommended Models for Natural Logarithm of Normalized PCT Boron and Sodium Loss from LAW Glasses

The 22-term bcPQM models discussed in Sections 3.3.5 and 3.4.5 are recommended as the best of the currently available models for predicting $\ln(PCT_B^{NL})$ and $\ln(PCT_{Na}^{NL})$ of LAW glasses. These models yield unbiased predictions near the WTP contract limit of 2 g/m² ($\sim 0.693 \ln[\text{g/m}^2]$). Although these models have statistically significant LOFs, they predict $\ln(PCT_B^{NL})$ and $\ln(PCT_{Na}^{NL})$ values of LAW glasses within the range of prediction uncertainty. Therefore, they are suitable for implementation in the WTP LAW Facility.

The ranges of single-component concentrations in the 691-glass dataset used for modeling normalized PCT boron and sodium losses from LAW glasses is listed in Table 3.15. These ranges can be used to determine model validity ranges.

Table 3.15. Data Component Concentration Ranges (mass fraction) for LAW Glasses Used in Final Natural Logarithm of Normalized PCT Boron and Sodium Loss Models

Component	20-component		15-component	
	Min	Max	Min	Max
Al ₂ O ₃	0.034972	0.147521	0.034972	0.147521
B ₂ O ₃	0.050009	0.151474	0.050009	0.151474
CaO	0	0.128136	0	0.128136
Cl	0	0.011722	NA ^(a)	NA
Cr ₂ O ₃	0	0.006304	NA	NA
F	0	0.013007	NA	NA
Fe ₂ O ₃	0	0.119838	0	0.119838
K ₂ O	0	0.08093	0	0.08093
Li ₂ O	0	0.063294	0	0.063294
MgO	0	0.050222	0	0.050222
Na ₂ O	0.024707	0.265729	0.024707	0.265729
P ₂ O ₅	0	0.047523	NA	NA
SO ₃	0	0.016	NA	NA
SiO ₂	0.332925	0.559206	0.332925	0.559206
SnO ₂	0	0.050299	0	0.050299
TiO ₂	0	0.040048	0	0.040048
V ₂ O ₅	0	0.057118	0	0.057118
ZnO	0	0.058152	0	0.058152
ZrO ₂	0	0.067534	0	0.067534
Others ^(b)	0	0.005421	0.00149	0.057991

(a) NA = not applicable or component not included as term.

(b) Note: Others for the 15-components are composed of all the NA components as well as Others for the 20 components.

4.0 Models Relating Vapor Hydration Test Results to LAW Glass Compositions

This section documents the development, evaluation, and validation of LAW glasses property-composition models and corresponding uncertainty expressions for predicting pass/fail VHT results (e.g., fail is classified as $r_a^{VHT} \geq 50 \text{ g/m}^2/\text{d}$). Pass/fail labels for glasses based on their VHT values are modeled using a logistic model, a GLM with a logit link and a binomial distribution for the response, as a function of LAW glass composition.

The VHT response for LAW glasses is a numerical value measuring the thickness of a corroded layer on a test glass coupon under high-temperature and high-humidity conditions for a specified amount of time (Buechele et al. 2002; Jiricka et al. 2001). However, the variety of test conditions, and the length of time covered by the LAW glass data used in this work, resulted in inconsistent values for measured thicknesses, making the resulting comprehensive dataset, with thickness as the response, unsuitable for modeling. The reported thickness for each glass can be transformed into a pass/fail binary response that can be modeled as a function of glass composition. The property-composition models and corresponding uncertainty expressions for a pass/fail VHT presented in this section were developed and validated using composition and VHT data collected for simulated and actual LAW glasses having VHT responses.

The 699 simulated and actual LAW glasses available for VHT model development, evaluation, and validation remaining after eliminating 89 CCC glasses are discussed in Section 4.1. Section 4.2 presents the model forms for pass/fail VHT that were investigated. Section 4.3 summarizes the results for VHT model forms investigated and the model forms ultimately recommended. Section 4.4 illustrates the calculation of pass/fail VHT predictions and the uncertainties in those predictions using selected models and corresponding uncertainty equations. Section 4.5 discusses the suitability of the recommended pass/fail VHT models for use by the WTP LAW Facility. Appendix B discusses the statistical methods and summary statistics used to develop, evaluate, and validate the several model forms investigated, as well as statistical equations for quantifying the uncertainties in pass/fail VHT predictions.

4.1 VHT Data from LAW Glasses Used for Model Development, Evaluation, and Validation

The data used to develop pass/fail VHT models as functions of LAW glass composition are discussed in Section 4.1.1. The approaches and data used for evaluating and validating the models are discussed in Sections 4.1.2 and 4.1.3, respectively.

4.1.1 Model Development Data for Pass/Fail VHT on LAW Glasses

The data available for developing property-composition models for the pass/fail VHT response consists of composition and pass/fail VHT responses from 699 quenched LAW glass samples. These glasses and their normalized compositions based on measured (or estimated) SO_3 values are discussed in Section 2.0. The corresponding pass/fail VHT values are presented in Table A.3 of Appendix A. A pass/fail determination was made by assessing the 24-day VHT glass alteration layer thickness. A pass (0) was assigned if the alteration thickness was $< 453 \text{ }\mu\text{m}$ and a fail (1) if $\geq 453 \text{ }\mu\text{m}$ or if the glass was fully dissolved. For glasses that were tested for multiple times, the 24-day results were used.

4.1.1.1 Assessment of Available LAW Glasses with Pass/Fail VHT data

The database of 699 glasses with pass/fail VHT values contains statistically designed as well as actively designed glasses. Some actively designed glasses are outside the composition region covered by the majority of the LAW compositions. Such glasses are not ideal for inclusion in a modeling dataset because they can be influential when fitting models to data. Hence, it was decided to (i) graphically assess the 699 simulated and actual LAW glass compositions with pass/fail VHT values and (ii) remove from the modeling dataset any compositions considered to be outlying or non-representative of glasses of interest for the WTP LAW Facility.

Figure 4.1 displays plots of the mass fraction values for 19 “main components” plus the Others component (the sum of all remaining components) in the 699 LAW glasses with VHT data. These 20 components (including Others) have sufficient ranges and distributions of mass fraction values to support separate model terms if so desired. Figure 4.2 displays similar plots for the remaining “minor components.” On each plot in Figure 4.1 and Figure 4.2, the x-axis represents the mass fraction values of LAW glass components. The y-axis shows an index value representing each LAW Glass #, which aids in spreading out the data points to avoid over-plotting. The plotting symbols in Figure 4.1 and Figure 4.2 correspond to the six groups of LAW glasses discussed in Section 2.3. For comparison purposes, the vertical lines in Figure 4.1 and Figure 4.2 represent the ranges over which the LAW glass components were varied in the PNNL (i) LAW Phase 1 outer-layer study (blue lines), (ii) Phase 2 outer-layer study (pink lines), and (iii) Phase 3 study (pink lines), as shown in Table 2.1. The PNNL Phases 2 and 3 focused on LAW glasses with high Na₂O waste loadings, whereas Phase 1 explored a larger LAW GCR with higher waste loadings.

Figure 4.1 shows that several of the 699 glasses have components with outlying mass fraction values compared to the remaining glasses and to the component ranges studied in the PNNL LAW Phase 1, Phase 2, and Phase 3 studies (e.g., MgO). Figure 4.2 shows what appear to be outliers for some “minor components,” but the values and ranges of those components are small and hence the glass compositions were not considered to be outliers (e.g., NiO). Table 4.1 lists the 13 LAW glasses excluded from the pass/fail VHT modeling dataset, and the reason each glass was excluded.

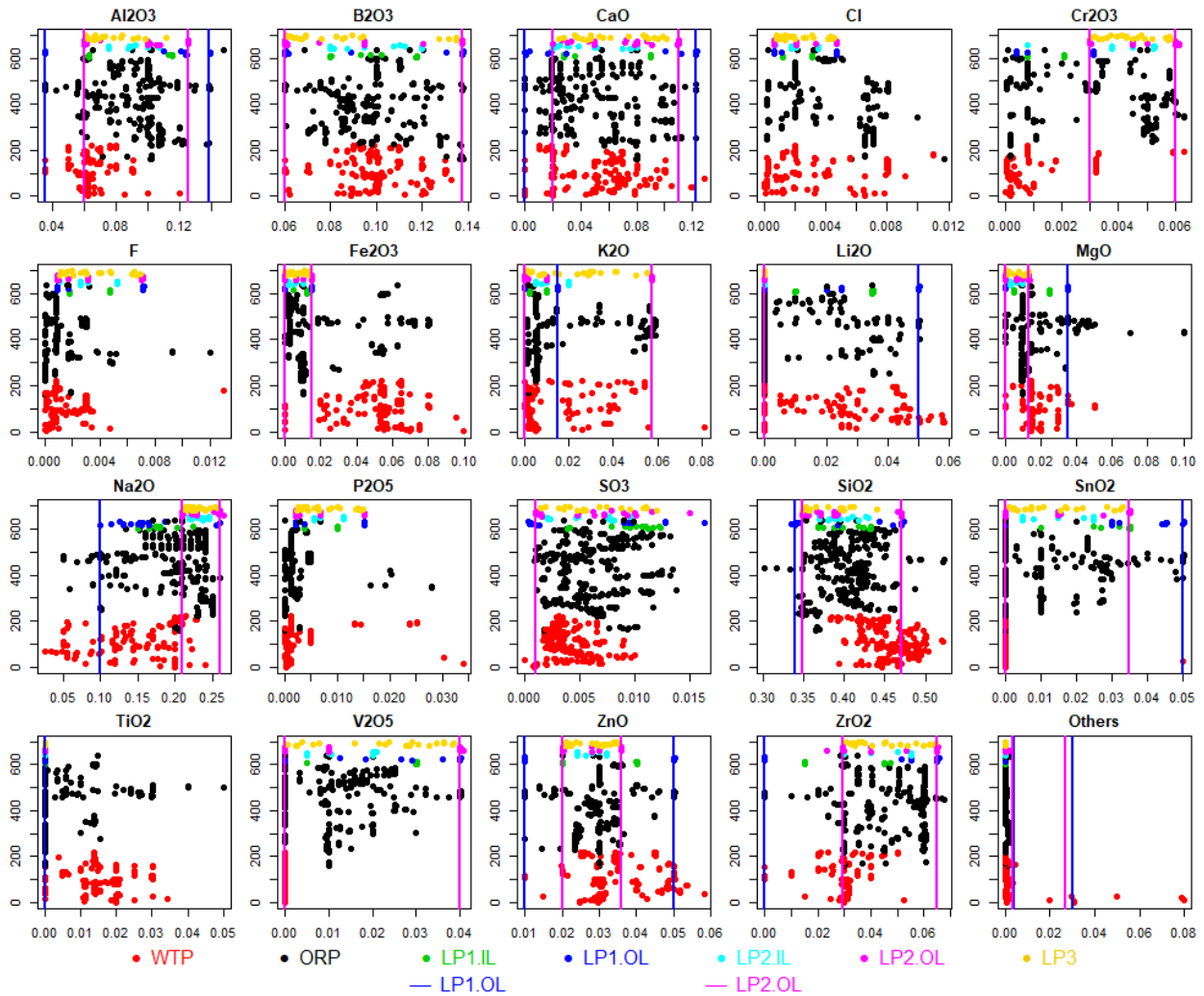


Figure 4.1. Distributions of 20 Main Components (in mass fractions) for 699 LAW Glass Compositions with Pass/Fail VHT Data. The vertical lines (when present) represent the lower and upper limits for each component from the PNNL LAW Phase 1 (blue lines) and Phase 2 (pink lines) outer-layer studies (see Table 2.1). In cases where two limits are the same, pink lines over plot the blue lines.

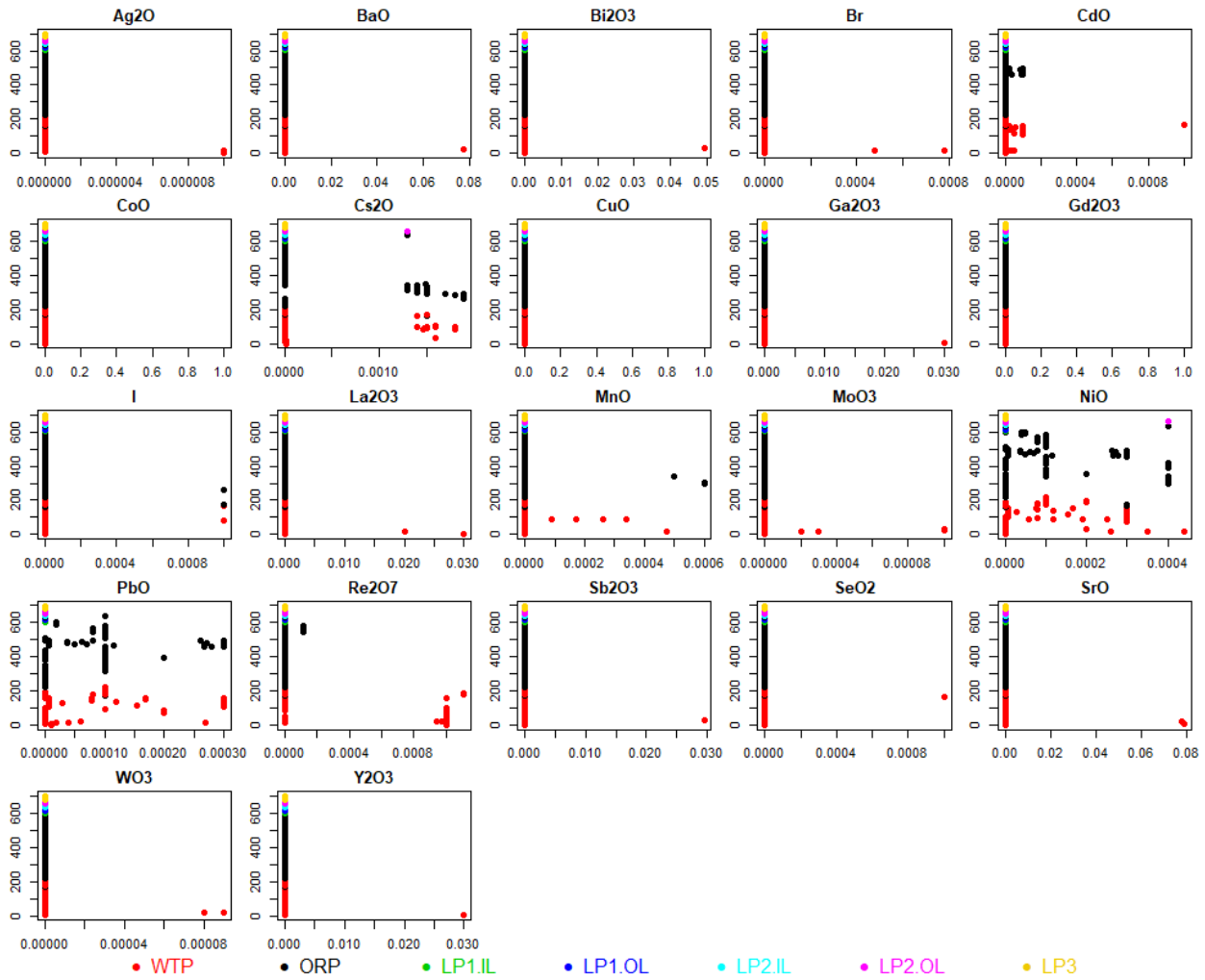


Figure 4.2. Distributions of 21 Minor Components (in mass fraction) for 699 LAW Glass Compositions with Pass/Fail VHT Data. The vertical lines (when present) represent the lower and upper limits for each component from the PNNL LAW Phase 1 (blue lines) and Phase 2 (pink lines) outer-layer studies (see Table 2.1). In cases where two limits are the same, pink lines over plot the blue lines.

Table 4.1. Thirteen LAW Glasses with Non-representative Compositions Excluded from the Modeling Datasets for Pass/Fail VHT

Glass ID	Glass #	Reason Glass Excluded from VHT Modeling Datasets ^(a)
ORPLA28	739	MgO > 0.06 (=0.070146) mf
ORPLA29	740	MgO > 0.06 (=0.100218) mf
ORPLA31	742	MgO > 0.06 (=0.070146) mf
ORPLA32	743	MgO > 0.06 (=0.100218) mf
LAWA46	12	Others > 0.019 (= 0.031025) mf
LAWA47	13	Others > 0.019 (= 0.031025) mf
LAWA48	14	Others > 0.019 (= 0.031025) mf
LAWA64	20	Others > 0.019 (= 0.079852) mf
LAWABP1	43	Others > 0.019 (= 0.020001) mf
LAWA54	90	Others > 0.019 (= 0.078579) mf
LAWA55	91	Others > 0.019 (=0.078630) mf
LAWA58	94	Others > 0.019 (=0.049942) mf
LAWA59	95	Others > 0.019 (=0.029906) mf
(a) mf = mass fraction		

Figure 4.3 and Figure 4.4 (corresponding to Figure 4.1 and Figure 4.2, respectively) show plots of component distributions after the 13 outlying and non-representative glasses were removed from the VHT dataset containing 699 glasses. Figure 4.3 shows that for the remaining 686 LAW glasses all 19 LAW glass “main components” have sufficient ranges and distributions of values within those ranges to support terms for modeling VHT. Figure 4.4 confirms that none of the “minor components” have sufficient ranges and distributions of values within their ranges to support model terms for those components. Based on Figure 4.3 and Figure 4.4, it was decided to use 20 components for initial pass/fail VHT modeling work. These components were Al₂O₃, B₂O₃, CaO, Cl, Cr₂O₃, F, Fe₂O₃, K₂O, Li₂O, MgO, Na₂O, P₂O₅, SO₃, SiO₂, SnO₂, TiO₂, V₂O₅, ZnO, ZrO₂, and Others (the sum of all remaining components). These are the same 20 components for all models except for melter SO₃ tolerance.

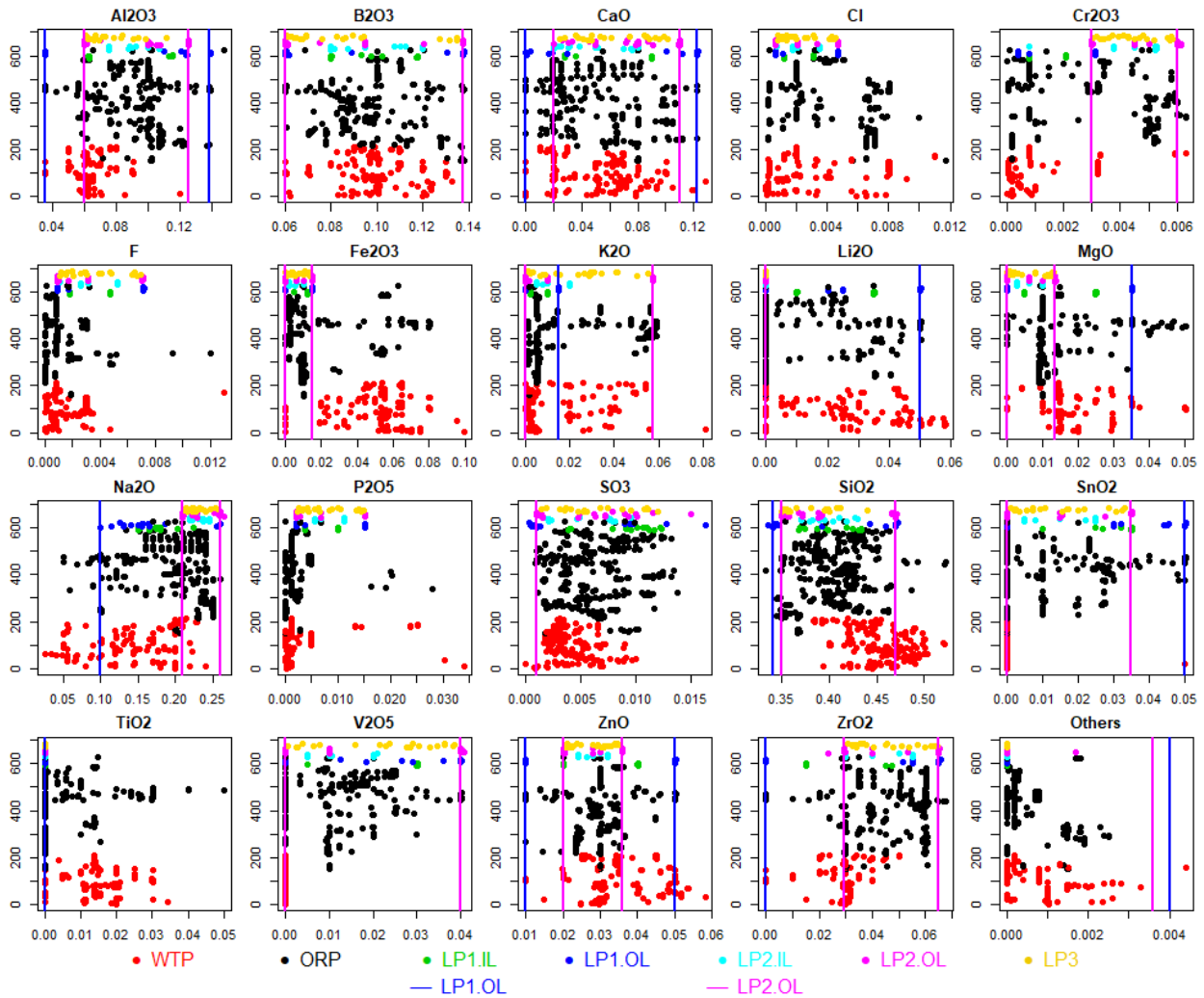


Figure 4.3. Distributions of 20 Main Components (in mass fractions) for 686 LAW Glass Compositions with Data for Pass/Fail VHT that Remain after Excluding the 13 Glasses in Table 4.1. The vertical lines (when present) represent the lower and upper limits for each component from the PNNL LAW Phase 1 (blue lines) and Phase 2 (pink lines) outer-layer studies (see Table 2.1). In cases where two limits are the same, pink lines overplot the blue lines.

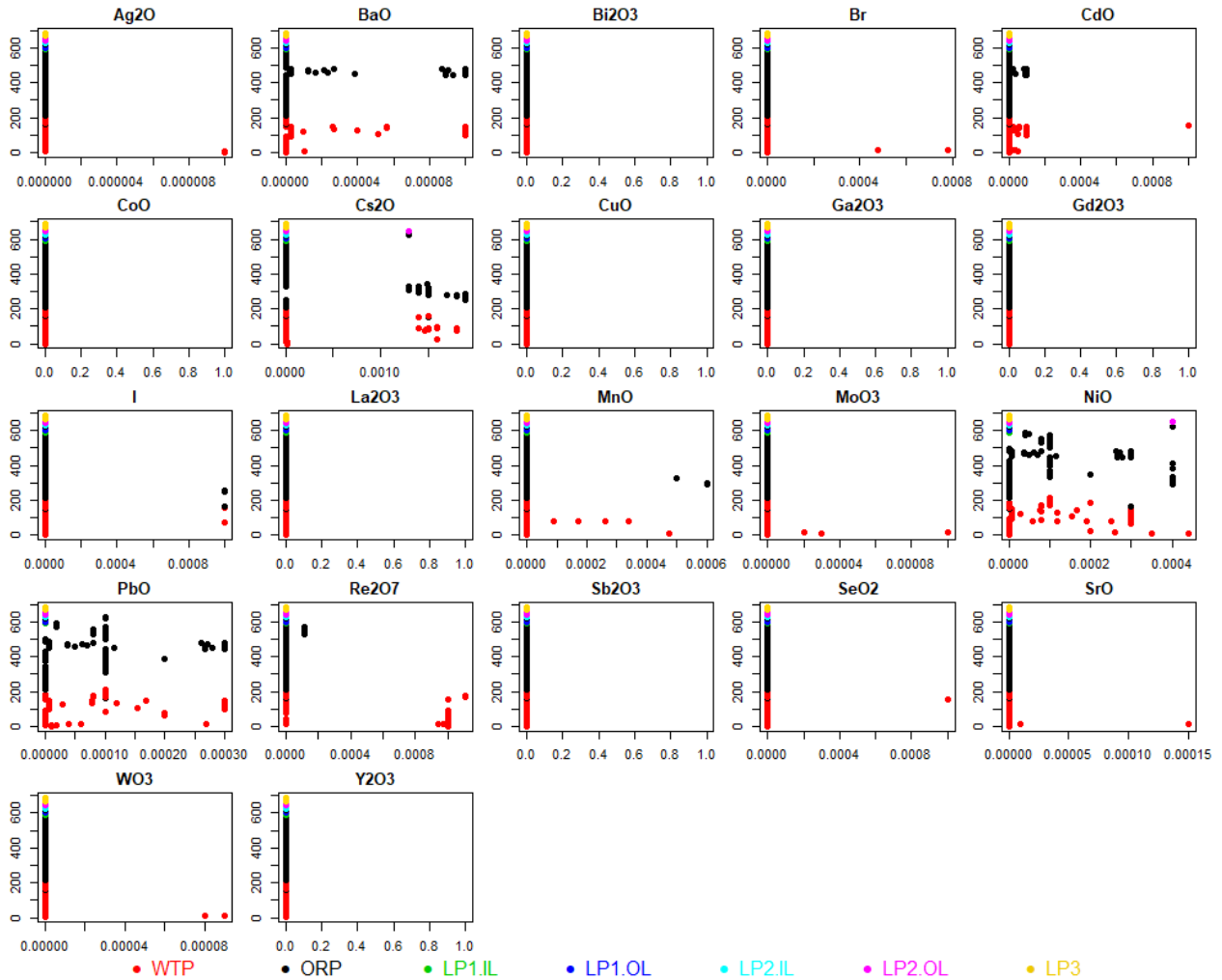


Figure 4.4. Distributions of 21 Minor Components (in weight percent) for 686 LAW Glass Compositions with Data for Pass/Fail VHT that Remain after Excluding the 13 Glasses in Table 4.1. The vertical lines (when present) represent the lower and upper limits for each component from the PNNL LAW Phase 1 (blue lines) and Phase 2 (pink lines) outer-layer studies (see Table 2.1). In cases where two limits are the same, pink lines over plot the blue lines.

Figure 4.5 shows a scatterplot matrix of the 686 glasses remaining in the VHT modeling dataset after removing the 13 non-representative compositions. High correlations in the predictors make parameter values difficult to estimate and result in inflated prediction uncertainties, so pairwise correlation coefficients were calculated. These can vary from -1.0 (perfect negative correlation) to 0 (no linear correlation) to 1.0 (perfect positive correlation). The only component pair with correlation larger (in absolute value) than 0.60 was Li_2O and Na_2O with a correlation of -0.8588 . See Section 9.7 for further information on these highly correlated component concentrations.

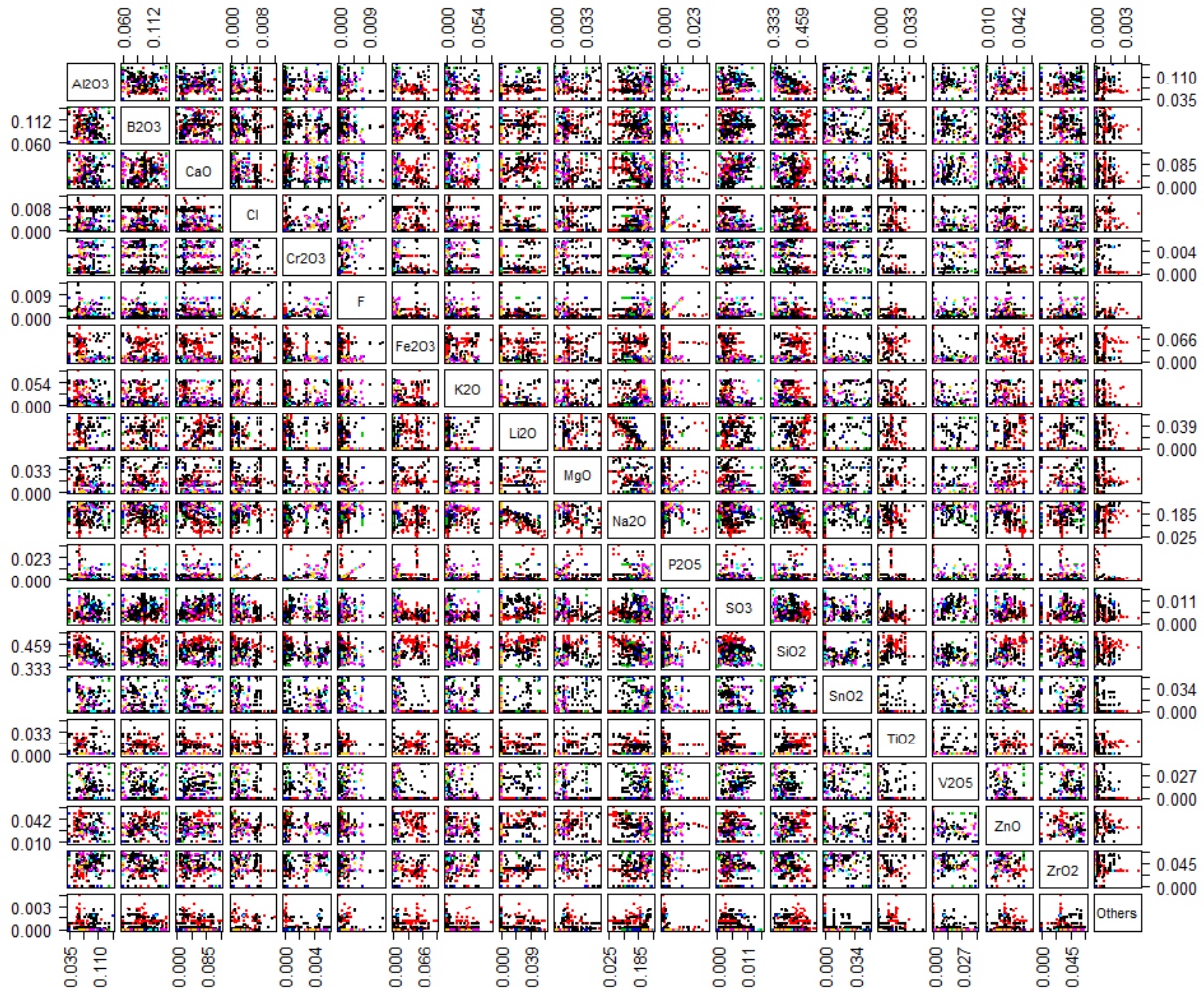


Figure 4.5. Scatterplot Matrix of 20 Components (mass fractions) for the 686 LAW Glasses with Pass/Fail Data that Remain after Excluding the 13 Glasses in Table 4.1

High pairwise correlations can make it difficult for regression methods to properly separate the effects of the components on the response variable. Thus, the high pairwise correlation between Li₂O and Na₂O needs to be kept in mind in developing and applying LAW glass property-composition models for the pass/fail VHT response.

4.1.1.2 Modeling Dataset for the Pass/Fail VHT Response

Table A.4 in Appendix A lists the Glass IDs, as well as pass/fail VHT values, for the 686 remaining simulated LAW glasses used for model development. The VHT values for non-representative glasses excluded from the 686-glass modeling dataset (see Table 4.1) are marked with an asterisk in Table A.3. The compositions for these 686 LAW glasses are included in Table A.2. The glass compositions are the normalized mass fractions of the 20 components previously identified as having sufficient data to support a separate model term if needed.

4.1.1.3 Replicate and Near-Replicate VHT Data on LAW Glasses

The changes to the LAW glass compositions caused by the renormalization associated with using measured (or estimated) SO₃ values (see Section 2.2) resulted in some replicate glasses not having exactly equal normalized compositions. Such compositions are near-replicates. For ease of discussion, henceforth both replicates and near-replicates are referred to as replicates.

Table 4.2 lists the replicate sets of LAW glasses in the VHT modeling dataset and the corresponding pass/fail VHT values. Table 4.2 also lists whether the glasses within a replicate set consistently have a single value (either pass or fail).

Table 4.2. Agreement in the VHT Pass (0)/Fail (1) Response for Replicate and Near-Replicate Glasses

Replicate Set Glass #s	Replicate Set Glass IDs	Replicate Set VHT Pass (0)/Fail (1)	Agreement in Replicate Set	Replicate Set #
993	EWG-LAW-Centroid-1	0	Yes	5
995	EWG-LAW-Centroid-2	0		
636	LAWA137	0	Yes	17
637	LAWA137	0		
285	LAWA137 (A3-AN104)	0	Yes	18
632	LAWA137 (A3-AN104)	0		
633	LAWA137 (A3-AN104)	0		
397	LAWA161	0	Yes	19
398	LAWA161	0		
516	LAWA187S1	0	Yes	20
517	LAWA187S1	0		
538	LAWA187S2	1	Yes	21
539	LAWA187S2	1		
737	LAWA187S2	1		
541	LAWA187S3	1	No	22
543	LAWA187S3	0		
28	LAWA88	0	Yes	34
389	LAWA88	0		
227	LAWB83	0	Yes	40
229	LAWB83	0		
284	LAWB83	0		
430	LAWB96	0	Yes	42
431	LAWB96	0		
442	LAWC100	0	Yes	43
443	LAWC100	0		
447	LAWC100	0		
125	LAWC21	0	Yes	45
437	LAWC21	0		
75	LAWC22	0	Yes	47
249	LAWC22	0		
272	LAWC22	0		
279	LAWC22	0		
456	LAWCrP1	0	Yes	51
457	LAWCrP1	0		

Table 4.2. Agreement in the VHT Pass (0)/Fail (1) Response for Replicate and Near-Replicate Glasses, cont.

638	LAWCrP11	0		
639	LAWCrP11	0	Yes	52
642	LAWCrP12	0		
643	LAWCrP12	0	Yes	53
458	LAWCrP2	0		
459	LAWCrP2	0	Yes	54
460	LAWCrP3	0		
461	LAWCrP3	0	Yes	55
462	LAWCrP4	0		
463	LAWCrP4	0	Yes	56
668	LAW18	1		
669	LAW18	1	Yes	57
670	LAW19	0		
671	LAW19	0	Yes	58
672	LAW19	0		
673	LAW20	1		
674	LAW20	1	Yes	59
675	LAW21	0		
676	LAW21	0	Yes	60
677	LAW22	0		
678	LAW22	0	Yes	61
679	LAW23	0		
680	LAW23	0	Yes	62
681	LAW24	1		
682	LAW24	0	No	63
683	LAW25	0		
684	LAW25	1	No	64
685	LAW26	0		
686	LAW26	1	No	65
451	LAW7H	0		
624	LAW7H	0	Yes	66
652	LAW9HCr1	0		
653	LAW9HCr1	0	Yes	67
654	LAW9HCr2	0		
655	LAW9HCr2	0	Yes	68
331	LAWM1	0		
383	LAWM1	0	Yes	69
342	LAWM12	1		
385	LAWM12	1	Yes	70
365	LAWM35	0		
386	LAWM35	0	Yes	71
380	LAWM50	0		
381	LAWM50	0	Yes	72
339	LAWM9	0		
384	LAWM9	0	Yes	73
846	ORLEC12	0		
865	ORLEC12	0	Yes	85
866	ORLEC12	0		

Table 4.2. Agreement in the VHT Pass (0)/Fail (1) Response for Replicate and Near-Replicate Glasses, cont.

848	ORLEC14	0	Yes	86
887	ORLEC14	0		
850	ORLEC16	0	Yes	87
888	ORLEC16	0		
889	ORLEC16	0		
853	ORLEC19	0	Yes	88
890	ORLEC19	0		
856	ORLEC22	0	Yes	89
891	ORLEC22	0		
859	ORLEC25	1	Yes	90
860	ORLEC25	1		
861	ORLEC25	1		
862	ORLEC26	0	Yes	91
867	ORLEC26	0		
868	ORLEC26	0		
863	ORLEC27	0	No	92
869	ORLEC27	1		
870	ORLEC27	0		
864	ORLEC28	0	Yes	93
871	ORLEC28	0		
872	ORLEC28	0		
877	ORLEC33	0	Yes	94
903	ORLEC33	0		
878	ORLEC34	0	Yes	95
904	ORLEC34	0		
893	ORLEC44	0	Yes	96
905	ORLEC44	0		
895	ORLEC46	0	Yes	97
906	ORLEC46	0		
897	ORLEC48R	0	Yes	98
907	ORLEC48R	0		
908	ORLEC48R	0		
616	ORPLA15	1	Yes	100
617	ORPLA15	1		
618	ORPLB4	1	Yes	105
619	ORPLB4	1		
589	ORPLC2	1	Yes	106
591	ORPLC2	1		
590	ORPLC2S4	1	Yes	107
592	ORPLC2S4	1		
595	ORPLC5	0	Yes	108
620	ORPLC5	0		
621	ORPLC5	0		
597	ORPLD1	0	Yes	109
622	ORPLD1	0		
997	ORPLD1	0		
999	ORPLD1	0		
1035	ORPLD1	0		

Table 4.2. Agreement in the VHT Pass (0)/Fail (1) Response for Replicate and Near-Replicate Glasses, cont.

766	ORPLG27	0	No	114
768	ORPLG27	1		
1022	LP2.Centroid	1	No	116
1028	LP2.Centroid	0		
1031	LP2.Centroid	0		
1049	LP2.Centroid	0		
1034	LP2.OL.Rep	0	Yes	117
1038	LP2.OL.Rep	0		
Proportion of replicate sets with consistent (pass or fail) results			88.14%	

The results in Table 4.2 show that, of the 138 glasses in 59 replicate sets, there is agreement (all observations in a particular set of replicates being either fail or pass) in 121, or 87.68% of the glasses in replicate sets with multiple glasses. Table 4.2 also shows that slightly over 88% (52 out of 59) of the sets have glasses with consistent (all pass or all fail) observations. This is an indication that the pass/fail response is reliable across a variety of glasses.

4.1.2 Model Validation Approach and Data for the VHT on LAW Glasses

The validation approach for the pass/fail VHT model was based on splitting the 686-glass dataset for model development into five modeling/validation subsets. The five modeling/validation splits of the 686 glasses in the VHT modeling dataset were formed as follows.

- The 59 replicate sets with multiple glasses (138 glasses) were set aside so they would always be included in each of the five model development datasets. This was done so that glasses in replicate sets would not be split between modeling and validation subsets, thus negating the intent to have validation glasses different than model development glasses.
- The remaining 548 glasses were ordered from smallest to largest according to their VHT values ($\text{g/m}^2/\text{d}$). The ordered glasses were numbered 1, 2, 3, 4, 5, 1, 2, 3, 4, 5, etc. All of the 1's formed the first model validation set, while all of the remaining points formed the first model development dataset. Similarly, all of the 2's, 3's, 4's, and 5's respectively formed the second, third, fourth, and fifth model validation sets. In each case, the remaining non-2's, non-3's, non-4's, and non-5's formed the second, third, fourth, and fifth model development datasets.
- The 138 replicate glasses were added to each of the split modeling subsets so that each of the five splits contained a balanced number of 548 glasses for modeling and 109 or 110 glasses for validation.

Data splitting was chosen as the validation approach because the VHT modeling dataset contains all compositions that (i) are in the LAW glass composition region of interest, (ii) meet QA requirements, and (iii) have pass/fail VHT data. Having a separate validation dataset not used for modeling is desirable, but that desire was over-riden by wanting the VHT models developed using all appropriate data including the data near the pass/fail boundary (which is relatively sparse).

4.1.3 Subsets of LAW Glasses to Evaluate Prediction Performance of Pass/Fail VHT Models

Section 2.4 discusses six subsets of LAW glasses for evaluating the prediction performance of LAW glass property-composition models, including subsets of glasses with higher waste loadings. The subsets, as discussed in Section 2.4, are denoted WTP, ORP, LP2OL, LP123, HiNa_2O , and HiSO_3 . The VHT modeling dataset of 686 LAW glasses (see Section 4.1.1) contains 202, 392, 134, 92, 285, and 108 glasses with pass/fail VHT values in these six evaluation subsets, respectively. The “Glass #s” of these six evaluation subsets of LAW glasses are listed in Table C.2 in Appendix C. The normalized LAW glass compositions and pass/fail values for the glasses with these “Glass #s” are listed in Tables A.2 and A.3, respectively, of Appendix A.

4.2 Model Forms and Accuracy Measures for the Vapor Hydration Test on LAW Glasses

Mixture models (Cornell 2002) are used to relate LAW glass compositions to the pass/fail VHT response. Empirical models of this type use existing data to estimate coefficients in a predictive equation such that certain goodness-of-fit criteria are optimized. Section B.1 of Appendix B discusses mixture experiments and several general forms of mixture experiment models.

Because of the binary nature of the VHT response, a logistic model was used to relate the binary (pass/fail) VHT response to the composition of glasses in the modeling set. A logistic model takes as input the composition of a glass and produces a *score*, a number between 0 and 1, that can be used to classify it as a pass or fail for VHT. The score represents a threshold for classification, where glasses with scores at or above a selected threshold are predicted as “fail” and those with scores below the threshold are classified as “pass.”

Different models may produce different scores for a given glass composition, and different thresholds can be used to decide whether a glass is classified as “fail” or “pass.” The objective addressed in this section is to select a model with foundations in glass science and a threshold that produces an optimal rate of classification. The optimal rate of classification can include practical considerations such as minimizing the number of “fail” VHT glasses that are classified as “pass,” maximizing overall accuracy (number of glasses correctly classified/total number of glasses predicted), or other considerations.

For the models developed in this work, higher scores are associated with “fail” glasses and lower scores are associated with “pass” glasses. This distinction is arbitrary, and the opposite could have been chosen by changing the labeling of the VHT response.

The accuracy measures of interest for the pass/fail VHT models are the overall accuracy

$$\frac{\# \text{ Glasses correctly classified}}{\text{Total number of glasses in set}}$$

the false negative rate (FNR)

$$\frac{\# \text{ Fail glasses classified as Pass}}{\# \text{ Fail glasses in set}}$$

and the false positive rate (FPR)

$$\frac{\# \text{ Pass glasses classified as Fail}}{\# \text{ Pass glasses in set}}$$

Other accuracy measures, such as true-positive and true-negative rates can also be calculated, but the overall accuracy, FNR and FPR sufficiently convey the quality of predictive models for this work. The optimality criterion used to select a threshold for classification is seeking a model with the highest overall accuracy constrained on maintaining FNR at or below 0.1. This FNR value was selected to maintain a 90% accuracy rate in predicting fail VHT glasses similar to that maintained in the WTP baseline GFA (Kim and Vienna 2012).

Section 4.2.1 contains the development of logistic models in the context of mixture experiments for predicting the pass/fail VHT response of LAW glasses.

4.2.1 Mixture Experiment Model Forms for a Binary Pass/Fail VHT Response on LAW Glasses

FLM and PQM model forms introduced in Section B.1 of Appendix B have been used in the past (e.g., Piepel et al. 2007; Muller et al. 2014) to model glass properties as functions of LAW glass composition. For this work, a GLM (Myers et al. 2002) using a binomial distribution for the response and a logit function to link the mixture portion of the data to the mean of the pass/fail VHT response are used. The logistic model form is given by

$$\ln\left(\frac{P(\mathbf{g})}{1 - P(\mathbf{g})}\right) = \sum_{i=1}^q \beta_i g_i + e \quad (4.1)$$

while the PQM model form is given by

$$\ln\left(\frac{P(\mathbf{g})}{1 - P(\mathbf{g})}\right) = \sum_{i=1}^q \beta_i g_i + \text{Selected} \left\{ \sum_{i=1}^q \beta_{ii} g_i^2 + \sum_{i < j}^{q-1} \sum_j^q \beta_{ij} g_i g_j \right\} + e \quad (4.2)$$

In Eqs. (4.1) and (4.2)

- $P(\mathbf{g})$ = probability in a Bernoulli trial for the normalized glass composition given by \mathbf{g}
- g_i = normalized mass fraction of the i^{th} glass oxide or halogen component
($i = 1, 2, \dots, q$) such that $\sum_{i=1}^q g_i = 1$
- β_i = coefficient of the i^{th} linear blending term ($i = 1, 2, \dots, q$)
- β_{ii} and β_{ij} = coefficients of selected quadratic (squared or crossproduct) blending terms to be estimated from the data
- e = random error for each data point.

The logistic models employed here, one in the family of GLMs (Myers et al. 2002), are useful for creating predictive equations when the response is binary. In a logistic model, the linear portion of the model, the right-hand side portion of Eq. (4.2), is related to the response using a link function such as the logit function shown as the left-hand side of Eq. (4.1). In Eq. (4.2), “Selected” means that only some of the terms in curly brackets are included in the model. The subset is selected using stepwise regression or a

different variable selection method (Draper and Smith 1998; Montgomery et al. 2012). PQM models are discussed in more detail and illustrated by Piepel et al. (2002) and Smith (2005).

Model selection for the pass/fail VHT response using a logistic PQM involves incorporating different combinations of glass components as linear, two-factor interactions and pure quadratic terms, and searching for an appropriate threshold that optimizes overall classification accuracy while maintaining the desired false negative rate.

4.3 Property-Composition Model Results for a Pass/Fail VHT Response on LAW Glasses

This section discusses the results of fitting several different mixture experiment models using a logistic equation to relate the pass/fail VHT response to LAW glass compositions. Section 4.3.1 presents the results of modeling the binary VHT response using a 20-component FLM model and a logit link. Section 4.3.2 presents results of modeling the binary VHT response using a logistic PQM model with a logit link function based on a reduced set of 16 mixture components. Then, Section 4.3.3 recommends a logistic model for future use and evaluation.

4.3.1 Results from the 20-Component Full Linear Mixture Logistic Model for the Pass/Fail Response for the VHT on LAW Glasses

As the initial step in model development for the pass/fail VHT response, an FLM model in the 20 components identified in Section 4.1.1 was fit to the modeling data (686 glasses) using a GLM and a logit function linking the pass/fail VHT response to the 20 glass components. This model form was a reasonable starting point based on previous work modeling other responses for LAW glasses (Piepel et al. 2007) and provided a basis for appropriate model modifications.

Table 4.3 contains the results from the 20-component FLM logistic model for the pass/fail VHT. Table 4.4 lists the model coefficients, standard deviations of the coefficients, and model performance summaries for the (i) 20-component logistic FLM model using the modeling dataset (686 LAW glasses), (ii) evaluation of model predictions for the six evaluation subsets (see Section 4.1.3), and (iii) the data splitting validation subsets labeled DS1, DS2, DS3, DS4, and DS5 (see Section 4.1.2) and a threshold for classification selected as 0.3 for illustration purposes because it resulted in a reasonably good performance. This threshold means that glasses with score values equal to or greater than the selected threshold are classified as fail and classified as pass otherwise. Table 4.3 also shows average performance statistics for the five validation sets.

Table 4.3. Coefficients and Performance Summary for the 20-Component Logistic Full Linear Mixture Model on the Pass/Fail VHT response on LAW Glasses Using a Threshold for Classification of 0.3

$\ln(\frac{P(g)}{1-P(g)})$		
20-Component FLM Model Term	Coefficient Estimate	Coefficient Stand. Err.
Al ₂ O ₃	-41.3243	8.5361
B ₂ O ₃	-8.0741	7.2244
CaO	-54.3502	8.0095
Cl	106.0113	63.6601
Cr ₂ O ₃	-81.9437	94.7179
F	-85.6558	100.6878
Fe ₂ O ₃	-33.8841	12.1827
K ₂ O	113.5594	12.5968
Li ₂ O	191.76	28.5713
MgO	33.0593	19.1647
Na ₂ O	103.765	11.3361
P ₂ O ₅	26.1474	53.1005
SO ₃	77.1368	66.3941
SiO ₂	-33.0163	4.3556
SnO ₂	-57.2678	15.6566
TiO ₂	-105.693	28.3877
V ₂ O ₅	24.0616	16.6005
ZnO	-46.9714	20.4829
ZrO ₂	-114.124	15.3502
Others ^(c)	932.0578	227.8075

Modeling Data Statistic, 686 Glasses ^(a)		Value
Overall Accuracy Rate		0.8630
False Positive Rate		0.1326
False Negative Rate		0.1519
Model LOF p-value ^(g)		>0.99

Evaluation Set (# Glasses) ^(b)			
	Acc.	FPR ^(e)	FNR ^(f)
WTP (202)	0.9505	0.0546	0
ORP (392)	0.8342	0.1622	0.1771
LP2OL (134)	0.8333	0.1875	0.1250
LP123 (92)	0.7935	0.2449	0.1628
HiNa ₂ O (285)	0.7965	0.2373	0.1481
HiSO ₃ (108)	0.9352	0.0667	0.0556

Data Splitting Statistic ^(a,d)	DS1	DS2	DS3	DS4	DS5	Average
Overall Accuracy	0.8300	0.8500	0.8300	0.8800	0.8400	0.8460
False Positive Rate	0.1867	0.1579	0.1467	0.1067	0.0959	0.1388
False Negative Rate	0.1200	0.1250	0.2400	0.1600	0.3333	0.1957

(a) The model evaluation statistics are defined in Section 4.2.

(b) The six sets of LAW evaluation glasses are discussed in Section 2.4 and Section 4.1.3.

(c) For the 20-component FLM model, the “Others” component includes any components not separately listed.

(d) The evaluation and validation statistics calculated for data-splits are defined the same as for separate modeling and validation sets. Section 4.1.2 describes how the modeling dataset was split into modeling and validation subsets.

(e) False positive rate

(f) False negative rate

(g) The logistic lack-of-fit (LOF) test uses the statistic $\chi^2 = \sum_{i=1}^m \frac{(y_i - n_i \hat{P}_i)^2}{n \hat{P}_i (1 - \hat{P}_i)}$, where y_i is the observed pass/fail response, \hat{P}_i is the model-predicted score, $n_i = 1$ in this work and m is the number of observations. If the pass/fail VHT response can be adequately modeled using a logistic model of the type developed in this work, this statistic is asymptotically distributed as χ^2_{m-p} , where p is the number of model parameters. A p -value for this statistic less than or equal to 0.05 indicates significant LOF.

The overall accuracy statistics in Table 4.3 indicate that the 20-component FLM model produces fairly good results for the 686-glass modeling dataset using the 0.3 threshold for classification. The overall accuracy, FPR, and FNR are also fairly good for the evaluation and validation sets. The worst overall accuracy of 0.7935 occurs for the LP123 evaluation set, while the best accuracy (0.9505) was for the

WTP evaluation set. Table 4.3 also indicates that the FLM does not have significant LOF. Figure 4.6 graphically demonstrates the model performance with a majority of fail glasses above the threshold and a majority of pass glasses below the threshold.

False positive and false negative rates are not too large for the FLM, which is also an indication that the model structure is highly consistent with the data. However, the FNR is in most cases above the desired target of 0.1. Results in Table 4.3 apply only to the combination of FLM and threshold selected, and different accuracy statistics will be found if a different classification threshold is employed.

Figure 4.7 and Figure 4.8 show that, for the 0.3 threshold used as an illustration for classification, the FLM produces results where, in general, glasses that fail have higher scores and glasses that pass have lower ones.

Results in Table 4.3, Figure 4.6, Figure 4.7, and Figure 4.8 indicate that the FLM with a threshold for classification of 0.3 is a reasonably good classifier. Results in Table 4.3 do not take into consideration uncertainty in model predictions. To account for uncertainty in model scores, confidence intervals can be computed for each observation. Confidence intervals can be used to help decide if a glass should be classified as pass, fail, or “uncertain.” Instead of comparing the score value directly to the threshold to make a classification, the limits of a confidence interval can be used. Intervals that do not overlap the threshold can be more clearly classified as the class assigned by the model than those whose confidence intervals are on both sides of the threshold.

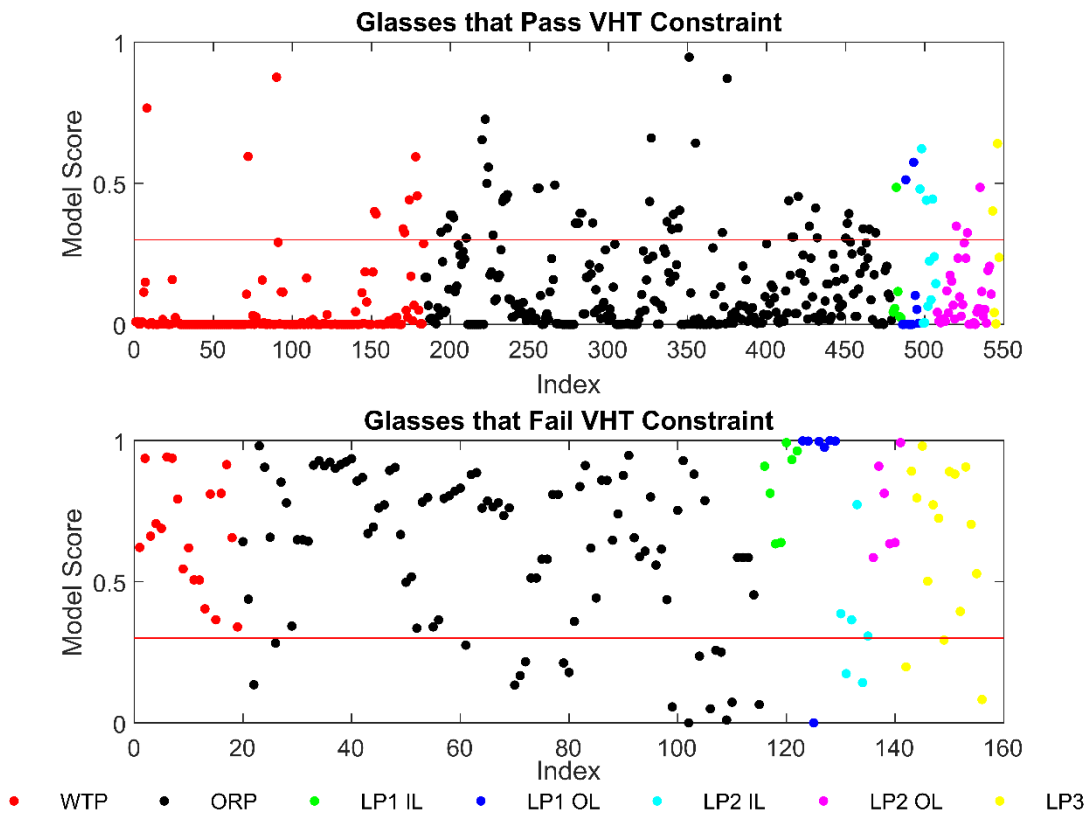


Figure 4.6. Scores (y-axes) for Glasses that Pass (upper panel) and Fail (lower panel) Generated by the 20-term VHT FLM. The x-axes show glasses on an index to avoid overcrowding. The 0.3 threshold value for classification (used for illustration purposes only) is shown as a red horizontal line.

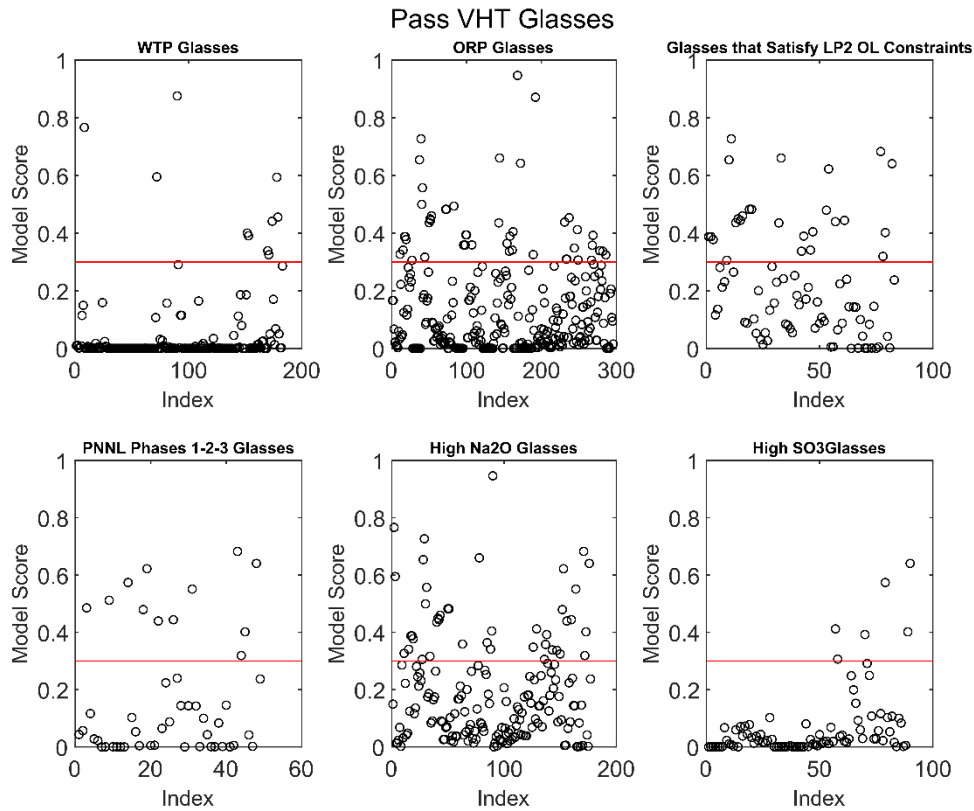


Figure 4.7. Plots of the Scores Produced by the 20-term FLM for Six Sets of Glasses that Pass the Vapor Hydration Constraint. The 0.3 threshold value for classification (used for illustration purposes only) is shown as a red horizontal line.

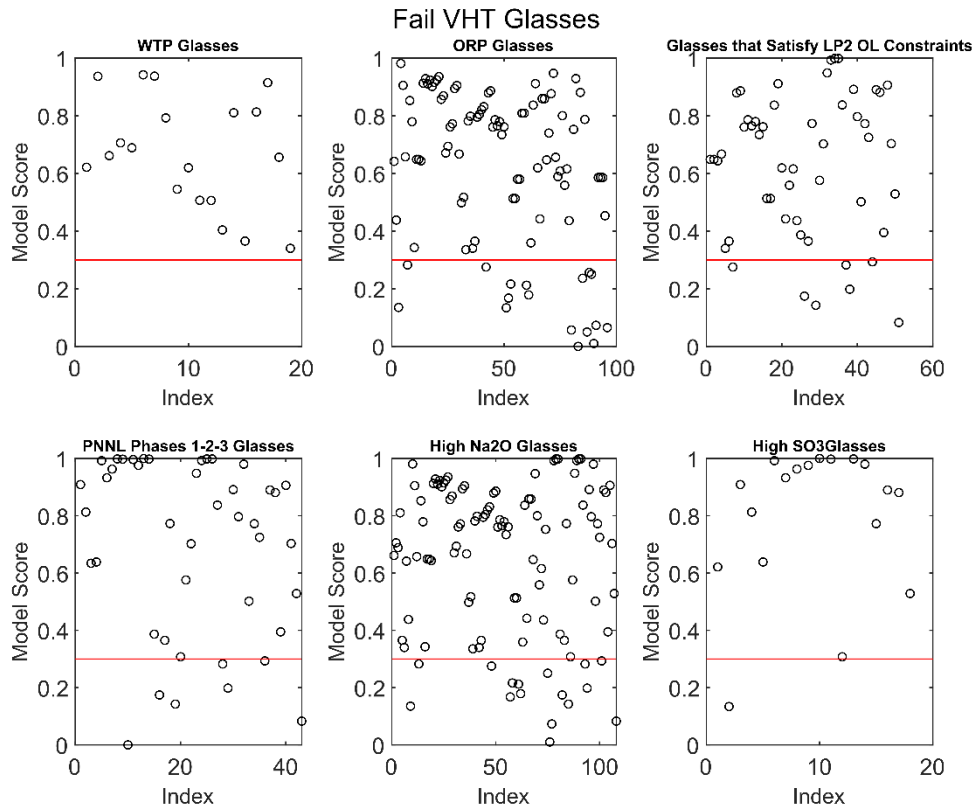


Figure 4.8. Plots of the Scores Produced by the 20-term FLM for Six Sets of Glasses that Fail the Vapor Hydration Constraint. The 0.3 threshold value for classification (used for illustration purposes only) is shown as a red horizontal line.

A classification strategy for VHT needs to involve selecting a combination of models and thresholds where the FNR achieves the desired value of 0.1 after taking into consideration the calculated confidence intervals. Conditional on achieving the desired FNR, the classification strategy should also minimize the FPR. This means that given two model/threshold options that satisfy the FNR target, the one giving the lowest FPR should be selected.

Results in Table 4.3 indicate that the 20-term FLM does not in general achieve the targeted FNR, even without considering confidence intervals. Achieving the desired FNR while considering the uncertainty in score values brought in by including confidence intervals will result in lower overall accuracy for the selected model. This suggests that models should be sought with improved performance. Based on previous experience, addition of non-linear terms to the model should be pursued to build a model that achieves the target FNR while remaining as accurate, overall, as possible.

4.3.2 Results from the Development of a 19-Term Partial Quadratic Mixture Model for Pass/Fail VHT on LAW Glasses

The full 20-component FLM model for the pass/fail VHT response presented in Section 4.3.1 does not in general produce the desired FNR, even without considering prediction uncertainty, so searching for a different model was the next step of the model development.

The first step in the search for alternative models consists of reducing the number of terms in the purely linear portion of the model. This is achieved by incorporating components that may not significantly affect the pass/fail VHT response into the “Others” term. Components that can be incorporated into the Others term in the model are any among Cl, Cr₂O₃, F, Fe₂O₃, SO₃, and ZnO that have been previously shown to have relatively small effects on VHT (Piepel et al. 2007; Vienna et al. 2013, 2016).

Next, performance of models with different combinations of two- and three-factor interaction, purely quadratic terms, and different thresholds for classification were evaluated, using different components incorporated into the Others term. This process produced a large number of models, which were sorted by FNR values as a function of classification threshold.

A model with Cl, Cr₂O₃, Fe₂O₃, and SO₃ incorporated into the Others term, two two-factor interactions (Li₂O × Na₂O and TiO₂ × ZrO₂) plus one purely quadratic term (Li₂O × Li₂O), produced acceptable results using a threshold of 0.19. These terms are generally expected based on past VHT response modeling for LAW glasses that showed second-order terms involving Li₂O, Na₂O and ZrO₂ (Piepel et al. 2007, Vienna et al. 2013, Vienna et al. 2016). Second order terms containing TiO₂ are not commonly found and warrant further investigation. Performance of this model is shown graphically in Figure 4.9 and Figure 4.10 and has the parameters and performance shown in Table 4.4.

Table 4.4. Coefficients and Performance Summary for the 19-Component Logistic Partially Quadratic Mixture Model on the Pass/Fail VHT response on LAW Glasses Using a Threshold for Classification of 0.19

$\ln(\frac{P(g)}{1-P(g)})$			Modeling Data Statistic, 686 Glasses ^(a)			
19-Component PQM Model Term	Coefficient Estimate	Coefficient Stand. Err.				Value
Al ₂ O ₃	-33.2908	7.8647	Overall Accuracy Rate			0.7974
B ₂ O ₃	-10.2672	6.8058	False Positive Rate			0.2424
CaO	-57.3456	8.1289	False Negative Rate			0.0696
F	47.6668	94.4440	Model LOF p-value ^(g)			>0.99
K ₂ O	97.7116	11.4808				
Li ₂ O	435.0046	133.7388				
MgO	30.6084	18.7840				
Na ₂ O	108.6944	12.0704				
P ₂ O ₅	-42.4271	49.1953				
SiO ₂	-34.1488	4.6266				
SnO ₂	-59.3127	13.0947				
TiO ₂	-72.6017	50.4728				
V ₂ O ₅	20.7981	15.1745				
ZnO	-48.7954	19.8328				
ZrO ₂	-102.7010	16.0042				
Others	-20.9574	11.4096				
Li ₂ O × Na ₂ O	-983.3257	451.7071				
TiO ₂ × ZrO ₂	-1488.9830	1093.0960				
Li ₂ O × Li ₂ O	-2124.0889	1671.6355				
Data Splitting Statistic ^(a,d)	DS1	DS2	DS3	DS4	DS5	Average
Overall Accuracy	0.7700	0.7800	0.8100	0.8500	0.8300	0.8080
False Positive Rate	0.2800	0.2500	0.2267	0.1867	0.2055	0.2298
False Negative Rate	0.0800	0.1250	0.0800	0.0400	0.0741	0.0798

(a) The model evaluation statistics are defined in Section 4.2.

(b) The six sets of LAW evaluation glasses are discussed in Section 2.4 and Section 4.1.3.

(c) For the 16-component PQM model, the “Others” component includes any components not separately listed. This is equivalent to the “Others” component in the 20-component FLM model plus the concentrations of Cl, Cr₂O₃, Fe₂O₃, and SO₃.

(d) The evaluation and validation statistics calculated for data-splits are defined the same as for separate modeling and validation sets. Section 4.1.2 describes how the modeling dataset was split into modeling and validation subsets.

(e) False Positive Rate

(f) False Negative Rate

(g) The logistic lack-of-fit (LOF) test uses the statistic $\chi^2 = \sum_{i=1}^m \frac{(y_i - n_i \hat{p}_i)^2}{n \hat{p}_i (1 - \hat{p}_i)}$, where y_i is the observed pass/fail response, \hat{p}_i is the model-predicted score, $n_i = 1$ in this work and m is the number of observations. If the pass/fail VHT response can be adequately modeled using a logistic model of the type developed in this work, $t\chi^2_{m-p}$ where p is the number of model parameters. A p -value for this statistic less than or equal to 0.05 indicates significant LOF.

Results in Table 4.4 show that the 19-term PQM generally achieves an FNR close to or below the target of 0.1 except for the DS2 validation set. The threshold score used for classifying a glass as fail using the model in Table 4.4 is very low (0.19) as a result of trying to maintain an overall FNR close to 0.1 after

incorporating the uncertainty produced by considering 90% CIs into the model predictions. Table 4.4 also indicates that the 19-term PQM does not have significant LOF.

Performance of the 19-term PQM model for the pass/fail VHT response is shown graphically in Figure 4.9, Figure 4.10, and Figure 4.11.

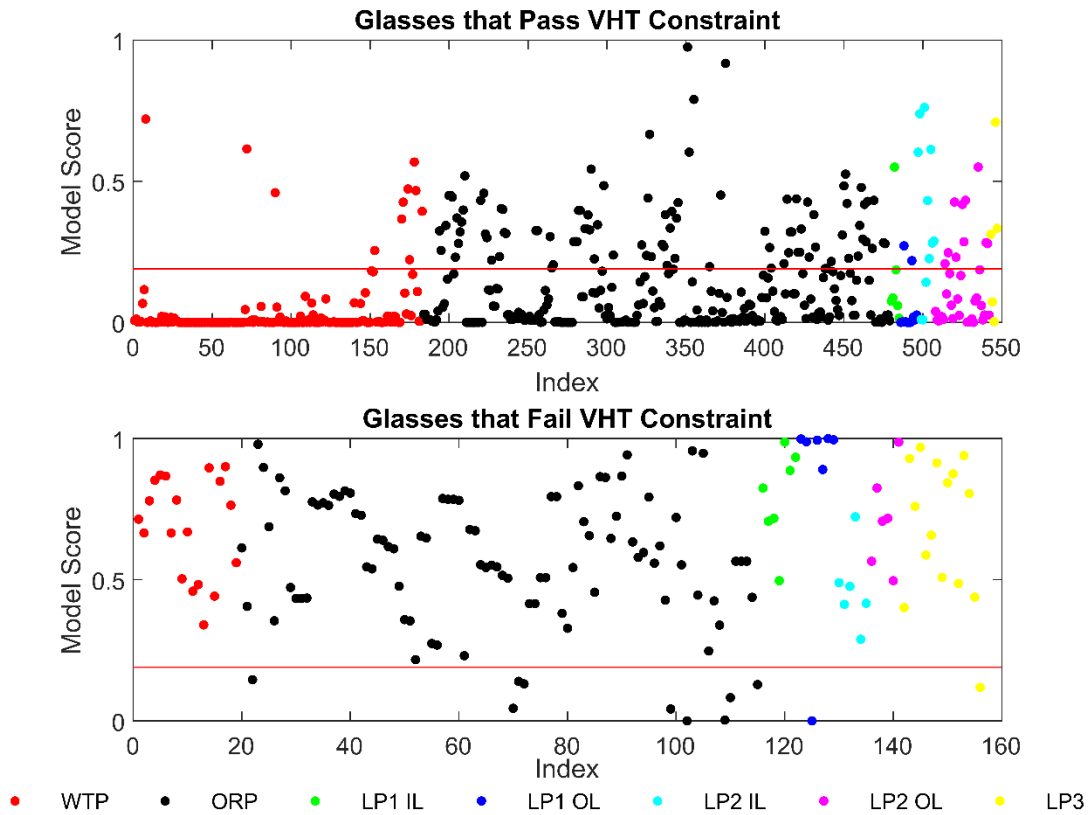


Figure 4.9. Scores (y-axes) for Glasses that Pass (upper panel) and Fail (lower panel) Generated by the 19-term VHT PQM. The x-axes show glasses on an index to avoid overcrowding. The 0.19 value used as threshold for classification is shown as a red horizontal line.

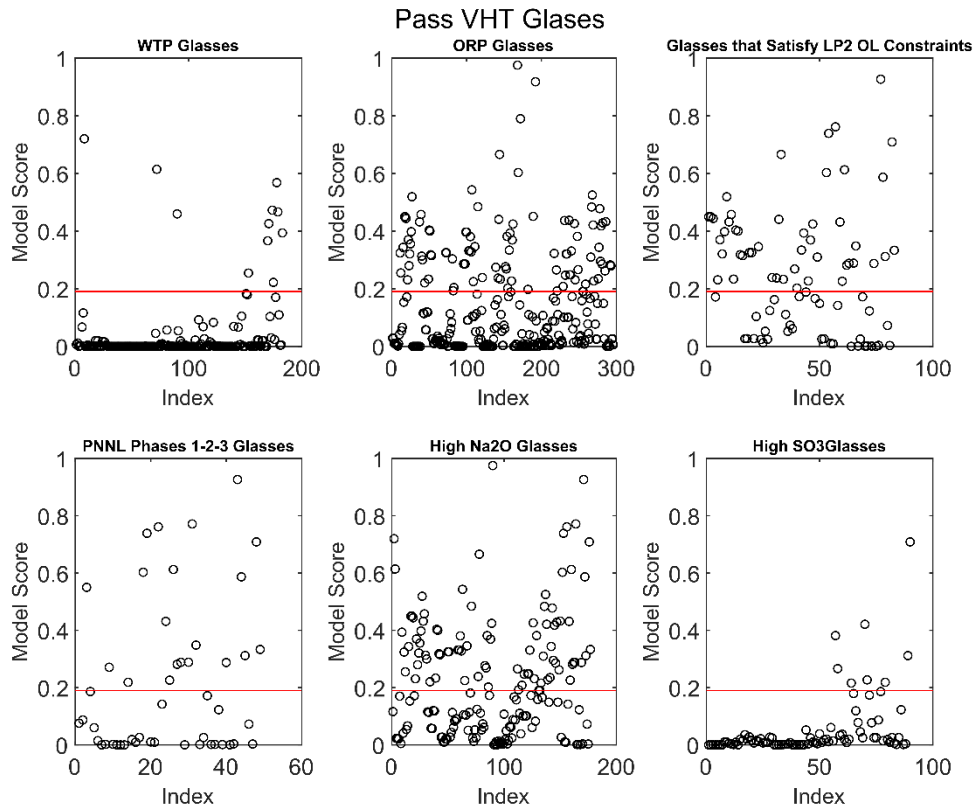


Figure 4.10. Model Scores (y-axes) Produced by the 19-term PQM Pass/Fail VHT Model for the Pass Glasses in Six Different Evaluation Sets. Glasses below the 0.19 threshold are correctly classified as Pass.

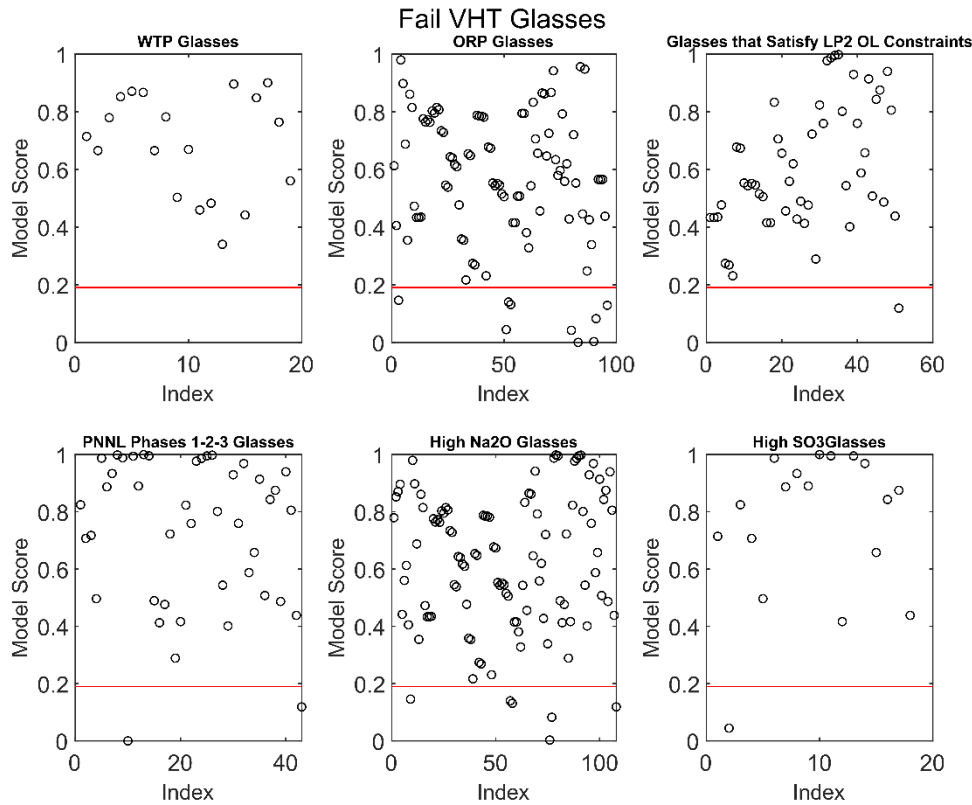


Figure 4.11. Model Scores (y-axes) Produced by the 19-term PQM Pass/Fail VHT Model for the Fail Glasses in Six Different Evaluation Sets. Glasses above the 0.19 threshold are correctly classified as Fail.

The plots in Figure 4.9, Figure 4.10, and Figure 4.11 show that very few fail glasses are classified as pass, which is a desired objective. This reduction in wrongly classified fail glasses comes at the expense of an increased rate of misclassification for pass glasses, which is necessary so that the desired FNR, considering prediction uncertainty, can be achieved. The model with parameters shown in Table 4.4 has one of the highest classification thresholds for achieving the desired FNR, ensuring that it simultaneously minimizes misclassification of pass glasses. Figure 4.12 shows the response trace plot for the 19-term PQM VHT model.

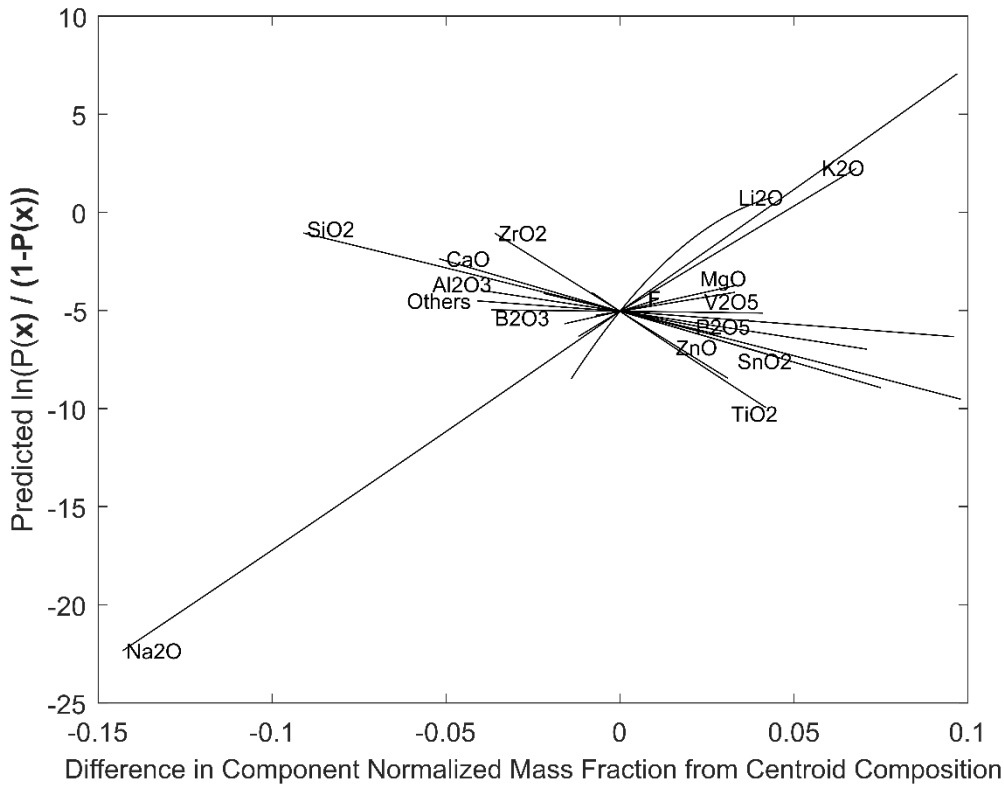


Figure 4.12. Response Trace Plot for the 19-term PQM Pass/Fail VHT Model

The response trace plot in Figure 4.12 shows that Li_2O , Na_2O , and K_2O have the largest effect on increasing the probability of VHT failure. TiO_2 , ZrO_2 , SnO_2 , and SiO_2 have the largest effects on decreasing the probability of VHT failure, with most of the other components exhibiting relatively small effect. The curvature produced by the Li_2O term is evident in Figure 4.12.

The PQM model in Table 4.4 has a two-factor interaction between Li_2O and Na_2O , two highly correlated compounds. The PQM also has a quadratic term involving Li_2O , which is also highly correlated with Na_2O (correlation value -0.8057). Such high correlations in the predictors make parameter values difficult to estimate and result in inflated prediction uncertainties (Montgomery et al. 2012). However, predictions obtained under conditions of high multicollinearity can still be accurate, provided they are made in the region where the multicollinearity holds.

4.3.3 Recommended Model for Pass/Fail VHT on LAW Glasses

Based on the results in Table 4.3 and Table 4.4 and discussions in Sections 4.3.1 and 4.3.2, the 19-term reduced PQM model (listed in Table 4.4) with a threshold for classification of 0.19 is recommended for predicting the pass/fail VHT response of LAW glasses.

Other model-threshold combinations can be used that produce similar results to those presented in this document for the recommended model. Varying the threshold selected for classification while maintaining the recommended model is the simplest way to alter prediction performance if project requirements change.

4.4 Example Illustrating VHT Model Predictions and Statistical Intervals

This section contains examples to illustrate using the recommended 19-term PQM model (Section 4.3.2) to obtain predicted pass/fail VHT values, and corresponding 90% CIs for a specific LAW glass composition as described in Section B.6 of Appendix B. The confidence level associated with 90% CIs was chosen for illustration purposes only. The WTP LAW facility can use an appropriate confidence level depending on the use of the VHT-composition model and the type of statistical uncertainty expression.

The glass composition used in this example is denoted REFMIX, as listed in Table 2.3. The 20-component composition of REFMIX for VHT modeling is given in Table 4.5 in mass fraction format. To apply the recommended VHT model to this composition, the mass fractions of the 20 components must be converted to mass fractions (that sum to 1.0) of the 16 LAW glass components contained in the recommended pass/fail VHT model. This involves adding to the mass fraction of Others (denoted Others₂₀ for the 20-component case) the mass fractions of the 4 of 20 components not contained in the recommended VHT model. This produces a new Others mass fraction, denoted Others₁₆. Mass fractions of the relevant components are then multiplied to obtain the quadratic terms of the PQM models. Table 4.5 contains the composition of REFMIX prepared for use in the VHT model for LAW glasses.

For each of the presented VHT models, predicted pass/fail VHT values are obtained by multiplying the composition in the format needed for that model by the coefficients for that model, then summing the results. That is, the predicted values are calculated by first calculating

$$\hat{y}(\mathbf{g}) = \mathbf{g}^T \mathbf{b} \quad (4.3)$$

where \mathbf{g} is the composition of REFMIX formatted to match the terms in a given model (from Table 4.6), the superscript T represents a matrix transpose (or vector transpose in this case), and \mathbf{b} is the vector of coefficients for a given model. The predicted score and pass/fail values for REFMIX using the VHT models are listed in the second column of Table 4.5. The predicted pass/fail score values are calculated by first computing

$$\widehat{P}(\mathbf{g}) = \exp(\mathbf{g}^T \mathbf{b}) / (1 + \exp(\mathbf{g}^T \mathbf{b})) \quad (4.4)$$

where $\widehat{P}(\mathbf{g})$ is the model-estimated score for the glass. The predicted score is then compared to the selected threshold of 0.19. Values equal or greater than the threshold classify the glass as fail. The glass is classified as pass otherwise.

Because of the monotonic relationship between the logit link and the linear portion of the model, a two-sided interval on $\mathbf{g}^T \mathbf{b}$ with $(1 - \alpha) \times 100\%$ confidence level is given by Myers et al. (2002):

$$\mathbf{g}^T \mathbf{b} \pm z_{\alpha/2} \sqrt{\mathbf{g}^T (\mathbf{G}^T \mathbf{V} \mathbf{G})^{-1} \mathbf{g}} \quad (4.5)$$

where $(\mathbf{G}^T \mathbf{V} \mathbf{G})^{-1}$ is the variance-covariance matrix of glass compositions, $z_{\alpha/2}$ is the value of a standard normal distribution that leaves an area of $\alpha/2$ to its right. For the example calculations presented in Table 4.6, the z -statistic value needed for Eq. (4.5) with $\alpha=0.10$ is 1.644854. The following cell formula can be used to obtain the z -statistic value with Excel: =NORM.INV(0.95,0,1). As discussed in Section B.6.5 of Appendix B, these confidence intervals rely on the fact that $\mathbf{g}^T \mathbf{b}$ is asymptotically normally distributed. An estimate on the confidence interval of the model score can be obtained by transforming the resulting values from Eq. (4.5) in the way shown in Eq. (4.4). A two-sided confidence interval on the model score

is a conservative estimate of the FNR needed because observations can cross the threshold used for classification from below (glasses with scores predicting them as pass, but where the upper limit of the confidence interval crosses into the fail side of the threshold), or from above (glasses with scores predicting them as fail, but where the lower limit of the confidence interval crosses into the pass side of the threshold). In Eq. (4.5), matrix **G** is formed from the data matrix used in the regression that generated a given VHT model. Matrix **G** has the number of rows in the VHT modeling dataset (686) and the number of columns corresponding to the number of terms in a given VHT model. Each column is calculated according to the corresponding term in the model using the LAW glass compositions in the VHT modeling dataset.

To obtain a 90% lower confidence interval (LCI) on the mean VHT score, only the ‘-’ of the ‘±’ in Eq. (4.5) is used, using z_α with $\alpha = 0.10$. Using the LCI essentially makes “fail” VHT glasses less likely to end up in the uncertain zone and makes the LCI an optimistic estimate for the FNR of this glass property.

Table 4.5. REFMIX Composition in Formats Used with Models of $\ln\left(\frac{P(g)}{1-P(g)}\right)$ for Predicting Pass/Fail VHT for LAW Glasses

Model Term	REFMIX Composition ^(a) (mass fractions)	REFMIX Composition (mass fractions) to Use in 19-Component PQM Model for $\ln\left(\frac{P(g)}{1-P(g)}\right)$ ^(b)
Al ₂ O ₃	0.075760	0.075760
B ₂ O ₃	0.097257	0.097257
CaO	0.052514	0.052514
Cl	0.003376	NA
Cr ₂ O ₃	0.002041	NA
F	0.001348	0.001348
Fe ₂ O ₃	0.029727	NA
K ₂ O	0.012064	0.012064
Li ₂ O	0.014802	0.014802
MgO	0.016989	0.016989
Na ₂ O	0.168395	0.168395
P ₂ O ₅	0.003239	0.003239
SO ₃	0.005542	NA
SiO ₂	0.424565	0.424565
SnO ₂	0.007587	0.007587
TiO ₂	0.008034	0.008034
V ₂ O ₅	0.007499	0.007499
ZnO	0.031997	0.031997
ZrO ₂	0.036219	0.036219
Others	0.001045	0.041731
Li ₂ O × Na ₂ O	NA	0.00249258
TiO ₂ × ZrO ₂	NA	0.00029098
(Li ₂ O) ²	NA	0.00021910

(a) The composition in mass fractions is from Table 2.3.
(b) See Table 4.4.
(c) NA = not applicable because the model does not contain this term

Table 4.6. Predicted $\ln\left(\frac{\overline{P(g)}}{1-\overline{P(g)}}\right)$ and $\overline{P(g)}$ and Confidence Interval for the REFMIX Composition Used in the Recommended 19-term Model for VHT

Model for $\ln\left(\frac{\overline{P(g)}}{1-\overline{P(g)}}\right)$ ^(a)	Predicted $\ln\left(\frac{\overline{P(g)}}{1-\overline{P(g)}}\right)$	Predicted $\overline{P(g)}$	90% CI ^(b) on Mean $\ln\left(\frac{\overline{P(g)}}{1-\overline{P(g)}}\right)$	90% CI ^(b) on Mean $\overline{P(g)}$
19-Term PQM Model	-5.045 ^(c)	0.006/Pass ^(c)	(-6.129, -3.961)	(0.002, 0.019)

(a) The model in this column is given in Table 4.4 (19-term PQM model).

(b) CI = two-sided confidence interval (see Section B.6 of Appendix B).

(c) All calculations were performed using the REFMIX glass composition, model coefficients, and variance-covariance matrix values given in tables of this report. The calculated $\ln\left(\frac{\overline{P(g)}}{1-\overline{P(g)}}\right)$ values were rounded to three decimal places in this table.

4.5 Suitability of the Recommended Model for Pass/Fail VHT Responses for Application by the WTP LAW Facility

The 19-term model and threshold for predicting pass/fail discussed in Section 4.3.2 is recommended for use by the WTP LAW Facility as the best model currently available for predicting pass/fail VHT from LAW glasses with higher waste loadings. This model yields predictions of pass/fail VHT that achieve an $\text{FNR} \leq 10\%$ while simultaneously maximizing overall accuracy. The selected model does not show significant LOF and generally has uniform performance across evaluation and validation datasets.

The VHT models presented in this document rely on the selection of a threshold for classifying a glass as pass or fail that satisfies the FNR constraint. Relaxing or modifying the FNR constraint can lead to the selection of different models that may improve overall accuracy by reducing the FPR while not increasing the FNR beyond a reasonable value.

The range of single component concentrations in the 686-glass dataset used for modeling is listed in Table 4.7 and discussed in Section 9.7. These ranges can be used to determine model validity ranges.

Table 4.7. Data Component Concentration Ranges (mass fraction) for LAW Glasses Used in Final VHT Pass/Fail Models

Component	20-component		16-component	
	Min	Max	Min	Max
Al ₂ O ₃	0.034972	0.147521	0.034972	0.147521
B ₂ O ₃	0.059952	0.138294	0.059952	0.138294
CaO	0.000000	0.128136	0.000000	0.128136
Cl	0.000000	0.011701	NA ^(a)	NA
Cr ₂ O ₃	0.000000	0.006304	NA	NA
F	0.000000	0.013007	0.000000	0.013007
Fe ₂ O ₃	0.000000	0.099815	NA	NA
K ₂ O	0.000000	0.080930	0.000000	0.080930
Li ₂ O	0.000000	0.058246	0.000000	0.058246
MgO	0.000000	0.050222	0.000000	0.050222
Na ₂ O	0.024707	0.265729	0.024707	0.265729
P ₂ O ₅	0.000000	0.034072	0.000000	0.034072
SO ₃	0.000000	0.016290	NA	NA
SiO ₂	0.332925	0.522624	0.332925	0.522624
SnO ₂	0.000000	0.050299	0.000000	0.050299
TiO ₂	0.000000	0.050058	0.000000	0.050058
V ₂ O ₅	0.000000	0.040885	0.000000	0.040885
ZnO	0.009980	0.058152	0.009980	0.058152
ZrO ₂	0.000000	0.067534	0.000000	0.067534
Others ^(b)	0.000000	0.004401	0.001600	0.108458

(a) NA = not applicable or component not included as term.

(b) Note: Others for the 16-components are composed of all the NA components as well as Others for the 20 components.

5.0 Models Relating Viscosity at 1150 °C to LAW Glass Composition

This section documents the development, evaluation, and validation of LAW glass property-composition models and corresponding uncertainty expressions for predicting the $\ln(\eta_{1150})$ as a function of LAW glass composition. The property-composition models and corresponding uncertainty expressions for $\ln(\eta_{1150})$ presented in this section were developed, evaluated, and validated using compositions and η_{1150} values for simulated LAW glasses. Viscosity was not measured on any of the LAW glasses made from actual waste samples, and therefore they were not included.

Section 5.1 discusses the LAW glasses available and used for $\ln(\eta_{1150})$ -composition model development, evaluation, and validation. Section 5.2 presents the models for $\ln(\eta_{1150})$ that were investigated. Section 5.3 summarizes the results for the selected linear and quadratic mixture model forms for $\ln(\eta_{1150})$ and identifies the recommended model. Section 5.4 illustrates the calculation of η_{1150} predictions and the uncertainties in those predictions using selected $\ln(\eta_{1150})$ models and corresponding uncertainty equations. Section 5.5 discusses the suitability of the recommended $\ln(\eta_{1150})$ model for use by the WTP LAW Facility. Appendix B discusses the statistical methods and summary statistics used to develop, evaluate, and validate the several $\ln(\eta_{1150})$ model forms investigated, as well as statistical models/equations used for quantifying the uncertainties in $\ln(\eta_{1150})$ model predictions.

5.1 Viscosity at 1150 °C Data Used for Model Development, Evaluation, and Validation

The data available and used for developing $\ln(\eta_{1150})$ models as functions of LAW glass composition are discussed in Section 5.1.1. The approaches and data used for validating and evaluating the models are discussed in Sections 5.1.2 and 5.1.3, respectively.

5.1.1 Model Development Data for Viscosity at 1150 °C

The data available for developing $\ln(\eta_{1150})$ -composition models consist of composition and η_{1150} values from 549 LAW glasses (see Table 2.2). These glasses and their normalized compositions based on measured (or estimated) SO_3 values are discussed in Section 2.0. The corresponding η_{1150} values are presented in Table A.3 of Appendix A.

5.1.1.1 Assessment of Available Glasses with Data for Viscosity at 1150 °C

The database of 549 glasses with η_{1150} results contains statistically designed as well as actively designed LAW glasses. Some actively designed glasses are outside the composition region covered by the majority of the LAW compositions. Such glasses are not ideal for inclusion in a modeling dataset because they can be influential when fitting models to data. Hence, it was decided to (i) graphically assess the 549 available LAW glass compositions with η_{1150} values and (ii) remove from the modeling dataset any compositions considered to be outlying (with respect to the composition region covered by most available data). Reasons for removing glasses from the assessment are described subsequently.

Figure 5.1 displays plots of the mass fractions for 19 “main components” plus the Others component (defined as the sum of all remaining components) in the 549 LAW glasses with η_{1150} data. These 20 components (including Others) have sufficient ranges and distributions of mass fraction values to support

separate model terms if desired. Figure 5.2 displays similar plots for the remaining “minor components.” On each plot in Figure 5.1 and Figure 5.2, the x-axis represents the mass fraction values of a LAW glass component. The y-axis shows an index value representing each LAW glass composition, which aids in spreading out the data points to avoid over-plotting. The plotting symbols in Figure 5.1 and Figure 5.2 correspond to the six groups of LAW glasses discussed in Section 2.3. For comparison purposes, the vertical lines in Figure 5.1 represent the ranges over which the LAW glass components were varied in the PNNL (i) LAW Phase 1 outer-layer study (blue lines), (ii) LAW Phase 2 outer-layer study (pink lines), and (iii) LAW Phase 3 study (pink lines, the same as LAW Phase 2 outer-layer study), as shown in Table 2.1. Phases 2 and 3 focused on LAW glasses with high Na₂O waste loadings, whereas Phase 1 explored a larger LAW GCR with higher waste loadings including higher SO₃.

Figure 5.1 shows that several of the 549 LAW glasses have “main components” (e.g., F) with outlying mass fraction values compared to the remaining glasses and to the component ranges in the PNNL LAW Phase 1, Phase 2, and Phase 3 studies. Figure 5.2 shows what appear to be outliers for some “minor components,” (e.g., SrO), but the values and ranges of those components are small and hence the glasses were not considered to be outliers and were retained. Table 5.1 lists the 15 LAW glasses excluded from the η_{1150} modeling dataset and the reason each glass was excluded. Finally, none of the 10 outlying glasses excluded from the viscosity modeling work by Piepel et al. (2007) are excluded in Table 5.1. None of those glasses appear as outliers in Figure 5.1, because of the larger compositional region covered by the current η_{1150} modeling dataset. Also, none of those glasses were identified as outliers by statistical modeling diagnostics.

Figure 5.3 and Figure 5.4 (corresponding to Figure 5.1 and Figure 5.2, respectively) show plots of component distributions after the 15 outlying glasses were removed from the η_{1150} dataset containing 549 glasses. Figure 5.3 shows that for the remaining 534 LAW glasses, all 19 LAW glass “main components” have sufficient ranges and distributions of values within those ranges to support terms for modeling η_{1150} . Figure 5.4 confirms that none of the “minor components” have sufficient ranges and distributions of values within their ranges to support model terms for those components. Based on Figure 5.3 and Figure 5.4, it was decided to use 20 components for initial η_{1150} modeling work. These components were Al₂O₃, B₂O₃, CaO, Cl, Cr₂O₃, F, Fe₂O₃, K₂O, Li₂O, MgO, Na₂O, P₂O₅, SO₃, SiO₂, SnO₂, TiO₂, V₂O₅, ZnO, ZrO₂, and Others (the sum of all remaining components) and were the same as those used for initial modeling of all other properties (except for melter SO₃ tolerance, which normalized out SO₃).

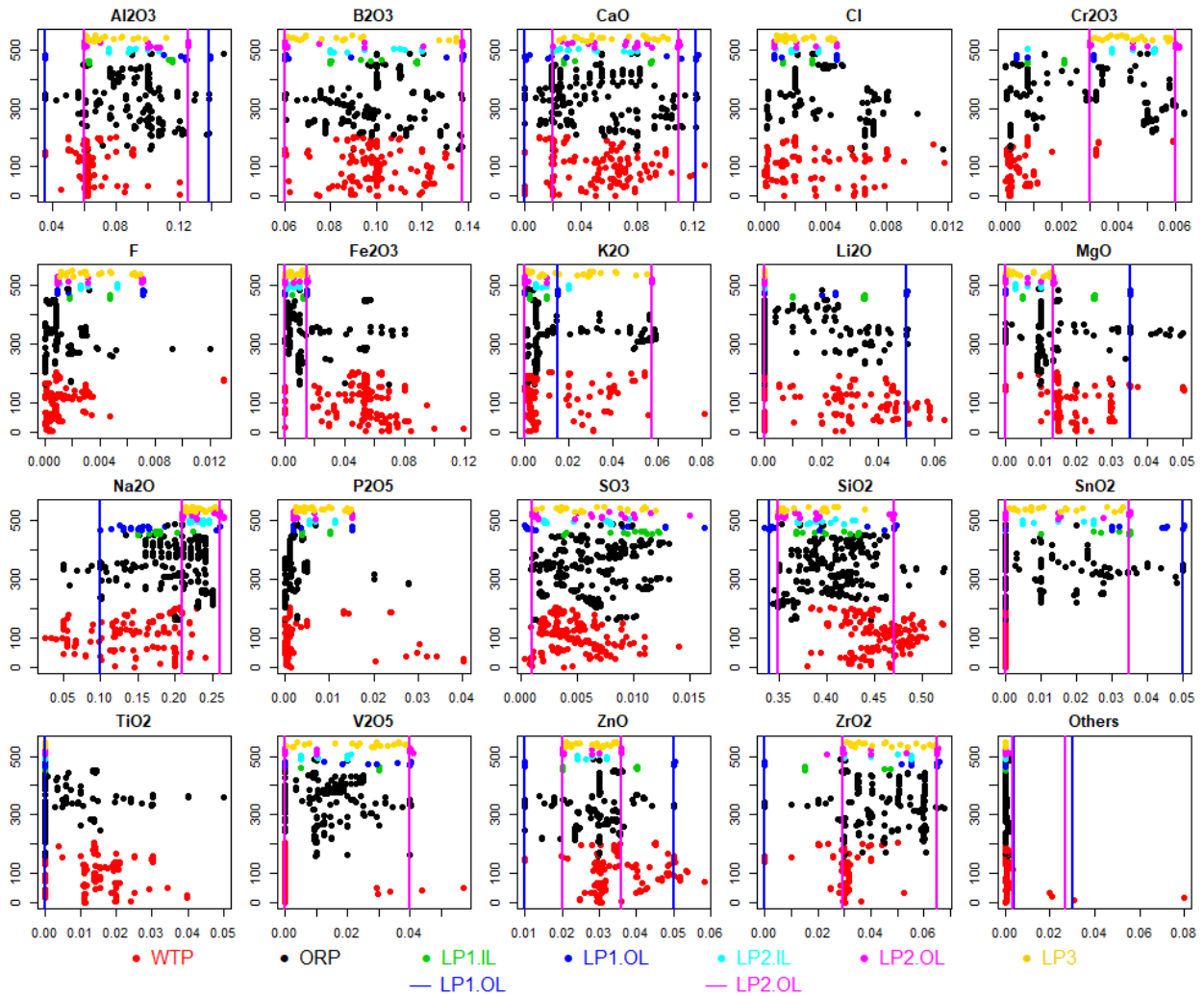


Figure 5.1. Distributions of 20 Main Components (in mass fractions) for 549 LAW Glass Compositions with Data for Viscosity at 1150 °C. The vertical lines (when present) represent the lower and upper limits for each component from the PNNL LAW Phase 1 outer-layer study (blue lines), Phase 2 outer-layer study (pink lines), and Phase 3 study (also shown by the same pink lines), as shown in Table 2.1. In cases where two limits are the same, pink lines over plot the blue lines. The x-axis represents the mass fraction values of a LAW glass component. The y-axis shows an index value representing each LAW glass composition, which aids in spreading out the data points to avoid over-plotting.

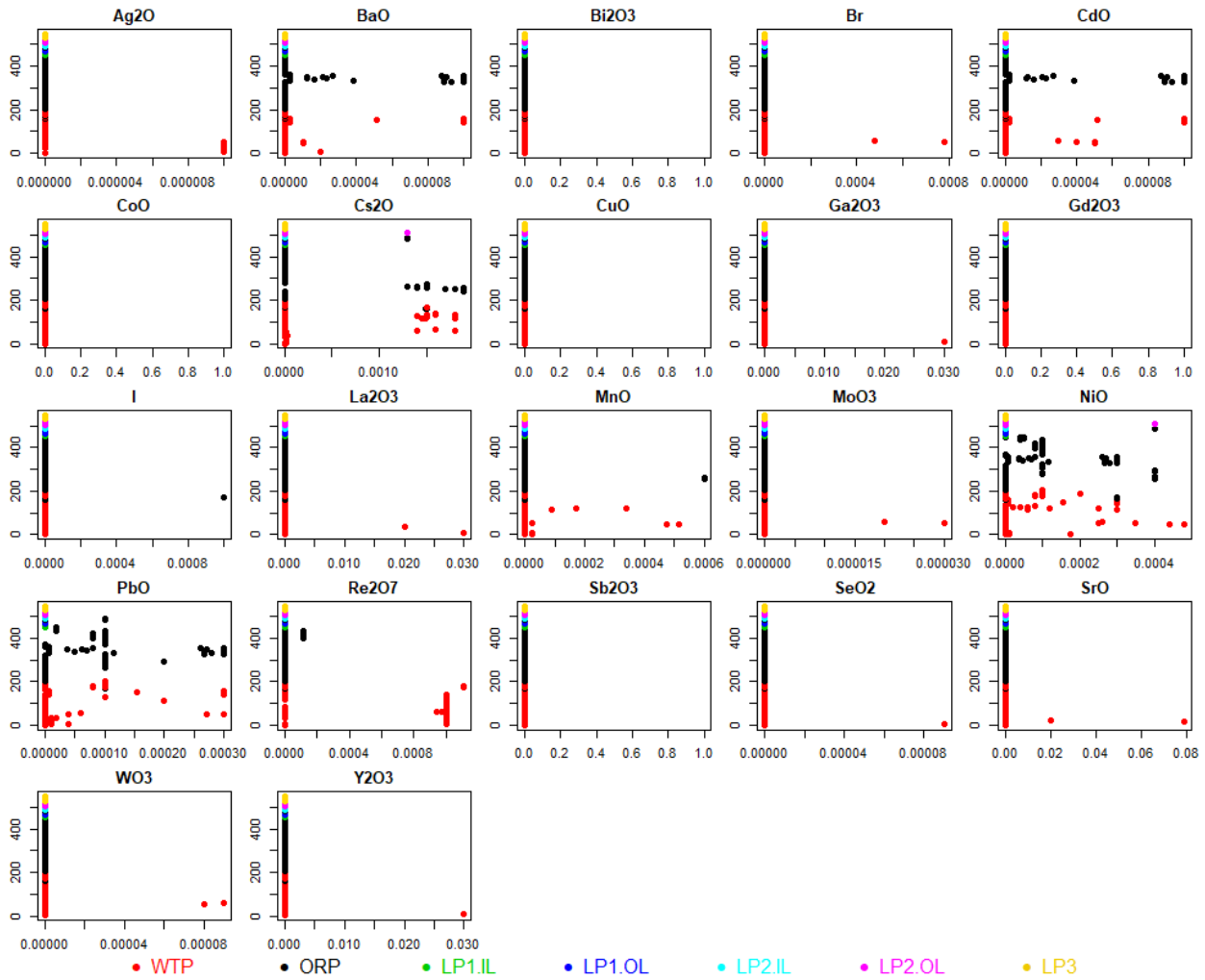


Figure 5.2. Distributions of 17 Minor Components (in mass fractions) for the 549 LAW Glass Compositions with Data for Viscosity at 1150 °C. The x-axis represents the mass fraction values of a LAW glass component. The y-axis shows an index value representing each LAW glass composition, which aids in spreading out the data points to avoid over-plotting.

Table 5.1. Fifteen LAW Glasses Excluded from the Modeling Dataset for Viscosity at 1150 °C (η_{1150})

Glass #	Glass ID	Reason Glass Excluded from η_{1150} Modeling Dataset
450	DWV-G-51B	$F > 0.0091$ (= 0.013) mf ^(a)
453	BWV-G-142B	$F > 0.0091$ (= 0.013006) mf
626	FWV-G-108B	$F > 0.0091$ (= 0.012001) mf
628	GWV-G-36D	$F > 0.0091$ (= 0.009306) mf
629	GWV-G-65A	$F > 0.0091$ (= 0.009303) mf
80	LAWC25	$K_2O > 0.06$ (= 0.080927) mf
67	LAWC14	$V_2O_5 > 0.05$ (= 0.057118) mf
12	LAWA46	Others > 0.02 (= 0.031024) mf
13	LAWA47	Others > 0.02 (= 0.031024) mf
14	LAWA48	Others > 0.02 (= 0.031024) mf
20	LAWA64	Others > 0.02 (= 0.079852) mf
25	LAWA85	Others > 0.02 (= 0.020963) mf
43	LAWABP1	Others > 0.02 (= 0.020001) mf
327	LA44PNCC	Container-centerline-cooled glass
57	LAWB42S	Identified as outlier in model development work

(a) mf = mass fraction

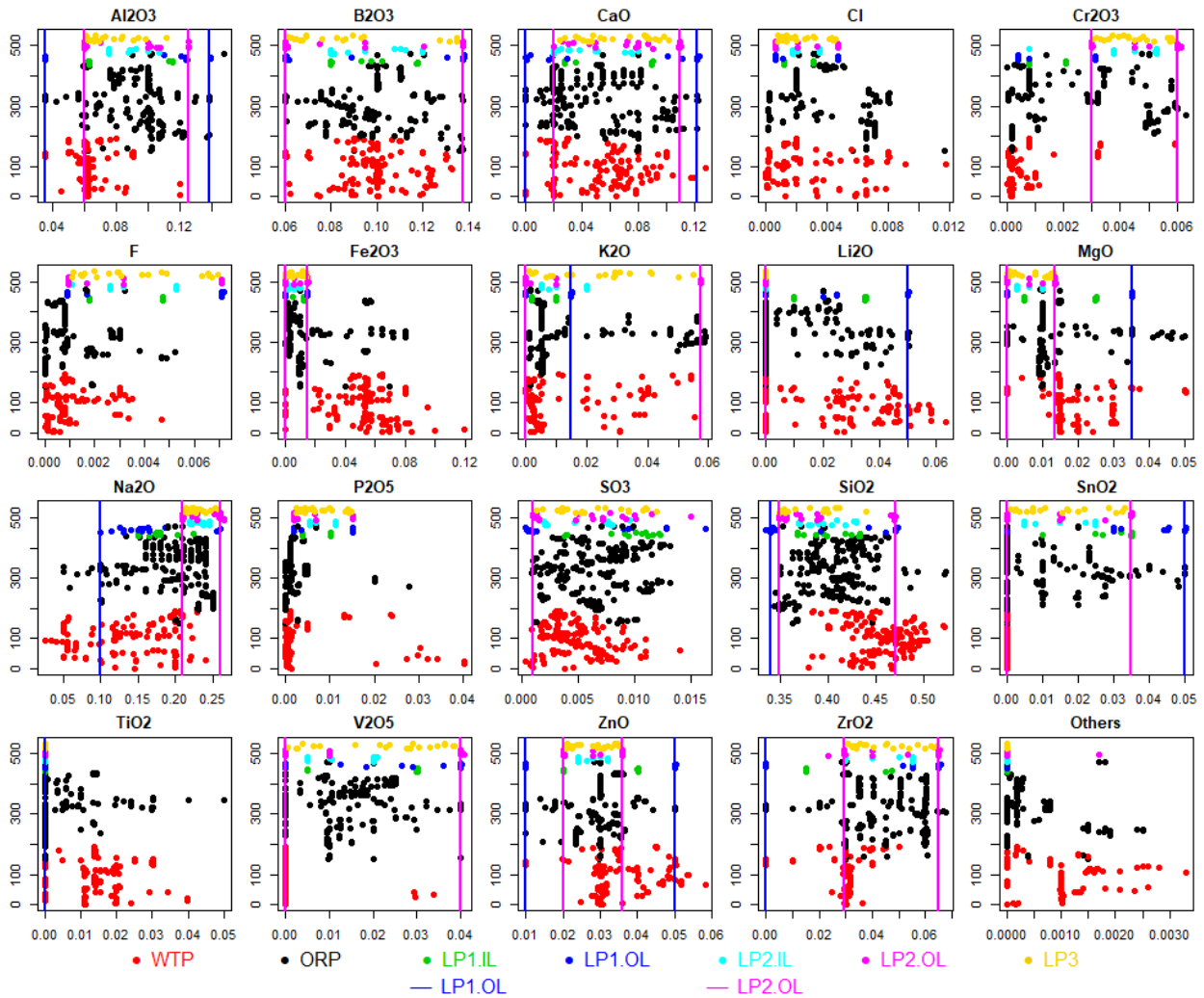


Figure 5.3. Distributions of 20 Main Components (in mass fractions) for 534 LAW Glass Compositions with Data for Viscosity at 1150 °C that Remain after Excluding the 15 Glasses in Table 5.1. The vertical lines (when present) represent the lower and upper limits for each component from the PNNL LAW Phase 1 outer-layer study (blue lines), Phase 2 outer-layer study (pink lines), and Phase 3 study (pink lines), as shown in Table 2.1. In cases where two limits are the same, pink lines over plot the blue lines. The x-axis represents the mass fraction values of a LAW glass component. The y-axis shows an index value representing each LAW glass composition, which aids in spreading out the data points to avoid over-plotting.

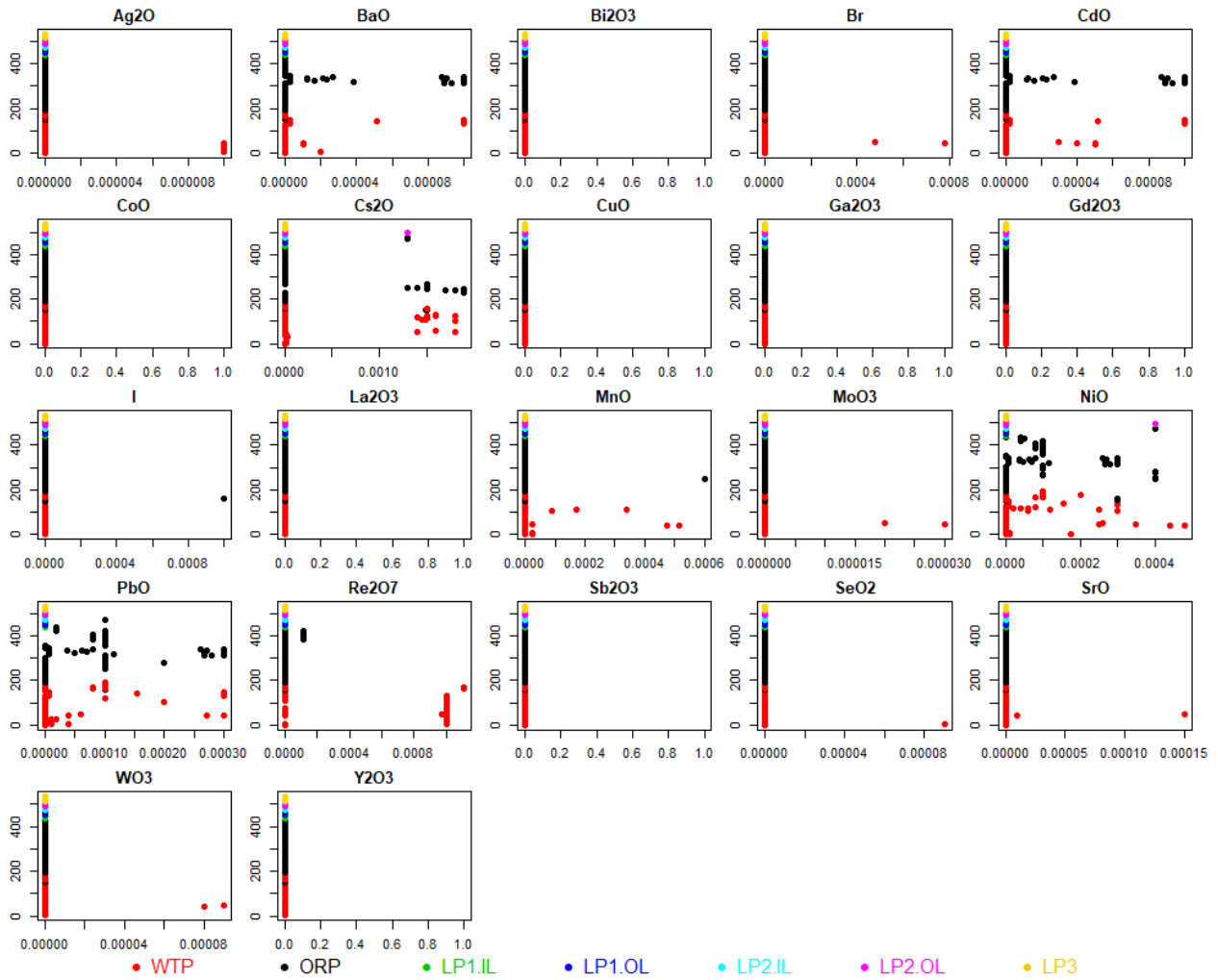


Figure 5.4. Distributions of 17 Minor Components (in mass fractions) for the 534 LAW Glass Compositions with Data for Viscosity at 1150 °C that Remain after Excluding the 15 Glasses in Table 5.1. The x-axis represents the mass fraction values of a LAW glass component. The y-axis shows an index value representing each LAW glass composition, which aids in spreading out the data points to avoid over-plotting.

Figure 5.5 shows a scatterplot matrix of the 534 glasses remaining in the η_{1150} modeling dataset after removing the 15 outlying glasses. High correlations between some pairs of components are evident, so pairwise correlation coefficients were calculated. These can vary from -1.0 (perfect negative correlation) to 0 (no correlation) to 1.0 (perfect positive correlation). There were two component pairs with correlations equal to or larger than 0.60 (in absolute value): Na_2O and Li_2O (-0.876) and Na_2O and SiO_2 (-0.600). Such high pairwise correlations, especially the one for the Na_2O and Li_2O relationship, can make it difficult for regression methods to properly separate the effects of correlated components on the response variable (e.g., η_{1150}). Further, such high correlations in the predictors make parameter values difficult to estimate and result in inflated prediction uncertainties. Thus, these high pairwise correlations need to be kept in mind when developing and interpreting LAW glass property-composition models for η_{1150} . See Section 9.7 for further discussion of highly correlated component concentrations.

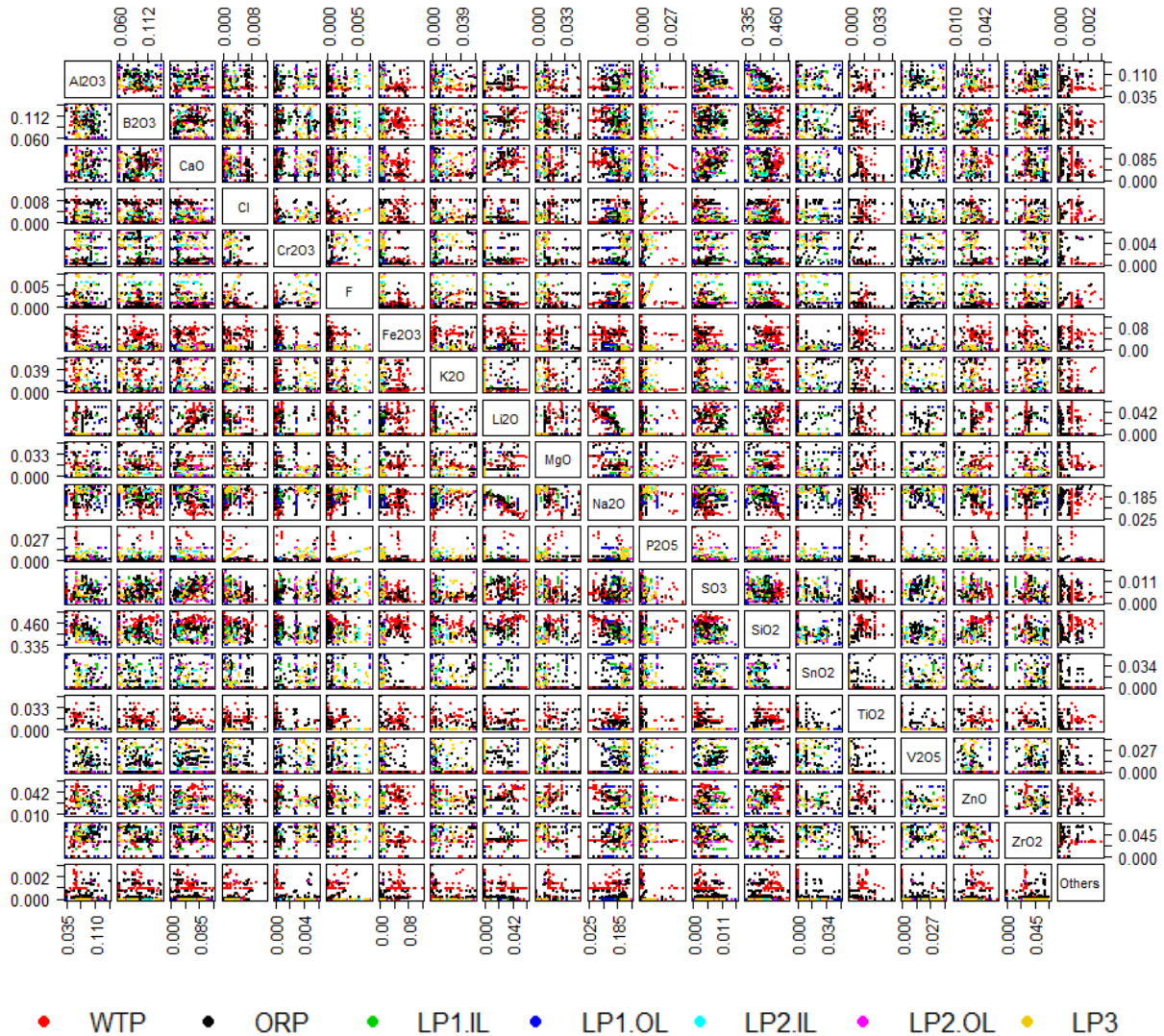


Figure 5.5. Scatterplot Matrix of 20 Components (mass fractions) for the 534 LAW Glasses with Viscosity at 1150°C Data that Remain after Excluding the 15 Glasses in Table 5.1

5.1.1.2 Viscosity at 1150 °C Modeling Dataset

Table A.3 in Appendix A lists the Glass #s, Glass IDs, and η_{1150} values for the 534 remaining simulated LAW glasses used for η_{1150} model development. The η_{1150} values for the 15 glasses excluded as outliers from the 549-glass modeling dataset (see Table 5.1) are marked with an asterisk in Table A.3. The compositions for these 534 LAW glasses are included in Table A.2. The glass compositions in Table A.2 are the normalized mass fractions (mf) of the 20 components previously identified as having sufficient data to support a separate model term if needed. The LAW glass compositions in Table A.2 were normalized so that the total mass fractions of all 20 components for each glass equaled precisely 1.000000 as discussed in Section 2.2.

Section 2.3 discusses how the η_{1150} values in Table A.3 were obtained from viscosity versus temperature data. The values of η_{1150} in Table A.3 for the 534 glasses in the modeling dataset range from 4.70 to 259.69 poise.

5.1.1.3 Replicate and Near-Replicate Data for Viscosity at 1150 °C

Changes to the LAW glass compositions caused by the renormalization associated with using measured (or estimated) SO_3 values (see Section 2.2) resulted in some replicate glasses not having exactly equal normalized compositions. Such compositions are near-replicates. For ease of discussion, henceforth both replicates and near-replicates are referred to as replicates.

Table 5.2 lists the replicate sets of LAW glasses in the η_{1150} modeling dataset and the corresponding η_{1150} values. Table 5.2 also lists estimates of (i) %RSDs [calculated using η_{1150} values in original poise units] and (ii) SDs [calculated using $\ln(\eta_{1150})$ values in $\ln(\text{poise})$ units] for each replicate set. The %RSD values for 21 of the 28 replicate sets range from 0% to 14.79%, with the %RSD values for the other 7 replicate sets ranging from 22.63% to 48.38%. The four replicate sets (Glass # 456-457, 458-459, 460-461, and 462-463 pairs) of the seven sets with higher %RSD values exhibited a consistent trend between η_{1150} , ε_{1150} , and r_a^{VHT} , that is, the replicate glasses had lower η_{1150} , higher ε_{1150} and higher r_a^{VHT} values than the original glasses. This trend agrees with the observation that all four replicate glasses had higher measured Na_2O concentration than the original glasses. However, this trend may not be enough to justify excluding these four replicate sets. No reasons for the higher %RSD values for the remaining three replicate sets could be found in the data-source reports. Hence, it was assumed that periodically there may be larger uncertainties in batching and melting glasses and determining glass properties including η_{1150} .

Table 5.2 also lists pooled estimates of %RSDs and SDs calculated over all replicate sets. A pooled %RSD or SD combines the separate %RSD or SD estimates from each replicate set, so that a more precise combined estimate of %RSD or SD is obtained. These pooled %RSDs and SDs include uncertainties due to fabricating glasses, determining SO_3 measured or estimated values, and the process of determining η_{1150} values. The magnitudes of the pooled SD = 0.1655 [in $\ln(\text{poise})$ units] and pooled %RSD = 16.26 [in percentage relative to $\ln(\text{poise})$ units] in Table 5.2 indicate there is approximately a 16% total relative uncertainty in the η_{1150} values over the replicate glasses. The pooled estimates of replicate uncertainty for η_{1150} in Table 5.2 are used subsequently to assess LOF of the various $\ln(\eta_{1150})$ models considered.

Table 5.2. Uncertainty in Viscosity at 1150 °C Responses for Replicate and Near-Replicate Sets

Replicate Set Glass #s	Replicate Set Glass IDs	Replicate Set η_{1150} (poise) Values	%RSD ^(a)	SD [ln(poise)]
993	EWG-LAW-Centroid-1	28.25	1.77	0.0177
995	EWG-LAW-Centroid-2	27.55		
9	LAWA44	69	2.02	0.0202
326	LAWA44R10	71		
227	LAWB83	54	2.90	0.0291
229	LAWB84	51		
284	B1-AZ101(LAWB83)	53		
442	LAWC100	32	14.79	0.1425
443	LAWC100R1	25		
447	WVY-G-95A	25		
75	LAWC22	39	8.39	0.0854
272	C22AN107	44		
279	C1-AN107(LAWC22)	46		
456	LAWCrP1	87	22.63	0.2282
457	LAWCrP1R	63		
458	LAWCrP2	66	26.76	0.2708
459	LAWCrP2R	45		
460	LAWCrP3	95	36.53	0.3737
461	LAWCrP3R	56		
462	LAWCrP4	67	27.78	0.2814
463	LAWCrP4R	45		
451	LAWC7H	21	29.35	0.2978
624	FWV-G-63B	32		
331	LAWM1	36	30.74	0.3124
383	LAWM53	56		
365	LAWM35	25	48.38	0.5041
386	LAWM56	51		
846	ORLEC12	60	11.47	0.1149
865	OWV-G-144E	51		
848	ORLEC14	66	7.92	0.0793
887	QWV-G-107B	59		
850	ORLEC16	77	9.82	0.0984
888	PWV-G-130C	67		
853	ORLEC19	76	4.81	0.0481
890	QWV-G-29C	71		
856	ORLEC22	34	4.29	0.0429
891	QWV-G-75B	32		
862	ORLEC26	62	7.19	0.0720
867	OWV-G-109B	56		
863	ORLEC27	61	14.01	0.1406
869	PWV-G-43E	50		
864	ORLEC28	65	11.79	0.1181
871	PWV-G-93A	55		
877	ORLEC33	58	0.00	0.00
903	RWV-G-9C	58		
878	ORLEC34	55	6.73	0.0674
904	RWV-G-48D	50		

Table 5.2. Uncertainty in Viscosity at 1150 °C Responses for Replicate and Near-Replicate Sets, cont.

Replicate Set Glass #s	Replicate Set Glass IDs	Replicate Set η_{1150} (poise) Values	%RSD	SD [ln(poise)]
893	ORLEC44	36	1.94	0.0194
905	RWV-G-79C	37		
895	ORLEC46	27	0.00	0.0000
906	RWV-G-120D	27		
897	ORLEC48R	24	2.89	0.0289
907	SWV-G-17A	25		
597	ORPLD1	33	5.63	0.0550
997	LAW-ORP-LD1(1)	29.37		
999	LAW-ORP-LD1(2)	29.46		
1035	LP2-OL-07	30.01		
1022	LP2-IL-10	47.13	9.84	0.0964
1028	LP2-IL-16	43.53		
1031	LP2-OL-02	52.56		
1049	LP2-OL-21	42.41		
1034	LP2-OL-05	66.51	3.46	0.0346
1038	LP2-OL-10-MOD	63.33		
Pooled Over All 28 Replicate Sets with 35 total DF^(b)			16.26	0.1655

(a) %RSD = $100 \times (\text{Standard Deviation} / \text{Mean})$.
(b) DF = degrees of freedom.

5.1.2 Model Validation Approach and Data for Viscosity at 1150 °C of LAW Glasses

The validation approach for η_{1150} models was based on splitting the 534-glass dataset for model development into five modeling/validation subsets. Of the 534 model-development glasses, 63 were in 28 replicate sets. The five modeling/validation splits of the 534 glasses in the η_{1150} modeling dataset were formed as follows.

- The 63 replicate glasses in 28 replicate sets were set aside so they would always be included in each of the five model development datasets. This was done so that replicate sets would not be split between modeling and validation subsets, thus negating the intent to have validation glasses different than model development glasses.
- The remaining 471 glasses were ordered from smallest to largest according to their η_{1150} values (poise). The 471 glasses were numbered 1, 2, 3, 4, 5, 1, 2, 3, 4, 5, etc. All of the 1's formed the first model validation set, while all of the remaining points formed the first model development dataset. Similarly, all of the 2's, 3's, 4's, and 5's respectively formed the second, third, fourth, and fifth model validation sets. In each case, the remaining non-2's, non-3's, non-4's, and non-5's formed the second, third, fourth, and fifth model development datasets respectively. Because 471 is not evenly divisible by 5, the five modeling and validation subsets did not all contain the same numbers of glasses. One of the five splits contained 95 glasses for validation and 376 glasses for modeling. The other four splits contained 94 glasses for validation and 377 for modeling. Note that these numbers of glasses in the modeling subsets do not yet include the 63 replicates.
- The 63 replicate glasses were added to each of the split modeling subsets. Including the replicates, one split contained 439 glasses for modeling and 95 for validation, while the other four splits contained 440 glasses for modeling and 94 for validation.

Data splitting was chosen as the validation approach because the η_{1150} modeling dataset contains all compositions that (i) are in the LAW GCR of interest, (ii) meet QA requirements, and (iii) have η_{1150} data. Having a separate validation dataset not used for modeling is desirable, but that desire was over-ridden by wanting η_{1150} models to be developed using all appropriate data.

5.1.3 Subsets of LAW Glasses to Evaluate Prediction Performance of Models for Viscosity at 1150 °C

Section 2.4 discusses six subsets of LAW glasses for evaluating the prediction performance of LAW glass property-composition models, including subsets of glasses with higher waste loadings. The subsets, as discussed in Section 2.4, are denoted WTP, ORP, LP2OL, LP123, HiNa_2O , and HiSO_3 . The η_{1150} modeling dataset of 534 LAW glasses (see Section 5.1.1) contains 182, 260, 102, 92, 200, and 104 glasses with η_{1150} values in these six evaluation subsets, respectively. Note that glasses can be in more than one of these evaluation sets. The “Glass #s” of these six evaluation subsets of LAW glasses are listed in Table C.3 of Appendix C; normalized LAW glass compositions and η_{1150} values for the glasses with these “Glass #s” are listed in Tables A.2 and A.3, respectively, of Appendix A.

Model performance/prediction summary statistics denoted R^2_{Eval} and $\text{RMSE}_{\text{Eval}}$ (see Section B.3 of Appendix B), as well as predicted versus measured plots (see Section B.3), are subsequently used to assess the prediction performance of the η_{1150} models (presented in later subsections) for the six evaluation subsets listed in Table C.3 of Appendix C.

5.2 Model Forms for Viscosity at 1150 °C of LAW Glasses

Ideally, a property-composition model for η_{1150} would use known mechanisms of η_{1150} as a function of LAW glass composition. However, no such mechanisms are known. Empirical models for η_{1150} with coefficients estimated from model development data have been shown in the past to perform well. The empirical model forms used are from the general class of *mixture experiment models* (Cornell 2002), which includes models linear in composition as well as non-linear in composition. Section B.1 of Appendix B discusses mixture experiments and several general forms of mixture experiment models.

Section 5.2.1 discusses the forms of mixture experiment models used for η_{1150} of LAW glasses. Section 5.2.2 discusses using natural-log-transformed η_{1150} values as the response variable for η_{1150} modeling.

5.2.1 Mixture Experiment Model Forms for Viscosity at 1150 °C of LAW Glasses

The LM and PQM model forms introduced in Section B.1 of Appendix B were chosen for use in modeling $\ln(\eta_{1150})$ as a function of LAW glass composition. These models have been used in the past (e.g., Piepel et al. 2007; Muller et al. 2014) to model the compositional dependence of $\ln(\eta)$ -composition-temperature models. However, the present work considered LM and PQM models for $\ln(\eta_{1150})$ as functions of LAW glass composition. The LM model form is given by

$$\ln(\eta_{1150}) = \sum_{i=1}^q \beta_i g_i + e \quad (5.1)$$

while the PQM model form is given by

$$\ln(\eta_{1150}) = \sum_{i=1}^q \beta_i g_i + \text{Selected} \left\{ \sum_{i=1}^q \beta_{ii} g_i^2 + \sum_{i < j}^{q-1} \sum_j^q \beta_{ij} g_i g_j \right\} + e \quad (5.2)$$

where in Eqs. (5.1) and (5.2)

$\ln(\eta_{1150})$ = natural logarithm of η_{1150} (in poise)

g_i = normalized mass fraction of the i^{th} glass oxide or halogen component

($i = 1, 2, \dots, q$), such that $\sum_{i=1}^q g_i = 1$

β_i = coefficient of the i^{th} linear blending term ($i = 1, 2, \dots, q$)

β_{ii} and β_{ij} = coefficients of selected quadratic (squared or crossproduct) blending terms to be estimated from the data

e = random error for each data point.

Many statistical methods exist for the case where the E is statistically independent (i.e., not correlated) and normally distributed with mean 0 and standard deviation σ . In Eq. (5.2), “Selected” denotes that only some of the terms in curly brackets are included in the model. The subset is selected using stepwise regression or other variable selection methods (Draper and Smith 1998; Montgomery et al. 2012). PQM models are discussed in more detail and illustrated by Piepel et al. (2002) and Smith (2005).

Cornell (2002) discusses many other empirical mixture model forms that could have been considered for η_{1150} -composition modeling. However, these other mixture model forms were not investigated because the special blending effects of components associated with those models were judged not to apply for η_{1150} . The model forms in Eqs. (5.1) and (5.2) are widely used in many application areas (including waste glass property modeling) and often predict the response very well.

5.2.2 Transformation of Viscosity at 1150 °C for LAW Glasses

In modeling η_{1150} , it is advantageous to use the natural logarithm transformation of the η_{1150} values. The advantages of this transformation include the following:

- The η_{1150} values for the 534 LAW glasses in the η_{1150} modeling dataset range from 4.70 to 259.69 poise. This range is significantly more than one order of magnitude. In such cases, typically the uncertainty in making glasses and determining η_{1150} leads to smaller absolute uncertainties for smaller η_{1150} values and larger absolute uncertainties for larger η_{1150} values. Hence, the OLS regression assumption of equal variances for all response variable values (see Section B.2.1 of Appendix B) is violated. After a logarithmic transformation, variances of η_{1150} values tend to be approximately equal as required for OLS regression.
- A logarithmic transformation tends to linearize the compositional dependence of η_{1150} data and reduce the need for non-linear terms in the model form.
- A natural logarithm transformation is preferred over a common logarithm (or other base logarithm) transformation because of the approximate relationship

$$\text{SD} [\ln(y)] \cong \text{RSD} (y) \quad (5.3)$$

where SD denotes standard deviation, RSD denotes relative standard deviation (i.e., the standard deviation divided by the mean), and y denotes η_{1150} . Eq. (5.3) results from applying the first-order variance propagation formula [Eq. (7-7) of Hahn and Shapiro (1967)] to the function $z = \ln(y)$. The relationship in Eq. (5.3) is very useful, in that uncertainties of the natural logarithm of the response variable y can be interpreted as approximate RSDs of the untransformed response variable y .

For these reasons, the natural logarithmic transformation was employed for all η_{1150} model forms.

5.3 Property-Composition Model Results for Viscosity at 1150 °C of LAW Glasses

This section discusses the results of fitting several different mixture experiment models using natural logarithms of η_{1150} (poise) as functions of LAW glass compositions. Section 5.3.1 presents the results of modeling $\ln(\eta_{1150})$ using a 20-component FLM model. Sections 5.3.2 and 5.3.3 present the results of modeling $\ln(\eta_{1150})$ using an RLM and PQM models based on a reduced set of mixture components. Finally, Section 5.3.4 compares the results from the three models and recommends a $\ln(\eta_{1150})$ model for future use and evaluation.

5.3.1 Results from the 20-Component Full Linear Mixture Model for the Natural Logarithm of Viscosity at 1150 °C with LAW Glasses

As the initial step in $\ln(\eta_{1150})$ -composition model development, a FLM model with the 20 components identified in Section 5.1.1.1 was fit to the modeling data (534 LAW glasses). Table 5.3 contains the results for the 20-component FLM model of $\ln(\eta_{1150})$. Table 5.3 lists the estimated model coefficients, standard errors-deviations of the coefficients (i.e., the standard deviation of the coefficients), and model fit summary statistics for the 20-component FLM of $\ln(\eta_{1150})$ model using the viscosity modeling dataset (534 LAW glasses). Table 5.3 also contains the results from the (i) data-splitting validation approach (see Section 5.1.2), and (ii) evaluation of model predictions for the six evaluation subsets (see Section 5.1.3). In the data-splitting validation portion of the results at the bottom of Table 5.3, the columns are labeled DS1, DS2, DS3, DS4, and DS5 to denote the five modeling/validation splits of the data as described in Section 5.1.2. The last column of this part of Table 5.3 shows the averages for the different statistics over the five splits.

The $R^2 = 0.9429$, $R^2_A = 0.9408$, and $R^2_P = 0.9367$ statistics (see Section B.3 of Appendix B) in Table 5.3 show that (i) the 20-component FLM model fits the $\ln(\eta_{1150})$ data in the 534-glass modeling dataset quite well, (ii) there are not a large number of unneeded model terms (evidenced by the small standard errors relative to the reported coefficient estimates and by the fact that the R^2 -adjusted value is very close to the R^2 value for this model), and (iii) there are not any highly influential data points (confirmed in the diagnostic graphics described in Section B.3 and by the fact that the R^2 -predicted value is close to the R^2 -adjusted and R^2 values for this model). The RMSE = 0.1375 is smaller than the pooled glass batching and η_{1150} determination uncertainty ($SD = 0.1655$ in $\ln(\text{poise})$ units) estimated from replicates in Table 5.2. This suggests that the 20-component FLM model does not have a statistically significant LOF, which is confirmed by the model LOF p-value = 0.9641 in Table 5.3. See Section B.3 for discussion of the statistical test for model LOF.

At the bottom right of Table 5.3, the average model-fit statistics (R^2 , R^2_A , R^2_P , and RMSE) over the five data-split validation sets are close to the statistics obtained from fitting the 20-component FLM model for $\ln(\eta_{1150})$ to all 534 glasses in the modeling dataset. The data-split validation statistics (R^2_V and $RMSE_V$) are also relatively close to the R^2 and RMSE (i) values from fitting the model to the full dataset, and (ii)

averages from fitting the model to the data-split modeling subsets. This indicates that the 20-component FLM model maintains its predictive performance for data not used to fit the model.

Table 5.3. Coefficient Estimates and Performance Summary Statistics for the 20-Component Full Linear Mixture Model on the Natural Logarithm of Viscosity at 1150 °C for LAW Glasses

ln(η_{1150}) 20-Component FLM Model Term	Coefficient Estimate	Coefficient Stand. Err.
Al ₂ O ₃	14.5193	0.2980
B ₂ O ₃	-5.4984	0.3032
CaO	-5.3544	0.2174
Cl	16.2018	2.8450
Cr ₂ O ₃	-8.8081	3.7163
F	-15.4524	4.5598
Fe ₂ O ₃	1.3668	0.3338
K ₂ O	-2.1876	0.4030
Li ₂ O	-30.0761	0.7601
MgO	-1.7309	0.7054
Na ₂ O	-7.2036	0.2312
P ₂ O ₅	11.0895	1.2958
SO ₃	6.4926	2.4104
SiO ₂	11.2176	0.1274
SnO ₂	7.2550	0.5668
TiO ₂	-0.9824	0.8528
V ₂ O ₅	-1.1043	0.6253
ZnO	-1.1794	0.7184
ZrO ₂	8.7008	0.4739
Others ^(c)	37.0390	10.2775

Modeling Data Statistic, 534 Glasses ^(a)			Value
R ²			0.9429
R ² _A			0.9408
R ² _P			0.9367
RMSE			0.1375
Model LOF p-value			0.9641

Evaluation Set (# Glasses) ^(b)			R ² _{Eval}	RMSE _{Eval}
WTP (182)			0.8569	0.1634
ORP (260)			0.9571	0.1079
LP2OL (102)			0.9515	0.1336
LP123 (92)			0.9437	0.1898
HiNa ₂ O (200)			0.9438	0.1309
HiSO ₃ (104)			0.9375	0.1378

Data Splitting Statistic ^(a,d)	DS1	DS2	DS3	DS4	DS5	Average
R ²	0.9399	0.9416	0.9451	0.9402	0.9449	0.9424
R ² _A	0.9372	0.9390	0.9427	0.9375	0.9424	0.9398
R ² _P	0.9317	0.9336	0.9379	0.9325	0.9373	0.9346
RMSE	0.1365	0.1414	0.1325	0.1400	0.1370	0.1375
R ² _V	0.9457	0.9465	0.9300	0.9503	0.9273	0.9399
RMSE _V	0.1464	0.1209	0.1631	0.1306	0.1443	0.1411

(a) The model evaluation statistics are defined in Section B.3 of Appendix B. The model validation statistics are defined in Section B.5.

(b) The six sets of LAW evaluation glasses are discussed in Section 2.4 and Section 5.1.3.

(c) For the 20-component FLM model, the “Others” component includes any components not separately listed.

(d) The evaluation and validation statistics calculated for data-splits are defined the same as for separate modeling and validation sets. Section 5.1.2 describes how the modeling dataset was split into modeling and validation subsets.

The statistics from evaluating the predictive performance of the 20-component FLM model for ln(η_{1150}) on the six evaluation subsets of modeling glasses (see Section 5.1.3) are given on the right side of Table 5.3. The R² statistics for five of the six evaluation subsets (0.9375 to 0.9571) are close to the R² statistic for the whole modeling dataset (0.9429). The exception is the WTP evaluation subset, with R² = 0.8569, which is still relatively high. The new models in this report are intended/expected to predict well for LAW glasses with higher waste loadings, and still predict acceptably well for glasses with lower waste loadings (the older WTP glasses).

Figure 5.6 shows the PvM plot for the 534-glass modeling dataset using the 20-component FLM model for $\ln(\eta_{1150})$. The plot illustrates that the 20-component FLM model predicts $\ln(\eta_{1150})$ quite well, but with a slight tendency to under-predict (i) above $\ln(\eta_{1150}) \sim 4.65$ ($\eta_{1150} \sim 104.58$ poise) and (ii) possibly below $\ln(\eta_{1150}) \sim 2.10$ ($\eta_{1150} \sim 8.17$ poise). However, the model predicts without bias within the WTP LAW Facility operating limits for η_{1150} (20 to 100 poise), shown by the red lines in Figure 5.6.

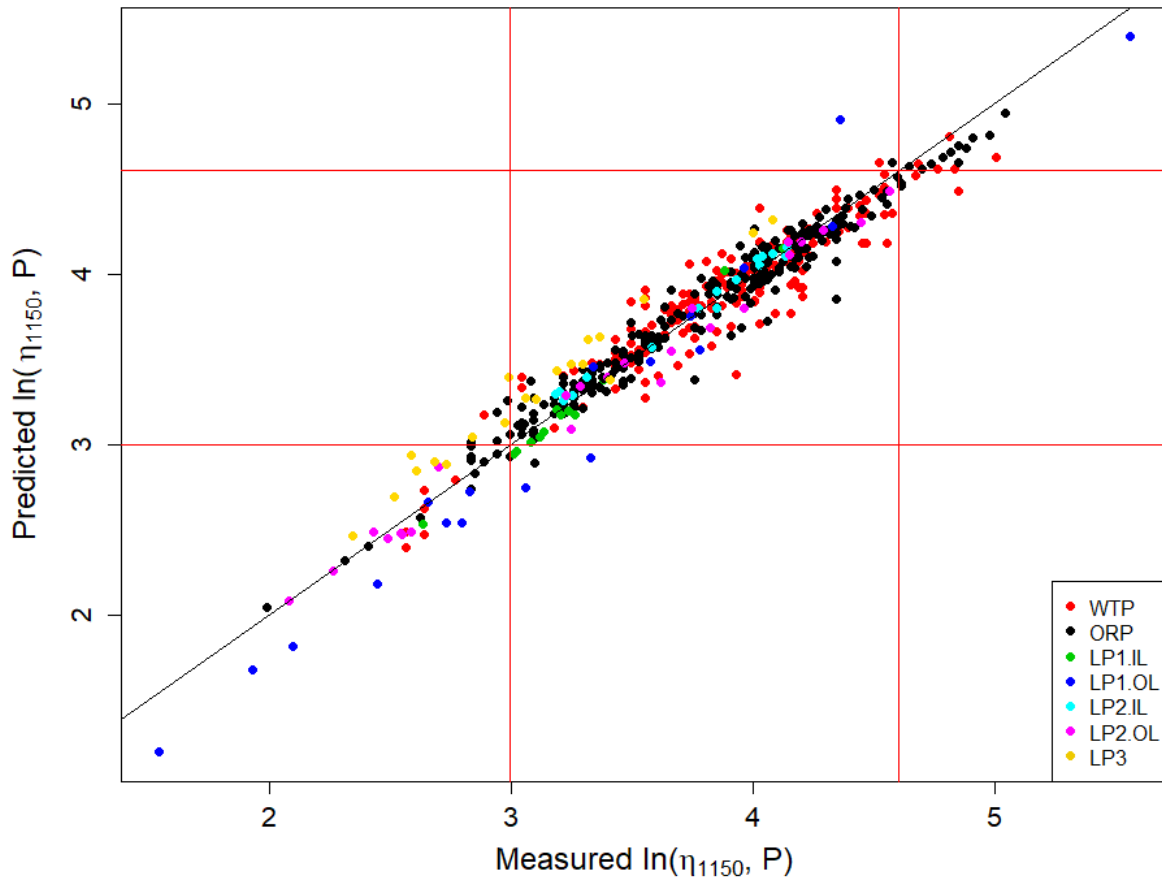


Figure 5.6. Predicted versus Measured Plot for the 534-Glass Modeling Dataset Using the 20-Component Full Linear Mixture Model on the Natural Logarithm of Viscosity at 1150 °C for LAW Glasses. The red lines represent the WTP LAW Facility operating limits for viscosity at 1150 °C (20 to 100 poise).

Figure 5.7 displays PvM plots using the 20-component FLM model for $\ln(\eta_{1150})$ in Table 5.3 applied to the six evaluation subsets discussed in Section 5.1.3. Each plot in the figure contains the evaluation R^2 and RMSE values for the corresponding evaluation subset. Figure 5.7 shows that the 20-component FLM model for $\ln(\eta_{1150})$ fit to the 534-glass modeling dataset generally predicts very well for the six evaluation subsets. In particular, the model predicts very well for the evaluation subsets containing glasses with higher waste loadings (LP2OL, LP123, HiNa_2O , and HSO_3). The plot for the WTP evaluation set (which contains older data for glasses with lower waste loadings) shows more scatter, resulting in an evaluation R^2 that is not as large as for the other evaluation sets. This is understandable and acceptable, since the new models presented in this report need to predict well for glasses with higher-waste loadings.

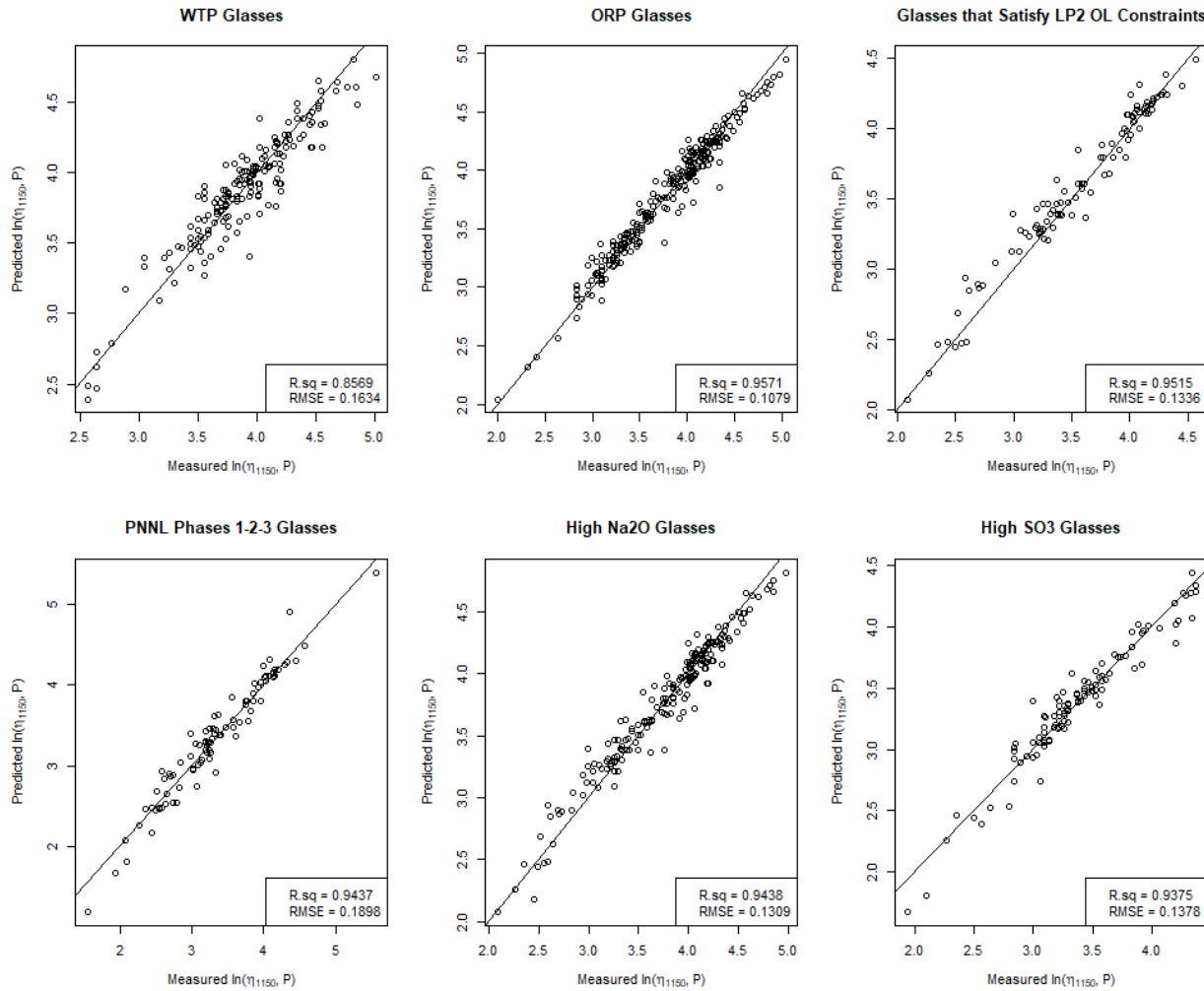


Figure 5.7. Predicted versus Measured Plots for the Six Evaluation Subsets Using the 20-Component Full Linear Mixture Model on the Natural Logarithm of Viscosity at 1150 °C for LAW Glasses

The model in Table 5.3 fits the 534-glass modeling dataset well enough, with no statistically significant LOF, to provide guidance for reducing the FLM model [i.e., removing separate terms for components that do not significantly influence $\ln(\eta_{1150})$]. Hence, the 20-component FLM model was used to produce the response trace plot (see Section B.4.1 in Appendix B) shown in Figure 5.8. The average glass composition of the 1074 glasses in the compiled database discussed in Section 2.5 was used as the REFMIX (see Section B.4.1) in response trace plots for every property. The glass composition of the REFMIX is listed in Table 2.3.

The response trace plot in Figure 5.8 shows (based on the sign and magnitude of the slopes of the respective traces) that Li₂O, Na₂O, CaO, B₂O₃, and K₂O are predicted to decrease $\ln(\eta_{1150})$ the most, while SiO₂, Al₂O₃, and P₂O₅ are predicted to increase $\ln(\eta_{1150})$ the most. The remaining components have predicted response traces with small to negligible slopes, indicating those components are predicted to have small to negligible effects on $\ln(\eta_{1150})$.

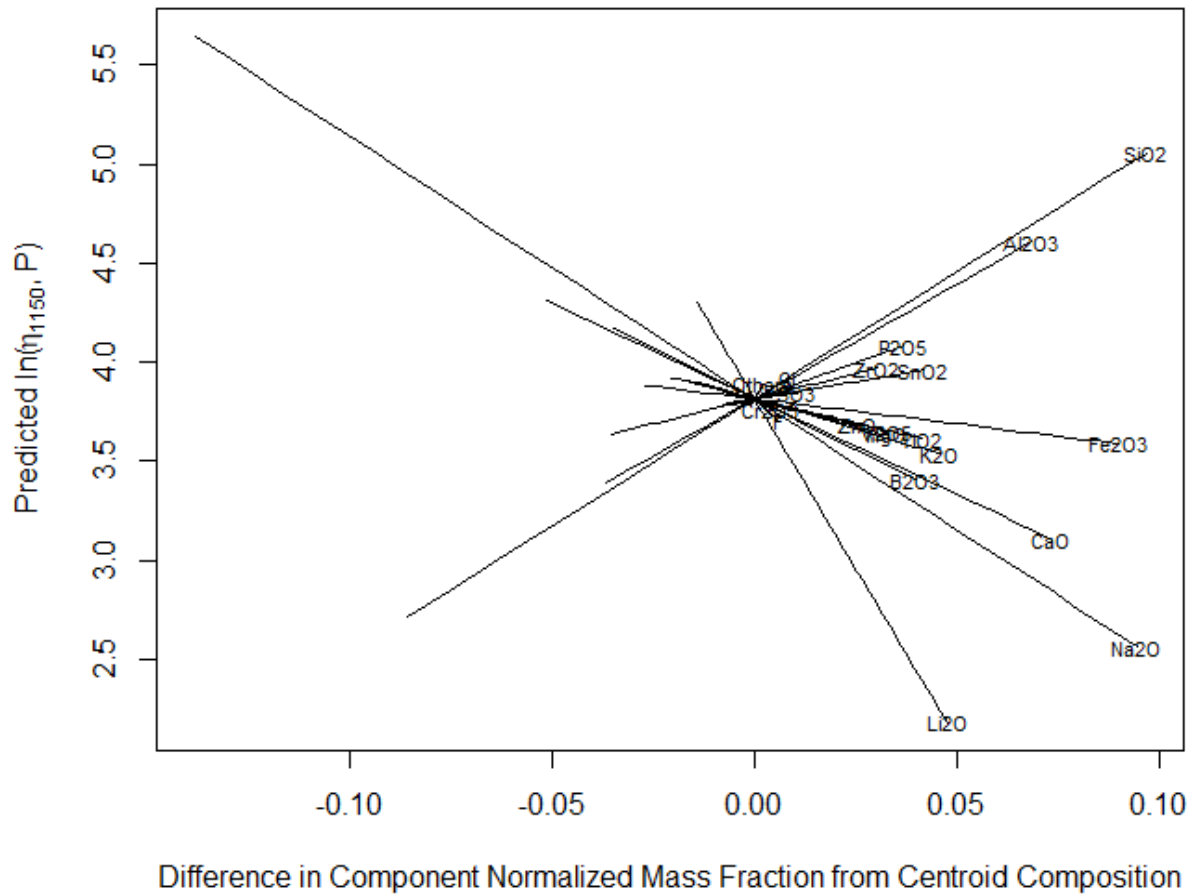


Figure 5.8. Response Trace Plot for the 20-Component Full Linear Mixture Model on the Natural Logarithm of Viscosity at 1150 °C for LAW Glasses

5.3.2 Results from a Reduced Linear Mixture Model for the Natural Logarithm of Viscosity at 1150 °C with LAW Glasses

The 20-component FLM model for $\ln(\eta_{1150})$ presented in Section 5.3.1 may contain components that do not significantly contribute to predicting $\ln(\eta_{1150})$, so model reduction, while still maintaining goodness of fit and predictive ability, was the next step of the model development approach. Thus, RLM models for $\ln(\eta_{1150})$ involving fewer than the 20 components were considered. The sequential F-test model reduction approach (see Section B.4.1 of Appendix B; Piepel and Cooley 2006) was used.

5.3.2.1 Numerical Results for the 18-Component Reduced Linear Mixture Model on the Natural Logarithm of Viscosity at 1150 °C for LAW Glasses

The RLM model for $\ln(\eta_{1150})$ was obtained using the backward-elimination F-test method discussed in Section B.4.1 of Appendix B. Glass scientists provided inputs on LAW glass components that should be retained in the model, and the method determined whether the remaining components should be kept as separate linear terms or combined into Others. The resulting RLM model for $\ln(\eta_{1150})$ contained terms for 18 components: Al_2O_3 , B_2O_3 , CaO , Cr_2O_3 , F , Fe_2O_3 , K_2O , Li_2O , MgO , Na_2O , P_2O_5 , SiO_2 , SnO_2 , TiO_2 ,

V₂O₅, ZnO, ZrO₂, and Others. So, Cl, and SO₃ were combined into Others. Note that the resulting Others is 1 minus the sum of all remaining components, and thus differs from the Others in the 20-component FLM model discussed in Section 5.3.1. Table 5.4 contains the results for the 18-component RLM model of $\ln(\eta_{1150})$. Table 5.4 lists the model coefficients, standard deviations of the coefficients, and model fit statistics for the 18-component RLM model using the modeling dataset (534 LAW glasses). Table 5.4 also contains the results from the (i) data-splitting validation approach (see Section 5.1.2), and (ii) evaluation of model predictions for the six evaluation subsets (see Section 5.1.3). In the data-splitting validation portion of the results at the bottom of Table 5.4, the columns are labeled DS1, DS2, DS3, DS4, and DS5 to denote the five modeling/validation splits of the data as described in Section 5.1.2. The last column of this part of Table 5.4 shows the averages for the different statistics over the five splits.

The $R^2 = 0.9410$, $R^2_A = 0.9390$, and $R^2_P = 0.9350$ statistics (see Section B.3 of Appendix B) in Table 5.4 show that (i) the 18-component RLM model fits the $\ln(\eta_{1150})$ data in the 534-glass modeling dataset quite well, (ii) there are not a large number of unneeded model terms, and (iii) there are no highly influential data points. The RMSE = 0.1395 is smaller than the pooled glass batching and η_{1150} determination uncertainty (SD = 0.1655 in $\ln(\text{poise})$ units) estimated from replicates in Table 5.2.

This suggests that the 18-component RLM model does not have a statistically significant LOF, which is confirmed by the model LOF p-value = 0.9510 in Table 5.4. See Section B.3 for discussion of the statistical test for modeling LOF.

At the bottom right of Table 5.4, the average model-fit statistics (R^2 , R^2_A , R^2_P , and RMSE) over the five data-splits are close to the statistics obtained from fitting the 18-component RLM model for $\ln(\eta_{1150})$ to all 534 glasses in the modeling dataset. The data-split validation statistics (R^2_V and RMSE_V) are also relatively close to the R^2 and RMSE (i) values from fitting the model to the full dataset, and (ii) averages from fitting the model to the data-split modeling subsets. This indicates that the 18-component RLM model for $\ln(\eta_{1150})$ maintains its predictive performance for data not used to fit the model.

Table 5.4. Coefficients and Performance Summary for the 18-Component Reduced Linear Mixture Model on the Natural Logarithm of Viscosity at 1150 °C for LAW Glasses

ln(η_{1150}) 18-Component RLM Model Term	Coefficient Estimate	Coefficient Stand. Err.	Modeling Data Statistic, 534 Glasses^(a)				Value
Al ₂ O ₃	14.5774	0.3005	R ²				0.9410
B ₂ O ₃	-5.5973	0.3066	R ² _A				0.9390
CaO	-5.5234	0.2167	R ² _P				0.9350
Cr ₂ O ₃	-8.4860	3.7659	RMSE				0.1395
F	-12.2861	4.5537	Model LOF p-value				0.9510
Fe ₂ O ₃	1.7297	0.3268					
K ₂ O	-2.4149	0.4049	Evaluation Set				
Li ₂ O	-30.5381	0.7621	(# Glasses)^(b)				
MgO	-1.3605	0.7087	R²_{Eval}				
Na ₂ O	-7.2055	0.2331	RMSE_{Eval}				
P ₂ O ₅	10.5192	1.2863	WTP (182)		0.8589		0.1609
SiO ₂	11.2259	0.1260	ORP (260)		0.9552		0.1097
SnO ₂	7.3765	0.5646	LP2OL (102)		0.9437		0.1424
TiO ₂	-0.6572	0.8463	LP123 (92)		0.9385		0.1972
V ₂ O ₅	-1.6274	0.6214	HiNa ₂ O (200)		0.9372		0.1369
ZnO	-1.3903	0.7267	HiSO ₃ (104)		0.9368		0.1374
ZrO ₂	8.8836	0.4782					
Others ^(c)	11.8195	1.9263					
Data Splitting Statistic^(a,d)							Average
R ²	0.9383	0.9394	0.9437	0.9374	0.9437		0.9405
R ² _A	0.9358	0.9369	0.9415	0.9348	0.9414		0.9381
R ² _P	0.9303	0.9316	0.9370	0.9295	0.9365		0.9330
RMSE	0.1380	0.1437	0.1339	0.1430	0.1381		0.1393
R ² _V	0.9425	0.9466	0.9263	0.9530	0.9220		0.9381
RMSE _V	0.1506	0.1208	0.1673	0.1270	0.1495		0.1430

- (a) The model evaluation statistics are defined in Section B.3 of Appendix B. The model validation statistics are defined in Section B.5.
- (b) The six sets of LAW evaluation glasses are discussed in Section 2.4 and Section 5.1.3.
- (c) For the 18-component RLM model, the “Others” component includes any components not separately listed.
- (d) The evaluation and validation statistics calculated for data-splits are defined the same as for separate modeling and validation sets. Section 5.1.2 describes how the modeling dataset was split into modeling and validation subsets.

The statistics from evaluating the predictive performance of the 18-component RLM model for ln(η_{1150}) on the six evaluation subsets of modeling glasses (see Section 5.1.3) are given on the right side of Table 5.4. The R² statistics for five of the six evaluation subsets (0.9368 to 0.9552) are close to the R² statistic for the whole modeling dataset (0.9410). The exception is the WTP evaluation subset, with R² = 0.8589, which is still relatively high. The new models in this report are intended to predict well for LAW glasses with higher waste loadings, and still predict acceptably well for glasses with lower waste loadings (the older WTP glasses).

5.3.2.2 Graphical Results for the 18-Component Reduced Linear Mixture Model on the Natural Logarithm of Viscosity at 1150 °C for LAW Glasses

Diagnostic plots for the 18-component RLM model (not included in this report) support the assumption of normally distributed errors in the $\ln(\eta_{1150})$ data (see Section B.3 of Appendix B). Figure 5.9 displays the 18-component RLM model of the $\ln(\eta_{1150})$ standardized residuals plotted versus the data index (a sequential numbering of the modeling data points), with different plotting symbols representing the different groups of LAW glasses discussed in Section 2.3. Figure 5.9 yields the following observations:

- The WTP and LP1.OL (PNNL Phase 1 outer layer) datasets have a wider scatter of standardized residuals, indicating a wider range of $\ln(\eta_{1150})$ model prediction uncertainty. This is likely a result of the WTP and LP1.OL glasses spanning wider subregions of LAW glass compositions.
- The 18-component RLM model (i) tends to under-predict $\ln(\eta_{1150})$ [corresponding to positive standardized residuals] for the LP2.OL glasses, and (ii) over-predicts $\ln(\eta_{1150})$ [corresponding to negative standardized residuals] for the LP3 glasses. The PNNL LP2.OL and LP3 studies were investigated and no reason for biased η_{1150} values was found. The differences in standardized residuals for these two studies may be a result of longer-term random uncertainty.
- Three glasses have standardized residuals near 4 in absolute value. Although outlying, these data points did not have a major impact on the 18-component RLM model for $\ln(\eta_{1150})$ and hence were retained in the modeling dataset.

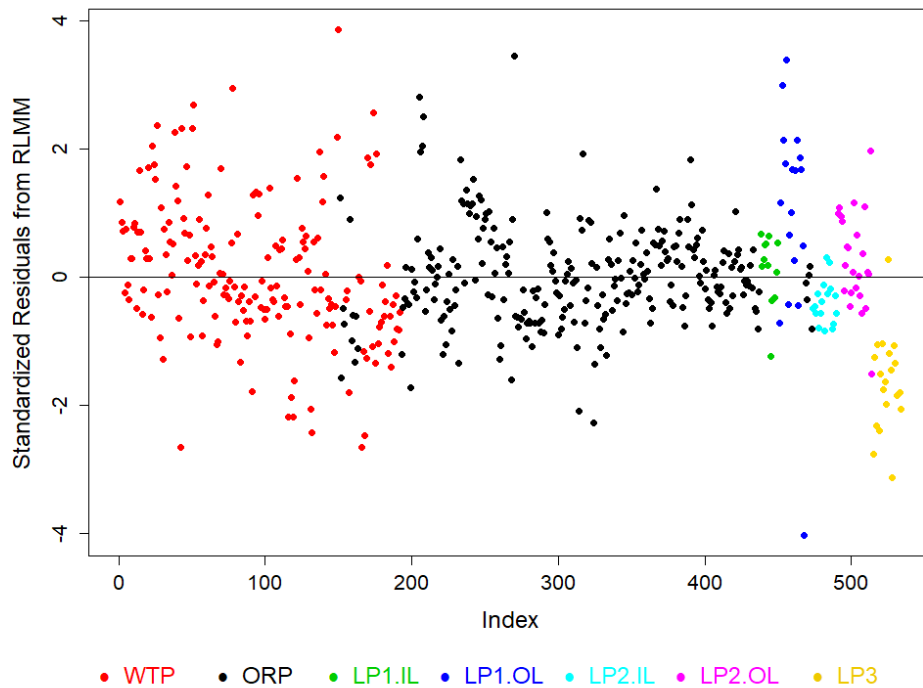


Figure 5.9. Standardized Residuals Plot for the 18-Component Reduced Linear Mixture Model on the Natural Logarithm of Viscosity at 1150 °C for LAW Glasses

Figure 5.10 displays the PvM plot for the 534-glass modeling dataset using the 18-component RLM model for $\ln(\eta_{1150})$. Figure 5.10 is nearly identical to the PvM plot for the 20-component FLM model in Figure 5.6. Hence, as in Figure 5.6, Figure 5.10 illustrates that the 18-component RLM model predicts $\ln(\eta_{1150})$ quite well, but with a slight tendency to under-predict (i) above $\ln(\eta_{1150}) \sim 4.65$ ($\eta_{1150} \sim 104.58$ poise) and (ii) possibly below $\ln(\eta_{1150}) \sim 2.10$ ($\eta_{1150} \sim 8.17$ poise). However, the model predicts without bias within the WTP LAW Facility operating limits for η_{1150} (20 to 100 poise), shown by the red lines in Figure 5.10.

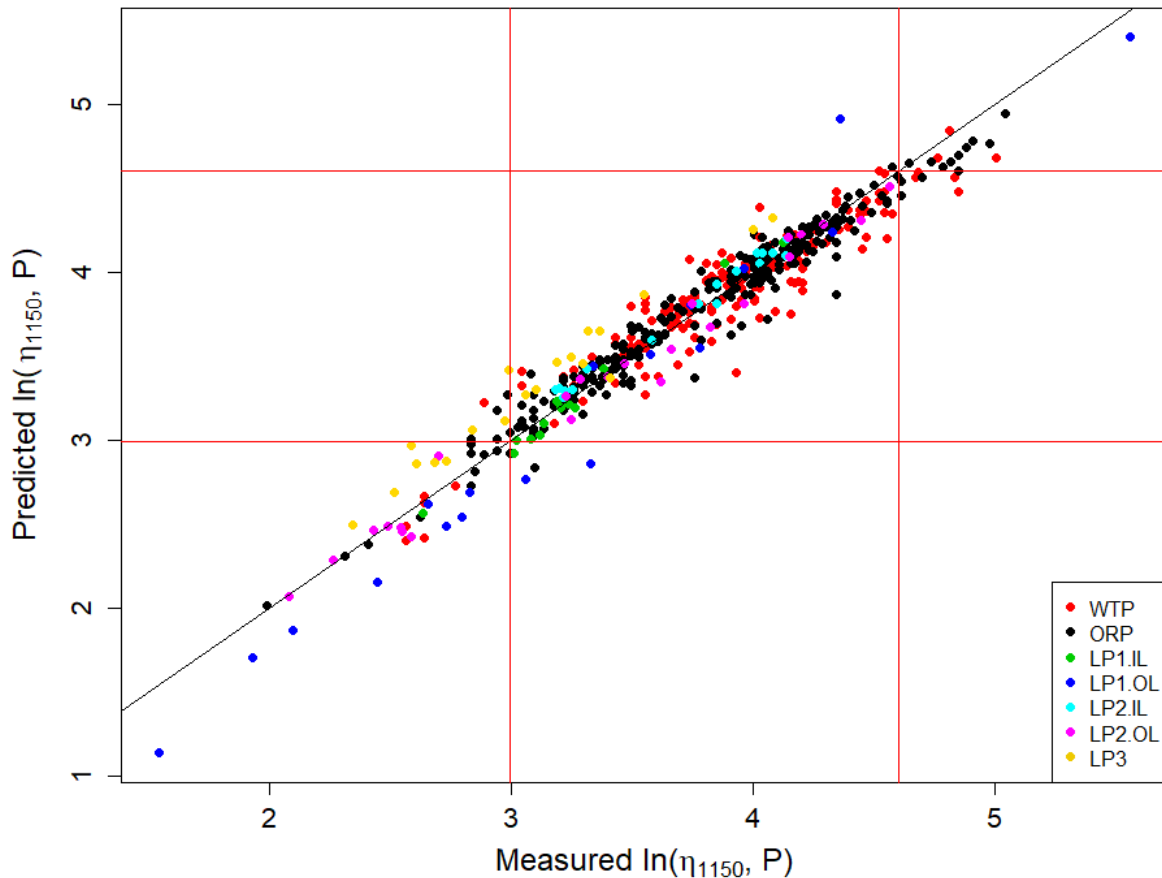


Figure 5.10. Predicted versus Measured Plot for the 534-Glass Modeling Dataset Using the 18-Component Reduced Linear Mixture Model on the Natural Logarithm of Viscosity at 1150 °C for LAW Glasses. The red lines represent the WTP LAW Facility operating limits for viscosity at 1150 °C (20 to 100 poise).

Figure 5.11 displays PvM plots using the 18-component RLM model for $\ln(\eta_{1150})$ in Table 5.4 applied to the six evaluation subsets discussed in Section 5.1.3. Each plot in the figure contains the evaluation R^2 and RMSE values for the corresponding evaluation subset. Figure 5.11 shows that the 18-component RLM model for $\ln(\eta_{1150})$ fit to the 534-glass modeling dataset generally predicts very well for the six evaluation subsets. In particular, the model predicts very well for the evaluation subsets containing glasses with higher waste loadings (LP2OL, LP123, HiNa_2O , and HiSO_3). The plot for the WTP evaluation set (which contains older data for glasses with lower waste loadings) shows more scatter, thus resulting in an evaluation R^2 that is not as large as for the other evaluation sets. This is understandable and

acceptable, since the new models presented in this report need to predict well for glasses with higher waste loadings.

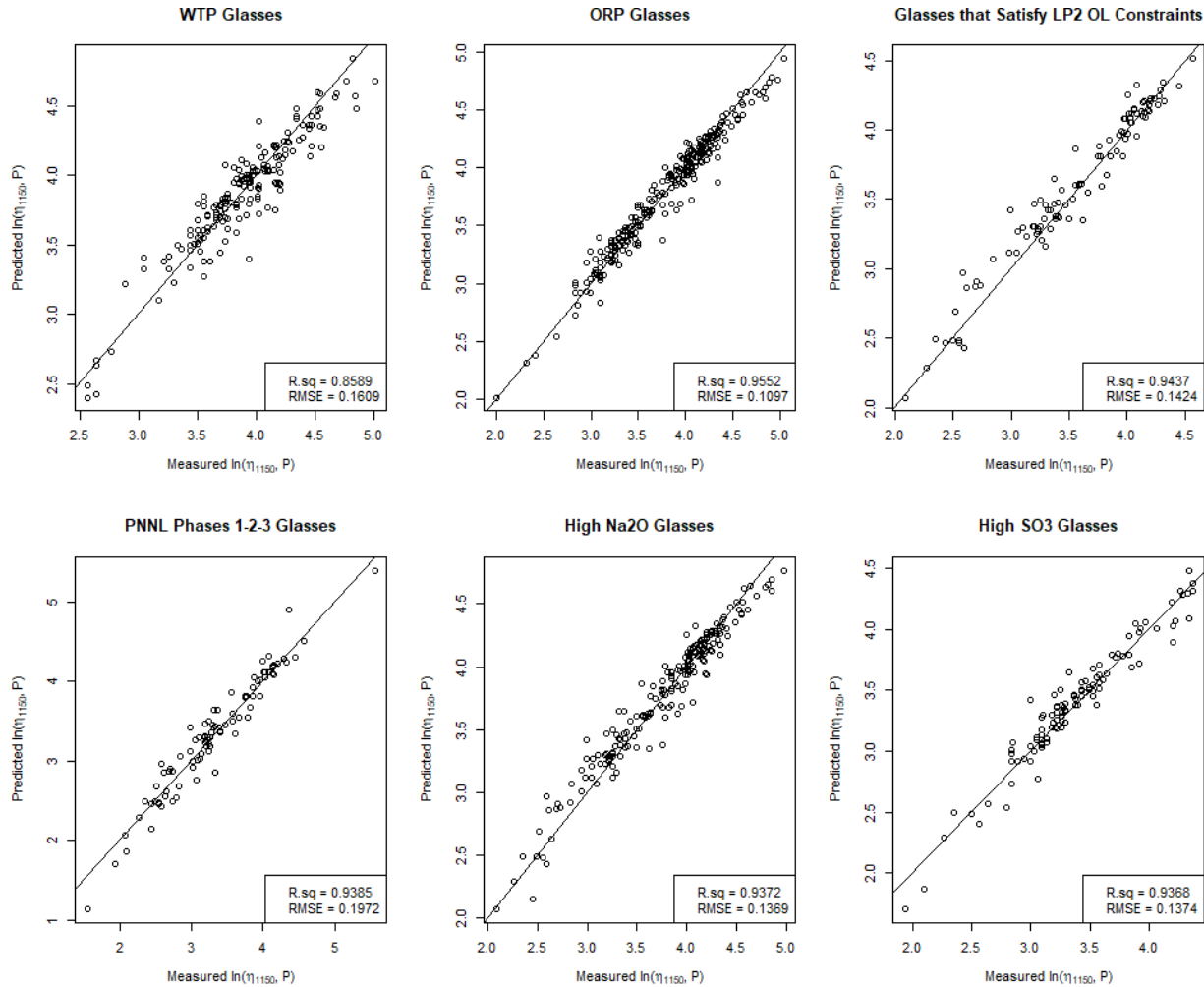


Figure 5.11. Predicted versus Measured Plots for the Six Evaluation Subsets Using the 18-Component Reduced Linear Mixture Model on the Natural Logarithm of Viscosity at 1150 °C for LAW Glasses

Figure 5.12 displays the response trace plot (see Section B.4.1 in Appendix B) for the 18-component RLM model of $\ln(\eta_{1150})$. The glass composition of the REF MIX (see Section B.4.1) used is listed in Table 2.3. Figure 5.12 shows that Li_2O , Na_2O , CaO , B_2O_3 , and K_2O are predicted to decrease $\ln(\eta_{1150})$ the most, while SiO_2 , Al_2O_3 , and P_2O_5 are predicted to increase $\ln(\eta_{1150})$ the most. The remaining components have predicted response traces with small to negligible slopes, indicating those components are predicted to have small to negligible effects on $\ln(\eta_{1150})$.

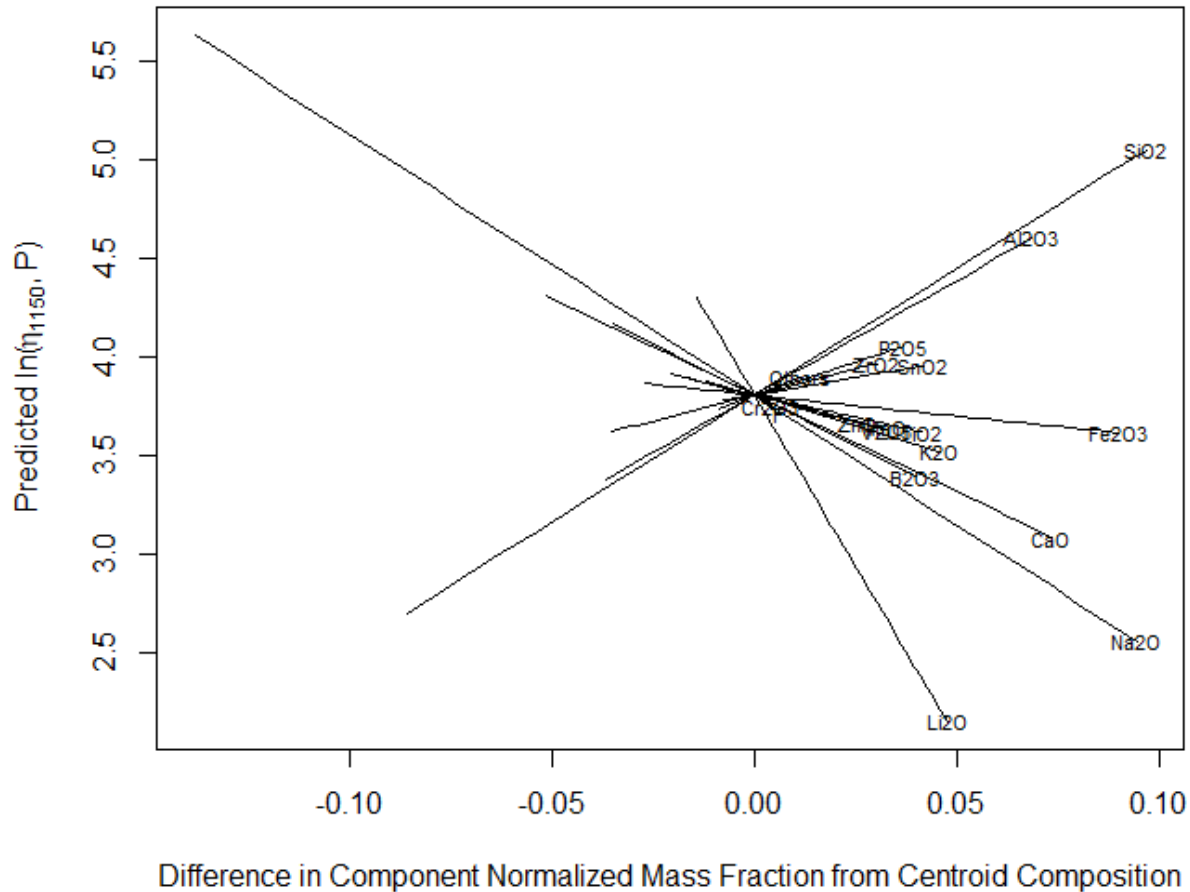


Figure 5.12. Response Trace Plot for the 18-Component Reduced Linear Mixture Model on the Natural Logarithm of Viscosity at 1150 °C for LAW Glasses

5.3.3 Results from a Reduced Partial Quadratic Mixture Model for the Natural Logarithm of Viscosity at 1150 °C with LAW Glasses

Reduced PQM models (see Section 5.2.1) were investigated in an effort to improve on the 18-component RLM model for $\ln(\eta_{1150})$. For example, the tendency for under-prediction from the FLM and RLM for viscosity, as observed in Figure 5.6 and Figure 5.10, might suggest some quadratic trend that second-order model terms would address. Previous experience with developing and validating PQM models has indicated that adding too many quadratic terms tends to over-fit the model development dataset and degrade predictive performance for new glasses. Therefore, the components that could form quadratic terms were limited to those with strong linear effects and a glass science basis. So, a process of identifying as few as possible second-order terms while improving model fit statistics was performed as follows:

1. Regressions were performed to fit reduced partial quadratic models involving all possible subsets of 1, 2, 3, or 4 second-order terms.
2. The resulting model summary/performance statistics (R^2 and RMSE values) were then examined to see which second-order terms were most beneficial to model performance and how many second-order terms to include.

3. The RMSE values from the top candidate models were plotted as a function of the number of second-order terms (0 to 4) to identify where the point of diminishing returns was.
4. The reduced PQM model with the number of terms just before the point of diminishing returns was selected as the final reduced PQM model.

The MAXR criterion (a selection approach aimed at maximizing R^2 , see Section B.4.2 of Appendix B) was also attempted as a means of selecting second-order terms. However, the terms selected by that method were not always intuitively obvious and the performance was not substantively better than the chosen approach.

Ultimately, a 21-term PQM model for $\ln(\eta_{1150})$ with 18 linear terms (from the RLM) and 3 quadratic terms ($\text{Al}_2\text{O}_3 \times \text{Na}_2\text{O}$, $(\text{Li}_2\text{O})^2$, and $\text{Li}_2\text{O} \times \text{Na}_2\text{O}$) was selected as including enough quadratic terms to improve the model fit, without over-fitting the model development data. These terms are generally expected based on past viscosity response modeling for LAW glasses that showed $\text{Li}_2\text{O} \times \text{Li}_2\text{O}$ (Piepel et al. 2007). Interactions between Al_2O_3 and Na_2O are expected due to the charge balancing of 4-coordinated Al_2O_3 that is primarily due to Na_2O and between Li_2O and Na_2O due to the mixed alkali effect. Table 5.5 contains the coefficients of the 21-term PQM model for $\ln(\eta_{1150})$ and the coefficient standard deviations. Table 5.5 also includes model performance statistics for the 21-term PQM model using the (i) 534-glass modeling data, (ii) data-split modeling data (as a model validation approach), and (iii) six evaluation subsets of modeling glasses discussed in Section 5.1.3 (as a model evaluation approach).

5.3.3.1 Numerical Results for the 21-Term Reduced Partial Quadratic Mixture Model on the Natural Logarithm of Viscosity at 1150 °C

In Table 5.5, the $\ln(\eta_{1150})$ model fit statistics $R^2 = 0.9487$, $R^2_A = 0.9467$, $R^2_P = 0.9426$, and $\text{RMSE} = 0.1304$ for the 21-term PQM model are small improvements over the corresponding statistics for the 18-component RLM model in Table 5.4. The small decrease in values from R^2_A to R^2_P suggests that the $\ln(\eta_{1150})$ modeling dataset does not have any highly influential data points for the 21-term reduced PQM model. In any case, $R^2_P = 0.9426$ provides an estimate of the fraction of variation in $\ln(\eta_{1150})$ values for future datasets over the same GCR that might be accounted for by this 21-term reduced PQM model.

The RMSE in Table 5.5 is an estimate of the uncertainty [in $\ln(\eta_{1150})$ units] in fabricating simulated LAW glasses and determining η_{1150} if the 21-term reduced PQM model for $\ln(\eta_{1150})$ does not have statistically significant LOF. The $\text{RMSE} = 0.1304$ for the reduced PQM model fitted to the 534-glass modeling dataset is smaller than the corresponding value for the 18-component RLM model ($\text{RMSE} = 0.1375$) in Table 5.4, indicating a better fit to the data by PQM. The RMSE value is also smaller than the pooled replicate SD in $\ln(\text{poise})$ units of 0.1655 in Table 5.2. These observations suggest that the 21-term reduced PQM model for $\ln(\eta_{1150})$ does not have model LOF, which is confirmed by the LOF test p-value = 0.9903 in Table 5.5. See Section B.3 of Appendix B for discussion of the statistical test for model LOF.

At the bottom right of Table 5.5, the average model-fit statistics (R^2 , R^2_A , R^2_P , and RMSE) over the five data-splits are close to the statistics obtained from fitting the 21-term reduced PQM model for $\ln(\eta_{1150})$ to all 534 glasses in the modeling dataset. The data-split validation statistics (R^2_V and RMSE_V) are also relatively close to the R^2 and RMSE (i) values from fitting the model to the full dataset, and (ii) averages from fitting the model to the data-split modeling subsets. This indicates that the 21-term reduced PQM model maintains its predictive performance for data not used to fit the model.

The statistics from evaluating the predictive performance of the 21-term reduced PQM model for $\ln(\eta_{1150})$ on the six evaluation subsets of modeling glasses (see Section 5.1.3) are given on the right side of Table

5.5. The R^2 statistics for five of the six evaluation subsets (0.9504 to 0.9640) are greater than the R^2 statistic for the whole modeling dataset (0.9487). The exception is the WTP evaluation subset, with $R^2 = 0.8658$, which is still relatively high. The new models in this report are intended to predict well for LAW glasses with higher waste loadings, and still predict acceptably well for glasses with lower waste loadings (the older WTP glasses).

Table 5.5. Coefficients and Performance Summary for 21-Term Reduced Partial Quadratic Mixture Model on the Natural Logarithm of Viscosity at 1150 °C for LAW Glasses

ln(η_{1150}) 21-Term PQM Model Term	Coefficient Estimate	Coefficient Stand. Err.	Modeling Data Statistic, 534 Glasses^(a)				Value
Al ₂ O ₃	10.4974	0.8471	R^2				0.9487
B ₂ O ₃	-5.4755	0.2910	R^2_A				0.9467
CaO	-4.6710	0.2256	R^2_P				0.9426
Cr ₂ O ₃	-6.4633	3.5965	RMSE				0.1304
F	-13.1106	4.3218	Model LOF p-value				0.9903
Fe ₂ O ₃	2.2898	0.3165					
K ₂ O	-2.0094	0.3983	Evaluation Set				
Li ₂ O	-53.7860	3.2603	(# Glasses)^(b)				
MgO	-0.5599	0.6714	R^2_{Eval}				
Na ₂ O	-10.3153	0.4506	RMSE _{Eval}				
P ₂ O ₅	11.2378	1.2104	WTP (182)				0.8658
SiO ₂	12.1422	0.1609	ORP (260)				0.9640
SnO ₂	7.6387	0.5316	LP2OL (102)				0.9579
TiO ₂	-0.3143	0.7932	LP123 (92)				0.9509
V ₂ O ₅	-1.1041	0.5891	HiNa ₂ O (200)				0.9506
ZnO	-0.9600	0.6866	HiSO ₃ (104)				0.9504
ZrO ₂	9.7255	0.4649					
Others ^(c)	10.8166	1.8174					
Al ₂ O ₃ × Na ₂ O	28.5242	4.9642					
(Li ₂ O) ²	265.7235	38.4830					
Li ₂ O × Na ₂ O	80.3767	11.4996					
Data Splitting Statistic^(a,d)	DS1	DS2	DS3	DS4	DS5	Average	
R^2	0.9433	0.9473	0.9522	0.9466	0.9503	0.9479	
R^2_A	0.9406	0.9448	0.9499	0.9440	0.9479	0.9455	
R^2_P	0.9344	0.9395	0.9457	0.9389	0.9429	0.9403	
RMSE	0.1327	0.1345	0.1238	0.1325	0.1302	0.1308	
R^2_V	0.9607	0.9523	0.9322	0.9530	0.9355	0.9467	
RMSE _V	0.1245	0.1141	0.1605	0.1270	0.1360	0.1324	

- (a) The model evaluation statistics are defined in Section B.3 of Appendix B. The model validation statistics are defined in Section B.5.
- (b) The six sets of LAW evaluation glasses are discussed in Section 2.4 and Section 5.1.3.
- (c) For the 21-component reduced PQM model, the “Others” component includes any components not separately listed.
- (d) The evaluation and validation statistics calculated for data-splits are defined the same as for separate modeling and validation sets. Section 5.1.2 describes how the modeling dataset was split into modeling and validation subsets.

5.3.3.2 Graphical Results for the 21-Term Reduced Partial Quadratic Mixture Model on the Natural Logarithm of Viscosity at 1150 °C for LAW Glasses

Diagnostic plots for the 21-term reduced PQM model (not included in this report) support the assumption of normally distributed errors in the $\ln(\eta_{1150})$ data (see Section B.3 of Appendix B). Figure 5.13 displays the standardized residuals of the 21-term reduced PQM model of $\ln(\eta_{1150})$ plotted versus the data index (a sequential numbering of the modeling data points), with different plotting symbols representing the different groups of LAW glasses discussed in Section 2.3. Figure 5.13 is very similar to Figure 5.9, so the observations on Figure 5.13 are the same as discussed in Section 5.3.2.2 for Figure 5.9.

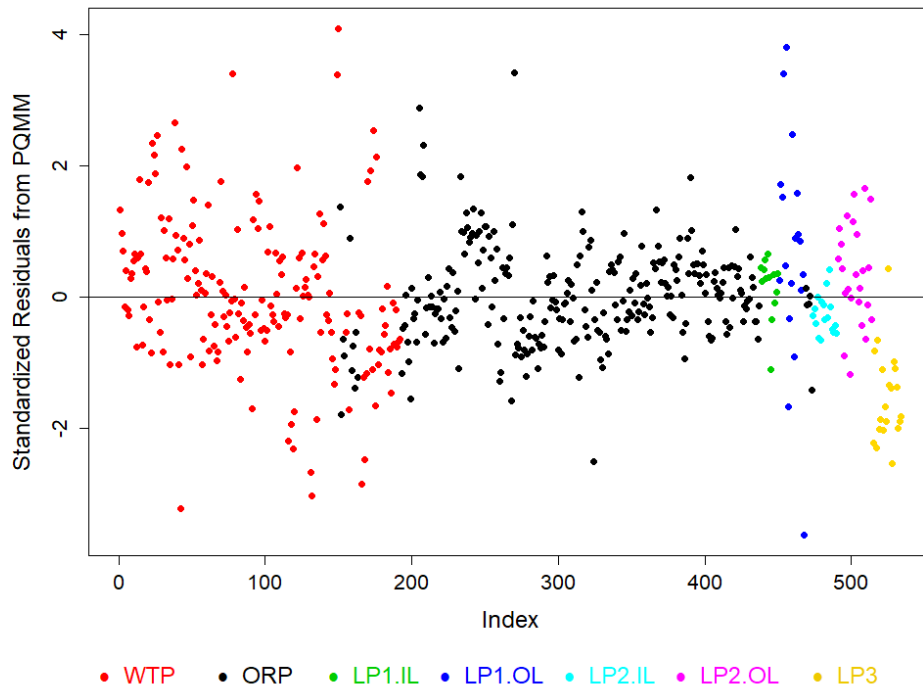


Figure 5.13. Standardized Residuals Plot for the 21-Term Reduced Partial Quadratic Mixture Model on the Natural Logarithm of Viscosity at 1150 °C for LAW Glasses

Figure 5.14 displays the PvM plot for the 534-glass modeling dataset using the 21-term reduced PQM model for $\ln(\eta_{1150})$. Figure 5.14 is nearly identical to the PvM plot for the 18-component RLM model in Figure 5.10. Hence, as in Figure 5.10, Figure 5.14 illustrates that the 21-term reduced PQM model predicts $\ln(\eta_{1150})$ quite well, but with a slight tendency to under-predict (i) above $\ln(\eta_{1150}) \sim 4.60$ ($\eta_{1150} \sim 99.17$ poise) and (ii) possibly below $\ln(\eta_{1150}) \sim 2.10$ ($\eta_{1150} \sim 8.17$ poise). However, the model predicts with little bias within the WTP LAW Facility operating limits for η_{1150} (20 to 100 poise), shown by the red lines in Figure 5.14.

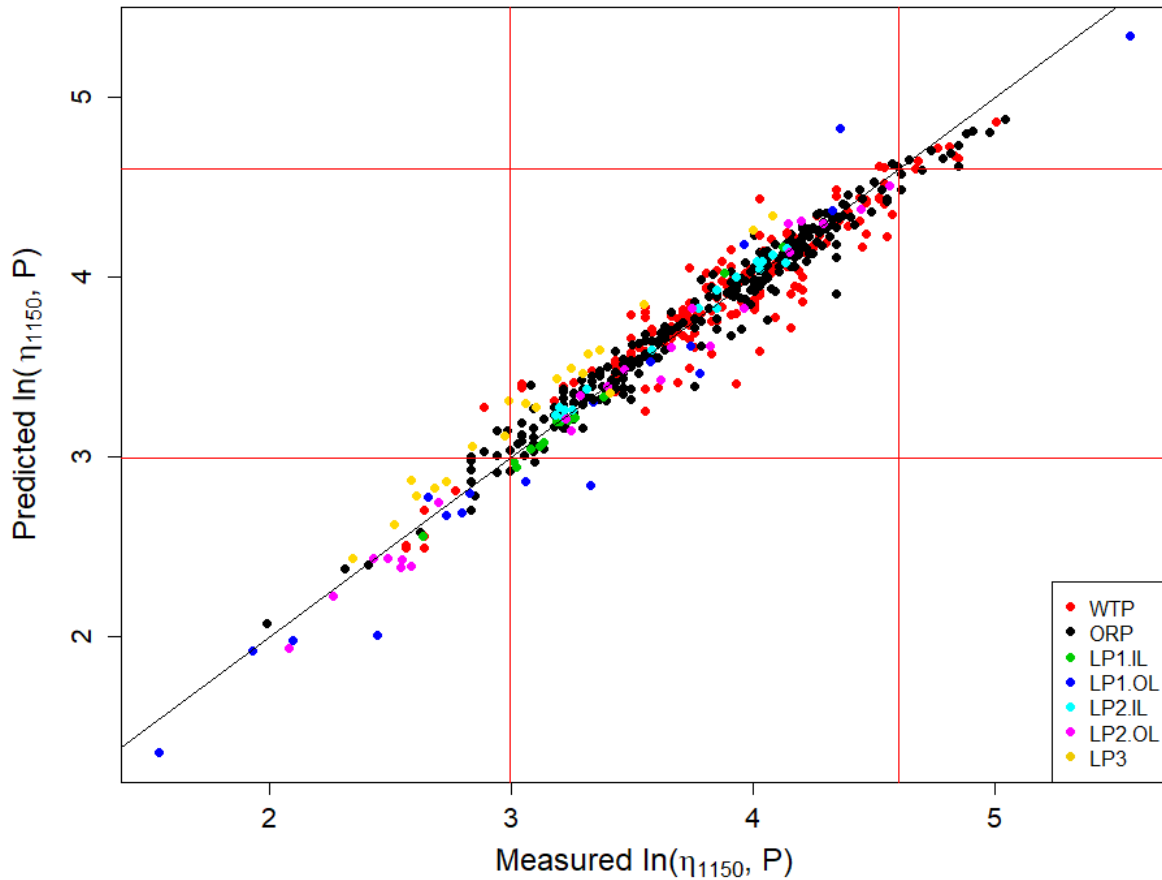


Figure 5.14. Predicted versus Measured Plot for the 516-glass Modeling Dataset Using the 21-term Reduced Partial Quadratic Mixture Model on the Natural Logarithm of Viscosity at 1150 °C for LAW glasses. The red lines represent the WTP LAW Facility operating limits for viscosity at 1150 °C (20 to 100 poise).

Figure 5.15 displays PvM plots using the 21-term reduced PQM model for $\ln(\eta_{1150})$ in Table 5.5 applied to the six evaluation subsets discussed in Section 5.1.3. Each plot in the figure contains the evaluation R^2 and RMSE values for the corresponding evaluation subset. Figure 5.15 shows that the 21-term reduced PQM model for $\ln(\eta_{1150})$ fit to the 534-glass modeling dataset generally predicts very well for the six evaluation subsets. In particular, the model predicts very well for the evaluation subsets containing glasses with higher waste loadings (LP2OL, LP123, HiNa_2O , and HiSO_3). The plot for the WTP evaluation set (which contains older data for glasses with lower waste loadings) shows more scatter, resulting in an evaluation R^2 that is not as large as for the other evaluation sets. This is understandable and acceptable, since the new models presented in this report need to predict well for glasses with higher waste loadings.

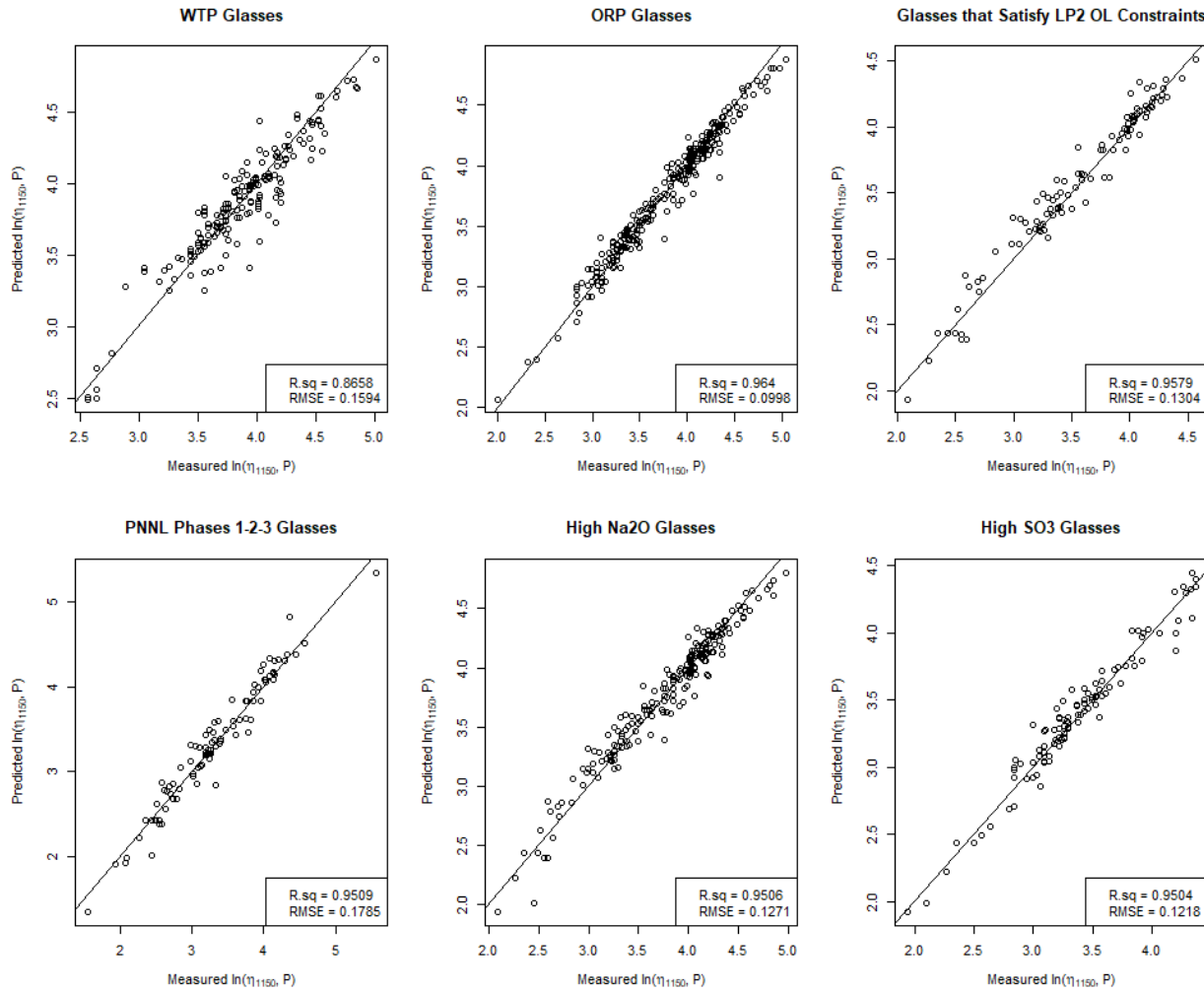


Figure 5.15. Predicted versus Measured Plots for the Six Evaluation Subsets Using the 21-term Reduced Partial Quadratic Mixture Model on the Natural Logarithm of Viscosity at 1150 °C for LAW Glasses

Figure 5.16 displays the response trace plot (see Section B.4.1 of Appendix B) for the 21-term reduced PQM model for $\ln(\eta_{1150})$. Figure 5.16 shows that Li_2O , Na_2O , CaO , B_2O_3 , and K_2O are predicted to decrease $\ln(\eta_{1150})$ the most, while SiO_2 , Al_2O_3 , and P_2O_5 are predicted to increase $\ln(\eta_{1150})$ the most. The remaining components have predicted response traces with small to negligible slopes, indicating those components are predicted to have small to negligible effects on $\ln(\eta_{1150})$.

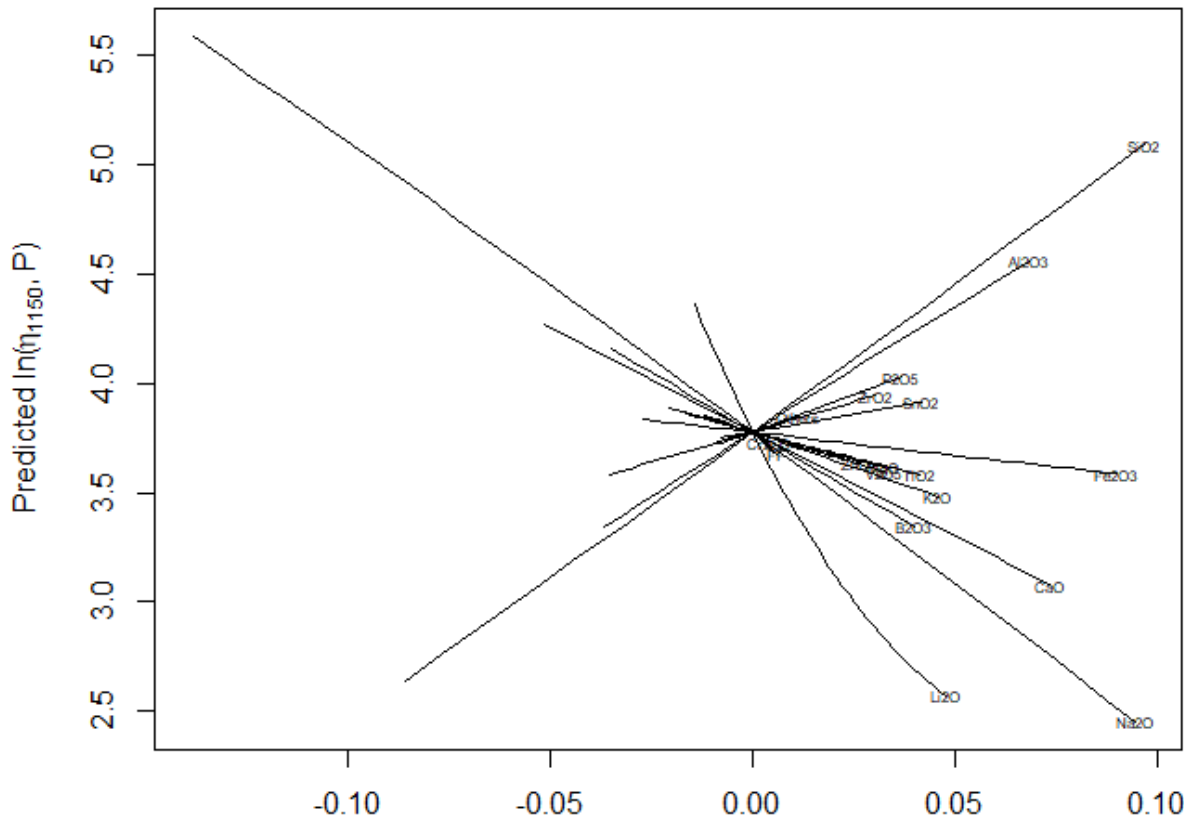


Figure 5.16. Response Trace Plot for 21-Term Reduced Partial Quadratic Mixture Model on the Natural Logarithm of Viscosity at 1150 °C for LAW Glasses

5.3.4 Recommended Model for the Natural Logarithm of Viscosity at 1150 °C for LAW Glasses

Table 5.6 summarizes the following primary $\ln(\eta_{1150})$ model evaluation and validation results for the 20-component FLM model, the 18-component RLM model, and the 21-term reduced PQM model from Table 5.3, Table 5.4, and Table 5.5, respectively:

- Model goodness-of-fit for the $\ln(\eta_{1150})$ -composition modeling data of 534 simulated LAW glasses
- Model validation using the data-splitting approach
- Model evaluation for six subsets of the 534-glass modeling dataset

Based on the summarized results in Table 5.6 and discussions in Sections 5.3.1 to 5.3.3, the 21-term reduced PQM model (listed in Table 5.5) is recommended for predicting $\ln(\eta_{1150})$ of LAW glasses. As a baseline for comparison, the 18-component RLM model (listed in Table 5.3) will be used.

Table 5.6. Performance Summary of Three Models for the Natural Logarithm of Viscosity at 1150 °C for LAW Glasses

	ln(η_{1150}) Model					
Summary Statistics from Model Fit to 534 Glasses ^(a)	20-Component FLM Model	18-Component RLM Model	21-Term Reduced PQM Model (recommended)			
R ²	0.9429	0.9410	0.9487			
R ² _A	0.9408	0.9390	0.9467			
R ² _P	0.9367	0.9350	0.9426			
RMSE	0.1375	0.1395	0.1304			
LOF p-value	0.9641	0.9510	0.9903			
Linear Terms	20 (See Table 5.3)	18 (See Table 5.4)	18 (See Table 5.5)			
Selected Quadratic Terms in Model	NA	NA	Al ₂ O ₃ × Na ₂ O (Li ₂ O) ² Li ₂ O × Na ₂ O			
# Model Terms	20	18	21			
Summary Statistics for Six Evaluation Subsets of LAW Glasses ^(a)						
Evaluation Set (# Glasses) ^(b)	R ² _{Eval}	RMSE _{Eval}	R ² _{Eval}	RMSE _{Eval}	R ² _{Eval}	RMSE _{Eval}
WTP (182)	0.8569	0.1634	0.8589	0.1609	0.8658	0.1594
ORP (260)	0.9571	0.1079	0.9552	0.1097	0.9640	0.0998
LP2OL (102)	0.9515	0.1336	0.9437	0.1424	0.9579	0.1304
LP123 (92)	0.9437	0.1898	0.9385	0.1972	0.9509	0.1785
HiNa ₂ O (200)	0.9438	0.1309	0.9372	0.1369	0.9506	0.1271
HiSO ₃ (104)	0.9375	0.1378	0.9368	0.1374	0.9504	0.1218
Validation Summary Statistics Averaged Over 5 Data-Splitting Sets ^(b)						
R ²	0.9424		0.9405		0.9479	
R ² _A	0.9398		0.9381		0.9455	
R ² _P	0.9346		0.9330		0.9403	
RMSE	0.1375		0.1393		0.1308	
R ² _V	0.9399		0.9381		0.9467	
RMSE _V	0.1411		0.1430		0.1324	

(a) The model evaluation statistics are defined in Section B.3 of Appendix B.

(b) Model validation statistics are defined in Section B.5 of Appendix B.

5.4 Example Illustrating Model Predictions and Statistical Intervals for Viscosity at 1150 °C

This section contains examples that illustrate the application of the recommended 21-term PQM model for $\ln(\eta_{1150})$ in Table 5.5 to the REFMIX glass composition listed in Table 2.3 to obtain predicted η_{1150} values and two-sided statistical intervals. Formulas for two-sided 90% CIs and two-sided 90% prediction intervals (PIs) are discussed in Section B.6 of Appendix B. Two-sided intervals are illustrated because η_{1150} will have lower and upper operating limits during the WTP LAW Facility operation. For comparison purposes, the same results are presented for the 18-component RLM model in Table 5.4 (although it was not a recommended model). The 90% CIs and 90% PIs were chosen for illustration purposes only. The WTP LAW Facility can use an appropriate confidence level depending on the use of the $\ln(\eta_{1150})$ -composition model and the type of statistical interval (uncertainty expression) desired.

The glass composition used in this example is denoted REFMIX, as listed in Table 2.3. The 20-component composition (mass fractions) of REFMIX for η_{1150} modeling is given in Table 5.7. To apply the 21-term reduced PQM and 18-component RLM models for $\ln(\eta_{1150})$ to the REFMIX composition, the mass fractions of the 20 components must be converted to mass fractions (that sum to

1.0) of the 18 LAW glass components contained in both models. This involves adding the mass fractions of the 2 of 20 components (Cl and SO₃) not contained in the ln(η_{1150}) RLM and reduced PQM models to the mass fraction of the Others component of the original 20 components, thereby producing the Others component for the reduced set of 18 components. Mass fractions of the relevant components are then multiplied to obtain the three quadratic terms of the 21-term reduced PQM model. Table 5.7 contains the composition of REFMIX prepared for use in the two ln(η_{1150}) models for LAW glasses.

For each of the two ln(η_{1150}) models, predicted ln(η_{1150} , poise) values are obtained by multiplying the composition in the format needed for that model by the coefficients for that model, then summing the results. That is, the predicted values are calculated by

$$\hat{y}(\mathbf{g}) = \mathbf{g}^T \mathbf{b} \quad (5.4)$$

where \mathbf{g} is the composition of REFMIX formatted to match the terms in a given model (from Table 5.7), the superscript T represents a vector transpose, and \mathbf{b} is the vector of coefficient estimates for a given model. The predicted ln(η_{1150}) values for REFMIX using the two ln(η_{1150}) models are listed in the second column of Table 5.8. The predicted ln(η_{1150}) values in ln(poise) units are easily converted to η_{1150} values (poise) by exponentiation. The third column of Table 5.8 contains the predicted η_{1150} values (poise). When used with CIs as discussed in Section B.6 of Appendix B, these back-transformed η_{1150} predictions in poise should be considered estimates of the true median (not the true mean) of the distribution of η_{1150} values that would result if viscosity measurements at 1150 °C were repeated multiple times on separately batched and melted samples of the REFMIX glass composition. When used with PIs, the back-transformed η_{1150} predictions should be considered estimates of individual test results for the REFMIX glass composition.

The predicted η_{1150} values for REFMIX in Table 5.8 are 44.86 poise for the 18-component RLM model and 43.74 poise for the recommended 21-term reduced PQM model. Statistical confidence intervals and prediction intervals for these predictions are discussed next.

Table 5.7. REFMIX Composition in Formats Used with Models of Natural Logarithm of Viscosity at 1150 °C for LAW Glasses

Model Term	REFMIX Composition ^(a) (mass fractions)	REFMIX Composition (mass fractions) to Use in 18-Component RLM Model for $\ln(\eta_{1150})$ ^(b)	REFMIX Composition (mass fractions) to Use in 21-Term PQM Model for $\ln(\eta_{1150})$ ^(c)
Al ₂ O ₃	0.075760	0.075761	0.075761
B ₂ O ₃	0.097257	0.097257	0.097257
CaO	0.052514	0.052514	0.052514
Cl	0.003376	NA ^(d)	NA
Cr ₂ O ₃	0.002041	0.002041	0.002041
F	0.001348	0.001349	0.001349
Fe ₂ O ₃	0.029727	0.029727	0.029727
K ₂ O	0.012064	0.012064	0.012064
Li ₂ O	0.014802	0.014802	0.014802
MgO	0.016989	0.016989	0.016989
Na ₂ O	0.168395	0.168395	0.168395
P ₂ O ₅	0.003239	0.003239	0.003239
SO ₃	0.005542	NA	NA
SiO ₂	0.424565	0.424565	0.424565
SnO ₂	0.007587	0.007587	0.007587
TiO ₂	0.008034	0.008034	0.008034
V ₂ O ₅	0.007499	0.007499	0.007499
ZnO	0.031997	0.031997	0.031997
ZrO ₂	0.036219	0.036219	0.036219
Others	0.001045	0.009963	0.009963
Al ₂ O ₃ ×Na ₂ O	NA	NA	0.01275761
(Li ₂ O) ²	NA	NA	0.00021910
Li ₂ O×Na ₂ O	NA	NA	0.00249258

(a) The composition in mass fractions is from Table 2.3.

(b) See Table 5.4.

(c) See Table 5.5.

(d) NA = not applicable, because the model does not contain this term.

Table 5.8. Predicted Viscosity at 1150 °C, Standard Deviation, and Statistical Intervals for the REFMIX Composition Used in Two Models for Viscosity at 1150 °C

Model for $\ln(\eta_{1150})^{(a)}$	Predicted $\ln(\widehat{\eta_{1150}})$ [ln(poise)]	Predicted $\widehat{\eta_{1150}}$ [poise]	Standard Deviation of Predicted $\ln(\eta_{1150})^{(b)}$ [ln(poise)]	90% CI ^(c) on Mean $\ln(\widehat{\eta_{1150}})$ [ln(poise)]	90% CI ^(c) on Median $\widehat{\eta_{1150}}$ [poise]	90% PI ^(c) on Individual $\ln(\widehat{\eta_{1150}})$ [ln(poise)]	90% PI ^(c) on Individual $\widehat{\eta_{1150}}$ [poise]
21-Term PQM Model	3.778 ^(d)	43.74 ^(d)	0.0111	(3.760, 3.796)	(42.94, 44.54)	(3.562, 3.994)	(35.25, 54.27)
18-Comp. RLM Model	3.804	44.86	0.0068	(3.792, 3.815)	(44.36, 45.36)	(3.573, 4.034)	(35.64, 56.47)

(a) The two $\ln(\eta_{1150})$ models in this column are given in Table 5.5 (21-term PQM model) and Table 5.4 (18-component RLM model), respectively.

(b) The standard deviation is for the $\ln(\eta_{1150})$ prediction considered to be the mean from many such results for the REFMIX glass.

(c) CI = two-sided confidence interval, PI = two-sided prediction interval (see Section B.6 of Appendix B).

(d) All calculations were performed using the REFMIX glass composition, model coefficients, and variance-covariance matrix values given in tables of this report. The calculated $\ln(\text{poise})$ values were rounded to three decimal places in this table. The poise values were calculated by exponentiating the $\ln(\text{poise})$ values before rounding, then rounding the resulting values to two decimal places in this table.

Eq. (B.21a) in Appendix B can be used to calculate a two-sided 90% CI for the true mean of $\ln(\eta_{1150})$ values for the REFMIX glass composition with each of the $\ln(\eta_{1150})$ models. Similarly, Eq. (B.22a) can be used to calculate a two-sided 90% PI for an individual test value of $\ln(\eta_{1150})$ for the REFMIX glass composition with each of the $\ln(\eta_{1150})$ models. In the notation of these equations:

- $100(1-\alpha)\% = 90\%$, so that $\alpha = 0.10$ for a 90% CI in Eq. (B.21a) and a 90% PI in Eq. (B.22a).
- The vector \mathbf{g} contains entries corresponding to the terms in a given $\ln(\eta_{1150})$ model, which are calculated using the composition of REFMIX in Table 5.7.
- Matrix \mathbf{G} is formed from the data matrix used in the regression that generated a given $\ln(\eta_{1150})$ model. Matrix \mathbf{G} has the number of rows in the η_{1150} modeling dataset (534 glasses) and the number of columns corresponding to the number of terms in a given $\ln(\eta_{1150})$ model. Each column is calculated according to the corresponding term in the model using the LAW normalized glass composition in the η_{1150} modeling dataset.

To calculate a two-sided $100(1-\alpha)\%$ CI, the quantity margin-of-error $t_{1-\alpha/2, n-p} \sqrt{MSE_{OLS} \mathbf{g}^T (\mathbf{G}^T \mathbf{G})^{-1} \mathbf{g}}$ is subtracted from and added to the predicted $\ln(\eta_{1150})$ [denoted $\hat{y}(\mathbf{g})$], as indicated by Eq. (B.21a). To calculate a two-sided $100(1-\alpha)\%$ PI, the quantity $t_{1-\alpha/2, n-p} \sqrt{MSE_{OLS} (1 + \mathbf{g}^T (\mathbf{G}^T \mathbf{G})^{-1} \mathbf{g})}$ is subtracted from and added to the predicted $\ln(\eta_{1150})$ [denoted $\hat{y}(\mathbf{g})$], as indicated by Eq. (B.22a). The $MSE_{OLS} (\mathbf{G}^T \mathbf{G})^{-1}$ portion of these expressions is an estimate of the variance-covariance matrix for the estimated model coefficients, as discussed near the end of Section B.6 of Appendix B, and $t_{1-\alpha/2, n-p}$ is the Students- t statistic corresponding to the intended confidence level with $n-p$ degrees of freedom. For the example calculations presented in Table 5.8, the Students- t statistic value needed for both the CI and PI formulas describing the 18-component RLM model is 1.647812. This is based on $n=534$ and $p=18$. The following cell formula can be used to obtain the t -statistic value with Excel: =T.INV(0.95,534-18). For the CI and PI calculations associated with the 21-term PQM model described in Table 5.8, the Students- t statistic is 1.647829=T.INV(0.95,534-21). The variance-covariance matrices for the 18-component RLM model and the recommended 21-term PQM model are respectively listed in Tables D.8 and D.9 of Appendix D. The quantity $\sqrt{MSE_{OLS} \mathbf{g}^T (\mathbf{G}^T \mathbf{G})^{-1} \mathbf{g}}$ is the estimated standard deviation of a model prediction (for a given composition vector \mathbf{a} expressed in a given model form); the value for each model is given in the fourth column of Table 5.7.

The 90% CIs and 90% PIs for the true mean and individual test result, respectively, of $\ln(\eta_{1150})$ in units of $\ln(\text{poise})$ for the REFMIX composition based on the two $\ln(\eta_{1150})$ models are given in the fifth and seventh columns of Table 5.7. Exponentiating the resulting 90% CIs for the mean $\ln(\eta_{1150})$ values in $\ln(\text{poise})$ units yields 90% CIs for the median η_{1150} (poise) (Montgomery and Peck 1992). These values are in the sixth column of Table 5.8. Exponentiating the 90% PIs for individual $\ln(\eta_{1150})$ test results in $\ln(\text{poise})$ units yields 90% PIs on individual η_{1150} test results (poise) for REFMIX. These values are in the seventh column of Table 5.7.

5.5 Suitability of the Recommended Viscosity at 1150 °C Model for Application by the WTP LAW Facility

The 21-term PQM model for $\ln(\eta_{1150})$ discussed in Section 5.3.3 is recommended for use by the WTP LAW Facility as the best model currently available for predicting η_{1150} for LAW glasses. This model yields unbiased predictions of η_{1150} over the WTP LAW Facility operating limits (20 to 100 poise) for η_{1150} values, both for the whole modeling dataset (see Figure 5.14) and for various subsets of the data,

including subsets of glasses with high waste loadings (see Figure 5.15). The recommended 21-term PQM model does not have a statistically significant LOF, so that a η_{1150} prediction within and somewhat outside the operating limits should be within the uncertainty of what would be obtained by batching and melting a LAW glass, measuring viscosity at several temperatures for the LAW glass, and determining the estimated value of η_{1150} for the LAW glass (as discussed in Section 2.3).

The magnitudes of uncertainties in η_{1150} model predictions should be small enough that they will not unduly restrict the formulation and processing of LAW glasses in the WTP LAW Facility. Figure 5.17 displays the $\ln(\eta_{1150})$ prediction standard deviations versus predicted values [both in $\ln(\text{poise})$ units] for the LAW glass compositions in the η_{1150} modeling dataset. The $\ln(\eta_{1150})$ prediction standard deviations for the η_{1150} modeling dataset of 534 LAW glasses range from approximately 0.01 to 0.055 $\ln(\text{poise})$ for the recommended 21-term PQM model. Note that predicted standard deviations will be larger for LAW glass compositions as their distance from glasses in the η_{1150} modeling dataset increases. Also, the total uncertainty in predictions with the recommended 21-term PQM model will depend on the type of statistical interval used (see Section B.6 of Appendix B).

Work to assess the impact of LAW glass composition and model uncertainties for the recommended $\ln(\eta_{1150})$ model (Sections 5.3.3 and 5.3.4) on satisfying the WTP LAW Facility processing requirements for LAW glasses must be performed in the future. The impacts of these uncertainties on glass formulation and processability are planned to be addressed as part of the second iteration of the LAW GFA development work. The first iteration of that work (Kim and Vienna 2012) used a viscosity model from Piepel et al. (2007). A more recent evaluation, performed by Gervasio et al. (2018), used a preliminary viscosity model from Vienna et al. (2016).

The range of single component concentrations in the 534-glass dataset used for modeling is listed in Table 5.9 and discussed in Section 9.7. These ranges can be used to determine model validity ranges.

Table 5.9. Data Component Concentration Ranges (mass fraction) for LAW Glasses Used in Final Viscosity Models

Component	20-component		18-component	
	Min	Max	Min	Max
Al ₂ O ₃	0.034972	0.147521	0.034972	0.147521
B ₂ O ₃	0.059952	0.138294	0.059952	0.138294
CaO	0.000000	0.127789	0.000000	0.127789
Cl	0.000000	0.011722	NA ^(a)	NA
Cr ₂ O ₃	0.000000	0.006303	0.000000	0.006303
F	0.000000	0.007197	0.000000	0.007197
Fe ₂ O ₃	0.000000	0.119838	0.000000	0.119838
K ₂ O	0.000000	0.058846	0.000000	0.058846
Li ₂ O	0.000000	0.063294	0.000000	0.063294
MgO	0.000000	0.050182	0.000000	0.050182
Na ₂ O	0.024707	0.265729	0.024707	0.265729
P ₂ O ₅	0.000000	0.040256	0.000000	0.040256
SO ₃	0.000360	0.016290	NA	NA
SiO ₂	0.335164	0.522624	0.335164	0.522624
SnO ₂	0.000000	0.050299	0.000000	0.050299
TiO ₂	0.000000	0.050058	0.000000	0.050058
V ₂ O ₅	0.000000	0.040885	0.000000	0.040885
ZnO	0.009992	0.058152	0.009992	0.058152
ZrO ₂	0.000000	0.067534	0.000000	0.067534
Others ^(b)	0.000000	0.003296	0.000963	0.021612

(a) NA = not applicable or component not included as term.

(b) Note: Others for the 18-components are composed of all the NA components as well as Others for the 20 components.

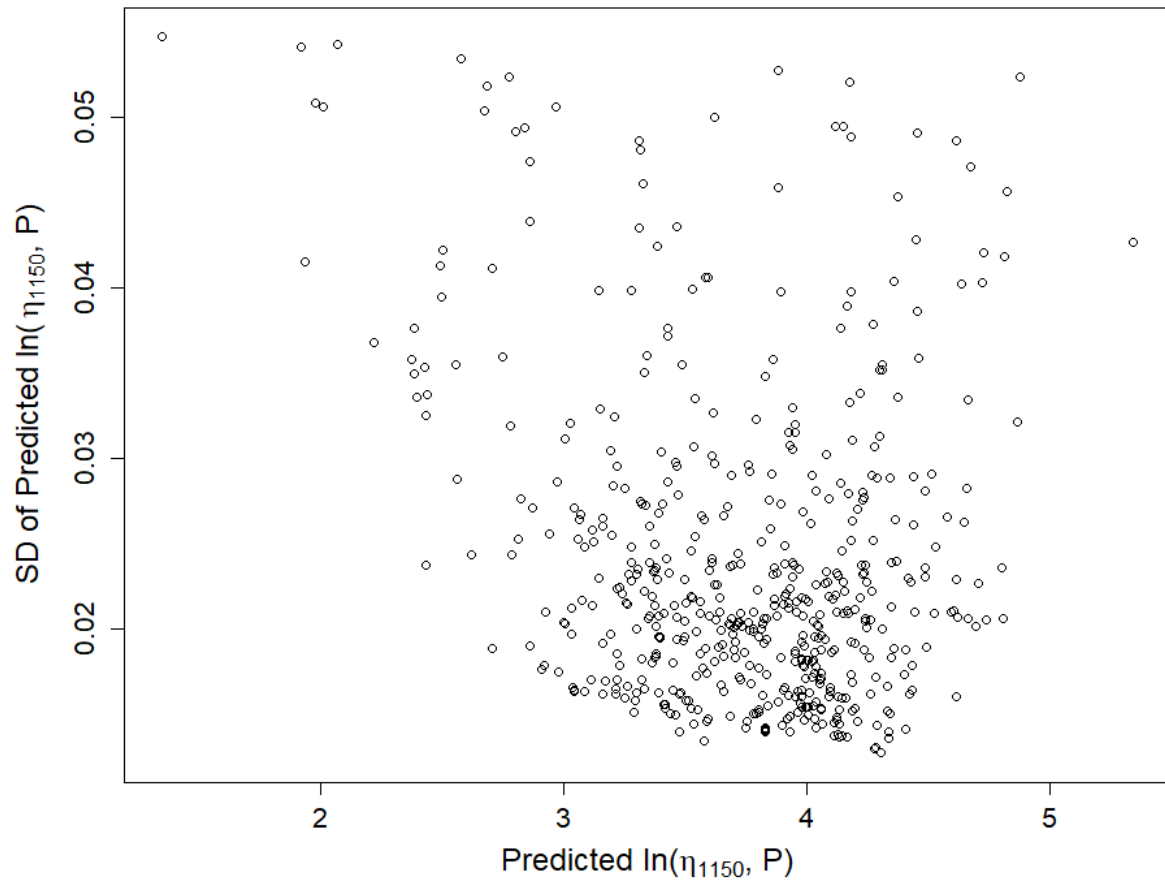


Figure 5.17. Prediction Standard Deviations versus Predicted Values over the LAW Glass Compositions in the 534-Glass Modeling Dataset for the Recommended 21-term PQM Model for the Natural Logarithm of Viscosity at 1150 °C

6.0 Models Relating Electrical Conductivity at 1150 °C to LAW Glass Composition

This section documents the development, evaluation, and validation of LAW glass property-composition models and corresponding uncertainty expressions for predicting the ϵ_{1150} in the form of $\ln(\epsilon_{1150})$ modeled as a function of LAW glass composition. The property-composition models and corresponding uncertainty expressions for $\ln(\epsilon_{1150})$ presented in this section were developed, evaluated, and validated using compositions and ϵ_{1150} values for simulated LAW glasses.

Section 6.1 discusses the LAW glasses available and used for $\ln(\epsilon_{1150})$ -composition model development, evaluation, and validation. Section 6.2 presents the model forms for $\ln(\epsilon_{1150})$ that were investigated. Section 6.3 summarizes the results for the selected linear and quadratic mixture model forms for $\ln(\epsilon_{1150})$ and identifies the recommended model. Section 6.4 illustrates the calculation of ϵ_{1150} predictions and the uncertainties in those predictions using selected $\ln(\epsilon_{1150})$ models and corresponding uncertainty equations. Section 6.5 discusses the suitability of the recommended $\ln(\epsilon_{1150})$ model for use by the WTP LAW Facility. Appendix B discusses the statistical methods and summary statistics used to develop, evaluate, and validate the several $\ln(\epsilon_{1150})$ model forms investigated, as well as statistical equations for quantifying the uncertainties in $\ln(\epsilon_{1150})$ model predictions.

6.1 Electrical Conductivity at 1150 °C Data Used for Model Development, Evaluation, and Validation

The data available and used for developing $\ln(\epsilon_{1150})$ models as functions of LAW glass composition are discussed in Section 6.1.1. The approaches and data used for validating and evaluating the models are discussed in Sections 6.1.2 and 6.1.3, respectively.

6.1.1 Model Development Data for Electrical Conductivity at 1150 °C

The data available for developing $\ln(\epsilon_{1150})$ -composition models consist of composition and ϵ_{1150} values from 542 LAW glasses (see Table 2.2). These glasses and their normalized compositions based on measured (or estimated) SO_3 values are discussed in Section 2.0. The corresponding ϵ_{1150} values are presented in Table A.3 of Appendix A.

6.1.1.1 Assessment of Available Glasses with Data for Electrical Conductivity at 1150 °C

The dataset of 542 glasses with ϵ_{1150} results contains statistically designed as well as actively designed LAW glasses. Some actively designed glasses are outside the composition region covered by the majority of the LAW compositions. Such glasses are not ideal for inclusion in a modeling dataset because they can be influential when fitting models to data. Hence, it was decided to (i) graphically assess the 542 available LAW glass compositions with ϵ_{1150} values and (ii) remove from the modeling dataset any compositions considered to be outlying or non-representative of LAW glasses of interest for the WTP LAW Facility.

Figure 6.1 displays plots of the mass fractions for 19 “main components” plus the Others component (the sum of all remaining components) in the 542 LAW glasses with ϵ_{1150} data. These 20 components (including Others) have sufficient ranges and distributions of mass fraction values to support separate model terms if so desired. Figure 6.2 displays similar plots for the remaining “minor components.” On

each plot in Figure 6.1 and Figure 6.2, the x-axis represents the mass fraction values of a LAW glass component. The y-axis shows an index value representing each LAW glass composition, which aids in spreading out the data points to avoid over-plotting. The plotting symbols in Figure 6.1 and Figure 6.2 correspond to the six groups of LAW glasses discussed in Section 2.3. For comparison purposes, the vertical lines in Figure 6.1 and Figure 6.2 represent the ranges over which the LAW glass components were varied in the PNNL (i) LAW Phase 1 outer-layer study (blue lines), (ii) LAW Phase 2 outer-layer study (pink lines), and (iii) LAW Phase 3 study (pink lines, the same as LAW Phase 2 outer-layer study), as shown in Table 2.1. Phases 2 and 3 focused on LAW glasses with high Na₂O waste loadings, whereas Phase 1 explored a larger LAW GCR with higher waste loadings.

Figure 6.1 shows that several of the 542 LAW glasses have “main components” with outlying mass fraction values (e.g., F) compared to the remaining glasses and to the component ranges in the PNNL LAW Phase 1, Phase 2, and Phase 3 studies. Figure 6.2 shows what appear to be outliers for some “minor components” (e.g., La₂O₃), but the values and ranges of those components are small and hence the glass compositions were not considered to be outliers. Table 6.1 lists the 16 LAW glasses excluded from the ϵ_{1150} modeling dataset. Finally, none of the 10 outlying glasses excluded from the EC modeling work by Piepel et al. (2007) are excluded in Table 6.1. None of those glasses appear as outliers in Figure 6.1, because of the Table 6.1 data included in the current ϵ_{1150} modeling dataset. Also, none of those glasses were identified as outliers by statistical modeling diagnostics.

Figure 6.3 and Figure 6.4 (corresponding to Figure 6.1 and Figure 6.2, respectively) show plots of component distributions after the 16 outlying glasses were removed from the ϵ_{1150} dataset containing 542 glasses. Figure 6.3 shows that for the remaining 526 LAW glasses, all 19 LAW glass “main components” have sufficient ranges and distributions of values within those ranges to support terms for modeling ϵ_{1150} . Figure 6.4 confirms that none of the “minor components” have sufficient ranges and distributions of values within their ranges to support model terms for those components. Based on Figure 6.3 and Figure 6.4, it was decided to use 20 components for initial ϵ_{1150} modeling work. These components are Al₂O₃, B₂O₃, CaO, Cl, Cr₂O₃, F, Fe₂O₃, K₂O, Li₂O, MgO, Na₂O, P₂O₅, SO₃, SiO₂, SnO₂, TiO₂, V₂O₅, ZnO, ZrO₂, and Others (the sum of all remaining components). These are the same 20 components for initial modeling of all other properties (except for melter SO₃ tolerance, which normalized out SO₃).

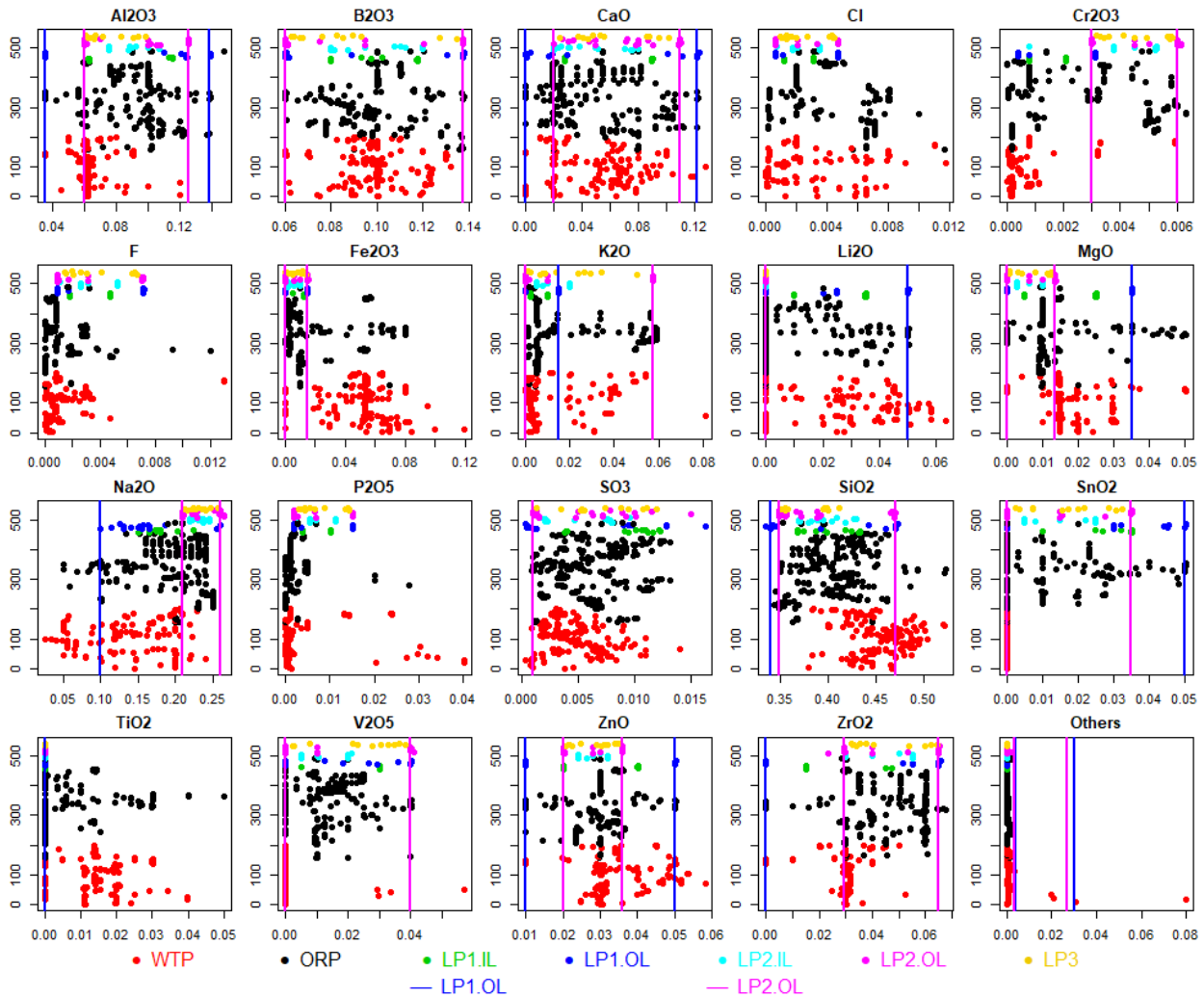


Figure 6.1. Distributions of 20 Main Components (in mass fractions) for 542 LAW Glass Compositions with Data for Electrical Conductivity at 1150 °C. The vertical lines (when present) represent the lower and upper limits for each component from the PNNL LAW Phase 1 outer-layer study (blue lines), Phase 2 outer-layer study (pink lines), and Phase 3 study (pink lines), as shown in Table 2.1. In cases where two limits are the same, pink lines over plot the blue lines. The x-axis represents the mass fraction values of a LAW glass component. The y-axis shows an index value representing each LAW glass composition, which aids in spreading out the data points to avoid over-plotting.

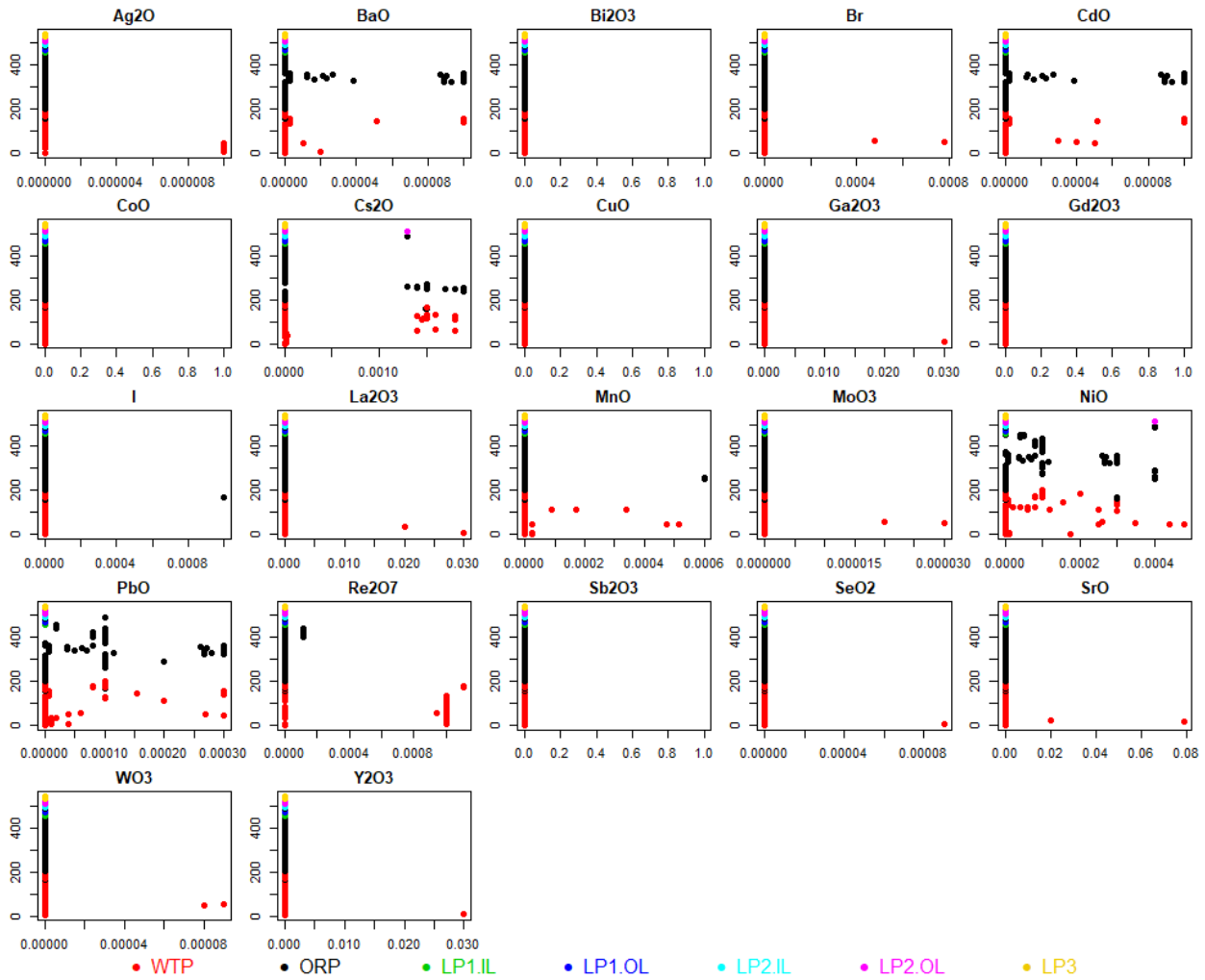


Figure 6.2. Distributions of 17 Minor Components (in mass fractions) for 542 LAW Glass Compositions with Data for Electrical Conductivity at 1150 °C. The x-axis represents the mass fraction values of a LAW glass component. The y-axis shows an index value representing each LAW glass composition, which aids in spreading out the data points to avoid over-plotting.

Table 6.1. Sixteen LAW Glasses Excluded from the Modeling Dataset for Electrical Conductivity at 1150 °C (ϵ_{1150})

Glass #	Glass ID	Reason Glass Excluded from ϵ_{1150} Modeling Dataset
450	DWV-G-51B	$F > 0.0091$ (= 0.013) mf ^(a)
453	BWV-G-142B	$F > 0.0091$ (= 0.013006) mf
626	FWV-G-108B	$F > 0.0091$ (= 0.012001) mf
628	GWV-G-36D	$F > 0.0091$ (= 0.009306) mf
629	GWV-G-65A	$F > 0.0091$ (= 0.009303) mf
80	LAWC25	$K_2O > 0.06$ (= 0.080927) mf
67	LAWC14	$V_2O_5 > 0.05$ (= 0.057118) mf
12	LAWA46	Others > 0.02 (= 0.031024) mf
13	LAWA47	Others > 0.02 (= 0.031024) mf
14	LAWA48	Others > 0.02 (= 0.031024) mf
20	LAWA64	Others > 0.02 (= 0.079852) mf
25	LAWA85	Others > 0.02 (= 0.020963) mf
43	LAWABP1	Others > 0.02 (= 0.020001) mf
327	LA44PNCC	CCC glass
337	LAWM7	Identified as outlier in model development work
339	LAWM9	Identified as outlier in model development work

(a) mf = mass fraction

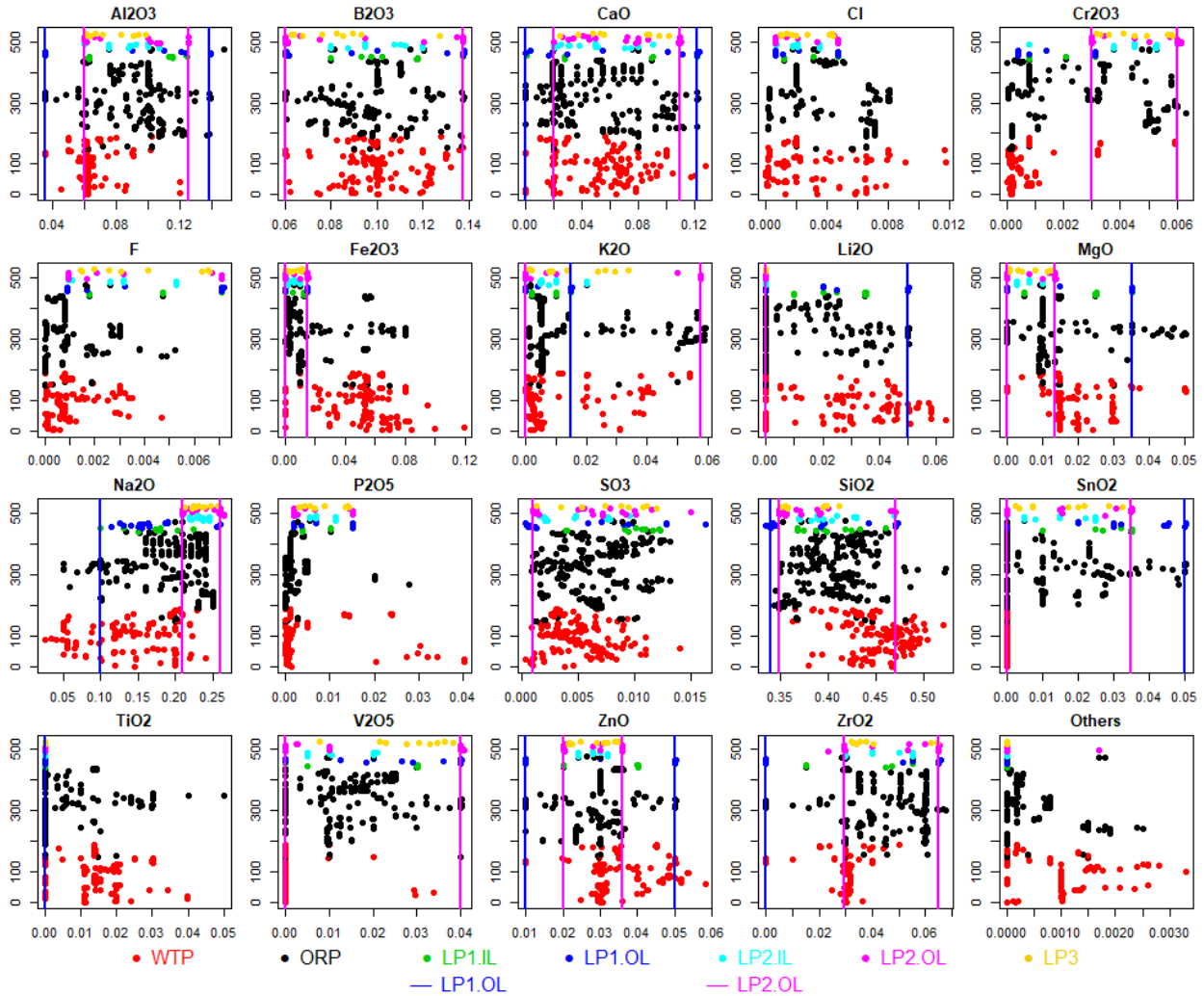


Figure 6.3. Distributions of 20 Main Components (in mass fractions) for 526 LAW Glass Compositions with Data for Electrical Conductivity at 1150 °C that Remain after Excluding the 16 Glasses in Table 6.1. The vertical lines (when present) represent the lower and upper limits for each component from the PNNL LAW Phase 1 outer-layer study (blue lines), Phase 2 outer-layer study (pink lines), and Phase 3 study (pink lines), as shown in Table 2.1. In cases where two limits are the same, pink lines over plot the blue lines. The x-axis represents the mass fraction values of a LAW glass component. The y-axis shows an index value representing each LAW glass composition, which aids in spreading out the data points to avoid over-plotting.

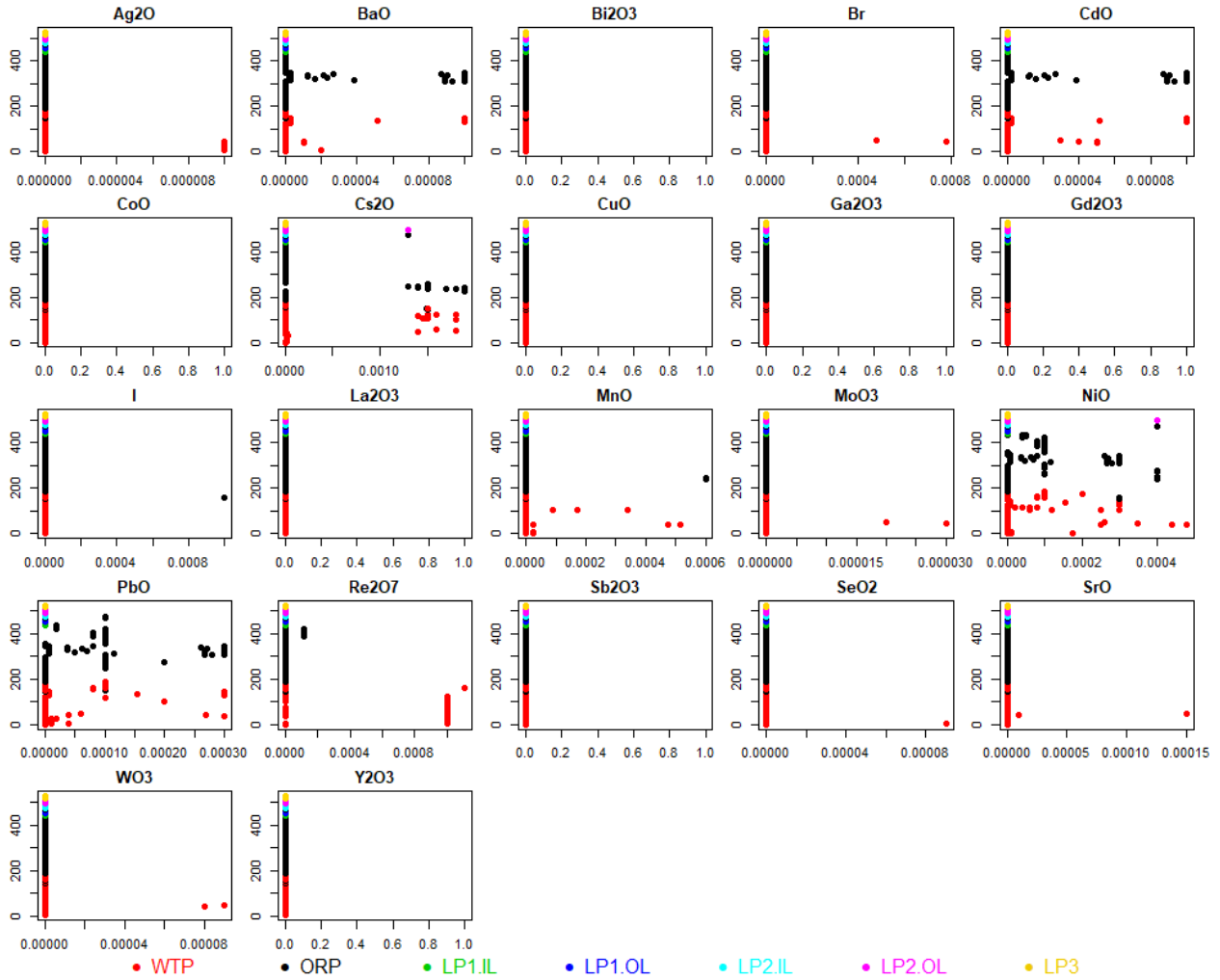


Figure 6.4. Distributions of 17 Minor Components (in mass fractions) for 526 LAW Glass Compositions with Data for Electrical Conductivity at 1150 °C that Remain after Excluding the 16 Glasses in Table 6.1. The x-axis represents the mass fraction values of a LAW glass component. The y-axis shows an index value representing each LAW glass composition, which aids in spreading out the data points to avoid over-plotting.

Figure 6.5 shows a scatterplot matrix of the 526 glasses remaining in the ϵ_{1150} modeling dataset after removing the 16 outlying compositions. High correlations between some pairs of components are evident, so pairwise correlation coefficients were calculated. These can vary from -1.0 (perfect negative correlation) to 0 (no correlation) to 1.0 (perfect positive correlation). The only component pair with correlation larger (in absolute value) than 0.60 was Na₂O and Li₂O with correlation -0.878 . Such high correlations in the predictors make parameter values difficult to estimate and result in inflated prediction uncertainties. Thus, this high pairwise correlation needs to be kept in mind when developing and interpreting LAW glass property-composition models for ϵ_{1150} . See Section 9.7 for further discussion on treatment of highly correlated component concentrations.

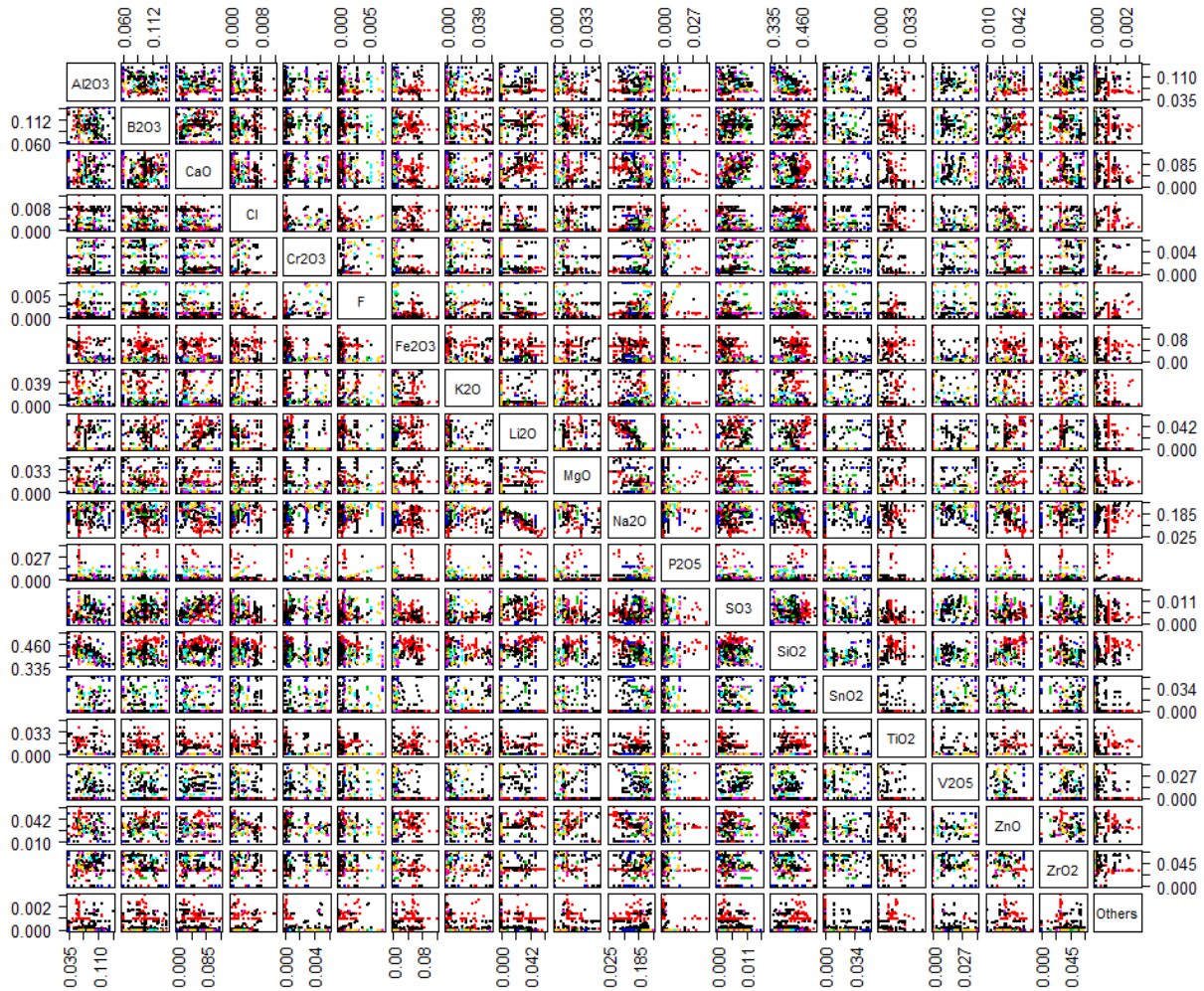


Figure 6.5. Scatterplot Matrix of 20 Components (mass fractions) for 526 LAW Glasses with Electrical Conductivity at 1150 °C Data that Remain after Excluding the 16 Glasses in Table 6.1

6.1.1.2 Electrical Conductivity at 1150 °C Modeling Dataset

Table A.3 in Appendix A lists the Glass #s, Glass IDs, and ϵ_{1150} values for the 526 remaining simulated LAW glasses used for ϵ_{1150} model development. The ϵ_{1150} values for the 16 glasses excluded as outliers from the 526-glass modeling dataset (see Table 6.1) are marked with an asterisk in Table A.3. The compositions for these 526 LAW glasses are included in Table A.2. The glass compositions in Table A.2 are the normalized mass fractions of the 20 components previously identified as having sufficient data to support a separate model term if needed. The LAW glass compositions in Table A.2 were normalized so that the total mass fractions of all 20 components for each glass equaled precisely 1.000000 as discussed in Section 2.2.

Section 2.3 discusses how the ϵ_{1150} values in Table A.3 were obtained from ϵ_{1150} versus temperature data. The values of ϵ_{1150} in Table A.3 for the 526 glasses in the modeling dataset range from 0.130 to 0.789 S/cm.

6.1.1.3 Replicate and Near-Replicate Data for Electrical Conductivity at 1150 °C

The changes to the LAW glass compositions caused by the renormalization associated with using measured (or estimated) SO_3 values (see Section 2.2) resulted in some replicate glasses not having exactly equal normalized compositions. Such compositions are near-replicates. For ease of discussion, henceforth both replicates and near-replicates are referred to as replicates.

Table 6.2 lists the replicate sets of LAW glasses in the ϵ_{1150} modeling dataset and the corresponding ϵ_{1150} values. Table 6.2 also lists estimates of (i) %RSDs [calculated using ϵ_{1150} values in original S/cm units] and (ii) SDs [calculated using $\ln(\epsilon_{1150})$ values in $\ln(\text{S/cm})$ units] for each replicate set. The %RSD values for 21 of the 28 replicate sets range from 0.75% to 18.64%, with the %RSD values for the other 7 replicate sets ranging from 24.75% to 62.83%. As discussed in Section 5.1.1.3, although four replicate sets (Glass # 456-457, 458-459, 460-461, and 462-463 pairs) exhibited a consistent trend between the ϵ_{1150} and measured Na_2O concentration, it was determined that this trend may not be enough to justify excluding these four replicate sets. No reasons for the higher %RSD values for the remaining three replicate sets could be found in the data-source reports. Hence, it was assumed that periodically there may be larger uncertainties in batching and melting glasses and determining ϵ_{1150} .

Table 6.2 also lists pooled estimates of %RSDs and SDs calculated over all replicate sets. A pooled %RSD or SD combines the separate %RSD or SD estimates from each replicate set, so that a more precise combined estimate of the %RSD or SD is obtained. These pooled %RSDs and SDs include uncertainties due to fabricating glasses, determining SO_3 measured or estimated values, and the process of determining ϵ_{1150} values. The magnitudes of the pooled $\text{SD} = 0.2006$ [calculated in $\ln(\text{S/cm})$ units] and $\text{\%RSD} = 19.95$ [calculated in S/cm units] in Table 6.2 indicate roughly a 20% total relative uncertainty in the ϵ_{1150} values over the replicate glasses. The pooled estimates of replicate uncertainty for ϵ_{1150} in Table 6.2 are used subsequently to assess LOF of the various $\ln(\epsilon_{1150})$ models considered.

Table 6.2. Uncertainty in Electrical Conductivity at 1150 °C Responses for Replicate and Near-Replicate Sets

Replicate Set Glass #s	Replicate Set Glass IDs	Replicate Set ϵ_{1150} (S/cm) Values	%RSD ^(a)	SD [ln(S/cm)]
993	EWG-LAW-Centroid-1	0.388	2.86	0.0286
995	EWG-LAW-Centroid-2	0.404		
9	LAWA44	0.516	40.10	0.4123
326	LAWA44R10	0.288		
227	LAWB83	0.233	7.21	0.0734
229	LAWB84	0.230		
284	B1-AZ101(LAWB83)	0.200		
442	LAWC100	0.290	9.45	0.0962
443	LAWC100R1	0.330		
447	WVY-G-95A	0.350		
75	LAWC22	0.448	18.64	0.1793
272	C22AN107	0.340		
279	C1-AN107(LAWC22)	0.320		
456	LAWCrP1	0.294	39.76	0.4086
457	LAWCrP1R	0.524		
458	LAWCrP2	0.381	37.70	0.3864
459	LAWCrP2R	0.658		
460	LAWCrP3	0.339	29.67	0.3012
461	LAWCrP3R	0.519		
462	LAWCrP4	0.363	45.20	0.4684
463	LAWCrP4R	0.704		
451	LAWC7H	0.400	2.15	0.0215
624	FWV-G-63B	0.388		
331	LAWM1	0.162	62.83	0.6753
383	LAWM53	0.421		
365	LAWM35	0.304	24.75	0.2501
386	LAWM56	0.433		
846	ORLEC12	0.431	3.83	0.0383
865	OWV-G-144E	0.455		
848	ORLEC14	0.567	0.75	0.0075
887	QWV-G-107B	0.561		
850	ORLEC16	0.531	1.97	0.0197
888	PWV-G-130C	0.546		
853	ORLEC19	0.350	11.85	0.1187
890	QWV-G-29C	0.414		
856	ORLEC22	0.393	6.85	0.0685
891	QWV-G-75B	0.433		
862	ORLEC26	0.514	8.61	0.0862
867	OWV-G-109B	0.455		
863	ORLEC27	0.431	1.78	0.0178
869	PWV-G-43E	0.442		
864	ORLEC28	0.485	3.59	0.0359
871	PWV-G-93A	0.461		
877	ORLEC33	0.501	6.98	0.0698
903	RWV-G-9C	0.533		
878	ORLEC34	0.477	1.47	0.0147
904	RWV-G-48D	0.487		

Table 6.2. Uncertainty in Electrical Conductivity at 1150 °C Responses for Replicate and Near-Replicate Sets (cont.)

Replicate Set		Replicate Set		SD
Glass #s	Replicate Set Glass IDs	ϵ_{1150} (S/cm) Values	%RSD ^(a)	[ln(S/cm)]
893	ORLEC44	0.432	8.03	0.0804
905	RWV-G-79C	0.484		
895	ORLEC46	0.456	0.78	0.0078
906	RWV-G-120D	0.451		
897	ORLEC48R	0.423	3.42	0.0342
907	SWV-G-17A	0.403		
597	ORPLD1	0.347	8.35	0.0825
997	LAW-ORP-LD1(1)	0.340		
999	LAW-ORP-LD1(2)	0.407		
1035	LP2-OL-07	0.377		
1022	LP2-IL-10	0.523	8.23	0.0825
1028	LP2-IL-16	0.562		
1031	LP2-OL-02	0.462		
1049	LP2-OL-21	0.498		
1034	LP2-OL-05	0.357	2.34	0.0234
1038	LP2-OL-10-MOD	0.369		
Pooled Over All 28 Replicate Sets with 35 total DF^(b)			19.95	0.2066
(a) %RSD = $100 \times (\text{Standard Deviation} / \text{Mean})$.				
(b) DF = degrees of freedom				

6.1.2 Model Validation Approach and Data for Electrical Conductivity at 1150 °C of LAW Glasses

The validation approach for ϵ_{1150} modeling was based on splitting the 526-glass dataset for model development into five modeling/validation subsets. Of the 526 model development glasses, 63 were in 28 replicate sets. The five modeling/validation splits of the 526 glasses in the ϵ_{1150} modeling dataset were formed as follows.

- The 63 replicate glasses in 28 replicate sets were set aside so they would always be included in each of the five model development datasets. This was done so that replicate sets would not be split between modeling and validation subsets, thus negating the intent to have validation glasses different than model development glasses.
- The remaining 463 glasses were ordered from smallest to largest according to their ϵ_{1150} values (S/cm). The 463 glasses were numbered 1, 2, 3, 4, 5, 1, 2, 3, 4, 5, etc. All of the 1's formed the first model validation set, while all of the remaining points formed the first model development dataset. Similarly, all of the 2's, 3's, 4's, and 5's respectively formed the second, third, fourth, and fifth model validation sets. In each case, the remaining non-2's, non-3's, non-4's, and non-5's formed the second, third, fourth, and fifth model development datasets. Because 463 is not evenly divisible by 5, the five modeling and validation subsets did not all contain the same numbers of glasses. Three of the five splits contained 93 glasses for validation and 370 glasses for modeling. The other two splits contained 92 glasses for validation and 371 for modeling. Note that these numbers of glasses in the modeling subsets do not yet include the 63 replicates.
- The 63 replicate glasses were added to each of the split modeling subsets. Including the replicates, three splits contained 433 glasses for modeling and 93 for validation, while the other two splits contained 434 glasses for modeling and 92 for validation.

Data splitting was chosen as the validation approach because the ϵ_{1150} modeling dataset contains all compositions that (i) are in the LAW GCR of interest, (ii) meet QA requirements, and (iii) have ϵ_{1150} data. Having a separate validation dataset not used for modeling is desirable, but that desire was over-ridden by wanting ϵ_{1150} models developed using all appropriate data.

6.1.3 Subsets of LAW Glasses to Evaluate Prediction Performance of Models for Electrical Conductivity at 1150 °C

Section 2.4 discusses six subsets of LAW glasses for evaluating the prediction performance of LAW glass property-composition models, including subsets of glasses with higher waste loadings. The subsets, as discussed in Section 2.4, are denoted WTP, ORP, LP2OL, LP123, HiNa_2O , and HiSO_3 . The ϵ_{1150} modeling dataset of 526 LAW glasses (see Section 5.1.1) contains 177, 267, 93, 82, 191, and 101 glasses with ϵ_{1150} values in these six evaluation subsets, respectively. The “Glass #s” of these six evaluation subsets of LAW glasses are listed in Table C.4 of Appendix C. The normalized LAW glass compositions and ϵ_{1150} values for the glasses with these “Glass #s” are listed in Tables A.2 and A.3, respectively, of Appendix A.

Summary statistics denoted R_{Eval}^2 and $RMSE_{Eval}$ (see Section B.3 of Appendix B), as well as predicted versus measured plots (see Section B.3), are subsequently used to assess the prediction performance of the ϵ_{1150} models (presented in later subsections) for the six evaluation subsets listed in Table C.4 of Appendix C.

6.2 Model Forms for Electrical Conductivity at 1150 °C of LAW Glasses

Ideally, a property-composition model for ϵ_{1150} would use known mechanisms of ϵ_{1150} as a function of LAW glass composition. However, no such mechanisms are known. Empirical models for ϵ_{1150} with coefficients estimated from model development data have been shown in the past to perform well. The empirical model forms used are from the general class of *mixture experiment models* (Cornell 2002), which includes models linear in composition as well as non-linear in composition. Section B.1 of Appendix B discusses mixture experiments and several general forms of mixture experiment models.

Section 6.2.1 discusses the forms of mixture experiment models used for ϵ_{1150} of LAW glasses. Section 6.2.2 discusses using natural-log transformed ϵ_{1150} values as the response variable for ϵ_{1150} modeling.

6.2.1 Mixture Experiment Model Forms for Electrical Conductivity at 1150 °C of LAW Glasses

The LM and PQM model forms introduced in Section B.1 of Appendix B were chosen for use in modeling $\ln(\epsilon_{1150})$ as a function of LAW glass composition. These models have been used in the past (Piepel et al. 2007; Muller et al. 2014) to model the compositional dependence of $\ln(\epsilon)$ -composition-temperature models. However, the present work considered LM and PQM models for $\ln(\epsilon_{1150})$ as functions of LAW glass composition. The LM model form is given by

$$\ln(\epsilon_{1150}) = \sum_{i=1}^q \beta_i g_i + e \quad (6.1)$$

while the PQM model form is given by

$$\ln(\varepsilon_{1150}) = \sum_{i=1}^q \beta_i g_i + \text{Selected} \left\{ \sum_{i=1}^q \beta_{ii} g_i^2 + \sum_{i < j}^{q-1} \sum_j^q \beta_{ij} g_i g_j \right\} + e \quad (6.2)$$

where in Eqs. (6.1) and (6.2):

- $\ln(\varepsilon_{1150})$ = natural logarithm of ε_{1150} (in S/cm)
- g_i = normalized mass fraction of the i^{th} glass oxide or halogen component
($i = 1, 2, \dots, q$), such that $\sum_{i=1}^q g_i = 1$
- β_i = coefficient of the i^{th} linear blending term ($i = 1, 2, \dots, q$)
- β_{ii} and β_{ij} = coefficients of selected quadratic (squared or crossproduct) blending terms to be estimated from the data
- e = random error for each data point

Many statistical methods exist for the case where the E are statistically independent (i.e., not correlated) and normally distributed with mean 0 and standard deviation σ . In Eq. (6.2), “Selected” means that only some of the terms in curly brackets are included in the model. The subset is selected using stepwise regression or other variable selection methods (Draper and Smith 1998; Montgomery et al. 2012). PQM models are discussed in more detail and illustrated by Piepel et al. (2002) and Smith (2005).

Cornell (2002) discusses many other empirical mixture model forms that could have been considered for ε_{1150} -composition modeling. However, these other mixture model forms were not investigated because the special blending effects of components associated with those models were judged not to apply for ε_{1150} . The model forms in Eqs. (6.1) and (6.2) are widely used in many application areas (including waste glass property modeling) and often predict the response very well.

6.2.2 Transformation of Electrical Conductivity at 1150 °C for LAW Glasses

In modeling ε_{1150} , it is advantageous to use the natural logarithm transformation of the ε_{1150} values. The advantages of this transformation include the following:

- The ε_{1150} values for the 526 LAW glasses in the ε_{1150} modeling dataset range from 0.130 to 0.789 S/cm. This range is not one full order of magnitude, but still the uncertainty in making glasses and determining ε_{1150} leads to smaller absolute uncertainties for smaller ε_{1150} values and larger absolute uncertainties for larger ε_{1150} values. Hence, the OLS regression assumption of equal variances for all response variable values (see Section B.2.1 of Appendix B) is violated. After a logarithmic transformation, variances of ε_{1150} tend to be approximately equal as required for OLS regression.
- A logarithmic transformation tends to linearize the compositional dependence of ε_{1150} data and reduce the need for non-linear terms in the model form.
- A natural logarithm transformation is preferred over a common logarithm (or other base logarithm) transformation because of the approximate relationship

$$SD [\ln(y)] \cong RSD (y) \quad (6.3)$$

where SD denotes standard deviation, RSD denotes relative standard deviation (i.e., the standard deviation divided by the mean), and y denotes ϵ_{1150} . Eq. (6.3) results from applying the first-order variance propagation formula [Eq. (7-7) of Hahn and Shapiro (1967)] to the function $z = \ln(y)$. The relationship in Eq. (6.3) is very useful, in that uncertainties of the natural logarithm of the response variable y can be interpreted as approximate RSDs of the untransformed response variable y .

For these reasons, the natural logarithmic transformation was employed for all ϵ_{1150} model forms.

6.3 Property-Composition Model Results for Electrical Conductivity at 1150 °C of LAW Glasses

This section discusses the results of fitting several different mixture experiment models using natural logarithms of ϵ_{1150} (S/cm) as functions of LAW glass compositions. Section 6.3.1 presents the results of modeling $\ln(\epsilon_{1150})$ using a 20-component FLM model. Sections 6.3.2 and 6.3.3 present the results of modeling $\ln(\epsilon_{1150})$ using RLM and PQM models based on a reduced set of mixture components. Finally, Section 6.3.4 compares the results from the three models and recommends a $\ln(\epsilon_{1150})$ model for future use and evaluation.

6.3.1 Results from the 20-Component Full Linear Mixture Model for the Natural Logarithm of Electrical Conductivity at 1150 °C of LAW Glasses

As the initial step in $\ln(\epsilon_{1150})$ -composition model development, an FLM model with the 20 components identified in Section 6.1.1 was fit to the modeling data (526 LAW glasses). Table 6.3 contains the results for the 20-component FLM model of $\ln(\epsilon_{1150})$. Table 6.3 lists the estimated model coefficients, standard deviation errors of the coefficients (i.e., the standard deviation of the coefficients), and model fit summary statistics for the 20-component FLM model on $\ln(\epsilon_{1150})$ using the modeling dataset (526 LAW glasses). Table 6.3 also contains the results from the (i) data-splitting validation approach (see Section 6.1.2), and (ii) evaluation of model predictions for the six evaluation subsets (see Section 6.1.3). In the data-splitting validation portion of the results at the bottom of Table 6.3, the columns are labeled DS1, DS2, DS3, DS4, and DS5 to denote the five modeling/validation splits of the data as described in Section 6.1.2. The last column of this part of Table 6.3 shows the averages for the different statistics over the five splits.

The $R^2 = 0.8359$, $R^2_A = 0.8298$, and $R^2_P = 0.8182$ statistics (see Section B.3 of Appendix B) in Table 6.3 show that (i) the 20-component FLM model fits the $\ln(\epsilon_{1150})$ data in the 526-glass modeling dataset reasonably well, (ii) there are not a large number of unneeded model terms, and (iii) there are not any highly influential data points (confirmed in the diagnostic graphics described in Section B.3). The RMSE = 0.1417 is smaller than the pooled glass batching and ϵ_{1150} determination uncertainty [$SD = 0.2066$ in $\ln(\text{S/cm})$ units] estimated from replicates in Table 6.2. This suggests that the 20-component FLM model does not have a statistically significant LOF, which is confirmed by the model LOF p-value > 0.9999 in Table 6.3. See Section B.3 for discussion of the statistical test for model LOF.

At the bottom right of Table 6.3, the average model-fit statistics (R^2 , R^2_A , R^2_P , and RMSE) over the five data-split validation sets are close to the statistics obtained from fitting the 20-component FLM model for $\ln(\epsilon_{1150})$ to all 526 glasses in the modeling dataset. The data-split validation statistics (R^2_V and $RMSE_V$) are also relatively close to the R^2 and RMSE (i) values from fitting the model to the full dataset, and

(ii) averages from fitting the model to the data-split modeling subsets. This indicates that the 20-component FLM model maintains its predictive performance for data not used to fit the model.

Table 6.3. Coefficients and Performance Summary for the 20-Component Full Linear Mixture Model on the Natural Logarithm of Electrical Conductivity at 1150 °C for LAW Glasses

ln(ϵ_{1150}) 20-Component FLM Model Term	Coefficient Estimate	Coefficient Stand. Err.
Al ₂ O ₃	-3.4665	0.2923
B ₂ O ₃	-3.0511	0.3198
CaO	-3.4203	0.2228
Cl	-2.5182	2.9297
Cr ₂ O ₃	7.8412	3.8548
F	-16.8531	4.7818
Fe ₂ O ₃	-0.9435	0.3308
K ₂ O	-0.5211	0.4190
Li ₂ O	15.4252	0.7680
MgO	-3.9090	0.7187
Na ₂ O	6.8513	0.2315
P ₂ O ₅	-2.3760	1.3379
SO ₃	0.4282	2.5079
SiO ₂	-2.9632	0.1341
SnO ₂	-4.4727	0.5660
TiO ₂	-1.3880	0.8712
V ₂ O ₅	-2.4194	0.6215
ZnO	-2.4630	0.7218
ZrO ₂	-1.9047	0.4791
Others ^(c)	21.2636	10.6379

Modeling Data Statistic, 526 Glasses ^(a)			Value
R ²			0.8359
R ² _A			0.8298
R ² _P			0.8182
RMSE			0.1417
Model LOF p-value			>0.9999

Evaluation Set (# Glasses) ^(b)			R ² _{Eval}	RMSE _{Eval}
WTP (177)			0.6876	0.1813
ORP (267)			0.8535	0.1073
LP2OL (93)			0.3498	0.1361
LP123 (82)			0.6881	0.1866
HiNa ₂ O (191)			0.1924	0.1259
HiSO ₃ (101)			0.6768	0.1440

Data Splitting Statistic ^(a,d)	DS1	DS2	DS3	DS4	DS5	Average
R ²	0.8249	0.8357	0.8331	0.8254	0.8439	0.8326
R ² _A	0.8168	0.8282	0.8254	0.8174	0.8368	0.8249
R ² _P	0.7999	0.8137	0.8120	0.8022	0.8230	0.8102
RMSE	0.1455	0.1412	0.1408	0.1454	0.1414	0.1429
R ² _V	0.8716	0.8305	0.8380	0.8767	0.7715	0.8377
RMSE _V	0.1287	0.1461	0.1500	0.1255	0.1486	0.1398

(a) The model evaluation statistics are defined in Section B.3 of Appendix B. The model validation statistics are defined in Section B.5.

(b) The six sets of LAW evaluation glasses are discussed in Section 2.4 and Section 6.1.3.

(c) For the 20-component FLM model, the “Others” component includes any components not separately listed.

(d) The evaluation and validation statistics calculated for data-splits are defined the same as for separate modeling and validation sets. Section 6.1.2 describes how the modeling dataset was split into modeling and validation subsets.

The statistics from evaluating the predictive performance of the 20-component FLM model for ln(ϵ_{1150}) on the six evaluation subsets of modeling glasses (see Section 6.1.3) are given on the right side of Table 6.3. Four of the six evaluation subsets (HiSO₃, WTP, LP123, and ORP) have R²_{Eval} statistics ranging from 0.6768 to 0.8535. These values are from notably below to slightly above the R² statistic for the whole modeling dataset (0.8359). The other two evaluation subsets (LP2OL and HiNa₂O) have R²_{Eval} values of 0.3498 and 0.1924, respectively, which are substantially below 0.8359. The R²_{Eval} values that are moderately to substantially lower than the R² for the whole modeling dataset are because ϵ_{1150} depends

very heavily on the mass fractions of Na_2O and Li_2O in a LAW glass composition. Hence, the less variation in mass fractions of Na_2O and Li_2O there is in an evaluation subset, the less dependent $\ln(\epsilon_{1150})$ will be on the mass fractions of Na_2O and Li_2O . This statement is discussed further in Section 6.3.3.

Figure 6.6 shows the PvM plot for the 526-glass modeling dataset using the 20-component FLM model on $\ln(\epsilon_{1150})$. The plot illustrates that the 20-component FLM model predicts $\ln(\epsilon_{1150})$ fairly well with notable scatter, but with tendencies to (i) under-predict below $\ln(\epsilon_{1150}) \sim -1.50$ ($\epsilon_{1150} \sim 0.223$ S/cm) and (ii) over-predict above $\ln(\epsilon_{1150}) \sim -0.40$ ($\epsilon_{1150} \sim 0.670$ S/cm). The tendency of this model to over-predict low ϵ_{1150} values is within the WTP LAW Facility operating limits shown by the red lines in Figure 6.6, which is nominally undesirable. This topic is further discussed in Sections 6.3.2, 6.3.3, 6.4, and 6.5.

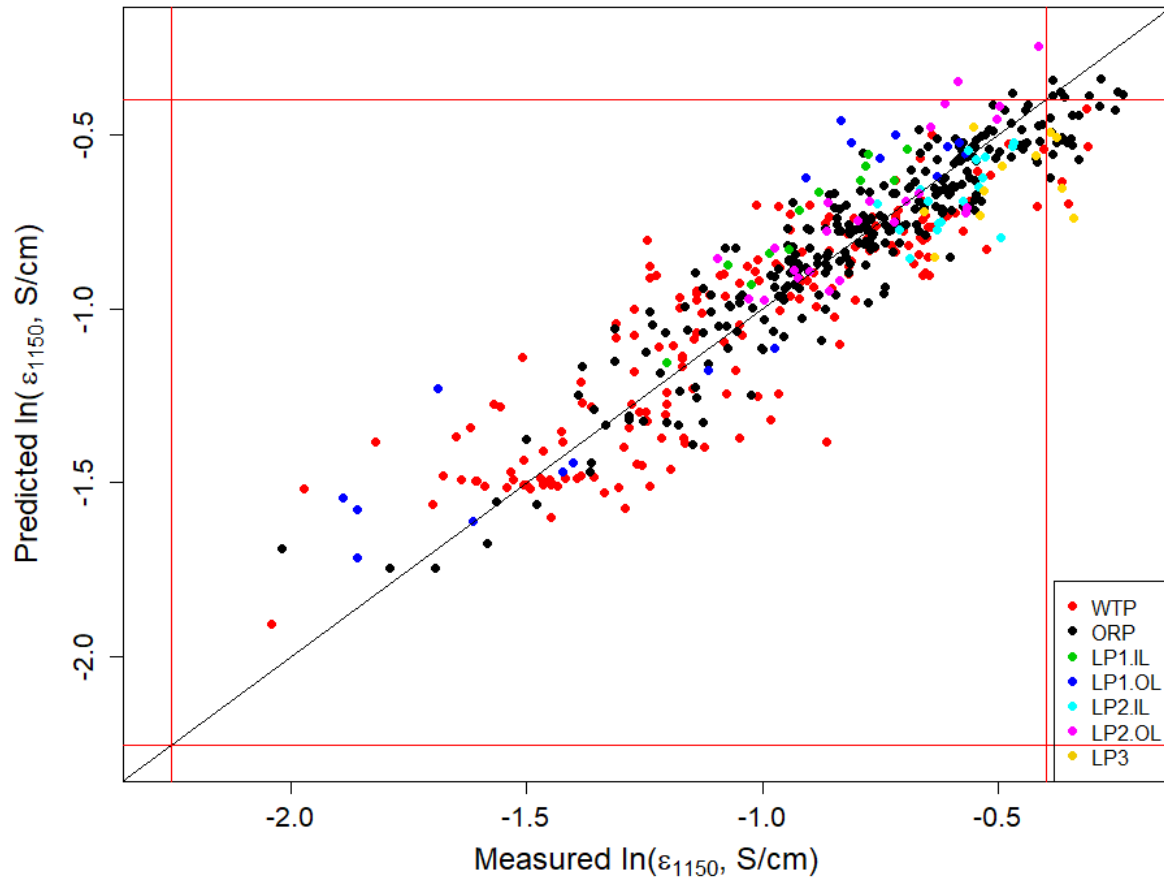


Figure 6.6. Predicted versus Measured Plot for the 526-Glass Modeling Dataset Using the 20-Component Full Linear Mixture Model on the Natural Logarithm of Electrical Conductivity at 1150 °C of LAW Glasses. The red lines represent WTP LAW Facility operating limits for electrical conductivity at 1150 °C (0.105 to 0.671 S/cm).

Figure 6.7 displays PvM plots using the 20-component FLM model for $\ln(\epsilon_{1150})$ in Table 6.3 applied to the six evaluation subsets discussed in Section 6.1.3. Each plot in the figure contains the evaluation R^2 and RMSE values for the corresponding evaluation subset. Figure 6.7 shows that the 20-component FLM model for $\ln(\epsilon_{1150})$ fit to the 526-glass modeling dataset predicts with different amounts of scatter and sometimes ranges of under- or over-prediction in the PvM plots for the six evaluation subsets. In particular, the model predicts with the tightest scatter for the ORP evaluation set, though there is some

tendency to under-predict the largest $\ln(\epsilon_{1150})$ values. Figure 6.7 shows that the largest scatter (and thus smallest R^2_{Eval} values) occurs for the HiNa₂O and LP2OL evaluation sets. As noted previously, these evaluation sets contain only high-Na₂O glasses, which reduces the R^2_{Eval} values. The prediction performances for the six evaluation sets using the model that is ultimately recommended are discussed in more detail in Section 6.5.

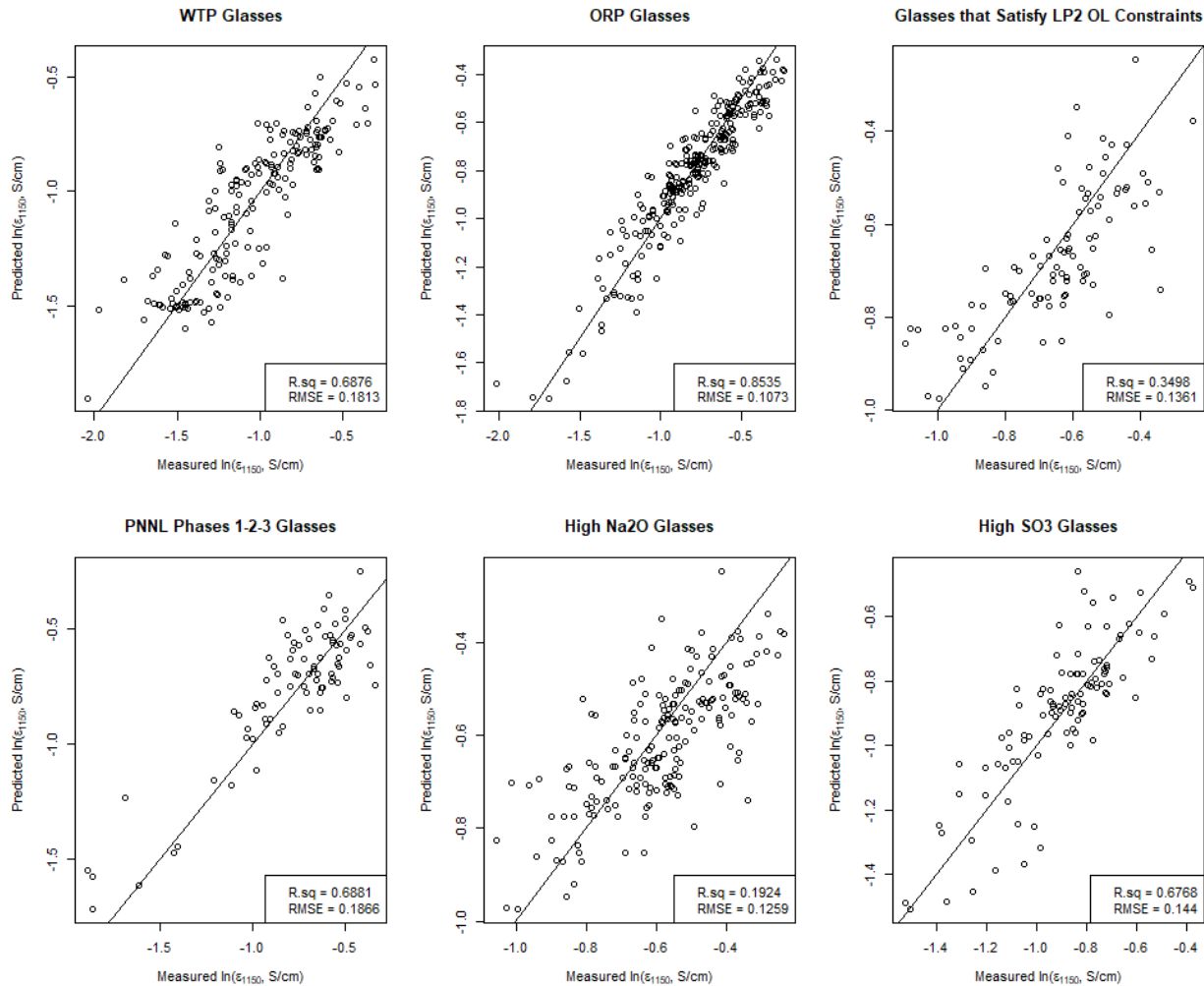


Figure 6.7. Predicted versus Measured Plots for the Six Evaluation Subsets Using the 20-Component Full Linear Mixture Model on the Natural Logarithm of Electrical Conductivity at 1150 °C for LAW Glasses

The model in Table 6.3 fits the 526-glass modeling dataset well enough, with no statistically significant LOF, to provide guidance for reducing the FLM model [i.e., removing separate terms for components that do not significantly influence $\ln(\epsilon_{1150})$]. Hence, the 20-component FLM model was used to produce the response trace plot (see Section B.4.1 in Appendix B shown in Figure 6.8. The average glass composition of the 1074 glasses in the compiled database discussed in Section 2.3 was used as the REFMIX (see Section B.4.1) in response trace plots for every modeled property. The glass composition of the REFMIX is listed in Table 2.3.

The response trace plot shown in Figure 6.8 shows that Li_2O and Na_2O are predicted to have the strongest effects of any component, with both predicted to increase $\ln(\epsilon_{1150})$. The components SiO_2 , Al_2O_3 , CaO , and SnO_2 are predicted to have much smaller decreasing effects on $\ln(\epsilon_{1150})$. The component F is predicted to have the steepest decreasing effect on $\ln(\epsilon_{1150})$, but over a small range. Hence, the predicted effect of F may not be real. The remaining components have predicted response traces with small to negligible slopes, indicating those components are predicted to have small to negligible effects on $\ln(\epsilon_{1150})$.

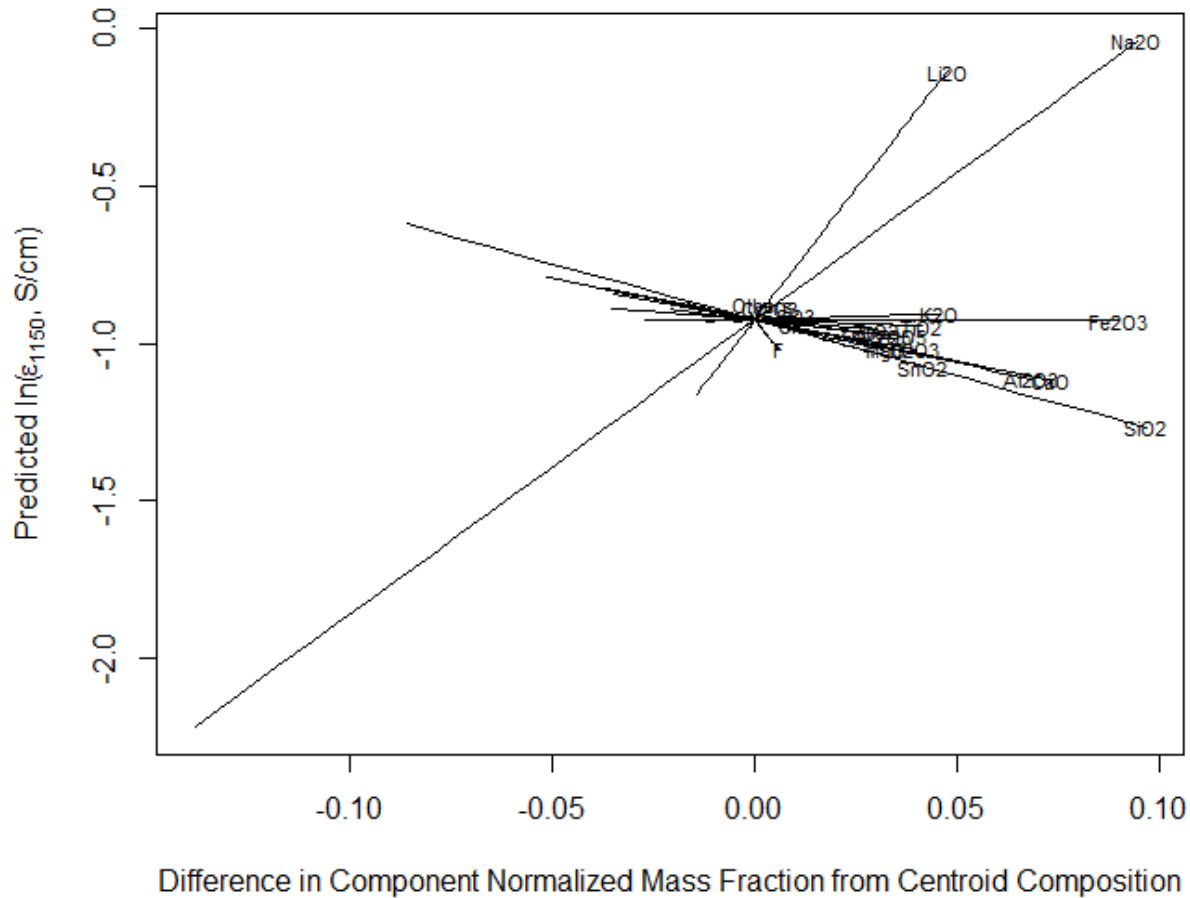


Figure 6.8. Response Trace Plot for 20-Component Full Linear Mixture Model on the Natural Logarithm of Electrical Conductivity at 1150 °C for LAW Glasses

6.3.2 Results from a Reduced Linear Mixture Model for Electrical Conductivity at 1150 °C for LAW Glasses

The 20-component FLM model for $\ln(\epsilon_{1150})$ presented in Section 6.3.1 likely contains components that do not significantly contribute to predicting $\ln(\epsilon_{1150})$, so model component reduction was the next step of the model development approach. Thus, RLM models for $\ln(\epsilon_{1150})$ involving fewer than the 20 components were considered. The sequential F-test model reduction approach (see Section B.5.1 of Appendix B; Piepel and Cooley 2006) was used.

6.3.2.1 Numerical Results for the 11-Component Reduced Linear Mixture Model on the Natural Logarithm of Electrical Conductivity at 1150 °C for LAW Glasses

The RLM model for $\ln(\epsilon_{1150})$ was obtained using the backward-elimination, F-test method discussed in Section B.4.1 of Appendix B. Glass scientists provided inputs on LAW glass components that should be retained in the model, and the method determined whether the remaining components should be kept as separate linear terms or combined into Others. The resulting RLM model for $\ln(\epsilon_{1150})$ contained terms for 11 components: Al_2O_3 , B_2O_3 , CaO , K_2O , Li_2O , MgO , Na_2O , SiO_2 , SnO_2 , V_2O_5 , and Others. So, Cl, Cr_2O_3 , F, Fe_2O_3 , P_2O_5 , SO_3 , TiO_2 , ZnO , and ZrO_2 were combined into the Others component. Note that the resulting Others component is 1 minus the sum of all remaining components, and thus differs from the Others in the 20-component FLM model discussed in Section 6.3.1.

Table 6.4 contains the results for the 11-component RLM model of $\ln(\epsilon_{1150})$. Table 6.4 lists the model coefficients, standard deviations of the coefficients, and model fit statistics for the 11-component RLM model using the modeling dataset (526 LAW glasses). Table 6.4 also contains the results from the (i) data-splitting validation approach (see Section 6.1.2), and (ii) evaluation of model predictions for the six evaluation subsets (see Section 6.1.3). In the data-splitting validation portion of the results at the bottom of Table 6.4, the columns are labeled DS1, DS2, DS3, DS4, and DS5 to denote the five modeling/validation splits of the data as described in Section 6.1.2. The last column of this part of Table 6.4 shows the averages for the different statistics over the five splits.

The $R^2 = 0.8267$, $R^2_A = 0.8233$, and $R^2_P = 0.8159$ statistics (see Section B.3 of Appendix B) in Table 6.4 show that (i) the 11-component RLM model fits the $\ln(\epsilon_{1150})$ data in the 526-glass modeling dataset reasonably well, (ii) there are not a large number of unneeded model terms, and (iii) there are not any highly influential data points. The $\text{RMSE} = 0.1444$ is smaller than the pooled glass batching and ϵ_{1150} determination uncertainty ($\text{SD} = 0.2066$ in $\ln(\text{S/cm})$ units) estimated from replicates in Table 6.2. This suggests that the 11-component RLM model does not have a statistically significant LOF, which is confirmed by the model LOF p-value = 0.9999 in Table 6.4. See Section B.3 for discussion of the statistical test for model LOF.

At the bottom right of Table 6.4, the average model-fit statistics (R^2 , R^2_A , R^2_P , and RMSE) over the five data-splits are close to the statistics obtained from fitting the 11-component RLM model for $\ln(\epsilon_{1150})$ to all 526 glasses in the modeling dataset. The data-split validation statistics (R^2_V and RMSE_V) are also relatively close to the R^2 and RMSE (i) values from fitting the model to the full dataset, and (ii) averages from fitting the model to the data-split modeling subsets. This indicates that the 11-component RLM model for $\ln(\epsilon_{1150})$ maintains its predictive performance for data not used to fit the model.

Table 6.4. Coefficients and Performance Summary for the 11-Component Reduced Linear Mixture Model on the Natural Logarithm of Electrical Conductivity at 1150 °C for LAW Glasses

ln(ϵ_{1150}) 11-Component RLM Model Term	Coefficient Estimate	Coefficient Stand. Err.	Modeling Data Statistic, 526 Glasses^(a)				Value
Al ₂ O ₃	-3.4135	0.2862	R ²				0.8267
B ₂ O ₃	-3.1506	0.3162	R ² _A				0.8233
CaO	-3.4901	0.2132	R ² _P				0.8159
K ₂ O	-0.5435	0.4073	RMSE				0.1444
Li ₂ O	15.1955	0.7544	Model LOF p-value				0.9999
MgO	-4.1430	0.7050					
Na ₂ O	6.7435	0.2151	Evaluation Set (# Glasses)^(b)				
SiO ₂	-2.9087	0.1264		R²_{Eval}		RMSE_{Eval}	
SnO ₂	-4.7892	0.5266	WTP (177)	0.6843			0.1755
V ₂ O ₅	-3.0055	0.5913	ORP (267)	0.8372			0.1100
Others ^(c)	-1.4542	0.2358	LP2OL (93)	0.4420			0.1185
			LP123 (82)	0.6096			0.1887
			HiNa ₂ O (191)	0.0798			0.1243
			HiSO ₃ (101)	0.6737			0.1416
Data Splitting Statistic^(a,d)	DS1	DS2	DS3	DS4	DS5	Average	
R ²	0.8154	0.8259	0.8248	0.8167	0.8321	0.8230	
R ² _A	0.8111	0.8217	0.8206	0.8124	0.8281	0.8188	
R ² _P	0.8009	0.8125	0.8120	0.8030	0.8190	0.8095	
RMSE	0.1477	0.1439	0.1427	0.1474	0.1451	0.1454	
R ² _V	0.8680	0.8273	0.8278	0.8652	0.7831	0.8343	
RMSE _V	0.1305	0.1475	0.1546	0.1313	0.1448	0.1417	

(a) The model evaluation statistics are defined in Section B.3 of Appendix B. The model validation statistics are defined in Section B.5.

(b) The six sets of LAW evaluation glasses are discussed in Section 2.4 and Section 6.1.3.

(c) For the 11-component RLM model, the “Others” component includes any components not separately listed.

(d) The evaluation and validation statistics calculated for data-splits are defined the same as for separate modeling and validation sets. Section 6.1.2 describes how the modeling dataset was split into modeling and validation subsets.

The statistics from evaluating the predictive performance of the 11-component RLM model for ln(ϵ_{1150}) on the six evaluation subsets of modeling glasses (see Section 6.1.3) are given on the right side of Table 6.4. Four of the six evaluation subsets (HiSO₃, WTP, LP123, and ORP) have R²_{Eval} statistics ranging from 0.6096 to 0.8372. These values are from notably below to slightly above the R² statistic for the whole modeling dataset (0.8267). The other two evaluation subsets (LP2OL and HiNa₂O) have R²_{Eval} values of 0.4420 and 0.0798, respectively, which are substantially below 0.8267. The R²_{Eval} values that are moderately to substantially lower than the R² for the whole modeling dataset are because ϵ_{1150} depends very heavily on the mass fraction of Na₂O and Li₂O in a LAW glass composition. Hence, the less variation in mass fractions of Na₂O and Li₂O there is in an evaluation subset, the less dependent ln(ϵ_{1150}) will be on the mass fractions of Na₂O and Li₂O. This statement is discussed further in Section 6.3.3.

6.3.2.2 Graphical Results for the 11-Component Reduced Linear Mixture Model on the Natural Logarithm of Electrical Conductivity at 1150 °C for LAW Glasses

Diagnostic plots for the 11-component RLM model (not included in this report) support the assumption of normally distributed errors in the ln(ϵ_{1150}) data (see Section B.3 of Appendix B). Figure 6.9 displays the standardized residuals for the 11-component RLM model of the ln(ϵ_{1150}) plotted versus the data index (a

sequential numbering of the modeling data points) with different plotting symbols representing the different groups of LAW glasses discussed in Section 2.3. Figure 6.9 yields the following observations:

- The WTP and LP1.OL (PNNL Phase 1 outer layer) datasets have a wider scatter of standardized residuals, indicating a wider range of $\ln(\epsilon_{1150})$ model prediction uncertainty. This is likely a result of the WTP and LP1.OL glasses spanning wider subregions of LAW glass compositions.
- The 11-component RLM model (i) tends to over-predict $\ln(\epsilon_{1150})$ [corresponding to negative standardized residuals] for the LP1.OL and LP2.OL glasses, and (ii) under-predicts $\ln(\epsilon_{1150})$ [corresponding to positive standardized residuals] for the LP3 glasses. The PNNL LP2.OL and LP3 studies were investigated and no reason for biased ϵ_{1150} values was found. The differences in standardized residuals for these two studies may be a result of longer-term random uncertainty.
- Two glasses have standardized residuals near -4 . Although outlying, these data points did not have a major impact on the 11-component RLM model for $\ln(\epsilon_{1150})$ and hence were retained in the modeling dataset.

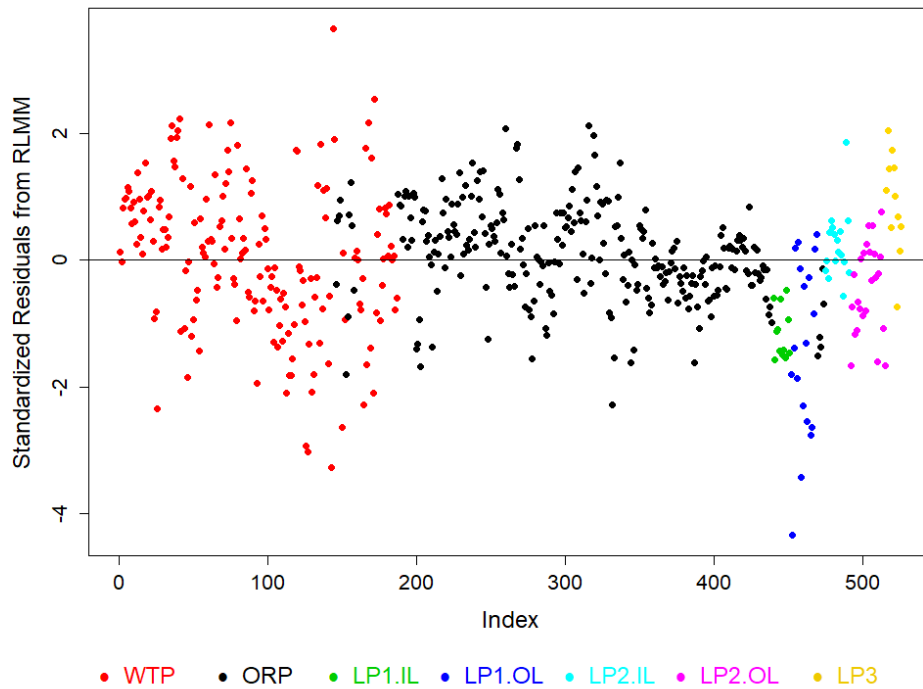


Figure 6.9. Standardized Residuals Plot for the 11-Component Reduced Linear Mixture Model on the Natural Logarithm of Electrical Conductivity at 1150 °C for LAW Glasses

Figure 6.10 displays the PvM plot for the 526-glass modeling dataset using the 11-component RLM model for $\ln(\epsilon_{1150})$. The plot illustrates that the 11-component RLM model predicts $\ln(\epsilon_{1150})$ fairly well with notable scatter, but with tendencies to (i) over-predict below $\ln(\epsilon_{1150}) \sim -1.50$ ($\epsilon_{1150} \sim 0.223$ S/cm) and (ii) under-predict above $\ln(\epsilon_{1150}) \sim -0.40$ ($\epsilon_{1150} \sim 0.670$ S/cm). The tendency of this model to over-predict low ϵ_{1150} values is within the WTP LAW Facility operating limits shown by the red lines in Figure 6.6, which is nominally undesirable. The tendency to underpredict high values occurs above the upper WTP LAW Facility operating limit. This topic is further discussed in Sections 6.3.3, 6.4, and 6.5.

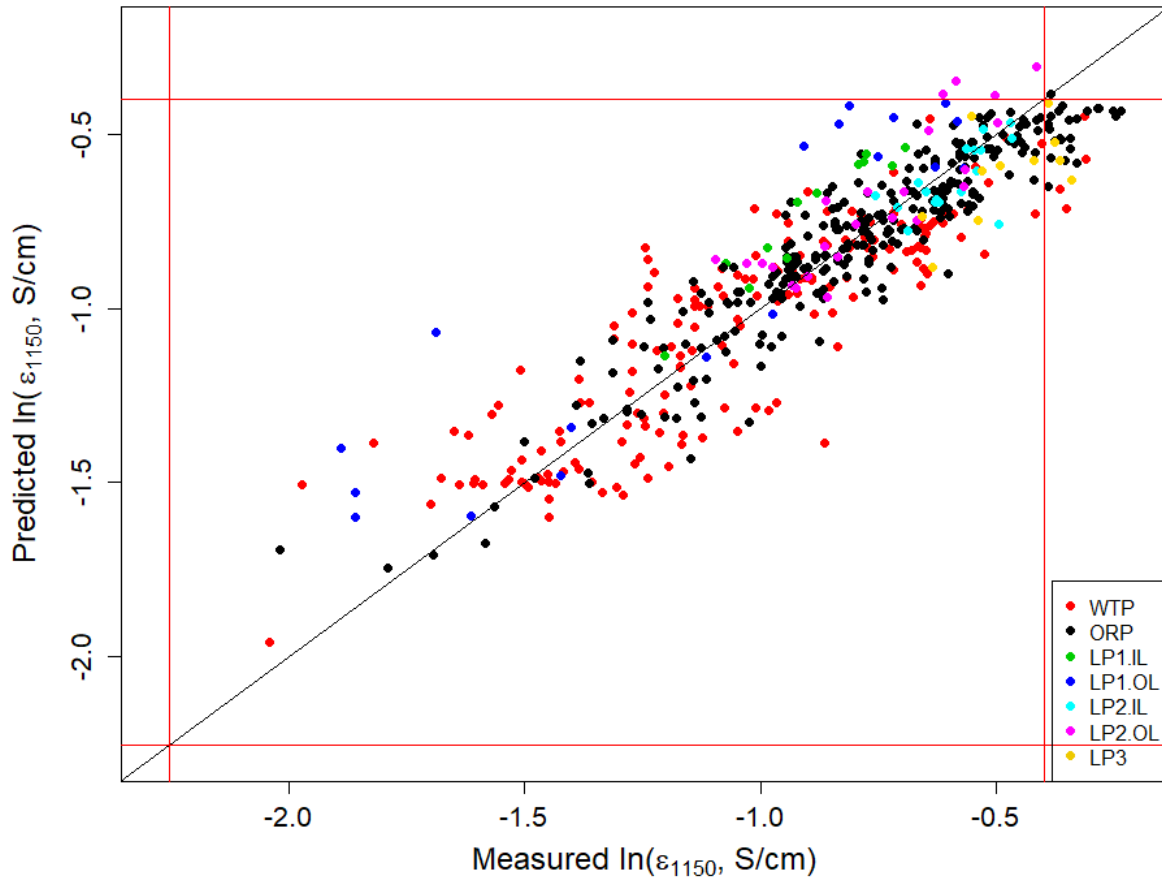


Figure 6.10. Predicted versus Measured Plot for the 526-Glass Modeling Dataset Using the 11-Component Reduced Linear Mixture Model on the Natural Logarithm of Electrical Conductivity at 1150 °C for LAW Glasses. The red lines represent the WTP LAW Facility operating limits for electrical conductivity at 1150 °C (0.105 to 0.671 S/cm).

Figure 6.11 displays PvM plots using the 11-component RLM model for $\ln(\epsilon_{1150})$ in Table 6.4 applied to the six evaluation subsets discussed in Section 6.1.3. Each plot in the figure contains the evaluation R^2 and RMSE values for the corresponding evaluation subset. Figure 6.11 shows that the 11-component RLM model for $\ln(\epsilon_{1150})$ fit to the 526-glass modeling dataset predicts with different amounts of scatter and sometimes ranges of under- or over-prediction in the PvM plots for the six evaluation subsets. In particular, the model predicts with the tightest scatter for the ORP evaluation set, though there is some tendency to under-predict the largest $\ln(\epsilon_{1150})$ values. Figure 6.11 shows that the largest scatter (and thus smallest R^2_{Eval} values) occurs for the HiNa_2O and LP2OL evaluation sets. As noted previously, these evaluation sets contain only high- Na_2O glasses, which reduces the R^2_{Eval} values. The prediction performances for the six evaluation sets using the model that is ultimately recommended are discussed in more detail in Section 6.5.

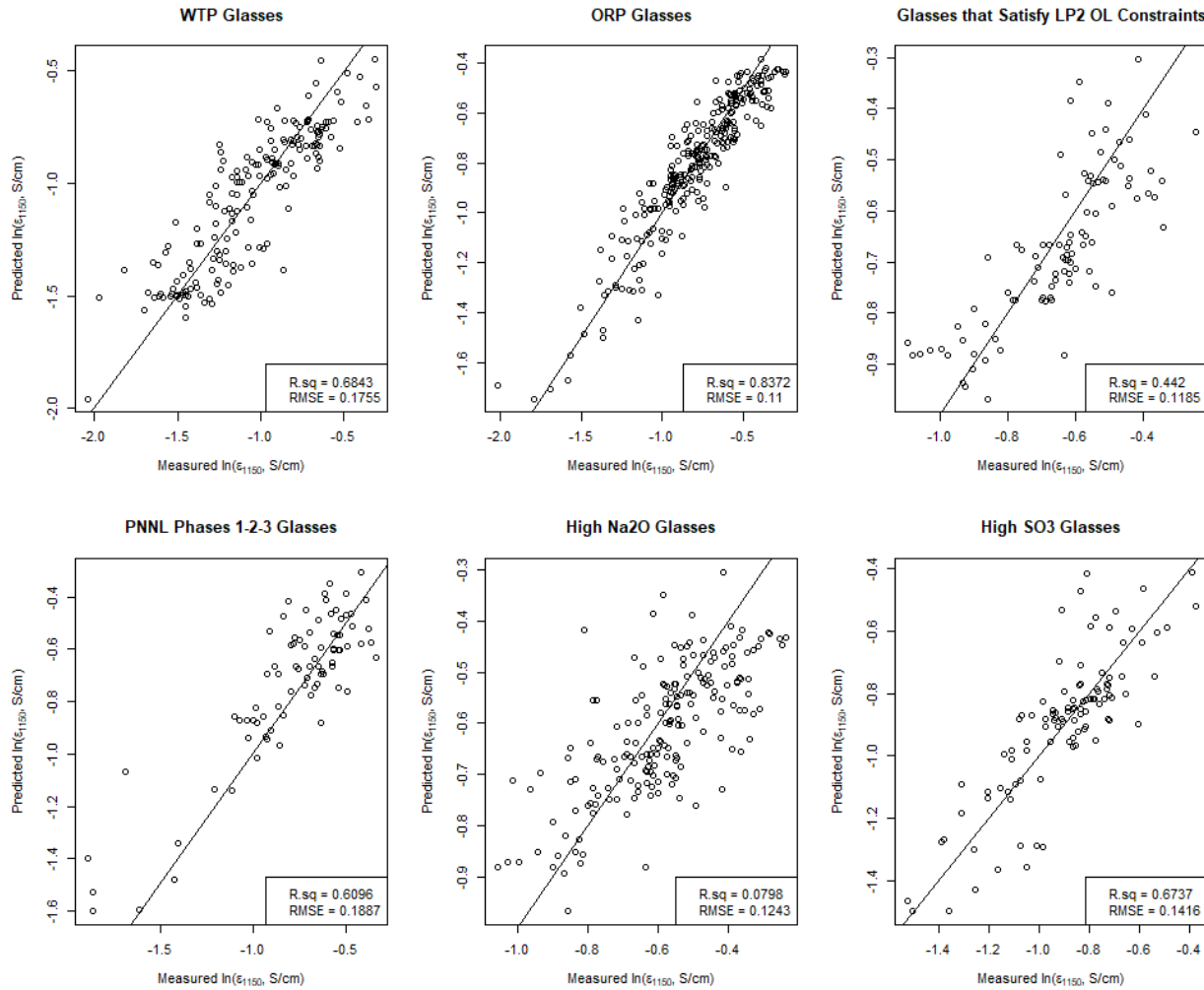


Figure 6.11. Predicted versus Measured Plots for the Six Evaluation Sets Using the 11-Component Reduced Linear Mixture Model on the Natural Logarithm of Electrical Conductivity at 1150 °C for LAW Glasses

Figure 6.12 displays the response trace plot (see Section B.4.1 in Appendix B) for the 11-component RLM model for $\ln(\epsilon_{1150})$. The glass composition of the REFMIX (see Section B.4.1) used is listed in Table 2.3. Figure 6.12 (for the 11-component RLM model) is similar to Figure 6.8 (for the 20-component FLM model), except that nine components no longer have response traces because they were included in Others. Figure 6.12 shows that Li_2O and Na_2O are predicted to have the strongest effects of any component, with both predicted to increase $\ln(\epsilon_{1150})$. The components SiO_2 , Al_2O_3 , CaO , and SnO_2 are predicted to have much smaller decreasing effects on $\ln(\epsilon_{1150})$. The component F was predicted to have the steepest decreasing effect on $\ln(\epsilon_{1150})$ over a small range in Figure 6.8, but F no longer has a response trace in Figure 6.12 after being combined into Others. The remaining components (K_2O , Others, V_2O_5 , B_2O_3 , and MgO) have predicted response traces with small to negligible slopes, indicating those components are predicted to have small to negligible effects on $\ln(\epsilon_{1150})$.

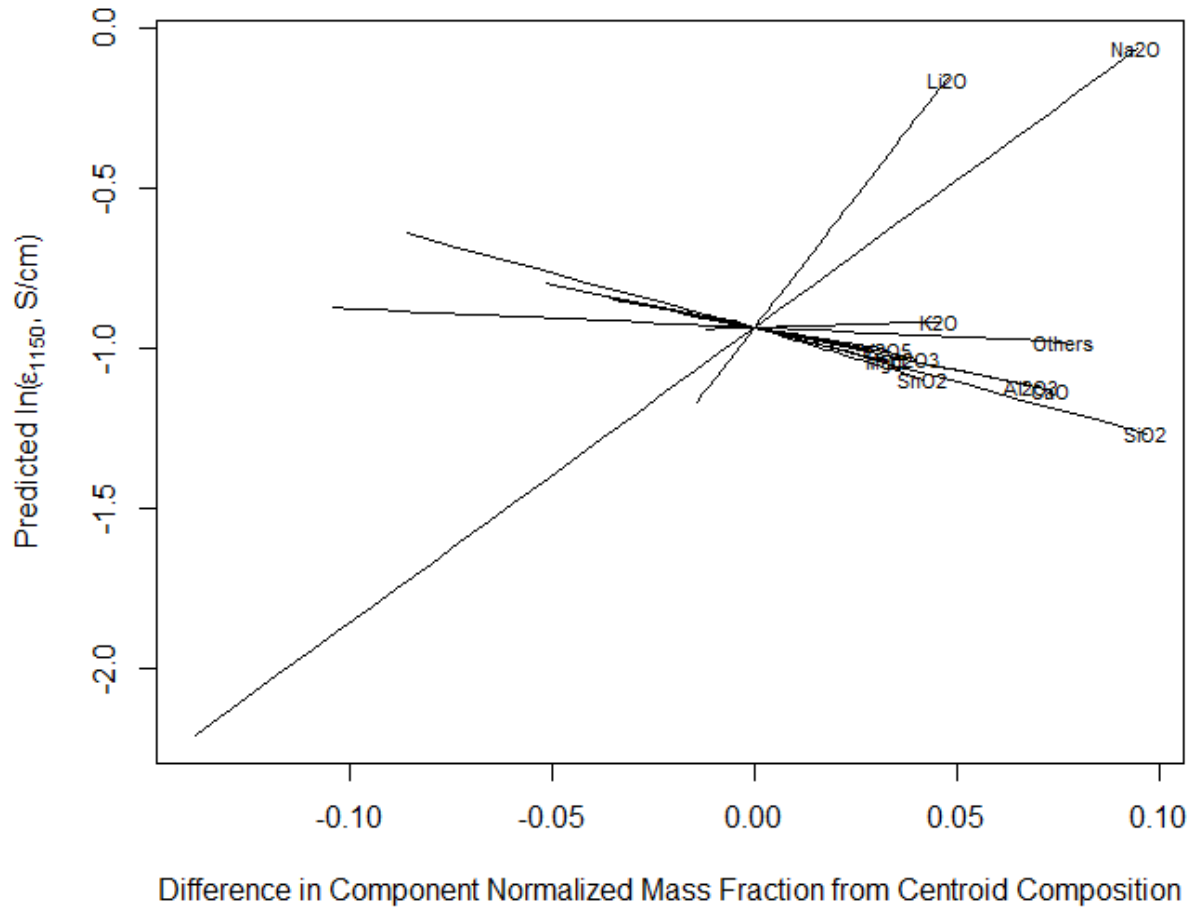


Figure 6.12. Response Trace Plot for 11-Component Reduced Linear Mixture Model on the Natural Logarithm of Electrical Conductivity at 1150 °C for LAW Glasses

6.3.3 Results from a Reduced Partial Quadratic Mixture Model for the Natural Logarithm of Electrical Conductivity at 1150 °C with LAW Glasses

Reduced PQM models (see Section 6.2.1) were investigated in an effort to improve on the 11-component RLM model for $\ln(\epsilon_{1150})$. Previous experience with developing and validating PQM models has indicated that adding too many quadratic terms tends to over-fit the model development dataset and degrade predictive performance for new glasses. Therefore, the components that could form quadratic terms were limited to those with strong linear effects and a glass science basis. So, a process of identifying as few as possible second-order terms while improving model fit statistics was performed as follows:

1. Regressions were performed to fit reduced partial quadratic models involving all possible subsets of 1, 2, 3, or 4 second-order terms.
2. The resulting model summary/performance statistics (R^2 and RMSE values) were then examined to see which second-order terms were most beneficial to model performance and how many second-order terms to include.

3. The RMSE values from the top candidate models were plotted as a function of the number of second-order terms (0 to 4) to identify where the point of diminishing returns was.
4. The reduced PQM model with the number of terms just before the point of diminishing returns was selected as the final reduced PQM model.

The MAXR criterion (see Section B.4.2 of Appendix B) was also attempted as a means of selecting second-order terms. However, the terms selected by that method were not always intuitively obvious and the performance was not substantively better than the chosen approach.

Ultimately, a 13-term PQM model for $\ln(\epsilon_{1150})$ with 11 linear terms and 2 quadratic terms ($\text{Li}_2\text{O} \times \text{Na}_2\text{O}$ and $\text{Na}_2\text{O} \times \text{Na}_2\text{O}$) was selected as including enough quadratic terms to improve the model fit, without over-fitting the model development data. These terms are generally expected based on past viscosity response modeling for LAW glasses that showed second-order terms including Li_2O and Na_2O (Piepel et al. 2007). The first of these terms is associated with the mixed alkali effect. Table 6.5 contains the coefficients of the 13-term PQM model for $\ln(\epsilon_{1150})$ and the coefficient standard deviations. Table 6.5 also includes model performance statistics for the 13-term PQM model using the (i) 526-glass modeling dataset, (ii) data-split modeling data (as a model validation approach), and (iii) six evaluation subsets of modeling glasses discussed in Section 6.1.3 (as a model evaluation approach).

6.3.3.1 Numerical Results for the 13-Term Reduced Partial Quadratic Mixture Model on the Natural Logarithm of Electrical Conductivity at 1150 °C

In Table 6.5, the $\ln(\epsilon_{1150})$ model evaluation statistics $R^2 = 0.8563$, $R^2_A = 0.8529$, $R^2_P = 0.8461$, and $\text{RMSE} = 0.1318$ for the 13-term PQM model are small improvements over the corresponding statistics for the 11-component RLM model in Table 6.4. The small drop in values from R^2_A to R^2_P suggests that the $\ln(\epsilon_{1150})$ modeling dataset does not have any highly influential data points for the 13-term reduced PQM model. In any case, $R^2_P = 0.8461$ provides an estimate of the fraction of variation in $\ln(\epsilon_{1150})$ values for future datasets over the same GCR that might be accounted for by this 13-term reduced PQM model.

The RMSE in Table 6.5 is an estimate of the uncertainty [in $\ln(\text{S/cm})$ units] in fabricating simulated LAW glasses and determining ϵ_{1150} if the 13-term reduced PQM model does not have statistically significant LOF. The $\text{RMSE} = 0.1318$ for the reduced PQM model fitted to the 526-glass modeling dataset is smaller than the corresponding value for the 11-component RLM model ($\text{RMSE} = 0.1444$) in Table 6.4, indicating a better fit to the data by PQM. The RMSE value is also smaller than the pooled replicate SD in $\ln(\text{poise})$ units of 0.2066 in Table 6.2. These observations suggest that the 13-term reduced PQM model for $\ln(\epsilon_{1150})$ does not have model LOF, which is confirmed by the LOF test p-value > 0.9999 in Table 6.5. See Section B.3 of Appendix B for discussion of the statistical test for model LOF.

At the bottom right of Table 6.5, the average model-fit statistics (R^2 , R^2_A , R^2_P , and RMSE) over the five data-splits are close to the statistics obtained from fitting the 13-term reduced PQM model for $\ln(\epsilon_{1150})$ to all 526 glasses in the modeling dataset. The data-split validation statistics (R^2_V and RMSE_V) are also relatively close to the R^2 and RMSE (i) values from fitting the model to the full dataset, and (ii) averages from fitting the model to the data-split modeling subsets. This indicates that the 13-term reduced PQM model maintains its predictive performance for data not used to fit the model.

The statistics from evaluating the predictive performance of the 13-term reduced PQM model for $\ln(\epsilon_{1150})$ on the six evaluation subsets of modeling glasses (see Section 6.1.3) are given on the right side of Table 6.5. Four of the six evaluation subsets (H_2SO_3 , WTP, LP123, and ORP) have R^2_{Eval} statistics ranging from 0.7455 to 0.8497. These values are from notably below to slightly above the R^2 statistic for the whole

modeling dataset (0.8563). The other two evaluation subsets (LP2OL and HiNa₂O) have R^2_{Eval} values of 0.4528 and -0.0013, respectively. The R^2_{Eval} values that are moderately to substantially lower than the R^2 for the whole modeling dataset are because ϵ_{1150} depends very heavily on the mass fractions of Na₂O and Li₂O in a LAW glass composition. Hence, the less variation in mass fractions of Na₂O and Li₂O there is in an evaluation subset, the less dependent $\ln(\epsilon_{1150})$ will be on the mass fractions of other components for glasses in that evaluation subset, which reduces the R^2_{Eval} values.

Table 6.5. Coefficients and Performance Summary for the 13-Term Reduced Partial Quadratic Mixture Model on the Natural Logarithm of Electrical Conductivity at 1150 °C for LAW Glasses

ln(ϵ_{1150}) 13-Term PQM Model Term	Coefficient Estimate	Coefficient Stand. Err.	Modeling Data Statistic, 526 Glasses ^(a)					
Al ₂ O ₃	-4.4821	0.2916	R ²		0.8563			
B ₂ O ₃	-3.7135	0.3355	R ² _A		0.8529			
CaO	-4.2790	0.2349	R ² _P		0.8461			
K ₂ O	-1.4916	0.4351	RMSE		0.1318			
Li ₂ O	34.1609	2.4870	Model LOF p-value		>0.9999			
MgO	-4.5173	0.6444						
Na ₂ O	14.4633	1.5225						
SiO ₂	-3.9157	0.1976						
SnO ₂	-5.3792	0.4898						
V ₂ O ₅	-2.8106	0.5615						
Others ^(c)	-2.4484	0.2665						
Li ₂ O × Na ₂ O	-136.2023	17.1208						
(Na ₂ O) ²	-19.7143	4.3633						
			Evaluation Set					
			# Glasses ^(b)		R ² _{Eval}	RMSE _{Eval}		
			WTP (177)		0.7455	0.1566		
			ORP (267)		0.8497	0.1108		
			LP2OL (93)		0.4528	0.1134		
			LP123 (82)		0.7457	0.1598		
			HiNa ₂ O (191)		-0.0013 ^(d)	0.1203		
			HiSO ₃ (101)		0.6857	0.1262		
Data Splitting Statistic ^(a,e)			DS1	DS2	DS3	DS4	DS5	Average
R ²			0.8425	0.8548	0.8540	0.8477	0.8585	0.8515
R ² _A			0.8380	0.8506	0.8498	0.8434	0.8545	0.8472
R ² _P			0.8283	0.8417	0.8424	0.8345	0.8462	0.8386
RMSE			0.1368	0.1317	0.1306	0.1347	0.1336	0.1335
R ² _V			0.9093	0.8598	0.8581	0.8882	0.8360	0.8703
RMSE _V			0.1082	0.1329	0.1404	0.1196	0.1259	0.1254

- (a) The model evaluation statistics are defined in Section B.3 of Appendix B. The model validation statistics are defined in Section B.5.
- (b) The six sets of LAW evaluation glasses are discussed in Section 2.4 and Section 6.1.3.
- (c) For the 13-term reduced PQM model, the Others component includes any components not separately listed.
- (d) A negative R^2_{Eval} value occurs when the model predicts the property values for glasses in the evaluation set less well than a “constant” model.
- (e) The evaluation and validation statistics calculated for data-splits are defined the same as for separate modeling and validation sets. Section 6.1.2 describes how the modeling dataset was split into modeling and validation subsets.

6.3.3.2 Graphical Results for the 13-Term Reduced Partial Quadratic Mixture Model on the Natural Logarithm of Electrical Conductivity at 1150 °C

Diagnostic plots for the 13-term reduced PQM model (not included in this report) support the assumption of normally distributed errors in the $\ln(\epsilon_{1150})$ data (see Section B.3 of Appendix B). Figure 6.13 displays the standardized residuals for the 13-term reduced PQM model of $\ln(\epsilon_{1150})$ plotted versus the data index (a

sequential numbering of the modeling data points) with different plotting symbols representing the different groups of LAW glasses discussed in Section 2.3. Figure 6.9 yields the following observations:

- The WTP and LP1.OL (PNNL Phase 1 outer layer) datasets have a wider scatter of standardized residuals, indicating a wider range of $\ln(\epsilon_{1150})$ model prediction uncertainty. This is likely a result of the WTP and LP1.OL glasses spanning wider subregions of LAW glass compositions.
- The 13-term reduced PQM model (i) tends to over-predict $\ln(\epsilon_{1150})$ [corresponding to negative standardized residuals] for the LP1.OL and LP2.OL glasses, and (ii) under-predicts $\ln(\epsilon_{1150})$ [corresponding to positive standardized residuals] for the LP3 glasses. The PNNL LP2.OL and LP3 studies were investigated and no reason for biased ϵ_{1150} values was found. The differences in standardized residuals for these two studies may be a result of longer-term random uncertainty.
- Three glasses have standardized residuals near 4 in absolute value. Although outlying, these data points did not have a major impact on the 13-term reduced PQM model for $\ln(\epsilon_{1150})$ and hence were retained in the modeling dataset.

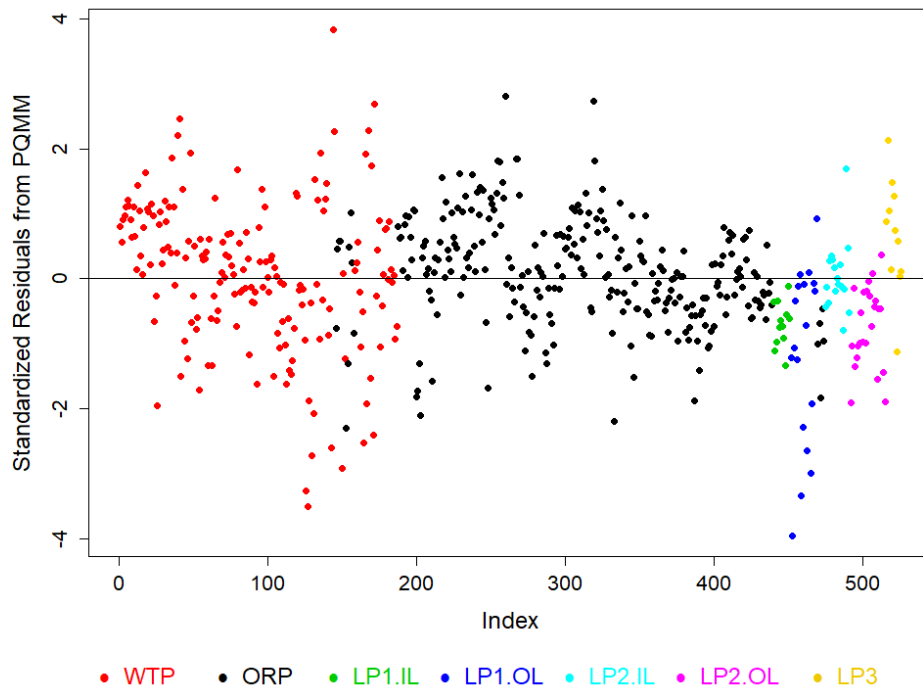


Figure 6.13. Standardized Residuals Plot for the 13-Term Reduced Partial Quadratic Mixture Model on the Natural Logarithm of Electrical Conductivity at 1150 °C for LAW Glasses

Figure 6.14 displays the PvM plot for the 526-glass modeling dataset using the 13-term reduced PQM model on $\ln(\epsilon_{1150})$. The plot illustrates that the 13-term reduced PQM model predicts $\ln(\epsilon_{1150})$ fairly well with notable scatter, but with tendencies to (i) over-predict below $\ln(\epsilon_{1150}) \sim -1.50$ ($\epsilon_{1150} \sim 0.223$ S/cm) and (ii) under-predict above $\ln(\epsilon_{1150}) \sim -0.40$ ($\epsilon_{1150} \sim 0.670$ S/cm). The tendency of this model to over-predict low ϵ_{1150} values is within the WTP LAW Facility operating limits shown by the red lines in Figure 6.14, and this would be the case even after accounting for model prediction uncertainty. However, the tendency to over-predict low ϵ_{1150} values will not cause an issue in operating the WTP LAW Facility. The tendency to underpredict high values above the upper WTP LAW Facility operating limit could result in judging LAW glasses to meet the upper WTP LAW Facility operating limit when they do not. However,

the WTP LAW Facility will be operated so that no adverse effect of high EC will be experienced (although at the potential cost of lower throughput).

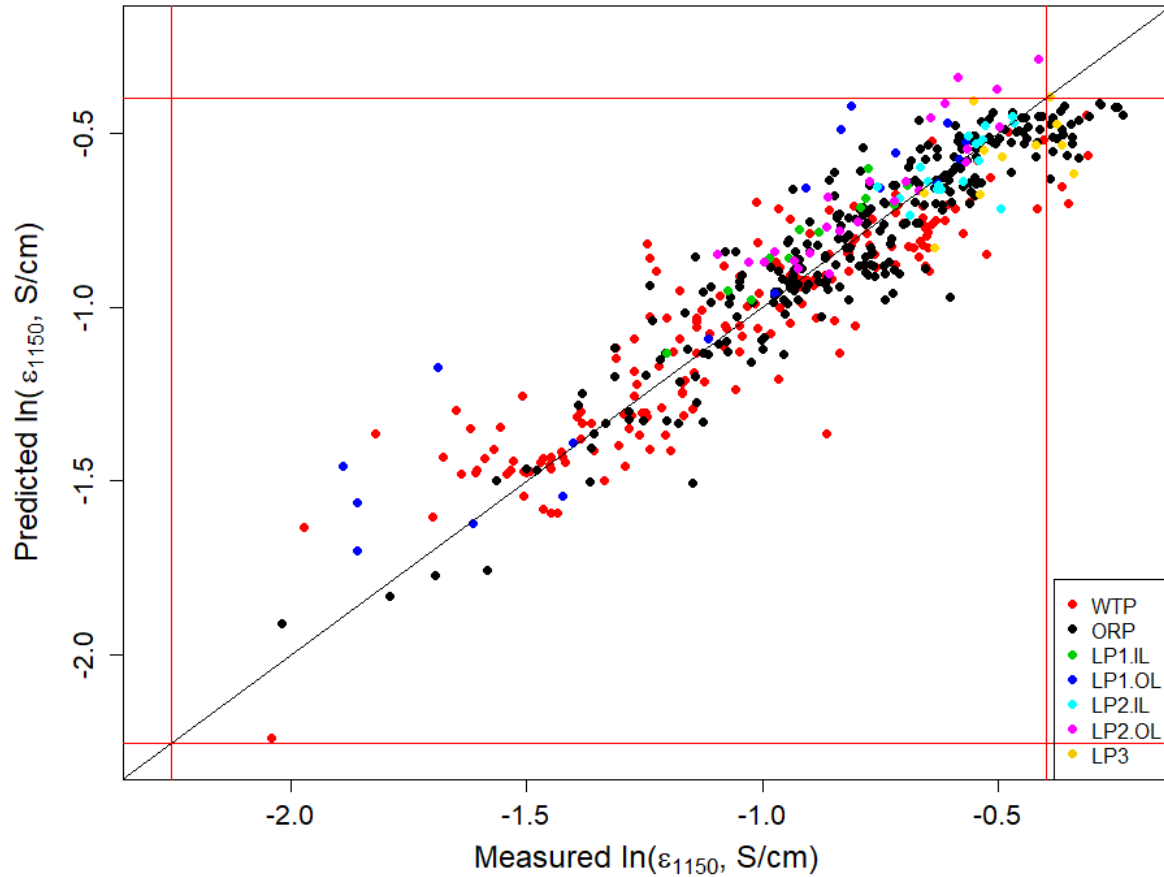


Figure 6.14. Predicted versus Measured Plot for the 526-glass Modeling Dataset Using the 13-term Reduced Partial Quadratic Mixture Model on the Natural Logarithm of Electrical Conductivity at 1150 °C for LAW Glasses. The red lines represent the WTP LAW Facility operating limits for electrical conductivity at 1150 °C (0.105 – 0.671 S/cm).

Figure 6.15 displays PvM plots using the 13-term reduced PQM model for $\ln(\epsilon_{1150})$ in Table 6.5 applied to the six evaluation subsets discussed in Section 6.1.3. Each plot in the figure contains the evaluation R^2 and RMSE values for the corresponding evaluation subset. Figure 6.15 shows that the 13-term RLM model for $\ln(\epsilon_{1150})$ fit to the 526-glass modeling dataset predicts with different amounts of scatter and sometimes ranges of under- or over-prediction in the PvM plots for the six evaluation subsets. In particular, the model predicts with the tightest scatter for the ORP evaluation set, though there is some tendency to under-predict the largest $\ln(\epsilon_{1150})$ values. Figure 6.15 shows that the largest scatter (and thus smallest R^2_{Eval} values) occurs for the HiNa_2O and LP2OL evaluation sets. As noted previously, these evaluation sets contain only high- Na_2O glasses, which reduces the R^2_{Eval} values. The prediction performances for the six evaluation sets using the model that is ultimately recommended are discussed in more detail in Section 6.5.

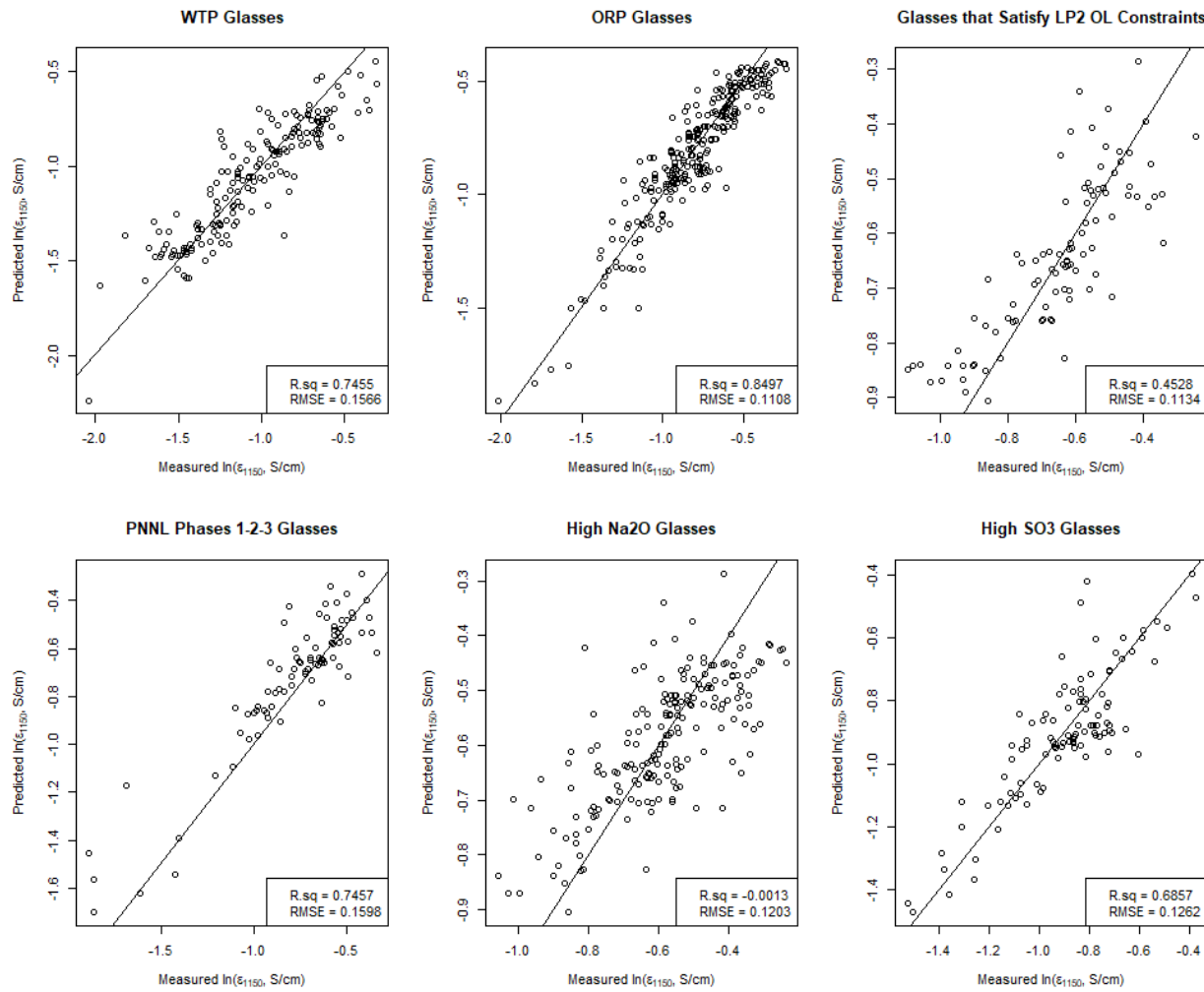


Figure 6.15. Predicted versus Measured Plots for the Six Evaluation Sets Using the 13-Term Reduced Partial Quadratic Mixture Model on the Natural Logarithm of Electrical Conductivity at 1150 °C for LAW Glasses

Figure 6.16 displays the response trace plot (see Section B.4.1 of Appendix B) for the 13-term reduced PQM model for $\ln(\epsilon_{1150})$. The glass composition of the REFMIX (see Section B.4.1) used is listed in Table 2.3. Figure 6.16 shows that Li_2O and Na_2O are predicted to have the strongest effects of any component, with both predicted to increase $\ln(\epsilon_{1150})$. The components SiO_2 , Al_2O_3 , CaO , and SnO_2 are predicted to have much smaller decreasing effects on $\ln(\epsilon_{1150})$. The remaining components (K_2O , Others, V_2O_5 , B_2O_3 , and MgO) have predicted response traces with small to negligible slopes, indicating those components are predicted to have small to negligible effects on $\ln(\epsilon_{1150})$.

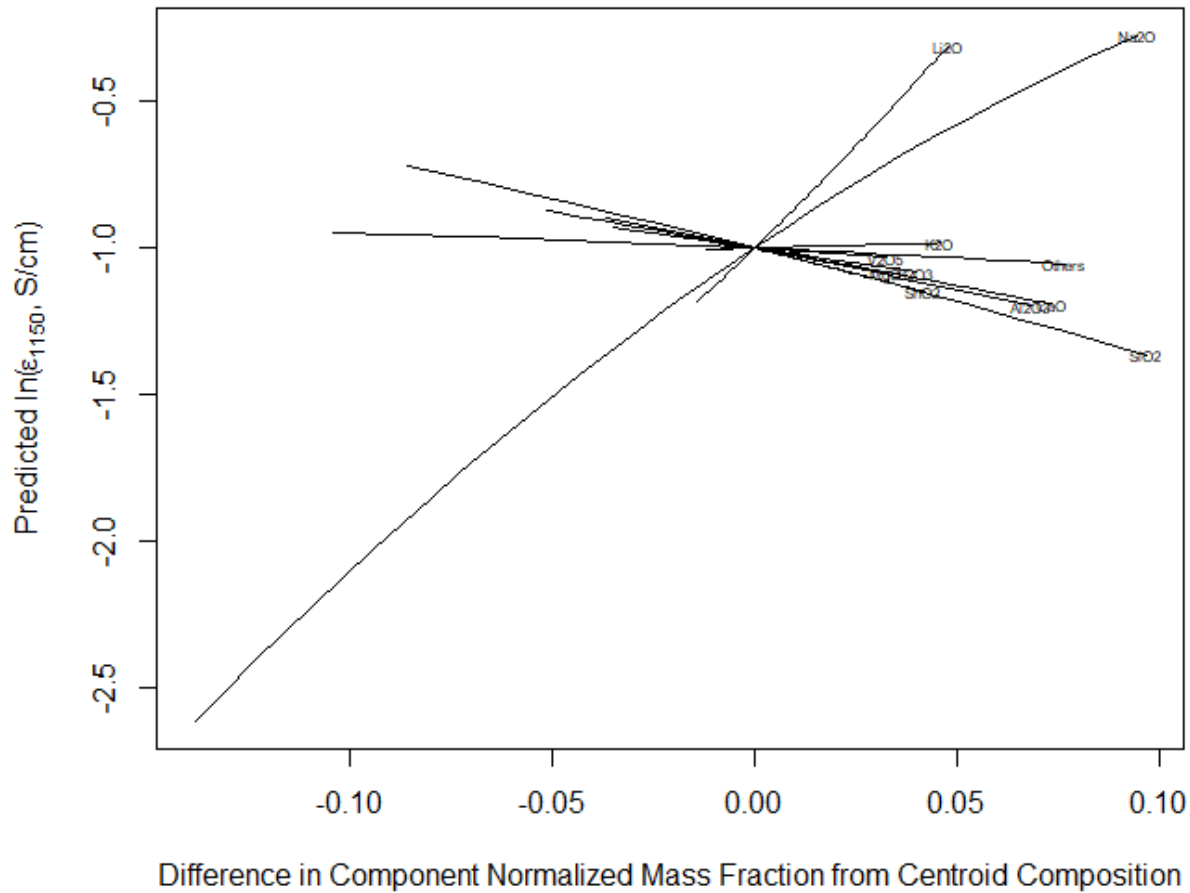


Figure 6.16. Response Trace Plot for 13-Term Reduced Partial Quadratic Mixture Model on the Natural Logarithm of Electrical Conductivity at 1150 °C for LAW Glasses

6.3.4 Recommended Model for the Natural Logarithm of Electrical Conductivity at 1150 °C for LAW Glasses

Table 6.6 summarizes the primary $\ln(\epsilon_{1150})$ model evaluation and validation results for the 20-component FLM model, the 11-component RLM model, and the 13-term reduced PQM model from Table 6.3 to Table 6.5, respectively, as follows:

- Model goodness-of-fit for the $\ln(\epsilon_{1150})$ -composition modeling data of 526 simulated LAW glasses
- Model validation using the data-splitting approach
- Model evaluation for six subsets of the 526-glass modeling dataset

Based on the summarized results in Table 6.6 and discussions in Sections 6.3.1 to 6.3.3, the 13-term reduced PQM model (listed in Table 6.5) is recommended for predicting $\ln(\epsilon_{1150})$ of LAW glasses. As a baseline for comparison, the 11-component RLM model (listed in Table 6.4) will be used.

Table 6.6. Performance Summary of Three Models for the Natural Logarithm of Electrical Conductivity at 1150 °C for LAW Glasses

	ln(ϵ_{1150}) Model					
Summary Statistics from Model Fit to 526 Glasses ^(a)	20-Component FLM Model	11-Component RLM Model	13-Term Reduced PQM Model (Recommended)			
R ²	0.8359	0.8267	0.8563			
R ² _A	0.8298	0.8233	0.8529			
R ² _P	0.8182	0.8159	0.8461			
RMSE	0.1417	0.1444	0.1318			
LOF p-value	>0.9999	0.9999	>0.9999			
Linear Terms	20 (See Table 6.3)	11 (See Table 6.4)	11 (See Table 6.5)			
Selected Quadratic Terms in Model	NA	NA	Li ₂ O × Na ₂ O (Li ₂ O) ²			
# Model Terms	20	11	13			
Summary Statistics for Six Evaluation Subsets of LAW Glasses ^(a)						
Evaluation Set (# Glasses) ^(b)	R ² _{Eval}	RMSE _{Eval}	R ² _{Eval}	RMSE _{Eval}	R ² _{Eval}	RMSE _{Eval}
WTP (177)	0.6876	0.1813	0.6843	0.1755	0.7455	0.1566
ORP (267)	0.8535	0.1073	0.8372	0.1100	0.8497	0.1108
LP2OL (93)	0.3498	0.1361	0.4420	0.1185	0.4528	0.1134
LP123 (82)	0.6881	0.1866	0.6096	0.1887	0.7457	0.1598
HiNa ₂ O (191)	0.1924	0.1259	0.0798	0.1243	-0.0013 ^(c)	0.1203
HiSO ₃ (101)	0.6768	0.1440	0.6737	0.1416	0.6857	0.1262
Validation Summary Statistics Averaged Over 5 Data-Splitting Sets ^(a)						
R ²	0.8326		0.8230		0.8515	
R ² _A	0.8249		0.8188		0.8472	
R ² _P	0.8102		0.8095		0.8386	
RMSE	0.1429		0.1454		0.1335	
R ² _V	0.8377		0.8343		0.8703	
RMSE _V	0.1398		0.1417		0.1254	

(a) The model evaluation statistics are defined in Section B.3 of Appendix B.

(b) Model validation statistics are defined in Section B.5 of Appendix B.

(c) A negative R^2_{Eval} value occurs when the model predicts the property values for glasses in the evaluation set less well than a “constant” model.

6.4 Example Illustrating Model Predictions and Statistical Intervals for Electrical Conductivity at 1150 °C

This section contains examples that illustrate the application of the recommended 13-term PQM model for $\ln(\epsilon_{1150})$ in Table 6.5 to the REFMIX glass composition listed in Table 2.3 to obtain predicted ϵ_{1150} values and two-sided statistical intervals. Formulas for two-sided 90% CIs and two-sided 90% PIs are discussed in Section B.6 of Appendix B. Two-sided intervals are illustrated because ϵ_{1150} will have lower and upper operating limits during the WTP LAW Facility operation. For comparison purposes, the same results are presented for the 11-component RLM model in Table 6.4 (although it was not a recommended model). The 90% CIs and 90% PIs were chosen for illustration purposes only. The WTP LAW Facility

can use an appropriate confidence level depending on the use of the $\ln(\epsilon_{1150})$ -composition model and the type of statistical interval (uncertainty expression) desired.

The glass composition used in this example is denoted REFMIX, as listed in Table 2.3. The 20-component composition (mass fractions) of REFMIX for ϵ_{1150} modeling is given in Table 6.7. To apply the 13-term reduced PQM and 11-component RLM models for $\ln(\epsilon_{1150})$ to the REFMIX composition, the mass fractions of the 20 components must be converted to mass fractions (that sum to 1.0) of the 11 LAW glass components contained in both models. This involves adding the mass fractions of the 9 of 20 components not contained in the RLM and reduced PQM $\ln(\epsilon_{1150})$ models to the mass fraction of Others (one of the original 20 components) to obtain a new Others component (one of the reduced sets of 11 components). Mass fractions of the relevant components are then multiplied to obtain the two quadratic terms of the 13-term PQM model. Table 6.7 contains the composition of REFMIX prepared for use in the two $\ln(\epsilon_{1150})$ models for LAW glasses.

For each of the two $\ln(\epsilon_{1150})$ models, predicted $\ln(\epsilon_{1150}, \text{S/cm})$ values are obtained by multiplying the composition in the format needed for that model by the coefficients for that model, then summing the results. That is, the predicted values are calculated by

$$\hat{y}(\mathbf{g}) = \mathbf{g}^T \mathbf{b} \quad (6.4)$$

where \mathbf{g} is the composition of REFMIX formatted to match the terms in a given model (from Table 6.7), the superscript T represents a matrix transpose (or vector transpose in this case), and \mathbf{b} is the vector of coefficients for a given model. The predicted $\ln(\epsilon_{1150})$ values for REFMIX using the two $\ln(\epsilon_{1150})$ models are listed in the second column of Table 6.8. The predicted $\ln(\epsilon_{1150})$ values in $\ln(\text{S/cm})$ units are easily converted to ϵ_{1150} values (S/cm) by exponentiation. The third column of Table 6.8 contains the predicted ϵ_{1150} values (S/cm). When used with CIs, as discussed in Section B.6 of Appendix B, these back-transformed ϵ_{1150} values in S/cm should be considered estimates of the true median (not the true mean) of the distribution of ϵ_{1150} values that would result if EC measurements at 1150 °C were repeated multiple times on separately batched and melted samples of the REFMIX glass composition. When used with PIs, the back-transformed ϵ_{1150} predictions should be considered estimates of individual test results for the REFMIX glass composition.

The predicted ϵ_{1150} values for REFMIX in Table 6.8 are 0.392 S/cm for the 11-component RLM model and 0.367 S/cm for the recommended 13-term PQM model. Statistical confidence intervals and prediction intervals for these predictions are discussed next.

Table 6.7. REFMIX Composition in Formats Used with Models of Natural Logarithm of Electrical Conductivity at 1150 °C for LAW Glasses

Model Term	REFMIX Composition ^(a) (mass fractions)	REFMIX Composition (mass fractions) to Use in 11-Component RLM Model for $\ln(\epsilon_{1150})$ ^(b)	REFMIX Composition (mass fractions) to Use in 13-Term PQM Model for $\ln(\epsilon_{1150})$ ^(c)
Al ₂ O ₃	0.075760	0.075761	0.075761
B ₂ O ₃	0.097257	0.097257	0.097257
CaO	0.052514	0.052514	0.052514
Cl	0.003376	NA	NA
Cr ₂ O ₃	0.002041	NA	NA
F	0.001348	NA	NA
Fe ₂ O ₃	0.029727	NA	NA
K ₂ O	0.012064	0.012064	0.012064
Li ₂ O	0.014802	0.014802	0.014802
MgO	0.016989	0.016989	0.016989
Na ₂ O	0.168395	0.168395	0.168395
P ₂ O ₅	0.003239	NA	NA
SO ₃	0.005542	NA	NA
SiO ₂	0.424565	0.424565	0.424565
SnO ₂	0.007587	0.007587	0.007587
TiO ₂	0.008034	NA	NA
V ₂ O ₅	0.007499	0.007499	0.007499
ZnO	0.031997	NA	NA
ZrO ₂	0.036219	NA	NA
Others	0.001045	0.122568	0.122568
Li ₂ O×Na ₂ O	NA	NA	0.00249258
(Na ₂ O) ²	NA	NA	0.02835688

(a) The composition in mass fractions is from Table 2.3.

(b) See Table 6.4

(c) See Table 6.5

(d) NA = not applicable, because the model does not contain this term.

Table 6.8. Predicted Electrical Conductivity at 1150 °C, Standard Deviation, and Statistical Intervals for the REFMIX Composition Used in Two Models for Electrical Conductivity at 1150 °C

Model for $\ln(\widehat{\epsilon}_{1150})^{(a)}$	Predicted $\ln(\widehat{\epsilon}_{1150})$ [ln(S/cm)]	Predicted $\widehat{\epsilon}_{1150}$ [S/cm]	Standard Deviation of Predicted $\ln(\widehat{\epsilon}_{1150})^{(b)}$ [ln(S/cm)]	90% CI ^(c) on Mean $\ln(\widehat{\epsilon}_{1150})$ [ln(S/cm)]	90% CI ^(c) on Median $\widehat{\epsilon}_{1150}$ [S/cm]	90% PI ^(c) on Individual $\ln(\widehat{\epsilon}_{1150})$ [ln(S/cm)]	90% PI ^(c) on Individual $\widehat{\epsilon}_{1150}$ [S/cm]
13-Term PQM Model	-1.0019 ^(d)	0.367 ^(d)	0.00958	(-1.0177, -0.9861)	(0.361, 0.373)	(-1.2196, -0.7843)	(0.295, 0.456)
11-Comp. RLM Model	-0.9368	0.392	0.00657	(-0.9476, -0.9260)	(0.388, 0.396)	(-1.1750, -0.6986)	(0.309, 0.497)

(a) The two $\ln(\epsilon_{1150})$ models in this column are given in Table 6.5 (13-term PQM model) and Table 6.4 (11-component RLM model), respectively.

(b) The standard deviation is for the $\ln(\epsilon_{1150})$ prediction considered to be the mean from many such results for the REFMIX glass.

(c) CI = two-sided confidence interval, PI = two-sided prediction interval (see Section B.6 of Appendix B).

(d) All calculations were performed using the REFMIX glass composition, model coefficients, and variance-covariance matrix values given in tables of this report. The calculated ln(S/cm) values were rounded to four decimal places in this table. The S/cm values were calculated by exponentiating the ln(S/cm) values before rounding, then rounding the resulting values to three decimal places in this table.

Eq. (B.21a) in Appendix B can be used to calculate a two-sided 90% CI for the true mean of $\ln(\epsilon_{1150})$ values for the REFMIX glass composition with each of the $\ln(\epsilon_{1150})$ models. Similarly, Eq. (B.22a) can be used to calculate a two-sided 90% PI for an individual test value of $\ln(\epsilon_{1150})$ for the REFMIX glass composition with each of the $\ln(\epsilon_{1150})$ models. In the notation of these equations:

- $100(1-\alpha)\% = 90\%$, so that $\alpha = 0.10$ for a 90% CI in Eq. (B.21a) and a 90% PI in Eq. (B.22a).
- The vector \mathbf{g} contains entries corresponding to the terms in a given $\ln(\epsilon_{1150})$ model, which are calculated using the composition of REFMIX in Table 6.7.
- Matrix \mathbf{G} is formed from the data matrix used in the regression that generated a given $\ln(\epsilon_{1150})$ model. Matrix \mathbf{G} has the number of rows in the ϵ_{1150} modeling dataset (526 glasses) and the number of columns corresponding to the number of terms in a given $\ln(\epsilon_{1150})$ model. Each column is calculated according to the corresponding term in the model using the LAW normalized glass composition in the ϵ_{1150} modeling dataset.

To calculate a two-sided $100(1-\alpha)\%$ CI, the quantity margin-of-error $t_{1-\frac{\alpha}{2}, n-p} \sqrt{MSE_{OLS} \mathbf{g}^T (\mathbf{G}^T \mathbf{G})^{-1} \mathbf{g}}$ is subtracted from and added to the predicted $\ln(\epsilon_{1150})$ [denoted $\hat{y}(\mathbf{g})$] described above, as indicated by Eq. (B.21a). To calculate a two-sided $100(1-\alpha)\%$ PI, the quantity $t_{1-\frac{\alpha}{2}, n-p} \sqrt{MSE_{OLS} \mathbf{g}^T (\mathbf{G}^T \mathbf{G})^{-1} \mathbf{g}}$ is subtracted from and added to the predicted $\ln(\epsilon_{1150})$ [denoted $\hat{y}(\mathbf{g})$], as indicated by Eq. (B.22a). The $MSE_{OLS} (\mathbf{G}^T \mathbf{G})^{-1}$ portion of these expressions is an estimate of the variance-covariance matrix for the estimated model coefficients, as discussed near the end of Section B.6 of Appendix B. For the example calculations presented in Table 6.8, the Students- t statistic value needed for both the CI and PI formulas describing the 11-component RLM model is 1.647818. This is based on $n=526$ and $p=11$. The following cell formula can be used to obtain the t -statistic value with Excel: =T.INV(0.95,526-11). For the CI and PI calculations associated with the 13-term PQM model described in Table 6.8, the Students- t statistic is 1.647829=T.INV(0.95,526-13). The variance-covariance matrices for the 11-component RLM model and the recommended 13-term PQM model are respectively listed in Tables D.10 and D.11 of Appendix D. The quantity $\sqrt{MSE_{OLS} \mathbf{g}^T (\mathbf{G}^T \mathbf{G})^{-1} \mathbf{g}}$ is the standard deviation of a model prediction (for a given composition vector \mathbf{g} expressed in a given model form); the value for each model is given in the fourth column of Table 6.8.

The 90% CIs and 90% PIs for the true mean and individual test result, respectively, of $\ln(\epsilon_{1150})$ in units of $\ln(\text{S/cm})$ for the REFMIX composition based on the two $\ln(\epsilon_{1150})$ models are given in the fifth and seventh columns of Table 6.8. Exponentiating the resulting 90% CIs for the mean $\ln(\epsilon_{1150})$ values in $\ln(\text{S/cm})$ units yields 90% CIs for the median ϵ_{1150} (S/cm). These values are in the sixth column of Table 6.8. Exponentiating the 90% PIs for individual $\ln(\epsilon_{1150})$ test results in $\ln(\text{S/cm})$ units yields 90% PIs on individual ϵ_{1150} test results (S/cm) for REFMIX. These values are in the seventh column of Table 6.8.

6.5 Suitability of the Recommended Electrical Conductivity at 1150 °C Model for Application by the WTP LAW Facility

The 13-term PQM model for $\ln(\epsilon_{1150})$ discussed in Section 6.3.3 is recommended for use by the WTP LAW Facility as the best model currently available for predicting ϵ_{1150} for LAW glasses. This model yields mostly unbiased predictions of ϵ_{1150} over the WTP LAW Facility operating limits (0.105 to 0.671 S/cm) of ϵ_{1150} values, both for the whole modeling dataset (see Figure 6.14) and for various subsets of the data, including subsets of glasses with high waste loadings (see Figure 6.15). These figures show some tendencies to under-predict the highest ϵ_{1150} values for some LAW glass compositions, but this often occurs beyond the upper limit of the operating range for the WTP LAW Facility. There are also

tendencies to over-predict the lowest ϵ_{1150} values, which had limited data for model development. The WTP LAW Facility is not expected to formulate LAW glass compositions with such low ϵ_{1150} values, so one option is to set a larger lower limit for the operating range of ϵ_{1150} .

The recommended 13-term PQM model does not have a statistically significant LOF. Hence, a ϵ_{1150} prediction should be within the uncertainty of what would be obtained by batching and melting a LAW glass, measuring EC at several temperatures for the LAW glass, and determining the estimated value of ϵ_{1150} for the LAW glass (as discussed in Section 2.3).

The magnitudes of uncertainties in ϵ_{1150} model predictions are moderate in size but should not unduly restrict the formulation and processing of LAW glasses in the WTP LAW Facility. Figure 6.17 displays the $\ln(\epsilon_{1150})$ prediction standard deviations versus predicted values [both in $\ln(\text{S/cm})$ units] for the LAW glass compositions in the ϵ_{1150} modeling dataset. The $\ln(\epsilon_{1150})$ prediction standard deviations for the ϵ_{1150} modeling dataset of 526 LAW glasses range from approximately 0.01 to 0.05 $\ln(\text{S/cm})$ for the recommended 13-term PQM model. Note that prediction standard deviations will be larger for LAW glass compositions as their distance from glasses in the ϵ_{1150} modeling dataset increases. Also, the total uncertainty in predictions with the recommended 13-term PQM model will depend on the type of statistical interval used (see Section B.6 of Appendix B).

Work to assess the impact of LAW glass composition and model uncertainties for the recommended $\ln(\epsilon_{1150})$ model (Sections 6.3.3 and 6.3.4) on satisfying the WTP LAW Facility's processing requirements for LAW glasses must be addressed in the future. The impacts of these uncertainties on glass formulation and processability are planned to be addressed as part of the second iteration of the LAW GFA development work. The first iteration of that work (Kim and Vienna 2012) used an EC model from Piepel et al. (2007). A more recent evaluation, performed by Gervasio et al. (2018), used a preliminary EC model from Vienna et al. (2016).

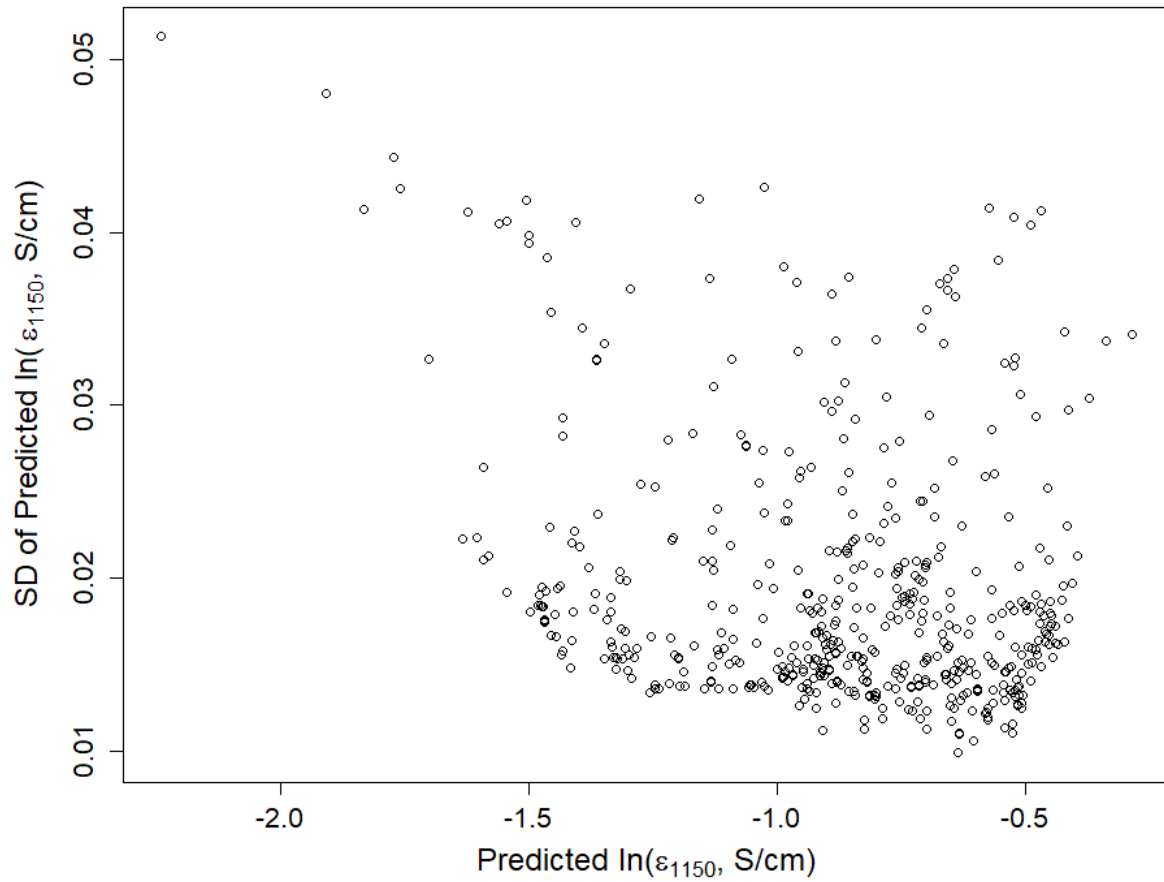


Figure 6.17. Prediction Standard Deviations versus Predicted Values over the LAW Glass Compositions in the 518-Glass Modeling Dataset for the Recommended 13-Term PQM Model for the Natural Logarithm of Electrical Conductivity at 1150 °C

The range of single component concentrations in the 526-glass dataset used for modeling is listed in Table 6.9 and discussed in Section 9.7. These ranges can be used to determine model validity ranges.

Table 6.9. Data Component Concentration Ranges (mass fraction) for LAW Glasses Used in Final Electrical Conductivity Models

Component	20-component		13-component	
	Min	Max	Min	Max
Al ₂ O ₃	0.034972	0.147521	0.034972	0.147521
B ₂ O ₃	0.059952	0.138294	0.059952	0.138294
CaO	0.000000	0.127789	0.000000	0.127789
Cl	0.000000	0.011722	NA ^(a)	NA
Cr ₂ O ₃	0.000000	0.006303	NA	NA
F	0.000000	0.007197	NA	NA
Fe ₂ O ₃	0.000000	0.119838	NA	NA
K ₂ O	0.000000	0.059085	0.000000	0.059085
Li ₂ O	0.000000	0.063294	0.000000	0.063294
MgO	0.000000	0.050222	0.000000	0.050222
Na ₂ O	0.024707	0.265729	0.024707	0.265729
P ₂ O ₅	0.000000	0.040256	NA	NA
SO ₃	0.000360	0.016290	NA	NA
SiO ₂	0.335164	0.522624	0.335164	0.522624
SnO ₂	0.000000	0.050299	0.000000	0.050299
TiO ₂	0.000000	0.050058	NA	NA
V ₂ O ₅	0.000000	0.040885	0.000000	0.040885
ZnO	0.009992	0.058152	NA	NA
ZrO ₂	0.000000	0.067534	NA	NA
Others ^(b)	0.000000	0.003296	0.015168	0.203562

(a) NA = not applicable or component not included as term.
(b) Note: Others for the 13-components are composed of all the NA components as well as Others for the 20 components.

7.0 Models Relating Melter SO₃ Tolerance at 1150 °C to LAW Glass Composition

This section documents the development, evaluation, and validation of LAW glass property-composition models and corresponding expressions of uncertainty for predicting melter SO₃ tolerance modeled as a function of LAW glass composition. The property-composition models and corresponding expressions of uncertainty for melter SO₃ tolerance presented in this section were developed, evaluated, and validated using compositions and melter SO₃ tolerance and solubility values for simulated LAW glasses.

Section 7.1 discusses the LAW glasses available and used for melter SO₃ tolerance model development, evaluation, and validation. Section 7.2 presents the models for melter SO₃ tolerance that were investigated. Section 7.3 summarizes the results for the selected linear and quadratic mixture model forms for melter SO₃ tolerance and identifies the recommended model. Section 7.4 illustrates the calculation of melter SO₃ tolerance predictions and the uncertainties in those predictions using selected melter SO₃ tolerance models and corresponding uncertainty equations. Section 7.5 discusses the suitability of the recommended melter SO₃ tolerance model for use by the WTP LAW Facility. Appendix B discusses the statistical methods and summary statistics used to develop, evaluate, and validate the several melter SO₃ tolerance model forms investigated, as well as statistical models/equations used for quantifying the uncertainties in melter SO₃ tolerance model predictions.

7.1 Melter SO₃ Tolerance and Solubility at 1150 °C Data Used for Melter SO₃ Tolerance Model Development, Evaluation, and Validation

The data available and used for developing melter SO₃ tolerance models as functions of LAW glass composition are discussed in Section 7.1.1. The approaches and data used for evaluating and validating the models are discussed in Sections 7.1.2 and 7.1.3.

7.1.1 Model Development Data for Melter SO₃ Tolerance at 1150 °C

The data available for developing melter SO₃ tolerance-composition models consist of composition and melter SO₃ tolerance and solubility values from 601 LAW glasses (see Table 2.2). Note that some glasses have more than one measurement by different methods and there are 660 melter SO₃ tolerance and solubility measurements that are accounted for by the 601 LAW glasses in the table. These glasses and their normalized compositions based on measured (or estimated) SO₃ values are discussed in Section 2.0. The corresponding melter SO₃ tolerance and SO₃ solubility values are presented in Table A.3 of Appendix A.

As shown in Table 2.2 and Table A.3, four different methods – batch saturation (BS), saturation re-melting (SR), bubbling (Bub), and three-time saturation (3TS) – were used to measure crucible-scale SO₃ solubility in glass. Because the SO₃ solubility in glass is one of the two major factors that determine the melter SO₃ tolerance of a specific glass (SO₃ solubility – thermodynamic equilibrium; and dissolution rate – kinetics), a reasonable proportionality between melter SO₃ tolerance and SO₃ solubility is expected. When the amount of sulfate salts added to the glass is beyond what the glass can hold (the glass saturation point), so that sulfate salts form on the glass, this is considered the melter tolerance point. Therefore, melter tolerance can be measured by determining how much sulfate can be contained within the glass.

However, the extent of SO₃ saturation in a final glass depends on the SO₃ solubility measurement method/technique employed.

There is a very minor difference between BS and SR methods: Excess sulfate is added to the glass raw materials in BS method, while it is added to a pre-melted glass in SR method. This minor difference is not expected to affect the saturated SO₃ concentration in a final glass. Vienna et al. (2014) found a reasonable match between the melter SO₃ tolerance and solubility by the Bub method; however, it was shown that a constant offset is needed between the melter SO₃ tolerance and solubility by BS or SR method. Jin et al. (2019) argued that the reason for this offset is because the BS or SR method that applies only one time melting with excess sulfate does not fully saturate the glass. The Bub method can fully saturate the glass, but it requires significantly more experimental time and effort. Recently, Jin et al. (2019) developed a simple and inexpensive 3TS method that uses three-time re-melting of glass mixed with excess sulfate to ensure near equilibrium saturation of SO₃. Although both the Bub and 3TS methods are designed to fully saturate the glass, they involve different loss or addition of other glass components during SO₃ saturation process, which makes it necessary to use an offset between them and increases the uncertainties of SO₃ solubility data (Skidmore et al. 2019).

7.1.1.1 Assessment of Available Glasses with Data for Melter SO₃ Tolerance and Solubility at 1150 °C

The database of 601 glasses with melter SO₃ tolerance and solubility results contains statistically designed as well as actively designed LAW glasses. Some actively designed glasses are outside the composition region covered by the majority of the LAW glass compositions. Such glasses are not ideal for inclusion in a modeling dataset because they can be influential when fitting models to data. Hence, it was decided to (i) graphically assess the 601 available LAW glass compositions with melter SO₃ tolerance and solubility values and (ii) remove from the modeling dataset any compositions considered to be outlying or non-representative of LAW glasses of interest for the WTP LAW Facility. Reasons for excluding glasses are reported in Table 7.1.

Figure 7.1 displays plots of the mass fractions for 19 “main components” plus the Others component (defined as the sum of all remaining components) in the 601 LAW glasses with melter SO₃ tolerance and solubility data. These 20 components (including Others) have sufficient ranges and distributions of mass fraction values to support separate model terms if so desired. Figure 7.2 displays similar plots for the remaining “minor components.” On each plot in Figure 7.1 and Figure 7.2, the x-axis represents the mass fraction values of a LAW glass component. The y-axis shows an index value representing each LAW glass composition, which aids in spreading out the data points to avoid over-plotting. The plotting symbols in Figure 7.1 and Figure 7.2 correspond to the seven groups of LAW glasses discussed in Section 2.3. For comparison purposes, the vertical lines in Figure 7.1 and Figure 7.3 represent the ranges over which the LAW glass components were varied in the PNNL (i) LAW Phase 1 outer-layer study (blue lines), (ii) LAW Phase 2 outer-layer study (pink lines), and (iii) LAW Phase 3 study (pink lines), as shown in Table 2.1. LAW Phases 2 and 3 focused on glasses with high Na₂O waste loadings, whereas Phase 1 explored a larger GCR with higher waste loadings.

Figure 7.1 shows several of the 601 LAW glasses have “main components” with outlying mass fraction values compared to the remaining glasses and to the component ranges in the PNNL LAW Phase 1, Phase 2, and Phase 3 studies (e.g., Cr₂O₃). Figure 7.2 shows what appear to be outliers for some “minor components,” but the values and ranges of those components are small and hence the glass compositions were not considered to be outliers (e.g., PbO). Table 7.1 lists the 25 LAW glasses excluded from the melter SO₃ tolerance and SO₃ solubility modeling dataset and the reason each glass was excluded.

Figure 7.3 and Figure 7.4 (corresponding to Figure 7.1 and Figure 7.2, respectively) show plots of component distributions after the 25 outlying glasses were removed from the melter SO_3 tolerance and solubility dataset containing 601 LAW glasses. Figure 7.3 shows that for the remaining 576 LAW glasses, all 19 LAW glass “main components” have sufficient ranges and distributions of values within those ranges to support terms for modeling melter SO_3 tolerance. Figure 7.4 confirms that none of the “minor components” have sufficient ranges and distributions of values within their ranges to support model terms for those components. Based on Figure 7.3 and Figure 7.4, it was decided to use 19 components for initial melter SO_3 tolerance modeling work (measured SO_3 was removed). These components were Al_2O_3 , B_2O_3 , CaO , Cl , Cr_2O_3 , F , Fe_2O_3 , K_2O , Li_2O , MgO , Na_2O , P_2O_5 , SiO_2 , SnO_2 , TiO_2 , V_2O_5 , ZnO , ZrO_2 , and Others (the sum of all remaining components except SO_3) and were the same as those used for initial modeling of all other properties (except for melter SO_3 tolerance normalized out measured SO_3).

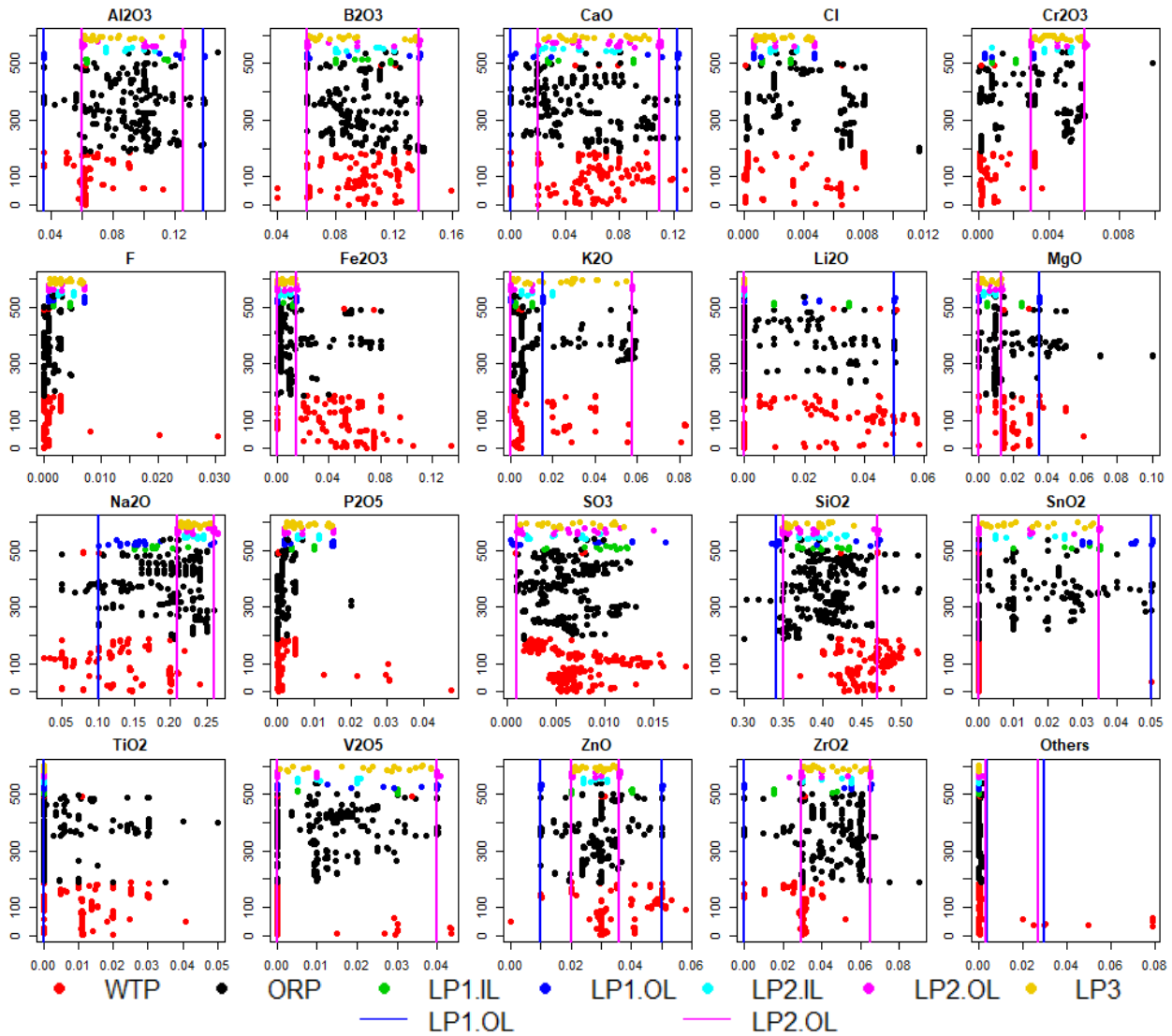


Figure 7.1. Distributions of 20 Main Components (in mass fractions) for 601 LAW Glass Compositions with Melter SO₃ Tolerance and Solubility Measurements at 1150 °C. The vertical lines (when present) represent the lower and upper limits for each component from the PNNL LAW Phase 1 outer-layer study (blue lines), LAW Phase 2 outer-layer study (pink lines), and LAW Phase 3 study (pink lines), as shown in Table 2.1. In cases where two limits are the same, blue lines over plot the pink lines.

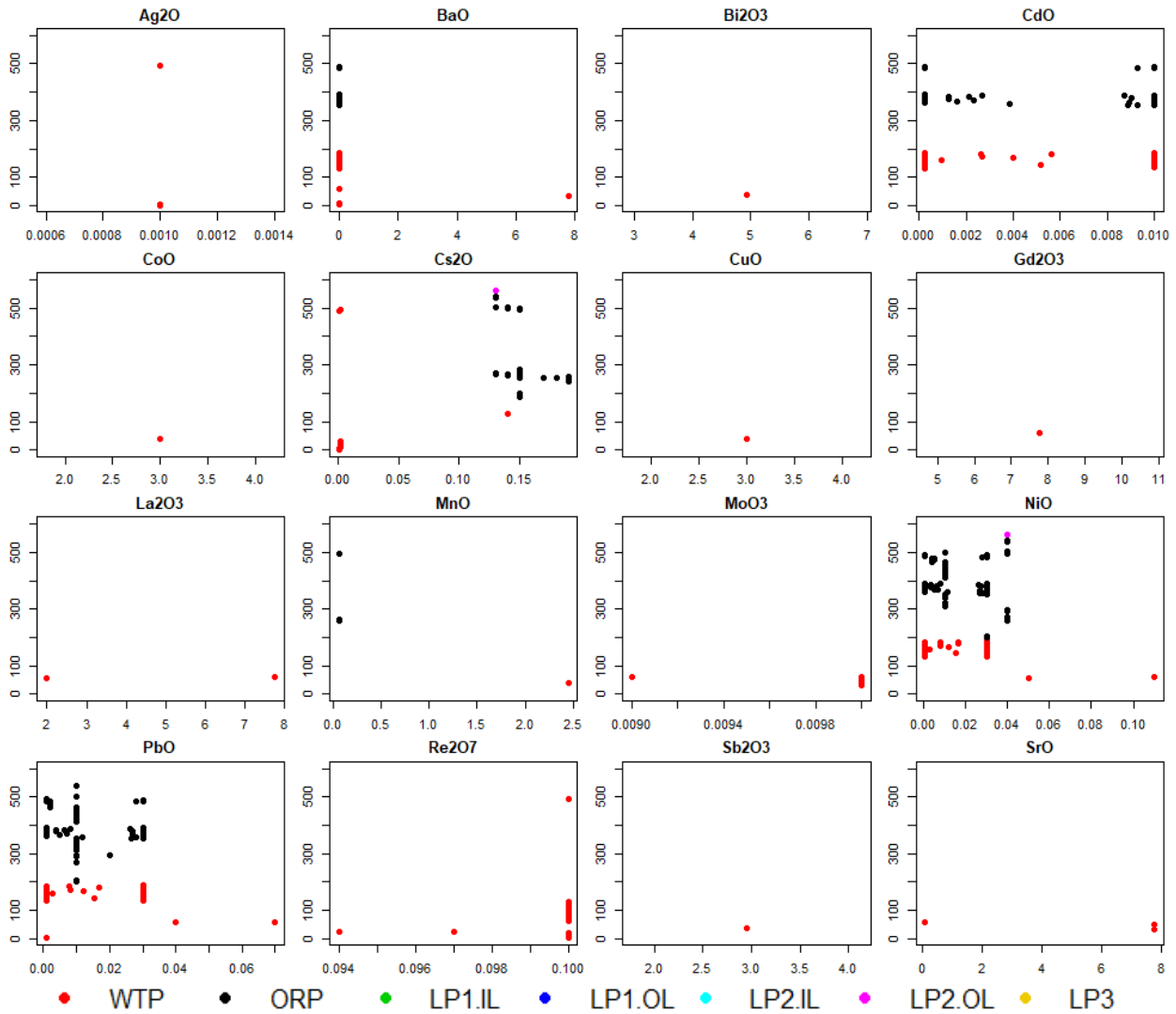


Figure 7.2. Distributions of 16 Minor Components (in mass fractions) for the 601 LAW Glasses with Melter SO₃ Tolerance and Solubility Values at 1150 °C.

Table 7.1. Twenty-five LAW Glasses Excluded from the Modeling Dataset for Melter SO₃ Tolerance and Solubility at 1150 °C

Glass #	Glass ID	Reason Glass Excluded from Melter SO ₃ Tolerance and Solubility Modeling Datasets ^(a)
81	LAWC25S	K ₂ O > 0.07 (= 0.080670) mf
90	LAWA54	Others > 0.019 (0.078579) mf
91	LAWA55	Others > 0.019 (0.078630) mf
94	LAWA58	Others > 0.019 (0.049942) mf
95	LAWA59	Others > 0.019 (0.029906) mf
96	LAWA61	Others > 0.019 (0.024981) mf
97	LAWA62	Others > 0.019 (0.030415) mf
98	LAWA63	Others > 0.019 (0.030430) mf
99	LAWA65	MgO > 0.06 (0.060380) mf
106	LAWA72	Others > 0.019 (0.078721) mf
115	LAWABPS	Others > 0.019 (0.019928) mf
118	LAWA91	Others > 0.019 (0.078713) mf
119	LAWA92	Others > 0.019 (0.078709) mf
167	LAWA120S1	K ₂ O > 0.07 (0.082850) mf
168	LAWA120S2	K ₂ O > 0.07 (0.082775) mf
169	LAWA121S1	K ₂ O > 0.07 (0.082841) mf
170	LAWA121S2	K ₂ O > 0.07 (0.082742) mf
739	ORPLA28	MgO > 0.06 (0.070146) mf
740	ORPLA29	MgO > 0.06 (0.100218) mf
742	ORPLA31	MgO > 0.06 (0.070146) mf
743	ORPLA32	MgO > 0.06 (0.100218) mf
727	ORPLG9CrS4	Cr ₂ O ₃ > 0.008 (0.009864) mf
100	LAWA66	Identified as outlier in preliminary modeling work
197	LAWB67S4	Identified as outlier in preliminary modeling work
959	New-OL-14844	Identified as outlier in preliminary modeling work

(a) mf = mass fraction

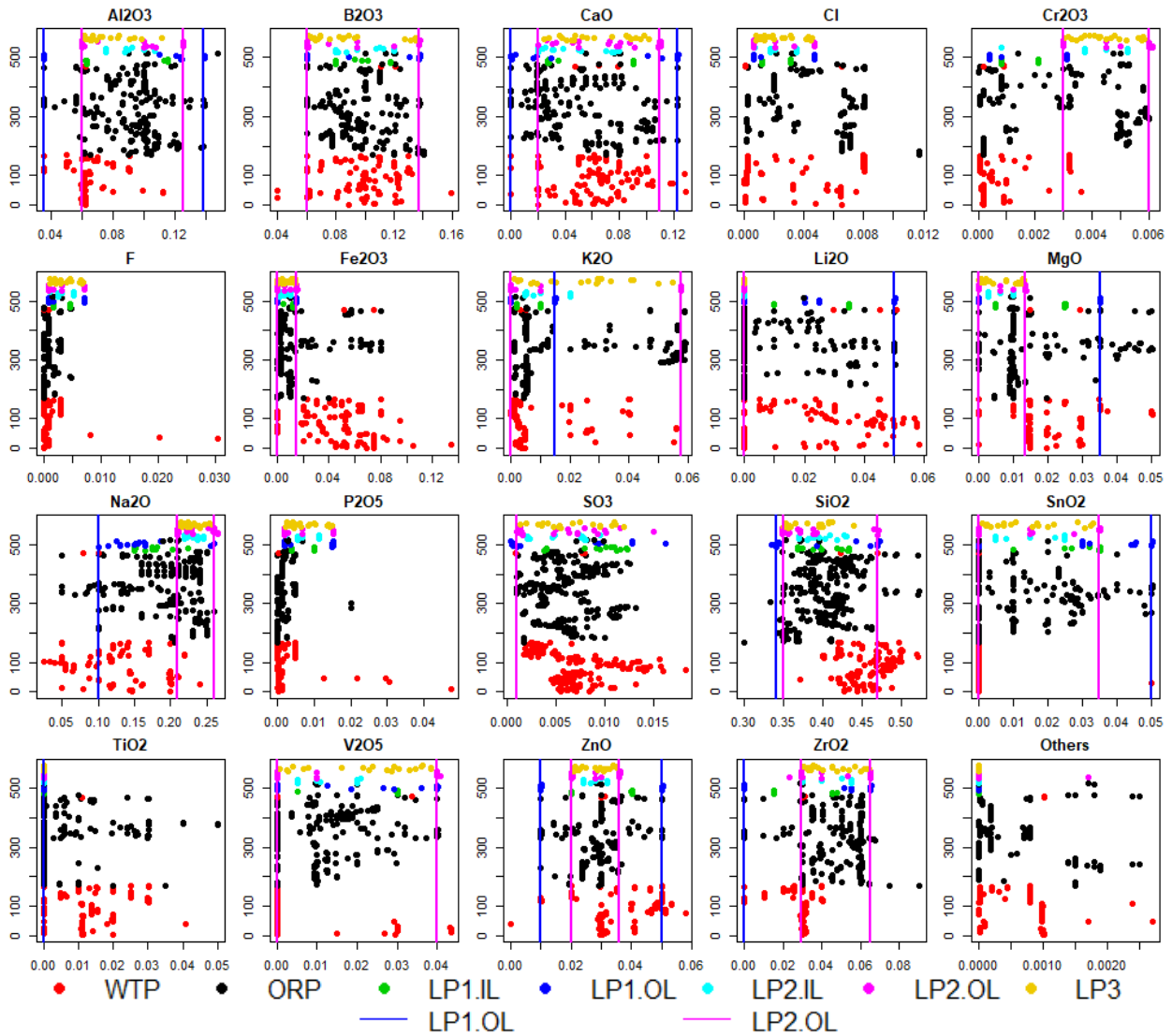


Figure 7.3. Distributions of 20 Main Components (in mass fractions) for 576 LAW Glass Compositions with Melter SO₃ Tolerance and Solubility Measurements at 1150 °C that Remain after Excluding the 25 Glasses in Table 7.1. The vertical lines (when present) represent the lower and upper limits for each component from the PNNL LAW Phase 1 outer-layer study (blue lines), LAW Phase 2 outer-layer study (pink lines), and LAW Phase 3 study (pink lines), as shown in Table 2.1. In cases where two limits are the same, blue lines over plot the pink lines.

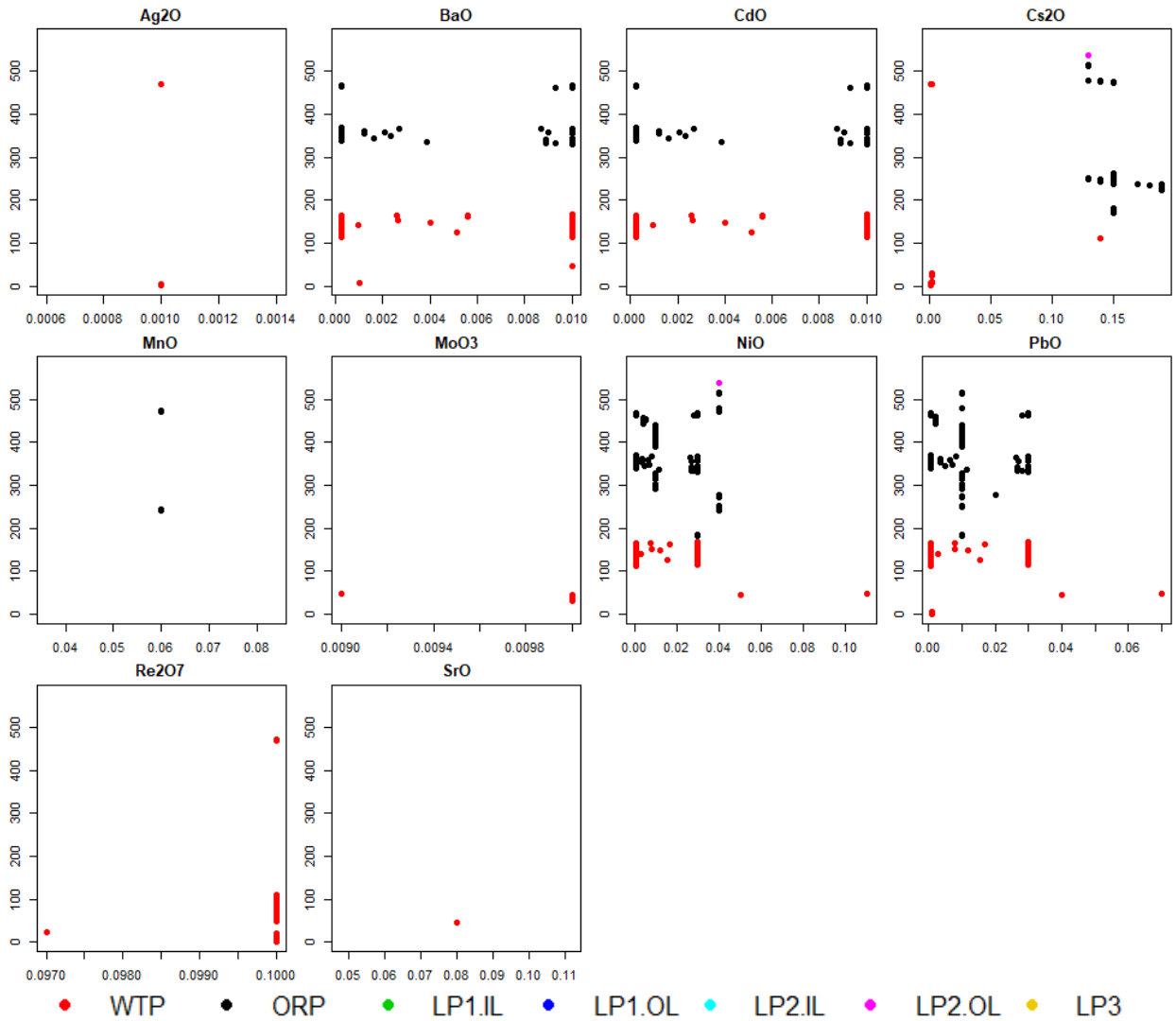


Figure 7.4. Distributions of 10 Minor Components (in mass fractions) for the 576 LAW Glass Compositions with Data for Melter SO_3 Tolerance and Solubility at 1150 °C that Remain after Excluding the 25 Glasses in Table 7.1

Figure 7.5 shows a scatterplot matrix of the 576 glasses remaining in the melter SO_3 tolerance and solubility modeling dataset after removing the 25 outlying glass compositions. Based on preliminary modeling work and the work of Vienna et al. (2014) and Skidmore et al. (2019), it was decided that melter SO_3 tolerance would be modeled by applying offsets for some of the SO_3 solubility at 1150 °C measurements. It was decided that BS and SR would be combined for one offset, 3TS would have another offset, and Bub and MT would be combined without an offset – namely, that it would be the model of interest. For each different offset model, the correlation among the components was assessed. High correlations between some pairs of components are evident, so pairwise correlation coefficients were calculated. These can vary from -1.0 (perfect negative correlation) to 0 (no correlation) to 1.0 (perfect positive correlation). For the BS and SR offset model, there were 468 SO_3 solubility measurements, and the component pairs with correlations larger (in absolute value) than 0.60 were Al_2O_3 and SiO_2 with correlation of -0.616 and Li_2O and Na_2O with correlation of -0.835 . Such high correlations in the predictors make parameter values difficult to estimate and result in inflated prediction uncertainties. Thus,

this high pairwise correlation needs to be kept in mind when developing and interpreting LAW glass property-composition models for melter SO_3 tolerance. For the Bub and MT model, there were only 69 melter SO_3 tolerance and solubility measurements, so the Pearson correlations are less stable and only those larger than 0.80 in magnitude are mentioned here. For the Bub and MT no offset model, the only component pair with correlations larger (in absolute value) than 0.80 was Li_2O and Na_2O with correlation of -0.925 . Thus, this high pairwise correlation needs to be kept in mind when developing and interpreting LAW glass property-composition models for melter SO_3 tolerance.

Further, such high correlations in the predictors make parameter values difficult to estimate and result in inflated prediction uncertainties. For the 3TS offset model, there were only 98 SO_3 solubility measurements, so the Pearson correlations are less stable and only those larger than 0.80 in magnitude are mentioned here. For the 3TS offset model, the component pairs with correlations larger (in absolute value) than 0.80 were Cl and F with correlation of 0.962, Cl and P_2O_5 with correlation of 0.954, and F and P_2O_5 with a correlation of 1.00. Because of this, although F and P_2O_5 are not strongly correlated in the other offset models, it is recommended that neither component be included in the RLM model for the melter SO_3 tolerance model. Such high pairwise correlations can make it difficult for regression methods to properly separate the effects of Cl and F (and Cl and P_2O_5) on the response variable (e.g., melter SO_3 tolerance). Thus, this high pairwise correlation needs to be kept in mind when developing and interpreting LAW glass property-composition models for melter SO_3 tolerance.

Finally, the correlations for the model as a whole, including glasses for each SO_3 solubility or melter tolerance measurement methods and the offsets for BS and SR, and 3TS were examined. This was essentially the independent variables matrix for the Full Linear Mixture (FLM) model discussed in Section 7.3.1 below. As 576 glasses (representing a total of 635 measurements as some glasses had multiple methods applied) were included, only those Pearson correlations with absolute values larger than 0.60 are mentioned here. Looking first at the components, only Li_2O and Na_2O with a correlation of -0.818 was larger in absolute value than 0.60 which agrees with the BS and SR, and Bub and MT subsets discussed above. See Section 9.7 for further discussion on treatment of the $\text{Li}_2\text{O}:\text{Na}_2\text{O}$ correlations. In addition, the BS and SR offset and 3TS offset had a correlation of -0.715 . This high correlation is largely because not all glasses were measured by all methods.

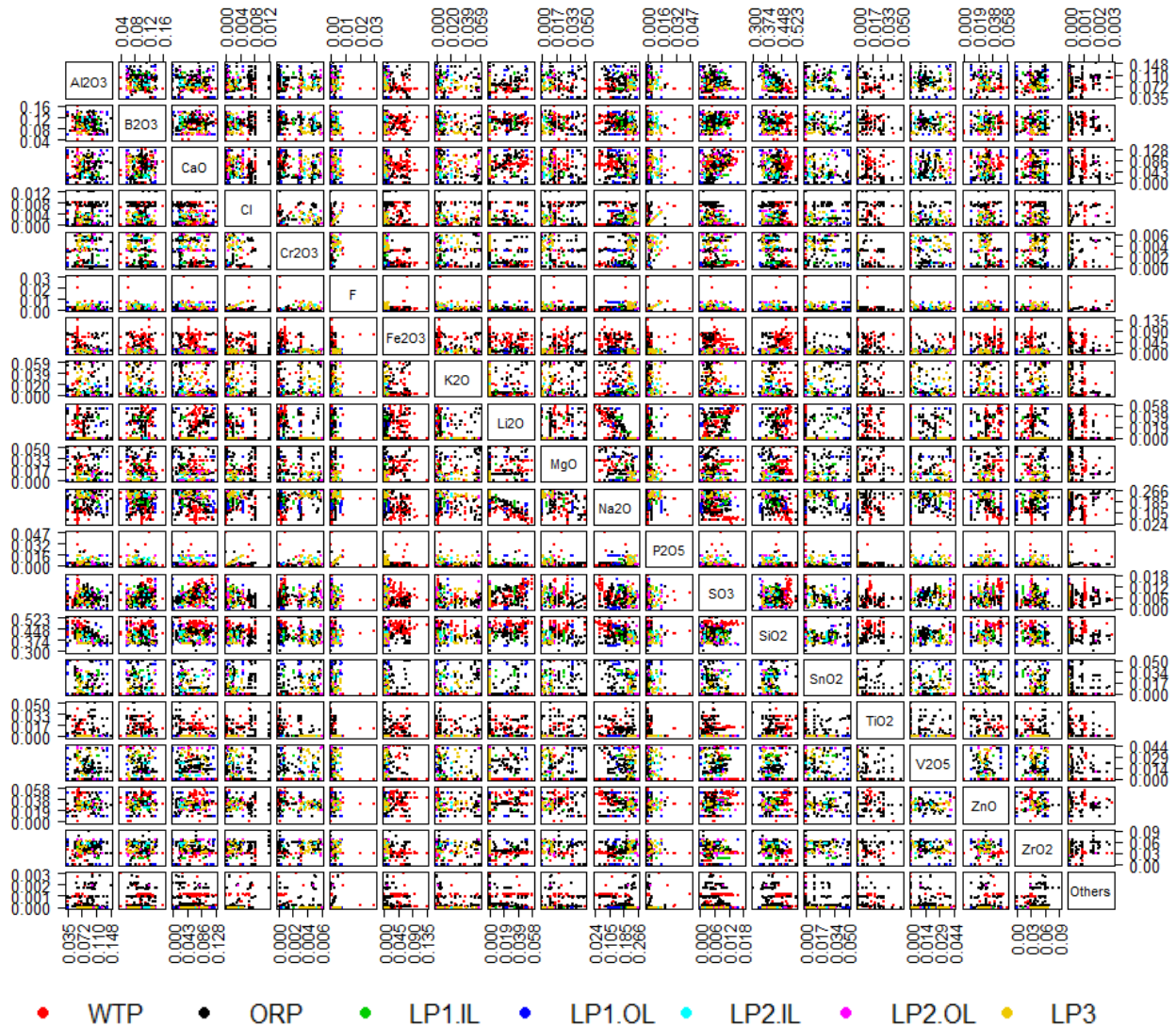


Figure 7.5. Scatterplot Matrix of 20 Components (mass fractions) for the 576 LAW Glasses with Melter SO₃ Tolerance and Solubility at 1150 °C Data that Remain after Excluding the 25 Glasses in Table 7.1

7.1.1.2 Melter SO₃ Tolerance and Solubility at 1150 °C Dataset Used for Modeling

Table A.3 in Appendix A lists the Glass #s, Glass IDs, and SO₃ solubility and melter tolerance values for the 576 remaining simulated LAW glasses used for melter SO₃ tolerance model development. The SO₃ solubility and melter tolerance values for the 25 glasses excluded as outliers from the 601-glass modeling dataset (see Table 7.1) are marked with an asterisk in Table A.3. The compositions for these 576 LAW glasses are included in Table A.2. The glass compositions in Table A.2 are the normalized mass fractions of the 20 components previously identified as having sufficient data to support a separate model term if needed. The LAW glass compositions in Table A.2 were normalized so that the total mass fractions of all 20 components for each glass equaled precisely 1.000000 as discussed in Section 2.2.

The values of melter SO_3 tolerance and solubility in Table A.3 for the 576 glasses in the modeling dataset range from 0.150 to 2.603 wt%.

7.1.1.3 Replicate and Near-Replicate Data for Melter SO_3 Tolerance and Solubility at 1150 °C

The changes to the LAW glass compositions caused by the renormalization associated with using measured (or estimated) SO_3 values (see Section 2.2) resulted in some replicate glasses not having exactly equal normalized compositions. Such compositions are near-replicates. For ease of discussion, henceforth both replicates and near-replicates are referred to as replicates.

Table 7.2 lists the replicate sets of LAW glasses in the SO_3 solubility modeling dataset and the corresponding melter SO_3 tolerance and solubility values. Table 7.2 also lists estimates of (i) %RSDs [calculated using SO_3 solubility values in wt%] and (ii) SDs [calculated using SO_3 solubility values in wt% units] for each replicate set. While the %RSD values are presented, it was determined that no transformation of the response variable was necessary, so only the pooled SD (and not the %RSD) should be used. When multiple melter SO_3 tolerance and solubility values are given, the %RSD and SD are computed within a melter SO_3 tolerance and solubility method given in parentheses in the table. The %RSD values for 22 replicate sets range from 0.81% to 35.36%. The SDs ranged from 0.0071 to 0.2440, with most of the larger SDs being associated with the 3TS method.

Table 7.2 also lists pooled estimates of SDs calculated over all replicate sets. A pooled SD combines the separate SD estimates from each replicate set so that a more precise combined estimate of SD is obtained. These pooled SDs include uncertainties due to fabricating glasses, determining SO_3 measured or estimated values, and the process of determining melter SO_3 tolerance and solubility values. The magnitudes of the pooled SD = 0.1067 [in wt% units] in Table 7.2 indicate there is approximately a 0.1067 wt% uncertainty in the melter SO_3 tolerance and solubility measurements over the replicate glasses. The pooled estimates of replicate uncertainty for melter SO_3 tolerance and solubility in Table 7.2 are used subsequently to assess LOF of the various melter SO_3 tolerance models considered.

Table 7.2. Uncertainty in SO₃ Solubility at 1150 °C Responses for Replicate and Near-Replicate Sets

Replicate Set Glass #s	Replicate Set Glass IDs	Rep. Set BS	Rep. Set SR	Rep. Set Bub	Rep. Set MT	Rep. Set 3TS	%RSD ^(a)	SD
164	LAWA118S2	0.62	--	--	--	--	7.56	0.0495
165	LAWA119S1	0.69	--	--	--	--	5.34 ^(BS)	0.0283 ^(BS)
10	LAWA44S	0.55	--	0.60	--	--		
144	LAWA44S1	0.51	--	--	--	--		
331	LAWM1	--	0.87	--	--	--	0.81	0.0071
383	LAWM53	--	0.88	--	--	--		
342	LAWM12	--	0.77	--	--	--	3.58	0.0283
385	LAWM55	--	0.81	--	--	--		
365	LAWM35	--	0.41	--	--	--	25.46	0.1273
386	LAWM56	--	0.59	--	--	--		
380	LAWM50	--	0.57	--	--	--	1.23	0.0071
381	LAWM51	--	0.58	--	--	--		
339	LAWM9	--	0.44	--	--	--	14.14	0.0566
384	LAWM54	--	0.36	--	--	--		
769	LORPM1	--	0.73	--	--	--	9.07	0.0707
1003	LORPM1R1	--	0.83	--	--	--		
778	LORPM10R1	--	1.47	--	--	--	3.29	0.0495
1007	LORPM10R1-repeat	--	1.54	--	--	--		
779	LORPM11	--	0.15	--	--	--	35.36	0.0707
1008	LORPM11-repeat	--	0.25	--	--	--		
786	LORPM18	--	0.36	--	--	--	25.71	0.1131
1009	LORPM18-repeat	--	0.52	--	--	--		
808	LORPM38	--	0.42	--	--	--	12.30	0.0566
1010	LORPM38R1	--	0.50	--	--	--		
772	LORPM4R1	--	0.82	--	--	--	4.99	0.0424
1004	LORPM4R2	--	0.88	--	--	--		
810	LORPM40	--	0.31	--	--	--	29.01	0.1131
1011	LORPM40R1	--	0.47	--	--	--		
777	LORPM9	--	0.31	--	--	--	8.57	0.0283
1006	LORPM9	--	0.35	--	--	--		
590	ORPLC2S4	--	0.68	--	--	--	5.40	0.0354
592	ORPLC3S4	--	0.63	--	--	--		
983	New-OL-108249Mod	--	--	--	--	1.295	1.55	0.0198
985	New-OL-108249Mod(PNNL)	--	--	--	--	1.267		
986	New-OL-116208Mod	--	--	--	--	1.271	9.98	0.1365
988	New-OL-116208Mod(PNNL)	--	--	--	--	1.464		
597	ORPLD1	--	--	--	1.10	--		
997	LAW-ORP-LD1(1)	--	--	--	--	1.253	14.61 ^(3TS)	0.2046 ^(3TS)
999	LAW-ORP-LD1(2)	--	--	--	--	1.314		
1035	LP2-OL-07	--	--	--	--	1.634		
930	New-IL-1721	--	--	--	--	1.647	2.90	0.0488
932	New-IL-1721(PNNL)	--	--	--	--	1.716		
1022	LP2-IL-10	--	--	--	--	1.337		
1028	LP2-IL-16	--	--	--	--	1.338	10.65	0.1304
1031	LP2-OL-02	--	--	--	--	1.098		
1049	LP2-OL-21	--	--	--	--	1.127		
1034	LP2-OL-05	--	--	--	--	1.427	19.45	0.2440
1038	LP2-OL-10-MOD	--	--	--	--	1.082		
Pooled Over All 22 Replicate Sets With 25 Total DF^(b)							14.60	0.1067
(a) %RSD = 100 × (Standard Deviation / Mean)								
(b) DF = degrees of freedom								

7.1.2 Model Validation Approach and Data for Melter SO₃ Tolerance Model at 1150 °C of LAW Glasses

The validation approach for melter SO₃ tolerance models was based on splitting the 576-glass dataset for model development into five modeling/validation subsets. Of the 576 model-development glasses, 48 were in 22 replicate sets. The five modeling/validation splits of the 576 glasses in the melter SO₃ tolerance and solubility modeling dataset were formed as follows:

- The 48 replicate glasses in 22 replicate sets were set aside so they would always be included in each of the five model development datasets. This was done so that replicate sets would not be split between modeling and validation subsets, thus negating the intent to have validation glasses different than model development glasses.
- The remaining 528 glasses were ordered from smallest to largest according to their melter SO₃ tolerance and solubility values (wt%). If there were multiple values for one glass, the SO₃ solubility measurements were prioritized (taken first) in the following order: MT, Bub, 3TS, SR, and BS. The 528 glasses were numbered 1, 2, 3, 4, 5, 1, 2, 3, 4, 5, etc. All of the 1's formed the first model validation set, while all of the remaining points formed the first model development dataset. Similarly, all of the 2's, 3's, 4's, and 5's respectively formed the second, third, fourth, and fifth model validation sets. In each case, the remaining non-2's, non-3's, non-4's, and non-5's formed the second, third, fourth, and fifth model development datasets. Because 528 is not evenly divisible by 5, the five modeling and validation subsets did not all contain the same numbers of glasses. Three of the five splits contained 106 glasses for validation and 422 glasses for modeling. The other two splits contained 105 glasses for validation and 423 glasses for modeling. Note that these numbers of glasses in the modeling subsets do not yet include the 48 replicates.
- The 48 replicate glasses were added to each of the split modeling subsets. Including the replicates, three of the five splits contained 470 glasses for modeling and 106 for validation, while the other two splits contained 471 glasses for modeling and 105 for validation.

Data splitting was chosen as the validation approach because the melter SO₃ tolerance and solubility modeling dataset contains all compositions that (i) are in the LAW GCR of interest, (ii) meet QA requirements, and (iii) have melter SO₃ tolerance and solubility data. Having a separate validation dataset not used for modeling is desirable, but that desire was overridden by wanting melter SO₃ tolerance models developed using all appropriate data.

7.1.3 Subsets of LAW Glasses to Evaluate Prediction Performance of Models for Melter SO₃ Tolerance at 1150 °C

Section 2.4 discusses six subsets of LAW glasses for evaluating the prediction performance of LAW glass property-composition models, including subsets of glasses with higher waste loadings. The subsets, as discussed in Section 2.4, are denoted WTP, ORP, LP2OL, LP123, HiNa₂O, and HiSO₃. The melter SO₃ tolerance modeling dataset of 576 LAW glasses (see Section 7.1.1) contains 171, 311, 115, 94, 223, and 135 glasses with melter SO₃ tolerance and solubility values in these six evaluation subsets, respectively. The Glass #s of these six evaluation subsets of LAW glasses are listed in Table C.5 of Appendix C. The normalized LAW glass compositions and melter SO₃ tolerance and solubility values for the glasses with these Glass #s are listed in Tables A.2 and A.3, respectively, of Appendix A.

Model performance/prediction statistics denoted R_{Eval}^2 and $RMSE_{Eval}$ (see Section B.3 of Appendix B), as well as predicted versus measured plots (see Section B.3), are subsequently used to assess the prediction performance of the melter SO_3 tolerance models (presented in later subsections) for the six evaluation subsets listed in Table C.5 of Appendix C.

7.2 Model Forms for Melter SO_3 Tolerance at 1150 °C of LAW Glasses

The empirical model forms used are from the general class of *mixture experiment models* (Cornell 2002), which includes models linear in composition as well as non-linear in composition. Section B.1 of Appendix B discusses mixture experiments and several general forms of mixture experiment models.

Section 7.2.1 discusses the forms of mixture experiment models used for melter SO_3 tolerance of LAW glasses. Section 7.2.2 discusses use of melter SO_3 tolerance and solubility values as the response variable for melter SO_3 tolerance modeling with offsets for some of the different SO_3 solubility methods.

7.2.1 Mixture Experiment Model Forms for Melter SO_3 Tolerance at 1150 °C of LAW Glasses

The LM and PQM model forms introduced in Section B.1 of Appendix B were chosen for use in modeling melter SO_3 tolerance as a function of LAW glass composition. Compositions were normalized after removing SO_3 content so that SO_3 content formed a true independent parameter. This approach (LM and PQM of normalized compositions) was used in the past (e.g., Vienna et al. 2014; Muller et al. 2014) to model the compositional dependence of melter SO_3 tolerance-composition or SO_3 solubility-composition models. The following equation was used to normalize the compositions.

$$x_i = \frac{g_i}{1 - g_{SO_3}} \quad (7.1)$$

where g_i is the i^{th} component mass fraction in glass and x_i is the i^{th} component so that the normalized concentrations of all components ($i = 1, \dots, q$) except SO_3 sum to 1.

The LM model form is given by

$$w_{SO_3}^{MT} = \sum_{i=1}^q \beta_i x_i + e \quad (7.2)$$

while the PQM model form is given by

$$w_{SO_3}^{MT} = \sum_{i=1}^q \beta_i x_i + \text{Selected} \left\{ \sum_{i=1}^q \beta_{ii} x_i^2 + \sum_{i < j}^{q-1} \sum_j^q \beta_{ij} x_i x_j \right\} + e \quad (7.3)$$

where in Eqs. (7.2) and (7.3)

- $w_{SO_3}^{MT}$ = melter SO₃ tolerance
- x_i = normalized mass fraction of the i^{th} glass oxide or halogen component
($i = 1, 2, \dots, q$) except measured SO₃, such that $\sum_{i=1}^q x_i = 1$
- β_i = coefficient of the i^{th} linear blending term ($i = 1, 2, \dots, q$)
- β_{ii} and β_{ij} = coefficients of selected quadratic (squared or crossproduct) blending terms to be estimated from the data
- e = random error for each data point.

Many statistical methods exist for the case where the E are statistically independent (i.e., not correlated) and normally distributed with mean 0 and standard deviation σ . In Eq. (7.3), “Selected” means that only some of the terms in curly brackets are included in the model. The subset is selected using stepwise regression or other variable selection methods (Draper and Smith 1998; Montgomery et al. 2012). PQM models are discussed in more detail and illustrated by Piepel et al. (2002) and Smith (2005).

Cornell (2002) discusses many other empirical mixture model forms that could have been considered for melter SO₃ tolerance-composition modeling. However, these other mixture model forms were not investigated because the special blending effects of components associated with those models were judged not to apply for melter SO₃ tolerance. The model forms in Eqs. (7.2) and (7.3) are widely used in many application areas (including waste glass property modeling) and usually predict the response very well.

7.2.2 Offsets for Melter SO₃ Tolerance Model at 1150 °C for LAW Glasses

In modeling melter SO₃ tolerance, it is advantageous to use the SO₃ solubility values from other methods. However, in previous work (Vienna et al. 2014) it was ascertained that SO₃ solubility measurements from other methods such as BS, SR, Bub, and 3TS sometimes require the use of offsets. The advantage of using these offsets, where appropriate, is that it allows the use of all the melter SO₃ tolerance and solubility measurements instead of only the much more limited melter SO₃ tolerance dataset, which in this case only had 13 observations.

Based on preliminary modeling and previous work (Vienna et al. 2014; Skidmore et al. 2019), it was determined that (i) the BS and SR SO₃ solubility data could be combined into one offset, (ii) MT and Bub SO₃ solubility data could be combined into the main model without any offset, and (iii) 3TS SO₃ solubility data would form the second offset.

The LM model form is then given by

$$w_{SO_3}^{MT} = w_{SO_3} = C_S H_S + C_3 H_3 + \sum_{i=1}^q \beta_i x_i + e \quad (7.4)$$

while the PQM model form is given by

$$w_{SO_3}^{MT} = C_S H_S + C_3 H_3 + \sum_{i=1}^q \beta_i x_i + \text{Selected} \left\{ \sum_{i=1}^q \beta_{ii} x_i^2 + \sum_{i < j}^{q-1} \sum_j^q \beta_{ij} x_i x_j \right\} + e. \quad (7.5)$$

In Eqs. (7.4) and (7.5)

- $w_{SO_3}^{MT}$ = melter SO₃ tolerance and solubility measurements
- H_S = 1 if the SO₃ solubility method was BS or SR, 0 otherwise
- H_3 = 1 if the SO₃ solubility method was 3TS, 0 otherwise
- x_i = normalized mass fraction of the i^{th} glass oxide or halogen component
($i = 1, 2, \dots, q$) except measured SO₃, such that $\sum_{i=1}^q x_i = 1$
- C_S = first offset, or coefficient for BS and SR SO₃ solubility methods
- C_3 = second offset, or coefficient for 3TS SO₃ solubility methods
- β_i = coefficient of the i^{th} linear blending term ($i = 1, 2, \dots, q$)
- β_{ii} and β_{ij} = coefficients of selected quadratic (squared or crossproduct) blending terms to be estimated from the data
- e = random error for each data point.

Notice that without the offsets (or when the melter SO₃ tolerance method is used), the model forms in Eqs. (7.4) and (7.5) reduce to the melter SO₃ tolerance model given in Eqs. (7.2) and (7.3), respectively.

7.3 Property-Composition Model Results for Melter SO₃ Tolerance at 1150 °C of LAW Glasses

This section discusses the results of fitting several different mixture experiment models using melter SO₃ tolerance and solubility data from five methods (BS, SR, Bub, MT, and 3TS) as functions of LAW glass compositions normalized after the removal of measured SO₃. Section 7.3.1 presents the results of modeling melter SO₃ tolerance using a 19-component FLM model. Sections 7.3.2 and 7.3.3 present the results of modeling melter SO₃ tolerance using RLM and PQM models based on a reduced set of mixture components. Finally, Section 7.3.4 compares the results from the three models and recommends a melter SO₃ tolerance model for future use and evaluation.

7.3.1 Results from the 19-Component Full Linear Mixture Model for Melter SO₃ Tolerance at 1150 °C with LAW Glasses

As the initial step for developing an FLM melter SO₃ tolerance-composition model, the 20 components identified in Section 7.1.1.1 were renormalized with measured SO₃ removed and were fit to the modeling data (576 LAW glasses). Table 7.3 contains the results for the 19-component FLM model of melter SO₃ tolerance. Table 7.3 lists the model coefficients, standard deviations of the coefficients, and model fit statistics for the 19-component FLM model on melter SO₃ tolerance with appropriate indicator vectors for the SO₃ method using the modeling dataset (576 LAW glasses). Table 7.3 also contains the results from the (i) data-splitting validation approach (see Section 7.1.2), and (ii) evaluation of model predictions for the six evaluation subsets (see Section 7.1.3). In the data-splitting validation portion of the results at the bottom of Table 7.3, the columns are labeled DS1, DS2, DS3, DS4, and DS5 to denote the five modeling/validation splits of the data as described in Section 7.1.2. The last column of this part of Table 7.3 shows the averages for the different statistics over the five splits.

The $R^2 = 0.8281$, $R^2_A = 0.8225$, and $R^2_P = 0.8125$ statistics (see Section B.3 of Appendix B) in Table 7.3 show that (i) the 19-component FLM model fits the melter SO₃ tolerance and solubility data in the 576-glass modeling dataset well, (ii) there are not a large number of unneeded model terms, and (iii) there are not any highly influential data points. The RMSE = 0.1769 is larger than the pooled glass batching and melter SO₃ tolerance and solubility determination uncertainty (SD = 0.1067 in wt% units) estimated from replicates in Table 7.2. This suggests that the 19-component FLM model does have a statistically significant LOF, which is confirmed by the model LOF p-value < 0.002 in Table 7.3. See Section B.3 for discussion of the statistical test for model LOF. This p-value indicates that the model LOF is significant at more than the 99.8% confidence level. This indicates that a model with additional term(s) may be necessary. However, the FLM model includes all reasonable linear terms. Addition of higher order terms (quadratic and two-way interactions) to a reduced linear model is investigated further in Section 7.3.3.

At the bottom right of Table 7.3, the average model-fit statistics (R^2 , R^2_A , R^2_P , and RMSE) over the five data-splits are very close to the statistics obtained from fitting the 19-component FLM model for melter SO₃ tolerance to all 576 glasses in the modeling dataset. This indicates that the model, despite its statistically significant LOF, maintains its performance for data not used to fit the model. The data-split validation statistics (R^2_V and RMSE_V) are also relatively close to the R^2 and RMSE (i) values from fitting the model to the full dataset, and (ii) averages from fitting the model to the data-split modeling subsets. The data-split validation statistics (R^2_V and RMSE_V) indicate that the 19-component FLM model mostly maintains its predictive performance for data not used to fit the model.

Table 7.3. Coefficients and Performance Summary for the 19-Component Full Linear Mixture Model on the Melter SO₃ Tolerance at 1150 °C for LAW Glasses

Melter SO ₃ Tolerance with Offsets						
19-Component FLM Model Term	Coefficient Estimate	Coefficient Stand. Err.	Modeling Data Statistic, 576 Glasses ^(a)			
BS or SR offset	-0.2041	0.0243	R ² 0.8281			
3TS offset	0.4233	0.0341	R ² _A 0.8225			
Al ₂ O ₃	-2.2987	0.3316	R ² _P 0.8125			
B ₂ O ₃	2.7737	0.3307	RMSE 0.1769			
CaO	4.7158	0.2430	Model LOF p-value ^(e) < 0.002			
Cl	-15.9895	3.0354				
Cr ₂ O ₃	2.2991	4.2240				
F	2.2255	4.0808	Evaluation Set (# Glasses) ^(b) R ² _{Eval} RMSE _{Eval}			
Fe ₂ O ₃	-1.8939	0.3573	WTP (171) 0.5883 0.1973			
K ₂ O	0.6084	0.4803	ORP (311) 0.8273 0.1398			
Li ₂ O	10.6810	0.7434	LP2OL (115) 0.8721 0.1803			
MgO	0.2821	0.7399	LP123 (94) 0.5343 0.2378			
Na ₂ O	2.8286	0.2420	HiNa ₂ O (223) 0.8777 0.1552			
P ₂ O ₅	-0.7042	2.1628	HiSO ₃ (135) 0.5556 0.1947			
SiO ₂	0.1730	0.1470				
SnO ₂	-4.9273	0.6516				
TiO ₂	1.0214	0.9376				
V ₂ O ₅	5.6346	0.6418				
ZnO	1.5752	0.8026				
ZrO ₂	-1.8679	0.5176				
Others ^(c)	-23.3768	12.8549				
Data Splitting Statistic ^(a,d)	DS1	DS2	DS3	DS4	DS5	Average
R ²	0.8105	0.8496	0.8392	0.7977	0.7525	0.8099
R ² _A	0.7701	0.8195	0.8073	0.7532	0.7004	0.7701
R ² _P	0.5807	0.7506	0.6847	0.6380	0.4319	0.6172
RMSE	0.2036	0.1789	0.1892	0.2023	0.2284	0.2005
R ² _V	0.8290	0.8221	0.8229	0.8330	0.8348	0.8283
RMSE _V	0.1840	0.1626	0.1721	0.1823	0.2067	0.1816

- (a) The model evaluation statistics are defined in Section B.3 of Appendix B. The model validation statistics are defined in Section B.5.
- (b) The six sets of LAW evaluation glasses are discussed in Section 2.4 and Section 7.1.3.
- (c) For the 19-component FLM model, the “Others” component includes any components not separately listed except for SO₃.
- (d) The evaluation and validation statistics calculated for data-splits are defined the same as for separate modeling and validation sets. Section 7.1.2 describes how the modeling dataset was split into modeling and validation subsets.
- (e) A CCP for the appropriate LOF test in this case is currently being worked on.

The statistics from evaluating the predictive performance of the 19-component FLM model for melter SO_3 tolerance on the six evaluation subsets of modeling glasses (see Section 7.1.3) are given on the right side of Table 7.3. The R^2 statistics for three of the six evaluation subsets (0.8273 to 0.8777) are close to or better than the R^2 statistic for the whole modeling dataset (0.8281). The exceptions are (i) the WTP evaluation subset, with $R^2 = 0.5883$; (ii) the LP123 evaluation subset, with $R^2 = 0.5343$; and (iii) HiSO_3 , with $R^2 = 0.5556$; all of which are still above the worst $R^2_p (= 0.4319)$ for the data splitting statistics. The

R^2_{Eval} values that are moderately to substantially lower than the R^2 for the whole modeling dataset are because melter SO_3 tolerance and solubility depends very heavily on the mass fractions of Cl, Li_2O , Fe_2O_3 , and ZrO_2 in a LAW glass composition. Hence, the less variation in mass fractions of Cl, Li_2O , Fe_2O_3 , and ZrO_2 there is in an evaluation subset, the less dependent melter SO_3 tolerance and solubility will be on the mass fractions of other components for glasses in that evaluation subset, which reduces the R^2_{Eval} values.

Figure 7.6 shows the PvM plot for the 576-glass modeling dataset using the 19-component FLM model for melter SO_3 tolerance. The plot illustrates that the 19-component FLM model predicts melter SO_3 tolerance fits well, but with a tendency to under-predict (i) above 1.8 wt% melter SO_3 tolerance and (ii) possibly below 0.7 wt% melter SO_3 tolerance. Note that the under-predictions mainly have to do with the BS, SR, or 3TS SO_3 solubility method data, and the MT and Bub methods data are much tighter around the line, indicating a better fit for these methods, although there is some under-prediction of MT and Bub methods above 1.2 wt% melter SO_3 tolerance. The underprediction will result in conservative estimates of melter SO_3 tolerance and, although non-ideal, can still be useful in the WTP LAW Facility operation.

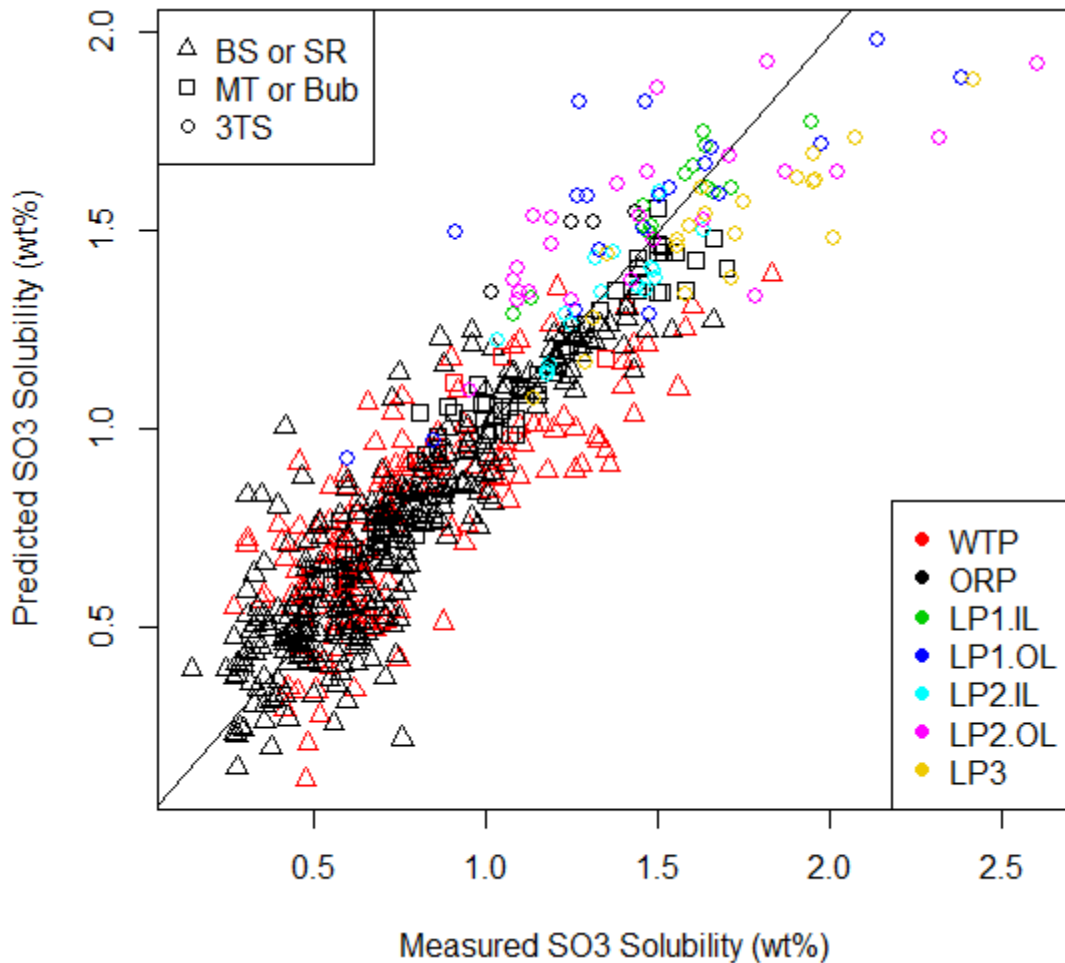


Figure 7.6. Predicted versus Measured Plot for the 576-Glass Modeling Dataset Using the 19-Component Full Linear Mixture Model on Melter SO_3 Tolerance at 1150 °C for LAW Glasses

Figure 7.7 displays PvM plots using the 19-component FLM model for melter SO_3 tolerance in Table 7.3 applied to the six evaluation subsets discussed in Section 7.1.3. Each plot in the figure contains the evaluation R^2 and RMSE values for the corresponding evaluation subset. Figure 7.7 shows that the 19-component FLM model for melter SO_3 tolerance fit to the 576-glass modeling dataset generally predicts well for three of the six evaluation subsets. In particular, the model predicts well for some of the evaluation subsets containing glasses with higher waste loadings (LP2OL and HiNa_2O). However, some of the evaluation subsets containing glasses with higher waste loadings (LP123 and HiSO_3) do not fit as well. The 3TS method has greater variability than the other methods, likely explaining the worse fit for the LP123 glasses, which were all 3TS measurements. Similarly, most of the data explaining the worse fit for the HiSO_3 evaluation set may be due to the 3TS method SO_3 solubility data. The plot for the WTP evaluation set (which contains older data for glasses with lower waste loadings) shows more scatter, resulting in an evaluation R^2 that is not as large as for the other evaluation sets. This is understandable and acceptable, since the new models presented in this report need to predict well for glasses with higher-waste loadings.

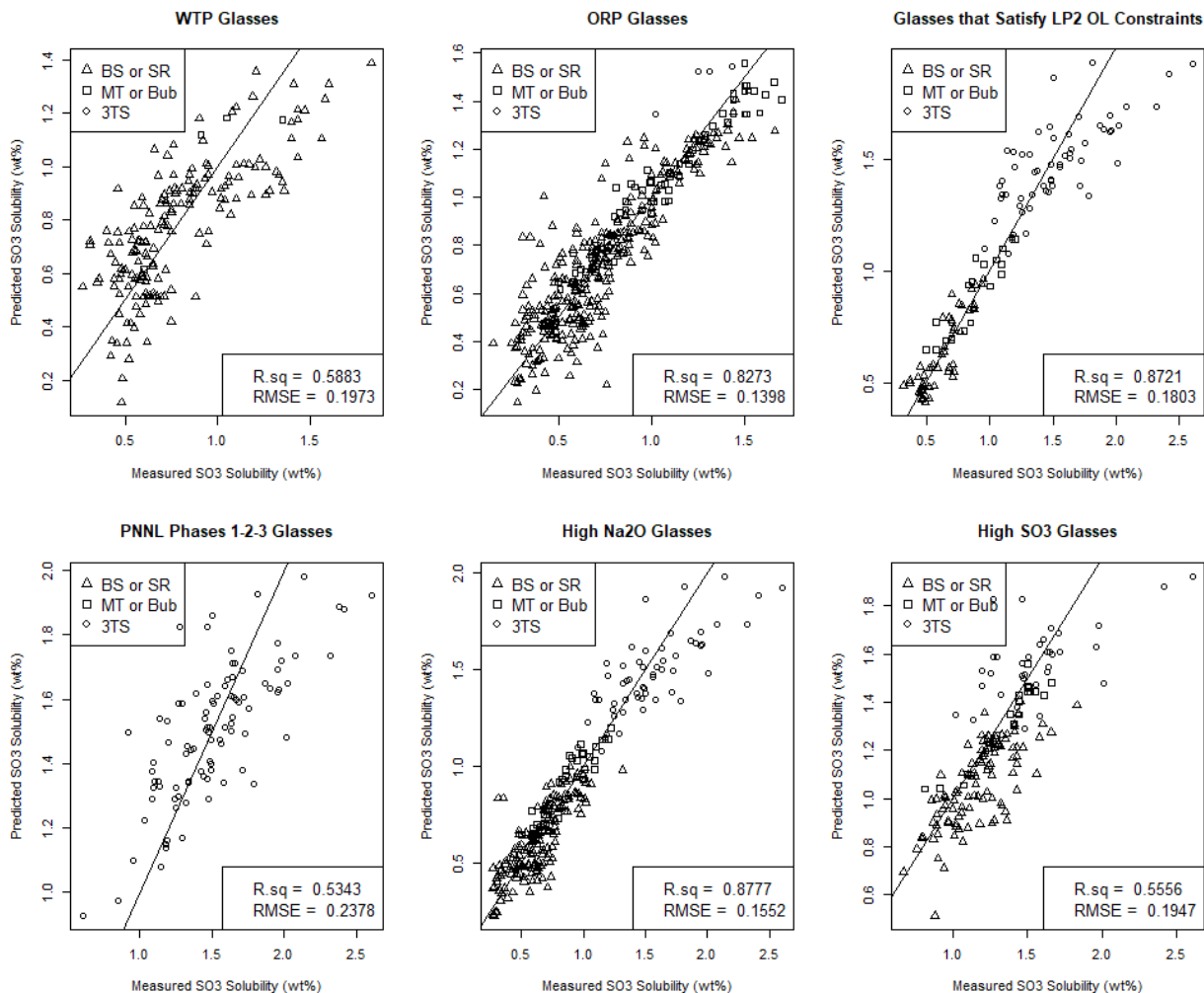


Figure 7.7. Predicted versus Measured Plots for the Six Evaluation Subsets Using the 19-Component Full Linear Mixture Model on the Melter SO_3 Tolerance at 1150 °C for LAW Glasses

The model in Table 7.3 does not fit the 576-glass modeling dataset well enough, as there is a statistically significant LOF (p-value = 0.0001), indicating that adding terms to the model, such as developing a PQM model (or a model with quadratic terms), may fit the modeling dataset better. However, there are no more linear terms that can be added to the FLM model (they can only be removed), so to provide guidance for reducing the FLM model (i.e., removing separate terms for components that do not significantly influence melter SO_3 tolerance), the 19-component FLM model was used to produce the response trace plot (see Section B.4.1 in Appendix B) shown in Figure 7.8. The average glass composition of the 1074 glasses in the compiled database discussed in Section 2.3 was used as the REFMIX (see Section B.4.1) in response trace plots for every property. The glass composition of the REFMIX is listed in Table 2.3; however, SO_3 was normalized out of the composition to agree with what was done for the model.

The response trace plot in Figure 7.8 shows that Cl , SnO_2 , Al_2O_3 , Fe_2O_3 , ZrO_2 , and SiO_2 are predicted to increase melter SO_3 tolerance the most, while Li_2O , V_2O_5 , CaO , Na_2O , B_2O_3 , and P_2O_5 are predicted to decrease melter SO_3 tolerance the most. The remaining components have predicted response traces with small to negligible slopes, indicating that those components are predicted to have small to negligible effects on melter SO_3 tolerance.

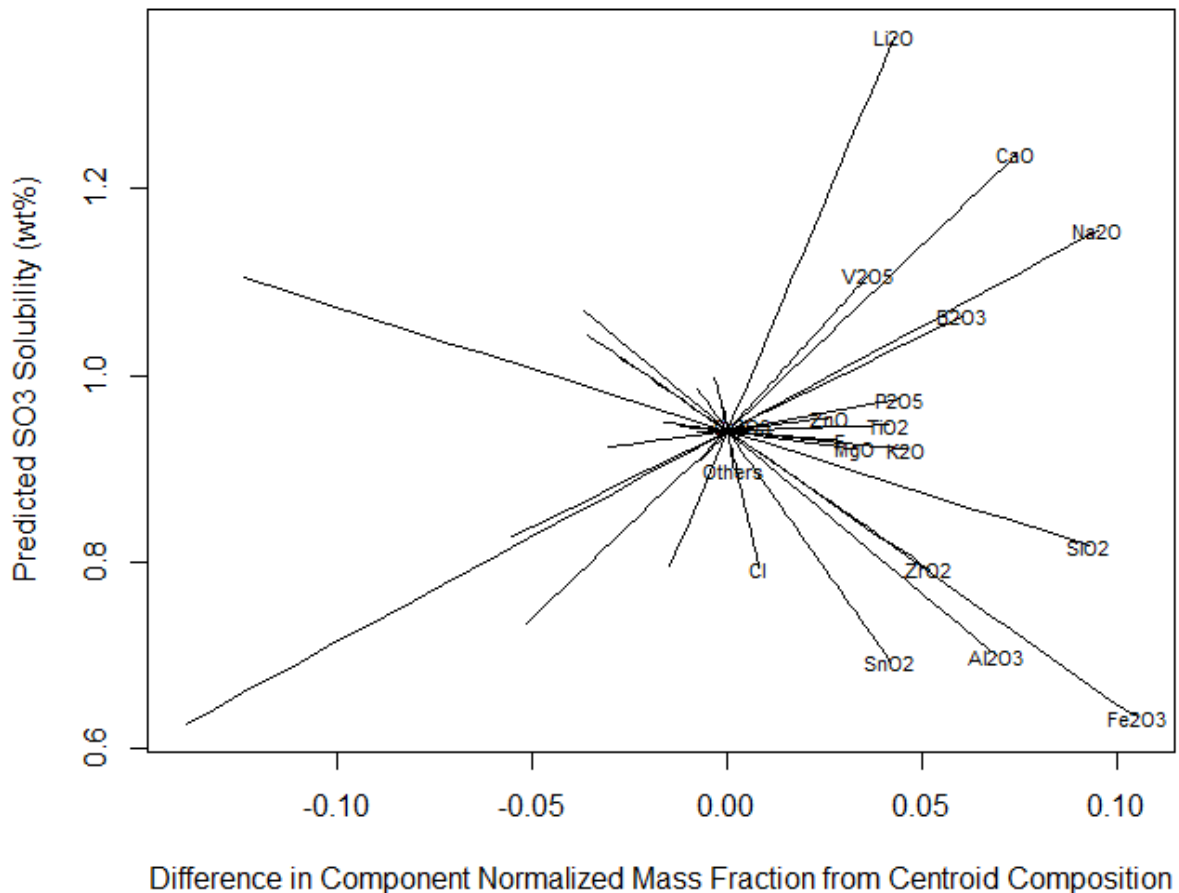


Figure 7.8. Response Trace Plot for the 19-Component Full Linear Mixture Model on Melter SO_3 Tolerance at 1150 °C for LAW Glasses

7.3.2 Results from a Reduced Linear Mixture Model for the Melter SO₃ Tolerance at 1150 °C with LAW Glasses

The 19-component FLM model for melter SO₃ tolerance presented in Section 5.3.1 likely contains components that do not significantly contribute to predicting melter SO₃ tolerance, so model reduction was the next step of the model development approach. Thus, RLM models for melter SO₃ tolerance involving fewer than the 19 components were considered. The sequential F-test model reduction approach (see Section B.4.1 of Appendix B; Piepel and Cooley 2006) was used.

7.3.2.1 Numerical Results for the 10-Component Reduced Linear Mixture Model on the Melter SO₃ Tolerance at 1150 °C for LAW Glasses

The RLM model for melter SO₃ tolerance was obtained using a combination of (i) glass scientist expertise looking at the slope terms and (ii) the backward-elimination, F-test method discussed in Section B.4.1 of Appendix B. Glass scientists provided inputs on LAW glass components that should be retained in the model, and the method determined whether the remaining components should be kept as separate linear terms or combined into Others. The resulting RLM model for melter SO₃ tolerance contained terms for 10 components: Al₂O₃, B₂O₃, CaO, Cl, Li₂O, Na₂O, P₂O₅, SiO₂, V₂O₅, and Others. Note that Others is the sum of all remaining components except SO₃, and thus differs from the Others in the 19-component FLM model discussed in Section 7.3.1.

Table 7.4 contains the results for the 10-component RLM model of melter SO₃ tolerance. Table 7.4 lists the model coefficients, standard deviations of the coefficients, and model fit statistics for the 10-component RLM model using the modeling dataset (576 LAW glasses). Table 7.4 also contains the results from the (i) data-splitting validation approach (see Section 7.1.2), and (ii) evaluation of model predictions for the six evaluation subsets (see Section 7.1.3). In the data-splitting validation portion of the results at the bottom of Table 7.4, the columns are labeled DS1, DS2, DS3, DS4, and DS5 to denote the five modeling/validation splits of the data as described in Section 7.1.2. The last column of this part of Table 7.4 shows the averages for the different statistics over the five splits.

The $R^2 = 0.8073$, $R^2_A = 0.8038$, and $R^2_P = 0.7965$ statistics (see Section B.3 of Appendix B) in Table 7.4 show that (i) the 10-component RLM model fits the melter SO₃ tolerance and solubility data in the 576-glass modeling dataset well, (ii) there are not a large number of unneeded model terms, and (iii) there are not any highly influential data points. The RMSE = 0.1860 is larger than the pooled glass batching melter SO₃ tolerance and solubility determination uncertainty (SD = 0.1067 in wt% units) estimated from replicates in Table 7.2. This suggests that the 10-component RLM model does have a statistically significant LOF, which is confirmed by the model LOF p-value < 0.002 in Table 7.4. This p-value indicates that the model LOF is significant at more than the 99.8% confidence level. This indicates that a model with additional term(s) may be necessary. Additions of higher order terms (quadratic and two-way interactions) to a reduced liner model is investigated further in Section 7.3.3. See Section B.3 for discussion of the statistical test for model LOF.

Table 7.4. Coefficients and Performance Summary for the 10-Component Reduced Linear Mixture Model on the Melter SO₃ Tolerance at 1150 °C for LAW Glasses

Melter SO ₃ Tolerance 10-Component RLM Model Term			Modeling Data Statistic, 576 Glasses ^(a)			
	Coefficient Estimate	Coefficient Stand. Err.				Value
BS or SR offset	-0.2026	0.0252	R ²			0.8073
3TS offset	0.3999	0.0336	R ² _A			0.8038
Al ₂ O ₃	-2.1233	0.3433	R ² _P			0.7965
B ₂ O ₃	2.8670	0.3339	RMSE			0.1860
CaO	4.8693	0.2465	Model LOF p-value ^(e)			< 0.002
Cl	-16.3356	2.8852				
Li ₂ O	9.4777	0.7230	Evaluation Set (# Glasses)^(b)			
Na ₂ O	2.3261	0.2165		R ² _{Eval}	RMSE _{Eval}	
P ₂ O ₅	0.6116	2.0905	WTP (171)	0.5819	0.1988	
SiO ₂	0.4894	0.1367	ORP (311)	0.7943	0.1525	
V ₂ O ₅	5.4924	0.6632	LP2OL (115)	0.8550	0.1920	
Others ^(c)	-1.0916	0.1856	LP123 (94)	0.4593	0.2563	
			HiNa ₂ O (223)	0.8551	0.1689	
			HiSO ₃ (135)	0.4776	0.2111	
Data Splitting Statistic ^(a,d)			DS1	DS2	DS3	Average
R ²	0.8096	0.8348	0.8075	0.7862	0.7861	0.8048
R ² _A	0.7892	0.8181	0.7883	0.7627	0.7635	0.7844
R ² _P	0.7239	0.7766	0.7224	0.6990	0.7002	0.7244
RMSE	0.1949	0.1795	0.1983	0.1983	0.2029	0.1948
R ² _V	0.8044	0.8000	0.8056	0.8103	0.8104	0.8061
RMSE _V	0.1845	0.1704	0.1883	0.1874	0.1921	0.1845

(a) The model evaluation statistics are defined in Section B.3 of Appendix B. The model validation statistics are defined in Section B.5.

(b) The six sets of LAW evaluation glasses are discussed in Section 2.4 and Section 7.1.3.

(c) For the 10-component RLM model, the “Others” component includes any components not separately listed except for SO₃.

(d) The evaluation and validation statistics calculated for data-splits are defined the same as for separate modeling and validation sets. Section 7.1.2 describes how the modeling dataset was split into modeling and validation subsets.

(e) A CCP for the appropriate LOF test in this case is currently being worked on.

At the bottom right of Table 7.4, the average model-fit statistics (R², R²_A, R²_P, and RMSE) over the five data-splits are close to (although a little less than) the statistics obtained from fitting the 10-component RLM model for melter SO₃ tolerance to all 576 glasses in the modeling dataset. This indicates that the model, despite its statistically significant LOF, maintains its performance for data not used to fit the model. The data-split validation statistics (R²_V and RMSE_V) are also relatively close to the R² and RMSE (i) values from fitting the model to the full dataset, and (ii) averages from fitting the model to the data-split modeling subsets. This indicates that the 10-component RLM model for melter SO₃ tolerance mostly maintains its predictive performance for data not used to fit the model.

The statistics from evaluating the predictive performance of the 10-component RLM model for melter SO₃ tolerance on the six evaluation subsets of modeling glasses (see Section 7.1.3) are given on the right side of Table 7.4. The R² statistics for three of the six evaluation subsets (0.7943 to 0.8551) are close to the R² statistic for the whole modeling dataset (0.8073). These values are from notably below to slightly above the R² statistics for the whole modeling dataset (0.8073). The exceptions are (i) the WTP

evaluation subset, with $R^2 = 0.5819$; (ii) the LP123 evaluation subset, with $R^2 = 0.4593$; and (iii) the HiSO_3 evaluation subset, with $R^2 = 0.4776$; all of which are relatively low. The R^2_{Eval} values that are moderately to substantially lower than the R^2 for the whole modeling dataset are because melter SO_3 tolerance depends very heavily on the mass fractions of Cl , Li_2O , Al_2O_3 , and CaO in a LAW glass composition. Hence, the less variation in mass fractions of Cl , Li_2O , Al_2O_3 , and CaO there is in an evaluation subset, the less dependent melter SO_3 tolerance will be on the mass fractions of other components for glasses in that evaluation subset, which reduces the R^2_{Eval} values.

7.3.2.2 Graphical Results for the 10-Component Reduced Linear Mixture Model on Melter SO_3 Tolerance at 1150 °C for LAW Glasses

While the RLM model exhibits significant LOF, it does have adequate performance, as indicated by the model-fit statistics (R^2 , R^2_{A} , R^2_{P} , and RMSE). Therefore, diagnostic plots for the 10-component RLM model (not included in this report) were investigated and support the assumption of normally distributed errors in the melter SO_3 tolerance and solubility data (see Section B.3 of Appendix B). Figure 7.9 displays for the 10-component RLM model of melter SO_3 tolerance the standardized residuals plotted versus the data index (a sequential numbering of the modeling data points for each melter SO_3 tolerance and solubility – 635 points because of multiple measurements on some of the glasses) with different plotting symbols representing the different groups of LAW glasses discussed in Section 2.3. Figure 7.9 yields the following observations:

- The LP3 (PNNL Phase 3) datasets have a narrower scatter of standardized residuals, indicating a narrower range of melter SO_3 tolerance model prediction uncertainty. This is likely because these glasses span narrower subregions of LAW glass compositions.
- The 10-component RLM model tends to under-predict melter SO_3 tolerance (corresponding to positive standardized residuals) for the LP3 glasses. The PNNL LP3 studies were investigated and no reason for biased SO_3 3TS values was found. The differences in standardized residuals for this study may be a result of longer-term random uncertainty.
- One glass has standardized residual over 4. Although outlying, this data point did not have a major impact on the 10-component RLM model for melter SO_3 tolerance and hence was retained in the modeling dataset.

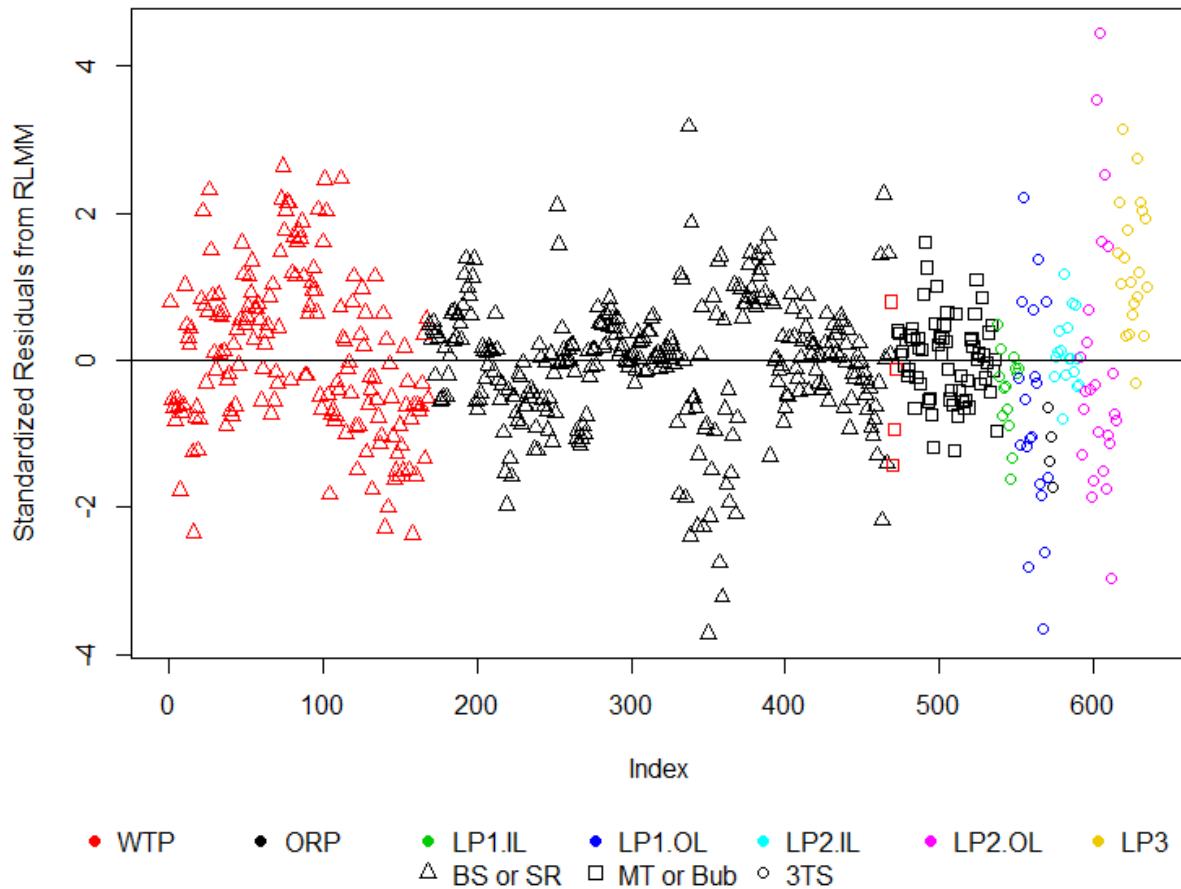


Figure 7.9. Standardized Residuals Plot for the 10-Component Reduced Linear Mixture Model on Melter SO_3 Tolerance at 1150 °C for LAW Glasses

Figure 7.10 displays the PvM plot for the 576-glass modeling dataset using the 10-component RLM model on melter SO_3 tolerance. Figure 7.10 is nearly identical to the PvM plot for the 19-component FLM model in Figure 7.6. Hence, as in Figure 7.6, Figure 7.10 illustrates that the 10-component RLM model predicts melter SO_3 tolerance well, but with a tendency to under-predict (i) above 1.8 wt% melter SO_3 tolerance and (ii) possibly below 0.8 wt% melter SO_3 tolerance. The underprediction will result in conservative estimates of melter SO_3 tolerance and, although non-ideal, can still be useful in the WTP LAW Facility operation.

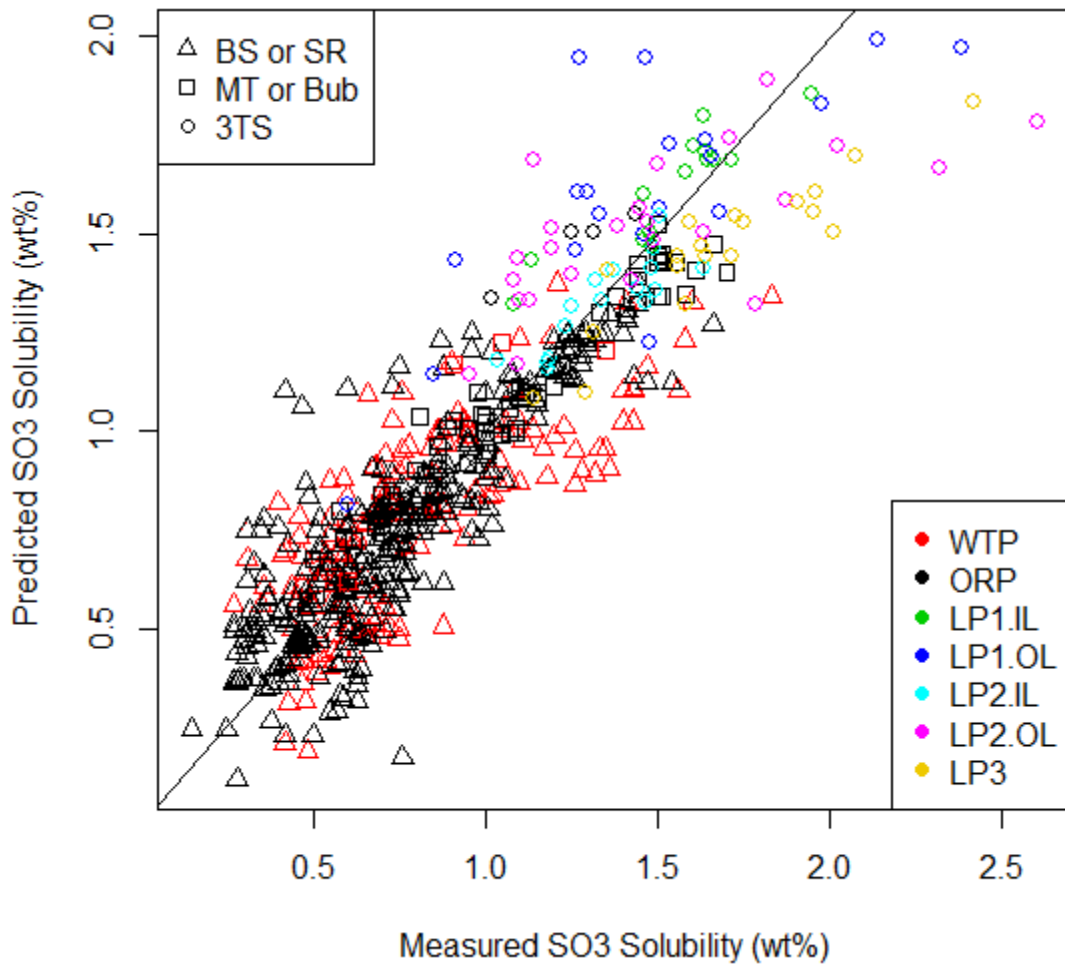


Figure 7.10. Predicted versus Measured Plot for the 576-Glass Modeling Dataset Using the 10-Component Reduced Linear Mixture Model on Melter SO_3 Tolerance at 1150 °C for LAW Glasses

Figure 7.11 displays PvM plots using the 10-component RLM model for melter SO_3 tolerance in Table 7.4 applied to the six evaluation subsets discussed in Section 7.1.3. Each plot in the figure contains the evaluation R^2 and RMSE values for the corresponding evaluation subset. Figure 7.11 shows that the 10-component RLM model for melter SO_3 tolerance fit to the 576-glass modeling dataset generally predicts well for three of the six evaluation subsets. In particular, the model predicts well for two of the evaluation subsets containing glasses with higher waste loadings (LP2OL and HiNa_2O). The model also predicts well for the ORP evaluation subset. The plot for the WTP (which contains older data for glasses with lower waste loadings), LP123, and HiSO_3 evaluation sets show more scatter, resulting in an evaluation R^2 that is not as large as for the other evaluation sets. However, most of the scatter in the LP123 and HiSO_3 evaluation sets is due to the 3TS SO_3 solubility data having greater variability. Despite this greater variability, the models will be used to predict melter tolerance that has better performance across these evaluation sets.

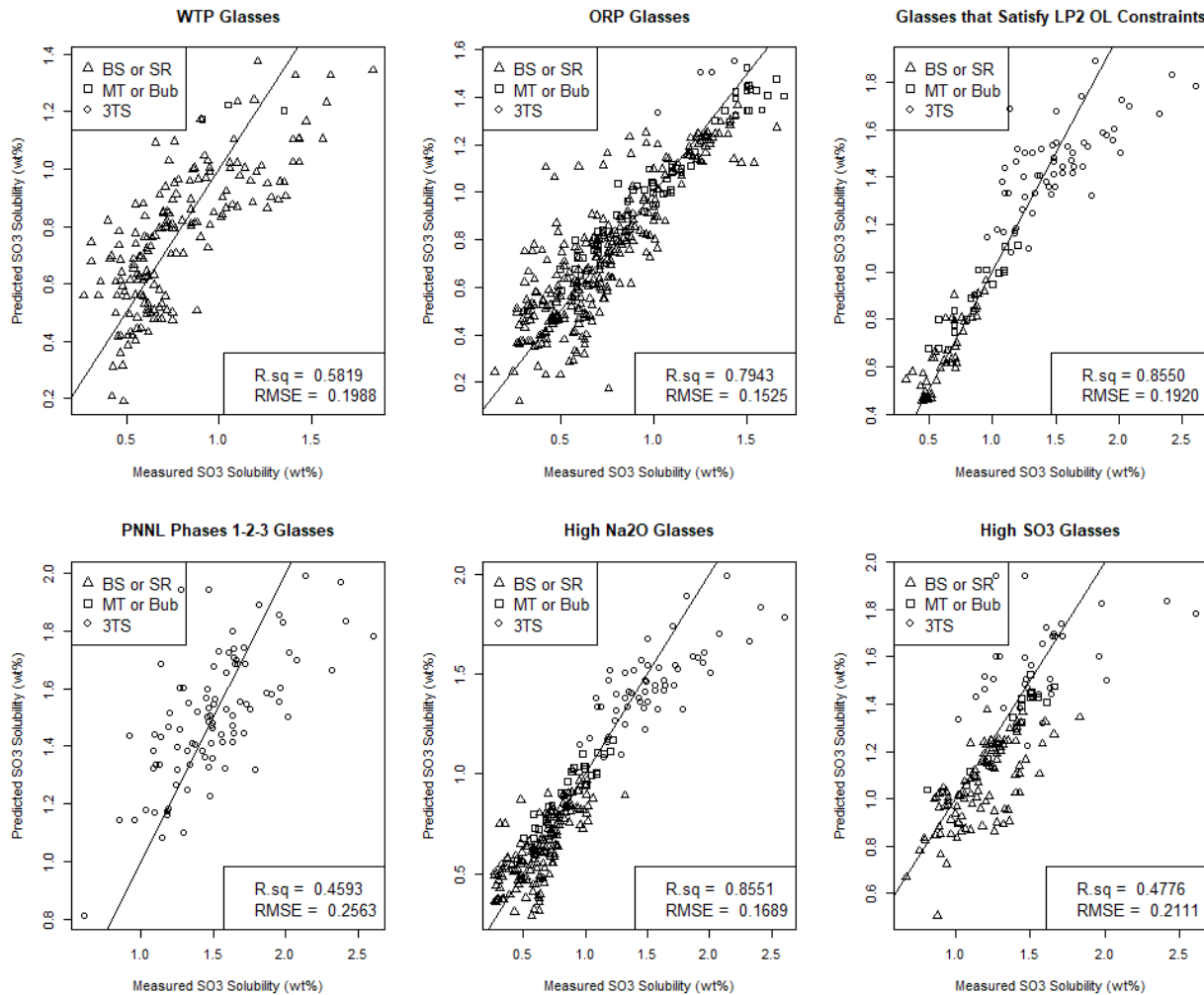


Figure 7.11. Predicted versus Measured Plots for the Six Evaluation Subsets Using the 10-Component Reduced Linear Mixture Model on Melter SO₃ Tolerance at 1150 °C for LAW Glasses

Figure 7.12 displays the response trace plot (see Section B.4.1 in Appendix B) for the 10-component RLM model of melter SO₃ tolerance. The glass composition of the REFMIX (see Section B.4.1) used is listed in Table 2.3. Figure 7.12 shows that Cl, Al₂O₃, SiO₂, and Others are predicted to increase melter SO₃ tolerance the most, while Li₂O, V₂O₅, CaO, B₂O₃, and Na₂O are predicted to decrease melter SO₃ tolerance the most. The remaining components have predicted response traces with small to negligible slopes, indicating that those components are predicted to have small to negligible effects on melter SO₃ tolerance.

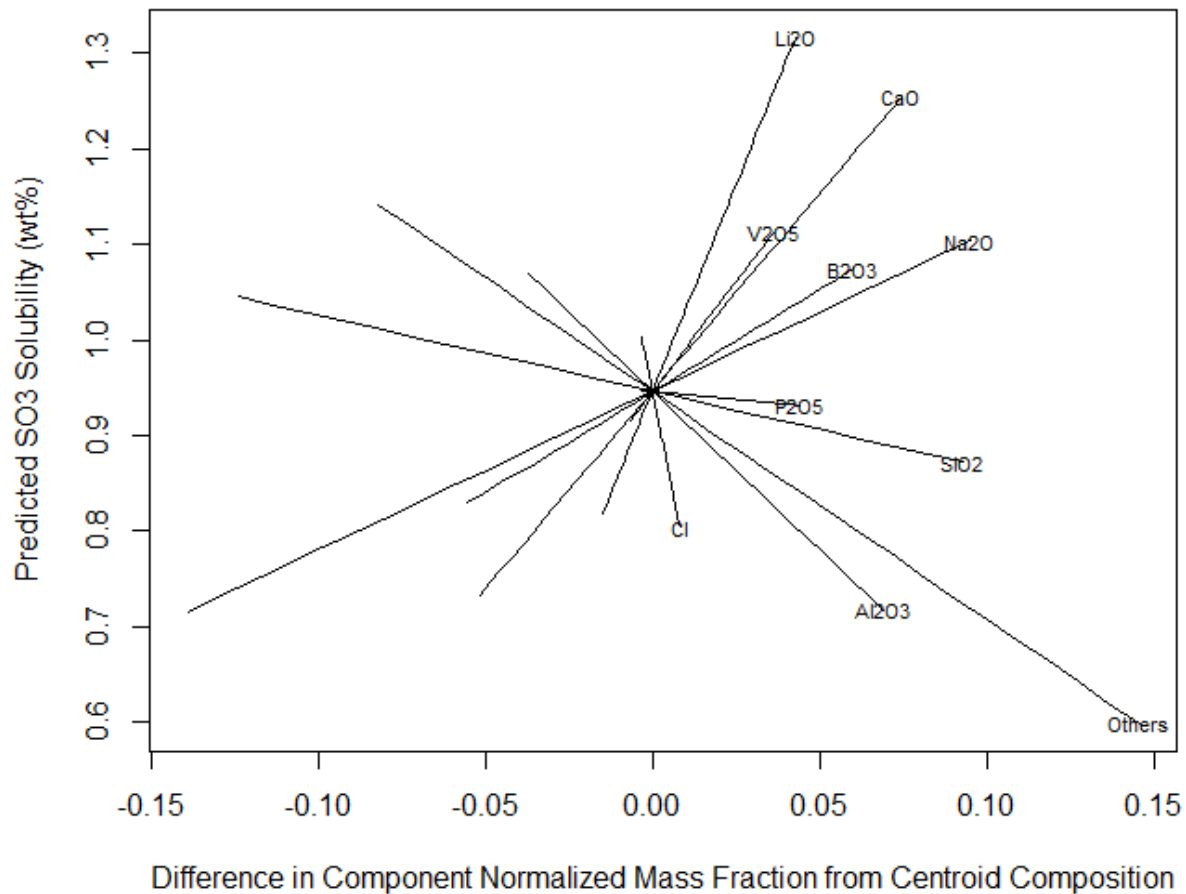


Figure 7.12. Response Trace Plot for the 10-Component Reduced Linear Mixture Model on Melter SO₃ Tolerance at 1150 °C for LAW Glasses

7.3.3 Results from a Reduced Partial Quadratic Mixture Model for Melter SO₃ Tolerance at 1150 °C with LAW Glasses

Reduced PQM models (see Section 7.2.1) were investigated in an effort to improve the 10-component RLM model for melter SO₃ tolerance presented in Section 7.3.2. Reduced PQM models were generated using the MAXR criterion (see Section B.4.2 of Appendix B) and plots of RMSE versus the number of quadratic terms to select a small number of quadratic (crossproduct and/or squared) terms to augment the 10 linear terms from the RLM model. Also, the components that could form quadratic terms were limited to those with strong linear effects and a glass science basis. Ultimately, an 11-term PQM model for melter SO₃ tolerance with 10 linear terms and 1 quadratic term (Na₂O × Li₂O) was selected as including enough quadratic terms to improve the model fit, without over-fitting the model development data. This term is generally expected based on past sulfur solubility modeling for LAW glasses that showed Li₂O × Li₂O (Vienna et al. 2014). Interactions between Li₂O and Na₂O are expected due to the mixed alkali effect. Table 7.5 contains the coefficients of the 11-term PQM model for melter SO₃ tolerance and the coefficient standard deviations. Table 7.5 also includes model performance statistics for the 11-term PQM model using the (i) 576-glass modeling data, (ii) data-split modeling data (as a model validation approach), and (iii) six evaluation subsets of modeling glasses discussed in Section 7.1.3 (as a model evaluation approach).

7.3.3.1 Numerical Results for the 11-Term Reduced Partial Quadratic Mixture Model on Melter SO₃ Tolerance at 1150 °C

In Table 7.5, the melter SO₃ tolerance model fit statistics $R^2 = 0.8303$, $R^2_A = 0.8270$, $R^2_P = 0.8190$, and $RMSE = 0.1747$ for the 11-term PQM model are small improvements over the corresponding statistics for the 10-component RLM model in Table 7.4. The small drop in values from R^2_A to R^2_P suggests that the melter SO₃ tolerance modeling dataset does not have any highly influential data points for the 11-term reduced PQM model. In any case, $R^2_P = 0.8190$ provides an estimate of the fraction of variation in melter SO₃ tolerance values for future datasets over the same GCR that might be accounted for by this 11-term reduced PQM model.

The RMSE in Table 7.5 is an estimate of the uncertainty (in wt% units) in fabricating simulated LAW glasses and determining melter SO₃ tolerance if the 11-term reduced PQM model for melter SO₃ tolerance does have statistically significant LOF. The $RMSE = 0.1747$ for the reduced PQM model fitted to the 576-glass modeling dataset is smaller than the corresponding value for the 10-component RLM model ($RMSE = 0.1860$) in Table 7.4. The RMSE value is larger than the pooled replicate SD in wt% units of 0.1067 in Table 7.2. These observations suggest that the 11-term reduced PQM model for melter SO₃ tolerance does have model LOF, which is confirmed by the LOF test p-value < 0.002 in Table 7.5. This p-value indicates that the model LOF is significant at more than the 99.8% confidence level. This indicates that a model with additional term(s) may be necessary; however, additional partial quadratic terms did not appear to improve the model much in terms of the model fit statistics. Future work is planned to see if the model fit can be improved. See Section B.3 of Appendix B for discussion of the statistical test for model LOF.

At the bottom right of Table 7.5, the average model-fit statistics (R^2 , R^2_A , R^2_P , and $RMSE$) over the five data-splits are close to the statistics obtained from fitting the 11-term reduced PQM model for melter SO₃ tolerance to all 576 glasses in the modeling dataset. This indicates that the model, despite its statistically significant LOF, maintains its performance for data not used to fit the model. The data-split validation statistics (R^2_V and $RMSE_V$) are also relatively close to the R^2 and $RMSE$ (i) values from fitting the model to the full dataset, and (ii) averages from fitting the model to the data-split modeling subsets. This indicates that the 11-term reduced PQM model maintains its predictive performance for data not used to fit the model.

The statistics from evaluating the predictive performance of the 11-term reduced PQM model for melter SO₃ tolerance on the six evaluation subsets of modeling glasses (see Section 2.4) are given on the right side of Table 7.5. The R^2 statistics for two of the six evaluation subsets (0.8636 to 0.8656) are greater than the R^2 statistic for the whole modeling dataset (0.8303). The exceptions are (i) the WTP evaluation subset, with $R^2 = 0.7239$; (ii) the ORP evaluation subset, with $R^2 = 0.7754$; (iii) LP123 evaluation subset, with $R^2 = 0.5515$; and (iv) the HiSO₃ evaluation subset, with $R^2 = 0.6081$; all of which are a little low but better than the RLM model. The R^2_{Eval} values that are moderately to substantially lower than the R^2 for the whole modeling dataset are because melter SO₃ tolerance and solubility depends very heavily on the mass fractions of Cl, Li₂O, Al₂O₃, and CaO in a LAW glass composition. Hence, the less variation in mass fractions of Cl, Li₂O, Al₂O₃, and CaO there is in an evaluation subset, the less dependent melter SO₃ tolerance will be on the mass fractions of other components for glasses in that evaluation subset, which reduces the R^2_{Eval} values.

Table 7.5. Coefficients and Performance Summary for 11-Term Reduced Partial Quadratic Mixture Model on Melter SO₃ Tolerance at 1150 °C for LAW Glasses

Melter SO₃ Tolerance			Modeling Data Statistic, 576 Glasses^(a)			
11-Term PQM Model Term	Coefficient Estimate	Coefficient Stand. Err.	Value			
BS or SR offset	-0.2030	0.0237	R ²			0.8303
3TS offset	0.3938	0.0315	R ² _A			0.8270
Al ₂ O ₃	-2.5573	0.3258	R ² _P			0.8190
B ₂ O ₃	3.0315	0.3141	RMSE			0.1747
CaO	4.8032	0.2316	Model LOF p-value ^(e)			< 0.002
Cl	-17.7273	2.7139				
Li ₂ O	19.3989	1.2761	Evaluation Set			
Na ₂ O	3.0912	0.2197	(# Glasses)^(b)			
P ₂ O ₅	2.1968	1.9709		R²_{Eval}	RMSE_{Eval}	
SiO ₂	0.2258	0.1316	WTP (171)	0.7239	0.1615	
V ₂ O ₅	6.2143	0.6278	ORP (311)	0.7754	0.1594	
Others ^(c)	-1.2757	0.1754	LP2OL (115)	0.8656	0.1849	
Li ₂ O × Na ₂ O	-77.5811	8.4488	LP123 (94)	0.5515	0.2334	
			HiNa ₂ O (223)	0.8636	0.1639	
			HiSO ₃ (135)	0.6081	0.1829	
Data Splitting Statistic^(a,d)						
	DS1	DS2	DS3	DS4	DS5	Average
R ²	0.8315	0.8591	0.8345	0.7933	0.8077	0.8252
R ² _A	0.8117	0.8434	0.8163	0.7682	0.7853	0.8050
R ² _P	0.7399	0.8011	0.7562	0.6674	0.7088	0.7347
RMSE	0.1842	0.1666	0.1847	0.1960	0.1933	0.1850
R ² _V	0.8275	0.8229	0.8272	0.8360	0.8345	0.8296
RMSE _V	0.1735	0.1574	0.1746	0.1843	0.1822	0.1744

(a) The model evaluation statistics are defined in Section B.3 of Appendix B. The model validation statistics are defined in Section B.5.

(b) The six sets of LAW evaluation glasses are discussed in Section 2.4 and Section 7.1.3.

(c) For the 11-component reduced PQM model, the “Others” component includes any components not separately listed except for SO₃.

(d) The evaluation and validation statistics calculated for data-splits are defined the same as for separate modeling and validation sets. Section 7.1.2 describes how the modeling dataset was split into modeling and validation subsets.

(e) A CCP for the appropriate LOF test in this case is currently being worked on.

7.3.3.2 Graphical Results for the 11-Term Reduced Partial Quadratic Mixture Model on Melter SO₃ Tolerance at 1150 °C for LAW Glasses

Diagnostic plots for the 11-term reduced PQM model (not included in this report) support the assumption of normally distributed errors in the melter SO₃ tolerance and solubility data (see Section B.3 of Appendix B). Figure 7.13 displays for the 11-term reduced PQM model of melter SO₃ tolerance the standardized residuals plotted versus the data index (a sequential numbering of the melter SO₃ tolerance and solubility modeling data points – 635 points) with different plotting symbols representing the different groups of LAW glasses discussed in Section 2.3. Figure 7.13 is very similar to Figure 7.9, so the observations on Figure 7.13 are the same as discussed in Section 7.3.2.2 for Figure 7.9 (although there is now a point < -4 in standardized residual).

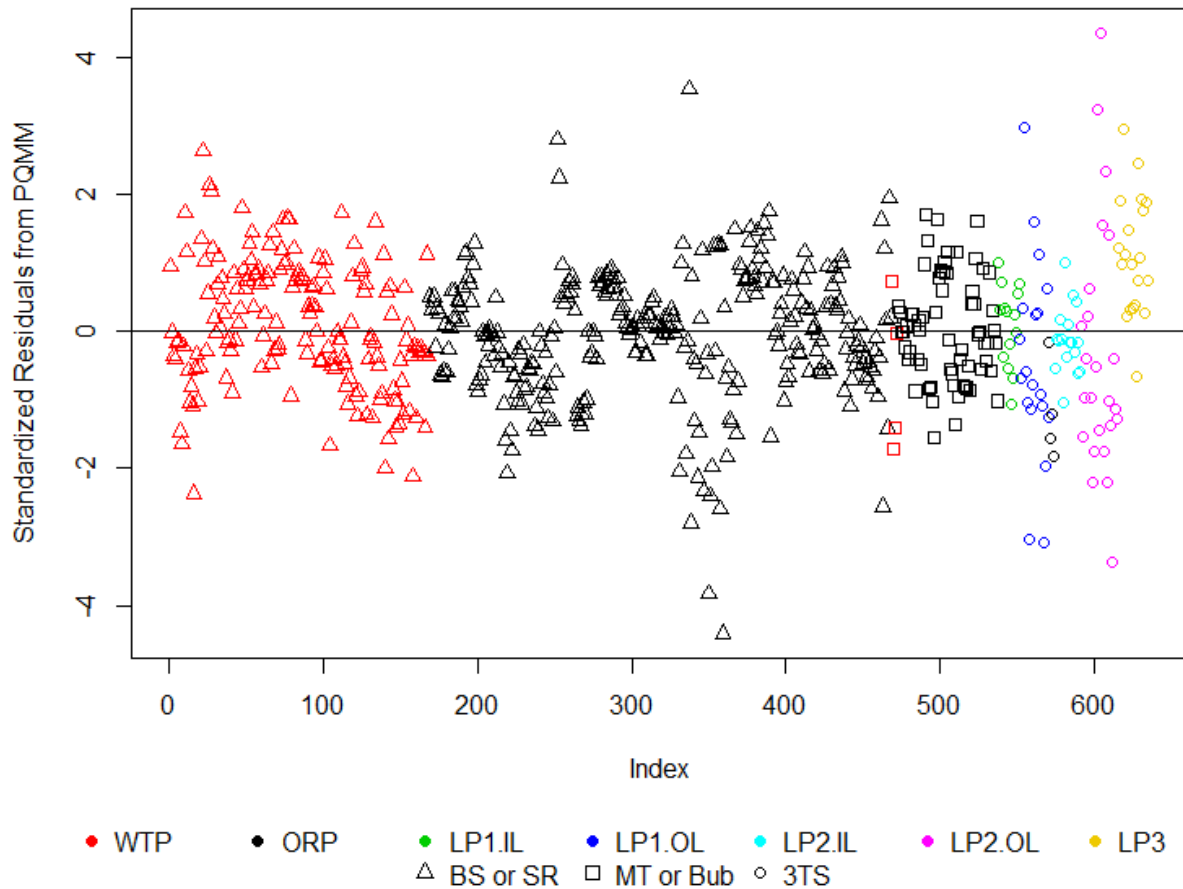


Figure 7.13. Standardized Residuals Plot for the 11-Term Reduced Partial Quadratic Mixture Model on Melter SO₃ Tolerance at 1150 °C for LAW Glasses

Figure 7.14 displays the PvM plot for the 576-glass modeling dataset using the 11-term reduced PQM model on melter SO₃ tolerance. Figure 7.14 is nearly identical to the PvM plot for the 10-component RLM model in Figure 7.10. Hence, as in Figure 7.10, Figure 7.14 illustrates that the 11-term reduced PQM model predicts melter SO₃ tolerance well, but with a tendency to under-predict (i) above 1.8 wt% melter SO₃ tolerance and (ii) possibly below 0.8 wt% melter SO₃ tolerance. The underprediction will result in conservative estimates of melter SO₃ tolerance and, although non-ideal, can still be useful in the WTP LAW Facility operation.

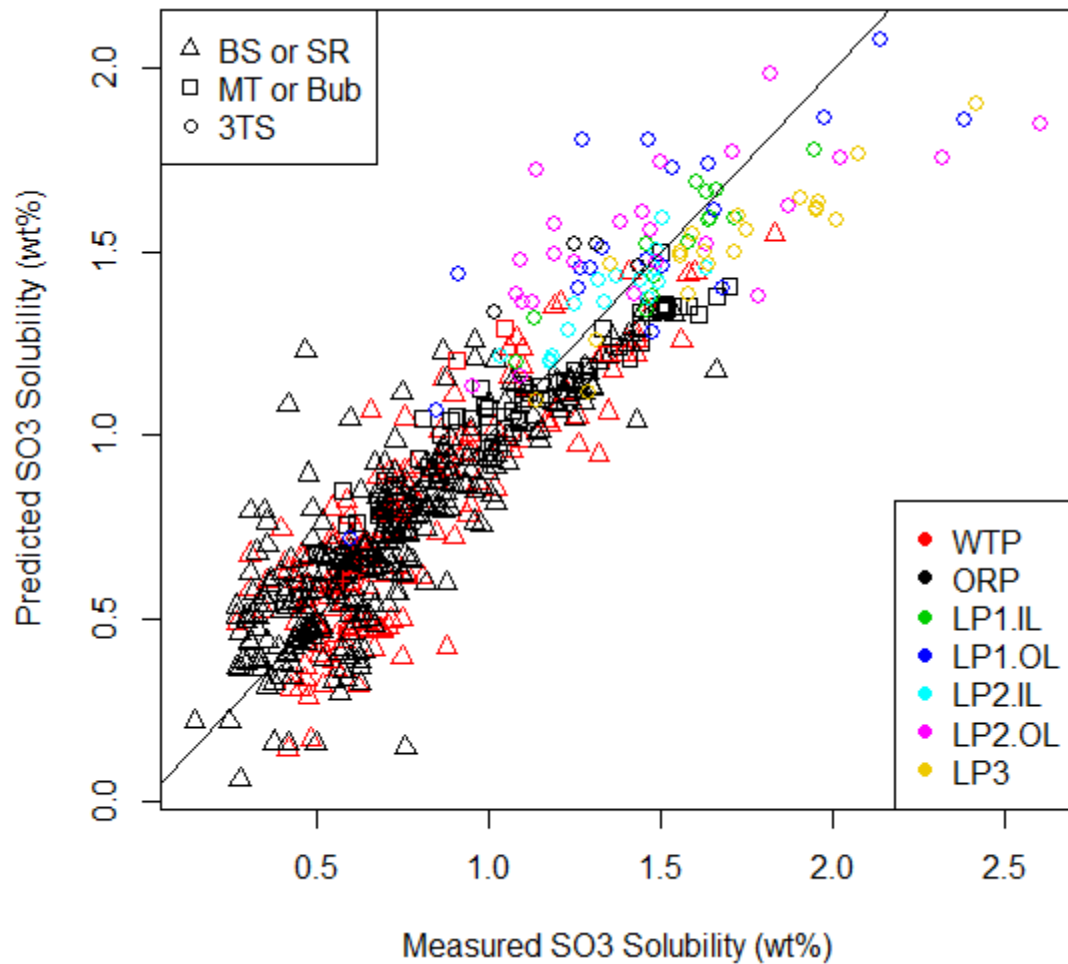


Figure 7.14. Predicted versus Measured Plot for the 576-Glass Modeling Dataset Using the 11-Term Reduced Partial Quadratic Mixture Model on Melter SO_3 Tolerance at 1150 °C for LAW Glasses

Figure 7.15 displays PvM plots using the 11-term reduced PQM model for melter SO_3 tolerance in Table 7.5 applied to the six evaluation subsets discussed in Section 7.1.3. Each plot in the figure contains the evaluation R^2 and RMSE values for the corresponding evaluation subset. Figure 7.15 shows that the 11-term reduced PQM model for melter SO_3 tolerance fit to the 576-glass modeling dataset generally predicts well for four of the six evaluation subsets. In particular, the model predicts well for two of the evaluation subsets containing glasses with higher waste loadings (LP2OL and HiNa_2O), and not so well for two of the other evaluation subsets containing glasses with higher waste loadings (LP123 and HiSO_3). The plot for the WTP, LP123, and HiSO_3 evaluation sets shows more scatter, resulting in evaluation R^2 values that are not as large as for the other evaluation sets. For the LP123 and HiSO_3 , the greater scatter is largely due to the 3TS SO_3 solubility data having greater variability. Despite this greater variability, this model has better performance across these evaluation sets compared to FLM and RLM models.

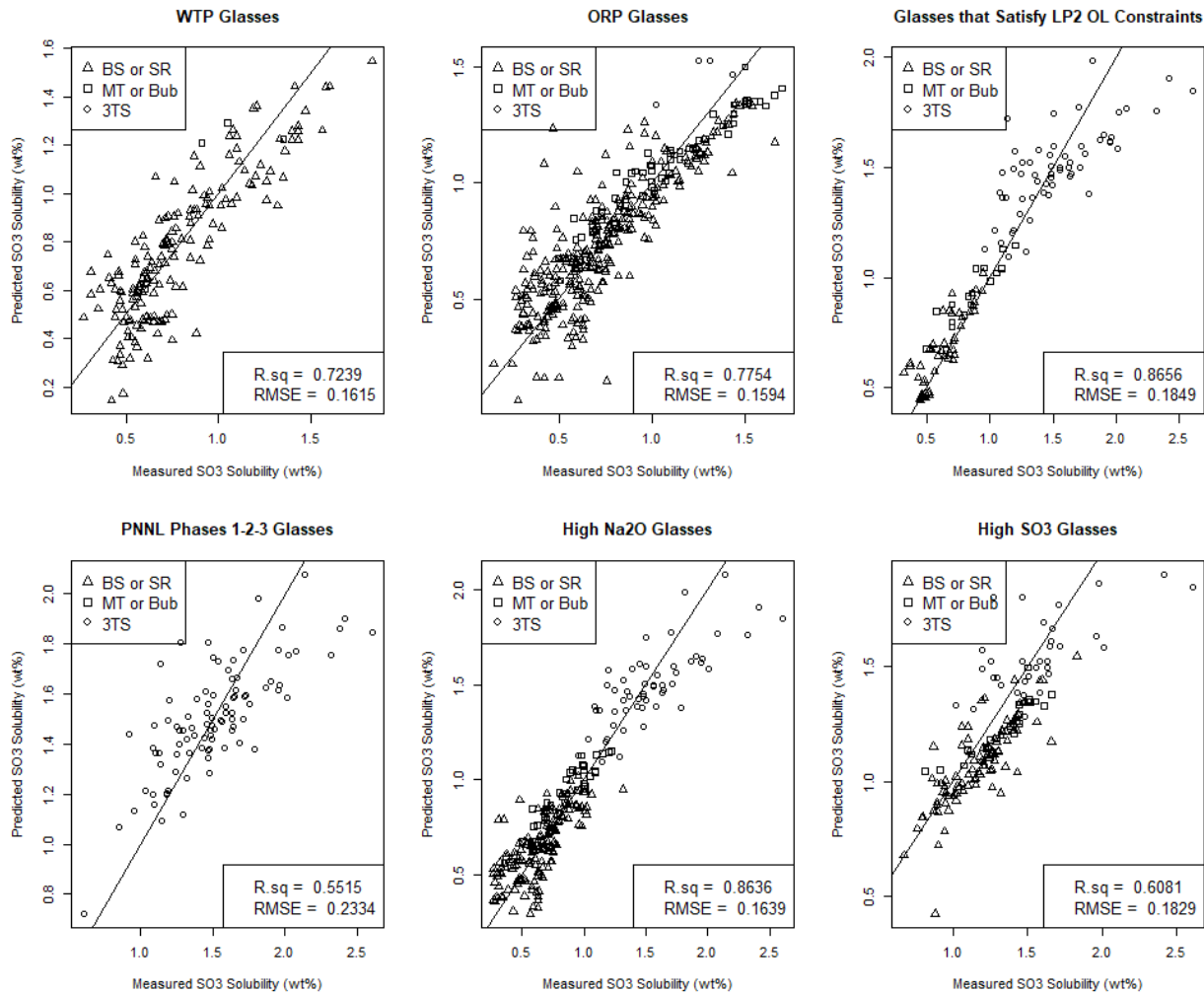


Figure 7.15. Predicted versus Measured Plots for the Six Evaluation Subsets Using the 11-Term Reduced Partial Quadratic Mixture Model on Melter SO₃ Tolerance at 1150 °C for LAW Glasses

Figure 7.16 displays the response trace plot (see Section B.4.1 of Appendix B) for the 11-term reduced PQM model on melter SO₃ tolerance. Figure 7.16 shows that Cl, Al₂O₃, Others, and SiO₂ are predicted to increase melter SO₃ tolerance the most, while Li₂O, V₂O₅, Na₂O, CaO, B₂O₃, Na₂O, and P₂O₅ are predicted to decrease melter SO₃ tolerance the most. It is unexpected that Others has such a large effect in the response trace plot. It is believed that this has more to do with the choice of REFMIX than an actual effect, as the Others coefficient (given the standard error) was not as large as for other terms in Table 7.5.

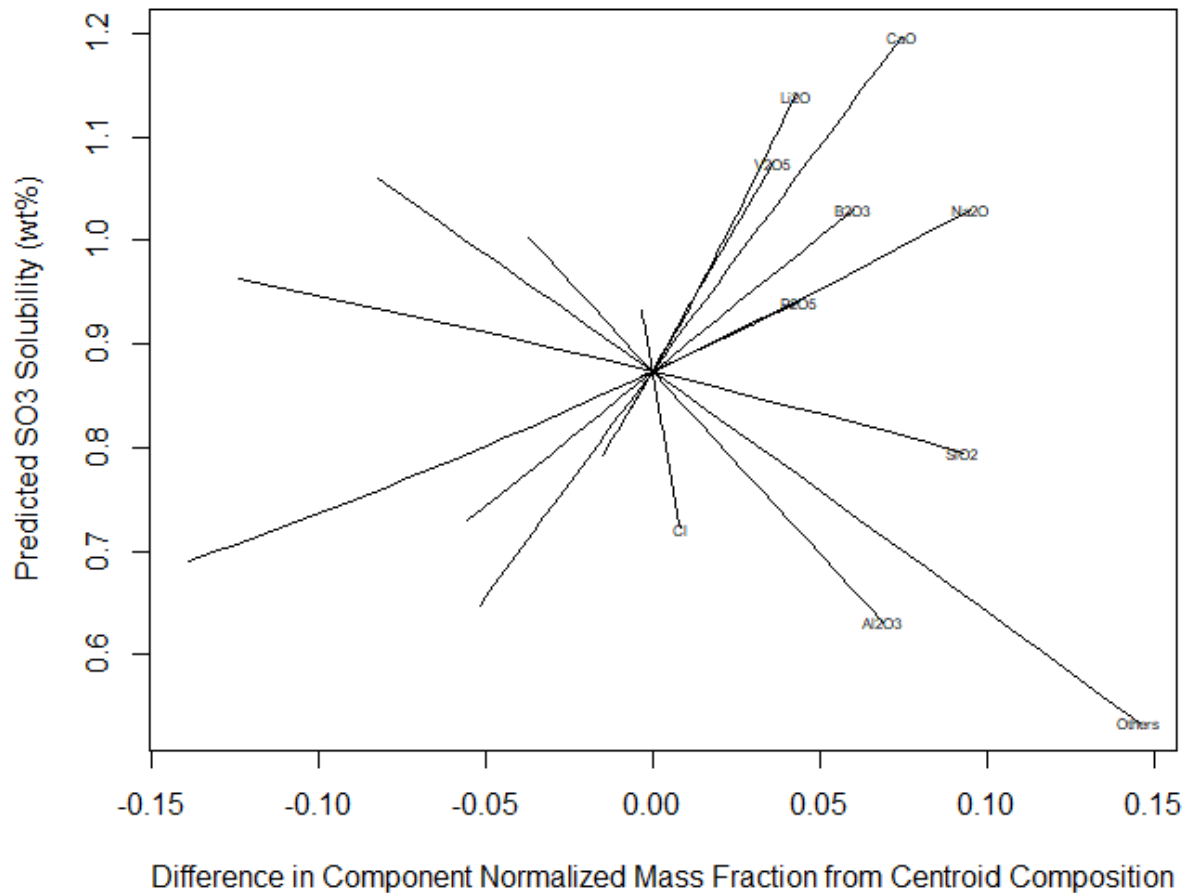


Figure 7.16. Response Trace Plot for 11-Term Reduced Partial Quadratic Mixture Model on Melter SO₃ Tolerance at 1150 °C for LAW Glasses

7.3.4 Recommended Model for Melter SO₃ Tolerance at 1150 °C for LAW Glasses

Table 7.6 summarizes the primary melter SO₃ tolerance model evaluation and validation results for the 19-component FLM model, the 10-component RLM model, and the 11-term reduced PQM model from Table 7.3, and Table 7.5, respectively, for the following:

- Model goodness-of-fit for the melter SO₃ tolerance-composition modeling data of 576 simulated LAW glasses
- Model validation using the data-splitting approach
- Model evaluation for six subsets of the 576-glass modeling dataset

Based on the summarized results in Table 7.6 and discussions in Sections 7.3.1 to 7.3.3, the 11-term reduced PQM model (listed in Table 7.5) is recommended for predicting melter SO₃ tolerance of LAW glasses. As a baseline for comparison, the 10-component RLM model (listed in Table 7.4) will be used.

Table 7.6. Performance Summary of Three Models for Melter SO₃ Tolerance at 1150 °C for LAW Glasses

	Melter SO ₃ Tolerance Model					
Summary Statistics from Model Fit to 576 Glasses ^(a)	19-Component FLM Model	10-Component RLM Model	11-Term Reduced PQM Model (Recommended)			
R ²	0.8281	0.8073	0.8303			
R ² _A	0.8225	0.8038	0.8270			
R ² _P	0.8125	0.7965	0.8190			
RMSE	0.1769	0.1860	0.1747			
LOF p-value	< 0.002	< 0.002	< 0.002			
Linear Terms	19 (See Table 7.3)	10 (See Table 7.4)	10 (See Table 7.5)			
Selected Quadratic Terms in Model	NA	NA	Li ₂ O × Na ₂ O			
# Model Terms	19	10	11			
Summary Statistics for Six Evaluation Subsets of LAW Glasses ^(a)						
Evaluation Set (# Glasses) ^(b)	R ² _{Eval}	RMSE _{Eval}	R ² _{Eval}	RMSE _{Eval}	R ² _{Eval}	RMSE _{Eval}
WTP (171)	0.5883	0.1973	0.5819	0.1988	0.7239	0.1615
ORP (311)	0.8273	0.1398	0.7943	0.1525	0.7754	0.1594
LP2OL (115)	0.8721	0.1803	0.8550	0.1920	0.8656	0.1849
LP123 (94)	0.5343	0.2378	0.4593	0.2563	0.5515	0.2334
HiNa ₂ O (223)	0.8777	0.1552	0.8551	0.1689	0.8636	0.1639
HiSO ₃ (135)	0.5556	0.1947	0.4776	0.2111	0.6081	0.1829
Validation Summary Statistics Averaged Over 5 Data-Splitting Sets ^(b)						
R ²	0.8099		0.8048		0.8252	
R ² _A	0.7701		0.7844		0.8050	
R ² _P	0.6172		0.7244		0.7347	
RMSE	0.2005		0.1948		0.1850	
R ² _V	0.8283		0.8061		0.8296	
RMSE _V	0.1816		0.1845		0.1744	

(a) The model evaluation statistics are defined in Section B.3 of Appendix B.

(b) Model validation statistics are defined in Section B.5 of Appendix B.

7.4 Example Illustrating Model Predictions and Statistical Intervals for Melter SO₃ Tolerance at 1150 °C

This section contains examples that illustrate application of the recommended 11-term PQM model for melter SO₃ tolerance in Table 7.5 to the REFMIX glass composition listed in Table 2.3 to obtain predicted melter SO₃ tolerance values and one-sided statistical intervals. Formulas for one-sided 90% CIs and one-sided 90% PIs are discussed in Section B.6 of Appendix B. One-sided intervals are illustrated because melter SO₃ tolerance will have upper operating limits during WTP LAW Facility operation. For comparison purposes, the same results are presented for the 10-component RLM model in Table 7.4 (although it is not a recommended model). The 90% CIs and 90% PIs were chosen for illustration purposes only. The WTP LAW Facility can use an appropriate confidence level depending on the use of the melter SO₃ tolerance-composition model and the type of statistical interval (uncertainty expression) desired.

The glass composition used in this example is denoted REFMIX, as listed in Table 2.3. The 19-component composition (mass fractions) of REFMIX for melter SO₃ tolerance modeling is given in Table 7.7 after normalizing out SO₃. To apply the 11-term reduced PQM model and 10-component RLM model for melter SO₃ tolerance to the REFMIX composition, the mass fractions of the 19 components

must be converted to mass fractions (that sum to 1.0) of the 10 LAW glass components contained in both models. This involves adding the mass fractions of the 9 of 19 components not contained in the melter SO₃ tolerance models to the mass fraction of Others (one of the original 19 components) to obtain Others (one of the reduced sets of 10 components). Mass fractions of the relevant components are then multiplied to obtain the one quadratic term of the 11-term reduced PQM model. Table 7.7 contains the composition of REFMIX prepared for use in the two melter SO₃ tolerance models for LAW glasses.

For each of the two melter SO₃ tolerance models, predicted melter SO₃ tolerance wt% values are obtained by multiplying the composition in the format needed for that model by the coefficients for that model, then summing the results. That is, the predicted values are calculated by

$$\hat{y}(\mathbf{d}) = \mathbf{d}^T \mathbf{b} \quad (7.6)$$

where \mathbf{d} is the composition of REFMIX formatted to match the terms in a given model (from Table 7.4 or Table 7.5 as appropriate, with 0's in \mathbf{d} corresponding to the offsets because we are interested in predicting melter SO₃ tolerance), the superscript T represents a vector transpose, and \mathbf{b} is the vector of coefficients for a given model. The predicted melter SO₃ tolerance values for REFMIX using the two melter SO₃ tolerance models are listed in the second column of Table 7.8.

The predicted melter SO₃ tolerance values for REFMIX in Table 7.8 are 0.946 wt% for the 10-component RLM model and 0.874 wt% for the recommended 11-term reduced PQM model. Statistical confidence intervals and prediction intervals for these predictions are discussed next.

Table 7.7. REFMIX Composition in Formats Used with Models of Melter SO₃ Tolerance at 1150 °C for LAW Glasses

Model Term	REFMIX Composition ^(a) (mass fractions)	REFMIX Composition (mass fractions) to Use in 10-Component RLM Model for melter SO ₃ tolerance ^(b)	REFMIX Composition (mass fractions) to Use in 11-Term PQM Model for melter SO ₃ tolerance ^(c)
Al ₂ O ₃	0.076182	0.076182	0.076182
B ₂ O ₃	0.097799	0.097799	0.097799
CaO	0.052807	0.052807	0.052807
Cl	0.003395	0.003395	0.003395
Cr ₂ O ₃	0.002052	NA	NA
F	0.001356	NA	NA
Fe ₂ O ₃	0.029893	NA	NA
K ₂ O	0.012131	NA	NA
Li ₂ O	0.014884	0.014884	0.014884
MgO	0.017084	NA	NA
Na ₂ O	0.169333	0.169334	0.169334
P ₂ O ₅	0.003257	0.003257	0.003257
SiO ₂	0.426931	0.426931	0.426931
SnO ₂	0.007629	NA	NA
TiO ₂	0.008079	NA	NA
V ₂ O ₅	0.007541	0.007541	0.007541
ZnO	0.032175	NA	NA
ZrO ₂	0.036421	NA	NA
Others	0.001051	0.147870	0.147870
Li ₂ O × Na ₂ O	NA	NA	0.00252037

(a) The composition in mass fractions is from Table 2.3 after normalizing out measured SO₃.
(b) See Table 7.4
(c) See Table 7.5.
(d) NA = not applicable, because the model does not contain this term.

Table 7.8. Predicted Melter SO₃ Tolerance at 1150 °C, Standard Deviation, and Statistical Intervals for the REFMIX Composition Used in Two Models for Melter SO₃ Tolerance at 1150 °C

Model for Melter SO ₃ Tolerance ^(a)	Predicted Melter SO ₃ Tolerance (wt%)	Standard Deviation of Predicted Melter SO ₃ Tolerance ^(b) (wt%)	90% upper CI ^(c) on Mean Melter SO ₃ Tolerance (wt%)	90% upper PI ^(c) on Individual Melter SO ₃ Tolerance (wt%)
11-Term PQM Model	0.874	0.024	0.904	1.100
10-Comp. RLM Model	0.946	0.024	0.977	1.187

(a) The two melter SO₃ tolerance models in this column are given in Table 7.5 (11-term PQM model) and (10-component RLM model), respectively.
(b) The standard deviation is for the melter SO₃ tolerance prediction considered to be the mean from many such results for the REFMIX glass.
(c) CI = one-sided upper confidence interval, PI = one-sided upper prediction interval (see Section B.6 of Appendix B).
(d) All calculations were performed using the REFMIX glass composition, model coefficients, and variance-covariance matrix values given in tables of this report. The calculated melter SO₃ tolerance values were rounded to three decimal places in this table.

Eq. (B.19a) can be used to calculate a one-sided 90% CI for the true mean of melter SO₃ tolerance values for the REFMIX glass composition with each of the melter SO₃ tolerance models. Similarly, based on the discussion in Section B.6.3, modifying Eq. (B.22a) by replacing “ \mp ” with “+” and replacing $t_{1-\alpha/2, n-p}$ with $t_{1-\alpha, n-p}$ can be used to calculate a one-sided 90% PI for an individual test value of melter SO₃ tolerance for the REFMIX glass composition with each of the melter SO₃ tolerance models. In the notation of these equations:

- 100(1- α)% = 90%, so that $\alpha = 0.10$ for a 90% CI in Eq. (B.19a) and a one-sided 90% PI based on the discussion following Eq. (B.22b) that describes the modified version of Eq. (B.22a).
- The vector **d** contains entries corresponding to the terms in a given melter SO₃ tolerance model, which are calculated using the composition of REFMIX in Table 7.7 with 0's for the BS or SR offset term and 3TS offset term.
- Matrix **D** is formed from the data matrix used in the regression that generated a given melter SO₃ tolerance model. Matrix **D** has the number of rows in the SO₃ modeling dataset (576 glasses, which equates to 635 melter SO₃ tolerance and solubility measurements – so the number of rows is 635) and the number of columns corresponding to the number of terms in a given melter SO₃ tolerance model. Each column is calculated according to the corresponding term in the model using two indicator columns (where for the first column it is 1 if the SO₃ solubility measurement came from the BS or SR method, 0 otherwise, and for the second column it is 1 if the SO₃ solubility measurement came from the 3TS method, 0 otherwise), followed by the LAW normalized glass composition in the melter SO₃ tolerance and solubility modeling dataset.

To calculate a one-sided 100(1 - α)% CI, the quantity $t_{1-\alpha, n-p} \sqrt{\mathbf{d}^T [(\mathbf{D}^T \mathbf{D})^{-1} MSE_{OLS}] \mathbf{d}}$ is added to the predicted melter SO₃ tolerance [denoted $\hat{y}(\mathbf{d})$], as indicated by Eq. (B.19a). To calculate a one-sided 100(1 - α)% PI, the quantity $t_{1-\alpha, n-p} \sqrt{MSE_{OLS} (1 + \mathbf{d}^T (\mathbf{D}^T \mathbf{D})^{-1} \mathbf{d})}$ is added to the predicted melter SO₃ tolerance [denoted $\hat{y}(\mathbf{d})$], as indicated by the modification of Eq. (B.22a) mentioned on page B.17 in the text just following Eq. (B.22b). The $MSE_{OLS} (\mathbf{D}^T \mathbf{D})^{-1}$ portion of these expressions is an estimate of the variance-covariance matrix for the estimated model coefficients, as discussed near the end of Section B.6 of Appendix B. For the example calculations presented in Table 7.8, the Students-*t* statistic value needed for both the one-sided upper CI and PI formulas describing the 10-component RLM model is 1.283049. This is based on $n=576$ and $p=10$. The following cell formula can be used to obtain the *t*-statistic value with Excel: =T.INV(0.90,576-10). For the UCI and UPI calculations associated with the 11-term PQM model described in Table 7.8, the Students-*t* statistic is 1.283052=T.INV(0.90,576-11). The variance-covariance matrices for the 10-component RLM model and the recommended 11-term PQM model are respectively listed in Tables D.8 and D.9 of Appendix D. The quantity $\sqrt{MSE_{OLS} \mathbf{d}^T (\mathbf{D}^T \mathbf{D})^{-1} \mathbf{d}}$ is the standard deviation of a model prediction (for a given composition vector **a** expressed in a given model form); the value for each model is given in the third column of Table 7.8. Using **D** instead of **G** in these equations as the offset terms are part of the data, not only the glass compositions themselves (**G**).

The 90% CIs and 90% PIs for the true mean and individual test result, respectively, of melter SO₃ tolerance in units of wt% for the REFMIX composition based on the two melter SO₃ tolerance models are given in the fourth and fifth columns of Table 7.8.

7.5 Suitability of the Recommended Melter SO_3 Tolerance at 1150 °C Model for Application by the WTP LAW Facility

The 11-term PQM model for melter SO_3 tolerance discussed in Section 7.3.3 is recommended for use by the WTP LAW Facility as the best model currently available for predicting melter SO_3 tolerance for LAW glasses. This model yields unbiased predictions of melter SO_3 tolerance over the full range of measured values with moderate scatter and some under-prediction at or above 1.8 wt% SO_3 solubility (see Figure 7.14). One reason for the moderate scatter and some non-linearity is the significant LOF of the recommended melter SO_3 tolerance model. Despite this LOF, the model maintains good performance for data not included in the model, as seen in the data splitting model statistics being close to the overall model statistics in Table 7.5. It is recommended that this model be revisited in the future to better address this LOF. Two of the evaluation subsets containing glasses with higher waste loadings (LP123 and Hi SO_3) did not perform all that well; however, part of the reason for this is that the 3TS SO_3 solubility method had greater variability (see Figure 7.15). The other four evaluation sets (WTP, ORP, LP2OL, and Hi Na_2O) performed well. The recommended 11-term PQM model does have a statistically significant LOF, so that a melter SO_3 tolerance prediction within and somewhat outside the operating limits may not be within the uncertainty of what would be obtained by batching and melting a LAW glass, measuring melter SO_3 tolerance at 1150 °C for the LAW glass, and determining the estimated value of melter SO_3 tolerance for the LAW glass (as discussed in Section 2.3). It's clear that 3TS results show larger scatter and are underpredicted by the model. However, it was not determined if there would be a LOF for models excluding 3TS data. That approach wasn't pursued because of the significant increase in SO_3 solubility afforded by including the 3TS data. There was a high (in absolute value) correlation between Li_2O and Na_2O of -0.818 and this may make some of the coefficient estimates not as interpretable as they would be otherwise. There was also a relatively high correlation between the offset indicators for BS and SR, and 3TS of -0.715 likely because MT and Bub were chosen as the reference (to have an offset of 0). This may have the effect of making the ratio of the coefficient estimates divided by the standard errors for the offset terms smaller than if a different reference was used. But these ratios were already quite large in absolute value (> 8) and show that the offset terms are highly significant. Although high correlation among predictors may make precise estimation of model parameters more difficult, predictions of new observations should still behave similarly to those available as long as they remain within the same space as the data used to fit the model (model validity ranges are summarized in Section 9.7).

Because of LOF of the recommended melter SO_3 tolerance models, prediction uncertainties for the models are moderate. Figure 7.17 displays the melter SO_3 tolerance prediction standard deviations versus predicted values (both in wt% units) for the LAW glass compositions in the melter SO_3 tolerance modeling dataset. The melter SO_3 tolerance prediction standard deviations for the melter SO_3 tolerance modeling dataset of 576 LAW glasses range from approximately 0.013 to 0.095 wt% for the recommended 11-term PQM model (range from approximately 0.013 to 0.60 wt% for all but LAW36S WTP glass). Note that prediction standard deviations will be larger for LAW glass compositions as their distance from glasses in the melter SO_3 tolerance modeling dataset increases. Also, the total uncertainty in predictions with the recommended 11-term PQM model will depend on the type of statistical interval used (see Section B.6 of Appendix B).

Work to assess the impact of LAW glass composition and model uncertainties for the recommended melter SO_3 tolerance model (Sections 7.3.3 and 7.3.4) on satisfying the WTP LAW Facility processing requirements for LAW glasses must be performed in the future.

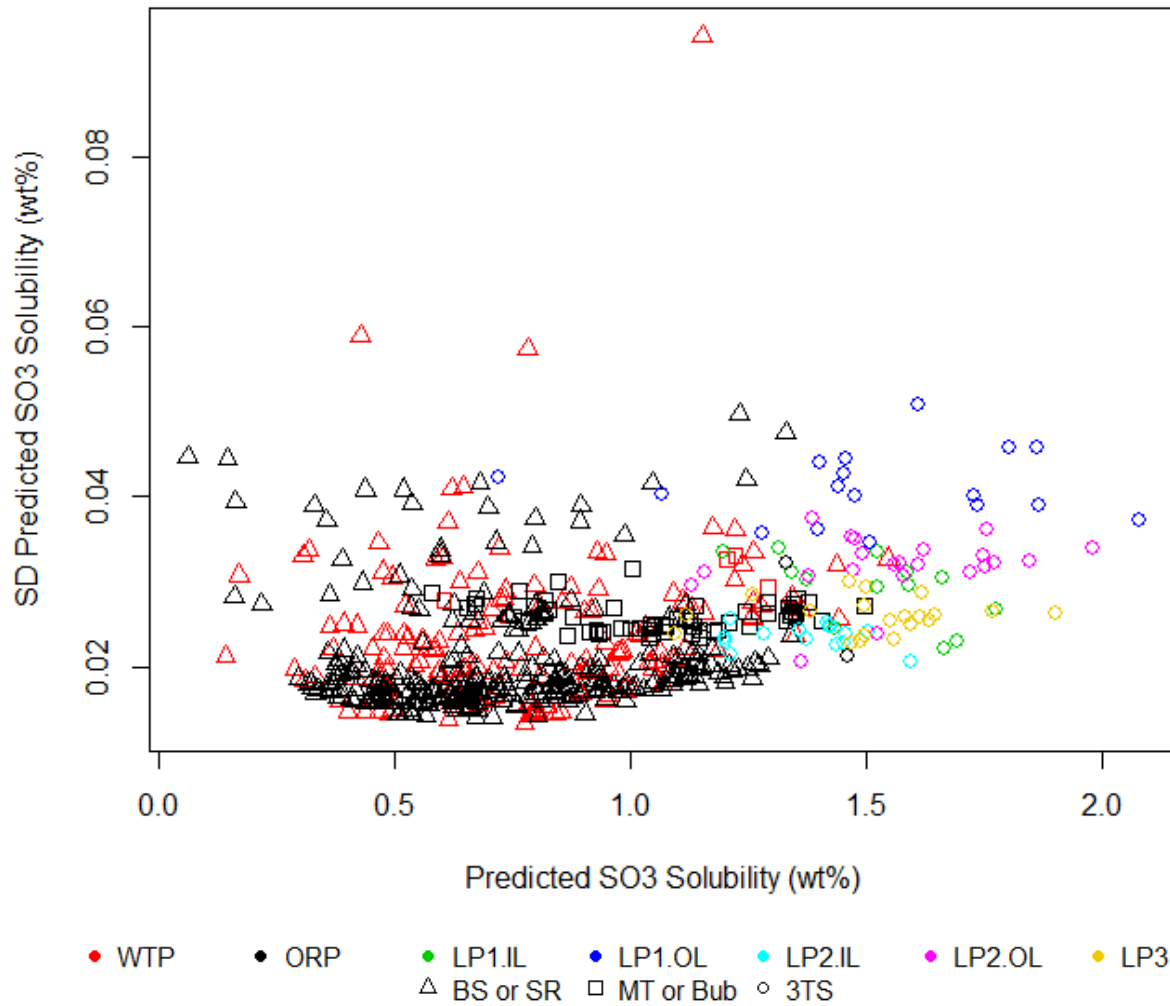


Figure 7.17. Prediction Standard Deviations versus Predicted Values over the LAW Glass Compositions in the 576-Glass Modeling Dataset for the Recommended 11-Term PQM Model for Melter SO₃ Tolerance at 1150 °C

The range of single component concentrations in the 576-glass dataset used for modeling is listed in Table 7.9. These ranges can be used to determine model validity ranges.

Table 7.9. Data Component Concentration Ranges (mass fraction) for LAW Glasses Used in Final Melter SO₃ Tolerance at 1150 °C Models

Component	20-component		19-component ^(b)		10-component ^(b)	
	Min	Max	Min	Max	Min	Max
Al ₂ O ₃	0.034972	0.147521	0.035031	0.148855	0.035031	0.148855
B ₂ O ₃	0.039670	0.159702	0.039891	0.160569	0.039891	0.160569
CaO	0.000000	0.128509	0.000000	0.129356	0.000000	0.129356
Cl	0.000000	0.011701	0.000000	0.011722	0.000000	0.011722
Cr ₂ O ₃	0.000000	0.006131	0.000000	0.006170	NA	NA
F	0.000000	0.030446	0.000000	0.030590	NA	NA
Fe ₂ O ₃	0.000000	0.134737	0.000000	0.135441	NA	NA
K ₂ O	0.000000	0.059085	0.000000	0.059394	NA	NA
Li ₂ O	0.000000	0.058352	0.000000	0.058977	0.000000	0.058977
MgO	0.000000	0.050222	0.000000	0.050505	NA	NA
Na ₂ O	0.024493	0.265729	0.024831	0.267422	0.024831	0.267422
P ₂ O ₅	0.000000	0.047463	0.000000	0.047880	0.000000	0.047880
SO ₃	0.000360	0.018300	NA	NA	NA	NA
SiO ₂	0.300014	0.522624	0.300541	0.525253	0.300541	0.525253
SnO ₂	0.000000	0.050299	0.000000	0.050756	NA	NA
TiO ₂	0.000000	0.050058	0.000000	0.050353	NA	NA
V ₂ O ₅	0.000000	0.043668	0.000000	0.043937	0.000000	0.043937
ZnO	0.000000	0.057806	0.000000	0.058645	NA	NA
ZrO ₂	0.000000	0.090004	0.000000	0.090162	NA	NA
Others ^(c)	0.000000	0.002707	0.000000	0.002720	0.065266	0.298376

(a) NA = not applicable, because the model does not contain this term.

(b) 19-component and 10-component ranges were calculated after normalizing without measured SO₃.

(c) Note: Others for the 10-components are composed of all the NA components except for measured SO₃ as well as Others for the 19-components.

8.0 Models Relating K-3 Refractory Corrosion to LAW Glass Composition

This section documents the development, evaluation, and validation of property-composition models and corresponding uncertainty expressions for predicting the 6-day K-3 refractory neck corrosion at 1208 °C (k_{1208}) of LAW glasses. Actually, $\ln(k_{1208})$ is modeled as a function of LAW glass composition, as discussed subsequently. The property-composition models and corresponding uncertainty expressions for $\ln(k_{1208})$ presented in this section were developed, evaluated, and validated using compositions and k_{1208} values for simulated LAW glasses.

Section 8.1 discusses the LAW glasses available and used for $\ln(k_{1208})$ -composition model development, evaluation, and validation. Section 8.2 presents the model forms for $\ln(k_{1208})$ that were investigated. Section 8.3 summarizes the results for the selected linear and quadratic mixture model forms for $\ln(k_{1208})$ and identifies the recommended model. Section 8.4 illustrates the calculation of k_{1208} predictions and the uncertainties in those predictions using selected $\ln(k_{1208})$ models and corresponding uncertainty equations. Section 8.5 discusses the suitability of the recommended $\ln(k_{1208})$ model for use by the WTP LAW Facility. Appendix B discusses the statistical methods and summary statistics used to develop, evaluate, and validate the several $\ln(k_{1208})$ model forms investigated, as well as statistical equations for quantifying the uncertainties in $\ln(k_{1208})$ model predictions.

8.1 K-3 Corrosion at 1208 °C Data Used for Model Development, Evaluation, and Validation

The data available and used for developing $\ln(k_{1208})$ models as functions of LAW glass composition are discussed in Section 8.1.1. The approaches and data used for validating and evaluating the models are discussed in Sections 8.1.2 and 8.1.3, respectively.

8.1.1 Model Development Data for K-3 Corrosion at 1208 °C

The data available for developing $\ln(k_{1208})$ -composition models consist of composition and k_{1208} values from 344 LAW glasses (see Table 2.2). These glasses and their normalized compositions based on measured (or estimated) SO_3 values are discussed in Section 2.0 and listed in Table A.4 of Appendix A. The corresponding k_{1208} values are presented in Table A.5.

8.1.1.1 Assessment of Available Glasses with Data for K-3 Corrosion at 1208 °C

The database of 344 glasses with k_{1208} results contains statistically designed as well as actively designed LAW glasses. Some actively designed glasses are outside the composition region covered by most of the LAW compositions. Such glasses are not ideal for inclusion in a modeling dataset because they can be influential when fitting models to data. Hence, it was decided to (i) graphically assess the 344 available LAW glass compositions with k_{1208} values and (ii) remove from the modeling dataset any compositions considered to be outlying or non-representative of LAW glasses of interest for the WTP LAW Facility.

Figure 8.1 displays plots of the mass fractions for 19 “main components” plus the Others component (the sum of all remaining components) in the 344 LAW glasses with k_{1208} data. These 20 components (including Others) have sufficient ranges and distributions of mass fraction values to support separate model terms if so desired. In Figure 8.1, the x-axis represents the mass fraction values of a LAW glass

component. The y-axis shows an index value representing each LAW glass composition, which aids in spreading out the data points to avoid over-plotting. The plotting symbols in Figure 8.1 correspond to the six groups of LAW glasses discussed in Section 2.3. For comparison purposes, the vertical lines in Figure 8.1 represent the ranges over which the LAW glass components were varied in the PNNL (i) LAW Phase 1 outer-layer study (blue lines), (ii) LAW Phase 2 outer-layer study (pink lines), and (iii) LAW Phase 3 study (pink lines), as shown in Table 2.1. Phases 2 and 3 focused on LAW glasses with high Na₂O waste loadings, whereas Phase 1 explored a larger LAW GCR with higher waste loadings.

Figure 8.1 shows that some of the 344 LAW glasses have “main components” with outlying mass fraction values compared to the remaining glasses and to the component ranges in the PNNL LAW Phase 1 (e.g., MgO), Phase 2, and Phase 3 studies. Table 8.1 lists the 11 LAW glasses excluded from the k_{1208} modeling dataset and the reason each glass was excluded.

Figure 8.2 show plots of component distributions after the 11 outlying glasses were removed from the k_{1208} dataset containing 344 glasses. Figure 8.2 shows for the remaining 333 LAW glasses that all 19 LAW glass “main components” have sufficient ranges and distributions of values within those ranges to support terms for modeling k_{1208} . Based on Figure 8.2, it was decided to use 20 components for initial k_{1208} modeling work. These components are Al₂O₃, B₂O₃, CaO, Cl, Cr₂O₃, F, Fe₂O₃, K₂O, Li₂O, MgO, Na₂O, P₂O₅, SO₃, SiO₂, SnO₂, TiO₂, V₂O₅, ZnO, ZrO₂, and Others (the sum of all remaining components). Note that these are the same 20 components chosen for initial modeling work for all other properties except melter SO₃ tolerance.

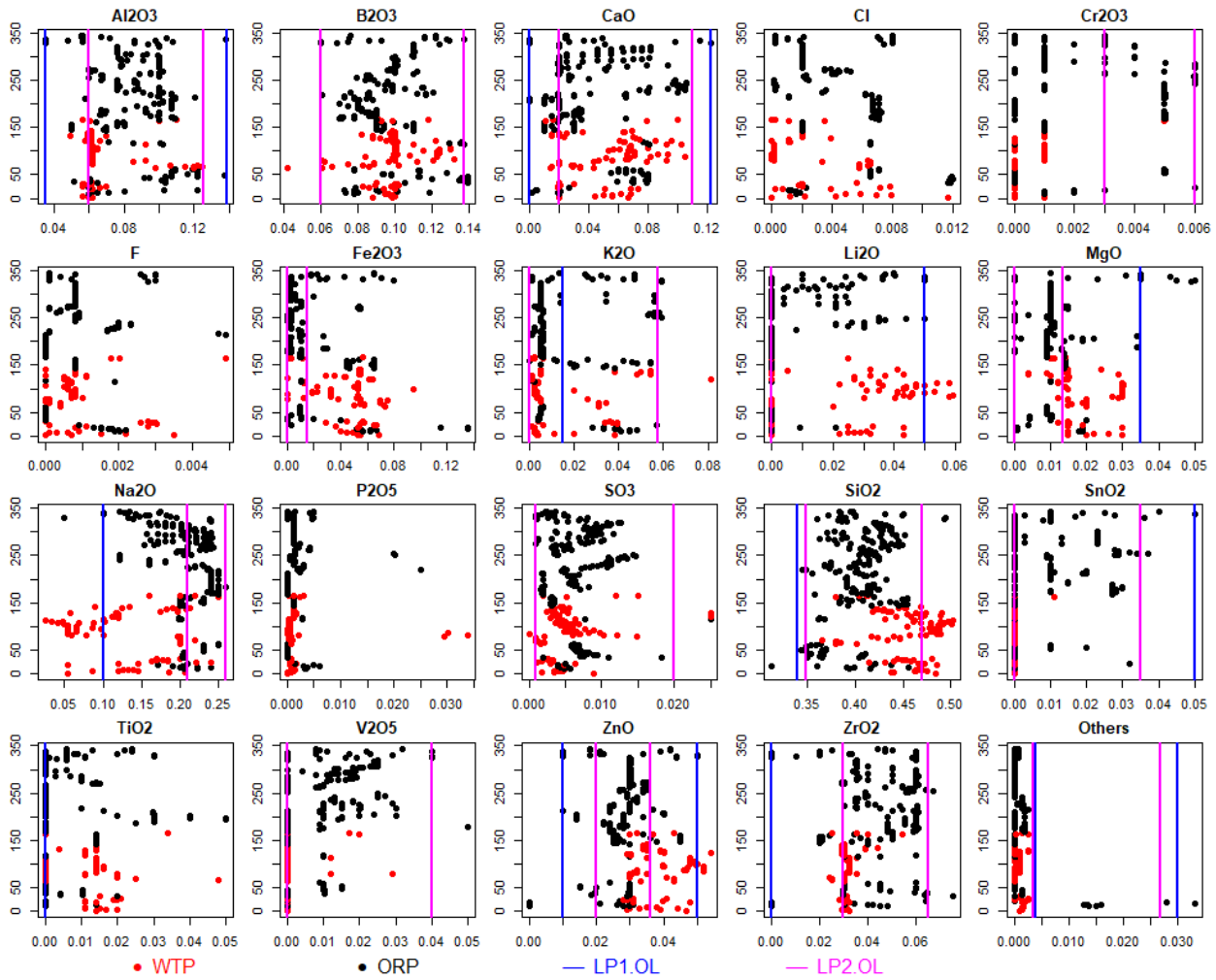


Figure 8.1. Distributions of 20 Main Components (in mass fractions) for 344 LAW Glass Compositions with Data for K-3 Corrosion at 1208 °C. The vertical lines (when present) represent the lower and upper limits for each component from the PNNL LAW Phase 1 outer-layer study (blue lines), Phase 2 outer-layer study (pink lines), and Phase 3 study (pink lines), as shown in Table 2.1. In cases where two limits are the same, pink lines over plot the blue lines.

Table 8.1. Eleven LAW Glasses Excluded from the Modeling Dataset for K-3 Corrosion at 1208 °C

Glass #	Glass ID	Reason Glass Excluded from k_{1208} Modeling Dataset ^(a)
k022	AY102D2-01	Others > 0.02 (= 0.0332) mf
k023	AY102D2-05	Others > 0.02 (= 0.0332) mf
k024	AY102D2-06	Others > 0.02 (= 0.0279) mf
k128	LAWC25S	K ₂ O > 0.065 (= 0.081) mf
k255	ORPLA20HV	V ₂ O ₅ > 0.04 (= 0.05) mf
k079	LAWA44PNCC	Container-centerline-cooled glass
k080	LAWA44PNCC-repeat	Container-centerline-cooled glass
k093	LAWB67	Outlier in response < 0.003 (= 0.001) inch
k189	LORPM4R2	Outlier in response < 0.003 (= 0.001) inch
k174	LORPM11	Outlier in response < 0.003 (= 0.001) inch
k187	LORPM38	Outlier in response < 0.003 (= 0.001) inch

(a) mf = mass fraction.

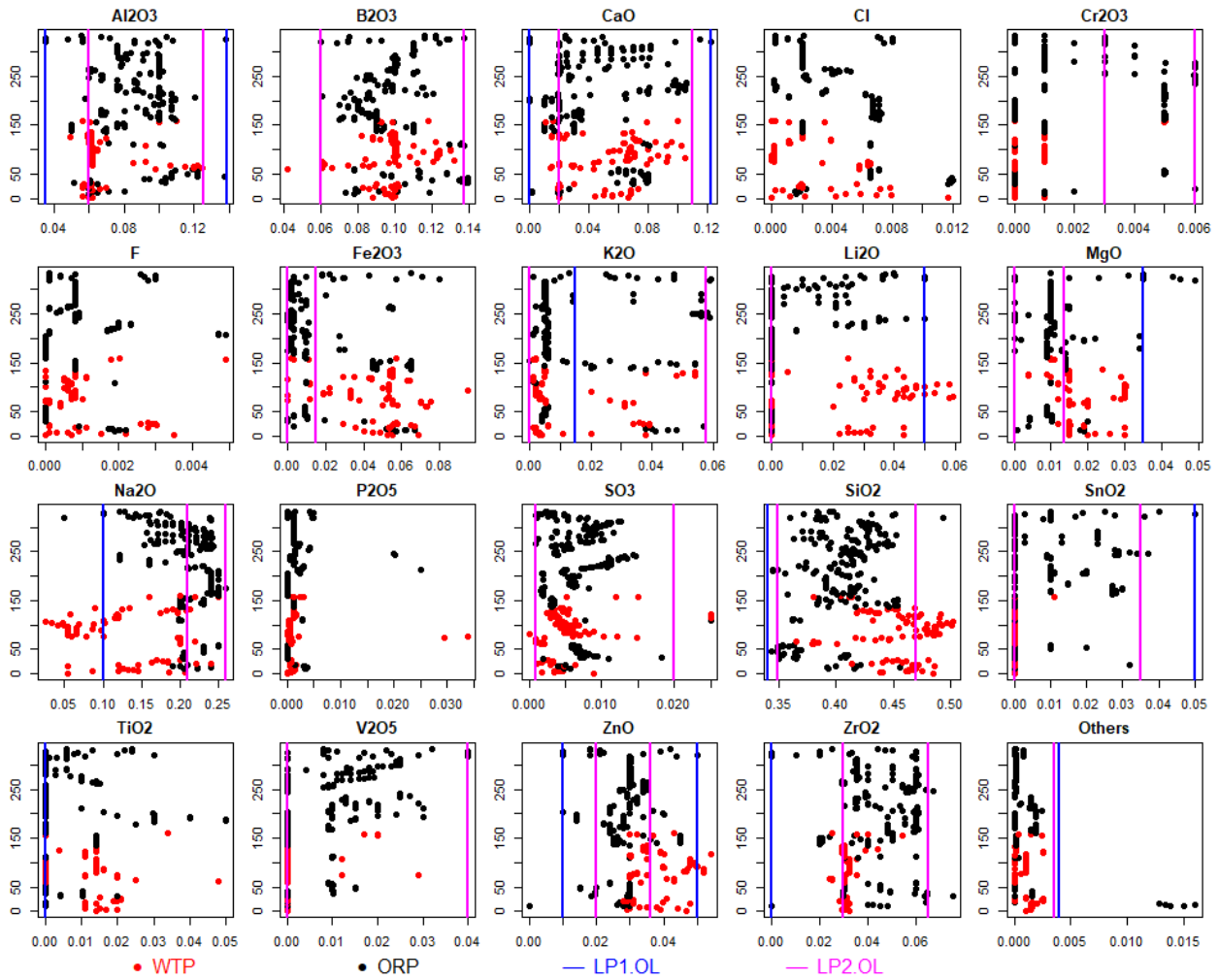


Figure 8.2. Distributions of 20 Main Components (in mass fractions) for 333 LAW Glass Compositions with Data for K-3 Corrosion at 1208 °C that Remain after Excluding the 11 Glasses in Table 8.1. The vertical lines (when present) represent the lower and upper limits for each component from the PNNL LAW Phase 1 outer-layer study (blue lines), Phase 2 outer-layer study (pink lines), and Phase 3 study (pink lines), as shown in Table 2.1. In cases where two limits are the same, pink lines over plot the blue lines.

Figure 8.3 shows a scatterplot matrix of the 333 glasses remaining in the k_{1208} modeling dataset after removing the 11 outlying compositions. High correlations between some pairs of components are evident, so pairwise correlation coefficients were calculated. These can vary from -1.0 (perfect negative correlation) to 0 (no correlation) to 1.0 (perfect positive correlation). There were four component pairs with correlations larger (in absolute value) than 0.60 : Na_2O and Li_2O (-0.917), Al_2O_3 and SiO_2 (-0.6968), Na_2O and MgO (-0.614), and Na_2O and SiO_2 (-0.690). Such high pairwise correlations, especially the one for Na_2O - Li_2O , can make it difficult for regression methods to properly estimate the effects of correlated components on the response variable (e.g., k_{1208}). Further, such high correlations in the predictors make parameter values difficult to estimate and result in inflated prediction uncertainties. Thus, these high pairwise correlations need to be kept in mind when developing and interpreting LAW

glass property-composition models for k_{1208} . See Section 9.7 for further detail on treatment of highly correlated component concentrations.

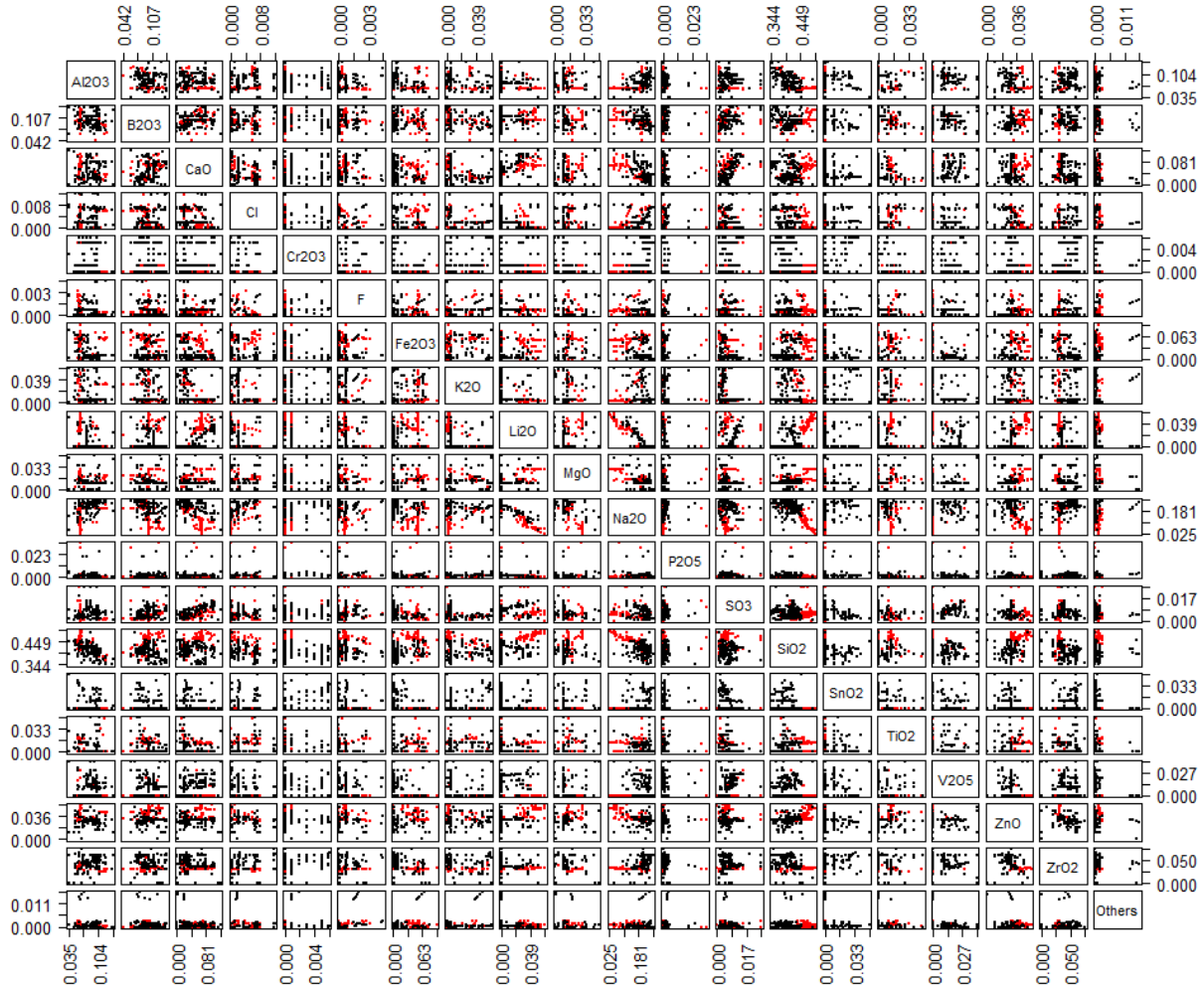


Figure 8.3. Scatterplot Matrix of 20 Components (mass fractions) for the 333 LAW Glasses with K-3 Corrosion at 1208 °C Data that Remain after Excluding the 11 Glasses in Table 8.1

8.1.1.2 K-3 Corrosion at 1208 °C Modeling Dataset

Table A.4 in Appendix A lists the Glass #s, Glass IDs, and k_{1208} values for the 333 remaining simulated LAW glasses used for k_{1208} model development. The k_{1208} values for the 11 glasses excluded as outliers from the 344-glass modeling dataset (see Table 8.1) are marked with an asterisk in Table A.5. The compositions for these 333 LAW glasses are included in Table A.4. The glass compositions in Table A.4 are the normalized mass fractions (mf) of the 20 components previously identified as having sufficient data to support a separate model term if needed. The normalized LAW glass compositions in Table A.4 were obtained as discussed in Section 2.2. Specifically, starting with the target mass fractions for all 20 components, the measured (or estimated) SO_3 mass fractions (see Section 2.2) were substituted for the target SO_3 mass fractions, and the mass fractions of the remaining 19 components were normalized so the total mass fractions of all 20 components for each glass equaled precisely 1.000000.

The values of k_{1208} in Table A.5 for the 333 glasses in the modeling dataset range from 0.003 to 0.145 inch.

8.1.1.3 Replicate and Near-Replicate Data for K-3 Corrosion at 1208 °C

The changes to the LAW glass compositions caused by the renormalization associated with using measured (or estimated) SO_3 values (see Section 2.2) resulted in some replicate glasses not having exactly equal normalized compositions. Such compositions are near-replicates. For ease of discussion, henceforth both replicates and near-replicates are referred to as replicates.

Table 8.2 lists the replicate sets of LAW glasses in the k_{1208} modeling dataset and the corresponding k_{1208} values. Table 8.2 also lists estimates of (i) %RSDs [calculated using k_{1208} values in original inch units] and (ii) SDs [calculated using $\ln(k_{1208})$ values in $\ln(\text{inch})$ units] for each replicate set. The %RSD values for 17 of the 24 replicate sets range from 5.16% to 32.64%; one set had a 1.99 %RSD while the %RSD values for the other 6 replicate sets ranged from 40.41% to 60.61%. No reasons for these higher %RSD values for the 6 replicate sets could be found in the data-source reports. Hence, it was assumed that periodically there may be larger uncertainties in batching and melting glasses and determining k_{1208} . Table 8.2 also lists pooled estimates of %RSDs and SDs calculated over all replicate sets. A pooled %RSD or SD combines the separate %RSD or SD estimates from each replicate set, so that a more precise combined estimate of %RSD or SD is obtained. These pooled %RSDs and SDs include uncertainties due to fabricating glasses, and the process of determining k_{1208} values. The magnitudes of the pooled SD = 0.3311 [in $\ln(\text{inch})$ units] and pooled %RSD = 30.27 [in percentage relative to $\ln(k_{1208})$ units] in Table 8.2 indicate there is a total relative uncertainty of approximately 30% in the k_{1208} values over the replicate glasses. The pooled estimates of replicate uncertainty for k_{1208} in Table 8.2 are used subsequently to assess LOF of the various $\ln(k_{1208})$ models considered.

Table 8.2. Uncertainty in K-3 Corrosion at 1208 °C Responses for Replicate and Near-Replicate Sets

Replicate Set		Replicate Set		SD [ln(in)]
Glass #s	Replicate Set Glass IDs	k_{1208} (inch) Values	%RSD ^(a)	
k025	B1-AZ101	0.0065		
k092	LAWB65	0.0030		
k107	LAWB83	0.0095	43.40	0.5434
k108	LAWB84	0.0095		
k002	A2-AP101	0.0255		
k031	LAWA126	0.0140	29.03	0.3206
k032	LAWA126R3	0.0230		
k040	LAWA152S2	0.0240		
k051	LAWA168S2	0.0330	22.33	0.2252
k044	LAWA160S2	0.0155		
k050	LAWA167S2	0.0290	42.90	0.4430
k059	LAWA187	0.0327		
k060	LAWA187R1	0.0660	47.71	0.4966
k078	LAWA44-3	0.0190		
k081	LAWA44R11	0.0250		
k079	LAWA44PNCC ^(b)	0.0135 ^(b)	19.28	0.1941
k080	LAWA44PNCC-repeat ^(b)	0.0095 ^(b)		
k098	LAWB72	0.0075		
k105	LAWB81	0.0120	32.64	0.3323
k131	LAWC31	0.0175		
k132	LAWC31R2	0.0180	1.99	0.0199
k254	ORPLA20	0.0330		
k256	ORPLA20R1	0.0395	12.68	0.1271
k267	ORPLA43	0.0230		
k268	ORPLA43R1-1	0.0345	28.31	0.3019
k269	ORPLA43R1-2	0.0415		
k272	ORPLA46	0.0470		
k273	ORPLA46-Repeat	0.0385	14.06	0.1411
k313	ORPLE4	0.0865		
k314	ORPLE4-Repeat 2010	0.0935	5.50	0.0550
k319	ORPLF10	0.0090		
k320	ORPLF10-Repeat	0.0050	40.41	0.4156
k321	ORPLF13	0.0125		
k322	ORPLF14	0.0170	21.57	0.2174
k324	ORPLF7	0.0100		
k325	ORPLF7-Repeat	0.0200	47.14	0.4901
k028	I10-G-130B	0.0240		
k333	ORPLG27	0.0340	24.38	0.2463
k335	ORPLG6	0.0225		
k336	ORPLG7	0.0265	11.54	0.1157
k013	AP105DLAW6	0.0200		
k015	AP105DLAW8	0.0320	32.64	0.3323
k197	ORLEC13	0.0110		
k210	ORLEC26	0.0275	60.61	0.6479
k222	ORLEC37	0.0300		
k229	ORLEC43	0.0250	12.86	0.1289
k223	ORLEC38	0.0405		
k230	ORLEC44	0.0350	10.30	0.1032
k227	ORLEC41	0.0395		
k233	ORLEC47	0.0360	6.56	0.0656
k228	ORLEC42	0.0355		
k234	ORLEC48R	0.0330	5.16	0.0516
k235	ORLEC49	0.0210		
k236	ORLEC49-Repeat	0.0250	12.30	0.1233
k189	LORPM4R2-Repeat	0.0030		
k190	LORPM4R2 ^(b)	0.0010 ^(b)	NA	NA
Pooled Over All 24 Replicate Sets with 28 total DF^(c)			30.27	0.3311

(a) %RSD = 100 × (Standard Deviation / Mean).
(b) Outlier data points excluded from modeling and from replicate set pooled standard deviations.
(c) DF = degrees of freedom.

8.1.2 Model Validation Approach and Data for K-3 Corrosion at 1208 °C of LAW Glasses

The validation approach for k_{1208} models was based on splitting the 333-glass dataset for model development into five modeling/validation subsets. Of the 333 model-development glasses, 52 were in 24 replicate sets. The five modeling/validation splits of the 333 glasses in the k_{1208} modeling dataset were formed as follows:

- The 52 replicate glasses in 24 replicate sets were set aside so they would always be included in each of the five model development datasets. This was done so that replicate sets would not be split between modeling and validation subsets, thus negating the intent to have validation glasses different than model development glasses.
- The remaining 281 glasses were ordered from smallest to largest according to their k_{1208} values (inch). The 281 glasses were numbered 1, 2, 3, 4, 5, 1, 2, 3, 4, 5, etc. All of the 1's formed the first model validation set, while all of the remaining points formed the first model development dataset. Similarly, all of the 2's, 3's, 4's, and 5's respectively formed the second, third, fourth, and fifth model validation sets. In each case, the remaining non-2's, non-3's, non-4's, and non-5's formed the second, third, fourth, and fifth model development datasets. Because 281 is not evenly divisible by 5, the five modeling and validation subsets did not all contain the same numbers of glasses. One of the five splits contained 57 glasses for validation and 224 glasses for modeling. The other four splits contained 56 glasses for validation and 225 for modeling. Note that these numbers of glasses in the modeling subsets do not yet include the 52 replicates.
- The 52 replicate glasses were added to each of the split modeling subsets. Including the replicates, one split contained 276 glasses for modeling and 57 for validation, while the other four splits contained 277 glasses for modeling and 56 for validation.

Data splitting was chosen as the validation approach because the k_{1208} modeling dataset contains all compositions that (i) are in the LAW GCR of interest, (ii) meet QA requirements, and (iii) have k_{1208} data. Having a separate validation dataset not used for modeling is desirable, but it was necessary to develop k_{1208} models using all appropriate data.

8.1.3 Subsets of LAW Glasses to Evaluate Prediction Performance of Models for K-3 Corrosion at 1208 °C

Section 2.4 discusses six subsets of LAW glasses for evaluating the prediction performance of LAW glass property-composition models, including subsets of glasses with higher waste loadings. The subsets, as discussed in Section 2.4, are denoted WTP, ORP, LP2OL, LP123, HiNa₂O, and HiSO₃. The k_{1208} modeling dataset of 333 LAW glasses (see Section 8.1.1) contains 98, 235, 40, 0, 136, and 65 glasses with k_{1208} values in these six evaluation subsets, respectively. The “Glass #s” of these six evaluation subsets of LAW glasses are listed in Table C.6 of Appendix C. The normalized LAW glass compositions and k_{1208} values for the glasses with these “Glass #s” are listed in Tables A.4 and A.5, respectively, of Appendix A.

Model performance/prediction summary statistics denoted R^2_{Eval} and $RMSE_{Eval}$ (see Section B.3 of Appendix B), as well as predicted versus measured plots (see Section B.3), are subsequently used to assess the prediction performance of the k_{1208} models (presented in later subsections) for the five evaluation subsets listed in Table C.6 of Appendix C.

8.2 Model Forms for K-3 Corrosion at 1208 °C of LAW Glasses

Ideally, a property-composition model for k_{1208} would use known mechanisms of k_{1208} as a function of LAW glass composition. However, no such mechanisms are known. Empirical models for k_{1208} with coefficients estimated from model development data have been shown in the past to perform well. The empirical model forms used are from the general class of *mixture experiment models* (Cornell 2002), which includes models linear in composition as well as non-linear in composition. Section B.1 of Appendix B discusses mixture experiments and several general forms of mixture experiment models.

Section 8.2.1 discusses the forms of mixture experiment models used for k_{1208} of LAW glasses. Section 8.2.2 discusses the use of natural-log-transformed k_{1208} values as the response variable for k_{1208} modeling.

8.2.1 Mixture Experiment Model Forms for K-3 Corrosion at 1208 °C of LAW Glasses

The LM and PQM model forms introduced in Section B.1 of Appendix B were chosen for use in modeling $\ln(k_{1208})$ as a function of LAW glass composition. These models have been used in the past (e.g., Muller et al. 2018) to model the compositional dependence of $\ln(k_{1208})$ -composition. The LM model form is given by

$$\ln(k_{1208}) = \sum_{i=1}^q \beta_i g_i + e \quad (8.1)$$

while the PQM model form is given by

$$\ln(k_{1208}) = \sum_{i=1}^q \beta_i g_i + \text{Selected} \left\{ \sum_{i=1}^q \beta_{ii} g_i^2 + \sum_{i < j}^{q-1} \beta_{ij} g_i g_j \right\} + e \quad (8.2)$$

where in Eqs.(8.1) and (8.2):

- $\ln(k_{1208})$ = natural logarithm of k_{1208} (in inches)
- g_i = normalized mass fraction of the i^{th} glass oxide or halogen component
- $(i = 1, 2, \dots, q)$, such that $\sum_{i=1}^q g_i = 1$
- β_i = coefficient of the i^{th} linear blending term ($i = 1, 2, \dots, q$)
- β_{ii} and β_{ij} = coefficients of selected quadratic (squared or crossproduct) blending terms to be estimated from the data
- e = random error for each data point.

Many statistical methods exist for the case where the e is statistically independent (i.e., not correlated) and normally distributed with mean 0 and standard deviation σ . In Eq. (8.2), “Selected” means that only some of the terms in curly brackets are included in the model. The subset is selected using stepwise regression or other variable selection methods (Draper and Smith 1998; Montgomery et al. 2012). PQM models are discussed in more detail and illustrated by Piepel et al. (2002) and Smith (2005).

Cornell (2002) discusses many other empirical mixture model forms that could have been considered for k_{1208} -composition modeling. However, these other mixture model forms were not investigated because the

special blending effects of components associated with those models were judged not to apply for k_{1208} . The model forms in Eqs. (8.1) and (8.2) are widely used in many application areas (including waste glass property modeling) and often predict the response very well.

8.2.2 Transformation of K-3 Corrosion at 1208 °C for LAW Glasses

In modeling k_{1208} , it is advantageous to use the natural logarithm transformation of the k_{1208} values. The advantages of this transformation include the following:

- The k_{1208} values for the 333 LAW glasses in the k_{1208} modeling dataset range from 0.003 to 0.145 inch. This range is significantly more than one order of magnitude. In such cases, typically the uncertainty in making glasses and determining k_{1208} leads to smaller absolute uncertainties for smaller k_{1208} values and larger absolute uncertainties for larger k_{1208} values. Hence, the OLS regression assumption of equal variances for all response variable values (see Section B.2.1 of Appendix B) is violated. After a logarithmic transformation, variances of k_{1208} values tend to be approximately equal as required for OLS regression.
- A logarithmic transformation tends to linearize the compositional dependence of k_{1208} data and reduce the need for non-linear terms in the model form.
- A natural logarithm transformation is preferred over a common logarithm (or other base logarithm) transformation because of the approximate relationship

$$SD [\ln(y)] \cong RSD (y) \quad (8.3)$$

where SD denotes standard deviation, RSD denotes relative standard deviation (i.e., the standard deviation divided by the mean), and y denotes k_{1208} . Eq. (8.3) results from applying the first-order variance propagation formula [Eq. (7-7) of Hahn and Shapiro (1967)] to the function $z = \ln(y)$. The relationship in Eq. (8.3) is very useful, in that uncertainties of the natural logarithm of the response variable y can be interpreted as approximate RSDs of the untransformed response variable y .

For these reasons, the natural logarithmic transformation was employed for all k_{1208} model forms.

8.3 Property-Composition Model Results for K-3 Corrosion at 1208 °C of LAW Glasses

This section discusses the results of fitting several different mixture experiment models using natural logarithms of k_{1208} (inch) as functions of LAW glass compositions. Section 8.3.1 presents the results of modeling $\ln(k_{1208})$ using a 20-component LM model. Sections 8.3.2 and 8.3.3 present the results of modeling $\ln(k_{1208})$ using LM and PQM models based on a reduced set of mixture components. Finally, Section 8.3.4 compares the results from the three models and recommends a $\ln(k_{1208})$ model for future use and evaluation.

8.3.1 Results from the 20-Component Full Linear Mixture Model for the Natural Logarithm of K-3 Corrosion at 1208 °C with LAW Glasses

As the initial step in $\ln(k_{1208})$ -composition model development, a FLM model in the 20 components identified in Section 8.1.1.1 was fit to the modeling data (333 LAW glasses). Table 8.3 contains the results for the 20-component FLM model of $\ln(k_{1208})$. Table 8.3 lists the model coefficients, standard deviations of the coefficients, and model fit statistics for the 20-component FLM model on $\ln(k_{1208})$ using the modeling dataset (333 LAW glasses). Table 8.3 also contains the results from the (i) data-splitting

validation approach (see Section 8.1.2), and (ii) evaluation of model predictions for the five evaluation subsets (see Section 8.1.3). In the data-splitting validation portion of the results at the bottom of Table 8.3, the columns are labeled DS1, DS2, DS3, DS4, and DS5 to denote the five modeling/validation splits of the data as described in Section 8.1.2. The last column of this part of Table 8.3 shows the averages for the different statistics over the five splits.

The $R^2 = 0.8162$, $R^2_A = 0.8050$, and $R^2_P = 0.7875$ statistics (see Section B.3 of Appendix B) in Table 8.3 show that (i) the 20-component FLM model fits the $\ln(k_{1208})$ data in the 333-glass modeling dataset reasonably well, (ii) there are not a large number of unneeded model terms, and (iii) there are not any highly influential data points. The RMSE = 0.3305 is slightly smaller than the pooled glass batching and k_{1208} determination uncertainty [$SD = 0.3311$ in $\ln(\text{inch})$ units] estimated from replicates in Table 8.3. The model LOF p-value = 0.5361 in Table 8.3 does not indicate that the 20-component FLM model has a significant LOF. However, the fact that the RMSE and pooled SD are noticeably higher than similar values for properties such as viscosity and EC, combined with the fact that the model LOF p-value is noticeably smaller than similar values for viscosity and EC, indicates that the 20-component FLM model does involve relatively high random error and has the potential for some degree of model LOF. See Section B.3 for discussion of the statistical test for model LOF.

At the bottom right of Table 8.3, the average model-fit statistics (R^2 , R^2_A , R^2_P , and RMSE) over the five data-splits are close to the statistics obtained from fitting the 20-component FLM model for $\ln(k_{1208})$ to all 333 glasses in the modeling dataset. The data-split validation statistics (R^2_V and $RMSE_V$) are also relatively close to the R^2 and RMSE (i) values from fitting the model to the full dataset, and (ii) averages from fitting the model to the data-split modeling subsets. This indicates that the 20-component FLM model maintains its predictive performance for data not used to fit the model.

Table 8.3. Coefficients and Performance Summary for the 20-Component Full Linear Mixture Model on the Natural Logarithm of K-3 Corrosion at 1208 °C for LAW Glasses

$\ln(k_{1208})$ 20-Component LM Model Term	Coefficient Estimate	Coefficient Stand. Err.
Al ₂ O ₃	-22.0645	1.3325
B ₂ O ₃	-3.5622	1.1660
CaO	8.6463	1.0901
Cl	-30.7667	9.0089
Cr ₂ O ₃	-96.6545	12.8159
F	6.8661	26.3477
Fe ₂ O ₃	0.1346	1.3399
K ₂ O	5.8944	1.4174
Li ₂ O	47.1575	3.5501
MgO	-5.6774	3.2280
Na ₂ O	22.3786	1.0641
P ₂ O ₅	-12.0946	5.9963
SO ₃	-13.3407	5.9777
SiO ₂	-12.8906	0.5359
SnO ₂	-1.0459	2.9400
TiO ₂	-2.9130	2.3023
V ₂ O ₅	-23.5116	2.8286
ZnO	-9.7077	3.0036
ZrO ₂	-7.8000	2.1744
Others ^(c)	-2.1388	10.7755

Modeling Data Statistic, 333 Glasses ^(a)		
		Value
R ²		0.8162
R ² _A		0.8050
R ² _P		0.7875
RMSE		0.3305
Model LOF p-value		0.5361

Evaluation Set (# Glasses) ^(b)		
	R ² _{Eval}	RMSE _{Eval}
WTP (98)	0.8399	0.3305
ORP (235)	0.5774	0.3455
LP2OL (40)	-0.6198	0.5306
LP123 (0)	NA	NA
HiNa ₂ O (136)	0.3865	0.3954
HiSO ₃ (65)	0.7163	0.3885

Data Splitting Statistic ^(a,d)	DS1	DS2	DS3	DS4	DS5	Average
R ²	0.8215	0.8220	0.8071	0.8245	0.8092	0.8169
R ² _A	0.8083	0.8088	0.7928	0.8115	0.7951	0.8033
R ² _P	0.7889	0.7876	0.7694	0.7890	0.7691	0.7808
RMSE	0.3299	0.3302	0.3387	0.3217	0.3340	0.3309
R ² _V	0.7533	0.7655	0.8435	0.7285	0.8338	0.7849
RMSE _V	0.3595	0.3442	0.3034	0.3965	0.3254	0.3458

(a) The model evaluation statistics are defined in Section B.3 of Appendix B. The model validation statistics are defined in Section B.5.

(b) The six sets of LAW evaluation glasses are discussed in Section 2.4. Five of these sets are applicable to k_{1208} models as described in Section 8.1.3.

(c) For the 20-component FLM model, the “Others” component includes any components not separately listed.

(d) The evaluation and validation statistics calculated for data-splits are defined the same as for separate modeling and validation sets. Section 8.1.2 describes how the modeling dataset was split into modeling and validation subsets.

for glasses with lower waste loadings (the older WTP glasses). The low R^2_{Eval} values and the significantly reduced model validity region for the k_{1208} model (compared to other models in this report) suggest that further data and modeling are required before directly applying this constraint in formulation of glasses for the WTP LAW Facility. We therefore recommend this model be used for indication only.

Figure 8.4 shows the PvM plot for the 333-glass modeling dataset using the 20-component FLM model for $\ln(k_{1208})$. The plot illustrates that the 20-component FLM model predicts $\ln(k_{1208})$ reasonably well, with only a slight tendency to under-predict high values and over predict low values.

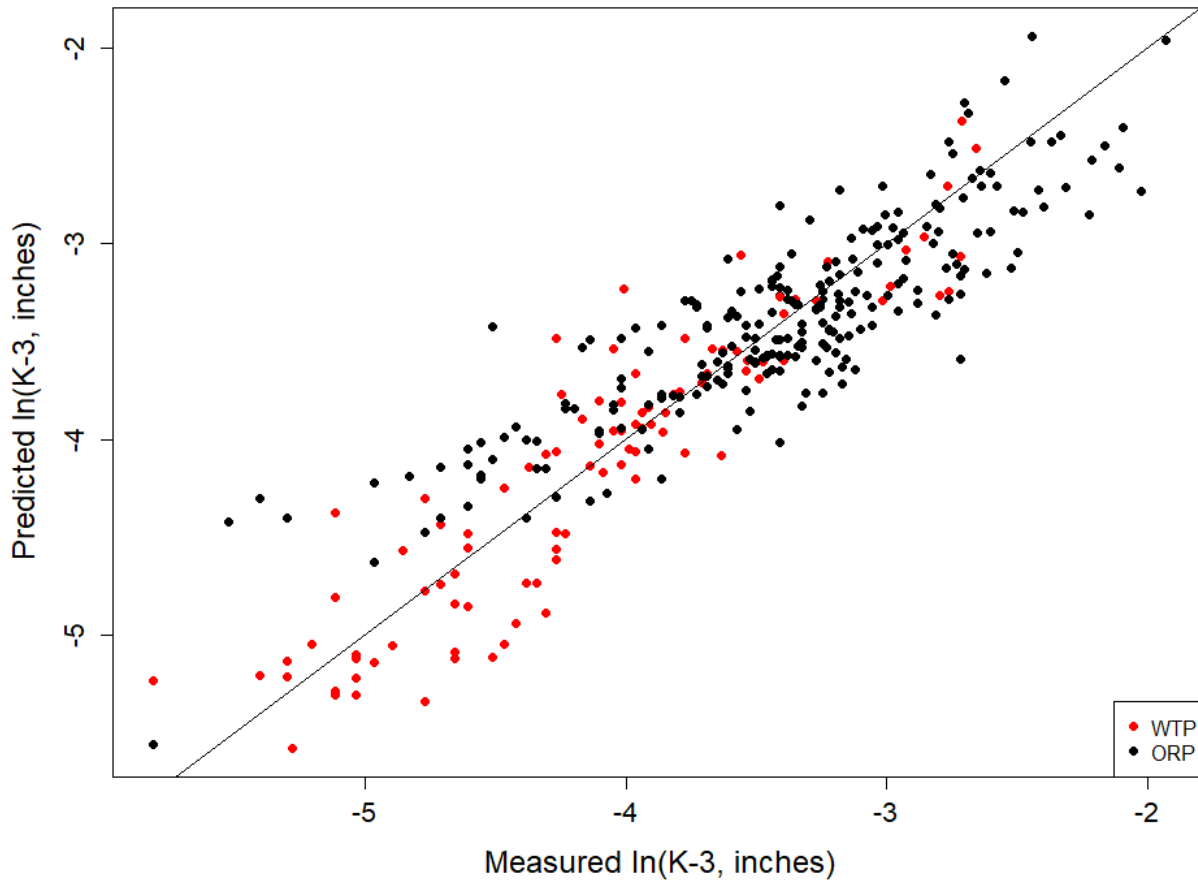


Figure 8.4. Predicted versus Measured Plot for the 333-Glass Modeling Dataset Using the 20-Component Full Linear Mixture Model on the Natural Logarithm of K-3 Corrosion at 1208 °C for LAW Glasses

Figure 8.5 displays PvM plots using the 20-component FLM model for $\ln(k_{1208})$ in Table 8.3 applied to the five evaluation subsets discussed in Section 8.1.3. Each plot in the figure contains the evaluation R^2 and RMSE values for the corresponding evaluation subset. Figure 8.5 shows that the 20-component FLM model for $\ln(k_{1208})$ fit to the 333-glass modeling dataset generally predicts reasonably well for the WTP and HiSO_3 evaluation subsets. The fits to the ORP and HiNa_2O subsets show more scatter with perhaps a slight bias for the ORP subset. The model did not well predict to the LP2OL subset.

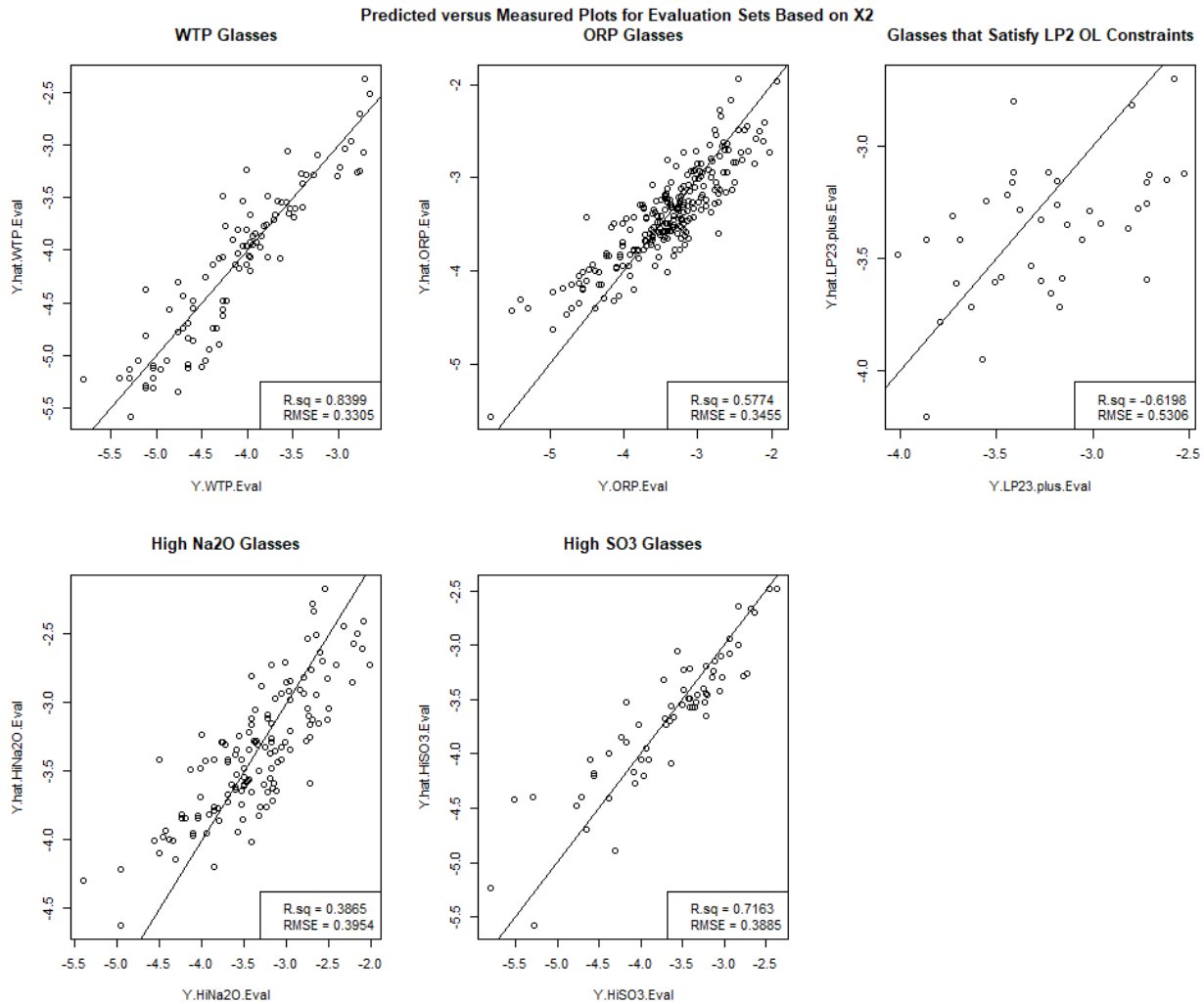


Figure 8.5. Predicted versus Measured Plots for the Five Evaluation Subsets Using the 20-Component Full Linear Mixture Model on the Natural Logarithm of K-3 Corrosion at 1208 °C for LAW Glasses

The model in Table 8.3, fit to the 333-glass modeling dataset, provides a starting point for reducing the LM model [i.e., removing separate terms for components that do not significantly influence $\ln(k_{1208})$]. Hence, the 20-component LM model was used to produce the response trace plot (see Section B.4.1 in Appendix B) shown in Figure 8.6. The average glass composition of the 1074 glasses in the compiled database discussed in Section 2.3 was used as the REFMIX (see Section B.4.1) in response trace plots for every property. The glass composition of the REFMIX is listed in Table 2.3.

The response trace plot in Figure 8.6 shows that Li₂O, Na₂O, CaO, and K₂O are predicted to increase $\ln(k_{1208})$ the most, while Cr₂O₃, Cl, V₂O₅, Al₂O₃, and SiO₂ are predicted to decrease $\ln(k_{1208})$ the most. The remaining components have predicted response traces with small to negligible slopes, indicating that those components are predicted to have small to negligible effects on $\ln(k_{1208})$.

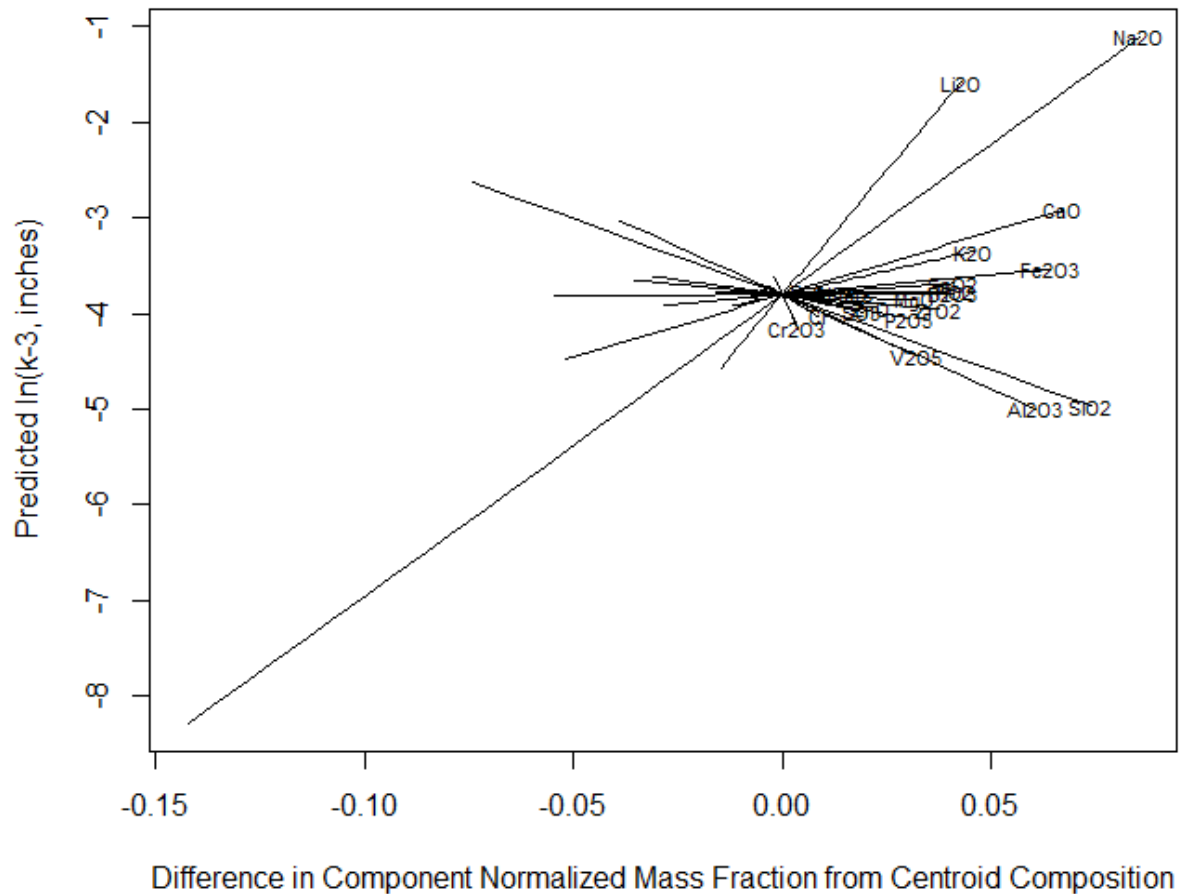


Figure 8.6. Response Trace Plot for the 20-Component Full Linear Mixture Model on the Natural Logarithm of K-3 Corrosion at 1208 °C for LAW Glasses

8.3.2 Results from a Reduced Linear Mixture Model for the Natural Logarithm of K-3 Corrosion at 1208 °C with LAW Glasses

The 20-component FLM model for $\ln(k_{1208})$ presented in Section 8.3.1 likely contains components that do not significantly contribute to predicting $\ln(k_{1208})$, so model reduction was the next step of the model development approach. Thus, LM models for $\ln(k_{1208})$ involving fewer than the 20 components were considered. The sequential F-test model reduction approach (see Section B.4.1 of Appendix B; Piepel and Cooley 2006) was used.

8.3.2.1 Numerical Results for the 11-Component Reduced Linear Mixture Model on the Natural Logarithm of K-3 Corrosion at 1208 °C for LAW Glasses

The RLM model for $\ln(k_{1208})$, using the F-test approach and a significance level of 0.001 while forcing B_2O_3 and K_2O in as model terms, contained terms for 11 components: Al_2O_3 , B_2O_3 , CaO , Cr_2O_3 , K_2O , Li_2O , Na_2O , SiO_2 , V_2O_5 , ZrO_2 , and Others. Note that Others is the sum of all remaining components, and thus differs from the Others in the 20-component LM model discussed in Section 8.3.1. Table 8.4 contains the results for the 11-component RLM model of $\ln(k_{1208})$. Table 8.4 lists the model coefficients, standard deviations of the coefficients, and model fit statistics for the 11-component RLM model using

the modeling dataset (333 LAW glasses). Table 8.4 also contains the results from the (i) data-splitting validation approach (see Section 8.1.2), and (ii) evaluation of model predictions for the five evaluation subsets (see Section 8.1.3). In the data-splitting validation portion of the results at the bottom of Table 8.4, the columns are labeled DS1, DS2, DS3, DS4, and DS5 to denote the five modeling/validation splits of the data as described in Section 8.1.2. The last column of this part of Table 8.4 shows the averages for the different statistics over the five splits.

The $R^2 = 0.8001$, $R^2_A = 0.7939$, and $R^2_P = 0.7837$ statistics (see Section B.3 of Appendix B) in Table 8.4 show that (i) the 11-component RLM model fits the $\ln(k_{1208})$ data in the 333-glass modeling dataset reasonably well, (ii) there are not a large number of unneeded model terms, and (iii) there are not any highly influential data points. The RMSE = 0.3397 is slightly larger than the pooled glass batching and k_{1208} determination uncertainty [SD = 0.3311 in $\ln(\text{inch})$ units] estimated from replicates in Table 8.2. The model LOF p-value = 0.4510 in Table 8.4 does not indicate that the 11-component RLM model has a significant LOF. However, the fact that the RMSE and pooled SD are noticeably higher than similar values for properties such as viscosity and EC, combined with the fact that the model LOF p-value is noticeably smaller than similar values for viscosity and EC, indicates that the 11-component RLM model does involve relatively high random error and has the potential for some degree of model LOF. See Section B.3 for discussion of the statistical test for model LOF.

At the bottom right of Table 8.4, the average model-fit statistics (R^2 , R^2_A , R^2_P , and RMSE) over the five data-splits are close to the statistics obtained from fitting the 11-component RLM model for $\ln(k_{1208})$ to all 333 glasses in the modeling dataset. The data-split validation statistics (R^2_V and RMSE_V) are also relatively close to the R^2 and RMSE (i) values from fitting the model to the full dataset, and (ii) averages from fitting the model to the data-split modeling subsets. This indicates that the model does not have statistically significant LOF and maintains its performance for data not used to fit the model.

Table 8.4. Coefficients and Performance Summary for the 11-Component Reduced Linear Mixture Model on the Natural Logarithm of K-3 Corrosion at 1208 °C for LAW Glasses

$\ln(k_{1208})$ 11-Component LM Model Term	Coefficient Estimate	Coefficient Stand. Err.	Modeling Data Statistic, 333 Glasses ^(a)				Value
Al ₂ O ₃	-23.6166	1.1934	R ²				0.8001
B ₂ O ₃	-4.9660	1.1254	R ² _A				0.7939
CaO	6.9274	0.9471	R ² _P				0.7837
Cr ₂ O ₃	-91.2882	10.6679	RMSE				0.3397
K ₂ O	7.7892	1.3435	Model LOF p-value				0.4510
Li ₂ O	51.0712	3.3918					
Na ₂ O	23.0767	0.9806	Evaluation Set				
SiO ₂	-12.8612	0.4783	(# Glasses)^(b)				
V ₂ O ₅	-25.9092	2.5140	R²_{Eval}				
ZrO ₂	-10.9683	1.9626	RMSE_{Eval}				
Others ^(c)	-3.5945	0.8602	WTP (98)		0.8340		0.3196
			ORP (235)		0.5075		0.3553
			LP2OL (40)		-0.4899		0.4520
			LP123 (0)		NA		NA
			HiNa ₂ O (136)		0.3723		0.3830
			HiSO ₃ (65)		0.6737		0.3743
Data Splitting Statistic^(a,d)	DS1	DS2	DS3	DS4	DS5	Average	
R ²	0.8067	0.8029	0.7889	0.8080	0.7941	0.8001	
R ² _A	0.7994	0.7955	0.7810	0.8008	0.7864	0.7926	
R ² _P	0.7873	0.7825	0.7678	0.7890	0.7740	0.7801	
RMSE	0.3374	0.3415	0.3483	0.3308	0.3410	0.3398	
R ² _V	0.7486	0.7736	0.8406	0.7311	0.8162	0.7820	
RMSE _V	0.3629	0.3382	0.3062	0.3946	0.3422	0.3488	

(a) The model evaluation statistics are defined in Section B.3 of Appendix B. The model validation statistics are defined in Section B.5.

(b) The six sets of LAW evaluation glasses are discussed in Section 2.4 and Section 8.1.3.

(c) For the 11-component RLM model, the “Others” component includes any components not separately listed.

(d) The evaluation and validation statistics calculated for data-splits are defined the same as for separate modeling and validation sets. Section 8.1.2 describes how the modeling dataset was split into modeling and validation subsets.

The statistics from evaluating the predictive performance of the 11-component RLM model for $\ln(k_{1208})$ on the five applicable evaluation subsets of modeling glasses (see Section 8.1.3) are given on the right side of Table 8.4. The R² statistics for two of the five evaluation subsets (0.6737 and 0.8340) are close to the R² statistic for the whole modeling dataset (0.8001). However, the remaining three evaluation sets resulted in significantly lower R^2_{Eval} values (−0.4899, 0.3723, and 0.5075). The new models in this report are intended to predict well for LAW glasses with higher waste loadings, and still predict acceptably well for glasses with lower waste loadings (the older WTP glasses). Like the 20-component FLM model, the low evaluation R² values and the significantly reduced model validity region for the $\ln(k_{1208})$ model (compared to other models in this report) suggest that further data and modeling are required before directly applying this constraint in formulation of glasses for the WTP LAW Facility. We therefore recommend this model be used for indication only.

8.3.2.2 Graphical Results for the 11-Component Reduced Linear Mixture Model on the Natural Logarithm of K-3 Corrosion at 1208 °C for LAW Glasses

Diagnostic plots for the 11-component RLM model (not included in this report) support the assumption of normally distributed errors in the $\ln(k_{1208})$ data (see Section B.3 of Appendix B). Figure 8.7 displays for the 11-component RLM model of $\ln(k_{1208})$ the standardized residuals plotted versus the data index (a sequential numbering of the modeling data points), with different plotting symbols representing the different groups of LAW glasses discussed in Section 2.3. Figure 8.7 indicates that the ORP datasets have a slightly wider scatter of standardized residuals, indicating a wider range of $\ln(k_{1208})$ model prediction uncertainty than the WTP datasets. This is likely a result of the ORP glasses spanning a wider subregion of LAW glass compositions. Only 2 of the 333 model glasses show a standardized residual greater than 3 on an absolute scale. Although these data points could be considered borderline outliers, they did not have a major impact on the 11-component RLM model for $\ln(k_{1208})$ and hence were retained in the modeling dataset. There is also a noticeable trend (rainbow shape) in the index versus standardized residual. Since the index for k_{1208} was data sorted in alphabetical order of Glass ID, the trend is not meaningful.

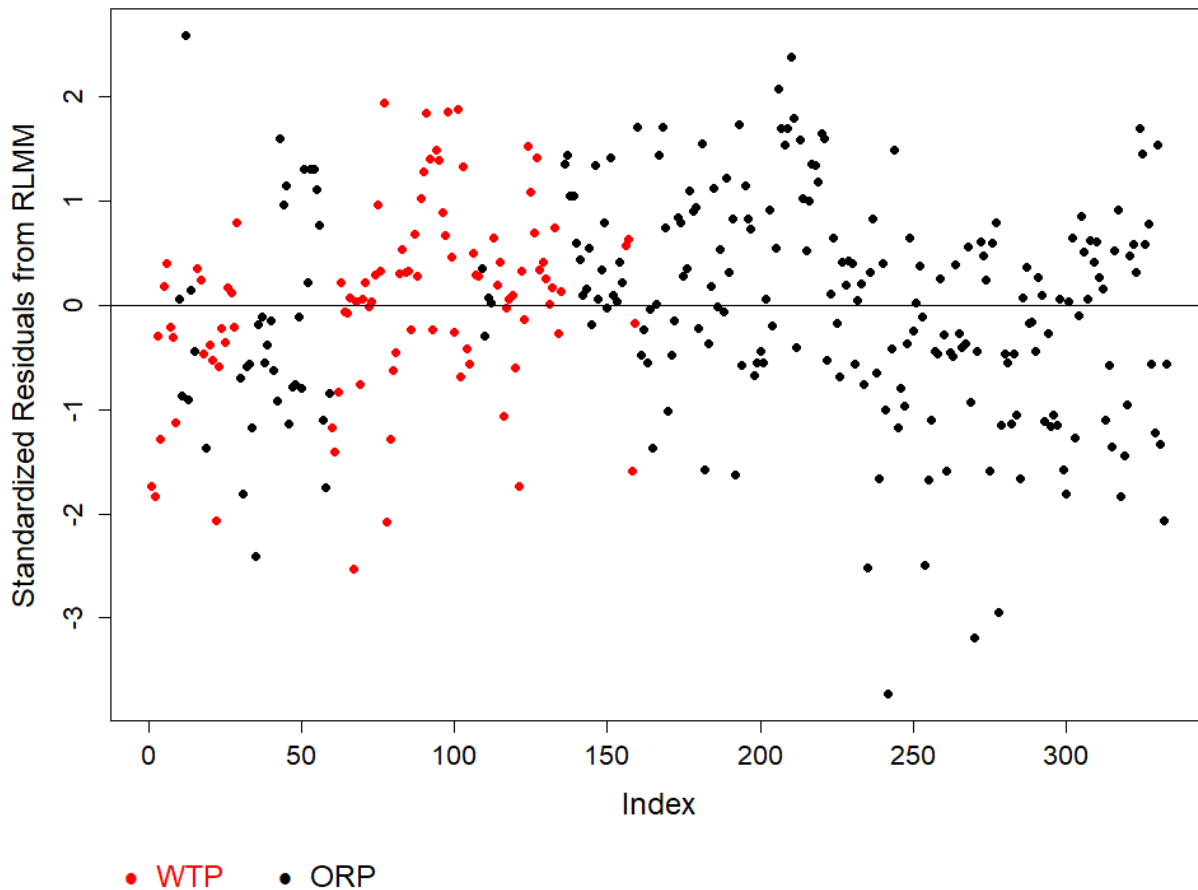


Figure 8.7. Standardized Residuals Plot for the 11-Component Reduced Linear Mixture Model on the Natural Logarithm of K-3 Corrosion at 1208 °C for LAW Glasses

Figure 8.8 displays the PvM plot for the 333-glass modeling dataset using the 11-component RLM model on $\ln(k_{1208})$. Figure 8.8 is similar to the PvM plot for the 20-component FLM model in Figure 8.4. Hence, as in Figure 8.4, Figure 8.8 illustrates that the 11-component RLM model predicts $\ln(k_{1208})$ moderately well, but with a slight tendency to under-predict above $\ln(k_{1208}) \sim -3$ ($k_{1208} \sim 0.05$ inch). However, the model predicts without bias near the WTP LAW Facility target operating limit for k_{1208} (0.04 inch, $\ln[k_{1208}] \sim -3.22 \ln[\text{inch}]$).

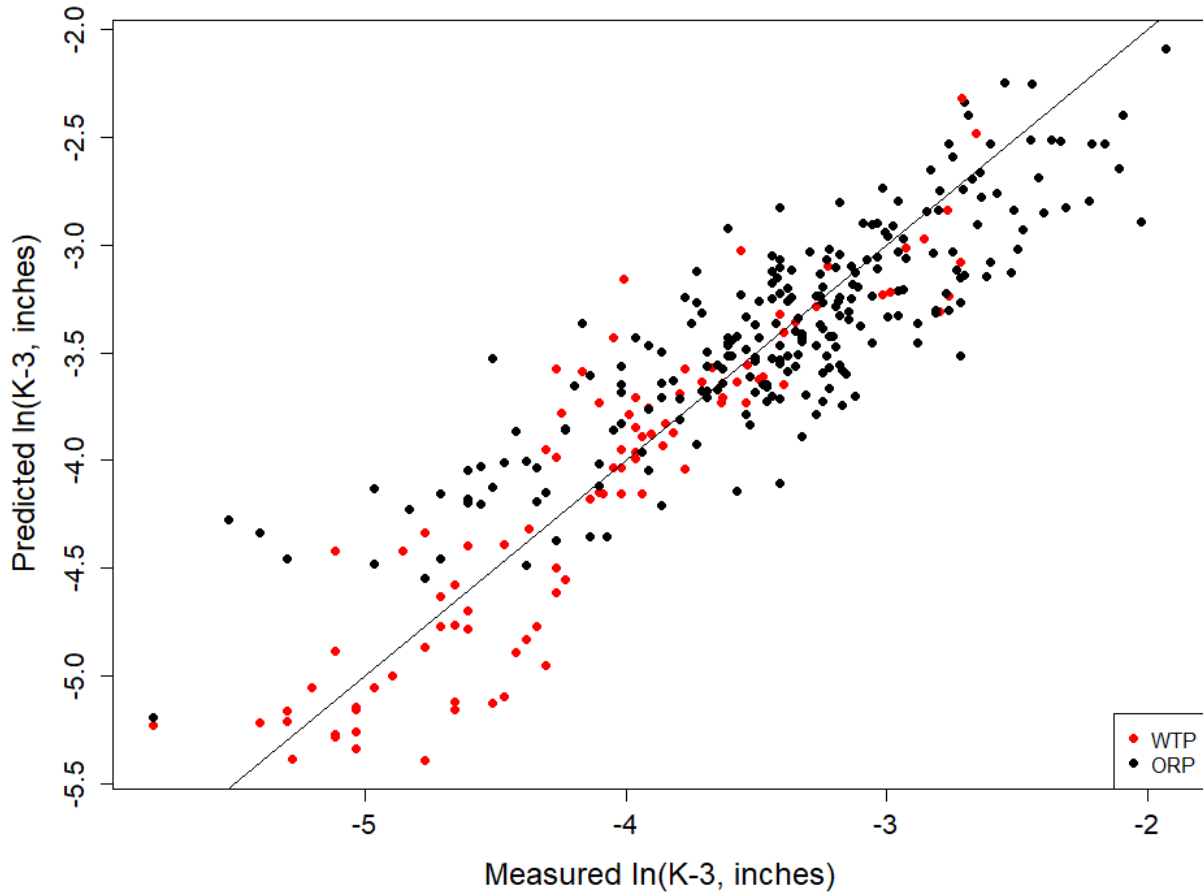


Figure 8.8. Predicted versus Measured Plot for the 333-Glass Modeling Dataset Using the 11-Component Reduced Linear Mixture Model on the Natural Logarithm of K-3 Corrosion at 1208 °C for LAW Glasses

Figure 8.9 displays PvM plots using the 11-component RLM model for $\ln(k_{1208})$ in Table 8.4 applied to the five evaluation subsets discussed in Section 8.1.3. Each plot in the figure contains the evaluation R^2 and RMSE values for the corresponding evaluation subset. Figure 8.9 shows that the 11-component RLM model for $\ln(k_{1208})$ fit to the 333-glass modeling dataset generally predicts reasonably well for the WTP and HiSO_3 evaluation subsets. The fits to the ORP and HiNa_2O subsets show more scatter with perhaps a slight bias for the ORP subset. The model did not fit the LP2OL subset well.

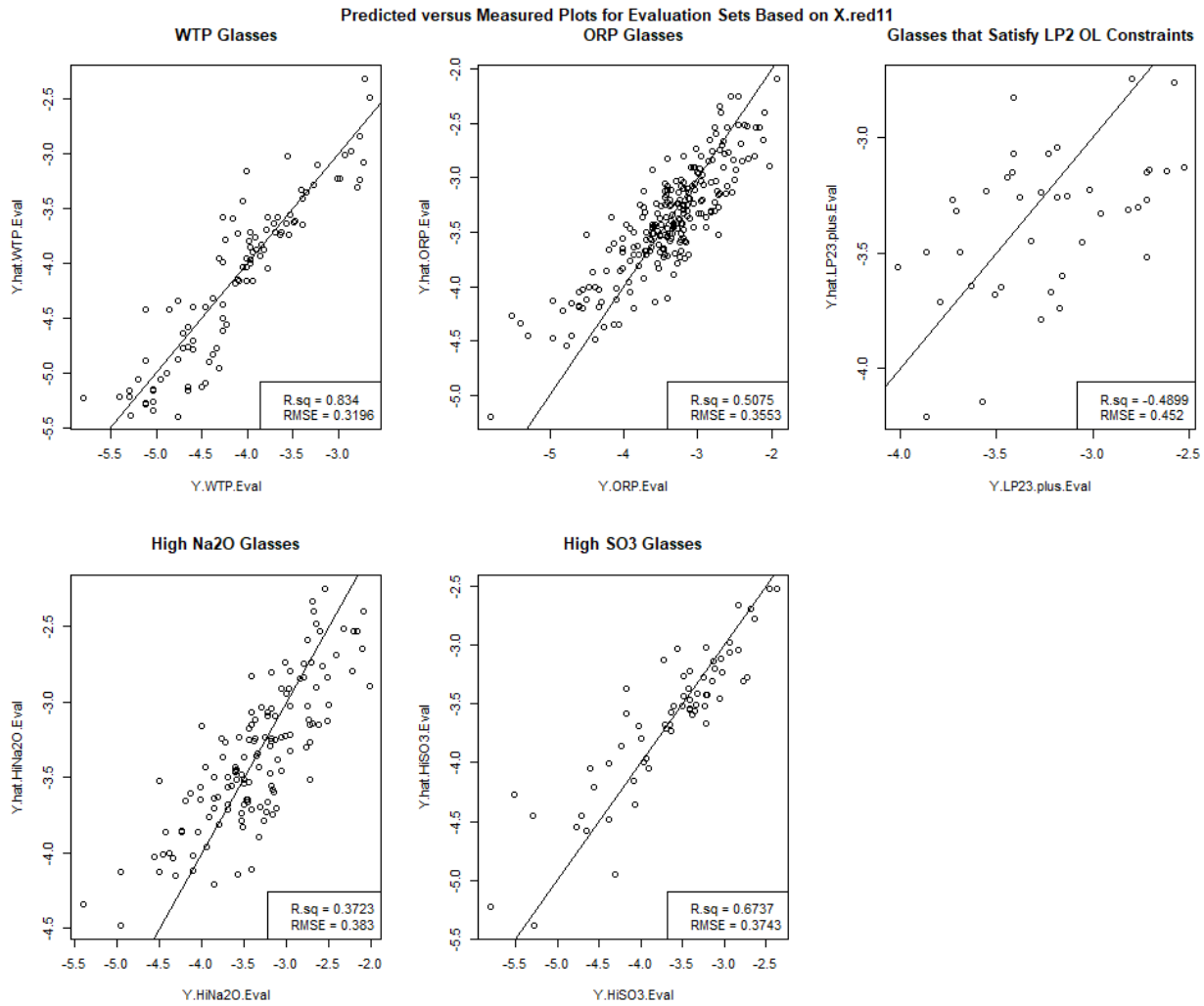


Figure 8.9. Predicted versus Measured Plots for the Five Evaluation Subsets Using the 11-Component Reduced Linear Mixture Model on the Natural Logarithm of K-3 Corrosion at 1208 °C for LAW Glasses

Figure 8.10 displays the response trace plot (see Section B.4.1 in Appendix B) for the 11-component RLM model of $\ln(k_{1208})$. The glass composition of the REFMIX glass (see Section B.4.1) used is listed in Table 2.3. Figure 8.10 shows that Li₂O and Na₂O (and CaO and K₂O to a lesser extent) are predicted to increase $\ln(k_{1208})$ the most, while Cr₂O₃, V₂O₅, Al₂O₃, and SiO₂ (and ZrO₂ to a lesser extent) are predicted to decrease $\ln(k_{1208})$ the most. B₂O₃ and Others have predicted response traces with small to negligible slopes, indicating those components are predicted to have small to negligible effects on $\ln(k_{1208})$.

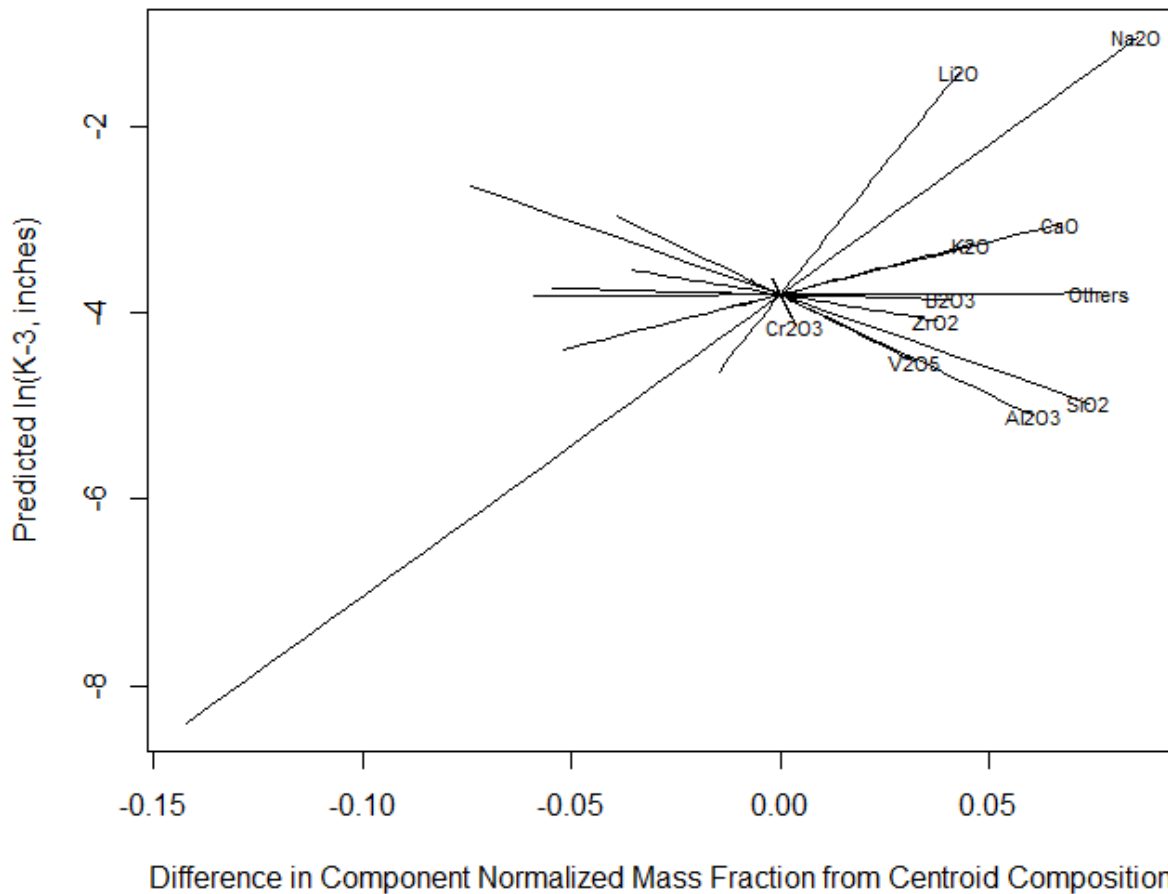


Figure 8.10. Response Trace Plot for the 11-Component Reduced Linear Mixture Model on the Natural Logarithm of K-3 Corrosion at 1208 °C for LAW Glasses

8.3.3 Results from a Reduced Partial Quadratic Mixture Model for the Natural Logarithm of K-3 Corrosion at 1208 °C with LAW Glasses

Reduced PQM models (see Section 8.2.1) were investigated in an effort to improve the 11-component RLM model for $\ln(k_{1208})$. Past experience with developing and validating PQM models has indicated that adding too many quadratic terms tends to over-fit the model development dataset and degrade predictive performance for new glasses. So, a process of identifying as few as possible second-order terms while improving model fit statistics was performed as follows:

1. Regressions were performed to fit reduced partial quadratic models involving all possible subsets of 1, 2, 3, or 4 second-order terms.
2. The resulting model performance statistics (R-squared and RMSE values) were then examined to see which second-order terms were most beneficial to model performance and how many second-order terms to include.
3. The RMSE values from the top candidate models were plotted as a function of the number of second order terms (0 to 4) to identify where the point of diminishing returns was.
4. The reduced PQM model with the number of terms just before the point of diminishing returns was selected as the final reduced PQM model.

The MAXR criterion (see Section B.4.2 of Appendix B) was also attempted as a means of selecting second-order terms. However, the terms selected by that method were not always intuitively obvious and the performance was not substantively better than the chosen approach.

Ultimately, a 13-term PQM model for $\ln(k_{1208})$ with 11 linear terms and 2 quadratic terms ($\text{Li}_2\text{O} \times \text{Li}_2\text{O}$ and $\text{Na}_2\text{O} \times \text{SiO}_2$) was selected as including enough quadratic terms to improve the model fit, without over-fitting the model development data. There is little past experience to judge if these second-order terms are to be expected. However, $\text{Li}_2\text{O} \times \text{Li}_2\text{O}$ and $\text{Na}_2\text{O} \times \text{SiO}_2$ are often observed cross products in waste glass models for other properties (e.g., Piepel et al. 2007, Vienna et al. 2013, Vienna et al. 2016). Table 8.5 contains the coefficients of the 13-term PQM model for $\ln(k_{1208})$ and the coefficient standard deviations. Table 8.5 also includes model performance statistics for the 13-term PQM model using the (i) 333-glass modeling data, (ii) data-split modeling data (as a model validation approach), and (iii) five evaluation subsets of modeling glasses discussed in Section 8.1.3 (as a model evaluation approach).

8.3.3.1 Numerical Results for the 13-Term Reduced Partial Quadratic Mixture Model on the Natural Logarithm of K-3 Corrosion at 1208 °C

In Table 8.5, the $\ln(k_{1208})$ model fit statistics $R^2 = 0.8245$, $R^2_A = 0.8179$, $R^2_P = 0.8081$, and $\text{RMSE} = 0.3193$ for the 13-term PQM model are small improvements over the corresponding statistics for the 11-component RLM model in Table 8.4. The small drop in values from R^2_A to R^2_P suggests that the $\ln(k_{1208})$ modeling dataset does not have any highly influential data points for the 13-term reduced PQM model. In any case, $R^2_P = 0.8081$ provides an estimate of the fraction of variation in $\ln(k_{1208})$ values for future datasets over the same GCR that might be accounted for by this 13-term reduced PQM model.

The RMSE in Table 8.5 is an estimate of the uncertainty [in $\ln(\text{inch})$ units] in fabricating simulated LAW glasses and determining k_{1208} if the 13-term reduced PQM model for $\ln(k_{1208})$ does not have a statistically significant LOF. The $\text{RMSE} = 0.3193$ is slightly smaller than the pooled glass batching and k_{1208} determination uncertainty [$\text{SD} = 0.3311$ in $\ln(\text{inch})$ units] estimated from replicates in Table 8.2. The model LOF p-value = 0.6415 in Table 8.5 does not indicate that the 13-term reduced PQM model has a significant LOF. However, the fact that the RMSE and pooled SD are noticeably higher than similar values for properties such as viscosity and EC, combined with the fact that the model LOF p-value is noticeably smaller than similar values for viscosity and EC, indicates that the 13-term reduced PQM model does involve relatively high random error and has the potential for some degree of model LOF. See Section B.3 for discussion of the statistical test for model LOF.

At the bottom right of Table 8.5, the average model-fit statistics (R^2 , R^2_A , R^2_P , and RMSE) over the five data-splits are close to the statistics obtained from fitting the 13-term reduced PQM model for $\ln(k_{1208})$ to all 333 glasses in the modeling dataset. The data-split validation statistics (R^2_V and RMSE_V) are also relatively close to the R^2 and RMSE (i) values from fitting the model to the full dataset, and (ii) averages from fitting the model to the data-split modeling subsets. This indicates that the 13-term reduced PQM model maintains its predictive performance for data not used to fit the model.

The statistics from evaluating the predictive performance of the 13-term reduced PQM model for $\ln(k_{1208})$ on the five evaluation subsets of modeling glasses (see Section 8.1.3) are given on the right side of Table 8.5. The R^2 statistic for the WTP evaluation subset (0.8311) is close to the R^2 statistic for the whole modeling dataset (0.8245). However, the remaining four evaluation sets resulted in significantly lower R^2 values (0.6470, 0.0328, 0.5371, and 0.7538). The new models in this report are intended to predict well for LAW glasses with higher waste loadings, and still predict acceptably well for glasses with lower waste loadings (the older WTP glasses). Like the 11-component RLM model, the low evaluation R^2 values and the significantly reduced model validity region for the $\ln(k_{1208})$ model (compared to other

models in this report) suggest that further data and modeling are required before directly applying this constraint in formulation of glasses for the WTP LAW Facility. We therefore recommend this model be used for indication only.

Table 8.5. Coefficients and Performance Summary for 13-Term Reduced Partial Quadratic Mixture Model on the Natural Logarithm of K-3 Corrosion at 1208 °C for LAW Glasses

$\ln(k_{1208})$ 11-Term PQM Model Term	Coefficient Estimate	Coefficient Stand. Err.	Modeling Data Statistic, 333 Glasses ^(a)				Value
Al ₂ O ₃	-33.3105	1.8903	R ²				0.8245
B ₂ O ₃	-12.0828	1.5356	R ² _A				0.8179
CaO	-0.6772	1.4473	R ² _P				0.8081
Cr ₂ O ₃	-101.3429	10.3063	RMSE				0.3193
K ₂ O	4.8322	1.3384	Model LOF p-value				0.6415
Li ₂ O	64.3499	4.9227					
Na ₂ O	54.7839	4.9832					
SiO ₂	-4.2539	1.3952					
V ₂ O ₅	-27.1194	2.3701					
ZrO ₂	-20.5035	2.3936					
Others	-11.0123	1.4175					
Li ₂ O×Li ₂ O	-438.1673	102.2222					
Na ₂ O×SiO ₂	-84.6857	12.9803					
			Evaluation Set (# Glasses) ^(b)				
				R ² _{Eval}	RMSE _{Eval}		
			WTP (98)	0.8311	0.3123		
			ORP (235)	0.6470	0.3312		
			LP2OL (40)	0.0328	0.4315		
			LP123 (0)	NA	NA		
			HiNa ₂ O (136)	0.5371	0.3664		
			HiSO ₃ (65)	0.7538	0.3442		
Data Splitting Statistic ^(a,d)	DS1	DS2	DS3	DS4	DS5	Average	
R ²	0.8294	0.8265	0.8111	0.8401	0.8178	0.8250	
R ² _A	0.8216	0.8186	0.8025	0.8329	0.8095	0.8170	
R ² _P	0.8103	0.8061	0.7896	0.8222	0.7971	0.8050	
RMSE	0.3182	0.3216	0.3307	0.3030	0.3220	0.3191	
R ² _V	0.7830	0.8024	0.8766	0.7194	0.8446	0.8052	
RMSE _V	0.3372	0.3160	0.2694	0.4031	0.3147	0.3281	

(a) The model evaluation statistics are defined in Section B.3 of Appendix B. The model validation statistics are defined in Section B.5.

(b) The six sets of LAW evaluation glasses (five of which apply) are discussed in Section 2.4 and Section 8.1.3.

(c) For the 13-component reduced PQM model, the “Others” component includes any components not separately listed.

(d) The evaluation and validation statistics calculated for data-splits are defined the same as for separate modeling and validation sets. Section 8.1.2 describes how the modeling dataset was split into modeling and validation subsets.

8.3.3.2 Graphical Results for the 13-Term Reduced Partial Quadratic Mixture Model on the Natural Logarithm of K-3 Corrosion at 1208 °C for LAW Glasses

Diagnostic plots for the 13-term reduced PQM model (not included in this report) support the assumption of normally distributed errors in the ln(k_{1208}) data (see Section B.3 of Appendix B). Figure 8.11 displays for the 13-term reduced PQM model of ln(k_{1208}) the standardized residuals plotted versus the data index (a sequential numbering of the modeling data points), with different plotting symbols representing the different groups of LAW glasses discussed in Section 2.3. Figure 8.11 is very similar to Figure 8.7, so the observations on Figure 8.11 are the same as discussed in Section 8.3.2.2 for Figure 8.7.

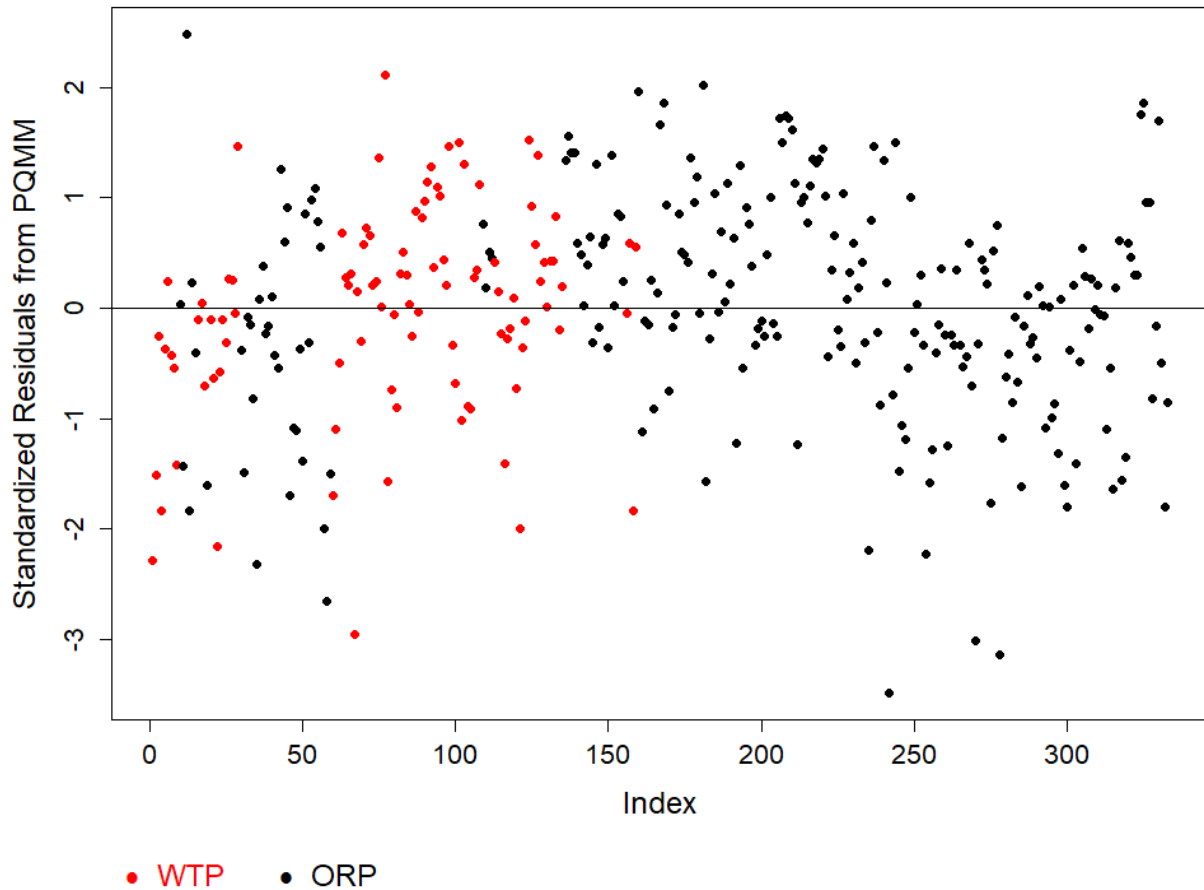


Figure 8.11. Standardized Residuals Plot for the 13-Term Reduced Partial Quadratic Mixture Model on the Natural Logarithm of K-3 Corrosion at 1208 °C for LAW Glasses

Figure 8.12 displays the PvM plot for the 333-glass modeling dataset using the 13-term reduced PQM model on $\ln(k_{1208})$. Figure 8.12 is similar to the PvM plot for the 11-component RLM model in Figure 8.8. However, comparing Figure 8.8 and Figure 8.12 illustrates that the 13-term reduced PQM model predicts $\ln(k_{1208})$ with less of a tendency to under-predict above $\ln(k_{1208}) \sim -3$ ($k_{1208} \sim 0.05$ inch). Also, the model predicts without bias near the WTP LAW Facility target operating limit for k_{1208} (0.04 inch, $\ln[k_{1208}] \sim -3.22 \ln[\text{inch}]$).

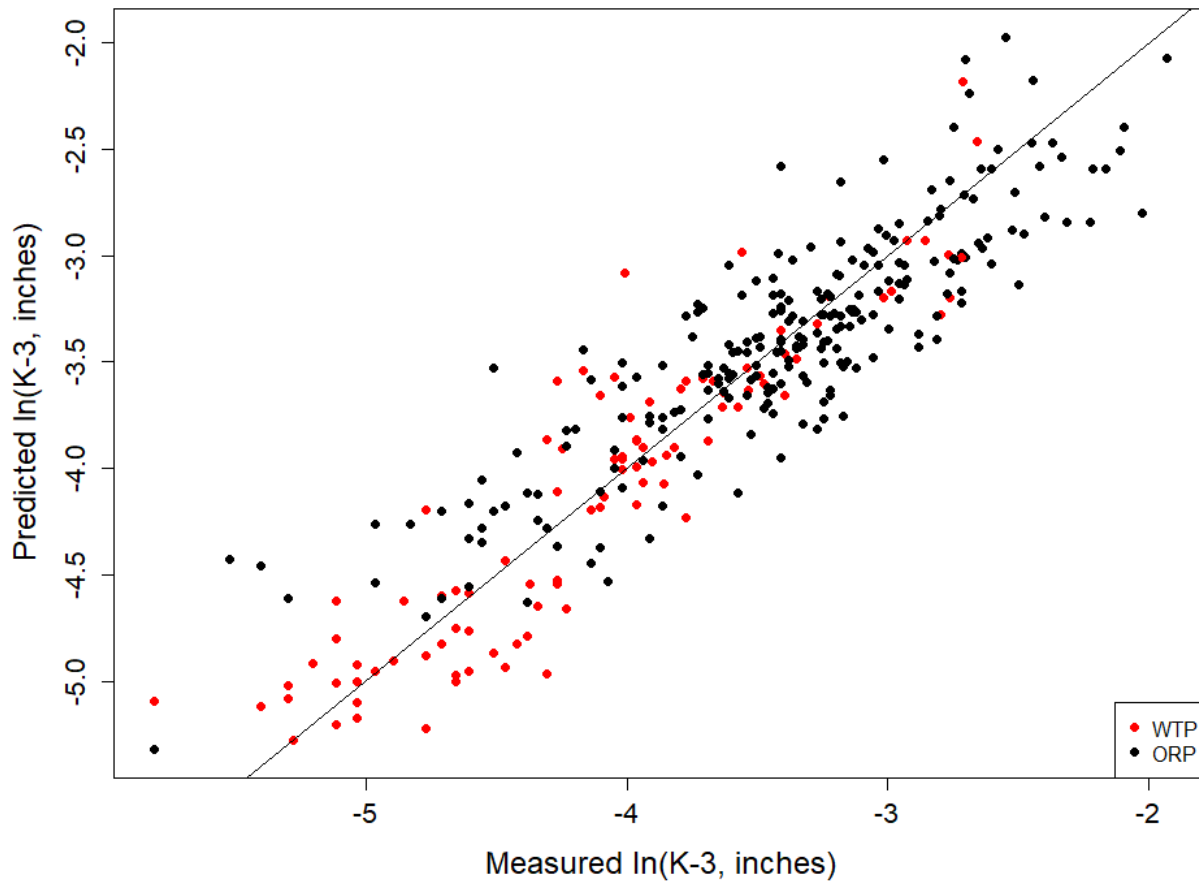


Figure 8.12. Predicted versus Measured Plot for the 333-Glass Modeling Dataset Using the 13-Term Reduced Partial Quadratic Mixture Model on the Natural Logarithm of K-3 Corrosion at 1208 °C for LAW Glasses

Figure 8.13 displays PvM plots using the 13-term reduced PQM model for $\ln(k_{1208})$ in Table 8.5 applied to the five evaluation subsets discussed in Section 8.1.3. Each plot in the figure contains the evaluation R^2 and RMSE values for the corresponding evaluation subset. Figure 8.13 shows that the 13-component reduced PQM model for $\ln(k_{1208})$ fit to the 333-glass modeling dataset generally predicts reasonably well for the WTP and HiSO_3 evaluation subsets. The fits to the ORP and HiNa_2O subsets show more scatter with perhaps a slight bias for the ORP subset. The model did not fit to the LP2OL subset well.

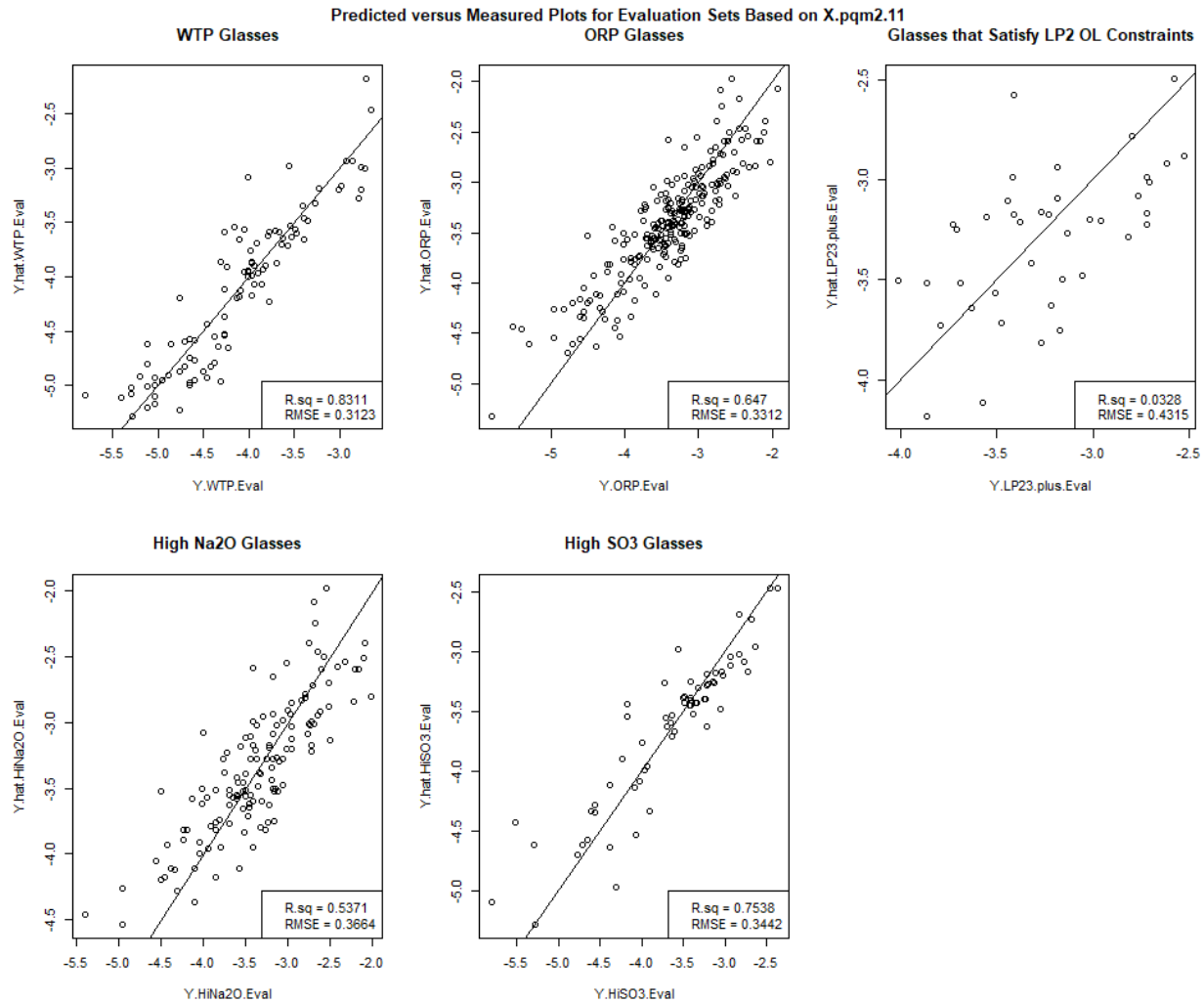


Figure 8.13. Predicted versus Measured Plots for the Five Evaluation Subsets Using the 13-Term Reduced Partial Quadratic Mixture Model on the Natural Logarithm of K-3 Corrosion at 1208 °C for LAW Glasses

Figure 8.14 displays the response trace plot (see Section B.4.1 of Appendix B) for the 13-term reduced PQM model on $\ln(k_{1208})$. Figure 8.14 shows that Li_2O and Na_2O (K_2O and CaO to a lesser extent) are predicted to increase $\ln(k_{1208})$ the most, while Cr_2O_3 , Al_2O_3 , V_2O_5 , SiO_2 , and ZrO_2 are predicted to decrease $\ln(k_{1208})$ the most. B_2O_3 and Others have predicted response traces with small to negligible slopes, indicating those components are predicted to have small to negligible effects on $\ln(k_{1208})$. The curvature in Li_2O effect is also evident with a high slope at low Li_2O concentrations and lower slope at higher Li_2O concentrations.

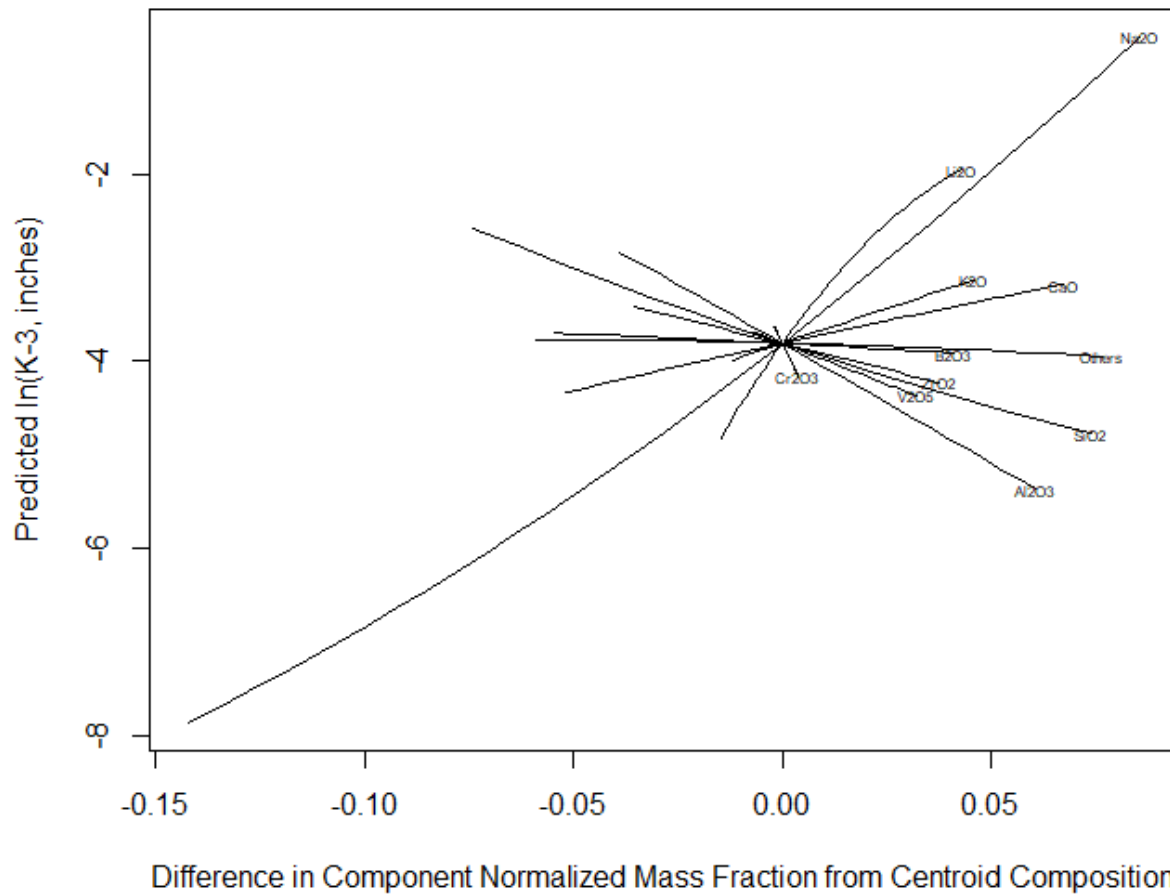


Figure 8.14. Response Trace Plot for 13-Term Reduced Partial Quadratic Mixture Model on the Natural Logarithm of K-3 Corrosion at 1208 °C for LAW Glasses

8.3.4 Recommended Model for the Natural Logarithm of K-3 Corrosion at 1208 °C for LAW Glasses

Table 8.6 summarizes the primary $\ln(k_{1208})$ model evaluation and validation results for the 20-component FLM model, the 11-component RLM model, and the 13-term reduced PQM model from Table 8.3, Table 8.4, and Table 8.5, respectively, for the following:

- Model goodness-of-fit for the $\ln(k_{1208})$ -composition modeling data of 333 simulated LAW glasses
- Model validation using the data-splitting approach
- Model evaluation for six subsets of the 333-glass modeling dataset

Based on the summarized results in Table 8.6 and discussions in Sections 8.3.1 to 8.3.3, the 13-term reduced PQM model (listed in Table 8.5) is recommended for predicting $\ln(k_{1208})$ of LAW glasses. However, this model is recommended to be used as information only at this time due to lack of data. As a baseline for comparison, the 11-component RLM model (listed in Table 8.3) will be used.

Table 8.6. Performance Summary of Three Models for the Natural Logarithm of K-3 Corrosion at 1208 °C for LAW Glasses

Summary Statistics from Model Fit to 333 Glasses ^(a)	ln(<i>k</i> ₁₂₀₈) Model					
	20-Component FLM	11-Component RLM	13-Term Reduced PQM (Recommended)			
R ²	0.8162	0.8001	0.8245			
R ² _A	0.8050	0.7939	0.8179			
R ² _P	0.7875	0.7837	0.8081			
RMSE	0.3305	0.3397	0.3193			
LOF p-value	0.5361	0.4510	0.6415			
Linear Terms	20 (See Table 8.3)	11 (See Table 8.4)	11 (See Table 8.5)			
Selected Quadratic Terms in Model	NA	NA	Li ₂ O × Li ₂ O Na ₂ O × SiO ₂			
# Model Terms	20	11	13			
Summary Statistics for Five Evaluation Subsets of LAW Glasses ^(a)						
Evaluation Set (# Glasses) ^(b)	R ² _{Eval}	RMSE _{Eval}	R ² _{Eval}	RMSE _{Eval}	R ² _{Eval}	RMSE _{Eval}
WTP (98)	0.8399	0.3305	0.8340	0.3196	0.8311	0.3123
ORP (235)	0.5774	0.3455	0.5075	0.3553	0.6470	0.3312
LP2OL (40)	-0.6198	0.5306	-0.4899	0.4520	0.0328	0.4315
LP123 (0)	NA	NA	NA	NA	NA	NA
HiNa ₂ O (136)	0.3865	0.3954	0.3723	0.3830	0.5371	0.3664
HiSO ₃ (65)	0.7163	0.3885	0.6737	0.3743	0.7538	0.3442
Validation Summary Statistics Averaged Over 5 Data-Splitting Sets ^(b)						
R ²	0.8169		0.8001		0.8250	
R ² _A	0.8033		0.7926		0.8170	
R ² _P	0.7808		0.7801		0.8050	
RMSE	0.3309		0.3398		0.3191	
R ² _V	0.7849		0.7820		0.8052	
RMSE _V	0.3458		0.3488		0.3281	

(a) The model evaluation statistics are defined in Section B.3 of Appendix B.

(b) Model validation statistics are defined in Section B.5 of Appendix B.

8.4 Example Illustrating Model Predictions and Statistical Intervals for K-3 Corrosion at 1208 °C

This section contains examples to illustrate using the recommended 13-term PQM model (Section 8.3.3) to obtain predicted k_{1208} values and corresponding 90% UCIs for a specific LAW glass composition as described in Section B.6 of Appendix B. For comparison purposes, the same results are presented for the 11-component RLM model in Section 8.3.2 (although it was not a recommended model). The 90% confidence levels associated with UCIs were chosen for illustration purposes only. The WTP LAW Facility can use an appropriate confidence level depending on the use of the ln(k_{1208})-composition model and the type of statistical uncertainty expression.

The common glass composition selected for example calculations for all properties in this report (denoted REFMIX) is listed in Table 2.3. The 20-component composition (mass fractions) for k_{1208} modeling is given in Table 8.7. To apply the 13-term reduced PQM and 11-component RLM models for ln(k_{1208}) to the glass composition, the mass fractions of the 20 components must be converted to mass fractions (that sum to 1.0) of the 11 LAW glass components contained in both models. This involves adding the mass fractions of the 9 of 20 components not contained in the ln(k_{1208}) models to the mass fraction of Others (one of the original 20 components) to obtain Others (one of the reduced sets of 11 components). Mass

fractions of the relevant components are then multiplied to obtain the two quadratic terms of the 13-term reduced PQM model. Table 8.7 contains the composition of the glass prepared for use in the two $\ln(k_{1208})$ models for LAW glasses.

For each of the two $\ln(k_{1208})$ models, predicted $\ln(k_{1208}, \text{inch})$ values are obtained by multiplying the composition in the format needed for that model by the coefficients for that model, then summing the results. That is, the predicted values are calculated by

$$\hat{y}(\mathbf{g}) = \mathbf{g}^T \mathbf{b} \quad (8.4)$$

where \mathbf{g} is the composition of REFMIX formatted to match the terms in a given model (from Table 8.7), the superscript T represents a vector transpose, and \mathbf{b} is the vector of coefficients for a given model. The predicted $\ln(k_{1208})$ values for REFMIX using the two $\ln(k_{1208})$ models are listed in the second column of Table 8.8. The predicted $\ln(k_{1208})$ values in $\ln(\text{inch})$ units are easily converted to k_{1208} values (inch) by exponentiation. The third column of Table 8.8 contains the predicted k_{1208} values (inch). However, as discussed in Section B.6 of Appendix B, these back-transformed k_{1208} predictions in inch should be considered estimates of the true median (not the true mean) of the distribution of k_{1208} values that would result if K-3 corrosion measurements at 1208 °C were repeated multiple times on separately batched and melted samples of the REFMIX glass composition.

The predicted k_{1208} values for REFMIX in Table 8.8 are 0.0223 inch for the 11-component RLM model and 0.0222 inch for the recommended 13-term reduced PQM model.

Table 8.7. REFMIX Glass Composition in Formats Used with Models of Natural Logarithm of K-3 Corrosion at 1208 °C for LAW Glasses

Model Term	Example Glass Composition ^(a) (mass fractions)	Example Glass Composition (mass fractions) to Use in 11-Component LM Model for $\ln(k_{1208})$ ^(b)	Example Glass Composition (mass fractions) to Use in 13-Term PQM Model for $\ln(k_{1208})$ ^(c)
Al ₂ O ₃	0.075760	0.07576	0.07576
B ₂ O ₃	0.097257	0.097257	0.097257
CaO	0.052514	0.052514	0.052514
Cl	0.003376	NA	NA
Cr ₂ O ₃	0.002041	0.002041	0.002041
F	0.001348	NA	NA
Fe ₂ O ₃	0.029727	NA	NA
K ₂ O	0.012064	0.012064	0.012064
Li ₂ O	0.014802	0.014802	0.014802
MgO	0.016989	NA	NA
Na ₂ O	0.168395	0.168395	0.168395
P ₂ O ₅	0.003239	NA	NA
SO ₃	0.005542	NA	NA
SiO ₂	0.424565	0.424565	0.424565
SnO ₂	0.007587	NA	NA
TiO ₂	0.008034	NA	NA
V ₂ O ₅	0.007499	0.007499	0.007499
ZnO	0.031997	NA	NA
ZrO ₂	0.036219	0.036219	0.036219
Others	0.001045	0.108884	0.108884
Li ₂ O×Li ₂ O	NA	NA	0.00021910
Na ₂ O×SiO ₂	NA	NA	0.07149462

(a) The composition in mass fractions is from Table 2.3.

(b) See Table 8.4.

(c) See Table 8.5.

(d) NA = not applicable, because the model does not contain this term.

Table 8.8. Predicted K-3 Corrosion at 1208 °C, Standard Deviation, and Statistical Intervals for the REFMIX Glass Composition Used in Two Models for K-3 Corrosion at 1208 °C

Model for $\ln(k_{1208})^{(a)}$	Predicted $\ln(\widehat{k_{1208}})$ [ln(inch)]	Predicted $\widehat{k_{1208}}$ [inch]	Standard Deviation of Predicted $\ln(\widehat{k_{1208}})^{(b)}$ [ln(inch)]	90% UCI ^(c) on Mean $\ln(\widehat{k_{1208}})$ [ln(inch)]	90% UCI ^(c) on Median $\widehat{k_{1208}}$ [inch]
13-Term PQM Model	-3.8067 ^(d)	0.0222 ^(d)	0.0392	-3.7563	0.0234
11-Comp. LM Model	-3.8022	0.0223	0.0231	-3.7725	0.0230

(a) The two $\ln(k_{1208})$ models in this column are given in Table 8.5 (13-term PQM) and Table 8.4 (11-component LM), respectively.

(b) The standard deviation is for the $\ln(k_{1208})$ prediction considered to be the mean of such values for the example glass.

(c) UCI = upper confidence interval (see Section B.6 of Appendix B).

(d) All calculations were performed using the example glass composition, model coefficients, and variance-covariance matrix values given in tables of this report. The calculated ln(inch) values were rounded to four decimal places in this table. The inch values were calculated by exponentiating the ln(inch) values before rounding, then rounding the resulting values to four decimal places in this table.

Eq. (B.19a) can be used to calculate a 90% UCI for the true mean of $\ln(k_{1208})$ values for the example glass composition with each of the $\ln(k_{1208})$ models. In the notation of these equations:

- $100(1-\alpha)\% = 90\%$, so that $\alpha = 0.10$ for a 90% UCI in Eq. (B.19a).
- The vector \mathbf{g} contains entries corresponding to the terms in a given $\ln(k_{1208})$ model, which are calculated using the composition of the example glass in Table 8.7.
- Matrix \mathbf{G} is formed from the data matrix used in the regression that generated a given $\ln(k_{1208})$ model. Matrix \mathbf{G} has the number of rows in the k_{1208} modeling dataset (333 glasses) and the number of columns corresponding to the number of terms in a given $\ln(k_{1208})$ model. Each column is calculated according to the corresponding term in the model using the LAW normalized glass composition in the k_{1208} modeling dataset.

To calculate a 90% UCI in $\ln(k_{1208})$ units of $\ln(\text{inch})$, the margin-of-error $t_{1-\alpha, n-p} \sqrt{MSE_{OLS} \mathbf{g}^T (\mathbf{G}^T \mathbf{G})^{-1} \mathbf{g}}$ is added to the predicted $\ln(k_{1208})$ [denoted $\hat{y}(\mathbf{g})$] described above. The calculations are given by

Eq. (B.19a). The $MSE_{OLS} (\mathbf{G}^T \mathbf{G})^{-1}$ portion of these expressions is an estimate of the variance-covariance matrix for the estimated model coefficients, as discussed near the end of Section B.6 of Appendix B. For the example calculations presented in Table 8.8, the Students- t statistic value needed for the one-sided upper CI formula describing the 11-component LM model is 1.284186. This is based on $n=333$ and $p=11$. The following cell formula can be used to obtain the t -statistic value with Excel: $=T.INV(0.90, 333-11)$. For the UCI calculations associated with the 13-term PQM model described in Table 8.8, the Students- t statistic is 1.284203 $=T.INV(0.90, 333-13)$. The variance-covariance matrices for the 11-component LM model and the recommended 13-term PQM model are respectively listed in Tables D.14 and D.15 of Appendix D. The quantity $\sqrt{MSE_{OLS} \mathbf{g}^T (\mathbf{G}^T \mathbf{G})^{-1} \mathbf{g}}$ is the standard deviation of a model prediction (for a given composition vector \mathbf{g} expressed in a given model form); the value for each model is given in the fourth column of Table 8.8.

The 90% UCI value for the true mean $\ln(k_{1208})$ in units of $\ln(\text{inch})$ for the example glass composition based on the two $\ln(k_{1208})$ models is given in the fifth column of Table 8.8. Exponentiating the resulting 90% UCIs for the mean $\ln(k_{1208})$ values in $\ln(\text{inch})$ units yields 90% UCIs, for the median k_{1208} (inch). These values are in the sixth column of Table 8.8. For example, the recommended 13-term PQM model for $\ln(k_{1208})$ has -3.7536 $\ln(\text{inch})$ as the 90% UCI on the true mean $\ln(k_{1208})$ for the example glass. Then $e^{-3.7536} = 0.0234$ inch is the 90% UCI on the true median for k_{1208} .

8.5 Suitability of the Recommended K-3 Corrosion at 1208 °C Model for Application by the WTP LAW Facility

The 13-term PQM model for $\ln(k_{1208})$ discussed in Section 8.3.3 is recommended as the best of the currently available models for predicting k_{1208} for LAW glasses. This model yields unbiased predictions of k_{1208} near the operating limit (0.04 inch), for the whole modeling dataset (see Figure 8.12). However, the k_{1208} model is recommended to be used for indication only rather than to constrain glass compositions in the WTP LAW Facility operations, for several reasons:

1. The model predictions are not as good for the five evaluation sets that are intended to demonstrate the ability to predict for glasses of interest to the WTP LAW Facility, including high-waste-loaded glasses.

2. The composition region for k_{1208} model validity is reduced compared to the models for other glass properties.
3. The melter operating temperature is 1150 °C rather than 1208 °C at which the testing was performed and the corrosion rate is likely to decrease with longer times compared to a single point at 6 days, suggesting the data may not be the most effective way to constrain glass composition.
4. The magnitude of the uncertainties (both measurement and prediction) are sufficiently high as to unduly restrict the processing envelope.

It is recommended that additional testing and modeling be performed to support the inclusion of a K-3 corrosion model for plant operation. In the meantime, the 13-term k_{1208} model is a useful tool to estimate potential impacts of composition on corrosivity of a melt and may be applied in system planning type calculations.

The ranges of single-component concentrations in the 333-glass dataset used for modeling are listed in Table 8.9. These ranges can be used to determine model validity ranges.

Table 8.9. Data Component Concentration Ranges (mass fraction) for LAW Glasses Used in Final Natural Logarithm K-3 Corrosion at 1208 °C Models

Component	20-component		11-component	
	Min	Max	Min	Max
Al ₂ O ₃	0.035000	0.138111	0.035000	0.138111
B ₂ O ₃	0.042017	0.139530	0.042017	0.139530
CaO	0.000000	0.122135	0.000000	0.122135
Cl	0.000000	0.011992	NA	NA
Cr ₂ O ₃	0.000000	0.006005	0.000000	0.006005
F	0.000000	0.004902	NA	NA
Fe ₂ O ₃	0.000000	0.094981	NA	NA
K ₂ O	0.000000	0.059065	0.000000	0.059065
Li ₂ O	0.000000	0.059065	0.000000	0.059065
MgO	0.000000	0.048970	NA	NA
Na ₂ O	0.024982	0.259714	0.024982	0.259714
P ₂ O ₅	0.000000	0.033986	NA	NA
SO ₃	0.000100	0.025000	NA	NA
SiO ₂	0.343965	0.501647	0.343965	0.501647
SnO ₂	0.000000	0.050000	NA	NA
TiO ₂	0.000000	0.050015	NA	NA
V ₂ O ₅	0.000000	0.040044	0.000000	0.040044
ZnO	0.000000	0.054032	NA	NA
ZrO ₂	0.000000	0.075105	0.000000	0.075105
Others ^(b)	0.000000	0.015987	0.046231	0.190102

(a) NA = not applicable or component not included as term.
(b) Note: Others for the 11-components are composed of all the NA components as well as Others for the 20 components.

9.0 Summary and Conclusions for LAW Glass Property-Composition Models

This report documents the development of property models for LAW glasses and the data used to develop the models. Models have been developed to relate

- PCT responses for boron and sodium,
- The VHT constraint pass/fail,
- Viscosity at 1150 °C,
- Electrical conductivity at 1150 °C,
- melter SO₃ tolerance at 1150 °C, and
- K-3 refractory neck corrosion extent after 6 days at 1208 °C

to LAW glass compositions.

The property-composition models and formulas for uncertainties in model predictions for the full current range of LAW glasses (spanning the compositions for WTP contract baseline formulation through the high waste-loaded enhanced glasses) resulting from this work can be used for numerous purposes. These include (i) formulating LAW glasses for specific LAW waste compositions, (ii) developing LAW GFAs to make process step decisions during operation of the LAW WTP Facility, (iii) assessing whether proposed LAW glass compositions or LAW glass compositions calculated by process simulation codes will satisfy property specifications (PCT and VHT) and processing requirements (viscosity, EC, melter SO₃ tolerance), and (iv) as the basis for any future ILAW glass formulation and model development work, if needed.

The datasets available to develop property-composition models for PCT, VHT, viscosity at 1150 °C, EC at 1150 °C, melter SO₃ tolerance at 1150 °C, and K-3 refractory corrosion at 1208 °C are composed of data from different LAW glass studies conducted over several years by PNNL, VSL, and SRNL. The number of data points available for modeling varied by property because not every property was measured on every glass. The different studies from which data were drawn for ILAW property modeling are discussed in Section 2.0. Some of these studies used statistical experimental design methods to select some or all of the test matrix glasses. Glasses in parts or all of some studies were “actively designed” using glass science knowledge and experience to achieve the desired purpose for the study or individual glasses in the study. The various samples encompass the effects of testing scale (from crucible melts of a few hundred grams to samples collected from continuous melter tests producing many thousands of kilograms of glass), post-melt treatment such as container cooling, and the use of actual radioactive waste as well as waste simulants. The datasets available for modeling LAW glass properties were assessed to remove outlying and non-representative compositions from the modeling datasets. The LAW glass compositions and their property values in the available dataset and modeling dataset for each property are presented in tables in this report and its associated appendices.

All data in the modeling dataset for a given property were used to develop models for that property. Model validation was accomplished by data-splitting. To accomplish this, the modeling dataset was split into five sets of modeling and validation subsets, using roughly 80% of the data for modeling and 20% for validation in each split of the dataset. The goodness of fit was evaluated for six different evaluation

subsets of the data to determine likely model performance in different composition spaces. Based on the performance of the models that were investigated, recommended models were selected.

Sections 9.1 to 9.6 summarize the model development data and work for PCT, VHT, viscosity, EC, melter SO₃ tolerance, and K-3 corrosion of LAW glasses; respectively. For each property, the recommended model is mentioned, and any limitations of the model noted. Section 9.7 summarizes the model validity region for each of the modeled LAW glass properties. Section 9.8 summarizes the component effects on the properties. Section 9.9 lists additional constraints. Section 9.10 makes recommendations for any future property-composition modeling work for LAW glasses.

9.1 Summary of LAW Glass PCT Modeling

Data on PCT were available for 703 simulated and actual quenched LAW glasses from the six data groups discussed in Section 2.0. Normalized loss values vary from 0.08 to 17.84 g/m² for PCT_B^{NL} and 0.01 to 13.41 for PCT_{Na}^{NL} . Assessment of the ranges and distributions of the component values over the 703 LAW glasses with PCT data led to designating 11 glasses as having outlying compositions. An additional two glasses for each PCT_B^{NL} and PCT_{Na}^{NL} were identified as outliers, leaving 691 total glasses with data suitable for PCT modeling (690 for PCT_B^{NL} and 690 for PCT_{Na}^{NL}). Of the 691 glasses with PCT modeling data, only 40 exceeded the 2 g/m² constraint for PCT_B^{NL} and 33 for PCT_{Na}^{NL} .

The LAW glass composition and PCT data are listed in Appendix A, Tables A.2 and A.3, respectively. Over these 691 simulated and actual LAW glasses, the component ranges and distributions of 20 components (Al₂O₃, B₂O₃, CaO, Cl, Cr₂O₃, F, Fe₂O₃, K₂O, Li₂O, MgO, Na₂O, P₂O₅, SO₃, SiO₂, SnO₂, TiO₂, V₂O₅, ZnO, ZrO₂, and Others) were sufficient to support separate model terms if needed.

Several property-composition model forms for PCT response were explored. In this study as in previous studies, it was determined that a natural logarithm transformation (e.g., $\ln[PCT_j^{NL}]$) improved modeling efforts. Therefore, models to predict $\ln(PCT_B^{NL})$ and $\ln(PCT_{Na}^{NL})$ were explored, included FLM, RLM, PQM, partial cubic, k-nearest neighbors, support vector machine, local linear regression, Gaussian process regression, and GLMs. None of these modeling approaches were found to represent PCT response with unbiased predictions across the entire range of data. Therefore, PQM models with bias correction at the high response range were selected – bcPQM.

Although FLM model, RLM model, and PQM model were reported, only the bcPQMs were fully developed and recommended with the form

$$\ln(PCT_B^{NL}) \text{ or } \ln(PCT_{Na}^{NL}) = \begin{cases} \mathbf{g}^T \boldsymbol{\beta} & \text{if } \mathbf{g}^T \boldsymbol{\beta} \leq C \\ \mathbf{g}^T \boldsymbol{\beta} + (\mathbf{g}^T \boldsymbol{\beta} - C)s & \text{if } \mathbf{g}^T \boldsymbol{\beta} > C \end{cases} + e \quad (9.1)$$

As described in Sections 3.3.5 and 3.4.5. The recommended models include the following:

- A 22-term bcPQM model for PCT_B^{NL} (Table 3.7) with 15 first-order terms (combining Cl, Cr₂O₃, P₂O₅, and SO₃ into Others), four nonlinear terms (Al₂O₃×Al₂O₃, Al₂O₃×Li₂O, CaO×CaO, and CaO×V₂O₅), a bias correction slope (*s*) and cutoff (*c*). Overall R² and RMSE values of 0.7762 and 0.3954 were obtained.
- A 22-term bcPQM model for PCT_{Na}^{NL} (Table 3.11) with 15 first-order terms (combining Cl, Cr₂O₃, P₂O₅, and SO₃ into Others), four nonlinear terms (Al₂O₃×Al₂O₃, Al₂O₃×Na₂O, CaO×CaO, and CaO×V₂O₅), a bias correction slope (*s*) and cutoff (*c*). An overall R² and RMSE of 0.7556 and 0.3574 were obtained.

Results for the recommended 21-term models are given in Table 3.7 and Table 3.11 and discussed in Sections 3.3.5 and 3.4.5 for boron and sodium, respectively. Methods for making PCT predictions and quantifying the uncertainties in the predictions are discussed and illustrated in Section 3.6.

After bias correction, the selected models do not show significant bias across the full range of PCT responses, although there appears to be higher uncertainty at the PCT response values above the 2 g/m² limit ($\sim 0.693 \ln[\text{g/m}^2]$) due to a lack of data. There is a statistically significant LOF in the PCT models as obtained in previous modeling efforts for this property (e.g., Piepel et al. 2007). However, the models are practically able to predict PCT responses.

9.2 Summary of LAW VHT Modeling

Data on VHT were available for 699 simulated and actual quenched LAW glasses from the six data groups discussed in Section 2.0. Numerical r_a^{VHT} values vary from 0.1 to 1529.1 g/m²/d. However, in this report it is the binary response of pass corresponding to $r_a^{VHT} < 50 \text{ g/m}^2/\text{d}$ and fail corresponding to $r_a^{VHT} \geq 50 \text{ g/m}^2/\text{d}$ that is modeled. This is due to the difficulty in predicting the r_a^{VHT} as functions of composition for the broader range of data needed for this phase of modeling. Of the 699 glasses with measured VHT responses, only 162 exceeded the 50 g/m²/d constraint.

Assessment of the ranges and distributions of the component values over the 699 LAW glasses with VHT data led to designating 13 glasses as having outlying compositions. The remaining 686 glass composition/VHT pass/fail data were used in modeling efforts. The LAW glass composition and VHT data are listed in Appendix A, Tables A.2 and A.3, respectively. Over these 686 LAW glasses, the component ranges and distributions of 20 components (Al₂O₃, B₂O₃, CaO, Cl, Cr₂O₃, F, Fe₂O₃, K₂O, Li₂O, MgO, Na₂O, P₂O₅, SO₃, SiO₂, SnO₂, TiO₂, V₂O₅, ZnO, ZrO₂, and Others) were sufficient to support separate model terms if needed.

Several property-composition model forms for VHT response were explored. In this study as in previous studies, it was determined that a natural logarithm transformation (i.e., $\ln(r_a^{VHT})$) improved modeling efforts. Therefore, models to predict $\ln(r_a^{VHT})$ were explored, included FLM, RLM, PQM, partial cubic, k-nearest neighbors, support vector machine, local linear regression, Gaussian process regression, and artificial neural network. None of these modeling approaches were found to predict $\ln(r_a^{VHT})$ of validation sets near the limit ($3.912 \ln[\text{g/m}^2/\text{d}]$) with low uncertainty and insignificant bias. Therefore, a logistic regression approach was adopted to predict the binary pass/fail data; pass being data with $r_a^{VHT} < 50 \text{ g/m}^2/\text{d}$ (represented by 0) and fail being data with $r_a^{VHT} \geq 50 \text{ g/m}^2/\text{d}$ (represented by 1).

A logit function was used to link the binary response to the mixture portion of the data, which was represented by either FLM or PQM model forms. As VHT P/F is a binary response, the measures of goodness of fit differ from the other models. FPR, FNR, and accuracy were optimized by changing the mixture model parameters and classification threshold.

Two models were ultimately selected for reporting:

- A 20-term FLM model (Table 4.4) with an overall accuracy of 86.30%, a FPR of 13.26%, and a FNR of 15.19%.
- A 19-term PQM model (Table 4.6) formed by combining Cl, Cr₂O₃, Fe₂O₃, and SO₃ into the Others component and adding three non-linear terms ($\text{TiO}_2 \times \text{ZrO}_2$, $(\text{Li}_2\text{O})^2$, and $\text{Li}_2\text{O} \times \text{Na}_2\text{O}$). This PQM model has an overall accuracy of 79.74%, a FPR of 24.24%, and a FNR of 6.96%.

Based on model fitting and validation results, the 19-term PQM model with three non-linear terms is the recommended model for LAW glass VHT P/F classification. This model has 16 linear composition terms of the form g_i (Al_2O_3 , B_2O_3 , CaO , F , K_2O , Li_2O , MgO , Na_2O , P_2O_5 , SiO_2 , SnO_2 , TiO_2 , V_2O_5 , ZnO , ZrO_2 , and Others); three quadratic terms of the form $g_i g_j$ or g_i^2 ($\text{TiO}_2 \times \text{ZrO}_2$, $(\text{Li}_2\text{O})^2$, and $\text{Li}_2\text{O} \times \text{Na}_2\text{O}$), a logit linking function, and a classification threshold of 0.19. Results for the recommended 19-term VHT P/F model are given in Table 4.6 and discussed in Section 4.3.2. Methods for making VHT P/F predictions and quantifying the uncertainties in the predictions are discussed and illustrated in Section 4.4.

The recommended VHT classification model yields predictions of pass/fail VHT that achieve the $\text{FNR} \leq 10\%$ while simultaneously maximizing overall accuracy. The selected model does not show significant LOF and has generally uniform performance across evaluation and validation datasets, so that VHT classifications can be expected to be within the uncertainty of what would be obtained by batching and melting glasses and measuring the VHT response.

9.3 Summary of LAW Viscosity Modeling

Data on viscosity were available for 549 LAW glass melts from the six data groups discussed in Section 2.0. Viscosity was measured at between three and eight temperatures for each LAW glass melt, generally 900 °C and 1250 °C. A VFT model¹ was generally used to interpolate the viscosity value at 1150 °C. The η_{1150} values vary from 4.70 to 353 poise.

Assessment of the ranges and distributions of the component values over the 549 LAW glasses with viscosity data led to designating 13 glasses as having outlying compositions. One glass was excluded from modeling since it was a CCC specimen of a previous glass, and one glass was identified as an outlier during the model development work. The remaining 534 glass composition/ η_{1150} data were used in modeling efforts. The LAW glass composition and viscosity data are listed in Appendix A, Tables A.2 and A.3, respectively. Over these 534 LAW glasses, the component ranges and distributions of 20 components (Al_2O_3 , B_2O_3 , CaO , Cl , Cr_2O_3 , F , Fe_2O_3 , K_2O , Li_2O , MgO , Na_2O , P_2O_5 , SO_3 , SiO_2 , SnO_2 , TiO_2 , V_2O_5 , ZnO , ZrO_2 , and Others) were sufficient to support separate model terms if needed.

Several property-composition model forms for η_{1150} were explored. In this study as in previous studies, it was determined that a natural logarithm transformation (i.e., $\ln(\eta_{1150})$) improved modeling efforts. Three models were ultimately selected for reporting:

- A 20-term FLM model (Table 5.4) with R^2 and RMSE values of 0.9429 and 0.1375
- An 18-term RLM model (Table 5.6) formed by combining Cl and SO_3 into the “Others” component, with R^2 and RMSE values of 0.9410 and 0.1395
- A 21-term PQM model (Table 5.7) formed by adding three non-linear terms to the RLM model ($\text{Al}_2\text{O}_3 \times \text{Na}_2\text{O}$, $(\text{Li}_2\text{O})^2$, and $\text{Li}_2\text{O} \times \text{Na}_2\text{O}$), with R^2 and RMSE values of 0.9487 and 0.1304

Based on model fitting and validation results, the 21-term PQM model with three non-linear terms is the recommended model for viscosity of LAW glasses. This model has 18 linear composition terms of the form g_i (Al_2O_3 , B_2O_3 , CaO , Cr_2O_3 , F , Fe_2O_3 , K_2O , Li_2O , MgO , Na_2O , P_2O_5 , SiO_2 , SnO_2 , TiO_2 , ZnO , ZrO_2 , and Others) and three quadratic terms of the form $g_i g_j$ or g_i^2 ($\text{Al}_2\text{O}_3 \times \text{Na}_2\text{O}$, $(\text{Li}_2\text{O})^2$, and $\text{Li}_2\text{O} \times \text{Na}_2\text{O}$). Results for the recommended 21-term $\ln(\eta_{1150})$ model are given in Table 5.7 and discussed in Section

¹ The Vogel-Tamman-Fulcher model describes temperature effect on viscosity: $\ln[\eta_T] = A + \frac{B}{T - T_0}$, where A , B , and T_0 are fit parameters and T is temperature in °C.

5.3.3. Methods for making viscosity predictions and quantifying the uncertainties in the predictions are discussed and illustrated in Section 5.4.

The recommended viscosity model provides unbiased predictions over the full range of measured viscosity values in the modeling dataset, with relatively tight scatter for most data points about the fitted model, and moderate scatter for some data points (see Figure 5.14). The recommended viscosity model does not have a statistically significant LOF, so that viscosity predictions can be expected to be within the uncertainty of what would be obtained by batching and melting glasses and measuring the viscosity. The magnitudes of uncertainties in $\ln(\eta_{1150})$ model predictions should be small enough that they will not unduly restrict the formulation and processing of LAW glasses in the LAW WTP Facility. However, separate work to confirm this is planned, as discussed in Section 9.10.

9.4 Summary of LAW Electrical Conductivity Modeling

EC data were available for 542 LAW glass melts from the six data groups discussed in Section 2.0. EC was measured at between three and eight temperatures for each LAW glass melt, generally 900 °C and 1250 °C. A VFT model¹ was generally used to interpolate the EC value at 1150 °C. The ϵ_{1150} values vary from 0.0770 to 0.789 S/cm.

Assessment of the ranges and distributions of the component values over the 542 LAW glasses with EC data led to designating 13 glasses as having outlying compositions. One glass was excluded from modeling since it was a CCC specimen of a previous glass and two glasses were identified as an outlier during the model development work. The remaining 526 glass composition/ ϵ_{1150} data were used in modeling efforts. The LAW glass composition and EC data are listed in Appendix A, Tables A.2 and A.3, respectively. Over these 526 LAW glasses, the component ranges and distributions of 20 components (Al_2O_3 , B_2O_3 , CaO , Cl , Cr_2O_3 , F , Fe_2O_3 , K_2O , Li_2O , MgO , Na_2O , P_2O_5 , SO_3 , SiO_2 , SnO_2 , TiO_2 , V_2O_5 , ZnO , ZrO_2 , and Others) were sufficient to support separate model terms if needed.

Several property-composition model forms for ϵ_{1150} were explored. In this study as in previous studies, it was determined that a natural logarithm transformation (i.e., $\ln(\epsilon_{1150})$) improved modeling efforts. Three models were ultimately selected for reporting:

- A 20-term FLM model (Table 6.3) with R^2 and RMSE values of 0.8359 and 0.1417
- An 11-term RLM model (Table 6.4) formed with individual terms for Al_2O_3 , B_2O_3 , CaO , K_2O , Li_2O , MgO , Na_2O , SiO_2 , SnO_2 , and V_2O_5 , with all remaining components combined into the Others component, with R^2 and RMSE values of 0.8267 and 0.1444
- A 13-term PQM model (Table 6.5) formed by adding two non-linear terms to the RLM model ($(\text{Na}_2\text{O})^2$ and $\text{Li}_2\text{O} \times \text{Na}_2\text{O}$), with R^2 and RMSE values of 0.8563 and 0.1318

Based on model fitting and validation results, the 13-term PQM model with two non-linear terms is the recommended model for viscosity of LAW glasses. This model has 11 linear composition terms of the form g_i (Al_2O_3 , B_2O_3 , CaO , K_2O , Li_2O , MgO , Na_2O , SiO_2 , SnO_2 , V_2O_5 , and Others) and two quadratic terms of the form $g_i g_j$ or g_i^2 ($(\text{Na}_2\text{O})^2$ and $\text{Li}_2\text{O} \times \text{Na}_2\text{O}$). Results for the recommended 13-term $\ln(\epsilon_{1150})$ model are given in Table 6.5 and discussed in Section 6.3.3. Methods for making EC predictions and quantifying the uncertainties in the predictions are discussed and illustrated in Section 6.4.

¹ The Vogel-Tamman-Fulcher model describes temperature effect on EC: $\ln(\epsilon_T) = A + \frac{B}{T - T_0}$, where A , B , and T_0 are fit parameters and T is temperature in °C.

The recommended EC model provides unbiased predictions over the full range of measured EC values in the modeling dataset, with relatively moderate scatter for most data points about the fitted model, and larger scatter for some data points (see Figure 6.14). The recommended EC model does not have a statistically significant LOF. The magnitudes of uncertainties in $\ln(\varepsilon_{1150})$ model predictions should be small enough that they will not unduly restrict the formulation and processing of LAW glasses in the LAW WTP Facility. However, separate work to confirm this is planned, as discussed in Section 9.10.

9.5 Summary of LAW Melter SO₃ Tolerance Modeling

Data related to melter SO₃ tolerance and SO₃ solubility in glass melts was measured using variants of five primary techniques: batch saturation (BS), saturation re-melting (SR), bubbling (Bub), and three-time saturation (3TS), and melter tolerance (MT) (see Section 7.1.1). The first four, based on crucible test methods, were used for modeling in this study. At least one of these techniques was performed on 601 LAW glass compositions from the six data groups discussed in Section 2.0. Table 9.1 summarizes these data.

The melter SO₃ tolerance and solubility results were found to depend on measurement method. A nearly constant offset was identified between data from different groups of methods such that 3TS > Bub = MT > BS = SR. Since, the property of interest is MT, it was decided to model a separate offset for 3TS and BS+SR data with no offset for MT or Bub data. For several glasses, multiple different measurements were performed. It was decided to include each measurement as a separate model entry with the appropriate offset, if applicable, resulting in 660 individual measurements. The LAW glass composition and melter SO₃ tolerance and solubility data are listed in Appendix A, Tables A.2 and A.3, respectively.

Table 9.1. Summary of Melter SO₃ Tolerance and Solubility Data

Method	# of Data	Min Value	Max Value	Approximate Offset ^(a)
BS	131	0.425 wt%	1.83 wt%	-0.2 wt%
SR	360	0.15	1.66	-0.2
Bub	57	0.51	1.7	0
MT	13	0.5	1.5	0
3TS	99	0.602	2.603	0.4
Total glasses	601			
Total data	660	0.15	2.603	

(a) Offset depends on model, refer to specific model for precise value

Assessment of the ranges and distributions of the component values over the 601 LAW glasses with melter SO₃ tolerance or solubility data led to designating 22 glasses as having outlying compositions. Three glasses were identified as outliers during the model development work (Table 7.1). The remaining 576 glass were used in melter SO₃ tolerance modeling efforts. Each of the outlying glasses were measured by only one technique, resulting in 635 melter SO₃ tolerance and solubility data points for modeling (112 BS, 356 SR, 56 Bub, 13 MT, and 98 3TS). Over these 576 LAW glasses, the component ranges and distributions of 19 re-normalized components (Al₂O₃, B₂O₃, CaO, Cl, Cr₂O₃, F, Fe₂O₃, K₂O, Li₂O, MgO, Na₂O, P₂O₅, SiO₂, SnO₂, TiO₂, V₂O₅, ZnO, ZrO₂, and Others) were sufficient to support separate model terms if needed.

Several property-composition model forms for melter SO₃ tolerance were explored. In each case, the glass composition was adjusted by removing measured SO₃ and renormalizing the remaining components.

After evaluating offsets for BS+SR and 3TS data compared to Bub+MT, it was determined that constant offset best reflected the trends in data. Setting the offset for MT+Bub data to zero allows the direct prediction of the property of interest in plant operation, namely MT. Three models were ultimately selected for reporting:

- A 19-term FLM model (Table 7.3) with R^2 and RMSE values of 0.8281 and 0.1769
- A 10-term RLM model (Table 7.4) formed with individual terms for Al_2O_3 , B_2O_3 , CaO , Cl , Li_2O , Na_2O , P_2O_5 , SiO_2 , and V_2O_5 with all remaining components combined into the Others component, with R^2 and RMSE values of 0.8073 and 0.1860
- An 11-term PQM model (Table 7.5) formed by adding one cross-product term to the RLM model ($\text{Li}_2\text{O} \times \text{Na}_2\text{O}$), with R^2 and RMSE values of 0.8303 and 0.1747

Based on model fitting and validation results, the 11-term PQM model with one non-linear term is the recommended model for $w_{\text{SO}_3}^{\text{MT}}$ of LAW glasses. This model has 10 linear composition terms of the form of normalized component concentrations, x_i (Al_2O_3 , B_2O_3 , CaO , Cl , Li_2O , Na_2O , P_2O_5 , SiO_2 , V_2O_5 , and Others) and one cross-product terms of the form $x_i x_j$ ($\text{Li}_2\text{O} \times \text{Na}_2\text{O}$). Results for the recommended 11-term $w_{\text{SO}_3}^{\text{MT}}$ model are given in Table 7.5 and discussed in Section 7.3.3. Methods for making melter SO_3 tolerance predictions and quantifying the uncertainties in the predictions are discussed and illustrated in Section 7.4.

The recommended $w_{\text{SO}_3}^{\text{MT}}$ model provides unbiased predictions over most of the measured $w_{\text{SO}_3}^{\text{MT}}$ range with relatively high scatter for most data points about the fitted model (see Figure 7.14). There is a slight under-prediction of $w_{\text{SO}_3}^{\text{MT}}$ above a predicted value of roughly 1.5 wt%, which will yield conservative results. The magnitudes of uncertainties in $w_{\text{SO}_3}^{\text{MT}}$ model predictions are likely to be high enough that they will restrict the formulation and processing of LAW glasses in the LAW WTP Facility, suggesting future testing and modeling efforts may be beneficial. Separate work to confirm this is planned, as discussed in Section 9.10.

9.6 Summary of LAW K-3 Refractory Corrosion Modeling

Data related to K-3 refractory corrosion in glass melts were measured at 1208 °C for 6 days (k_{1208}). Data on k_{1208} were available for 344 LAW glass melts from the six data groups discussed in Section 2. The k_{1208} values ranged from 0.001 to 0.145 inch generally distributed in a log-normal pattern.

Assessment of the ranges and distributions of the component values over the 344 LAW glasses with k_{1208} data led to designating five glasses as having outlying compositions. Two glasses were excluded from modeling since they were tested on a CCC specimen of a previous glass and four glasses were identified as having outlying k_{1208} values (< 0.003 inch) and were also found to be outliers during model development work (Table 8.1). The remaining 333 glass composition/ k_{1208} data were used in modeling efforts. The LAW glass composition and k_{1208} data are listed in Appendix A, Tables A.4 and A.5, respectively. Over these 333 LAW glasses, the component ranges and distributions of 20 components (Al_2O_3 , B_2O_3 , CaO , Cl , Cr_2O_3 , F , Fe_2O_3 , K_2O , Li_2O , MgO , Na_2O , P_2O_5 , SO_3 , SiO_2 , SnO_2 , TiO_2 , V_2O_5 , ZnO , ZrO_2 , and Others) were sufficient to support separate model terms if needed.

Several property-composition model forms for k_{1208} data were explored. In this study as in previous studies, it was determined that a natural logarithm transformation (i.e., $\ln(k_{1208})$) improved modeling efforts. Three models were ultimately selected for reporting:

- A 20-term FLM model (Table 8.4) with R^2 and RMSE values of 0.8162 and 0.3305
- An 11-term RLM model (Table 8.6) formed with individual terms for Al_2O_3 , B_2O_3 , CaO , Cr_2O_3 , K_2O , Li_2O , Na_2O , SiO_2 , V_2O_5 , and ZrO_2 with all remaining components combined into the Others component, with R^2 and RMSE values of 0.8001 and 0.3397
- A 13-term PQM model (Table 8.7) formed by adding two non-linear terms to the RLM model $((\text{Li}_2\text{O})^2$ and $\text{Na}_2\text{O} \times \text{SiO}_2$), with R^2 and RMSE values of 0.8245 and 0.3193

Based on model fitting and validation results, the 13-term PQM model with two non-linear terms is the recommended model for k_{1208} of LAW glasses. This model has 11 linear composition terms of the form g_i (Al_2O_3 , B_2O_3 , CaO , Cr_2O_3 , K_2O , Li_2O , Na_2O , SiO_2 , V_2O_5 , ZrO_2 , and Others) and two quadratic terms of the form $g_i g_j$ or g_i^2 ($(\text{Li}_2\text{O})^2$ and $\text{Na}_2\text{O} \times \text{SiO}_2$). Results for the recommended 13-term $\ln[k_{1208}]$ model are given in Table 8.7 and discussed in Section 8.3.3. Methods for making k_{1208} predictions and quantifying the uncertainties in the predictions are discussed and illustrated in Section 8.4.

The recommended k_{1208} model provides unbiased predictions over the full range of measured k_{1208} values in the modeling dataset, with relatively moderate scatter for most data points about the fitted model, and larger scatter for some data points (see Figure 8.12). It is recommended that the k_{1208} model be used as an indicator only and not to limit the composition of LAW glasses to be produced in the WTP LAW Facility for the following reasons:

- The recommended k_{1208} model has a statistically significant LOF.
- The magnitudes of uncertainties in $\ln(k_{1208})$ model predictions are large enough that they will restrict the formulation and processing of LAW glasses in the LAW Facility.
- The model validity ranges for k_{1208} are sufficiently narrower than for other models in this report, which will limit the flexibility to process the full range of LAW glasses.

Future testing and modeling efforts are recommended to improve upon the k_{1208} model. Separate work to confirm this is planned, as discussed in Section 9.10.

9.7 Summary of Model Validity Regions for Recommended LAW Glass Property Models

The LAW glass property-composition models recommended in this report were obtained by estimating coefficients of models using least squares regression methods. Models developed in this way should only be applied to LAW glass compositions inside the composition region over which the models were developed and demonstrated to yield unbiased predictions. Such regions are referred to as *model validity regions*, which are typically defined using single- and multiple-component constraints on glass components.

The single-component concentration ranges for data used to develop each of the recommended models are summarized in Table 9.2. The single-component model validity constraints vary from model to model as all properties were not measured on all glasses. For practical application of these models in glass formulation, a single set of model validity constraints must be applied. The ranges were compared and overall model validity constraints across the models for application in glass design were determined. Relatively large differences between the overall component concentration ranges and those for individual properties are marked in bold and either red or green font to represent if the component range for the property is narrower or broader than the overall range for that component, respectively. Values marked with gray font are for components not in the recommended model. With the previously described

exception of the K-3 corrosion model, those values with narrower ranges than the overall range are few. With only a few exceptions, the overall range is not significantly broader than any individual model range for components found to be significant for the recommended model (e.g., term in the recommended model). Those exceptions include the following:

- TiO_2 for PCT responses with a maximum value of 4 wt% compared to 5.01 wt% in the overall validity range. This is a reasonable extrapolation with relatively small and linear effect of TiO_2 on $\ln(PCT_B^{NL})$ and $\ln(PCT_{Na}^{NL})$ responses and it's a relatively small extrapolation (1.01 wt%).
- P_2O_5 for VHT responses with a maximum value of 3.41 wt% compared to 4.03 wt% in the overall validity range. This is a reasonable extrapolation as P_2O_5 has a small linear effect on VHT P/F and it's a relatively small extrapolation (0.62 wt%).
- F for viscosity with a maximum value of 0.72 wt% compared to 1.3 wt% in the overall validity range. This is a reasonable extrapolation considering the general linearity and goodness of fit for viscosity and relatively small extrapolation (0.58 wt%).
- ZnO for viscosity with a minimum value of 1 wt% compared to 0 wt% for the overall validity range. The linearity and goodness of fit for viscosity model, the relatively low impact of ZnO on melt viscosity, and the relatively small extrapolation (1 wt%) suggest this extrapolation can be safely made.

For selected models there were also strong pairwise correlations between components with some portions of two- and higher-component space being sparsely covered with data. For example, there is a significant negative correlation between Li_2O and Na_2O concentrations in glasses for each of the models. This is understandable as the primary LAW waste component is Na_2O which makes the alkali needed to successfully process glass while Li_2O is added in the cases that loading limitations (primarily due to high SO_3 in the waste) reduce the Na_2O concentration.

Table 9.2. Data Component Concentration Ranges (mass fraction) for LAW Glasses Used in Models

Model	PCT-Na		PCT-B		VHT		Viscosity		EC		SO ₃		<i>k</i> ₁₂₀₈		Overall	
mass fraction	Min	Max	Min	Max	Min	Max	Min	Max	Min	Max	Min	Max	Min	Max	Min	Max
Al ₂ O ₃	0.0350	0.1475	0.0350	0.1475	0.0350	0.1475	0.0350	0.1475	0.0350	0.1475	0.0350	0.1475	0.0350	0.1381^(b)	0.0350	0.1475
B ₂ O ₃	0.0500^(a)	0.1515	0.0500	0.1515	0.0600	0.1383	0.0600	0.1383	0.0600	0.1383	0.0397	0.1597	0.0420	0.1395	0.0600	0.1383
CaO	0.0000	0.1281	0.0000	0.1281	0.0000	0.1281	0.0000	0.1278	0.0000	0.1278	0.0000	0.1285	0.0000	0.1221	0.0000	0.1278
Cl	0.0000 ^(c)	0.0117	0.0000	0.0117	0.0000	0.0117	0.0000	0.0117	0.0000	0.0117	0.0000	0.0117	0.0000	0.0120	0.0000	0.0117
Cr ₂ O ₃	0.0000	0.0063	0.0000	0.0063	0.0000	0.0063	0.0000	0.0063	0.0000	0.0063	0.0000	0.0061	0.0000	0.0060	0.0000	0.0063
F	0.0000	0.0130	0.0000	0.0130	0.0000	0.0130	0.0000	0.0072	0.0000	0.0072	0.0000	0.0304	0.0000	0.0049	0.0000	0.0130
Fe ₂ O ₃	0.0000	0.1198	0.0000	0.1198	0.0000	0.0998	0.0000	0.1198	0.0000	0.1198	0.0000	0.1347	0.0000	0.0950	0.0000	0.1198
K ₂ O	0.0000	0.0809	0.0000	0.0809	0.0000	0.0809	0.0000	0.0588	0.0000	0.0591	0.0000	0.0591	0.0000	0.0591	0.0000	0.0590
Li ₂ O	0.0000	0.0633	0.0000	0.0633	0.0000	0.0582	0.0000	0.0633	0.0000	0.0633	0.0000	0.0584	0.0000	0.0591	0.0000	0.0584
MgO	0.0000	0.0502	0.0000	0.0502	0.0000	0.0502	0.0000	0.0502	0.0000	0.0502	0.0000	0.0502	0.0000	0.0490	0.0000	0.0502
Na ₂ O	0.0247	0.2657	0.0247	0.2657	0.0247	0.2657	0.0247	0.2657	0.0247	0.2657	0.0245	0.2657	0.0250	0.2597	0.0247	0.2657
P ₂ O ₅	0.0000	0.0475	0.0000	0.0475	0.0000	0.0341	0.0000	0.0403	0.0000	0.0403	0.0000	0.0475	0.0000	0.0340	0.0000	0.0403
SO ₃	0.0000	0.0160	0.0000	0.0160	0.0000	0.0163	0.0004	0.0163	0.0004	0.0163	NA ^(d)	NA	0.0001	0.0250	0.0000	0.0163
SiO ₂	0.3329	0.5592	0.3329	0.5592	0.3329	0.5226	0.3352	0.5226	0.3352	0.5226	0.3000	0.5226	0.3440	0.5016	0.3352	0.5226
SnO ₂	0.0000	0.0503	0.0000	0.0503	0.0000	0.0503	0.0000	0.0503	0.0000	0.0503	0.0000	0.0503	0.0000	0.0500	0.0000	0.0503
TiO ₂	0.0000	0.0400	0.0000	0.0400	0.0000	0.0501	0.0000	0.0501	0.0000	0.0501	0.0000	0.0501	0.0000	0.0500	0.0000	0.0501
V ₂ O ₅	0.0000	0.0571	0.0000	0.0571	0.0000	0.0409	0.0000	0.0409	0.0000	0.0409	0.0000	0.0437	0.0000	0.0400	0.0000	0.0409
ZnO	0.0000	0.0582	0.0000	0.0582	0.0100	0.0582	0.0100	0.0582	0.0100	0.0582	0.0000	0.0578	0.0000	0.0540	0.0000	0.0582
ZrO ₂	0.0000	0.0675	0.0000	0.0675	0.0000	0.0675	0.0000	0.0675	0.0000	0.0675	0.0000	0.0900	0.0000	0.0751	0.0000	0.0675
Others Rec ^(e)	0.0015	0.0580	0.0015	0.0580	0.0016	0.1085	0.0010	0.0216	0.0152	0.2036	0.0653	0.2984	0.0462	0.1901	NA	NA
Others20 ^(f)	0.0000	0.0054	0.0000	0.0054	0.0000	0.0044	0.0000	0.0033	0.0000	0.0033	0.0000	0.0027	0.0000	0.0160	NA	NA
Property (transformed)	-2.3026	2.5958	-2.5257	2.8814	0.0000	1.0000	1.5476	5.5595	-2.0402	-0.2370	0.1500	2.6030	-5.8091	-1.9310	NA	NA
property (untransformed)	0.1	13.407	0.08	17.84	0.1	1529.1	4.7	259.69	0.13	0.789	0.15	2.603	0.003	0.145	NA	NA

(a) Green entries represent higher values than overall mv limits.

(b) Red entries represent significantly lower values than overall mv limits.

(c) Gray entries represent components not in the recommended models.

(d) NA represents non-applicable entries.

(e) Others Rec is the concentration of Others in the final recommended models.

(f) Others20 represents the Others in the full 20-component modeling dataset.

To address this and other pairwise (i.e., 2-D) correlations, the combined data that was used in at least one of the models was evaluated for correlations. Three pairs were found to show significant correlations (with absolute values near or greater than 0.6) – $\text{Li}_2\text{O}:\text{Na}_2\text{O}$ (-0.8572), $\text{Al}_2\text{O}_3:\text{SiO}_2$ (-0.5914), and $\text{Na}_2\text{O}:\text{SiO}_2$ (-0.6288). Figure 9.1 shows the data correlation between Li_2O and NaK ($= g_{\text{Na}_2\text{O}} + 0.66g_{\text{K}_2\text{O}}$). A similar but broader correlation exists between Li_2O and Na_2O , but since most glass formulations are designed to an optimum value of NaK (Muller et al. 2017b), the correlation is tighter and more useful as a constraint. Roughly 98% of the model database falls within the range shown by the two slanted lines on the plot. These lines have a parallel slope of precisely -1/2.07 which is equivalent to $-MW_{\text{Na}_2\text{O}}/MW_{\text{Li}_2\text{O}}$. These lines therefore translate to a limit in the range of NaK ($= g_{\text{Na}_2\text{O}} + 0.66g_{\text{K}_2\text{O}}$) of:

$$0.13500 \leq \text{NaK} \leq 0.27018 \quad (9.1)$$

Figure 9.2 shows the data correlation between Al_2O_3 and SiO_2 . Most of the glasses (roughly 98%) in the model database falls below the red line on the plot. This line has a slope of precisely -1/1.697 which is equivalent to $-MW_{\text{Al}_2\text{O}_3}/MW_{\text{SiO}_2}$. The line therefore translates to a limit of:

$$g_{\text{SiO}_2} + 1.697g_{\text{Al}_2\text{O}_3} \leq 0.6160 \quad (9.2)$$

Figure 9.3 shows the data correlation between Na_2O and SiO_2 . In this figure the vertical lines represent the model validity range for SiO_2 given in Table 9.2. Although there is a clear cluster of glass from the upper left to lower right of the figure, the full two-dimensional composition region is reasonably covered. So, no further constraints are recommended.

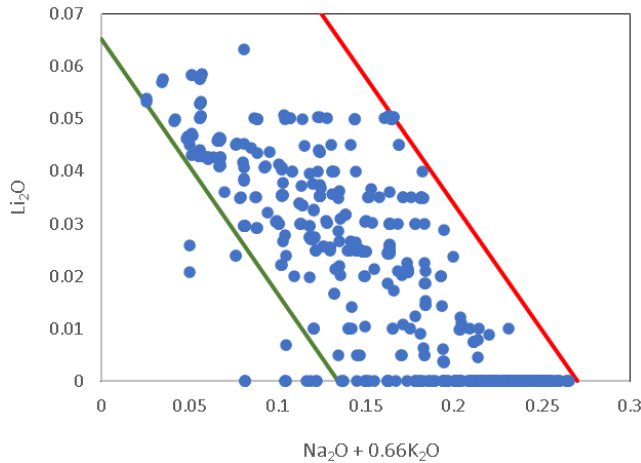


Figure 9.1. Concentrations of NaK ($= g_{\text{Na}_2\text{O}} + 0.66g_{\text{K}_2\text{O}}$) and Li_2O of modeling database in mass fractions.

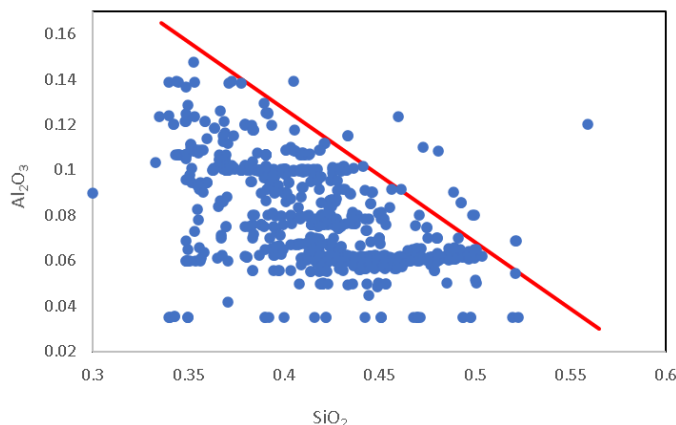


Figure 9.2. Concentrations of SiO_2 and Al_2O_3 of modeling database in mass fractions.

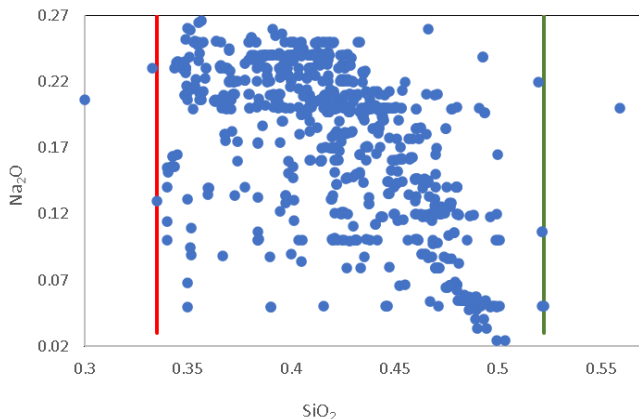


Figure 9.3. Concentrations of Na_2O and SiO_2 of modeling database in mass fractions.

Just as pairwise (2-D) correlations were identified in the modeling dataset, there are likely to be similar higher dimensional correlations in the data. This is partially due to the inherent constraint that test glasses must be fabricated in a certain temperature range and within a relatively narrow viscosity range, and they target immobilizing Hanford LAW, which is inherently compositionally correlated.

High correlation among variables used as predictors, or multicollinearity, has the effect of inflating the variances of parameter estimates of the predictors (see Myers and Montgomery, 1995, especially Appendix 2). In the context of this work, the inflated variances produced by multicollinearity can lead to poor estimates of model parameters, making interpretation of component effects difficult.

Assessing the level of multicollinearity in a dataset can be done in a variety of ways, but they all essentially determine if two or more predictors are involved in a linear or near-linear constraint such as the one shown in Figure 9.1. Naturally, this type of constraint is always present in the glass composition portion of the models in this document because the sum of the mass fractions over the glass components is always equal to unity. In addition, as shown in the analysis leading to the results in Figures 9.1 to 9.3, other multicomponent constraints needed to make usable glass for Hanford LAW are present in the data.

Multicollinearity can be diminished by collecting data in a way to systematically ‘break’ linear relationships that are present (one such way is the use of statistically designed glass formulations, as was

done for a number of the glasses in this work), by appropriately rescaling the predictors (although this may be of limited benefit in our case since rescaling will not eliminate some of the fundamental constraints present), by estimating model parameters using a method that is less sensitive to multicollinearity than least squares (like ridge regression), or by performing model selection in a way that deletes certain predictors from the model. Although multicollinearity can have a detrimental effect on the precision of parameter estimates, the models can produce accurate predictions, particularly in the space where the multicollinearity is in effect. This is because, while individual parameters may be poorly estimated, the data place constraints on the combination of model parameters, $\sum_i b_i g_i$, and this combination may be estimated very well (Transtrum et al. 2015). This means that predictions on new or existing glass compositions that remain in the space defined by the data are likely to have similar performance as those used during validation.

One important characteristic of the models developed in this work, which may reduce the impact of multicollinearity, is that model development has been guided by glass science and by previous efforts to statistically design new glass formulations. Knowledge of the effects that certain components have on the responses of interest was employed to select and discriminate between competing models, while the use of statistically designed glasses lessens the effect of multicollinearity as much as possible.

In conclusion, it is recommended that the 1-D model validity constraints given in Table 9.2 and the 2-D model validity constraints given in Equations (9.1) and (9.2) be used to constrain the application of the glass property-composition models recommended in this report.

9.8 Component Effects on Properties

Component effects (dP/dg_i , where P is transformed property) on the properties modeled in this report are calculated at the REFMIX composition and listed in Table 9.3. A semi-graphical representation of these effects is given in Table 9.4 where arrows represent the relative effects of components on a given property. In this latter representation, there is subjectivity in determining which effects are to be considered significant as statistically all terms in the models (with the occasional exception of “Others”) are significant. Therefore, the graphical representation given in Table 9.4 should be taken as a rough indication only.

Table 9.3. Component effect “slopes” for each of the recommended models taken at the REFMIX composition

	$\ln(PCT_B^{NL}, \text{g/m}^2)$	$\ln(PCT_{Na}^{NL}, \text{g/m}^2)$	VHT P/F x_b	$\ln(\epsilon_{1150}, \text{S/cm})$	$\ln(\eta_{1150}, \text{P})$	Melter SO ₃ Tolerance, wt%	$\ln(k_{1208}, \text{inch})$
Al ₂ O ₃	-13.85	-12.47	-26.94	-2.79	11.79	-3.52	-25.27
B ₂ O ₃	7.36	3.52	-2.07	-2.01	-10.94	2.62	-2.35
CaO	-2.40	0.34	-51.66	-2.51	-9.57	4.38	9.79
Cl	n/a	n/a	n/a	n/a	n/a	-18.57	n/a
Cr ₂ O ₃	n/a	n/a	n/a	n/a	-10.89	n/a	-91.57
F	n/a	n/a	56.14	n/a	-17.53	n/a	n/a
Fe ₂ O ₃	1.66	-0.19	n/a	n/a	-2.18	n/a	n/a
K ₂ O	7.53	7.69	107.40	0.41	-6.49	n/a	14.97
Li ₂ O	13.30	13.52	218.16	13.32	-37.34	5.70	62.26
MgO	14.80	8.88	39.68	-2.66	-5.05	n/a	n/a
Na ₂ O	11.23	11.35	123.30	9.27	-13.67	1.52	34.62
P ₂ O ₅	n/a	n/a	-34.14	n/a	6.86	1.53	n/a
SO ₃	n/a	n/a	n/a	n/a	n/a	n/a	n/a
SiO ₂	-6.61	-5.64	-44.76	-3.50	13.45	-0.79	-14.87
SnO ₂	-7.01	-5.53	-51.31	-3.51	3.26	n/a	n/a
TiO ₂	-8.09	-3.62	-119.09	n/a	-4.75	n/a	n/a
V ₂ O ₅	2.53	2.96	29.41	-0.92	-5.55	5.61	-17.29
ZnO	-1.47	-1.32	-41.74	n/a	-5.54	n/a	n/a
ZrO ₂	1.16	-0.51	-110.26	n/a	5.52	n/a	-10.94
Others	0.69	0.66	-13.11	-0.62	6.48	-2.32	-1.18

Table 9.4. General Direction of Component Effects on Properties^(a) (For Information Only)

	PCT	VHT	ϵ_{1150}	η_{1150}	SO ₃	k_{1208}
Al ₂ O ₃	↓↔	↔	↔	↑	↓	↓
B ₂ O ₃	↔	↔	↔	↓	↑	↔
CaO	↔	↓	↔	↓	↑	↑
Cl	n/a	n/a	n/a	n/a	↓	n/a
Cr ₂ O ₃	n/a	n/a	n/a	↓	n/a	↓
F	n/a	↑	n/a	↓	n/a	n/a
Fe ₂ O ₃	↔	n/a	n/a	↔	n/a	n/a
K ₂ O	↑	↑	↔	↓	n/a	↑
Li ₂ O	↑	↑	↑	↓	↑	↑
MgO	↑	↔	↔	↔	n/a	n/a
Na ₂ O	↑	↑	↑	↓	↑	↑
P ₂ O ₅	n/a	↔	n/a	↑	↑	n/a
SO ₃	n/a	n/a	n/a	n/a	n/a	n/a
SiO ₂	↓	↓	↔	↑	↓	↓
SnO ₂	↓	↓	↔	↔	n/a	n/a
TiO ₂	↓	↓	n/a	↔	n/a	n/a
V ₂ O ₅	↔↑	↔	↔	↔	↑	↓
ZnO	↔	↔	n/a	↔	n/a	n/a
ZrO ₂	↔	↓	n/a	↔	n/a	↓
Others	↔	↔	↔	↔	↓	↔

(a) ↑ - component significantly increases property value, ↓ - component significantly decreases property value, ↔ component has a relatively small effect on property, n/a – component not included in model, ↓↔ - Al₂O₃ significantly decreases PCT response when added at low concentrations and has negligible effects when added at higher concentrations.

9.9 Additional Constraints

Not all properties of interest to LAW processing and product acceptance were fitted as functions of composition in the sections above. For example, glass property-composition models were generated to predict PCT responses (Section 3.0) and VHT responses (Section 4.0) of quenched glasses and not for CCC glasses. Additional constraints were developed, as discussed in Section 9.9.1, to ensure glasses will not have significantly poorer performance after CCC heat-treatment compared to quenched glasses. Likewise, with the broader composition regions available by applying the models reported here, there is the possibility for crystallization in the melter. Section 9.9.2 describes constraints needed to avoid the deleterious effects of that crystallization.

9.9.1 Slow-Cooled Glass Crystallization Constraint

The LAW glass property-composition models presented in this work primarily focus on quenched glass samples. These are sufficient for melt properties such as viscosity, EC, melter SO₃ tolerance, and K-3 corrosion. However, glass properties such as PCT and VHT may be changed by slow cooling inside the LAW containers. Slow cooling tends to reduce the PCT and VHT responses (makes glass more durable) so long as significant phase changes are avoided. When some components participate in crystallization or immiscible phase separation, their concentration reduction in bulk glass will have significant effects on glass properties (e.g., PCT and VHT).

The rate of cooling in a LAW glass container is bounded by typical quenching that is performed as part of normal laboratory glass sample preparation on one side and by simulated CCC on the other side (Petkus 2003). The PCT and VHT responses have been measured on selected glass samples exposed to both CCC and quench preparation. The composition space in which crystallization occurs during CCC of LAW glasses to a sufficient degree as to affect PCT or VHT is relatively small. For WTP baseline glass formulation approach, no glasses were found with significantly degraded PCT or VHT on CCC. Therefore, no constraint was necessary to avoid the potentially adverse effects of crystallization in the container (Latham 2018; Kim and Vienna 2012). As the GCR expanded, some LAW glasses were found to crystallize sufficiently during CCC as to degrade PCT and/or VHT. In the 2016 modeling effort, a crystallization constraint was introduced to avoid such concentration range (Vienna et al. 2016):

$g_{ZrO_2} + g_{SnO_2} + g_{Al_2O_3} \leq 0.17$. This ad-hoc constraint was found to be insufficient when compared to data developed after 2016; therefore, a new crystallization constraint was needed.

All the glasses with PCT and VHT measured for both quenched and simulated CCC treated samples were collected from established databases, including the one described in Section 2.1. There were two crystal groups identified to have a noticeable negative effect on PCT and VHT responses: Na-Al silicate and Na-Ca (also covering Na-Ca-Al) silicate groups. Na-Al silicate group included nepheline (nominal chemical formula of NaAlSiO₄) and nosean [Na₈Al₆Si₆O₂₄(SO₄)] while Na-Ca silicate group included combeite (Na₂Ca₂Si₃O₉), hauyne [Na₃CaAl₃Si₃O₁₂(SO₄)], and lazurite [Na₃CaAl₃Si₃O₁₂(SO₄, S, Cl, OH)]. The following CCC crystallization constraints (Eqn. 9.3 and 9.4), were developed to prevent formation of Na-Al and Na-Ca group crystals, respectively, and thus to avoid the potential negative effect of slow cooling in a LAW glass container on PCT and VHT responses.

$$g_{Al_2O_3} \leq 0.158 - 0.28(g_{Na_2O} + 0.66g_{K_2O}) \quad (9.3)$$

$$g_{CaO} \leq 0.2084 - 0.528(g_{Na_2O} + 0.66g_{K_2O}) \quad (9.4)$$

The detailed description of data collection and constraints development is treated in a separate report (Lonergan et al. 2021).

9.9.2 Melt Crystallization Constraint

Excessive crystallization in the LAW melter may be detrimental to both melter operation and product quality. Crystals that form in the glass melt, if of sufficient density, particle size, and amount, may settle and cause pouring problems in the pour-spout riser (Matyáš et al. 2012). This is a well-established issue for HLW glass melts where spinel crystals are ubiquitous (Jain and Barnes 1991; Vienna et al. 2001; Annamalai et al. 2004; Jantzen and Brown 2007; Matlack et al. 2009b; Matyáš et al. 2010; and Lonergan et al. 2019). For Hanford HLW glass melts, ad-hoc constraints of 1 vol% (Kot and Pegg 2001) or 2 vol% (Vienna et al. 2013) of spinel at 950 °C were adopted as conservative constraints.

Crystallization in the melt has not traditionally been an issue in LAW glass melts which rarely precipitate spinel or other phases. However, in an attempt to maximize alkali loading while maintaining satisfactory VHT and PCT responses, SnO₂ has been added to the melt, creating a potential challenge with exceeding the liquidus temperature of cassiterite (SnO₂). With a density higher than spinel (~7 g/cm³ compared to ~5 g/cm³ for typical HLW glass spinels), settling may be an issue. Also, as SnO₂ is specifically added to reduce VHT response and glasses containing SnO₂ are typically formulated at or near the VHT response limit, loss of SnO₂ due to crystallization may impact waste form acceptance.

All the glass crystal content vs. composition and isothermal heat treatment data from glasses described in Section 2.1 were collected by Lonergan et al. (2022). They also tested additional glasses to fill gaps in the data primarily for glass compositions with intermediate to high SnO₂ content. An evaluation of the results identified two constraints to significantly reduce the risk of ≥ 1 vol% of either Cassiterite (SnO₂) or zirconia-containing phases (e.g., Baddeleyite, Zircon, Parakelydshite). These constraints include:

$$g_{SnO_2} \leq 0.045 \quad (9.5)$$

$$g_{Al_2O_3} + 0.677g_{SnO_2} + 0.827g_{ZrO_2} \leq 0.1655. \quad (9.6)$$

9.9.3 Lithia and Zirconia Targets

The models and constraints documented in this report were used to develop a set of optimized glasses for example Hanford LAW feeds (Lu et al. 2021). It was observed that optimizing glass composition for maximum waste loading resulted in a few glasses with Li₂O concentrations above those previously observed to cause a change in the mechanism of K-3 refractory corrosion (Muller et al. 2004a). Therefore, a maximum Li₂O concentration constraint is recommended:

$$g_{Li_2O} \leq 0.043. \quad (9.7)$$

Several glasses with optimized LAW loading also reduced ZrO₂ concentrations to zero which is below the concentration for virtually all of the actively designed glasses and in a region prone to relatively poor VHT and PCT responses. Therefore, a minimum ZrO₂ concentration constraint is recommended:

$$g_{ZrO_2} \geq 0.02. \quad (9.8)$$

9.10 Status and Recommendation of Future Work

The work in this report to develop, validate, and quantify the uncertainty in property-composition models for LAW glasses has succeeded in meeting the objectives of this study. Models have been developed and validated for key properties of interest to the LAW Facility operation and waste form qualification, including VHT, PCT, viscosity, EC, and melter SO_3 tolerance. These models incorporate the data developed since the last plant operations modeling effort in 2007 (Piepel et al. 2007). The composition ranges over which these new models were developed are significantly broader than those in current use.

However, there are many areas where improvements to the models can significantly reduce the risk and open the operating window for operation. These include the following:

- Develop methods and models to control composition of LAW glasses to reduce the risk of disposal performance shortfalls and thereby replace the current most-restrictive constraint of VHT response.
- Develop data and models to extend the composition region over which k_{1208} models are valid. This would allow the models to be implemented directly as a formulation constraint without exceeding model validity range and thereby reduce risk of premature melter failure due to refractory corrosion (see Section 8.3.4).
- Develop viscosity and EC models as functions of temperature. This would provide LAW Facility operators with direct data to evaluate the impact of changing operating temperature due to upset conditions or idling. Viscosity predictions as a function of temperature would also be useful in evaluating crystallinity and vitrification processing rates. Example viscosity and EC models as functions of both composition and temperature are given in Appendix E.
- Develop data and models to improve VHT response prediction to reduce conservatism and expand the LAW Facility operating window. Advanced machine learning techniques could be employed.
- Develop data and models that cover broader composition regions to further open the plant processing window and reduce conservatism in glass formulation.
- More detailed analyses of replicate glass and near-replicate glass data is warranted due to the relatively large differences (%RSDs) for some near replicate pairs for some properties.
- Statistical analyses suggested significant and unexpected effects of some minor components on a number of glass properties. Most notably, the impacts of Cr_2O_3 and SO_3 on viscosity, PCT, and VHT responses were unexpectedly significant. In some cases, these components were combined in Others despite significant statistical evidence for effects, while in other cases their effects are reflected in the models. Experimental testing aimed specifically at determining the impacts of these components on properties of LAW glasses is needed to better predict composition effects. Statistical design of new test glasses can be used to decrease the impact of multicollinearity, which may be at least in part responsible for the unexpected significant effect of these minor components.
- Update the GFA(s) to allow for direct implementation of these new models and associated glass formulation approaches in plant operations.
- Update the glass formulation methods in system planning and dynamic flowsheet models to better predict the composition and amounts of LAW glasses and schedule of LAW vitrification.

- Develop data and models for other key glass and melt properties such as density, thermal expansion, thermal conductivity, melter volatility (partitioning to off-gas stream) all as functions of temperature to support various LAW product qualification and plant operations activities.

10.0 References

- Annamalai S, H Gan, M Chaudhuri, WK Kot, and IL Pegg. 2004. "Spinel Crystallization in HLW Glass Melts: Cation Exchange Systematics and the Role of Rh_2O_3 in Spinel Formation." *Ceramic Transactions*, pp. 279-288. American Ceramic Society, Westerville, Ohio.
- ASME. 2000. *Quality Assurance Requirements for Nuclear Facility Applications*. ASME NQA-1-2000, American Society of Mechanical Engineers, New York, New York.
- ASTM. 2014. *Standard Test Methods for Determining Chemical Durability of Nuclear, Hazardous, and Mixed Waste Glasses and Multiphase Glass Ceramics: The Product Consistency Test (PCT)*. ASTM C1285-14, ASTM International, West Conshohocken, Pennsylvania.
- Buechele AC, CT Mooers, and IL Pegg. 2002. "Vapor Hydration Testing of Nuclear Waste Glasses Using D_2O and H_2O ." *Microscopy and Microanalysis* 8(S02):1312-1313.
- Cornell JA. 2002. *Experiments with Mixtures: Designs, Models, and the Analysis of Mixture Data*, 3rd Edition. John Wiley and Sons, New York, New York.
- DOE. 2000. *Design, Construction, and Commissioning of the Hanford Tank Waste Treatment and Immobilization Plant*. U.S. Department of Energy, Office of River Protection, Richland, Washington.
- DOE. 2011. *Quality Assurance*. DOE O 414.1D. U.S. Department of Energy, Washington, D.C.
- DOE. 2013. *Nuclear Safety Management*. 10CFR830. U.S. Department of Energy, Washington, D.C.
- Draper NR and H Smith. 1998. *Applied Regression Analysis*, 3rd Edition. John Wiley and Sons, New York, New York.
- Feng, X and TB Metzger. 1996. "A Structural Bond Strength Model for Glass Durability," *Ceramic Transactions*, Vol. 72, 51–60 pp.
- Freund RJ and RC Littell. 2003. *SAS System for Regression*, Second Edition (SAS Series in Statistical Applications) 2nd Edition, SAS Institute, Inc., Cary, North Carolina.
- Freund RJ, RC Littell, and L Creighton. 2003. *Regression Using JMP*. SAS Institute, Inc., Cary, North Carolina.
- Gan H, X Lu, I Vidensky, C Paul, IL Pegg, IS Muller, AC Buechele, P Branch, L Su, C Mooers, E Malone, G Bazemore, and M Ing. 2001. *Corrosion of K-3 Refractory and Metal Alloys in RPP-WTP LAW Glasses*. VSL-01R3540-1, Vitreous State Laboratory, The Catholic University of America, Washington, D.C.
- Gervasio V, JD Vienna, DS Kim, and AA Kruger. 2018. *Impacts of Process and Prediction Uncertainties on Projected Hanford Waste Glass Amount*. PNNL-26996, EWG-RPT-015, Rev. 0.0, Pacific Northwest National Laboratory, Richland, Washington.
- Gilbert RO. 1987. *Statistical Methods for Environmental Pollution Monitoring*. Van Nostrand Reinhold, New York, New York.
- Gin, S, M Wang, N Bisbrouck, M Taron, X Lu, L Deng, F Angeli, T Charpentier, JM Delaye, J Du, and M Bauchy. 2020. "Can a Simple Topological-Constraints-Based Model Predict the Initial Dissolution Rate of Borosilicate and Aluminosilicate Glasses?," *npj-Materials Degradation*, 4(6). 10.1038/s41529-020-0111-4.

- Goodman, LA. 1960. "On the Exact Variance of Products." *Journal of the American Statistical Association*, **55**(292):708-713
- Hahn GJ and SS Shapiro. 1967. *Statistical Models in Engineering*, John Wiley and Sons, New York, New York.
- Hrma, P, GF Piepel, MJ Schweiger, DE Smith, DS Kim, PE Redgate, JD Vienna, CA LoPresti, DB Simpson, DK Peeler, and MH Langowski. 1994. Property/Composition Relationships for Hanford High-Level Waste Glasses Melting at 1150°C, PNL-10359, Pacific Northwest Laboratory, Richland, WA.
- Ihaka R, R Gentleman 1996. "R: A Language for Data Analysis and Graphics." *Journal of Computational and Graphical Statistics*, **5**(3):299-314
- Jain V and SM Barnes. 1991. "Effect of Glass Pour Cycle on the Crystallization Behavior in the Canistered Product at the West Valley Demonstration Project." *Nuclear Waste Management IV* 23.
- Jantzen, CM., JB Pickett, KG Brown, TB Edwards, and DC Beam. 1995. *Process/Product Models for the Defense Waste Processing Facility (DWPF): Part I. Predicting Glass Durability from Composition Using a Thermodynamic Hydration Energy Reaction Model (Thermo)*, WSRC-TR-93-0672, Westinghouse Savannah River Company, Aiken, SC.
- Jantzen CM and KG Brown. 2007. "Predicting the Spinel-Nepheline Liquidus for Application to Nuclear Waste Glass Processing: Part I. Primary Phase Analysis, Liquidus Measurement, and Quasicrystalline Approach." *Journal of the American Ceramic Society* **90**(6):1866-1879.
- Jin T, D Kim, LP Darnell, B Weese, M Bliss, N Canfield, MJ Schweiger, JD Vienna, and AA Kruger. 2019. "A Crucible Salt Saturation Method for Determining Sulfur Solubility in Glass Melt." *International Journal of Applied Glass Science* **10**(1):92-102. <https://doi.org/10.1111/ijag.12366>
- Jiricka A, JD Vienna, P Hrma, and DM Strachan. 2001. "The Effect of Experimental Conditions and Evaluation Techniques on the Alteration of Low Activity Glasses by Vapor Hydration." *Journal of Non-Crystalline Solids* **292**(1-3):25-43.
- Kim DS and JD Vienna. 2012. *Preliminary ILAW Formulation Algorithm Description: 24590-LAW-RPT-RT-04-0003, Rev. 1*. ORP-56321, River Protection Project, Hanford Tank Waste Treatment and Immobilization Plant, Richland, Washington.
- Kot WK and IL Pegg. 2001. *Glass Formulation and Testing with Rpp-WTP HLW Simulants*, VSL-01R2540-2, Rev. 0, Vitreous State Laboratory, The Catholic University of America, Washington, D.C.
- Lonergan CE, JL George, D Cutforth, T Jin, P Cholsaipant, SE Sannoh, CH Skidmore, BA Stanfill, SK Cooley, GF Piepel, RL Russell, and JD Vienna. 2019. *Enhanced Hanford Low-Activity Waste Glass Property Data Development: Phase 3*. PNNL-29847, Pacific Northwest National Laboratory, Richland, Washington.
- Lonergan CE, JL George, D Cutforth, T Jin, P Cholsaipant, SE Sannoh, CH Skidmore, BA Stanfill, SK Cooley, GF Piepel, R Russell, and JD Vienna. 2020. *Enhanced Hanford Low-Activity Waste Glass Property Data Development: Phase 3*. PNNL-29847, Rev. 0, EWG-RPT-026, Pacific Northwest National Laboratory, Richland, Washington.
- Lonergan CE, T Jin, DS Kim, and JD Vienna. 2021. *LAW Glass Crystallization Constraints for WTP Operations: Assessment of CCC Impacts on VHT and PCT*, PNNL-31138, Pacific Northwest National Laboratory, Richland, Washington.
- Lonergan, CE, EL Rivers, SM Baird, SE Sannoh, DS Kim and JD Vienna. 2021b. *Glass Crystallization Constraints for WTP LAW Operations: Assessment of Isothermal Treatments on Crystal Formation*. PNNL-31334, Pacific Northwest National Laboratory, Richland, Washington.

Lu X, DS Kim and JD Vienna. 2021. "Impacts of Constraints and Uncertainties on Projected Amount of Hanford Low-Activity Waste Glasses," *Nuclear Engineering and Design*, **385**, DOI: 10.1016/j.nucengdes.2021.111543.

MathWorks 2019. *MatLab R2019b*. The MathWorks, Inc. Natick Massachusetts.

Matlack KS, SP Morgan, and IL Pegg. 2000. *Melter Tests with LAW Envelope B Simulants to Support Enhanced Sulfate Incorporation*. VSL-00R3501-1, Rev. 0, Vitreous State Laboratory, The Catholic University of America, Washington, D.C.

Matlack KS, SP Morgan, and IL Pegg. 2001. *Melter Tests with LAW Envelope A and C Simulants to Support Enhanced Sulfate Incorporation*. VSL-01R3501-2, Rev. 0, Vitreous State Laboratory, The Catholic University of America, Washington, D.C.

Matlack KS, W Gong, and IL Pegg. 2003. *Compositional Variation Tests on DuraMelter 100 with LAW Sub-Envelope A3 Feed in Support of the LAW Pilot Melter*. VSL-01R62N0-1, Rev. 2, Vitreous State Laboratory, The Catholic University of America, Washington, D.C.

Matlack KS, M Chaudhuri, H Gan, IS Muller, WK Kot, W Gong, and IL Pegg. 2004a. *Glass Formulation Testing to Increase Sulfate Incorporation*. VSL-04R4960-1, ORP-51808, Vitreous State Laboratory, The Catholic University of America, Washington, D.C.

Matlack KS, W Gong, and IL Pegg. 2004b. *Glass Formulation Testing to Increase Sulfate Volatilization from Melter*. VSL-04R4970-1, Rev. 0, Vitreous State Laboratory, The Catholic University of America, Washington, DC.

Matlack KS, W Gong, and IL Pegg. 2004c. *Small Scale Melter Testing with LAW Simulants to Assess the Impact of Higher Temperature Melter Operations*. VSL-04R4980-1, Rev. 0, Vitreous State Laboratory, The Catholic University of America, Washington, D.C.

Matlack KS, W Gong, IS Muller, I Joseph, and IL Pegg. 2006a. *LAW Envelope A and B Glass Formulations Testing to Increase Waste Loading*. VSL-06R6900-1, ORP-56322, Vitreous State Laboratory, The Catholic University of America, Washington, D.C.

Matlack KS, W Gong, IS Muller, I Joseph, and IL Pegg. 2006b. *LAW Envelope C Glass Formulation Testing to Increase Waste Loading*. VSL-05R5900-1, ORP-56323, Vitreous State Laboratory, The Catholic University of America, Washington, D.C.

Matlack KS, IS Muller, W Gong, and IL Pegg. 2006c. *DuraMelter 100 Tests to Support LAW Glass Formulation Correlation Development*. VSL-06R6480-1, ORP-56324, Vitreous State Laboratory, The Catholic University of America, Washington, D.C.

Matlack KS, I Joseph, W Gong, IS Muller, and IL Pegg. 2007a. *Enhanced LAW Glass Formulation Testing*. VSL-07R1130-1. ORP-56293, Vitreous State Laboratory, The Catholic University of America, Washington, D.C.

Matlack KS, IS Muller, W Gong, and IL Pegg. 2007b. *Small Scale Melter Testing of LAW Salt Phase Separation*. VSL-07R7480-1, Rev. 0, Vitreous State Laboratory, The Catholic University of America, Washington, D.C.

Matlack KS, I Joseph, W Gong, IS Muller, and IL Pegg. 2009a. *Glass Formulation Development and DM10 Melter Testing with ORP LAW Glasses*. VSL-09R1510-2, ORP-56296, Vitreous State Laboratory, The Catholic University of America, Washington, D.C.

Matlack KS, WK Kot, W Gong, W Lutze, IL Pegg, and I Joseph. 2009b. *Effects of High Spinel and Chromium Oxide Crystal Contents on Simulated HLW Vitrification in DM100 Melter Tests*.

VSL-09R1520-1, ORP-56327, Vitreous State Laboratory, The Catholic University of America, Washington, D.C.

Matlack KS, IS Muller, I Joseph, and IL Pegg. 2014. *Melter Tests to Define LAW Halide, Chromium and Phosphate Concentrations*. VSL-14R3070-1, Vitreous State Laboratory, The Catholic University of America, Washington, D.C.

Matlack KS, IS Muller, H Abramowitz, I Joseph, and IL Pegg. 2017a. *Support to Direct Feed LAW FlowSheet Development*. VSL-17R4250-1, Rev. 0, Vitreous State Laboratory, The Catholic University of America, Washington, D.C.

Matlack KS, H Abramowitz, IS Muller, I Joseph, and IL Pegg. 2017b. *DFLAW Glass and Feed Qualifications to Support WTP Start-Up and Flow-Sheet Development*. VSL-17R4330-1, Rev. 0, Vitreous State Laboratory, The Catholic University of America, Washington, D.C.

Matyáš J, AR Huckleberry, CP Rodriguez, JB Lang, AT Owen, and AA Kruger. 2012. *HLW Glass Studies: Development of Crystal Tolerant HLW Glasses*. PNNL-21308, Pacific Northwest National Laboratory, Richland, Washington.

Matyáš J, JD Vienna, A Kimura, M Schaible, and RM Tate. 2010. "Development of Crystal-Tolerant Waste Glasses." *Advances in Materials Science for Environmental and Nuclear Technology* 222:41-50.

Montgomery, DC, EA Peck. 1992. *Introduction to Linear Regression Analysis*, Second Edition., John Wiley & Sons, Inc., New York, New York

Montgomery, DC, EA Peck, and GG Vining. 2012. *Introduction to Linear Regression Analysis*, Fifth Edition. Wiley & Sons, New York, New York

Muller IS, AC Buechele, and IL Pegg. 2001. *Glass Formulation and Testing with RPP-WTP LAW Simulants*. VSL-01R3560-2, ORP-56327, Vitreous State Laboratory, The Catholic University of America, Washington, D.C.

Muller IS and IL Pegg. 2003a. *Baseline LAW Glass Formulation Testing*. VSL-03R3460-1, ORP-55237, Vitreous State Laboratory, The Catholic University of America, Washington, D.C.

Muller IS and IL Pegg. 2003b. *LAW Glass Formulation to Support Melter Runs with Simulants*. VSL-03R3460-2, ORP-55237, Vitreous State Laboratory, The Catholic University of America, Washington, D.C.

Muller IS, IL Pegg, D McKeown, A Buechele, E Rielley, K Hight, G Bazemore, I Carranza, C Mooers, S Grant, and L Su. 2003c. *LAW Glass Formulation to Support AZ-102 Actual Waste Testing*. VSL-03R3470-1, ORP- 63493, Vitreous State Laboratory, The Catholic University of America, Washington, D.C.

Muller IS and IL Pegg. 2003d. *LAW Glass Formulation to Support AP-101 Actual Waste Testing*. VSL-03R3470-2, Vitreous State Laboratory, The Catholic University of America, Washington, D.C.

Muller IS and IL Pegg. 2003e. *LAW Glass Formulation to Support AZ-101 Actual Waste Testing*. VSL-03R3470-3, Rev. 0, Vitreous State Laboratory, The Catholic University of America, Washington, D.C.

Muller IS, IL Pegg, E Rielley, K Hight, G Bazemore, M Chaudhuri, H Gan, E Kashnikov, J Cheron, R Cecil, KD Derr, S Watt, C Mooers, and S-T Lai. 2003f. *LAW Glass Formulation to Support SY-101/AP-104 Actual Waste Testing*. VSL-03R4470-1, ORP- 63495, Vitreous State Laboratory, The Catholic University of America, Washington, D.C.

Muller IS, L Goloski, IL Pegg, T Moncrief, M Chaudhuri, J Berger, D Horton, JB Martin, J Singh, R Cecil, C Viragh, C Boice, L Su, ST Lai, E Kashnikov, J Cheron, C Mooers, S Watt, and CF Feng. 2004.

LAW Glass Formulation to Support AN-104 Actual Waste Testing. VSL-04R4470-1, Vitreous State Laboratory, The Catholic University of America, Washington, D.C.

Muller IS, G Diener, I Joseph, and IL Pegg. 2004a. *Proposed Approach for Development of LAW Glass Formulation Correlation.* VSL-04L4460-1, Vitreous State Laboratory, The Catholic University of America, Washington, D.C.

Muller IS, I Joseph, and IL Pegg. 2005. *Comparison of LAW Simulant, Actual Waste, and Melter Glasses.* VSL-05R5460-1, Rev. 0, Vitreous State Laboratory, The Catholic University of America, Washington, D.C.

Muller IS, I Joseph, and IL Pegg. 2006a. *Preparation and Testing of LAW High Phosphorus and High-Chromium Glasses.* VSL-06R6480-2, Rev. 0, Vitreous State Laboratory, The Catholic University of America, Washington, D.C.

Muller IS, I Joseph, and IL Pegg. 2006b. *Preparation and Testing of LAW High-Alkali Correlation and Augmentation Matrix Glasses.* VSL-06R6480-3, ORP-63500, Vitreous State Laboratory, The Catholic University of America, Washington, D.C.

Muller IS, I Joseph, F Perez-Cardenas, and IL Pegg. 2008. *LAW Glass Testing and VHT Model Assessment.* VSL-08R1410-1, Rev. 0, Vitreous State Laboratory, The Catholic University of America, Washington, D.C.

Muller IS, KS Matlack, H Gan, I Joseph, and IL Pegg. 2010. *Waste Loading Enhancements for Hanford LAW Glasses.* VSL-10R1790-1, ORP-48578, Vitreous State Laboratory, The Catholic University of America, Washington, D.C.

Muller IS, K Gilbo, I Joseph, and IL Pegg. 2013. *Enhanced LAW Glass Property-Composition Models – Phase 1.* VSL-13R2940-1, Vitreous State Laboratory, The Catholic University of America, Washington, D.C.

Muller IS, K Gilbo, I Joseph, and IL Pegg. 2014. *Enhanced LAW Glass Property-Composition Models – Phase 2.* VSL-14R3050-1, Vitreous State Laboratory, The Catholic University of America, Washington, D.C.

Muller IS, KS Matlack, IL Pegg, and I Joseph. 2015a. *Test Plan: Enhanced LAW Glass Correlation.* VSL-15T3680-1, Vitreous State Laboratory, The Catholic University of America, Washington, D.C.

Muller IS, H Gan, K Gilbo, IL Pegg, and I Joseph. 2015b. *LAW Glass Property-Composition Models for K-3 Refractory Corrosion and Sulfate Solubility.* VSL-15R3270-1, Vitreous State Laboratory, The Catholic University of America, Washington, D.C.

Muller IS, M Chaudhuri, H Gan, A Buechele, X Xie, IL Pegg, and I Joseph. 2015c. *Improved High-Alkali Low-Activity Waste Formulations.* VSL-15R3290-1, Rev.0, Vitreous State Laboratory, The Catholic University of America, Washington, D.C.

Muller IS, KS Matlack, IL Pegg, and I Joseph. 2016. *Enhanced LAW Glass Correlation - Phase 1.* VSL-16R4000-1, Vitreous State Laboratory, The Catholic University of America, Washington, D.C.

Muller IS, KS Matlack, IL Pegg, and I Joseph. 2017a. *Enhanced LAW Glass Correlation - Phase 2.* VSL-17R4140-1, Vitreous State Laboratory, The Catholic University of America, Washington, D.C.

Muller IS, KS Matlack, IL Pegg, and I Joseph. 2017b. *Enhanced LAW Glass Correlation - Phase 3.* VSL-17R4230-1, Vitreous State Laboratory, The Catholic University of America, Washington, D.C.

- Muller IS, K Gilbo, M Chaudhuri, and IL Pegg. 2018. *K-3 Refractory Corrosion and Sulfate Solubility Model Enhancement*. VSL-18R4360-1, Rev. 0, Vitreous State Laboratory, The Catholic University of America, Washington, D.C.
- Myers, R.H. and Montgomery, D.C. 1995. *Response Surface Methodology. Process and Product Optimization Using Designed Experiments*, John Wiley & Sons, New York, New York.
- Myers RH, DC Montgomery, and GG Vining. 2002. *Generalized Linear Models: with Applications in Engineering and the Sciences*. John Wiley & Sons, New York, New York.
- Latham, A 2018. *ILAW Product Qualification Report*, 24590-LAW-RPT-PENG-17-008, Rev. 2, River Protection Project, Waste Treatment Plant, Richland, Washington.
- Perez JM. 2006. *Practical and Historical Bases for a Glass Viscosity Range for Joule-Heater Ceramic Melter Operation*. Email to JD Vienna, Dec. 22, 2006, CCN: 150054, River Protection Project, Hanford Waste Treatment and Immobilization Plant, Richland, Washington.
- Perez-Cardenas, F, H Gan and IL Pegg. 2003. *Summary and Recommendations on PCT Model Form to Support LAW Vitrification*, VSL-03L4480-1, Rev. 0, Vitreous State Laboratory, The Catholic University of America, Washington, DC.
- Petkus LL. 2003. *Low Activity Container Centerline Cooling Data*, to CA Musick, CCN: 074181, Oct. 16, 2003, River Protection Project, Hanford Waste Treatment and Immobilization Plant, Richland, Washington.
- Piepel GF, JM Szychowski, and JL Loeppky. 2002. "Augmenting Scheffé Linear Mixture Models with Squared and/or Crossproduct Terms." *Journal of Quality Technology* 34:297-314.
- Piepel GF, A Heredia-Langner, and SK Cooley. 2008. "Property-Composition-Temperature Modeling of Waste Glass Melt Data Subject to a Randomization Restriction." *Journal of the American Ceramic Society* 91(10):3222-3228.
- Piepel GF, SK Cooley, IS Muller, H Gan, I Joseph, and IL Pegg. 2007. *ILAW PCT, VHT, Viscosity, and Electrical Conductivity Model Development*. VSL-07R1230-4, Rev. 0, ORP-56502, Vitreous State Laboratory, The Catholic University of America, Washington, D.C.
- Piepel GF and SK Cooley. 2006. "Automated Method for Reducing Scheffé Linear Mixture Experiment Models." *Quality Technology and Quantitative Management* 6:255-270.
- Piepel GF, SK Cooley, JD Vienna, and JV Crum. 2016. *Experimental Design for Hanford Low-Activity Waste Glasses with High Waste Loading*, PNNL-24391, EWG-RPT-006, Rev. 1, Pacific Northwest National Laboratory, Richland, Washington.
- Piepel GF and T Redgate. 1997. "Mixture techniques for reducing the number of components applied for modeling waste glass sodium release." *Journal of the American Ceramic Society* 80:3038-3044.
- R Core Team. 2019. *A language and environment for statistical computing*. R Foundation for Statistical Computing, Vienna, Austria. <http://www.r-project.org/index.html>
- Rielly E, IS Muller and IL Pegg. 2004. *Preparation and Testing of LAW Matrix Glasses to Support WTP Property-Composition Model Development*. VSL-04R4480-1, ORP-63497, Vitreous State Laboratory, The Catholic University of America, Washington, D.C.
- Russell RL, T Jin, BP McCarthy, LP Darnell, DE Rinehart, CC Bonham, V Gervasio, JM Mayer, CL Arendt, JB Lang, MJ Schweiger, and JD Vienna. 2017. *Enhanced Hanford Low-Activity Waste Glass Property Data Development: Phase 1*. PNNL-26630, EWG-RPT-012, Pacific Northwest National Laboratory, Richland, Washington.

Russell RL, McCarthy BP, Cooley SK, Piepel GF, Cordova EA, Sannoh SE, Gervasio V, Schweiger MJ, Lang JB, Skidmore CH, Lonergan CE, Stanfill BA, Meline JM, and Vienna JD. 2020. *Enhanced Hanford Low-Activity Waste Glass Property Data Development: Phase 2*. PNNL-28838, EWG-RPT-021, Rev. 2. Pacific Northwest National Laboratory, Richland, Washington.

Skidmore CH, JD Vienna, T Jin, DS Kim, BA Stanfill, KM Fox, and AA Kruger. 2019. "Sulfur Solubility in Low Activity Waste Glass and Its Correlation to Melter Tolerance." *International Journal of Applied Glass Science* 10(4):558-568. doi:10.1111/IJAG.13272

Smith WF. 2005. *Experimental Design for Formulation*. ASA-SIAM Series on Statistics and Applied Probability, SIAM, Philadelphia, Pennsylvania, and ASA, Alexandria, Virginia.

Tilanus SN, LM Bergman, RO Lokken, AJ Schubick, EB West, RT Jasper, SL Orcutt, TM Holh, AN Praga, MN Wells, KW Burnett, CS Smalley, JK Bernards, SD Reaksecker, and TL Waldo. 2017. *River Protection Project System Plan*. ORP-11242, Rev. 8, U.S. Department of Energy, Office of River Protection, Richland, Washington.

Transtrum, M.K., Machta, B.B., Brown, K.S., Daniels, B.C., Myers, C.R. and Sethna, J.P., 2015. Perspective: Sloppiness and emergent theories in physics, biology, and beyond. *The Journal of chemical physics*, 143(1), p.07B201_1.

Vienna JD, A Jiříčka, PR Hrma, DE Smith, TH Lorier, RL Schulz, and IA Reamer. 2001. *Hanford Immobilized LAW Product Acceptance Testing: Tanks Focus Area Results*. PNNL-13744, Pacific Northwest National Laboratory, Richland, Washington.

Vienna JD, DS Kim, DC Skorski, and J Matyas. 2013. *Glass Property Models and Constraints for Estimating the Glass to Be Produced at Hanford by Implementing Current Advanced Glass Formulation Efforts*. PNNL-22631, Rev. 1, ORP-58289, Pacific Northwest National Laboratory, Richland, Washington.

Vienna, JD. 2014. "Compositional Models of Glass/Melt Properties and Their Use for Glass Formulation," *Procedia Materials Science*, 7(0):148-155. <http://dx.doi.org/10.1016/j.mspro.2014.10.020>.

Vienna, JD and DS Kim. 2014. *Preliminary IHLW Formulation Algorithm Description*, 24590-HLW-RPT-RT-05-001, Rev. 1, River Protection Project, Hanford Tank Waste Treatment and Immobilization Plant, Richland, WA.

Vienna JD, DS Kim, IS Muller, GF Piepel, and AA Kruger. 2014. "Toward Understanding the Effect of Low-Activity Waste Glass Composition on Sulfur Solubility." *Journal of the American Ceramic Society*, 97(10):3135–3142. DOI: 10.1111/jace.13125.

Vienna JD, GF Piepel, DS Kim, JV Crum, CE Lonergan, BA Stanfill, BJ Riley, SK Cooley, and T Jin. 2016. *2016 Update of Hanford Glass Property Models and Constraints for Use in Estimating the Glass Mass to be Produced at Hanford by Implementing Current Enhanced Glass Formulation Efforts*. PNNL-25835, Pacific Northwest National Laboratory, Richland, Washington.

Vienna, J.D. and J.V. Crum. 2018. "Non-Linear Effects of Alumina Concentration on Product Consistency Test Response of Waste Glasses," *Journal of Nuclear Materials*, **511**(12):396-405. [10.1016/j.jnucmat.2018.09.040](http://dx.doi.org/10.1016/j.jnucmat.2018.09.040).

Weier, DR and GF Piepel. 2003. *Methodology for Adjusting and Normalizing Analyzed Glass Compositions*, PNWD-3260, Battelle, Pacific Northwest Division, Richland, WA.

Working, H and H Hotelling. 1929. "Application of the Theory of Error to the Interpretation of Trends," *Journal of the American Statistical Association*, Supplement, (24):73-85.

Appendix A – LAW Glass Data for Developing Property-Composition Models

This appendix summarizes the complete dataset compiled to develop property-composition models for low-activity waste (LAW) glasses. Properties for which data were compiled include Product Consistency Test (PCT), Vapor Hydration Test (VHT), η_{1150} , ϵ_{1150} , melter SO_3 tolerance at 1150 °C, and the neck corrosion loss of K-3 refractory at 1208 °C.

Table A.1 summarizes the range of Glass #s in the compiled database of LAW glass compositions and properties discussed in Section 2.1. Table A.1 also lists the technical reports from which the data were compiled.

Table A.2 lists the normalized (as discussed in Section 2.2) compositions of the LAW glasses in the compiled database, including the concentrations (mass fractions) of 19 “major” LAW glass components plus Others, which is the total of all remaining “minor” components. The 19 components were selected as ones that have sufficient distributions of LAW glass concentration values (mass fractions) to support separate terms in LAW glass property-composition models. The LAW glass compositions in Table A.2 were rounded and listed to six decimal places in a way that guarantees that the mass fractions of the 20 components for each glass sum exactly to 1.000000. Six decimal places was chosen because mass fraction values for some components had the first significant figure in the fifth decimal place. Listing the mass fractions to six decimal places avoided relative rounding differences being too large for such values.

Table A.3 lists the values of properties (PCT, VHT, η_{1150} , ϵ_{1150} , and melter SO_3 tolerance and solubilities at 1150 °C) for the LAW glasses from the compiled literature data. Not all properties are available for all glasses in Table A.3. Those properties without measured properties are labelled “-”. Glasses with one or more component values assessed to be outliers were not used in modeling. Glasses whose property values were assessed as outliers (as discussed in the main body section for each property) were also not used in modeling. Those glasses that were not used for modeling have their property values marked with an asterisk in Table A.3.

Table A.4 lists the normalized compositions of 344 LAW glasses with data for the neck corrosion loss of K-3 refractory at 1208 °C (k_{1208}). Similar to Table A.2, these compositions are listed using the same 20 components (19 plus Others), with mass fractions to six decimal places summing exactly to 1.000000. Table A.5 lists the k_{1208} values in inches. These LAW normalized glass compositions and K-3 corrosion values are all from Muller et al. (2018).

Table A.1. Reference and Glass # Range for Each LAW Glass Dataset in the Compiled Literature Data

Group(a)	Report(b)	Reference	# of Glasses	Glass # Range
WTP	VSL-00R3501-1	Matlack et al. 2000	1	1
WTP	VSL-01R3501-2	Matlack et al. 2001	4	2 – 5
WTP	VSL-01R3560-2	Muller et al. 2000	121	6 - 126
WTP	VSL-01R3540-1	Gan et al. 2001	15	127 – 141
WTP	VSL-01R62N0-1, Rev. 2	Matlack et al. 2003	2	142 – 143
WTP	VSL-03R3460-1	Muller and Pegg 2003 ^a	122	144 – 265
WTP	VSL-03R3460-2	Muller and Pegg 2003 ^b	42	266 – 307
WTP	VSL-03R3470-1	Muller and Pegg 2003 ^c	6	308 – 313
WTP	VSL-03R3470-2	Muller and Pegg 2003 ^d	10	314 – 323
WTP	VSL-03R3470-3	Muller and Pegg 2003 ^e	2	324 – 325
WTP	VSL-03R4470-1	Muller and Pegg 2003 ^f	3	326 – 328
WTP	VSL-04R4470-1	Muller et al. 2004	2	329 – 330
WTP	VSL-04R4480-1	Rielley et al. 2004	60	331 – 390
ORP	VSL-04R4960-1	Matlack et al. 2004 ^a	17	391 – 407
ORP	VSL-04R4970-1	Matlack et al. 2004 ^b	3	408 – 410
WTP	VSL-04R4980-1	Matlack et al. 2004 ^c	1	411
WTP	VSL-05R5460-1	Muller et al. 2005	30	412 – 441
ORP	VSL-05R5900-1	Matlack et al. 2005	6	442 – 447
WTP	VSL-06R6480-1	Matlack et al. 2006 ^a	8	448 – 455
WTP	VSL-06R6480-2	Muller et al. 2006 ^a	18	456 – 473
WTP	VSL-06R6480-3	Muller et al. 2006 ^b	26	474 – 499
ORP	VSL-06R6900-1	Matlack et al. 2006 ^b	45	500 – 544
ORP	VSL-07R1130-1	Matlack et al. 2007 ^a	78	545 – 622
ORP	VSL-07R7480-1	Matlack et al. 2007 ^b	9	623 – 631
ORP	VSL-08R1410-1	Muller et al. 2008	56	632 – 686, 1012
ORP	VSL-09R1510-2	Matlack et al. 2009	50	687 – 736
ORP	VSL-10R1790-1	Muller et al. 2010	32	737 – 768
ORP	VSL-13R2940-1	Muller et al. 2013	20	769 – 788
ORP	VSL-14R3050-1	Muller et al. 2014	22	789 – 810
ORP	VSL-15R3290-1	Muller et al. 2015	24	811 – 834
ORP	VSL-16R4000-1	Muller et al. 2016	38	835 – 872
ORP	VSL-17R4140-1	Muller et al. 2017 ^a	19	873 – 891
ORP	VSL-17R4230-1	Muller et al. 2017 ^b	17	892 – 908
ORP	VSL-17R4250-1	Matlack et al. 2017 ^a	11	909 – 919
ORP	VSL-17R4330-1	Matlack et al. 2017 ^b	8	920 – 927
ORP	PNNL-26630 (PNNL Ph. 1)	Russell et al. 2017	75	928 – 1002
ORP	VSL-18R4360-1	Muller et al. 2018	9	1003 – 1011
ORP	PNNL-28838 (PNNL Ph. 2)	Russell et al. 2020, Rev. 2	41(c)	1013-1053
ORP	PNNL-29847 (PNNL Ph. 3)	Lonergan et al. 2020	22(d)	1054-1075

(a) WTP denotes data for LAW glass compositions to support cold commissioning, hot commissioning, and initial

(b) All reports are Rev. 0 unless otherwise noted.

(c) The PNNL LAW Phase 2 test matrices were designed to have a total of 42 glasses. However, a homogenous glass could not be made (even with modifications) for test matrix glass LP2-OL-06. Hence, no property data were collected for that glass. Thus, LP2-OL-06 does not appear in the glass composition and property value listings.

(d) The PNNL LAW Phase 3 test matrix was designed to contain 20 glasses, but replicate glasses were made for duplicate PCTs of two glasses, resulting in 22 glasses

Table A.2. Normalized Compositions (in mass fractions) of 1075 LAW Glasses in the Database of Compiled Literature Data

#	Glass ID	Al ₂ O ₃	B ₂ O ₃	CaO	Cl	Cr ₂ O ₃	F	Fe ₂ O ₃	K ₂ O	Li ₂ O	MgO	Na ₂ O	P ₂ O ₅	SO ₃	SiO ₂	SnO ₂	TiO ₂	V ₂ O ₅	ZnO	ZrO ₂	Others
1	LB100-G-83A	0.061486	0.123774	0.066501	0.000100	0.000702	0.000802	0.052759	0.002608	0.046340	0.029790	0.065197	0.000301	0.006400	0.480050	0.000000	0.000000	0.000000	0.031595	0.031595	0.000000
2	LAWA102	0.060538	0.100063	0.050732	0.003302	0.000200	0.000300	0.054134	0.002602	0.025016	0.014909	0.144691	0.001301	0.003873	0.466094	0.000000	0.011407	0.000000	0.030619	0.030219	0.000000
3	LAWC21	0.061221	0.100830	0.064055	0.001236	0.000200	0.000599	0.064736	0.001506	0.027319	0.015081	0.118690	0.001179	0.004581	0.467030	0.000000	0.011204	0.000000	0.030163	0.030191	0.000179
4	A100-G-115A	0.060557	0.100030	0.050664	0.003298	0.000200	0.000300	0.054162	0.002598	0.024982	0.014990	0.144698	0.001299	0.003600	0.466173	0.000000	0.011492	0.000000	0.030678	0.030279	0.000000
5	C100-G-136B	0.061268	0.100912	0.064071	0.001201	0.000200	0.000601	0.064772	0.001502	0.027330	0.015117	0.118731	0.001201	0.004300	0.467216	0.000000	0.011212	0.000000	0.030133	0.030233	0.000000
6	LAWA41	0.062039	0.075011	0.019963	0.005791	0.000170	0.000360	0.069841	0.031015	0.000000	0.019943	0.200031	0.000780	0.000956	0.434127	0.000000	0.019953	0.000000	0.029935	0.029955	0.000130
7	LAWA42	0.062034	0.090336	0.024042	0.005790	0.000170	0.000360	0.084106	0.031012	0.000010	0.024022	0.200014	0.000780	0.000956	0.380026	0.000000	0.024022	0.000000	0.030643	0.030673	0.000204
8	LAWA43	0.120010	0.073896	0.019672	0.005790	0.000170	0.000360	0.068795	0.031012	0.000010	0.019652	0.200016	0.000780	0.000956	0.380030	0.000000	0.019652	0.000000	0.029482	0.029512	0.000205
9	LAWA44	0.062019	0.089033	0.019943	0.006521	0.000200	0.000100	0.069820	0.005011	0.000000	0.019943	0.200030	0.000340	0.000892	0.445596	0.000000	0.019943	0.000000	0.029654	0.029925	0.001030
10	LAWA44S	0.061733	0.088623	0.019851	0.006491	0.000199	0.000100	0.069498	0.004988	0.000000	0.019851	0.199107	0.000338	0.005500	0.443541	0.000000	0.019851	0.000000	0.029518	0.029786	0.001025
11	LAWA45	0.062019	0.119028	0.000000	0.006521	0.000200	0.000100	0.069820	0.005011	0.000000	0.014772	0.200030	0.000340	0.000892	0.445596	0.000000	0.019943	0.000000	0.024774	0.029924	0.001030
12	LAWA46	0.062019	0.089033	0.000000	0.006521	0.000200	0.000100	0.069820	0.005011	0.000000	0.014772	0.200030	0.000340	0.000892	0.445596	0.000000	0.019943	0.000000	0.024774	0.029924	0.031025
13	LAWA47	0.062019	0.089033	0.000000	0.006521	0.000200	0.000100	0.069820	0.005011	0.000000	0.014772	0.200030	0.000340	0.000892	0.445596	0.000000	0.019943	0.000000	0.024774	0.029924	0.031025
14	LAWA48	0.062019	0.089033	0.000000	0.006521	0.000200	0.000100	0.069820	0.005011	0.000000	0.014772	0.200030	0.000340	0.000892	0.445596	0.000000	0.019943	0.000000	0.024774	0.029924	0.031025
15	LAWA49	0.062019	0.089033	0.000000	0.006521	0.000200	0.000100	0.099815	0.005011	0.000000	0.014772	0.200030	0.000340	0.000892	0.445596	0.000000	0.019943	0.000000	0.024774	0.029924	0.001030
16	LAWA50	0.062019	0.089033	0.000000	0.006521	0.000200	0.000100	0.119838	0.005011	0.000000	0.014772	0.200030	0.000340	0.000892	0.425573	0.000000	0.019943	0.000000	0.024774	0.029924	0.001030
17	LAWA51	0.062027	0.119755	0.000000	0.005861	0.000180	0.000090	0.069978	0.004511	0.000000	0.014842	0.180022	0.000300	0.000809	0.465766	0.000000	0.019962	0.000000	0.024883	0.029984	0.001030
18	LAWA52	0.061800	0.061920	0.078832	0.006521	0.000200	0.000100	0.075062	0.005011	0.000000	0.014772	0.200031	0.000340	0.000892	0.422547	0.000000	0.011082	0.000000	0.029945	0.029925	0.001020
19	LAWA60	0.085293	0.112308	0.043217	0.006521	0.000200	0.000100	0.000000	0.005011	0.000000	0.019943	0.200032	0.000340	0.000892	0.445600	0.000000	0.019943	0.000000	0.029655	0.029925	0.001020
20	LAWA64	0.061800	0.061920	0.000000	0.006521	0.000200	0.000100	0.075062	0.005011	0.000000	0.014772	0.200031	0.000340	0.000892	0.422547	0.000000	0.011082	0.000000	0.029945	0.029925	0.079852
21	LAWA81	0.062019	0.089033	0.039896	0.006521	0.000200	0.000100	0.069820	0.005011	0.000000	0.019943	0.200030	0.000340	0.000892	0.445596	0.000000	0.000000	0.000000	0.029654	0.029925	0.001020
22	LAWA82	0.062019	0.089033	0.000000	0.006521	0.000200	0.000100	0.069820	0.005011	0.000000	0.019943	0.200030	0.000340	0.000892	0.445596	0.000000	0.039896	0.000000	0.029654	0.029925	0.001020
23	LAWA83	0.062021	0.089035	0.019943	0.006521	0.000200	0.000100	0.049868	0.005011	0.000000	0.019943	0.200034	0.020284	0.000892	0.445605	0.000000	0.019943	0.000000	0.029655	0.029925	0.001020
24	LAWA84	0.062020	0.089034	0.019943	0.006521	0.000200	0.000100	0.029925	0.005011	0.000000	0.019943	0.200032	0.040236	0.000892	0.445600	0.000000	0.019943	0.000000	0.029655	0.029925	0.001020
25	LAWA85	0.062021	0.089035	0.000000	0.006521	0.000200	0.000100	0.049868	0.005011	0.000000	0.019943	0.200034	0.020283	0.000892	0.445605	0.000000	0.019943	0.000000	0.029655	0.029925	0.020964
26	LAWA86	0.062020	0.089034	0.000000	0.006521	0.000200	0.000100	0.029925	0.005011	0.000000	0.019943	0.200032	0.040236	0.000892	0.445600	0.000000	0.019943	0.000000	0.029655	0.029925	0.020963
27	LAWA87	0.044808	0.088736	0.019914	0.003291	0.000090	0.000000	0.069703	0.025835	0.000000	0.019914	0.200037	0.000700	0.001966	0.444632	0.000000	0.019914	0.000000	0.029575	0.029875	0.001010
28	LAWA88	0.060811	0.096997	0.019913	0.003291	0.000090	0.000000	0.055320	0.025834	0.000000	0.014753	0.200035	0.000700	0.001966	0.439987	0.000000	0.019913	0.000000	0.029505	0.029875	0.001010
29	LAWA89	0.060811	0.096997	0.000000	0.003290	0.000090	0.000000	0.055320	0.025834	0.000000	0.014753	0.200035	0.000700	0.001966	0.439987	0.000000	0.039827	0.000000	0.029505	0.029875	0.001010
30	LAWA90	0.060811	0.096997	0.039827	0.003290	0.000090	0.000000	0.055320	0.025834	0.000000	0.014753	0.200035	0.000700	0.001966	0.439987	0.000000	0.000000	0.000000	0.029505	0.029875	0.001010
31	LAWA93	0.061800	0.110977	0.078832	0.006521	0.000200	0.000100	0.075062	0.005011	0.050678	0.014772	0.100296	0.000340	0.000892	0.422547	0.000000	0.011082	0.000000	0.029945	0.029925	0.001020
32	LAWA96	0.062050	0.079101	0.039915	0.006524	0.000200	0.000100	0.029939	0.005013	0.000000	0.019953	0.200128	0.040256	0.000400	0.435839	0.000000	0.019953	0.000000	0.029669	0.029939	0.001021
33	LAWA97S	NA	NA	NA	NA	NA	NA	NA	NA	NA	NA	NA	NA	NA	NA	NA	NA	NA	NA	NA	NA
34	LAWA98S	0.059938	0.106681	0.050479	0.004789	0.000149	0.000070	0.074516	0.003686	0.030446	0.014826	0.147064	0.000248	0.007100	0.427260	0.000000	0.011219	0.000000	0.030466	0.030049	0.001014
35	LAWA98S0	0.060367	0.107444	0.050840	0.004824	0.000150	0.000070	0.075048	0.003713	0.030664	0.014932	0.148115	0.000250	0.000000	0.430316	0.000000	0.011299	0.000000	0.030684	0.030263	0.001021
36	LAWA99S	0.059859	0.106539	0.060811	0.004783	0.000149	0.000069	0.044815	0.003682	0.020006	0.014806	0.146868	0.000248	0.008400	0.426692	0.000000	0.011204	0.029612	0.030426	0.030009	0.001022
37	LAWA100S	0.059998	0.106787	0.060953	0.004794	0.000149	0.000070	0.074590	0.003690	0.020053	0.014840	0.147211	0.000249	0.006100	0.427686	0.000000	0.011230	0.000000	0.030496	0.030079	0.001025
38	LAWA101S	0.059992	0.106777	0.070574	0.004794	0.000149	0.000070	0.074582	0.003690	0.010423	0.014839	0.147196	0.000249	0.006200	0.427643	0.000000	0.011229	0.000000	0.030493	0.030076	0.001024
39	LAWA102S	0.060332	0.099610	0.050482	0.003316	0.000179	0.000259	0.053888	0.002589	0.024907	0.014889	0.144286	0.001325	0.006800	0.464099	0.000000	0.011393	0.000000	0.030514	0.030116	0.001016
40	LAWA103S	0.060411	0.099740	0.050548	0.003321	0.000180	0.000259	0.049880	0.002593	0.024940	0.014908	0.144475	0.001326	0.005500	0.453787	0.000000	0.011408	0.014998	0.030554	0.030155	0.001017
41	LAWA104	0.066142	0.085915	0.019244	0.007171	0.000220	0.000110	0.067362	0.005511	0.000000	0.019243	0.220039	0.000370	0.000984	0.429936	0.000000	0.019243	0.000000	0.028605	0.028865	0.001040
42	LAWA105	0.070271	0.082804	0.018543	0.007821	0.000240	0.000120	0.064901	0.006011	0.000000	0.018543	0.240039	0.000400	0.001067	0.414268	0.000000	0.018543	0.000000	0.027564	0.027815	0.001050
43	LAWABP1	0.100006	0.092506	0.000000	0.005800	0.000200	0.000400	0.025002	0.022001	0.000000	0.010001	0.200012	0.000800	0.000938	0.418926	0.000000	0.024902	0.000000	0.026002	0.025203	0.020001
44	LAWB29																				

Table A.2. (cont.) Normalized Compositions (in mass fractions) of 1075 LAW Glasses in the Database of Compiled Literature Data

#	Glass ID	Al ₂ O ₃	B ₂ O ₃	CaO	Cl	Cr ₂ O ₃	F	Fe ₂ O ₃	K ₂ O	Li ₂ O	MgO	Na ₂ O	P ₂ O ₅	SO ₃	SiO ₂	SnO ₂	TiO ₂	V ₂ O ₅	ZnO	ZrO ₂	Others
67	LAWC14	0.061350	0.061751	0.055123	0.002006	0.000231	0.000983	0.034776	0.002467	0.000000	0.015433	0.200556	0.001895	0.003290	0.424548	0.000000	0.015433	0.057118	0.030876	0.030876	0.001288
68	LAWC15	0.062279	0.089387	0.020084	0.000779	0.000030	0.004696	0.070143	0.001419	0.000000	0.020104	0.199838	0.000150	0.001090	0.447607	0.000000	0.020024	0.000000	0.029936	0.030086	0.002348
69	LAWC16S	0.061066	0.100574	0.063466	0.001235	0.000199	0.000598	0.074893	0.001504	0.039548	0.015042	0.117549	0.001176	0.001100	0.443678	0.000000	0.011177	0.000000	0.030085	0.030114	0.000996
70	LAWC17S	0.061098	0.100627	0.073387	0.001236	0.000199	0.000598	0.044822	0.001505	0.029672	0.015050	0.117610	0.001176	0.006600	0.443910	0.000000	0.011183	0.030100	0.030100	0.030130	0.000997
71	LAWC18S	0.061042	0.100534	0.073320	0.001235	0.000199	0.000597	0.074863	0.001504	0.029644	0.015036	0.117503	0.001175	0.007500	0.443503	0.000000	0.011173	0.000000	0.030073	0.030103	0.000996
72	LAWC19S	0.061053	0.100554	0.083224	0.001235	0.000199	0.000598	0.074878	0.001504	0.019770	0.015039	0.117525	0.001175	0.007300	0.443588	0.000000	0.011175	0.000000	0.030079	0.030108	0.000996
73	LAWC20S	0.061165	0.100737	0.073467	0.001237	0.000200	0.000599	0.074585	0.001507	0.000000	0.015067	0.117740	0.001177	0.005500	0.444397	0.000000	0.011195	0.030133	0.030133	0.030163	0.000998
74	LAWC21S	0.061023	0.100504	0.063850	0.001234	0.000199	0.000597	0.064527	0.001503	0.027236	0.015032	0.118263	0.001175	0.007000	0.465536	0.000000	0.011169	0.000000	0.030063	0.030093	0.000996
75	LAWC22	0.060740	0.100533	0.051087	0.000480	0.000120	0.003361	0.054248	0.000830	0.025058	0.015135	0.144048	0.000670	0.002891	0.466304	0.000000	0.011434	0.000000	0.030700	0.030270	0.002091
76	LAWC23	0.061158	0.100734	0.063987	0.001230	0.000200	0.000600	0.064677	0.002880	0.000000	0.015065	0.118528	0.001180	0.003873	0.467484	0.000000	0.011196	0.000000	0.030129	0.030159	0.001000
77	LAWC23S	0.060960	0.100408	0.063780	0.001226	0.000199	0.000598	0.064467	0.002870	0.000000	0.015016	0.118144	0.001176	0.007100	0.465970	0.000000	0.011160	0.000000	0.030032	0.030062	0.000996
78	LAWC24	0.059531	0.098051	0.062293	0.001201	0.000190	0.000580	0.062953	0.055569	0.000000	0.014668	0.115381	0.001151	0.003687	0.454179	0.000000	0.010896	0.000000	0.029335	0.029365	0.000970
79	LAWC24S	0.059226	0.097548	0.061973	0.001194	0.000189	0.000577	0.062630	0.055284	0.000000	0.014592	0.114788	0.001145	0.008800	0.451848	0.000000	0.010840	0.000000	0.029185	0.029215	0.000966
80	LAWC25	0.057939	0.095417	0.060620	0.001171	0.000190	0.000570	0.061260	0.080930	0.000000	0.014277	0.112276	0.001121	0.003597	0.441969	0.000000	0.010605	0.000000	0.028544	0.028574	0.000940
81	LAWC25S	0.057752	0.095111	0.060425	0.001167	0.000190	0.000569	0.061063	0.080670	0.000000	0.014231	0.111915	0.001117	0.006800	0.440548	0.000000	0.010571	0.000000	0.028452	0.028482	0.000937
82	LAWN1aIS	0.061726	0.100863	0.047131	0.000071	0.000885	0.000986	0.051331	0.003194	0.000000	0.029180	0.119861	0.000366	0.009000	0.460030	0.000000	0.000000	0.043541	0.040845	0.030970	0.000020
83	LAWN2a	0.061819	0.080643	0.047202	0.000071	0.000886	0.000988	0.041223	0.003199	0.000000	0.029224	0.160787	0.000367	0.007500	0.450540	0.000000	0.000000	0.043607	0.040907	0.031017	0.000020
84	LAWN3a	0.061682	0.060137	0.047098	0.000071	0.000884	0.000986	0.030968	0.003191	0.000000	0.029159	0.201085	0.000366	0.009700	0.439378	0.000000	0.000000	0.043510	0.040817	0.030948	0.000020
85	LAWN4a	0.061464	0.039670	0.046931	0.000071	0.000881	0.000982	0.020731	0.003180	0.000000	0.029056	0.240884	0.000365	0.013200	0.427698	0.000000	0.000000	0.043356	0.040672	0.030839	0.000020
86	LAWN5a	0.061819	0.101015	0.047202	0.000071	0.000886	0.000988	0.095016	0.003199	0.000000	0.029224	0.120043	0.000367	0.007500	0.460726	0.000000	0.000000	0.000000	0.040907	0.031017	0.000020
87	LAWN6a	0.061863	0.080700	0.047236	0.000071	0.000887	0.000989	0.084889	0.003201	0.000000	0.029244	0.160901	0.000367	0.006800	0.450858	0.000000	0.000000	0.000000	0.040936	0.031038	0.000020
88	LAWN7a	0.061925	0.060374	0.047283	0.000072	0.000888	0.000990	0.074771	0.003204	0.000000	0.029274	0.201877	0.000367	0.005800	0.441108	0.000000	0.000000	0.000000	0.040977	0.031070	0.000020
89	LAWA53	0.061525	0.061727	0.078497	0.000646	0.000202	0.000101	0.074760	0.004950	0.000000	0.014750	0.199224	0.000303	0.005900	0.420876	0.000000	0.011012	0.000000	0.029803	0.029803	0.000101
90	LAWA54	0.061510	0.061712	0.000000	0.000644	0.000202	0.000101	0.074741	0.004949	0.000000	0.014746	0.199174	0.000303	0.006150	0.420770	0.000000	0.011009	0.000000	0.029795	0.029795	0.078579
91	LAWA55	0.061550	0.061752	0.000000	0.000648	0.000202	0.000101	0.074790	0.004952	0.000000	0.014756	0.199304	0.000303	0.005500	0.421046	0.000000	0.011016	0.000000	0.029815	0.029815	0.078630
92	LAWA56	0.061513	0.120500	0.019696	0.000644	0.000202	0.000101	0.074745	0.004949	0.000000	0.014747	0.199184	0.000303	0.006100	0.420791	0.000000	0.011010	0.000000	0.029797	0.029797	0.000101
93	LAWA57	0.061593	0.061796	0.028723	0.000643	0.000202	0.000101	0.074842	0.004956	0.000000	0.014766	0.199445	0.000303	0.004800	0.421342	0.000000	0.011024	0.000000	0.029836	0.029836	0.000101
94	LAWA58	0.061568	0.061771	0.028712	0.000640	0.000202	0.000101	0.074812	0.004954	0.000000	0.014760	0.199364	0.000303	0.005200	0.421173	0.000000	0.011020	0.000000	0.029824	0.029824	0.049942
95	LAWA59	0.061528	0.061730	0.048697	0.000646	0.000202	0.000101	0.074763	0.004951	0.000000	0.014751	0.199234	0.000303	0.005850	0.420897	0.000000	0.011013	0.000000	0.029804	0.029804	0.029906
96	LAWA61	0.061897	0.062100	0.048481	0.000650	0.000203	0.000102	0.075212	0.004980	0.000000	0.014839	0.200429	0.000305	0.005500	0.423421	0.000000	0.011079	0.000000	0.029983	0.029983	0.024981
97	LAWA62	0.061537	0.061740	0.048199	0.000647	0.000202	0.000101	0.074775	0.004951	0.000000	0.014753	0.199264	0.000303	0.005700	0.420961	0.000000	0.011014	0.000000	0.029809	0.029809	0.030415
98	LAWA63	0.061568	0.061771	0.048224	0.000640	0.000202	0.000101	0.074812	0.004954	0.000000	0.014760	0.199364	0.000303	0.005200	0.421173	0.000000	0.011020	0.000000	0.029824	0.029824	0.030430
99	LAWA65	0.061593	0.061795	0.032971	0.000643	0.000202	0.000101	0.074842	0.004956	0.000000	0.060380	0.199445	0.000303	0.004800	0.421342	0.000000	0.011024	0.000000	0.029836	0.029836	0.000101
100	LAWA66	0.061469	0.061671	0.048146	0.000640	0.000202	0.000101	0.074692	0.004946	0.000000	0.014736	0.199044	0.030583	0.006800	0.420495	0.000000	0.011002	0.000000	0.029776	0.029776	0.000101
101	LAWA67	0.061488	0.061690	0.048160	0.000642	0.000202	0.000101	0.074714	0.004947	0.000000	0.014741	0.199104	0.000303	0.006500	0.420622	0.000000	0.011005	0.030290	0.029785	0.029785	0.000101
102	LAWA68	0.061599	0.061802	0.031963	0.000643	0.000202	0.030446	0.074850	0.004956	0.000000	0.014768	0.199465	0.000303	0.004700	0.437669	0.000000	0.011025	0.000000	0.029839	0.029839	0.000101
103	LAWA69	0.061574	0.110005	0.000000	0.000641	0.000202	0.000101	0.074820	0.004954	0.000000	0.014762	0.199384	0.030636	0.005100	0.421215	0.000000	0.011021	0.000000	0.029827	0.029827	0.000101
104	LAWA70	0.061572	0.061774	0.058336	0.000641	0.000202	0.020322	0.074816	0.004954	0.000000	0.014761	0.199374	0.000303	0.005150	0.421194	0.000000	0.011020	0.000000	0.029825	0.029825	0.000101
105	LAWA71	0.061590	0.109729	0.078580	0.000643	0.000202	0.000101	0.074839	0.004956	0.000000	0.014766	0.151598	0.000303	0.004750	0.421320	0.000000	0.011024	0.000000	0.029834	0.029834	0.000101
106	LAWA72	0.061621	0.109784	0.000000	0.000646	0.000202	0.000101	0.074876	0.004958	0.000000	0.014773	0.151675	0.000304	0.004250	0.421532	0.000000	0.011029	0.000000	0.029849	0.029849	0.078721
107	LAWA73	0.061541	0.061743	0.078517	0.000647	0.000202	0.000101	0.074778	0.004952	0.000000	0.014754	0.199274	0.000303	0.005650	0.420982	0.000000	0.040825	0.000000	0.000000	0.029810	0.000101
108	LAWA74	0.061506	0.069485	0.078474	0.000644	0.000202	0.000101	0.082109	0.004949	0.000000	0.022118	0.199164	0.000303	0.006100	0.420749	0.000000	0.018381	0.000000	0.000000	0.029794	0.000101
109	LAWA75	0.061556	0.159702	0.078537	0.000649	0.000202	0.000101	0.074797	0.004953	0.000000	0.014757	0.101381	0.0003								

Table A.2. (cont.) Normalized Compositions (in mass fractions) of 1075 LAW Glasses in the Database of Compiled Literature Data

#	Glass ID	Al ₂ O ₃	B ₂ O ₃	CaO	Cl	Cr ₂ O ₃	F	Fe ₂ O ₃	K ₂ O	Li ₂ O	MgO	Na ₂ O	P ₂ O ₅	SO ₃	SiO ₂	SnO ₂	TiO ₂	V ₂ O ₅	ZnO	ZrO ₂	Others
133	LAWA95	0.061326	0.061527	0.056233	0.006472	0.000191	0.000091	0.037834	0.004972	0.000000	0.014665	0.198513	0.029662	0.009400	0.419279	0.000000	0.011001	0.029329	0.029722	0.029692	0.000091
134	LAWA102	0.060423	0.099708	0.050552	0.003320	0.000200	0.000259	0.053942	0.002593	0.024927	0.014956	0.144478	0.001296	0.005708	0.464641	0.000000	0.011367	0.000000	0.030511	0.030112	0.001007
135	LAWA104	0.066142	0.085915	0.019244	0.007171	0.000220	0.000110	0.067362	0.005511	0.000000	0.019243	0.220039	0.000370	0.000984	0.429936	0.000000	0.019243	0.000000	0.028605	0.028865	0.001040
136	LAWA105	0.070271	0.082804	0.018543	0.007821	0.000240	0.000120	0.064901	0.006011	0.000000	0.018543	0.240039	0.000400	0.001067	0.414268	0.000000	0.018543	0.000000	0.027564	0.027815	0.001050
137	LAWABP1	0.100006	0.092506	0.000000	0.005800	0.000200	0.000400	0.025002	0.022001	0.000000	0.010001	0.200012	0.000800	0.000938	0.418926	0.000000	0.024902	0.000000	0.026002	0.025203	0.020001
138	LAWB37	0.061721	0.121197	0.047138	0.000700	0.000882	0.000992	0.051618	0.003197	0.029628	0.029176	0.079181	0.034028	0.008003	0.470205	0.000000	0.000000	0.000000	0.030971	0.030971	0.001022
139	LAWC21	0.061093	0.100620	0.063924	0.001236	0.000199	0.000598	0.064601	0.001505	0.027268	0.015049	0.118400	0.001176	0.005852	0.466074	0.000000	0.011182	0.000000	0.030098	0.030128	0.000997
140	LAWC25	0.057939	0.095417	0.060620	0.001171	0.000190	0.000190	0.061260	0.080930	0.000000	0.014277	0.112276	0.001121	0.003597	0.441969	0.000000	0.010605	0.000000	0.028544	0.028574	0.000940
141	OD2-G-50A	0.109907	0.091355	0.016045	0.000000	0.000201	0.000000	0.057460	0.001705	0.000000	0.013839	0.200560	0.000301	0.001842	0.403727	0.000000	0.034195	0.000000	0.042819	0.024569	0.001475
142	LAWA102 + 15% Additive	0.058490	0.102358	0.051880	0.003005	0.000200	0.000200	0.055385	0.002304	0.025539	0.015324	0.128698	0.000000	0.003466	0.477735	0.000000	0.011718	0.000000	0.031348	0.030948	0.001402
143	LAWA102 + 15% Simulant	0.062638	0.097159	0.049230	0.003702	0.000200	0.000300	0.052632	0.002902	0.024315	0.014609	0.161599	0.001501	0.004192	0.452977	0.000000	0.011107	0.000000	0.029718	0.029418	0.001801
144	LAWA44S1	0.061845	0.088734	0.019918	0.005577	0.000199	0.000398	0.069514	0.004282	0.000000	0.019918	0.199179	0.000996	0.005100	0.443971	0.000000	0.019918	0.000000	0.029578	0.029877	0.000996
145	LAWA44S2	0.061833	0.088716	0.019914	0.005576	0.000199	0.000398	0.069500	0.004281	0.000000	0.019914	0.199139	0.000996	0.005300	0.443881	0.000000	0.019914	0.000000	0.029572	0.029871	0.000996
146	LAWA44SX	0.060887	0.087360	0.019610	0.005491	0.000196	0.000392	0.068437	0.004216	0.000000	0.019609	0.210802	0.000981	0.005800	0.437095	0.000000	0.019609	0.000000	0.029120	0.029414	0.000981
147	LAWA88S1	0.060514	0.096543	0.019806	0.003284	0.000100	0.000000	0.055040	0.025678	0.000000	0.014631	0.199058	0.000697	0.006900	0.437828	0.000000	0.019806	0.000000	0.029361	0.029759	0.000995
148	LAWA88S2	0.060538	0.096582	0.019814	0.003286	0.000099	0.000000	0.055062	0.025689	0.000000	0.014637	0.199138	0.000697	0.006500	0.438004	0.000000	0.019814	0.000000	0.029373	0.029771	0.000996
149	LAWA88SX	0.059699	0.095244	0.019540	0.003240	0.000098	0.000000	0.054299	0.025333	0.000000	0.014434	0.209144	0.000687	0.007500	0.431936	0.000000	0.019540	0.000000	0.028966	0.029358	0.000982
150	LAWA102R1	0.060454	0.099759	0.050478	0.003292	0.000199	0.000299	0.053870	0.002594	0.024940	0.014864	0.145149	0.001297	0.006800	0.463979	0.000000	0.011373	0.000000	0.030526	0.030127	0.000000
151	LAWA108S1	0.061677	0.123255	0.019796	0.006466	0.000199	0.000100	0.060000	0.004974	0.000000	0.019796	0.198959	0.000299	0.006600	0.477898	0.000000	0.019796	0.000000	0.029446	0.029744	0.000995
152	LAWA108S2	0.061683	0.123267	0.019798	0.006467	0.000199	0.000100	0.060000	0.004974	0.000000	0.019798	0.198979	0.000299	0.006500	0.477947	0.000000	0.019798	0.000000	0.029449	0.029747	0.000995
153	LAWA109S1	0.061690	0.105967	0.019800	0.006467	0.000199	0.000100	0.034725	0.004975	0.000000	0.019800	0.198999	0.000299	0.006300	0.460682	0.000000	0.019800	0.000000	0.029452	0.029750	0.000995
154	LAWA109S2	0.061690	0.105967	0.019800	0.006467	0.000199	0.000100	0.034725	0.004975	0.000000	0.019800	0.198999	0.000299	0.006300	0.460682	0.000000	0.019800	0.000000	0.029452	0.029750	0.000995
155	LAWA110S1	0.073217	0.100176	0.031436	0.006466	0.000199	0.000100	0.034718	0.004974	0.000000	0.019796	0.198959	0.000298	0.006500	0.443180	0.000000	0.019796	0.000000	0.029446	0.029744	0.000995
156	LAWA110S2	0.073246	0.100216	0.031448	0.006469	0.000199	0.000100	0.034732	0.004976	0.000000	0.019804	0.199039	0.000299	0.006100	0.443359	0.000000	0.019804	0.000000	0.029458	0.029756	0.000995
157	LAWA111S1	0.061634	0.088474	0.089270	0.006462	0.000199	0.000099	0.000000	0.004971	0.000000	0.019782	0.198819	0.000298	0.007200	0.442868	0.000000	0.019782	0.000000	0.029425	0.029723	0.000994
158	LAWA111S2	0.061584	0.088403	0.089198	0.006456	0.000199	0.000099	0.000000	0.004967	0.000000	0.019767	0.198658	0.000298	0.008000	0.442511	0.000000	0.019767	0.000000	0.029401	0.029699	0.000993
159	LAWA112S1	0.060258	0.096135	0.074529	0.003271	0.000000	0.000000	0.000000	0.000000	0.000000	0.014668	0.198216	0.000694	0.011000	0.435977	0.000000	0.019722	0.000000	0.029237	0.029633	0.000991
160	LAWA112S2	0.060410	0.096378	0.074718	0.003279	0.000099	0.000000	0.000000	0.000000	0.000000	0.014705	0.198717	0.000695	0.008500	0.437079	0.000000	0.019722	0.000000	0.029311	0.029708	0.000994
161	LAWA112B14	0.060945	0.098611	0.076431	0.003797	0.000200	0.000099	0.000000	0.000000	0.000000	0.014787	0.199820	0.000999	0.001600	0.442201	0.000000	0.019982	0.000000	0.029673	0.030073	0.000999
162	LAWA112B15	0.061545	0.098012	0.076031	0.003097	0.000100	0.000899	0.000000	0.024078	0.000000	0.014787	0.199820	0.000500	0.001100	0.439804	0.000000	0.019882	0.000000	0.029473	0.029873	0.000999
163	LAWA118S1	0.060336	0.099829	0.050563	0.003291	0.000200	0.000299	0.053953	0.027525	0.000000	0.014959	0.144408	0.001297	0.006000	0.464339	0.000000	0.011369	0.000000	0.030517	0.030118	0.000997
164	LAWA118S2	0.060324	0.099809	0.050553	0.003290	0.000199	0.000299	0.053943	0.027520	0.000000	0.014956	0.144379	0.001296	0.006200	0.464245	0.000000	0.011367	0.000000	0.030511	0.030112	0.000997
165	LAWA119S1	0.060282	0.099738	0.050517	0.003288	0.000199	0.000299	0.053905	0.027500	0.000000	0.014946	0.144277	0.001295	0.006900	0.463918	0.000000	0.011359	0.000000	0.030490	0.030091	0.000996
166	LAWA119S2	0.060263	0.099708	0.050430	0.003287	0.000199	0.000299	0.053890	0.027492	0.000000	0.014941	0.144234	0.001295	0.007200	0.463778	0.000000	0.011356	0.000000	0.030480	0.030082	0.000996
167	LAWA120S1	0.058025	0.092820	0.046958	0.003290	0.000199	0.000299	0.050149	0.082850	0.000000	0.013858	0.144364	0.001296	0.006300	0.431597	0.000000	0.010568	0.000000	0.028414	0.028016	0.000997
168	LAWA120S2	0.057972	0.092736	0.046916	0.003287	0.000199	0.000299	0.050103	0.082775	0.000000	0.013846	0.144233	0.001295	0.007200	0.431206	0.000000	0.010559	0.000000	0.028388	0.027990	0.000996
169	LAWA121S1	0.058019	0.092810	0.046907	0.003290	0.000199	0.000299	0.050000	0.082841	0.000000	0.013857	0.144350	0.001296	0.006400	0.431554	0.000000	0.010567	0.000000	0.028411	0.028013	0.000997
170	LAWA121S2	0.057949	0.092698	0.046900	0.003286	0.000199	0.000299	0.050000	0.082742	0.000000	0.013840	0.144175	0.001294	0.007600	0.431032	0.000000	0.010554	0.000000	0.028377	0.027979	0.000996
171	LAWA122S2	0.059074	0.096033	0.048614	0.003287	0.000199	0.000299	0.051901	0.056185	0.000000	0.014345	0.144348	0.001295	0.006700	0.447389	0.000000	0.010958	0.000000	0.029388	0.028989	0.000996
172	LAWA123S1	0.059086	0.096052	0.048615	0.003288	0.000199	0.000299	0.051901	0.056186	0.000000	0.014348	0.144277	0.001295	0.006900	0.447079	0.000000	0.010960	0.000000	0.029394	0.028995	0.000997
173	LAWA123S2	0.059044	0.095984	0.048616	0.003286	0.000199	0.000299	0.051901	0.056187	0.000000	0.014338	0.144175	0.001294	0.007600	0.446764	0.000000	0.010953	0.000000	0.029373	0.028974	0.000996
174	LAWA130	0.060252	0.089428	0.020783	0.001998	0.000200	0.002998	0.028577	0.038769	0.000000	0.011791	0.184452	0.000799	0.003300	0.460530	0.000000	0.020883	0.000000	0.041367	0.031275	0.002598
175	LAWA133	0.062038																			

Table A.2. (cont.) Normalized Compositions (in mass fractions) of 1075 LAW Glasses in the Database of Compiled Literature Data

#	Glass ID	Al ₂ O ₃	B ₂ O ₃	CaO	Cl	Cr ₂ O ₃	F	Fe ₂ O ₃	K ₂ O	Li ₂ O	MgO	Na ₂ O	P ₂ O ₅	SO ₃	SiO ₂	SnO ₂	TiO ₂	V ₂ O ₅	ZnO	ZrO ₂	Others
199	LAWB69	0.061513	0.123325	0.104621	0.000100	0.000500	0.000800	0.000000	0.002301	0.046109	0.029706	0.066213	0.000500	0.006500	0.479597	0.000000	0.000000	0.000000	0.045709	0.031506	0.001000
200	LAWB69S4	0.061178	0.122655	0.104052	0.000099	0.000497	0.000796	0.000000	0.002288	0.045859	0.029545	0.065853	0.000497	0.011900	0.476990	0.000000	0.000000	0.000000	0.045461	0.031335	0.000995
201	LAWB70	0.061587	0.123474	0.066293	0.000100	0.000501	0.003256	0.000230	0.002303	0.046165	0.029742	0.066293	0.000501	0.005400	0.480176	0.000000	0.000000	0.000000	0.051573	0.031544	0.001001
202	LAWB70S4	0.061159	0.122617	0.065833	0.000099	0.000497	0.000796	0.003230	0.002287	0.045845	0.029536	0.065833	0.000497	0.012300	0.476845	0.000000	0.000000	0.000000	0.051215	0.031326	0.000995
203	LAWB71	0.061624	0.108017	0.066333	0.000100	0.000501	0.000802	0.003256	0.002305	0.046193	0.029760	0.066333	0.000501	0.004800	0.480466	0.000000	0.015531	0.000000	0.051604	0.031563	0.001002
204	LAWB71S4	0.061141	0.107171	0.065813	0.000099	0.000497	0.000795	0.003210	0.002287	0.045831	0.029527	0.065813	0.000497	0.012600	0.476700	0.000000	0.015410	0.000000	0.051199	0.031316	0.000994
205	LAWB72	0.061543	0.123387	0.071250	0.000100	0.000500	0.000801	0.003253	0.002302	0.041129	0.029721	0.066247	0.000500	0.006100	0.479838	0.000000	0.000000	0.000000	0.051536	0.031522	0.001001
206	LAWB72S4	0.061178	0.122654	0.070827	0.000100	0.000497	0.000796	0.003230	0.002288	0.040885	0.029545	0.065853	0.000497	0.012000	0.476990	0.000000	0.000000	0.000000	0.051230	0.031335	0.000995
207	LAWB73	0.061931	0.099471	0.093449	0.000000	0.001004	0.000703	0.019071	0.002610	0.050489	0.029711	0.054905	0.000100	0.009000	0.485312	0.000000	0.013952	0.000000	0.046674	0.031618	0.000000
208	LAWB73S4	0.061619	0.098969	0.092977	0.000000	0.000999	0.000699	0.018975	0.002597	0.050234	0.029561	0.054628	0.000100	0.014000	0.482863	0.000000	0.013882	0.000000	0.046439	0.031458	0.000000
209	LAWB74	0.062183	0.101084	0.087277	0.000000	0.001008	0.000705	0.019149	0.002620	0.053314	0.029831	0.055128	0.000101	0.007700	0.487281	0.000000	0.014009	0.000000	0.046864	0.031746	0.000000
210	LAWB74S4	0.061600	0.102833	0.086460	0.000000	0.000998	0.000699	0.018969	0.002596	0.052814	0.029552	0.054611	0.000100	0.014300	0.482716	0.000000	0.013878	0.000000	0.046425	0.031449	0.000000
211	LAWB75	0.061869	0.117922	0.086837	0.000000	0.001003	0.000702	0.019052	0.002607	0.053045	0.015041	0.054849	0.000100	0.010000	0.484822	0.000000	0.013938	0.000000	0.046627	0.031586	0.000000
212	LAWB75S4	0.061575	0.117362	0.086424	0.000000	0.000998	0.000699	0.018961	0.002595	0.052793	0.014970	0.054589	0.000100	0.014700	0.482520	0.000000	0.013872	0.000000	0.046406	0.031436	0.000000
213	LAWB76	0.061926	0.118032	0.086918	0.000000	0.001004	0.000702	0.019070	0.002609	0.058113	0.015055	0.054901	0.000100	0.009075	0.494208	0.000000	0.000000	0.000000	0.046671	0.031616	0.000000
214	LAWB76S4	0.061506	0.117231	0.086328	0.000000	0.000997	0.000698	0.018940	0.002592	0.057718	0.014953	0.054528	0.000100	0.015800	0.490854	0.000000	0.000000	0.000000	0.046354	0.031401	0.000000
215	LAWB77	0.061599	0.123499	0.066307	0.000100	0.000501	0.000801	0.022035	0.002304	0.041166	0.029748	0.066307	0.000501	0.005200	0.480272	0.000000	0.015525	0.000000	0.051583	0.031551	0.001001
216	LAWB77S4	0.061197	0.122692	0.065873	0.000099	0.000498	0.000796	0.021891	0.002289	0.040897	0.029553	0.065873	0.000498	0.011700	0.477134	0.000000	0.015424	0.000000	0.051246	0.031345	0.000995
217	LAWB78	0.061605	0.123511	0.071322	0.000100	0.000501	0.003256	0.002304	0.002309	0.030552	0.029751	0.097967	0.000501	0.005100	0.470805	0.000000	0.000000	0.000000	0.040068	0.031554	0.001002
218	LAWB78S4	0.061345	0.122990	0.071021	0.000100	0.000499	0.000798	0.032418	0.002294	0.030423	0.029625	0.097554	0.000499	0.009300	0.468817	0.000000	0.000000	0.000000	0.039899	0.031421	0.000997
219	LAWB79	0.061562	0.123424	0.071272	0.000100	0.000500	0.000801	0.032533	0.002302	0.035135	0.029730	0.086287	0.000501	0.005800	0.477480	0.000000	0.000000	0.000000	0.040040	0.031532	0.001001
220	LAWB79S4	0.061333	0.122965	0.071006	0.000100	0.000499	0.000798	0.032412	0.002294	0.035004	0.029619	0.085966	0.000499	0.009500	0.475703	0.000000	0.000000	0.000000	0.039891	0.031414	0.000997
221	LAWB80	0.061556	0.123412	0.071265	0.000100	0.000500	0.000801	0.032529	0.001918	0.035132	0.029727	0.066260	0.000500	0.005800	0.479934	0.000000	0.000000	0.000000	0.040036	0.031529	0.001001
222	LAWB80S4	0.061171	0.122841	0.070935	0.000100	0.000498	0.000797	0.032379	0.0019826	0.034969	0.029589	0.065953	0.000498	0.010400	0.477714	0.000000	0.000000	0.000000	0.039851	0.031383	0.000996
223	LAWB81	0.061550	0.123399	0.071257	0.000100	0.000501	0.000801	0.032526	0.002302	0.042634	0.029724	0.066253	0.000501	0.006000	0.479886	0.000000	0.000000	0.000000	0.050040	0.031525	0.001001
224	LAWB81S4	0.061215	0.122729	0.070870	0.000100	0.000498	0.000796	0.032350	0.002289	0.042403	0.029563	0.065893	0.000498	0.011400	0.477279	0.000000	0.000000	0.000000	0.049768	0.031354	0.000995
225	LAWB82	0.061624	0.101003	0.071343	0.000100	0.000501	0.000802	0.095191	0.002305	0.042686	0.014830	0.066333	0.000501	0.004800	0.455315	0.000000	0.000000	0.000000	0.050101	0.031563	0.001002
226	LAWB82S4	0.061258	0.100404	0.070920	0.000100	0.000498	0.000797	0.094627	0.002291	0.042433	0.014742	0.065940	0.000498	0.010700	0.452616	0.000000	0.000000	0.000000	0.049804	0.031376	0.000996
227	LAWB83	0.061831	0.100350	0.067834	0.000100	0.000400	0.000600	0.052927	0.001901	0.043122	0.029715	0.054728	0.000400	0.004900	0.486244	0.000000	0.013907	0.000000	0.048424	0.031616	0.001001
228	LAWB83S4	0.061489	0.099796	0.067459	0.000100	0.000398	0.000597	0.052634	0.001890	0.042883	0.029551	0.054425	0.000398	0.010400	0.483557	0.000000	0.013830	0.000000	0.048157	0.031441	0.000995
229	LAWB84	0.061868	0.100411	0.066874	0.000100	0.000400	0.000601	0.052959	0.001902	0.040409	0.029733	0.054760	0.000400	0.004400	0.486538	0.000000	0.013915	0.000000	0.048454	0.031635	0.001001
230	LAWB84S4	0.061458	0.099745	0.066431	0.000099	0.000398	0.000597	0.052607	0.001890	0.043757	0.029536	0.054398	0.000398	0.011000	0.483312	0.000000	0.013823	0.000000	0.048132	0.031425	0.000994
231	LAWB85	0.061837	0.115270	0.052832	0.000100	0.000400	0.000600	0.052932	0.001901	0.043126	0.029718	0.054733	0.000400	0.004900	0.486293	0.000000	0.013909	0.000000	0.048429	0.031619	0.001001
232	LAWB85S4	0.061514	0.114667	0.052556	0.000100	0.000398	0.000597	0.052655	0.001891	0.042901	0.029563	0.054447	0.000398	0.010100	0.483752	0.000000	0.013836	0.000000	0.048176	0.031454	0.000995
233	LAWB86	0.061881	0.124262	0.057375	0.000100	0.000401	0.000601	0.052969	0.001902	0.043557	0.029739	0.054772	0.000401	0.004300	0.486635	0.000000	0.000000	0.000000	0.048463	0.031641	0.001001
234	LAWB86S4	0.061514	0.123526	0.057035	0.000100	0.000398	0.000597	0.052655	0.001891	0.043299	0.029563	0.054447	0.000398	0.010200	0.483752	0.000000	0.000000	0.000000	0.048176	0.031454	0.000995
235	LAWB89	0.061821	0.100334	0.067823	0.000100	0.000400	0.000600	0.052918	0.001901	0.050017	0.029710	0.040814	0.000400	0.005060	0.493169	0.000000	0.013905	0.000000	0.048417	0.031611	0.001000
236	LAWB89S4	0.061340	0.099554	0.067296	0.000099	0.000397	0.000595	0.052506	0.001886	0.049628	0.029479	0.040496	0.000397	0.012800	0.489332	0.000000	0.013797	0.000000	0.048040	0.031365	0.000993
237	LAWB90	0.061878	0.100426	0.067885	0.000100	0.000401	0.000601	0.052967	0.001902	0.036145	0.029737	0.068786	0.000401	0.004150	0.479602	0.000000	0.013917	0.000000	0.048461	0.031640	0.001001
238	LAWB91	0.061905	0.100471	0.067916	0.000100	0.000401	0.000601	0.052990	0.001903	0.029250	0.029751	0.087349	0.000401	0.003700	0.468199	0.000000	0.013924	0.000000	0.048483	0.031654	0.001002
239	LAWB91S4	0.061695	0.100129	0.067684	0.000100	0.000399	0.000599	0.052810	0.001897	0.029150	0.029649	0.087051	0.000399	0.007100	0.466601	0.000000	0.013876	0.000000	0.048317	0.031546	0.000998
240	LAWB92	0.061868	0.100411	0.067875	0.000100	0.000400	0.000601	0.052959	0.001902	0.022225	0.029733	0.101212	0.000400	0.004300	0.461009	0.000000	0.013915	0.000000	0.048454	0.031635	0.001001
241	LAWB92S4	0.061738	0.100199	0.067732	0.000100	0.000400	0.000599														

Table A.2. (cont.) Normalized Compositions (in mass fractions) of 1075 LAW Glasses in the Database of Compiled Literature Data

#	Glass ID	Al ₂ O ₃	B ₂ O ₃	CaO	Cl	Cr ₂ O ₃	F	Fe ₂ O ₃	K ₂ O	Li ₂ O	MgO	Na ₂ O	P ₂ O ₅	SO ₃	SiO ₂	SnO ₂	TiO ₂	V ₂ O ₅	ZnO	ZrO ₂	Others
265	LAWC33	0.061462	0.101001	0.069470	0.001101	0.000200	0.000500	0.044445	0.001401	0.027528	0.015115	0.120121	0.001101	0.003700	0.469772	0.000000	0.011311	0.000000	0.040441	0.030330	0.001001
266	LAWA44(Crucible)	0.062025	0.089036	0.019908	0.006503	0.000200	0.000100	0.069828	0.005002	0.000000	0.019908	0.200080	0.000300	0.001000	0.445678	0.000000	0.019908	0.000000	0.029612	0.029912	0.001000
267	A88AP101R1	0.060957	0.088231	0.019986	0.001299	0.000200	0.000200	0.055461	0.0021385	0.000000	0.014790	0.199860	0.000699	0.002300	0.440991	0.000000	0.019986	0.000000	0.029579	0.029979	0.001999
268	A88SI+15	0.061412	0.094819	0.019304	0.001400	0.000200	0.002501	0.053511	0.0023705	0.000000	0.014303	0.221844	0.000800	0.002900	0.425585	0.000000	0.019304	0.000000	0.028506	0.028906	0.001000
269	A88SI-15	0.060548	0.102182	0.020717	0.001101	0.000100	0.002001	0.057646	0.018815	0.000000	0.015412	0.176742	0.000600	0.001900	0.458668	0.000000	0.020717	0.000000	0.030725	0.031125	0.001001
270	LAWB96	0.061795	0.100291	0.067794	0.000100	0.000400	0.000600	0.052895	0.001900	0.043096	0.029697	0.054695	0.000400	0.005489	0.485956	0.000000	0.013899	0.000000	0.048396	0.031597	0.001000
271	LAWC22(Crucible)	0.060651	0.100419	0.051059	0.000500	0.000100	0.003397	0.054157	0.000799	0.024980	0.015088	0.143884	0.000699	0.004600	0.465726	0.000000	0.011391	0.000000	0.030675	0.030276	0.001599
272	C22AN107	0.061055	0.100791	0.051146	0.000801	0.000200	0.001401	0.055850	0.000901	0.025123	0.015114	0.144330	0.001201	0.002700	0.466121	0.000000	0.011410	0.000000	0.030628	0.030227	0.001001
273	C22SI+15	0.060327	0.098182	0.049940	0.000899	0.000200	0.001598	0.054734	0.000999	0.024471	0.014682	0.161705	0.001298	0.003100	0.454153	0.000000	0.011087	0.000000	0.029864	0.029465	0.003296
274	C22SI-15	0.061731	0.103252	0.052326	0.000700	0.000200	0.001301	0.057029	0.000700	0.025713	0.015508	0.125663	0.001000	0.002300	0.477439	0.000000	0.011706	0.000000	0.031416	0.031016	0.001000
275	A1-AN105R2(LAWA44)	0.061031	0.088385	0.019643	0.011722	0.000170	0.000030	0.068682	0.004411	0.000000	0.019643	0.206655	0.000000	0.001700	0.438255	0.000000	0.019643	0.000000	0.029175	0.029395	0.001460
276	A1C1-1	0.060875	0.091252	0.027417	0.009132	0.000150	0.000860	0.065006	0.003471	0.006232	0.018494	0.191656	0.000330	0.002100	0.444757	0.000000	0.017584	0.000000	0.029507	0.029557	0.001620
277	A1C1-2	0.060722	0.094139	0.035208	0.006543	0.000130	0.001691	0.061332	0.002541	0.012477	0.017339	0.176702	0.000660	0.002300	0.451345	0.000000	0.015538	0.000000	0.029836	0.029736	0.001761
278	A1C1-3	0.060552	0.096985	0.042975	0.003951	0.000110	0.002521	0.057641	0.001611	0.018707	0.016186	0.161658	0.000990	0.002900	0.457745	0.000000	0.013475	0.000000	0.030161	0.029901	0.001931
279	C1-AN107(LAWC22)	0.060418	0.099905	0.050788	0.001361	0.000090	0.003353	0.053991	0.000681	0.024954	0.015044	0.146730	0.001311	0.002800	0.464483	0.000000	0.011431	0.000000	0.030499	0.030079	0.002082
280	A2-AP101(LAWA126)	0.056209	0.098278	0.019884	0.004243	0.000210	0.003502	0.055348	0.0038136	0.000000	0.014770	0.184748	0.000771	0.003330	0.440175	0.000000	0.019874	0.000000	0.029400	0.029631	0.001491
281	A2B1-1	0.057605	0.098782	0.031836	0.003224	0.000240	0.002833	0.054732	0.029073	0.010752	0.018531	0.152313	0.000681	0.003500	0.451682	0.000000	0.018401	0.000000	0.034169	0.030144	0.001502
282	A2B1-2	0.058982	0.099245	0.043786	0.002202	0.000270	0.002152	0.054077	0.019981	0.021503	0.022284	0.119796	0.000591	0.004200	0.462958	0.000000	0.016918	0.000000	0.038911	0.030642	0.001502
283	A2B1-3	0.060370	0.099715	0.055734	0.001191	0.000310	0.001482	0.053432	0.010893	0.032257	0.026040	0.087291	0.000501	0.004700	0.474318	0.000000	0.015448	0.000000	0.034660	0.031146	0.001512
284	B1-AZ101(LAWB83)	0.061758	0.100197	0.067696	0.000170	0.000340	0.000801	0.052787	0.001802	0.043015	0.029798	0.054789	0.000411	0.005200	0.485855	0.000000	0.013968	0.000000	0.048411	0.031660	0.001512
285	A3-AN104(LAWA137)	0.060531	0.099209	0.050290	0.007871	0.000210	0.000060	0.053670	0.003281	0.024785	0.014803	0.146438	0.001120	0.003500	0.460968	0.000000	0.011342	0.000000	0.030416	0.030016	0.001490
286	A3C2-1	0.060593	0.097983	0.056110	0.006884	0.000190	0.000330	0.049257	0.002691	0.026724	0.014838	0.139816	0.001241	0.003800	0.464002	0.000000	0.011206	0.000000	0.032798	0.030016	0.001521
287	A3C2-2	0.060663	0.096771	0.061945	0.005886	0.000160	0.000601	0.044847	0.002092	0.028670	0.014865	0.133209	0.001351	0.004000	0.467118	0.000000	0.011072	0.000000	0.035187	0.030021	0.001542
288	A3C2-3	0.060682	0.095476	0.067737	0.004883	0.000140	0.004008	0.001501	0.003601	0.014880	0.126488	0.001471	0.004900	0.469836	0.000000	0.010928	0.000000	0.037536	0.030001	0.001661	
289	C2-AN102C35	0.060733	0.094232	0.073554	0.003883	0.000120	0.001141	0.035982	0.000911	0.032539	0.014903	0.119835	0.001591	0.005400	0.472794	0.000000	0.010789	0.000000	0.039915	0.029996	0.001682
290	LAWC35S2	0.060474	0.089566	0.073227	0.003885	0.000100	0.001096	0.028992	0.000897	0.037659	0.009963	0.119354	0.001594	0.008900	0.481502	0.000000	0.010760	0.000000	0.039752	0.029888	0.002391
291	WVG-G-10B	0.065822	0.086329	0.019106	0.006202	0.000200	0.000300	0.067022	0.004902	0.000000	0.019106	0.221474	0.000700	0.002368	0.427642	0.000000	0.019106	0.000000	0.028410	0.028710	0.002601
292	WVF-G-81A	0.057505	0.093308	0.020702	0.004900	0.000200	0.000200	0.072406	0.003900	0.000000	0.020702	0.176914	0.000600	0.002019	0.461938	0.000000	0.020702	0.000000	0.030702	0.031002	0.002300
293	WVF-G-21B	0.060816	0.098026	0.019905	0.001300	0.000200	0.002301	0.055415	0.0021306	0.000000	0.014804	0.200154	0.000700	0.003134	0.440117	0.000000	0.019905	0.000000	0.029508	0.029908	0.002501
294	WVE-G-108A	0.061313	0.094521	0.019204	0.001400	0.000200	0.002501	0.053412	0.023605	0.000000	0.014203	0.221848	0.000800	0.003384	0.424392	0.000000	0.019204	0.000000	0.028506	0.028806	0.002701
295	WVE-G-27D	0.060407	0.101812	0.020703	0.001100	0.000100	0.002000	0.057507	0.018802	0.000000	0.015302	0.176821	0.000600	0.002882	0.457054	0.000000	0.020702	0.000000	0.030704	0.031104	0.002400
296	WVB-G-124B	0.060359	0.099833	0.050566	0.003298	0.000200	0.000300	0.053964	0.002598	0.024983	0.014890	0.144302	0.001299	0.003873	0.464786	0.000000	0.011392	0.000000	0.030579	0.030180	0.002598
297	WVB-G-93A	0.062575	0.097062	0.049181	0.003699	0.000200	0.000300	0.052579	0.002899	0.024291	0.014594	0.161436	0.001499	0.004192	0.452522	0.000000	0.011096	0.000000	0.029688	0.029388	0.002799
298	WVA-G-100B	0.058361	0.102132	0.051765	0.002998	0.000200	0.000200	0.055263	0.002299	0.025483	0.015290	0.128414	0.001199	0.003466	0.476682	0.000000	0.011692	0.000000	0.031279	0.030879	0.002398
299	WVJ-G-109D	0.061663	0.100102	0.067669	0.000100	0.000400	0.000601	0.052754	0.001902	0.043044	0.029730	0.054656	0.000400	0.005489	0.485193	0.000000	0.013914	0.000000	0.048349	0.031532	0.002502
300	WVK-G-41A	0.062069	0.099010	0.066874	0.000100	0.000401	0.000701	0.052358	0.002203	0.042647	0.029333	0.062069	0.000400	0.005995	0.480234	0.000000	0.013815	0.000000	0.047853	0.031235	0.002703
301	WVN-G-110A	0.061274	0.099521	0.067181	0.000100	0.000400	0.000501	0.052464	0.001302	0.042752	0.029536	0.058571	0.000100	0.005995	0.484087	0.000000	0.013817	0.000000	0.048259	0.031538	0.002803
302	WVO-G-44B	0.061960	0.100597	0.067965	0.000100	0.000300	0.000200	0.053051	0.001001	0.043041	0.029829	0.050749	0.000100	0.005043	0.489171	0.000000	0.014013	0.000000	0.048647	0.031931	0.002302
303	WVD-G-25A	0.060275	0.098060	0.049879	0.000900	0.000200	0.001599	0.054677	0.001000	0.024390	0.014694	0.162133	0.001299	0.003711	0.453613	0.000000	0.011095	0.000000	0.029788	0.029388	0.003299
304	WVC-G-107B	0.061546	0.103077	0.052239	0.000701	0.000200	0.001301	0.056943	0.000701	0.025719	0.015412	0.126095	0.001001	0.003050	0.476658	0.000000	0.011709	0.000000	0.031324	0.030923	0.001401
305	WVH-G-57B	0.061112	0.100319	0.074014	0.001100	0.000200	0.000500	0.044208	0.001400	0.027305	0.015003	0.119022	0.001000	0.004113	0.466788	0.000000	0.011202	0.000000	0.040108	0.030106	0.002500
306	WVG-G-88D	0.061089	0.098282	0.072487	0.001300	0.000200	0.000600	0.043292	0.001500	0.026695	0.014697	0.134475	0.001200	0.004584	0.457115	0.000000	0.010998	0.000000	0.039293	0.029494	0.002699
307	WV																				

Table A.2. (cont.) Normalized Compositions (in mass fractions) of 1075 LAW Glasses in the Database of Compiled Literature Data

#	Glass ID	Al ₂ O ₃	B ₂ O ₃	CaO	Cl	Cr ₂ O ₃	F	Fe ₂ O ₃	K ₂ O	Li ₂ O	MgO	Na ₂ O	P ₂ O ₅	SO ₃	SiO ₂	SnO ₂	TiO ₂	V ₂ O ₅	ZnO	ZrO ₂	Others
331	LAWM1	0.090436	0.060291	0.100485	0.000201	0.000081	0.000075	0.080388	0.040194	0.045218	0.000000	0.050243	0.000125	0.005200	0.446655	0.000000	0.030146	0.000000	0.050242	0.000000	0.000020
332	LAWM2	0.035117	0.060200	0.100333	0.000820	0.003225	0.003004	0.080266	0.000000	0.045150	0.050167	0.050167	0.005006	0.006700	0.471566	0.000000	0.030100	0.000000	0.050167	0.000000	0.000083
333	LAWM3	0.090327	0.060218	0.100364	0.000201	0.000081	0.000075	0.080291	0.000000	0.044863	0.050182	0.115217	0.000125	0.006400	0.401455	0.000000	0.000000	0.000000	0.010036	0.040145	0.000020
334	LAWM4	0.035156	0.130578	0.100444	0.000201	0.000081	0.000075	0.055646	0.040178	0.045200	0.000000	0.050222	0.000125	0.005600	0.415941	0.000000	0.030133	0.000000	0.050222	0.040178	0.000020
335	LAWM5	0.090409	0.060273	0.057962	0.000201	0.000081	0.000075	0.080364	0.040182	0.045205	0.000000	0.050227	0.000125	0.005500	0.489013	0.000000	0.030136	0.000000	0.010045	0.040182	0.000020
336	LAWM6	0.090018	0.106121	0.100020	0.000200	0.000081	0.000075	0.080016	0.040008	0.000000	0.050010	0.090018	0.000125	0.003200	0.400080	0.000000	0.030006	0.000000	0.010002	0.000000	0.000020
337	LAWM7	0.054544	0.069596	0.100283	0.000201	0.000081	0.000075	0.080226	0.000000	0.025873	0.050141	0.050141	0.000125	0.007200	0.521471	0.000000	0.030085	0.000000	0.010028	0.000000	0.000020
338	LAWM8	0.090273	0.130394	0.064495	0.000204	0.003210	0.003009	0.000000	0.000000	0.020863	0.050151	0.050152	0.000125	0.007000	0.446248	0.000000	0.030091	0.000000	0.050152	0.040121	0.000802
339	LAWM9	0.035056	0.060096	0.100161	0.008015	0.003219	0.002999	0.080129	0.040064	0.023939	0.000000	0.050080	0.004998	0.002400	0.497899	0.000000	0.000000	0.000000	0.050080	0.040064	0.000801
340	LAWM10	0.090045	0.130065	0.100050	0.008006	0.003216	0.002995	0.000000	0.000000	0.045023	0.000000	0.130766	0.004993	0.002300	0.401701	0.000000	0.030015	0.000000	0.010005	0.040020	0.000800
341	LAWM11	0.035035	0.130131	0.094095	0.000200	0.000081	0.000075	0.053154	0.040040	0.045046	0.000000	0.114916	0.000125	0.009000	0.468072	0.000000	0.000000	0.000000	0.010010	0.000000	0.000020
342	LAWM12	0.035014	0.130052	0.000000	0.008005	0.003216	0.002995	0.023109	0.040016	0.045018	0.019708	0.142557	0.004992	0.002300	0.422169	0.000000	0.030012	0.000000	0.050020	0.040016	0.000801
343	LAWM13	0.035007	0.060012	0.100020	0.004122	0.001656	0.001542	0.080016	0.037908	0.000000	0.000000	0.220044	0.002570	0.005000	0.400081	0.000000	0.030006	0.000000	0.021604	0.000000	0.000412
344	LAWM14	0.034996	0.059994	0.020498	0.000075	0.000080	0.000000	0.000000	0.000000	0.008799	0.049995	0.219978	0.000125	0.005300	0.519948	0.000000	0.029997	0.000000	0.049995	0.000000	0.000020
345	LAWM15	0.089991	0.093591	0.000000	0.008001	0.003214	0.002994	0.062794	0.000000	0.000000	0.037196	0.219978	0.004998	0.001700	0.434756	0.000000	0.029997	0.000000	0.009999	0.000000	0.000800
346	LAWM16	0.080056	0.120084	0.080056	0.000200	0.000081	0.000075	0.065046	0.001001	0.030021	0.000077	0.100700	0.000125	0.003300	0.424798	0.000000	0.025018	0.000000	0.050035	0.010007	0.000020
347	LAWM17	0.050020	0.120048	0.022109	0.000200	0.000080	0.000075	0.065026	0.020008	0.005002	0.035014	0.170068	0.000125	0.002000	0.420169	0.000000	0.005002	0.000000	0.050020	0.035014	0.000020
348	LAWM18	0.080048	0.120072	0.080048	0.008005	0.003202	0.003002	0.065039	0.001001	0.030018	0.010006	0.100060	0.005003	0.003400	0.420253	0.000000	0.025015	0.000000	0.020012	0.025015	0.000801
349	LAWM19	0.079976	0.119964	0.079976	0.007998	0.003199	0.001994	0.019994	0.004999	0.009997	0.131660	0.004998	0.003600	0.419874	0.000000	0.004998	0.000000	0.049985	0.034989	0.000800	
350	LAWM20	0.050015	0.070021	0.080024	0.008002	0.003201	0.003001	0.020006	0.020006	0.022607	0.030011	0.170051	0.005001	0.002100	0.420126	0.000000	0.005002	0.000000	0.050015	0.035011	0.000800
351	LAWM21	0.050050	0.109010	0.080081	0.000200	0.000080	0.000075	0.065066	0.020020	0.030030	0.010101	0.100101	0.000125	0.004600	0.420422	0.000000	0.025025	0.000000	0.050050	0.035035	0.000020
352	LAWM22	0.080027	0.070023	0.020007	0.008003	0.003201	0.003001	0.065022	0.020007	0.005001	0.035012	0.170057	0.005002	0.002966	0.420140	0.000000	0.006702	0.000000	0.050017	0.035012	0.000800
353	LAWM23	0.050111	0.070155	0.080177	0.008018	0.003207	0.003007	0.020044	0.020044	0.030066	0.010022	0.100221	0.005011	0.003400	0.485472	0.000000	0.025055	0.000000	0.050111	0.035077	0.000802
354	LAWM24	0.080008	0.120012	0.020002	0.000200	0.000080	0.000075	0.065007	0.020002	0.006401	0.010001	0.170017	0.000125	0.002300	0.470747	0.000000	0.005000	0.000000	0.020002	0.010001	0.000020
355	LAWM25	0.080112	0.120169	0.020028	0.008011	0.003205	0.003004	0.036852	0.020028	0.030042	0.035049	0.100141	0.005007	0.002600	0.499902	0.000000	0.005007	0.000000	0.020028	0.010014	0.000801
356	LAWM26	0.080056	0.120084	0.049735	0.008006	0.003202	0.003002	0.020014	0.001001	0.030021	0.010007	0.100070	0.005004	0.004900	0.499051	0.000000	0.005004	0.000000	0.050035	0.010007	0.000801
357	LAWM27	0.080056	0.070049	0.080056	0.008006	0.003202	0.003002	0.065046	0.020014	0.005003	0.035025	0.133794	0.005003	0.002500	0.420295	0.000000	0.025018	0.000000	0.033123	0.010007	0.000801
358	LAWM28	0.050101	0.120241	0.080161	0.000201	0.000080	0.000075	0.065131	0.007014	0.006914	0.010020	0.100201	0.000125	0.003600	0.501006	0.000000	0.025050	0.000000	0.020040	0.010020	0.000020
359	LAWM29	0.075668	0.070063	0.020018	0.000761	0.000304	0.006509	0.020018	0.030027	0.035032	0.100090	0.000476	0.003100	0.468923	0.000000	0.005023	0.000000	0.050045	0.035032	0.000076	
360	LAWM30	0.080032	0.120048	0.020008	0.000200	0.000080	0.000075	0.065026	0.001001	0.020208	0.010004	0.170068	0.000125	0.002000	0.420169	0.000000	0.005902	0.000000	0.050020	0.035014	0.000020
361	LAWM31	0.050020	0.070028	0.080032	0.008003	0.003201	0.003001	0.065026	0.001001	0.030012	0.010004	0.167567	0.005002	0.003000	0.423270	0.000000	0.025010	0.000000	0.020008	0.035014	0.000801
362	LAWM32	0.051415	0.070021	0.020006	0.008004	0.003215	0.002006	0.020006	0.030009	0.035011	0.165150	0.004991	0.003200	0.500151	0.000000	0.005002	0.000000	0.050015	0.010003	0.000800	
363	LAWM33	0.050020	0.120048	0.080032	0.000200	0.000080	0.000075	0.065026	0.017207	0.009004	0.010004	0.170068	0.000125	0.002900	0.420169	0.000000	0.025010	0.000000	0.020008	0.010004	0.000020
364	LAWM34	0.050015	0.083525	0.080024	0.000200	0.000080	0.000075	0.062919	0.020006	0.030009	0.010003	0.170051	0.000125	0.003000	0.420126	0.000000	0.014805	0.000000	0.020006	0.035011	0.000020
365	LAWM35	0.050030	0.120072	0.061837	0.008007	0.003216	0.002996	0.044127	0.001001	0.005003	0.035021	0.170102	0.004993	0.001800	0.420253	0.000000	0.025015	0.000000	0.020012	0.025715	0.000800
366	LAWM36	0.070021	0.110033	0.070021	0.003201	0.001280	0.001200	0.050015	0.003001	0.025008	0.015004	0.120036	0.002001	0.003700	0.450136	0.000000	0.020006	0.000000	0.035011	0.020006	0.000020
367	LAWM37	0.067554	0.110088	0.070056	0.000200	0.000080	0.000075	0.050040	0.003003	0.025020	0.025020	0.120097	0.000125	0.003200	0.450362	0.000000	0.010008	0.000000	0.035028	0.030024	0.000020
368	LAWM38	0.069986	0.079984	0.069986	0.007998	0.003199	0.002999	0.029994	0.001500	0.024995	0.014997	0.139972	0.004999	0.003700	0.479904	0.000000	0.009998	0.000000	0.034993	0.019996	0.000800
369	LAWM39	0.070070	0.090591	0.050050	0.008008	0.003203	0.003003	0.030030	0.001001	0.025025	0.025025	0.140141	0.005005	0.002500	0.480482	0.000000	0.010010	0.000000	0.035035	0.020020	0.000801
370	LAWM40	0.060036	0.110066	0.050030	0.002121	0.000849	0.000796	0.050030	0.001001	0.010006	0.015009	0.140084	0.001326	0.003100	0.480289	0.000000	0.010006	0.000000	0.035021	0.030018	0.000212
371	LAWM41	0.070021	0.080024	0.070021	0.008002	0.003201	0.003001	0.050015	0.003001	0.010003	0.025008	0.140042	0.005002	0.003400	0.450135	0.000000	0.010003	0.000000	0.046014	0.022307	0.000800
372	LAWM42	0.060042	0.080056	0.050035	0.008006	0.003202	0.003002	0.040328	0.001001	0.025018	0.015011	0.140098	0.005003	0.003000	0.480337	0.000000	0.020014	0.000000	0.035025	0.030021	0.000801
373	LAWM43	0.070021	0.086826	0.050015	0.008002	0.003201	0.003001	0.050015	0.003001	0.025008	0.025008	0.120036	0.005001	0.003900							

Table A.2. (cont.) Normalized Compositions (in mass fractions) of 1075 LAW Glasses in the Database of Compiled Literature Data

#	Glass ID	Al ₂ O ₃	B ₂ O ₃	CaO	Cl	Cr ₂ O ₃	F	Fe ₂ O ₃	K ₂ O	Li ₂ O	MgO	Na ₂ O	P ₂ O ₅	SO ₃	SiO ₂	SnO ₂	TiO ₂	V ₂ O ₅	ZnO	ZrO ₂	Others
397	LAWA161	0.101605	0.136706	0.079904	0.011701	0.000200	0.000000	0.010001	0.004400	0.000000	0.010001	0.206610	0.000000	0.001753	0.365817	0.000000	0.000000	0.010000	0.029901	0.029901	0.001500
398	LAWA161R	0.101605	0.136706	0.079904	0.011701	0.000200	0.000000	0.010001	0.004400	0.000000	0.010001	0.206610	0.000000	0.001753	0.365817	0.000000	0.000000	0.010000	0.029901	0.029901	0.001500
399	LAWA161S2	0.100918	0.135782	0.079364	0.011622	0.000199	0.000000	0.009933	0.004370	0.000000	0.009933	0.205213	0.000000	0.008500	0.363345	0.000000	0.000000	0.009933	0.029699	0.029699	0.001490
400	LAWA162	0.061003	0.140007	0.070003	0.011701	0.000200	0.000000	0.010000	0.004400	0.000000	0.004600	0.206610	0.000000	0.001753	0.409019	0.000000	0.000000	0.000000	0.019201	0.060003	0.001500
401	LAWA163	0.061003	0.140007	0.070003	0.011701	0.000200	0.000000	0.000000	0.004400	0.000000	0.004600	0.206610	0.000000	0.001753	0.409019	0.000000	0.000000	0.010000	0.019201	0.060003	0.001500
402	LAWA164	0.061003	0.120006	0.070003	0.011701	0.000200	0.000000	0.010001	0.004400	0.000000	0.004600	0.206610	0.000000	0.001753	0.410019	0.000000	0.004600	0.010000	0.019201	0.064403	0.001500
403	LAWA165	0.091604	0.136706	0.079904	0.011701	0.000200	0.000000	0.010001	0.004400	0.000000	0.010001	0.206610	0.000000	0.001753	0.355817	0.000000	0.000000	0.010000	0.029901	0.049902	0.001500
404	LAWA166	0.094604	0.140207	0.079904	0.011701	0.000200	0.000000	0.002800	0.004400	0.000000	0.010001	0.206610	0.000000	0.001753	0.356517	0.000000	0.000000	0.010000	0.029901	0.049902	0.001500
405	LAWA167	0.104605	0.140207	0.079904	0.011701	0.000200	0.000000	0.002800	0.004400	0.000000	0.010001	0.206610	0.000000	0.001753	0.366517	0.000000	0.000000	0.010000	0.029901	0.029901	0.001500
406	LAWA168	0.104605	0.140207	0.079904	0.011701	0.000200	0.000000	0.002800	0.004400	0.000000	0.010001	0.206610	0.000000	0.001753	0.366517	0.000000	0.010000	0.000000	0.029901	0.029901	0.001500
407	WVW-G-11A	0.101831	0.137848	0.080562	0.005618	0.000200	0.000000	0.010133	0.004414	0.000000	0.010133	0.199147	0.000000	0.009281	0.368999	0.000000	0.000000	0.010133	0.030098	0.030098	0.001505
408	LAWA143	0.062048	0.089866	0.019976	0.005642	0.000180	0.000030	0.069840	0.004481	0.000000	0.019976	0.200058	0.000000	0.001200	0.445649	0.000000	0.000000	0.020006	0.029669	0.029889	0.001490
409	LAWA144	0.062048	0.089866	0.019976	0.005642	0.000180	0.000030	0.069840	0.004481	0.000000	0.029976	0.200058	0.000000	0.001200	0.445649	0.000000	0.000000	0.010003	0.029669	0.029889	0.001490
410	LAWA145	0.062042	0.089857	0.019974	0.005641	0.000180	0.000030	0.039827	0.004481	0.000000	0.029976	0.200038	0.000000	0.001300	0.445605	0.000000	0.000000	0.040007	0.029666	0.029886	0.001490
411	LAWA140	0.062012	0.089917	0.019904	0.005601	0.000200	0.000300	0.044809	0.004401	0.000000	0.014903	0.200439	0.000700	0.002106	0.480293	0.000000	0.014903	0.000000	0.029706	0.029806	0.000000
412	AN-103 Actual	0.062204	0.089506	0.020101	0.003100	0.000100	0.000200	0.070204	0.006000	0.000000	0.020101	0.200013	0.000500	0.000938	0.446828	0.000000	0.020101	0.000000	0.030002	0.030102	0.000000
413	AW-101 Actual	0.060806	0.097110	0.019902	0.000800	0.000100	0.000000	0.055406	0.025803	0.000000	0.014801	0.200020	0.000700	0.002100	0.440544	0.000000	0.019902	0.000000	0.029503	0.029903	0.002600
414	AP-101 Actual	0.056600	0.098500	0.020000	0.001700	0.000300	0.002700	0.055600	0.038200	0.000000	0.014900	0.184600	0.000900	0.003100	0.442700	0.000000	0.020100	0.000000	0.029700	0.030100	0.000300
415	AZ-101 Actual	0.062100	0.100400	0.067900	0.000800	0.000300	0.005290	0.001800	0.043100	0.029900	0.053500	0.000500	0.005500	0.487000	0.000000	0.000000	0.014000	0.000000	0.048500	0.031700	0.000100
416	AZ-102 Actual	0.064961	0.129921	0.079951	0.000100	0.000600	0.000500	0.021987	0.002099	0.046872	0.014091	0.049970	0.000200	0.008500	0.499697	0.000000	0.000000	0.000000	0.048670	0.031881	0.000000
417	AZ-102 Actual CCC	0.064961	0.129921	0.079951	0.000100	0.000600	0.000500	0.021987	0.002099	0.046872	0.014091	0.049970	0.000200	0.008500	0.499697	0.000000	0.000000	0.000000	0.048670	0.031881	0.000000
418	AN-107 Actual	0.062306	0.089409	0.020102	0.000800	0.000000	0.004701	0.070207	0.001400	0.000000	0.020202	0.200020	0.000200	0.001300	0.447845	0.000000	0.020002	0.000000	0.029903	0.030103	0.001500
419	AN-102 Actual LC Melter	0.061475	0.100959	0.064274	0.000900	0.000200	0.000500	0.064974	0.000700	0.027489	0.015194	0.117953	0.000800	0.003600	0.467812	0.000000	0.011295	0.000000	0.030388	0.030388	0.001099
420	AN-102 Actual	0.061500	0.101300	0.064200	0.001200	0.000200	0.000600	0.064900	0.000900	0.027400	0.015200	0.118000	0.001300	0.003600	0.467500	0.000000	0.011300	0.000000	0.030300	0.030300	0.000300
421	LA44CCCR2	0.061720	0.088729	0.019806	0.005702	0.000700	0.002201	0.069622	0.002601	0.000000	0.019706	0.200064	0.003501	0.002281	0.444642	0.000000	0.019706	0.000000	0.029109	0.029910	0.000000
422	I2U-G-86A	0.061619	0.089527	0.019806	0.005602	0.000200	0.000200	0.069421	0.004401	0.000000	0.019806	0.199660	0.000700	0.002300	0.443333	0.000000	0.019806	0.000000	0.029509	0.029709	0.004401
423	I2U-G-86ACCC	0.061619	0.089527	0.019806	0.005602	0.000200	0.000200	0.069421	0.004401	0.000000	0.019806	0.199660	0.000700	0.002300	0.443333	0.000000	0.019806	0.000000	0.029509	0.029709	0.004401
424	LAWA170	0.060525	0.096661	0.019810	0.003285	0.000100	0.000000	0.055150	0.030561	0.000000	0.014733	0.199096	0.000697	0.001931	0.438509	0.000000	0.019810	0.000000	0.029367	0.029765	0.000000
425	LA126CCC	0.056515	0.098526	0.020005	0.002001	0.000200	0.003001	0.055615	0.038811	0.000000	0.014804	0.184649	0.000800	0.003134	0.442318	0.000000	0.020005	0.000000	0.029608	0.030008	0.000000
426	WVM-G-142C	0.056128	0.098149	0.019910	0.004202	0.000200	0.003502	0.055328	0.038119	0.000000	0.014707	0.184493	0.000800	0.003500	0.439621	0.000000	0.019810	0.000000	0.029415	0.029615	0.002501
427	LAWA102R2	0.060567	0.100110	0.050656	0.003304	0.000200	0.000300	0.054060	0.002603	0.025028	0.015016	0.144960	0.001301	0.003300	0.466315	0.000000	0.011413	0.000000	0.030634	0.030233	0.000000
428	WVR-G-127A	0.060482	0.099070	0.050185	0.007898	0.000200	0.000100	0.053584	0.003299	0.024792	0.014795	0.146256	0.001100	0.003800	0.460261	0.000000	0.011297	0.000000	0.030391	0.029991	0.002499
429	LB83CCC-I	0.062154	0.100487	0.067959	0.000000	0.000300	0.000801	0.052946	0.001802	0.043137	0.029926	0.053747	0.000500	0.004738	0.487222	0.000000	0.014012	0.000000	0.048542	0.031727	0.000000
430	LAWB96	0.061705	0.100271	0.067716	0.000100	0.000301	0.000200	0.052890	0.001202	0.042973	0.029751	0.054794	0.000100	0.004800	0.487433	0.000000	0.013924	0.000000	0.048583	0.031754	0.001503
431	GTSD-1126	0.061830	0.100412	0.067843	0.000100	0.000301	0.000200	0.053012	0.001203	0.043091	0.029763	0.054916	0.000100	0.004500	0.488430	0.000000	0.013929	0.000000	0.048603	0.031767	0.000000
432	GTSD-1126CCC	0.061830	0.100412	0.067843	0.000100	0.000301	0.000200	0.053012	0.001203	0.043091	0.029763	0.054916	0.000100	0.004500	0.488430	0.000000	0.013929	0.000000	0.048603	0.031767	0.000000
433	LB88SRCC-2	0.065052	0.129805	0.079764	0.000100	0.000601	0.000500	0.022018	0.002002	0.046938	0.014111	0.050040	0.000200	0.007300	0.500804	0.000000	0.000000	0.000000	0.048839	0.031926	0.000000
434	LAWB88CCC	0.064878	0.130057	0.079897	0.000100	0.000601	0.000501	0.022027	0.002002	0.046957	0.014117	0.050060	0.000200	0.006800	0.501005	0.000000	0.000000	0.000000	0.048859	0.031939	0.000000
435	AZ-102 Surrogate	0.064196	0.129790	0.079572	0.000000	0.000599	0.000998	0.021965	0.001997	0.046824	0.014077	0.050718	0.000200	0.009300	0.499914	0.000000	0.000000	0.000000	0.048721	0.031849	0.000000
436	I2S-G-85C	0.060800	0.100500	0.050900	0.000800	0.000200	0.001400	0.055600	0.000800	0.025000	0.015100	0.144300	0.001200	0.003800	0.464300	0.000000	0.011400	0.000000	0.030600	0.030100	0.000300
437	LAWC21	0.061388	0.101045	0.064192	0.001202	0.000200	0.000601	0.064893	0.001502	0.027439	0.015122	0.118971	0.001202	0.002870	0.467671	0.000000	0.011216	0.000000	0.030243	0.030243	0.000000
438	LAWC21Rev2	0.061388	0.101045	0.064192	0.001202	0.000200	0.000601	0.064893	0.001502	0.027439	0.015122	0.118971	0.001202	0.002870	0.467671	0.000000	0.011216	0.000000	0.030243	0.030243	0.000000
439	Surrogate #2 for AN-102	0.061418	0.101431	0.																	

Table A.2. (cont.) Normalized Compositions (in mass fractions) of 1075 LAW Glasses in the Database of Compiled Literature Data

#	Glass ID	Al ₂ O ₃	B ₂ O ₃	CaO	Cl	Cr ₂ O ₃	F	Fe ₂ O ₃	K ₂ O	Li ₂ O	MgO	Na ₂ O	P ₂ O ₅	SO ₃	SiO ₂	SnO ₂	TiO ₂	V ₂ O ₅	ZnO	ZrO ₂	Others
463	LAWCrP4R	0.060988	0.099980	0.021096	0.001899	0.005899	0.001000	0.054989	0.002699	0.000000	0.014797	0.209958	0.023795	0.003700	0.420216	0.000000	0.013997	0.000000	0.034993	0.029994	0.000000
464	LAWCrP5	0.061061	0.100101	0.058158	0.001401	0.005906	0.000701	0.055055	0.000901	0.026427	0.014915	0.143945	0.013313	0.003800	0.434937	0.000000	0.014014	0.000000	0.035035	0.030030	0.000300
465	LAWCrP6	0.061031	0.100050	0.069435	0.001401	0.006303	0.000700	0.055028	0.000900	0.041721	0.025513	0.080040	0.025113	0.005800	0.447625	0.000000	0.014007	0.000000	0.035018	0.030015	0.000300
466	LAWCrP7	0.061031	0.100050	0.069835	0.001401	0.006303	0.000700	0.055028	0.000900	0.043022	0.029315	0.054027	0.025113	0.006600	0.467335	0.000000	0.014007	0.000000	0.035018	0.030015	0.000300
467	LAWCrP8CCC	0.061043	0.100070	0.069449	0.001401	0.004303	0.000700	0.055039	0.000901	0.041729	0.025518	0.080056	0.025118	0.005600	0.449717	0.000000	0.014010	0.000000	0.035025	0.030021	0.000300
468	LAWCrP9CCC	0.061055	0.100091	0.069863	0.001401	0.004304	0.000701	0.055050	0.000901	0.043039	0.029326	0.054049	0.025123	0.006200	0.469525	0.000000	0.014013	0.000000	0.035032	0.030027	0.000300
469	LAWCrP10CCC	0.060994	0.099990	0.069793	0.001400	0.003300	0.000700	0.054994	0.000900	0.042996	0.029297	0.082991	0.013299	0.007200	0.481851	0.000000	0.013999	0.000000	0.034996	0.029997	0.000300
470	LAWE3Cr2CCC	0.061031	0.100050	0.020210	0.002001	0.014007	0.000800	0.055028	0.004925	0.000000	0.014807	0.183194	0.001201	0.003300	0.416509	0.000000	0.014007	0.000000	0.035018	0.030015	0.000200
471	LAWE9HC1CCC	0.060585	0.099340	0.068697	0.002003	0.006008	0.000801	0.054577	0.005408	0.040857	0.023633	0.089426	0.001202	0.005500	0.463352	0.000000	0.013920	0.000000	0.034749	0.029742	0.000200
472	LAWE9HC2CCC	0.060604	0.099370	0.068718	0.002003	0.004508	0.000801	0.054593	0.005409	0.040870	0.023640	0.089453	0.001202	0.005200	0.464995	0.000000	0.013924	0.000000	0.034759	0.029751	0.000200
473	LAWE10HC1CCC	0.060810	0.099681	0.069726	0.002004	0.003506	0.000802	0.054900	0.005410	0.042677	0.029453	0.057304	0.001202	0.006200	0.487383	0.000000	0.013925	0.000000	0.034863	0.029954	0.000200
474	LAWE3H	0.059424	0.097439	0.019708	0.002001	0.000800	0.000800	0.053621	0.054122	0.000000	0.014406	0.197479	0.001200	0.003301	0.418568	0.000000	0.013605	0.000000	0.034114	0.029212	0.000200
475	LAWE12	0.069514	0.087517	0.019704	0.002000	0.000800	0.000800	0.043609	0.054111	0.000000	0.014403	0.197440	0.001200	0.003200	0.418484	0.000000	0.013703	0.000000	0.034107	0.039208	0.000200
476	LAWE13	0.069514	0.097519	0.019704	0.002000	0.000800	0.000800	0.053611	0.054111	0.000000	0.004401	0.197440	0.001200	0.003200	0.418484	0.000000	0.003701	0.000000	0.034107	0.039208	0.000200
477	LAWE14	0.049515	0.097529	0.014705	0.002001	0.000800	0.000800	0.053616	0.054116	0.000000	0.004401	0.197460	0.001200	0.003100	0.433531	0.000000	0.013704	0.000000	0.034110	0.039212	0.000200
478	LAWE15	0.059518	0.087526	0.014705	0.002001	0.000800	0.000800	0.053616	0.054116	0.000000	0.009403	0.197460	0.001200	0.003100	0.428529	0.000000	0.013704	0.000000	0.034110	0.039212	0.000200
479	LAWE16	0.059428	0.082401	0.014682	0.001998	0.000799	0.000799	0.053535	0.054035	0.000000	0.009389	0.197162	0.001199	0.004600	0.427884	0.000000	0.013683	0.000000	0.034059	0.044147	0.000200
480	LAWM57	0.070007	0.110011	0.030003	0.002000	0.000800	0.000800	0.046605	0.038004	0.000000	0.014402	0.206121	0.001200	0.003200	0.392639	0.000000	0.013701	0.000000	0.030303	0.040004	0.000200
481	LAWM58	0.070014	0.092919	0.010302	0.002000	0.000800	0.000800	0.065013	0.038008	0.000000	0.014403	0.205341	0.001200	0.003200	0.416484	0.000000	0.013703	0.000000	0.025605	0.040008	0.000200
482	LAWM59	0.068421	0.090127	0.029609	0.002001	0.000800	0.000800	0.064920	0.020006	0.000000	0.014404	0.200060	0.001200	0.003100	0.445534	0.000000	0.013704	0.000000	0.025108	0.020006	0.000200
483	LAWM60	0.050020	0.110044	0.017107	0.002001	0.000800	0.000800	0.045018	0.020008	0.000000	0.014406	0.200180	0.001201	0.003000	0.453482	0.000000	0.013706	0.000000	0.028011	0.040016	0.000200
484	LAWM61	0.050005	0.110011	0.010001	0.002000	0.000800	0.000800	0.045005	0.032903	0.000000	0.014402	0.200020	0.001200	0.003300	0.450545	0.000000	0.013701	0.000000	0.045005	0.020102	0.000200
485	LAWM62	0.050010	0.090018	0.010002	0.002000	0.000800	0.000800	0.065013	0.033807	0.000000	0.014403	0.200040	0.001200	0.003200	0.443389	0.000000	0.013703	0.000000	0.038408	0.033007	0.000200
486	LAWM63	0.069993	0.093991	0.010399	0.002000	0.000800	0.000800	0.046995	0.020598	0.000000	0.014398	0.229977	0.001200	0.003400	0.425957	0.000000	0.013699	0.000000	0.044995	0.020598	0.000200
487	LAWM64	0.069928	0.109844	0.030012	0.002001	0.000800	0.000800	0.065026	0.020008	0.000000	0.014406	0.200480	0.001201	0.003000	0.383754	0.000000	0.013706	0.000000	0.044918	0.039916	0.000200
488	LAWM65	0.050005	0.090009	0.029603	0.002000	0.000800	0.000800	0.045005	0.020002	0.000000	0.014401	0.227923	0.001200	0.003400	0.435944	0.000000	0.013701	0.000000	0.025003	0.040004	0.000200
489	LAWM66	0.075915	0.106321	0.010002	0.002001	0.000800	0.000800	0.063113	0.040481	0.000000	0.014403	0.229946	0.001200	0.003200	0.383577	0.000000	0.013703	0.000000	0.045009	0.045009	0.000200
490	LAWM67	0.080008	0.106011	0.015502	0.002000	0.000800	0.000800	0.046005	0.054005	0.000000	0.014401	0.201320	0.001200	0.003200	0.383639	0.000000	0.013701	0.000000	0.027203	0.050005	0.000200
491	LAWM68	0.050000	0.090000	0.030000	0.002000	0.000800	0.000800	0.065000	0.048000	0.000000	0.014400	0.200100	0.001200	0.003300	0.408100	0.000000	0.013700	0.000000	0.035600	0.036800	0.000200
492	LAWM69	0.079792	0.109889	0.029997	0.002000	0.000800	0.000800	0.063694	0.018298	0.000000	0.014398	0.200880	0.001200	0.003400	0.395960	0.000000	0.013699	0.000000	0.044995	0.019998	0.000200
493	LAWM70	0.049995	0.093991	0.010499	0.002000	0.000800	0.000800	0.064993	0.054595	0.000000	0.014399	0.200080	0.001200	0.003300	0.453454	0.000000	0.013699	0.000000	0.024997	0.020098	0.000200
494	LAWM71	0.050100	0.090000	0.010000	0.002000	0.000800	0.000800	0.045000	0.054000	0.000000	0.014400	0.200000	0.001200	0.003400	0.449400	0.000000	0.013700	0.000000	0.045000	0.020000	0.000200
495	LAWM72	0.080008	0.110011	0.029403	0.002000	0.000800	0.000800	0.064507	0.041804	0.000000	0.014402	0.200420	0.001200	0.003200	0.391639	0.000000	0.013701	0.000000	0.025003	0.020902	0.000200
496	LAWM73	0.080008	0.090009	0.030003	0.002000	0.000800	0.000800	0.048805	0.012201	0.000000	0.014402	0.230023	0.001200	0.003200	0.403841	0.000000	0.013701	0.000000	0.044905	0.023902	0.000200
497	LAWM74	0.075838	0.090045	0.010005	0.002001	0.000800	0.000800	0.045023	0.000000	0.000000	0.014407	0.213307	0.001201	0.002900	0.453728	0.000000	0.013707	0.000000	0.026013	0.050025	0.000200
498	LAWM75	0.080032	0.091537	0.030012	0.002001	0.000800	0.000800	0.064926	0.010804	0.000000	0.014406	0.206883	0.001201	0.003100	0.384554	0.000000	0.013706	0.000000	0.045018	0.050020	0.000200
499	LAWM76	0.064019	0.099230	0.019206	0.002001	0.000800	0.000800	0.054216	0.026008	0.000000	0.014404	0.214065	0.001201	0.003100	0.418826	0.000000	0.013704	0.000000	0.034210	0.034010	0.000200
500	LAWA171	0.101682	0.136910	0.056546	0.006505	0.000200	0.000000	0.010008	0.005104	0.000000	0.010008	0.230186	0.000000	0.006700	0.366095	0.000000	0.000000	0.010008	0.030024	0.030024	0.000000
501	LAWA172	0.106554	0.127964	0.079940	0.006503	0.000200	0.000000	0.009105	0.005102	0.000000	0.009105	0.230116	0.000000	0.006800	0.348776	0.000000	0.000000	0.009805	0.030015	0.030015	0.000000
502	LAWA173	0.106575	0.112980	0.079956	0.006505	0.000200	0.000000	0.009106	0.005104	0.000000	0.009106	0.230162	0.000000	0.006600	0.348846	0.000000	0.000000	0.009807	0.030021	0.045032	0.000000
503	LAWA174	0.106543	0.097939	0.079932	0.006503	0.000200	0.000000	0.009104	0.005102	0.000000	0.009104	0.230093	0.000000	0.006900	0.348740	0.000000	0.000000	0.009804	0.030012	0.060024	0.000000
504	LAWA175	0.121525	0.112923	0.079916	0.006501	0.000200	0.000000	0.009102	0.005101	0.000000	0.009102	0.230046	0.000000	0.007100	0.348670	0.000000	0.000000	0.009802	0.030006	0.030006	0.000000
505	LAWA176	0.136583	0.097959	0.079948	0.006504	0.000200	0.000000	0.009105	0.005103												

Table A.2. (cont.) Normalized Compositions (in mass fractions) of 1075 LAW Glasses in the Database of Compiled Literature Data

#	Glass ID	Al ₂ O ₃	B ₂ O ₃	CaO	Cl	Cr ₂ O ₃	F	Fe ₂ O ₃	K ₂ O	Li ₂ O	MgO	Na ₂ O	P ₂ O ₅	SO ₃	SiO ₂	SnO ₂	TiO ₂	V ₂ O ₅	ZnO	ZrO ₂	Others
529	LAWB97	0.091629	0.100241	0.092130	0.000100	0.001102	0.000701	0.011516	0.004106	0.035450	0.011516	0.100141	0.000300	0.006300	0.461450	0.000000	0.000000	0.012418	0.035450	0.035450	0.000000
530	LAWB98	0.101694	0.110311	0.092176	0.000100	0.001102	0.000701	0.011522	0.004108	0.035468	0.011522	0.100191	0.000301	0.005800	0.441644	0.000000	0.000000	0.012424	0.035468	0.035468	0.000000
531	LAWB99	0.101623	0.110233	0.102223	0.000100	0.001101	0.000701	0.011514	0.004105	0.035443	0.011514	0.100121	0.000300	0.006400	0.431321	0.000000	0.000000	0.012415	0.035443	0.035443	0.000000
532	LAWB100	0.091565	0.115281	0.107176	0.000100	0.001101	0.000700	0.011508	0.004103	0.035425	0.011508	0.100070	0.000300	0.006900	0.431004	0.000000	0.000000	0.012409	0.035425	0.035425	0.000000
533	LAWB101	0.101694	0.100292	0.112315	0.000100	0.001102	0.000701	0.011522	0.004108	0.035468	0.011522	0.100191	0.000300	0.005700	0.431625	0.000000	0.000000	0.012424	0.035468	0.035468	0.000000
534	LAWB102	0.091731	0.100352	0.122408	0.000100	0.001103	0.000702	0.011529	0.004110	0.035489	0.011529	0.100252	0.000301	0.005100	0.431885	0.000000	0.000000	0.012431	0.035489	0.035489	0.000000
535	LAWB103	0.091633	0.100251	0.092139	0.000100	0.001102	0.000701	0.011517	0.004106	0.040461	0.011517	0.100151	0.000301	0.006100	0.425689	0.000000	0.000000	0.012419	0.035454	0.035454	0.000000
536	LAWB104	0.101428	0.100029	0.112021	0.000100	0.001099	0.000700	0.011492	0.004097	0.040372	0.011492	0.099929	0.000300	0.008200	0.425600	0.000000	0.000000	0.012391	0.035375	0.035375	0.000000
537	LAWB105	0.061630	0.130476	0.092195	0.000100	0.001102	0.000701	0.011524	0.004109	0.035475	0.011524	0.100212	0.000301	0.005500	0.461775	0.000000	0.000000	0.012426	0.035475	0.035475	0.000000
538	EWV-G-89B	0.106361	0.127693	0.064798	0.006510	0.005208	0.000000	0.009014	0.005108	0.000000	0.009014	0.229647	0.000000	0.008000	0.348026	0.010015	0.000000	0.009715	0.029945	0.029945	0.010101
539	EWV-G-89B	0.106361	0.127693	0.064798	0.006510	0.005208	0.000000	0.009014	0.005108	0.000000	0.009014	0.229647	0.000000	0.008000	0.348026	0.010015	0.000000	0.009715	0.029945	0.029945	0.010101
540	EWV-G-89BCCC	0.106361	0.127693	0.064798	0.006510	0.005208	0.000000	0.009014	0.005108	0.000000	0.009014	0.229647	0.000000	0.008000	0.348026	0.010015	0.000000	0.009715	0.029945	0.029945	0.010101
541	EWV-G-93B	0.106393	0.127732	0.064818	0.006512	0.005209	0.000000	0.009016	0.005109	0.000000	0.009016	0.229717	0.000000	0.007700	0.348132	0.010018	0.000000	0.009718	0.029954	0.029954	0.010102
542	EWV-G-93BCCC	0.106393	0.127732	0.064818	0.006512	0.005209	0.000000	0.009016	0.005109	0.000000	0.009016	0.229717	0.000000	0.007700	0.348132	0.010018	0.000000	0.009718	0.029954	0.029954	0.010102
543	EWV-G-108B	0.106329	0.127655	0.064778	0.006508	0.005206	0.000000	0.009011	0.005106	0.000000	0.009011	0.229578	0.000000	0.008300	0.347921	0.010012	0.000000	0.009712	0.029936	0.029936	0.010101
544	DWW-G-123C	0.100896	0.109421	0.101398	0.000100	0.001103	0.000702	0.011434	0.004012	0.035304	0.011434	0.099893	0.000301	0.011700	0.428557	0.000000	0.000000	0.012336	0.035203	0.035203	0.010103
545	ORPLA1	0.100000	0.090000	0.035000	0.007100	0.000200	0.000000	0.010100	0.005600	0.000000	0.013500	0.250000	0.000000	0.001900	0.413100	0.000000	0.000000	0.000000	0.023600	0.048000	0.010190
546	ORPLA1S4	0.099709	0.089739	0.034898	0.007079	0.000199	0.000000	0.010071	0.005584	0.000000	0.013461	0.249274	0.000000	0.004800	0.411900	0.000000	0.000000	0.000000	0.023531	0.047861	0.010189
547	ORPLA2	0.100000	0.090000	0.025000	0.007100	0.000200	0.000000	0.010100	0.005600	0.000000	0.013500	0.250000	0.000000	0.001900	0.413100	0.010000	0.000000	0.000000	0.023600	0.048000	0.010190
548	ORPLA2S4	0.099769	0.089793	0.024942	0.007084	0.000199	0.000000	0.010077	0.005587	0.000000	0.013469	0.249424	0.000000	0.004200	0.412148	0.009977	0.000000	0.000000	0.023546	0.047889	0.010186
549	ORPLA3	0.099990	0.089991	0.030397	0.007099	0.000489	0.000000	0.010099	0.005599	0.000000	0.013499	0.249975	0.000000	0.001900	0.413059	0.000000	0.000000	0.000000	0.023598	0.047995	0.010190
550	ORPLA3S4	0.099769	0.089793	0.030330	0.007084	0.000489	0.000000	0.010077	0.005587	0.000000	0.013469	0.249424	0.000000	0.004100	0.412148	0.000000	0.000000	0.000000	0.023546	0.047889	0.010189
551	ORPLA4	0.079776	0.089973	0.034989	0.007088	0.000200	0.000000	0.030191	0.005598	0.000000	0.013496	0.249925	0.000000	0.002100	0.412976	0.000000	0.000000	0.000000	0.023593	0.047986	0.010189
552	ORPLA4S4	0.079792	0.089766	0.034909	0.007081	0.000199	0.000000	0.030121	0.005585	0.000000	0.013465	0.249349	0.000000	0.004400	0.412024	0.000000	0.000000	0.000000	0.023539	0.047875	0.010189
553	ORPLA5	0.100020	0.070014	0.010002	0.007101	0.004901	0.000000	0.010102	0.005601	0.000000	0.013503	0.250050	0.000000	0.002000	0.433187	0.010002	0.000000	0.000000	0.033607	0.048010	0.010190
554	ORPLA5S4	0.099880	0.069916	0.009988	0.007091	0.004894	0.000000	0.010088	0.005593	0.000000	0.013484	0.249699	0.000000	0.003400	0.432579	0.009988	0.000000	0.000000	0.033560	0.047942	0.010190
555	ORPLA6	0.100800	0.077800	0.010000	0.007100	0.004900	0.000000	0.009400	0.005600	0.000000	0.009100	0.250000	0.000000	0.001900	0.419200	0.010000	0.000000	0.000000	0.033600	0.060700	0.010190
556	ORPLA6S4	0.100848	0.077691	0.009986	0.007090	0.004893	0.000000	0.009387	0.005592	0.000000	0.009087	0.249649	0.000000	0.003300	0.418612	0.009986	0.000000	0.000000	0.023567	0.060615	0.010189
557	ORPLA7	0.100800	0.077800	0.014700	0.007100	0.004900	0.000000	0.009400	0.005600	0.000000	0.009100	0.250000	0.000000	0.002000	0.405000	0.010000	0.000000	0.009400	0.023600	0.060700	0.010190
558	ORPLA7S4	0.100813	0.077738	0.014688	0.007094	0.004896	0.000000	0.009392	0.005596	0.000000	0.009093	0.249800	0.000000	0.002800	0.404675	0.009992	0.000000	0.009392	0.023581	0.060651	0.010189
559	ORPLA8	0.058177	0.084766	0.000000	0.007097	0.004898	0.000000	0.026989	0.005598	0.000000	0.033687	0.249900	0.000000	0.002300	0.420831	0.019392	0.015494	0.000000	0.009996	0.058976	0.010189
560	ORPLA8S4	0.058083	0.084630	0.000000	0.007086	0.004890	0.000000	0.026946	0.005589	0.000000	0.033633	0.249499	0.000000	0.003900	0.420156	0.019361	0.015469	0.000000	0.009980	0.058882	0.010186
561	ORPLA9	0.109022	0.078016	0.065213	0.007101	0.004901	0.000000	0.009102	0.005601	0.000000	0.009102	0.250050	0.000000	0.001800	0.355171	0.020004	0.000000	0.009402	0.023605	0.050010	0.010190
562	ORPLA9S4	0.100818	0.077727	0.064971	0.007075	0.004883	0.000000	0.009068	0.005580	0.000000	0.009068	0.249123	0.000000	0.005500	0.353855	0.019930	0.000000	0.009367	0.023517	0.049825	0.010189
563	ORPLA10	0.109000	0.078000	0.065200	0.007100	0.004900	0.000000	0.009100	0.005600	0.000000	0.009100	0.250000	0.000000	0.001900	0.357800	0.026800	0.000000	0.000000	0.023600	0.050000	0.010190
564	ORPLA10S4	0.100872	0.077765	0.065004	0.007079	0.004885	0.000000	0.009073	0.005583	0.000000	0.009073	0.249249	0.000000	0.004900	0.356725	0.026719	0.000000	0.000000	0.023529	0.049850	0.010189
565	ORPLA11	0.108989	0.069993	0.019998	0.007099	0.004900	0.000000	0.009099	0.005599	0.000000	0.009099	0.249975	0.000000	0.001900	0.401460	0.026997	0.000000	0.000000	0.023598	0.059394	0.010190
566	ORPLA11S4	0.108880	0.069923	0.019978	0.007092	0.004895	0.000000	0.009090	0.005594	0.000000	0.009090	0.249724	0.000000	0.002900	0.401058	0.026970	0.000000	0.000000	0.023574	0.059334	0.010189
567	ORPLA12	0.107689	0.071293	0.020298	0.006799	0.005000	0.000000	0.009299	0.005399	0.000000	0.009299	0.239976	0.000000	0.001700	0.409959	0.027497	0.000000	0.000000	0.024498	0.059494	0.010180
568	ORPLA12S4	0.107581	0.071221	0.020278	0.006793	0.004994	0.000000	0.009290	0.005394	0.000000	0.009290	0.239736	0.000000	0.002700	0.409548	0.027470	0.000000	0.000000	0.024473	0.059434	0.010178
569	ORPLA13	0.100831	0.070707	0.020102	0.006901	0.004900	0.000000	0.009201	0.005501	0.000000	0.009201	0.245024	0.000000	0.001900	0.406141	0.027203	0.000000	0.000000	0.024202	0.058906	0.010180
570	ORPLA13S4	0.100819	0.070629	0.020080	0.006893	0.004895	0.000000	0.009191	0.005494	0.000000	0.009191	0.244755	0.000000	0.003000	0.405693	0.027173	0.000000	0.000000	0.024176	0.058841	0.010178
571	ORPLA14	0.107011	0.072007	0.020502	0.006601																

Table A.2. (cont.) Normalized Compositions (in mass fractions) of 1075 LAW Glasses in the Database of Compiled Literature Data

#	Glass ID	Al ₂ O ₃	B ₂ O ₃	CaO	Cl	Cr ₂ O ₃	F	Fe ₂ O ₃	K ₂ O	Li ₂ O	MgO	Na ₂ O	P ₂ O ₅	SO ₃	SiO ₂	SnO ₂	TiO ₂	V ₂ O ₅	ZnO	ZrO ₂	Others
595	ORPLC5	0.100440	0.085234	0.019108	0.006202	0.005302	0.000100	0.009704	0.005402	0.000000	0.009304	0.235795	0.001901	0.004800	0.401161	0.010004	0.000000	0.020008	0.023710	0.060424	0.001401
596	ORPLC5S4	0.100360	0.085166	0.019092	0.006198	0.005298	0.000100	0.009696	0.005398	0.000000	0.009296	0.235605	0.001899	0.005600	0.400839	0.009996	0.000000	0.019992	0.023690	0.060376	0.001399
597	ORPLD1	0.101815	0.120755	0.080370	0.003307	0.005011	0.001704	0.010021	0.001603	0.000000	0.010021	0.210445	0.002906	0.007601	0.372488	0.000000	0.000000	0.010021	0.030064	0.030064	0.001804
598	ORPLD1S4	0.101877	0.120828	0.080419	0.003309	0.005014	0.001705	0.010027	0.001604	0.000000	0.010027	0.210573	0.002908	0.007000	0.372713	0.000000	0.000000	0.010027	0.030082	0.030082	0.001805
599	ORPLD2	0.091275	0.076246	0.080354	0.003306	0.005010	0.001703	0.007514	0.001603	0.000754	0.010019	0.210403	0.002906	0.007700	0.394756	0.010019	0.000000	0.010019	0.025148	0.052701	0.001804
600	ORPLD2S4	0.091229	0.076208	0.080313	0.003305	0.005007	0.001702	0.007511	0.001602	0.000751	0.010014	0.210297	0.002904	0.008200	0.394557	0.010014	0.000000	0.010014	0.025135	0.052674	0.001803
601	ORPLD3	0.081198	0.086204	0.100321	0.003304	0.005006	0.001702	0.007509	0.001602	0.000759	0.010012	0.210255	0.002904	0.008400	0.394477	0.000000	0.000000	0.010012	0.025131	0.042652	0.001802
602	ORPLD3S4	0.081157	0.086161	0.100271	0.003302	0.005004	0.001701	0.007505	0.001601	0.000750	0.010012	0.210149	0.002902	0.008900	0.394279	0.000000	0.000000	0.010007	0.025118	0.042630	0.001801
603	ORPLE1	0.076085	0.098610	0.104717	0.000200	0.001001	0.002002	0.002403	0.005506	0.030033	0.010512	0.160178	0.001201	0.011300	0.414561	0.000000	0.000000	0.012514	0.032236	0.035439	0.001502
604	ORPLE2	0.100262	0.114786	0.080530	0.000200	0.001002	0.002003	0.002404	0.005509	0.030049	0.010517	0.160259	0.001202	0.010900	0.398645	0.000000	0.000000	0.012520	0.032252	0.035457	0.001503
605	ORPLE3	0.100232	0.114751	0.104738	0.000200	0.001001	0.002003	0.002403	0.005507	0.030039	0.010514	0.160211	0.001202	0.011100	0.374392	0.000000	0.000000	0.012516	0.032242	0.035447	0.001502
606	ORPLE4	0.076539	0.098279	0.104490	0.000301	0.001102	0.002304	0.002304	0.006111	0.021038	0.010519	0.180328	0.001403	0.010800	0.404136	0.000000	0.000000	0.012122	0.031357	0.035364	0.001503
607	ORPLE5	0.076069	0.096188	0.102493	0.000300	0.001301	0.002502	0.002302	0.006806	0.011010	0.009909	0.200182	0.001502	0.011500	0.399864	0.000000	0.000000	0.011811	0.029627	0.035132	0.001502
608	ORPLE6	0.076092	0.098620	0.099821	0.000200	0.005006	0.002002	0.002403	0.005507	0.030037	0.010513	0.160194	0.001202	0.011300	0.414603	0.000000	0.000000	0.012515	0.032239	0.036244	0.001502
609	ORPLE7	0.076085	0.098610	0.104716	0.000200	0.005006	0.002002	0.002403	0.005506	0.026029	0.010512	0.160178	0.001201	0.011300	0.414561	0.000000	0.000000	0.012514	0.032236	0.035439	0.001502
610	ORPLE8	0.076085	0.094605	0.100612	0.000200	0.001001	0.002002	0.010512	0.005506	0.030033	0.010512	0.160178	0.001201	0.011300	0.414561	0.000000	0.000000	0.012514	0.032236	0.035440	0.001502
611	ORPLE9	0.076085	0.090601	0.096607	0.000200	0.005006	0.002002	0.010512	0.005506	0.030033	0.010512	0.160178	0.001201	0.011300	0.414561	0.000000	0.000000	0.012514	0.032236	0.039444	0.001502
612	ORPLE10	0.088278	0.104930	0.092792	0.000201	0.001003	0.002006	0.002408	0.005517	0.030095	0.010533	0.160505	0.001204	0.009281	0.409389	0.000000	0.000000	0.012539	0.032302	0.035512	0.001505
613	ORPLE11	0.076100	0.098630	0.104738	0.000200	0.001001	0.002003	0.002403	0.005507	0.025033	0.010514	0.160211	0.001201	0.011100	0.414645	0.000000	0.000000	0.017523	0.032242	0.035447	0.001502
614	ORPLE12	0.076154	0.098700	0.100704	0.000200	0.005010	0.002004	0.002405	0.005511	0.025051	0.010521	0.160324	0.001202	0.010500	0.414939	0.000000	0.000000	0.017535	0.032265	0.035472	0.001503
615	Q10-G-134A	0.076000	0.098630	0.100633	0.000200	0.002503	0.002003	0.002403	0.005407	0.025033	0.010514	0.160211	0.001202	0.013800	0.414647	0.000000	0.000100	0.017523	0.032265	0.035447	0.001502
616	R10-G-91E	0.094985	0.086441	0.033371	0.006835	0.004925	0.000000	0.009247	0.005428	0.000000	0.009247	0.241232	0.000000	0.001100	0.394514	0.027440	0.000000	0.000000	0.024425	0.059403	0.001407
617	R10-G-155A	0.094605	0.086095	0.033237	0.006808	0.004905	0.000000	0.009210	0.005406	0.000000	0.009210	0.240266	0.000000	0.005100	0.392934	0.027330	0.000000	0.000000	0.024327	0.059165	0.001402
618	S10-G-45A	0.099840	0.084834	0.018908	0.001100	0.005302	0.004702	0.009604	0.001100	0.000000	0.009304	0.240097	0.002201	0.008100	0.398961	0.010004	0.000000	0.019908	0.023610	0.060124	0.002301
619	S10-G-45AR	0.099840	0.084834	0.018908	0.001100	0.005302	0.004702	0.009604	0.001100	0.000000	0.009304	0.240097	0.002201	0.008100	0.398961	0.010004	0.000000	0.019908	0.023610	0.060124	0.002301
620	S10-G-101B	0.100271	0.085060	0.019113	0.006204	0.005304	0.000100	0.009707	0.005404	0.000000	0.009307	0.235866	0.001801	0.006100	0.400382	0.010007	0.000000	0.020014	0.023617	0.060342	0.001401
621	T10-G-101BR	0.100271	0.085060	0.019113	0.006204	0.005304	0.000100	0.009707	0.005404	0.000000	0.009307	0.235866	0.001801	0.006100	0.400382	0.010007	0.000000	0.020014	0.023617	0.060342	0.001401
622	T10-G-16A	0.101705	0.120443	0.080262	0.003307	0.005010	0.001703	0.010020	0.001603	0.000000	0.010020	0.210425	0.002806	0.008900	0.371850	0.000000	0.000000	0.010020	0.030061	0.030061	0.001804
623	FWV-G-35B	0.060391	0.098949	0.069205	0.004307	0.000801	0.005482	0.005408	0.005408	0.042364	0.029244	0.057287	0.001202	0.006300	0.486434	0.000000	0.013821	0.000000	0.034652	0.029745	0.000200
624	FWV-G-63B	0.060130	0.098650	0.063032	0.002001	0.000800	0.001901	0.054227	0.005403	0.031716	0.014907	0.135368	0.001201	0.005300	0.447125	0.000000	0.013807	0.000000	0.034617	0.029615	0.000200
625	LAWE4H	0.059322	0.097236	0.024409	0.002001	0.000800	0.000800	0.053420	0.005402	0.000000	0.014405	0.212779	0.001201	0.003630	0.447466	0.000000	0.013605	0.000000	0.034113	0.029211	0.000200
626	FWV-G-108B	0.057806	0.094810	0.023802	0.010001	0.000800	0.012001	0.052105	0.005301	0.000000	0.014002	0.212721	0.001200	0.003800	0.436344	0.000000	0.013301	0.000000	0.033303	0.028503	0.000200
627	FWV-G-138A	0.058624	0.096039	0.024110	0.003201	0.006303	0.003801	0.052721	0.005402	0.000000	0.014206	0.212785	0.001200	0.003700	0.441777	0.000000	0.013405	0.000000	0.033714	0.028812	0.000200
628	GWV-G-36D	0.055734	0.091455	0.022914	0.007705	0.006304	0.009306	0.050230	0.005403	0.000000	0.013508	0.212828	0.027917	0.003500	0.420653	0.000000	0.012808	0.000000	0.032119	0.027416	0.000200
629	GWV-G-65A	0.059918	0.098330	0.019806	0.007702	0.000800	0.009303	0.054016	0.049015	0.000000	0.014505	0.182155	0.001200	0.003200	0.422127	0.000000	0.013804	0.000000	0.034410	0.029509	0.000200
630	GWV-G-110A	0.060594	0.099290	0.020098	0.002000	0.006299	0.000800	0.054594	0.049795	0.000000	0.014699	0.182082	0.001200	0.003600	0.426357	0.000000	0.013899	0.000000	0.034696	0.029797	0.000200
631	GWV-G-133B	0.058100	0.095200	0.019200	0.003200	0.006300	0.003800	0.052400	0.049800	0.000000	0.014100	0.182100	0.027900	0.003500	0.409000	0.000000	0.013300	0.000000	0.033300	0.028600	0.000200
632	A3-AN104	0.060531	0.099209	0.050290	0.007871	0.000210	0.000060	0.053670	0.003281	0.024785	0.014803	0.146438	0.001120	0.003500	0.460968	0.000000	0.011342	0.000000	0.030416	0.030016	0.001490
633	A3-AN104	0.060531	0.099209	0.050290	0.007871	0.000210	0.000060	0.053670	0.003281	0.024785	0.014803	0.146438	0.001120	0.003500	0.460968	0.000000	0.011342	0.000000	0.030416	0.030016	0.001490
634	LA137SRCCC	0.060506	0.099110	0.050305	0.007601	0.000300	0.000200	0.053605	0.006201	0.024803	0.014801	0.146415	0.001100	0.002700	0.460646	0.000000	0.011301	0.000000	0.030403	0.030003	0.000000
635	LA137SRCCC	0.060506	0.099110	0.050305	0.007601	0.000300	0.000200	0.053605	0.006201	0.024803	0.014801	0.146415	0.001100	0.002700	0.460646	0.000000	0.011301	0.000000	0.030403	0.030003	0.000000
636	LAWA137	0.060470	0.099050	0.050275	0.007596	0.000300	0.000200	0.053573	0.006197	0.024787	0.014793	0.146327	0.001099	0.003300	0.460369	0.000000	0.011294	0.000000	0.030385	0.029985	0.000000
637	LAWA137	0.060470	0.099050	0.050275	0.007596																

Table A.2. (cont.) Normalized Compositions (in mass fractions) of 1075 LAW Glasses in the Database of Compiled Literature Data

#	Glass ID	Al ₂ O ₃	B ₂ O ₃	CaO	Cl	Cr ₂ O ₃	F	Fe ₂ O ₃	K ₂ O	Li ₂ O	MgO	Na ₂ O	P ₂ O ₅	SO ₃	SiO ₂	SnO ₂	TiO ₂	V ₂ O ₅	ZnO	ZrO ₂	Others
661	LAWM25R1CCC	0.080112	0.120169	0.020028	0.008011	0.003205	0.003004	0.036852	0.020028	0.030042	0.035049	0.100141	0.005007	0.002600	0.499902	0.000000	0.005007	0.000000	0.020028	0.010014	0.000801
662	LAWM39CCC	0.070070	0.090591	0.050050	0.008008	0.003203	0.003003	0.030030	0.001001	0.025025	0.025025	0.140141	0.005005	0.002500	0.480482	0.000000	0.010010	0.000000	0.030535	0.020020	0.000801
663	LAWM39CCC	0.070070	0.090591	0.050050	0.008008	0.003203	0.003003	0.030030	0.001001	0.025025	0.025025	0.140141	0.005005	0.002500	0.480482	0.000000	0.010010	0.000000	0.030535	0.020020	0.000801
664	LAWM41CCC	0.070021	0.080024	0.070021	0.008002	0.003201	0.003001	0.050015	0.003001	0.010003	0.025008	0.140042	0.005002	0.003400	0.450135	0.000000	0.010003	0.000000	0.046014	0.022307	0.000800
665	LAWM41CCC	0.070021	0.080024	0.070021	0.008002	0.003201	0.003001	0.050015	0.003001	0.010003	0.025008	0.140042	0.005002	0.003400	0.450135	0.000000	0.010003	0.000000	0.046014	0.022307	0.000800
666	LAWM43CCC	0.070021	0.086826	0.050015	0.008002	0.003201	0.003001	0.050015	0.003001	0.025008	0.025008	0.120036	0.005001	0.003900	0.450136	0.000000	0.020006	0.000000	0.046014	0.030009	0.000800
667	LAWM43CCC	0.070021	0.086826	0.050015	0.008002	0.003201	0.003001	0.050015	0.003001	0.025008	0.025008	0.120036	0.005001	0.003900	0.450136	0.000000	0.020006	0.000000	0.046014	0.030009	0.000800
668	LAWE18	0.059258	0.082342	0.014690	0.001999	0.000800	0.000799	0.053562	0.053962	0.000000	0.009393	0.202058	0.001199	0.005100	0.422703	0.000000	0.013690	0.000000	0.034076	0.044169	0.000200
669	LAWE18	0.059258	0.082342	0.014690	0.001999	0.000800	0.000799	0.053562	0.053962	0.000000	0.009393	0.202058	0.001199	0.005100	0.422703	0.000000	0.013690	0.000000	0.034076	0.044169	0.000200
670	LAWE19	0.059264	0.082350	0.024685	0.001999	0.000800	0.000800	0.053568	0.053968	0.000000	0.009394	0.197081	0.001199	0.005000	0.417748	0.000000	0.013692	0.000000	0.034079	0.044173	0.000200
671	LAWE19	0.059264	0.082350	0.024685	0.001999	0.000800	0.000800	0.053568	0.053968	0.000000	0.009394	0.197081	0.001199	0.005000	0.417748	0.000000	0.013692	0.000000	0.034079	0.044173	0.000200
672	LAWE19	0.059264	0.082350	0.024685	0.001999	0.000800	0.000800	0.053568	0.053968	0.000000	0.009394	0.197081	0.001199	0.005000	0.417748	0.000000	0.013692	0.000000	0.034079	0.044173	0.000200
673	LAWE20	0.059364	0.087447	0.014691	0.001999	0.000800	0.000800	0.053668	0.054067	0.000000	0.009394	0.207375	0.001199	0.003700	0.418348	0.000000	0.013692	0.000000	0.034080	0.039176	0.000200
674	LAWE20	0.059364	0.087447	0.014691	0.001999	0.000800	0.000800	0.053668	0.054067	0.000000	0.009394	0.207375	0.001199	0.003700	0.418348	0.000000	0.013692	0.000000	0.034080	0.039176	0.000200
675	LAWE21	0.074363	0.072464	0.014693	0.001999	0.000799	0.000800	0.053673	0.054073	0.000000	0.009395	0.197401	0.001199	0.003600	0.423885	0.000000	0.013693	0.000000	0.034083	0.039180	0.000200
676	LAWE21	0.074363	0.072464	0.014693	0.001999	0.000799	0.000800	0.053673	0.054073	0.000000	0.009395	0.197401	0.001199	0.003600	0.423885	0.000000	0.013693	0.000000	0.034083	0.039180	0.000200
677	LAWE22	0.075854	0.106336	0.009994	0.001999	0.000799	0.000800	0.063062	0.004797	0.000000	0.014391	0.224865	0.001199	0.003700	0.388366	0.000000	0.013692	0.000000	0.044973	0.044973	0.000200
678	LAWE22	0.075854	0.106336	0.009994	0.001999	0.000799	0.000800	0.063062	0.004797	0.000000	0.014391	0.224865	0.001199	0.003700	0.388366	0.000000	0.013692	0.000000	0.044973	0.044973	0.000200
679	LAWE23	0.075839	0.106315	0.000000	0.001998	0.000799	0.000799	0.063049	0.009792	0.000000	0.014389	0.229816	0.001199	0.003900	0.388288	0.000000	0.013689	0.000000	0.044964	0.044964	0.000200
680	LAWE23	0.075839	0.106315	0.000000	0.001998	0.000799	0.000799	0.063049	0.009792	0.000000	0.014389	0.229816	0.001199	0.003900	0.388288	0.000000	0.013689	0.000000	0.044964	0.044964	0.000200
681	LAWE24	0.079952	0.090046	0.029982	0.001999	0.000799	0.000799	0.048771	0.012193	0.000000	0.014391	0.224864	0.001199	0.003700	0.408654	0.000000	0.013692	0.000000	0.044873	0.023886	0.000200
682	LAWE24	0.079952	0.090046	0.029982	0.001999	0.000799	0.000799	0.048771	0.012193	0.000000	0.014391	0.224864	0.001199	0.003700	0.408654	0.000000	0.013692	0.000000	0.044873	0.023886	0.000200
683	LAWE25	0.079952	0.090046	0.039976	0.001999	0.000799	0.000799	0.048771	0.012193	0.000000	0.014391	0.224864	0.001199	0.003700	0.398660	0.000000	0.013692	0.000000	0.044873	0.023886	0.000200
684	LAWE25	0.079952	0.090046	0.039976	0.001999	0.000799	0.000799	0.048771	0.012193	0.000000	0.014391	0.224864	0.001199	0.003700	0.398660	0.000000	0.013692	0.000000	0.044873	0.023886	0.000200
685	LAWE26	0.079952	0.090046	0.029982	0.001999	0.000799	0.000799	0.048771	0.017190	0.000000	0.014391	0.224864	0.001199	0.003700	0.403657	0.000000	0.013692	0.000000	0.044873	0.023886	0.000200
686	LAWE26	0.079952	0.090046	0.029982	0.001999	0.000799	0.000799	0.048771	0.017190	0.000000	0.014391	0.224864	0.001199	0.003700	0.403657	0.000000	0.013692	0.000000	0.044873	0.023886	0.000200
687	ORPLA18	0.097000	0.088000	0.033400	0.006800	0.005000	0.003000	0.005400	0.000000	0.009300	0.240000	0.000000	0.001700	0.395200	0.027600	0.000000	0.000000	0.000000	0.027600	0.060000	0.000000
688	ORPLA19	0.097000	0.088000	0.033400	0.006800	0.005000	0.003000	0.005400	0.000000	0.009300	0.240000	0.000000	0.001700	0.395200	0.048300	0.000000	0.000000	0.000000	0.027600	0.039300	0.000000
689	ORPLA20	0.067013	0.088018	0.033407	0.006801	0.005001	0.003001	0.005401	0.000000	0.009302	0.240048	0.000000	0.001600	0.425185	0.027605	0.000000	0.000000	0.000000	0.027606	0.060012	0.000000
690	ORPLA21	0.069100	0.086400	0.032800	0.007100	0.005000	0.002900	0.005600	0.000000	0.009100	0.250000	0.000000	0.001800	0.417200	0.027100	0.000000	0.000000	0.000000	0.027100	0.058800	0.000000
691	ORPLA22	0.094609	0.088009	0.035504	0.006801	0.005000	0.000000	0.005401	0.000000	0.000000	0.240024	0.000000	0.001700	0.402940	0.030003	0.000000	0.000000	0.000000	0.030003	0.060006	0.000000
692	ORPLA23	0.094609	0.088009	0.035504	0.006801	0.005000	0.000000	0.005401	0.000000	0.000000	0.240024	0.000000	0.001700	0.402940	0.050005	0.000000	0.000000	0.000000	0.030003	0.040004	0.000000
693	ORPLA24	0.093409	0.085509	0.035203	0.007101	0.005000	0.000000	0.005601	0.000000	0.000000	0.250025	0.000000	0.001700	0.397040	0.030003	0.000000	0.000000	0.000000	0.029403	0.060006	0.000000
694	ORPLA25	0.091718	0.083917	0.034507	0.007302	0.004901	0.000000	0.005801	0.000000	0.000000	0.260052	0.000000	0.001800	0.391078	0.030006	0.000000	0.000000	0.000000	0.028906	0.060012	0.000000
695	ORPLD4	0.101934	0.120858	0.080405	0.003304	0.005007	0.001702	0.003004	0.001602	0.000000	0.010013	0.210276	0.002904	0.008500	0.379698	0.000000	0.000000	0.000000	0.010013	0.030139	0.000501
696	ORPLD5	0.101954	0.100452	0.080422	0.003305	0.005008	0.001703	0.003005	0.001602	0.000000	0.010015	0.210318	0.002904	0.008300	0.379774	0.000000	0.000000	0.000000	0.020030	0.030146	0.000501
697	ORPLD6	0.101384	0.098880	0.079244	0.003506	0.005009	0.001803	0.003005	0.001703	0.000000	0.009918	0.220400	0.003005	0.008200	0.373979	0.000000	0.000000	0.000000	0.019736	0.039973	0.000501
698	ORPLD7	0.100943	0.098840	0.079212	0.003505	0.005007	0.001803	0.003004	0.001702	0.000000	0.009914	0.220311	0.003004	0.008700	0.373828	0.010014	0.000000	0.000000	0.010014	0.029742	0.039956
699	ORPLD8	0.100532	0.095220	0.073670	0.003608	0.005012	0.001904	0.002907	0.001804	0.000000	0.009722	0.230532	0.003107	0.008213	0.368249	0.010023	0.000000	0.000000	0.014634	0.029969	0.040293
700	ORPLD9	0.085898	0.095220	0.073670	0.003608	0.005012	0.001904	0.002907	0.001804	0.000000	0.009722	0.230532	0.003107	0.008213	0.368249	0.010023	0.000000	0.000000	0.029969	0.040293	0.000601
701	ORPLF1	0.100993	0.098174	0.100691	0.000101	0.005538	0.000705	0.003121	0.004128	0.037759	0.010170	0.100691	0.000302	0.009200	0.436496	0.008861	0.000000	0.012586	0.030207	0.040277	0.000000
702	ORPLF2	0.099544	0.096726	0.099243	0.000101	0.005536	0.000805	0.003020	0.004529	0.037241	0.009964	0.110717	0.000302	0.011500	0.430185	0.008656	0.000000	0.012481	0.029793	0.039657	0.000000
703	ORPLF3	0.098585	0.095757	0.098181	0.000101	0.005657	0.000808	0.003030	0.00505												

Table A.2. (cont.) Normalized Compositions (in mass fractions) of 1075 LAW Glasses in the Database of Compiled Literature Data

#	Glass ID	Al ₂ O ₃	B ₂ O ₃	CaO	Cl	Cr ₂ O ₃	F	Fe ₂ O ₃	K ₂ O	Li ₂ O	MgO	Na ₂ O	P ₂ O ₅	SO ₃	SiO ₂	SnO ₂	TiO ₂	V ₂ O ₅	ZnO	ZrO ₂	Others
727	ORPLG9CrS4	0.067155	0.084592	0.026802	0.002292	0.009864	0.000897	0.002790	0.057291	0.000000	0.009465	0.209238	0.001395	0.003630	0.406021	0.028197	0.000000	0.000000	0.033777	0.056395	0.000199
728	ORPLG10	0.067214	0.084017	0.026605	0.002400	0.005901	0.000900	0.002801	0.058812	0.000000	0.009402	0.215043	0.001500	0.004000	0.403581	0.028006	0.000000	0.000000	0.033607	0.056011	0.000200
729	ORPLG11	0.067507	0.085709	0.039604	0.002300	0.005901	0.000000	0.0056106	0.000000	0.000000	0.009400	0.205020	0.001400	0.003800	0.411541	0.028603	0.000000	0.000000	0.034303	0.057106	0.000200
730	ORPLG12	0.067520	0.085726	0.027108	0.002301	0.005902	0.000900	0.002901	0.056117	0.000000	0.009603	0.205062	0.020006	0.003500	0.411624	0.028608	0.000000	0.000000	0.034310	0.038612	0.000200
731	Y10-G-146C	0.066567	0.087488	0.033233	0.006707	0.005005	0.000000	0.001902	0.050305	0.000000	0.009209	0.240242	0.000000	0.006100	0.423726	0.027428	0.000000	0.000000	0.027428	0.059660	0.000000
732	Z10-G-60C	0.100839	0.098440	0.078852	0.003498	0.004997	0.001799	0.002798	0.001699	0.000000	0.009994	0.219866	0.002998	0.012600	0.372174	0.000000	0.000000	0.019588	0.029582	0.039776	0.000500
733	10A-G-53C	0.100849	0.098450	0.078860	0.003498	0.004997	0.001799	0.002799	0.001699	0.000000	0.009995	0.219889	0.002998	0.012500	0.372212	0.000000	0.000000	0.019590	0.029585	0.039780	0.000500
734	Z10-G-122B	0.087253	0.096358	0.098660	0.000100	0.005703	0.0002301	0.005003	0.004127	0.000000	0.009906	0.120073	0.000400	0.007600	0.427559	0.000000	0.000000	0.025315	0.029518	0.039324	0.000000
735	Z10-G-153B	0.086623	0.095736	0.097939	0.000100	0.005608	0.000801	0.002303	0.005007	0.043862	0.009914	0.120171	0.000401	0.013500	0.424502	0.000000	0.000000	0.025136	0.029342	0.039055	0.000000
736	10A-G-43B	0.067593	0.085092	0.026997	0.002300	0.005899	0.000900	0.002000	0.057594	0.000000	0.009599	0.209979	0.001400	0.002100	0.409159	0.028397	0.000000	0.000000	0.033997	0.056794	0.000200
737	ORPLA26	0.105849	0.127881	0.064792	0.006409	0.005207	0.000913	0.005107	0.000000	0.000000	0.009013	0.230325	0.000000	0.008300	0.348492	0.010014	0.000000	0.009714	0.029942	0.029942	0.000000
738	ORPLA27	0.103494	0.122229	0.061916	0.006412	0.005009	0.000000	0.008616	0.005110	0.000000	0.040075	0.230432	0.000000	0.007538	0.332925	0.009618	0.000000	0.009318	0.028654	0.028654	0.000000
739	ORPLA28	0.101210	0.116642	0.059123	0.006413	0.004810	0.000000	0.008217	0.005111	0.000000	0.070146	0.230479	0.000000	0.007538	0.317760	0.009119	0.000000	0.008918	0.027257	0.027257	0.000000
740	ORPLA29	0.098915	0.111042	0.056323	0.006414	0.004510	0.000000	0.007817	0.005111	0.000000	0.100218	0.230502	0.000000	0.007538	0.302559	0.008719	0.000000	0.008418	0.025957	0.025957	0.000000
741	ORPLA30	0.095799	0.117544	0.054413	0.006413	0.005211	0.000000	0.009019	0.005111	0.000000	0.040083	0.230479	0.000000	0.007538	0.348725	0.010021	0.000000	0.009720	0.029962	0.029962	0.000000
742	ORPLA31	0.086680	0.107022	0.043991	0.006413	0.005211	0.000000	0.009019	0.005111	0.000000	0.070146	0.230479	0.000000	0.007538	0.348725	0.010021	0.000000	0.009720	0.029962	0.029962	0.000000
743	ORPLA32	0.077469	0.096611	0.033473	0.006414	0.005211	0.000000	0.009020	0.005111	0.000000	0.100218	0.230502	0.000000	0.007538	0.348760	0.010022	0.000000	0.009721	0.029965	0.029965	0.000000
744	ORPLA33	0.061731	0.089690	0.032068	0.006414	0.005011	0.000000	0.002605	0.005111	0.000000	0.010121	0.231890	0.000000	0.007601	0.425800	0.024752	0.000000	0.009420	0.028761	0.059025	0.000000
745	ORPLA33-1	0.067427	0.089167	0.031860	0.006412	0.005009	0.000000	0.002605	0.005110	0.000000	0.010019	0.230432	0.000000	0.007538	0.423094	0.024646	0.000000	0.009317	0.028654	0.058710	0.000000
746	ORPLA34	0.072746	0.100903	0.042185	0.006413	0.005010	0.000000	0.004709	0.005110	0.000000	0.020141	0.232168	0.000000	0.007601	0.395998	0.019740	0.000000	0.009419	0.028858	0.048999	0.000000
747	ORPLA35	0.083852	0.112103	0.052395	0.006512	0.005009	0.000000	0.006712	0.005109	0.000000	0.030355	0.232321	0.000000	0.007601	0.366064	0.014727	0.000000	0.009417	0.028852	0.038971	0.000000
748	ORPLA36	0.063648	0.088005	0.031473	0.006716	0.004911	0.000000	0.002606	0.005312	0.000000	0.009923	0.242064	0.000000	0.007788	0.417874	0.024257	0.000000	0.009222	0.028266	0.057935	0.000000
749	ORPLA37	0.063648	0.082793	0.031473	0.006716	0.004911	0.000000	0.002606	0.005312	0.000000	0.019846	0.242064	0.000000	0.007788	0.413163	0.024257	0.000000	0.009222	0.028266	0.057935	0.000000
750	ORPLA38	0.063642	0.082784	0.031470	0.006715	0.004911	0.000000	0.002606	0.005312	0.000000	0.009922	0.242039	0.000000	0.007788	0.417932	0.026860	0.000000	0.009221	0.028263	0.060535	0.000000
751	ORPLA38-1	0.069555	0.082283	0.031270	0.006715	0.004911	0.000000	0.002606	0.005312	0.000000	0.009822	0.240536	0.000000	0.007788	0.415226	0.026659	0.000000	0.009120	0.028063	0.060134	0.000000
752	ORPLG13	0.065407	0.082808	0.026203	0.002200	0.005701	0.000900	0.002800	0.054705	0.000000	0.040404	0.200020	0.001400	0.003700	0.397640	0.027603	0.000000	0.000000	0.033103	0.055206	0.000200
753	ORPLG14	0.065307	0.082008	0.026003	0.002300	0.005701	0.000900	0.002700	0.056106	0.000000	0.040004	0.205021	0.001400	0.003700	0.393839	0.027303	0.000000	0.000000	0.032803	0.054705	0.000200
754	ORPLG15	0.065107	0.081208	0.025703	0.002300	0.005701	0.000900	0.002700	0.057506	0.000000	0.039604	0.210021	0.001400	0.003900	0.390039	0.027103	0.000000	0.000000	0.032503	0.054105	0.000200
755	ORPLG16	0.055217	0.082625	0.027308	0.002301	0.005902	0.000900	0.002901	0.056417	0.000000	0.020506	0.206162	0.001400	0.003600	0.413925	0.028709	0.000000	0.000000	0.034510	0.057417	0.000200
756	ORPLG17	0.055222	0.082633	0.027311	0.002301	0.005902	0.000900	0.002901	0.056423	0.000000	0.020508	0.206183	0.001401	0.003500	0.413966	0.032313	0.000000	0.000000	0.027311	0.061025	0.000200
757	ORPLG18	0.055222	0.080432	0.027311	0.002301	0.005902	0.000900	0.002901	0.056423	0.000000	0.019708	0.206183	0.001401	0.003600	0.422570	0.027311	0.000000	0.000000	0.027311	0.060324	0.000200
758	ORPLG19	0.055139	0.079656	0.027019	0.002301	0.005904	0.000901	0.002802	0.057841	0.000000	0.019514	0.211348	0.001401	0.003600	0.418594	0.027019	0.000000	0.000000	0.027019	0.059742	0.000200
759	ORPLG20	0.060412	0.080016	0.027106	0.002301	0.005901	0.000900	0.002901	0.056111	0.000000	0.009602	0.205041	0.001400	0.003700	0.420184	0.037108	0.000000	0.000000	0.027105	0.060012	0.000200
760	ORPLG21	0.060424	0.080032	0.027111	0.002301	0.005902	0.000900	0.002901	0.056123	0.000000	0.009604	0.205082	0.001401	0.003500	0.430273	0.027111	0.000000	0.000000	0.027111	0.060024	0.000200
761	ORPLG22	0.060430	0.080040	0.027114	0.002301	0.005903	0.000900	0.002902	0.056128	0.000000	0.004602	0.205103	0.001401	0.003400	0.420311	0.034617	0.000000	0.000000	0.027114	0.067534	0.000200
762	ORPLG23	0.060430	0.080040	0.027114	0.002301	0.005903	0.000900	0.002902	0.056128	0.000000	0.004602	0.205103	0.001401	0.003400	0.425313	0.032116	0.000000	0.000000	0.027114	0.060533	0.000200
763	ORPLG24	0.060324	0.079232	0.026911	0.002301	0.005902	0.000900	0.002801	0.057523	0.000000	0.009404	0.210084	0.001401	0.003600	0.416167	0.036915	0.000000	0.000000	0.026911	0.059424	0.000200
764	ORPLG25	0.060330	0.079240	0.026913	0.002301	0.005903	0.000900	0.002801	0.057529	0.000000	0.009405	0.210105	0.001401	0.003500	0.426214	0.026914	0.000000	0.000000	0.026914	0.059430	0.000200
765	ORPLG26	0.060336	0.079248	0.026916	0.002301	0.005904	0.000900	0.002802	0.057535	0.000000	0.004403	0.210126	0.001401	0.003400	0.416251	0.034421	0.000000	0.000000	0.026916	0.066940	0.000200
766	ORPLG27	0.060330	0.079240	0.026914	0.002301	0.005903	0.000901	0.002801	0.057529	0.000000	0.004402	0.210105	0.001401	0.003500	0.421211	0.031916	0.000000	0.000000	0.026914	0.064432	0.000200
767	J10-G-24B	0.069528	0.082233	0.031313	0.006603	0.004902	0.000000	0.002601	0.005202	0.000000	0.009804	0.240097	0.000000	0.007600	0.415667	0.026711	0.000000	0.009204	0.028211	0.060324	0.000000
768	J10-G-135A	0.060230	0.079140	0.026814	0.002301	0.005903	0.000900	0.002801	0.057429	0.000000	0.004402	0.210106	0.001401	0.004700	0.420711	0.031816	0.000000	0.000000	0.026814	0.064332	0.000200
769	LORPM1	0.068894	0.082904	0.012776	0.008025																

Table A.2. (cont.) Normalized Compositions (in mass fractions) of 1075 LAW Glasses in the Database of Compiled Literature Data

#	Glass ID	Al ₂ O ₃	B ₂ O ₃	CaO	Cl	Cr ₂ O ₃	F	Fe ₂ O ₃	K ₂ O	Li ₂ O	MgO	Na ₂ O	P ₂ O ₅	SO ₃	SiO ₂	SnO ₂	TiO ₂	V ₂ O ₅	ZnO	ZrO ₂	Others
793	LORPM25	0.138472	0.127545	0.000000	0.000980	0.000394	0.000367	0.009968	0.026255	0.023665	0.043321	0.182703	0.000611	0.001200	0.371386	0.003049	0.000000	0.000000	0.009998	0.059988	0.000098
794	LORPM26	0.100997	0.060303	0.100887	0.008043	0.003230	0.003009	0.072323	0.053328	0.000000	0.000000	0.109741	0.005015	0.004100	0.351766	0.050252	0.025950	0.000000	0.050252	0.000000	0.000000
795	LORPM27	0.129382	0.060327	0.011905	0.000205	0.000082	0.000077	0.080436	0.054043	0.050273	0.046361	0.087424	0.000128	0.004600	0.389634	0.000000	0.014720	0.000000	0.010055	0.060327	0.000021
796	LORPM28	0.034972	0.137190	0.000000	0.007216	0.002898	0.002700	0.002998	0.001099	0.049960	0.000000	0.142995	0.004500	0.001800	0.451079	0.049960	0.000000	0.039968	0.009992	0.059952	0.000721
797	LORPM28R1	0.034972	0.137190	0.000000	0.007216	0.002898	0.002700	0.002998	0.001099	0.049960	0.000000	0.142995	0.004500	0.001800	0.451079	0.049960	0.000000	0.039968	0.009992	0.059952	0.000721
798	LORPM28R1	0.034972	0.137190	0.000000	0.007216	0.002898	0.002700	0.002998	0.001099	0.049960	0.000000	0.142995	0.004500	0.001800	0.451079	0.049960	0.000000	0.039968	0.009992	0.059952	0.000721
799	LORPM29	0.094335	0.099661	0.000000	0.008045	0.003231	0.003010	0.003015	0.059085	0.050242	0.046645	0.088979	0.005017	0.005200	0.351697	0.050242	0.030146	0.000000	0.046223	0.054423	0.000804
800	LORPM30	0.034989	0.059982	0.122363	0.001676	0.000673	0.007997	0.058782	0.043577	0.029991	0.043577	0.049985	0.001045	0.001300	0.349895	0.049985	0.005019	0.039988	0.009997	0.059982	0.000168
801	LORPM31	0.109833	0.101750	0.000000	0.008035	0.003227	0.003006	0.064034	0.001105	0.043720	0.006346	0.094952	0.005011	0.005900	0.351450	0.050207	0.000000	0.040166	0.050207	0.060248	0.000803
802	LORPM32	0.055767	0.116030	0.024510	0.000985	0.000396	0.000369	0.043382	0.047317	0.035743	0.035042	0.100121	0.000614	0.004800	0.430970	0.010012	0.024029	0.010843	0.038947	0.020024	0.000099
803	LORPM33	0.117847	0.115767	0.024490	0.008005	0.003215	0.023019	0.012645	0.040016	0.031713	0.100040	0.004992	0.002000	0.405483	0.010004	0.006003	0.020938	0.020008	0.050020	0.000800	0.000800
804	LORPM34	0.071780	0.121926	0.024497	0.008008	0.003216	0.002996	0.018413	0.047293	0.040028	0.035025	0.100851	0.004994	0.003500	0.384270	0.018993	0.024017	0.021875	0.020644	0.046873	0.000801
805	LORPM35	0.103713	0.075448	0.049242	0.000196	0.000079	0.000073	0.018397	0.032385	0.028885	0.031275	0.172972	0.000122	0.003000	0.383938	0.009999	0.013338	0.008929	0.017997	0.049992	0.000020
806	LORPM36	0.066557	0.121872	0.024486	0.006976	0.002802	0.002610	0.018405	0.025087	0.040010	0.035009	0.128203	0.004350	0.002500	0.397514	0.024856	0.022046	0.008002	0.018005	0.050013	0.000697
807	LORPM37	0.055706	0.116252	0.024482	0.002145	0.000861	0.000802	0.021612	0.047265	0.036594	0.035004	0.121982	0.001337	0.002300	0.394750	0.040004	0.024002	0.008001	0.042004	0.024683	0.000214
808	LORPM38	0.055835	0.075642	0.024539	0.008021	0.003222	0.003001	0.064756	0.047374	0.010024	0.035085	0.134233	0.005002	0.003600	0.397548	0.010024	0.024058	0.008019	0.042101	0.047114	0.000802
809	LORPM39	0.055694	0.121828	0.024478	0.000200	0.000080	0.000075	0.064593	0.012639	0.039996	0.009999	0.173823	0.000125	0.002500	0.383961	0.009999	0.005999	0.031997	0.017998	0.043996	0.000020
810	LORPM40	0.117812	0.075468	0.024482	0.000200	0.000080	0.000075	0.057106	0.047265	0.040004	0.035003	0.100010	0.000125	0.002300	0.384038	0.010001	0.006001	0.008001	0.042004	0.050005	0.000020
811	ORPLA39	0.066554	0.082266	0.033227	0.006705	0.000200	0.000000	0.026922	0.050304	0.000000	0.009308	0.240193	0.000000	0.006200	0.418637	0.027422	0.000000	0.000000	0.022418	0.054644	0.000000
812	ORPLA40	0.066547	0.082258	0.033223	0.006705	0.000200	0.000000	0.001901	0.005304	0.000000	0.009307	0.240169	0.000000	0.006300	0.418595	0.027419	0.025018	0.000000	0.022416	0.054638	0.000000
813	ORPLA41	0.066574	0.082291	0.033237	0.006707	0.000200	0.000000	0.001902	0.005306	0.000000	0.009338	0.240266	0.000000	0.005900	0.418763	0.027430	0.000000	0.000000	0.022425	0.054661	0.000000
814	ORPLA42	0.091537	0.082233	0.033213	0.006703	0.000200	0.000000	0.001901	0.005302	0.000000	0.009304	0.240097	0.000000	0.006600	0.418468	0.027411	0.000000	0.000000	0.022409	0.054622	0.000000
815	ORPLA43	0.066233	0.080293	0.020023	0.006708	0.000200	0.000000	0.001902	0.005306	0.000000	0.009311	0.240278	0.000000	0.005852	0.390751	0.015017	0.030035	0.000000	0.028032	0.059669	0.000000
816	ORPLA43R1	0.06597	0.080273	0.020018	0.006706	0.000200	0.000000	0.001902	0.005305	0.000000	0.009308	0.240217	0.000000	0.006100	0.390654	0.015014	0.030027	0.000000	0.028025	0.059654	0.000000
817	ORPLA43R1	0.06597	0.080273	0.020018	0.006706	0.000200	0.000000	0.001902	0.005305	0.000000	0.009308	0.240217	0.000000	0.006100	0.390654	0.015014	0.030027	0.000000	0.028025	0.059654	0.000000
818	ORPLA44	0.106629	0.080297	0.020024	0.006708	0.000200	0.000000	0.001902	0.005307	0.000000	0.009311	0.240290	0.000000	0.005800	0.390772	0.015018	0.030036	0.014017	0.014017	0.059672	0.000000
819	ORPLA45	0.086587	0.080281	0.020020	0.006707	0.000200	0.000000	0.001902	0.005305	0.000000	0.009310	0.240242	0.000000	0.006000	0.390693	0.015015	0.050050	0.000000	0.028028	0.059660	0.000000
820	ORPLA46	0.106623	0.075287	0.020023	0.006708	0.000200	0.000000	0.001902	0.005306	0.000000	0.009311	0.240278	0.000000	0.005852	0.390751	0.015018	0.050058	0.000000	0.028032	0.059669	0.000000
821	ORPLA46	0.106564	0.075246	0.020012	0.006704	0.000200	0.000000	0.001901	0.005303	0.000000	0.009306	0.240145	0.000000	0.006400	0.390536	0.015000	0.050030	0.000000	0.028017	0.059636	0.000000
822	ORPLA47	0.106629	0.080297	0.020024	0.006708	0.000200	0.000000	0.001902	0.005307	0.000000	0.009311	0.240290	0.000000	0.005800	0.390772	0.015018	0.030036	0.015018	0.028034	0.059672	0.000000
823	ORPLA48	0.106629	0.080297	0.020024	0.006708	0.000200	0.000000	0.001902	0.005307	0.000000	0.009311	0.240290	0.000000	0.005800	0.390772	0.015018	0.030036	0.015018	0.028034	0.059672	0.000000
824	ORPLA49	0.096587	0.080273	0.020018	0.006706	0.000200	0.000000	0.001902	0.005305	0.000000	0.009308	0.240218	0.000000	0.006100	0.390654	0.015014	0.030027	0.000000	0.028025	0.059654	0.000000
825	ORPLA50	0.096578	0.080265	0.020016	0.006705	0.000200	0.000000	0.001902	0.005304	0.000000	0.009308	0.240193	0.000000	0.006200	0.389614	0.015000	0.040032	0.030024	0.014011	0.059648	0.000000
826	ORPLA51	0.101623	0.080297	0.010012	0.006708	0.000200	0.000000	0.001902	0.005307	0.000000	0.019323	0.240290	0.000000	0.005800	0.390772	0.010012	0.040048	0.000000	0.028034	0.059672	0.000000
827	ORPLA52	0.101582	0.080265	0.010008	0.006705	0.000200	0.000000	0.001902	0.005304	0.000000	0.019316	0.240193	0.000000	0.006200	0.390614	0.010008	0.020016	0.020016	0.028023	0.059648	0.000000
828	ORPLA53	0.101613	0.080289	0.010011	0.006708	0.000200	0.000000	0.001902	0.005306	0.000000	0.019321	0.240266	0.000000	0.005900	0.390732	0.010011	0.030033	0.010011	0.028031	0.059666	0.000000
829	ORPLA54	0.101613	0.080289	0.010011	0.006707	0.000200	0.000000	0.001902	0.005306	0.000000	0.019321	0.240266	0.000000	0.005900	0.390732	0.010011	0.030033	0.024027	0.014016	0.059666	0.000000
830	ORPLA55	0.106682	0.080337	0.000000	0.006712	0.000200	0.000000	0.001803	0.005309	0.000000	0.002003	0.240411	0.000000	0.005300	0.411003	0.010017	0.030051	0.000000	0.040069	0.060103	0.000000
831	ORPLA56	0.106629	0.080297	0.020024	0.006708	0.000200	0.000000	0.001802	0.005306	0.000000	0.022027	0.240290	0.000000	0.005800	0.410796	0.010000	0.000000	0.000000	0.040048	0.060073	0.000000
832	ORPLA57	0.106586	0.080565	0.015012	0.006706	0.000200	0.000000	0.000501	0.005304	0.000000	0.000000	0.240193	0.000000	0.006200	0.408629	0.000000	0.030024	0.000000	0.040032	0.060048	0.000000
833	ORPLA58	0.106623	0.087601	0.000000	0.006708	0.000200	0.000000	0.002503	0.005306	0.000000	0.015518	0.240277	0.000000	0.005852	0.409273	0.000000	0.030035	0.000000	0.030035	0.060069	0.000000
834	ORPLA20R1	0.067013	0.088018	0.033407	0.006801	0.005001	0.000000	0.003001	0.005401	0.000000	0.009302	0.240048	0.000000	0.001600	0.425185	0.027605	0.000000	0.000000	0.027605	0.060012	0.000000
835	ORLEC1	0.100000	0.100000	0.019500	0.002000	0.005800	0.000800	0.010000													

Table A.2. (cont.) Normalized Compositions (in mass fractions) of 1075 LAW Glasses in the Database of Compiled Literature Data

#	Glass ID	Al ₂ O ₃	B ₂ O ₃	CaO	Cl	Cr ₂ O ₃	F	Fe ₂ O ₃	K ₂ O	Li ₂ O	MgO	Na ₂ O	P ₂ O ₅	SO ₃	SiO ₂	SnO ₂	TiO ₂	V ₂ O ₅	ZnO	ZrO ₂	Others
859	ORLEC25	0.100080	0.100080	0.019516	0.002002	0.003403	0.000801	0.003403	0.056445	0.000000	0.010008	0.206266	0.001201	0.005100	0.370898	0.023319	0.003403	0.003503	0.030024	0.060348	0.000200
860	ORLEC25	0.100080	0.100080	0.019516	0.002002	0.003403	0.000801	0.003403	0.056445	0.000000	0.010008	0.206266	0.001201	0.005100	0.370898	0.023319	0.003403	0.003503	0.030024	0.060348	0.000200
861	ORLEC25	0.100080	0.100080	0.019516	0.002002	0.003403	0.000801	0.003403	0.056445	0.000000	0.010008	0.206266	0.001201	0.005100	0.370898	0.023319	0.003403	0.003503	0.030024	0.060348	0.000200
862	ORLEC26	0.100020	0.100020	0.019504	0.002001	0.004401	0.000800	0.006001	0.005001	0.000000	0.010002	0.240048	0.001200	0.003800	0.387378	0.023305	0.006001	0.000000	0.030006	0.060312	0.000200
863	ORLEC27	0.100010	0.100010	0.019502	0.002000	0.004400	0.000800	0.006001	0.005606	0.000000	0.010001	0.206121	0.001200	0.003900	0.369837	0.023302	0.006001	0.000000	0.030003	0.060306	0.000200
864	ORLEC28	0.100030	0.100030	0.019506	0.002001	0.004401	0.000800	0.006002	0.003610	0.000000	0.010003	0.221167	0.001200	0.003700	0.377714	0.023307	0.006002	0.000000	0.030009	0.060318	0.000200
865	OWV-G-144E	0.099923	0.099923	0.019485	0.001998	0.005796	0.000799	0.009992	0.056357	0.000000	0.009992	0.205941	0.001199	0.001800	0.363020	0.023282	0.009992	0.000000	0.029977	0.060253	0.000271
866	OWV-G-144E	0.099923	0.099923	0.019485	0.001998	0.005796	0.000799	0.009992	0.056357	0.000000	0.009992	0.205941	0.001199	0.001800	0.363020	0.023282	0.009992	0.000000	0.029977	0.060253	0.000271
867	OWV-G-109B	0.100054	0.100054	0.019511	0.002001	0.004402	0.000801	0.006003	0.005003	0.000000	0.010005	0.240130	0.001201	0.003500	0.387510	0.023313	0.006003	0.000000	0.030016	0.060333	0.000160
868	OWV-G-109B	0.100054	0.100054	0.019511	0.002001	0.004402	0.000801	0.006003	0.005003	0.000000	0.010005	0.240130	0.001201	0.003500	0.387510	0.023313	0.006003	0.000000	0.030016	0.060333	0.000160
869	PWV-G-43E	0.100023	0.100023	0.019505	0.002001	0.004401	0.000800	0.006001	0.056413	0.000000	0.010002	0.206148	0.001200	0.003800	0.369785	0.023305	0.006001	0.000000	0.030007	0.060314	0.000271
870	PWV-G-43E	0.100023	0.100023	0.019505	0.002001	0.004401	0.000800	0.006001	0.056413	0.000000	0.010002	0.206148	0.001200	0.003800	0.369785	0.023305	0.006001	0.000000	0.030007	0.060314	0.000271
871	PWV-G-93A	0.100063	0.100063	0.019512	0.002001	0.004403	0.000801	0.006004	0.033621	0.000000	0.010006	0.221240	0.001201	0.003400	0.377738	0.023315	0.006004	0.000000	0.030019	0.060338	0.000271
872	PWV-G-93A	0.100063	0.100063	0.019512	0.002001	0.004403	0.000801	0.006004	0.033621	0.000000	0.010006	0.221240	0.001201	0.003400	0.377738	0.023315	0.006004	0.000000	0.030019	0.060338	0.000271
873	ORLEC29	0.100217	0.110239	0.025054	0.002004	0.000802	0.000802	0.002004	0.005011	0.000000	0.010022	0.230500	0.001203	0.007850	0.410089	0.000000	0.000000	0.013529	0.030065	0.050409	0.000200
874	ORLEC30	0.100258	0.110284	0.036494	0.002005	0.000802	0.000802	0.002005	0.005013	0.000000	0.010026	0.220568	0.001203	0.008448	0.415570	0.000000	0.000000	0.015841	0.030077	0.040404	0.000200
875	ORLEC31	0.090962	0.110318	0.045932	0.002006	0.000802	0.000802	0.002006	0.005014	0.000000	0.010029	0.210606	0.001204	0.008846	0.428333	0.000000	0.000000	0.017751	0.030087	0.035101	0.000201
876	ORLEC32	0.081456	0.110347	0.055073	0.002006	0.000802	0.000803	0.002006	0.005016	0.000000	0.010032	0.200632	0.001204	0.009281	0.436273	0.000000	0.000000	0.019662	0.030095	0.035111	0.000201
877	ORLEC33	0.092500	0.110239	0.025054	0.002004	0.000802	0.000802	0.002004	0.005011	0.000000	0.010022	0.230500	0.001203	0.007850	0.410289	0.000000	0.000000	0.021046	0.030065	0.050409	0.000200
878	ORLEC34	0.083807	0.110273	0.036490	0.002005	0.000802	0.000802	0.002005	0.005013	0.000000	0.010025	0.220545	0.001203	0.008448	0.425151	0.000000	0.000000	0.022756	0.030074	0.040400	0.000201
879	ORLEC35	0.076292	0.110423	0.045976	0.002008	0.000803	0.000803	0.002008	0.005019	0.000000	0.010038	0.210807	0.001205	0.007900	0.437476	0.000000	0.000000	0.023791	0.030115	0.035135	0.000201
880	ORLEC36	0.076339	0.110490	0.055145	0.002009	0.000803	0.000804	0.002009	0.005022	0.000000	0.010044	0.200891	0.001205	0.008100	0.437139	0.000000	0.000000	0.024509	0.030134	0.035156	0.000201
881	ORLEC37	0.076208	0.110300	0.045925	0.002005	0.000802	0.000802	0.002005	0.005014	0.007922	0.010027	0.210574	0.001203	0.009000	0.429069	0.000000	0.000000	0.023765	0.030082	0.035096	0.000201
882	ORLEC38	0.076200	0.110290	0.055045	0.002005	0.000802	0.000802	0.002005	0.005013	0.012232	0.010026	0.200527	0.001203	0.009000	0.424114	0.000000	0.000000	0.024464	0.030079	0.035092	0.000201
883	ORLEC39	0.076416	0.110602	0.062540	0.002011	0.000804	0.000804	0.002011	0.005027	0.003720	0.010055	0.191040	0.001207	0.007700	0.435570	0.000000	0.000000	0.024936	0.030164	0.035192	0.000201
884	ORLEC40	0.076277	0.110402	0.069653	0.002007	0.000803	0.000803	0.002007	0.005018	0.014553	0.010037	0.180657	0.001204	0.010100	0.425949	0.000000	0.000000	0.025091	0.030110	0.035128	0.000201
885	ORLEC41	0.076270	0.110391	0.076069	0.002007	0.000803	0.000803	0.002007	0.005018	0.021476	0.010035	0.170604	0.001204	0.010700	0.422093	0.000000	0.000000	0.025089	0.030106	0.035124	0.000201
886	ORLEC42	0.076278	0.110402	0.081697	0.002007	0.000803	0.000803	0.002007	0.005018	0.024589	0.010037	0.160585	0.001204	0.011100	0.422940	0.000000	0.000000	0.025091	0.030110	0.035128	0.000201
887	QWV-G-107B	0.100023	0.100023	0.019505	0.002001	0.003401	0.000800	0.003301	0.005001	0.000000	0.010002	0.240055	0.001200	0.005900	0.388089	0.023305	0.003301	0.003501	0.030007	0.060314	0.000271
888	PWV-G-130C	0.100155	0.100154	0.025039	0.002003	0.001502	0.000801	0.002003	0.005008	0.000000	0.010016	0.230355	0.001202	0.008400	0.408830	0.013321	0.000000	0.010516	0.030046	0.050378	0.000271
889	PWV-G-130C	0.100155	0.100154	0.025039	0.002003	0.001502	0.000801	0.002003	0.005008	0.000000	0.010016	0.230355	0.001202	0.008400	0.408830	0.013321	0.000000	0.010516	0.030046	0.050378	0.000271
890	QWV-G-29C	0.081111	0.100013	0.054907	0.002000	0.000800	0.000800	0.002000	0.005001	0.000000	0.010001	0.200022	0.001200	0.012300	0.449659	0.000000	0.000000	0.014902	0.030004	0.035005	0.000271
891	QWV-G-75B	0.078074	0.100094	0.075871	0.002002	0.000801	0.000801	0.002002	0.005005	0.021420	0.010009	0.170160	0.001201	0.013200	0.436111	0.000000	0.000000	0.017917	0.030028	0.035033	0.000271
892	ORLEC43	0.076192	0.110278	0.045916	0.002005	0.000802	0.000802	0.002005	0.005013	0.004511	0.010025	0.210531	0.001203	0.009200	0.432391	0.000000	0.000000	0.023760	0.030076	0.035089	0.000201
893	ORLEC44	0.076254	0.110368	0.055083	0.002007	0.000803	0.000803	0.002007	0.005017	0.009933	0.010033	0.200668	0.001204	0.009200	0.426721	0.000000	0.000000	0.024481	0.030100	0.035117	0.000201
894	ORLEC45	0.076139	0.110201	0.062313	0.002004	0.000801	0.000801	0.002004	0.005009	0.014326	0.010018	0.190347	0.001202	0.011300	0.423371	0.000000	0.000000	0.024845	0.030055	0.035064	0.000200
895	ORLEC46	0.076223	0.110323	0.069604	0.002006	0.000802	0.000802	0.002006	0.005015	0.018655	0.010029	0.180529	0.001204	0.010800	0.421536	0.000000	0.000000	0.025074	0.030088	0.035103	0.000201
896	ORLEC47	0.076116	0.110167	0.075915	0.002003	0.000801	0.000801	0.002003	0.005008	0.022534	0.010015	0.170259	0.001202	0.012600	0.420239	0.000000	0.000000	0.025038	0.030046	0.035053	0.000200
897	ORLEC48R	0.076185	0.110268	0.081598	0.002005	0.000802	0.000802	0.002005	0.005012	0.025863	0.010024	0.160390	0.001203	0.012300	0.421123	0.000000	0.000000	0.025061	0.030073	0.035085	0.000201
898	ORLEC49	0.100020	0.110022	0.019504	0.002001	0.004401	0.000800	0.006001	0.005001	0.000000	0.010002	0.240048	0.001200	0.003800	0.390679	0.010002	0.006001	0.000000	0.030006	0.060312	0.000200
899	ORLEC49R	0.100020	0.110022	0.019504	0.002001	0.004401	0.000800	0.006001	0.005001	0.000000	0.010002	0.240048	0.001200	0.003800	0.390679	0.010002	0.006001	0.000000	0.030006	0.060312	0.000200
900	ORLEC50	0.100060	0.110066	0.019512	0.002001	0.003402	0.000801	0.003402	0.005003	0.000000	0.010006	0.240145	0.001201	0.005300	0.386133	0.010006	0.003402	0.009006	0.030018	0.060336	0.000200
901	ORLEC51	0.100101	0.110111	0.019520	0.002002	0.002502															

Table A.2. (cont.) Normalized Compositions (in mass fractions) of 1075 LAW Glasses in the Database of Compiled Literature Data

#	Glass ID	Al ₂ O ₃	B ₂ O ₃	CaO	Cl	Cr ₂ O ₃	F	Fe ₂ O ₃	K ₂ O	Li ₂ O	MgO	Na ₂ O	P ₂ O ₅	SO ₃	SiO ₂	SnO ₂	TiO ₂	V ₂ O ₅	ZnO	ZrO ₂	Others
925	WDFL2H	0.059999	0.098398	0.051399	0.003500	0.000400	0.000600	0.054099	0.004200	0.021099	0.014600	0.165497	0.002000	0.005300	0.441191	0.000000	0.013800	0.000000	0.034399	0.029499	0.000020
926	WDFL2+15%	0.060393	0.097488	0.050894	0.003900	0.000400	0.000700	0.053594	0.004399	0.020898	0.014398	0.171079	0.002300	0.005600	0.437047	0.000000	0.013598	0.000000	0.034096	0.029196	0.000020
927	WDFL2-15%	0.061730	0.102750	0.053626	0.003101	0.000300	0.000600	0.056527	0.003402	0.022011	0.015207	0.133264	0.001801	0.003800	0.460722	0.000000	0.014407	0.000000	0.035917	0.030815	0.000020
928	New-IL-456	0.062504	0.080006	0.090006	0.001200	0.000800	0.001800	0.012501	0.002000	0.035003	0.025002	0.150011	0.003800	0.003830	0.431530	0.035003	0.000000	0.030002	0.020001	0.015001	0.000000
929	New-IL-456CCC	0.062504	0.080006	0.090006	0.001200	0.000800	0.001800	0.012501	0.002000	0.035003	0.025002	0.150011	0.003800	0.003830	0.431530	0.035003	0.000000	0.030002	0.020001	0.015001	0.000000
930	New-IL-1721	0.062615	0.117715	0.027550	0.003106	0.002104	0.004709	0.012523	0.010018	0.035064	0.005009	0.164802	0.010119	0.011190	0.433293	0.035064	0.000000	0.030055	0.020037	0.015027	0.000000
931	New-IL-1721CCC	0.062615	0.117715	0.027550	0.003106	0.002104	0.004709	0.012523	0.010018	0.035064	0.005009	0.164802	0.010119	0.011190	0.433293	0.035064	0.000000	0.030055	0.020037	0.015027	0.000000
932	New-IL-1721(PNNL)	0.062615	0.117715	0.027550	0.003106	0.002104	0.004709	0.012523	0.010018	0.035064	0.005009	0.164802	0.010119	0.011190	0.433293	0.035064	0.000000	0.030055	0.020037	0.015027	0.000000
933	New-IL-5253	0.062714	0.117902	0.027594	0.001204	0.000803	0.001806	0.012543	0.002007	0.035120	0.025085	0.150514	0.003813	0.009520	0.398861	0.035120	0.000000	0.030103	0.040137	0.045154	0.000000
934	New-IL-5253CCC	0.062714	0.117902	0.027594	0.001204	0.000803	0.001806	0.012543	0.002007	0.035120	0.025085	0.150514	0.003813	0.009520	0.398861	0.035120	0.000000	0.030103	0.040137	0.045154	0.000000
935	New-IL-5255	0.062578	0.117646	0.027534	0.001202	0.000801	0.001802	0.012516	0.002002	0.035044	0.025031	0.180224	0.003805	0.011670	0.367958	0.035044	0.000000	0.030037	0.040050	0.045056	0.000000
936	New-IL-5255CCC	0.062578	0.117646	0.027534	0.001202	0.000801	0.001802	0.012516	0.002002	0.035044	0.025031	0.180224	0.003805	0.011670	0.367958	0.035044	0.000000	0.030037	0.040050	0.045056	0.000000
937	New-IL-42295	0.062495	0.117490	0.027498	0.001200	0.000800	0.001800	0.012499	0.002000	0.034997	0.024998	0.174786	0.003800	0.003980	0.424166	0.009999	0.000000	0.029998	0.019998	0.047496	0.000000
938	New-IL-42295CCC	0.062495	0.117490	0.027498	0.001200	0.000800	0.001800	0.012499	0.002000	0.034997	0.024998	0.174786	0.003800	0.003980	0.424166	0.009999	0.000000	0.029998	0.019998	0.047496	0.000000
939	New-IL-70316	0.062534	0.080044	0.090049	0.001201	0.000800	0.001801	0.012507	0.010006	0.010005	0.025014	0.202411	0.003802	0.012360	0.387412	0.035019	0.000000	0.030016	0.020011	0.015008	0.000000
940	New-IL-70316CCC	0.062534	0.080044	0.090049	0.001201	0.000800	0.001801	0.012507	0.010006	0.010005	0.025014	0.202411	0.003802	0.012360	0.387412	0.035019	0.000000	0.030016	0.020011	0.015008	0.000000
941	New-IL-87749	0.114980	0.079986	0.089985	0.001200	0.000800	0.001800	0.012498	0.009998	0.034994	0.004999	0.174870	0.003799	0.004070	0.374036	0.026995	0.000000	0.029995	0.019997	0.014998	0.000000
942	New-IL-87749CCC	0.114980	0.079986	0.089985	0.001200	0.000800	0.001800	0.012498	0.009998	0.034994	0.004999	0.174870	0.003799	0.004070	0.374036	0.026995	0.000000	0.029995	0.019997	0.014998	0.000000
943	New-IL-93907	0.115241	0.117746	0.027558	0.001203	0.000802	0.001804	0.012526	0.010021	0.035073	0.005010	0.151517	0.003808	0.009130	0.433405	0.035073	0.000000	0.005010	0.020042	0.015031	0.000000
944	New-IL-93907CCC	0.115241	0.117746	0.027558	0.001203	0.000802	0.001804	0.012526	0.010021	0.035073	0.005010	0.151517	0.003808	0.009130	0.433405	0.035073	0.000000	0.005010	0.020042	0.015031	0.000000
945	New-IL-94020	0.115252	0.080175	0.035377	0.001203	0.000802	0.001804	0.012527	0.002004	0.035077	0.025055	0.150329	0.003808	0.007930	0.433448	0.035077	0.000000	0.005011	0.040088	0.015033	0.000000
946	New-IL-94020CCC	0.115252	0.080175	0.035377	0.001203	0.000802	0.001804	0.012527	0.002004	0.035077	0.025055	0.150329	0.003808	0.007930	0.433448	0.035077	0.000000	0.005011	0.040088	0.015033	0.000000
947	New-IL-103151	0.062460	0.079948	0.027482	0.001199	0.000799	0.001799	0.012492	0.009993	0.009994	0.024984	0.224754	0.003798	0.012240	0.418129	0.024984	0.000000	0.029981	0.039974	0.014990	0.000000
948	New-IL-103151CCC	0.062460	0.079948	0.027482	0.001199	0.000799	0.001799	0.012492	0.009993	0.009994	0.024984	0.224754	0.003798	0.012240	0.418129	0.024984	0.000000	0.029981	0.039974	0.014990	0.000000
949	New-IL-151542	0.062648	0.097630	0.090212	0.003107	0.002105	0.004711	0.012529	0.002005	0.010024	0.025059	0.174110	0.010124	0.010670	0.394830	0.035083	0.000000	0.030071	0.020047	0.015035	0.000000
950	New-IL-151542CCC	0.062648	0.097630	0.090212	0.003107	0.002105	0.004711	0.012529	0.002005	0.010024	0.025059	0.174110	0.010124	0.010670	0.394830	0.035083	0.000000	0.030071	0.020047	0.015035	0.000000
951	New-IL-166697	0.112720	0.102400	0.027554	0.003106	0.002104	0.004709	0.012524	0.010020	0.035068	0.005010	0.175242	0.010120	0.010970	0.368219	0.035068	0.000000	0.030059	0.040078	0.015029	0.000000
952	New-IL-166697CCC	0.112720	0.102400	0.027554	0.003106	0.002104	0.004709	0.012524	0.010020	0.035068	0.005010	0.175242	0.010120	0.010970	0.368219	0.035068	0.000000	0.030059	0.040078	0.015029	0.000000
953	New-IL-166731	0.115301	0.093343	0.027572	0.003108	0.002106	0.004712	0.005013	0.002005	0.035092	0.025065	0.180671	0.010126	0.010120	0.368460	0.032084	0.000000	0.030078	0.040105	0.015039	0.000000
954	New-IL-166731CCC	0.115301	0.093343	0.027572	0.003108	0.002106	0.004712	0.005013	0.002005	0.035092	0.025065	0.180671	0.010126	0.010120	0.368460	0.032084	0.000000	0.030078	0.040105	0.015039	0.000000
955	New-OL-8445	0.124089	0.137488	0.122389	0.004699	0.003100	0.007099	0.000000	0.014999	0.020098	0.034997	0.099991	0.015099	0.000990	0.339969	0.000000	0.000000	0.000000	0.009999	0.064994	0.000000
956	New-OL-8445CCC	0.124089	0.137488	0.122389	0.004699	0.003100	0.007099	0.000000	0.014999	0.020098	0.034997	0.099991	0.015099	0.000990	0.339969	0.000000	0.000000	0.000000	0.009999	0.064994	0.000000
957	New-OL-8788Mod	0.123506	0.060003	0.000500	0.004700	0.003100	0.007100	0.015001	0.015001	0.025001	0.035002	0.130007	0.015101	0.000950	0.460023	0.000000	0.000000	0.000000	0.050002	0.055003	0.000000
958	New-OL-8788ModCCC	0.123506	0.060003	0.000500	0.004700	0.003100	0.007100	0.015001	0.015001	0.025001	0.035002	0.130007	0.015101	0.000950	0.460023	0.000000	0.000000	0.000000	0.050002	0.055003	0.000000
959	New-OL-14844	0.034990	0.061482	0.122363	0.004699	0.003099	0.007098	0.000000	0.014996	0.049985	0.034989	0.155053	0.015095	0.001300	0.339898	0.000000	0.000000	0.039988	0.049985	0.064980	0.000000
960	New-OL-14844CCC	0.034990	0.061482	0.122363	0.004699	0.003099	0.007098	0.000000	0.014996	0.049985	0.034989	0.155053	0.015095	0.001300	0.339898	0.000000	0.000000	0.039988	0.049985	0.064980	0.000000
961	New-OL-15493	0.034994	0.059990	0.122379	0.000600	0.000400	0.000900	0.000000	0.014997	0.000000	0.034994	0.255057	0.002000	0.001270	0.392433	0.029995	0.000000	0.039993	0.009998	0.000000	0.000000
962	New-OL-15493CCC	0.034994	0.059990	0.122379	0.000600	0.000400	0.000900	0.000000	0.014997	0.000000	0.034994	0.255057	0.002000	0.001270	0.392433	0.029995	0.000000	0.039993	0.009998	0.000000	0.000000
963	New-OL-17130	0.035000	0.137499	0.016500	0.004700	0.003100	0.007100	0.015000	0.000000	0.049999	0.000000	0.164998	0.015100	0.010110	0.469995	0.030000	0.000000	0.039999	0.010000	0.000000	0.000000
964	New-OL-17130CCC	0.035000	0.137499	0.016500	0.004700	0.003100	0.007100	0.015000	0.000000	0.049999	0.000000	0.164998	0.015100	0.010110	0.469995	0.030000	0.000000	0.039999	0.010000	0.000000	0.000000
965	New-OL-45748	0.138564	0.060028	0.122456	0.004702	0.003101	0.007103	0.015007	0.000000	0.050023	0.000000	0.114053	0.015107	0.000540	0.340157	0.050023	0.000000	0.029113	0.050023	0.000000	0.000000
966	New-OL-45748CCC	0.138564	0.060028	0.122456	0.004702	0.003101	0.007103	0.015007	0.000000	0.050023	0.000000	0.114053	0.015107	0.000540	0.340157	0.050023	0.000000	0.029113			

Table A.2. (cont.) Normalized Compositions (in mass fractions) of 1075 LAW Glasses in the Database of Compiled Literature Data

#	Glass ID	Al ₂ O ₃	B ₂ O ₃	CaO	Cl	Cr ₂ O ₃	F	Fe ₂ O ₃	K ₂ O	Li ₂ O	MgO	Na ₂ O	P ₂ O ₅	SO ₃	SiO ₂	SnO ₂	TiO ₂	V ₂ O ₅	ZnO	ZrO ₂	Others
991	New-OL-127708Mod	0.110032	0.138294	0.003017	0.000603	0.000402	0.000905	0.015087	0.015087	0.020216	0.035202	0.125722	0.002012	0.000360	0.472714	0.050289	0.000000	0.000000	0.010058	0.000000	0.000000
992	New-OL-127708ModCCC	0.110032	0.138294	0.003017	0.000603	0.000402	0.000905	0.015087	0.015087	0.020216	0.035202	0.125722	0.002012	0.000360	0.472714	0.050289	0.000000	0.000000	0.010058	0.000000	0.000000
993	EWG-LAW-Centroid-1	0.090099	0.100110	0.055060	0.002102	0.001402	0.003204	0.010011	0.004004	0.020022	0.015016	0.190209	0.006807	0.005910	0.395934	0.020022	0.000000	0.020022	0.030033	0.030033	0.000000
994	EWG-LAW-Centroid-1CCC	0.090099	0.100110	0.055060	0.002102	0.001402	0.003204	0.010011	0.004004	0.020022	0.015016	0.190209	0.006807	0.005910	0.395934	0.020022	0.000000	0.020022	0.030033	0.030033	0.000000
995	EWG-LAW-Centroid-2	0.089991	0.099990	0.054994	0.002100	0.001400	0.003200	0.009999	0.004000	0.019998	0.014998	0.189981	0.006799	0.007100	0.395460	0.019998	0.000000	0.019998	0.029997	0.029997	0.000000
996	EWG-LAW-Centroid-2CCC	0.089991	0.099990	0.054994	0.002100	0.001400	0.003200	0.009999	0.004000	0.019998	0.014998	0.189981	0.006799	0.007100	0.395460	0.019998	0.000000	0.019998	0.029997	0.029997	0.000000
997	LAW-ORP-LD1(1)	0.101558	0.120469	0.080146	0.003302	0.005003	0.001701	0.010006	0.001601	0.000000	0.010006	0.209921	0.002902	0.009930	0.371614	0.000000	0.000000	0.010006	0.030017	0.030017	0.001801
998	LAW-ORP-LD1(1)CCC	0.101558	0.120469	0.080146	0.003302	0.005003	0.001701	0.010006	0.001601	0.000000	0.010006	0.209921	0.002902	0.009930	0.371614	0.000000	0.000000	0.010006	0.030017	0.030017	0.001801
999	LAW-ORP-LD1(2)	0.101741	0.120686	0.080290	0.003308	0.005012	0.001704	0.010024	0.001604	0.000000	0.010024	0.210298	0.002907	0.008150	0.372282	0.000000	0.000000	0.010024	0.030071	0.030071	0.001804
1000	LAW-ORP-LD1(2)CCC	0.101741	0.120686	0.080290	0.003308	0.005012	0.001704	0.010024	0.001604	0.000000	0.010024	0.210298	0.002907	0.008150	0.372282	0.000000	0.000000	0.010024	0.030071	0.030071	0.001804
1001	LAW-ORP-LD1(M)	0.147521	0.114369	0.076088	0.003135	0.004749	0.001615	0.009499	0.001520	0.000000	0.009499	0.199291	0.002755	0.008960	0.352796	0.000000	0.000000	0.009499	0.028497	0.028497	0.001710
1002	LAW-ORP-LD1(M)CCC	0.147521	0.114369	0.076088	0.003135	0.004749	0.001615	0.009499	0.001520	0.000000	0.009499	0.199291	0.002755	0.008960	0.352796	0.000000	0.000000	0.009499	0.028497	0.028497	0.001710
1003	LORPM1R1	0.068908	0.082921	0.012779	0.008026	0.003224	0.003003	0.013671	0.011103	0.050152	0.000000	0.106732	0.005005	0.007000	0.521576	0.025668	0.004754	0.034524	0.050152	0.000000	0.000802
1004	LORPM4R2	0.094524	0.123903	0.050590	0.007453	0.002994	0.003003	0.003003	0.005885	0.000000	0.049269	0.139709	0.004648	0.006400	0.360069	0.000000	0.010811	0.040040	0.044194	0.000000	0.000745
1005	LORPM4R2 (K3-R)	0.094524	0.123903	0.050590	0.007453	0.002994	0.003003	0.005885	0.005885	0.000000	0.049269	0.139709	0.004648	0.006400	0.360069	0.000000	0.010811	0.040040	0.044194	0.000000	0.000745
1006	LORPM9-repeat	0.085812	0.069344	0.000000	0.000200	0.000080	0.003000	0.008469	0.000000	0.000000	0.023895	0.000125	0.001100	0.492936	0.000000	0.000000	0.039996	0.049996	0.009889	0.000020	
1007	LORPM10R1-repeat	0.035027	0.060047	0.122495	0.008008	0.003216	0.002996	0.080062	0.058846	0.050039	0.045055	0.050039	0.004994	0.008100	0.390213	0.000000	0.030023	0.040031	0.010008	0.000000	0.000801
1008	LORPM11-repeat	0.035000	0.060000	0.000000	0.008002	0.003214	0.002994	0.003000	0.001100	0.000000	0.050000	0.196200	0.004990	0.001000	0.493700	0.000000	0.030000	0.000000	0.050000	0.000000	0.000800
1009	LORPM18-repeat	0.055698	0.075458	0.024479	0.000200	0.000080	0.000075	0.018399	0.001260	0.033449	0.031729	0.105827	0.000125	0.002800	0.478876	0.039999	0.023999	0.031999	0.017999	0.046149	0.000020
1010	LORPM38R1	0.055806	0.075604	0.024527	0.008017	0.003220	0.003000	0.064724	0.047350	0.010019	0.035067	0.134166	0.005000	0.004100	0.397348	0.010019	0.024046	0.008015	0.042080	0.047090	0.000802
1011	LORPM40R1	0.117753	0.075430	0.024470	0.000200	0.000080	0.005707	0.047241	0.047241	0.039984	0.039986	0.009960	0.000125	0.002800	0.383846	0.009996	0.005997	0.007997	0.041983	0.049980	0.000020
1012	LAW17	0.064961	0.068559	0.079952	0.000200	0.000100	0.000100	0.062862	0.019988	0.034979	0.009994	0.169997	0.000100	0.003600	0.414950	0.000000	0.014691	0.000000	0.019988	0.034979	0.000000
1013	LP2-IL-01	0.074995	0.079995	0.076165	0.001740	0.005250	0.002630	0.002000	0.019999	0.000000	0.003000	0.236786	0.005629	0.008060	0.379757	0.005000	0.000000	0.019999	0.023998	0.054997	0.000000
1014	LP2-IL-02	0.075006	0.081297	0.020002	0.001740	0.005250	0.002630	0.005771	0.020002	0.000000	0.003000	0.219973	0.005630	0.007920	0.418114	0.025002	0.000000	0.005000	0.026312	0.055004	0.000000
1015	LP2-IL-03	0.087240	0.087310	0.019998	0.003470	0.005249	0.005259	0.002000	0.007579	0.000000	0.003000	0.244973	0.011269	0.002110	0.403556	0.024997	0.000000	0.004999	0.031997	0.054994	0.000000
1016	LP2-IL-04	0.074978	0.079977	0.074918	0.003469	0.005249	0.005268	0.009997	0.019994	0.000000	0.009997	0.236731	0.011267	0.002290	0.381889	0.024993	0.000000	0.004999	0.023997	0.029991	0.000000
1017	LP2-IL-05	0.074991	0.119986	0.070242	0.003470	0.005259	0.002630	0.002000	0.004999	0.000000	0.003000	0.219973	0.011269	0.002120	0.369955	0.024997	0.000000	0.004999	0.023997	0.054993	0.000000
1018	LP2-IL-06	0.106819	0.120022	0.020004	0.003471	0.005251	0.005261	0.002000	0.020004	0.000000	0.010002	0.220040	0.011272	0.007820	0.370667	0.008201	0.000000	0.010752	0.024004	0.055010	0.000000
1019	LP2-IL-07	0.075014	0.120022	0.051479	0.003471	0.003751	0.002000	0.020004	0.020004	0.000000	0.010002	0.223310	0.011272	0.007820	0.394571	0.005001	0.000000	0.005001	0.032006	0.030005	0.000000
1020	LP2-IL-08	0.075028	0.080030	0.080030	0.003471	0.005252	0.005262	0.010004	0.005002	0.000000	0.010004	0.220082	0.011274	0.007630	0.389895	0.005002	0.000000	0.005002	0.032012	0.055020	0.000000
1021	LP2-IL-09	0.074991	0.119986	0.019998	0.001730	0.005249	0.002630	0.009999	0.004999	0.000000	0.009999	0.243701	0.005629	0.002120	0.369955	0.022027	0.000000	0.019998	0.031996	0.054993	0.000000
1022	LP2-IL-10	0.100031	0.095030	0.050015	0.002081	0.004501	0.003161	0.006002	0.010003	0.000000	0.006502	0.230072	0.006762	0.006490	0.388121	0.015005	0.000000	0.010003	0.028009	0.040012	0.000000
1023	LP2-IL-11	0.090001	0.080001	0.030800	0.003470	0.003750	0.005260	0.010000	0.020000	0.000000	0.003000	0.220002	0.011270	0.001990	0.388454	0.025000	0.000000	0.020000	0.032001	0.055001	0.000000
1024	LP2-IL-12	0.074995	0.079995	0.031168	0.003470	0.003750	0.005270	0.002000	0.005000	0.000000	0.009999	0.237856	0.011269	0.002060	0.429174	0.005000	0.000000	0.019999	0.023998	0.054997	0.000000
1025	LP2-IL-13	0.075001	0.112551	0.023200	0.001740	0.005250	0.002630	0.010000	0.020000	0.000000	0.003000	0.220002	0.005630	0.001990	0.430005	0.005000	0.000000	0.005000	0.024000	0.055001	0.000000
1026	LP2-IL-14	0.087979	0.120040	0.038313	0.003471	0.003751	0.005262	0.010003	0.005002	0.000000	0.003001	0.245081	0.011274	0.007670	0.370123	0.005002	0.000000	0.005002	0.024008	0.055018	0.000000
1027	LP2-IL-15	0.075044	0.107584	0.020012	0.003472	0.005273	0.005253	0.010006	0.005003	0.000000	0.003002	0.220131	0.011277	0.007410	0.427474	0.025015	0.000000	0.020012	0.024014	0.030018	0.000000
1028	LP2-IL-16	0.100014	0.095013	0.050007	0.002080	0.004501	0.003161	0.006001	0.010001	0.000000	0.006501	0.230032	0.006761	0.004860	0.388055	0.015002	0.000000	0.010001	0.028004	0.040006	0.000000
1029	LP2-IL-17	0.092313	0.110051	0.025012	0.000730	0.008080	0.001101	0.002001	0.005002	0.000000	0.010005	0.230107	0.002371	0.009540	0.409620	0.000000	0.000000	0.021010	0.030014	0.050323	0.000000
1030	LP2-OL-01	0.059967	0.059968	0.090851	0.000620	0.005997	0.000000	0.000000	0.000000	0.000000	0.013493	0.209886	0.002029	0.001540	0.469746	0.000000	0.000000	0.000000	0.019989	0.064965	0.000000
1031	LP2-OL-02	0.100021	0.095020	0.050011	0.002080	0.004501	0.003161	0.006001	0.010002	0.000000	0.006501	0.230049	0.006761	0.004790	0.388082	0.015003	0.000000	0.010002	0.028006	0.040009	0.000000
1032	LP2-OL-03-MOD2	0.107411	0.061088	0.109082	0.000630	0.006112	0.000970	0.000000	0.000000	0.000000	0.013744	0.264717	0.002071	0.007250	0.355334	0.027798	0.000000	0.000000	0.020366		

Table A.2. (cont.) Normalized Compositions (in mass fractions) of 1075 LAW Glasses in the Database of Compiled Literature Data

#	Glass ID	Al ₂ O ₃	B ₂ O ₃	CaO	Cl	Cr ₂ O ₃	F	Fe ₂ O ₃	K ₂ O	Li ₂ O	MgO	Na ₂ O	P ₂ O ₅	SO ₃	SiO ₂	SnO ₂	TiO ₂	V ₂ O ₅	ZnO	ZrO ₂	Others
1057	LAWPH3-04	0.063676	0.127662	0.095308	0.002011	0.004944	0.003052	0.003673	0.008956	0.000000	0.004153	0.222260	0.006525	0.012030	0.358287	0.003493	0.000000	0.027580	0.022446	0.033944	0.000000
1058	LAWPH3-05 mod6	0.062360	0.084946	0.024684	0.004397	0.004497	0.006596	0.010593	0.029282	0.000000	0.011393	0.227256	0.014191	0.009530	0.395049	0.020187	0.000000	0.032979	0.021486	0.040574	0.000000
1059	LAWPH3-06	0.090177	0.067261	0.101596	0.001000	0.005829	0.001510	0.002390	0.023937	0.000000	0.011378	0.212640	0.003239	0.003550	0.357720	0.032525	0.000000	0.023037	0.028946	0.033265	0.000000
1060	LAWPH3-07	0.098065	0.076119	0.088452	0.004151	0.003291	0.006312	0.005251	0.007822	0.000000	0.000700	0.238920	0.013503	0.005320	0.350728	0.007332	0.000000	0.030508	0.030958	0.032568	0.000000
1061	LAWPH3-08	0.066728	0.064828	0.061427	0.004560	0.004680	0.006931	0.001060	0.015152	0.000000	0.001850	0.212456	0.014822	0.003590	0.439923	0.005691	0.000000	0.000500	0.032914	0.062888	0.000000
1062	LAWPH3-09	0.078230	0.085981	0.092272	0.002570	0.003051	0.003911	0.008421	0.054987	0.000000	0.002050	0.212878	0.008361	0.009510	0.355177	0.002360	0.000000	0.006441	0.022893	0.050907	0.000000
1063	LAWPH3-10	0.082534	0.063629	0.055807	0.000950	0.003611	0.001441	0.007892	0.026268	0.000000	0.003381	0.235999	0.003081	0.010740	0.355124	0.017195	0.000000	0.038371	0.031879	0.062098	0.000000
1064	LAWPH3-11	0.093342	0.093302	0.037719	0.002719	0.005648	0.004119	0.000520	0.013716	0.000000	0.008167	0.247516	0.008817	0.001380	0.354883	0.007458	0.000000	0.034560	0.021863	0.064271	0.000000
1065	LAWPH3-12	0.111198	0.135093	0.027604	0.003199	0.004269	0.004859	0.010708	0.002290	0.000000	0.012588	0.214277	0.010388	0.003150	0.351300	0.009338	0.000000	0.038452	0.027904	0.033383	0.000000
1066	LAWPH3-12-2	0.111198	0.135093	0.027604	0.003199	0.004269	0.004859	0.010708	0.002290	0.000000	0.012588	0.214277	0.010388	0.003150	0.351300	0.009338	0.000000	0.038452	0.027904	0.033383	0.000000
1067	LAWPH3-13	0.071219	0.062449	0.085958	0.001690	0.005800	0.002570	0.000690	0.034029	0.000000	0.012510	0.230375	0.005490	0.011110	0.398382	0.002720	0.000000	0.007860	0.035009	0.032139	0.000000
1068	LAWPH3-14	0.066353	0.082668	0.052978	0.004302	0.003181	0.006542	0.000330	0.002091	0.000000	0.000870	0.256518	0.013995	0.008830	0.395726	0.021687	0.000000	0.021397	0.024809	0.037723	0.000000
1069	LAWPH3-15	0.072964	0.094299	0.086661	0.001050	0.004299	0.001600	0.012457	0.041351	0.000000	0.000080	0.217032	0.003419	0.004090	0.353352	0.016916	0.000000	0.016036	0.029414	0.044980	0.000000
1070	LAWPH3-16	0.061103	0.069171	0.074150	0.001930	0.004249	0.002939	0.003329	0.040809	0.000000	0.007918	0.231957	0.006288	0.001920	0.365481	0.001150	0.000000	0.036220	0.034321	0.057065	0.000000
1071	LAWPH3-17	0.061675	0.061255	0.098614	0.001910	0.003921	0.002901	0.013953	0.003281	0.000000	0.013273	0.253721	0.006201	0.006750	0.380852	0.007532	0.000000	0.023886	0.023746	0.036529	0.000000
1072	LAWPH3-17-2	0.061675	0.061255	0.098614	0.001910	0.003921	0.002901	0.013953	0.003281	0.000000	0.013273	0.253721	0.006201	0.006750	0.380852	0.007532	0.000000	0.023886	0.023746	0.036529	0.000000
1073	LAWPH3-18	0.083707	0.060726	0.035766	0.003089	0.004778	0.004698	0.003939	0.029449	0.000000	0.013025	0.222373	0.010046	0.003630	0.407690	0.033007	0.000000	0.004028	0.034587	0.045462	0.000000
1074	LAWPH3-19 mod1	0.067000	0.068895	0.084855	0.000768	0.003731	0.001157	0.013605	0.030762	0.000000	0.002105	0.214156	0.002494	0.011000	0.407935	0.010783	0.000000	0.029106	0.021106	0.030542	0.000000
1075	LAWPH3-20	0.060342	0.089328	0.047574	0.001320	0.004089	0.002000	0.011219	0.001270	0.000000	0.000740	0.224291	0.004289	0.007430	0.411926	0.028626	0.000000	0.036385	0.033876	0.035295	0.000000

Table A.3. Properties of LAW Glasses in the Compiled Literature Database (Glasses # 1-1075).

Glass #	Glass ID	η_{1150} , P ^(a)	ε_{1150} , S/cm	PCT Response, g/m ²		VHT Response		SO ₃ Solubility and Melter SO ₃ Tolerance, wt%				
				NL _B	NL _{Na}	r _a , g/m ² /d	P/F ^(b)	BS ^(c)	SR ^(d)	Bub ^(e)	MT ^(f)	3TS ^(g)
1	LB100-G-83A	-	-	0.725	0.62	-	-	-	-	-	-	-
2	LAWA102	55	0.39	-	-	-	-	-	-	-	-	-
3	LAWC21	56	0.31	-	-	-	-	-	-	-	-	-
4	A100-G-115A	-	-	0.48	0.458	-	-	-	-	-	-	-
5	C100-G-136B	-	-	0.368	0.405	-	-	-	-	-	-	-
6	LAWA41	68	0.526	0.47	0.52	-	-	-	-	-	-	-
7	LAWA42	31	0.554	0.78	0.695	-	-	-	-	-	-	-
8	LAWA43	87	0.521	0.385	0.43	-	-	-	-	-	-	-
9	LAWA44	69	0.516	0.37	0.36	1	P	-	-	-	-	-
10	LAWA44S	-	-	-	-	-	-	0.55	-	-	-	-
11	LAWA45	64	0.514	0.77	0.515	-	-	-	-	-	-	-
12	LAWA46	89*	0.55	0.425*	0.355*	16.6	P	-	-	-	-	-
13	LAWA47	85*	0.499	0.375*	0.335*	0.6	P	-	-	-	-	-
14	LAWA48	81*	0.554	0.395*	0.335*	3.2	P	-	-	-	-	-
15	LAWA49	87	0.52	0.31	0.29	3.3	P	-	-	-	-	-
16	LAWA50	72	0.517	0.315	0.3	-	-	-	-	-	-	-
17	LAWA51	107	0.412	0.355	0.26	0.6	P	-	-	-	-	-
18	LAWA52	52	0.466	0.425	0.55	7.4	P	-	-	-	-	-
19	LAWA60	63	0.398	0.29	0.31	6.2	P	-	-	-	-	-
20	LAWA64	61*	0.498	0.38*	0.5*	28.5	P	-	-	-	-	-
21	LAWA81	70	0.512	0.39	0.42	-	-	-	-	-	-	-
22	LAWA82	97	0.523	0.34	0.335	-	-	-	-	-	-	-
23	LAWA83	92	0.461	0.31	0.34	-	-	-	-	-	-	-
24	LAWA84	92	0.444	0.295	0.335	-	-	-	-	-	-	-
25	LAWA85	86*	0.473	0.34*	0.35*	-	-	-	-	-	-	-
26	LAWA86	-	-	0.39*	0.385*	-	-	-	-	-	-	-
27	LAWA87	49	0.517	0.595	0.55	-	-	-	-	-	-	-
28	LAWA88	60	0.562	0.435	0.425	1.3	P	-	-	-	-	-
29	LAWA89	65	0.542	0.585	0.465	-	-	-	-	-	-	-
30	LAWA90	65	0.501	0.485	0.485	-	-	-	-	-	-	-
31	LAWA93	16	0.442	0.525	0.535	-	-	-	-	1.35	-	-
32	LAWA96	77	0.507	0.31	0.375	-	-	-	-	-	-	-
33	LAWA97S	76*	0.431*	-	-	-	-	-	-	-	-	-
34	LAWA98S	35	0.468	0.36	0.28	-	-	0.71	-	-	-	-
35	LAWA98S0	-	-	0.735	0.545	-	-	-	-	-	-	-
36	LAWA99S	40	0.309	-	-	-	-	0.84	-	-	-	-
37	LAWA100S	42	0.329	0.54	0.375	-	-	0.61	-	-	-	-
38	LAWA101S	60	0.221	0.43	0.32	-	-	0.62	-	-	-	-
39	LAWA102S	-	-	0.275	0.22	-	-	0.68	-	-	-	-
40	LAWA103S	-	-	-	-	-	-	0.55	-	-	-	-
41	LAWA104	53	0.596	0.58	0.525	6.5	P	-	-	-	-	-
42	LAWA105	38	0.731	0.96	0.795	39.6	P	-	-	-	-	-
43	LAWABP1	140*	0.469	0.285*	0.31*	5.1	P	-	-	-	-	-
44	LAWB29	43	0.339	-	-	-	-	-	-	-	-	-
45	LAWB30	31	0.287	0.24	0.24	-	-	-	-	-	-	-
46	LAWB31	-	-	0.21	0.105	-	-	-	-	-	-	-
47	LAWB32	-	-	0.245	0.14	-	-	-	-	-	-	-
48	LAWB33	-	-	0.19	0.115	-	-	-	-	-	-	-
49	LAWB34	85	0.238	0.215	0.125	-	-	-	-	-	-	-
50	LAWB35	-	-	0.5	0.34	-	-	-	-	-	-	-
51	LAWB36S	-	-	-	-	-	-	0.87	-	-	-	-
52	LAWB37	92	0.231	0.26	0.18	1.5	P	-	-	-	-	-
53	LAWB38	65	0.277	0.255	0.18	-	-	-	-	-	-	-
54	LAWB39	66	0.235	0.505	0.4	-	-	-	-	0.91	-	-
55	LAWB40	24	0.517	1.585	1.175	-	-	-	-	-	-	-
56	LAWB41	35	0.381	0.85	0.705	-	-	-	-	1.05	-	-
57	LAWB42S	353*	-	-	-	-	-	0.61	-	-	-	-
58	LAWB43S	-	-	-	-	-	-	0.62	-	-	-	-
59	LAWB44S	-	-	-	-	-	-	0.52	-	-	-	-
60	LAWB45	43	0.311	-	-	-	-	-	-	-	-	-
61	LAWB51S	67	-	0.475	0.33	-	-	1.06	-	-	-	-
62	LAWB52S	50	0.341	0.49	0.335	-	-	1.06	-	-	-	-
63	LAWB53S	47	0.364	0.42	0.265	-	-	1.1	-	-	-	-
64	LAWC11 for AN107	59	0.694	-	-	-	-	-	-	-	-	-
65	LAWC12 for AN107	56	0.591	0.42	0.409	1.8	P	-	-	-	-	-

Table A.3. Properties of LAW Glasses in the Compiled Literature Database (Glasses # 1-1075).

Glass #	Glass ID	η_{1150} , P ^(a)	ε_{1150} , S/cm	PCT Response, g/m ²		VHT Response		SO ₃ Solubility and Melter SO ₃ Tolerance, wt%				
				NL _B	NL _{Na}	r _a , g/m ² /d	P/F ^(b)	BS ^(c)	SR ^(d)	Bub ^(e)	MT ^(f)	3TS ^(g)
66	LAWC13	86	0.364	0.355	0.37	-	-	-	-	-	-	-
67	LAWC14	49*	0.561	0.54	3.609*	-	-	-	-	-	-	-
68	LAWC15	74	0.522	0.329	0.336	0.5	P	-	-	-	-	-
69	LAWC16S	31	0.336	0.584	0.409	-	-	0.71	-	-	-	-
70	LAWC17S	-	-	0.399	0.294	-	-	0.66	-	-	-	-
71	LAWC18S	46	0.318	0.413	0.295	-	-	0.75	-	-	-	-
72	LAWC19S	48	0.208	0.232	0.226	-	-	0.73	-	-	-	-
73	LAWC20S	-	-	0.244	0.189	-	-	0.55	-	-	-	-
74	LAWC21S	56	0.31	0.15	0.172	2.9	P	0.7	-	-	-	-
75	LAWC22	39	0.448	0.518	0.469	7.7	P	-	-	-	-	-
76	LAWC23	149	-	0.239	0.274	-	P	-	-	-	-	-
77	LAWC23S	-	-	-	-	-	-	0.71	-	-	-	-
78	LAWC24	128	-	0.221	0.282	-	P	-	-	-	-	-
79	LAWC24S	-	-	-	-	-	-	0.88	-	-	-	-
80	LAWC25	96*	0.209	0.32	0.385	-	P	-	-	-	-	-
81	LAWC25S	-	-	-	-	-	-	0.68*	-	-	-	-
82	LAWNa1S	-	-	-	-	-	-	0.9	-	-	-	-
83	LAWNa2	-	-	-	-	-	-	0.75	-	-	-	-
84	LAWNa3	-	-	-	-	-	-	0.97	-	-	-	-
85	LAWNa4	-	-	-	-	-	-	1.32	-	-	-	-
86	LAWNa5	-	-	-	-	-	-	0.75	-	-	-	-
87	LAWNa6	-	-	-	-	-	-	0.68	-	-	-	-
88	LAWNa7	-	-	-	-	-	-	0.58	-	-	-	-
89	LAWA53	-	-	-	-	0.8	P	0.59	-	-	-	-
90	LAWA54	-	-	-	-	4.9	P	0.615*	-	-	-	-
91	LAWA55	-	-	-	-	40.9	P	0.55*	-	-	-	-
92	LAWA56	-	-	-	-	1.7	P	0.61	-	-	-	-
93	LAWA57	-	-	-	-	0.1	P	0.48	-	-	-	-
94	LAWA58	-	-	-	-	0.9	P	0.52*	-	-	-	-
95	LAWA59	-	-	-	-	0.8	P	0.585*	-	-	-	-
96	LAWA61	-	-	-	-	-	-	0.55*	-	-	-	-
97	LAWA62	-	-	-	-	-	-	0.57*	-	-	-	-
98	LAWA63	-	-	-	-	-	-	0.52*	-	-	-	-
99	LAWA65	-	-	-	-	-	-	0.48*	-	-	-	-
100	LAWA66	-	-	-	-	-	-	0.68*	-	-	-	-
101	LAWA67	-	-	-	-	-	-	0.65	-	-	-	-
102	LAWA68	-	-	-	-	-	-	0.47	-	-	-	-
103	LAWA69	-	-	-	-	-	-	0.51	-	-	-	-
104	LAWA70	-	-	-	-	-	-	0.515	-	-	-	-
105	LAWA71	-	-	-	-	-	-	0.475	-	-	-	-
106	LAWA72	-	-	-	-	-	-	0.425*	-	-	-	-
107	LAWA73	-	-	-	-	-	-	0.565	-	-	-	-
108	LAWA74	-	-	-	-	-	-	0.61	-	-	-	-
109	LAWA75	-	-	-	-	-	-	0.54	-	-	-	-
110	LAWA76	-	-	0.71	0.66	-	-	0.86	-	-	-	-
111	LAWA77	-	-	-	-	-	-	0.455	-	-	-	-
112	LAWA78	-	-	-	-	-	-	0.655	-	-	-	-
113	LAWA79	-	-	-	-	-	-	0.56	-	-	-	-
114	LAWA80	-	-	-	-	-	-	0.55	-	-	-	-
115	LAWABPS	-	-	-	-	-	-	0.46*	-	-	-	-
116	LAWBF99	-	-	-	-	-	-	0.68	-	-	-	-
117	LAWPC99	-	-	-	-	-	-	0.485	-	-	-	-
118	LAWA91	-	-	-	-	-	-	0.445*	-	-	-	-
119	LAWA92	-	-	-	-	-	-	0.45*	-	-	-	-
120	LAWA95	-	-	-	-	-	-	0.94	-	-	-	-
121	PNLREF (LD6-5412)	-	-	0.105	0.275	-	-	-	-	-	-	-
122	TFA-BASE (HLP-01)	-	-	0.395	0.325	9.5	P	-	-	-	-	-
123	A100-G-115A	-	-	0.485	0.45	13	P	-	-	-	-	-
124	A100CC	-	-	0.355*	0.325*	9.7*	P	-	-	-	-	-
125	C100-G-136B	-	-	0.368	0.349	2.5	P	-	-	-	-	-
126	C100GCC	-	-	0.232*	0.243*	6.4*	P	-	-	-	-	-
127	LAWA41-3	-	-	-	-	-	-	-	-	-	-	-
128	LAWA44-3	-	-	-	-	-	-	-	-	-	-	-
129	LAWA52-2	-	-	-	-	-	-	-	-	-	-	-
130	LAWA60	-	-	-	-	-	-	-	-	-	-	-

Table A.3. Properties of LAW Glasses in the Compiled Literature Database (Glasses # 1-1075).

Glass #	Glass ID	η_{1150} , P ^(a)	ε_{1150} , S/cm	PCT Response, g/m ²		VHT Response		SO ₃ Solubility and Melter SO ₃ Tolerance, wt%				
				NL _B	NL _{Na}	r _a , g/m ² /d	P/F ^(b)	BS ^(c)	SR ^(d)	Bub ^(e)	MT ^(f)	3TS ^(g)
131	LAWA64	-	-	-	-	-	-	-	-	-	-	-
132	LAWA88	-	-	-	-	-	-	-	-	-	-	-
133	LAWA95	-	-	-	-	-	-	-	-	-	-	-
134	LAWA102	-	-	-	-	-	-	-	-	-	-	-
135	LAWA104	-	-	-	-	-	-	-	-	-	-	-
136	LAWA105	-	-	-	-	-	-	-	-	-	-	-
137	LAWABP1	-	-	-	-	-	-	-	-	-	-	-
138	LAWB37	-	-	-	-	-	-	-	-	-	-	-
139	LAWC21	-	-	-	-	-	-	-	-	-	-	-
140	LAWC25	-	-	-	-	-	-	-	-	-	-	-
141	OD2-G-50A	-	-	-	-	-	-	-	-	-	-	-
142	LAWA102 + 15% Additive	59	0.28	-	-	-	-	-	-	-	-	-
143	LAWA102 + 15% Simulant	39	0.39	-	-	-	-	-	-	-	-	-
144	LAWA44S1	-	-	-	-	-	-	0.51	-	0.6	-	-
145	LAWA44S2	-	-	-	-	-	-	0.53	-	-	-	-
146	LAWA44SX	-	-	-	-	-	-	0.58	-	-	-	-
147	LAWA88S1	-	-	-	-	-	-	0.69	-	-	-	-
148	LAWA88S2	-	-	-	-	-	-	0.65	-	-	-	-
149	LAWA88SX	-	-	-	-	-	-	0.75	-	-	-	-
150	LAWA102R1	-	-	-	-	3.8	P	-	-	-	-	-
151	LAWA108S1	81	0.426	-	-	-	-	-	-	-	-	-
152	LAWA108S2	-	-	-	-	-	-	0.65	-	-	-	-
153	LAWA109S1	-	0.378	-	-	-	-	0.63	-	-	-	-
154	LAWA109S2	-	-	-	-	-	-	0.63	-	-	-	-
155	LAWA110S1	81	0.382	-	-	-	-	0.65	-	-	-	-
156	LAWA110S2	-	-	-	-	-	-	0.61	-	-	-	-
157	LAWA111S1	46	0.309	-	-	-	-	0.72	-	-	-	-
158	LAWA111S2	-	-	-	-	-	-	0.8	-	-	-	-
159	LAWA112S1	36	0.441	-	-	-	-	-	-	-	-	-
160	LAWA112S2	-	-	0.53	0.64	-	-	0.85	-	-	-	-
161	LAWA112B14	-	-	0.39	0.54	-	-	-	-	-	-	-
162	LAWA112B15	-	-	0.39	0.52	-	-	-	-	-	-	-
163	LAWA118S1	-	-	-	-	-	-	0.6	-	-	-	-
164	LAWA118S2	-	-	-	-	-	-	0.62	-	-	-	-
165	LAWA119S1	-	-	-	-	-	-	0.69	-	-	-	-
166	LAWA119S2	-	-	-	-	-	-	0.72	-	-	-	-
167	LAWA120S1	-	-	-	-	-	-	0.63*	-	-	-	-
168	LAWA120S2	-	-	-	-	-	-	0.72*	-	-	-	-
169	LAWA121S1	-	-	-	-	-	-	0.64*	-	-	-	-
170	LAWA121S2	-	-	-	-	-	-	0.76*	-	-	-	-
171	LAWA122S2	-	-	-	-	-	-	0.67	-	-	-	-
172	LAWA123S1	-	-	-	-	-	-	0.69	-	-	-	-
173	LAWA123S2	-	-	-	-	-	-	0.76	-	-	-	-
174	LAWA130	71	0.41	0.46	0.46	0.7	P	-	-	-	-	-
175	LAWA133	-	-	0.54	0.565	0.6	P	-	-	-	-	-
176	LAWA133S2	-	-	-	-	-	-	0.57	-	-	-	-
177	LAWA134	66	0.382	0.46	0.39	0.2	P	-	-	-	-	-
178	LAWA135	78	0.352	0.435	0.37	0.3	P	-	-	-	-	-
179	LAWA136	-	-	0.38	0.355	0.3	P	-	-	-	-	-
180	LAWB60	-	-	-	-	7.5	P	-	-	-	-	-
181	LAWB60S2	35	0.257	-	-	-	-	1.41	-	-	-	-
182	LAWB60S4	-	-	0.26	0.255	-	-	1.6	-	-	-	-
183	LAWB61	36	0.3	0.39	0.335	-	-	-	-	-	-	-
184	LAWB61S4	-	-	-	-	-	-	1.43	-	-	-	-
185	LAWB62	27	0.35	0.165	0.18	4.1	P	-	-	-	-	-
186	LAWB62S4	-	-	-	-	-	-	1.83	-	-	-	-
187	LAWB63	41	0.248	0.18	0.175	7.9	P	-	-	-	-	-
188	LAWB63S4	-	-	-	-	-	-	1.43	-	-	-	-
189	LAWB64	34	0.3	0.28	0.245	1.7	P	-	-	-	-	-
190	LAWB64S0	-	-	-	-	-	-	-	-	-	-	-
191	LAWB64S4	-	-	-	-	-	-	1.4	-	-	-	-
192	LAWB65	53	0.222	0.28	0.24	1.1	P	-	-	-	-	-
193	LAWB65S4	-	-	-	-	-	-	1.26	-	-	-	-
194	LAWB66	46	0.263	0.295	0.275	1.9	P	-	-	-	-	-
195	LAWB66S4	-	-	-	-	-	-	1.35	-	-	-	-

Table A.3. Properties of LAW Glasses in the Compiled Literature Database (Glasses # 1-1075).

Glass #	Glass ID	η_{1150} , P ^(a)	ϵ_{1150} , S/cm	PCT Response, g/m ²		VHT Response		SO ₃ Solubility and Melter SO ₃ Tolerance, wt%				
				NL _B	NL _{Na}	r _a , g/m ² /d	P/F ^(b)	BS ^(c)	SR ^(d)	Bub ^(e)	MT ^(f)	3TS ^(g)
196	LAWB67	77	0.217	0.245	0.14	1.7	P	-	-	-	-	-
197	LAWB67S4	-	-	-	-	-	-	1.42*	-	-	-	-
198	LAWB68	58	0.214	0.25	0.24	2	P	-	-	-	-	-
199	LAWB69	37	0.25	0.245	0.24	14.1	P	-	-	-	-	-
200	LAWB69S4	-	-	-	-	-	-	1.19	-	-	-	-
201	LAWB70	38	0.274	0.56	0.47	3.4	P	-	-	-	-	-
202	LAWB70S4	-	-	-	-	-	-	1.23	-	-	-	-
203	LAWB71	39	0.297	0.32	0.275	1.3	P	-	-	-	-	-
204	LAWB71S4	-	-	-	-	-	-	1.26	-	-	-	-
205	LAWB72	42	0.234	0.44	0.385	2.5	P	-	-	-	-	-
206	LAWB72S4	-	-	-	-	-	-	1.2	-	-	-	-
207	LAWB73	36	0.285	0.205	0.19	3.4	P	-	-	-	-	-
208	LAWB73S4	-	-	-	-	-	-	1.4	-	-	-	-
209	LAWB74	34	0.325	0.225	0.2	5.7	P	-	-	-	-	-
210	LAWB74S4	-	-	-	-	-	-	1.43	-	-	-	-
211	LAWB75	33	0.312	0.17	0.145	6.5	P	-	-	-	-	-
212	LAWB75S4	-	-	-	-	-	-	1.47	-	-	-	-
213	LAWB76	34	0.374	0.21	0.18	8.6	P	-	-	-	-	-
214	LAWB76S4	-	-	-	-	-	-	1.58	-	-	-	-
215	LAWB77	64	0.242	0.36	0.3	1.9	P	-	-	-	-	-
216	LAWB77S4	-	-	-	-	-	-	1.17	-	-	-	-
217	LAWB78	42	0.241	0.615	0.555	2.5	P	-	-	-	-	-
218	LAWB78S4	-	-	-	-	-	-	0.93	-	-	-	-
219	LAWB79	40	0.231	0.545	0.49	1.2	P	-	-	-	-	-
220	LAWB79S4	-	-	-	-	-	-	0.95	-	-	-	-
221	LAWB80	55	0.183	0.44	0.365	1.1	P	-	-	-	-	-
222	LAWB80S4	-	-	-	-	-	-	1.04	-	-	-	-
223	LAWB81	39	0.303	0.45	0.395	2.7	P	-	-	-	-	-
224	LAWB81S4	-	-	-	-	-	-	1.14	-	-	-	-
225	LAWB82	33	0.288	0.25	0.23	3.5	P	-	-	-	-	-
226	LAWB82S4	-	-	-	-	-	-	1.07	-	-	-	-
227	LAWB83	54	0.223	0.305	0.265	1.8	P	-	-	-	-	-
228	LAWB83S4	-	-	-	-	-	-	1.04	-	-	-	-
229	LAWB84	51	0.23	0.34	0.28	1.7	P	-	-	-	-	-
230	LAWB84S4	-	-	-	-	-	-	1.1	-	-	-	-
231	LAWB85	55	0.235	0.325	0.25	1.2	P	-	-	-	-	-
232	LAWB85S4	-	-	-	-	-	-	1.01	-	-	-	-
233	LAWB86	47	0.225	0.625	0.505	1.7	P	-	-	-	-	-
234	LAWB86S4	-	-	-	-	-	-	1.02	-	-	-	-
235	LAWB89	48	0.271	0.3	0.235	1.8	P	-	-	-	-	-
236	LAWB89S4	-	-	-	-	-	-	1.28	-	-	-	-
237	LAWB90	-	-	0.31	0.275	1.5	P	-	-	-	-	-
238	LAWB91	-	-	0.395	0.345	1.3	P	-	-	-	-	-
239	LAWB91S4	-	-	-	-	-	-	0.71	-	-	-	-
240	LAWB92	54	0.222	0.455	0.395	1.1	P	-	-	-	-	-
241	LAWB92S4	-	-	-	-	-	-	0.64	-	-	-	-
242	LAWB93	50	0.204	0.43	0.25	1.7	P	-	-	-	-	-
243	LAWB93S4	-	-	-	-	-	-	1.18	-	-	-	-
244	LAWB94	48	0.235	0.355	0.235	1.5	P	-	-	-	-	-
245	LAWB94S4	-	-	-	-	-	-	1.36	-	-	-	-
246	LAWB95	55	0.282	0.335	0.22	1.2	P	-	-	-	-	-
247	LAWB95S4	-	-	-	-	-	-	1.33	-	-	-	-
248	C21REV2	-	-	0.345	0.36	-	-	-	-	-	-	-
249	C22AN107	-	-	0.57	0.555	1	P	-	-	-	-	-
250	LAWC26	51	-	0.34	0.33	2.4	P	-	-	-	-	-
251	LAWC26S2	67	0.251	-	-	-	-	0.94	-	-	-	-
252	LAWC27	51	0.256	0.19	0.22	19.5	P	-	-	-	-	-
253	LAWC27S2	55	0.211	-	-	-	-	0.76	-	-	-	-
254	LAWC28	-	-	0.145	0.22	10.2	P	-	-	-	-	-
255	LAWC28S2	31	0.283	-	-	-	-	1.1	-	-	-	-
256	LAWC29	40	0.279	0.15	0.205	11.7	P	-	-	-	-	-
257	LAWC29S2	-	-	-	-	-	-	0.92	-	-	-	-
258	LAWC30	43	0.347	0.3	0.33	6.6	P	-	-	-	-	-
259	LAWC30S2	-	-	-	-	-	-	0.7	-	-	-	-
260	LAWC31	41	0.28	0.275	0.315	10.5	P	-	-	-	-	-

Table A.3. Properties of LAW Glasses in the Compiled Literature Database (Glasses # 1-1075).

Glass #	Glass ID	η_{1150} , P ^(a)	ϵ_{1150} , S/cm	PCT Response, g/m ²		VHT Response		SO ₃ Solubility and Melter SO ₃ Tolerance, wt%				
				NL _B	NL _{Na}	r _{as} , g/m ² /d	P/F ^(b)	BS ^(c)	SR ^(d)	Bub ^(e)	MT ^(f)	3TS ^(g)
261	LAWC31R2	-	-	-	-	-	-	-	-	-	-	-
262	LAWC31S2	-	-	-	-	-	-	0.77	-	-	-	-
263	LAWC32	39	0.317	0.21	0.275	22.7	P	-	-	-	-	-
264	LAWC32S2	-	-	-	-	-	-	0.95	-	-	-	-
265	LAWC33	-	-	0.32	0.34	1.9	P	-	-	-	-	-
266	LAWA44(Crucible)	-	-	0.54	0.47	-	-	-	-	-	-	-
267	A88AP101R1	-	-	0.685	0.585	1.4	P	-	-	-	-	-
268	A88Si+15	42	0.58	1.24	1	32	P	-	-	-	-	-
269	A88Si-15	94	0.35	0.325	0.325	0.4	P	-	-	-	-	-
270	LAWB96	-	-	0.275	0.285	-	-	-	-	-	-	-
271	LAWC22(Crucible)	-	-	0.48	0.435	-	-	-	-	-	-	-
272	C22AN107	44	0.34	0.57	0.555	1.1	P	-	-	-	-	-
273	C22Si+15	35	0.42	0.635	0.83	2.5	P	-	-	-	-	-
274	C22Si-15	54	0.31	0.465	0.345	3.2	P	-	-	-	-	-
275	A1-AN105R2(LAWA44)	70	0.39	0.525	0.515	-	-	-	-	-	-	-
276	A1C1-1	58	0.44	0.435	0.435	0.7	P	-	-	-	-	-
277	A1C1-2	49	0.4	0.41	0.445	3.4	P	-	-	-	-	-
278	A1C1-3	-	-	0.455	0.42	0.7	P	-	-	-	-	-
279	C1-AN107(LAWC22)	46	0.32	0.515	0.53	8.8	P	-	-	-	-	-
280	A2-AP101(LAWA126)	60	0.35	0.78	0.56	0.8	P	-	-	-	-	-
281	A2B1-1	61	0.32	0.355	0.325	0.6	P	-	-	-	-	-
282	A2B1-2	54	0.25	0.34	0.3	0.7	P	-	-	-	-	-
283	A2B1-3	53	0.24	0.415	0.33	-	-	-	-	-	-	-
284	B1-AZ101(LAWB83)	53	0.2	0.39	0.265	1.5	P	-	-	-	-	-
285	A3-AN104(LAWA137)	35	0.29	0.54	0.53	0.7	P	-	-	-	-	-
286	A3C2-1	41	0.32	0.55	0.535	-	-	-	-	-	-	-
287	A3C2-2	35	0.28	0.545	0.555	-	-	-	-	-	-	-
288	A3C2-3	33	0.27	0.415	0.43	-	-	-	-	-	-	-
289	C2-AN102C35	35	0.27	0.34	0.375	17	P	-	-	-	-	-
290	LAWC35S2	46	0.32	-	-	9.6	P	0.89	-	-	-	-
291	WVG-G-10B	-	-	0.745	0.645	-	-	-	-	-	-	-
292	WVF-G-81A	-	-	0.315	0.29	-	-	-	-	-	-	-
293	WVF-G-21B	-	-	0.415	0.365	-	-	-	-	-	-	-
294	WVE-G-108A	-	-	0.585	0.515	-	-	-	-	-	-	-
295	WVE-G-27D	-	-	0.3	0.285	-	-	-	-	-	-	-
296	WVB-G-124B	-	-	0.425	0.415	-	-	-	-	-	-	-
297	WVB-G-93A	-	-	0.475	0.48	-	-	-	-	-	-	-
298	WVA-G-100B	-	-	0.395	0.37	-	-	-	-	-	-	-
299	WVJ-G-109D	-	-	0.245	0.22	-	-	-	-	-	-	-
300	WVK-G-41A	-	-	0.25	0.23	-	-	-	-	-	-	-
301	WVN-G-110A	-	-	0.28	0.27	-	-	-	-	-	-	-
302	WVO-G-44B	-	-	0.22	0.23	-	-	-	-	-	-	-
303	WVD-G-25A	-	-	0.46	0.46	-	-	-	-	-	-	-
304	WVC-G-107B	-	-	0.285	0.26	-	-	-	-	-	-	-
305	WVH-G-57B	-	-	0.24	0.245	-	-	-	-	-	-	-
306	WVG-G-88D	-	-	0.315	0.345	-	-	-	-	-	-	-
307	WVH-G-13A	-	-	0.195	0.22	-	-	-	-	-	-	-
308	LAWB53FCC	-	-	-	-	8.5*	P	-	-	-	-	-
309	LAWB87	64	0.29	0.265	0.21	1.2	P	-	-	-	-	-
310	LAWB87S	-	-	-	-	-	-	1.11	-	-	-	-
311	LAWB88	52	0.275	0.195	0.16	3.8	P	-	-	-	-	-
312	LAWB88S	-	-	-	-	-	-	1.56	-	-	-	-
313	LB88SRCC-2	-	-	-	-	3.4*	P	-	-	-	-	-
314	LAWA125	42	0.464	0.964	0.809	37.9	P	-	-	-	-	-
315	LAWA126	63	0.395	0.598	0.524	2.4	P	-	-	-	-	-
316	LAWA126R3	-	-	-	-	-	-	-	-	-	-	-
317	PNLA126CC	-	-	0.448*	0.393*	1.4*	P	-	-	-	-	-
318	LAWA127R1	85	0.295	0.334	0.342	-	-	-	-	-	-	-
319	LAWA127R2	-	-	0.365	0.353	0.4	P	-	-	-	-	-
320	LAWA128	-	-	0.314	0.434	0.9	P	-	-	-	-	-
321	LAWA128R1	94	0.393	-	-	-	-	-	-	-	-	-
322	LAWA129	-	-	0.271	0.372	-	-	-	-	-	-	-
323	LAWA129R1	108	0.323	-	-	2.4	P	-	-	-	-	-
324	LB83PNCC	-	-	0.235*	0.23*	1.5*	P	-	-	-	-	-
325	LB83PNCC	-	-	-	-	1.7*	P	-	-	-	-	-

Table A.3. Properties of LAW Glasses in the Compiled Literature Database (Glasses # 1-1075).

Glass #	Glass ID	η_{1150} , P ^(a)	ϵ_{1150} , S/cm	PCT Response, g/m ²		VHT Response		SO ₃ Solubility and Melter SO ₃ Tolerance, wt%				
				NL _B	NL _{Na}	r _a , g/m ² /d	P/F ^(b)	BS ^(c)	SR ^(d)	Bub ^(e)	MT ^(f)	3TS ^(g)
326	LAWA44R10	71	0.288	-	-	-	-	-	-	-	-	-
327	LA44PNCC	58*	0.283*	0.335*	0.335*	0.8*	P	-	-	-	-	-
328	LA44PNCC	-	-	-	-	-	-	-	-	-	-	-
329	LA137SRCCC	-	-	0.54*	0.485*	5.5*	P	-	-	-	-	-
330	A3-AN104	-	-	-	-	-	-	-	-	-	-	-
331	LAWM1	36	0.162	0.075	0.145	9.1	P	-	0.87	-	-	-
332	LAWM2	21	0.187	0.335	0.43	8.3	P	-	0.85	-	-	-
333	LAWM3	18	0.365	0.4	0.58	3.8	P	-	0.78	-	-	-
334	LAWM4	13	0.192	0.23	0.3	0.6	P	-	1.08	-	-	-
335	LAWM5	123	0.198	0.125	0.14	0.8	P	-	0.62	-	-	-
336	LAWM6	50	0.13	0.275	0.355	2.1	P	-	0.49	-	-	-
337	LAWM7	117	0.077	0.125	0.215	2.9	P	-	0.95	-	-	-
338	LAWM8	-	-	0.16	0.14	1.4	P	-	0.72	-	-	-
339	LAWM9	126	0.091	0.105	0.255	0.1	P	-	0.44	-	-	-
340	LAWM10	14	0.424	0.12	0.22	12.6	P	-	0.9	-	-	-
341	LAWM11	13	0.487	0.58	0.705	77.3	F	-	1.21	-	-	-
342	LAWM12	14	0.526	14.85	8.045	-	F	-	0.77	-	-	-
343	LAWM13	14	0.733	1.24	2.465	-	F	-	1.02	-	-	-
344	LAWM14	47	0.488	1	1.08	-	F	-	0.74	-	-	-
345	LAWM15	65	0.57	1.085	0.77	94.5	F	-	0.43	-	-	-
346	LAWM16	26	0.299	0.145	0.21	7.8	P	-	0.68	-	-	-
347	LAWM17	33	0.428	6.265	3.99	0.3	P	-	0.45	-	-	-
348	LAWM18	-	-	0.215	0.255	1.7	P	-	0.75	-	-	-
349	LAWM19	-	-	0.25	0.275	0.1	P	-	0.56	-	-	-
350	LAWM20	-	-	1.335	1.36	12.8	P	-	0.46	-	-	-
351	LAWM21	-	-	0.445	0.48	1	P	-	0.85	-	-	-
352	LAWM22	-	-	0.195	0.31	0.2	P	-	0.42	-	-	-
353	LAWM23	-	-	0.14	0.255	1	P	-	0.63	-	-	-
354	LAWM24	-	-	0.525	0.41	13.6	P	-	0.47	-	-	-
355	LAWM25	-	-	0.41	0.29	4.5	P	-	0.35	-	-	-
356	LAWM26	-	-	0.21	0.18	3.4	P	-	0.55	-	-	-
357	LAWM27	-	-	0.345	0.425	5	P	-	0.56	-	-	-
358	LAWM28	-	-	0.185	0.265	0.7	P	-	0.4	-	-	-
359	LAWM29	-	-	0.25	0.245	1	P	-	0.47	-	-	-
360	LAWM30	-	-	0.59	0.51	20	P	-	0.31	-	-	-
361	LAWM31	-	-	1.135	1.095	5.3	P	-	0.85	-	-	-
362	LAWM32	42	0.407	1	0.92	-	F	-	0.52	-	-	-
363	LAWM33	-	-	2.14	2.055	3.8	P	-	0.76	-	-	-
364	LAWM34	-	-	2.61	2.135	46.4	P	-	0.73	-	-	-
365	LAWM35	25	0.304	5.265	3.315	0.4	P	-	0.41	-	-	-
366	LAWM36	-	-	0.245	0.305	11.8	P	-	0.6	-	-	-
367	LAWM37	-	-	0.62	0.495	1.1	P	-	0.59	-	-	-
368	LAWM38	-	-	0.19	0.345	18.9	P	-	0.6	-	-	-
369	LAWM39	-	-	0.27	0.23	12.4	P	-	0.47	-	-	-
370	LAWM40	-	-	0.385	0.365	0.3	P	-	0.42	-	-	-
371	LAWM41	-	-	0.18	0.295	4.7	P	-	0.59	-	-	-
372	LAWM42	-	-	0.265	0.29	0.8	P	-	0.54	-	-	-
373	LAWM43	-	-	0.33	0.325	1	P	-	0.5	-	-	-
374	LAWM44	-	-	0.25	0.285	2.2	P	-	0.46	-	-	-
375	LAWM45	-	-	0.215	0.295	4.9	P	-	0.54	-	-	-
376	LAWM46	77	0.139	0.24	0.235	0.3	P	-	0.31	-	-	-
377	LAWM47	-	-	0.26	0.365	2.8	P	-	0.61	-	-	-
378	LAWM48	-	-	0.235	0.285	0.6	P	-	0.27	-	-	-
379	LAWM49	-	-	0.27	0.25	2.5	P	-	0.48	-	-	-
380	LAWM50	-	-	0.325	0.315	0.4	P	-	0.57	-	-	-
381	LAWM51	-	-	0.345	0.36	0.6	P	-	0.58	-	-	-
382	LAWM52	-	-	0.725	0.58	3.1	P	-	0.44	-	-	-
383	LAWM53	56	0.421	0.09	0.135	9.9	P	-	0.88	-	-	-
384	LAWM54	-	-	0.185	0.185	0.3	P	-	0.36	-	-	-
385	LAWM55	-	-	17.835	11.47	-	F	-	0.81	-	-	-
386	LAWM56	51	0.433	7.29	4.89	0.7	P	-	0.59	-	-	-
387	LAWA53	-	-	0.405	0.535	-	-	-	-	-	-	-
388	LAWA56	-	-	0.87	0.59	-	-	-	-	-	-	-
389	LAWA88R1	-	-	0.815	0.65	1.4	P	-	-	-	-	-
390	LAWA102R1	-	-	0.43	0.365	-	-	-	-	-	-	-

Table A.3. Properties of LAW Glasses in the Compiled Literature Database (Glasses # 1-1075).

Glass #	Glass ID	η_{1150} , P ^(a)	ε_{1150} , S/cm	PCT Response, g/m ²		VHT Response		SO ₃ Solubility and Melter SO ₃ Tolerance, wt%				
				NL _B	NL _{Na}	r _a , g/m ² /d	P/F ^(b)	BS ^(c)	SR ^(d)	Bub ^(e)	MT ^(f)	3TS ^(g)
391	LAWA147	-	-	-	-	-	-	-	0.6	-	-	-
392	LAWA149	-	-	-	-	-	-	-	0.61	-	-	-
393	LAWA152	-	-	-	-	-	-	-	0.82	-	-	-
394	LAWA155	-	-	-	-	-	-	-	0.89	-	-	-
395	LAWA159	-	-	-	-	-	-	-	0.69	-	-	-
396	LAWA160	-	-	-	-	-	-	-	0.88	-	-	-
397	LAWA161	-	-	0.672	0.667	24.6	P	-	0.85	1.07	1	-
398	LAWA161R	-	-	-	-	25.4	P	-	-	-	-	-
399	LAWA161S2	33	0.374	-	-	-	-	-	-	-	-	-
400	LAWA162	-	-	-	-	-	-	-	0.69	-	-	-
401	LAWA163	-	-	-	-	-	-	-	0.76	-	-	-
402	LAWA164	-	-	-	-	-	-	-	0.69	-	-	-
403	LAWA165	-	-	-	-	-	-	-	0.82	-	-	-
404	LAWA166	-	-	-	-	-	-	-	0.71	-	-	-
405	LAWA167	-	-	-	-	-	-	-	0.77	-	-	-
406	LAWA168	-	-	-	-	-	-	-	0.75	-	-	-
407	WVW-G-11A	-	-	0.63	0.57	12.5	P	-	-	-	-	-
408	LAWA143	55	0.463	-	-	-	-	-	-	-	-	-
409	LAWA144	64	0.463	-	-	-	-	-	-	-	-	-
410	LAWA145	56	0.458	-	-	-	-	-	-	-	-	-
411	LAWA140	94	0.29	0.42	0.5	4	P	-	-	-	-	-
412	AN-103 Actual	-	-	0.37	0.4	-	-	-	-	-	-	-
413	AW-101 Actual	-	-	0.57	0.59	-	-	-	-	-	-	-
414	AP-101 Actual	-	-	0.65	0.65	-	-	-	-	-	-	-
415	AZ-101 Actual	-	-	0.26	0.25	-	-	-	-	-	-	-
416	AZ-102 Actual	-	-	0.2	0.16	-	-	-	-	-	-	-
417	AZ-102 Actual CCC	-	-	0.16*	0.14*	-	-	-	-	-	-	-
418	AN-107 Actual	-	-	0.35	0.42	-	-	-	-	-	-	-
419	AN-102 Actual LC Melter	-	-	0.21	0.26	-	-	-	-	-	-	-
420	AN-102 Actual	-	-	0.3	0.35	-	-	-	-	-	-	-
421	LA44CCCR2	-	-	0.33*	0.36*	0.9*	P	-	-	-	-	-
422	12U-G-86A	-	-	0.4	0.38	1.7	P	-	-	-	-	-
423	12U-G-86ACCC	-	-	-	-	1.9*	P	-	-	-	-	-
424	LAWA170	53	0.459	0.65	0.64	14.5	P	-	-	-	-	-
425	LA126CCC	-	-	0.47*	0.43*	4*	P	-	-	-	-	-
426	WVM-G-142C	-	-	0.57	0.52	-	-	-	-	-	-	-
427	LAWA102R2	-	-	0.38	0.44	-	-	-	-	-	-	-
428	WVR-G-127A	-	-	0.4	0.4	-	-	-	-	-	-	-
429	LB83CCC-1	-	-	0.26*	0.22*	1.1*	P	-	-	-	-	-
430	LAWB96	45	0.194	-	-	4.5	P	-	-	-	-	-
431	GTSD-1126	-	-	0.29	0.28	1.1	P	-	-	-	-	-
432	GTSD-1126CCC	-	-	-	-	1.5*	P	-	-	-	-	-
433	LB88SRCC-2	-	-	0.15*	0.14*	-	-	-	-	-	-	-
434	LAWB88CCC	-	-	-	-	3.8*	P	-	-	-	-	-
435	AZ-102 Surrogate	-	-	0.22	0.2	-	-	-	-	-	-	-
436	12S-G-85C	-	-	0.34	0.33	-	-	-	-	-	-	-
437	LAWC21	-	-	0.33	0.36	13.7	P	-	-	-	-	-
438	LAWC21Rev2	-	-	0.35	0.36	-	-	-	-	-	-	-
439	Surrogate #2 for AN-102	-	-	0.22	0.26	-	-	-	-	-	-	-
440	GTSD-1437	-	-	0.35	0.37	-	-	-	-	-	-	-
441	PLTC35CCC	-	-	0.25*	0.31*	6.1*	P	-	-	-	-	-
442	LAWC100	32	0.29	0.525	0.435	10.5	P	-	1	1.15	1.1	-
443	LAWC100R1	25	0.33	0.84	0.755	15.9	P	-	-	-	-	-
444	LAWC101	29	0.42	0.68	0.625	7.4	P	-	0.9	1.07	-	-
445	LAWC102	22	0.46	0.91	0.82	15.6	P	-	1.02	1.12	-	-
446	LAWC103	22	0.43	1.075	0.97	0.6	P	-	0.97	1.1	-	-
447	WVY-G-95A	25	0.35	0.92	0.78	11.3	P	-	-	-	-	-
448	LAWE3	52	0.404	0.955	0.705	14.2	P	-	-	-	-	-
449	WVZ-G-61D	52	0.41	0.71	0.685	19.3	P	-	-	-	-	-
450	DWV-G-51B	44*	0.404	1.405	1.135	11	P	-	-	-	-	-
451	LAWE7H	21	0.4	0.535	0.515	16.8	P	-	-	-	-	-
452	AWV-G-78A	26	0.362	0.54	0.51	9.6	P	-	-	-	-	-
453	BWV-G-142B	27*	0.374	0.49	0.535	7	P	-	-	-	-	-
454	LAWE10H	42	0.201	0.23	0.215	1.9	P	-	-	-	-	-
455	BWV-G-32B	50	0.216	0.245	0.26	2.2	P	-	-	-	-	-

Table A.3. Properties of LAW Glasses in the Compiled Literature Database (Glasses # 1-1075).

Glass #	Glass ID	η_{1150} , P ^(a)	ϵ_{1150} , S/cm	PCT Response, g/m ²		VHT Response		SO ₃ Solubility and Melter SO ₃ Tolerance, wt%				
				NL _B	NL _{Na}	r _a , g/m ² /d	P/F ^(b)	BS ^(c)	SR ^(d)	Bub ^(e)	MT ^(f)	3TS ^(g)
456	LAWCrP1	87	0.294	0.276	0.326	0.2	P	-	-	-	-	-
457	LAWCrP1R	63	0.524	0.283	0.328	3.5	P	-	-	-	-	-
458	LAWCrP2	66	0.381	0.303	0.328	1.8	P	-	-	-	-	-
459	LAWCrP2R	45	0.658	0.558	0.519	23.9	P	-	-	-	-	-
460	LAWCrP3	95	0.339	0.285	0.326	0.2	P	-	-	-	-	-
461	LAWCrP3R	56	0.519	0.376	0.424	8.7	P	-	-	-	-	-
462	LAWCrP4	67	0.363	0.436	0.409	0.7	P	-	-	-	-	-
463	LAWCrP4R	45	0.704	0.437	0.437	22.1	P	-	-	-	-	-
464	LAWCrP5	29	0.356	0.733	0.734	0.9	P	-	-	-	-	-
465	LAWCrP6	-	-	0.335	0.288	1.4	P	-	-	-	-	-
466	LAWCrP7	-	-	0.242	0.178	1.3	P	-	-	-	-	-
467	LAWCrP8CCC	-	-	0.333*	0.243*	1.7*	P	-	-	-	-	-
468	LAWCrP9CCC	-	-	0.244*	0.143*	1.3*	P	-	-	-	-	-
469	LAWCrP10CCC	-	-	0.147*	0.146*	1.1*	P	-	-	-	-	-
470	LAWCrP11CCC	-	-	0.584*	0.549*	20.5*	P	-	-	-	-	-
471	LAWCrP12CCC	-	-	0.203*	0.228*	7.5*	P	-	-	-	-	-
472	LAWCrP13CCC	-	-	0.253*	0.245*	10.2*	P	-	-	-	-	-
473	LAWCrP14CCC	-	-	0.133*	0.143*	3.1*	P	-	-	-	-	-
474	LAWCrP15H	-	-	-	-	71.1	F	-	-	-	-	-
475	LAWCrP16H	48	0.496	1.201	1.06	81.4	F	-	-	-	-	-
476	LAWCrP17H	51	0.531	1.258	0.989	67.9	F	-	-	-	-	-
477	LAWCrP18H	43	0.424	1.494	1.203	-	F	-	-	-	-	-
478	LAWCrP19H	51	0.455	1.138	1.026	53.6	F	-	-	-	-	-
479	LAWCrP20H	60	0.487	0.829	0.816	50.7	F	-	-	-	-	-
480	LAWCrP21H	28	0.545	1.316	1.032	15.7	P	-	-	-	-	-
481	LAWCrP22H	-	-	1.103	0.822	17.3	P	-	-	-	-	-
482	LAWCrP23H	57	0.484	0.385	0.45	14.8	P	-	-	-	-	-
483	LAWCrP24H	47	0.448	1.184	0.895	3.3	P	-	-	-	-	-
484	LAWCrP25H	-	-	1.83	1.379	39.9	P	-	-	-	-	-
485	LAWCrP26H	-	-	0.751	0.627	12.7	P	-	-	-	-	-
486	LAWCrP27H	40	0.668	1.246	0.958	72.3	F	-	-	-	-	-
487	LAWCrP28H	-	-	0.979	0.78	3	P	-	-	-	-	-
488	LAWCrP29H	-	-	1.319	1.139	57.6	F	-	-	-	-	-
489	LAWCrP30H	31	0.619	1.102	0.784	49.1	P	-	-	-	-	-
490	LAWCrP31H	-	-	1.348	0.992	28.7	P	-	-	-	-	-
491	LAWCrP32H	32	0.49	2.428	1.749	25.8	P	-	-	-	-	-
492	LAWCrP33H	-	-	0.795	0.665	31.2	P	-	-	-	-	-
493	LAWCrP34H	-	-	1.609	1.305	89.8	F	-	-	-	-	-
494	LAWCrP35H	43	0.487	2.194	1.758	108.2	F	-	-	-	-	-
495	LAWCrP36H	-	-	1.58	1.315	54.7	F	-	-	-	-	-
496	LAWCrP37H	33	0.514	0.994	1.06	52.1	F	-	-	-	-	-
497	LAWCrP38H	-	-	0.53	0.572	1.5	P	-	-	-	-	-
498	LAWCrP39H	42	0.447	0.562	0.587	0.8	P	-	-	-	-	-
499	LAWCrP40H	-	-	1.188	0.978	9.9	P	-	-	-	-	-
500	LAWCrP41H	21	0.585	1.315	1.025	-	F	-	0.94	-	-	-
501	LAWCrP42H	19	0.563	0.855	0.805	-	F	-	1.01	1.15	-	-
502	LAWCrP43H	24	0.576	0.98	0.93	76.9	F	-	0.93	1	-	-
503	LAWCrP44H	32	0.548	0.96	1.12	27.7	P	-	0.83	-	-	-
504	LAWCrP45H	26	0.572	0.885	1.075	45.8	P	-	0.96	1	-	-
505	LAWCrP46H	35	0.576	0.43	0.685	16.8	P	-	0.96	1.01	-	-
506	LAWCrP47H	19	0.637	3.34	2.33	-	F	-	1.02	-	-	-
507	LAWCrP48H	22	0.693	1.5	1.7	-	F	-	1.06	-	-	-
508	LAWCrP49H	26	0.678	1.2	1.46	-	F	-	0.98	-	-	-
509	LAWCrP50H	33	0.661	1.01	1.47	64.6	F	-	0.87	-	-	-
510	LAWCrP51H	28	0.695	1.02	1.375	-	F	-	1.01	-	-	-
511	LAWCrP52H	43	0.686	0.58	1.135	-	F	-	0.98	-	-	-
512	LAWCrP53H	43	0.428	0.565	0.505	25.4	P	-	0.7	-	-	-
513	LAWCrP54H	52	0.424	0.605	0.615	7.7	P	-	0.68	-	-	-
514	LAWCrP55H	50	0.428	0.375	0.49	14.2	P	-	0.73	-	-	-
515	LAWCrP56H	58	0.392	0.43	0.535	9.9	P	-	0.73	-	-	-
516	LAWCrP57H	21	0.541	1.71	1.46	25.4	P	-	0.84	1.09	0.95	-
517	LAWCrP58H	-	-	-	-	36.9	P	-	-	-	-	-
518	LAWCrP59H	-	-	1.03*	0.84*	-	-	-	-	-	-	-
519	LAWCrP60H	25	0.548	1.665	1.305	10.6	P	-	0.77	1	-	-
520	LAWCrP61H	26	0.576	1.165	1.185	14.9	P	-	0.76	0.89	-	-

Table A.3. Properties of LAW Glasses in the Compiled Literature Database (Glasses # 1-1075).

Glass #	Glass ID	η_{1150} , P ^(a)	ε_{1150} , S/cm	PCT Response, g/m ²		VHT Response		SO ₃ Solubility and Melter SO ₃ Tolerance, wt%				
				NL _B	NL _{Na}	r _a , g/m ² /d	P/F ^(b)	BS ^(c)	SR ^(d)	Bub ^(e)	MT ^(f)	3TS ^(g)
521	LAWA190	34	0.538	1.3	1.135	26.4	P	-	0.72	0.86	-	-
522	LAWA191	28	0.529	1.065	1.13	18.9	P	-	0.78	1.05	-	-
523	LAWA192	38	0.512	1.11	0.985	27.8	P	-	0.75	0.95	-	-
524	LAWA193	35	0.508	1.375	1.225	22.9	P	-	0.71	0.83	-	-
525	LAWA194	37	0.513	0.935	1.36	22.9	P	-	0.72	-	-	-
526	LAWA195	37	0.643	1.06	1.415	25.3	P	-	0.64	-	-	-
527	LAWA196	49	0.665	0.76	0.955	78.6	F	-	0.76	-	-	-
528	LAWA197	50	0.599	0.78	0.975	23.4	P	-	0.64	-	-	-
529	LAWB97	47	0.277	0.12	0.19	19	P	-	1.05	1.33	-	-
530	LAWB98	38	0.286	0.12	0.175	16	P	-	1	-	-	-
531	LAWB99	35	0.324	0.12	0.205	14.9	P	-	1.08	1.51	1.5	-
532	LAWB100	27	0.3	0.135	0.215	13	P	-	1.02	1.7	-	-
533	LAWB101	36	0.264	0.11	0.205	13.4	P	-	0.88	-	-	-
534	LAWB102	31	0.308	0.135	0.225	17.2	P	-	0.87	-	-	-
535	LAWB103	39	0.319	0.135	0.205	6.8	P	-	1.07	1.58	-	-
536	LAWB104	28	0.309	0.11	0.205	30.1	P	-	0.96	-	-	-
537	LAWB105	29	0.277	0.26	0.33	3.3	P	-	0.96	-	-	-
538	EWV-G-89B	-	-	1.06	0.95	81.3	F	-	-	-	-	-
539	EWV-G-89B	-	-	-	-	100	F	-	-	-	-	-
540	EWV-G-89BCCC	-	-	1.125*	0.85*	25.4*	P	-	-	-	-	-
541	EWV-G-93B	-	-	-	-	79.4	F	-	-	-	-	-
542	EWV-G-93BCCC	-	-	-	-	24.6*	P	-	-	-	-	-
543	EWV-G-108B	-	-	-	-	32.1	P	-	-	-	-	-
544	DWV-G-123C	-	-	0.09	0.165	21.9	P	-	-	-	-	-
545	ORPLA1	57	0.719	0.92	0.775	-	F	-	-	-	-	-
546	ORPLA1S4	-	-	-	-	-	F	-	0.48	-	-	-
547	ORPLA2	67	0.677	0.99	0.785	130.2	F	-	-	-	-	-
548	ORPLA2S4	-	-	-	-	94.7	F	-	0.42	-	-	-
549	ORPLA3	61	0.681	0.9	0.75	114.7	F	-	-	-	-	-
550	ORPLA3S4	-	-	-	-	133.8	F	-	0.41	-	-	-
551	ORPLA4	39	0.697	1.19	1.07	113.8	F	-	-	-	-	-
552	ORPLA4S4	-	-	-	-	101.4	F	-	0.44	-	-	-
553	ORPLA5	128	0.735	0.655	0.745	103.1	F	-	-	-	-	-
554	ORPLA5S4	-	-	-	-	-	F	-	0.34	-	-	-
555	ORPLA6	124	0.789	0.575	0.63	90.7	F	-	-	-	-	-
556	ORPLA6S4	-	-	-	-	61.9	F	-	0.33	-	-	-
557	ORPLA7	101	0.624	0.655	0.655	67.7	F	-	-	-	-	-
558	ORPLA7S4	-	-	-	-	75.1	F	-	0.28	-	-	-
559	ORPLA8	55	0.753	1.43	1.025	98.7	F	-	-	-	-	-
560	ORPLA8S4	-	-	-	-	-	F	-	0.39	-	-	-
561	ORPLA9	44	0.615	0.895	0.94	56.8	F	-	-	-	-	-
562	ORPLA9S4	-	-	-	-	37.5	P	-	0.55	-	-	-
563	ORPLA10	47	0.709	0.87	0.965	15	P	-	-	-	-	-
564	ORPLA10S4	-	-	-	-	12.6	P	-	0.49	-	-	-
565	ORPLA11	110	0.645	0.485	0.605	-	F	-	-	-	-	-
566	ORPLA11S4	-	-	-	-	-	F	-	0.29	-	-	-
567	ORPLA12	128	0.579	0.375	0.505	16	P	-	-	-	-	-
568	ORPLA12S4	-	-	-	-	18.6	P	-	0.27	-	-	-
569	ORPLA13	120	0.623	0.44	0.545	20.2	P	-	-	-	-	-
570	ORPLA13S4	-	-	-	-	76.7	F	-	0.3	-	-	-
571	ORPLA14	145	0.623	0.32	0.46	8.5	P	-	-	-	-	-
572	ORPLA14S4	-	-	-	-	0.6	P	-	0.28	-	-	-
573	ORPLA15	65	0.702	0.66	0.68	25.4	P	-	-	-	-	-
574	ORPLA15S4	-	-	-	-	30.8	P	-	0.27	-	-	-
575	ORPLA16	95	0.691	0.75	0.695	107.7	F	-	-	-	-	-
576	ORPLA16S4	-	-	-	-	112.2	F	-	0.3	-	-	-
577	ORPLA17	71	0.599	0.775	0.67	74.4	F	-	-	-	-	-
578	ORPLA17S4	-	-	-	-	94.7	F	-	0.32	-	-	-
579	ORPLB1	83	0.776	0.605	0.655	-	F	-	-	0.62	-	-
580	ORPLB1S4	-	-	-	-	-	F	-	0.56	-	-	-
581	ORPLB2	77	0.751	0.845	0.77	109.9	F	-	-	0.68	-	-
582	ORPLB2S4	-	-	-	-	58.1	F	-	0.58	-	-	-
583	ORPLB3	65	0.709	0.55	0.575	38	P	-	-	-	-	-
584	ORPLB3S4	-	-	-	-	88	F	-	0.54	-	-	-
585	ORPLB4	75	0.644	0.705	0.665	40.7	P	-	-	0.7	0.85	-

Table A.3. Properties of LAW Glasses in the Compiled Literature Database (Glasses # 1-1075).

Glass #	Glass ID	η_{1150} , P ^(a)	ε_{1150} , S/cm	PCT Response, g/m ²		VHT Response		SO ₃ Solubility and Melter SO ₃ Tolerance, wt%				
				NL _B	NL _{Na}	r _a , g/m ² /d	P/F ^(b)	BS ^(c)	SR ^(d)	Bub ^(e)	MT ^(f)	3TS ^(g)
586	ORPLB4S4	-	-	-	-	35.3	P	-	0.52	-	-	-
587	ORPLC1	59	0.782	-	-	123.2	F	-	-	0.58	-	-
588	ORPLC1S4	-	-	-	-	117.7	F	-	0.59	-	-	-
589	ORPLC2	27	0.559	1.12	1.125	-	F	-	-	-	-	-
590	ORPLC2S4	-	-	-	-	83.1	F	-	0.68	-	-	-
591	ORPLC3	-	-	1.74	1.28	-	F	-	-	-	-	-
592	ORPLC3S4	-	-	-	-	-	F	-	0.63	-	-	-
593	ORPLC4	-	-	1.045	1.03	-	F	-	-	1.09	-	-
594	ORPLC4S4	-	-	-	-	-	F	-	0.7	-	-	-
595	ORPLC5	74	0.532	0.85	0.745	40	P	-	-	-	0.7	-
596	ORPLC5S4	-	-	-	-	24.7	P	-	0.56	-	-	-
597	ORPLD1	33	0.347	0.66	0.72	10.9	P	-	-	-	1.1	-
598	ORPLD1S4	-	-	-	-	15.6	P	-	0.7	-	-	-
599	ORPLD2	-	-	0.57	0.75	10.9	P	-	-	-	-	-
600	ORPLD2S4	-	-	-	-	3.8	P	-	0.82	-	-	-
601	ORPLD3	-	-	0.42	0.655	10.9	P	-	-	-	-	-
602	ORPLD3S4	-	-	-	-	23.1	P	-	0.89	-	-	-
603	ORPLE1	20	0.458	0.27	0.64	19.9	P	-	1.66	1.66	-	-
604	ORPLE2	22	0.477	0.355	0.455	29.2	P	-	1.43	1.38	-	-
605	ORPLE3	17	0.467	0.295	0.505	18.9	P	-	1.24	1.51	-	-
606	ORPLE4	19	0.481	0.28	0.525	41.5	P	-	1.3	1.44	-	-
607	ORPLE5	23	0.482	0.365	0.72	104.9	F	-	1.18	-	-	-
608	ORPLE6	17	0.486	0.225	0.46	24.4	P	-	1.24	1.5	-	-
609	ORPLE7	17	0.485	0.215	0.43	40.6	P	-	1.23	1.52	-	-
610	ORPLE8	17	0.52	0.12	0.38	34.8	P	-	1.26	-	-	-
611	ORPLE9	22	0.463	0.17	0.375	27.4	P	-	1.19	1.44	-	-
612	ORPLE10	20	0.492	0.225	0.37	32.4	P	-	1.24	-	-	-
613	ORPLE11	22	0.442	0.155	0.345	31.5	P	-	1.29	-	-	-
614	ORPLE12	22	0.547	0.25	0.395	30.6	P	-	1.2	1.55	1.5	-
615	Q10-G-134A	-	-	0.255	0.385	33.2	P	-	-	-	-	-
616	R10-G-91E	-	-	-	-	61.2	F	-	-	-	-	-
617	R10-G-155A	-	-	0.935	0.83	82.9	F	-	-	-	-	-
618	S10-G-45A	-	-	0.815	0.705	53.1	F	-	-	-	-	-
619	S10-G-45AR	-	-	-	-	66.7	F	-	-	-	-	-
620	S10-G-101B	-	-	0.675	0.605	32.2	P	-	-	-	-	-
621	S10-G-101BR	-	-	-	-	26.5	P	-	-	-	-	-
622	T10-G-16A	-	-	0.345	0.395	10.9	P	-	-	-	-	-
623	FWV-G-35B	56	0.228	0.16	0.17	1	P	-	-	-	-	-
624	FWV-G-63B	32	0.388	0.14	0.245	9.7	P	-	-	-	-	-
625	LAW4H	44	0.455	0.63	0.6	16.2	P	-	-	-	-	-
626	FWV-G-108B	49*	0.496	0.53	0.455	2.1	P	-	-	-	-	-
627	FWV-G-138A	54	0.508	0.52	0.47	6.7	P	-	-	-	-	-
628	GWV-G-36D	53*	0.543	0.445	0.445	10.2	P	-	-	-	-	-
629	GWV-G-65A	58*	0.429	0.655	0.53	4	P	-	-	-	-	-
630	GWV-G-110A	77	0.392	0.74	0.565	8.7	P	-	-	-	-	-
631	GWV-G-133B	46	0.397	0.7	0.51	21	P	-	-	-	-	-
632	A3-AN104	-	-	-	-	1.2	P	-	-	-	-	-
633	A3-AN104	-	-	-	-	0.6	P	-	-	-	-	-
634	LA137SRCCC	-	-	-	-	3.8*	P	-	-	-	-	-
635	LA137SRCCC	-	-	-	-	1.4*	P	-	-	-	-	-
636	LAWA137	-	-	-	-	13	P	-	-	-	-	-
637	LAWA137	-	-	-	-	17.9	P	-	-	-	-	-
638	LAWCrP11	-	-	0.341	0.323	1.3	P	-	-	-	-	-
639	LAWCrP11	-	-	-	-	1.2	P	-	-	-	-	-
640	LAWCrP11CCC	-	-	0.333*	0.293*	8.2*	P	-	-	-	-	-
641	LAWCrP11CCC	-	-	-	-	7.8*	P	-	-	-	-	-
642	LAWCrP12	-	-	0.378	0.363	1.2	P	-	-	-	-	-
643	LAWCrP12	-	-	-	-	1.1	P	-	-	-	-	-
644	LAWCrP12CCC	-	-	0.334*	0.31*	10.9*	P	-	-	-	-	-
645	LAWCrP12CCC	-	-	-	-	11.8*	P	-	-	-	-	-
646	LAWCrP6CCC	-	-	0.269*	0.231*	1.5*	P	-	-	-	-	-
647	LAWCrP6CCC	-	-	-	-	1.3*	P	-	-	-	-	-
648	LAWCrP7CCC	-	-	0.217*	0.116*	0.3*	P	-	-	-	-	-
649	LAWCrP7CCC	-	-	-	-	0.8*	P	-	-	-	-	-
650	LAW10HCr1CCC	-	-	0.326*	0.213*	3.8*	P	-	-	-	-	-

Table A.3. Properties of LAW Glasses in the Compiled Literature Database (Glasses # 1-1075).

Glass #	Glass ID	η_{1150} , P ^(a)	ϵ_{1150} , S/cm	PCT Response, g/m ²		VHT Response		SO ₃ Solubility and Melter SO ₃ Tolerance, wt%				
				NL _B	NL _{Na}	r _a , g/m ² /d	P/F ^(b)	BS ^(c)	SR ^(d)	Bub ^(e)	MT ^(f)	3TS ^(g)
651	LAW10HCr1CCC	-	-	-	-	1.8*	P	-	-	-	-	-
652	LAW9HCr1	-	-	0.165	0.211	1	P	-	-	-	-	-
653	LAW9HCr1	-	-	-	-	2.4	P	-	-	-	-	-
654	LAW9HCr2	-	-	0.311	0.319	1.1	P	-	-	-	-	-
655	LAW9HCr2	-	-	-	-	7.8	P	-	-	-	-	-
656	LAWM2CCC	-	-	0.414*	0.318*	13.4*	P	-	-	-	-	-
657	LAWM2CCC	-	-	-	-	15.5*	P	-	-	-	-	-
658	LAWM7CCC	-	-	0.062*	0.125*	1.4*	P	-	-	-	-	-
659	LAWM7CCC	-	-	-	-	1.1*	P	-	-	-	-	-
660	LAWM25R1CCC	-	-	0.295*	0.254*	4.4*	P	-	-	-	-	-
661	LAWM25R1CCC	-	-	-	-	7.6*	P	-	-	-	-	-
662	LAWM39CCC	-	-	0.246*	0.252*	8.2*	P	-	-	-	-	-
663	LAWM39CCC	-	-	-	-	8.2*	P	-	-	-	-	-
664	LAWM41CCC	-	-	0.207*	0.239*	7.1*	P	-	-	-	-	-
665	LAWM41CCC	-	-	-	-	7.8*	P	-	-	-	-	-
666	LAWM43CCC	-	-	0.232*	0.253*	0.8*	P	-	-	-	-	-
667	LAWM43CCC	-	-	-	-	3.6*	P	-	-	-	-	-
668	LAW18	-	-	-	-	61.4	F	-	-	-	-	-
669	LAW18	-	-	-	-	57.9	F	-	-	-	-	-
670	LAW19	-	-	-	-	23.4	P	-	-	-	-	-
671	LAW19	-	-	-	-	19.3	P	-	-	-	-	-
672	LAW19	-	-	-	-	12	P	-	-	-	-	-
673	LAW20	-	-	-	-	107.3	F	-	-	-	-	-
674	LAW20	-	-	-	-	72.8	F	-	-	-	-	-
675	LAW21	-	-	-	-	34.2	P	-	-	-	-	-
676	LAW21	-	-	-	-	38.4	P	-	-	-	-	-
677	LAW22	-	-	-	-	18.4	P	-	-	-	-	-
678	LAW22	-	-	-	-	25.2	P	-	-	-	-	-
679	LAW23	-	-	-	-	42.2	P	-	-	-	-	-
680	LAW23	-	-	-	-	42.6	P	-	-	-	-	-
681	LAW24	-	-	-	-	64.6	F	-	-	-	-	-
682	LAW24	-	-	-	-	45.1	P	-	-	-	-	-
683	LAW25	-	-	-	-	45.1	P	-	-	-	-	-
684	LAW25	-	-	-	-	76.6	F	-	-	-	-	-
685	LAW26	-	-	-	-	44.3	P	-	-	-	-	-
686	LAW26	-	-	-	-	56.8	F	-	-	-	-	-
687	ORPLA18	60	0.719	0.555	0.58	35.8	P	-	0.3	-	-	-
688	ORPLA19	57	0.677	0.66	0.695	22.3	P	-	0.32	-	-	-
689	ORPLA20	54	0.681	0.725	0.735	7.2	P	-	0.37	-	0.7	-
690	ORPLA21	-	-	0.95	0.945	42.7	P	-	0.37	-	-	-
691	ORPLA22	-	-	0.525	0.63	2.7	P	-	0.33	-	-	-
692	ORPLA23	-	-	0.455	0.59	12	P	-	0.36	-	-	-
693	ORPLA24	-	-	0.605	0.74	12.5	P	-	0.35	-	-	-
694	ORPLA25	-	-	0.845	0.975	42.1	P	-	0.41	-	-	-
695	ORPLD4	28	0.42	0.58	0.66	13.5	P	-	0.94	-	-	-
696	ORPLD5	36	0.439	0.505	0.63	14.5	P	-	0.86	-	-	-
697	ORPLD6	30	0.456	0.565	0.675	18.1	P	-	0.89	-	1.2	-
698	ORPLD7	31	0.407	0.575	0.7	14.8	P	-	0.87	-	-	-
699	ORPLD8	29	0.487	0.69	0.79	12.8	P	-	0.88	-	-	-
700	ORPLD9	23	0.542	0.755	0.84	41.6	P	-	0.95	-	-	-
701	ORPLF1	40	0.249	0.08	0.26	4.7	P	-	1.26	-	-	-
702	ORPLF2	34	0.269	0.08	0.325	18.6	P	-	1.23	-	-	-
703	ORPLF3	33	0.269	0.14	0.305	14.5	P	-	1.24	-	-	-
704	ORPLF4	27	0.299	0.15	0.245	21.3	P	-	1.32	-	-	-
705	ORPLF4(Rep-K3)	-	-	-	-	-	-	-	-	-	-	-
706	ORPLF5	-	-	0.16	0.595	15.2	P	-	1.19	-	-	-
707	ORPLF6	-	-	0.165	0.345	16.7	P	-	1.28	-	-	-
708	ORPLF7	21	0.42	0.165	0.355	18.1	P	-	1.44	-	1.5	-
709	ORPLF7(Rep-K3)	-	-	-	-	-	-	-	-	-	-	-
710	ORPLF8	18	0.442	0.185	0.325	10.5	P	-	1.45	-	-	-
711	ORPLF9	29	0.341	0.31	0.37	30.1	P	-	1.4	-	-	-
712	ORPLF10	24	0.314	0.18	0.46	13.5	P	-	1.41	-	-	-
713	ORPLF10(Rep-K3)	-	-	-	-	-	-	-	-	-	-	-
714	ORPLF11	-	-	0.165	0.29	26.1	P	-	1.35	-	-	-
715	ORPLF12	27	0.335	0.175	0.31	24.5	P	-	1.33	-	-	-

Table A.3. Properties of LAW Glasses in the Compiled Literature Database (Glasses # 1-1075).

Glass #	Glass ID	η_{1150} , P ^(a)	ε_{1150} , S/cm	PCT Response, g/m ²		VHT Response		SO ₃ Solubility and Melter SO ₃ Tolerance, wt%				
				NL _B	NL _{Na}	r _{as} , g/m ² /d	P/F ^(b)	BS ^(c)	SR ^(d)	Bub ^(e)	MT ^(f)	3TS ^(g)
716	ORPLF13	26	0.324	0.1	0.25	11.9	P	-	1.36	-	-	-
717	ORPLF14	26	0.369	0.13	0.275	10.4	P	-	1.41	-	-	-
718	ORPLG1	132	0.312	0.235	0.32	1.9	P	-	0.36	-	-	-
719	ORPLG2	114	0.324	0.81	0.835	2.4	P	-	0.38	-	-	-
720	ORPLG3	-	-	0.46	0.645	11.6	P	-	0.4	-	-	-
721	ORPLG4	101	0.377	0.485	0.63	20.4	P	-	0.43	-	-	-
722	ORPLG5	99	0.38	0.285	0.43	4	P	-	0.4	-	-	-
723	ORPLG6	66	0.394	0.3	0.44	11.3	P	-	0.45	-	-	-
724	ORPLG7	66	0.388	0.305	0.46	16.5	P	-	0.44	-	-	-
725	ORPLG8	57	0.459	0.295	0.455	34.8	P	-	0.46	-	-	-
726	ORPLG9	51	0.539	0.51	0.59	45.3	P	-	0.48	0.65	-	-
727	ORPLG9CrS4	-	-	-	-	-	-	-	-	0.55*	-	-
728	ORPLG10	43	0.535	0.475	0.565	87.8	F	-	0.49	-	-	-
729	ORPLG11	52	0.457	0.55	0.61	8.6	P	-	0.48	-	-	-
730	ORPLG12	53	0.512	0.745	0.765	91.1	F	-	0.47	-	-	-
731	Y10-G-146C	-	-	0.65	0.66	15.5	P	-	-	-	-	-
732	Z10-G-60C	-	-	0.625	0.79	-	-	-	-	-	-	-
733	10A-G-53C	-	-	0.49	0.565	27.2	P	-	-	-	-	-
734	Z10-G-122B	-	-	0.205	0.295	23.1	P	-	-	-	-	-
735	Z10-G-153B	-	-	0.215	0.315	25.8	P	-	-	-	-	-
736	10A-G-43B	-	-	0.65	0.78	-	F	-	-	-	-	-
737	ORPLA26	-	-	0.92	0.775	50.7	F	-	0.88	-	-	-
738	ORPLA27	-	-	2.745	1.975	144.1	F	-	0.79	-	-	-
739	ORPLA28	-	-	4.66*	3.5*	111.7	F	-	0.62*	-	-	-
740	ORPLA29	-	-	3.475*	2.775*	69.9	F	-	0.44*	-	-	-
741	ORPLA30	-	-	2.86	1.84	145.8	F	-	0.72	-	-	-
742	ORPLA31	-	-	7.76*	5.335*	150.2	F	-	0.62*	-	-	-
743	ORPLA32	-	-	5.84*	4.11*	108.4	F	-	0.56*	-	-	-
744	ORPLA33	-	-	0.965	0.81	0.6	P	-	0.68	-	-	-
745	ORPLA33-1	58	0.541	0.67	0.605	0.9	P	-	0.67	-	-	-
746	ORPLA34	-	-	1.3	1.03	11.4	P	-	0.65	-	-	-
747	ORPLA35	-	-	2.75	2.015	117.7	F	-	0.7	-	-	-
748	ORPLA36	-	-	1.425	1.095	6.3	P	-	0.71	-	-	-
749	ORPLA37	-	-	2.295	1.59	13.8	P	-	0.68	-	-	-
750	ORPLA38	-	-	0.83	0.74	9.9	P	-	0.72	-	-	-
751	ORPLA38-1	56	0.641	0.73	0.675	7.8	P	-	0.71	-	0.8	-
752	ORPLG13	-	-	4.86	3.325	136.5	F	-	0.42	-	-	-
753	ORPLG14	-	-	5.155	3.51	125.7	F	-	0.42	-	-	-
754	ORPLG15	-	-	5.415	3.675	119.4	F	-	0.44	-	-	-
755	ORPLG16	-	-	2.715	1.995	-	F	-	0.45	-	-	-
756	ORPLG17	-	-	2.285	1.66	-	F	-	0.48	-	-	-
757	ORPLG18	-	-	2.465	1.78	-	F	-	0.48	-	-	-
758	ORPLG19	-	-	3.48	2.405	-	F	-	0.48	-	-	-
759	ORPLG20	-	-	0.615	0.735	3.4	P	-	0.49	-	-	-
760	ORPLG21	67	0.496	0.695	0.765	45.8	P	-	0.46	-	-	-
761	ORPLG22	69	0.499	0.47	0.72	3.5	P	-	0.49	-	-	-
762	ORPLG23	72	0.51	0.455	0.705	5.7	P	-	0.47	-	-	-
763	ORPLG24	56	0.538	0.69	0.845	71.6	F	-	0.52	-	-	-
764	ORPLG25	63	0.518	0.695	0.8	79.7	F	-	0.52	-	-	-
765	ORPLG26	62	0.571	0.635	0.765	3.5	P	-	0.46	-	-	-
766	ORPLG27	58	0.531	0.665	0.77	3.8	P	-	0.49	0.58	0.5	-
767	J10-G-24B	-	-	0.875	0.825	-	-	-	-	-	-	-
768	I10-G-135A	-	-	0.93	1.02	72.7	F	-	-	-	-	-
769	LORPM1	71.97	0.475	0.235	0.185	54.9	F	-	0.73	-	-	-
770	LORPM2R1	51.71	0.167	0.139	0.192	3.8	P	-	0.33	-	-	-
771	LORPM3	19.84	0.656	0.784	0.796	66.5	F	-	0.71	-	-	-
772	LORPM4R1	29.83	0.255	0.943	0.83	76	F	-	0.82	-	-	-
773	LORPM5	154.81	0.328	0.132	0.1	10.7	P	-	0.56	-	-	-
774	LORPM6	22.15	0.184	0.839	0.882	-	P	-	0.49	-	-	-
775	LORPM7R1	63.36	0.397	0.226	0.266	11	P	-	0.34	-	-	-
776	LORPM8R1	-	0.205	0.176	0.152	35.7	P	-	0.76	-	-	-
777	LORPM9	97.29	0.658	0.844	0.842	43.1	P	-	0.31	-	-	-
778	LORPM10R1	7.32	0.359	1.787	2.047	13.3	P	-	1.47	-	-	-
779	LORPM11	135.34	0.398	0.735	0.663	0.1	P	-	0.15	-	-	-
780	LORPM12R1	72.63	0.209	0.445	0.369	0.8	P	-	0.49	-	-	-

Table A.3. Properties of LAW Glasses in the Compiled Literature Database (Glasses # 1-1075).

Glass #	Glass ID	η_{1150} , P ^(a)	ϵ_{1150} , S/cm	PCT Response, g/m ²		VHT Response		SO ₃ Solubility and Melter SO ₃ Tolerance, wt%				
				NL _B	NL _{Na}	r _a , g/m ² /d	P/F ^(b)	BS ^(c)	SR ^(d)	Bub ^(e)	MT ^(f)	3TS ^(g)
781	LORPM13	-	0.317	0.328	0.252	51.5	F	-	0.36	-	-	-
782	LORPM14R1	11.15	0.477	0.701	0.874	9.4	P	-	0.75	-	-	-
783	LORPM15	21.79	0.368	0.681	0.7	0.5	P	-	0.67	-	-	-
784	LORPM16R1	32.95	0.367	0.281	0.248	11.8	P	-	0.57	-	-	-
785	LORPM17R1	50.47	0.443	0.538	0.549	-	F	-	0.6	-	-	-
786	LORPM18	80.8	0.32	0.205	0.253	0.4	P	-	0.36	-	-	-
787	LORPM19R1	37.34	0.385	0.325	0.313	0.4	P	-	0.52	-	-	-
788	LORPM20R1	33.13	0.465	0.39	0.401	85.8	F	-	0.6	-	-	-
789	LORPM21	26.93	0.257	0.194	0.34	2.3	P	-	0.42	-	-	-
790	LORPM22	16.99	0.549	0.184	0.697	1.3	P	-	0.48	-	-	-
791	LORPM23	-	0.376	0.295	0.274	8.8	P	-	0.36	-	-	-
792	LORPM24	-	0.223	0.259	0.353	1.6	P	-	0.28	-	-	-
793	LORPM25	45.44	0.439	0.74	0.588	60.7	F	-	0.34	-	-	-
794	LORPM26	-	0.133	0.142	0.211	9	P	-	0.38	-	-	-
795	LORPM27	56.69	0.319	0.292	0.311	3.2	P	-	0.58	-	-	-
796	LORPM28	24.96	0.571	-	-	-	-	-	-	-	-	-
797	LORPM28R1	-	-	3.845	2.094	19.5	P	-	0.6	-	-	-
798	LORPM28R1	-	-	3.709	2.124	-	-	-	-	-	-	-
799	LORPM29	-	0.4	0.418	0.37	3.4	P	-	0.55	-	-	-
800	LORPM30	13.84	0.256	0.474	0.659	0.2	P	-	0.47	-	-	-
801	LORPM31	-	0.417	0.297	0.168	44.6	P	-	0.6	-	-	-
802	LORPM32	25.16	0.342	0.576	0.521	56.4	F	-	0.6	-	-	-
803	LORPM33	54.98	0.296	0.261	0.208	2.6	P	-	0.31	-	-	-
804	LORPM34	21.22	0.348	0.501	0.436	1.2	P	-	0.6	-	-	-
805	LORPM35	30.4	0.476	0.63	0.673	37.1	P	-	0.4	-	-	-
806	LORPM36	20.66	0.396	0.396	0.375	0.5	P	-	0.43	-	-	-
807	LORPM37	17.32	0.385	0.52	0.479	60.4	F	-	0.52	-	-	-
808	LORPM38	56.26	0.251	0.371	0.389	0.2	P	-	0.42	-	-	-
809	LORPM39	10.1	0.68	2.672	1.99	35.2	P	-	0.73	-	-	-
810	LORPM40	45.61	0.291	0.302	0.309	1.1	P	-	0.31	-	-	-
811	ORPLA39	-	-	-	-	-	-	-	0.74	-	-	-
812	ORPLA40	-	-	-	-	-	-	-	0.73	-	-	-
813	ORPLA41	-	-	-	-	-	-	-	0.66	-	-	-
814	ORPLA42	-	-	-	-	-	-	-	0.67	-	-	-
815	ORPLA43	89	0.595	0.295	0.475	2.4	P	-	0.52	-	-	-
816	ORPLA43R1	-	-	-	-	-	-	-	-	-	-	-
817	ORPLA43R1	-	-	-	-	-	-	-	-	-	-	-
818	ORPLA44	-	-	-	-	11.1	P	-	0.63	-	-	-
819	ORPLA45	-	-	-	-	-	-	-	0.64	-	-	-
820	ORPLA46	67	0.595	-	-	1.9	P	-	0.63	-	-	-
821	ORPLA46	-	-	-	-	-	-	-	-	-	-	-
822	ORPLA47	-	-	-	-	30.9	P	-	0.66	-	-	-
823	ORPLA48	63	0.589	0.35	0.555	34	P	-	0.6	-	-	-
824	ORPLA49	-	-	-	-	26.3	P	-	0.63	-	-	-
825	ORPLA50	-	-	-	-	38.1	P	-	0.72	-	-	-
826	ORPLA51	70	0.662	0.37	0.54	2.1	P	-	0.59	-	-	-
827	ORPLA52	72	0.638	0.475	0.585	37.7	P	-	0.67	-	-	-
828	ORPLA53	69	0.634	0.245	0.445	17.6	P	-	0.62	-	-	-
829	ORPLA54	74	0.63	0.42	0.575	42.6	P	-	0.64	-	-	-
830	ORPLA55	104	0.707	0.36	0.55	19	P	-	0.57	-	-	-
831	ORPLA56	93	0.556	0.47	0.63	104.7	F	-	0.58	-	-	-
832	ORPLA57	85	0.585	0.215	0.5	74.6	F	-	0.63	-	-	-
833	ORPLA58	90	0.553	0.305	0.495	24.8	P	-	0.63	-	-	-
834	ORPLA20R1	-	-	-	-	-	-	-	-	-	-	-
835	ORLEC1	55	0.523	0.49	0.525	26.2	P	-	0.27	-	-	-
836	ORLEC2	69	0.551	0.45	0.46	52.2	F	-	0.75	-	-	-
837	ORLEC3	73	0.475	0.41	0.415	33.3	P	-	0.78	-	-	-
838	ORLEC4	79	0.438	0.315	0.33	26.9	P	-	0.67	-	-	-
839	ORLEC5	78	0.393	0.31	0.32	2.7	P	-	0.76	-	-	-
840	ORLEC6	63	0.381	0.3	0.32	0.7	P	-	0.77	-	-	-
841	ORLEC7	35	0.413	0.3	0.375	21.7	P	-	0.95	-	-	-
842	ORLEC8	25	0.421	0.3	0.39	25.5	P	-	1.06	-	-	-
843	ORLEC9	21	0.393	0.285	0.365	20.8	P	-	1.21	-	-	-
844	ORLEC10	57	0.532	0.36	0.45	1.3	P	-	0.33	-	-	-
845	ORLEC11	55	0.502	0.405	0.47	29.4	P	-	0.31	-	-	-

Table A.3. Properties of LAW Glasses in the Compiled Literature Database (Glasses # 1-1075).

Glass #	Glass ID	η_{1150} , P ^(a)	ε_{1150} , S/cm	PCT Response, g/m ²		VHT Response		SO ₃ Solubility and Melter SO ₃ Tolerance, wt%				
				NL _B	NL _{Na}	r _{as} , g/m ² /d	P/F ^(b)	BS ^(c)	SR ^(d)	Bub ^(e)	MT ^(f)	3TS ^(g)
846	ORLEC12	60	0.431	0.635	0.605	41.1	P	-	0.28	-	-	-
847	ORLEC13	64	0.561	0.42	0.475	4.6	P	-	0.43	-	-	-
848	ORLEC14	66	0.567	0.475	0.48	1.6	P	-	0.61	0.68	-	-
849	ORLEC15	64	0.579	0.49	0.495	2.5	P	-	0.75	-	-	-
850	ORLEC16	77	0.531	0.435	0.435	20.9	P	-	0.77	0.73	-	-
851	ORLEC17	82	0.459	0.425	0.415	38.4	P	-	0.77	-	-	-
852	ORLEC18	79	0.443	0.36	0.38	23.6	P	-	0.76	-	-	-
853	ORLEC19	76	0.35	0.33	0.365	17.9	P	-	0.79	0.81	-	-
854	ORLEC20	67	0.36	0.3	0.365	22.1	P	-	0.82	-	-	-
855	ORLEC21	41	0.39	0.31	0.4	33.9	P	-	1.02	-	-	-
856	ORLEC22	34	0.393	0.28	0.39	35.5	P	-	1.14	1.41	-	-
857	ORLEC23	31	0.397	0.265	0.36	40.7	P	-	1.25	-	-	-
858	ORLEC24	65	0.504	0.46	0.47	2.3	P	-	0.61	-	-	-
859	ORLEC25	61	0.448	0.81	0.715	74.4	F	-	0.57	-	-	-
860	ORLEC25	-	-	-	-	78.8	F	-	-	-	-	-
861	ORLEC25	-	-	-	-	75.7	F	-	-	-	-	-
862	ORLEC26	62	0.514	0.365	0.445	0.6	P	-	0.45	0.59	-	-
863	ORLEC27	61	0.431	0.68	0.64	38.8	P	-	0.43	0.51	-	-
864	ORLEC28	65	0.485	0.51	0.51	6.5	P	-	0.46	0.61	-	-
865	OWV-G-144E	51	0.455	0.84	0.61	21.9	P	-	-	-	-	-
866	OWV-G-144E	-	-	-	-	27.8	P	-	-	-	-	-
867	OWV-G-109B	56	0.455	0.615	0.515	1.7	P	-	-	-	-	-
868	OWV-G-109B	-	-	-	-	0.9	P	-	-	-	-	-
869	PWV-G-43E	50	0.442	1.39	0.945	71.7	F	-	-	-	-	-
870	PWV-G-43E	-	-	-	-	48.5	P	-	-	-	-	-
871	PWV-G-93A	55	0.461	0.765	0.585	2.5	P	-	-	-	-	-
872	PWV-G-93A	-	-	-	-	1.5	P	-	-	-	-	-
873	ORLEC29	70	0.452	0.555	0.44	38.1	P	-	0.74	0.8	-	-
874	ORLEC30	65	0.453	0.51	0.42	39.4	P	-	0.8	-	-	-
875	ORLEC31	77	0.413	0.435	0.395	20.4	P	-	0.8	0.91	-	-
876	ORLEC32	68	0.384	0.39	0.385	16.9	P	-	0.89	-	-	-
877	ORLEC33	58	0.501	0.74	0.55	28.8	P	-	0.7	0.86	-	-
878	ORLEC34	55	0.477	0.9	0.68	27.1	P	-	0.85	0.99	-	-
879	ORLEC35	56	0.389	0.755	0.62	28.7	P	-	0.82	0.98	-	-
880	ORLEC36	58	0.352	0.515	0.46	10.5	P	-	0.86	-	-	-
881	ORLEC37	38	0.433	0.875	0.755	34.9	P	-	1.01	1.22	-	-
882	ORLEC38	32	0.472	-	-	42.6	P	-	1.15	1.29	-	-
883	ORLEC39	53	0.344	0.39	0.375	24.7	P	-	0.87	-	-	-
884	ORLEC40	34	0.405	0.36	0.385	29.4	P	-	1.1	-	-	-
885	ORLEC41	26	0.389	0.34	0.38	38.5	P	-	1.2	-	-	-
886	ORLEC42	26	0.377	0.31	0.35	27.8	P	-	1.28	-	-	-
887	QWV-G-107B	59	0.561	0.425	0.49	1.1	P	-	-	-	-	-
888	PWV-G-130C	67	0.546	0.49	0.445	0.5	P	-	-	-	-	-
889	PWV-G-130C	-	-	-	-	1.8	P	-	-	-	-	-
890	QWV-G-29C	71	0.414	0.365	0.37	12.3	P	-	-	-	-	-
891	QWV-G-75B	32	0.433	0.31	0.405	33.3	P	-	-	-	-	-
892	ORLEC43	44	0.434	0.875	0.745	35.3	P	-	1	-	-	-
893	ORLEC44	36	0.432	0.49	0.52	30	P	-	1.03	1.25	-	-
894	ORLEC45	31	0.464	0.505	0.465	28.9	P	-	1.15	-	-	-
895	ORLEC46	27	0.456	0.345	0.405	26.6	P	-	1.13	1.44	-	-
896	ORLEC47	25	0.422	0.35	0.38	47.3	P	-	1.28	-	-	-
897	ORLEC48R	24	0.423	0.275	0.435	45.8	P	-	1.3	1.61	-	-
898	ORLEC49	55	0.574	0.61	0.48	0.6	P	-	0.45	-	-	-
899	ORLEC49R	-	-	-	-	-	-	-	-	-	-	-
900	ORLEC50	54	0.595	0.795	0.58	2.1	P	-	0.62	-	-	-
901	ORLEC51	47	0.607	0.87	0.725	2.2	P	-	0.71	-	-	-
902	ORLEC52	47	0.602	0.845	0.71	17.1	P	-	0.77	-	-	-
903	RWV-G-9C	58	0.553	0.72	0.525	24.5	P	-	-	-	-	-
904	RWV-G-48D	50	0.487	0.97	0.735	22.2	P	-	-	-	-	-
905	RWV-G-79C	37	0.484	0.695	0.63	31.4	P	-	-	-	-	-
906	RWV-G-120D	27	0.451	0.5	0.54	23.7	P	-	-	-	-	-
907	SWV-G-17A	25	0.403	0.315	0.395	30.5	P	-	-	-	-	-
908	SWV-G-17A	-	-	-	-	28.3	P	-	-	-	-	-
909	AP105DLAW1	95	0.463	-	-	11.8	P	-	0.48	-	-	-
910	AP105DLAW2	76	0.578	-	-	16.6	P	-	0.54	-	-	-

Table A.3. Properties of LAW Glasses in the Compiled Literature Database (Glasses # 1-1075).

Glass #	Glass ID	η_{1150} , P ^(a)	ε_{1150} , S/cm	PCT Response, g/m ²		VHT Response		SO ₃ Solubility and Melter SO ₃ Tolerance, wt%				
				NL _B	NL _{Na}	r _a , g/m ² /d	P/F ^(b)	BS ^(c)	SR ^(d)	Bub ^(e)	MT ^(f)	3TS ^(g)
911	AP105DLAW3	68	0.519	0.64	0.5	24.3	P	-	0.59	-	-	-
912	AP105DLAW4	57	0.558	-	-	28.2	P	-	0.57	-	-	-
913	AP105DLAW5	77	0.568	0.47	0.46	24.1	P	-	0.59	-	-	-
914	AP105DLAW6	64	0.576	0.585	0.52	30.9	P	-	0.6	-	-	-
915	AP105DLAW7	80	0.561	0.445	0.445	23.8	P	-	0.65	-	-	-
916	AP105DLAW8	69	0.575	0.52	0.5	32.3	P	-	0.59	-	-	-
917	AP105DLAW9	-	-	-	-	-	-	-	0.58	-	-	-
918	AP105DLAW10	-	-	-	-	-	-	-	0.59	-	-	-
919	AP105DLAW11	53	0.563	0.695	0.55	27.3	P	-	0.43	-	-	-
920	WDFL1	58	0.455	0.51	0.445	14	P	-	0.4	-	-	-
921	WDFL1H	47	0.552	0.77	0.62	12.3	P	-	0.5	-	-	-
922	WDFL1+15%	43	0.574	0.865	0.68	19	P	-	0.48	-	-	-
923	WDFL1-15%	86	0.343	-	-	0.5	P	-	0.33	-	-	-
924	WDFL2	38	0.386	0.29	0.31	12.2	P	-	0.58	-	-	-
925	WDFL2H	32	0.392	-	-	2.4	P	-	0.64	-	-	-
926	WDFL2+15%	29	0.42	0.405	0.41	13.3	P	-	0.67	-	-	-
927	WDFL2-15%	50	0.287	-	-	2.1	P	-	0.51	-	-	-
928	New-IL-456	22.66	0.359	0.25	0.451	19.2	P	-	-	-	-	1.949
929	New-IL-456CCC	-	-	0.254*	0.382*	-	-	-	-	-	-	-
930	New-IL-1721	25.45	0.398	1.276	1.091	95.6	F	-	-	-	-	1.647
931	New-IL-1721CCC	-	-	0.8*	0.701*	-	-	-	-	-	-	-
932	New-IL-1721(PNNL)	-	-	-	-	-	-	-	-	-	-	1.716
933	New-IL-5253	23.04	0.373	0.8	0.725	10.3	P	-	-	-	-	1.459
934	New-IL-5253CCC	-	-	1.105*	0.904*	-	-	-	-	-	-	-
935	New-IL-5255	13.93	0.5	6.597	5.12	95.2	F	-	-	-	-	1.584
936	New-IL-5255CCC	-	-	6.286*	4.504*	-	-	-	-	-	-	-
937	New-IL-42295	21.78	0.457	9.727	6.598	60	F	-	-	-	-	1.639
938	New-IL-42295CCC	-	-	8.15*	5.815*	-	-	-	-	-	-	-
939	New-IL-70316	20.61	0.389	0.313	0.674	66.6	F	-	-	-	-	1.602
940	New-IL-70316CCC	-	-	0.301*	0.633*	-	-	-	-	-	-	-
941	New-IL-87749	20.29	0.414	0.229	0.492	19.1	P	-	-	-	-	1.633
942	New-IL-87749CCC	-	-	0.156*	0.434*	-	-	-	-	-	-	-
943	New-IL-93907	48.47	0.342	0.214	0.26	37.9	P	-	-	-	-	1.134
944	New-IL-93907CCC	-	-	0.223*	0.233*	-	-	-	-	-	-	-
945	New-IL-94020	61.98	0	0.249	0.334	16.6	P	-	-	-	-	1.081
946	New-IL-94020CCC	-	-	0.204*	0.282*	-	-	-	-	-	-	-
947	New-IL-103151	29.43	0.46	1.055	1.013	287.7	F	-	-	-	-	1.48
948	New-IL-103151CCC	-	-	0.844*	0.944*	-	-	-	-	-	-	-
949	New-IL-151542	24.23	0.3	0.317	0.475	8	P	-	-	-	-	1.664
950	New-IL-151542CCC	-	-	0.336*	0.469*	-	-	-	-	-	-	-
951	New-IL-166697	24.64	0.486	0.4	0.448	80.8	F	-	-	-	-	1.474
952	New-IL-166697CCC	-	-	0.377*	0.43*	-	-	-	-	-	-	-
953	New-IL-166731	26.19	0.452	0.406	0.502	165.4	F	-	-	-	-	1.462
954	New-IL-166731CCC	-	-	2.351*	1.457*	-	-	-	-	-	-	-
955	New-OL-8445	28.21	0.156	0.265	0.319	2	P	-	-	-	-	1.459
956	New-OL-8445CCC	-	-	0.208*	0.248*	-	-	-	-	-	-	-
957	New-OL-8788Mod	259.69	0.185	0.156	0.202	1.4	P	-	-	-	-	0.602
958	New-OL-8788ModCCC	-	-	0.261*	0.211*	-	-	-	-	-	-	-
959	New-OL-14844	4.7	0.544	3.805	3.687	2.9	P	-	-	-	-	1.403*
960	New-OL-14844CCC	-	-	3.499*	3.394*	-	-	-	-	-	-	-
961	New-OL-15493	11.55	0.566	0.476	1.617	167	F	-	-	-	-	2.138
962	New-OL-15493CCC	-	-	44.793*	20.679*	-	-	-	-	-	-	-
963	New-OL-17130	15.4	0.488	11.385	8.464	262.5	F	-	-	-	-	2.379
964	New-OL-17130CCC	-	-	10.719*	8.17*	-	-	-	-	-	-	-
965	New-OL-45748	27.88	0.377	0.113	0.201	7.4	P	-	-	-	-	1.637
966	New-OL-45748CCC	-	-	0.481*	0.184*	-	-	-	-	-	-	-
967	New-OL-54017	52.72	0.199	0.181	0.258	0.3	P	-	-	-	-	1.331
968	New-OL-54017CCC	-	-	0.101*	0.226*	-	-	-	-	-	-	-
969	New-OL-57284	76.04	0.151	0.854	0.778	283.9	F	-	-	-	-	0.916
970	New-OL-57284CCC	-	-	1.113*	0.904*	-	-	-	-	-	-	-
971	New-OL-62380	16.91	0.156	0.165	0.251	0.1	P	-	-	-	-	1.532
972	New-OL-62380CCC	-	-	0.126*	0.227*	-	-	-	-	-	-	-
973	New-OL-62909Mod	43.78	0.246	0.211	0.305	3.9	P	-	-	-	-	1.265
974	New-OL-62909ModCCC	-	-	0.132*	0.224*	-	-	-	-	-	-	-
975	New-OL-65959Mod	14.3	0.472	1.67	1.218	262.2	F	-	-	-	-	1.68

Table A.3. Properties of LAW Glasses in the Compiled Literature Database (Glasses # 1-1075).

Glass #	Glass ID	η_{1150} , P ^(a)	ϵ_{1150} , S/cm	PCT Response, g/m ²		VHT Response		SO ₃ Solubility and Melter SO ₃ Tolerance, wt%				
				NL _B	NL _{Na}	r _a , g/m ² /d	P/F ^(b)	BS ^(c)	SR ^(d)	Bub ^(e)	MT ^(f)	3TS ^(g)
976	New-OL-65959ModCCC	-	-	23.234*	9.191*	-	-	-	-	-	-	-
977	New-OL-80309	8.14	0.434	11.52	7.563	287.7	F	-	-	-	-	1.657
978	New-OL-80309CCC	-	-	5.587*	3.562*	-	-	-	-	-	-	-
979	New-OL-90780	21.39	0.532	2.419	1.465	176.6	F	-	-	-	-	1.506
980	New-OL-90780CCC	-	-	14.07*	5.992*	-	-	-	-	-	-	-
981	New-OL-100210	42.2	0.444	1.033	1.41	1529.1	F	-	-	-	-	1.478
982	New-OL-100210CCC	-	-	0.98*	1.232*	-	-	-	-	-	-	-
983	New-OL-108249Mod	16.39	0.403	0.164	0.42	7.3	P	-	-	-	-	1.295
984	New-OL-108249ModCCC	-	-	8.055*	2.279*	-	-	-	-	-	-	-
985	New-OL-108249Mod(PNNL)	-	-	-	-	-	-	-	-	-	-	1.267
986	New-OL-116208Mod	6.91	0.558	4.303	3.935	0.7	P	-	-	-	-	1.271
987	New-OL-116208ModCCC	-	-	9.033*	5.722*	-	-	-	-	-	-	-
988	New-OL-116208Mod(PNNL)	-	-	-	-	-	-	-	-	-	-	1.464
989	New-OL-122817	35.68	0.328	0.147	0.538	34.7	P	-	-	-	-	1.977
990	New-OL-122817CCC	-	-	0.22*	0.466*	-	-	-	-	-	-	-
991	New-OL-127708Mod	78.25	0.241	0.276	0.269	2.9	P	-	-	-	-	0.85
992	New-OL-127708ModCCC	-	-	0.26*	0.219*	-	-	-	-	-	-	-
993	EWG-LAW-Centroid-1	28.25	0.388	0.402	0.524	16.1	P	-	-	-	-	-
994	EWG-LAW-Centroid-1CCC	-	-	0.444*	0.521*	-	-	-	-	-	-	-
995	EWG-LAW-Centroid-2	27.55	0.404	0.398	0.527	27.4	P	-	-	-	-	1.435
996	EWG-LAW-Centroid-2CCC	-	-	0.446*	0.526*	-	-	-	-	-	-	-
997	LAW-ORP-LD1(1)	29.37	0.34	0.467	0.596	6.2	P	-	-	-	-	1.253
998	LAW-ORP-LD1(1)CCC	-	-	0.285*	0.368*	-	-	-	-	-	-	-
999	LAW-ORP-LD1(2)	29.46	0.407	0.424	0.517	26.8	P	-	-	-	-	1.314
1000	LAW-ORP-LD1(2)CCC	-	-	0.322*	0.414*	-	-	-	-	-	-	-
1001	LAW-ORP-LD1(M)	46.18	0.33	0.303	0.354	2.5	P	-	-	-	-	1.019
1002	LAW-ORP-LD1(M)CCC	-	-	0.231*	0.299*	-	-	-	-	-	-	-
1003	LORPM1R1	-	-	-	-	-	-	-	0.83	-	-	-
1004	LORPM4R2	-	-	-	-	-	-	-	0.88	-	-	-
1005	LORPM4R2 (K3-R)	-	-	-	-	-	-	-	-	-	-	-
1006	LORPM9-repeat	-	-	-	-	-	-	-	0.35	-	-	-
1007	LORPM10R1-repeat	-	-	-	-	-	-	-	1.54	-	-	-
1008	LORPM11-repeat	-	-	-	-	-	-	-	0.25	-	-	-
1009	LORPM18-repeat	-	-	-	-	-	-	-	0.52	-	-	-
1010	LORPM38R1	-	-	-	-	-	-	-	0.5	-	-	-
1011	LORPM40R1	-	-	-	-	-	-	-	0.47	-	-	-
1012	LAWE17	-	-	-	-	-	F	-	-	-	-	-
1013	LP2-IL-01	25.14	0.569	0.688	0.927	49.8	F	-	-	-	-	1.503
1014	LP2-IL-02	62.72	0.578	0.57	0.66	0.8	P	-	-	-	-	1.18
1015	LP2-IL-03	56.64	0.59	0.384	0.556	169.4	F	-	-	-	-	1.18
1016	LP2-IL-04	25	0.582	0.68	0.954	1	P	-	-	-	-	1.484
1017	LP2-IL-05	24.53	0.502	0.502	0.569	5.2	P	-	-	-	-	1.489
1018	LP2-IL-06	46.91	0.537	1.261	0.934	132.9	F	-	-	-	-	1.035
1019	LP2-IL-07	25.9	0.534	1.474	1.281	113.2	F	-	-	-	-	1.632
1020	LP2-IL-08	35.98	0.491	0.659	0.786	12.3	P	-	-	-	-	1.373
1021	LP2-IL-09	24.21	0.626	1.734	1.347	31.6	P	-	-	-	-	1.444
1022	LP2-IL-10	47.13	0.523	0.441	0.573	106.6	F	-	-	-	-	1.337
1023	LP2-IL-11	59.28	0.532	0.291	0.48	27.2	P	-	-	-	-	1.189
1024	LP2-IL-12	62.44	0.586	0.692	0.749	45.9	P	-	-	-	-	1.468
1025	LP2-IL-13	56.11	0.469	1.011	0.816	2.1	P	-	-	-	-	1.236
1026	LP2-IL-14	27.55	0.625	1.456	1.178	39.3	P	-	-	-	-	1.496
1027	LP2-IL-15	55.56	0.61	0.89	0.681	6.3	P	-	-	-	-	1.252
1028	LP2-IL-16	43.53	0.562	0.486	0.599	47.6	P	-	-	-	-	1.338
1029	LP2-IL-17	50.87	0.514	0.889	0.706	62.7	F	-	-	-	-	1.321
1030	LP2-OL-01	85.59	0.334	0.333	0.57	0.5	P	-	-	-	-	1.489
1031	LP2-OL-02	52.56	0.462	0.469	0.523	1.2	P	-	-	-	-	1.098
1032	LP2-OL-03-MOD2	25.82	0.607	0.371	1.276	23.2	P	-	-	-	-	1.445
1033	LP2-OL-04	39.05	0.423	0.766	1.058	2.7	P	-	-	-	-	1.092
1034	LP2-OL-05	66.51	0.357	0.16	0.363	5.2	P	-	-	-	-	1.427
1035	LP2-OL-07	30.01	0.377	0.437	0.501	15.8	P	-	-	-	-	1.634
1036	LP2-OL-08-MOD	12.76	0.66	1.268	2.261	109.4	F	-	-	-	-	1.816
1037	LP2-OL-09	63.66	0.393	1.559	0.922	10.2	P	-	-	-	-	1.096
1038	LP2-OL-10-MOD	63.33	0.369	0.17	0.405	8.7	P	-	-	-	-	1.082
1039	LP2-OL-11	11.41	0.486	3.869	3.605	55.4	F	-	-	-	-	1.47
1040	LP2-OL-12	8.02	0.605	17.112	13.407	252.3	F	-	-	-	-	2.319

Table A.3. Properties of LAW Glasses in the Compiled Literature Database (Glasses # 1-1075).

Glass #	Glass ID	η_{1150} , P ^(a)	ϵ_{1150} , S/cm	PCT Response, g/m ²		VHT Response		SO ₃ Solubility and Melter SO ₃ Tolerance, wt%				
				NL _B	NL _{Na}	r _a , g/m ² /d	P/F ^(b)	BS ^(c)	SR ^(d)	Bub ^(e)	MT ^(f)	3TS ^(g)
1041	LP2-OL-13	13.31	0.567	0.516	1.943	50.8	F	-	-	-	-	1.5
1042	LP2-OL-14	9.64	0.512	7.233	6.38	-	F	-	-	-	-	2.603
1043	LP2-OL-15	12.83	0.397	0.276	0.438	1.2	P	-	-	-	-	2.022
1044	LP2-OL-16-MOD	72.96	0.421	1.304	1.306	3.8	P	-	-	-	-	1.19
1045	LP2-OL-17	25.18	0.565	5.617	4.744	-	F	-	-	-	-	1.786
1046	LP2-OL-18	26.74	0.433	1.183	1.186	9.5	P	-	-	-	-	1.195
1047	LP2-OL-19	95.88	0.45	0.389	0.913	121.1	F	-	-	-	-	0.956
1048	LP2-OL-20	45.86	0.541	0.27	1.091	261	F	-	-	-	-	1.87
1049	LP2-OL-21	42.41	0.498	0.451	0.521	24.6	P	-	-	-	-	1.127
1050	LP2-OL-22	32.19	0.406	0.198	0.539	1.4	P	-	-	-	-	1.139
1051	LP2-OL-23	12.1	0.424	0.481	0.597	2.1	P	-	-	-	-	1.707
1052	LP2-OL-24	37.31	0.525	0.457	0.873	13.9	P	-	-	-	-	1.385
1053	LP2-OL-25	14.92	0.556	2.574	1.932	27.7	P	-	-	-	-	1.248
1054	LAWPH3-01	13.29	0.657	4.505	3.734	-	F	-	-	-	-	1.714
1055	LAWPH3-02	12.38	-	7.529	6.559	-	F	-	-	-	-	1.95
1056	LAWPH3-03	34.88	0.712	3.751	3.257	-	F	-	-	-	-	1.29
1057	LAWPH3-04	10.47	0.583	1.282	1.628	30	P	-	-	-	-	2.416
1058	LAWPH3-05 mod6	27.64	0.588	6.64	5.19	242.3	F	-	-	-	-	1.58
1059	LAWPH3-06	21.35	0.53	<0.3205*	0.993	6.3	P	-	-	-	-	1.592
1060	LAWPH3-07	19.61	0.693	0.501	1.168	-	F	-	-	-	-	1.905
1061	LAWPH3-08	59.26	-	0.344	0.654	0.6	P	-	-	-	-	1.317
1062	LAWPH3-09	17.16	-	1.138	1.653	55.3	F	-	-	-	-	1.641
1063	LAWPH3-10	24.34	0.686	0.835	1.234	47	P	-	-	-	-	1.557
1064	LAWPH3-11	30.2	0.575	1.623	1.471	-	F	-	-	-	-	1.559
1065	LAWPH3-12	27.02	-	1.36	0.96	79.9	F	-	-	-	-	1.353
1066	LAWPH3-12-2	-	-	1.558	1.075	-	-	-	-	-	-	-
1067	LAWPH3-13	22.25	0.611	0.405	1.287	-	F	-	-	-	-	1.628
1068	LAWPH3-14	19.91	0.676	0.797	1.32	54.1	F	-	-	-	-	2.01
1069	LAWPH3-15	15.39	-	0.873	1.475	32.9	F	-	-	-	-	1.749
1070	LAWPH3-16	14.66	-	2.747	3.408	203.7	F	-	-	-	-	1.95
1071	LAWPH3-17	13.6	-	0.532	1.713	39	F	-	-	-	-	2.076
1072	LAWPH3-17-2	-	-	0.591	1.324	-	-	-	-	-	-	-
1073	LAWPH3-18	54.74	-	0.451	0.841	3.4	P	-	-	-	-	1.143
1074	LAWPH3-19 mod1	25.83	-	0.502	1.096	39	F	-	-	-	-	1.96
1075	LAWPH3-20	28.94	0.518	0.481	0.741	8.7	F	-	-	-	-	1.727
(a) Most η_{1150} values were obtained from VSL reports where the values were calculated and rounded to zero decimal places. However, some η_{1150} values were calculated from VFT models fit to viscosity at temperature data, evaluated at 1150°C, and rounded to two decimal places. That is the number of decimal places usually recorded for viscosity (Poise) at temperature data.												
(b) P/F = Pass/Fail, where P = Pass and F = Fail. This refers to whether the VHT Alteration Rate passes or fails the WTP contractual limit of 50 g/m ² /d.												
(c) BS = Batch saturation. Excess sulfate is added to raw materials batch and melted to fabricate glass while saturating glass with sulfate.												
(d) SR = Saturation re-melting. Pre-melted glass is mixed with excess sulfate and melted to saturate glass.												
(e) Bub = Bubbling. Molten glass is bubbled with SO ₂ and O ₂ gas mixture to saturate glass.												
(f) MT = Melter tolerance. Maximum target SO ₃ concentration (glass basis) in the melter feed without salt segregation.												
(g) 3TS = Three-time saturation. Like the saturation re-melting method, but re-melted three times to fully saturate glass.												
(h) LP2-OL-06 (Mod2) did not form a glass upon melting even after two modifications of the original composition, and hence no property data could be collected for this composition.												
(i) A modified composition of glass LP2-OL-18 was investigated, but ultimately the original composition was used for all property measurements. Still, the records from data collection show this glass as modified, so for consistency with those records, “-MOD” was included in the Glass ID.												

Table A.4. Normalized compositions (in mass fractions) of 344 LAW glasses with K-3 Corrosion data.

K-3 ID Number	Glass Number from Database	Glass ID	Al ₂ O ₃	B ₂ O ₃	CaO	Cl	Cr ₂ O ₃	F	Fe ₂ O ₃	K ₂ O	Li ₂ O	MgO	Na ₂ O	P ₂ O ₅	SO ₃	SiO ₂	SuO ₂	TiO ₂	V ₂ O ₅	ZnO	ZrO ₂	Others
k001	N/A	A1-AN105R2	0.061000	0.088000	0.020000	0.011700	0.000000	0.000000	0.069000	0.004000	0.000000	0.020000	0.207000	0.000000	0.001800	0.438000	0.000000	0.020000	0.000000	0.029000	0.029000	0.001500
k002	N/A	A2-AP101	0.056028	0.098049	0.020010	0.004202	0.000000	0.003502	0.055028	0.038019	0.000000	0.015007	0.185093	0.000800	0.003500	0.440221	0.000000	0.020010	0.000000	0.029015	0.030015	0.001501
k003	282	A2B1-2	0.058959	0.098930	0.043969	0.002198	0.000000	0.002198	0.053962	0.019986	0.021984	0.021985	0.119916	0.000600	0.004200	0.462675	0.000000	0.016988	0.000000	0.038973	0.030978	0.001499
k004	283	A2B1-3	0.060097	0.100161	0.056090	0.001202	0.000000	0.001502	0.053085	0.011018	0.032052	0.026042	0.087140	0.000501	0.004700	0.474763	0.000000	0.015024	0.000000	0.044071	0.031050	0.001502
k005	330	A3-AN104	0.061055	0.099089	0.050045	0.007907	0.000000	0.000100	0.054049	0.003003	0.025023	0.015014	0.146132	0.001101	0.003500	0.461417	0.000000	0.011010	0.000000	0.030027	0.030027	0.001501
k006	286	A3C2-1	0.060957	0.097931	0.055961	0.006895	0.000000	0.000300	0.048966	0.002998	0.026981	0.014989	0.139902	0.001199	0.003800	0.463674	0.000000	0.010992	0.000000	0.032977	0.029979	0.001499
k007	287	A3C2-2	0.060975	0.096961	0.061975	0.005898	0.000000	0.000600	0.044982	0.001999	0.028988	0.014994	0.132947	0.001399	0.004000	0.466813	0.000000	0.010996	0.000000	0.034986	0.029988	0.001499
k008	288	A3C2-3	0.060951	0.094924	0.067945	0.004896	0.000000	0.000899	0.039968	0.001998	0.030975	0.014988	0.125899	0.001499	0.004900	0.469622	0.000000	0.010991	0.000000	0.037970	0.029976	0.001599
k009	919	AP105DLAW11	0.101847	0.111832	0.019970	0.005192	0.004993	0.000100	0.006989	0.004993	0.000000	0.009985	0.243633	0.001997	0.003100	0.393408	0.000000	0.000000	0.000000	0.030953	0.060908	0.000100
k010	910	AP105DLAW2	0.088982	0.109978	0.019996	0.003999	0.003999	0.000300	0.002000	0.005999	0.000000	0.009998	0.225955	0.003999	0.004900	0.434913	0.000000	0.000000	0.007998	0.029994	0.046990	0.000000
k011	911	AP105DLAW3	0.095048	0.110055	0.019010	0.004102	0.003002	0.000400	0.002001	0.006003	0.000000	0.010005	0.233117	0.004102	0.005900	0.414208	0.000000	0.000000	0.009005	0.030015	0.054027	0.000000
k012	912	AP105DLAW4	0.100071	0.110078	0.020014	0.004203	0.003002	0.000400	0.002001	0.006004	0.000000	0.010007	0.240169	0.004203	0.005500	0.394278	0.000000	0.000000	0.010007	0.030021	0.060042	0.000000
k013	914	AP105DLAW6	0.100051	0.100050	0.020010	0.004202	0.003002	0.000400	0.002001	0.006003	0.000000	0.010005	0.239120	0.004202	0.005700	0.405204	0.000000	0.000000	0.010005	0.030015	0.060030	0.000000
k014	915	AP105DLAW7	0.094924	0.099919	0.019984	0.004097	0.000000	0.000400	0.001998	0.005995	0.000000	0.009992	0.232813	0.004097	0.005200	0.427656	0.000000	0.000000	0.008993	0.029976	0.053956	0.000000
k015	916	AP105DLAW8	0.100081	0.100081	0.020016	0.004103	0.000000	0.000400	0.002002	0.006005	0.000000	0.010008	0.239192	0.004203	0.005500	0.408329	0.000000	0.000000	0.010008	0.030024	0.060048	0.000000
k016	N/A	AY102D1-01	0.059928	0.077906	0.019976	0.001598	0.000999	0.001898	0.056931	0.040951	0.000000	0.018977	0.204753	0.003196	0.005700	0.415498	0.000000	0.000000	0.000000	0.029964	0.047942	0.013783
k017	N/A	AY102D1-02	0.065066	0.073074	0.019019	0.001702	0.001001	0.002002	0.062062	0.045045	0.000000	0.018018	0.223224	0.003504	0.004800	0.393395	0.000000	0.000000	0.000000	0.028028	0.045045	0.015015
k018	N/A	AY102D1-03	0.064941	0.118893	0.001998	0.001699	0.000999	0.001998	0.061944	0.044959	0.000000	0.000999	0.222799	0.003497	0.004700	0.455588	0.000000	0.000000	0.000000	0.000000	0.014986	
k019	N/A	AY102D1-04	0.070943	0.079936	0.001998	0.001899	0.001998	0.002198	0.066946	0.047962	0.000000	0.000999	0.240807	0.003797	0.004900	0.391685	0.000000	0.000000	0.000000	0.025979	0.041966	0.015987
k020	N/A	AY102D1-05	0.080048	0.091055	0.020012	0.001601	0.001001	0.001801	0.055033	0.040024	0.000000	0.019011	0.200121	0.003202	0.004400	0.399241	0.000000	0.000000	0.000000	0.030018	0.040024	0.013408
k021	N/A	AY102D1-06R	0.062062	0.101102	0.021021	0.001502	0.001001	0.001702	0.052052	0.038038	0.000000	0.019019	0.190191	0.003003	0.004000	0.417419	0.000000	0.014014	0.000000	0.031031	0.030030	0.012813
k022	N/A	AY102D2-01	0.121975	0.089982	0.004999	0.001300	0.002999	0.001500	0.135973	0.032993	0.000000	0.001000	0.202959	0.005999	0.005200	0.359928	0.000000	0.000000	0.000000	0.000000	0.033193	
k023	N/A	AY102D2-05	0.122000	0.073000	0.005000	0.001300	0.003000	0.001500	0.136000	0.033000	0.009000	0.001000	0.203000	0.006000	0.005000	0.313000	0.000000	0.000000	0.000000	0.021000	0.034000	0.033200
k024	N/A	AY102D2-06	0.102969	0.077976	0.003999	0.001100	0.001999	0.001300	0.114965	0.027992	0.002094	0.001000	0.170948	0.004998	0.004000	0.437868	0.000000	0.000000	0.000000	0.000000	0.027892	
k025	N/A	B1-AZ101	0.061950	0.099920	0.067945	0.000200	0.000000	0.000799	0.052957	0.001998	0.042966	0.029976	0.054956	0.000400	0.004900	0.485610	0.000000	0.013989	0.000000	0.047961	0.031974	0.001499
k026	N/A	C1-AN107R1	0.061018	0.100030	0.051015	0.000700	0.000000	0.002801	0.054016	0.001000	0.025008	0.015005	0.145044	0.001301	0.002900	0.466140	0.000000	0.011003	0.000000	0.031009	0.030009	0.002001
k027	289	C2-AN102C35	0.060969	0.093953	0.072963	0.003898	0.000000	0.001099	0.035982	0.001000	0.032983	0.014992	0.119940	0.001599	0.006300	0.471763	0.000000	0.010995	0.000000	0.039980	0.029985	0.001599
k028	N/A	I10-G-130B	0.060018	0.079024	0.002700	0.002301	0.006002	0.000900	0.003001	0.057017	0.000000	0.004001	0.210063	0.001401	0.005000	0.421127	0.032010	0.000000	0.000000	0.027008	0.064019	0.000100
k029	41	LAWA104	0.066079	0.086103	0.019023	0.007209	0.000000	0.000100	0.067081	0.006007	0.000000	0.019023	0.220265	0.000400	0.001100	0.430517	0.000000	0.019023	0.000000	0.029035	0.029035	0.000000
k030	42	LAWA105	0.069972	0.082967	0.018992	0.007797	0.000000	0.000100	0.064974	0.005998	0.000000	0.018992	0.239904	0.000400	0.001100	0.413834	0.000000	0.018992	0.000000	0.027989	0.027989	0.000000
k031	315	LAWA126	0.056197	0.098345	0.020071	0.002007	0.000000	0.003011	0.055194	0.039137	0.000000	0.015053	0.184648	0.000803	0.003100	0.440547	0.000000	0.020070	0.000000	0.029102	0.030106	0.002609
k032	316	LAWA126R3	0.056186	0.098325	0.020066	0.002007	0.000000	0.003010	0.055183	0.039130	0.000000	0.015050	0.184611	0.000803	0.003300	0.440458	0.000000	0.020066	0.000000	0.029096	0.030100	0.002609
k033	318	LAWA127R1	0.056977	0.101959	0.020992	0.001799	0.000000	0.002599	0.057977	0.033986	0.000000	0.014994	0.162935	0.000700	0.001800	0.457816	0.000000	0.020992	0.000000	0.030987	0.030988	0.002499
k034	174	LAWA130	0.060018	0.089027	0.021006	0.002001	0.000000	0.003001	0.029009	0.039012	0.000000	0.012004	0.184055	0.000800	0.003300	0.461139	0.000000	0.021006	0.000000	0.041012	0.031009	0.002601
k035	177	LAWA134	0.056084	0.100151	0.020030	0.002003	0.000000	0.002904	0.056084	0.037056	0.000000	0.015023	0.177267	0.000801	0.002800	0.448675	0.000000	0.020030	0.000000	0.030045	0.030045	0.001002
k036	178	LAWA135	0.057051	0.101091	0.020018	0.001902	0.000000	0.002803	0.057051	0.036032	0.000000	0.015014	0.170154	0.000701	0.002700	0.453409	0.000000	0.020018	0.000000	0.030027	0.031028	0.001001
k037	179	LAWA136	0.057051	0.101091	0.030027	0.001902	0.000000	0.002803	0.057051	0.036032	0.000000	0.015014	0.170154	0.000701	0.002700	0.443400	0.000000	0.020018	0.000000	0.030027	0.031028	0.001001
k038	N/A	LAWA140R3	0.062019	0.090027	0.020006	0.005602	0.000000	0.000000	0.045014	0.004001	0.000000	0.015004	0.200600	0.000700	0.002400	0.480144	0.000000	0.015005	0.000000	0.030009	0.030009	0.000000
k039	392	LAWA149	0.065091	0.105148	0.070098	0.011716	0.000000	0.000000	0.040056	0.004006	0.000000	0.020028	0.207291	0.000000	0.001900	0.350492	0.000000	0.020028	0.000000	0.029041	0.075105	0.000000
k040	N/A	LAWA152S2	0.103394	0.139224	0.078825	0.011875	0.000000	0.000000	0.000000	0.004095	0.000000	0.010237	0.204741	0.000000	0.011000	0.365462	0.000000	0.010237	0.000000	0.029687	0.029687	0.001536
k041	N/A	LAWA155S2	0.060523	0.137459	0.068729	0.011797	0.000000	0.000000	0.000000	0.004103	0.000000	0.004103	0.203110	0.000000	0.018300	0.404169	0.000000	0.004103	0.000000	0.018465	0.063600	0.001539
k042	N/A	LAWA156S2																				

Table A.4. (cont.) Normalized compositions (in mass fractions) of 344 LAW glasses with K-3 Corrosion data

K-3 ID Number	Glass Number from Database	Glass ID	Al ₂ O ₃	B ₂ O ₃	CaO	Cl	Cr ₂ O ₃	F	Fe ₂ O ₃	K ₂ O	Li ₂ O	MgO	Na ₂ O	P ₂ O ₅	SO ₃	SiO ₂	SuO ₂	TiO ₂	V ₂ O ₅	ZnO	ZrO ₂	Others
k056	513	LAWA184	0.106968	0.093972	0.076977	0.006498	0.000000	0.000000	0.008997	0.004999	0.000000	0.008997	0.229931	0.000000	0.006800	0.365889	0.000000	0.000000	0.014995	0.014995	0.059982	0.000000
k057	514	LAWA185	0.121939	0.097951	0.079960	0.006497	0.000000	0.000000	0.008995	0.004998	0.000000	0.008995	0.229884	0.000000	0.007000	0.368814	0.000000	0.000000	0.014992	0.019990	0.029985	0.000000
k058	515	LAWA186	0.116094	0.093075	0.080065	0.006505	0.000000	0.000000	0.009007	0.005004	0.000000	0.009007	0.230185	0.000000	0.006700	0.369298	0.000000	0.000000	0.015012	0.015012	0.045036	0.000000
k059	516	LAWA187	0.107032	0.128039	0.065020	0.006502	0.005001	0.000000	0.009003	0.005002	0.000000	0.009003	0.230069	0.000000	0.006200	0.349105	0.010003	0.000000	0.010003	0.030009	0.030009	0.000000
k060	N/A	LAWA187R1	0.107032	0.128039	0.065020	0.006502	0.005001	0.000000	0.009003	0.005002	0.000000	0.009003	0.230069	0.000000	0.006200	0.349105	0.010003	0.000000	0.010003	0.030009	0.030009	0.000000
k061	519	LAWA188	0.107043	0.128051	0.055022	0.006503	0.005002	0.000000	0.009004	0.005002	0.000000	0.009004	0.230093	0.000000	0.006100	0.349140	0.020008	0.000000	0.010004	0.030012	0.030012	0.000000
k062	520	LAWA189	0.107043	0.113045	0.075030	0.006503	0.005002	0.000000	0.009004	0.005002	0.000000	0.009004	0.230093	0.000000	0.006100	0.349140	0.000000	0.000000	0.010004	0.030012	0.045018	0.000000
k063	521	LAWA190	0.122074	0.113068	0.060036	0.006504	0.005003	0.000000	0.009006	0.005003	0.000000	0.009005	0.230139	0.000000	0.005900	0.349211	0.000000	0.000000	0.010006	0.030018	0.045027	0.000000
k064	522	LAWA191	0.122049	0.113045	0.075030	0.006503	0.005002	0.000000	0.009004	0.005002	0.000000	0.009004	0.230093	0.000000	0.006100	0.349140	0.000000	0.000000	0.010004	0.030012	0.030012	0.000000
k065	523	LAWA192	0.121963	0.112966	0.059982	0.006498	0.000000	0.000000	0.008997	0.004998	0.000000	0.008997	0.229931	0.000000	0.006800	0.358892	0.000000	0.000000	0.009997	0.029991	0.039988	0.000000
k066	525	LAWA194	0.108901	0.077929	0.069937	0.007094	0.000000	0.000000	0.008992	0.005994	0.000000	0.008992	0.249774	0.000000	0.005800	0.353680	0.009991	0.000000	0.008992	0.023978	0.059946	0.000000
k067	526	LAWA195	0.108901	0.077929	0.064941	0.007094	0.004995	0.000000	0.008992	0.005995	0.000000	0.008992	0.249774	0.000000	0.005800	0.353680	0.009991	0.000000	0.008992	0.023978	0.059946	0.000000
k068	527	LAWA196	0.118845	0.077898	0.059922	0.007091	0.000000	0.000000	0.008988	0.005992	0.000000	0.008988	0.249673	0.000000	0.006200	0.363524	0.000000	0.000000	0.008988	0.023969	0.059922	0.000000
k069	N/A	LAWA23C	0.098039	0.042017	0.043017	0.005803	0.000000	0.000400	0.073029	0.031013	0.020008	0.020008	0.200080	0.000800	0.001600	0.401161	0.000000	0.000000	0.000000	0.033013	0.030012	0.000000
k070	N/A	LAWA28	0.119916	0.060957	0.033976	0.005796	0.000000	0.000400	0.072949	0.030978	0.000000	0.019986	0.199860	0.000799	0.001600	0.379734	0.000000	0.000000	0.000000	0.042970	0.029979	0.000100
k071	N/A	LAWA28Ti	0.119856	0.060927	0.013983	0.005793	0.000000	0.000399	0.049940	0.030963	0.000000	0.014982	0.199760	0.000799	0.002100	0.379544	0.000000	0.000000	0.047942	0.000000	0.029964	0.000100
k072	N/A	LAWA29	0.124912	0.065954	0.033976	0.005796	0.000000	0.000400	0.057959	0.030978	0.000000	0.019986	0.199860	0.000800	0.001600	0.384730	0.000000	0.000000	0.000000	0.042970	0.029979	0.000100
k073	N/A	LAWA30	0.119988	0.085991	0.028997	0.005799	0.000000	0.000400	0.057994	0.030997	0.000000	0.019998	0.199980	0.000800	0.001000	0.379962	0.000000	0.000000	0.000000	0.042996	0.024998	0.000100
k074	N/A	LAWA32	0.115104	0.086078	0.015013	0.005805	0.000000	0.000400	0.055050	0.031028	0.000000	0.016014	0.200180	0.000801	0.001000	0.380343	0.000000	0.025022	0.000000	0.043039	0.025023	0.000100
k075	N/A	LAWA34	0.105989	0.101990	0.029997	0.005799	0.000000	0.000000	0.054994	0.030997	0.000000	0.019998	0.199980	0.000800	0.001000	0.379962	0.000000	0.000000	0.000000	0.042996	0.024998	0.000100
k076	N/A	LAWA36	0.122024	0.083017	0.028006	0.006401	0.000000	0.000400	0.055011	0.034007	0.000000	0.019004	0.220044	0.000900	0.001100	0.365073	0.000000	0.000000	0.000000	0.041008	0.024005	0.000000
k077	127	LAWA41-3	0.062019	0.075023	0.020006	0.005802	0.000000	0.000100	0.070021	0.031009	0.000000	0.020006	0.200060	0.000800	0.001000	0.434130	0.000000	0.020006	0.000000	0.030009	0.030009	0.000000
k078	128	LAWA44-3	0.062006	0.089009	0.020002	0.006501	0.000000	0.000100	0.070007	0.005000	0.000000	0.020002	0.200020	0.000300	0.001000	0.446045	0.000000	0.020002	0.000000	0.030003	0.030003	0.000000
k079	N/A	LAWA44PNCC	0.062013	0.089018	0.020004	0.006501	0.000000	0.000000	0.070014	0.005001	0.000000	0.020004	0.200040	0.000300	0.001000	0.446089	0.000000	0.020004	0.000000	0.030006	0.030006	0.000000
k080	N/A	LAWA44PNCC-repeat	0.062013	0.089018	0.020004	0.006501	0.000000	0.000000	0.070014	0.005001	0.000000	0.020004	0.200040	0.000300	0.001000	0.446089	0.000000	0.020004	0.000000	0.030006	0.030006	0.000000
k081	N/A	LAWA44R11	0.062013	0.089018	0.020004	0.006501	0.000000	0.000000	0.070014	0.005001	0.000000	0.020004	0.200040	0.000300	0.001000	0.446089	0.000000	0.020004	0.000000	0.030006	0.030006	0.000000
k082	129	LAWA52-2	0.062006	0.062006	0.079008	0.006501	0.000000	0.000100	0.075008	0.005000	0.000000	0.015002	0.200020	0.000300	0.001000	0.423042	0.000000	0.011001	0.000000	0.030003	0.030003	0.000000
k083	130	LAWA60	0.085094	0.112123	0.043047	0.006507	0.000000	0.000100	0.070014	0.005006	0.000000	0.020022	0.200221	0.000300	0.001000	0.446492	0.000000	0.020022	0.000000	0.030033	0.030033	0.000000
k084	132	LAWA88	0.060994	0.096990	0.019998	0.003300	0.000000	0.000000	0.054994	0.025997	0.000000	0.014999	0.199980	0.000700	0.002100	0.439956	0.000000	0.019998	0.000000	0.029997	0.029997	0.000000
k085	120	LAWA95	0.060950	0.060950	0.055955	0.006395	0.000000	0.000100	0.037969	0.004996	0.000000	0.014988	0.196840	0.029476	0.014800	0.416662	0.000000	0.010991	0.028976	0.029976	0.029976	0.000000
k086	535	LAWB103	0.092074	0.100080	0.092074	0.000100	0.001001	0.000701	0.012010	0.004003	0.012010	0.100081	0.000300	0.000300	0.006100	0.457368	0.000000	0.000000	0.012010	0.035028	0.035028	0.000000
k087	138	LAWB37	0.061975	0.120951	0.046981	0.000100	0.001000	0.001000	0.051979	0.002999	0.029988	0.028988	0.078968	0.033986	0.010300	0.468811	0.000000	0.000000	0.030987	0.030987	0.000000	0.000000
k088	N/A	LAWB45-S	0.062013	0.132027	0.065013	0.000100	0.001000	0.000800	0.053011	0.004001	0.045009	0.027005	0.059012	0.002200	0.012100	0.473096	0.000000	0.000000	0.000000	0.032007	0.031006	0.000600
k089	183	LAWB61	0.061881	0.099809	0.066872	0.000000	0.000998	0.000699	0.052899	0.002994	0.057889	0.029943	0.054895	0.000100	0.007100	0.485072	0.000000	0.013973	0.000000	0.031939	0.031939	0.000998
k090	189	LAWB64	0.061900	0.099839	0.066892	0.000000	0.000998	0.000699	0.052947	0.002995	0.057889	0.029952	0.054912	0.000100	0.006800	0.485218	0.000000	0.013978	0.000000	0.051916	0.031949	0.000998
k091	190	LAWB64S0	0.062068	0.100110	0.067074	0.000000	0.001001	0.000701	0.033036	0.003003	0.059065	0.030033	0.055061	0.000100	0.000100	0.489539	0.000000	0.014016	0.000000	0.052057	0.032035	0.001001
k092	192	LAWB65	0.061894	0.098830	0.066885	0.000000	0.000998	0.000699	0.052909	0.002995	0.042926	0.029949	0.054906	0.000100	0.008900	0.484170	0.000000	0.013976	0.000000	0.046920	0.031945	0.000998
k093	196	LAWB67	0.061900	0.098840	0.051916	0.000000	0.000998	0.000699	0.052915	0.002995	0.042931	0.029952	0.054911	0.030151	0.009700	0.484218	0.000000	0.013978	0.000000	0.031948	0.031948	0.000000
k094	198	LAWB68	0.061931	0.083907	0.081909	0.000000	0.000999	0.000699	0.052941	0.002997	0.042952	0.029967	0.054939	0.000100	0.008300	0.484463	0.000000	0.013984	0.000000	0.046948	0.031965	0.000999
k095	199	LAWB69	0.061882	0.122765	0.104800	0.000100	0.000998	0.000798	0.000000	0.001996	0.045912	0.029943	0.065874	0.000499	0.006500	0.479084	0.000000	0.000000	0.000000	0.045912	0.031939	0.000998
k096	201	LAWB70	0.061950	0.122901	0.065947	0.000100	0.000999	0.000799	0.032974	0.001999	0.045963	0.029976	0.065947	0.000500	0.005400	0.479614	0.000000	0.000000	0.000000	0.051958	0.031974	0.000999
k097	203	LAWB71	0.061925	0.107870	0.065920	0.000																

Table A.4. (cont.) Normalized compositions (in mass fractions) of 344 LAW glasses with K-3 Corrosion data

K-3 ID Number	Glass Number from Database	Glass ID	Al ₂ O ₃	B ₂ O ₃	CaO	Cl	Cr ₂ O ₃	F	Fe ₂ O ₃	K ₂ O	Li ₂ O	MgO	Na ₂ O	P ₂ O ₅	SO ₃	SiO ₂	SuO ₂	TiO ₂	V ₂ O ₅	ZnO	ZrO ₂	Others
k111	309	LAWB87	0.065033	0.130065	0.061031	0.000100	0.001000	0.000500	0.050025	0.002001	0.047024	0.014007	0.050025	0.000200	0.005700	0.492248	0.000000	0.000000	0.000000	0.049025	0.032016	0.000000
k112	311	LAWB88	0.064961	0.129921	0.079952	0.000100	0.000999	0.000500	0.021987	0.001999	0.046972	0.013991	0.049970	0.000200	0.006800	0.500697	0.000000	0.000000	0.000000	0.048970	0.031981	0.000000
k113	N/A	LAWB89R1	0.061938	0.099899	0.067931	0.000100	0.000000	0.000000	0.052947	0.001998	0.049950	0.029970	0.040959	0.000399	0.006500	0.492504	0.000000	0.013986	0.000000	0.047952	0.031968	0.000999
k114	N/A	LAWB90R1	0.061432	0.100708	0.067475	0.000101	0.000000	0.000604	0.053375	0.002014	0.036255	0.030213	0.068482	0.000403	0.004900	0.479372	0.000000	0.014099	0.000000	0.048340	0.031220	0.001007
k115	N/A	LAWB91R1	0.062394	0.100636	0.067426	0.000101	0.000000	0.000604	0.053337	0.002013	0.029185	0.030191	0.087554	0.000403	0.003600	0.467959	0.000000	0.014089	0.000000	0.048305	0.031197	0.001006
k116	N/A	LAWB92R1	0.062376	0.100606	0.067406	0.000101	0.000000	0.000604	0.053321	0.002012	0.022133	0.030182	0.101612	0.000402	0.003900	0.460775	0.000000	0.014085	0.000000	0.048291	0.031188	0.001006
k117	242	LAWB93	0.061963	0.099940	0.067959	0.000100	0.000000	0.000599	0.052968	0.001999	0.046972	0.029982	0.047971	0.000400	0.004500	0.489705	0.000000	0.013991	0.000000	0.047971	0.031981	0.000999
k118	244	LAWB94	0.061931	0.099890	0.067925	0.000100	0.000000	0.000599	0.052941	0.001998	0.053940	0.029967	0.033962	0.000400	0.005000	0.496451	0.000000	0.013985	0.000000	0.047947	0.031965	0.000999
k119	246	LAWB95	0.061956	0.099930	0.067952	0.000100	0.000000	0.000600	0.052963	0.001999	0.057959	0.029979	0.024982	0.000400	0.004600	0.501647	0.000000	0.013990	0.000000	0.047966	0.031978	0.000999
k120	529	LAWB97	0.092148	0.100161	0.092148	0.000100	0.001002	0.000701	0.012019	0.004007	0.035057	0.012019	0.100161	0.000301	0.006300	0.461744	0.000000	0.000000	0.012019	0.035057	0.035056	0.000000
k121	531	LAWB99	0.102154	0.110166	0.102154	0.000100	0.001002	0.000701	0.012018	0.004006	0.035053	0.012018	0.100151	0.000301	0.006400	0.431652	0.000000	0.000000	0.012018	0.035053	0.035053	0.000000
k122	442	LAWC100	0.101979	0.136972	0.080984	0.000499	0.000000	0.001900	0.009998	0.002000	0.000998	0.009998	0.200959	0.002699	0.007700	0.367926	0.000000	0.000000	0.009998	0.029994	0.029994	0.000400
k123	N/A	LAWC101S2	0.100979	0.128973	0.078984	0.006499	0.000000	0.000000	0.009998	0.001000	0.000000	0.009998	0.197959	0.002699	0.025000	0.361926	0.000000	0.000000	0.009998	0.029994	0.035993	0.000000
k124	N/A	LAWC102S2	0.085070	0.135111	0.079065	0.006505	0.000000	0.000000	0.010008	0.001001	0.000000	0.010008	0.198163	0.002702	0.025000	0.362297	0.000000	0.000000	0.010008	0.030025	0.045037	0.000000
k125	N/A	LAWC103S2	0.070985	0.135972	0.076984	0.006499	0.000000	0.000000	0.009998	0.001000	0.000000	0.009998	0.197959	0.002699	0.025000	0.362926	0.000000	0.000000	0.009998	0.029994	0.059988	0.000000
k126	438	LAWC21REV2	0.061086	0.101142	0.064090	0.001102	0.000000	0.000501	0.064090	0.001001	0.027038	0.015021	0.120169	0.001102	0.002900	0.468658	0.000000	0.011015	0.000000	0.030042	0.030042	0.001001
k127	N/A	LAWC21S	0.059939	0.098899	0.062935	0.001199	0.000000	0.000599	0.062935	0.000999	0.026972	0.014985	0.115881	0.001199	0.025000	0.457531	0.000000	0.010989	0.000000	0.029969	0.029969	0.000000
k128	81	LAWC25S	0.058064	0.095105	0.061067	0.000000	0.000000	0.000601	0.061067	0.081090	0.000000	0.014016	0.112124	0.001101	0.004100	0.442489	0.000000	0.011012	0.000000	0.029032	0.029032	0.000100
k129	252	LAWC27	0.061074	0.122147	0.085103	0.001101	0.000000	0.000501	0.000000	0.001001	0.027033	0.015018	0.120145	0.001101	0.004100	0.489590	0.000000	0.011013	0.000000	0.030036	0.030036	0.001001
k130	256	LAWC29	0.066040	0.100600	0.096058	0.001101	0.000000	0.000500	0.000000	0.001001	0.027016	0.015009	0.120072	0.001101	0.003700	0.472284	0.000000	0.011007	0.000000	0.054032	0.030018	0.001001
k131	260	LAWC31	0.061147	0.100242	0.074179	0.001103	0.000000	0.000501	0.044106	0.001002	0.027065	0.015036	0.120290	0.001103	0.003900	0.468128	0.000000	0.011027	0.000000	0.040097	0.030072	0.001002
k132	261	LAWC31R2	0.061147	0.100242	0.074179	0.001103	0.000000	0.000501	0.044106	0.001002	0.027065	0.015036	0.120290	0.001103	0.003900	0.468128	0.000000	0.011027	0.000000	0.040097	0.030072	0.001002
k133	N/A	LAWC34S2	0.059926	0.097880	0.071911	0.003895	0.000000	0.001099	0.042947	0.000999	0.026967	0.014982	0.116856	0.001598	0.025000	0.454441	0.000000	0.010986	0.000000	0.038952	0.028964	0.002597
k134	290	LAWC35S2	0.059988	0.091981	0.071985	0.003899	0.000000	0.001100	0.034993	0.001000	0.031993	0.014997	0.116976	0.001600	0.025000	0.462905	0.000000	0.010998	0.000000	0.038992	0.028994	0.002599
k135	N/A	LAWC36S2	0.059932	0.087901	0.071919	0.003896	0.000000	0.000000	0.028967	0.000999	0.036958	0.009989	0.117867	0.001598	0.025000	0.473466	0.000000	0.010988	0.000000	0.038956	0.028967	0.002597
k136	454	LAWE10H	0.060963	0.099940	0.069958	0.001999	0.000999	0.000799	0.054967	0.004997	0.042974	0.028982	0.056966	0.001199	0.005400	0.490704	0.000000	0.013992	0.000000	0.034979	0.029982	0.000200
k137	N/A	LAWE11	0.060957	0.099930	0.022984	0.001999	0.000999	0.000799	0.054961	0.047966	0.000000	0.014990	0.173878	0.001199	0.002500	0.437693	0.000000	0.013990	0.000000	0.034976	0.029979	0.000200
k138	476	LAWE13	0.069902	0.097863	0.019972	0.001997	0.000999	0.000799	0.053924	0.053924	0.000000	0.003995	0.196724	0.001198	0.003200	0.418412	0.000000	0.003994	0.000000	0.033952	0.038945	0.000200
k139	477	LAWE14	0.048985	0.097970	0.014995	0.001999	0.001000	0.000800	0.053984	0.053984	0.000000	0.003999	0.196941	0.001200	0.003100	0.433869	0.000000	0.013996	0.000000	0.033990	0.038988	0.000200
k140	478	LAWE15	0.058982	0.087973	0.014995	0.001999	0.001000	0.000800	0.053984	0.053984	0.000000	0.008997	0.196941	0.001200	0.003100	0.428871	0.000000	0.013996	0.000000	0.033990	0.038988	0.000200
k141	479	LAWE16	0.059012	0.082016	0.015003	0.002000	0.001000	0.000800	0.054011	0.054011	0.000000	0.009002	0.197040	0.001200	0.004600	0.428086	0.000000	0.014003	0.000000	0.034007	0.044009	0.000200
k142	N/A	LAWE2H	0.059922	0.097872	0.019974	0.001997	0.000999	0.000799	0.053930	0.037950	0.000000	0.013982	0.207729	0.001198	0.003100	0.423448	0.000000	0.013982	0.000000	0.033956	0.028962	0.000200
k143	448	LAWE3	0.060976	0.099960	0.019992	0.001999	0.001000	0.000800	0.054978	0.049980	0.000000	0.014994	0.181927	0.001199	0.003200	0.429827	0.000000	0.013994	0.000000	0.034986	0.029988	0.000200
k144	474	LAWE3H	0.059024	0.097039	0.020008	0.002001	0.001000	0.000800	0.054022	0.054022	0.000000	0.014005	0.197079	0.001200	0.003400	0.419168	0.000000	0.014006	0.000000	0.034014	0.029012	0.000200
k145	625	LAWE4H	0.059958	0.097931	0.024982	0.001999	0.000999	0.000799	0.053962	0.004997	0.000000	0.014989	0.212851	0.001199	0.003500	0.444688	0.000000	0.013990	0.000000	0.033976	0.028980	0.000200
k146	N/A	LAWE5H	0.060018	0.098030	0.036011	0.002001	0.001000	0.000800	0.054016	0.005001	0.005002	0.015005	0.190057	0.001200	0.003500	0.451136	0.000000	0.014004	0.000000	0.034010	0.029009	0.000200
k147	N/A	LAWE7	0.061074	0.100121	0.064077	0.002002	0.001001	0.000000	0.055067	0.005006	0.032039	0.015018	0.125151	0.001202	0.005500	0.453547	0.000000	0.014017	0.000000	0.035042	0.030036	0.000100
k148	451	LAWE7H	0.060006	0.099010	0.063006	0.002000	0.001000	0.000800	0.054005	0.005001	0.032003	0.015002	0.135014	0.001200	0.004700	0.448045	0.000000	0.014001	0.000000	0.035004	0.030003	0.000200
k149	N/A	LAWE9H	0.060908	0.098851	0.068896	0.001997	0.000999	0.000799	0.054917	0.004992	0.040938	0.023964	0.089865	0.001198	0.004300	0.468295	0.000000	0.013979	0.000000	0.034947	0.029955	0.000200
k150	480	LAWM57	0.069972	0.109956	0.029988	0.001999	0.001000	0.000800	0.046981	0.037985	0.000000	0.013994	0.205917	0.001200	0.003200	0.392842	0.000000	0.013994	0.000000	0.029988	0.039984	0.000200
k151	481	LAWM58	0.069972	0.092963	0.009996	0.001999	0.001000	0.000800	0.064974	0.037985	0.000000	0.013994	0.204918	0.001199	0.003200	0.416833	0.000000	0.013994	0.000000	0.025989	0.039984	0.000200
k152	482	LAWM59	0.067979	0.089973	0.029991	0.001999	0.0															

Table A.4. (cont.) Normalized compositions (in mass fractions) of 344 LAW glasses with K-3 Corrosion data

K-3 ID Number	Glass Number from Database	Glass ID	Al ₂ O ₃	B ₂ O ₃	CaO	Cl	Cr ₂ O ₃	F	Fe ₂ O ₃	K ₂ O	Li ₂ O	MgO	Na ₂ O	P ₂ O ₅	SO ₃	SiO ₂	SrO ₂	TiO ₂	V ₂ O ₅	ZnO	ZrO ₂	Others
k166	496	LAWM73	0.079968	0.089964	0.029988	0.001999	0.001000	0.000800	0.048980	0.011995	0.000000	0.013994	0.229908	0.001200	0.003200	0.403838	0.000000	0.013994	0.000000	0.044982	0.023990	0.000200
k167	497	LAWM74	0.075992	0.089991	0.009999	0.002000	0.001000	0.000800	0.044995	0.000000	0.000000	0.013999	0.212979	0.001200	0.002900	0.453954	0.000000	0.013999	0.000000	0.025997	0.049995	0.000200
k168	498	LAWM75	0.079896	0.091880	0.029961	0.001997	0.000999	0.000799	0.064915	0.010986	0.000000	0.013982	0.206730	0.001198	0.003100	0.384499	0.000000	0.013982	0.000000	0.044941	0.049935	0.000200
k169	499	LAWM76	0.064045	0.099070	0.019013	0.002001	0.001001	0.000801	0.054038	0.026018	0.000000	0.014010	0.214150	0.001201	0.003100	0.419294	0.000000	0.014010	0.000000	0.034024	0.034024	0.000200
k170	N/A	LAWSNa1-3	0.100000	0.093000	0.011000	0.001100	0.005000	0.004900	0.011000	0.001000	0.000000	0.011000	0.250000	0.002300	0.005200	0.380000	0.011000	0.000000	0.022000	0.037000	0.054000	0.002500
k171	N/A	LAWSNa2-2	0.060895	0.098830	0.078864	0.003494	0.004991	0.001797	0.002995	0.001997	0.000000	0.009983	0.219622	0.002995	0.012000	0.411292	0.000000	0.000000	0.019966	0.029949	0.039931	0.000399
k172	N/A	LAWSNa3-2	0.056063	0.118132	0.100112	0.000200	0.005005	0.002002	0.002002	0.006007	0.025028	0.010011	0.160179	0.001201	0.015000	0.413462	0.000000	0.000000	0.017019	0.032036	0.035039	0.001502
k173	778	LORPM11	0.035039	0.060067	0.122135	0.008009	0.003003	0.003003	0.080089	0.059065	0.050056	0.045050	0.050056	0.005006	0.008100	0.390433	0.000000	0.030033	0.040044	0.010011	0.000000	0.000801
k174	779	LORPM11	0.035007	0.060012	0.000000	0.008002	0.003000	0.003001	0.003001	0.001000	0.000000	0.050010	0.196039	0.005001	0.001000	0.494099	0.000000	0.030006	0.000000	0.050010	0.060012	0.000800
k175	782	LORPM14R1	0.056000	0.075000	0.098000	0.000200	0.000000	0.000100	0.024000	0.047000	0.036000	0.035000	0.133000	0.000100	0.002600	0.384000	0.036000	0.006000	0.029000	0.018000	0.020000	0.000000
k176	785	LORPM17R1	0.108033	0.075023	0.027008	0.000200	0.000000	0.000100	0.057017	0.042013	0.010003	0.035011	0.187056	0.000100	0.005300	0.386117	0.010003	0.008002	0.008002	0.021006	0.020006	0.000000
k177	787	LORPM19R1	0.085871	0.092860	0.042935	0.001897	0.000999	0.000699	0.028956	0.027958	0.016975	0.022965	0.146779	0.001198	0.003500	0.400397	0.016975	0.019970	0.022965	0.033949	0.031952	0.000200
k178	788	LORPM20R1	0.097872	0.085888	0.036952	0.000200	0.000000	0.000100	0.029961	0.034954	0.029961	0.014980	0.154798	0.000100	0.004900	0.400477	0.027963	0.008988	0.016978	0.021971	0.032957	0.000000
k179	789	LORPM21	0.048029	0.129077	0.115069	0.000200	0.000000	0.000100	0.071043	0.010006	0.000000	0.000000	0.160096	0.000100	0.001000	0.449270	0.000000	0.006004	0.000000	0.010006	0.000000	0.000000
k180	793	LORPM25	0.138111	0.128103	0.000000	0.001001	0.000000	0.000400	0.010008	0.026021	0.024019	0.043034	0.183147	0.000601	0.001200	0.371297	0.003002	0.000000	0.000000	0.010008	0.060048	0.000000
k181	797	LORPM28R1	0.035000	0.137000	0.000000	0.007200	0.003000	0.002700	0.003000	0.001000	0.050000	0.000000	0.143000	0.004500	0.001800	0.451000	0.050000	0.000000	0.040000	0.010000	0.060000	0.000800
k182	802	LORPM32	0.056011	0.116023	0.025005	0.001000	0.000000	0.000400	0.043009	0.047010	0.036007	0.035007	0.100020	0.000600	0.004800	0.431087	0.010002	0.024005	0.011002	0.039008	0.020004	0.000000
k183	804	LORPM34	0.072051	0.122086	0.024017	0.008006	0.003002	0.003002	0.018013	0.047033	0.040028	0.035025	0.101071	0.005003	0.003500	0.384270	0.019013	0.024017	0.022015	0.021015	0.047033	0.000800
k184	805	LORPM35	0.104167	0.075121	0.049079	0.000200	0.000000	0.000100	0.018029	0.032051	0.029047	0.031050	0.173278	0.000100	0.003000	0.384617	0.010016	0.013021	0.009015	0.018029	0.050080	0.000000
k185	806	LORPM36	0.066987	0.121976	0.023995	0.006999	0.002999	0.002999	0.017996	0.024995	0.039992	0.034993	0.127974	0.004299	0.002500	0.397920	0.024995	0.021996	0.007998	0.017996	0.049990	0.000800
k186	807	LORPM37	0.055961	0.115919	0.023983	0.002099	0.000999	0.000799	0.021985	0.046967	0.036974	0.034975	0.121914	0.001299	0.002300	0.394723	0.039972	0.023983	0.007994	0.041971	0.024983	0.000200
k187	808	LORPM38	0.055978	0.075969	0.024990	0.007997	0.002999	0.002999	0.064974	0.046981	0.009996	0.034986	0.133946	0.004998	0.003600	0.397840	0.009996	0.023990	0.007997	0.041983	0.046981	0.000800
k188	809	LORPM39	0.055950	0.121890	0.023978	0.000200	0.000000	0.000100	0.064941	0.012988	0.039964	0.009991	0.173843	0.000100	0.002500	0.383654	0.009991	0.005991	0.031971	0.017984	0.043960	0.000000
k189	1004	LORPM4R2	0.093943	0.123925	0.050969	0.007396	0.002998	0.002798	0.002998	0.058964	0.000000	0.048970	0.139916	0.004597	0.007000	0.359783	0.000000	0.010993	0.039976	0.043974	0.000000	0.000800
k190	N/A	LORPM4R2-Repeat	0.093943	0.123925	0.050969	0.007396	0.002998	0.002798	0.002998	0.058964	0.000000	0.048970	0.139916	0.004597	0.007000	0.359783	0.000000	0.010993	0.039976	0.043974	0.000000	0.000800
k191	777	LORPM9	0.086043	0.069035	0.000000	0.000200	0.000000	0.000100	0.003001	0.008004	0.000000	0.000000	0.239120	0.000100	0.001100	0.493247	0.000000	0.000000	0.040020	0.050025	0.010005	0.000000
k192	N/A	OD2-G-50A	0.110132	0.091110	0.016019	0.000000	0.000000	0.000000	0.057069	0.002002	0.000000	0.014017	0.200241	0.000300	0.002000	0.403485	0.000000	0.034041	0.000000	0.043052	0.025030	0.001502
k193	835	ORLEC1	0.099980	0.099980	0.019996	0.001999	0.005999	0.000800	0.009998	0.004999	0.000000	0.009998	0.239952	0.001200	0.001000	0.380924	0.022995	0.009998	0.000000	0.029994	0.059988	0.000200
k194	844	ORLEC10	0.100050	0.100050	0.019010	0.002001	0.006003	0.000800	0.010005	0.014007	0.000000	0.010005	0.234117	0.001201	0.001300	0.378189	0.023012	0.010005	0.000000	0.030015	0.060030	0.000200
k195	845	ORLEC11	0.100070	0.100070	0.019013	0.002002	0.006004	0.000801	0.010007	0.034024	0.000000	0.010007	0.221155	0.001201	0.001100	0.371260	0.023016	0.010007	0.000000	0.030021	0.060042	0.000200
k196	846	ORLEC12	0.100060	0.100060	0.020012	0.002001	0.006004	0.000800	0.010006	0.056034	0.000000	0.010006	0.206124	0.001201	0.001200	0.363218	0.023014	0.010006	0.000000	0.030018	0.060036	0.000200
k197	847	ORLEC13	0.100171	0.100171	0.019032	0.002003	0.005009	0.000801	0.007012	0.005009	0.000000	0.010017	0.240410	0.001202	0.003100	0.385658	0.023039	0.007012	0.000000	0.030051	0.060103	0.000200
k198	848	ORLEC14	0.100141	0.100141	0.020028	0.002003	0.003004	0.000801	0.003004	0.005007	0.000000	0.010014	0.241340	0.001202	0.005400	0.390550	0.023033	0.003004	0.000000	0.030042	0.061086	0.000200
k199	849	ORLEC15	0.100101	0.100101	0.020020	0.002002	0.002002	0.000801	0.002002	0.005005	0.000000	0.010010	0.240242	0.001201	0.006800	0.388391	0.023023	0.000000	0.008008	0.030030	0.060061	0.000200
k200	850	ORLEC16	0.100091	0.100091	0.025023	0.002002	0.002002	0.000801	0.002002	0.005004	0.000000	0.010009	0.230209	0.001201	0.007900	0.409371	0.013012	0.000000	0.011010	0.030027	0.050045	0.000200
k201	851	ORLEC17	0.100111	0.100111	0.036040	0.002002	0.001001	0.000801	0.002002	0.005006	0.000000	0.010011	0.221246	0.001202	0.008700	0.426473	0.003003	0.000000	0.012013	0.030033	0.040045	0.000200
k202	852	ORLEC18	0.090972	0.099970	0.045986	0.001999	0.001000	0.000800	0.001999	0.004999	0.000000	0.009997	0.210936	0.001200	0.008100	0.442866	0.000000	0.000000	0.013996	0.029991	0.034989	0.000200
k203	853	ORLEC19	0.082008	0.101010	0.055006	0.002000	0.001000	0.000800	0.002000	0.005001	0.000000	0.010001	0.201020	0.001200	0.008700	0.452046	0.000000	0.000000	0.013001	0.030003	0.035004	0.000200
k204	836	ORLEC2	0.100000	0.100000	0.022000	0.002000	0.001000	0.000800	0.010000	0.005000	0.000000	0.010000	0.231000	0.001200	0.007800	0.395000	0.013000	0.010000	0.011000	0.030000	0.050000	0.000200
k205	854	ORLEC20	0.078047	0.100061	0.063038	0.002001	0.001001	0.000800	0.002001	0.005003	0.004002	0.010006	0.191116	0.001201	0.008200	0.452274	0.000000	0.000000	0.016010	0.030018	0.035021	0.000200
k206	855	ORLEC21	0.078039	0.100050	0.070035	0.002001	0.001001	0.000800	0.002001	0.005003	0.015008	0.010005	0.181091	0.001201	0.009300	0.442223	0.000000	0.000000	0.017009	0.030015	0.035018	0.000200
k207	856	ORLEC22	0.078063	0.100081	0.076061	0.0																

Table A.4. (cont.) Normalized compositions (in mass fractions) of 344 LAW glasses with K-3 Corrosion data

K-3 ID Number	Glass Number from Database	Glass ID	Al ₂ O ₃	B ₂ O ₃	CaO	Cl	Cr ₂ O ₃	F	Fe ₂ O ₃	K ₂ O	Li ₂ O	MgO	Na ₂ O	P ₂ O ₅	SO ₃	SiO ₂	SuO ₂	TiO ₂	V ₂ O ₅	ZnO	ZrO ₂	Others
k221	880	ORLEC36	0.076054	0.110078	0.055039	0.002001	0.001001	0.000800	0.002001	0.005003	0.000000	0.010007	0.201142	0.001201	0.008100	0.437309	0.000000	0.000000	0.025018	0.030021	0.035025	0.000200
k222	881	ORLEC37	0.075985	0.109978	0.045991	0.001999	0.001000	0.000800	0.002000	0.004999	0.007998	0.009998	0.210957	0.001200	0.009000	0.428913	0.000000	0.000000	0.023995	0.029994	0.034993	0.000200
k223	882	ORLEC38	0.076069	0.110100	0.055050	0.002002	0.001001	0.000801	0.002002	0.005004	0.012011	0.010009	0.201183	0.001201	0.009900	0.424386	0.000000	0.000000	0.024022	0.030027	0.035032	0.000200
k224	883	ORLEC39	0.075931	0.110900	0.062943	0.001998	0.000999	0.000799	0.001998	0.004996	0.003996	0.009991	0.190827	0.001199	0.007700	0.435605	0.000000	0.000000	0.024977	0.029973	0.034968	0.000200
k225	838	ORLEC4	0.100050	0.100050	0.033017	0.002001	0.001001	0.000800	0.010005	0.005003	0.000000	0.010005	0.211106	0.001201	0.007300	0.429216	0.000000	0.010005	0.014007	0.030015	0.035018	0.000200
k226	884	ORLEC40	0.075977	0.109967	0.069979	0.001999	0.001000	0.000800	0.001999	0.004999	0.014995	0.009997	0.180945	0.001200	0.010100	0.425871	0.000000	0.000000	0.024992	0.029991	0.034989	0.000200
k227	885	ORLEC41	0.076085	0.110123	0.076085	0.002002	0.001001	0.000801	0.002002	0.005006	0.021023	0.010011	0.171190	0.001201	0.010700	0.422470	0.000000	0.000000	0.025028	0.030033	0.035039	0.000200
k228	886	ORLEC42	0.075977	0.109967	0.081975	0.001999	0.001000	0.000800	0.001999	0.004999	0.024992	0.009997	0.160951	0.001200	0.011100	0.422872	0.000000	0.000000	0.024992	0.029991	0.034989	0.000200
k229	892	ORLEC43	0.075969	0.109956	0.045981	0.001999	0.001000	0.000800	0.001999	0.004998	0.004998	0.009996	0.210915	0.001199	0.009200	0.431826	0.000000	0.000000	0.023990	0.029988	0.034986	0.000200
k230	893	ORLEC44	0.076046	0.110067	0.055033	0.002001	0.001001	0.000800	0.002001	0.005003	0.010006	0.010006	0.201122	0.001201	0.009200	0.427259	0.000000	0.000000	0.024015	0.030018	0.035021	0.000200
k231	894	ORLEC45	0.076115	0.110167	0.062094	0.002003	0.001002	0.000801	0.002003	0.005008	0.014021	0.010015	0.190289	0.001202	0.011300	0.423643	0.000000	0.000000	0.025038	0.030046	0.035053	0.000200
k232	895	ORLEC46	0.075923	0.109889	0.069929	0.001998	0.000999	0.000799	0.001998	0.004995	0.018981	0.009990	0.180817	0.001199	0.010800	0.421574	0.000000	0.000000	0.024975	0.029970	0.034964	0.000200
k233	896	ORLEC47	0.076015	0.110022	0.076015	0.002001	0.001000	0.000800	0.002001	0.005001	0.023005	0.010002	0.170035	0.001200	0.012600	0.420085	0.000000	0.000000	0.025005	0.030006	0.035007	0.000200
k234	897	ORLEC48R	0.076038	0.110056	0.082042	0.002001	0.001000	0.000800	0.002001	0.005003	0.026013	0.010005	0.160081	0.001201	0.012300	0.421213	0.000000	0.000000	0.025013	0.030015	0.035018	0.000200
k235	898	ORLEC49	0.100000	0.110000	0.020000	0.002000	0.004000	0.000800	0.006000	0.005000	0.000000	0.010000	0.240000	0.001200	0.003800	0.391000	0.010000	0.006000	0.000000	0.030000	0.060000	0.000200
k236	N/A	ORLEC49-Repeat	0.100000	0.100000	0.020000	0.002000	0.004000	0.000800	0.006000	0.005000	0.000000	0.010000	0.240000	0.001200	0.003800	0.391000	0.010000	0.006000	0.000000	0.030000	0.060000	0.000200
k237	900	ORLEC50	0.100151	0.110166	0.020030	0.002003	0.003004	0.000801	0.003005	0.005008	0.000000	0.010015	0.240362	0.001202	0.005300	0.386583	0.010015	0.003005	0.009014	0.030045	0.060091	0.000200
k238	901	ORLEC51	0.099990	0.109989	0.019998	0.002000	0.003000	0.000800	0.002000	0.004999	0.000000	0.009999	0.239976	0.001200	0.006900	0.381961	0.009999	0.001000	0.015998	0.029997	0.059994	0.000200
k239	902	ORLEC52	0.099090	0.110100	0.020018	0.002002	0.002002	0.000801	0.002002	0.005005	0.000000	0.010009	0.238216	0.001201	0.007900	0.386350	0.008007	0.000000	0.019017	0.030027	0.058053	0.000200
k240	840	ORLEC6	0.077984	0.100980	0.052989	0.002000	0.001000	0.000800	0.009998	0.004999	0.003999	0.009998	0.190961	0.001200	0.007000	0.444910	0.000000	0.009998	0.015997	0.029994	0.034993	0.000200
k241	841	ORLEC7	0.078079	0.100101	0.066067	0.002002	0.001001	0.000801	0.010010	0.005005	0.015015	0.010010	0.181183	0.001201	0.008800	0.428432	0.000000	0.010010	0.017017	0.030030	0.035036	0.000200
k242	842	ORLEC8	0.078071	0.100091	0.079072	0.002002	0.001001	0.000801	0.010009	0.005005	0.021019	0.010009	0.171156	0.001201	0.009900	0.417379	0.000000	0.010009	0.018016	0.030027	0.035032	0.000200
k243	843	ORLEC9	0.079120	0.101153	0.093141	0.002003	0.001001	0.000801	0.010015	0.005008	0.025038	0.000000	0.162246	0.001202	0.010300	0.413627	0.000000	0.010015	0.019029	0.030046	0.036055	0.000200
k244	545	ORPLA1	0.099910	0.089919	0.034968	0.007094	0.000000	0.000000	0.009991	0.005995	0.000000	0.013987	0.249775	0.000000	0.001900	0.412628	0.000000	0.000000	0.000000	0.023978	0.047957	0.001898
k245	563	ORPLA10	0.108902	0.077930	0.064941	0.007094	0.004995	0.000000	0.008992	0.005995	0.000000	0.008992	0.249775	0.000000	0.001900	0.357677	0.026976	0.000000	0.000000	0.023978	0.049955	0.001898
k246	565	ORPLA11	0.109011	0.070007	0.020002	0.007101	0.005000	0.000000	0.009001	0.006001	0.000000	0.009001	0.250025	0.000000	0.001900	0.401040	0.027003	0.000000	0.000000	0.024002	0.059006	0.001900
k247	567	ORPLA12	0.108293	0.071193	0.020054	0.006818	0.005014	0.000000	0.009024	0.005014	0.000000	0.009024	0.240651	0.000000	0.001700	0.411112	0.027073	0.000000	0.000000	0.024065	0.059160	0.001805
k248	569	ORPLA13	0.108043	0.071028	0.020008	0.006903	0.005002	0.000000	0.009003	0.006002	0.000000	0.009004	0.245098	0.000000	0.001900	0.406163	0.027011	0.000000	0.000000	0.024010	0.059024	0.001801
k249	571	ORPLA14	0.107000	0.072000	0.021000	0.006600	0.005000	0.000000	0.009000	0.005000	0.000000	0.009000	0.235000	0.000000	0.001700	0.414000	0.028000	0.000000	0.000000	0.025000	0.060000	0.001700
k250	573	ORPLA15	0.095277	0.086251	0.033096	0.006820	0.005014	0.000000	0.009026	0.005015	0.000000	0.009026	0.240699	0.000000	0.001800	0.396151	0.027079	0.000000	0.000000	0.024070	0.059172	0.001504
k251	575	ORPLA16	0.098931	0.077945	0.014989	0.007095	0.004996	0.000000	0.008994	0.005996	0.000000	0.008994	0.249825	0.000000	0.001700	0.415708	0.009993	0.000000	0.008994	0.023983	0.059958	0.001899
k252	577	ORPLA17	0.098990	0.087991	0.029997	0.006799	0.005000	0.000000	0.008999	0.004999	0.000000	0.008999	0.239976	0.000000	0.001800	0.399960	0.009999	0.000000	0.009999	0.023998	0.060994	0.001500
k253	547	ORPLA2	0.099910	0.089919	0.024977	0.007094	0.000000	0.000000	0.009991	0.005995	0.000000	0.013987	0.249775	0.000000	0.001900	0.412628	0.009991	0.000000	0.000000	0.023978	0.047957	0.001898
k254	689	ORPLA20	0.067040	0.088053	0.033020	0.006804	0.005003	0.000000	0.003002	0.005003	0.000000	0.009005	0.240144	0.000000	0.001600	0.425256	0.028017	0.000000	0.000000	0.028017	0.060036	0.000000
k255	N/A	ORPLA20HV	0.066080	0.087105	0.022027	0.006808	0.005006	0.000000	0.000000	0.005006	0.000000	0.000000	0.240290	0.000000	0.007000	0.423512	0.000000	0.000000	0.050060	0.027033	0.060073	0.000000
k256	834	ORPLA20R1	0.067040	0.088053	0.033020	0.006804	0.005003	0.000000	0.003002	0.005003	0.000000	0.009005	0.240144	0.000000	0.001600	0.425256	0.028017	0.000000	0.000000	0.028017	0.060036	0.000000
k257	690	ORPLA21	0.069007	0.086009	0.033003	0.007101	0.005000	0.000000	0.003000	0.006000	0.000000	0.009001	0.250025	0.000000	0.001800	0.417042	0.027003	0.000000	0.000000	0.027003	0.059006	0.000000
k258	693	ORPLA24	0.093019	0.086017	0.035007	0.007101	0.005001	0.000000	0.000000	0.006001	0.000000	0.000000	0.250050	0.000000	0.001700	0.397080	0.030006	0.000000	0.000000	0.029006	0.060012	0.000000
k259	694	ORPLA25	0.091899	0.083908	0.034961	0.007292	0.004994	0.000000	0.000000	0.005993	0.000000	0.000000	0.259714	0.000000	0.001800	0.390570	0.029967	0.000000	0.000000	0.028968	0.059934	0.000000
k260	549	ORPLA3	0.100010	0.090009	0.030003	0.007101	0.005001	0.000000	0.010001	0.006001	0.000000	0.013001	0.250025	0.000000	0.001900	0.413041	0.000000	0.000000	0.000000	0.024002	0.048005	0.001900
k261	751	ORPLA38-1	0.070000	0.082000	0.031000	0.006700	0.005000	0.000000	0.003000	0.005000	0.000000	0.010000	0.240000	0.000000	0.008300	0.415000	0.027000	0.000000	0.009000	0.028000	0.060000	0.000000
k262	811	ORPLA39	0.067074	0.082091	0.033037																	

Table A.4. (cont.) Normalized compositions (in mass fractions) of 344 LAW glasses with K-3 Corrosion data

K-3 ID Number	Glass Number from Database	Glass ID	Al ₂ O ₃	B ₂ O ₃	CaO	Cl	Cr ₂ O ₃	F	Fe ₂ O ₃	K ₂ O	Li ₂ O	MgO	Na ₂ O	P ₂ O ₅	SO ₃	SiO ₂	SuO ₂	TiO ₂	V ₂ O ₅	ZnO	ZrO ₂	Others
k276	824	ORPLA49	0.097020	0.080016	0.020004	0.006701	0.000000	0.000000	0.002000	0.005001	0.000000	0.009002	0.240048	0.000000	0.006100	0.391079	0.000000	0.040008	0.015003	0.028006	0.060012	0.000000
k277	553	ORPLA5	0.099900	0.069930	0.009990	0.007093	0.004995	0.000000	0.009990	0.005994	0.000000	0.013986	0.249750	0.000000	0.002000	0.432566	0.009990	0.000000	0.000000	0.033966	0.047952	0.001898
k278	825	ORPLA50	0.097010	0.080008	0.020002	0.006701	0.000000	0.000000	0.002000	0.005001	0.000000	0.009001	0.240024	0.000000	0.006200	0.390039	0.000000	0.040004	0.030003	0.014001	0.060006	0.000000
k279	826	ORPLA51	0.102051	0.080040	0.010005	0.006703	0.000000	0.000000	0.002001	0.005003	0.000000	0.019101	0.240121	0.000000	0.005800	0.391197	0.010005	0.040020	0.000000	0.028014	0.060030	0.000000
k280	827	ORPLA52	0.102010	0.080008	0.010001	0.006701	0.000000	0.000000	0.002000	0.005001	0.000000	0.019002	0.240024	0.000000	0.006200	0.391039	0.010001	0.020002	0.022002	0.028003	0.060006	0.000000
k281	828	ORPLA53	0.102041	0.080032	0.010004	0.006703	0.000000	0.000000	0.002001	0.005002	0.000000	0.019008	0.240097	0.000000	0.005900	0.391157	0.010004	0.030012	0.010004	0.028011	0.060024	0.000000
k282	829	ORPLA54	0.102041	0.080032	0.010004	0.006703	0.000000	0.000000	0.002001	0.005002	0.000000	0.019008	0.240096	0.000000	0.005900	0.391157	0.010004	0.030012	0.024010	0.014006	0.060024	0.000000
k283	830	ORPLA55	0.107108	0.080080	0.000000	0.006707	0.000000	0.000000	0.002002	0.005005	0.000000	0.002002	0.240242	0.000000	0.005300	0.411414	0.010010	0.030030	0.000000	0.040040	0.060060	0.000000
k284	831	ORPLA56	0.107054	0.080040	0.020010	0.006703	0.000000	0.000000	0.002001	0.005003	0.000000	0.022011	0.240121	0.000000	0.005800	0.411207	0.000000	0.000000	0.000000	0.040020	0.060030	0.000000
k285	832	ORPLA57	0.106903	0.080927	0.014986	0.006694	0.000000	0.000000	0.000999	0.004995	0.000000	0.000000	0.239783	0.000000	0.006200	0.408630	0.000000	0.029973	0.000000	0.039964	0.059946	0.000000
k286	833	ORPLA58	0.106828	0.087858	0.000000	0.006689	0.000000	0.000000	0.002995	0.004992	0.000000	0.015974	0.239614	0.000000	0.006900	0.408342	0.000000	0.029952	0.000000	0.029952	0.059904	0.000000
k287	555	ORPLA6	0.108902	0.077930	0.009991	0.007094	0.004995	0.000000	0.008992	0.005995	0.000000	0.008992	0.249775	0.000000	0.001900	0.418622	0.009991	0.023978	0.000000	0.060945	0.001898	
k288	557	ORPLA7	0.108891	0.077922	0.014985	0.007093	0.004995	0.000000	0.008991	0.005994	0.000000	0.008991	0.249750	0.000000	0.002000	0.404594	0.009990	0.000000	0.008991	0.023976	0.060939	0.001898
k289	559	ORPLA8	0.057948	0.084923	0.000000	0.007094	0.004995	0.000000	0.026976	0.005995	0.000000	0.033969	0.249775	0.000000	0.001900	0.420621	0.018983	0.015985	0.000000	0.009991	0.058947	0.001898
k290	561	ORPLA9	0.109022	0.078016	0.065013	0.007101	0.005001	0.000000	0.009002	0.006001	0.000000	0.009002	0.250050	0.000000	0.001800	0.355071	0.020004	0.000000	0.009002	0.024005	0.050010	0.001900
k291	579	ORPLB1	0.120048	0.073029	0.011005	0.006101	0.005002	0.004902	0.011004	0.001000	0.000000	0.011004	0.250101	0.002301	0.004800	0.380153	0.011004	0.000000	0.020008	0.037015	0.054022	0.002501
k292	581	ORPLB2	0.100040	0.073029	0.011005	0.006101	0.005002	0.004902	0.011004	0.001000	0.000000	0.011004	0.250101	0.002301	0.004800	0.400161	0.011004	0.000000	0.020008	0.037015	0.054022	0.002501
k293	583	ORPLB3	0.099050	0.086043	0.030015	0.006101	0.005002	0.004702	0.010005	0.001000	0.000000	0.009005	0.240121	0.002201	0.004700	0.401202	0.010005	0.000000	0.010005	0.024012	0.060030	0.001801
k294	585	ORPLB4	0.100171	0.085145	0.019032	0.006102	0.005009	0.004708	0.010017	0.001002	0.000000	0.009015	0.240411	0.002204	0.004500	0.401686	0.010017	0.000000	0.020034	0.024041	0.060103	0.001803
k295	587	ORPLC1	0.094981	0.060988	0.029994	0.006598	0.004999	0.000100	0.009998	0.005999	0.000000	0.009998	0.249950	0.001999	0.005000	0.382923	0.019996	0.009998	0.029994	0.029994	0.044991	0.001500
k296	589	ORPLC2	0.106957	0.116953	0.063974	0.006198	0.004998	0.000100	0.008996	0.004998	0.000000	0.008996	0.234906	0.001799	0.004900	0.344861	0.009996	0.000000	0.014994	0.029988	0.034986	0.001400
k297	591	ORPLC3	0.106903	0.116894	0.040963	0.006194	0.004996	0.000100	0.008992	0.004996	0.000000	0.008992	0.234788	0.024977	0.005200	0.344688	0.009991	0.000000	0.014986	0.029973	0.034968	0.001399
k298	593	ORPLC4	0.106935	0.111932	0.064961	0.006196	0.004997	0.000100	0.008995	0.004997	0.000000	0.008995	0.234858	0.001799	0.005100	0.348790	0.009994	0.000000	0.014991	0.029982	0.034979	0.001399
k299	595	ORPLC5	0.100161	0.085137	0.019031	0.006210	0.005008	0.000100	0.010016	0.005008	0.000000	0.009014	0.236380	0.001903	0.004800	0.401646	0.010016	0.000000	0.020032	0.024039	0.060097	0.001402
k300	597	ORPLD1	0.101897	0.120878	0.079919	0.003297	0.004995	0.001698	0.009990	0.001998	0.000000	0.009990	0.210788	0.002897	0.007300	0.372625	0.000000	0.000000	0.009990	0.029970	0.029970	0.001798
k301	599	ORPLD2	0.090963	0.075969	0.079968	0.003299	0.004998	0.001699	0.007997	0.001999	0.007997	0.009996	0.209915	0.002899	0.007700	0.394841	0.009996	0.000000	0.009996	0.024990	0.052979	0.001799
k302	601	ORPLD3	0.080992	0.085991	0.099990	0.003300	0.004999	0.001700	0.007999	0.002000	0.007999	0.009999	0.209979	0.002900	0.008400	0.393960	0.000000	0.000000	0.009999	0.024997	0.042996	0.001800
k303	697	ORPLD6	0.100837	0.098840	0.078872	0.003494	0.004992	0.001797	0.002995	0.001997	0.000000	0.009984	0.219645	0.002995	0.010800	0.372398	0.000000	0.000000	0.019968	0.029952	0.039935	0.000499
k304	698	ORPLD7	0.100949	0.098950	0.078960	0.003498	0.004997	0.001799	0.002999	0.001999	0.000000	0.009995	0.219889	0.002999	0.008700	0.373811	0.009995	0.000000	0.009995	0.029985	0.039980	0.000500
k305	699	ORPLD8	0.099939	0.094942	0.073955	0.003598	0.004997	0.001899	0.002998	0.001999	0.000000	0.009994	0.229861	0.003098	0.009400	0.367777	0.009994	0.000000	0.014991	0.029982	0.039976	0.000600
k306	700	ORPLD9	0.085904	0.094894	0.073918	0.003596	0.004994	0.001898	0.002997	0.001998	0.000000	0.009989	0.229745	0.003096	0.009900	0.367592	0.009989	0.000000	0.028968	0.029967	0.039956	0.000599
k307	603	ORPLE1	0.075908	0.098880	0.104873	0.000200	0.000999	0.001997	0.001998	0.005993	0.029964	0.010987	0.159806	0.001198	0.011300	0.414497	0.000000	0.000000	0.012984	0.031961	0.034957	0.001498
k308	612	ORPLE10	0.088009	0.105011	0.093010	0.000200	0.001000	0.002000	0.002000	0.006001	0.030003	0.011001	0.160016	0.001200	0.010000	0.409041	0.000000	0.000000	0.013001	0.032003	0.035004	0.001500
k309	613	ORPLE11	0.075923	0.098900	0.104894	0.000200	0.000999	0.001998	0.001998	0.005994	0.024975	0.010989	0.159838	0.001199	0.011100	0.414581	0.000000	0.000000	0.017982	0.031968	0.034964	0.001498
k310	614	ORPLE12	0.075969	0.098960	0.100959	0.000200	0.004998	0.001999	0.001999	0.005998	0.024990	0.010996	0.159935	0.001200	0.010500	0.414832	0.000000	0.000000	0.017993	0.031987	0.034986	0.001499
k311	604	ORPLE2	0.099919	0.114907	0.080935	0.000200	0.000999	0.001998	0.001998	0.005995	0.029976	0.010991	0.159871	0.001199	0.010900	0.398678	0.000000	0.000000	0.012989	0.031974	0.034972	0.001499
k312	605	ORPLE3	0.100000	0.115000	0.105000	0.000200	0.001000	0.002000	0.002000	0.006000	0.030000	0.011000	0.160000	0.001200	0.011100	0.374000	0.000000	0.000000	0.013000	0.032000	0.035000	0.001500
k313	606	ORPLE4	0.077133	0.098169	0.104179	0.000301	0.001002	0.002304	0.002003	0.006010	0.021036	0.011019	0.180310	0.001402	0.010800	0.404695	0.000000	0.000000	0.012021	0.031053	0.035060	0.001503
k314	N/A	ORPLE4-Repeat 2010	0.077133	0.098169	0.104179	0.000301	0.001002	0.002304	0.002003	0.006010	0.021036	0.011019	0.180310	0.001402	0.010800	0.404695	0.000000	0.000000	0.012021	0.031053	0.035060	0.001503
k315	608	ORPLE6	0.075908	0.098880	0.099879	0.000200	0.004994	0.001997	0.001998	0.005993	0.029964	0.010987	0.159806	0.001198	0.011300	0.414497	0.000000	0.000000	0.012984	0.031961	0.035956	0.001498
k316	609	ORPLE7	0.075908	0.098880	0.104873	0.000200	0.004994	0.001998	0.001998	0.005993	0.025968	0.010987	0.159806	0.001198	0.011300	0.414497	0.000000	0.000000	0.012984	0.031961	0.034957	0.001498
k317	610	ORPLE8	0.075831	0.094789	0.100776	0.000199	0.0															

Table A.4. (cont.) Normalized compositions (in mass fractions) of 344 LAW glasses with K-3 Corrosion data

K-3 ID Number	Glass Number from Database	Glass ID	Al ₂ O ₃	B ₂ O ₃	CaO	Cl	Cr ₂ O ₃	F	Fe ₂ O ₃	K ₂ O	Li ₂ O	MgO	Na ₂ O	P ₂ O ₅	SO ₃	SiO ₂	SnO ₂	TiO ₂	V ₂ O ₅	ZnO	ZrO ₂	Others
k331	763	ORPLG24	0.060036	0.079048	0.027016	0.002301	0.006004	0.000901	0.003002	0.058035	0.000000	0.009005	0.210126	0.001401	0.003600	0.416251	0.037022	0.000000	0.000000	0.027016	0.059036	0.000200
k332	765	ORPLG26	0.060048	0.079063	0.027022	0.002302	0.006005	0.000901	0.003002	0.058047	0.000000	0.004003	0.210169	0.001401	0.003400	0.416334	0.034027	0.000000	0.000000	0.027022	0.067054	0.000200
k333	766	ORPLG27	0.060042	0.079055	0.027019	0.002302	0.006004	0.000901	0.003002	0.058041	0.000000	0.004003	0.210148	0.001401	0.003500	0.421296	0.032022	0.000000	0.000000	0.027019	0.064045	0.000200
k334	722	ORPLG5	0.100000	0.087000	0.028000	0.002100	0.006000	0.000800	0.000000	0.053000	0.000000	0.000000	0.195000	0.001300	0.003600	0.408000	0.029000	0.000000	0.000000	0.028000	0.058000	0.000200
k335	723	ORPLG6	0.067843	0.086800	0.027936	0.002195	0.005986	0.000898	0.002993	0.053876	0.000000	0.009977	0.197544	0.001397	0.003600	0.417037	0.028933	0.000000	0.000000	0.034919	0.057866	0.000200
k336	724	ORPLG7	0.067823	0.086774	0.026930	0.002194	0.005984	0.000898	0.002992	0.054857	0.000000	0.009974	0.199479	0.001396	0.003900	0.414917	0.028925	0.000000	0.000000	0.034909	0.057849	0.000199
k337	725	ORPLG8	0.067905	0.085879	0.026962	0.002297	0.005992	0.000899	0.002996	0.055921	0.000000	0.009986	0.204712	0.001398	0.003600	0.411422	0.028959	0.000000	0.000000	0.033952	0.056920	0.000200
k338	726	ORPLG9	0.066906	0.084881	0.026962	0.002297	0.005991	0.000899	0.002996	0.057919	0.000000	0.009986	0.209705	0.001398	0.003600	0.407427	0.027961	0.000000	0.000000	0.033952	0.056920	0.000200
k339	920	WDFL1	0.061024	0.100040	0.021008	0.004502	0.000000	0.000100	0.055022	0.004002	0.000000	0.015006	0.210084	0.001701	0.003300	0.445179	0.000000	0.014006	0.000000	0.035014	0.030012	0.000000
k340	N/A	WDFL1+15	0.063019	0.096029	0.020006	0.005002	0.001000	0.000100	0.053016	0.004001	0.000000	0.014004	0.233070	0.001901	0.003700	0.429129	0.000000	0.013004	0.000000	0.034010	0.029009	0.000000
k341	921	WDFL1H	0.059952	0.097921	0.019984	0.004396	0.000999	0.000100	0.053957	0.003997	0.000000	0.014988	0.227817	0.001699	0.003600	0.432652	0.000000	0.014988	0.000000	0.033973	0.028977	0.000000
k342	924	WDFL2	0.061018	0.100030	0.052016	0.003501	0.000000	0.000600	0.055017	0.004001	0.021006	0.015005	0.153046	0.002101	0.004500	0.449135	0.000000	0.014004	0.000000	0.035011	0.030009	0.000000
k343	N/A	WDFL2+15	0.060091	0.097147	0.051077	0.003906	0.000000	0.000701	0.054082	0.004006	0.021032	0.014021	0.171258	0.002303	0.005600	0.437660	0.000000	0.014021	0.000000	0.034051	0.029044	0.000000
k344	925	WDFL2H	0.059970	0.098950	0.051974	0.003498	0.000000	0.000600	0.053973	0.001999	0.020989	0.014992	0.165917	0.002099	0.005300	0.441778	0.000000	0.013993	0.000000	0.033983	0.029985	0.000000

Table A.5. Values of K-3 Refractory Corrosion Neck Loss at 1208°C for 344 LAW glasses.

K-3 ID Number	Glass Number from Database	Glass ID	Neck Loss (inch)
k001	N/A	A1-AN105R2	0.0175
k002	N/A	A2-AP101	0.0255
k003	282	A2B1-2	0.0085
k004	283	A2B1-3	0.009
k005	330	A3-AN104	0.0305
k006	286	A3C2-1	0.0245
k007	287	A3C2-2	0.0225
k008	288	A3C2-3	0.0165
k009	919	AP105DLAW11	0.026
k010	910	AP105DLAW2	0.007
k011	911	AP105DLAW3	0.012
k012	912	AP105DLAW4	0.018
k013	914	AP105DLAW6	0.02
k014	915	AP105DLAW7	0.021
k015	916	AP105DLAW8	0.032
k016	N/A	AY102D1-01	0.048
k017	N/A	AY102D1-02	0.068
k018	N/A	AY102D1-03	0.132
k019	N/A	AY102D1-04	0.078
k020	N/A	AY102D1-05	0.035
k021	N/A	AY102D1-06R	0.028
k022	N/A	AY102D2-01	0.02*
k023	N/A	AY102D2-05	0.021*
k024	N/A	AY102D2-06	0.0155*
k025	N/A	B1-AZ101	0.0065
k026	N/A	C1-AN107R1	0.0265
k027	289	C2-AN102C35	0.02
k028	N/A	I10-G-130B	0.024
k029	41	LAWA104	0.0398
k030	42	LAWA105	0.07
k031	315	LAWA126	0.014*
k032	316	LAWA126R3	0.023
k033	318	LAWA127R1	0.0115
k034	174	LAWA130	0.019
k035	177	LAWA134	0.022
k036	178	LAWA135	0.0165
k037	179	LAWA136	0.018
k038	N/A	LAWA140R3	0.023
k039	392	LAWA149	0.063
k040	N/A	LAWA152S2	0.024
k041	N/A	LAWA155S2	0.04
k042	N/A	LAWA156S2	0.0455
k043	N/A	LAWA159S2	0.032
k044	N/A	LAWA160S2	0.0155
k045	399	LAWA161S2	0.0325
k046	N/A	LAWA162S2	0.05

Table A.5. Values of K-3 Refractory Corrosion Neck Loss at 1208°C for 344 LAW glasses.

K-3 ID Number	Glass Number from Database	Glass ID	Neck Loss (inch)
k047	N/A	LAWA164S2	0.034
k048	N/A	LAWA165S2	0.0385
k049	N/A	LAWA166S2	0.039
k050	N/A	LAWA167S2	0.029
k051	N/A	LAWA168S2	0.033
k052	502	LAWA173	0.121
k053	504	LAWA175	0.081
k054	505	LAWA176	0.065
k055	512	LAWA183	0.0415
k056	513	LAWA184	0.037
k057	514	LAWA185	0.0345
k058	515	LAWA186	0.0435
k059	516	LAWA187	0.0327
k060	N/A	LAWA187R1	0.066
k061	519	LAWA188	0.0413
k062	520	LAWA189	0.067
k063	521	LAWA190	0.0425
k064	522	LAWA191	0.052
k065	523	LAWA192	0.052
k066	525	LAWA194	0.067
k067	526	LAWA195	0.033
k068	527	LAWA196	0.049
k069	N/A	LAWA23C	0.0664
k070	N/A	LAWA28	0.0143
k071	N/A	LAWA28Ti	0.014
k072	N/A	LAWA29	0.0211
k073	N/A	LAWA30	0.0213
k074	N/A	LAWA32	0.0202
k075	N/A	LAWA34	0.0292
k076	N/A	LAWA36	0.0182
k077	127	LAWA41-3	0.0379
k078	128	LAWA44-3	0.019
k079	N/A	LAWA44PNCC	0.0135*
k080	N/A	LAWA44PNCC-rep	0.0095*
k081	N/A	LAWA44R11	0.025
k082	129	LAWA52-2	0.0628
k083	130	LAWA60	0.019
k084	132	LAWA88	0.0335
k085	120	LAWA95	0.0264
k086	535	LAWB103	0.0145
k087	138	LAWB37	0.0051
k088	N/A	LAWB45-S	0.0135
k089	183	LAWB61	0.006
k090	189	LAWB64	0.0078
k091	190	LAWB64S0	0.01
k092	192	LAWB65	0.003

Table A.5. Values of K-3 Refractory Corrosion Neck Loss at 1208°C for 344 LAW glasses.

K-3 ID Number	Glass Number from Database	Glass ID	Neck Loss (inch)
k093	196	LAWB67	0.001*
k094	198	LAWB68	0.0055
k095	199	LAWB69	0.014
k096	201	LAWB70	0.01
k097	203	LAWB71	0.0095
k098	205	LAWB72	0.0075
k099	207	LAWB73	0.0095
k100	209	LAWB74	0.014
k101	215	LAWB77	0.007
k102	217	LAWB78	0.014
k103	219	LAWB79	0.013
k104	221	LAWB80	0.011
k105	223	LAWB81	0.012
k106	225	LAWB82	0.009
k107	227	LAWB83	0.0095
k108	229	LAWB84	0.0095
k109	231	LAWB85	0.0065
k110	233	LAWB86	0.0065
k111	309	LAWB87	0.0085
k112	311	LAWB88	0.006
k113	N/A	LAWB89R1	0.005
k114	N/A	LAWB90R1	0.0115
k115	N/A	LAWB91R1	0.006
k116	N/A	LAWB92R1	0.0125
k117	242	LAWB93	0.005
k118	244	LAWB94	0.0045
k119	246	LAWB95	0.006
k120	529	LAWB97	0.0085
k121	531	LAWB99	0.01
k122	442	LAWC100	0.036
k123	N/A	LAWC101S2	0.027
k124	N/A	LAWC102S2	0.039
k125	N/A	LAWC103S2	0.044
k126	438	LAWC21REV2	0.0195
k127	N/A	LAWC21S	0.0168
k128	81	LAWC25S	0.0128*
k129	252	LAWC27	0.018
k130	256	LAWC29	0.0135
k131	260	LAWC31	0.0175
k132	261	LAWC31R2	0.018
k133	N/A	LAWC34S2	0.019
k134	290	LAWC35S2	0.0185
k135	N/A	LAWC36S2	0.0155
k136	454	LAWC10H	0.0065
k137	N/A	LAWC11	0.0195
k138	476	LAWC13	0.061

Table A.5. Values of K-3 Refractory Corrosion Neck Loss at 1208°C for 344 LAW glasses.

K-3 ID Number	Glass Number from Database	Glass ID	Neck Loss (inch)
k139	477	LAWE14	0.066
k140	478	LAWE15	0.0505
k141	479	LAWE16	0.063
k142	N/A	LAWE2H	0.0575
k143	448	LAWE3	0.031
k144	474	LAWE3H	0.0535
k145	625	LAWE4H	0.035
k146	N/A	LAWE5H	0.028
k147	N/A	LAWE7	0.0335
k148	451	LAWE7H	0.033
k149	N/A	LAWE9H	0.016
k150	480	LAWM57	0.084
k151	481	LAWM58	0.056
k152	482	LAWM59	0.04
k153	483	LAWM60	0.039
k154	484	LAWM61	0.043
k155	485	LAWM62	0.0415
k156	486	LAWM63	0.0605
k157	487	LAWM64	0.0437
k158	488	LAWM65	0.0967
k159	489	LAWM66	0.0495
k160	490	LAWM67	0.0625
k161	491	LAWM68	0.071
k162	492	LAWM69	0.0385
k163	493	LAWM70	0.053
k164	494	LAWM71	0.046
k165	495	LAWM72	0.074
k166	496	LAWM73	0.0667
k167	497	LAWM74	0.0165
k168	498	LAWM75	0.039
k169	499	LAWM76	0.052
k170	N/A	LAWSNa1-3	0.029
k171	N/A	LAWSNa2-2	0.049
k172	N/A	LAWSNa3-2	0.0285
k173	778	LORPM10R1	0.032
k174	779	LORPM11	0.001*
k175	782	LORPM14R1	0.145
k176	785	LORPM17R1	0.038
k177	787	LORPM19R1	0.014
k178	788	LORPM20R1	0.056
k179	789	LORPM21	0.06
k180	793	LORPM25	0.024
k181	797	LORPM28R1	0.032
k182	802	LORPM32	0.018
k183	804	LORPM34	0.01
k184	805	LORPM35	0.099

Table A.5. Values of K-3 Refractory Corrosion Neck Loss at 1208°C for 344 LAW glasses.

K-3 ID Number	Glass Number from Database	Glass ID	Neck Loss (inch)
k185	806	LORPM36	0.02
k186	807	LORPM37	0.027
k187	808	LORPM38	0.001*
k188	809	LORPM39	0.087
k189	1004	LORPM4R2	0.001*
k190	N/A	LORPM4R2-Repea	0.003
k191	777	LORPM9	0.007
k192	N/A	OD2-G-50A	0.0126
k193	835	ORLEC1	0.025
k194	844	ORLEC10	0.016
k195	845	ORLEC11	0.0315
k196	846	ORLEC12	0.0315
k197	847	ORLEC13	0.011
k198	848	ORLEC14	0.0235
k199	849	ORLEC15	0.027
k200	850	ORLEC16	0.0175
k201	851	ORLEC17	0.0125
k202	852	ORLEC18	0.0135
k203	853	ORLEC19	0.0105
k204	836	ORLEC2	0.0315
k205	854	ORLEC20	0.009
k206	855	ORLEC21	0.026
k207	856	ORLEC22	0.033
k208	857	ORLEC23	0.0265
k209	858	ORLEC24	0.029
k210	862	ORLEC26	0.0275
k211	863	ORLEC27	0.0295
k212	864	ORLEC28	0.03
k213	873	ORLEC29	0.0145
k214	837	ORLEC3	0.013
k215	874	ORLEC30	0.0165
k216	875	ORLEC31	0.011
k217	876	ORLEC32	0.0105
k218	877	ORLEC33	0.0145
k219	878	ORLEC34	0.0195
k220	879	ORLEC35	0.0105
k221	880	ORLEC36	0.008
k222	881	ORLEC37	0.03
k223	882	ORLEC38	0.0405
k224	883	ORLEC39	0.01
k225	838	ORLEC4	0.0045
k226	884	ORLEC40	0.0245
k227	885	ORLEC41	0.0395
k228	886	ORLEC42	0.0355
k229	892	ORLEC43	0.025
k230	893	ORLEC44	0.035

Table A.5. Values of K-3 Refractory Corrosion Neck Loss at 1208°C for 344 LAW glasses.

K-3 ID Number	Glass Number from Database	Glass ID	Neck Loss (inch)
k231	894	ORLEC45	0.033
k232	895	ORLEC46	0.04
k233	896	ORLEC47	0.036
k234	897	ORLEC48R	0.033
k235	898	ORLEC49	0.021
k236	N/A	ORLEC49-Repeat	0.025
k237	900	ORLEC50	0.018
k238	901	ORLEC51	0.03
k239	902	ORLEC52	0.033
k240	840	ORLEC6	0.013
k241	841	ORLEC7	0.034
k242	842	ORLEC8	0.043
k243	843	ORLEC9	0.0445
k244	545	ORPLA1	0.108
k245	563	ORPLA10	0.064
k246	565	ORPLA11	0.0275
k247	567	ORPLA12	0.0175
k248	569	ORPLA13	0.025
k249	571	ORPLA14	0.0115
k250	573	ORPLA15	0.0355
k251	575	ORPLA16	0.039
k252	577	ORPLA17	0.042
k253	547	ORPLA2	0.0705
k254	689	ORPLA20	0.033
k255	N/A	ORPLA20HV	0.0385*
k256	834	ORPLA20R1	0.0395
k257	690	ORPLA21	0.061
k258	693	ORPLA24	0.064
k259	694	ORPLA25	0.089
k260	549	ORPLA3	0.041
k261	751	ORPLA38-1	0.0435
k262	811	ORPLA39	0.115
k263	551	ORPLA4	0.123
k264	812	ORPLA40	0.109
k265	813	ORPLA41	0.074
k266	814	ORPLA42	0.082
k267	815	ORPLA43	0.023
k268	N/A	ORPLA43R1-1	0.0345
k269	N/A	ORPLA43R1-2	0.0415
k270	818	ORPLA44	0.0415
k271	819	ORPLA45	0.058
k272	820	ORPLA46	0.047
k273	N/A	ORPLA46-Repeat	0.0385
k274	822	ORPLA47	0.042
k275	823	ORPLA48	0.036
k276	824	ORPLA49	0.045

Table A.5. Values of K-3 Refractory Corrosion Neck Loss at 1208°C for 344 LAW glasses.

K-3 ID Number	Glass Number from Database	Glass ID	Neck Loss (inch)
k277	553	ORPLA5	0.015
k278	825	ORPLA50	0.044
k279	826	ORPLA51	0.032
k280	827	ORPLA52	0.0365
k281	828	ORPLA53	0.041
k282	829	ORPLA54	0.029
k283	830	ORPLA55	0.021
k284	831	ORPLA56	0.027
k285	832	ORPLA57	0.027
k286	833	ORPLA58	0.022
k287	555	ORPLA6	0.0225
k288	557	ORPLA7	0.0295
k289	559	ORPLA8	0.051
k290	561	ORPLA9	0.076
k291	579	ORPLB1	0.033
k292	581	ORPLB2	0.036
k293	583	ORPLB3	0.038
k294	585	ORPLB4	0.028
k295	587	ORPLC1	0.066
k296	589	ORPLC2	0.08
k297	591	ORPLC3	0.03
k298	593	ORPLC4	0.073
k299	595	ORPLC5	0.021
k300	597	ORPLD1	0.031
k301	599	ORPLD2	0.05
k302	601	ORPLD3	0.091
k303	697	ORPLD6	0.04
k304	698	ORPLD7	0.047
k305	699	ORPLD8	0.066
k306	700	ORPLD9	0.063
k307	603	ORPLE1	0.059
k308	612	ORPLE10	0.053
k309	613	ORPLE11	0.0595
k310	614	ORPLE12	0.0305
k311	604	ORPLE2	0.0305
k312	605	ORPLE3	0.0715
k313	606	ORPLE4	0.0865
k314	N/A	ORPLE4-Repeat 20	0.0935
k315	608	ORPLE6	0.0535
k316	609	ORPLE7	0.033
k317	610	ORPLE8	0.069
k318	611	ORPLE9	0.048
k319	712	ORPLF10	0.009
k320	N/A	ORPLF10-Repeat	0.005
k321	716	ORPLF13	0.0125
k322	717	ORPLF14	0.017

Table A.5. Values of K-3 Refractory Corrosion Neck Loss at 1208°C for 344 LAW glasses.

K-3 ID Number	Glass Number from Database	Glass ID	Neck Loss (inch)
k323	704	ORPLF4	0.0085
k324	708	ORPLF7	0.01
k325	N/A	ORPLF7-Repeat	0.02
k326	710	ORPLF8	0.018
k327	711	ORPLF9	0.004
k328	728	ORPLG10	0.0415
k329	729	ORPLG11	0.06
k330	730	ORPLG12	0.0245
k331	763	ORPLG24	0.032
k332	765	ORPLG26	0.0285
k333	766	ORPLG27	0.034
k334	722	ORPLG5	0.016
k335	723	ORPLG6	0.0225
k336	724	ORPLG7	0.0265
k337	725	ORPLG8	0.036
k338	726	ORPLG9	0.038
k339	920	WDFL1	0.019
k340	N/A	WDFL1+15	0.052
k341	921	WDFL1H	0.047
k342	924	WDFL2	0.034
k343	N/A	WDFL2+15	0.048
k344	925	WDFL2H	0.041

(a) k_{1208} = Neck corrosion distance in 6-day test at 1208°C (in inches).

Appendix B – Statistical Methods to Develop, Evaluate, and Validate Property-Compositions Models Fit to Experimental Data

This appendix presents statistical methods used for developing, evaluating, and validating waste glass property-composition models. Section B.1 discusses mixture experiments and corresponding model forms. Section B.2 discusses the least squares regression methods used to fit models to data and the corresponding assumptions. Section B.3 discusses the statistical methods and summary statistics used for model evaluation based on the data used to fit a model. Section B.4 discusses statistical methods for model augmentation (i.e., adding terms to a model) and model reduction (i.e., removing unneeded terms from a model). Section B.5 discusses the statistical methods and summary statistics used for model validation based on data not used to fit a model. Section B.6 discusses several statistical intervals used to quantify uncertainties in model predictions. Draper and Smith (1998) and Montgomery et al. (2012) are textbook references that discuss statistical methods for evaluating and validating models.

B.1 Mixture Experiments and Model Forms

A *mixture experiment* involves mixing two or more components in various proportions, and then measuring one or more response variables for the resulting end-product mixtures. If the proportions of q mixture components are denoted g_i , $i = 1, 2, \dots, q$, then these proportions are subject to the basic mixture constraints

$$0 \leq g_i \leq 1 \forall i \quad \text{and} \quad \sum_{i=1}^q g_i = 1. \quad (\text{B.1})$$

Often in practice, the component proportions may be subject to additional single-component constraints (SCCs)

$$0 \leq L_i \leq g_i \leq U_i \leq 1 \quad (\text{B.2})$$

and/or multiple-component constraints (MCCs) that can be written in the general form

$$\sum_{i=1}^q A_{ki} g_i + A_{k0} \geq 0, \quad k = 1, 2, \dots, K. \quad (\text{B.3})$$

In Eq. (B.2), L_i and U_i denote, respectively, the lower and upper constraints on the i^{th} component ($i = 1, 2, \dots, q$). In Eq. (B.3), the A_{ki} ($i = 1, 2, \dots, q$) and A_{k0} denote the coefficients of the k^{th} MCC. The MCC in Eq. (B.3) is a linear function of glass composition, but MCCs may also involve nonlinear functions of glass composition. Cornell (2002) provides a comprehensive discussion of statistical methods for the design, modeling, and data analysis of mixture experiments.

The linear mixture (LM) model and partial quadratic mixture (PQM) model forms for mixture experiment data were used in this work. The LM model form is given by

$$f(y) = \sum_{i=1}^q \beta_i g_i + e \quad (\text{B.4})$$

while the PQM model form is given by

$$f(y) = \sum_{i=1}^q \beta_i g_i + \text{Selected} \left\{ \sum_{i=1}^q \beta_{ii} g_i^2 + \sum_{i=1}^{q-1} \sum_{j=i+1}^q \beta_{ij} g_i g_j \right\} + e. \quad (\text{B.5})$$

In Eqs. (B.4) and (B.5), y is a property or response variable that can be measured for each end-product mixture; $f(y)$ is some mathematical transformation of y (which could be the identity transformation); the g_i ($i = 1, 2, \dots, q$) are proportions of q components subject to the constraints in Eq. (B.1) and possibly constraints of the forms in Eqs. (B.2) and/or (B.3); the b_i ($i = 1, 2, \dots, q$), the b_{ii} (selected), and the b_{ij} (selected) are coefficients to be estimated from data; and E is a random experimental and property measurement error for each data point. Estimates of model coefficients and related statistics can be obtained using well-established statistical methods. More traditional statistical methods are used for the case where the E are independent (i.e., not correlated) and normally distributed with mean 0 and standard deviation σ , but other techniques, also discussed in this document, exist for cases with more complex error structures. In Eq. (B.5), “Selected” means that only some of the terms in curly brackets are included in the model. The subset is selected using standard stepwise regression or related methods (Draper and Smith 1998; Montgomery et al. 2012). LM models and PQM models are discussed in more detail and illustrated, respectively, by Cornell (2002) and Piepel et al. (2002).

Cornell (2002) discusses many other empirical mixture model forms that can be more appropriate than models of the forms in Eqs. (B.4) and (B.5) in certain specialized conditions. However, models of the form in Eqs. (B.4) and (B.5) are widely used in many application areas (including waste glass property modeling) and have been shown to perform very well (Hrma et al. 1994, Piepel et al. 2007, Piepel et al. 2008, Vienna et al. 2013, Vienna 2014, Vienna et al. 2016). Selection of LM and PQM models is often informed by knowledge of the effects of specific components on the response gained through experience or scientific discoveries.

B.2 Least Squares Regression Methods and Assumptions for Fitting Models

Empirical or semi-empirical property-composition models are typically fitted to datasets using ordinary least squares (OLS) or weighted least squares (WLS) regression. Generalized linear models (GLMs) have also been used in this work in the form of a logistic model for VHT, and as one of the techniques employed to find good predictive models for the PCT response. Section B.2.1 discusses OLS and WLS regression, while Section B.2.2 discusses GLMs. Draper and Smith (1998), Montgomery et al. (2012), and Myers et al. (2002) provide additional discussion of the OLS, WLS, and GLM topics.

B.2.1 Ordinary and Weighted Least Squares Regression

The underlying assumptions of OLS and WLS regression are as follows:

- i. The predictor variable values (e.g., mass fractions of glass components) are known or measured without uncertainty or at least the uncertainty is small relative to the uncertainty in response variable (glass property) values. This assumption is expected to hold for the work of modeling glass properties using glass compositions as predictors because glass composition is usually known accurately, and any significant biases can generally be corrected.
- ii. The testing and/or measurement errors in a response variable (glass property) over a model development dataset are independently distributed (i.e., the errors are not correlated across measurements). For OLS regression, the additional assumption is made that the errors are

identically distributed (i.e., with zero mean and the same variance). For WLS regression, the errors are also assumed to have zero mean, but the variance can be different for different data points.

- iii. The errors from (ii) are normally (Gaussian) distributed.

Regarding assumption (i), the true compositions of glasses in a model development dataset are generally not known, and so any representation of glass composition selected (e.g., target compositions, analyzed compositions, or adjusted and normalized versions of analyzed compositions) will be subject to uncertainty. Weier and Piepel (2003) discuss a procedure for performing adjustments and weighted normalization of analyzed glass compositions that corrects for biases and reduces uncertainties in analyzed glass compositions. If representations of glass composition do not have significant biases (or those biases are appropriately corrected), it is generally expected that uncertainties in glass compositions will be small compared to uncertainties in glass property values. Further, uncertainties in glass compositions are expected to be small compared to errors in using empirical or semi-empirical model forms to approximate the true (but unknown) property-composition relationships. Hence, assumption (i) is sufficiently satisfied for most waste glass property-composition modeling situations.

The portion of assumption (ii) having to do with the independence of errors in testing and measuring properties may not be completely satisfied when model development datasets are composed of subsets of data generated at different times or locations (e.g., different laboratories). There is the potential for errors (uncertainties) in testing and measuring properties to vary for different subsets of data and be more alike within the same subset of data. However, this issue has generally not been a problem in many past property-composition modeling efforts (Vienna and Kim 2014). If needed, generalized least squares (GLS; Myers et al. 2002) methods that account for correlations among data points could be applied.

The “identically distributed errors” portion of assumption (ii) for OLS regression is not valid for some properties, because the variance of errors in testing and measurement of properties depends on the value of the property. For example, the variances of viscosity and durability results for waste glasses tend to increase as the values of these properties increase. In cases where the equal variance (identically distributed errors) assumption is violated, it can often be remedied by applying an appropriate mathematical transformation to the property values (e.g., a logarithmic transformation). The Box-Cox family of transformations contains transformations (including the logarithmic transformation) appropriate for many models (see Draper and Smith 1998). Such transformations also often yield better-fitting empirical or semi-empirical property-composition models. In some cases, a property transformation used in a particular model form may be preferred for some reason (e.g., provides a better fit), but does not satisfy the constant variance assumption of (ii). Or, it may be that the difference in variances across response values in the modeling dataset cannot be rectified by a response transformation. In such cases, other regression methods such as WLS regression or GLS regression (Myers et al. 2002) could be applied.

The assumption of normally distributed measurement and testing errors in the measured response variable values allows the use of normal theory regression tests, estimation of the standard errors of the coefficients, and uncertainty equations associated with the fitted regression model and resulting predictions. For example, normal theory confidence intervals and prediction intervals can be used (see Section B.6).

As discussed previously, OLS regression requires that all response values for the modeling data have constant variance (i.e., uncertainty). WLS regression accounts for response values having different variations by using a weight for each data point (w_i). Often, w_i is chosen to be proportional to the reciprocal of the variance (squared standard deviation) of the response for the i^{th} data point (y_i).

$$w_i = \frac{\lambda}{\text{var}(y_i)} = \frac{\lambda}{[SD(y_i)]^2} \quad (\text{B.6})$$

where λ is a proportionality constant (which could be 1). Thus, in such a WLS regression the weighted response values $\sqrt{w_i}y_i$ then have equal variance. However, other methods for selecting weights can be applicable for various situations.

In summary, assumptions of OLS regression may not be completely satisfied for typical property-composition datasets and models. Violations of the constant variance assumption for property values over a modeling dataset can sometimes be addressed by appropriate property transformations so that OLS regression may be used. Other violations may be small enough that OLS regression methods can still be used without significant consequence. However, if there are large enough differences in variances of property values across a modeling dataset that cannot be addressed by a property transformation, then WLS regression methods should be used. If there are correlations among data points in a regression set, GLS methods are needed, as discussed in the following subsection.

B.2.2 Regression Using Generalized Linear Models (GLM)

The underlying assumptions of GLM regression are as follows:

- i. The predictor variable values (e.g., mass fractions of glass components) are known or measured without uncertainty, or at least the uncertainty is small relative to the uncertainty in response variable (glass property) values.
- ii. The responses of a variable (glass property), y_1, y_2, \dots, y_n over a model development dataset are independent with means $\mu_1, \mu_2, \dots, \mu_n$, respectively.
- iii. The observation y_i has a distribution that is a member of the exponential family. The exponential family of distributions includes normal, binomial, Poisson, gamma, and inverse gaussian. OLS is a special case where responses are independent and normally distributed.

A GLM for a linear mixture model is built using a linear predictor

$$\eta = \sum_{i=1}^q \beta_i g_i \quad (\text{B.7})$$

while the PQM model form for a GLM is built using the linear predictor

$$\eta = \sum_{i=1}^q \beta_i g_i + \text{Selected} \left\{ \sum_{i=1}^q \beta_{ii} g_i^2 + \sum_i^{q-1} \sum_j^q \beta_{ij} g_i g_j \right\}. \quad (\text{B.8})$$

The model is found using a link function

$$\eta_i = h(\mu_i), i = 1, 2, \dots, n$$

so that the expected response for a linear mixture model is found through

$$E(y_i) = h^{-1}(\eta_i) = h^{-1}\left(\sum_{i=1}^q \beta_i g_i\right) \quad (\text{B.9})$$

and the expected response for the PQM model is found through

$$E(y_i) = h^{-1}(\eta_i) = h^{-1}\left(\sum_{i=1}^q \beta_i g_i + \text{Selected} \left\{ \sum_{i=1}^q \beta_{ii} g_i^2 + \sum_{i=1}^{q-1} \sum_j^q \beta_{ij} g_i g_j \right\}\right). \quad (\text{B.10})$$

The link function $h(\cdot)$ can take many forms, including an identity function, a logarithmic function, a reciprocal function, or another monotonic differentiable function. The variance σ_i^2 ($i = 1, 2, \dots, n$) of the observations is a function of the mean μ_i . Model parameters for GLMs are obtained using weighted least squares iteratively.

B.3 Statistical Methods for Model Evaluation

There are many statistical methods (both numerical and graphical) for assessing models. *Evaluation methods* assess a model with the data used to develop the model. Such data are referred to as *model development data*. The goals of model evaluation are to assess (i) how well a model fits the data used to develop it, (ii) how well the least squares or other regression method assumptions are satisfied (see Section B.2), and (iii) whether there are any outlying or influential data points that significantly affect the fitted model.

Problems detected by model evaluation such as violation of assumptions, detection of outlying data points, or detection of model inadequacy require implementation of various remedies in the model development process until the problem(s) are corrected. When the model being evaluated acceptably fits the data used to develop the model, *model validation* methods should be applied using data not used to develop the model. Such data are referred to as *model validation data*. If model validation data are not available, *cross-validation methods* can be applied using the model development data. Cross-validation methods leave out one or more data points at a time, so that some of the data are used for model development and some for model validation. Such methods are also referred to as data-splitting validation methods, where part of the data is used for model development and evaluation, while the other part is used for validation. Draper and Smith (1998) and Montgomery et al. (2012) discuss statistical methods for evaluating and validating models.

Model evaluation techniques include predicted versus measured (PvM) property plots, standardized residual plots, outlier diagnostics, three R^2 statistics, root mean squared error (*RMSE*), and statistical lack-of-fit (LOF) tests. Each of these is explained briefly below. The following notation is used in the subsequent descriptions and definitions:

- n = the number of data points used to fit a model
- p = the number of parameters (coefficients) in a model form estimated via regression on the data
- y_i = the measured property value (mathematically transformed, if appropriate for the model form used) for the i^{th} data point
- \hat{y}_i = the predicted property value (mathematically transformed, if appropriate for the model form used) for the i^{th} data point made using the model fitted to all n data points
- r_i = the residual for the i^{th} data point = $y_i - \hat{y}_i$

- $\hat{y}_{(i)}$ = the predicted property value (mathematically transformed, if appropriate for the model form used) for the i^{th} data point made using a model fitted to all n data points except the i^{th}
- w_i = the weight applied to the i^{th} data point in cases where WLS regression is used. Typically, w_i is proportional to the reciprocal of the variance of the response variable for the i^{th} data point
- \bar{y} = the unweighted average (mean) of the n measured property values (mathematically transformed, if appropriate for the model form used)
- \bar{y}_w = the weighted average (mean) of the n measured property values (mathematically transformed, if appropriate for the model form used)

$$\bar{y}_w = \frac{\sum_{i=1}^n w_i y_i}{\sum_{i=1}^n w_i} \quad (B.11)$$

The model evaluation methods are now briefly described.

- PvM property plots show how well model predicted values, \hat{y}_i , compare to the measured values, y_i , for the glasses in the model development dataset. Predicted property values, \hat{y}_i , are plotted on the y-axis and measured property values (mathematically transformed, if appropriate for the model form used), y_i , are plotted on the x-axis. A line with a slope of 1 and an intercept of 0 is included in the plot for reference purposes and represents the ideal situation of predicted values equaling measured values. Plotted points falling above this line correspond to glasses for which the model over-predicts the property, while plotted points falling below this line represent glasses for which the model under-predicts the property. A preponderance of plotted points in a portion of the plot falling above or below the line indicates that the model tends to yield biased predictions for that range of property values. Plotted points far from the line are outlying or potentially influential data points.

For WLS regression, an *ordinary (unweighted) PvM plot* of \hat{y}_i versus y_i could be viewed as is done for OLS regression. Or, a *weighted PvM plot* of $\sqrt{w_i}\hat{y}_i$ versus $\sqrt{w_i}y_i$ could be viewed. The ordinary (unweighted) PvM plot has the advantage of retaining the units of the response (or its transformation), but the disadvantage that points with smaller weights (i.e., higher uncertainties) may appear farther from the line with a slope of 1 and an intercept of 0. However, rather than considering this a disadvantage, it may be better thought of as showing the penalty paid in obtaining predictions having more uncertainty for modeling data points with smaller weights (i.e., higher uncertainty). The weighted PvM plot would show the model predictive performance for the modeling data points after accounting for (i.e., removing the scatter due to) the differing weights (i.e., uncertainties).

- RMSE for OLS regression is given by

$$RMSE_{OLS} = \sqrt{\frac{\sum_{i=1}^n (\hat{y}_i - y_i)^2}{n-p}} \quad (B.12a)$$

and for WLS regression

$$RMSE_{WLS} = \sqrt{\frac{\sum_{i=1}^n w_i (\hat{y}_i - y_i)^2}{n-p}} \quad (B.12b)$$

If the fitted model is adequate and does not have a statistically significant LOF, this statistic provides an estimate of the experimental and measurement uncertainty standard deviation associated with melting glasses and measuring the associated property. The statistic $RMSE$ is included as standard output in most regression software, and has units the same as the property values y_i (including any mathematical transformation of the property in the model form) for OLS regression and the units of $\sqrt{w_i}y_i$ for WLS regression.

- Standardized residual plots display standardized residuals (s_i , differences in predicted and measured property values divided by their standard deviations) versus various quantities, such as normalized glass component mass fractions (g_i), predicted property values (\hat{y}_i), or an index associated with each data point. The formula for a standardized residual is given by

$$s_i = \frac{r_i}{RMSE_{OLS}[1 - \mathbf{g}_i^T (\mathbf{G}^T \mathbf{G})^{-1} \mathbf{g}_i]^{0.5}} \quad (\text{B.13a})$$

for OLS regression and by

$$s_i = \frac{\sqrt{w_i} r_i}{RMSE_{WLS}[1 - \mathbf{g}_i^T (\mathbf{G}^T \mathbf{W} \mathbf{G})^{-1} \mathbf{g}_i]^{0.5}} \quad (\text{B.13b})$$

for WLS regression.

In Eqs. (B.13a) and (B.13b): s_i , w_i , and r_i are as previously described; $RMSE_{OLS}$ and $RMSE_{WLS}$ are respectively given by Eqs. (B.12a) and (B.12b); \mathbf{g}_i is the composition (column) vector for the i^{th} modeling data point expanded in the form of the model; \mathbf{G} is an $n \times p$ matrix of the compositions in the modeling dataset expanded in the form of the model; and \mathbf{W} is an $n \times n$ matrix with the weights, w_i , along the main diagonal, and zeros elsewhere.

Patterns in the s_i versus \hat{y}_i plot can indicate a violation of the least squares regression assumptions and suggest a property transformation to remedy the situation. Patterns in the s_i versus x_i plots can indicate inadequacies of the model or least squares assumptions. Patterns in s_i versus data indices can indicate subsets of the data for which a model may be inadequate. Standardized residuals are typically used in residual plots because the majority should fall within the range of ± 2.0 and almost all should fall within ± 3.0 . Comparing standardized residuals to such a range provides an easy criterion for judging whether a data point is outlying.

- Normality plots display normal scores versus the ordered (from smallest to largest) standardized residuals [from Eqs. (B.13a) and (B.13b) for OLS and WLS, respectively] for the n data points used to fit the model being assessed. Normal scores are the expected values of a sample of size n from standard normal distribution (with mean 0 and standard deviation 1). The plotted points are compared to the ideal of a straight line corresponding to a normal distribution. A straight middle portion of the plot with curved “tails” on each end of the plot indicates the presence of outlying data points, which cause a heavier-tailed distribution than the normal distribution.
- Outlier diagnostics and plots indicate data points that are outlying or influential with respect to property value or composition. There are too many of these diagnostics and plots to discuss here, but several produced by the R software (Ihaka and Gentleman 1996; R Core Team 2019) and MatLab (Mathworks 2019) were considered in this work. Draper and Smith (1998) and Montgomery et al. (2012) discuss outlier diagnostics and plots for OLS regression, but software such as R (R Core Team

2019) and SAS (SASTM Software SAS Institute Inc., Cary, NC) produce the appropriate versions of diagnostics and plots for WLS as well as OLS regression.

- R^2 statistics quantify the proportion of variation in the property values (mathematically transformed, if appropriate for the model form used) y_i (for OLS regression) or weighted property values $\sqrt{w_i}y_i$ (for WLS regression) accounted for by the fitted model. Three R^2 statistics are used, as discussed later in this section.
- A statistical lack-of-fit (LOF) test checks whether the differences (for OLS regression) or weighted differences (for WLS regression) between measured and predicted property values from a fitted model are larger than expected based on the experimental and measurement uncertainty in the data. If the predicted versus measured differences are larger than data uncertainty at a high enough statistical confidence (e.g., greater than 90%), the model is said to have a statistically significant LOF. Replicate data points containing all applicable sources of experimental and measurement uncertainty¹ are required to perform statistical LOF tests. This process is conducted using a LOF F-test given by

$$F = \frac{(SSE - SSPE)/(n - p - f)}{SSPE/f}$$

$$= \frac{\left[\left(\sum_{i=1}^n (\hat{y}_i - y_i)^2 - \sum_{k=1}^K \sum_{j=1}^{m_k} (y_{kj} - \bar{y}_k)^2 \right) / (n - p - f) \right]}{\sum_{k=1}^K \sum_{j=1}^{m_k} (y_{kj} - \bar{y}_k)^2 / f} \quad (\text{B.14a})$$

for OLS regression, and by

$$F = \frac{(SSE - SSPE)/(n - p - f)}{SSPE/f}$$

$$= \frac{\left[\left(\sum_{i=1}^n w_i (\hat{y}_i - y_i)^2 - \sum_{k=1}^K \sum_{j=1}^{m_k} w_j (y_{kj} - \bar{y}_k)^2 \right) / (n - p - f) \right]}{\sum_{k=1}^K \sum_{j=1}^{m_k} w_j (y_{kj} - \bar{y}_k)^2 / f} \quad (\text{B.14b})$$

for WLS regression. In Eqs. (B.14a) and B.14b), SSE = sum of squares error; SSPE = sum of squared pure error (i.e., from replicates); n and p are as described previously such that $n-p$ is the degrees of freedom for SSE; and the degrees of freedom for pure error is given by $f = \sum_{k=1}^K (m_k - 1)$, where m_k is the number of replicate data points in the k^{th} replicate set, $k = 1, 2, \dots, K$. In practice, if the F-test for LOF is statistically significant at a significance level (often referred to as a p -value) of 0.05 or smaller (i.e., 95% confidence or higher), then it would be concluded that the fitted model has a

¹ To be appropriate replicate data points, two or more glass samples of the same composition must be batched and melted at different times, and have their properties measured at different times. It is insufficient, for example, to batch and melt a glass once and measure its properties two or more times (because the batching and melting sources of uncertainty are not included in the data). Similarly, replicate samples should not be measured at the same time (or close in time) because all sources of measurement uncertainty will not be included in the data.

statistically significant LOF for the modeling dataset. See Draper and Smith (1998) or Montgomery et al. (2012) for additional discussion of the statistical test for model LOF with OLS and WLS regression.

Even when a fitted model has a statistically significant LOF, the LOF may not be “practically significant.” An example of such a situation is when a fitted model yields biased predictions for higher and/or lower values of a property or in a particular subregion of compositions, but the model will not be applied to such areas in practice. Another example is when the model fits the data very well (e.g., $R^2 > 0.95$) without bias over the model’s region of validity, but the LOF is statistically significant because the experimental and measurement uncertainty is very small (e.g., because glasses can be batched, melted, and properties measured with excellent reproducibility). Finally, a statistically significant LOF may not be practically significant if the uncertainty in model predictions is considerably smaller than uncertainty that can be tolerated and still meet requirements.

The model evaluation techniques discussed in the preceding bullets are included in, or can be obtained from, the output of the R software (Ihaka and Gentleman 1996, R Core Team 2019), and MatLab R2019b, (2019). See Draper and Smith (1998) or Montgomery et al. (2012) for further discussion of the concepts.

Three different R^2 statistics are useful in evaluating models fitted to glass property-composition data. These are denoted as R^2 , R_A^2 , and R_P^2 , which are discussed subsequently. Formulas for these statistics are given when models are fitted by OLS or WLS.

The (*ordinary*) R^2 statistic is given by

$$R^2 = 1 - \frac{\sum_{i=1}^n (\hat{y}_i - y_i)^2}{\sum_{i=1}^n (y_i - \bar{y})^2} \quad (\text{B.15a})$$

for OLS regression, and by

$$R^2 = 1 - \frac{\sum_{i=1}^n w_i (\hat{y}_i - y_i)^2}{\sum_{i=1}^n w_i (y_i - \bar{y}_w)^2} \quad (\text{B.15b})$$

for WLS regression, where \bar{y}_w in Eq. (B.15b) is the weighted mean whose formula is given in Eq. (B.11). R^2 is interpreted as the fraction of variability in the unweighted (for OLS regression) or weighted (for WLS regression) property data (transformed if appropriate) accounted for by the fitted model. The *adjusted R^2 statistic* is given by

$$R_A^2 = 1 - \frac{\sum_{i=1}^n (\hat{y}_i - y_i)^2 / (n-p)}{\sum_{i=1}^n (y_i - \bar{y})^2 / (n-1)} \quad (\text{B.16a})$$

for OLS regression, and by

$$R_A^2 = 1 - \frac{\sum_{i=1}^n w_i (\hat{y}_i - y_i)^2 / (n-p)}{\sum_{i=1}^n w_i (y_i - \bar{y}_w)^2 / (n-1)} \quad (\text{B.16b})$$

for WLS regression. R_A^2 is interpreted as the adjusted fraction of variability in the unweighted or weighted property data (transformed if appropriate) accounted for by the fitted model. The adjustment is for the number of parameters (p) and number of data points (n) used in fitting the model.

The *predicted R^2 statistic* is given by

$$R_P^2 = 1 - \frac{\sum_{i=1}^n (\hat{y}_{(i)} - y_i)^2}{\sum_{i=1}^n (y_i - \bar{y})^2}, \quad (\text{B.17a})$$

for OLS regression, and by

$$R_P^2 = 1 - \frac{\sum_{i=1}^n w_i (\hat{y}_{(i)} - y_i)^2}{\sum_{i=1}^n w_i (y_i - \bar{y}_w)^2}, \quad (\text{B.17b})$$

for WLS regression. R_P^2 is interpreted as the leave-one-out cross-validation fraction of variability in the unweighted or weighted property data (transformed if appropriate) accounted for by the fitted model. This statistic is calculated by a method equivalent to leaving each data point out of the model fit, and then evaluating how well the model predicts the property for that data point. R_P^2 estimates the fraction of variability that would be explained in predicting new observations drawn from the same composition space. However, computational simplifications for OLS and WLS regression do not require re-fitting a model with each data point removed.

Generally, R^2 statistics take values between 0 and 1. However, R_A^2 and R_P^2 can take negative values for a poor-fitting model, a model that contains many more terms than needed to fit the data, or a model fitted to data with one or more very influential data points. Among the three R^2 statistics, typically $R^2 > R_A^2 > R_P^2$. More than a minor difference between R^2 and R_A^2 indicates that the model may contain more terms than needed to achieve the same goodness of fit. A substantial difference between R^2 and R_P^2 is indicative of one or more data points being very influential in determining the fit of the model. Some reduction from R^2 to R_P^2 is expected because R^2 corresponds to using all data to fit the model, whereas R_P^2 corresponds to leaving each data point out of the fit when evaluating the performance of the model for that point. In general, a model will tend to predict better for data used to fit it than for data not used to fit it. R_P^2 is a crossvalidation evaluation method.

B.4 Statistical Methods for Model Reduction and Augmentation

Section B.4.1 discusses methods for identifying and removing unnecessary terms from mixture experiment models. Section B.4.2 discusses methods for augmenting linear mixture models with quadratic terms or other nonlinear blending terms.

B.4.1 Statistical Methods for Reducing Mixture Experiment Models

In evaluating a fitted regression model, it may often be determined that there are unnecessary terms in the model. Such terms may not improve, and can even degrade, the predictive performance of the model in applications to data not used to develop the model. Also, unnecessary model terms can increase the uncertainties of model-predicted response values.

The most basic statistical method to identify unnecessary terms in a model is a *t-test* to perform a hypothesis test of whether the coefficient of a model term is statistically different from zero. The t-test computes a t-statistic equal to a model coefficient divided by the standard deviation of the coefficient. The t-statistic is then compared to the Student-t probability distribution to determine the probability of getting a t-statistic at least that large. The resulting probability is referred to as a *p-value* and represents the probability of incorrectly deciding a coefficient is significantly different than zero. Most regression software output includes estimated model coefficients, coefficient standard deviations, t-statistics, and p-values. Typically, practitioners require a p-value to be smaller than 0.05 or 0.01 as strong evidence that the coefficient is significantly different than zero, and thus that the corresponding model term is needed. If there are not too many potentially unnecessary terms in a model, a practitioner can assess the t-statistics

and p-values for the coefficients in a “full” model and remove the model term whose coefficient is least statistically significant. Then, the model would be refitted without that term, and the t-statistics and p-values again considered, deleting the model term with the least statistically significant coefficient. This process continues until all terms in the model have p-values lower than a certain value, e.g. 0.05. This approach, referred to as *backward elimination* (Draper and Smith 1998; Montgomery et al. 2012), is a widely used statistical method for removing unneeded terms from a model. This method basically automates the process just described, where the practitioner sets a stopping criterion.

Unfortunately, there are some model forms for which the model reduction methods just described are inappropriate. In general, these are model forms where a model coefficient being small (e.g., near zero) does not imply the corresponding model term is unneeded. Some model forms may have terms with significant effects even though the coefficients of those terms are small. One class of models in this category relevant to this work is the class of *mixture experiment models* (Cornell 2002), of which LM and PQM models are discussed in Section B.1. The LM model (or the linear blending portion of a PQM model) is of the form $\sum_{i=1}^q b_i g_i$, where the b_i are coefficients and the g_i are proportions of the mixture components (e.g., mass fractions of waste glass components) that must sum to one (i.e., $\sum_{i=1}^q g_i = 1$). When each g_i can vary from zero to one, the coefficient b_i represents the estimated response variable value for pure component i [i.e., when $g_i = 1$ and $g_j = 0$ ($j \neq i$)]. When the ranges of the mixture component proportions g_i are constrained, each b_i represents the extrapolated response value for pure component i . Because hypotheses concerning LM model coefficients (or the coefficients of linear terms in PQM models) equaling zero are not related to the importance or non-importance of a given component, it is inappropriate to use t-tests or the standard backward elimination method to reduce the linear portion of a mixture experiment model. However, mixture models can contain nonlinear terms in the components (such as in the PQM model form discussed in Section B.1), and it is appropriate to use t-tests or the standard stepwise, forward, or backward elimination *variable selection methods* (see Draper and Smith 1998 or Montgomery et al. 2012) on such terms.

Component response trace plots (Cornell 2002) provide for graphically assessing the effects of mixture components on a response variable of interest. These plots are generally produced using a fitted mixture model. The model is used to predict, for each component, the response for a series of compositions lying along an *effect direction* for that component. The most commonly used effect direction corresponds to subtracting or adding a component to a reference (or baseline) mixture. Along such a direction, the component of interest is varied within the allowable composition region of interest. The changes in the component of interest are offset by changes in the remaining components, such that they remain in the same relative proportions as in the REFMIX. The predicted response values along the effect direction for a given component form a *component response trace*. The response traces for the components varied in a mixture experiment plotted together form the *component response trace plot*. The predicted response values are plotted on the y-axis and changes in each component from its REFMIX value are plotted on the x-axis. Components with steeper response traces have stronger effects on the response. A response trace that is nearly horizontal indicates the corresponding component has little or no effect on the response. Components whose response traces are very close may have similar effects on the response. Thus, component response trace plots can be used to guide the reduction of components appearing in a mixture experiment model (e.g., see Piepel and Redgate 1997).

A special backward-elimination, F-test method for mixture experiments has been developed to reduce linear mixture models and linear portions of mixture models (Piepel and Cooley 2006). The reduction method is performed in stages. In general, at the end of each stage, either (i) a mixture component is dropped, and the remaining components are renormalized; or (ii) two components are combined. As an option, model reductions of the form (i) can be skipped and only reductions of the form (ii) considered.

This includes combining minor components into an “Others” component. For each stage, the process occurs as follows.

- If reductions of the form (i) are allowed, each mixture component still in the model is in turn dropped from the model; the remaining mixture component proportions are renormalized to sum to one. Then a linear mixture model without the dropped component is fitted to the data. The dropped mixture component that causes the smallest increase in the error sums of squares (the quantity being minimized in OLS regression) is then the component permanently dropped from the model at the current stage. After each component is dropped, the remaining components are renormalized according to the mixture experiment definition that a response variable depends only on the relative proportions of the mixture components that affect the response variable (Cornell 2002).
- For reductions of the form (ii), each allowable pair of components is combined, and the corresponding reduced linear mixture model is fitted. The pair of components causing the smallest increase in the error sum of squares is then permanently combined at the current stage.

Similar stages continue, with either one component dropped [option (i)] or one pair of components combined [option (ii)], until the stage in which a model reduction causes the full-reduced model F-test (Draper and Smith 1998; Montgomery et al. 2012) to declare a statistically significant increase in the error sum of squares. This then signals the stopping point for the backward elimination algorithm appropriate for linear mixture models. Note that the algorithm allows for the user specifying the components (if any) that can be dropped, and components that can be combined. These options provide for incorporating subject-matter knowledge into the model reduction process.

B.4.2 Statistical Methods for Adding Terms to Models

It is often of interest to add additional terms onto a starting model in the hopes of improving the predictive performance of the starting model. For example, a linear mixture model may be considered as a starting model. However, if it has a significant LOF, adding nonlinear composition terms may be considered in hopes of improving the predictive performance of the model. *Stepwise regression* is the most commonly used method to add terms to an existing starting model. In stepwise regression, certain terms can be forced into the model, and a candidate list of possible terms to add is identified. The procedure identifies the term from the candidate list that, if added to the model, would yield the greatest reduction in the error sum of squares (i.e., the sum of squared differences in measured and model-predicted values across the modeling dataset). If the reduction is statistically significant, that term is added to the model. Stepwise regression proceeds in stages, with one additional term being added at each stage unless the user-selected stopping criterion is reached. After adding a term, stepwise regression checks all other terms in the model to assess if they are still statistically significant. If not, a term can be removed during a stage.

The stepwise regression algorithm requires that a statistical significance level be specified for terms to enter the model, and that a statistical significance level be specified for terms to remain in the model. In each iteration of a stepwise regression application, t-tests are conducted for each term already in the model and for terms being considered for inclusion in the model. To describe the results of these t-tests, a p-value is calculated for each of the terms. Loosely speaking, the p-values represent the probability that the respective model terms do not make a significant contribution to the predictive ability of the model. Terms whose corresponding p-values are small (often <0.05 is considered sufficiently small) are considered important in the model. The statistical significance levels specified for the stepwise regression algorithm indicate how small p-values must be for the corresponding terms to be included in the model. The statistical literature generally indicates that the stepwise algorithm is somewhat liberal in allowing terms into models. Yet, models containing unnecessary terms are undesirable because they tend to have

inflated prediction uncertainties. Thus, it is typically advisable to use tight statistical significance levels, such as 0.05, 0.01, or even smaller in some cases, when applying the stepwise regression algorithm.

One variation of stepwise regression that can be used to select terms for model building is what the SAS statistical software package (SASTM Software, SAS Institute Inc., Cary, NC) refers to as the Maximum R-squared Improvement (MAXR) selection method. For the MAXR criterion (as with other criteria for stepwise regression), terms can enter and leave (being replaced by another term) the model. Sequential changes to the model are based on maximal increases to the model's R^2 value, and MAXR tries to find the "best" model having a specified number of terms. However, MAXR is not the same as the "best subsets" algorithm because it does not consider all possible models with a given number of terms. Therefore, MAXR is not guaranteed to find the model with the highest R^2 value among all models having a given number of terms. This method tends to have a better chance of finding more nearly optimal models than does the stepwise selection method using other criteria (Freund and Littell 2003). The MAXR method does not require significance levels to control model term selection but does require the user to identify any terms to force into the model and to specify the number of terms to include in models being considered. Graphical and other methods can be used to compare and choose among models with different numbers of terms.

The standard stepwise regression procedure (regardless of the criterion used for model term selection) is not appropriate for linear mixture models or linear portions of other mixture experiment models for similar reasons as described previously regarding the standard backward elimination method. However, it is appropriate for adding nonlinear mixture terms or non-mixture terms to mixture models.

B.5 Statistical Methods for Model Validation

Model validation methods assess how well a fitted model predicts property values for data not used in fitting the model. The glasses used for validation ideally should be in the same composition region as the data used to fit the property-composition models, because (in general) fitted empirical and semi-empirical models should not be used to extrapolate much beyond the region covered by the modeling data. Also, ideally the validation data should be evenly distributed over the model composition region of model validity to properly assess predictive ability over the region. However, this is difficult to achieve in practice because validation data are typically not designed, but often consist of whatever extra data are available.

Validation generally consists of using a fitted model to predict property values for a set of validation data, and then comparing the predicted property values to the measured values from the validation database. The following subsections describe several methods for comparing predicted and measured values of properties.

B.5.1 Validation R^2

Statistical summary comparisons of predicted and measured property values are also useful to see if differences are larger than their expected uncertainties. One such comparison is the *validation R^2* statistic, which in general is given by

$$R_V^2 = 1 - \frac{\sum_{i=1}^n (\hat{y}_i - y_i)^2}{\sum_{i=1}^n (y_i - \bar{y})^2}. \quad (\text{B.18a})$$

However, in cases where WLS regression is used to fit the model and corresponding weights are available for the validation data, a weighted version of the *validation* R^2 statistic is given by

$$R_V^2 = 1 - \frac{\sum_{i=1}^n w_i (\hat{y}_i - y_i)^2}{\sum_{i=1}^n w_i (y_i - \bar{y}_w)^2} \quad (\text{B.18b})$$

R_V^2 is interpreted as the fraction of variability in the unweighted or weighted property values (transformed if appropriate) in the validation data accounted for by the fitted model. Note that R_V^2 is defined exactly the same as the ordinary R^2 defined in Eqs. (B.15a) and (B.15b), except that model validation data are used to assess model predictive performance instead of the model development data. Hence, the y_i , \hat{y}_i , \bar{y} , w_i , and \bar{y}_w values in Eqs. (B.18a) and (B.18b) correspond to the model validation data.

Generally, the range is $R_V^2 \leq R_P^2 \leq R_A^2 \leq R^2 \leq 1$. However, R_V^2 can take negative values (when a model predicts a validation set very poorly) and can take values larger than R_P^2 , R_A^2 , or R^2 (when a model predicts a particular validation dataset better than estimated by these statistics based on the modeling data).

B.5.2 Validation RMSE

Another useful summary statistic for model validation is *validation RMSE* (RMSE_V). This statistic is calculated the same as given in Eq. (B.12a) for OLS-fitted models and as given in Eq. (B.12b) for WLS-fitted models.

B.5.3 Predicted versus Measured Plots for Validation

Predicted and measured values for a model validation dataset can be compared by plotting the predicted versus the measured property values for each data point. Such *PvM plots* are the same as described in Section B.3, except model validation data are used instead of model development data. Also, similarly as described in Section B.3, *unweighted PvM plots* or *weighted PvM plots* may be produced and viewed to validate models fitted by WLS regression.

Optionally, error bars consisting of two-sided prediction intervals (PIs) with a specified level of confidence (e.g. 95% PIs) on the predicted values can be included in the PvM plot for validation. Then, if the error bar for a given validation data point overlaps a line with slope one superimposed on the PvM plot, the model is validated for that data point. Draper and Smith (1998) and Montgomery et al. (2012) provide additional discussion of PIs for regression models. The formulas for a 95% two-sided PI in the OLS and WLS cases are given in Section B.6.

B.6 Statistical Intervals for Quantifying Uncertainties in Model Predictions

Several types of statistical intervals are available to quantify the uncertainty associated with model predictions. Each type of statistical interval has a particular interpretation. A common assumption for all statistical intervals based on regression models is that the model represents the true underlying response surface (property-composition relationship for waste glasses) without a statistically significant lack-of-fit.

The following subsections present the formulas for one-sided upper (or lower) confidence intervals (Section B.6.1), two-sided confidence intervals (Section B.6.2), and two-sided prediction intervals (Section B.6.3). These types of statistical intervals are used to describe the uncertainty associated with model predictions at a single specific composition. Section B.6.4 presents the formulas for simultaneous

upper confidence intervals, which are used to describe the uncertainty associated with model predictions at many glass compositions. The formulas for these types of statistical intervals are given in each subsection for the OLS and WLS cases. Section B.6.5 presents two-sided approximated intervals for GLMs. Section B.6.6 discusses aspects of using the statistical intervals.

B.6.1 One-Sided Confidence Interval for OLS and WLS regression

A $100(1-\alpha)\%$ upper confidence interval (UCI) for the true mean response value for a given glass composition $\mathbf{g} = (g_1, g_2, \dots, g_q)$ is given by

$$\begin{aligned}\hat{y}(\mathbf{g}) + t_{1-\alpha, n-p} \sqrt{\mathbf{g}^T \mathbf{C}_{OLS} \mathbf{g}} &= \hat{y}(\mathbf{g}) + t_{1-\alpha, n-p} \sqrt{\mathbf{g}^T [(\mathbf{G}^T \mathbf{G})^{-1} MSE_{OLS}] \mathbf{g}} \\ &= \hat{y}(\mathbf{g}) + t_{1-\alpha, n-p} RMSE_{OLS} \sqrt{\mathbf{g}^T (\mathbf{G}^T \mathbf{G})^{-1} \mathbf{g}},\end{aligned}\quad (\text{B.19a})$$

for OLS regression, and by

$$\begin{aligned}\hat{y}(\mathbf{g}) + t_{1-\alpha, n-p} \sqrt{\mathbf{g}^T \mathbf{C}_{WLS} \mathbf{g}} &= \hat{y}(\mathbf{g}) + t_{1-\alpha, n-p} \sqrt{\mathbf{g}^T [(\mathbf{G}^T \mathbf{W} \mathbf{G})^{-1} MSE_{WLS}] \mathbf{g}} \\ &= \hat{y}(\mathbf{g}) + t_{1-\alpha, n-p} RMSE_{WLS} \sqrt{\mathbf{g}^T (\mathbf{G}^T \mathbf{W} \mathbf{G})^{-1} \mathbf{g}},\end{aligned}\quad (\text{B.19b})$$

for WLS regression. In Eqs. (B.19a) and (B.19b), the superscript T notation indicates a vector or matrix transpose, not temperature. The other notations in Eqs. (B.19a) and (B.19b) are defined as follows.

$\hat{y}(\mathbf{g})$	=	model predicted property value at composition \mathbf{g}
$100(1-\alpha)$	=	desired confidence (e.g., 90%) for the confidence interval, where α denotes the statistical significance level (e.g., $\alpha = 0.10$ for 90% confidence)
$t_{1-\alpha, n-p}$	=	$100(1-\alpha)$ -percentile of the Student's t -distribution with $n - p$ degrees of freedom
n	=	number of data points used to fit the model
p	=	number of parameters estimated in the model
\mathbf{C}_{OLS}	=	estimated variance-covariance matrix for the estimated coefficients of a model fitted by OLS regression = $(\mathbf{G}^T \mathbf{G})^{-1} MSE_{OLS}$
\mathbf{C}_{WLS}	=	estimated variance-covariance matrix for the estimated coefficients of a model fitted by WLS regression = $(\mathbf{G}^T \mathbf{W} \mathbf{G})^{-1} MSE_{WLS}$
\mathbf{g}	=	the vector of the glass composition expanded in the form of the model terms
\mathbf{G}	=	the matrix of the data (consisting of glass compositions expanded in the form of the model terms)
\mathbf{W}	=	an $n \times n$ diagonal weight matrix with entries w_i , $i = 1, 2, \dots, n$ (i.e., the weights associated with the model development set of n data points)
MSE	=	mean squared error, which is obtained from the OLS (MSE_{OLS}) or WLS (MSE_{WLS}) regression fit of the model

$RMSE$ = the root mean squared error = \sqrt{MSE} , with $RMSE_{OLS}$ and $RMSE_{WLS}$ resulting from OLS and WLS regression fits of a model, respectively

A $100(1-\alpha)$ % UCI, as given by Eqs. (B.18a) and (B.18b), is appropriate when an uncertainty statement is desired about the true mean response for a given composition \mathbf{g} .

The formulas for a one-sided lower confidence interval (LCI) are the same as in Eqs. (B.18a) and (B.18b), except the plus signs following $\hat{y}(\mathbf{g})$ are changed to minus signs. Thus, a $100(1-\alpha)$ % LCI for the true mean response value for a given glass composition $\mathbf{g} = (g_1, g_2, \dots, g_q)$ is given by

$$\begin{aligned}\hat{y}(\mathbf{g}) - t_{1-\alpha, n-p} \sqrt{\mathbf{g}^T C_{OLS} \mathbf{g}} &= \hat{y}(\mathbf{g}) - t_{1-\alpha, n-p} \sqrt{\mathbf{g}^T [(\mathbf{G}^T \mathbf{G})^{-1} MSE_{OLS}] \mathbf{g}} \\ &= \hat{y}(\mathbf{g}) - t_{1-\alpha, n-p} RMSE_{OLS} \sqrt{\mathbf{g}^T (\mathbf{G}^T \mathbf{G})^{-1} \mathbf{g}},\end{aligned}\tag{B.20a}$$

for OLS regression, and by

$$\begin{aligned}\hat{y}(\mathbf{g}) - t_{1-\alpha, n-p} \sqrt{\mathbf{g}^T C_{WLS} \mathbf{g}} &= \hat{y}(\mathbf{g}) - t_{1-\alpha, n-p} \sqrt{\mathbf{g}^T [(\mathbf{G}^T \mathbf{W} \mathbf{G})^{-1} MSE_{WLS}] \mathbf{g}} \\ &= \hat{y}(\mathbf{g}) - t_{1-\alpha, n-p} RMSE_{WLS} \sqrt{\mathbf{g}^T (\mathbf{G}^T \mathbf{W} \mathbf{G})^{-1} \mathbf{g}},\end{aligned}\tag{B.20b}$$

for WLS regression.

B.6.2 Two-Sided Confidence Interval for OLS and WLS regression

A $100(1-\alpha)$ % two-sided confidence interval (CI) for the true mean response value for a given glass composition $\mathbf{g} = (g_1, g_2, \dots, g_q)$ is given by

$$\begin{aligned}\hat{y}(\mathbf{g}) \mp t_{1-\alpha/2, n-p} \sqrt{\mathbf{g}^T C_{OLS} \mathbf{g}} &= \hat{y}(\mathbf{g}) \mp t_{1-\alpha/2, n-p} \sqrt{\mathbf{g}^T [(\mathbf{G}^T \mathbf{G})^{-1} MSE_{OLS}] \mathbf{g}} \\ &= \hat{y}(\mathbf{g}) \mp t_{1-\alpha/2, n-p} RMSE_{OLS} \sqrt{\mathbf{g}^T (\mathbf{G}^T \mathbf{G})^{-1} \mathbf{g}},\end{aligned}\tag{B.21a}$$

for OLS regression, and by

$$\begin{aligned}\hat{y}(\mathbf{g}) \mp t_{1-\alpha/2, n-p} \sqrt{\mathbf{g}^T C_{WLS} \mathbf{g}} &= \hat{y}(\mathbf{g}) \mp t_{1-\alpha/2, n-p} \sqrt{\mathbf{g}^T [(\mathbf{G}^T \mathbf{W} \mathbf{G})^{-1} MSE_{WLS}] \mathbf{g}} \\ &= \hat{y}(\mathbf{g}) \mp t_{1-\alpha/2, n-p} RMSE_{WLS} \sqrt{\mathbf{g}^T (\mathbf{G}^T \mathbf{W} \mathbf{G})^{-1} \mathbf{g}},\end{aligned}\tag{B.21b}$$

for WLS regression. In Eqs. (B.21a) and (B.21b), the notation is all the same as described in Section B.6.1, except that $t_{1-\alpha/2, n-p}$ denotes the $100(1-\alpha/2)$ -percentile of the Student's t -distribution with $n - p$ degrees of freedom.

B.6.3 Two-Sided Prediction Interval for OLS and WLS regression

A $100(1-\alpha)$ % two-sided prediction interval (PI) for an individual response value for a given composition \mathbf{g} is given by

$$\hat{y}(\mathbf{g}) \mp t_{1-\alpha/2, n-p} \sqrt{MSE_{OLS} + \mathbf{g}^T \mathbf{C}_{OLS} \mathbf{g}} = \hat{y}(\mathbf{g}) \mp t_{1-\alpha/2, n-p} RMSE_{OLS} \sqrt{1 + \mathbf{g}^T (\mathbf{G}^T \mathbf{G})^{-1} \mathbf{g}} \quad (\text{B.22a})$$

for OLS regression, and by

$$\hat{y}(\mathbf{g}) \mp t_{1-\alpha/2, n-p} \sqrt{\frac{MSE_{WLS}}{w_i} + \mathbf{g}^T \mathbf{C}_{WLS} \mathbf{g}} = \hat{y}(\mathbf{g}) \mp t_{1-\alpha/2, n-p} RMSE_{WLS} \sqrt{\frac{1}{w_i} + \mathbf{g}^T (\mathbf{G}^T \mathbf{W} \mathbf{G})^{-1} \mathbf{g}} \quad (\text{B.22b})$$

for WLS regression. The remaining notations in Eqs. (B.22a) and (B.22b) are defined as given following the UCI formulas in Section B.6.1. The preceding equations for $100(1-\alpha)$ % two-sided PIs are easily converted to $100(1-\alpha)$ % one-sided PIs by replacing “ \mp ” with “ $-$ ” or “ $+$ ”, and replacing $t_{1-\alpha/2, n-p}$ with $t_{1-\alpha, n-p}$.

Note in Eq. (B.22b) that the w_i under the square root applies when PIs are calculated for modeling data, validation data, or application data (i.e., data used in applying the models and PIs) with weights. In situations where validation or application data do not have weights, w_i should be set to 1.

A $100(1-\alpha)$ % PI is appropriately used when comparing a model predicted response value for a given composition to an individual measurement of the response for that composition. This type of application arises in validating the predictive performance of a model for one or more glass compositions not used to fit the model. Specifically, Eqs. (B.21a) and (B.21b) can be used to produce 95% PIs displayed as error bars in PvM plots, as described at the end of Section B.5.

B.6.4 Simultaneous Upper Confidence Intervals for OLS and WLS Regression

At times it is desirable to describe the uncertainty associated with predictions obtained for a specified group of compositions. For example, a statement may be desired that indicates with high confidence that the predicted response value for every composition \mathbf{g} in a specified group of compositions (or composition region) is below a particular regulatory limit. Such a confidence statement requires a statistical interval called a simultaneous upper confidence interval. While several different approaches exist to calculate simultaneous confidence intervals, the Working-Hotelling methodology (Working and Hotelling, 1929) is relatively simple and is particularly useful when a large number of compositions is involved. The formula for a $100(1-\alpha)$ % simultaneous upper confidence interval (SUCI) associated with predictions on an unlimited number of compositions \mathbf{g} using the Working-Hotelling approach is given by

$$\hat{y}(\mathbf{g}) + \sqrt{pF_{1-2\alpha, (p, n-p)}} \sqrt{\mathbf{g}^T \mathbf{C}_{OLS} \mathbf{g}} = \hat{y}(\mathbf{g}) + RMSE_{OLS} \sqrt{pF_{1-2\alpha, (p, n-p)}} \sqrt{\mathbf{g}^T (\mathbf{G}^T \mathbf{G})^{-1} \mathbf{g}} \quad (\text{B.23a})$$

for OLS regression, and by

$$\hat{y}(\mathbf{g}) + \sqrt{pF_{1-2\alpha, (p, n-p)}} \sqrt{\mathbf{g}^T \mathbf{C}_{WLS} \mathbf{g}} = \hat{y}(\mathbf{g}) + RMSE_{WLS} \sqrt{pF_{1-2\alpha, (p, n-p)}} \sqrt{\mathbf{g}^T (\mathbf{G}^T \mathbf{W} \mathbf{G})^{-1} \mathbf{g}} \quad (\text{B.23b})$$

for WLS regression. In Eqs. (B.23a) and (B.23b), $F_{1-2\alpha, (p, n-p)} = 100(1-2\alpha)$ -percentile of the F -distribution with p and $n - p$ degrees of freedom.

The remaining notations are the same as defined previously.

B.6.5 Confidence Intervals for Generalized Linear Models

Inference on goodness-of-fit statistics for GLMs can be carried out in a manner analogous to OLS, and Wald inference can be applied in hypothesis testing and for building approximated confidence intervals.

Confidence intervals for GLMs can be estimated using the fact that, asymptotically (Myers et al. 2002),

$$\mathbf{g}^T \mathbf{b} \sim N \left[\mathbf{g}^T \mathbf{b}, \mathbf{g}^T (\mathbf{G}^T \mathbf{W} \mathbf{G})^{-1} \mathbf{g} \right] \quad (\text{B.24})$$

which leads to a confidence interval on $\mathbf{g}^T \mathbf{b}$ of

$$\mathbf{g}^T \mathbf{b} \pm z_{\alpha/2} \sqrt{\mathbf{g}^T (\mathbf{G}^T \mathbf{W} \mathbf{G})^{-1} \mathbf{g}}. \quad (\text{B.25})$$

If the inverse link function produces a monotonic function of $\mathbf{g}^T \mathbf{b}$, Eq. (B.25) can be used to attach an approximate $100(1 - \alpha)$ % confidence interval on the mean response, where $z_{\alpha/2}$ is the $100(1-\alpha/2)$ -percentile of the standard normal distribution.

One-sided confidence intervals for GLMs can be obtained with Eq. (B.25), using z_{α} , and

$$\mathbf{g}^T \mathbf{b} + z_{\alpha} \sqrt{\mathbf{g}^T (\mathbf{G}^T \mathbf{W} \mathbf{G})^{-1} \mathbf{g}} \quad (\text{B.26})$$

for an upper confidence interval, or

$$\mathbf{g}^T \mathbf{b} - z_{\alpha} \sqrt{\mathbf{g}^T (\mathbf{G}^T \mathbf{W} \mathbf{G})^{-1} \mathbf{g}} \quad (\text{B.27})$$

for a lower confidence interval.

B.6.6 Statistical Intervals in Transformed and Untransformed Units

Eqs. (B.19) through (B.23) yield statistical intervals in transformed units when a transformed property is modeled. For example, a natural logarithm transformation of a response y [i.e., $\ln(y)$] is often used for property-composition models. Hence, the statistical intervals calculated using the preceding equations would be in $\ln(y)$ units. The statistical intervals can be transformed back to the original units of y by exponentiating the endpoint(s) of the statistical interval. However, the process of back-transforming (exponentiating) a statistical interval can change its interpretation. For example, if a 90% UCI in $\ln(y)$ units has the value “ v ”, the back-transformed 90% UCI in the original units of y is given by e^v . The 90% UCI in units of $\ln(y)$ is a statement about the true mean response in $\ln(y)$ units for a given glass composition \mathbf{g} . However, the resulting back-transformed interval is a 90% UCI on the true median response value for the given composition \mathbf{g} , under the assumption that experimental errors in the data used to develop the model are lognormally distributed. This assumes that the experimental errors in the natural-log-transformed response data are normally distributed. This change in interpretation occurs

because the mean and median of a normal distribution are the same, but the mean of a lognormal distribution is larger than the median of a lognormal distribution.

Hence, back-transforming a 90% UCI on a mean response for a given composition \mathbf{g} in ln-units yields a 90% UCI on the median response for a given composition \mathbf{g} in original units. This then underestimates a 90% UCI on the mean response for a given composition \mathbf{g} in original units. Back-transforming $100(1-\alpha)\%$ *SUCIs* given by Eq. (B.23) in log-transformed units has a similar change in interpretation. Whereas the original $100(1-\alpha)\%$ *SUCIs* are statements about the true mean values of responses in log-transformed response units for multiple compositions \mathbf{g} , the back-transformed $100(1-\alpha)\%$ *SUCIs* are statements about the true median values of responses in original response units for multiple compositions \mathbf{g} . However, a $100(1-\alpha)\%$ *PI* given by Eq. (B.22) in log-transformed units does not have a change in interpretation when back-transforming, because the original statement (in log-transformed units) and the back-transformed statement (in original units) are both about a true individual response value.

Alternatives exist to using normal-theory-based Eqs. (B.19) through (B.23) and back-transforming them when a transformed response variable is modeled. One alternative is to modify the statistical interval equations so that the statistical statement is about the true mean response value in the original units for a given composition \mathbf{g} [e.g., Eq. (B.19) for an UCI] or a set of compositions \mathbf{g} [e.g., Eq. (B.23) for a SUCI]. Although this type of alternative is discussed in the literature for non-regression problems (e.g., Gilbert 1987), no references were found for the regression context. Another alternative, the *generalized linear model* regression approach (Myers et al. 2002), avoids directly transforming the response variable and instead uses the transformation indirectly. Confidence intervals for the generalized linear models (GLMs) used in this document are based on the fact that the linear predictor in the model, $\mathbf{g}^T\mathbf{b}$, is asymptotically normal and the logit link, the function used to link the linear predictor with the score or probability of failure for a glass, is a monotonic function of the linear predictor.

Note that Eqs. (B.19) through (B.23) require knowledge of the variance-covariance matrix $\mathbf{C}_{OLS} = MSE_{OLS}(\mathbf{G}^T\mathbf{G})^{-1}$ for OLS regression and $\mathbf{C}_W = MSE_{WLS}(\mathbf{G}^T\mathbf{W}\mathbf{G})^{-1}$ for WLS regression. The MSE_U and MSE_W are mean squared errors equal to the squares of $RMSE_U$ and $RMSE_W$ given by Eqs. (B.12a) and (B.12b). This information is included in the OLS or WLS regression software output that comes with the estimates of the p model coefficients. A variance-covariance matrix for estimated model coefficients is a $p \times p$ matrix with variances of estimated coefficients along the diagonal, and covariances between pairs of estimated model coefficients in the off-diagonal entries.

Appendix C – LAW Glass Numbers in Each of the Six Evaluation Subsets.

The specific glasses in each of the six evaluation subsets below are listed for each of the LAW glass properties modeled in this report:

- **WTP:** Older low-activity waste (LAW) glasses with lower waste loadings that were tested by the Vitreous State Laboratory (VSL), which were used by Piepel et al. (2007) for property-composition modeling. This classification was assigned when the database of 1075 LAW glasses was compiled (see Section 2.3).
- **ORP:** Newer LAW glasses with higher waste loadings that were tested by VSL. This classification was assigned when the database of 1075 LAW glasses was compiled (see Section 2.3).
- **LP2OL:** LAW glasses that satisfy slightly expanded (described subsequently) versions of the Pacific Northwest National Laboratory (PNNL) Phase 2 OL (and Phase 3) constraints specified in Table 2.1. Hence, this subset of evaluation glasses includes the LP2.OL, LP2.IL, and LP3 glasses, as well as any other LAW glasses that satisfy the expanded Phase 2 OL constraints. Note that the glasses in this evaluation set have high Na₂O waste loadings.
- **LP123:** LAW glasses from PNNL Phases 1, 2, and 3.
- **HiNa₂O:** LAW glasses with high concentrations of Na₂O (≥ 0.21 mf).
- **HiSO₃:** LAW glasses with high concentrations of SO₃ (≥ 0.0085 mf).

Table C.1 lists the glass numbers of LAW glasses with Product Consistency Test (PCT) data in the six evaluation subsets. Table C.2 lists the glass numbers of LAW glasses with Vapor Hydration Test (VHT) data in the six evaluation subsets. Table C.3 lists the glass numbers of LAW glasses with viscosity data in the six evaluation subsets. Table C.4 lists the glass numbers of LAW glasses with electrical conductivity data in the six evaluation subsets. Table C.5 lists the glass numbers of LAW glasses with melter SO₃ tolerance and solubility data in the six evaluation subsets. Table C.6 lists the glass numbers of LAW glasses with k_{1208} data in five of the six evaluation subsets.

Table C.1. Glass #s of LAW Glasses with PCT Data in Six Evaluation Subsets^(a)

Count	Evaluation Subset, Glass #s for PCT					
	WTP	ORP	LP2OL	LP123	HiNa ₂ O	HiSO ₃
1	1	397	516	928	41	61
2	4	407	519	930	42	62
3	5	442	520	933	268	63
4	6	443	521	935	291	110
5	7	444	522	937	294	182
6	8	445	524	939	343	185
7	9	446	526	941	344	192
8	11	447	528	943	345	196
9	15	500	538	945	458	207
10	16	501	561	947	459	211
11	17	502	577	949	462	213
12	18	503	583	951	486	341
13	19	504	585	953	488	407
14	21	505	589	955	489	435
15	22	506	591	957	496	443
16	23	507	593	959	497	444
17	24	508	595	961	499	445
18	27	509	597	963	500	446
19	28	510	618	965	501	447
20	29	511	620	967	502	544
21	30	512	622	969	503	603
22	31	513	689	971	504	604
23	32	514	690	973	505	605
24	34	515	695	975	506	606
25	35	516	696	979	507	607
26	37	519	697	981	508	608
27	38	520	698	983	509	609
28	39	521	699	986	510	610
29	41	522	700	989	511	611
30	42	523	723	991	512	612
31	45	524	724	1013	513	613
32	46	525	725	1014	514	614
33	47	526	726	1015	515	615
34	48	527	728	1016	516	622
35	49	528	729	1017	519	698
36	50	529	730	1018	520	701
37	52	530	731	1019	521	702
38	53	531	732	1020	522	703
39	54	532	733	1021	523	704
40	55	533	736	1022	524	706
41	56	534	737	1023	525	707
42	61	535	744	1024	526	708

Table C.1. Glass #s of LAW Glasses with PCT Data in Six Evaluation Subsets,^(a)
cont.

Evaluation Subset, Glass #s for PCT						
Count	WTP	ORP	LP2OL	LP123	HiNa ₂ O	HiSO ₃
43	62	536	745	1025	527	710
44	63	537	748	1026	528	711
45	65	538	750	1027	538	712
46	66	544	751	1028	545	714
47	67	545	759	1029	547	715
48	68	547	760	1030	549	716
49	69	549	761	1031	551	717
50	70	551	762	1032	553	732
51	71	553	763	1033	555	733
52	72	555	764	1034	557	735
53	73	557	765	1035	559	838
54	74	559	766	1036	561	841
55	75	561	767	1037	563	842
56	76	563	768	1038	565	843
57	78	565	898	1039	567	852
58	80	567	900	1040	569	853
59	110	569	919	1041	571	855
60	121	571	997	1042	573	856
61	122	573	999	1043	575	857
62	123	575	1013	1044	577	875
63	125	577	1014	1045	579	876
64	160	579	1015	1046	581	881
65	161	581	1016	1047	583	884
66	162	583	1017	1048	585	885
67	174	585	1018	1049	589	886
68	175	589	1019	1050	591	890
69	177	591	1020	1051	593	891
70	178	593	1021	1052	595	892
71	179	595	1022	1053	597	893
72	182	597	1023	1054	599	894
73	183	599	1024	1055	601	895
74	185	601	1025	1056	617	896
75	187	603	1026	1057	618	897
76	189	604	1027	1058	620	903
77	192	605	1028	1059	622	904
78	194	606	1030	1060	625	905
79	196	607	1031	1061	626	906
80	198	608	1033	1062	627	907
81	199	609	1034	1063	628	930
82	201	610	1035	1064	687	933
83	203	611	1036	1065	688	935
84	205	612	1037	1066	689	939

Table C.1. Glass #s of LAW Glasses with PCT Data in Six Evaluation Subsets,^(a)
cont.

Evaluation Subset, Glass #s for PCT						
Count	WTP	ORP	LP2OL	LP123	HiNa ₂ O	HiSO ₃
85	207	613	1038	1067	690	943
86	209	614	1039	1068	691	947
87	211	615	1040	1069	692	949
88	213	617	1041	1070	693	951
89	215	618	1042	1071	694	953
90	217	620	1043	1072	695	979
91	219	622	1044	1073	696	981
92	221	623	1045	1074	697	983
93	223	624	1046	1075	698	986
94	225	625	1047	--	699	989
95	227	626	1048	--	700	997
96	229	627	1049	--	726	1001
97	231	628	1050	--	728	1029
98	233	629	1051	--	731	1034
99	235	630	1052	--	732	1035
100	237	631	1053	--	733	1042
101	238	638	1054	--	737	1044
102	240	642	1055	--	738	1046
103	242	652	1056	--	741	1051
104	244	654	1057	--	744	1057
105	246	687	1059	--	745	1058
106	248	688	1060	--	746	1062
107	249	689	1061	--	747	1063
108	250	690	1062	--	748	1067
109	252	691	1063	--	749	1068
110	254	692	1064	--	750	1074
111	256	693	1065	--	751	--
112	258	694	1066	--	754	--
113	260	695	1067	--	758	--
114	263	696	1068	--	763	--
115	265	697	1069	--	764	--
116	266	698	1070	--	765	--
117	267	699	1071	--	766	--
118	268	700	1072	--	767	--
119	269	701	1073	--	768	--
120	270	702	1074	--	771	--
121	271	703	1075	--	777	--
122	272	704	--	--	790	--
123	273	706	--	--	815	--
124	274	707	--	--	823	--
125	275	708	--	--	826	--
126	276	710	--	--	827	--
127	277	711	--	--	828	--

Table C.1. Glass #s of LAW Glasses with PCT Data in Six Evaluation Subsets,^(a)
cont.

Evaluation Subset, Glass #s for PCT						
Count	WTP	ORP	LP2OL	LP123	HiNa ₂ O	HiSO ₃
128	278	712	--	--	829	--
129	279	714	--	--	830	--
130	280	715	--	--	831	--
131	281	716	--	--	832	--
132	282	717	--	--	833	--
133	283	718	--	--	835	--
134	284	719	--	--	836	--
135	285	720	--	--	837	--
136	286	721	--	--	838	--
137	287	722	--	--	844	--
138	288	723	--	--	845	--
139	289	724	--	--	847	--
140	291	725	--	--	848	--
141	292	726	--	--	849	--
142	293	728	--	--	850	--
143	294	729	--	--	851	--
144	295	730	--	--	852	--
145	296	731	--	--	858	--
146	297	732	--	--	862	--
147	298	733	--	--	864	--
148	299	734	--	--	867	--
149	300	735	--	--	871	--
150	301	736	--	--	873	--
151	302	737	--	--	874	--
152	303	738	--	--	875	--
153	304	741	--	--	877	--
154	305	744	--	--	878	--
155	306	745	--	--	879	--
156	307	746	--	--	881	--
157	309	747	--	--	887	--
158	311	748	--	--	888	--
159	314	749	--	--	892	--
160	315	750	--	--	898	--
161	318	751	--	--	900	--
162	319	752	--	--	901	--
163	320	753	--	--	902	--
164	322	754	--	--	903	--
165	331	755	--	--	904	--
166	332	756	--	--	911	--
167	333	757	--	--	913	--
168	334	758	--	--	914	--
169	335	759	--	--	915	--
170	336	760	--	--	916	--

Table C.1. Glass #s of LAW Glasses with PCT Data in Six Evaluation Subsets,^(a)
cont.

Evaluation Subset, Glass #s for PCT						
Count	WTP	ORP	LP2OL	LP123	HiNa ₂ O	HiSO ₃
171	337	761	--	--	919	--
172	338	762	--	--	921	--
173	339	763	--	--	922	--
174	340	764	--	--	947	--
175	341	765	--	--	961	--
176	342	766	--	--	981	--
177	343	767	--	--	999	--
178	344	768	--	--	1013	--
179	345	769	--	--	1014	--
180	346	770	--	--	1015	--
181	347	771	--	--	1016	--
182	348	772	--	--	1017	--
183	349	773	--	--	1018	--
184	350	774	--	--	1019	--
185	351	775	--	--	1020	--
186	352	776	--	--	1021	--
187	353	777	--	--	1022	--
188	354	778	--	--	1023	--
189	355	779	--	--	1024	--
190	356	780	--	--	1025	--
191	357	781	--	--	1026	--
192	358	782	--	--	1027	--
193	359	783	--	--	1028	--
194	360	784	--	--	1029	--
195	361	785	--	--	1031	--
196	362	786	--	--	1032	--
197	363	787	--	--	1034	--
198	364	788	--	--	1036	--
199	365	789	--	--	1038	--
200	366	790	--	--	1040	--
201	367	791	--	--	1041	--
202	368	792	--	--	1042	--
203	369	793	--	--	1044	--
204	370	794	--	--	1045	--
205	371	795	--	--	1046	--
206	372	797	--	--	1047	--
207	373	798	--	--	1048	--
208	374	799	--	--	1049	--
209	375	800	--	--	1051	--
210	376	801	--	--	1052	--
211	377	802	--	--	1053	--
212	378	803	--	--	1054	--
213	379	804	--	--	1055	--

Table C.1. Glass #s of LAW Glasses with PCT Data in Six Evaluation Subsets,^(a)
cont.

Evaluation Subset, Glass #s for PCT						
Count	WTP	ORP	LP2OL	LP123	HiNa ₂ O	HiSO ₃
214	380	805	--	--	1056	--
215	381	806	--	--	1057	--
216	382	807	--	--	1058	--
217	383	808	--	--	1059	--
218	384	809	--	--	1060	--
219	385	810	--	--	1061	--
220	386	815	--	--	1062	--
221	387	823	--	--	1063	--
222	388	826	--	--	1064	--
223	389	827	--	--	1065	--
224	390	828	--	--	1066	--
225	411	829	--	--	1067	--
226	412	830	--	--	1068	--
227	413	831	--	--	1069	--
228	414	832	--	--	1070	--
229	415	833	--	--	1071	--
230	416	835	--	--	1072	--
231	418	836	--	--	1073	--
232	419	837	--	--	1074	--
233	420	838	--	--	1075	--
234	422	839	--	--	--	--
235	424	840	--	--	--	--
236	426	841	--	--	--	--
237	427	842	--	--	--	--
238	428	843	--	--	--	--
239	431	844	--	--	--	--
240	435	845	--	--	--	--
241	436	846	--	--	--	--
242	437	847	--	--	--	--
243	438	848	--	--	--	--
244	439	849	--	--	--	--
245	440	850	--	--	--	--
246	448	851	--	--	--	--
247	449	852	--	--	--	--
248	450	853	--	--	--	--
249	451	854	--	--	--	--
250	452	855	--	--	--	--
251	453	856	--	--	--	--
252	454	857	--	--	--	--
253	455	858	--	--	--	--
254	456	859	--	--	--	--
255	457	862	--	--	--	--
256	458	863	--	--	--	--

Table C.1. Glass #s of LAW Glasses with PCT Data in Six Evaluation Subsets,^(a)
cont.

Count	Evaluation Subset, Glass #s for PCT					
	WTP	ORP	LP2OL	LP123	HiNa ₂ O	HiSO ₃
257	459	864	--	--	--	--
258	460	865	--	--	--	--
259	461	867	--	--	--	--
260	462	869	--	--	--	--
261	463	871	--	--	--	--
262	464	873	--	--	--	--
263	465	874	--	--	--	--
264	466	875	--	--	--	--
265	475	876	--	--	--	--
266	476	877	--	--	--	--
267	477	878	--	--	--	--
268	478	879	--	--	--	--
269	479	880	--	--	--	--
270	480	881	--	--	--	--
271	481	883	--	--	--	--
272	482	884	--	--	--	--
273	483	885	--	--	--	--
274	484	886	--	--	--	--
275	485	887	--	--	--	--
276	486	888	--	--	--	--
277	487	890	--	--	--	--
278	488	891	--	--	--	--
279	489	892	--	--	--	--
280	490	893	--	--	--	--
281	491	894	--	--	--	--
282	492	895	--	--	--	--
283	493	896	--	--	--	--
284	494	897	--	--	--	--
285	495	898	--	--	--	--
286	496	900	--	--	--	--
287	497	901	--	--	--	--
288	498	902	--	--	--	--
289	499	903	--	--	--	--
290	--	904	--	--	--	--
291	--	905	--	--	--	--
292	--	906	--	--	--	--
293	--	907	--	--	--	--
294	--	911	--	--	--	--
295	--	913	--	--	--	--
296	--	914	--	--	--	--
297	--	915	--	--	--	--
298	--	916	--	--	--	--
299	--	919	--	--	--	--

Table C.1. Glass #s of LAW Glasses with PCT Data in Six Evaluation Subsets,^(a)
cont.

Evaluation Subset, Glass #s for PCT						
Count	WTP	ORP	LP2OL	LP123	HiNa ₂ O	HiSO ₃
300	--	920	--	--	--	--
301	--	921	--	--	--	--
302	--	922	--	--	--	--
303	--	924	--	--	--	--
304	--	926	--	--	--	--
305	--	993	--	--	--	--
306	--	995	--	--	--	--
307	--	997	--	--	--	--
308	--	999	--	--	--	--
309	--	1001	--		--	

(a) The “Glass #” is a unique number assigned to each LAW glass composition, as shown in Table A.2 of Appendix A. The corresponding η_{1150} values of LAW glasses by Glass # are listed in Table A.3 of Appendix A.

Table C.2. Glass #s of LAW Glasses with Pass/Fail VHT Data in Six Evaluation Subsets^(a)

Count	Evaluation Subset, Glass #s for VHT					
	WTP	ORP	LP2OL	LP123	HiNa ₂ O	HiSO ₃
1	9	397	516	928	41	185
2	15	398	517	930	42	192
3	17	407	519	933	268	196
4	18	442	520	935	343	207
5	19	443	521	937	344	211
6	28	444	522	939	345	213
7	41	445	524	941	458	290
8	42	446	526	943	459	341
9	52	447	528	945	462	407
10	65	500	538	947	486	443
11	68	501	539	949	488	444
12	74	502	541	951	489	445
13	75	503	543	953	496	446
14	76	504	561	955	497	447
15	78	505	562	957	499	544
16	80	506	577	959	500	602
17	89	507	578	961	501	603
18	92	508	583	963	502	604
19	93	509	584	965	503	605
20	122	510	585	967	504	606
21	123	511	586	969	505	607
22	125	512	587	971	506	608
23	150	513	588	973	507	609
24	174	514	589	975	508	610
25	175	515	590	977	509	611
26	177	516	591	979	510	612
27	178	517	592	981	511	613
28	179	519	593	983	512	614
29	180	520	594	986	513	615
30	185	521	595	989	514	622
31	187	522	596	991	515	698
32	189	523	597	1013	516	701
33	192	524	598	1014	517	702
34	194	525	618	1015	519	703
35	196	526	619	1016	520	704
36	198	527	620	1017	521	706
37	199	528	621	1018	522	707
38	201	529	622	1019	523	708
39	203	530	689	1020	524	710
40	205	531	690	1021	525	711
41	207	532	695	1022	526	712
42	209	533	696	1023	527	714
43	211	534	697	1024	528	715
44	213	535	698	1025	538	716
45	215	536	699	1026	539	717
46	217	537	700	1027	541	733

Table C.2. Glass #s of LAW Glasses with Pass/Fail VHT Data in Six Evaluation Subsets^(a), cont.

Count	Evaluation Subset, Glass #s for VHT					
	WTP	ORP	LP2OL	LP123	HiNa ₂ O	HiSO ₃
47	219	538	723	1028	543	735
48	221	539	724	1029	545	838
49	223	541	725	1030	546	841
50	225	543	726	1031	547	842
51	227	544	728	1032	548	843
52	229	545	729	1033	549	852
53	231	546	730	1034	550	853
54	233	547	731	1035	551	855
55	235	548	733	1036	552	856
56	237	549	736	1037	553	857
57	238	550	737	1038	554	875
58	240	551	744	1039	555	876
59	242	552	745	1040	556	881
60	244	553	748	1041	557	882
61	246	554	750	1042	558	884
62	249	555	751	1043	559	885
63	250	556	759	1044	560	886
64	252	557	760	1045	561	890
65	254	558	761	1046	562	891
66	256	559	762	1047	563	892
67	258	560	763	1048	564	893
68	260	561	764	1049	565	894
69	263	562	765	1050	566	895
70	265	563	766	1051	567	896
71	267	564	768	1052	568	897
72	268	565	898	1053	569	903
73	269	566	900	1054	570	904
74	272	567	919	1055	571	905
75	273	568	997	1056	572	906
76	274	569	999	1057	573	907
77	276	570	1013	1058	574	908
78	277	571	1014	1059	575	930
79	278	572	1015	1060	576	933
80	279	573	1016	1061	577	935
81	280	574	1017	1062	578	939
82	281	575	1018	1063	579	943
83	282	576	1019	1064	580	947
84	284	577	1020	1065	581	949
85	285	578	1021	1067	582	951
86	289	579	1022	1068	583	953
87	290	580	1023	1069	584	977
88	309	581	1024	1070	585	979
89	311	582	1025	1071	586	981
90	314	583	1026	1073	587	983
91	315	584	1027	1074	588	986

Table C.2. Glass #s of LAW Glasses with Pass/Fail VHT Data in Six Evaluation Subsets^(a), cont.

Count	Evaluation Subset, Glass #s for VHT					
	WTP	ORP	LP2OL	LP123	HiNa ₂ O	HiSO ₃
92	319	585	1028	1075	589	989
93	320	586	1030	--	590	997
94	323	587	1031	--	591	1001
95	331	588	1033	--	592	1029
96	332	589	1034	--	593	1034
97	333	590	1035	--	594	1035
98	334	591	1036	--	595	1042
99	335	592	1037	--	596	1044
100	336	593	1038	--	597	1046
101	337	594	1039	--	598	1051
102	338	595	1040	--	599	1057
103	339	596	1041	--	600	1058
104	340	597	1042	--	601	1062
105	341	598	1043	--	602	1063
106	342	599	1044	--	616	1067
107	343	600	1045	--	617	1068
108	344	601	1046	--	618	1074
109	345	602	1047	--	619	--
110	346	603	1048	--	620	--
111	347	604	1049	--	621	--
112	348	605	1050	--	622	--
113	349	606	1051	--	625	--
114	350	607	1052	--	626	--
115	351	608	1053	--	627	--
116	352	609	1054	--	628	--
117	353	610	1055	--	677	--
118	354	611	1056	--	678	--
119	355	612	1057	--	679	--
120	356	613	1059	--	680	--
121	357	614	1060	--	681	--
122	358	615	1061	--	682	--
123	359	616	1062	--	683	--
124	360	617	1063	--	684	--
125	361	618	1064	--	685	--
126	362	619	1065	--	686	--
127	363	620	1067	--	687	--
128	364	621	1068	--	688	--
129	365	622	1069	--	689	--
130	366	623	1070	--	690	--
131	367	624	1071	--	691	--
132	368	625	1073	--	692	--
133	369	626	1074	--	693	--
134	370	627	1075	--	694	--
135	371	628	--	--	695	--
136	372	629	--	--	696	--
137	373	630	--	--	697	--

Table C.2. Glass #s of LAW Glasses with Pass/Fail VHT Data in Six Evaluation Subsets^(a), cont.

Count	Evaluation Subset, Glass #s for VHT					
	WTP	ORP	LP2OL	LP123	HiNa ₂ O	HiSO ₃
138	374	631	--	--	698	--
139	375	632	--	--	699	--
140	376	633	--	--	700	--
141	377	636	--	--	726	--
142	378	637	--	--	728	--
143	379	638	--	--	731	--
144	380	639	--	--	733	--
145	381	642	--	--	737	--
146	382	643	--	--	738	--
147	383	652	--	--	741	--
148	384	653	--	--	744	--
149	385	654	--	--	745	--
150	386	655	--	--	746	--
151	389	668	--	--	747	--
152	411	669	--	--	748	--
153	422	670	--	--	749	--
154	424	671	--	--	750	--
155	430	672	--	--	751	--
156	431	673	--	--	754	--
157	437	674	--	--	758	--
158	448	675	--	--	763	--
159	449	676	--	--	764	--
160	450	677	--	--	765	--
161	451	678	--	--	766	--
162	452	679	--	--	768	--
163	453	680	--	--	771	--
164	454	681	--	--	777	--
165	455	682	--	--	790	--
166	456	683	--	--	815	--
167	457	684	--	--	818	--
168	458	685	--	--	820	--
169	459	686	--	--	822	--
170	460	687	--	--	823	--
171	461	688	--	--	824	--
172	462	689	--	--	825	--
173	463	690	--	--	826	--
174	464	691	--	--	827	--
175	465	692	--	--	828	--
176	466	693	--	--	829	--
177	474	694	--	--	830	--
178	475	695	--	--	831	--
179	476	696	--	--	832	--
180	477	697	--	--	833	--
181	478	698	--	--	835	--
182	479	699	--	--	836	--
183	480	700	--	--	837	--

Table C.2. Glass #s of LAW Glasses with Pass/Fail VHT Data in Six Evaluation Subsets^(a), cont.

Count	Evaluation Subset, Glass #s for VHT					
	WTP	ORP	LP2OL	LP123	HiNa ₂ O	HiSO ₃
184	481	701	--	--	838	--
185	482	702	--	--	844	--
186	483	703	--	--	845	--
187	484	704	--	--	847	--
188	485	706	--	--	848	--
189	486	707	--	--	849	--
190	487	708	--	--	850	--
191	488	710	--	--	851	--
192	489	711	--	--	852	--
193	490	712	--	--	858	--
194	491	714	--	--	862	--
195	492	715	--	--	864	--
196	493	716	--	--	867	--
197	494	717	--	--	868	--
198	495	718	--	--	871	--
199	496	719	--	--	872	--
200	497	720	--	--	873	--
201	498	721	--	--	874	--
202	499	722	--	--	875	--
203	--	723	--	--	877	--
204	--	724	--	--	878	--
205	--	725	--	--	879	--
206	--	726	--	--	881	--
207	--	728	--	--	887	--
208	--	729	--	--	888	--
209	--	730	--	--	889	--
210	--	731	--	--	892	--
211	--	733	--	--	898	--
212	--	734	--	--	900	--
213	--	735	--	--	901	--
214	--	736	--	--	902	--
215	--	737	--	--	903	--
216	--	738	--	--	904	--
217	--	741	--	--	909	--
218	--	744	--	--	910	--
219	--	745	--	--	911	--
220	--	746	--	--	912	--
221	--	747	--	--	913	--
222	--	748	--	--	914	--
223	--	749	--	--	915	--
224	--	750	--	--	916	--
225	--	751	--	--	919	--
226	--	752	--	--	921	--
227	--	753	--	--	922	--
228	--	754	--	--	947	--
229	--	755	--	--	961	--

Table C.2. Glass #s of LAW Glasses with Pass/Fail VHT Data in Six Evaluation Subsets^(a), cont.

Count	Evaluation Subset, Glass #s for VHT					
	WTP	ORP	LP2OL	LP123	HiNa ₂ O	HiSO ₃
230	--	756	--	--	981	--
231	--	757	--	--	999	--
232	--	758	--	--	1013	--
233	--	759	--	--	1014	--
234	--	760	--	--	1015	--
235	--	761	--	--	1016	--
236	--	762	--	--	1017	--
237	--	763	--	--	1018	--
238	--	764	--	--	1019	--
239	--	765	--	--	1020	--
240	--	766	--	--	1021	--
241	--	768	--	--	1022	--
242	--	769	--	--	1023	--
243	--	770	--	--	1024	--
244	--	771	--	--	1025	--
245	--	772	--	--	1026	--
246	--	773	--	--	1027	--
247	--	774	--	--	1028	--
248	--	775	--	--	1029	--
249	--	776	--	--	1031	--
250	--	777	--	--	1032	--
251	--	778	--	--	1034	--
252	--	779	--	--	1036	--
253	--	780	--	--	1038	--
254	--	781	--	--	1040	--
255	--	782	--	--	1041	--
256	--	783	--	--	1042	--
257	--	784	--	--	1044	--
258	--	785	--	--	1045	--
259	--	786	--	--	1046	--
260	--	787	--	--	1047	--
261	--	788	--	--	1048	--
262	--	789	--	--	1049	--
263	--	790	--	--	1051	--
264	--	791	--	--	1052	--
265	--	792	--	--	1053	--
266	--	793	--	--	1054	--
267	--	794	--	--	1055	--
268	--	795	--	--	1056	--
269	--	797	--	--	1057	--
270	--	799	--	--	1058	--
271	--	800	--	--	1059	--
272	--	801	--	--	1060	--
273	--	802	--	--	1061	--
274	--	803	--	--	1062	--
275	--	804	--	--	1063	--

Table C.2. Glass #s of LAW Glasses with Pass/Fail VHT Data in Six Evaluation Subsets^(a), cont.

Count	Evaluation Subset, Glass #s for VHT					
	WTP	ORP	LP2OL	LP123	HiNa ₂ O	HiSO ₃
276	--	805	--	--	1064	--
277	--	806	--	--	1065	--
278	--	807	--	--	1067	--
279	--	808	--	--	1068	--
280	--	809	--	--	1069	--
281	--	810	--	--	1070	--
282	--	815	--	--	1071	--
283	--	818	--	--	1073	--
284	--	820	--	--	1074	--
285	--	822	--	--	1075	--
286	--	823	--	--	--	--
287	--	824	--	--	--	--
288	--	825	--	--	--	--
289	--	826	--	--	--	--
290	--	827	--	--	--	--
291	--	828	--	--	--	--
292	--	829	--	--	--	--
293	--	830	--	--	--	--
294	--	831	--	--	--	--
295	--	832	--	--	--	--
296	--	833	--	--	--	--
297	--	835	--	--	--	--
298	--	836	--	--	--	--
299	--	837	--	--	--	--
300	--	838	--	--	--	--
301	--	839	--	--	--	--
302	--	840	--	--	--	--
303	--	841	--	--	--	--
304	--	842	--	--	--	--
305	--	843	--	--	--	--
306	--	844	--	--	--	--
307	--	845	--	--	--	--
308	--	846	--	--	--	--
309	--	847	--	--	--	--
310	--	848	--	--	--	--
311	--	849	--	--	--	--
312	--	850	--	--	--	--
313	--	851	--	--	--	--
314	--	852	--	--	--	--
315	--	853	--	--	--	--
316	--	854	--	--	--	--
317	--	855	--	--	--	--
318	--	856	--	--	--	--
319	--	857	--	--	--	--
320	--	858	--	--	--	--
321	--	859	--	--	--	--

Table C.2. Glass #s of LAW Glasses with Pass/Fail VHT Data in Six Evaluation Subsets^(a), cont.

Count	Evaluation Subset, Glass #s for VHT					
	WTP	ORP	LP2OL	LP123	HiNa ₂ O	HiSO ₃
322	--	860	--	--	--	--
323	--	861	--	--	--	--
324	--	862	--	--	--	--
325	--	863	--	--	--	--
326	--	864	--	--	--	--
327	--	865	--	--	--	--
328	--	866	--	--	--	--
329	--	867	--	--	--	--
330	--	868	--	--	--	--
331	--	869	--	--	--	--
332	--	870	--	--	--	--
333	--	871	--	--	--	--
334	--	872	--	--	--	--
335	--	873	--	--	--	--
336	--	874	--	--	--	--
337	--	875	--	--	--	--
338	--	876	--	--	--	--
339	--	877	--	--	--	--
340	--	878	--	--	--	--
341	--	879	--	--	--	--
342	--	880	--	--	--	--
343	--	881	--	--	--	--
344	--	882	--	--	--	--
345	--	883	--	--	--	--
346	--	884	--	--	--	--
347	--	885	--	--	--	--
348	--	886	--	--	--	--
349	--	887	--	--	--	--
350	--	888	--	--	--	--
351	--	889	--	--	--	--
352	--	890	--	--	--	--
353	--	891	--	--	--	--
354	--	892	--	--	--	--
355	--	893	--	--	--	--
356	--	894	--	--	--	--
357	--	895	--	--	--	--
358	--	896	--	--	--	--
359	--	897	--	--	--	--
360	--	898	--	--	--	--
361	--	900	--	--	--	--
362	--	901	--	--	--	--
363	--	902	--	--	--	--
364	--	903	--	--	--	--
365	--	904	--	--	--	--
366	--	905	--	--	--	--
367	--	906	--	--	--	--

Table C.2. Glass #s of LAW Glasses with Pass/Fail VHT Data in Six Evaluation Subsets^(a), cont.

Count	Evaluation Subset, Glass #s for VHT					
	WTP	ORP	LP2OL	LP123	HiNa ₂ O	HiSO ₃
368	--	907	--	--	--	--
369	--	908	--	--	--	--
370	--	909	--	--	--	--
371	--	910	--	--	--	--
372	--	911	--	--	--	--
373	--	912	--	--	--	--
374	--	913	--	--	--	--
375	--	914	--	--	--	--
376	--	915	--	--	--	--
377	--	916	--	--	--	--
378	--	919	--	--	--	--
379	--	920	--	--	--	--
380	--	921	--	--	--	--
381	--	922	--	--	--	--
382	--	923	--	--	--	--
383	--	924	--	--	--	--
384	--	925	--	--	--	--
385	--	926	--	--	--	--
386	--	927	--	--	--	--
387	--	993	--	--	--	--
388	--	995	--	--	--	--
389	--	997	--	--	--	--
390	--	999	--	--	--	--
391	--	1001	--	--	--	--
392	--	1012	--	--	--	--

(a) The “Glass #” is a unique number assigned to each LAW glass composition, as shown in Table A.2 of Appendix A. The corresponding pass/fail VHT values of LAW glasses by Glass # are listed in Table A.3 of Appendix A.

Table C.3. Glass #s of LAW Glasses with Viscosity at 1150 °C Data in Six Evaluation Subsets^(a)

Count	Evaluation Subset, Glass #s for η_{1150}					
	WTP	ORP	LP2OL	LP123	HiNa ₂ O	HiSO ₃
1	2	399	516	928	41	61
2	3	408	519	930	42	62
3	6	409	520	933	64	63
4	7	410	521	935	268	159
5	8	442	522	937	343	181
6	9	443	524	939	344	185
7	11	444	526	941	345	192
8	15	445	528	943	458	196
9	16	446	561	945	459	207
10	17	447	577	947	462	211
11	18	500	583	949	486	213
12	19	501	585	951	489	251
13	21	502	587	953	496	255
14	22	503	589	955	500	290
15	23	504	595	957	501	341
16	24	505	597	959	502	443
17	27	506	689	961	503	444
18	28	507	695	963	504	445
19	29	508	696	965	505	446
20	30	509	697	967	506	447
21	31	510	698	969	507	603
22	32	511	699	971	508	604
23	34	512	700	973	509	605
24	36	513	723	975	510	606
25	37	514	724	977	511	607
26	38	515	725	979	512	608
27	41	516	726	981	513	609
28	42	519	728	983	514	610
29	44	520	729	986	515	611
30	45	521	730	989	516	612
31	49	522	745	991	519	613
32	52	523	751	1013	520	614
33	53	524	760	1014	521	698
34	54	525	761	1015	522	701
35	55	526	762	1016	523	702
36	56	527	763	1017	524	703
37	60	528	764	1018	525	704
38	61	529	765	1019	526	708
39	62	530	766	1020	527	710
40	63	531	898	1021	528	711
41	64	532	900	1022	545	712
42	65	533	919	1023	547	715
43	66	534	997	1024	549	716
44	68	535	999	1025	551	717

Table C.3. Glass #s of LAW Glasses with Viscosity at 1150 °C Data in Six Evaluation Subsets,^(a) cont.

Count	Evaluation Subset, Glass #s for η_{1150}					
	WTP	ORP	LP2OL	LP123	HiNa ₂ O	HiSO ₃
45	69	536	1013	1026	553	838
46	71	537	1014	1027	555	841
47	72	545	1015	1028	557	842
48	74	547	1016	1029	559	843
49	75	549	1017	1030	561	852
50	76	551	1018	1031	563	853
51	78	553	1019	1032	565	855
52	142	555	1020	1033	567	856
53	143	557	1021	1034	569	857
54	151	559	1022	1035	571	875
55	155	561	1023	1036	573	876
56	157	563	1024	1037	575	881
57	159	565	1025	1038	577	882
58	174	567	1026	1039	579	884
59	177	569	1027	1040	581	885
60	178	571	1028	1041	583	886
61	181	573	1030	1042	585	890
62	183	575	1031	1043	587	891
63	185	577	1033	1044	589	892
64	187	579	1034	1045	595	893
65	189	581	1035	1046	597	894
66	192	583	1036	1047	625	895
67	194	585	1037	1048	627	896
68	196	587	1038	1049	687	897
69	198	589	1039	1050	688	903
70	199	595	1040	1051	689	904
71	201	597	1041	1052	695	905
72	203	603	1042	1053	696	906
73	205	604	1043	1054	697	907
74	207	605	1044	1055	698	930
75	209	606	1045	1056	699	933
76	211	607	1046	1057	700	935
77	213	608	1047	1058	726	939
78	215	609	1048	1059	728	943
79	217	610	1049	1060	745	947
80	219	611	1050	1061	751	949
81	221	612	1051	1062	763	951
82	223	613	1052	1063	764	953
83	225	614	1053	1064	765	977
84	227	623	1054	1065	766	979
85	229	624	1055	1067	771	981
86	231	625	1056	1068	777	983
87	233	627	1057	1069	790	986
88	235	630	1059	1070	815	989
89	240	631	1060	1071	820	997
90	242	687	1061	1073	823	1001

Table C.3. Glass #s of LAW Glasses with Viscosity at 1150 °C Data in Six Evaluation Subsets,^(a) cont.

Count	Evaluation Subset, Glass #s for η_{1150}					
	WTP	ORP	LP2OL	LP123	HiNa ₂ O	HiSO ₃
91	244	688	1062	1074	826	1029
92	246	689	1063	1075	827	1034
93	250	695	1064	--	828	1035
94	251	696	1065	--	829	1042
95	252	697	1067	--	830	1044
96	253	698	1068	--	831	1046
97	255	699	1069	--	832	1051
98	256	700	1070	--	833	1057
99	258	701	1071	--	835	1058
100	260	702	1073	--	836	1062
101	263	703	1074	--	837	1063
102	268	704	1075	--	838	1067
103	269	708	--	--	844	1068
104	272	710	--	--	845	1074
105	273	711	--	--	847	--
106	274	712	--	--	848	--
107	275	715	--	--	849	--
108	276	716	--	--	850	--
109	277	717	--	--	851	--
110	279	718	--	--	852	--
111	280	719	--	--	858	--
112	281	721	--	--	862	--
113	282	722	--	--	864	--
114	283	723	--	--	867	--
115	284	724	--	--	871	--
116	285	725	--	--	873	--
117	286	726	--	--	874	--
118	287	728	--	--	875	--
119	288	729	--	--	877	--
120	289	730	--	--	878	--
121	290	745	--	--	879	--
122	309	751	--	--	881	--
123	311	760	--	--	887	--
124	314	761	--	--	888	--
125	315	762	--	--	892	--
126	318	763	--	--	898	--
127	321	764	--	--	900	--
128	323	765	--	--	901	--
129	326	766	--	--	902	--
130	331	769	--	--	903	--
131	332	770	--	--	904	--
132	333	771	--	--	909	--
133	334	772	--	--	910	--
134	335	773	--	--	911	--
135	336	774	--	--	912	--
136	337	775	--	--	913	--

Table C.3. Glass #s of LAW Glasses with Viscosity at 1150 °C Data in Six Evaluation Subsets,^(a) cont.

Count	Evaluation Subset, Glass #s for η_{1150}					
	WTP	ORP	LP2OL	LP123	HiNa ₂ O	HiSO ₃
137	339	777	--	--	914	--
138	340	778	--	--	915	--
139	341	779	--	--	916	--
140	342	780	--	--	919	--
141	343	782	--	--	921	--
142	344	783	--	--	922	--
143	345	784	--	--	947	--
144	346	785	--	--	961	--
145	347	786	--	--	981	--
146	362	787	--	--	999	--
147	365	788	--	--	1013	--
148	376	789	--	--	1014	--
149	383	790	--	--	1015	--
150	386	793	--	--	1016	--
151	411	795	--	--	1017	--
152	424	796	--	--	1018	--
153	430	800	--	--	1019	--
154	448	802	--	--	1020	--
155	449	803	--	--	1021	--
156	451	804	--	--	1022	--
157	452	805	--	--	1023	--
158	454	806	--	--	1024	--
159	455	807	--	--	1025	--
160	456	808	--	--	1026	--
161	457	809	--	--	1027	--
162	458	810	--	--	1028	--
163	459	815	--	--	1029	--
164	460	820	--	--	1031	--
165	461	823	--	--	1032	--
166	462	826	--	--	1034	--
167	463	827	--	--	1036	--
168	464	828	--	--	1038	--
169	475	829	--	--	1040	--
170	476	830	--	--	1041	--
171	477	831	--	--	1042	--
172	478	832	--	--	1044	--
173	479	833	--	--	1045	--
174	480	835	--	--	1046	--
175	482	836	--	--	1047	--
176	483	837	--	--	1048	--
177	486	838	--	--	1049	--
178	489	839	--	--	1051	--
179	491	840	--	--	1052	--
180	494	841	--	--	1053	--
181	496	842	--	--	1054	--
182	498	843	--	--	1055	--

Table C.3. Glass #s of LAW Glasses with Viscosity at 1150 °C Data in Six Evaluation Subsets,^(a) cont.

Count	Evaluation Subset, Glass #s for η_{1150}					
	WTP	ORP	LP2OL	LP123	HiNa ₂ O	HiSO ₃
183	--	844	--	--	1056	--
184	--	845	--	--	1057	--
185	--	846	--	--	1058	--
186	--	847	--	--	1059	--
187	--	848	--	--	1060	--
188	--	849	--	--	1061	--
189	--	850	--	--	1062	--
190	--	851	--	--	1063	--
191	--	852	--	--	1064	--
192	--	853	--	--	1065	--
193	--	854	--	--	1067	--
194	--	855	--	--	1068	--
195	--	856	--	--	1069	--
196	--	857	--	--	1070	--
197	--	858	--	--	1071	--
198	--	859	--	--	1073	--
199	--	862	--	--	1074	--
200	--	863	--	--	1075	--
201	--	864	--	--	--	--
202	--	865	--	--	--	--
203	--	867	--	--	--	--
204	--	869	--	--	--	--
205	--	871	--	--	--	--
206	--	873	--	--	--	--
207	--	874	--	--	--	--
208	--	875	--	--	--	--
209	--	876	--	--	--	--
210	--	877	--	--	--	--
211	--	878	--	--	--	--
212	--	879	--	--	--	--
213	--	880	--	--	--	--
214	--	881	--	--	--	--
215	--	882	--	--	--	--
216	--	883	--	--	--	--
217	--	884	--	--	--	--
218	--	885	--	--	--	--
219	--	886	--	--	--	--
220	--	887	--	--	--	--
221	--	888	--	--	--	--
222	--	890	--	--	--	--
223	--	891	--	--	--	--
224	--	892	--	--	--	--
225	--	893	--	--	--	--
226	--	894	--	--	--	--
227	--	895	--	--	--	--
228	--	896	--	--	--	--

Table C.3. Glass #s of LAW Glasses with Viscosity at 1150 °C Data in Six Evaluation Subsets,^(a) cont.

Count	Evaluation Subset, Glass #s for η_{1150}					
	WTP	ORP	LP2OL	LP123	HiNa ₂ O	HiSO ₃
229	--	897	--	--	--	--
230	--	898	--	--	--	--
231	--	900	--	--	--	--
232	--	901	--	--	--	--
233	--	902	--	--	--	--
234	--	903	--	--	--	--
235	--	904	--	--	--	--
236	--	905	--	--	--	--
237	--	906	--	--	--	--
238	--	907	--	--	--	--
239	--	909	--	--	--	--
240	--	910	--	--	--	--
241	--	911	--	--	--	--
242	--	912	--	--	--	--
243	--	913	--	--	--	--
244	--	914	--	--	--	--
245	--	915	--	--	--	--
246	--	916	--	--	--	--
247	--	919	--	--	--	--
248	--	920	--	--	--	--
249	--	921	--	--	--	--
250	--	922	--	--	--	--
251	--	923	--	--	--	--
252	--	924	--	--	--	--
253	--	925	--	--	--	--
254	--	926	--	--	--	--
255	--	927	--	--	--	--
256	--	993	--	--	--	--
257	--	995	--	--	--	--
258	--	997	--	--	--	--
259	--	999	--	--	--	--
260	--	1001	--	--	--	--

(a) The “Glass #” is a unique number assigned to each LAW glass composition, as shown in Table A.2 of Appendix A. The corresponding η_{1150} values of LAW glasses by Glass # are listed in Table A.3 of Appendix A.

Table C.4. Glass #s of LAW Glasses with Electrical Conductivity at 1150 °C Data in Six Evaluation Subsets^(a)

Number of Glasses	Evaluation Subset, Glass #s for ϵ_{1150}					
	WTP	ORP	LP2OL	LP123	HiNa ₂ O	HiSO ₃
1	2	399	516	928	41	62
2	3	408	519	930	42	63
3	6	409	520	933	64	159
4	7	410	521	935	268	181
5	8	442	522	937	343	185
6	9	443	524	939	344	192
7	11	444	526	941	345	196
8	15	445	528	943	458	207
9	16	446	561	947	459	211
10	17	447	577	949	462	213
11	18	500	583	951	486	251
12	19	501	585	953	489	255
13	21	502	587	955	496	290
14	22	503	589	957	500	341
15	23	504	595	959	501	443
16	24	505	597	961	502	444
17	27	506	689	963	503	445
18	28	507	695	965	504	446
19	29	508	696	967	505	447
20	30	509	697	969	506	603
21	31	510	698	971	507	604
22	32	511	699	973	508	605
23	34	512	700	975	509	606
24	36	513	723	977	510	607
25	37	514	724	979	511	608
26	38	515	725	981	512	609
27	41	516	726	983	513	610
28	42	519	728	986	514	611
29	44	520	729	989	515	612
30	45	521	730	991	516	613
31	49	522	745	1013	519	614
32	52	523	751	1014	520	698
33	53	524	760	1015	521	701
34	54	525	761	1016	522	702
35	55	526	762	1017	523	703
36	56	527	763	1018	524	704
37	60	528	764	1019	525	708
38	62	529	765	1020	526	710
39	63	530	766	1021	527	711
40	64	531	898	1022	528	712
41	65	532	900	1023	545	715
42	66	533	919	1024	547	716
43	68	534	997	1025	549	717
44	69	535	999	1026	551	838
45	71	536	1013	1027	553	841

Table C.4. Glass #s of LAW Glasses with Electrical Conductivity at 1150 °C Data in Six Evaluation Subsets,^(a) cont.

Number of Glasses	Evaluation Subset, Glass #s for ϵ_{1150}					
	WTP	ORP	LP2OL	LP123	HiNa ₂ O	HiSO ₃
46	72	537	1014	1028	555	842
47	74	545	1015	1029	557	843
48	75	547	1016	1030	559	852
49	142	549	1017	1031	561	853
50	143	551	1018	1032	563	855
51	151	553	1019	1033	565	856
52	153	555	1020	1034	567	857
53	155	557	1021	1035	569	875
54	157	559	1022	1036	571	876
55	159	561	1023	1037	573	881
56	174	563	1024	1038	575	882
57	177	565	1025	1039	577	884
58	178	567	1026	1040	579	885
59	181	569	1027	1041	581	886
60	183	571	1028	1042	583	890
61	185	573	1030	1043	585	891
62	187	575	1031	1044	587	892
63	189	577	1033	1045	589	893
64	192	579	1034	1046	595	894
65	194	581	1035	1047	597	895
66	196	583	1036	1048	625	896
67	198	585	1037	1049	627	897
68	199	587	1038	1050	687	903
69	201	589	1039	1051	688	904
70	203	595	1040	1052	689	905
71	205	597	1041	1053	695	906
72	207	603	1042	1054	696	907
73	209	604	1043	1056	697	930
74	211	605	1044	1057	698	933
75	213	606	1045	1058	699	935
76	215	607	1046	1059	700	939
77	217	608	1047	1060	726	943
78	219	609	1048	1063	728	947
79	221	610	1049	1064	745	949
80	223	611	1050	1067	751	951
81	225	612	1051	1068	763	953
82	227	613	1052	1075	764	977
83	229	614	1053	--	765	979
84	231	623	1054	--	766	981
85	233	624	1056	--	771	983
86	235	625	1057	--	777	986
87	240	627	1059	--	790	989
88	242	630	1060	--	815	997
89	244	631	1063	--	820	1001
90	246	687	1064	--	823	1029

Table C.4. Glass #s of LAW Glasses with Electrical Conductivity at 1150 °C Data in Six Evaluation Subsets,^(a) cont.

Number of Glasses	Evaluation Subset, Glass #s for ϵ_{1150}					
	WTP	ORP	LP2OL	LP123	HiNa ₂ O	HiSO ₃
91	251	688	1067	--	826	1034
92	252	689	1068	--	827	1035
93	253	695	1075	--	828	1042
94	255	696	--	--	829	1044
95	256	697	--	--	830	1046
96	258	698	--	--	831	1051
97	260	699	--	--	832	1057
98	263	700	--	--	833	1058
99	268	701	--	--	835	1063
100	269	702	--	--	836	1067
101	272	703	--	--	837	1068
102	273	704	--	--	838	--
103	274	708	--	--	844	--
104	275	710	--	--	845	--
105	276	711	--	--	847	--
106	277	712	--	--	848	--
107	279	715	--	--	849	--
108	280	716	--	--	850	--
109	281	717	--	--	851	--
110	282	718	--	--	852	--
111	283	719	--	--	858	--
112	284	721	--	--	862	--
113	285	722	--	--	864	--
114	286	723	--	--	867	--
115	287	724	--	--	871	--
116	288	725	--	--	873	--
117	289	726	--	--	874	--
118	290	728	--	--	875	--
119	309	729	--	--	877	--
120	311	730	--	--	878	--
121	314	745	--	--	879	--
122	315	751	--	--	881	--
123	318	760	--	--	887	--
124	321	761	--	--	888	--
125	323	762	--	--	892	--
126	326	763	--	--	898	--
127	331	764	--	--	900	--
128	332	765	--	--	901	--
129	333	766	--	--	902	--
130	334	769	--	--	903	--
131	335	770	--	--	904	--
132	336	771	--	--	909	--
133	340	772	--	--	910	--
134	341	773	--	--	911	--
135	342	774	--	--	912	--
136	343	775	--	--	913	--

Table C.4. Glass #s of LAW Glasses with Electrical Conductivity at 1150 °C Data in Six Evaluation Subsets,^(a) cont.

Number of Glasses	Evaluation Subset, Glass #s for ϵ_{1150}					
	WTP	ORP	LP2OL	LP123	HiNa ₂ O	HiSO ₃
137	344	776	--	--	914	--
138	345	777	--	--	915	--
139	346	778	--	--	916	--
140	347	779	--	--	919	--
141	362	780	--	--	921	--
142	365	781	--	--	922	--
143	376	782	--	--	947	--
144	383	783	--	--	961	--
145	386	784	--	--	981	--
146	411	785	--	--	999	--
147	424	786	--	--	1013	--
148	430	787	--	--	1014	--
149	448	788	--	--	1015	--
150	449	789	--	--	1016	--
151	451	790	--	--	1017	--
152	452	791	--	--	1018	--
153	454	792	--	--	1019	--
154	455	793	--	--	1020	--
155	456	794	--	--	1021	--
156	457	795	--	--	1022	--
157	458	796	--	--	1023	--
158	459	799	--	--	1024	--
159	460	800	--	--	1025	--
160	461	801	--	--	1026	--
161	462	802	--	--	1027	--
162	463	803	--	--	1028	--
163	464	804	--	--	1029	--
164	475	805	--	--	1031	--
165	476	806	--	--	1032	--
166	477	807	--	--	1034	--
167	478	808	--	--	1036	--
168	479	809	--	--	1038	--
169	480	810	--	--	1040	--
170	482	815	--	--	1041	--
171	483	820	--	--	1042	--
172	486	823	--	--	1044	--
173	489	826	--	--	1045	--
174	491	827	--	--	1046	--
175	494	828	--	--	1047	--
176	496	829	--	--	1048	--
177	498	830	--	--	1049	--
178	--	831	--	--	1051	--
179	--	832	--	--	1052	--
180	--	833	--	--	1053	--
181	--	835	--	--	1054	--
182	--	836	--	--	1056	--

Table C.4. Glass #s of LAW Glasses with Electrical Conductivity at 1150 °C Data in Six Evaluation Subsets,^(a) cont.

Number of Glasses	Evaluation Subset, Glass #s for ϵ_{1150}					
	WTP	ORP	LP2OL	LP123	HiNa ₂ O	HiSO ₃
183	--	837	--	--	1057	--
184	--	838	--	--	1058	--
185	--	839	--	--	1059	--
186	--	840	--	--	1060	--
187	--	841	--	--	1063	--
188	--	842	--	--	1064	--
189	--	843	--	--	1067	--
190	--	844	--	--	1068	--
191	--	845	--	--	1075	--
192	--	846	--	--	--	--
193	--	847	--	--	--	--
194	--	848	--	--	--	--
195	--	849	--	--	--	--
196	--	850	--	--	--	--
197	--	851	--	--	--	--
198	--	852	--	--	--	--
199	--	853	--	--	--	--
200	--	854	--	--	--	--
201	--	855	--	--	--	--
202	--	856	--	--	--	--
203	--	857	--	--	--	--
204	--	858	--	--	--	--
205	--	859	--	--	--	--
206	--	862	--	--	--	--
207	--	863	--	--	--	--
208	--	864	--	--	--	--
209	--	865	--	--	--	--
210	--	867	--	--	--	--
211	--	869	--	--	--	--
212	--	871	--	--	--	--
213	--	873	--	--	--	--
214	--	874	--	--	--	--
215	--	875	--	--	--	--
216	--	876	--	--	--	--
217	--	877	--	--	--	--
218	--	878	--	--	--	--
219	--	879	--	--	--	--
220	--	880	--	--	--	--
221	--	881	--	--	--	--
222	--	882	--	--	--	--
223	--	883	--	--	--	--
224	--	884	--	--	--	--
225	--	885	--	--	--	--
226	--	886	--	--	--	--
227	--	887	--	--	--	--
228	--	888	--	--	--	--

Table C.4. Glass #s of LAW Glasses with Electrical Conductivity at 1150 °C Data in Six Evaluation Subsets,^(a) cont.

Number of Glasses	Evaluation Subset, Glass #s for ϵ_{1150}					
	WTP	ORP	LP2OL	LP123	HiNa ₂ O	HiSO ₃
229	--	890	--	--	--	--
230	--	891	--	--	--	--
231	--	892	--	--	--	--
232	--	893	--	--	--	--
233	--	894	--	--	--	--
234	--	895	--	--	--	--
235	--	896	--	--	--	--
236	--	897	--	--	--	--
237	--	898	--	--	--	--
238	--	900	--	--	--	--
239	--	901	--	--	--	--
240	--	902	--	--	--	--
241	--	903	--	--	--	--
242	--	904	--	--	--	--
243	--	905	--	--	--	--
244	--	906	--	--	--	--
245	--	907	--	--	--	--
246	--	909	--	--	--	--
247	--	910	--	--	--	--
248	--	911	--	--	--	--
249	--	912	--	--	--	--
250	--	913	--	--	--	--
251	--	914	--	--	--	--
252	--	915	--	--	--	--
253	--	916	--	--	--	--
254	--	919	--	--	--	--
255	--	920	--	--	--	--
256	--	921	--	--	--	--
257	--	922	--	--	--	--
258	--	923	--	--	--	--
259	--	924	--	--	--	--
260	--	925	--	--	--	--
261	--	926	--	--	--	--
262	--	927	--	--	--	--
263	--	993	--	--	--	--
264	--	995	--	--	--	--
265	--	997	--	--	--	--
266	--	999	--	--	--	--
267	--	1001	--	--	--	--

(a) The “Glass #” is a unique number assigned to each LAW glass composition, as shown in Table A.2 of Appendix A. The corresponding ϵ_{1150} values of LAW glasses by Glass # are listed in Table A.3 of Appendix A.

Table C.5. Glass #s of LAW Glasses with Melter SO₃ Tolerance and Solubility at 1150 °C Data in Six Evaluation Subsets^(a)

Count	Evaluation Subset, Glass #s for SO ₃ Solubility/Melter Tolerance					
	WTP	ORP	LP2OL	LP123	HiNa ₂ O	HiSO ₃
1	10	391	516	928	85	51
2	31	392	519	930	146	61
3	34	393	520	932	343	62
4	36	394	521	933	344	63
5	37	395	522	935	345	79
6	38	396	524	937	500	82
7	39	397	526	939	501	84
8	40	400	528	941	502	85
9	51	401	562	943	503	110
10	54	402	578	945	504	120
11	56	403	584	947	505	181
12	57	404	585	949	506	182
13	58	405	586	951	507	184
14	59	406	587	953	508	186
15	61	442	588	955	509	188
16	62	444	590	957	510	191
17	63	445	592	961	511	193
18	69	446	593	963	512	195
19	70	500	594	965	513	200
20	71	501	595	967	514	202
21	72	502	596	969	515	204
22	73	503	597	971	516	206
23	74	504	598	973	519	208
24	77	505	689	975	520	210
25	79	506	690	977	521	212
26	82	507	695	979	522	214
27	83	508	696	981	523	216
28	84	509	697	983	524	218
29	85	510	698	985	525	220
30	86	511	699	986	526	222
31	87	512	700	988	527	224
32	88	513	723	989	528	226
33	89	514	724	991	546	228
34	92	515	725	1013	548	230
35	93	516	726	1014	550	232
36	101	519	728	1015	552	234
37	102	520	729	1016	554	236
38	103	521	730	1017	556	243
39	104	522	737	1018	558	245
40	105	523	744	1019	560	247
41	107	524	745	1020	562	251
42	108	525	748	1021	564	255
43	109	526	750	1022	566	257
44	110	527	751	1023	568	264
45	111	528	759	1024	570	290

Table C.5. Glass #s of LAW Glasses with Melter SO₃ Tolerance and Solubility at 1150 °C Data in Six Evaluation Subsets,^(a) cont.

Count	Evaluation Subset, Glass #s for SO ₃ Solubility/Melter Tolerance					
	WTP	ORP	LP2OL	LP123	HiNa ₂ O	HiSO ₃
46	112	529	760	1025	572	310
47	113	530	761	1026	574	312
48	114	531	762	1027	576	341
49	116	532	763	1028	578	444
50	117	533	764	1029	579	445
51	120	534	765	1030	580	446
52	144	535	766	1031	581	602
53	145	536	898	1032	582	603
54	146	537	900	1033	584	604
55	147	546	919	1034	585	605
56	148	548	997	1035	586	606
57	149	550	999	1036	587	607
58	152	552	1013	1037	588	608
59	153	554	1014	1038	590	609
60	154	556	1015	1039	592	610
61	155	558	1016	1040	593	611
62	156	560	1017	1041	594	612
63	157	562	1018	1042	595	613
64	158	564	1019	1043	596	614
65	160	566	1020	1044	597	698
66	163	568	1021	1045	598	701
67	164	570	1022	1046	600	702
68	165	572	1023	1047	602	703
69	166	574	1024	1048	687	704
70	171	576	1025	1049	688	706
71	172	578	1026	1050	689	707
72	173	579	1027	1051	690	708
73	176	580	1028	1052	691	710
74	181	581	1030	1053	692	711
75	182	582	1031	1054	693	712
76	184	584	1033	1055	694	714
77	186	585	1034	1056	695	715
78	188	586	1035	1057	696	716
79	191	587	1036	1058	697	717
80	193	588	1037	1059	698	838
81	195	590	1038	1060	699	841
82	200	592	1039	1061	700	842
83	202	593	1040	1062	726	843
84	204	594	1041	1063	728	852
85	206	595	1042	1064	737	853
86	208	596	1043	1065	738	855
87	210	597	1044	1067	741	856
88	212	598	1045	1068	744	857
89	214	600	1046	1069	745	875
90	216	602	1047	1070	746	876

Table C.5. Glass #s of LAW Glasses with Melter SO₃ Tolerance and Solubility at 1150 °C Data in Six Evaluation Subsets,^(a) cont.

Count	Evaluation Subset, Glass #s for SO ₃ Solubility/Melter Tolerance					
	WTP	ORP	LP2OL	LP123	HiNa ₂ O	HiSO ₃
91	218	603	1048	1071	747	881
92	220	604	1049	1073	748	882
93	222	605	1050	1074	749	884
94	224	606	1051	1075	750	885
95	226	607	1052	--	751	886
96	228	608	1053	--	754	892
97	230	609	1054	--	758	893
98	232	610	1055	--	763	894
99	234	611	1056	--	764	895
100	236	612	1057	--	765	896
101	239	613	1059	--	766	897
102	241	614	1060	--	771	930
103	243	687	1061	--	777	932
104	245	688	1062	--	790	933
105	247	689	1063	--	811	935
106	251	690	1064	--	812	939
107	253	691	1065	--	813	943
108	255	692	1067	--	814	947
109	257	693	1068	--	815	949
110	259	694	1069	--	818	951
111	262	695	1070	--	819	953
112	264	696	1071	--	820	977
113	290	697	1073	--	822	979
114	310	698	1074	--	823	981
115	312	699	1075	--	824	983
116	331	700	--	--	825	985
117	332	701	--	--	826	986
118	333	702	--	--	827	988
119	334	703	--	--	828	989
120	335	704	--	--	829	997
121	336	706	--	--	830	1001
122	337	707	--	--	831	1029
123	338	708	--	--	832	1034
124	339	710	--	--	833	1035
125	340	711	--	--	835	1042
126	341	712	--	--	836	1044
127	342	714	--	--	837	1046
128	343	715	--	--	838	1051
129	344	716	--	--	844	1057
130	345	717	--	--	845	1058
131	346	718	--	--	847	1062
132	347	719	--	--	848	1063
133	348	720	--	--	849	1067
134	349	721	--	--	850	1068
135	350	722	--	--	851	1074
136	351	723	--	--	852	--

Table C.5. Glass #s of LAW Glasses with Melter SO₃ Tolerance and Solubility at 1150 °C Data in Six Evaluation Subsets,^(a) cont.

Count	Evaluation Subset, Glass #s for SO ₃ Solubility/Melter Tolerance					
	WTP	ORP	LP2OL	LP123	HiNa ₂ O	HiSO ₃
137	352	724	--	--	858	--
138	353	725	--	--	862	--
139	354	726	--	--	864	--
140	355	728	--	--	873	--
141	356	729	--	--	874	--
142	357	730	--	--	875	--
143	358	737	--	--	877	--
144	359	738	--	--	878	--
145	360	741	--	--	879	--
146	361	744	--	--	881	--
147	362	745	--	--	892	--
148	363	746	--	--	898	--
149	364	747	--	--	900	--
150	365	748	--	--	901	--
151	366	749	--	--	902	--
152	367	750	--	--	909	--
153	368	751	--	--	910	--
154	369	752	--	--	911	--
155	370	753	--	--	912	--
156	371	754	--	--	913	--
157	372	755	--	--	914	--
158	373	756	--	--	915	--
159	374	757	--	--	916	--
160	375	758	--	--	917	--
161	376	759	--	--	918	--
162	377	760	--	--	919	--
163	378	761	--	--	921	--
164	379	762	--	--	922	--
165	380	763	--	--	947	--
166	381	764	--	--	961	--
167	382	765	--	--	981	--
168	383	766	--	--	999	--
169	384	769	--	--	1006	--
170	385	770	--	--	1013	--
171	386	771	--	--	1014	--
172	--	772	--	--	1015	--
173	--	773	--	--	1016	--
174	--	774	--	--	1017	--
175	--	775	--	--	1018	--
176	--	776	--	--	1019	--
177	--	777	--	--	1020	--
178	--	778	--	--	1021	--
179	--	779	--	--	1022	--
180	--	780	--	--	1023	--
181	--	781	--	--	1024	--
182	--	782	--	--	1025	--

Table C.5. Glass #s of LAW Glasses with Melter SO₃ Tolerance and Solubility at 1150 °C Data in Six Evaluation Subsets,^(a) cont.

Count	Evaluation Subset, Glass #s for SO ₃ Solubility/Melter Tolerance					
	WTP	ORP	LP2OL	LP123	HiNa ₂ O	HiSO ₃
183	--	783	--	--	1026	--
184	--	784	--	--	1027	--
185	--	785	--	--	1028	--
186	--	786	--	--	1029	--
187	--	787	--	--	1031	--
188	--	788	--	--	1032	--
189	--	789	--	--	1034	--
190	--	790	--	--	1036	--
191	--	791	--	--	1038	--
192	--	792	--	--	1040	--
193	--	793	--	--	1041	--
194	--	794	--	--	1042	--
195	--	795	--	--	1044	--
196	--	797	--	--	1045	--
197	--	799	--	--	1046	--
198	--	800	--	--	1047	--
199	--	801	--	--	1048	--
200	--	802	--	--	1049	--
201	--	803	--	--	1051	--
202	--	804	--	--	1052	--
203	--	805	--	--	1053	--
204	--	806	--	--	1054	--
205	--	807	--	--	1055	--
206	--	808	--	--	1056	--
207	--	809	--	--	1057	--
208	--	810	--	--	1058	--
209	--	811	--	--	1059	--
210	--	812	--	--	1060	--
211	--	813	--	--	1061	--
212	--	814	--	--	1062	--
213	--	815	--	--	1063	--
214	--	818	--	--	1064	--
215	--	819	--	--	1065	--
216	--	820	--	--	1067	--
217	--	822	--	--	1068	--
218	--	823	--	--	1069	--
219	--	824	--	--	1070	--
220	--	825	--	--	1071	--
221	--	826	--	--	1073	--
222	--	827	--	--	1074	--
223	--	828	--	--	1075	--
224	--	829	--	--	--	--
225	--	830	--	--	--	--
226	--	831	--	--	--	--
227	--	832	--	--	--	--
228	--	833	--	--	--	--

Table C.5. Glass #s of LAW Glasses with Melter SO₃ Tolerance and Solubility at 1150 °C Data in Six Evaluation Subsets,^(a) cont.

Count	Evaluation Subset, Glass #s for SO ₃ Solubility/Melter Tolerance					
	WTP	ORP	LP2OL	LP123	HiNa ₂ O	HiSO ₃
229	--	835	--	--	--	--
230	--	836	--	--	--	--
231	--	837	--	--	--	--
232	--	838	--	--	--	--
233	--	839	--	--	--	--
234	--	840	--	--	--	--
235	--	841	--	--	--	--
236	--	842	--	--	--	--
237	--	843	--	--	--	--
238	--	844	--	--	--	--
239	--	845	--	--	--	--
240	--	846	--	--	--	--
241	--	847	--	--	--	--
242	--	848	--	--	--	--
243	--	849	--	--	--	--
244	--	850	--	--	--	--
245	--	851	--	--	--	--
246	--	852	--	--	--	--
247	--	853	--	--	--	--
248	--	854	--	--	--	--
249	--	855	--	--	--	--
250	--	856	--	--	--	--
251	--	857	--	--	--	--
252	--	858	--	--	--	--
253	--	859	--	--	--	--
254	--	862	--	--	--	--
255	--	863	--	--	--	--
256	--	864	--	--	--	--
257	--	873	--	--	--	--
258	--	874	--	--	--	--
259	--	875	--	--	--	--
260	--	876	--	--	--	--
261	--	877	--	--	--	--
262	--	878	--	--	--	--
263	--	879	--	--	--	--
264	--	880	--	--	--	--
265	--	881	--	--	--	--
266	--	882	--	--	--	--
267	--	883	--	--	--	--
268	--	884	--	--	--	--
269	--	885	--	--	--	--
270	--	886	--	--	--	--
271	--	892	--	--	--	--
272	--	893	--	--	--	--
273	--	894	--	--	--	--
274	--	895	--	--	--	--

Table C.5. Glass #s of LAW Glasses with Melter SO₃ Tolerance and Solubility at 1150 °C Data in Six Evaluation Subsets,^(a) cont.

Count	Evaluation Subset, Glass #s for SO ₃ Solubility/Melter Tolerance					
	WTP	ORP	LP2OL	LP123	HiNa ₂ O	HiSO ₃
275	--	896	--	--	--	--
276	--	897	--	--	--	--
277	--	898	--	--	--	--
278	--	900	--	--	--	--
279	--	901	--	--	--	--
280	--	902	--	--	--	--
281	--	909	--	--	--	--
282	--	910	--	--	--	--
283	--	911	--	--	--	--
284	--	912	--	--	--	--
285	--	913	--	--	--	--
286	--	914	--	--	--	--
287	--	915	--	--	--	--
288	--	916	--	--	--	--
289	--	917	--	--	--	--
290	--	918	--	--	--	--
291	--	919	--	--	--	--
292	--	920	--	--	--	--
293	--	921	--	--	--	--
294	--	922	--	--	--	--
295	--	923	--	--	--	--
296	--	924	--	--	--	--
297	--	925	--	--	--	--
298	--	926	--	--	--	--
299	--	927	--	--	--	--
300	--	995	--	--	--	--
301	--	997	--	--	--	--
302	--	999	--	--	--	--
303	--	1001	--	--	--	--
304	--	1003	--	--	--	--
305	--	1004	--	--	--	--
306	--	1006	--	--	--	--
307	--	1007	--	--	--	--
308	--	1008	--	--	--	--
309	--	1009	--	--	--	--
310	--	1010	--	--	--	--
311	--	1011	--	--	--	--

(a) The “Glass #” is a unique number assigned to each LAW glass composition, as shown in Table A.2 of Appendix A. The corresponding melter SO₃ tolerance and solubility values of LAW glasses by Glass # are listed in Table A.3 of Appendix A.

Table C.6. Glass #s of LAW Glasses with K-3 Corrosion at 1208 °C Data in Five of the Six Evaluation Subsets^(a)

Count	Glass # in Each Evaluation Set				
	WTP	ORP	LP2OL	HiNa ₂ O	HiSO ₃
1	k001	k009	k028	k009	k040
2	k002	k010	k059	k010	k041
3	k003	k011	k060	k011	k044
4	k004	k012	k061	k012	k045
5	k005	k013	k062	k013	k085
6	k006	k014	k063	k014	k087
7	k007	k015	k064	k015	k088
8	k008	k016	k067	k017	k092
9	k025	k017	k171	k018	k099
10	k026	k018	k235	k019	k123
11	k027	k019	k236	k028	k124
12	k029	k020	k237	k029	k125
13	k030	k021	k238	k030	k127
14	k031	k028	k252	k052	k133
15	k032	k039	k254	k053	k134
16	k033	k040	k256	k054	k135
17	k034	k041	k257	k055	k171
18	k035	k042	k261	k056	k172
19	k036	k043	k290	k057	k201
20	k037	k044	k293	k058	k203
21	k038	k045	k294	k059	k206
22	k069	k046	k295	k060	k207
23	k070	k047	k296	k061	k208
24	k071	k048	k298	k062	k213
25	k072	k049	k299	k063	k217
26	k073	k050	k300	k064	k219
27	k074	k051	k303	k065	k222
28	k075	k052	k304	k066	k223
29	k076	k053	k305	k067	k226
30	k077	k054	k306	k068	k227
31	k078	k055	k328	k076	k228
32	k081	k056	k329	k145	k229
33	k082	k057	k330	k156	k230
34	k083	k058	k331	k158	k231
35	k084	k059	k332	k159	k232
36	k085	k060	k333	k166	k233
37	k086	k061	k335	k167	k234
38	k087	k062	k336	k169	k241
39	k088	k063	k337	k170	k242
40	k089	k064	k338	k171	k243
41	k090	k065	--	k191	k303
42	k091	k066	--	k193	k304
43	k092	k067	--	k194	k305
44	k094	k068	--	k195	k306
45	k095	k122	--	k197	k307
46	k096	k123	--	k198	k308
47	k097	k124	--	k199	k309
48	k098	k125	--	k200	k310

Table C.6. Glass #s of LAW Glasses with K-3 Corrosion at 1208 °C Data in Five of the Six Evaluation Subsets^(a), cont.

Count	Glass # in Each Evaluation Set				
	WTP	ORP	LP2OL	HiNa ₂ O	HiSO ₃
49	k099	k150	--	k201	k311
50	k100	k151	--	k202	k312
51	k101	k152	--	k204	k313
52	k102	k153	--	k209	k314
53	k103	k154	--	k210	k315
54	k104	k155	--	k212	k316
55	k105	k156	--	k213	k317
56	k106	k157	--	k214	k318
57	k107	k158	--	k215	k319
58	k108	k159	--	k216	k320
59	k109	k160	--	k218	k321
60	k110	k161	--	k219	k322
61	k111	k162	--	k220	k323
62	k112	k163	--	k222	k324
63	k113	k164	--	k225	k325
64	k114	k165	--	k229	k326
65	k115	k166	--	k235	k327
66	k116	k167	--	k236	--
67	k117	k168	--	k237	--
68	k118	k169	--	k238	--
69	k119	k173	--	k239	--
70	k120	k175	--	k244	--
71	k121	k176	--	k245	--
72	k126	k177	--	k246	--
73	k127	k178	--	k247	--
74	k129	k179	--	k248	--
75	k130	k180	--	k249	--
76	k131	k181	--	k250	--
77	k132	k182	--	k251	--
78	k133	k183	--	k252	--
79	k134	k184	--	k253	--
80	k135	k185	--	k254	--
81	k136	k186	--	k256	--
82	k137	k188	--	k257	--
83	k138	k190	--	k258	--
84	k139	k191	--	k259	--
85	k140	k193	--	k260	--
86	k141	k194	--	k261	--
87	k142	k195	--	k262	--
88	k143	k196	--	k263	--
89	k144	k197	--	k264	--
90	k145	k198	--	k265	--
91	k146	k199	--	k266	--
92	k147	k200	--	k267	--
93	k148	k201	--	k268	--
94	k149	k202	--	k269	--
95	k170	k203	--	k270	--
96	k171	k204	--	k271	--

Table C.6. Glass #s of LAW Glasses with K-3 Corrosion at 1208 °C Data in Five of the Six Evaluation Subsets^(a), cont.

Count	Glass # in Each Evaluation Set				
	WTP	ORP	LP2OL	HiNa ₂ O	HiSO ₃
97	k172	k205	--	k272	--
98	k192	k206	--	k273	--
99	--	k207	--	k274	--
100	--	k208	--	k275	--
101	--	k209	--	k276	--
102	--	k210	--	k277	--
103	--	k211	--	k278	--
104	--	k212	--	k279	--
105	--	k213	--	k280	--
106	--	k214	--	k281	--
107	--	k215	--	k282	--
108	--	k216	--	k283	--
109	--	k217	--	k284	--
110	--	k218	--	k285	--
111	--	k219	--	k286	--
112	--	k220	--	k287	--
113	--	k221	--	k288	--
114	--	k222	--	k289	--
115	--	k223	--	k290	--
116	--	k224	--	k291	--
117	--	k225	--	k292	--
118	--	k226	--	k293	--
119	--	k227	--	k294	--
120	--	k228	--	k295	--
121	--	k229	--	k296	--
122	--	k230	--	k297	--
123	--	k231	--	k298	--
124	--	k232	--	k299	--
125	--	k233	--	k300	--
126	--	k234	--	k303	--
127	--	k235	--	k304	--
128	--	k236	--	k305	--
129	--	k237	--	k306	--
130	--	k238	--	k328	--
131	--	k239	--	k331	--
132	--	k240	--	k332	--
133	--	k241	--	k333	--
134	--	k242	--	k339	--
135	--	k243	--	k340	--
136	--	k244	--	k341	--
137	--	k245	--	--	--
138	--	k246	--	--	--
139	--	k247	--	--	--
140	--	k248	--	--	--
141	--	k249	--	--	--
142	--	k250	--	--	--
143	--	k251	--	--	--
144	--	k252	--	--	--
145	--	k253	--	--	--
146	--	k254	--	--	--

Table C.6. Glass #s of LAW Glasses with K-3 Corrosion at 1208 °C Data in Five of the Six Evaluation Subsets^(a), cont.

Count	Glass # in Each Evaluation Set				
	WTP	ORP	LP2OL	HiNa ₂ O	HiSO ₃
147	--	k256	--	--	--
148	--	k257	--	--	--
149	--	k258	--	--	--
150	--	k259	--	--	--
151	--	k260	--	--	--
152	--	k261	--	--	--
153	--	k262	--	--	--
154	--	k263	--	--	--
155	--	k264	--	--	--
156	--	k265	--	--	--
157	--	k266	--	--	--
158	--	k267	--	--	--
159	--	k268	--	--	--
160	--	k269	--	--	--
161	--	k270	--	--	--
162	--	k271	--	--	--
163	--	k272	--	--	--
164	--	k273	--	--	--
165	--	k274	--	--	--
166	--	k275	--	--	--
167	--	k276	--	--	--
168	--	k277	--	--	--
169	--	k278	--	--	--
170	--	k279	--	--	--
171	--	k280	--	--	--
172	--	k281	--	--	--
173	--	k282	--	--	--
174	--	k283	--	--	--
175	--	k284	--	--	--
176	--	k285	--	--	--
177	--	k286	--	--	--
178	--	k287	--	--	--
179	--	k288	--	--	--
180	--	k289	--	--	--
181	--	k290	--	--	--
182	--	k291	--	--	--
183	--	k292	--	--	--
184	--	k293	--	--	--
185	--	k294	--	--	--
186	--	k295	--	--	--
187	--	k296	--	--	--
188	--	k297	--	--	--
189	--	k298	--	--	--
190	--	k299	--	--	--
191	--	k300	--	--	--
192	--	k301	--	--	--
193	--	k302	--	--	--
194	--	k303	--	--	--
195	--	k304	--	--	--
196	--	k305	--	--	--

Table C.6. Glass #s of LAW Glasses with K-3 Corrosion at 1208 °C Data in Five of the Six Evaluation Subsets^(a), cont.

Count	Glass # in Each Evaluation Set				
	WTP	ORP	LP2OL	HiNa ₂ O	HiSO ₃
197	--	k306	--	--	--
198	--	k307	--	--	--
199	--	k308	--	--	--
200	--	k309	--	--	--
201	--	k310	--	--	--
202	--	k311	--	--	--
203	--	k312	--	--	--
204	--	k313	--	--	--
205	--	k314	--	--	--
206	--	k315	--	--	--
207	--	k316	--	--	--
208	--	k317	--	--	--
209	--	k318	--	--	--
210	--	k319	--	--	--
211	--	k320	--	--	--
212	--	k321	--	--	--
213	--	k322	--	--	--
214	--	k323	--	--	--
215	--	k324	--	--	--
216	--	k325	--	--	--
217	--	k326	--	--	--
218	--	k327	--	--	--
219	--	k328	--	--	--
220	--	k329	--	--	--
221	--	k330	--	--	--
222	--	k331	--	--	--
223	--	k332	--	--	--
224	--	k333	--	--	--
225	--	k334	--	--	--
226	--	k335	--	--	--
227	--	k336	--	--	--
228	--	k337	--	--	--
229	--	k338	--	--	--
230	--	k339	--	--	--
231	--	k340	--	--	--
232	--	k341	--	--	--
233	--	k342	--	--	--
234	--	k343	--	--	--
235	--	k344	--	--	--

(a) The “Glass #” is a unique number assigned to each LAW glass composition, as shown in Table A.4 of Appendix A. The corresponding k_{1208} values of LAW glasses by Glass # are listed in Table A.5 of Appendix A.

Appendix D – Variance-Covariance Matrices Associated with the Estimated Coefficients of LAW Glass Property-Composition

This appendix contains the variance-covariance matrices for the estimated model coefficients of selected property-composition models for low-activity waste (LAW) glasses discussed in this report. Included are variance-covariance matrices for Product Consistency Test (PCT), Vapor Hydration Test (VHT), viscosity at 1150 °C, electrical conductivity at 1150 °C, melter SO₃ tolerance at 1150 °C, and K-3 refractory corrosion at 1208 °C models, which are functions of LAW glass composition. Variances and covariances are listed to six decimal places, which was determined to be sufficient to obtain appropriate precision in calculated values of statistical intervals (see Section B.6).

Tables D.1 and D.2, respectively, contain the variance-covariance matrices for the $\ln(PCT_B^{NL}, \text{g/m}^2)$ and the $\ln(PCT_{Na}^{NL}, \text{g/m}^2)$ 22-term bias corrected partial quadratic mixture (bcPQM) models given in Tables 3.7 and 3.11.

Tables D.3 and D.4, respectively, contain the variance-covariance matrices for two VHT pass/fail models: (i) the 20-term FLM model given in Table 4.3 and (ii) the 19-term PQM model given in Table 4.4. The 20-term FLM model was judged as inadequate for predicting VHT pass/fail but provides a baseline for comparison to the PQM model. The 19-term PQM model is the recommended model for predicting VHT pass/fail.

Tables D.5 and D.6, respectively, contain the variance-covariance matrices for two $\ln(\eta_{1150}, P)$ models: (i) the 18-component reduced linear mixture (RLM) model given in Table 5.4, and (ii) the 21-term PQM model given in Table 5.5. The 18-component RLM model provides a baseline for comparison to the 21-term PQM model [which is the recommended model for $\ln(\eta_{1150}, P)$ prediction].

Tables D.7 and D.8, respectively, contain the variance-covariance matrices for two $\ln(\epsilon, \text{S/cm})$ models: (i) the 11-term RLM model given in Table 6.4, and (ii) the 13-term PQM model given in Table 6.5. The 11-term RLM model provides a baseline for comparison to the 13-term PQM model [which is the recommended model for $\ln(\epsilon, \text{S/cm})$ prediction].

Tables D.9 and D.10, respectively, contain the variance-covariance matrices for two melter SO₃ tolerance at 1150 °C (wt%) models: (i) the 10-component RLM model with two offsets given in Table 7.4, and (ii) the 11-term PQM model with two offsets given in Table 7.5. The 10-component RLM model with two offsets provides a baseline for comparison to the 11-term PQM model with two offsets (which is the recommended model for melter SO₃ tolerance at 1150 °C prediction).

Tables D.11 and D.12, respectively, contain the variance-covariance matrices for two $\ln(k_{1208}, \text{inch})$ (K-3 refractory corrosion at 1208 °C) models: (i) the 11-component RLM model given in Table 8.4, and (ii) the 13-term PQM model given in Table 8.5. The 11-component RLM model provides a baseline for comparison to the 13-term PQM model (which is the recommended model for k_{1208} prediction).

Table D.1. Variance-Covariance Matrix Associated With the Terms in the 19-term PQM model for ln(PCT-B) of LAW Glasses.

Term	Al ₂ O ₃	B ₂ O ₃	CaO	Fe ₂ O ₃	K ₂ O	Li ₂ O	MgO	Na ₂ O	SiO ₂	SnO ₂
Al ₂ O ₃	25.471817	-1.207720	-4.344667	-0.076427	-0.427823	2.856344	0.130499	-0.958991	-1.111311	0.207370
B ₂ O ₃	-1.207720	0.697856	0.005962	0.011418	0.003054	-0.512135	-0.081662	-0.017313	-0.032632	0.126531
CaO	-4.344667	0.005962	4.964385	-0.088406	0.221486	-1.273600	0.126360	0.148251	0.017220	0.469206
Fe ₂ O ₃	-0.076427	0.011418	-0.088406	0.646984	-0.050309	0.089730	-0.071668	0.029905	-0.073566	0.135234
K ₂ O	-0.427823	0.003054	0.221486	-0.050309	0.984784	0.528137	-0.035621	0.096838	-0.029786	-0.443486
Li ₂ O	2.856344	-0.512135	-1.273600	0.089730	0.528137	10.885676	-0.335643	0.558165	-0.384757	-0.217229
MgO	0.130499	-0.081662	0.126360	-0.071668	-0.035621	-0.335643	2.978226	0.134684	-0.094235	-0.256211
Na ₂ O	-0.958991	-0.017313	0.148251	0.029905	0.096838	0.558165	0.134684	0.314099	-0.050958	-0.192114
SiO ₂	-1.111311	-0.032632	0.017220	-0.073566	-0.029786	-0.384757	-0.094235	-0.050958	0.154299	0.001640
SnO ₂	0.207370	0.126531	0.469206	0.135234	-0.443486	-0.217229	-0.256211	-0.192114	0.001640	2.035562
TiO ₂	-1.170801	0.202408	1.437434	-0.608554	-0.192072	-0.551289	-0.811255	-0.051501	-0.078868	0.510089
V ₂ O ₅	0.737500	-0.398197	0.448745	0.104262	0.352062	-0.770961	0.222723	-0.023112	-0.052427	-0.663133
ZnO	-0.826343	-0.047286	-0.234892	0.116763	-0.058413	0.122506	-0.205850	0.082996	-0.164134	0.106165
ZrO ₂	-2.140986	0.092205	0.459892	0.164718	-0.182075	-1.155193	-0.039685	-0.109206	0.055001	-0.168246
Others	-0.331007	-0.028220	-0.100705	0.128850	0.041243	-0.233332	-0.248036	-0.141420	-0.024807	-0.247410
Al ₂ O ₃ × Al ₂ O ₃	-149.682999	6.487049	24.607478	0.923354	2.710410	-9.458567	-1.829832	4.615579	6.822777	-0.437623
Al ₂ O ₃ × Li ₂ O	-48.978214	5.142475	18.441405	-1.312134	-1.564051	-106.902332	1.744186	3.082478	1.957565	-5.696826
CaO × CaO	32.227590	-0.407089	-38.867320	0.986919	-1.020915	6.883273	0.091046	-0.699715	-0.320979	-4.077822
CaO × V ₂ O ₅	-20.884699	6.920648	-3.638362	0.930814	-6.658844	6.439389	-5.477255	-2.826332	1.872214	9.774779

Term	TiO ₂	V ₂ O ₅	ZnO	ZrO ₂	Others	Al ₂ O ₃ × Al ₂ O ₃	Al ₂ O ₃ × Li ₂ O	CaO × CaO	CaO × V ₂ O ₅
Al ₂ O ₃	-1.170801	0.737500	-0.826343	-2.140986	-0.331007	-149.682999	-48.978214	32.227590	-20.884699
B ₂ O ₃	0.202408	-0.398197	-0.047286	0.092205	-0.028220	6.487049	5.142475	-0.407089	6.920648
CaO	1.437434	0.448745	-0.234892	0.459892	-0.100705	24.607478	18.441405	-38.867320	-3.638362
Fe ₂ O ₃	-0.608554	0.104262	0.116763	0.164718	0.128850	0.923354	-1.312134	0.986919	0.930814
K ₂ O	-0.192072	0.352062	-0.058413	-0.182075	0.041243	2.710410	-1.564051	-1.020915	-6.658844
Li ₂ O	-0.551289	-0.770961	0.122506	-1.155193	-0.233332	-9.458567	-106.902332	6.883273	6.439389
MgO	-0.811255	0.222723	-0.205850	-0.039685	-0.248036	-1.829832	1.744186	0.091046	-5.477255
Na ₂ O	-0.051501	-0.023112	0.082996	-0.109206	-0.141420	4.615579	3.082478	-0.699715	-2.826332
SiO ₂	-0.078868	-0.052427	-0.164134	0.055001	-0.024807	6.822777	1.957565	-0.320979	1.872214
SnO ₂	0.510089	-0.663133	0.106165	-0.168246	-0.247410	-0.437623	-5.696826	-4.077822	9.774779
TiO ₂	5.182647	0.328957	-0.203718	0.508594	0.282370	6.903590	7.145730	-10.259386	2.247095
V ₂ O ₅	0.328957	6.834246	-0.071665	0.248785	-0.262637	-7.268965	3.548646	4.083478	-86.880557
ZnO	-0.203718	-0.071665	3.211062	-0.059927	-0.048268	5.010206	-2.099436	1.319312	5.352353
ZrO ₂	0.508594	0.248785	-0.059927	1.640204	0.215250	11.451765	12.054899	-2.770333	-0.272737
Others	0.282370	-0.262637	-0.048268	0.215250	3.353813	2.067308	0.719613	0.175947	-0.137760
Al ₂ O ₃ × Al ₂ O ₃	6.903590	-7.268965	5.010206	11.451765	2.067308	912.792737	160.712087	-188.874767	176.148561
Al ₂ O ₃ × Li ₂ O	7.145730	3.548646	-2.099436	12.054899	0.719613	160.712087	1502.468116	-121.775691	-101.283024
CaO × CaO	-10.259386	4.083478	1.319312	-2.770333	0.175947	-188.874767	-121.775691	343.956007	-140.035979
CaO × V ₂ O ₅	2.247095	-86.880557	5.352353	-0.272737	-0.137760	176.148561	-101.283024	-140.035979	1684.304327

Table D.2. Variance-Covariance Matrix Associated With the Terms in the 19-term PQM model for In(PCT-Na) of LAW Glasses.

Term	Al ₂ O ₃	B ₂ O ₃	CaO	Fe ₂ O ₃	K ₂ O	Li ₂ O	MgO	Na ₂ O	SiO ₂	SnO ₂
Al ₂ O ₃	19.670735	-0.878130	-2.702538	-0.256798	-0.601670	-0.591151	-0.027610	-0.043264	-0.936112	-0.217357
B ₂ O ₃	-0.878130	0.548792	-0.076026	0.025471	0.026011	-0.104573	-0.056078	-0.073860	-0.023700	0.137293
CaO	-2.702538	-0.076026	3.896607	-0.117397	0.104581	-0.024157	0.020720	0.327242	-0.043919	0.349539
Fe ₂ O ₃	-0.256798	0.025471	-0.117397	0.549966	0.007417	0.020785	-0.017928	-0.114327	-0.034115	0.149468
K ₂ O	-0.601670	0.026011	0.104581	0.007417	0.851005	0.367415	0.024952	-0.113206	0.009330	-0.293792
Li ₂ O	-0.591151	-0.104573	-0.024157	0.020785	0.367415	2.633428	-0.143000	0.524006	-0.181426	-0.457220
MgO	-0.027610	-0.056078	0.020720	-0.017928	0.024952	-0.143000	2.411566	-0.045657	-0.051923	-0.151167
Na ₂ O	-0.043264	-0.073860	0.327242	-0.114327	-0.113206	0.524006	-0.045657	0.800773	-0.135249	-0.325132
SiO ₂	-0.936112	-0.023700	-0.043919	-0.034115	0.009330	-0.181426	-0.051923	-0.135249	0.135838	0.038021
SnO ₂	-0.217357	0.137293	0.349539	0.149468	-0.293792	-0.457220	-0.151167	-0.325132	0.038021	1.656836
TiO ₂	-0.803216	0.139341	1.071276	-0.466985	-0.133721	-0.037300	-0.638324	-0.101428	-0.061292	0.441273
V ₂ O ₅	0.421815	-0.323719	0.267969	0.144107	0.353019	-0.403854	0.239032	-0.250625	-0.005944	-0.449356
ZnO	-0.786417	-0.027149	-0.187489	0.106099	-0.028948	-0.012197	-0.146655	0.012403	-0.118652	0.094169
ZrO ₂	-1.323664	0.033242	0.271802	0.127637	-0.152710	-0.250449	-0.054843	-0.058826	0.023010	-0.109826
Others	-0.409484	-0.007352	-0.165936	0.142299	0.089567	-0.114551	-0.156232	-0.270210	0.003950	-0.137684
Al ₂ O ₃ × Al ₂ O ₃	-109.232903	4.238075	20.032505	-0.328640	0.659912	0.662194	-2.844430	8.074418	4.482021	-1.252711
CaO × CaO	19.350960	0.332357	-31.079851	1.368604	0.046705	-0.831370	0.887187	-3.021430	0.303902	-2.747680
CaO × V ₂ O ₅	-19.536014	5.832578	-1.930647	0.671311	-5.373786	-0.531194	-4.282112	-2.091657	1.607184	7.413039
Al ₂ O ₃ × Na ₂ O	-9.868312	0.805614	-3.735750	2.171553	2.991749	1.484695	2.324207	-8.603005	1.412275	2.828242

Term	TiO ₂	V ₂ O ₅	ZnO	ZrO ₂	Others	Al ₂ O ₃ × Al ₂ O ₃	CaO × CaO	CaO × V ₂ O ₅	Al ₂ O ₃ × Na ₂ O
Al ₂ O ₃	-0.803216	0.421815	-0.786417	-1.323664	-0.409484	-109.232903	19.350960	-19.536014	-9.868312
B ₂ O ₃	0.139341	-0.323719	-0.027149	0.033242	-0.007352	4.238075	0.332357	5.832578	0.805614
CaO	1.071276	0.267969	-0.187489	0.271802	-0.165936	20.032505	-31.079851	-1.930647	-3.735750
Fe ₂ O ₃	-0.466985	0.144107	0.106099	0.127637	0.142299	-0.328640	1.368604	0.671311	2.171553
K ₂ O	-0.133721	0.353019	-0.028948	-0.152710	0.089567	0.659912	0.046705	-5.373786	2.991749
Li ₂ O	-0.037300	-0.403854	-0.012197	-0.250449	-0.114551	0.662194	-0.831370	-0.531194	1.484695
MgO	-0.638324	0.239032	-0.146655	-0.054843	-0.156232	-2.844430	0.887187	-4.282112	2.324207
Na ₂ O	-0.101428	-0.250625	0.012403	-0.058826	-0.270210	8.074418	-3.021430	-2.091657	-8.603005
SiO ₂	-0.061292	-0.005944	-0.118652	0.023010	0.003950	4.482021	0.303902	1.607184	1.412275
SnO ₂	0.441273	-0.449356	0.094169	-0.109826	-0.137684	-1.252711	-2.747680	7.413039	2.828242
TiO ₂	4.121145	0.306567	-0.146301	0.358200	0.226455	4.493527	-7.623558	2.146839	0.729139
V ₂ O ₅	0.306567	5.626140	-0.021968	0.162855	-0.171296	-7.979264	4.204437	-69.083049	3.440518
ZnO	-0.146301	-0.021968	2.561625	-0.037479	-0.022086	3.733824	1.152590	4.123675	0.884438
ZrO ₂	0.358200	0.162855	-0.037479	1.232209	0.149132	8.427631	-1.672206	0.464629	-0.754340
Others	0.226455	-0.171296	-0.022086	0.149132	2.718699	0.183102	1.043290	-0.005333	2.427738
Al ₂ O ₃ × Al ₂ O ₃	4.493527	-7.979264	3.733824	8.427631	0.183102	750.132224	-162.068997	150.269482	-72.455364
CaO × CaO	-7.623558	4.204437	1.152590	-1.672206	1.043290	-162.068997	280.225444	-118.071928	41.532013
CaO × V ₂ O ₅	2.146839	-69.083049	4.123675	0.464629	-0.005333	150.269482	-118.071928	1335.671950	0.287181
Al ₂ O ₃ × Na ₂ O	0.729139	3.440518	0.884438	-0.754340	2.427738	-72.455364	41.532013	0.287181	133.226339

Table D.3. Variance-Covariance Matrix Associated With the Terms in the 20-term FLM model for VHT of LAW Glasses.

Term	Al ₂ O ₃	B ₂ O ₃	CaO	Cl	Cr ₂ O ₃	F	Fe ₂ O ₃	K ₂ O	Li ₂ O	MgO
Al ₂ O ₃	72.864879	-14.590300	14.053565	-88.490250	86.325707	54.725349	31.389135	-31.140668	-93.099673	4.987143
B ₂ O ₃	-14.590300	52.192106	5.748860	-62.811826	-67.250255	12.315954	-6.232835	-5.894931	-22.692268	-4.603197
CaO	14.053565	5.748860	64.152211	-91.970960	-77.097336	2.310341	21.356298	-53.445791	-141.852804	8.959698
Cl	-88.490250	-62.811826	-91.970960	4052.609838	-359.240055	99.650542	-10.645844	197.498239	72.797211	-130.678698
Cr ₂ O ₃	86.325707	-67.250255	-77.097336	-359.240055	8971.486235	670.184293	182.904967	-193.238977	418.225680	-130.950658
F	54.725349	12.315954	2.310341	99.650542	670.184293	10138.035673	-17.958360	-112.015916	-20.846543	42.532115
Fe ₂ O ₃	31.389135	-6.232835	21.356298	-10.645844	182.904967	-17.958360	148.418215	-60.776443	-106.269225	30.481611
K ₂ O	-31.140668	-5.894931	-53.445791	197.498239	-193.238977	-112.015916	-60.776443	158.678939	201.799410	-11.612310
Li ₂ O	-93.099673	-22.692268	-141.852804	72.797211	418.225680	-20.846543	-106.269225	201.799410	816.316978	-117.621594
MgO	4.987143	-4.603197	8.959698	-130.678698	-130.950658	42.532115	30.481611	-11.612310	-117.621594	367.285143
Na ₂ O	-55.356464	-2.726577	-55.936977	2.600902	-112.360728	-4.729553	-55.221074	99.540986	261.925622	-11.096405
P ₂ O ₅	13.427138	11.461489	16.020891	-11.117062	-1562.131879	-3446.152061	-19.012297	35.696351	-191.729721	50.914819
SO ₃	-40.769607	-118.939811	-167.681907	698.223128	628.690125	-406.848406	92.873643	151.830170	298.032522	54.677440
SiO ₂	14.564024	-5.563613	14.648474	-6.829484	40.408285	10.838818	5.517184	-32.561622	-78.059420	-2.402235
SnO ₂	21.528680	18.291291	49.286290	-87.876864	-595.296998	-61.762157	60.950908	-77.050161	-249.233490	17.887080
TiO ₂	18.067479	16.762980	53.732213	-257.279224	443.036874	-23.693839	-126.243352	-61.592753	-49.025405	-166.717098
V ₂ O ₅	4.544394	-1.512083	-7.453724	176.529171	-65.798657	-237.658772	25.716499	32.107390	-102.022748	-9.541491
ZnO	1.936256	-11.983327	25.272883	104.140629	-55.310140	-202.274065	26.666410	-54.026795	-115.122616	-29.767031
ZrO ₂	30.186409	4.797640	72.492073	-58.422916	-106.393703	-2.692635	87.734213	-115.502069	-222.636050	16.554950
Others	-549.855631	270.692334	-100.781906	-1338.718704	-7607.056809	-7158.392700	-655.991772	1042.995627	809.939499	27.723706

Term	Na ₂ O	P ₂ O ₅	SO ₃	SiO ₂	SnO ₂	TiO ₂	V ₂ O ₅	ZnO	ZrO ₂	Others
Al ₂ O ₃	-55.356464	13.427138	-40.769607	14.564024	21.528680	18.067479	4.544394	1.936256	30.186409	-549.855631
B ₂ O ₃	-2.726577	11.461489	-118.939811	-5.563613	18.291291	16.762980	-1.512083	-11.983327	4.797640	270.692334
CaO	-55.936977	16.020891	-167.681907	14.648474	49.286290	53.732213	-7.453724	25.272883	72.492073	-100.781906
Cl	2.600902	-11.117062	698.223128	-6.829484	-87.876864	-257.279224	176.529171	104.140629	-58.422916	-1338.718704
Cr ₂ O ₃	-112.360728	-1562.131879	628.690125	40.408285	-595.296998	443.036874	-65.798657	-55.310140	-106.393703	-7607.056809
F	-4.729553	-3446.152061	-406.848406	10.838818	-61.762157	-23.693839	-237.658772	-202.274065	-2.692635	-7158.392700
Fe ₂ O ₃	-55.221074	-19.012297	92.873643	5.517184	60.950908	-126.243352	25.716499	26.666410	87.734213	-655.991772
K ₂ O	99.540986	35.696351	151.830170	-32.561622	-77.050161	-61.592753	32.107390	-54.026795	-115.502069	1042.995627
Li ₂ O	261.925622	-191.729721	298.032522	-78.059420	-249.233490	-49.025405	-102.022748	-115.122616	-222.636050	809.939499
MgO	-11.096405	50.914819	54.677440	-2.402235	17.887080	-166.717098	-9.541491	-29.767031	16.554950	27.723706
Na ₂ O	128.508237	-27.302244	95.649054	-38.506928	-69.529161	-30.192058	-18.797139	-57.329850	-114.276233	678.878388
P ₂ O ₅	-27.302244	2819.657991	164.463740	-2.946078	91.985339	1.245864	-22.524937	-6.985562	70.350344	4316.634230
SO ₃	95.649054	164.463740	4408.171766	-71.835865	-82.042694	18.853895	-257.792652	-63.685197	-2.864925	1409.779466
SiO ₂	-38.506928	-2.946078	-71.835865	18.971549	12.803635	0.870611	1.654148	-5.385855	19.716956	-320.098606
SnO ₂	-69.529161	91.985339	-82.042694	12.803635	245.129639	20.093168	35.827647	64.049037	67.853255	198.398381
TiO ₂	-30.192058	1.245864	18.853895	0.870611	20.093168	805.859962	-12.354580	-14.543634	65.037801	-161.974898
V ₂ O ₅	-18.797139	-22.524937	-257.792652	1.654148	35.827647	-12.354580	275.576987	49.685271	-5.208153	153.150652
ZnO	-57.329850	-6.985562	-63.685197	-5.385855	64.049037	-14.543634	49.685271	419.549414	65.605690	274.002647
ZrO ₂	-114.276233	70.350344	-2.864925	19.716956	67.853255	65.037801	-5.208153	65.605690	235.627392	-596.881614
Others	678.878388	4316.634230	1409.779466	-320.098606	198.398381	-161.974898	153.150652	274.002647	-596.881614	51896.238128

Table D.4. Variance-Covariance Matrix Associated With the Terms in the 19-term Partial-Quadratic Model for VHT of LAW Glasses.

Term	Al ₂ O ₃	B ₂ O ₃	CaO	F	K ₂ O	Li ₂ O	MgO	Na ₂ O	P ₂ O ₅	SiO ₂
Al ₂ O ₃	61.853735	-7.995062	11.994068	-26.224535	-18.268189	-402.107228	-3.913059	-50.704214	49.006524	12.518598
B ₂ O ₃	-7.995062	46.318296	3.117576	27.882688	-6.693278	-93.341664	-2.220724	-10.803966	-4.436338	-3.571706
CaO	11.994068	3.117576	66.078419	-12.679472	-56.193683	-455.858446	10.590620	-67.368698	17.160778	19.213611
F	-26.224535	27.882688	-12.679472	8919.670394	44.645687	1237.637900	66.077648	109.538919	-2803.354614	-41.288235
K ₂ O	-18.268189	-6.693278	-56.193683	44.645687	131.808032	554.660152	-10.653396	102.720522	-65.103318	-33.576814
Li ₂ O	-402.107228	-93.341664	-455.858446	1237.637900	554.660152	17886.056420	-485.020189	977.665269	9.022222	-363.634872
MgO	-3.913059	-2.220724	10.590620	66.077648	-10.653396	-485.020189	352.839596	-10.130859	35.983715	2.184334
Na ₂ O	-50.704214	-10.803966	-67.368698	109.538919	102.720522	977.665269	-10.130859	145.694467	-73.802189	-44.976646
P ₂ O ₅	49.006524	-4.436338	17.160778	-2803.354614	-65.103318	9.022222	35.983715	-73.802189	2420.179474	10.977073
SiO ₂	12.518598	-3.571706	19.213611	-41.288235	-33.576814	-363.634872	2.184334	-44.976646	10.977073	21.405482
SnO ₂	17.591088	8.661558	40.306765	-50.774622	-71.404937	-410.460550	-0.664785	-70.808660	4.786175	16.303868
TiO ₂	108.221307	38.812779	74.584688	-313.777454	-77.742128	-1785.636655	-240.100302	-119.583465	137.321538	5.235819
V ₂ O ₅	-3.542689	-11.524668	-23.210599	-234.024886	31.680709	-73.947152	-27.189419	3.066306	-57.577241	-2.356876
ZnO	-3.818794	-24.696057	20.541658	-110.689350	-53.702022	419.183968	-38.948076	-40.531242	-26.724807	-6.292719
ZrO ₂	27.436951	17.637137	72.398328	-121.138054	-102.829243	-594.314068	-12.777566	-126.280873	125.267503	19.803919
Others	9.241988	4.130961	10.658384	-104.030176	-27.739303	-52.086287	9.854105	-35.248093	68.198556	-1.797571
Li ₂ O × Na ₂ O	1316.070399	290.748160	1187.761355	-3872.860693	-1166.521691	-53811.961478	1367.670724	-2625.879428	289.865719	874.765044
TiO ₂ × ZrO ₂	-1350.943215	-956.595328	721.774789	6463.054670	-802.111211	21130.363769	2903.072101	527.549794	-1297.710941	690.450911
Li ₂ O × Li ₂ O	3168.018611	647.424934	3329.926080	-12695.902142	-4305.328516	-199028.461978	4643.348867	-7578.547971	-5386.851469	3553.404158

Term	SnO ₂	TiO ₂	V ₂ O ₅	ZnO	ZrO ₂	Others	Li ₂ O × Na ₂ O	TiO ₂ × ZrO ₂	Li ₂ O × Li ₂ O
Al ₂ O ₃	17.591088	108.221307	-3.542689	-3.818794	27.436951	9.241988	1316.070399	-1350.943215	3168.018611
B ₂ O ₃	8.661558	38.812779	-11.524668	-24.696057	17.637137	4.130961	290.748160	-956.595328	647.424934
CaO	40.306765	74.584688	-23.210599	20.541658	72.398328	10.658384	1187.761355	721.774789	3329.926080
F	-50.774622	-313.777454	-234.024886	-110.689350	-121.138054	-104.030176	-3872.860693	6463.054670	-12695.902142
K ₂ O	-71.404937	-77.742128	31.680709	-53.702022	-102.829243	-27.739303	-1166.521691	-802.111211	-4305.328516
Li ₂ O	-410.460550	-1785.636655	-73.947152	419.183968	-594.314068	-52.086287	-53811.961478	21130.363769	-199028.461978
MgO	-0.664785	-240.100302	-27.189419	-38.948076	-12.777566	9.854105	1367.670724	2903.072101	4643.348867
Na ₂ O	-70.808660	-119.583465	3.066306	-40.531242	-126.280873	-35.248093	-2625.879428	527.549794	-7578.547971
P ₂ O ₅	4.786175	137.321538	-57.577241	-26.724807	125.267503	68.198556	289.865719	-1297.710941	-5386.851469
SiO ₂	16.303868	5.235819	-2.356876	-6.292719	19.803919	-1.797571	874.765044	690.450911	3553.404158
SnO ₂	171.471306	27.988348	13.714619	47.384932	44.005541	50.036521	883.360276	1450.644484	2403.915485
TiO ₂	27.988348	2547.506704	-15.872043	-73.590286	347.777258	-153.848532	8197.672255	-42761.872997	10840.093574
V ₂ O ₅	13.714619	-15.872043	230.266027	16.884889	-10.329896	18.207349	-29.773818	1169.128215	882.703566
ZnO	47.384932	-73.590286	16.884889	393.341135	53.822375	25.544746	-1974.023596	682.042188	-5287.589919
ZrO ₂	44.005541	347.777258	-10.329896	53.822375	256.135473	61.777670	2178.867193	-5973.986292	1641.327386
Others	50.036521	-153.848532	18.207349	25.544746	61.777670	130.179622	375.195976	-55.057410	-1587.016141
Li ₂ O × Na ₂ O	883.360276	8197.672255	-29.773818	-1974.023596	2178.867193	375.195976	204039.285870	-136648.820610	489992.997092
TiO ₂ × ZrO ₂	1450.644484	-42761.872997	1169.128215	682.042188	-5973.986292	-55.057410	-136648.820610	1194858.926551	-97934.146142
Li ₂ O × Li ₂ O	2403.915485	10840.093574	882.703566	-5287.589919	1641.327386	-1587.016141	489992.997092	-97934.146142	2794365.341855

Table D.5. Variance-Covariance Matrix Associated With the Terms in the 18 Term Reduced Linear Mixture Model for $\ln(\eta_{1150}, P)$ of LAW Glasses

Term	Al ₂ O ₃	B ₂ O ₃	CaO	Cr ₂ O ₃	F	Fe ₂ O ₃	K ₂ O	Li ₂ O	MgO
Al ₂ O ₃	0.090300	-0.010841	-0.004987	-0.056727	0.076948	0.010154	-0.003006	-0.072427	-0.015731
B ₂ O ₃	-0.010841	0.094033	0.000027	0.067390	0.051160	0.004455	-0.000087	-0.018256	-0.011450
CaO	-0.004987	0.000027	0.046944	-0.057397	-0.086564	0.000392	0.001341	-0.019628	0.010834
Cr ₂ O ₃	-0.056727	0.067390	-0.057397	14.182375	-2.398374	0.164112	-0.234597	0.030457	0.270709
F	0.076948	0.051160	-0.086564	-2.398374	20.736063	0.051684	-0.203616	-0.308474	-0.110585
Fe ₂ O ₃	0.010154	0.004455	0.000392	0.164112	0.051684	0.106780	-0.015462	-0.021507	-0.025511
K ₂ O	-0.003006	-0.000087	0.001341	-0.234597	-0.203616	-0.015462	0.163970	0.060012	0.005464
Li ₂ O	-0.072427	-0.018256	-0.019628	0.030457	-0.308474	-0.021507	0.060012	0.580757	-0.031689
MgO	-0.015731	-0.011450	0.010834	0.270709	-0.110585	-0.025511	0.005464	-0.031689	0.502320
Na ₂ O	-0.031666	-0.005443	0.004370	-0.056863	-0.087798	-0.005375	0.014336	0.146675	0.022707
P ₂ O ₅	0.019807	-0.008239	0.012227	-0.788853	-2.777425	-0.023835	0.056323	0.045288	-0.047967
SiO ₂	0.003532	-0.014576	-0.005369	-0.020194	0.020703	-0.012189	-0.007699	-0.041124	-0.015721
SnO ₂	0.013639	0.011137	0.014707	-0.459111	-0.245432	0.022714	-0.052818	-0.131862	-0.054356
TiO ₂	0.012783	0.033329	0.037820	0.469778	0.057322	-0.067348	-0.052356	-0.006581	-0.110331
V ₂ O ₅	0.016646	-0.001273	-0.015447	0.233125	-0.343865	0.037570	-0.016854	-0.117611	-0.020331
ZnO	-0.002188	-0.018960	-0.002368	0.015053	-0.158478	0.016671	0.005554	-0.046028	0.000454
ZrO ₂	-0.013428	-0.006038	0.005359	-0.371492	0.224655	0.029615	-0.030825	-0.051799	-0.018617
Others	-0.043476	-0.067190	-0.072896	0.179918	-0.639464	0.114477	0.090754	-0.245791	-0.036662

Term	Na ₂ O	P ₂ O ₅	SiO ₂	SnO ₂	TiO ₂	V ₂ O ₅	ZnO	ZrO ₂	Others
Al ₂ O ₃	-0.031666	0.019807	0.003532	0.013639	0.012783	0.016646	-0.002188	-0.013428	-0.043476
B ₂ O ₃	-0.005443	-0.008239	-0.014576	0.011137	0.033329	-0.001273	-0.018960	-0.006038	-0.067190
CaO	0.004370	0.012227	-0.005369	0.014707	0.037820	-0.015447	-0.002368	0.005359	-0.072896
Cr ₂ O ₃	-0.056863	-0.788853	-0.020194	-0.459111	0.469778	0.233125	0.015053	-0.371492	0.179918
F	-0.087798	-2.777425	0.020703	-0.245432	0.057322	-0.343865	-0.158478	0.224655	-0.639464
Fe ₂ O ₃	-0.005375	-0.023835	-0.012189	0.022714	-0.067348	0.037570	0.016671	0.029615	0.114477
K ₂ O	0.014336	0.056323	-0.007699	-0.052818	-0.052356	-0.016854	0.005554	-0.030825	0.090754
Li ₂ O	0.146675	0.045288	-0.041124	-0.131862	-0.006581	-0.117611	-0.046028	-0.051799	-0.245791
MgO	0.022707	-0.047967	-0.015721	-0.054356	-0.110331	-0.020331	0.000454	-0.018617	-0.036662
Na ₂ O	0.054350	-0.001402	-0.014070	-0.037262	-0.012259	-0.041814	-0.003974	-0.030741	-0.114871
P ₂ O ₅	-0.001402	1.654660	-0.009648	0.015612	0.001725	-0.018681	0.015460	0.040561	0.132397
SiO ₂	-0.014070	-0.009648	0.015865	0.004642	-0.015419	0.006958	-0.035733	-0.004449	-0.016653
SnO ₂	-0.037262	0.015612	0.004642	0.318774	0.046492	-0.020533	0.037796	0.008652	0.168298
TiO ₂	-0.012259	0.001725	-0.015419	0.046492	0.716180	0.090310	-0.012272	0.029174	-0.162073
V ₂ O ₅	-0.041814	-0.018681	0.006958	-0.020533	0.090310	0.386148	0.030666	0.037593	-0.101142
ZnO	-0.003974	0.015460	-0.035733	0.037796	-0.012272	0.030666	0.528159	-0.009204	0.170709
ZrO ₂	-0.030741	0.040561	-0.004449	0.008652	0.029174	0.037593	-0.009204	0.228675	0.083592
Others	-0.114871	0.132397	-0.016653	0.168298	-0.162073	-0.101142	0.170709	0.083592	3.710757

Table D.6. Variance-Covariance Matrix Associated With the Terms in the 21 Term Partial Quadratic Mixture Model for $\ln(h_{1150}, P)$ of LAW Glasses

Term	Al ₂ O ₃	B ₂ O ₃	CaO	Cr ₂ O ₃	F	Fe ₂ O ₃	K ₂ O	Li ₂ O	MgO	Na ₂ O	P ₂ O ₅
Al ₂ O ₃	0.717602	-0.043274	-0.060347	-0.166514	-0.332527	-0.049073	-0.098431	0.063224	-0.070843	0.230974	-0.088181
B ₂ O ₃	-0.043274	0.084652	0.001822	0.048150	0.077623	0.006009	0.005494	0.028415	-0.008866	-0.013741	-0.001308
CaO	-0.060347	0.001822	0.050912	-0.019399	-0.076547	0.007605	0.007499	-0.251668	0.019311	-0.034138	0.020154
Cr ₂ O ₃	-0.166514	0.048150	-0.019399	12.934980	-2.287970	0.178625	-0.196710	-0.872359	0.292973	-0.199350	-0.682494
F	-0.332527	0.077623	-0.076547	-2.287970	18.677641	0.061504	-0.102945	1.257702	-0.102957	-0.117396	-2.361222
Fe ₂ O ₃	-0.049073	0.006009	0.007605	0.178625	0.061504	0.100173	-0.005760	-0.126897	-0.014068	-0.036323	-0.011642
K ₂ O	-0.098431	0.005494	0.007499	-0.196710	-0.102945	-0.005760	0.158651	0.127070	0.011291	-0.019819	0.065013
Li ₂ O	0.063224	0.028415	-0.251668	-0.872359	1.257702	-0.126897	0.127070	10.629705	-0.254035	0.865027	0.007577
MgO	-0.070843	-0.008866	0.019311	0.292973	-0.102957	-0.014068	0.011291	-0.254035	0.450713	-0.020535	-0.033087
Na ₂ O	0.230974	-0.013741	-0.034138	-0.199350	-0.117396	-0.036323	-0.019819	0.865027	-0.020535	0.203073	-0.043448
P ₂ O ₅	-0.088181	-0.001308	0.020154	-0.682494	-2.361222	-0.011642	0.065013	0.007577	-0.033087	-0.043448	1.465013
SiO ₂	-0.061862	-0.010703	0.006128	0.021969	0.019815	-0.002271	0.000853	-0.279771	-0.002544	-0.055053	0.002318
SnO ₂	-0.037026	0.012435	0.016658	-0.394182	-0.180529	0.024106	-0.038644	-0.102527	-0.043622	-0.050926	0.021706
TiO ₂	-0.018061	0.029772	0.037513	0.440930	0.050297	-0.054810	-0.042207	-0.093994	-0.091031	-0.029896	0.005911
V ₂ O ₅	-0.050998	0.003184	-0.007317	0.185134	-0.254142	0.037819	-0.005059	-0.140020	-0.013462	-0.061521	-0.004509
ZnO	-0.024184	-0.017716	0.003673	0.082567	-0.165541	0.020076	0.006557	-0.209757	0.009093	-0.028741	0.015873
ZrO ₂	-0.023604	-0.007463	0.013950	-0.258016	0.136009	0.031715	-0.028659	-0.415270	-0.005341	-0.059891	0.036868
Others	0.143878	-0.072026	-0.077307	0.177713	-0.702338	0.086261	0.051037	-0.281713	-0.043339	-0.038186	0.084534
Al ₂ O ₃ xNa ₂ O	-3.946554	0.198512	0.380492	0.942510	2.199756	0.376149	0.577486	-2.331489	0.391123	-1.712168	0.651165
Li ₂ OxLi ₂ O	0.584707	-0.373448	2.480365	1.562524	-16.346837	0.741448	-1.139271	-115.320597	1.884166	-6.776355	0.277500
Li ₂ OxNa ₂ O	-1.641575	-0.162145	0.889889	5.965481	-5.076567	0.571180	-0.069100	-33.700401	1.030654	-3.204304	0.225991

Term	SiO ₂	SnO ₂	TiO ₂	V ₂ O ₅	ZnO	ZrO ₂	Others	Al ₂ O ₃ xNa ₂ O	Li ₂ OxLi ₂ O	Li ₂ OxNa ₂ O
Al ₂ O ₃	-0.061862	-0.037026	-0.018061	-0.050998	-0.024184	-0.023604	0.143878	-3.946554	0.584707	-1.641575
B ₂ O ₃	-0.010703	0.012435	0.029772	0.003184	-0.017716	-0.007463	-0.070206	0.198512	-0.373448	-0.162145
CaO	0.006128	0.016658	0.037513	-0.007317	0.003673	0.013950	-0.077307	0.380492	2.480365	0.889889
Cr ₂ O ₃	0.021969	-0.394182	0.440930	0.185134	0.082567	-0.258016	0.177713	0.942510	1.562524	5.965481
F	0.019815	-0.180529	0.050297	-0.254142	-0.165541	0.136009	-0.702338	2.199756	-16.346837	-5.076567
Fe ₂ O ₃	-0.002271	0.024106	-0.054810	0.037819	0.020076	0.031715	0.086261	0.376149	0.741448	0.571180
K ₂ O	0.000853	-0.038644	-0.042207	-0.005059	0.006557	-0.028659	0.051037	0.577486	-1.139271	-0.069100
Li ₂ O	-0.279771	-0.102527	-0.093994	-0.140020	-0.209757	-0.415270	-0.281713	-2.331489	-115.320597	-33.700401
MgO	-0.002544	-0.043622	-0.091031	-0.013462	0.009093	-0.005341	-0.043339	0.391123	1.884166	1.030654
Na ₂ O	-0.055053	-0.050926	-0.029896	-0.061521	-0.028741	-0.059891	-0.038186	-1.712168	-6.776355	-3.204304
P ₂ O ₅	0.002318	0.021706	0.005911	-0.004509	0.015873	0.036868	0.084534	0.651165	0.277500	0.225991
SiO ₂	0.025900	0.008531	-0.008314	0.012722	-0.024304	0.006307	-0.029918	0.438343	2.432383	0.979568
SnO ₂	0.008531	0.282608	0.042735	-0.013014	0.034438	0.007684	0.133060	0.299146	-0.308944	0.053712
TiO ₂	-0.008314	0.042735	0.629105	0.080855	-0.006301	0.030390	-0.147430	0.196828	0.577983	0.459827
V ₂ O ₅	0.012722	-0.013014	0.080855	0.347009	0.025636	0.032487	-0.110279	0.402344	0.848683	0.038429
ZnO	-0.024304	0.034438	-0.006301	0.025636	0.471413	0.002238	0.149906	0.173039	0.885280	0.928863
ZrO ₂	0.006307	0.007684	0.030390	0.032487	0.002238	0.216095	0.076864	0.136196	3.560076	1.455479
Others	-0.029918	0.133060	-0.147430	-0.110279	0.149906	0.076864	3.302962	-1.099502	0.480692	0.158056
Al ₂ O ₃ xNa ₂ O	0.438343	0.299146	0.196828	0.402344	0.173039	0.136196	-1.099502	24.643517	12.450573	15.813503
Li ₂ OxLi ₂ O	2.432383	-0.308944	0.577983	0.848683	0.885280	3.560076	0.480692	12.450573	1480.941397	326.761218
Li ₂ OxNa ₂ O	0.979568	0.053712	0.459827	0.038429	0.928863	1.455479	0.158056	15.813503	326.761218	132.241786

Table D.7. Variance-Covariance Matrix Associated With the Terms in the 11 Term Reduced Linear Mixture Model for $\ln(\epsilon_{1150}, S/cm)$ of LAW Glasses

Term	Al ₂ O ₃	B ₂ O ₃	CaO	K ₂ O	Li ₂ O	MgO	Na ₂ O	SiO ₂	SnO ₂	V ₂ O ₅	Others
Al ₂ O ₃	0.081882	-0.014443	-0.005120	-0.004573	-0.065923	-0.009382	-0.030893	0.004436	0.001023	-0.003125	-0.000148
B ₂ O ₃	-0.014443	0.099955	-0.003503	0.005523	-0.026001	-0.002017	-0.008393	-0.017001	0.012620	-0.004376	0.003670
CaO	-0.005120	-0.003503	0.045449	0.004088	-0.032848	0.018474	-0.000356	-0.005517	0.011583	-0.015748	0.008470
K ₂ O	-0.004573	0.005523	0.004088	0.165860	0.061642	-0.004586	0.012627	-0.007023	-0.073823	0.001812	-0.016387
Li ₂ O	-0.065923	-0.026001	-0.032848	0.061642	0.569147	-0.038212	0.134537	-0.044965	-0.117092	-0.103918	-0.014490
MgO	-0.009382	-0.002017	0.018474	-0.004586	-0.038212	0.497074	0.024987	-0.016708	-0.026786	-0.022974	-0.033478
Na ₂ O	-0.030893	-0.008393	-0.000356	0.012627	0.134537	0.024987	0.046270	-0.014609	-0.033931	-0.033478	-0.004874
SiO ₂	0.004436	-0.017001	-0.005517	-0.007023	-0.044965	-0.016708	-0.014609	0.015973	0.009271	0.007062	-0.013955
SnO ₂	0.001023	0.012620	0.011583	-0.073823	-0.117092	-0.026786	-0.033931	0.009271	0.277348	-0.048842	0.011147
V ₂ O ₅	-0.003125	-0.004376	-0.015748	0.001812	-0.103918	-0.022974	-0.033478	0.007062	-0.048842	0.349663	0.029712
Others	-0.000148	0.003670	0.008470	-0.016387	-0.014490	-0.033478	-0.004874	-0.013955	0.011147	0.029712	0.055589

Table D.8. Variance-Covariance Matrix Associated With the Terms in the 13 Term Partial Quadratic Mixture Model for $\ln(\varepsilon_{1150}, S/\text{cm})$ of LAW Glasses

Term	Al ₂ O ₃	B ₂ O ₃	CaO	K ₂ O	Li ₂ O	MgO	Na ₂ O	SiO ₂	SnO ₂	V ₂ O ₅	Others	Li ₂ OxNa ₂ O	Na ₂ OxNa ₂ O
Al ₂ O ₃	0.085018	0.006285	0.012039	0.021850	-0.364754	-0.003096	-0.205586	0.023759	0.012718	0.007418	0.019571	2.220197	0.503974
B ₂ O ₃	0.006285	0.112567	0.018670	0.043215	-0.369219	0.002254	-0.260731	0.011849	0.025968	0.020370	0.028485	2.485316	0.741263
CaO	0.012039	0.018670	0.055195	0.032624	-0.331601	0.019455	-0.198190	0.016540	0.022175	0.001957	0.027756	2.177907	0.566888
K ₂ O	0.021850	0.043215	0.032624	0.189341	-0.432872	0.002011	-0.329562	0.029476	-0.040475	0.031666	0.020922	3.463494	0.987252
Li ₂ O	-0.364754	-0.369219	-0.331601	-0.432872	6.185229	-0.117155	3.486860	-0.411289	-0.318652	-0.285832	-0.378889	-40.915923	-9.490854
MgO	-0.003096	0.002254	0.019455	0.002011	-0.117155	0.415294	-0.022195	-0.008823	-0.019303	-0.017974	-0.022868	0.612103	0.116664
Na ₂ O	-0.205586	-0.260731	-0.198190	-0.329562	3.486860	-0.022195	2.317938	-0.252249	-0.170747	-0.215730	-0.239133	-24.149635	-6.573481
SiO ₂	0.023759	0.011849	0.016540	0.029476	-0.411289	-0.008823	-0.252249	0.039059	0.022990	0.023638	0.013626	2.676408	0.686153
SnO ₂	0.012718	0.025968	0.022175	-0.040475	-0.318652	-0.019303	-0.170747	0.022990	0.239952	-0.030042	0.024244	1.583304	0.407499
V ₂ O ₅	0.007418	0.020370	0.001957	0.031666	-0.285832	-0.017974	-0.215730	0.023638	-0.030042	0.315278	0.042039	1.421132	0.568413
Others	0.019571	0.028485	0.027756	0.020922	-0.378889	-0.022868	-0.239133	0.013626	0.024244	0.042039	0.071016	2.626137	0.671572
Li ₂ OxNa ₂ O	2.220197	2.485316	2.177907	3.463494	-40.915923	0.612103	-24.149635	2.676408	1.583304	1.421132	2.626137	293.120337	67.898493
Na ₂ OxNa ₂ O	0.503974	0.741263	0.566888	0.987252	-9.490854	0.116664	-6.573481	0.686153	0.407499	0.568413	0.671572	67.898493	19.038633

Table D.9. Variance-Covariance Matrix Associated With the Terms in the 10 Component Reduced Linear Mixture Model for Melter SO_3 Tolerance, wt% of LAW Glasses

Term	SR	3TS	Al_2O_3	B_2O_3	CaO	Cl	Li_2O	Na_2O	P_2O_5	SiO_2	V_2O_5	Others
SR	0.000637	0.000495	-0.000140	0.000347	-0.000108	-0.008400	0.000056	0.000022	0.000489	-0.000965	0.000387	-0.001021
3TS	0.000495	0.001127	0.000892	-0.000209	-0.001337	0.017849	-0.001781	-0.001823	-0.030053	0.000077	-0.002065	-0.001188
Al_2O_3	-0.000140	0.000892	0.117832	-0.025843	-0.007552	-0.056442	-0.074092	-0.038118	0.013647	0.004544	-0.017689	-0.002528
B_2O_3	0.000347	-0.000209	-0.025843	0.111503	-0.009082	-0.152745	-0.013175	-0.001626	0.060215	-0.021128	-0.004550	0.008459
CaO	-0.000108	-0.001337	-0.007552	-0.009082	0.060771	-0.052798	-0.018885	0.006402	0.036872	-0.009342	-0.002724	0.010933
Cl	-0.008400	0.017849	-0.056442	-0.152745	-0.052798	8.324525	0.092096	-0.155348	-1.709251	0.083292	0.265201	-0.073693
Li_2O	0.000056	-0.001781	-0.074092	-0.013175	-0.018885	0.092096	0.522786	0.114845	-0.079399	-0.041238	-0.085304	-0.005564
Na_2O	0.000022	-0.001823	-0.038118	-0.001626	0.006402	-0.155348	0.114845	0.046852	0.036286	-0.015242	-0.026507	0.002955
P_2O_5	0.000489	-0.030053	0.013647	0.060215	0.036872	-1.709251	-0.079399	0.036286	4.370267	-0.029369	-0.140084	-0.010662
SiO_2	-0.000965	0.000077	0.004544	-0.021128	-0.009342	0.083292	-0.041238	-0.015242	-0.029369	0.018686	0.002496	-0.012765
V_2O_5	0.000387	-0.002065	-0.017689	-0.004550	-0.002724	0.265201	-0.085304	-0.026507	-0.140084	0.002496	0.439848	0.013174
Others	-0.001021	-0.001188	-0.002528	0.008459	0.010933	-0.073693	-0.005564	0.002955	-0.010662	-0.012765	0.013174	0.034431

Table D.10. Variance-Covariance Matrix Associated With the Terms in the 11 Term Partial Quadratic Mixture Model for Melter SO₃ Melter (wt%) of LAW Glasses

Term	SR	3TS	Al ₂ O ₃	B ₂ O ₃	CaO	Cl	Li ₂ O	Na ₂ O	P ₂ O ₅	SiO ₂	V ₂ O ₅	Others	Li ₂ O x Na ₂ O
SR	0.000562	0.000437	-0.000121	0.000306	-0.000095	-0.007402	-0.000001	0.000016	0.000423	-0.000850	0.000338	-0.000900	0.000391
3TS	0.000437	0.000994	0.000818	-0.000197	-0.001174	0.015845	-0.002290	-0.001663	-0.026623	0.000087	-0.001873	-0.001035	0.005625
Al ₂ O ₃	-0.000121	0.000818	0.106166	-0.023641	-0.006321	-0.042622	-0.116415	-0.037560	0.003878	0.005365	-0.019318	-0.001282	0.399300
B ₂ O ₃	0.000306	-0.000197	-0.023641	0.098671	-0.008139	-0.137443	0.007740	0.000059	0.056206	-0.019151	-0.002605	0.007102	-0.151396
CaO	-0.000095	-0.001174	-0.006321	-0.008139	0.053655	-0.045479	-0.024439	0.005047	0.031280	-0.008033	-0.002969	0.009788	0.060851
Cl	-0.007402	0.015845	-0.042622	-0.137443	-0.045479	7.365518	-0.082514	-0.149650	-1.533789	0.077818	0.222002	-0.061961	1.280449
Li ₂ O	-0.000001	-0.002290	-0.116415	0.007740	-0.024439	-0.082514	1.628478	0.191322	0.116498	-0.067394	0.009706	-0.026574	-9.128442
Na ₂ O	0.000016	-0.001663	-0.037560	0.000059	0.005047	-0.149650	0.191322	0.048268	0.046391	-0.015836	-0.016830	0.000936	-0.703963
P ₂ O ₅	0.000423	-0.026623	0.003878	0.056206	0.031280	-1.533789	0.116498	0.046391	3.884548	-0.030861	-0.109986	-0.012867	-1.458618
SiO ₂	-0.000850	0.000087	0.005365	-0.019151	-0.008033	0.077818	-0.067394	-0.015836	-0.030861	0.017306	-0.000056	-0.010683	0.242571
V ₂ O ₅	0.000338	-0.001873	-0.019318	-0.002605	-0.002969	0.222002	0.009706	-0.016830	-0.109986	-0.000056	0.394144	0.010043	-0.664261
Others	-0.000900	-0.001035	-0.001282	0.007102	0.009788	-0.061961	-0.026574	0.000936	-0.012867	-0.010683	0.010043	0.030772	0.169424
Li ₂ OxNa ₂ O	0.000391	0.005625	0.399300	-0.151396	0.060851	1.280449	-9.128442	-0.703963	-1.458618	0.242571	-0.664261	0.169424	71.381920

Table D.11. Variance-Covariance Matrix Associated With the Terms in the 11 Term Reduced Linear Mixture Model for $\ln(k_{1208})$ in of LAW Glasses

Term	Al ₂ O ₃	B ₂ O ₃	CaO	Cr ₂ O ₃	K ₂ O	Li ₂ O	Na ₂ O	SiO ₂	V ₂ O ₅	ZrO ₂	Others
Al ₂ O ₃	1.424275	-0.196368	-0.181561	0.256397	0.147292	-1.184685	-0.621428	0.127750	-0.000326	-0.193765	-0.066503
B ₂ O ₃	-0.196368	1.266439	-0.330739	1.456241	-0.093675	0.249682	0.004383	-0.244115	-0.054948	-0.049840	0.066017
CaO	-0.181561	-0.330739	0.897014	-1.161892	0.183376	-0.827434	-0.014343	-0.055768	-0.190127	0.526020	0.210556
Cr ₂ O ₃	0.256397	1.456241	-1.161892	113.804199	-4.719855	-6.007136	-1.495310	0.231267	-0.452838	-4.890241	2.137992
K ₂ O	0.147292	-0.093675	0.183376	-4.719855	1.804941	0.801154	0.078904	-0.039017	-0.293128	0.137461	-0.389528
Li ₂ O	-1.184685	0.249682	-0.827434	-6.007136	0.801154	11.504028	2.890170	-0.880563	-3.259264	-2.440359	-0.686403
Na ₂ O	-0.621428	0.004383	-0.014343	-1.495310	0.078904	2.890170	0.961620	-0.260520	-0.923089	-0.844381	-0.093419
SiO ₂	0.127750	-0.244115	-0.055768	0.231267	-0.039017	-0.880563	-0.260520	0.228765	0.105843	-0.064394	-0.192954
V ₂ O ₅	-0.000326	-0.054948	-0.190127	-0.452838	-0.293128	-3.259264	-0.923089	0.105843	6.320087	1.500310	0.810594
ZrO ₂	-0.193765	-0.049840	0.526020	-4.890241	0.137461	-2.440359	-0.844381	-0.064394	1.500310	3.851941	0.485569
Others	-0.066503	0.066017	0.210556	2.137992	-0.389528	-0.686403	-0.093419	-0.192954	0.810594	0.485569	0.739875

Table D.12. Variance-Covariance Matrix Associated With the Terms in the 13 Term Partial Quadratic Mixture Model for $\ln(k_{1208}, \text{in})$ of LAW Glasses

Term	Al ₂ O ₃	B ₂ O ₃	CaO	Cr ₂ O ₃	K ₂ O	Li ₂ O	Na ₂ O	SiO ₂	V ₂ O ₅	ZrO ₂	Others	Li ₂ O x Li ₂ O	Na ₂ O x SiO ₂
Al ₂ O ₃	3.573147	1.519970	1.516088	3.246322	0.772305	-2.515171	-7.987438	-1.889312	0.253034	2.145784	1.712778	60.388215	19.666766
B ₂ O ₃	1.519970	2.357941	0.938047	3.479048	0.388767	-0.899775	-5.441480	-1.681855	0.137742	1.649922	1.354328	45.375048	14.402735
CaO	1.516088	0.938047	2.094815	0.769452	0.667521	-2.870531	-5.483996	-1.532965	0.038030	2.117489	1.468916	71.699047	14.594724
Cr ₂ O ₃	3.246322	3.479048	0.769452	106.220365	-3.511597	-2.447411	-10.651697	-2.258378	-0.169643	-1.185556	4.200548	-45.335949	24.097781
K ₂ O	0.772305	0.388767	0.667521	-3.511597	1.791339	-0.193112	-2.032416	-0.605337	-0.178361	0.752612	0.147252	29.579515	5.617009
Li ₂ O	-2.515171	-0.899775	-2.870531	-2.447411	-0.193112	24.233045	8.299026	0.902785	-3.315438	-3.316944	-1.728650	-379.754076	-16.764174
Na ₂ O	-7.987438	-5.441480	-5.483996	-10.651697	-2.032416	8.299026	24.832372	6.235704	-1.651070	-8.167206	-5.775041	-220.734103	-63.532158
SiO ₂	-1.889312	-1.681855	-1.532965	-2.258378	-0.605337	0.902785	6.235704	1.946707	-0.134198	-2.051280	-1.702693	-62.902963	-17.144585
V ₂ O ₅	0.253034	0.137742	0.038030	-0.169643	-0.178361	-3.315438	-1.651070	-0.134198	5.617225	1.572596	0.909986	13.760979	2.242051
ZrO ₂	2.145784	1.649922	2.117489	-1.185556	0.752612	-3.316944	-8.167206	-2.051280	1.572596	5.729554	2.202219	52.414480	19.584270
Others	1.712778	1.354328	1.468916	4.200548	0.147252	-1.728650	-5.775041	-1.702693	0.909986	2.202219	2.009430	46.172721	15.050488
Li ₂ O x Li ₂ O	60.388215	45.375048	71.699047	-45.335949	29.579515	-379.754076	-220.734103	-62.902963	13.760979	52.414480	46.172721	10449.375970	624.494574
Na ₂ O x SiO ₂	19.666766	14.402735	14.594724	24.097781	5.617009	-16.764174	-63.532158	-17.144585	2.242051	19.584270	15.050488	624.494574	168.489058

Appendix E Example Temperature and Composition Models for Viscosity and Electrical Conductivity

The recommended viscosity (Section 5) and EC (Section 6) models are based on isothermal 1150°C values. Although these values are appropriate for formulation of glasses to be produced at the WTP, there are occasions in which a model user would desire viscosity or electrical conductivity predictions at alternative temperatures. This appendix supplies example models to predict viscosity and EC as functions of both composition and temperature.

E.1 Viscosity-Composition-Temperature Models

Considerable effort has been devoted to the development of models describing silicate melt viscosities as functions of temperature and composition. Reviews and in-depth assessments of modeling approaches and technical underpinnings are readily found in the literature as summarized by Heredia-Langner et al. (2022) and Ferkl et al. (2022). Heredia-Langner et al. (2022) fitted the LAW glass viscosity-temperature-composition database to each of the model forms listed in Table E.1. and recommended the AR version of the model with a PQM form describing the composition dependence of the B term as most appropriate for use in design of glasses and control of melter operation at the Hanford Site. They also recommended an AR version of the model with RLM form describing the composition dependence of the B term as the most simplistic linear model with good predictability. The coefficients and fit statistics for these models are summarized in Table E.2. and the variance-covariance matrices are listed in Tables E.3. and E.4.

Table E.1. Some of the Most Frequently Referenced Viscosity-Temperature Models in Nuclear waste Glass Science. The table is not intended to be all-inclusive.

Model	Functions	Pros	Cons
Arrhenius (AR)	$\ln(\eta) = A + \frac{B}{T}$	<ul style="list-style-type: none"> • Fewer parameters • Linear fit 	<ul style="list-style-type: none"> • Only applicable over narrow range
Vogel, Fulcher, and Tammann (VF)	$\ln(\eta) = A + \frac{B}{T - T_0}$	<ul style="list-style-type: none"> • Reproduces curvature in data • Most widely used in literature 	<ul style="list-style-type: none"> • Requires non-linear fit
Mauro, Yue, Ellison, Gupta, and Allan (MY)	$\ln(\eta) = A + \frac{B}{T} \exp\left(\frac{C}{T}\right)$	<ul style="list-style-type: none"> • Reproduces curvature in data • Represents data well near glass transition 	<ul style="list-style-type: none"> • Non-linear fit
Avramov and Milchev (AM)	$\ln(\eta) = A + \left(\frac{B}{T}\right)^a$	<ul style="list-style-type: none"> • Reproduces curvature in data 	<ul style="list-style-type: none"> • Non-linear fit • Oddly scaled parameters

Table E.2. Component Coefficients for the AR and
AM Viscosity-Temperature-Composition Models*
(After Heredia-Langner et al. 2022)

Term	AM PQM	AR RLM
A	-2.1483	-10.63733
Al ₂ O ₃	4522.3515	37356.844
B ₂ O ₃	1020.4357	6527.8997
CaO	1260.0231	7494.2639
Fe ₂ O ₃	2762.4187	17545.756
K ₂ O	1673.1286	10224.607
Li ₂ O	-5264.2734	-33402.96
MgO	2373.9846	14905.896
Na ₂ O	291.4697	3393.0905
P ₂ O ₅	3984.1403	24547.678
SiO ₂	4921.0864	31721.392
SnO ₂	4388.7692	27793.878
TiO ₂	2401.3011	15507.64
V ₂ O ₅	1985.4762	12212.411
ZnO	1826.5884	11553.131
ZrO ₂	3659.8543	30364.115
Others	3503.1550	23380.133
Al ₂ O ₃ × Na ₂ O	7674.5414	n/a
SiO ₂ × ZrO ₂	2602.8079	n/a
Na ₂ O × Na ₂ O	-996.9091	n/a
a	2.2520	n/a
Fit R ²	0.9843	0.9797
Fit RMSE	0.1736	0.1973
Val R ²	0.9755	0.9643
Val RMSE	0.1762	0.2127
*Component concentrations expressed in mass fraction, temperature in K, and viscosity in P.		

Table E.3. Variance-Covariance Matrix for AM-PQM Model

Term	A	Al ₂ O ₃	B ₂ O ₃	CaO	Fe ₂ O ₃	K ₂ O	Li ₂ O	MgO
A	0.0162	-13.1402	-3.3438	-4.1711	-8.7570	-5.6134	15.1141	-7.6599
Al ₂ O ₃	-13.1402	21659.8171	2512.8958	2691.8855	6752.9313	3478.1091	-14485.5691	5454.6300
B ₂ O ₃	-3.3438	2512.8958	2128.7728	1220.6814	2160.9769	1603.4869	-2910.0889	1715.6931
CaO	-4.1711	2691.8855	1220.6814	2063.8432	2666.5243	1889.8270	-3748.5171	2627.0251
Fe ₂ O ₃	-8.7570	6752.9313	2160.9769	2666.5243	6087.3329	3284.5881	-8177.4862	4248.3517
K ₂ O	-5.6134	3478.1091	1603.4869	1889.8270	3284.5881	4131.5049	-3976.8921	3361.4442
Li ₂ O	15.1141	-14485.5691	-2910.0889	-3748.5171	-8177.4862	-3976.8921	21904.4624	-7171.6780
MgO	-7.6599	5454.6300	1715.6931	2627.0251	4248.3517	3361.4442	-7171.6780	10187.3463
Na ₂ O	-1.0512	1068.6323	-373.7232	144.7962	295.1780	-144.2031	774.6070	1249.0340
P ₂ O ₅	-12.6456	8892.9549	3005.5496	3816.5364	7066.3802	5106.8265	-10864.3786	6058.2314
SiO ₂	-15.0135	11639.3957	2615.8675	3457.8669	7777.8110	4900.1690	-15084.2454	6444.1596
SnO ₂	-14.0372	10801.5727	3549.0224	4344.5799	8388.4399	4467.2470	-14289.7969	6822.5684
TiO ₂	-7.7291	6131.2096	2442.3784	2879.4552	4101.6460	2894.5251	-7003.6709	3153.9123
V ₂ O ₅	-6.4437	4362.9325	1723.9419	1950.9839	4236.2164	2798.3556	-6735.3747	3279.0878
ZnO	-5.4476	4348.6204	1005.4142	1547.1672	3257.4972	1909.2329	-5616.6558	2928.2777
ZrO ₂	-9.9879	6510.6360	-4745.2354	-5211.7491	-986.8173	-3556.5166	-16253.9151	-5414.1455
Others	-10.8314	9881.1784	2106.6178	1947.1158	6967.4298	3583.4813	-12961.2649	5359.0413
Al ₂ O ₃ ×Na ₂ O	-26.3415	-35864.1984	6483.0503	11387.5808	18445.2176	16513.6644	-18106.8282	18397.4063
SiO ₂ ×ZrO ₂	-11.6628	12829.2791	19542.3232	23140.8831	23725.7034	20805.9783	4543.9378	31803.9077
Na ₂ O×Na ₂ O	2.8731	7317.8314	2029.9834	42.3444	-859.6593	865.6558	2395.3448	-3152.8864
a	0.0053	-4.3598	-1.0833	-1.3616	-2.8989	-1.8413	5.1036	-2.5301

Table E.3. Variance-Covariance Matrix for AM-PQM Model, Cont.

Term	Na ₂ O	P ₂ O ₅	SiO ₂	SnO ₂	TiO ₂	V ₂ O ₅	ZnO	ZrO ₂
A	-1.0512	-12.6456	-15.0135	-14.0372	-7.7291	-6.4437	-5.4476	-9.9879
Al ₂ O ₃	1068.6323	8892.9549	11639.3957	10801.5727	6131.2096	4362.9325	4348.6204	6510.6360
B ₂ O ₃	-373.7232	3005.5496	2615.8675	3549.0224	2442.3784	1723.9419	1005.4142	-4745.2354
CaO	144.7962	3816.5364	3457.8669	4344.5799	2879.4552	1950.9839	1547.1672	-5211.7491
Fe ₂ O ₃	295.1780	7066.3802	7777.8110	8388.4399	4101.6460	4236.2164	3257.4972	-986.8173
K ₂ O	-144.2031	5106.8265	4900.1690	4467.2470	2894.5251	2798.3556	1909.2329	-3556.5166
Li ₂ O	774.6070	-10864.3786	-15084.2454	-14289.7969	-7003.6709	-6735.3747	-5616.6558	-16253.9151
MgO	1249.0340	6058.2314	6444.1596	6822.5684	3153.9123	3279.0878	2928.2777	-5414.1455
Na ₂ O	3832.5612	311.5619	351.2347	397.6426	-48.7547	-723.8749	649.3130	-1743.7549
P ₂ O ₅	311.5619	21405.1278	11542.1379	11076.5469	6863.3102	5234.7058	4215.6480	1658.5054
SiO ₂	351.2347	11542.1379	14726.9797	12793.3155	6573.3623	5802.2989	4435.3060	17412.7313
SnO ₂	397.6426	11076.5469	12793.3155	16408.6563	8165.8386	6075.9101	5259.8792	-820.1045
TiO ₂	-48.7547	6863.3102	6573.3623	8165.8386	10792.2528	4492.3227	2741.2570	-4547.5009
V ₂ O ₅	-723.8749	5234.7058	5802.2989	6075.9101	4492.3227	7392.0787	2584.8941	-2340.1281
ZnO	649.3130	4215.6480	4435.3060	5259.8792	2741.2570	2584.8941	7895.0286	-1059.5727
ZrO ₂	-1743.7549	1658.5054	17412.7313	-820.1045	-4547.5009	-2340.1281	-1059.5727	176726.4001
Others	-341.5298	4743.4599	9816.8673	9138.4216	5732.9323	3298.1157	5066.0167	3622.5901
Al ₂ O ₃ ×Na ₂ O	-1502.8651	31952.9783	27785.2360	29580.7802	15292.8541	17124.4971	9969.2964	-4933.2250
SiO ₂ ×ZrO ₂	6813.7446	25870.9721	-9868.6006	34216.2908	30813.6201	22080.9285	15067.0503	-421890.1172
Na ₂ O×Na ₂ O	-10253.1139	-1738.0363	-3062.6994	-2317.8431	682.8208	936.2050	-1874.9293	-12579.0660
a	-0.3129	-4.1778	-4.9900	-4.6569	-2.5454	-2.1060	-1.7869	-3.2594

Table E.3. Variance-Covariance Matrix for AM-PQM Model, Cont.

Term	Others	Al ₂ O ₃ ×Na ₂ O	SiO ₂ ×ZrO ₂	Na ₂ O×Na ₂ O	<i>a</i>
A	-10.8314	-26.3415	-11.6628	2.8731	0.0053
Al ₂ O ₃	9881.1784	-35864.1984	12829.2791	7317.8314	-4.3598
B ₂ O ₃	2106.6178	6483.0503	19542.3232	2029.9834	-1.0833
CaO	1947.1158	11387.5808	23140.8831	42.3444	-1.3616
Fe ₂ O ₃	6967.4298	18445.2176	23725.7034	-859.6593	-2.8989
K ₂ O	3583.4813	16513.6644	20805.9783	865.6558	-1.8413
Li ₂ O	-12961.2649	-18106.8282	4543.9378	2395.3448	5.1036
MgO	5359.0413	18397.4063	31803.9077	-3152.8864	-2.5301
Na ₂ O	-341.5298	-1502.8651	6813.7446	-10253.1139	-0.3129
P ₂ O ₅	4743.4599	31952.9783	25870.9721	-1738.0363	-4.1778
SiO ₂	9816.8673	27785.2360	-9868.6006	-3062.6994	-4.9900
SnO ₂	9138.4216	29580.7802	34216.2908	-2317.8431	-4.6569
TiO ₂	5732.9323	15292.8541	30813.6201	682.8208	-2.5454
V ₂ O ₅	3298.1157	17124.4971	22080.9285	936.2050	-2.1060
ZnO	5066.0167	9969.2964	15067.0503	-1874.9293	-1.7869
ZrO ₂	3622.5901	-4933.2250	-42189.1172	-12579.0660	-3.2594
Others	34230.5621	11881.4070	16160.3760	-1263.0471	-3.6062
Al ₂ O ₃ ×Na ₂ O	11881.4070	386554.6211	77062.5819	-61788.7091	-8.8705
SiO ₂ ×ZrO ₂	16160.3760	77062.5819	1105814.3575	21479.5389	-4.0404
Na ₂ O×Na ₂ O	-1263.0471	-61788.7091	21479.5389	49094.4657	0.9727
<i>a</i>	-3.6062	-8.8705	-4.0404	0.9727	0.0018

Table E.4. Variance-Covariance Matrix for AR-RLM Model

Term	A	Al ₂ O ₃	B ₂ O ₃	CaO	Fe ₂ O ₃	K ₂ O	Li ₂ O	MgO
A	0.0016	-2.0927	-2.1857	-2.1669	-2.0844	-2.2829	-2.2270	-2.1980
Al ₂ O ₃	-2.0927	56342.8492	-4845.2086	-1903.3782	8142.1475	4554.3968	-35943.3106	-2199.5755
B ₂ O ₃	-2.1857	-4845.2086	56717.4522	2561.7520	4829.8564	4655.7938	-6521.4627	-4799.5070
CaO	-2.1669	-1903.3782	2561.7520	31460.5950	4904.7677	3319.9122	-11739.1902	11489.1995
Fe ₂ O ₃	-2.0844	8142.1475	4829.8564	4904.7677	59610.9301	-4325.7674	-7780.5002	-15132.7784
K ₂ O	-2.2829	4554.3968	4655.7938	3319.9122	-4325.7674	91934.2885	43446.6941	19439.3080
Li ₂ O	-2.2270	-35943.3106	-6521.4627	-11739.1902	-7780.5002	43446.6941	339532.6650	-20998.7647
MgO	-2.1980	-2199.5755	-4799.5070	11489.1995	-15132.7784	19439.3080	-20998.7647	310055.4582
Na ₂ O	-2.2741	-15647.4036	2.2753	5692.4728	-398.3989	12487.2291	87947.6220	13877.7692
P ₂ O ₅	-3.3289	23016.0905	7784.2870	10249.9848	-8318.6761	11407.4799	34385.1576	-17335.6370
SiO ₂	-2.1227	5133.5345	-5552.1821	-274.2281	-3916.3035	-2139.5709	-20761.2756	-7655.0664
SnO ₂	-2.6224	10331.5177	16392.2812	15305.1433	19179.6301	-40758.2977	-68552.8613	-22714.2204
TiO ₂	-2.5328	6189.4689	21657.3224	23475.1352	-29604.6808	-15805.7428	-6530.9734	-52679.1347
V ₂ O ₅	-2.9330	12033.3570	2092.7041	-4788.6138	24384.4761	1808.0133	-63548.7674	-6089.7450
ZnO	-2.2580	630.3841	-9433.6711	1233.9436	10748.2218	-244.3242	-29659.4981	3386.6484
ZrO ₂	-1.9564	-8458.6054	2468.1207	8997.1450	22568.7535	-17436.3674	-23041.3357	2755.3961
Others	-1.3494	-9518.9682	-12429.2741	-43616.0978	60099.1609	-5691.5620	-131110.7176	4891.0770

Table E.4. Variance-Covariance Matrix for AR-RLM Model, Cont.

Term	Na ₂ O	P ₂ O ₅	SiO ₂	SnO ₂	TiO ₂
A	-2.2741	-3.3289	-2.1227	-2.6224	-2.5328
Al ₂ O ₃	-15647.4036	23016.0905	5133.5345	10331.5177	6189.4689
B ₂ O ₃	2.2753	7784.2870	-5552.1821	16392.2812	21657.3224
CaO	5692.4728	10249.9848	-274.2281	15305.1433	23475.1352
Fe ₂ O ₃	-398.3989	-8318.6761	-3916.3035	19179.6301	-29604.6808
K ₂ O	12487.2291	11407.4799	-2139.5709	-40758.2977	-15805.7428
Li ₂ O	87947.6220	34385.1576	-20761.2756	-68552.8613	-6530.9734
MgO	13877.7692	-17335.6370	-7655.0664	-22714.2204	-52679.1347
Na ₂ O	34367.1046	7710.2014	-4912.0832	-16490.7390	-5608.3452
P ₂ O ₅	7710.2014	648024.5199	227.9365	-25767.9619	22865.4932
SiO ₂	-4912.0832	227.9365	11913.5498	6453.1250	-5917.7798
SnO ₂	-16490.7390	-25767.9619	6453.1250	189290.3081	48703.9191
TiO ₂	-5608.3452	22865.4932	-5917.7798	48703.9191	370738.1678
V ₂ O ₅	-20258.2764	-15314.1677	7974.7414	2250.8090	53368.0713
ZnO	1297.1175	-6354.0255	-17272.0492	15368.4540	-1950.5957
ZrO ₂	-13531.1631	26016.7020	-1901.0303	-4641.1864	34071.0729
Others	-63162.6313	-220458.1370	-3840.0681	-11628.2872	14896.0724

Table E.4. Variance-Covariance Matrix for AR-RLM Model, Cont.

Term	V ₂ O ₅	ZnO	ZrO ₂	Others
A	-2.9330	-2.2580	-1.9564	-1.3494
Al ₂ O ₃	12033.3570	630.3841	-8458.6054	-9518.9682
B ₂ O ₃	2092.7041	-9433.6711	2468.1207	-12429.2741
CaO	-4788.6138	1233.9436	8997.1450	-43616.0978
Fe ₂ O ₃	24384.4761	10748.2218	22568.7535	60099.1609
K ₂ O	1808.0133	-244.3242	-17436.3674	-5691.5620
Li ₂ O	-63548.7674	-29659.4981	-23041.3357	-131110.7176
MgO	-6089.7450	3386.6484	2755.3961	4891.0770
Na ₂ O	-20258.2764	1297.1175	-13531.1631	-63162.6313
P ₂ O ₅	-15314.1677	-6354.0255	26016.7020	-220458.1370
SiO ₂	7974.7414	-17272.0492	-1901.0303	-3840.0681
SnO ₂	2250.8090	15368.4540	-4641.1864	-11628.2872
TiO ₂	53368.0713	-1950.5957	34071.0729	14896.0724
V ₂ O ₅	230950.5780	19772.5709	35123.2430	-46394.7637
ZnO	19772.5709	318242.8355	-3601.5985	71529.7521
ZrO ₂	35123.2430	-3601.5985	136029.0332	7236.9486
Others	-46394.7637	71529.7521	7236.9486	1420446.7621

E.2 Electrical Conductivity-Composition-Temperature Models

Electrical conductivity-composition-temperature models of silicate-based waste glass melts as functions of temperature and composition are typically of the forms AR and VF (as those described in Table E.1. with ϵ replacing η). These two model forms were fitted to the LAW glass EC-temperature-composition database. An AR based model with the composition effects on the B term represented by a PQM is recommended as most appropriate for use in design of glasses and control of melter operation at the

Hanford Site. Table E.5. lists the model coefficients and summary statistics and Table E.6 gives the variance-covariance matrix.

Table E.5. Component Coefficients for the AR EC-
Temperature-Composition Models*

Term	Coefficient	Statistic	Value
A	4.2142345	R ² Fit	0.9371
Al ₂ O ₃	-11799.56	R ² Adj	0.9368
B ₂ O ₃	-9911.015	R ² Press	0.9314
CaO	-11790.3	R ² Val	0.8773
Fe ₂ O ₃	-7829.393	RMSE Fit	0.1404
K ₂ O	-6743.649	RMSE Press	0.1463
Li ₂ O	30637.593	RMSE Val	0.1755
MgO	-12411.88	n	3586
Na ₂ O	5895.8381	Mean of response	-1.1257
P ₂ O ₅	-10398.91		
SiO ₂	-10764.34		
SnO ₂	-12859.96		
TiO ₂	-9275.658		
V ₂ O ₅	-8540.411		
ZnO	-10217.12		
ZrO ₂	-10388.09		
Others	-7937.69		
Li ₂ O×Na ₂ O	-98110.49		

* EC in S/cm and component concentrations in mass fractions.

Table E.6. Variance-covariance Matrix for EC AR PQM Model

Term	A	Al ₂ O ₃	B ₂ O ₃	CaO	Fe ₂ O ₃	K ₂ O	Li ₂ O	MgO
A	0.0009	-1.1669	-1.3026	-1.1509	-1.2654	-1.1831	-1.3733	-1.1211
Al ₂ O ₃	-1.1669	28327.3814	-2495.4926	78.3926	3557.1500	1999.8238	-33494.7463	-2080.4450
B ₂ O ₃	-1.3026	-2495.4926	30391.5185	960.0687	1780.6233	2455.3009	4954.0218	-335.8192
CaO	-1.1509	78.3926	960.0687	15831.6033	3010.7666	2215.8793	-11867.4651	6355.8914
Fe ₂ O ₃	-1.2654	3557.1500	1780.6233	3010.7666	31666.8330	-1097.4079	-9033.4167	-7142.6801
K ₂ O	-1.1831	1999.8238	2455.3009	2215.8793	-1097.4079	47886.9787	29857.2739	4952.5237
Li ₂ O	-1.3733	-33494.7463	4954.0218	-11867.4651	-9033.4167	29857.2739	532419.8003	-36998.9861
MgO	-1.1211	-2080.4450	-335.8192	6355.8914	-7142.6801	4952.5237	-36998.9861	163729.9574
Na ₂ O	-1.1843	-8699.1518	1000.7743	1703.2333	-2.0754	6864.2961	83694.4627	4665.6880
P ₂ O ₅	-1.3931	10705.8265	3891.8899	4417.0981	-6370.1909	6295.4958	29849.2871	-10784.9985
SiO ₂	-1.2123	3489.2210	-2792.6990	234.2552	-1415.4531	-1276.6376	-21737.4823	-2886.2719
SnO ₂	-1.0927	3170.5242	7167.2575	6966.8189	7183.2890	-20884.2573	-32185.9583	-10004.1554
TiO ₂	-1.6608	3125.0795	11019.4397	13120.4251	-17097.5141	-7260.3529	4512.0288	-30974.7283
V ₂ O ₅	-1.3011	-410.7453	2316.9782	-1375.5684	8744.7550	3373.7354	7690.8650	-7428.0884
ZnO	-1.2296	930.3032	-5971.9689	1290.9756	6486.0579	88.3255	-36284.6400	-4597.3209
ZrO ₂	-1.2595	-3563.1609	638.1794	5663.7293	11514.5383	-8584.6525	-50735.9953	5422.6905
Others	-0.5692	-8796.5997	-9910.8522	-19907.4938	36912.5653	-3131.0202	-94210.1378	3225.8602
Li ₂ O× Na ₂ O	1.6951	123174.0817	-61552.3140	32788.8288	45000.2075	-65922.8199	-2505816.9192	176235.7770

Table E.6. Variance-covariance Matrix for EC AR PQM Model, Cont.

Term	Na ₂ O	P ₂ O ₅	SiO ₂	SnO ₂	TiO ₂	V ₂ O ₅	ZnO
A	-1.1843	-1.3931	-1.2123	-1.0927	-1.6608	-1.3011	-1.2296
Al ₂ O ₃	-8699.1518	10705.8265	3489.2210	3170.5242	3125.0795	-410.7453	930.3032
B ₂ O ₃	1000.7743	3891.8899	-2792.6990	7167.2575	11019.4397	2316.9782	-5971.9689
CaO	1703.2333	4417.0981	234.2552	6966.8189	13120.4251	-1375.5684	1290.9756
Fe ₂ O ₃	-2.0754	-6370.1909	-1415.4531	7183.2890	-17097.5141	8744.7550	6486.0579
K ₂ O	6864.2961	6295.4958	-1276.6376	-20884.2573	-7260.3529	3373.7354	88.3255
Li ₂ O	83694.4627	29849.2871	-21737.4823	-32185.9583	4512.0288	7690.8650	-36284.6400
MgO	4665.6880	-10784.9985	-2886.2719	-10004.1554	-30974.7283	-7428.0884	-4597.3209
Na ₂ O	21464.3517	4839.5087	-4022.3247	-6868.2968	-143.6704	-3422.1068	-624.0778
P ₂ O ₅	4839.5087	358144.2499	-676.2999	-15268.6849	14332.8574	-5236.1338	-3369.1550
SiO ₂	-4022.3247	-676.2999	6765.6393	3611.7532	-2211.0052	2430.3796	-8219.2292
SnO ₂	-6868.2968	-15268.6849	3611.7532	87330.2172	20298.2562	-4272.4410	2432.5827
TiO ₂	-143.6704	14332.8574	-2211.0052	20298.2562	195425.5732	26902.0357	-2798.8374
V ₂ O ₅	-3422.1068	-5236.1338	2430.3796	-4272.4410	26902.0357	110953.9374	5803.1233
ZnO	-624.0778	-3369.1550	-8219.2292	2432.5827	-2798.8374	5803.1233	166764.5976
ZrO ₂	-10494.0907	13139.8693	624.1073	-3415.2389	15174.5904	10339.5963	4140.9476
Others	-34589.5739	-125733.1555	-140.1960	-14010.4353	-10541.5068	-26134.3716	27661.2293
Li ₂ O× Na ₂ O	-271957.9704	-85655.1834	69971.7418	22655.0071	-27270.2141	-240988.8445	206309.3138

Table E.6. Variance-covariance Matrix for EC AR PQM Model, Cont.

Term	ZrO ₂	Others	Li ₂ O×Na ₂ O
A	-1.2595	-0.5692	1.6951
Al ₂ O ₃	-3563.1609	-8796.5997	123174.0817
B ₂ O ₃	638.1794	-9910.8522	-61552.3140
CaO	5663.7293	-19907.4938	32788.8288
Fe ₂ O ₃	11514.5383	36912.5653	45000.2075
K ₂ O	-8584.6525	-3131.0202	-65922.8199
Li ₂ O	-50735.9953	-94210.1378	-2505816.9192
MgO	5422.6905	3225.8602	176235.7770
Na ₂ O	-10494.0907	-34589.5739	-271957.9704
P ₂ O ₅	13139.8693	-125733.1555	-85655.1834
SiO ₂	624.1073	-140.1960	69971.7418
SnO ₂	-3415.2389	-14010.4353	22655.0071
TiO ₂	15174.5904	-10541.5068	-27270.2141
V ₂ O ₅	10339.5963	-26134.3716	-240988.8445
ZnO	4140.9476	27661.2293	206309.3138
ZrO ₂	71957.2052	15104.1194	272265.9151
Others	15104.1194	729994.9756	185900.9952
Li ₂ O× Na ₂ O	272265.9151	185900.9952	17645290.8306

E.3 References

Heredia-Langner A, V Gervasio, SK Cooley, CE Lonergan, DS Kim, AA Kruger, and JD Vienna. 2022. “Hanford Low-Activity Waste Glass Composition-Temperature-Melt Viscosity Relationships,” in *International Journal of Applied Glass Science*, **Under Revision**.

Ferkl P, P Hrma, and A Kruger. 2022. “Parsimonious viscosity–composition relationships for high-temperature multicomponent glass melts,” in *Journal of Asian Ceramic Societies*, DOI: 10.1080/21870764.2021.2012903.

Pacific Northwest National Laboratory

902 Battelle Boulevard
P.O. Box 999
Richland, WA 99354
1-888-375-PNNL (7665)

www.pnnl.gov